VOLUME 23 / NUMBER 23
DECEMBER 8, 1985
ACC. NOS. N85-34113 TO N85-35151

STAR
AN ABSTRACT JOURNAL

Scientific and Technical Aerospace Reports

PRODUCED BY THE
SCIENTIFIC AND TECHNICAL
INFORMATION
BRANCH

NASA

NATIONAL AERONAUTICS AND SPACE ADMINISTRATION

WHAT YOU CAN DO FOR *STAR*

All users of this abstract service are urged to forward reports to be considered for announcement in *STAR*. This will aid NASA in its efforts to provide the fullest possible coverage of all scientific and technical publications that might support aeronautics and space research and development. If you have prepared relevant reports (other than those that you will transmit to NASA, DoD, or DOE through the usual contract- or grant-reporting channels), please send them for consideration to the NASA Scientific and Technical Information Facility, P.O. Box 8757, B.W.I. Airport, Maryland 21240.

Reprints of journal articles, book chapters, and conference papers are also welcome. These will be considered for announcement in *STAR's* companion journal, *International Aerospace Abstracts*.

You may specify a particular source to be included in a report announcement if you wish; otherwise the report will be placed on public sale at the National Technical Information Service. Copyrighted publications will be announced but not distributed or sold.

PURCHASE OF *STAR*

The semimonthly issues are available for sale by the Superintendent of Documents, U.S. Government Printing Office, Washington, D.C. 20402.

PUBLISHED BY:

UNITED STATES GOVERNMENT
NATIONAL AERONAUTICS AND SPACE ADMINISTRATION
SCIENTIFIC AND TECHNICAL INFORMATION BRANCH
Scientific and Technical Aerospace Reports, Volume 23, is prepared by the NASA Scientific and Technical Information Facility operated for the National Aeronautics and Space Administration by RMS Associates.

The Administrator of the National Aeronautics and Space Administration has determined that the publication of this periodical is necessary in the transaction of the public business required by law of this Agency. Use of funds for printing this periodical has been approved by the Director of the Office of Management and Budget through March 22, 1988.

US ISSN 0036-8741

INTRODUCTION

Scientific and Technical Aerospace Reports (STAR) is a major component of a comprehensive National Aeronautics and Space Administration information system covering aeronautics, space, and supporting disciplines. *STAR* is issued on the 8th and 23rd of each month and announces current publications of the following types:

- NASA, NASA contractor, and NASA grantee reports
- Reports issued by other U.S. Government agencies, domestic and foreign institutions, universities, and private firms
- Translations in report form
- NASA-owned patents and patent applications
- Dissertations and theses

Cumulative index volumes are published annually.

Journal, book, and conference literature, cover-to-cover journal translations, and certain foreign dissertations are announced in a companion journal, *International Aerospace Abstracts (IAA)*, available on subscription from the American Institute of Aeronautics and Astronautics, Technical Information Service, 555 West 57th Street, 12th Floor, New York, New York 10019.

SUBJECT SCOPE

Subject scope of *STAR*, and *IAA* includes all aspects of aeronautics and space research and development, supporting basic and applied research, and applications. Aerospace aspects of earth resources, energy development, conservation, oceanography, environmental protection, urban transportation, and other topics of high national priority are also covered.

OTHER NASA PUBLICATIONS

Other NASA publications and information services are described in the publication, *The NASA Scientific and Technical Information System ... and How to Use It*, available without charge from the NASA Scientific and Technical Information Facility, P.O. Box 8757, B.W.I. Airport, Maryland 21240.

HOW TO USE *STAR* SUBJECT CATEGORIES

STAR is categorized by 10 major subject divisions divided into 74 specific subject categories and one general category/division. The major subject divisions are listed in the Table of Contents, together with a note for each that defines its scope and provides any cross-references. For example:

AERONAUTICS

Includes aeronautics (general); aerodynamics; air transportation and safety; aircraft communications and navigation; aircraft design, testing and performance; aircraft instrumentation; aircraft propulsion and power; aircraft stability and control; and research and support facilities (air).

For related information see also *Astronautics*.

Each major division is further divided into as many as nine specific categories, which are identified by category numbers.

Abstracts in *STAR* are grouped by specific category, the categories appearing in sequential order. Category breaks in the abstract section are identified by the category number and title, and a scope note. Cross-references to other categories are provided as appropriate. For example:

02 AERODYNAMICS

Includes aerodynamics of bodies, combinations, wings, rotors, and control surfaces; and internal flow in ducts and turbomachinery.

For related information see also *34 Fluid Mechanics and Heat Transfer*.

CROSS-REFERENCES

Individual *STAR* abstracts are not ordinarily cross-referenced, except for certain conference reports or book translations that have had separate abstracts written for their component papers or chapters. Citations and abstracts of the components follow immediately after those of the parent document. When the subject content of a component differs sufficiently from the general content of the parent, a cross-reference citation also is printed at the end of the category to which it normally would have been assigned if it were independent.

DOCUMENTS ON MICROFICHE

Documents on microfiche[1] are designated by a pound sign (#) following the accession number. The pound sign is used without regard to the source or quality of the microfiche.

AVAILABILITIES

One or more sources from which a document announced in *STAR* is available to the public is given in each citation. The most commonly indicated sources and their acronyms or abbreviations are listed below. If the publication is available from a source other than those listed, the publisher and his address will be displayed on the availability line or in combination with the corporate source line.

(1) A microfiche is a transparent sheet of film, 105 by 148 mm in size, containing as many as 60 to 98 pages of information reduced to micro images (not to exceed 26:1 reduction).

Avail: NTIS. Sold by the National Technical Information Service. Prices for hard copy (HC) and microfiche (MF) are indicated by a price code following the letters HC or MF in the *STAR* citation. Current values for the price codes are given in the tables on page vii.

Initially distributed microfiche under the NTIS SRIM (Selected Research in Microfiche) is available at greatly reduced unit prices. For this service and for information concerning subscription to NASA printed reports, consult the NTIS Subscription Section, Springfield, Va. 22161.

NOTE ON ORDERING DOCUMENTS: When ordering NASA publications (those followed by the * symbol), use the N accession number. NASA patent applications (only the specifications are offered) should be ordered by the US-Patent-Appl-SN number. Non-NASA publications (no asterisk) should be ordered by the AD, PB, or other *report* number shown on the last line of the citation, not by the N accession number. It is also advisable to cite the title and other bibliographic identification.

Avail: SOD (or GPO). Sold by the Superintendent of Documents, U.S. Government Printing Office, in hard copy. The current price and 'order number are given following the availability line. (NTIS will fill microfiche requests, as indicated above, for those documents identified by a # symbol.)

Avail: NASA Public Document Rooms. Documents so indicated may be examined at or purchased from the National Aeronautics and Space Adminstration, Public Documents Room (Room 126), 600 Independence Ave., S.W., Washington, D.C. 20546, or public document rooms located at each of the NASA research centers, the NASA Space Technology Laboratories, and the NASA Pasadena Office at the Jet Propulsion Laboratory.

Avail: DOE Depository Libraries. Organizations in U.S. cities and abroad that maintain collections of Department of Energy reports, usually in microfiche form, are listed in *Energy Research Abstracts*. Services available from the DOE and its depositories are described in a booklet, *DOE Technical Information Center - Its' Functions and Services* (TID-4660), which may be obtained without charge from the DOE Technical Information Center.

Avail: Univ. Microfilms. Documents so indicated are dissertations selected from *Dissertation Abstracts* and are sold by University Microfilms as xerographic copy (HC) and microfilm. All requests should cite the author and the Order Number as they appear in the citation.

Avail: USGS. Originals of many reports from the U.S. Geological Survey, which may contain color illustrations, or otherwise may not have the quality of illustrations preserved in the microfiche or facsimile reproduction, may be examined by the public at the libraries of the USGS field offices whose addresses are listed in this Introduction. The libraries may be queried concerning the availability of specific documents and the possible utilization of local copying services, such as color reproduction.

Avail: HMSO. Publications of Her Majesty's Stationery Office are sold in the U.S. by Pendragon House, Inc. (PHI), Redwood City, California. The U.S. price (including a service and mailing charge) is given, or a conversion table may be obtained from PHI.

Avail: BLL (formerly NLL): British Library Lending Division, Boston Spa, Wetherby, Yorkshire, England. Photocopies available from this organization at the price shown. (If none is given, inquiry should be addressed to the BLL.)

Avail: Fachinformationszentrum, Karlsruhe. Sold by the Fachinformationszentrum Energie, Physik, Mathematik GMBH, Eggenstein Leopoldshafen, Federal Republic of Germany, at the price shown in deutschmarks (DM).

Avail: Issuing Activity, or Corporate Author, or no indication of availability. Inquiries as to the availability of these documents should be addressed to the organization shown in the citation as the corporate author of the document.

Avail: U.S. Patent and Trademark Office. Sold by Commissioner of Patents and Trademarks, U.S. Patent and Trademark Office, at the standard price of 50 cents each, postage free. (See discussion of patents and patent applications below.)

Avail: ESDU. Pricing information on specific data, computer programs, and details on ESDU topic categories can be obtained from ESDU International Ltd. Requesters in North America should use the Virginia address while all other requesters should use the London address, both of which are on page vi.

NASA PATENTS AND PATENT APPLICATIONS

Patents and patent applications owned by NASA are announced in *STAR* under appropriate subject categories and are referenced in the *STAR* indexes. In the Report/Accession Number Index, patents are indexed by the NASA Case Number (which appears in lieu of the report number in other indexes), the U.S. Patent Number, the U.S. Patent Application Serial Number, and the U.S. Patent Class. Patent applications for which patents have not yet been issued are indexed by the NASA Case Number and the U.S. Patent Application Serial Number.

NASA *patent application specifications* are sold in paper copy by the National Technical Information Service at price code A02 ($7.00 domestic; $14.00 foreign). Microfiche are sold at price code A01 ($4.50 domestic; $9.00 foreign). The US-Patent-Appl-SN- number should be used in ordering either paper copy or microfiche from NTIS. Printed copies of *patents* (which are not microfiched) are available for purchase at 50 cents per copy from:

Commissioner of Patents and Trademarks
U.S. Patent and Trademark Office
Washington, D.C. 20231

When ordering patents, the U.S. Patent Number should be used, and payment must be remitted in advance, preferably by money order or check payable to the Commissioner of Patents and Trademarks. Prepaid purchase coupons for ordering are also available from the Patent and Trademark Office. The patents and patent applications announced in *STAR* are owned by NASA and are available for royalty-free licensing. Requests for licensing terms and further information should be addressed to:

Assistant General Counsel for Patent Matters/Code GP-1
National Aeronautics and Space Administration
Washington, D.C. 20546

ELIGIBILITY AND REGISTRATION FOR NASA INFORMATION PRODUCTS AND SERVICES

A variety of services is available to organizations of the following types that have registered with NASA to receive specific services or products:

1. NASA offices, research centers, contractors, subcontractors, grantees, and consultants;
2. Other U.S. Government agencies and their contractors;
3. Libraries in the United States that have arrangements with NASA to maintain collections of NASA documents for public reference;
4. Other organizations in the United States having a need for NASA documents in work related to aeronautics and space research;
5. Organizations abroad that have established reciprocal document exchange arrangements with NASA.

Only the central service points or central points of document acquisition and control within qualified organizations are eligible to register for NASA products and services. Domestic organizations that may be eligible to receive various classes of NASA publications and services should address their requests for registration or for further information to:

NASA Scientific and Technical Information Facility
ATTN: Registration Activity
P.O. Box 8757
B.W.I. Airport, Maryland 21240

Organizations abroad should direct requests to the same address, but to the attention of: International Exchange Program.

AVAILABILITY OF *STAR* ABSTRACTS ON MICROFICHE

Microfiche of the abstract sections of this issue and other issues of *STAR* are available on annual subscription from NTIS, Attn: Subscriptions, 5285 Port Royal Road, Springfield, Virginia 22161. Annual subscription rates are $60.00 North America; $120.00 foreign. Abstract sections for previous years retroactive to 1964 are available at the current rates. Microfiche for individual *STAR* issue abstract sections are not available.

PUBLIC COLLECTIONS OF NASA DOCUMENTS

DOMESTIC: NASA and NASA-sponsored documents and a large number of aerospace publications are available to the public for reference purposes at the library maintained by the American Institute of Aeronautics and Astronautics, Technical Information Service, 555 West 57th Street, 12th Floor, New York, New York 10019.

EUROPEAN: An extensive collection of NASA and NASA-sponsored publications is maintained by the British Library Lending Division, Boston Spa, Wetherby, Yorkshire, England for public access. The British Library Lending Division also has available many of the non-NASA publications cited in *STAR*. European requesters may purchase facsimile copy or microfiche of NASA and NASA-sponsored documents, those identified by both the symbols # and * from ESA - Information Retrieval Service European Space Agency, 8-10 rue Mario-Nikis, 75738 Paris CEDEX 15, France.

FEDERAL DEPOSITORY LIBRARY PROGRAM

In order to provide the general public with greater access to U.S. Government publications, Congress established the Federal Depository Library Program under the Government Printing Office (GPO), with 50 regional depositories responsible for permanent retention of material, inter-library loan, and reference services. Over 1,300 other depositories also exist. A list of the regional GPO libraries appears on the inside back cover of *STAR*.

ADDRESSES OF ORGANIZATIONS

American Institute of Aeronautics and Astronautics
Technical Information Service
555 West 57th Street, 12th Floor
New York, New York 10019

British Library Lending Division,
Boston Spa, Wetherby, Yorkshire,
England

Commissioner of Patents and Trademarks
U.S. Patent and Trademark Office
Washington, D.C. 20231

Department of Energy
Technical Information Center
P.O. Box 62
Oak Ridge, Tennessee 37830

ESA-Information Retrieval Service
ESRIN
Via Galileo Galilei
00044 Frascati (Rome) Italy

ESDU International, Ltd.
1495 Chain Bridge Road
McLean, Virginia 22101

ESDU International, Ltd.
251-259 Regent Street
London, W1R 7AD, England

Fachinformationszentrum Energie, Physik, Mathematik GMBH
7514 Eggenstein Leopoldshafen
Federal Republic of Germany

Her Majesty's Stationery Office
P.O. Box 569, S.E. 1
London, England

NASA Scientific and Technical Information Facility
P.O. Box 8757
B.W.I. Airport, Maryland 21240

National Aeronautics and Space Administration
Scientific and Technical Information Branch (NIT-1)
Washington, D.C. 20546

National Technical Information Service
5285 Port Royal Road
Springfield, Virginia 22161

Pendragon House, Inc.
899 Broadway Avenue
Redwood City, California 94063

Superintendent of Documents
U.S. Government Printing Office
Washington, D.C. 20402

University Microfilms
A Xerox Company
300 North Zeeb Road
Ann Arbor, Michigan 48106

University Microfilms, Ltd.
Tylers Green
London, England

U.S. Geological Survey Library
National Center – MS 950
12201 Sunrise Valley Drive
Reston, Virginia 22092

U.S. Geological Survey Library
2255 North Gemini Drive
Flagstaff, Arizona 86001

U.S. Geological Survey
345 Middlefield Road
Menlo Park, California 94025

U.S. Geological Survey Library
Box 25046
Denver Federal Center, MS 914
Denver, Colorado 80225

NTIS PRICE SCHEDULES

Schedule A

STANDARD PAPER COPY PRICE SCHEDULE

(Effective January 1, 1983)

Price Code	Page Range	North American Price	Foreign Price
A01	Microfiche	$ 4.50	$ 9.00
A02	001-025	7.00	14.00
A03	026-050	8.50	17.00
A04	051-075	10.00	20.00
A05	076-100	11.50	23.00
A06	101-125	13.00	26.00
A07	126-150	14.50	29.00
A08	151-175	16.00	32.00
A09	176-200	17.50	35.00
A10	201-225	19.00	38.00
A11	226-250	20.50	41.00
A12	251-275	22.00	44.00
A13	276-300	23.50	47.00
A14	301-325	25.00	50.00
A15	326-350	26.50	53.00
A16	351-375	28.00	56.00
A17	376-400	29.50	59.00
A18	401-425	31.00	62.00
A19	426-450	32.50	65.00
A20	451-475	34.00	68.00
A21	476-500	35.50	71.00
A22	501-525	37.00	74.00
A23	526-550	38.50	77.00
A24	551-575	40.00	80.00
A25	576-600	41.50	83.00
A99	601-up	-1	-2

1/ Add $1.50 for each additional 25 page increment or portion thereof for 601 pages up.

2/ Add $3.00 for each additional 25 page increment or portion thereof for 601 pages and more.

Schedule E

EXCEPTION PRICE SCHEDULE

Paper Copy & Microfiche

Price Code	North American Price	Foreign Price
E01	$ 6.50	$ 13.50
E02	7.50	15.50
E03	9.50	19.50
E04	11.50	23.50
E05	13.50	27.50
E06	15.50	31.50
E07	17.50	35.50
E08	19.50	39.50
E09	21.50	43.50
E10	23.50	47.50
E11	25.50	51.50
E12	28.50	57.50
E13	31.50	63.50
E14	34.50	69.50
E15	37.50	75.50
E16	40.50	81.50
E17	43.50	88.50
E18	46.50	93.50
E19	51.50	102.50
E20	61.50	123.50
E-99 - Write for quote		
N01	35.00	45.00

VOLUME 23 NUMBER 23 / DECEMBER 8, 1985

TABLE OF CONTENTS

AERONAUTICS

Includes aeronautics (general); aerodynamics; air transportation and safety; aircraft communications and navigation; aircraft design, testing and performance; aircraft instrumentation; aircraft propulsion and power; aircraft stability and control; and research and support facilities (air).

For related information see also *Astronautics*.

01 AERONAUTICS (GENERAL) **N.A.**

02 AERODYNAMICS **3893**

Includes aerodynamics of bodies, combinations, wings, rotors, and control surfaces; and internal flow in ducts and turbomachinery.

For related information see also *34 Fluid Mechanics and Heat Transfer*

03 AIR TRANSPORTATION AND SAFETY **3895**

Includes passenger and cargo air transport operations; and aircraft accidents.

For related information see also *16 Space Transportation* and *85 Urban Technology and Transportation*.

04 AIRCRAFT COMMUNICATIONS AND NAVIGATION **3895**

Includes digital and voice communication with aircraft; air navigation systems (satellite and ground based); and air traffic control.

For related information see also *17 Spacecraft Communications, Command and Tracking* and *32 Communications*.

05 AIRCRAFT DESIGN, TESTING AND PERFORMANCE **3896**

Includes aircraft simulation technology.

For related information see also *18 Spacecraft Design, Testing and Performance* and *39 Structural Mechanics*.

06 AIRCRAFT INSTRUMENTATION **3896**

Includes cockpit and cabin display devices; and flight instruments.

For related information see also *19 Spacecraft Instrumentation* and *35 Instrumentation and Photography*.

07 AIRCRAFT PROPULSION AND POWER **3897**

Includes prime propulsion systems and systems components, e.g., gas turbine engines and compressors; and on-board auxiliary power plants for aircraft.

For related information see also *20 Spacecraft Propulsion and Power, 28 Propellants and Fuels*, and *44 Energy Production and Conversion*.

08 AIRCRAFT STABILITY AND CONTROL **3898**

Includes aircraft handling qualities; piloting; flight controls; and autopilots.

09 RESEARCH AND SUPPORT FACILITIES (AIR) **3898**

Includes airports, hangars and runways; aircraft repair and overhaul facilities; wind tunnels; shock tube facilities; and engine test blocks.

For related information see also *14 Ground Support Systems and Facilities (Space)*.

ASTRONAUTICS

Includes astronautics (general); astrodynamics; ground support systems and facilities (space); launch vehicles and space vehicles; space transportation; spacecraft communications, command and tracking; spacecraft design, testing and performance; spacecraft instrumentation; and spacecraft propulsion and power.

For related information see also *Aeronautics*

12 ASTRONAUTICS (GENERAL) **3898**

For extraterrestrial exploration see *91 Lunar and Planetary Exploration*.

13 ASTRODYNAMICS **N.A.**

Includes powered and free-flight trajectories; and orbit and launching dynamics.

14 GROUND SUPPORT SYSTEMS AND FACILITIES (SPACE) **N.A.**

Includes launch complexes, research and production facilities; ground support equipment, e.g., mobile transporters; and simulators.

For related information see also *09 Research and Support Facilities (Air)*.

15 LAUNCH VEHICLES AND SPACE VEHICLES **3899**

Includes boosters; manned orbital laboratories; reusable vehicles; and space stations.

16 SPACE TRANSPORTATION **N.A.**

Includes passenger and cargo space transportation, e.g., shuttle operations; and rescue techniques.

For related information see also *03 Air Transportation and Safety* and *85 Urban Technology and Transportation*.

17 SPACECRAFT COMMUNICATION, COMMAND AND TRACKING **3899**

Includes telemetry; space communications networks; astronavigation; and radio blackout.

For related information see also *04 Aircraft Communications and Navigation* and *32 Communications*.

18 SPACECRAFT DESIGN, TESTING AND PERFORMANCE **3899**

Includes spacecraft thermal and environmental control; and attitude control.

For life support systems see *54 Man/System Technology and Life Support*. For related information see also *05 Aircraft Design, Testing and Performance* and *39 Structural Mechanics*.

19 SPACECRAFT INSTRUMENTATION **3900**

For related information see also *06 Aircraft Instrumentation* and *35 Instrumentation and Photography*.

20 SPACECRAFT PROPULSION AND POWER **3903**

Includes main propulsion systems and components, e.g., rocket engines; and spacecraft auxiliary power sources.

For related information see also *07 Aircraft Propulsion and Power, 28 Propellants and Fuels*, and *44 Energy Production and Conversion*.

CHEMISTRY AND MATERIALS

Includes chemistry and materials (general); composite materials; inorganic and physical chemistry; metallic materials; nonmetallic materials; and propellants and fuels.

23 CHEMISTRY AND MATERIALS (GENERAL) 3903
Includes biochemistry and organic chemistry.

24 COMPOSITE MATERIALS 3909
Includes laminates.

25 INORGANIC AND PHYSICAL CHEMISTRY 3911
Includes chemical analysis, e.g., chromatography; combustion theory; electrochemistry; and photochemistry.
For related information see also *77 Thermodynamics and Statistical Physics.*

26 METALLIC MATERIALS 3913
Includes physical, chemical, and mechanical properties of metals, e.g., corrosion; and metallurgy.

27 NONMETALLIC MATERIALS 3918
Includes physical, chemical, and mechanical properties of plastics, elastomers, lubricants, polymers, textiles, adhesives, and ceramic materials.

28 PROPELLANTS AND FUELS 3921
Includes rocket propellants, igniters, and oxidizers; storage and handling; and aircraft fuels.
For related information see also *07 Aircraft Propulsion and Power, 20 Spacecraft Propulsion and Power,* and *44 Energy Production and Conversion.*

ENGINEERING

Includes engineering (general); communications; electronics and electrical engineering; fluid mechanics and heat transfer; instrumentation and photography; lasers and masers; mechanical engineering; quality assurance and reliability; and structural mechanics.
For related information see also *Physics.*

31 ENGINEERING (GENERAL) 3923
Includes vacuum technology; control engineering; display engineering; and cryogenics.

32 COMMUNICATIONS 3925
Includes land and global communications; communications theory; and optical communications.
For related information see also *04 Aircraft Communications and Navigation* and *17 Spacecraft Communications, Command and Tracking.*

33 ELECTRONICS AND ELECTRICAL ENGINEERING 3926
Includes test equipment and maintainability; components, e.g., tunnel diodes and transistors; microminiaturization; and integrated circuity.
For related information see also *60 Computer Operations and Hardware* and *76 Solid-State Physics.*

34 FLUID MECHANICS AND HEAT TRANSFER 3929
Includes boundary layers; hydrodynamics; fluidics; mass transfer; and ablation cooling.
For related information see also *02 Aerodynamics* and *77 Thermodynamics and Statistical Physics.*

35 INSTRUMENTATION AND PHOTOGRAPHY 3933
Includes remote sensors; measuring instruments and gages; detectors; cameras and photographic supplies; and holography.
For aerial photography see *43 Earth Resources.* For related information see also *06 Aircraft Instrumentation* and *19 Spacecraft Instrumentation.*

36 LASERS AND MASERS 3936
Includes parametric amplifiers.

37 MECHANICAL ENGINEERING 3937
Includes auxiliary systems (non-power); machine elements and processes; and mechanical equipment.

38 QUALITY ASSURANCE AND RELIABILITY 3940
Includes product sampling procedures and techniques; and quality control.

39 STRUCTURAL MECHANICS 3940
Includes structural element design and weight analysis; fatigue; and thermal stress.
For applications see *05 Aircraft Design, Testing and Performance* and *18 Spacecraft Design, Testing and Performance.*

GEOSCIENCES

Includes geosciences (general); earth resources; energy production and conversion; environment pollution; geophysics; meteorology and climatology; and oceanography.
For related information see also *Space Sciences.*

42 GEOSCIENCES (GENERAL) N.A.

43 EARTH RESOURCES 3943
Includes remote sensing of earth resources by aircraft and spacecraft; photogrammetry; and aerial photography.
For instrumentation see *35 Instrumentation and Photography.*

44 ENERGY PRODUCTION AND CONVERSION 3944
Includes specific energy conversion systems, e.g., fuel cells and batteries; global sources of energy; fossil fuels; geophysical conversion; hydroelectric power; and wind power.
For related information see also *07 Aircraft Propulsion and Power, 20 Spacecraft Propulsion and Power, 28 Propellants and Fuels,* and *85 Urban Technology and Transportation.*

45 ENVIRONMENT POLLUTION 3947
Includes air, noise, thermal and water pollution; environment monitoring; and contamination control.

46 GEOPHYSICS 3948
Includes aeronomy; upper and lower atmosphere studies; ionospheric and magnetospheric physics; and geomagnetism.
For space radiation see *93 Space Radiation.*

47 METEOROLOGY AND CLIMATOLOGY 3950
Includes weather forecasting and modification.

48 OCEANOGRAPHY 3950
Includes biological, dynamic and physical oceanography; and marine resources.

LIFE SCIENCES

Includes sciences (general); aerospace medicine; behavioral sciences; man/system technology and life support; and planetary biology.

51 LIFE SCIENCES (GENERAL) **3951**
Includes genetics.

52 AEROSPACE MEDICINE **3952**
Includes physiological factors; biological effects of radiation; and weightlessness.

53 BEHAVIORAL SCIENCES **N.A.**
Includes psychological factors; individual and group behavior; crew training and evaluation; and psychiatric research.

54 MAN/SYSTEM TECHNOLOGY AND LIFE SUPPORT **N.A.**
Includes human engineering; biotechnology; and space suits and protective clothing.

55 PLANETARY BIOLOGY **N.A.**
Includes exobiology; and extraterrestrial life.

MATHEMATICAL AND COMPUTER SCIENCES

Includes mathematical and computer sciences (general); computer operations and hardware; computer programming and software; computer systems; cybernetics; numerical analysis; statistics and probability; systems analysis; and theoretical mathematics.

59 MATHEMATICAL AND COMPUTER SCIENCES (GENERAL) **3955**

60 COMPUTER OPERATIONS AND HARDWARE **3955**
Includes computer graphics and data processing.
For components see *33 Electronics and Electrical Engineering.*

61 COMPUTER PROGRAMMING AND SOFTWARE **3956**
Includes computer programs, routines, and algorithms.

62 COMPUTER SYSTEMS **3967**
Includes computer networks.

63 CYBERNETICS **3967**
Includes feedback and control theory.
For related information see also *54 Man/System Technology and Life Support.*

64 NUMERICAL ANALYSIS **3967**
Includes iteration, difference equations, and numerical approximation.

65 STATISTICS AND PROBABILITY **3968**
Includes data sampling and smoothing; Monte Carlo method; and stochastic processes.

66 SYSTEMS ANALYSIS **N.A.**
Includes mathematical modeling; network analysis; and operations research.

67 THEORETICAL MATHEMATICS **N.A.**
Includes topology and number theory.

PHYSICS

Includes physics (general); acoustics; atomic and molecular physics; nuclear and high-energy physics; optics; plasma physics; solid-state physics; and thermodynamics and statistical physics.
For related information see also *Engineering.*

70 PHYSICS (GENERAL) **N.A.**
For geophysics see *46 Geophysics.* For astrophysics see *90 Astrophysics.* For solar physics see *92 Solar Physics.*

71 ACOUSTICS **3968**
Includes sound generation, transmission, and attenuation.
For noise pollution see *45 Environment Pollution.*

72 ATOMIC AND MOLECULAR PHYSICS **3969**
Includes atomic structure and molecular spectra.

73 NUCLEAR AND HIGH-ENERGY PHYSICS **3969**
Includes elementary and nuclear particles; and reactor theory.
For space radiation see *93 Space Radiation.*

74 OPTICS **3973**
Includes light phenomena.

75 PLASMA PHYSICS **3974**
Includes magnetohydrodynamics and plasma fusion.
For ionospheric plasmas see *46 Geophysics.* For space plasmas see *90 Astrophysics.*

76 SOLID-STATE PHYSICS **3985**
Includes superconductivity.
For related information see also *33 Electronics and Electrical Engineering* and *36 Lasers and Masers.*

77 THERMODYNAMICS AND STATISTICAL PHYSICS **N.A.**
Includes quantum mechanics; and Bose and Fermi statistics.
For related information see also *25 Inorganic and Physical Chemistry* and *34 Fluid Mechanics and Heat Transfer.*

SOCIAL SCIENCES

Includes social sciences (general); administration and management; documentation and information science; economics and cost analysis; law and political science; and urban technology and transportation.

80 SOCIAL SCIENCES (GENERAL) **N.A.**
Includes educational matters.

81 ADMINISTRATION AND MANAGEMENT **3986**
Includes management planning and research.

82 DOCUMENTATION AND INFORMATION SCIENCE **N.A.**
Includes information storage and retrieval technology; micrography; and library science.
For computer documentation see *61 Computer Programming and Software.*

83 ECONOMICS AND COST ANALYSIS **N.A.**
Includes cost effectiveness studies.

84 LAW AND POLITICAL SCIENCE **3987**
Includes space law; international law; international cooperation; and patent policy.

85 URBAN TECHNOLOGY AND TRANSPORTATION **3987**
Includes applications of space technology to urban problems; technology transfer; technology assessment; and surface and mass transportation.
For related information see *03 Air Transportation and Safety, 16 Space Transportation,* and *44 Energy Production and Conversion.*

SPACE SCIENCES

Includes space sciences (general); astronomy; astrophysics; lunar and planetary exploration; solar physics; and space radiation.
For related information see also *Geosciences.*

88 SPACE SCIENCES (GENERAL) **N.A.**

89 ASTRONOMY **3987**
Includes radio and gamma-ray astronomy; celestial mechanics; and astrometry.

90 ASTROPHYSICS **3987**
Includes cosmology; and interstellar and interplanetary gases and dust.

91 LUNAR AND PLANETARY EXPLORATION **3989**
Includes planetology; and manned and unmanned flights.
For spacecraft design see *18 Spacecraft Design, Testing and Performance.* For space stations see *15 Launch Vehicles and Space Vehicles.*

92 SOLAR PHYSICS **3989**
Includes solar activity, solar flares, solar radiation and sunspots.

93 SPACE RADIATION **4012**
Includes cosmic radiation; and inner and outer earth's radiation belts.
For biological effects of radiation see *52 Aerospace Medicine.* For theory see *73 Nuclear and High-Energy Physics.*

GENERAL

99 GENERAL **4056**

Note: N.A. means that no abstracts were assigned to this category for this issue.

SUBJECT INDEX **I-1**
PERSONAL AUTHOR INDEX **I-67**
CORPORATE SOURCE INDEX **I-77**
CONTRACT NUMBER INDEX **I-91**
REPORT / ACCESSION NUMBER INDEX **I-93**

TYPICAL CITATION AND ABSTRACT

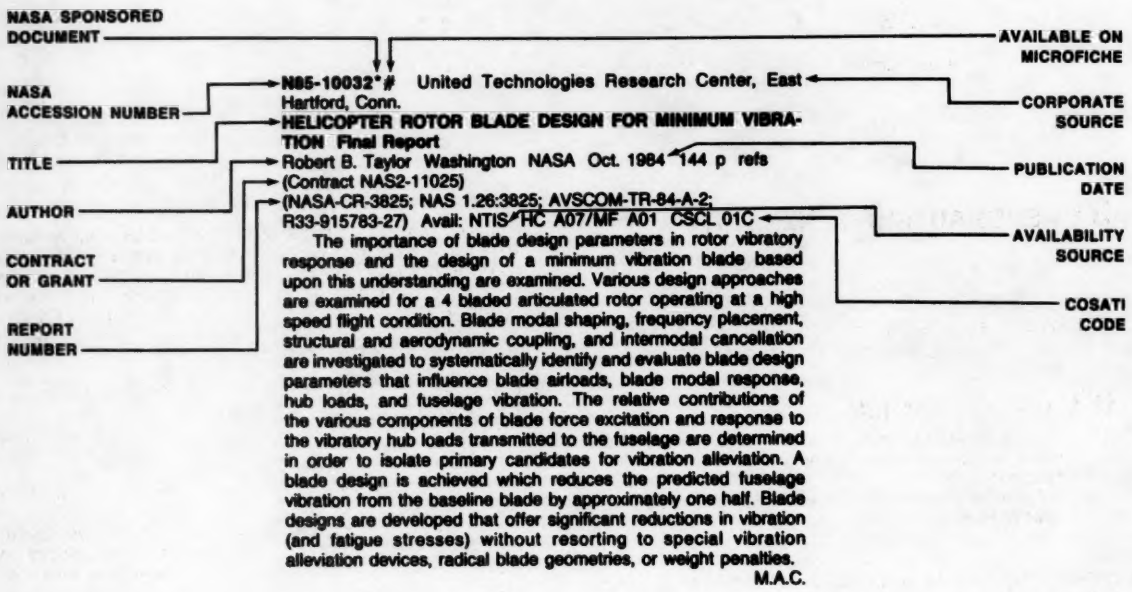
NASA SPONSORED DOCUMENT
AVAILABLE ON MICROFICHE
NASA ACCESSION NUMBER
N85-10032*# United Technologies Research Center, East Hartford, Conn.
CORPORATE SOURCE
TITLE
HELICOPTER ROTOR BLADE DESIGN FOR MINIMUM VIBRATION Final Report
AUTHOR
Robert B. Taylor Washington NASA Oct. 1984 144 p refs
PUBLICATION DATE
CONTRACT OR GRANT
(Contract NAS2-11025)
REPORT NUMBER
(NASA-CR-3825; NAS 1.26:3825; AVSCOM-TR-84-A-2; R33-915783-27) Avail: NTIS HC A07/MF A01 CSCL 01C
AVAILABILITY SOURCE
COSATI CODE
The importance of blade design parameters in rotor vibratory response and the design of a minimum vibration blade based upon this understanding are examined. Various design approaches are examined for a 4 bladed articulated rotor operating at a high speed flight condition. Blade modal shaping, frequency placement, structural and aerodynamic coupling, and intermodal cancellation are investigated to systematically identify and evaluate blade design parameters that influence blade airloads, blade modal response, hub loads, and fuselage vibration. The relative contributions of the various components of blade force excitation and response to the vibratory hub loads transmitted to the fuselage are determined in order to isolate primary candidates for vibration alleviation. A blade design is achieved which reduces the predicted fuselage vibration from the baseline blade by approximately one half. Blade designs are developed that offer significant reductions in vibration (and fatigue stresses) without resorting to special vibration alleviation devices, radical blade geometries, or weight penalties.
M.A.C.

VOLUME 23 NUMBER 23 / DECEMBER 8, 1985

Scientific and Technical Aerospace Reports

A Semimonthly Publication of the National Aeronautics and Space Administration

01 AERONAUTICS (GENERAL)

No abstracts in this category.

02 AERODYNAMICS

Includes aerodynamics of bodies, combinations, wings, rotors, and control surfaces; and internal flow in ducts and turbomachinery.

For related information see also *34 Fluid Mechanics and Heat Transfer.*

N85-34113*# Institute for Computer Application Research and Utilization in Science, Inc., Boston, Mass.
SCALAR/VECTOR POTENTIAL FORMULATION FOR COMPRESSIBLE VISCOUS UNSTEADY FLOWS Final Report
Luigi Morino Aug. 1985 44 p refs
(Contract NAS1-17317)
(NASA-CR-3921; NAS 1.26:3921; TR-84-01) Avail: NTIS HC A03/MF A01 CSCL 01A

A scalar/vector potential formulation for unsteady viscous compressible flows is presented. The scalar/vector potential formulation is based on the classical Helmholtz decomposition of any vector field into the sum of an irrotational and a solenoidal field. The formulation is derived from fundamental principles of mechanics and thermodynamics. The governing equations for the scalar potential and vector potential are obtained, without restrictive assumptions on either the equation of state or the constitutive relations or the stress tensor and the heat flux vector. Author

N85-34114*# Scientific Research Associates, Inc., Glastonbury, Conn.
A THREE-DIMENSIONAL VISCOUS FLOW ANALYSIS FOR THE HELICOPTER TIP VORTEX GENERATION PROBLEM Final Report
S-J. Lin, R. Levy, S. J. Shamroth, and T. R. Govindan Washington NASA Aug. 1985 69 p refs
(Contract NAS1-14904)
(NASA-CR-3906; NAS 1.26:3906) Avail: NTIS HC A04/MF A01 CSCL 01A

The tip vortex flow field occurring in the vicinity of the tip region of a a helicopter rotor blade is a very complicated three-dimensional, viscous flow phenomenon. The details of the flow in the tip region can have a major effect in determining the generated rotor noise and can significantly affect the performance and dynamic loading of the rotor blade. The three-dimensional viscous subsonic tip vortex generation processes is investigated by a numerical procedure which allows spatial forward-marching integration, utilizing flow approximations from the velocity-decomposition approach of Briley and McDonald. The approach has been applied to compute the laminar and turbulent tip vortex flows for a constant thickness slab airfoil with a square tip, a constant thickness slab airfoil with a half round tip and a NACA 0012 airfoil with a half round tip. The basic mechanism of the tip vortex generation process as well as the prediction of vortex appearance, strength and secondary flow shown by the calculations are in qualitative agreement with experimental results. Author

N85-34115*# National Aeronautics and Space Administration. Ames Research Center, Moffett Field, Calif.
AN EVALUATION OF THREE HELICOPTER ROTOR SECTIONS
Raymond M. Hicks and Leslie J. Collins (Informatics General Corp., Palo Alto, Calif.) Aug. 1985 122 p refs
(NASA-TM-86719; Rept-85219; NAS 1.15:86719) Avail: NTIS HC A06/MF A01 CSCL 01A

Three helicopter rotor sections were tested in the NASA Ames Research Center 2- by 2-Foot Transonic Wind Tunnel over a Mach range from 0.2 to 0.88. The sections tested had maximum thickness/chord ratios of 0.078, 0.09, and 0.10. The thickest section was of early technology and had been tested previously in other wind tunnels. This section was included in the investigation to establish a basis for comparing the two thinner sections, which were of recent design. The results of the investigation showed that the pitching-moment characteristics for the three airfoil sections were acceptable. The drag divergence Mach numbers for the three sections were 0.80, 0.825, and 0.845 in order of decreasing thickness. Author

N85-34116*# National Aeronautics and Space Administration. Ames Research Center, Moffett Field, Calif.
USE OF A HYPERBOLIC GRID GENERATION SCHEME IN SIMULATING SUPERSONIC VISCOUS FLOW ABOUT THREE-DIMENSIONAL WINGED CONFIGURATION
Yehia M. Rizk (Informatics General Corp., Palo Alto, Calif.), Joseph L. Steger, and Dennis S. Chaussee Jul. 1985 16 p refs
(NASA-TM-85344; Rept-85344; NAS 1.15:85344) Avail: NTIS HC A02/MF A01 CSCL 01A

The present paper describes a numerical mesh generation technique to be used with an implicit finite difference method for simulating visous supersonic flow about low-aspect-ratio wing body configurations using a single grid strategy. The computational domain is segmented into multiple regions, with borders located in supersonic areas to avoid the otherwise costly interfacing procedure between adjacent segments. The numerical procedure is applied to calculate the turbulent flow around the shuttle orbiter and a canard projectile at supersonic free stream Mach number. Author

N85-34117# Toronto Univ. (Ontario).
TABULAR AND GRAPHICAL SOLUTIONS OF REGULAR AND MACH REFLECTIONS IN PSEUDO-STATIONARY FROZEN AND VIBRATIONAL-EQUILIBRIUM FLOWS, PART 1
T. C. J. Hu and M. Shirouzu Jun. 1985 274 p refs Sponsored in part by Canadian Natural Sciences and Engineering Research Council
(Contract DNA001-83-C-0266; Grant AF-AFOSR-82-0096)

(UTIAS-283-Pt-1; ISSN-0082-5255) Avail: NTIS HC A12/MF A01

Flow properties of pseudostationary oblique shock wave reflections are given as solutions of two shock and three shock theories. The calculations were performed for Ar, air, CO2 and SF6 using both frozen and vibrational equilibrium gas assumptions. The flow properties are tabulated for initial shock Mach numbers 1.2 < M sub s < 10.0 and wedge angles 1 deg < theta sub w < 85 deg. The flow properties are plotted as a function of the incident shock Mach number for a series of wedge angles for both regular and Mach reflections. Another set of graphs is presented for Mach reflection with the flow properties plotted against the effective wedge angle theta prime sub w for a series of shock Mach numbers. The latter set is used when the effective wedge angle is chosen as the parameter for comparison. The second triple point system, which exists only in double Mach reflection, is solved numerically for the first time, and the solutions are presented both in tabular and graphical forms. The tables and graphs are designed to serve the analyst and experimenter working on oblique shock wave reflections. Author

N85-34118# Toronto Univ. (Ontario). Inst. for Aerospace Studies.

TABULAR AND GRAPHICAL SOLUTIONS OF REGULAR AND MACH REFLECTIONS IN PSEUDO-STATIONARY FROZEN AND VIBRATIONAL-EQUILIBRIUM FLOWS, PART 2

Jun. 1985 232 p refs Sponsored in part by Canadian Natural Sciences and Engineering Research Council.

(Contract DNA001-83-C-0266; Grant AF-AFOSR-001-83-C-0266) (UTIAS-283-Pt-2; ISSN-0082-5255) Avail: NTIS HC A11/MF A01

The plotted flow properties and graphs are continued. The actual sidewall pressure history and numerical results are presented in appendix A. And appendix B presents the computer program listing for the analytical solution of regular and Mach reflections. E.R.

N85-34119# Aeronautical Research Labs., Melbourne (Australia).

INTEGRAL EQUATION FORMULATION FOR THREE-DIMENSIONAL UNSTEADY TRANSONIC FLOW

J. A. Gear Feb. 1985 22 p refs

(ARL-Struc-R-416; AR-003-999) Avail: NTIS HC A02/MF A01

The unsteady transonic small perturbation differential equation is converted into an integro-differential equation by application of the classical Green's function method. It is shown that no contribution from shock waves explicitly appears in this integral equation, due to the shock capturing properties of the Green's function method. After assuming that the motion consists of small infinitesimal perturbations around a thin nearly-planar body, a simplified integral equation for the streamwise velocity component is obtained, which is suitable for fast numerical computations. Author

N85-34120# Glasgow Univ. (Scotland). Dept. of Aeronautics and Fluid Mechanics.

A DESIGN PROCEDURE TO MODIFY THE TRAILING EDGE UPPER SURFACE PRESSURE GRADIENT OF A GIVEN AEROFOIL

A. J. Niven and R. A. McD. Galbraith 10 Jul. 1984 29 p refs Sponsored by Westlands Helicopters Public Ltd. Company and UK Science and Engineering Research Council

(GU-AERO-8408) Avail: NTIS HC A03/MF A01

A method whereby the pressure gradient on the trailing edge upper surface of a given airfoil may be modified to enhance or reduce trailing-edge separation during dynamic stall, for a given section, while retaining the leading edge pressure distribution, is outlined. The NACA 23012 airfoil was modified to enhance the boundary layer separation at the trailing-edge. The modification procedure consists of three algorithms: a potential flow panel method allowing calculation of the original pressure gradient at any angle of attack; a procedure allowing the modification of this gradient; and an inverse potential flow panel method to calculate a new profile from the modified vorticity distribution. Author (ESA)

N85-34121# Glasgow Univ. (Scotland). Dept. of Aeronautics and Fluid Mechanics.

THE AERODYNAMIC CHARACTERISTICS OF A GU25-5(11)8 AEROFOIL FOR LOW REYNOLDS NUMBERS

R. A. McD. Galbraith 8 Nov. 1984 11 p refs

(GU-AERO-8410) Avail: NTIS HC A02/MF A01

Wind tunnel tests of an airfoil section used for the canards of microlights where low Reynolds numbers are common, over the Reynolds number range 50,000 to 610,000 are summarized. The airfoil exhibits severe degradation of performance below Re = 300,000, a phenomenon known to be quite general. Author (ESA)

N85-34122# Glasgow Univ. (Scotland). Dept. of Aeronautics and Fluid Mechanics.

MODELLING OF UNSTEADY, INCOMPRESSIBLE SEPARATION ON AN AEROFOIL USING AN INVISCID FLOW ALGORITHM

M. Vezza and R. A. McD. Galbraith 8 Nov. 1984 33 p refs

(GU-AERO-8412) Avail: NTIS HC A03/MF A01

A method for the prediction of unsteady, incompressible separated flow over a two dimensional airfoil is presented. The algorithm was developed from an unsteady potential flow model and uses an inviscid formulation for the flow field. The airfoil is represented by vortex panels of linearly varying strength, piecewise continuous at the corners. Discrete vortices with finite cores are used to model the separating shear layers. Unsteady separation modeling, the theoretical framework, and numerical implementation are discussed. Results for flows which tend asymptotically to the steady state are encouraging. Author (ESA)

N85-34123# Glasgow Univ. (Scotland). Dept. of Aeronautics and Fluid Mechanics.

THE COLLECTED DATA FOR RAMP FUNCTION TESTS ON A NACA 23012 AEROFOIL. VOLUME 1: DESCRIPTION AND PRESSURE DATA

L. Y. Setro and R. A. McD. Galbraith 8 Nov. 1984 58 p refs Sponsored by Westlands Helicopters Public Ltd. Company

(Contract MIN-DEF-2048/O26XR/STR)

(GU-AERO-8413-Vol-1) Avail: NTIS HC A04/MF A01

Data for wind tunnel tests in which a NACA 23012 airfoil was subjected to a variety of ramp type displacements in pitch about the quarter chord position are presented. The data clearly illustrate the effect of reduced frequency on airfoil characteristics and the chordal pressure distribution at the midspan position of the airfoil model. Author (ESA)

N85-34124# Glasgow Univ. (Scotland). Dept. of Aeronautics and Fluid Mechanics.

AN INVESTIGATION INTO THE THREE-DIMENSIONAL STALL DEVELOPMENT ON A MODIFIED NACA 23012 AEROFOIL

A. J. Niven and R. A. McD. Galbraith 22 Nov. 1984 19 p refs Sponsored by United Kingdom Science and Engineering Research Council

(Contract MIN-DEF-2048/026XR/STR)

(GU-AERO-8414) Avail: NTIS HC A02/MF A01

A numerical method of modifying the trailing edge upper surface pressure gradient of a given airfoil was applied to the NACA 23012 airfoil to enhance the trailing edge pressure gradient. The redesigned airfoil was tested in a subsonic wind tunnel. A flow visualization technique, using a fluorescent yellow oil-film, was used to indicate transition regions, laminar separation bubbles, and the positions of turbulent separation. The extent of three-dimensionality, reverse flow, and corner flow separation were also observed. Results show increased boundary layer separation of the modified airfoil, and vindicate the design method.Author (ESA)

N85-34125# Glasgow Univ. (Scotland).

COMMENTS ON THE PREDICTION OF DYNAMIC STALL

R. A. McD. Galbraith 20 Mar. 1985 25 p refs

(Contract DAJA45-84-M-0446)

(GU-AERO-8501) Avail: NTIS HC A02/MF A01

Navier-Stokes, discrete vortex, zonal, and empirical methods for predicting dynamic stall were reviewed. It is concluded that accepted test cases by which the performance of dynamic stall

methods may be assessed are needed. There is an unresolved dilemma as to which basic prediction philosophy should be adopted. Using the appropriate form of the Navier-Stokes equations in finite difference form requires large and expensive computing power, while the predominantly empirical procedures need little of such power but much expensive data. A summary table provides a quick reference to the methods. Author (ESA)

N85-34126# Aeronautical Research Inst. of Sweden, Stockholm. Aerodynamics Dept.

AEROELASTIC CONSTRAINTS FOR A WING WEIGHT MINIMIZATION PROCEDURE

Sven G. Hedman Feb. 1985 17 p refs

(Contract STU-81-4626)

(FFA-TN-1985-4) Avail: NTIS HC A02/MF A01

Basic formulas of aeroelastic relations for use as constraints in a wing weight optimization procedure are derived. Steady subsonic or supersonic flow is assumed, and a reference plane panel method is chosen as the aerodynamic load generator. Wing elastic deformation is assumed to be a linear function of the applied loads. The effect of changing the amount of wing material for each wing panel on the deformation properties is used in expressions for aeroelastic efficiency and induced drag. The formulas were successfully implemented for a high aspect ratio wing application. Author (ESA)

N85-34127# Institut Franco-Allemand de Recherches, St. Louis (France).

A COMPARISON OF LASER DOPPLER ANEMOMETRY AND PROBE MEASUREMENTS WITHIN THE BOUNDARY LAYER OF AN AIRFOIL AT SUBSONIC FLOW

P. Meyer, G. Koerber, H. Hoheisel (DFVLR, Brunswick), and M. Hoeger (DFVLR, Brunswick) 3 Sep. 1984 18 p refs Presented at 2nd Intern. Symp. on Appl. of Laser Anemometry to Fluid Mech., Lisbon, 2-4 Jul. 1984

(Contract DFVLR-IB-129-84/5)

(ISL-CO-219/84) Avail: NTIS HC A02

Measurements were performed with a Pitot probe and a laser Doppler anemometer in the boundary layer of a NACA 65-213 airfoil with a separation bubble on the suction side. Comparison of the results shows good agreement for attached laminar and turbulent boundary layers, at the separation point, and in the laminar separated region except for reverse flow. Differences between the two techniques are observed only near the reattachment point in flow areas with steep pressure gradients, where the presence of the probe may lead to disturbances in the flow field. The importance of a laminar separation bubble for the improvement of cascade flow and airfoils is discussed. Author (ESA)

N85-34128# Institut Franco-Allemand de Recherches, St. Louis (France).

STUDY OF BOUNDARY LAYER SEPARATION ON A SUPERCRITICAL PROFILE WITH A SPOILER BY MEANS OF A LASER DOPPLER VELOCIMETER

P. Meyer and G. Koerber 3 Sep. 1984 8 p refs Presented at 2nd Intern. Symp. on Appl. of Laser Anemometry to Fluid Mech., Lisbon, 2-4 Jul. 1984

(Contract DRET-82-318)

(ISL-CO-225/84) Avail: NTIS HC A02

A supercritical airfoil with a spoiler was studied by a two-dimensional laser Doppler velocimeter. Local and global mean velocity and shear evolutions are presented. Two different separation models can be observed as a function of the spoiler deflection angle: a separated region with one recirculating area (angle of 10 deg) a separated region with areas (angle of 20 and 40 deg). Flow visualizations show a Karman vortex street behind the spoiler. Boundary layer displacement and momentum thickness deduced from the measurements agree with calculations.

Author (ESA)

03 AIR TRANSPORTATION AND SAFETY

Includes passenger and cargo air transport operations; and aircraft accidents.

For related information see also *16 Space Transportation* and *85 Urban Technology and Transportation.*

N85-34129*# National Aeronautics and Space Administration, Washington, D. C.

A LIFE-SAVING DEVICE FOR SHIPS

P. Converti Sep. 1985 11 p Transl. into ENGLISH of "Dispositivo de salvataje para naves" patent description, Bueno Aires, 1985 11 p Transl. by The Corporate Word, Pittsburgh

(Contract NASw-4006)

(NASA-TM-77670; NAS 1.15:77670) Avail: NTIS HC A02/MF A01 CSCL 06K

A life-saving device is described which can be used on either ships or airplanes. The device consists of an airtight container for passengers equipped with elements needed for survival (oxygen, food, medicines, etc.), an energy source, and a parachute. This device can be ejected from the plane or ship when an emergency arises. Author

N85-34130# Committee on Public Works and Transportation (U.S. House).

AVIATION SAFETY (AIRCRAFT PASSENGER SURVIVABILITY AND CABIN SAFETY)

Washington GPO 1985 780 p refs Hearings before the Subcomm. on Invest. and Oversight of the Comm. on Public Works and Transportation, 98th Congr., 1st Sess., 12-14 Jul. and 1-2 Nov. 1983

(GPO-39-847) Avail: Subcommittee on Investigations and Oversight

Various issues relative to the survival of aircraft passengers are discussed. Aircraft construction materials, firefighting, fireproofing, toxic hazards, fire extinguishers and emergency life sustaining equipment are among the topics discussed. R.J.F.

04 AIRCRAFT COMMUNICATIONS AND NAVIGATION

Includes digital and voice communication with aircraft; air navigation systems (satellite and ground based); and air traffic control.

For related information see also *17 Spacecraft Communications, Command, and Tracking* and *32 Communications.*

N85-34131# Lincoln Lab., Mass. Inst. of Tech., Lexington.

EFFECT OF INTERFERENCE ON THE PERFORMANCE OF A MINIMUM TCAS 2

R. G. Sandholm 5 Sep. 1985 66 p refs

(Contracts DOT-FA77WAI-817; F19628-85-C-0002)

(FAA/PM-84/33; ATC-132) Avail: NTIS HC A04/MF A01

Minimum TCAS 2 equipment is required to operate reliably in all aircraft densities up to the 0.3 transponder-equipped aircraft per square nautical mile anticipated in the Los Angeles Basin in the year 2000. Prototype TCAS equipment has been developed and shown to be capable of providing reliable surveillance in today's highest densities, which reach an average of about 0.1 aircraft per square nmi. Since there are no existing environments that reach the density of asynchronous interference anticipated for the Los Angeles Basin in the year 2000, it is neccessary to generate simulated interference to determine the performance of the TCAS 2 design in that environment. A series of bench tests were conducted for this purpose. Special sources were used to generate asynchronous ATCRBS and Mode S rely signals (fruit) and TACAN DME squitter and interrogation signals Synchronous ATCRBS and Mode S reply sequences were also generated to simulate airborne encounters. The performance was evaluated by observing how

the interference signals either degrated the ability of a TCAS 2 unit to receive, process, and track the desired synchronous reply sequences, or caused the TCAS 2 unit to generate false tracks.
Author

N85-34132# Aeronautical Research Labs., Melbourne (Australia).
GUIDELINES FOR THE EVALUATION OF VISUAL APPROACH SLOPE INDICATORS
Jane Millar Sep. 1984 34 p refs
(ARL-Sys-R-32; AR-003-962) Avail: NTIS HC A03/MF A01

This report discusses techniques for evaluating the efficacy of Visual Approach Slope Indicators (VASIs) intended for transport aircraft landing at major runways. The discussion is predicated on the assumption that VASI signals should act as a substitute for the information the pilot sees in the natural scene, and a list of design requirements is developed accordingly. Several testing techniques and the utility of information likely to be obtained from each one is outlined. Various aspects of experimental design including the choice of aircraft, pilots, treatments and statistical analysis which can influence the validity of conclusions are highlighted. In many published evaluations to date there has been undue reliance on the subjective opinions of pilots instead of measurements describing flight paths in objective terms. Similarly, operational evaluations have been preferred to more informative experimental tests. Adequate testing of current VASIs could enable substantial improvements to be incorporated into VASI designs of the future, but unfortunately, previous tests have not always been adequate, restricting the pertinence of the findings and limiting the generality of conclusions which might otherwise have influenced subsequent designs. Author

05 AIRCRAFT DESIGN, TESTING AND PERFORMANCE

Includes aircraft simulation technology.

For related information see also *18 Spacecraft Design, Testing and Performance* and *39 Structural Mechanics.*

N85-34133*# Simula, Inc., Phoenix, Ariz.
DESIGN AND TESTING OF AN ENERGY-ABSORBING CREWSEAT FOR THE F/FB-111 AIRCRAFT, VOLUME 1 Final Report, May 1983 - May 1985
S. Joseph Shane Washington NASA 1985 150 p refs 3 Vol.
(Contract NAS1-17387)
(NASA-CR-3916; NAS 1.26:3916; TR-84428) Avail: NTIS HC A07/MF A01 CSCL 01C

A program to determine if the injury potential could be reduced by replacing the existing crewseats with energy absorbing crewseats is explored. An energy-absorbing test seat was designed using much of the existing seat hardware. An extensive dynamic seat test series, designed to duplicate various crew module ground impact conditions, was conducted at a sled test facility. Comparative tests with operational F-111 crewseats were also conducted. After successful dynamic testing of the seat, more testing was conducted with the seats mounted in an F-111 crew module. Both swing tests and vertical drop tests were conducted. The vertical drop tests were used to obtain comparative data between the energy-absorbing and operational seats. Volume 1 describes the energy absorbing test seat and testing conducted, and evaluates the data from both test series. Author

N85-34134*# Simula, Inc., Phoenix, Ariz.
DESIGN AND TESTING OF AN ENERGY-ABSORBING CREWSEAT FOR THE F/FB-111 AIRCRAFT. VOLUME 3: DATA FROM CREW MODULE TESTING Final Report, May 1983 - May 1985
S. Joseph Shane Washington NASA Aug. 1985 257 p 3 Vol.
(Contract NAS1-17387)
(NASA-CR-3918; NAS 1.26:3918; TR-84428) Avail: NTIS HC A12/MF A01 CSCL 01C

Over the past years, several papers and reports have documented the unacceptably high injury rate during the escape sequence (including the ejection and ground impact) of the crew module for F/FB-111 aircraft. This report documents a program to determine if the injury potential could be reduced by replacing the existing crewseats with energy absorbing crewseats. An energy absorbing test seat was designed using much of the existing seat hardware. An extensive dynamic seat test series, designed to duplicate various crew module ground impact conditions, was conducted at a sled test facility. Comparative tests with operational F-111 crewseats were also conducted. After successful dynamic testing of the seat, more testing was conducted with the seats mounted in an F-111 crew module. Both swing tests and vertical drop tests were conducted. The vertical drop tests were used to obtain comparative data between the energy absorbing and operational seats. B.W.

N85-34135*# National Aeronautics and Space Administration. Ames Research Center, Moffett Field, Calif.
FLIGHT TESTING THE FIXED-WING CONFIGURATION OF THE ROTOR SYSTEMS RESEARCH AIRCRAFT (RSRA)
G. Warren Hall and Patrick M. Morris (Army Aeromechanics Lab.) St. Louis, Mo. Army Aviation Systems Command Jun. 1985 17 p
(NASA-TM-86762; Rept-85283; NAS 1.15:86762; USAAVSCOM-TM-85-A-4) Avail: NTIS HC A02/MF A01 CSCL 01C

The Rotor Systems Research Aircraft (RSRA) is a unique research aircraft designed to flight test advanced helicopter rotor system. Its principal flight test configuration is as a compound helicopter. The fixed wing configuration of the RSRA was primarily considered an energy fly-home mode in the event it became necessary to sever an unstable rotor system in flight. While it had always been planned to flight test the fixed wing configuration, the selection of the RSRA as the flight test bed for the X-wing rotor accelerated this schedule. This paper discusses the build-up to, and the test of, the RSRA fixed wing configuration. It is written primarily from the test pilot's perspective. Author

N85-34136*# Hydraulic Research Textron, Irvine, Calif. Systems Engineering Div.
INTELLIGENT REDUNDANT ACTUATION SYSTEM REQUIREMENTS AND PRELIMINARY SYSTEM DESIGN
P. deFeo, L. J. Geiger, and J. Harris Sep. 1985 80 p
(Contract NAS2-12081)
(NASA-CR-177366; NAS 1.26:177366; HR-73600253) Avail: NTIS HC A05/MF A01 CSCL 01C

Several redundant actuation system configurations were designed and demonstrated to satisfy the stringent operational requirements of advanced flight control systems. However, this has been accomplished largely through brute force hardware redundancy, resulting in significantly increased computational requirements on the flight control computers which perform the failure analysis and reconfiguration management. Modern technology now provides powerful, low-cost microprocessors which are effective in performing failure isolation and configuration management at the local actuator level. One such concept, called an Intelligent Redundant Actuation System (IRAS), significantly reduces the flight control computer requirements and performs the local tasks more comprehensively than previously feasible. The requirements and preliminary design of an experimental laboratory system capable of demonstrating the concept and sufficiently flexible to explore a variety of configurations are discussed. R.J.F.

06 AIRCRAFT INSTRUMENTATION

Includes cockpit and cabin display devices; and flight instruments.

For related information see also *19 Spacecraft Instrumentation* and *35 Instrumentation and Photography.*

N85-34137# Aeronautical Research Labs., Melbourne (Australia).
DETERMINATION OF INSTRUMENT ERRORS BY COMPATIBIL-

ITY CHECKING: RESULTS FROM DYNAMIC FLIGHT TEST DATA
R. A. Feik Sep. 1984 30 p refs
(ARL-Aero-R-162; AR-003-968) Avail: NTIS HC A03/MF A01

The considerable potential benefits of compatibility checking of aircraft dynamic flight data have in the past not been fully realized when applied to real data. It is suggested in this report that this is partly due to the presence of errors in the real data which are not usually accounted for in computer simulation studies. When factors such as accelerometer offset from center of gravity, measurement time delays and other non-linearities are accounted for, good results can be achieved with moderate quality instrumentation. The effect of these factors on the identified instrument errors are studied in this report and confidence in the results established by a careful comparison with instrument calibrations and expected errors. Other considerations, such as the influence of maneuver shape the inclusion of altitude record, are also discussed, and the conditions for successful application of compatibility checking techniques to flight data are summarized. The importance of understanding the instrumentation system is highlighted. Author

07 AIRCRAFT PROPULSION AND POWER

Includes prime propulsion systems and systems components, e.g., gas turbine engines and compressors; and on-board auxiliary power plants for aircraft.

For related information see also *20 Spacecraft Propulsion and Power, 28 Propellants and Fuels,* and *44 Energy Production and Conversion.*

N85-34138*# General Electric Co., Cincinnati, Ohio. Aircraft Engine Business Group.
HIGH PRESSURE COMPRESSOR COMPONENT PERFORMANCE REPORT
S. J. Cline, W. Fesler, H. S. Liu, R. C. Lovell, and S. J. Shaffer Sep. 1983 170 p
(Contract NAS3-20643)
(NASA-CR-168245; NAS 1.26:168245; R82AEB437) Avail: NTIS HC A08/MF A01 CSCL 21E

A compressor optimization study defined a 10 stage configuration with a 22.6:1 pressure ratio, an adiabatic efficiency goal of 86.1%, and a polytropic efficiency of 90.6%; the corrected airflow is 53.5 kg/s. Subsequent component testing included three full scale tests: a six stage rig test, a 10 stage rig test, and another 10 stage rig test completed in the second quarter of 1982. Information from these tests is used to select the configuration for a core engine test and an integrated core/low spool test. The test results will also provide data base for the flight propulsion system. The results of the test series with both aerodynamic and mechanical performance of each compressor build are presented. The second 10 stage compressor adiabatic efficiency was 0.848 at a cruise operating point versus a test goal of 0.846. E.A.K.

N85-34139# Toronto Univ. (Ontario). Inst. for Aerospace Studies.
A MODEL OF HYPERSONIC TWO-DIMENSIONAL OBLIQUE DETONATION WAVE RAMJET
Y. Sheng and J. P. Sislian Jul. 1985 27 p refs
(UTIAS-TN-257; ISSN-0082-5263) Avail: NTIS HC A03/MF A01

The possibility of using an oblique detonation wave ramjet as a power plant for a hypersonic vehicle is examined. The performance of a model of a two dimensional oblique detonation wave ramjet is analyzed in terms of thrust, lift and fuel consumption. Author

N85-34140*# General Electric Co., Cincinnati, Ohio. Aircraft Engine Business Group.
COMPONENT-SPECIFIC MODELING Annual Status Report
R. L. McKnight May 1985 162 p refs
(Contract NAS3-23687)
(NASA-CR-174765; NAS 1.26:174765; ASR-1) Avail: NTIS HC A08/MF A01 CSCL 21E

A series of interdisciplinary modeling and analysis techniques that were specialized to address three specific hot section components are presented. These techniques will incorporate data as well as theoretical methods from many diverse areas including cycle and performance analysis, heat transfer analysis, linear and nonlinear stress analysis, and mission analysis. Building on the proven techniques already available in these fields, the new methods developed will be integrated into computer codes to provide an accurate, and unified approach to analyzing combustor burner liners, hollow air cooled turbine blades, and air cooled turbine vanes. For these components, the methods developed will predict temperature, deformation, stress and strain histories throughout a complete flight mission. Author

N85-34141*# General Electric Co., Cincinnati, Ohio. Aircraft Engine Business Group.
ENERGY EFFICIENT ENGINE. FAN AND QUARTER-STAGE COMPONENT PERFORMANCE REPORT
S. J. Cline, P. H. Halter, J. T. Kutney, Jr., and T. J. Sullivan Jan. 1983 71 p ref
(Contract NAS3-20643)
(NASA-CR-168070; NAS 1.26:168070; R82AEB408) Avail: NTIS HC A04/MF A01 CSCL 21E

The fan configuration for the general Electric/NASA Energy Efficient Engine was selected following an extensive preliminary design study. The fan has an iniet radius ratio of 0.342 and a specific flowrate of 208.9 Kg/sec/sq. m (42.8 1bm/sec/sq. ft). The design corrected tip speed is 411.5 m/sec (1350 ft/sec) producing a bypass flow total-pressure ratio of 1.65 and a core flow total-pressure ratio of 1.6. The design bypass ratio is 6.8. The aerodynamic design point corresponds to the maximum climb power setting at Mach 0.8 and 10.67 Km (35,000 ft) altitude. The fully-instrumented fan component was tested in the Lynn Large Fan Test Facility in 1981. The overall performance results, reported herein, showed excellent fan performance with the fan meeting all of its component test goals of flow, efficiency and stall margin. Author

N85-34142# Rolls-Royce Ltd., Derby (England). Manufacturing Labs.
PERFORMANCE IMPROVEMENTS FROM SURFACING IN AERO ENGINE COMPONENTS
J. A. S. Graham 8 Nov. 1984 5 p Presented at Surface Eng. Soc., Coventry, England, 8 Nov. 1984
(PNR-90257) Avail: NTIS HC A02/MF A01

Wear resistance of aircraft engine components is discussed, and abradable linings, thermal barrier coatings, and controlled atmospheric spraying are reviewed. It is shown that application of surface treatments and protectives is a cost effective manufacturing approach to promote performance improvements, i.e., integrity and life. At the forefront of such techniques is the flame or thermal spraying technique. Author (ESA)

N85-34143# Rolls-Royce Ltd., Derby (England). Mechanical Technology Div.
SHROUD SEGMENTS FOR UNSHROUDED BLADE TURBINES
R. S. Attwood 1 Feb. 1985 13 p
(PNR-90260) Avail: NTIS HC A02/MF A01

The thermal requirements of shroud segments for unshrouded blade turbines were assessed by examining the thermal gradient through various types of section. For sections involving ceramic coatings, coating thickness required is defined and related to the cost in terms of cooling air flow. A limitation associated with the use of a compliant layer, as a result of its relatively low conductivity, is discussed. Transpiration of cooling air through the porous compliant layer is suggested. A method of comparative assessment

of engine and rig thermal gradients and cycles was used to define a set of test conditions. Author (ESA)

08 AIRCRAFT STABILITY AND CONTROL

Includes aircraft handling qualities; piloting; flight controls; and autopilots.

N85-34144*# National Aeronautics and Space Administration. Langley Research Center, Hampton, Va.
GROUND-BASED AND IN-FLIGHT SIMULATOR STUDIES OF FLIGHT CHARACTERISTICS OF A TWIN-FUSELAGE PASSENGER TRANSPORT AIRPLANE DURING APPROACH AND LANDING
William D. Grantham, Paul M. Smith (PRC Kentron, Inc.), William R. Neely, Jr. (AFSC Liaison Office, Hampton, Va.), Perry L. Deal, and Kenneth R. Yenni Sep. 1985 55 p refs
(NASA-TP-2451; L-15941; NAS 1.60:2451) Avail: NTIS HC A04/MF A01 CSCL 01C

Six-degree-of-freedom ground-based and in-flight simulator studies were conducted to evaluate the low-speed flight characteristics of a twin-fuselage passenger transport airplane and to compare these characteristics with those of a large, single-fuselage (reference) transport configuration similar to the Lockheed C-5A airplane. The primary piloting task was the approach and landing task. The results of this study indicated that the twin-fuselage transport concept had acceptable but unsatisfactory longitudinal and lateral-directional low-speed flight characteristics, and that stability and control augmentation would be required in order to improve the handling qualities. Through the use of rate-command/attitude-hold augmentation in the pitch and roll axes, and the use of several turn coordination features, the handling qualities of the simulated transport were improved appreciably. The in-flight test results showed excellent agreement with those of the six-degree-of-freedom ground-based simulator handling qualities tests. As a result of the in-flight simulation study, a roll-control-induced normal-acceleration criterion was developed. The handling qualities of the augmented twin-fuselage passenger transport airplane exhibited an improvement over the handling characteristics of the reference (single-fuselage) transport. B.W.

09 RESEARCH AND SUPPORT FACILITIES (AIR)

Includes airports, hangars and runways; aircraft repair and overhaul facilities; wind tunnels; shock tube facilities; and engine test blocks.

For related information see also *14 Ground Support Systems and Facilities (Space).*

N85-34145 National Physical Lab., Teddington (England). Div. of Mechanical and Optical Metrology.
RECOMMENDATIONS FOR THE DESIGN AND EQUIPPING OF ENGINEERING METROLOGY LABORATORIES
Aug. 1984 28 p refs Revised
(NPL-MOM-22; ISSN-0309-3069) Copyright. Avail: Issuing Activity

Suggestions for size, site, general design features, atmospheric control, equipment, and other factors which affect the satisfactory functioning of an engineering metrology laboratory are made. A bibliography and a list of equipment suppliers are included. Author (ESA)

N85-34146*# National Aeronautics and Space Administration. Ames Research Center, Moffett Field, Calif.
PREDICTION OF THE FLOW-FIELD INTERFERENCE INDUCED BY THE LONG-RANGE LASER VELOCIMETER IN THE AMES 40- BY 80-FOOT AND THE 80- BY 120-FOOT WIND TUNNELS
Michael S. Reinath and James C. Ross Aug. 1985 20 p refs
(NASA-TM-86763; Rept-85286; NAS 1.15:86763) Avail: NTIS HC A02/MF A01 CSCL 14B

The predicted flow disturbances induced in the test sections of the Ames 40- by 80-Foot Wind Tunnels by the presence of the Long-Range Laser Velocimeter (LRLV) are presented. The predictions were made using a potential-flow paneling code to model the test section and the LRLV, and a calculation of the resulting flow field was made. The flow velocity and angularity were calculated at numerous locations in the flow field relative to the LRLV, and the results are presented. Author

12 ASTRONAUTICS (GENERAL)

For extraterrestrial exploration see *91 Lunar and Planetary Exploration.*

N85-34147*# Wilson (James E.), La Plata, Md.
STUDY TO ENCOURAGE AND FACILITATE INDUSTRIAL INVESTMENT AND INVOLVEMENT IN SPACE Final Report
James E. Wilson 29 Feb. 1984 13 p
(Contract NASw-3873)
(NASA-CR-176152; NAS 1.26:176152) Avail: NTIS HC A02/MF A01 CSCL 22A

A simple and efficient means to alert the Director, Space Station Commercialization Task Force (DSCTF) and the equivalent director of a permanent office for the same function, to actions required to assure comprehensive support of the NASA objectives for commercial uses of space during the annual budget cycle is described. G.L.C.

N85-35143*# Chicago Univ., Ill.
SPACE SCIENCE AND EXPLORATION: A HISTORICAL PERSPECTIVE
John A. Simpson *In* NASA, Washington A Spacefaring People 1985 p 3-31 refs (For primary document see N85-35142 23-99)
(Grant NGL-14-001-006)
Avail: NTIS HC A08/MF A01; also available SOD HC $3.50 as 033-000-009-33-0 CSCL 22A

13 ASTRODYNAMICS

Includes powered and free-flight trajectories; and orbit and launching dynamics.

No abstracts in this category.

14 GROUND SUPPORT SYSTEMS AND FACILITIES (SPACE)

Includes launch complexes, research and production facilities; ground support equipment, e.g., mobile transporters; and simulators.

For related information see also *09 Research Support Facilities (Air).*

No abstracts in this category.

15 LAUNCH VEHICLES AND SPACE VEHICLES

Includes boosters; manned orbital laboratories; reusable vehicles; and space stations.

N85-34148*# National Aeronautics and Space Administration. Marshall Space Flight Center, Huntsville, Ala.
SPACE STATION ROTATIONAL EQUATIONS OF MOTION
Mario H. Rheinfurth and Stanley N. Carroll Aug. 1985 21 p (NASA-TP-2511; NAS 1.60:2511) Avail: NTIS HC A02/MF A01 CSCL 22B

Dynamic equations of motion are developed which describe the rotational motion for a large space structure having rotating appendages. The presence of the appendages produce torque coupling terms which are dependent on the inertia properties of the appendages and the rotational rates for both the space structure and the appendages. These equations were formulated to incorporate into the Space Station Attitude Control and Stabilization Test Bed to accurately describe the influence rotating solar arrays and thermal radiators have on the dynamic behavior of the Space Station. Author

N85-34149*# National Aeronautics and Space Administration. Marshall Space Flight Center, Huntsville, Ala.
POTENTIAL SPIN-OFFS OF THE CARBON DIOXIDE OBSERVATIONAL PLATFORM SYSTEM (CO-OPS) FOR REMOTE SENSING OPPORTUNITIES
J. Briscoe Stephens 1985 36 p refs (NASA-TP-2510; NAS 1.60:2510) Avail: NTIS HC A03/MF A01 CSCL 22B

Alternate remote sensing techniques that could utilize the slight losses of energy from the microwave beam which powers the NASA/MSFC Carbon Dioxide Observational Platform System (CO-OPS) to achieve the objectives of the U.S. Department of Energy (DOE) Carbon Dioxide Research Program's regional observational data requirements, ODRs, are addressed heuristically. The opportunity for regional remote sensing of the carbon dioxide and water vapor constituents in the atmosphere are discussed as a potential spin off of the CO-OPS. The CO-OPS is envisioned as a high altitude (approx. 25 km) observational platform system powered by microwave energy for regional observational use by the DOE in their Carbon Dioxide Research Program. Author

16 SPACE TRANSPORTATION

Includes passenger and cargo space transportation, e.g., shuttle operations; and rescue techniques.

For related information see also *03 Air Transportation and Safety* and *85 Urban Technology and Transportation.*

No abstracts in this category.

17 SPACECRAFT COMMUNICATIONS, COMMAND AND TRACKING

Includes telemetry; space communications networks; astronavigation; and radio blackout.

For related information see also *04 Aircraft Communications and Navigation* and *32 Communications.*

N85-34150*# National Aeronautics and Space Administration. Lewis Research Center, Cleveland, Ohio.
TELECOMMUNICATIONS FORECAST FOR ITU REGION 2 TO THE YEAR 1995
James E. Hollansworth, Jack A. Salzman, and James R. Ramler Aug. 1985 131 p refs (NASA-TM-87077; E-2653; NAS 1.15:87077) Avail: NTIS HC A07/MF A01 CSCL 17B

Telecommunications activity was studied. The primary objective was to forecast the need for fixed service satellites (FSS) by countries within ITU Region 2 excluding the United States and Greenland. Forecasts of telecommunications equipment needs were developed as a yardstick of the relative level of telecommunications activity among developing countries within the region. A likely scenario for the implementation of domestic and regional communications satellites is forecasted to provide services to and among countries in ITU Region 2. By 1995, it is forecast that 15 fixed service satellites will be implemented. A forecast of the countries requirements indicates that, with the possible exception of Canada, this constellation of satellites will meet these countries' needs to beyond the year 2000. E.A.K.

N85-34151# Rolls-Royce Ltd., Derby (England).
DESIGN, DEVELOPMENT AND OPERATION OF A HIGH SIMULTANEOUS CAPACITY DIGITAL TELEMETRY SYSTEM
K. Bradley 25 Feb. 1985 33 p refs Presented at Von Karman Inst. for Fluid Dyn. Lecture Series on Meas. Techn. in Turbomachines, Rhode Saint-Genese, Belgium, 25 Feb.-1 Mar. 1985 (PNR-90261) Avail: NTIS HC A03/MF A01

A digital telemetry system for measuring pressures in interblade passages on large fan engines and model fan rigs was developed. The telemetry system incorporates on-rotor digitization and hybrid circuit techniques for temperature measurement in time division multiplexed systems and interblade shock patterns, respectively. The system proves to be satisfactory for dc and low frequency investigation. Author (ESA)

18 SPACECRAFT DESIGN, TESTING AND PERFORMANCE

Includes spacecraft thermal and environmental control; and attitude control.

For life support systems see *54 Man/System Technology and Life Support.* For related information see also *05 Aircraft Design, Testing and Performance* and *39 Structural Mechanics.*

N85-34152*# RCA Astro-Electronics Div., Princeton, N. J.
SPACECRAFT (MOBILE SATELLITE) CONFIGURATION DESIGN STUDY Final Report
14 Jun. 1985 129 p refs Sponsored by NASA Prepared in cooperation with JPL, Pasadena, Calif.
(NASA-CR-176153; NAS 1.26:176153) Avail: NTIS HC A07/MF A01 CSCL 22B

The relative costs to procure and operate a two-satellite mobile satellite system designed to operate either in the UHF band of the L Band, and with several antenna diameter options in each frequency band was investigated. As configured, the size of the spacecraft is limited to the current RCA Series 4000 Geosynchronous Communications Spacecraft bus, which spans the range from 4000 to 5800 pounds in the transfer orbit. The Series 4000 bus forms the basis around which the Mobile Satellite transponder and associated antennas were appended. Although the resultant configuration has little outward resemblance to the present Series 4000 microwave communications spacecraft, the structure, attitude control, thermal, power, and command and control subsystems of the Series 4000 spacecraft are all adapted to support the Mobile Satellite mission. G.L.C.

N85-34153*# National Academy of Sciences - National Research Council, Washington, D. C. Commission on Engineering and Technical Systems.
SPACE STATION ENGINEERING AND TECHNOLOGY DEVELOPMENT: PROCEEDINGS OF THE PANEL ON IN-SPACE ENGINEERING RESEARCH AND TECHNOLOGY DEVELOPMENT

May 1985 194 p Proc. held in Hampton, Va., 21-22 May 1985 (Contract NASw-4003)
(NASA-CR-176110; NAS 1.26:176110) Avail: NTIS HC A09/MF A01 CSCL 22B

In 1984 the ad hoc committee on Space Station Engineering and Technology Development of the Aeronautics and Space Engineering Board (ASEB) conducted a review of the National Aeronautics and Space Administration's (NASA's) space station program planning. The review addressed the initial operating configuration (IOC) of the station. The ASEB has reconstituted the ad hoc committee which then established panels to address each specific related subject. The participants of the panels come from the committee, industry, and universities. The proceedings of the Panel on In Space Engineering Research and Technology Development are presented in this report. Activities, and plans for identifying and developing R&T programs to be conducted by the space station and related in space support needs including module requirements are addressed. Consideration is given to use of the station for R&T for other government agencies, universities, and industry. B.W.

N85-34154*# National Aeronautics and Space Administration. Marshall Space Flight Center, Huntsville, Ala.
THE ROLE OF TETHERS ON SPACE STATION
Georg vonTiesenhausen, ed. Oct. 1985 155 p refs
(NASA-TM-86519; NAS 1.15:86519) Avail: NTIS HC A08/MF A01 CSCL 22B

The results of research and development that addressed the usefulness of tether applications in space, particularly for space station are described. A well organized and structured effort of considerable magnitude involving NASA, industry and academia have defined the engineering and technological requirements of space tethers and their broad range of economic and operational benefits. The work directed by seven NASA Field Centers is consolidated and structured to cover the general and specific roles of tethers in space as they apply to NASA's planned space station. This is followed by a description of tether systems and operations. A summary of NASA's plans for tether applications in space for years to come is given. Author

N85-34155*# National Aeronautics and Space Administration. Goddard Space Flight Center, Greenbelt, Md.
PERFORMANCE INTERFACE DOCUMENT FOR THE S-BAND DIPLEXER FOR SPACE USERS OF NASA NETWORKS
Larry G. Line Jun. 1985 39 p
(NASA-TM-86224; G85F-0299; NAS 1.15:86224) Avail: NTIS HC A03/MF A01 CSCL 22B

This report discusses the test results and interfacing information of the S-band diplexer development program supported by RTOP 310 funding. The program was implemented to reduce the S-band transponder noise figure by minimizing the receive channel insertion loss and to also provide Space Transportation System (STS) compatibility by providing 70-db rejection up to 16 GHz in the receive channel. This compatibility includes rejection of signals from the Shuttle S-band Data Link, the K-band Data Link, and the K-band Rendezvous Radar. The first of many projects to benefit from this accomplishment was the Earth Radiation Budget Satellite (ERBS). Author

N85-34156*# Martin Marietta Aerospace, Denver, Colo.
BOX TRUSS ANALYSIS AND TECHNOLOGY DEVELOPMENT. TASK 1: MESH ANALYSIS AND CONTROL Final Report
E. E. Bachtell, S. S. Bettadapur, and J. V. Coyner Aug. 1985 118 p
(Contract NAS1-17551)
(NASA-CR-172570; NAS 1.26:172570; MCR-85-533) Avail: NTIS HC A06/MF A01 CSCL 22B

An analytical tool was developed to model, analyze and predict RF performance of box truss antennas with reflective mesh surfaces. The analysis system is unique in that it integrates custom written programs for cord tied mesh surfaces, thereby drastically reducing the cost of analysis. The analysis system is capable of determining the RF performance of antennas under any type of manufacturing or operating environment by integrating together the various disciplines of design, finite element analysis, surface best fit analysis and RF analysis. The Integrated Mesh Analysis System consists of six separate programs: The Mesh Tie System Model Generator, The Loadcase Generator, The Model Optimizer, The Model Solver, The Surface Topography Solver and The RF Performance Solver. Additionally, a study using the mesh analysis system was performed to determine the effect of on orbit calibration, i.e., surface adjustment, on a typical box truss antenna. Author

N85-34157# Centre National d'Etudes Spatiales, Toulouse (France). Direction des Lanceurs.
THERMAL PROTECTION SYSTEMS FOR REENTRY VEHICLES [SYSTEMES DE PROTECTION THERMIQUE POUR VEHICULES DE RENTREE]
Maurice Desloire Dec. 1984 44 p In FRENCH; ENGLISH summary Report will also be announced as translation (ESA-TT-926)
(CNES-NT-113) Avail: NTIS HC A03/MF A01

French investigations for the Hermes European reentry vehicle design are summarized. Mass and the difficulties of possible systems were compared. The technological feasibility of low density ceramics, metallic radiative insulation, and low density ablatives are examined. Mass, life and technological factors suggest that French industry is able to develop the systems. Author (ESA)

N85-34168*# National Aeronautics and Space Administration. Marshall Space Flight Center, Huntsville, Ala.
ELECTRODYNAMIC TETHER Abstract Only
William T. Roberts *In* Alabama Univ. Coordinated Study of Solar-Terrestrial Payloads on Space Station 1985 2 p (For primary document see N85-34158 23-19)
Avail: NTIS HC A04/MF A01 CSCL 22B

19 SPACECRAFT INSTRUMENTATION

For related information see also *06 Aircraft Instrumentation* and *35 Instrumentation and Photography.*

N85-34158*# Alabama Univ., Huntsville.
COORDINATED STUDY OF SOLAR-TERRESTRIAL PAYLOADS ON SPACE STATION Interim Status Report, 10 Jul. 1984 - 31 Jul. 1985
S. T. Wu 1985 53 p refs Proc. of the Solar Terrestrial Observatory Mini-Workshop, Huntsville, Ala., 6 Jun. 1985
(Contract NAS8-488)
(NASA-CR-176160; NAS 1.26:176160) Avail: NTIS HC A04/MF A01 CSCL 14B

A review of the instruments to be placed on the initial Solar Terrestrial Observatory (STO) is given. Brief descriptive writeups of each instrument are included. The placement of these instruments is discussed. For individual titles, see N85-34159 through N85-34174.

N85-34159*# National Aeronautics and Space Administration. Marshall Space Flight Center, Huntsville, Ala.
SOFT X-RAY TELESCOPE (SXRT) Abstract Only
Ronald L. Moore *In* Alabama Univ. Coordinated Study of Solar-Terrestrial Payloads on Space Station 1985 2 p (For primary document see N85-34158 23-19)
Avail: NTIS HC A04/MF A01 CSCL 14B

The soft X-ray telescope (SXRT) will provide direct images of the solar corona with spatial resolution of about 1 arcsecond. These images will show the global structure of the corona, the location and area of coronal holes, and the presence of even the smallest active regions and flares. The good spatial resolution will show the fine scale magnetic structure and changes in these phenomena. These observations are essential for monitoring, predicting, and understanding the solar magnetic cycle, coronal heating, solar flares, coronal mass ejections, and the solar wind. These observations complement those of the White Light Corona-

graph and Ultra-Violet Coronal Spectrometer; the SXRT will detect active regions and coronal holes near the east limb, thereby giving a week or more of advanced warning for disturbed geomagnetic conditions at Earth. The instrument consists of a grazing incidence collecting mirror with a full disk film camera at the primary focus, and a secondary relay optic that feeds a CCD camera with a field of view about the size of an average active region. Author

N85-34160*# National Aeronautics and Space Administration. Marshall Space Flight Center, Huntsville, Ala.
SOLAR ULTRAVIOLET SPECTRAL IRRADIANCE MONITOR (SUSIM) Abstract Only
Ronald L. Moore *In* Alabama Univ. Coordinated Study of Solar-Terrestrial Payloads on Space Station 1985 2 p (For primary document see N85-34158 23-19)
Avail: NTIS HC A04/MF A01 CSCL 14B

The solar ultraviolet spectral irradiance monitor (SUSIM) measures the ultraviolet flux from the entire Sun with high absolute accuracy over the wavelength range 120 to 400 nm with a resolution of 0.1 nm. SUSIM consists of two identical double dispersion scanning spectrometers with 5 photodiodes, 2 photon counters, and a deuterium lamp calibration source, all sealed in a canister pressurized to 1.1 atmosphere of argon. One spectrometer is used almost continuously during sunlight, the other is used once per day as a calibration check. The observations will yield improved absolute measurements of the ultraviolet solar fluxes, provide an accurate reference for studies of variability of the solar fluxes on the time scales of the solar cycle and longer, and measure shorter term changes as well. These measurements complement the active cavity radiometer (ACR) measurements of the total solar irradiance. The data will be used to study the physical behavior of the Sun and the Earth's atmosphere, weather, and climate. Author

N85-34161*# National Aeronautics and Space Administration. Marshall Space Flight Center, Huntsville, Ala.
WHITE LIGHT CORONOGRAPH (WLC) AND ULTRA-VIOLET CORONAL SPECTROMETER (UVCS) Abstract Only
Ronald L. Moore *In* Alabama Univ. Coordinated Study of Solar-Terrestrial Payloads on Space Station 1985 2 p (For primary document see N85-34158 23-19)
Avail: NTIS HC A04/MF A01 CSCL 14B

The white light coronagraph (WLC) and ultraviolet coronal spectrometer (UVCS) together reveal the corona and the roots of the solar wind from 1.5 to 6 solar radii from Sun center. The WLC measures the plasma density and spatial structure of the corona and coronal mass ejections at a resolution of about 20 arcseconds. The UVCS, in combination with the WLC, measures the temperature and radial outflow speed of the coronal plasma. These instruments will detect mass ejections from active regions and high speed solar wind streams from coronal holes a few days before the source regions rotate onto the face of the Sun, thus giving a week or more of advanced warning for disturbed geomagnetic conditions at Earth. Author

N85-34162*# National Aeronautics and Space Administration. Marshall Space Flight Center, Huntsville, Ala.
HIGH RESOLUTION TELESCOPE AND SPECTROGRAPH (HRTS) Abstract Only
Ronald L. Moore *In* Alabama Univ. Coordinated Study of Solar-Terrestrial Payloads on Space Station 1985 2 p (For primary document see N85-34158 23-19)
Avail: NTIS HC A04/MF A01 CSCL 14B

The major objectives of the high resolution telescope and spectrograph (HRTS) are: (1) the investigation of the energy balance and mass balance of the temperature minimum, chromosphere, transition zone, and corona in quiet regions on the Sun as well as in plages, flares, and sunspots; (2) the investigation of the velocity field of the lower corona to study the origin of the solar wind; (3) the investigation of preflare and flare phenomena. The HRTS instruments consists of a telescope, an ultraviolet spectrograph, and ultraviolet spectroheliograph, and an H alpha slit display system, all housed in a thermal control canister mounted on an instrument pointing system. Author

N85-34163*# National Aeronautics and Space Administration. Marshall Space Flight Center, Huntsville, Ala.
ACTIVE CAVITY RADIOMETER (ACR) Abstract Only
Ronald L. Moore *In* Alabama Univ. Coordinated Study of Solar-Terrestrial Payloads on Space Station 1985 2 p (For primary document see N85-34158 23-19)
Avail: NTIS HC A04/MF A01 CSCL 14B

The active cavity radiometer (ACR) measures the total solar irradiance to determine the magnitude and direction of variations in the total solar radiative output. The ACR is an electrically self calibrating cavity pyroheliometer capable of measuring the total solar irradiance with an absolute accuracy better than 0.2% and capable of detecting changes in the total irradiance smaller than 0.001%. The data will be used to study the physical behavior of the Sun and the Earth's climate. Author

N85-34164*# TRW, Inc., Redondo Beach, Calif.
WAVES IN SPACE PLASMAS (WISP) Abstract Only
William W. L. Taylor *In* Alabama Univ. Coordinated Study of Solar-Terrestrial Payloads on Space Station 1985 2 p (For primary document see N85-34158 23-19)
Avail: NTIS HC A04/MF A01 CSCL 14B

Waves in space plasmas (WISP) utilizes powerful radio transmitters and sensitive receivers to probe the secrets of the magnetosphere, ionosphere and atmosphere. The scientific objective is to achieve a better understanding of the physical processes occurring in these regions. For example, audio frequency radio waves will be radiated from the long WISP antenna, will travel to the outer reaches of the magnetosphere, and will interact with Van Allen belt particles, releasing some of their energy which amplifies the waves. Study of this interaction will give us a better understanding of a major magnetospheric process, wave particle interactions. Radio waves from WISP at higher frequencies (AM radio and beyond) will be reflected by the ionosphere and will, for example, advance our understanding of bubbles in the equatorial ionosphere which affect satellite communications. Author

N85-34165*# National Aeronautics and Space Administration. Marshall Space Flight Center, Huntsville, Ala.
SPACE EXPERIMENTS WITH PARTICLE ACCELERATORS (SEPAC) Abstract Only
William T. Roberts *In* Alabama Univ. Coordinated Study of Solar-Terrestrial Payloads on Space Station 1985 2 p (For primary document see N85-34158 23-19)
Avail: NTIS HC A04/MF A01 CSCL 14B

The space experiments with particle accelerators (SEPAC) instruments consist of an electron accelerator, a plasma accelerator, a neutral gas (N2) release device, particle and field diagnostic instruments, and a low light level television system. These instruments are used to accomplish multiple experiments: to study beam particle interactions and other plasma processes; as probes to investigate magnetospheric processes; and as perturbation devices to study energy coupling mechanisms in the magnetosphere, ionosphere, and upper atmosphere. Author

N85-34166*# National Aeronautics and Space Administration. Marshall Space Flight Center, Huntsville, Ala.
THEORETICAL AND EXPERIMENTAL BEAM PLASMA PHYSICS (TEBPP) Abstract Only
William T. Roberts *In* Alabama Univ. Coordinated Study of Solar-Terrestrial Payloads on Space Station 1985 2 p (For primary document see N85-34158 23-19)
Avail: NTIS HC A04/MF A01 CSCL 14B

The theoretical and experimental beam plasma physics (TEBPP) consists of a package of five instruments to measure electric and magnetic fields, plasma density and temperature, neutral density, photometric emissions, and energetic particle spectra during firings of the particle injector (SEPAC) electron beam. The package is deployed on a maneuverable boom (or RMS) and is used to measure beam characteristics and induced perturbations in the near field (< 10 m) and mid field (10 m to 100 m) along the electron beam. The TEBPP package will be designed to investigate induced oscillations and induced electro-

magnetic mode waves, neutral and ion density and temperature effects, and beam characteristics as a function of axial distance.
Author

N85-34167*# National Aeronautics and Space Administration. Marshall Space Flight Center, Huntsville, Ala.
RECOVERABLE PLASMA DIAGNOSTICS PACKAGE (RPDP) Abstract Only
William T. Roberts *In* Alabama Univ. Coordinated Study of Solar-Terrestrial Payloads on Space Station 1985 2 p (For primary document see N85-34158 23-19)
Avail: NTIS HC A04/MF A01 CSCL 14B

The recoverable plasma diagnostics package (RPDP) is an ejectable and recoverable satellite with flight and ground support systems so that it can be utilized in three modes: attached to an remote manipulator system; tethered; or as a subsatellite. The satellite is well instrumented with particle and field diagnostic as well as optical sensors to: investigate the dynamics of the natural environment or ejected perturbations from particle beams; measure the characteristics and propagation of electrostatic and electromagnetic waves; study wave particle interactions; and study natural properties of the magnetosphere, ionosphere, and upper atmosphere.
Author

N85-34168*# National Aeronautics and Space Administration. Marshall Space Flight Center, Huntsville, Ala.
ELECTRODYNAMIC TETHER Abstract Only **c18**
William T. Roberts *In* Alabama Univ. Coordinated Study of Solar-Terrestrial Payloads on Space Station 1985 2 p (For primary document see N85-34158 23-19)
Avail: NTIS HC A04/MF A01 CSCL 22B

The electrodynamic tether consists of a satellite deployed to a distance of 20 km by an electrically conducting tether. The space station hardware consists of a 12 meter deployment boom, satellite cradle, tether reel and motor, and other tether support systems. The electrodynamic tether will be used to perform a variety of wave experiments by exciting a wide spectrum of low frequency waves in the ionospheric plasma. The system can also be used to artificially generate and study field aligned currents and associated plasma effects. Hydromagnetic waves generated by the passage of the system through the space plasma are of particular interest in space plasma research.
Author

N85-34169*# National Aeronautics and Space Administration. Marshall Space Flight Center, Huntsville, Ala.
IMAGING SPECTROMETRIC OBSERVATORY (ISO) Abstract Only
William T. Roberts *In* Alabama Univ. Coordinated Study of Solar-Terrestrial Payloads on Space Station 1985 2 p (For primary document see N85-34158 23-19)
Avail: NTIS HC A04/MF A01 CSCL 14B

The imaging spectrometric observatory (ISO) is discussed. The objectives of this instrument are to measure the spectral signatures of a large range of minor constituents, metastable, and excited species of both atomic and molecular ions, and neutrals in the atmosphere (from the stratosphere to the upper thermosphere). The instrument is composed of five identical spectrometers, each restricted to a given spectral range between 20 and 1200 nanometers designed for high speed operation as an imaging device. Each module is an imaging scanning spectrometer with coincident 0.5 x 0.007 degree field of view.
Author

N85-34170*# National Aeronautics and Space Administration. Marshall Space Flight Center, Huntsville, Ala.
ATMOSPHERIC EMISSION PHOTOMETRIC IMAGING (AEPI) Abstract Only
William T. Roberts *In* Alabama Univ. Coordinated Study of Solar-Terrestrial Payloads on Space Station 1985 2 p (For primary document see N85-34158 23-19)
Avail: NTIS HC A04/MF A01 CSCL 14B

The atmospheric emission photometric imaging (AEPI) consists of a dual channel, low light level video system with a filter wheel to isolate the emissions of interest, mounted on a stabilized, two axis gimbal system for pointing and control. The objectives are to produce images of various atmospheric emissions to: investigate ionospheric transport processes; observe induced emissions from artificial particle injection; measure electron impact cross sections of atmospheric species; study natural aurora at high spatial and temporal resolutions and in the ultraviolet.
Author

N85-34171*# Southwest Research Inst., San Antonio, Tex.
MAGNETOSPHERIC MULTIPROBES: MMP/CHEMSAT Abstract Only
James Burch *In* Alabama Univ. Coordinated Study of Solar-Terrestrial Payloads on Space Station 1985 2 p (For primary document see N85-34158 23-19)
Avail: NTIS HC A04/MF A01 CSCL 14B

The magnetospheric multiprobes (MMP) are a set of ejectable, self contained, limited lifetime free flyers which are designed to make plasma diagnostic measurements at multiple locations within telemetry range of the space station's coorbiting platform and polar platform. When configured as CHEMSATs, one or more MMP's will conduct chemical releases as tracers or modifiers of the local plasma and field environment, while diagnostic measurements are made from other MMP's and from the nearby platform. The probes will be battery powered and will have lifetimes of a few days to several weeks. Up to 12 probes would be placed on the coorbiting platform and the polar platform every six months and two years respectively for use in the campaign mode of operation.
Author

N85-34172*# National Aeronautics and Space Administration. Marshall Space Flight Center, Huntsville, Ala.
WIDE ANGLE MICHELSON DOPPLER IMAGING INTERFEROMETER (WAMDII) Abstract Only
William T. Roberts *In* Alabama Univ. Coordinated Study of Solar-Terrestrial Payloads on Space Station 1985 2 p (For primary document see N85-34158 23-19)
Avail: NTIS HC A04/MF A01 CSCL 14B

The wide angle Michelson Doppler imaging interferometer (WAMDII) is a specialized type of optical Michelson interferometer working at sufficiently long path difference to measure Doppler shifts and to infer Doppler line widths of naturally occurring upper atmospheric Gaussian line emissions. The instrument is intended to measure vertical profiles of atmospheric winds and temperatures within the altitude range of 85 km to 300 km. The WAMDII consists of a Michelson interferometer followed by a camera lens and an 85 x 106 charge coupled device photodiode array. Narrow band filters in a filter wheel are used to isolate individual line emissions and the lens forms an image of the emitting region on the charge coupled device array.
Author

N85-34173*# National Aeronautics and Space Administration. Marshall Space Flight Center, Huntsville, Ala.
VEHICLE CHARGING AND POTENTIAL (VCAP) Abstract Only
William T. Roberts *In* Alabama Univ. Coordinated Study of Solar-Terrestrial Payloads on Space Station 1985 2 p (For primary document see N85-34158 23-19)
Avail: NTIS HC A04/MF A01 CSCL 14B

The vehicle charging and potential (VCAP) payload includes a small electron accelerator capable of operating in a pulsed mode with firing pulses ranging from 600 nanoseconds to 107 seconds (100 milliamps at 1000 volts), a spherical retarding potential analyzer - Langmuir probe, and charge current probes. This instrumentation will support studies of beam plasma interactions and the electrical charging of the spacecraft. Active experiments may also be performed to investigate the fundamental processes of artificial aurora and ionospheric perturbations. In addition, by firing the beam up the geomagnetic field lines of force (away from the Earth) investigations of parallel electric field may be performed.
Author

N85-34174*# National Aeronautics and Space Administration. Marshall Space Flight Center, Huntsville, Ala.
INITIAL PLACEMENT OF STO INSTRUMENTS
In Alabama Univ. Coordinated Study of Solar-Terrestrial Payloads

on Space Station 1985 19 p refs (For primary document see N85-34158 23-19)
Avail: NTIS HC A04/MF A01 CSCL 14B

The current plans for the placement of the Solar Terrestrial Observatory (STO) space station will make use of each of the currently planned space station elements - the manned space station, the polar platform, and the coorbiting platform. A designation of the instrument placement on each element along with a summary of the mass, volume, power and data requirements which these instrument will impose is provided in tabular form. R.J.F.

20 SPACECRAFT PROPULSION AND POWER

Includes main propulsion systems and components, e.g., rocket engines; and spacecraft auxiliary power sources.

For related information see also *07 Aircraft Propulsion, 28 Propellants and Fuels,* and *44 Energy Production and Conversion.*

N85-34175*# National Aeronautics and Space Administration. Goddard Space Flight Center, Greenbelt, Md.
SOLAR MAXIMUM: SOLAR ARRAY DEGRADATION
Tom Miller Aug. 1985 20 p refs
(NASA-TM-86194; Rept-85B0257; NAS 1.15:86194) Avail: NTIS HC A02/MF A01 CSCL 10B

The 5-year in-orbit power degradation of the silicon solar array aboard the Solar Maximum Satellite was evaluated. This was the first spacecraft to use Teflon R FEP as a coverglass adhesive, thus avoiding the necessity of an ultraviolet filter. The peak power tracking mode of the power regulator unit was employed to ensure consistent maximum power comparisons. Telemetry was normalized to account for the effects of illumination intensity, charged particle irradiation dosage, and solar array temperature. Reference conditions of 1.0 solar constant at air mass zero and 301 K (28 C) were used as a basis for normalization. Beginning-of-life array power was 2230 watts. Currently, the array output is 1830 watts. This corresponds to a 16 percent loss in array performance over 5 years. Comparison of Solar Maximum Telemetry and predicted power levels indicate that array output is 2 percent less than predictions based on an annual 1.0 MeV equivalent election fluence of 2.34 x ten to the 13th power square centimeters space environment. Author

N85-34176*# National Aeronautics and Space Administration. Lewis Research Center, Cleveland, Ohio.
OPTICAL ANALYSIS OF PARABOLIC DISH CONCENTRATORS FOR SOLAR DYNAMIC POWER SYSTEMS IN SPACE
Kent S. Jefferies Aug. 1985 27 p refs
(NASA-TM-87080; E-2659; NAS 1.15:87080) Avail: NTIS HC A03/MF A01 CSCL 10B

An optical analysis of a parabolic solar collection system operating in Earth orbit was performed using ray tracing techniques. The analysis included the effects of: (1) solar limb darkening, (2) parametric variation of mirror surface error, (3) parametric variation of mirror rim angle, and (4) parametric variation of alignment and pointing error. This ray tracing technique used numerical integration to combine the effects of rays emanating from different parts of the sun at different intensities with the effects of normally distributed mirror-surface errors to compute the angular intensity distribution of rays leaving the mirror surface. A second numerical integration was then performed over the surface of the parabolic mirror to compute the radial distribution of brightness at the mirror focus. Major results of the analysis included: (1) solar energy can be collected at high temperatures with high efficiency, (2) higher absorber temperatures can be achieved at lower efficiencies, or higher efficiencies can be achieved at lower temperatures, and (3) collection efficiency is near its maximum level across a broad plateau of rim angles from 40 deg to 70 deg. Author

N85-34177*# National Aeronautics and Space Administration. Lewis Research Center, Cleveland, Ohio.
HEATERLESS IGNITION OF INERT GAS ION THRUSTER HOLLOW CATHODES
Michael F. Schatz 1985 23 p refs Presented at the 18th Intern. Elec. Propulsion Conf., Alexandria, Va., 30 Sep. - 2 Oct. 1985; sponsored by AIAA, JSASS and DGLR
(NASA-TM-87086; E-2672; NAS 1.15:87086) Avail: NTIS HC A02/MF A01 CSCL 21C

Heaterless inert gas ion thruster hollow cathodes were investigated with the aim of reducing ion thruster complexity and increasing ion thruster reliability. Cathodes heated by glow discharges are evaluated for power requirements, flowrate requirements, and life limiting mechanisms. An accelerated cyclic life test is presented. E.A.K.

N85-34178*# National Aeronautics and Space Administration. Lewis Research Center, Cleveland, Ohio.
ELECTRODE EROSION IN ARC DISCHARGES AT ATMOSPHERIC PRESSURE
Terry L. Hardy 1985 21 p refs Presented at the 18th Intern. Elec. Propulsion Conf., Alexandria, Va., 30 Sep. - 2 Oct. 1985; sponsored by AIAA, JSASS and DGLR
(NASA-TM-87087; E-2673; NAS 1.15:87087) Avail: NTIS HC A02/MF A01 CSCL 21C

An experimental investigation was performed in an effort to measure and increase lifetime of electrodes in an arcjet thruster. The electrode erosion of various anode and cathode materials was measured after tests in an atmospheric pressure nitrogen arc discharge at powers less than 1 kW. A free-burning arc configuration and a constricted arc configuration were used to test the materials. Lanthanum hexaboride and thoriated tungsten had low cathode erosion rates while thoriated tungsten and pure tungsten had the lowest anode erosion rates of the materials tested. Anode cooling, reverse gas flow, and external magnetic fields were all found to reduce electrode mass loss. Author

N85-34179*# National Aeronautics and Space Administration. Lewis Research Center, Cleveland, Ohio.
HOLLOW CATHODES IN HIGH PRESSURE ARC DISCHARGES
Terry L. Hardy and Francis M. Curran 1985 9 p refs Presented at the 18th Intern. Elec. Propulsion Conf., Alexandria, Va., 30 Sep. - 2 Oct. 1985; sponsored by AIAA, JSASS and DGLR
(NASA-TM-87098; E-2689; NAS 1.15:87098) Avail: NTIS HC A02/MF A01 CSCL 21C

An orified hallow cathode was tested at high pressure to improve lifetime and efficiency in arcjet thrusters. It is indicated that the arc would not operate with emission from the insert above 200 torr in nitrogen regardless of insert material, orifice diameter, or gas flow direction. Emission occurred from the insert in argon and xenon although it could not be ascertained whether diffuse or spot emission existed within the cathode. Over the extended range of configurations and operating parameters explored the desired diffuse emission mode could not be obtained at high enough pressures for orified hollow cathodes to operate in the range which is considered for arcjet applications. E.A.K.

23 CHEMISTRY AND MATERIALS (GENERAL)

Includes biochemistry and organic chemistry.

N85-34180# Society of Materials Science, Kyoto (Japan).
PROCEEDINGS OF THE TWENTY-SEVENTH JAPAN CONGRESS ON MATERIALS RESEARCH
Mar. 1984 302 p refs Congr. held in Tokyo, Sep. 1983 Previously announced in IAA as A85-23462
(ISSN-0368-3141) Avail: NTIS HC A14/MF A01

Among the topics discussed are stress wave behavior in a conical bar, negative flexural behavior of precast composite slabs with steel joints, the collapse of thick walled tubing under external

pressure and axial load, the high strain rate fragmentation of a closed vessel, the mechanical properties of plasma arc-cut steel, corrosion fatigue strength and crack growth in prestrained 0.16-percent carbon steel, the crystallographic orientation dependence of fatigue crack propagation in extremely low carbon steel. Many topics on cement and concrete are discussed, as are topics on ceramics, polymers and fiber reinforced plastics. For individual titles, see N85-34181 through N85-34216.

N85-34181# National Defence Academy, Tokyo (Japan).
ELECTRICAL RESISTIVITY AND HYSTERESIS OF THE EQUIATOMIC NICKEL-TITANIUM ALLOY NEAR THE MARTENSITIC TRANSFORMATION TEMPERATURE **c26**
Hitoshu Matsumoto and Shoso Dohi *In* Society of Materials Science Proc. of the 27th Japan Congr. on Mater. Res. Mar. 1984 p 1-5 refs Previously announced in IAA as A85-23463 (For primary document see N85-34180 23-23)
Avail: NTIS HC A14/MF A01

Because of the importance of the martensitic transformation to the shape memory effect and pseudoelasticity in equiatomic NiTi, attention is given to this material's structure-sensitive electrical resistivity using standard four-probe potentiometric methods at the thermal cycling rate of 25 C/hour. Within the transformation temperature region, the resistivity behavior is noted to exhibit hysteresis even when the heating temperature is on the upper and lower sides of the A(s) temperature. After complete thermal cycling, the resistivity peak observed on heating is significantly smaller than that noted on cooling. O.C.

N85-34182# Kobe Univ. (Japan). Faculty of Engineering.
BEHAVIORS OF STRESS WAVES IN A CONICAL BAR **c39**
Noritoshi Nakagawa, Yasuo Fujiwara (Kobe Steel Ltd.), and Ryoji Kawai *In* Society of Materials Science Proc. of the 27th Japan Congr. on Mater. Res. Mar. 1984 p 7-12 refs (For primary document see N85-34180 23-23)
Avail: NTIS HC A14/MF A01

The behaviors of strain waves in a conical bar subjected to impulsive loadings are investigated experimentally and numerically. The conical bar is composed of a cylindrical part and a conical part. Incident waves are measured by strain gages in the cylindrical part and the aspect of wave propagation in the concial part is observed. On the other hand the impact of the conical bar is analyzed three dimensionally by the finite element method. The behaviors of waves after reflection at the pointed end of the conical bar are investigated and compared with the experimental results. Influences of the half apex angle and the incident pulse length on the stress waves are also considered. Author

N85-34183# Kyushu Univ., Fukuoka (Japan). Faculty of Engineering.
NEGATIVE FLEXURAL BEHAVIOR OF PRECASE COMPOSITE SLABS WITH STEEL JOINT **c39**
Toshiaki Ohta, Shinichi Hino (Yamaguchi Univ.), Yutaka Yamamoto (Ishikawajima Kenzai Cogyo Co., Ltd.), Saburo Tomisawa (Ishikawajima Kenzai Cogyo Co., Ltd.), and Takayuki Nose *In* Society of Materials Science Proc. of the 27th Japan Congr. on Mater. Res. Mar. 1984 p 13-18 refs (For primary document see N85-34180 23-23)
Avail: NTIS HC A14/MF A01

Some fundamental information on developments in an effective method for jointing RC composite slab decks on the steel girder is provided. Two types of steel joint structures are proposed, and six composite slabs having proposed joints and a lapped joint and two corresponding monolithic slabs are tested in order to evaluate the efficiency of the joints in transfer of negative bending moment. Author

N85-34184# Hiroshima Univ. (Japan). Faculty of Engineering.
MECHANICAL RATCHETING BEHAVIORS OF A STEEL PIPE UNDER COMBINED CYCLIC AXIAL LOAD AND INTERNAL PRESSURE **c39**
Fusahito Yoshida, Yoichi Obataya (Fukui Univ.), and Eiryo Shiratori (Saitama Univ.) *In* Society of Materials Science Proc. of the 27th Japan Congr. on Mater. Res. Mar. 1984 p 13-24 refs (For primary document see N85-34180 23-23)
Avail: NTIS HC A14/MF A01

The test results of mechanical ratcheting in a carbon steel pipe under combined cyclic axial load and steady internal pressure is described. The effects of maximum effective stress, stress ratio and steady stress on the biaxial strain accumulating behaviors are discussed. Author

N85-34185# Musashi Inst. of Tech., Tokyo (Japan). Dept. of Civil Engineering.
MONOTONOUS STRESS-STRAIN PROPERTIES OF STRUCTURAL STEEL SUBJECTED TO NONSTATIONARY REPETITIVE PRE-LOADING **c39**
Masaru Minagawa, Takeo Nishiwaki, and Nobutoshi Masuda *In* Society of Materials Science Proc. of the 27th Japan Congr. on Mater. Res. Mar. 1984 p 25-31 refs Sponsored by the Ministry of Education, Science and Culture (For primary document see N85-34180 23-23)
Avail: NTIS HC A14/MF A01

Many researches on properties of structural steel subjected to inelastic monotonous loads or stationary repetitive loads have been performed with the purpose of ensuring the structural safety under such loading histories. According to the results, it is clear that mechanical properties of structural steel are affected by inelastic loading histories. However, mechanical properties of structural steel previously subjected to nonstationary repetition of stress or strain are not known in detail due to the lack of experimental data. In order to investigate the mechanical properties of structural steel which had previously been subjected to nonstationary repetitive uniaxial loads, monotonous tension or compression loading tests of steel specimens were carried out. Author

N85-34186# Osaka Univ. (Japan). Dept. of Mechanical Engineering.
EXPERIMENTAL STUDY OF COLLAPSE OF THICK-WALLED TUBE UNDER EXTERNAL PRESSURE AND AXIAL FORCE **c39**
Hiroshi Kitagawa, Yasunori Tanizawa (Sumitomo Metal Industries, Ltd.), and Masaya Okamoto *In* Society of Materials Science Proc. of the 27th Japan Congr. on Mater. Res. Mar. 1984 p 33-37 refs Sponsored in part by the Ministry of Education of Japan (For primary document see N85-34180 23-23)
Avail: NTIS HC A14/MF A01

According to the finite element analysis of the collapsing process under external pressure, axial force and/or bending moment, there is no remarkable dependence of the combinations of the load on the collapse strength (the maximum pressure endured) in appearance, but the collapsing processes are strongly influenced by the load combination. How thick walled tubes behaves in the collapsing process is examined and its influence on the collapse strength is shown based on the experimental measurements of the tube subjected to external pressure and axial force in various ratios. Comparisons of the experimental results with the theoretical ones obtained by a finite element simulation analysis are made. Author

N85-34187# General Dynamics International Corp., Tokyo (Japan).
ON HIGH STRAIN RATE FRAGMENTATION OF A CLOSED VESSEL **c39**
Jiro Yamamasu and Hiroshi Miyamoto (Science Univ. of Tokyo) *In* Society of Materials Science Proc. of the 27th Japan Congr. on Mater. Res. Mar. 1984 p 39-45 refs (For primary document see N85-34180 23-23)
Avail: NTIS HC A14/MF A01

The research on fragmentation phenomena principally aims to elucidate the relation between fragment weight distribution and the external explosive force applied to the system. Historically, the fragment weight distribution function has been derived from the probability theory on partition of a line element and inferred from the experiment. In general, the performance parameters involved in the function are determined as experimental constants which, therefore, are not able to show the relation with the external

force. The fragment weight distribution is reasonably analyzed by a fracture model having an analogy with the thermodynamic principle of increase of disorder. An experimental relationship between the distribution and the force agrees well with the theoretical prediction. Author

N85-34188# Ship Research Inst., Tokyo (Japan).
MECHANICAL PROPERTIES OF PLASMA ARC CUT STEEL **c26**

Shinya Hayashi and Tokuji Nagamatsu *In* Society of Materials Science Proc. of the 27th Japan Congr. on Mater. Res. Mar. 1984 p 47-51 refs (For primary document see N85-34180 23-23)
Avail: NTIS HC A14/MF A01

Plasma arc cutting, one of thermal cutting, has been developed for aluminum alloy or stainless steel which is not able to be cut by gas cutting. However, this cutting has been considerably put to use for steels for the reason of the advantage of a small quantity of yielded strain and quick cutting speed. However, metallographic aspects or mechanical properties of plasma arc cut edges have been scarcely studied. Mechanical properties of plasma arc cut edges, compared to those of gas cut edges, already reported are discussed. Temperature distribution at plasma arc cutting, change in contents of chemical composition of N2 and distribution of hardness in heat affected zone (HAZ) were measured. Author

N85-34189# Nagasaki Univ. (Japan). Faculty of Engineering.
ON THE METHODS TO DETERMINE THE STRESS INTENSITY FACTORS IN BOUNDARY ELEMENT METHOD **c39**

Hiroyuki Kisu, Ryoji Yuuki (Inst. of Industrial Science), and Hideo Kitagawa (Yokohame National Univ.) *In* Society of Materials Sciences Proc. of the 27th Japan Congr. on Mater. Res. Mar. 1984 p 53-56 refs Previously announced in IAA as A85-23464 (For primary document see N85-34180 23-23)
Avail: NTIS HC A14/MF A01

Two methods are proposed that are suitable for determining stress intensity factors in boundary element method (BEM) calculations, one of which uses stress near the crack tip, as proposed by Murakami (1979), while the other uses displacement near the crack tip. These methods are found to simply and accurately determine the values of K without requiring modification of existing BEM analysis calculation program. O.C.

N85-34190# Kyoto Univ. (Japan). Dept. of Mechanical Engineering.
THE INFLUENCE OF TEMPERATURE ON STATIC AND DYNAMIC SCC CRACK GROWTH BEHAVIOR IN ALUMINUM ALLOY **c26**

Kenjiro Komai, Kohji Minoshima, and Hiroshi Yukimachi *In* Society of Materials Science Proc. of the 27th Japan Congr. on Mater. Res. Mar. 1984 p 57-62 refs Previously announced in IAA as A85-23465 (For primary document see N85-34180 23-23)
Avail: NTIS HC A14/MF A01

The effects of temperature on static and dynamic stress corrosion cracking (SCC) crack growth behavior are studied in the high strength Al alloy ZK141, which has been noted to be sensitive to active path corrosion-type SCC. At the 278-343 K temperatures examined, an acceleration of dynamic SCC crack growth rate over the static SCC type is observed, together with a significant decrease of threshold stress intensity factor. Intergranular cracking dominates the fracture surface in static SCC at all temperatures. O.C.

N85-34191# Kyoto Univ. (Japan). Dept. of Mechanical Engineering.
A FRACTOGRAPHIC STUDY ON MODE 2 AND MODE 3 SCC CRACK GROWTH IN AN Al-Zn-Mg ALLOY **c26**

Kenjiro Komai and Eiji Usuki (Sumitomo Metals, Ltd.) *In* Society of Materials Science Proc. of the 27th Japan Congr. on Mater. Res. Mar. 1984 p 63-69 refs Previously announced in IAA as A85-23466 (For primary document see N85-34180 23-23)
Avail: NTIS HC A14/MF A01

Attention is given to the results of a fractographic study of modes 2 and 3 stress corrosion cracking (SCC) crack growth, in a 3.5-percent NaCl solution, for an Al-Zn-Mg alloy. Fracture surface morphologies are noted to be very different from mode 1 SCC under considerable influence from shearing loads. The most characteristic features are transgranular dissolution surfaces along a maximum shearing stress direction, accompanied by trench-like dissolution traces along slip planes, and slip traces. O.C.

N85-34192# Toyama Univ. (Japan). Dept. of Mechanical Engineering.
CORROSION FATIGUE STRENGTH AND CRACK GROWTH IN PRESTRAINED 0.16% C CARBON STEEL **c26**

Sotomi Ishihara, Ichiro Maekawa (Tohoku Univ.), Kazuaki Shiozawa, and Kazyu Miyao *In* Society of Materials Science Proc. of the 27th Japan Congr. on Mater. Res. Mar. 1984 p 71-77 refs (For primary document see N85-34180 23-23)
Avail: NTIS HC A14/MF A01

Very small and distributed cracks can be observed on the surface of smooth specimen subjected to corrosion fatigue. The fracture process can be characterized by the interaction and connection of these small and distributed cracks. The effects of tensile prestrain on fatigue life, particularly on the crack initiation and growth process is studied. Fatigue tests were performed with the specimen of 0.16% carbon steel under completely reversed plane bending fatigue in salt water of 3.0% NaCl. Initiation and growth of cracks in the surface of prestrained smooth specimen were observed in detail during corrosion fatigue tests. Author

N85-34193# Aoyamagakuin Univ., Tokyo (Japan). Dept. of Mechanical Engineering.
EXPERIMENTAL STUDY ON TIME AND TEMPERATURE DEPENDENT BEHAVIOR OF CRACK GROWTH IN VISCOELASTIC STRIP **c39**

Hidekazu Ohtsuka and Masahisa Takashi *In* Society of Materials Science Proc. of the 27th Japan Congr. on Mater. Res. Mar. 1984 p 79-83 refs (For primary document see N85-34180 23-23)
Avail: NTIS HC A14/MF A01

A new technique for measuring the increment of crack length, namely the method of slight impact superposition has been developed. Thus, the increment of crack length could be measured in accuracy of the order of micro-meter. As a consequence of improvement in measurement of crack length, it was, however, made clear that any evidences of discontinuous and/or abrupt phenomena which would define the threshold of crack growth, could not be observed at least in macroscopic range of crack length increment. It has been reported that crack growth behavior is expressed by a kind of power function of time over a wide range of increment of crack length. Time and temperature dependences of parameters which concern crack growth behavior, were compared quantitatively with the theoretical predictions by Shapery and by Misawa et al. And the possibility of application of time and temperature superposition for crack growth behavior was also discussed. Author

N85-34194# Suzuka Coll. of Technology (Japan).
FRACTOGRAPHIC ANALYSIS FOR NONPROPAGATING CONDITIONS OF FATIGUE CRACK AT HIGH STRESS RATIOS IN MILD STEEL **c26**

Kuniji Ichida and Teiichi Ohkouchi (Nagoya Inst. of Technology) *In* Society of Materials Science Proc. of the 27th Japan Congr. on Mater. Res. Mar. 1984 p 85-91 refs (For primary document see N85-34180 23-23)
Avail: NTIS HC A14/MF A01

The behavior of the nonpropagation is evaluated at high stress ratios near R=1.0 where crack fronts remain open since the stress intensity to close the crack becomes lower than the minimum stress intensity range. Oxide induced or roughness induced crack closure hardly occurs at such high stress ratios because the crack tip displacements exceed the order of the scales of the oxide deposits or the fracture roughness. The role of cyclic plasticity at blunted crack fronts under near threshold levels at high stress ratios near static tensile loading is discussed relative to other near threshold mechanisms, in light of fracture surface structures which contribute to transgranular or intergranular cracking. Author

N85-34195# Waseda Univ., Tokyo (Japan). School of Science and Engineering.
CRYSTALLOGRAPHIC ORIENTATION DEPENDENCE OF FATIGUE CRACK PROPAGATION IN EXTREMELY LOW CARBON STEEL **c26**
Ikuhiko Hayashi, Takayuki Suzuki, Hiromi Ishii, and Makoto Oiyama *In* Society of Materials Science Proc. of the 27th Japan Congr. on Mater. Res. Mar. 1984 p 93-98 refs (For primary document see N85-34180 23-23)
Avail: NTIS HC A14/MF A01

In polycrystalline metals, slip systems in each grain play an important role in the crack propagation. Since the activity of these slip systems depends on grain orientation and grain size, it seems certain that the direction of crack propagation is affected by the crystallographic orientation of each grain. In b.c.c. metals, it has not yet been made clear whether the direction of crack propagation depends on grain orientation. The effect of grain orientation on the direction of low cycle fatigue crack propagation in extremely low carbon steel was previously reported. The same problem in the case of high cycle fatigue crack propagation is investigated and the basic mechanism of the fatigue crack growth from the crystallographic viewpoint is made clear. Author

N85-34196# Waseda Univ., Tokyo (Japan). School of Science and Engineering.
FATIGUE CRACK RETARDATION PHENOMENON CAUSED BY SINGLE-MULTIPLE OVERLOADS IN 2017-T3 ALUMINUM ALLOW **c26**
Ikuhiko Hayashi, Yuji Suzuki, Eiichi Kusama, and Yasuhiro Majima *In* Society of Materials Science Proc. of the 27th Japan Congr. on Mater. Res. Mar. 1984 p 99-104 refs Previously announced in IAA as A85-23467 (For primary document see N85-34180 23-23)
Avail: NTIS HC A14/MF A01

The retardation phenomenon in fatigue crack propagation after single and multiple overloads in 2017-T3 Al alloy was investigated, with a view to retardation behavior prediction. The retardation effect is noted to have intensified with increasing overload magnitude, perhaps due to the extension of the compressive residual stress region generated by the overload. The effect also intensified with increasing numbers of overload cycles. It is suggested that this is caused by the increasing compressive residual stress, which acts on the crack surface with crack propagation during multiple overloads. Retardation behavior prediction was carried out by a simple crack propagation model, under the assumption that the effective residual stress acting on the crack surface caused the retardation. O.C.

N85-34197# Toshiba Corp., Fuchu (Japan). Heavy Apparatus Engineering Lab.
SAFETY AND RELIABILITY OF STEEL STRUCTURAL MATERIALS UNDER RANDOM SERVICE IMPACT LOADS **c26**
Nagatoshi Okabe, Toshiyuki Yano, and Tadao Mori *In* Society of Materials Science Proc. of the 27th Japan Congr. on Mater. Res. Mar. 1984 p 105-110 refs (For primary document see N85-34180 23-23)
Avail: NTIS HC A14/MF A01

In design of the machine, not forgetting the material strength, it is important to examine reliability of the steel structural materials by considering variations of impact load characteristics as well as those of material strengths, when fatigue strength and life to failure of the steel structural materials under these repeated service impact loads are determined. The fatigue strength of the structural carbon steels under random impact tension compression loads with a given stress ratio is analyzed along with the failure probability estimation based on their static tensile properties. Analytical results obtained show good agreement with the experimental results. The research performs reliability engineering approach on the failure probabilitical decision of the safety factor and allowable stress, and moreover the material selection is investigated from the viewpoint of optimum structural design considering safety and economy. Author

N85-34198# Kanazawa Inst. of Tech. (Japan). Material System Research Lab.
STATISTICAL POOLING METHOD OF FATIGUE DATA FOR RELIABILITY DESIGN **c39**
Hidetoshi Nakayasu and Tadashi Umerhara *In* Society of Materials Science Proc. of the 27th Japan Congr. on Mater. Res. Mar. 1984 p 111-117 refs Previously announced in IAA as A85-23468 (For primary document see N85-34180 23-23)
Avail: NTIS HC A14/MF A01

Attention is given to a fatigue data pooling method having its graphical basis in the regression equation's statistical significance test, which is fitted to the fatigue data on a log-log scale. The samples used must satisfy criteria of linearity, equality of residual squares, and equality of regression coefficients. O.C.

N85-34199# Tokyo Inst. of Tech. (Japan).
ANTI WEAR PROPERTY OF TWO PHASIC METAL COMPOSITE **c26**
Susumu Norose, Tadashi Sasada, and Keiichi Maruyama (Fuji Heavy Industry Ltd.) *In* Society of Materials Science Proc. of the 27th Japan Congr. on Mater. Res. Mar. 1984 p 119-124 refs (For primary document see N85-34180 23-23)
Avail: NTIS HC A14/MF A01

Forming metal layers composed of the mixture of sliding metals, the edge surface of piled thin plates of different metals using bonding agent were rubbed against other metal surface. By doing so, it was found that running-in phenomenon occurred more easily than in the case of rubbing different metals against each other and that the wear rate was decreased. It is considered that the results obtained using piled material should give several clues for understanding the wearing mechanisms of two phasic material. At the same time, it is also considered that such piled material itself should practically be useful as anti-wear material. Author

N85-34200# Tokyo Inst. of Tech. (Japan).
THREE BODY ABRASIVE WEAR IN VARIOUS METAL COMBINATIONS **c26**
Tadashi Sasada, Noibuhiko Emori (Komatsu Ltd.), and Mamoru Oike (National Aerospace Lab., Kakuda) *In* Society of Materials Science Proc. of the 27th Japan Congr. on Mater. Res. Mar. 1984 p 125-130 refs (For primary document see N85-34180 23-23)
Avail: NTIS HC A14/MF A01

The effect of the material of a rubbing part on the wear of the mating surface in three body abrasive wear was studied experimentally. If the cutting action of abrasives is kept ideal, the wear rate of a rubbing part concerned is kept constant irrespective of the mating materials. This simple relation is observable experimentally under such conditions as larger sized abrasives, smaller rubbing area and use of lubricant oil. But, if such conditions are not prepared, the adhesive action between metal and metal and between abrasives and metal becomes violent. As a result, the cutting action of abrasives is disturbed and the wear rate of the rubbing part concerned is reduced. Greater reduction of wear rate was observed in the case where the hardness of the opposite metal surface is lower. Author

N85-34201# Nihon Univ., Tokyo (Japan). Coll. of Science and Technology.
ELECTROLYTIC SYNTHESIS OF COLORED ETA ALUMINA FILM **c27**
Midori Yamada and Ikuo Mita (Tokyo Metropolitan Industrial Technology Center) *In* Society of Materials Science Proc. of the 27th Japan Congr. on Mater. Res. Mar. 1984 p 131-134 refs Sponsored in part by The Light Metal Educational Foundation, Inc. (For primary document see N85-34180 23-23)
Avail: NTIS HC A14/MF A01

White eta alumina film can be synthesized by anodic oxidation of aluminum in aq. solution of sodium carbonate added with sodium fluoride under high voltage. Colored eta alumina films were synthesized by electrolytic method. The methods were found of electrolytic synthesis of colored eta alumina film incorporated metal ions in the film on aluminum using aluminum alloys, electrolytic

coloring process and dipping process. Eta alumina film on aluminum has excellent mechanical properties and high resistance against alkaline and acid solution, compared with usual amorphous alumina film. UV and IR absorption spectra, X-ray diffraction patterns and thickness of the films were measured. The film surfaces were also observed by scanning electron microscope. Author

N85-34202# Meidensha Electric Mfg. Co. Ltd., Todyo (Japan).
X-RAY RESIDUAL STRESS ANALYSIS ON THE COARSE GRAIN OF COPPER AND ITS APPLICATION TO THE BRAZED COPPER **c26**
Masaki Koga, Hidemitsi Takebuchi, and Katsuaki Senba *In* Society of Materials Science Proc. of the 27th Japan Congr. on Mater. Res. Mar. 1984 p 135-140 refs (For primary document see N85-34180 23-23)
Avail: NTIS HC A14/MF A01

Hermetic seal techniques of ceramics to metals have been developed. As typified by vacuum interrupter, such techniques have been applied to various power electric equipments. Such hermetic seals are carried out in vacuum or in H2 gas by high temperature soldering, (brazing) between ceramics and metals. Recrystallization temperature of copper (about 400 C) is fairly even below, as compared with that of brazing heat treatment. As a result, it is supposed that the grain size of copper becomes coarse inevitably because of hermetic seal treatment. Consequently, reduction of residual stress based on annealing effect of copper is expected on the hermetic seal of ceramics to copper, nevertheless the difference among these thermal expansion coefficients is large. X-ray residual stress analysis of copper ring hermetic sealed to alumina ceramic disk is discussed. Author

N85-34203# Bunka Women's Univ. (Japan). Dept. of Domestic Science.
STUDY ON THE CORRELATION BETWEEN GRINDING CONDITIONS AND RESIDUAL STRESSES IN GROUND SURFACE OF STEEL BY THE X-RAY METHOD **c26**
Shigeo Zaima and Hideyuki Mitzutani (Chubu Inst. of Technology) *In* Society of Materials Science Proc. of the 27th Japan Congr. on Mater. Res. Mar. 1984 p 141-146 refs (For primary document see N85-34180 23-23)
Avail: NTIS HC A14/MF A01

The situation in which residual stresses occur in the ground surface is investigated by the X-ray method. When results were considered, influence of grinding direction on the residual stresses were regarded, and the relationship between grinding condition and the residual stresses was examined. As a result, a basic data to assist in the selection of optimum grinding conditions was obtained. Author

N85-34204# Musashi Inst. of Tech., Tokyo (Japan).
MULTIAXIAL STRESS ANALYSIS TAKING ACCOUNT OF PENETRATION DEPTH OF X-RAYS. A SOLUTION BY MEANS OF POLYNOMIAL APPROXIMATION **c39**
Yasuo Yoshioka, Toshihiko Sasaki, and Makoto Kuramoto (Inst. of Vocational Training) *In* Society of Materials Science Proc. of the 27th Japan Congr. on Mater. Res. Mar. 1984 p 147-152 refs (For primary document see N85-34180 23-23)
Avail: NTIS HC A14/MF A01

A method was previously proposed for an X-ray multiaxial stress analysis in which the effect of stress gradient was taken into account within the penetration depth of X-rays. The basic equation of this method was solved by an application of the integral method proposed by Lode and Peiter. The stress tensor in surface, and the stress gradient can be evaluated from the measured Bragg angle times measuring directions values. During a smoothing process it was found that the coefficients of this approximated function of sin sup 2 psi include the stress in surface, and stress gradient and all components can be solved without the use of integration. Attention is given to this method for the X-ray stress analysis by means of the polynomial approximation of sin sup 2 psi and its application to the plane stress problem. Author

N85-34205# Niihama Technical Coll. (Japan).
X-RAY MEASUREMENT OF THERMAL STRESSES IN TUNGSTEN FIBER-COPPER COMPOSITES **c26**
Yasukazu Keuchi and Haruo Fujiwara (Tokushima Univ.) *In* Society of Materials Sciences Proc. of the 27th Japan Congr. on Mater. Res. Mar. 1984 p 153-158 refs (For primary document see N85-34180 23-23)
Avail: NTIS HC A14/MF A01

The thermal stress behavior is clarified experimentally by measuring both the matrix and the fiber stresses in-situ in a well consolidated model system, tungsten fiber reinforced copper composite. An X-ray method, being nondestructive, has the great advantage of making repeated measurements possible on the same specimen even at an elevated temperature. The in-situ stress measurements at the temperatures up to 696 K are carried out in the direction parallel to the fiber axis by the X-ray method. The thermal stress induced in each phase during thermal cycling between 282 and 503 K is also measured in-situ. The thermal stress behavior of each phase in the composites is experimentally discussed. Author

N85-34206# Waseda Univ., Tokyo (Japan). Castings Research Lab.
EVALUATION METHODS OF CERAMIC FIBER REINFORCED METAL MATRIX COMPOSITE **c26**
Yutaka Kagawa and Eiichi Nakata *In* Society of Materials Science Proc. of the 27th Japan Congr. on Mater. Res. Mar. 1984 p 159-163 refs Previously announced in IAA as A85-23469 (For primary document see N85-34180 23-23)
Avail: NTIS HC A14/MF A01

The present evaluation method for metal matrix composite mechanical properties is applied to the case of an SiC fiber-reinforced aluminum matrix material whose fiber volume fraction was 0.35. The results obtained indicate that tensile fracture strength strongly depends on the stress concentration of the specimen. It is found that the different results produced by different test methods can be collectively evaluated by the use of the effective volume and the Weibull modulus of the composite. O.C.

N85-34207# Tokushima Univ. (Japan). Faculty of Engineering.
FRACTURE BEHAVIOR OF ALUMINUM COMPOSITES REINFORCED WITH FIBER **c24**
Kiyoshi Sakamaki, Masanori Hamada, and Masaharu Hasegawa *In* Society of Materials Science Proc. of the 27th Japan Congr. on Mater. Res. Mar. 1984 p 165-172 refs Previously announced in IAA as A85-23470 (For primary document see N85-34180 23-23)
Avail: NTIS HC A14/MF A01

An evaluation is made of the consequences for fracture behavior of the fiber-matrix reaction zone in copper or tungsten fiber-reinforced aluminum matrix composites. Attention is given to the initiation and propagation of microcracks with casting temperature, for the cases of 700, 800, and 900 C in the aluminum-tungsten system, which yielded higher strength than that predicted by the law of mixtures. The strength of the aluminum-copper system composites is noted to be lower than predicted by the law of mixtures, since they, unlike the aluminum-tungsten, did not develop an effective fiber-matrix interface. O.C.

N85-34208# Hiroshima Univ. (Japan). Faculty of Engineering.
ROTATING BENDING FATIGUE STRENGTH OF SILICON CARBIDE AND ALUMINA-FIBER REINFORCED ALUMINUM **c24**
Hideharu Fukunaga, Koichi Goda, and Tomoaki Tachihara *In* Society of Materials Science Proc. of the 27th Japan Congr. on Mater. Res. Mar. 1984 p 173-177 refs (For primary document see N85-34180 23-23)
Avail: NTIS HC A14/MF A01

Composite materials produced by a solid process, (diffusion bonding) have been used for the aircraft materials. The method, however, takes rather long time in the compositing process, and requires a secondary processing, causing a problem in productivity. The other method in which molten metal is forcibly charged into fiber bundle, (liquid process) may possibly cause the interfacial

reaction between fiber and matrix, but it has a characteristic of high productivity because of its short time process. For the purpose of providing the elemental data on mechanical properties of an inorganic fiber reinforced metal, the rotating bending fatigue behavior of the silicon carbide fiber reinforced aluminum and the alumina fiber reinforced aluminum fabricated by a liquid process is studied. Author

N85-34209# Hokkaido Industrial Research Inst. (Japan).
POLY-FUNCTIONAL BUILDING MATERIAL FROM FIBERGLASS (ITS FABRICATION AND PROPERTIES) **c27**
Keiichi Katsuse, Nobuhiro Naano, Toshihiko Maruyama, Toru Hirano, and Takuya Koga (Iwakura-Gumi Lumber Co., Ltd.) *In* Society of Materials Science Proc. of the 27th Japan Congr. on Mater. Res. Mar. 1984 p 253-256 ref (For primary document see N85-34180 23-23)
Avail: NTIS HC A14/MF A01

A poly-functional material for building parts mainly from shortcut fiberglass was previously reported. The combination of such functions as heat insulation, mechanical strength, stiffness, fire resistivity, water resistivity, lightness, some of which are believed to be mutually exclusive in a simple material was sought. Specimens for the poly-functional building material were fabricated and the properties are discussed, relating to the composite structure. Author

N85-34210# Osaka City Univ. (Japan). Faculty of Engineering.
STRESS DISTRIBUTION OF FIBERGLASS REINFORCED PLASTIC BEAM WITH A DELAMINATION UNDER THREE-POINT BENDING **c39**
Taichi Fujii and Qian Sun (Beijing FRP Research Inst.) *In* Society of Materials Science Proc. of the 27th Japan Congr. on Mater. Res. Mar. 1984 p 257-261 refs Previously announced in IAA as A85-23472 (For primary document see N85-34180 23-23)
Avail: NTIS HC A14/MF A01

When a fiber-reinforced plastic (FRP) beam possessing a delamination is subjected to flatwise flexure under three-point bending conditions, high stress concentration occurs in the vicinity of the edge of the delamination which is primarily due to the shearing stress at the edge as well as the stress exerted by the bending moment at the center of the delamination. The effect of the delamination's position becomes critical as it approaches the edge of the beam and as its distance increases from the neutral axis of the beam. The amount of interlaminar shearing stress is proportional to the difference between the inverse of the matrix Young's modulus and that of the reinforcement. O.C.

N85-34211# Aoyamagakuin Univ., Tokyo (Japan). Dept. of Mechanical Engineering.
INFLUENCE OF CYCLIC THERMAL LOADING ON INTERNAL STRESS IN CASTED EPOXY RESIN **c24**
Satoshi Koike, Masahisa Takashi, and Masaki Koga (Meidensha Electric Mfg. Co., Ltd.) *In* Society of Materials Science Proc. of the 27th Japan Congr. on Mater. Res. Mar. 1984 p 263-268 refs (For primary document see N85-34180 23-23)
Avail: NTIS HC A14/MF A01

Generated internal stress often bring about initiation and succeeding crack growth to fracture of molded products particularly in the vicinity of interface of an insert and a resin. Variation of photoviscoelastic fringe order was traced periodically during the curing process and the cooling-heating repetition of thermal loading. Standing upon quantitative evaluation of internal stress by the linear photoviscoelastic stress analysis the influence of difference in glass transition temperature of the resin and the effect of cyclic thermal loading, on the internal stress distribution near the insert, were investigated. Author

N85-34212# Kyoto Univ. (Japan). Industrial Arts and Textile Fibers.
STRENGTH PROPERTIES OF GLASSFIBER REINFORCED THERMOPLASTICS **c27**
Zenichiro Maekawa, Taichi Fujii (Osaka City Univ.), Teruaki Ikeda (Idemitsu Petrochemical Co.), and Toshio Yamada (Nippon Sheet Glass Co.) *In* Society of Materials Science Proc. of the 27th Japan Congr. on Mater. Res. Mar. 1984 p 269-273 refs (For primary document see N85-34180 23-23)
Avail: NTIS HC A14/MF A01

Glassfiber reinforced thermoplastics (GRTP) with high productivity have become of major interest, since these are structural materials formulated specifically for fabrication on stamping press and enable us to achieve fast molding cycles. These are composites of polypropylene/continuous glassfiber and are fabricated by the compression molding method. The experimental results of tensile test and flexural test of GRTP panels are described. Three kinds of GRTP are molded and shaped into square plates. The tensile strengths and flexural strengths at various points in the plate are measured. With the experiment and discussions, it is made clear the effect of the flow of fibers on the strength properties of GRTP. Author

N85-34213# Aoyamagakuin Univ., Tokyo (Japan). Dept. of Mechanical Engineering.
TIME AND TEMPERATURE DEPENDENCE OF FRACTURE SURFACE IN SOFT EPOXY RESIN **c24**
Akira Tanaka, Kazuo Ogawa, and Masahisa Takashi *In* Society of Materials Science Proc. of the 27th Japan Congr. on Mater. Res. Mar. 1984 p 275-279 refs (For primary document see N85-34180 23-23)
Avail: NTIS HC A14/MF A01

Fracture surface of soft epoxy resin is precisely investigated by a polarization and an interference microscope. In order to quantify the characteristic of fracture surface, roughness was measured by pattern analysis on interference fringes obtained through video photographs. The temperature dependence of roughness and its relation to the time and temperature dependent stress intensity factor, were also discussed. Author

N85-34214# Waseda Univ., Tokyo (Japan). School of Science and Engineering.
EFFECT OF STRAIN RATE ON THE INITIAL FAILURE OF NOTCHED GRP LAMINATES **c24**
Ikuhiko Hayashi, Hideo Takahashi, Hideki Kondo, Toshiya Ohta, and Shigeki Kataoka *In* Society of Materials Science Proc. of the 27th Japan Congr. on Mater. Res. Mar. 1984 p 281-287 refs Previously announced in IAA as A85-23473 (For primary document see N85-34180 23-23)
Avail: NTIS HC A14/MF A01

The present investigation of strain rate effects in the behavior of glass fiber-reinforced plastic (GRP) gave attention to mechanical properties, crack tip failure zones, and FEM analysis results. GRP laminates are noted to suffer from strain rate effects in a comparatively low range. Microscopic observation indicates the presence of extensive matrix cracking at high strain rate. FEM analysis of the failure propagation mechanism, including viscoelastic effects, indicated considerable matrix failures at high strain rate, in agreement with experimental results. O.C.

N85-34215# Waseda Univ., Tokyo (Japan). School of Science and Engineering.
IMPACT FRACTURE MECHANISM OF POLYMER PLATES CONTAINING A HEAVY INNER MATERIAL **c27**
Ikuhiko Hayashi, Hisashi Ishikawa, Keishi Takahashi, and Katsumi Kirao *In* Society of Materials Science Proc. of the 27th Japan Congr. on Mater. Res. Mar. 1984 p 289-294 refs (For primary document see N85-34180 23-23)
Avail: NTIS HC A14/MF A01

Impact fracture mechanism are studied. Experimental studies were carried out using two dimensional specimens containing a heavy inner material with specially manufactured impact instruments. Two kinds of polymers (epoxy and polyester) for filler material, and steel rod as the core, were evaluated. Based on the experimental results, the difference in the failure mode under static and impact load, and the difference in the fracture threshold of epoxy specimens and polyester ones under impact load were discussed. In addition to this, a finite element analysis was carried out to predict the stress distributions around the inner material

under static and impact load. The experimental results were compared with the analytical results. Author

N85-34216# Meidensha Electric Mfg. Co. Ltd., Todyo (Japan).
STUDY ON FRACTURE BEHAVIOR OF EPOXY RESIN c24
Masaki Koga, Masahisa Takashi (Aoyamagakuin Univ.), and Satoshi Koike (Aoyamagakuin Univ.) *In* Society of Materials Science Proc. of the 27th Japan Congr. on Mater. Res. Mar. 1984 p 295-299 refs (For primary document see N85-34180 23-23)
Avail: NTIS HC A14/MF A01

In a cooling and heat cycle test, the molded parts are in peril of cracking by the thermal stress, and the cracking causes some troubles in practical use. To cope with these obstacles, it is necessary to define the critical values concerning the mechanical properties and fracture behaviors. Both the temperature dependence of static tensile properties and the low cycle fatigue strength at the room temperature are discussed for two kinds of epoxy resins with different glass transition temperature. These properties are qualitatively interrelated with the macroscopic fracture patterns. Author

N85-34217# Brookhaven National Lab., Upton, N. Y.
ATMOSPHERIC MODELING OF ORGANICS FOR RISK ASSESSMENT: A CHEMIST'S VIEW
J. S. Gaffney 1985 7 p refs Presented at the DOE Workshop on Atmospheric Modeling 3: Toxic Org., La Jolla, Calif., 11 Feb. 1985
(Contract DE-AC02-76CH-00016)
(DE85-009770; BNL-36089; CONF-850280-1) Avail: NTIS HC A02/MF A01

An overview of some of the approaches used in the research of organic atmospheric chemistry is presented. Attention is given to the need for evaluation of secondary organic toxin production in the atmosphere, and to identification of areas where problems may occur in their modeling. DOE

N85-34218# Department of Energy, Washington, D. C.
METHOD OF DISTRIBUTING LIQUEFACTION CATALYSTS IN SOLID CARBONACEOUS MATERIAL Patent Application
S. W. Weller, inventor (to NASA) Filed 23 May 1984 14 p
(Contract DE-FG22-81PC-40781)
(DE85-005759; US-Patent-Appl-SN-612953) Avail: NTIS HC A02/MF A01

A method of dispersing a liquefaction catalyst within coal or other carbonaceous solids involves providing a suspension in oil of microcapsules containing the catalyst. An aqueous solution of a catalytic metal salt is emulsified in the water immiscible oil and the resulting minute droplets microencapsulated in polymeric shells by interfacial polycondensation. The catalyst is subsequently blended and dispersed throughout the powdered carbonaceous material to be liquefied. At liquefaction temperatures the polymeric microcapsules are destroyed and the catalyst converted to minute crystallites in intimate contact with the carbonaceous material. DOE

N85-34219# Department of Energy, Washington, D. C.
PROCESS FOR FUNCTIONALIZING ALKANES Patent Application
R. G. Bergman, A. H. Janowicz, and R. A. Periana-Pillai, inventors (to DOE) Filed 12 Jun. 1984 18 p
(Contract DE-AC03-76SF-00098)
(DE85-006420; US-Patent-Appl-SN-619886) Avail: NTIS HC A02/MF A01

Process for functionalizing saturated hydrocarbons selectively in the terminal position comprises: (1) reacting said saturated hydrocarbons with a metal complex CpRhPMe3H2 in the presence of ultraviolet radiation at -60 to -17 C to form a hydridoalkyl complex CpRhPMe3RH; (2) reacting said hydridoalkyl complex with a haloform CHX3 at -60 to -17 C to form the corresponding haloalkyl complex of step (1) CpRhPMe3RX; and (3) reacting said haloalkyl complex with halogen -60 to 25 C to form a functional haloalkyl compound. DOE

N85-34220# Department of Energy, Washington, D. C.
METHOD FOR EXTRACTING LANTHANIDES AND ACTINIDES FROM ACID SOLUTIONS BY MODIFICATION OF PUREX SOLVENT Patent Application
E. P. Horwitz and D. G. Kalina, inventors (to DOE) Filed 21 May 1984 30 p
(Contract W-31-109-eng-38)
(DE85-005763; US-Patent-Appl-SN-612199) Avail: NTIS HC A03/MF A01

The process has been developed for the extraction of multivalent lanthanide and actinide values from acidic waste solutions, and for the separation of these values from fission product and other values. The process utilizes a new series of neutral bi-functional extractants, the alkyl(phenyl)-N, N-dialkylcarbamoylmethylphosphine oxides, in combination with a phase modifier to form an extraction solution. The addition of the extractant to the Purex process extractant, tri-n-butylphosphate in normal paraffin hydrocarbon diluent, will permit the extraction of multivalent lanthanide and actinide values from 0.1 to 12.0 molar acid solutions. DOE

N85-34221# Department of Energy, Washington, D. C.
METHOD FOR CONTROLLING THE VISCOSITY OF SILOXANE OILS Patent Application
A. A. Carey (Martin Marietta Energy Systems) and J. T. Shor, inventors (to DOE) (Martin Marietta Energy Systems) Filed 12 Sep. 1984 8 p
(Contract DE-AC05-84OR-21400)
(DE85-011586; US-Patent-Appl-SN-649623) Avail: NTIS HC A02/MF A01

A method of controlling the viscosity of siloxane oils in the presence of lead by adding a small amount of a dione such as p-benzoquinone or 2,3-butanedione is described. DOE

24 COMPOSITE MATERIALS

Includes laminates.

N85-34222*# Sikorsky Aircraft, Stratford, Conn.
FLIGHT SERVICE EVALUATION OF COMPOSITE HELICOPTER COMPONENTS Contractor Final Report, May 1982 - Sep. 1983
Melvin J. Rich and David W. Lowry Apr. 1985 116 p refs
(Contract NAS1-16542)
(NASA-CR-172562; NAS 1.26:172562; SER-510117) Avail: NTIS HC A06/MF A01 CSCL 11D

An assessment of composite helicopter structures, exposed to environmental effects, after four years of commercial service is presented. This assessment is supported by test results of helicopter components and test panels which have been exposed to environmental effects since late 1979. Full scale static and fatigue tests are being conducted on composite components obtained from S-76 helicopters in commercial operations in the Gulf Coast region of Louisiana. Small scale tests are being conducted on coupons obtained from panels being exposed to outdoor conditions in Stratford, Connecticut and West Palm Beach, Florida. The panel layups represent S-76 components. Moisture evaluations and strength tests are being conducted, on the S-76 components and panels, over a period of eight years. Results are discussed for components and panels with up to four years of exposure. Author

N85-34223*# National Aeronautics and Space Administration. Lewis Research Center, Cleveland, Ohio.
MECHANICAL PROPERTIES OF SiC FIBER-REINFORCED REACTION-BONDED Si3N4 COMPOSITES
Ramakrishna T. Bhatt 1985 14 p refs Presented at the 21st Univ. Conf. on Ceram. Sci., University Park, Pa., 17-19 Jul. 1985; sponsored by Pennsylvania State Univ. Prepared in cooperation with Army Aviation Research and Development Command, Cleveland

(NASA-TM-87085; E-2671; NAS 1.15:87085; USAAVSCOM-TR-85-C-14) Avail: NTIS HC A02/MF A01 CSCL 11D

The room temperature mechanical and physical properties of silicon carbide fiber reinforced reaction-bonded silicon nitride composites (SiC/RBSN) have been evaluated. The composites contained 23 and 40 volume fraction of aligned 140 micro m diameter chemically vapor deposited SiC fibers. Preliminary results for composite tensile and bend strengths and fracture strain indicate that the composites displayed excellent properties when compared with unreinforced RBSN of comparable porosity. Fiber volume fraction showed little influence on matrix first cracking strain but did influence the stressed required for matrix first cracking and for ultimate composite fracture strength. It is suggested that by reducing matrix porosity and by increasing the volume fraction of the large diameter SiC fiber, it should be possible to further improve the composite stress at which the matrix first cracks. Author

N85-34224# Department of the Air Force, Washington, D.C.
CARBON/CARBON COMBUSTOR EXTERNAL INSULATION Patent Application
Bruns, inventor (to Air Force) Filed 18 Apr. 1985 22 p
(AD-D011719; US-Patent-Appl-SN-724719) Avail: NTIS HC A02/MF A01 CSCL 11/4

The combustion chambers of ramjet-powered missiles must be thermally insulated to protect adjacent equipment from combustion gas temperatures of 3000 F or greater. Thermal protection is accomplished in the present disclosure by the hot wall carbon/carbon combustor, and an intermediate-temperature insulation layer composed of MIN-K 2000 a proprietary product of the Manville Corp. A portion of the MIN-K 2000 insulation is allowed to experience temperatures greater than its maximum rated value of 2,000 F and thermally degrade in the one-time use to which the disclosure is put. However, virgin layers of the MIN-K insulation still protect the structure, fuel and electrical components adjacent to the combustion chamber from heat shorts. The present disclosure minimizes the weight and volume of the thermal protection system, resulting in increased missile performance. GRA

N85-34225# Delaware Univ., Newark. Dept. of Mechanical and Aerospace Engineering.
VISCOELASTIC BEHAVIOR OF SHORT-FIBER COMPOSITE MATERIALS
S. Nomura and T. W. Chou [1985] 21 p
(Contract DE-AC01-79ER-10511)
(DE85-011233; DOE/ER-10511/T6) Avail: NTIS HC A02/MF A01

This paper examines the viscoelastic behavior of unidirectional short-fiber composites. Each fiber is approximated by an ellipsoidal elastic inclusion embedded in a viscoelastic matrix. The static correspondence principle which relates the viscoelastic problem to the elastic problem is applied to the modified version of the effective elastic moduli of short-fiber composites originally derived by the authors. Numerical examples for various fiber aspect ratios are derived based upon the collocation approximation method as well as the self-consistent model. DOE

N85-34226# Department of Energy, Washington, D. C.
COMPOSITE DESICCANT STRUCTURE Patent Application
A. V. Fraioli and W. W. Schertz, inventors (to DOE) Filed 6 Jun. 1984 13 p
(Contract W-31-109-eng-38)
(DE85-006400; US-Patent-Appl-SN-617781) Avail: NTIS HC A02/MF A01

A composite formed of small desiccant particles retained in a dark matrix composed of a porous binder containing a transition metal oxide with pores to provide moisture transport with respect to the particles, and metallic fibers to remove the heat of condensation during dehumidification and provide heat for the removal of moisture during regeneration is presented. The moisture absorbing properties of the composite may be regenerated by exposure of the dark matrix to solar radiation with dehumidification occurring at night. DOE

N85-34227# Societe Nationale Industrielle Aerospatiale, Issac (France).
CENTRALIZED SURVEILLANCE OF FLEXIBLE WORKSHOPS FOR THE MANUFACTURING OF COMPOSITE MATERIALS [SURVEILLANCE CENTRALISEE D'ATELIERS FLEXIBLES DE FABRICATION DE MATERIAUX COMPOSITES]
J. F. Pere 1985 6 p In FRENCH Presented at Journees Europeennes des Composites, Paris, 20-21 Mar. 1985
(SNIAS-851-430-103) Avail: NTIS HC A02/MF A01

The reorganization of composite material manufacturing facilities in order to attain an extensive automation is described. The project includes the continuous utilization of the existing facilities, the integration of the process surveillance, the development of continuous measuring and control systems, increasing of the period of autonomous functioning, the installation of a local computer network, and the reprogramming of the maintenance. Author (ESA)

N85-34228# Societe Nationale Industrielle Aerospatiale, Issac (France). Div. Systemes Balistiques et Spatiaux.
PRODUCT DEFINITION: TECHNICAL SPECIFICATION OF NEEDS [LA DEFINITION DU PRODUIT: SPECIFICATIONS TECHNIQUES DE BESOIN]
Albert Phan 7 Dec. 1984 8 p In FRENCH Presented at Journees d'Etudes CODEMAC 84, 17 May 1984
(SNIAS-851-430-104; AQEF-783/84) Avail: NTIS HC A02/MF A01

A product definition method used in the aerospace industry was adapted to the manufacturing of sports goods in composite materials. The customer needs are translated into technical terms. The resulting specification describing the customer requirements must be adapted to the technological capability of the manufactures. A certain number of tests and measurements may be necessary to complete such technical specifications. Author (ESA)

N85-34207# Tokushima Univ. (Japan). Faculty of Engineering.
FRACTURE BEHAVIOR OF ALUMINUM COMPOSITES REINFORCED WITH FIBER
Kiyoshi Sakamaki, Masanori Hamada, and Masaharu Hasegawa *In* Society of Materials Science Proc. of the 27th Japan Congr. on Mater. Res. Mar. 1984 p 165-172 refs Previously announced in IAA as A85-23470 (For primary document see N85-34180 23-23)
Avail: NTIS HC A14/MF A01

N85-34208# Hiroshima Univ. (Japan). Faculty of Engineering.
ROTATING BENDING FATIGUE STRENGTH OF SILICON CARBIDE AND ALUMINA-FIBER REINFORCED ALUMINUM
Hideharu Fukunaga, Koichi Goda, and Tomoaki Tachihara *In* Society of Materials Science Proc. of the 27th Japan Congr. on Mater. Res. Mar. 1984 p 173-177 refs (For primary document see N85-34180 23-23)
Avail: NTIS HC A14/MF A01

N85-34211# Aoyamagakuin Univ., Tokyo (Japan). Dept. of Mechanical Engineering.
INFLUENCE OF CYCLIC THERMAL LOADING ON INTERNAL STRESS IN CASTED EPOXY RESIN
Satoshi Koike, Masahisa Takashi, and Masaki Koga (Meidensha Electric Mfg. Co., Ltd.) *In* Society of Materials Science Proc. of the 27th Japan Congr. on Mater. Res. Mar. 1984 p 263-268 refs (For primary document see N85-34180 23-23)
Avail: NTIS HC A14/MF A01

N85-34213# Aoyamagakuin Univ., Tokyo (Japan). Dept. of Mechanical Engineering.
TIME AND TEMPERATURE DEPENDENCE OF FRACTURE SURFACE IN SOFT EPOXY RESIN
Akira Tanaka, Kazuo Ogawa, and Masahisa Takashi *In* Society of Materials Science Proc. of the 27th Japan Congr. on Mater. Res. Mar. 1984 p 275-279 refs (For primary document see

N85-34180 23-23)
Avail: NTIS HC A14/MF A01

N85-34214# Waseda Univ., Tokyo (Japan). School of Science and Engineering.
EFFECT OF STRAIN RATE ON THE INITIAL FAILURE OF NOTCHED GRP LAMINATES
Ikuhiko Hayashi, Hideo Takahashi, Hideki Kondo, Toshiya Ohta, and Shigeki Kataoka *In* Society of Materials Science Proc. of the 27th Japan Congr. on Mater. Res. Mar. 1984 p 281-287 refs Previously announced in IAA as A85-23473 (For primary document see N85-34180 23-23)
Avail: NTIS HC A14/MF A01

N85-34216# Meidensha Electric Mfg. Co. Ltd., Todyo (Japan).
STUDY ON FRACTURE BEHAVIOR OF EPOXY RESIN
Masaki Koga, Masahisa Takashi (Aoyamagakuin Univ.), and Satoshi Koike (Aoyamagakuin Univ.) *In* Society of Materials Science Proc. of the 27th Japan Congr. on Mater. Res. Mar. 1984 p 295-299 refs (For primary document see N85-34180 23-23)
Avail: NTIS HC A14/MF A01

25 INORGANIC AND PHYSICAL CHEMISTRY

Includes chemical analysis, e.g., chromatography; combustion theory; electrochemistry; and photochemistry.

For related information see also *77 Thermodynamics and Statistical Physics.*

N85-34229# Notre Dame Univ., Ind. Dept. of Aerospace and Mechanical Engineering.
SCALING PARAMETERS OF FLASHOVER
A. M. Kanury Jul. 1985 49 p refs
(NBS-GCR-85-497) Avail: NTIS HC A03/MF A01

The topic of concern in this project is room fire growth to flashover. The objective is to develop scaling rules for flashover time and to apply these rules to certain existing room fire flashover test data. In this report, the scaling rules are deduced from first principles of energy and mass conservation describing the physics of fire growth. The nondimensional scaling parameters are all obtained in the desirable terms of fundamental combustion properties. Collection, estimation, and deduction of these fundamental properties for the materials involved in the concerned fire tests has to be done in the immediate future to evaluate the scaling parameters for correlating the test data. Author

N85-34230# Kentucky Univ., Lexington. Dept. of Chemistry.
ELECTRON PHOTOEJECTION IN CARBANIONS Final Report
L. M. Tolbert 1985 5 p
(Contract DE-AS05-79ER-10424)
(DE85-011747; DOE/ER-10424/5) Avail: NTIS HC A02/MF A01

The photochemistry of resonance-stabilized carbanions is investigated. This program is based on the fact that photoexcited carbanions are very strong reductants, and that such electron-transfer photosensitizers might find utility as models and, eventually, agents, for solar energy conversion devices. Initial work concentrated on evaluating the factors which control carbanion photochemistry and to select among the various decay pathways such as isomerization or electron ejection. Efforts in this area were rewarded, and now carbanions may soon be designed with specific types of photoreactivity. DOE

N85-34231# California Univ., Livermore. Lawrence Livermore Lab.
DESCRIPTION OF A TEST SITE FOR LARGE-SCALE HEAVY GAS DISPERSION AND COMBUSTION EXPERIMENTS
R. P. Koopman and D. Thompson Nov. 1984 20 p refs Presented at the 3rd Symp. on Heavy Gases and Risk Assessment, Bonn, 12 Nov. 1984
(Contract W-7405-eng-48)
(DE85-004987; UCRL-91831; CONF-8411134-1) Avail: NTIS HC A02/MF A01

The US Department of Energy (DOE) is constructing a facility at the Nevada Test Site (NTS) which will be capable of rapid release of large quantities of cryogenic, flammable, or toxic materials. The facility is being built in concert with, and in response to the needs of many industrial and government organizations. The capabilities of the facility and some of the proposed testing is described. In addition, the meteorological characteristics of the Frenchman Flat area of the NTS, an unusually favorable area for the dense gas dispersion testing, is presented. DOE

N85-34232# Pittsburgh Univ., Pa. Dept. of Chemistry.
INFRARED STUDIES OF THE INFLUENCE OF ALKALI METALS ON THE C-O BOND IN CHEMISORBED CARBON MONOXIDE Progress Report
J. T. Yates, Jr. 1985 2 p
(Contract DE-AC02-82ER-13017)
(DE85-005306; DOE/ER-13017/T1) Avail: NTIS HC A02/MF A01

A unique apparatus was constructed to carry out reflection in spectroscopy on single crystal surfaces. Three major types of adsorbate interaction were studied. These are: (1) interaction of vibrationally excited chemisorbed CO species with the lattice phonons in Ni via vibrational dephasing - a new physical phenomenon on surfaces; (2) through metal interaction of chemisorbed CO species with each other, leading to CO rehybridization at high CO surface coverages on Ni; and (3) interaction of chemisorbed CO with controlled coverages of an electronegative surface impurity - chemisorbed S - giving insight into the range of S poisoning on a Ni surface, and information about the detailed character of the S-Ni-CO interaction process. These studies illustrate the high potential of IR spectroscopy for understanding the details of surface bonding and interaction between surface species. The method is about 15 times in frequency resolution than the best high resolution electron energy loss spectroscopy practice anywhere in the world. DOE

N85-34233# Argonne National Lab., Ill.
DIRECT DETERMINATION OF METALS IN ORGANIC MATRICES BY INDUCTIVELY COUPLED PLASMA-ATOMIC EMISSION SPECTROMETRY (ICP-AES)
E. A. Huff Apr. 1985 19 p refs
(Contract W-31-109-eng-38)
(DE85-012015; ANL/ACL-85-2) Avail: NTIS HC A02/MF A01

The capability to do direct determination of metals in organic matrices by inductively coupled plasma atomic emission spectrometry was established. The method was optimized using xylene as the organic solvent, and data on the determination of elements in oils, tri-n-butyl phosphate, and his-(2-ethylhexyl) hydrogen phosphate reflect satisfactory detectability and precision. Although other solvents can be used, plasma properties are a function of solvent composition; thus, different operating conditions have to be generated. The preparation of standards by serial dilution and solvent extraction techniques was investigated with satisfactory results. DOE

N85-34234# Du Pont de Nemours (E. I.) and Co., Aiken, S.C.
DETERMINATION OF LOW CHLORIDE VALUES IN ROCKY FLATS SCRUB ALLOY SOLUTIONS AND OTHER COMPLEX MATRICES
H. P. Holcomb 1985 10 p refs Presented at the 9th Ann. Actinide Separations Workshop, Richland, Wash., 22 May 1985
(Contract DE-AC05-76SR-00001)
(DE85-011506; DP-MS-85-37; CONF-8505139-1) Avail: NTIS HC A02/MF A01

A turbidimetric method, using silver chloride, has been developed to determine low ppM quantities of chloride in Rocky Flats scrub alloy (RFSA) dissolver solutions. This analytical technique has also been applied to other complex matrices such as process 50% caustic and neutralized Purex low heat liquid waste concentrate. A controlled pH precipitation with NaOH, during which chloride remains in solution, is used to pretreat samples to minimize salt

effects from acids, bases, and/or hydrolyzable ions. Control of pH with bromocresol purple indicator also provides a more consistent pH for silver chloride formation, aiding in turbidity reproducibility. Disodium ethylenediaminetetracetic acid is employed to negate covalent bonding by Hg with chloride. The average standard deviation was + or - 17% for turbidity reproducibility in simulated sample aliquots containing a total of 10 to 100 (MU) g chloride. For actual RFSA samples, the relative standard deviation ranged from + or - 14% to + or - 26%, depending on initial chloride values. DOE

N85-34235# Brown Univ., Providence, R. I. Div. of Engineering.
TIME-RESOLVED AND INFRARED SPECTROSCOPY OF EXCITONS Final Report, Jul. 1981 - May 1984
A. V. Nurmikko and M. Glicksman Mar. 1985 22 p ref
(Contract DE-AC02-81ER-10877)
(DE85-011879; DOE/ER-10877/3) Avail: NTIS HC A02/MF A01

This report summarizes results of spectroscopic investigations of three related problems involving excitons in semiconductors. First, the infrared absorption spectra of laser-excited gallium phosphide has been measured as a function of temperature and found to contain a large contribution from intervalence band transition by photoexcited holes. Second, ultrashort laser pulse spectroscopy has yielded new information about the excitonic collisional processes in cuprous oxide, particularly the feature that slow velocity collisions are remarkably effective and possess large scattering cross sections for the 1S ground state. Third, photoluminescence from a mixed crystal zinc manganese telluride has been shown to lead to spectral broadening and lineshapes which demonstrate the role of alloy broadening and exciton electron-hole liquid transition. DOE

N85-34236# Pacific Northwest Lab., Richland, Wash.
SEPARATION OF GAS MIXTURES BY SUPPORTED COMPLEXES
[1985] 8 p refs
(Contract DE-AC06-76RL-01830)
(DE85-011996; DOE/RL-01830/T35) Avail: NTIS HC A02/MF A01

The objective of this program is to define the most advantageous materials (both complex and support), methods of material preparation, material properties, and the performance of feasible supportetd complex systems in applicable gas separations. DOE

N85-34237# Kentucky Univ., Lexington. Dept. of Chemistry.
ELECTRON PHOTOEJECTION IN CARBANIONS
L. M. Tolbert 1985 20 p refs
(Contract DE-AS05-79ER-10424)
(DE85-011748; DOE/ER-10424/4) Avail: NTIS HC A02/MF A01

The photochemistry of resonance stabilized carbanions is investigated. Photoexcited carbanions are very strong reductants, and such electron transfer photosensitizers might find utility as models and, eventually, agents, for solar energy conversion devices. Our initial work has concentrated on evaluating the factors which control carbanion photochemistry and select among the various decay pathways such as isomerization or electron ejection. A ground state carbanion has a specific and well defined space charge relationship such that the negative charge is not evenly distributed, but rather is localized at certain atoms in the molecule. In the excited state, a new space charge relationship exists, and the charge is redistributed to other atoms. It is this phenomenon which we believe dominates the photochemistry of such species and which provides a framework for this report of our work on carbanion photoreactivity. DOE

N85-34238# Ohio State Univ., Columbus. Dept. of Metallurgical Engineering.
EXPERIMENTAL EVALUATION OF THE THERMODYNAMIC PROPERTIES OF CONCENTRATED AQUEOUS POTASSIUM HYDROXIDE SOLUTIONS Final Report
W. B. Johnson, G. R. St.Pierre, D. D. MacDonald, and M. K. Malhotra Feb. 1985 70 p refs
(Contract DE-AC03-76SF-00098)
(DE85-010628; LBL-19146) Avail: NTIS HC A04/MF A01

The thermodynamic activity of water in a binary KOH H2O system has been measured using an electrochemical cell, Cell A (H2(Pt)/KOH in H2O/Hg, HgO(Pt), in the concentration range between 1 and 8 molal and the temperature range of 0 to 80 C. From the equilibrium voltage of cell (A), the activity of water can be directly calculated without making assumptions about the degree of dissociation of the solute or any other solution parameters. The measured values of activity are greater than those found in previous vapor pressure studies, but are consistent with previous EMF measurements of KOH concentration cells at 25 C. These values are invariant with temperature for concentrations up to 4.0 molal but between 6.0 and 8.0 molal the H2O activity first decreases by approximately 10% and then increases by approx. 15% as the temperature is increased. The general activity of water reported here can be used to define previous calculations on the theoretical efficiencies of alkaline battery systems. DOE

N85-34239# California Univ., Livermore. Lawrence Livermore Lab.
INVESTIGATION OF THE FLAME SPEEDS OF PROPANE/METHANOL GAS MIXTURES
K. L. Foote and J. Villareal 2 May 1985 16 p refs
(Contract W-7405-eng-48)
(DE85-012817; UCID-20385) Avail: NTIS HC A02/MF A01

A series of tests was conducted in an acoustically tuned flame tube in order to determine the laminar burning velocities in air of various propane/methanol gas mixtures. The experimental method is explained in detail, along with the tabular results. A 90% propane, 10% methanol mixture is shown to have a maximum burning velocity of 40.8 cm/s. A 65% propane, 35% methanol mixture has a maximum velocity of 41.8 cm/s. These maximum flame speeds are shown to be about the same as that of pure propane by the same method. Gulder has found evidence that the presence of methanol in some hydrocarbon fuels may actually inhibit combustion, but we see no apparent modifications in the combustion of propane when mixed with methanol. DOE

N85-34240# Sandia Labs., Livermore, Calif.
NUMERICAL MODEL OF A PULSE COMBUSTOR
H. A. Dwyer, T. T. Bramlette, J. O. Keller, and B. R. Sanders Apr. 1985 24 p refs Presented at the Central States Sect. and Western States Sect. of the Combustion Inst. Spring Tech. Meeting, San Antonio, 22 Apr. 1985
(Contract DE-AC04-76DR-00789)
(DE85-011717; SAND-84-8971; CONF-8504113-6) Avail: NTIS HC A02/MF A01

Pulse combustion devices can exhibit exceedingly high thermal efficiency and very low pollutant emission when used in heating applications. Broad application of these heating devices has been limited, however, because of a lack of understanding of the fundamental controlling physical and chemical processes governing pulse combustors. A theoretical and experimental research program has been initiated at Sandia National Laboratories to develop such insight. The theoretical results obtained by solving the one dimensional, unsteady, nonlinear gas dynamic equations for a variable area geometry are reported. The important effects of combustion, mixing, wall friction, heat transfer and valve dynamics have been modeled parametrically. One of the major conclusions of the study is that the wave pattern is very sensitive to changes in the system parameters (heat transfer, wall friction, etc.). In fact, the overall wave pattern in a pulse combustor appears to be the result of many destructive and constructive influences which take on the order of tens of cycles to form a periodic pattern. Therefore, it appears that a nonlinear approach which properly accounts for the system history and transport processes is mandatory. DOE

N85-34241# Department of Energy, Washington, D. C.
IMPROVED NEGATIVE ION SOURCE Patent Application
J. E. Delmore, inventor (to DOE) Filed 1 May 1984 35 p
(Contract DE-AC07-79ID-01675)
(DE85-006445; US-Patent-Appl-SN-606038) Avail: NTIS HC A03/MF A01

A method and apparatus for providing a negative ion source accelerates electrons away from a hot filament electron emitter into a region of crossed electric and magnetic fields arranged in a magnetron configuration. During a portion of the resulting cycloidal path, the electron velocity is reduced below its initial value. The electron accelerates as it leaves the surface at a rate of only slightly less than if there were no magnetic field, thereby preventing a charge buildup at the surface of the emitter. As the electron traverses the cycloid, it is decelerated during the second, third, and fourth quadrants, then reaccelerated as it approaches the end of the fourth quadrant to regain its original velocity. The minimum velocity occurs during the fourth quadrant, and corresponds to an electron temperature of 200 to 500 C for the electric and magnetic fields commonly encountered in the ion sources of magnetic sector mass spectrometers. An ion source using the above described thermalized electrons is also disclosed. DOE

N85-34242# Department of Energy, Washington, D. C.
METHOD FOR PREPARING HIGH PURITY VANADIUM Patent Application
F. Schmidt and O. N. Carlson, inventors (to DOE) Filed 16 May 1984 23 p
(Contract W-7405-eng-82)
(DE85-006412; US-Patent-Appl-SN-610905) Avail: NTIS HC A02/MF A01

A method for preparing high purity vanadium having a low silicon content was developed. Vanadium pentoxide is reduced with a stoichiometric, or slightly deficient amount of aluminum to produce a vanadium-aluminum alloy containing an excess of oxygen. Silicon is removed by electron-beam melting the alloy under oxidizing conditions to promote the formation of SiO which is volatile at elevated temperatures. Excess oxygen is removed by heating the alloy in the presence of calcium metal to form calcium oxide. DOE

N85-34243# Institute of Oceanographic Sciences, Wormley (England).
A MANUAL OF METHODS FOR THE CONTINUOUS FLOW DETERMINATION OF AMMONIA, NITRATE-NITRITE, PHOSPHATE AND SILICATE IN SEAWATER
D. J. Hydes 1984 33 p
(IOS-177) Avail: NTIS HC A03/MF A01

Information required to take to and run at sea the Chemlab continuous flow analysis system is provided. Background information on the system is given, along with the details of the chemistries involved, and a full listing of the chemicals and subsidiary equipment needed at sea. Author (ESA)

26 METALLIC MATERIALS

Includes physical, chemical, and mechanical properties of metals, e.g., corrosion; and metallurgy.

N85-34244 Electricity Council, London (England).
THE DEVELOPMENT OF TITANIUM PRODUCTION IN THE USSR
A. N. Petrunko 28 Jun. 1985 12 p refs Transl. into ENGLISH from Otechestvennaya Met. (USSR), 1983 p 252-259
(BLL-OA-Trans-3226-(6196.3)) Avail: British Library Lending Div., Boston Spa, Engl.

The titanium industry since the early 1950's is reviewed. Methods of improving the quality of sponge titanium are explored. Aspects mentioned include the design of ore-smelting furnaces for the treatment of titanium slag; improvements to the technology and equipment of the slag chlorination and titanium tetrachloride cleaning processes; new principles of electrolytic refining; powder metallurgy methods, and low-temperature plasma chemical reaction processes. B.W.

N85-34245 British Library Lending Div., Boston Spa (England).
ULTRA-TRACE ANALYSIS OF SINTER TANTALUM WITH SIMS
M. Grasserbauer, H. M. Ortner, P. Wilhartitz, M. Pimminger, and R. Leuprecht 19 Jul. 1985 25 p Transl. into ENGLISH from Z. Anal. Chem. (Berlin), v. 317, 1984 p 539-546
(BLL-RARDE-Tr-1220-(7291.7965)) Avail: British Library Lending Div., Boston Spa, Engl.

The technical significance and the analytical possibilities of characterizing trace elements which have a large influence on the properties of sinter-tantalum with SIMS are reported. It is shown that SIMS can successfully be used for the quantitative ultra-trace determination of the grain stabilizing element Y and for the semiquantitative multielement characterization of other impurities. The analytical results enable the study of the change of trace elements during sintering and of the influence of the Y-concentration on the microstructure of tantalum after annealing. G.L.C.

N85-34246 British Library Lending Div., Boston Spa (England).
THE STUDY OF THE EFFECT OF RESIDUAL MICROIMPURITIES ON THE FATIGUE STRENGTH OF 55S2 STEEL
V. I. Machkin, A. V. Kharchenko, and S. A. Onishchenko 19 Jul. 1985 3 p ref Transl. into ENGLISH from Izv. Vysshikh Uchebn. Zavedenii, Chernaya Met. (Moscow), no. 12, 1984 p 133
(BLL-M-36317-(5828.4)) Avail: British Library Lending Div., Boston Spa, Engl.

The harmful effects of the presence of micro-impurities on the properties of 55S2 steel are discussed, and the use of microalloying is suggested as a way of overcoming these effects. Author

N85-34247 British Library Lending Div., Boston Spa (England).
ENTHALPIES OF FORMATION OF LIQUID Fe-Ce-Si AND Fe-Ce-Al THREE-COMPONENT ALLOYS
Yu. O. Esin, E. D. Pletneva, A. P. Ermakov, and M. G. Valyshev 14 Aug. 1984 9 p refs Transl. into ENGLISH from Izv. Vysshikh Uchebn. Zavedenii, Chernaya Met. (Moscow), no. 12, 1984 p 1-4
(BLL-M-36296-(5828.4)) Avail: British Library Lending Div., Boston Spa, Engl.

The thermodynamic properties of ternary alloys of iron containing cerium as an alloying element have been investigated. The enthalpies of formation of the alloys can be found by various methods. The Gromakov method provides results which agree best with those of experiments. Author

N85-34248 British Library Lending Div., Boston Spa (England).
TOWARDS THE DEVELOPMENT OF TECHNOLOGICAL PROCESSES FOR THE PREPARATION OF CADMIUM PLATED STEEL ARTICLES
V. L. Kolmogorov, C. N. Curyanov, and A. A. Bogatov [1985] 3 p ref Transl. into ENGLISH from Izv. Vysshikh Uchebn. Zavedenii, Chernaya Met. (Moscow), no. 12, 1984 p 131
(BLL-M-36315-(5828.4)) Avail: British Library Lending Div., Boston Spa, Engl.

A study was made of the properties of cadmium plated wire and a noncoated control to determine the effect of temperature and speed of deformation on their plasticity with a view to perfecting techniques of cadmium coating for wire and similar products. Author

N85-34249 British Library Lending Div., Boston Spa (England).
CALCULATING THE INTERATOMIC PAIR POTENTIAL ALLOWING FOR RESONANCE INTERACTION IN TITANIUM, NICKEL AND VANADIUM
S. E. Balakir, Yu. S. Stark, and E. G. Guiskaya 24 Sep. 1984 5 p refs Transl. into ENGLISH from Izv. Vysshikh Uchebn. Zavedenii, Chernaya Met. (Moscow), no. 1, 1984 p 169-170
(BLL-M-35843-(5828.4)) Avail: British Library Lending Div., Boston Spa, Engl.

Effective paired energies of resonance interaction have been calculated, using an equation which has been deduced, for titanium nickel and vanadium. The energies are comparable with the interatomic paired potentials established for Phonon spectra. Author

N85-34250 British Library Lending Div., Boston Spa (England).
EFFECTS OF HOT DEFORMATION ON THE KINETICS OF THE

PEARLITE TRANSFORMATION IN EUTECTOID STEEL
O. V. Samedov and L. P. Sorkin 24 Sep. 1984 5 p refs Transl. into ENGLISH from Izv. Vysshikh Uchebn. Zavedenii, Chernaya Met. (Moscow), no. 1, 1984 p 170-171
(BLL-M-35844-(5828.4)) Avail: British Library Lending Div., Boston Spa, Engl.

The transformation of austenite pearlite during different hot reduction operations has been investigated. It has been found that the rate of initial formation of pearlite is very high and varies greatly, increasing with the degree of deformation. The decomposition of hot deformed austenite is very rapid in the pearlite region. The reason for the increased rate of initiation of pearlite lies in change in the intragranular structure of austenite. Author

N85-34251 British Library Lending Div., Boston Spa (England).
APPROXIMATE DETERMINATION OF THE EXTENT OF THE SOLID-LIQUID ZONE
E. M. Kitaev 24 Sep. 1984 11 p refs Transl. into ENGLISH from Izv. Vysshikh Uchebn. Zavedenii, Chernaya Met. (Moscow), no. 1, 1984 p 119-123
(BLL-M-35829-(5828.4)) Avail: British Library Lending Div., Boston Spa, Engl.

The solid-liquid zone in solidifying alloys is considered, and an approximate procedure is given for determining its extent. It is concluded that for the real conditions of steel-ingot solidification an impurity that precipitates ahead of the solidification front with a superheated melt is removed into the liquid phase. As the superheat is eliminated effective diffusion of the impurity decreases and it accumulates ahead of the solidification front. The impurity lowers the liquidus temperature and the alloy therefore acts as if it were superheated and development of the solid-liquid zone is retarded. Where the impurity concentration at the front is less the speed of the liquidus boundary is greater and the impurity is displaced in a direction perpendicular to growth. It forms local aggregates and promotes off-center chemical heterogeneity.
Author

N85-34252 British Library Lending Div., Boston Spa (England).
DYNAMICS OF THE MELTING OF CHROMIUM-MANGANESE ALLOYS IN MOLTEN STEEL
O. S. Bobkova, V. A. Krivandin, N. V. Panteleeva, and Yu. P. Filimonov 24 Sep. 1984 7 p refs Transl. into ENGLISH from Stal (Moscow), no. 2, 1984 p 27-28
(BLL-M-35850-(5828.4)) Avail: British Library Lending Div., Boston Spa, Engl.

Experiments were carried out to determine the relationships to the enthalpy and heat capacity of chromium-manganese alloys at 1600 to 2000 C to temperature, also their heat capacities and coefficients of thermal diffusivity and conductivity in the solid state. The manner in which small pieces of the alloy melt in molten steel was determined. The best ratio of amounts of alloy to feed into the furnace and the ladle can be found, and the greater the mount fed into the furnace the wider the range of chromium-manganese steels which can economically be melted in arc furnaces. Author

N85-34253 British Library Lending Div., Boston Spa (England).
CALCULATION OF ACTIVITIES OF COMPONENTS IN LIQUID ALLOYS OF IRON WITH YTTRIUM
M. S. Petrushevskii 24 Sep. 1984 7 p refs Transl. into ENGLISH from Izv. Vysshikh Uchebn. Zavedenii, Chernaya Met. (Moscow), no. 2, 1984 p 3-5
(BLL-M-35868-(5828.4)) Avail: British Library Lending Div., Boston Spa, Engl.

In recent years, yttrium and other rare earth metals have been used increasingly as different additions to steels and alloys. Here their effectiveness is ensured by their physiochemical and in particular their thermodynamic properties. The theory of regular solutions, quasichemical theory, and a method based on allowing for the concentration dependences of the energies of atomic interaction are used to investigate the activities of the components in Fe-Y melts at 1870 K. B.W.

N85-34254 British Library Lending Div., Boston Spa (England).
PHASE TRANSFORMATIONS TAKING PLACE IN AUSTENITIC STEEL DURING DEFORMATION AT DIFFERENT RATES
E. T. Shinkarenko and V. G. Khoroshailov 24 Sep. 1984 6 p refs Transl. into ENGLISH from Izv. Vysshikh Uchebn. Zavedenii, Chernaya Met. (Moscow), no. 2, 1984 p 65-66
(BLL-M-35875-(5828.4)) Avail: British Library Lending Div., Boston Spa, Engl.

The article describes experiments carried out to find the phase transformation which take place with different deformation rates and at different temperatures. Conclusions are drawn as to the transformations in austenitic steel. Author

N85-34255 British Library Lending Div., Boston Spa (England).
THE EFFECT OF PRE-HEATING ON THE STRUCTURE AND PROPERTIES OF CHROMIUM-MOLYBDENUM STEELS
V. Yu. Slyusarev, I. V. Leirikh, and A. I. Cherkaskin 24 Sep. 1984 4 p Transl. into ENGLISH from Izv. Vysshikh Uchebn. Zavedenii, Chernaya Met. (Moscow), no. 2, 1984 p 158
(BLL-M-35897-(5828.4)) Avail: British Library Lending Div., Boston Spa, Engl.

The effects of preparatory thermocyclic treatment of steel were investigated. Conditions under which this can have a beneficial effect on the microstructure and mechanical properties of the steel are noted. Author

N85-34256 British Library Lending Div., Boston Spa (England).
ACOUSTIC EMISSION DURING TRANSFORMATION OF AUSTENITE IN 38KhN3MF STEEL
S. A. Gladyshev and V. A. Plotnikov 24 Sep. 1984 6 p refs Transl. into ENGLISH from Izv. Vysshikh Uchebn. Zavedenii (Moscow), no. 1, 1984 p 92-94
(BLL-M-35825-(5828.4)) Avail: British Library Lending Div., Boston Spa, Engl.

Acoustic emission levels were analyzed during transformation of supercooled austenite in medium alloy 38KhN3MF steel. The acoustic emission curve showed three distinct sections of emission level, type of acoustic emission levels and observed temperature intervals definite the stages in transformation of austenite to upper bainite, lower bainite and martensite. Author

N85-34257 British Library Lending Div., Boston Spa (England).
INFLUENCE OF TECHNOLOGY OF ATOMIZATION OF NATURALLY ALLOYED IRON ON GRAIN-SIZE CHARACTERISTICS OF POWDER MATERIAL
N. A. Raspopov, V. B. Akimenko, G. L. Khazan, V. Ya. Bulanov, and E. S. Michkova 24 Sep. 1985 7 p refs Transl. into ENGLISH from Stal (Moscow), no. 1, 1984 p 77-78
(BLL-M-35810-(5828.4)) Avail: British Library Lending Div., Boston Spa, Engl.

The influence of the initial parameters of air atomization of naturally alloyed iron on the grain-size parameters of the obtained metal particles was determined in tests conducted with variation in the temperature of the melt, the pressure of the air blast, the diameter of the jet of melt, and the angle of collision of the gas streams. The obtained mathematical relationships enable optimum atomization conditions to be established. Author

N85-34258 British Library Lending Div., Boston Spa (England).
SPECIAL FEATURES OF THE FRACTURE OF BALL-BEARING STEEL CLOSE TO NON-METALLIC INCLUSION EUTECTICS
S. I. Gubenko, V. Ya. Grabovskii, Yu. V. Yatsenko, and A. M. Galkin 24 Sep. 1984 8 p refs Transl. into ENGLISH from Stal (Moscow), no. 1, 1984 p 75-76
(BLL-M-35809-(5828.4)) Avail: British Library Lending Div., Boston Spa, Engl.

The different types of chromium sulfide eutectic inclusions found in commercial ShKh15 ball-bearing steel are described. The behavior of these inclusions in the steel is discussed in some detail, leading to the manner in high microscopic breakdown occurs in the metal. The chromium sulfide and oxysulfide eutectic inclusions are found to lead to breakdown of the steel under low deformations, i.e., to red shortness developing. Author

N85-34259 British Library Lending Div., Boston Spa (England).
PROPERTIES OF TUNGSTEN-FREE STEEL FOR CUTTING TOOLS
K. A. Lanskaya 24 Sep. 1984 8 p refs Transl. into ENGLISH from Stal (Moscow), no. 1, 1984 p 73-75
(BLL-M-35808-(5828.4)) Avail: British Library Lending Div., Boston Spa, Engl.

The influence of various heat treatments on the properties of a new, tungsten-free steel 95Kh6M3F3T for cutting tools is discussed. After optimized heat treatment (oil quenching from 1220 to 1240 C and triple tempering at 550 to 560 C for 1 hour), the steel shows a good combination of hardness (64 to 65 HRC), red hardness (58 HRC at 620 C), bend strength (3100 to 3500 MPa) and impact strength (0.5 MJ/square meter on an unnotched specimen). Author

N85-34260 British Library Lending Div., Boston Spa (England).
CHROMIUM-BASE POWDER ALLOYS FOR WELDING CLADDING LAYER OF BIMETAL
V. N. Dikun, L. V. Duben, Zh. I. Dzneladze, V. N. Plechev, and R. P. Shchegoleva 14 Aug. 1984 8 p refs Transl. into ENGLISH from Stal (Moscow), no. 12, 1983 p 68-70
(BLL-M-35776-(5828.4)) Avail: British Library Lending Div., Boston Spa, Engl.

An investigation was made of technology for automatic submerged-arc welding of bimetal, during which the weld of the cladding layer (steel 10Kh17N13M3T) is formed in one pass, with high-alloy powders of high homogeneity and low impurities content introduced into the weldpool. The required composition of the cladding layer weld is obtained by means of separate feeding of the powder and electrode chromium-nickel-molybdenum wire of steel Sv-04Kh19N113. Results of study the microstructure of the cladding layer weld metal are discussed. Chemical inhomogeneity of the metal of welds was investigated by spectral analysis. The given technology makes it possible to produce weld joints with high corrosion resistance and the required mechanical properties. Author

N85-34261 British Library Lending Div., Boston Spa (England).
CHANGES IN LATTICE CELL PARAMETER OF FILM INTERMETALLIC COMPOUNDS RT2
L. M. Lyubushkina, V. A. Domyshev, V. B. Apkhanov, O. D. Glebova, V. A. Egorov, and N. A. Manakov 24 Sep. 1984 9 p refs Transl. into ENGLISH from Izv. Vysshikh Uchebn. Zavedenii, Chernaya Met. (Moscow), no. 2, 1984 p 54-57
(BLL-M-35874-(5828.4)) Avail: British Library Lending Div., Boston Spa, Engl.

An investigation was made of the influence of the substrate temperature during condensation of films, the temperature and time of annealing, the material of the film and substrate, and phase composition on the change in the lattice constants of film rare-earth intermetallic compounds compared with bulky specimens. The established change in the lattice cell parameter in the direction of the normal to the plane of the film is governed by structural and thermal mechanisms. Author

N85-34262 British Library Lending Div., Boston Spa (England).
THE INFLUENCE OF TEMPERATURE ON THE COMPOSITION DENSITY OF THE TRANSITION METALS
O. A. Evdokimenko, O. T. Malyuchkov, and L. I. Yastrebov 24 Sep. 1984 4 p refs Transl. into ENGLISH from Izv. Vyssh. Ucheb. Chern. Met. (USSR), no. 2, 1984 p 157
(BLL-M-35896-(5826.4)) Avail: British Library Lending Div., Boston Spa, Engl.

A model was constructed to explain the effects of temperature change on the molecular density composition of the transition metals which can be used in the analysis of data arrived at by X-ray or photoemission spectroscopy. E.A.K.

N85-34263 British Library Lending Div., Boston Spa (England).
THE PROPERTIES OF VSt3sp INOCULATED STEEL
V. I. Alimov, V. L. Zhuk, and G. P. Istratova 24 Sep. 1984 4 p Transl. into ENGLISH from Izv. Vysshikh Uchebn. Zavedenii, Chernaya Met. (Moscow), no. 2, 1984 p 155
(BLL-M-35894-(5828.4)) Avail: British Library Lending Div., Boston Spa, Engl.

A study was made of the effect of different modifiers on steel. Titanium and aluminum modification is shown to be the most cost effective type. The model produced can be used for the analysis of modifications to all types of high grade steel. Author

N85-34264*# Analytical Services and Materials, Inc., Tabb, Va.
AN X-RAY DIFFRACTION STUDY OF TITANIUM OXIDATION
K. E. Wiedemann and J. Unnam Warrendale, Pa. Metallurgical Society of AIME 1984 13 p refs
(NASA-CR-176263; NAS 1.26:176263; TMS-Paper-F84-14) Avail: NTIS HC A02/MF A01 CSCL 11F

Titanium specimens of commercial purity were exposed at 1100 to 1400 F to laboratory air for times up to 100 hours. The extent of substrate contamination by interstitial oxygen was was determined by a new X-ray diffraction analysis involving transformation of X-ray diffraction intensity bands. The oxygen solid-solubility at the oxide-metal interfaces and its variation with time at temperature were also determined. Diffusion coefficients are deduced from the oxygen depth profiles. Author

N85-34265*# National Aeronautics and Space Administration. Lewis Research Center, Cleveland, Ohio.
ALUMINUM WORK FUNCTION: EFFECT OF OXIDATION, MECHANICAL SCRAPING AND ION BOMBARDMENT
Pascal Vinet, Thierry Lemogne (Ecole Centrale de Lyon), and Henri Montes (Ecole Centrale de Lyon) 1985 17 p refs Presented at Eurotrib 85, 4th Intern. Tribology Symp., Lyon, 9-12 Sep. 1985; sponsored by La Societe Francaise de Tribologie and the International Tribology Council
(NASA-TM-87079; E-2657; NAS 1.15:87079) Avail: NTIS HC A02/MF A01 CSCL 11F

Surface studies have been performed on aluminum polycrystalline surfaces which have been mechanically scraped. Such studies were initiated in order to understand surface effects occurring in tribological processes which involve rubbing surfaces and the effects of adsorption of oxygen. To characterize the surfaces, the following three different experimental approaches have been used: (1) X.P.S. (X-ray photoelectron spectroscopy), in order to check the cleanliness of the surfaces and follow the adsorption and oxidation kinetics; (2) Analysis of the work function changes by following the energy spectra of secondary electrons emitted under low energy electron bombardment; and (3) Analysis of photoemission intensities under U.V. excitation. The reference state being chosen to be the surface cleaned by ion bombardment and exposures to oxygen atmospheres have been shown to lower the work function of clean polycrystalline aluminum by 1.2 eV. The oxygen pressure is found to affect only the kinetics of these experiments. Mechanical scraping has been shown to induce a decrease (> 0.3 eV) in the work function, which could sharply modify the kinetics of adsorption on the surface. Author

N85-34266*# National Aeronautics and Space Administration. Lewis Research Center, Cleveland, Ohio.
MICROSTRUCTURES IN RAPIDLY SOLIDIFIED Ni-Mo ALLOYS
N. Jayaraman (Cincinnati Univ.), S. N. Tewari, K. J. Hemker, and T. K. Glasgow 1985 8 p refs Presented at the Intern. Conf. on Rapidly Solidified Mater., San Diego, Calif., 3-5 Feb. 1985; sponsored by the American Society for Metals
(NASA-TM-87100; E-2694; NAS 1.15:87100) Avail: NTIS HC A02/MF A01 CSCL 11F

Ni-Mo alloys of compositions ranging from pure Ni to Ni-40 at % Mo were rapidly solidified by Chill Block Melt Spinning in vacuum and were examined by optical metallography, X-ray diffraction and transmission electron microscopy. Rapid solidification resulted in an extension of molybdenum solubility in nickel from 28 to 37.5 at %. A number of different phases and microstructures were seen at different depths (solidification conditions) from the quenched surface of the melt spun ribbons. Author

N85-34267# Department of Energy, Washington, D. C.
MANUFACTURING PROCESS TO REDUCE LARGE GRAIN GROWTH IN ZIRCONIUM ALLOYS Patent Application
P. M. Rosecrans, inventor (to NASA) (GE, Schenectady, N.Y.) Filed 1 Aug. 1984 11 p
(Contract DE-AC12-76SN-00052)
(DE85-011649; US-Patent-Appl-SN-636659) Avail: NTIS HC A02/MF A01

A procedure for desensitizing zirconium based alloys to large grain growth (LGG) during thermal treatment above the recrystallization temperature of the alloy is presented. A method for treating zirconium based alloys which have been cold worked in the range of 2 to 8% strain to reduce large grain growth is devised. A method for fabricating a zirconium alloy clad nuclear fuel element wherein the zirconium clad is resistant to large grain growth is given. DOE

N85-34268# Tennessee Univ., Knoxville.
SHAPE MEMORY EFFECT IN URANIUM-NIOBIUM ALLOYS BELOW ROOM TEMPERATURE Final Report
R. A. Vandermeer Mar. 1985 26 p
(Contract W-7405-eng-48)
(DE85-012964; UCRL-15666) Avail: NTIS HC A03/MF A01

The temperature dependence of the martensitic (GAMMA)(0) to (ALPHA)(11) phase transformation between 25(0)C and -198(0)C in water quenched uranium niobium alloys between 6.2 and 7.0 wt % niobium was determined using cold stage X-ray diffraction experiments. Lowering the temperature promoted the transformation to (ALPHA)(11) but complete transformation was never observed. The transformation was reversible with little or no hysteresis. Aging the alloys for two hours at 200(0)C stabilized the (GAMMA)(0) phase and retarded the martensitic transformation. The compositions where M sub s and M sub t equaled room temperature were 5.80 and 7.04 wt % Mb respectively. At -196(0)C these values were approximately 0.25 wt % higher. Two alloys were selected as potential candidates for a uranium alloy clamp. DOE

N85-34269# Indiana Univ., Bloomington. Dept. of Chemistry.
METAL ALKOXIDES: MODELS FOR METAL OXIDES. ALKOXIDE LIGANDS IN EARLY TRANSITION METAL ORGANOMETALLIC CHEMISTRY
M. H. Chisholm 1985 14 p
(Contract DE-AC02-80ER-10639)
(DE85-011368; DOE/ER-10639/T2) Avail: NTIS HC A02/MF A01

Structural analogies between polynuclear metal alkoxides and metal oxides are noted, with the former providing models for subunits within the extended networks of the latter. An extensive organometallic chemistry supported by alkoxy ligands is emerging. Their facile interconversion between terminal and bridging positions and between sigma(2) and (sigma(2) + (PI)(2) donors allows for easy uptake and release of substrate molecules. Key reports during the 1984 to 1985 period are: (1) the cleavage of C identical with O to carbido and oxo tungsten alkoxide clusters; (2) the coupling, co-coupling, and sometimes metathesis like reactions (M = W) between C identical with C, C identical with N and M identical with M bonds in M2(OR)6 compounds; (3) unusual (BETA)-hydrogen effects in dinuclear alkyl alkoxides or molybdenum; and (4) the isolation of Mo-Mo quadruply bonded compounds supported by alkoxide ligands. Recent developments have led to general synthesis of hydridoditungsten alkoxide anions W2((MU)-H)(ORB(-) which have been isolated as sodium salts. New nitrido and amido clusters have been discovered, Mo4((MU)3-N)2(OPr/sup i/)12 and W3((MU)3-NH)OPr/sup i/)10 which may provide models for the Haber synthesis of NH3 from N2 and H2. DOE

N85-34270# Rockwell International Corp., Richland, Wash.
REVIEW OF ZIRCONIUM-ZIRCALOY PYROPHORICITY
T. D. Cooper Nov. 1984 28 p refs
(Contract DE-AC06-77RL-01030)
(DE85-011169; RHO-RE-ST-31P) Avail: NTIS HC A03/MF A01

Massive zirconium metal scrap can be handled, shipped, and stored with no evidence of combustion or pyrophoricity hazards. Mechanically produced fine scrap such as shavings, turnings, or powders can burn but are not pyrophoric unless the particle diameter is less than 54 (MU)m. Powders with particle diameters less than 54 (MU)m can be both pyrophoric and explosive. Pyrophoric powders should be collected and stored underwater or under inert gas cover to reduce the flammability hazard. Opening sealed containers of zirconium stored underwater should be attempted with caution since hydrogen may be present. The factors that influence the ignition temperature have been explored in depth and recommendations are included for the safe handling, shipping, and storage of pyrophoric or flammable zirconium. DOE

N85-34271# Los Alamos Scientific Lab., N. Mex.
IRON AND MANGANESE IN OXIDE MINERALS AND IN GLASSES: PRELIMINARY CONSIDERATION OF Eh BUFFERING POTENTIAL AT YUCCA MOUNTAIN, NEVADA
F. A. Caporuscio and D. T. Vaniman Apr. 1985 31 p refs
(Contract W-7405-eng-36)
(DE85-011892; LA-10369-MS) Avail: NTIS HC A03/MF A01

The tuffs of Yucca Mountain at the Nevada Test Site are currently under investigation as a possible deep burial site for high level radioactive waste disposal. One of the main concerns is the effect of oxidizing groundwater on the transport of radionuclides. Rock components that may affect the oxygen content of groundwater include Fe-Ti oxides, Mn oxides, and glasses that contain ferrous iron. Some phenocryst Fe-Ti oxides at Yucca Mountain are in reduced states, whereas groundmass Fe-Ti oxides have been oxidized to hematite, rutile, and pseudobrookite (Fe(3+)-bearing phases) exclusively. Estimates of Fe(2+)-bearing oxides indicate that less than 0.33 vol% phenocrysts is available to act as solid buffering agents of Eh. Of this percentage, significant amounts of Fe-Ti oxides are isolated from effective interaction with groundwater because they occur in densely welded, devitrified tuffs that have low interstitial permeability. Manganese oxides occur primarily along fractures in the ash flow tuffs. Because the Mn oxides are concentrated along the same pathways (fractures) where transport has occurred in the past, there small volume percentages could act as buffers. DOE

N85-34272# Oak Ridge Y-12 Plant, Tenn.
EXPERIMENTAL ATTEMPT TO ACHIEVE MICROSTRUCTURE VARIATIONS THROUGH TEMPERATURE/TIME PERMUTATIONS FOR A NONWROUGHT POWDER METALLURGY URANIUM-6 NIOBIUM ALLOY
G. M. Alexander-Morrison 7 Jun. 1985 25 p refs
(Contract DE-AC05-84OS-21400)
(DE85-013166; Y/DV-427) Avail: NTIS HC A02/MF A01

The powder metallurgical processing of uranium-6 niobium (U-6Nb) alloy has undergone 3 years of characterization at the Oak Ridge Y-12 Plant. The current structure of the powder metallurgy (P/M) alloy has been described as duplex: a mixture of two or more distinct grain sizes. An experiment was conducted to determine a gamma stabilizing heat treatment (time and temperature combination) to produce a structure consisting of one gamma grain size. Two heat treatments were found to produce an irregular ASTM 4 grain size. Additional P/M U6Nb alloy material was hot pressed and characterized using the two new heat treatments; however, the resulting microstructures were size ASTM 8. Mechanical properties of the fine grained P/M material were characterized. Continued evaluation of these results did not determine the cause of the grain refinement. DOE

N85-34273# Virginia Polytechnic Inst. and State Univ., Blacksburg.
HYDROGEN EMBRITTLEMENT TESTING Final Report
[1985] 3 p
(Contract DE-AS05-78ER-06039)
(DE85-007352; DOE/ER-06039/T2) Avail: NTIS HC A02/MF A01

Several important hydrogen induced effects are established. These effects include the observation of hydrogen induced weakening of interfacial strength of boundaries such as twin boundaries, grain boundaries and slip bands. Impact and slow

bend testing of hydrogen charged samples illustrate that this weakening is inherent with hydrogen absorption and that dislocation transport of hydrogen is not necessary for interfacial embrittlement to occur. These observations help establish a phenomenological model for hydrogen embrittlement. DOE

N85-34274# Department of Energy, Washington, D. C.
METHOD FOR PREPARING HYDRIDE CONFIGURATIONS AND REACTIVE METAL SURFACE Patent Application
G. L. Silver, inventor (to DOE) Filed 18 May 1984 20 p
(Contract DE-AC04-76DP-00053)
(DE85-006443; US-Patent-Appl-SN-611773) Avail: NTIS HC A02/MF A01

A method for preparing reactive metal surfaces, particularly uranium surfaces is disclosed, whereby the metal is immediately reactive to hydrogen gas at room temperature and low pressure. The metal surfaces are first pretreated by exposure to an acid which forms an adherent hydride-bearing composition on the metal surface. Subsequent heating of the pretreated metal at a temperature sufficient to decompose the hydride coating in vacuum or inert gas renders the metal surface instantaneously reactive to hydrogen gas at room temperature and low pressure. DOE

N85-34275# Department of Energy, Washington, D. C.
NITRIDING OF SUPER ALLOYS FOR ENHANCING PHYSICAL PROPERTIES Patent Application
A. Purohit, inventor (to DOE) Filed 25 Jun. 1984 16 p
(Contract W-31-109-eng-38)
(DE85-005762; US-Patent-Appl-SN-624085) Avail: NTIS HC A02/MF A01

The invention teaches the improvement of certain super alloys by exposing the alloy to an atmosphere of elemental nitrogen at elevated temperatures in excess of 750(0)C but less than 1150(0)C for an extended duration, viz., by nitriding the surface of the alloy, to establish barrier nitrides of the order of 25 to 100 micrometers thickness. These barrier nitrides appear to shield the available oxidizing metallic species of the alloy for up to a sixfold improved resistance against oxidation and also appear to impede egress of surface dislocations for increase fatigue and creep strengths. DOE

N85-34276# Cincinnati Univ., Ohio. Dept. of Materials Science and Metallurgical Engineering.
INFLUENCE OF PARTICLE EROSION ON THE MICROSTRUCTURAL CHANGES IN METALS AND ALLOYS
John Moteff and Eduardo Rosa 1985 8 p refs Presented at the Gas Turbine Conf. and Exhibit, Houston, Tex., 18-21 Mar. 1985
(TI85-901384; M85901384; CONF-850351-6; Rept-85-GT-201) Avail: NTIS HC A02/MF A01

The microstructural changes that occur in metals and alloys exposed to pneumatic particle erosion conditions are determined through microhardness measurements performed on the cross-section of the target material. In particular, the hardness gradient in an inward direction normal to the eroded surface is determined for pure Cu, AISI 304 stainless steel, and for AISI 1020 steel having various degrees of cold-work. The elevated temperature erosion behavior of Ti-6Al-4V as a function of the elevated temperature surface microhardness and ductility clearly shows significant differences when evaluated above and below about one-half of the absolute melting temperature of this alloy. DOE

N85-34277# Argonne National Lab., Ill. Materials Science and Technology Div.
STRESS CORROSION CRACKING SUSCEPTIBILITY OF TYPES 316NG AND 316 STAINLESS STEEL IN AN IMPURITY ENVIRONMENT
P. S. Maiya and W. J. Shack Oct. 1984 13 p refs Presented at Corrosion 85, Boston, 25-29 Mar. 1985 Sponsored in part by Nuclear Regulatory Commission
(TI85-006884; CONF-850311-8) Avail: NTIS HC A02/MF A01

The relative stress corrosion cracking (SCC) susceptibility of heat treated Types 316NG and 316 stainless steel (SS) has been investigated by means of constant extension rate (CERT) tests over a range of strain rates from 10 to the minus 5th power to 10 to the minus 7th power S(-1) in simulated boiling water reactor environments that contain SO2-over 4 as an impurity. It is observed that, although Type 316NG SS is extremely resistant to intergranular SCC (IGSCC) even when subjected to severe heat treatments, it can become susceptible to transgranular SCC (TGSCC) in the presence of impurities. Sensitized Type 316 SS, however, is susceptible to IGSCC even in high-purity water containing 0.2 ppm O sub 2 and the addition of an impurity aggravates the IGSCC susceptibility. The SCC results obtained for both materials are discussed in terms of a phenomenological model that incorporates a slip-dissolution mechanism and elastic-plastic fracture mechanics. DOE

N85-34278# Rolls-Royce Ltd., Derby (England).
THE DEVELOPMENT AND EVALUATION OF THE CREEP AND CORROSION RESISTANT ALLOY IN6201
P. R. Hooper, R. L. Freelove, S. Shaw (INCO Alloy Products Ltd.), and A. Taylor (Admiralty Marine Technology Establishment) 15 Nov. 1984 46 p refs Presented at Workshop on Gas Turbines in a Marine Environ., Bath, England, 15-16 Nov. 1984
(PNR-90253) Avail: NTIS HC A03/MF A01

The beneficial effect on stress rupture strength of critical large boron additions to high chromium, nickel based superalloys, was exploited to develop an alloy for marine gas turbines (IN6201). The development of the alloy chemistry and physical properties, in terms of mechanical and corrosion/oxidation performance and its ensuing foundry capabilities related to structure and properties utilizing an experimental vehicle under conventional casting techniques is described. Corrosion/oxidation characteristics compare favorably with competitor alloys. Stress rupture properties can be superior if the alloy is cast to optimum parameters. Encouraging experimental data obtained from producing examples of directionally solidified components are mentioned. Author (ESA)

N85-34279# Rolls-Royce Ltd., Derby (England).
DIRECTIONALLY SOLIDIFIED GAS TURBINE ALLOYS
P. R. Beeley (Leeds Univ.) and D. Driver 1 Feb. 1985 51 p refs
(PNR-90264) Avail: NTIS HC A04/MF A01

Progress in directional solidification of superalloys, and applications to aircraft engine turbine blades are reviewed. Superalloy metallurgy and blade design; casting techniques for directional solidification; alloy development for conventional casting; and single crystal alloys are discussed. Author (ESA)

N85-34181# National Defence Academy, Tokyo (Japan).
ELECTRICAL RESISTIVITY AND HYSTERESIS OF THE EQUIATOMIC NICKEL-TITANIUM ALLOY NEAR THE MARTENSITIC TRANSFORMATION TEMPERATURE
Hitoshu Matsumoto and Shoso Dohi *In* Society of Materials Science Proc. of the 27th Japan Congr. on Mater. Res. Mar. 1984 p 1-5 refs Previously announced in IAA as A85-23463 (For primary document see N85-34180 23-23)
Avail: NTIS HC A14/MF A01

N85-34188# Ship Research Inst., Tokyo (Japan).
MECHANICAL PROPERTIES OF PLASMA ARC CUT STEEL
Shinya Hayashi and Tokuji Nagamatsu *In* Society of Materials Science Proc. of the 27th Japan Congr. on Mater. Res. Mar. 1984 p 47-51 refs (For primary document see N85-34180 23-23)
Avail: NTIS HC A14/MF A01

N85-34190# Kyoto Univ. (Japan). Dept. of Mechanical Engineering.
THE INFLUENCE OF TEMPERATURE ON STATIC AND DYNAMIC SCC CRACK GROWTH BEHAVIOR IN ALUMINUM ALLOY
Kenjiro Komai, Kohji Minoshima, and Hiroshi Yukimachi *In* Society of Materials Science Proc. of the 27th Japan Congr. on Mater. Res. Mar. 1984 p 57-62 refs Previously announced in IAA as A85-23465 (For primary document see N85-34180 23-23)
Avail: NTIS HC A14/MF A01

N85-34191# Kyoto Univ. (Japan). Dept. of Mechanical Engineering.
A FRACTOGRAPHIC STUDY ON MODE 2 AND MODE 3 SCC CRACK GROWTH IN AN Al-Zn-Mg ALLOY
Kenjiro Komai and Eiji Usuki (Sumitomo Metals, Ltd.) *In* Society of Materials Science Proc. of the 27th Japan Congr. on Mater. Res. Mar. 1984 p 63-69 refs Previously announced in IAA as A85-23466 (For primary document see N85-34180 23-23)
Avail: NTIS HC A14/MF A01

N85-34192# Toyama Univ. (Japan). Dept. of Mechanical Engineering.
CORROSION FATIGUE STRENGTH AND CRACK GROWTH IN PRESTRAINED 0.16% C CARBON STEEL
Sotomi ishihara, Ichiro Maekawa (Tohoku Univ.), Kazuaki Shiozawa, and Kazyu Miyao *In* Society of Materials Science Proc. of the 27th Japan Congr. on Mater. Res. Mar. 1984 p 71-77 refs (For primary document see N85-34180 23-23)
Avail: NTIS HC A14/MF A01

N85-34194# Suzuka Coll. of Technology (Japan).
FRACTOGRAPHIC ANALYSIS FOR NONPROPAGATING CONDITIONS OF FATIGUE CRACK AT HIGH STRESS RATIOS IN MILD STEEL
Kuniji Ichida and Teiichi Ohkouchi (Nagoya Inst. of Technology) *In* Society of Materials Science Proc. of the 27th Japan Congr. on Mater. Res. Mar. 1984 p 85-91 refs (For primary document see N85-34180 23-23)
Avail: NTIS HC A14/MF A01

N85-34195# Waseda Univ., Tokyo (Japan). School of Science and Engineering.
CRYSTALLOGRAPHIC ORIENTATION DEPENDENCE OF FATIGUE CRACK PROPAGATION IN EXTREMELY LOW CARBON STEEL
Ikuhiko Hayashi, Takayuki Suzuki, Hiromi Ishii, and Makoto Oiyama *In* Society of Materials Science Proc. of the 27th Japan Congr. on Mater. Res. Mar. 1984 p 93-98 refs (For primary document see N85-34180 23-23)
Avail: NTIS HC A14/MF A01

N85-34196# Waseda Univ., Tokyo (Japan). School of Science and Engineering.
FATIGUE CRACK RETARDATION PHENOMENON CAUSED BY SINGLE-MULTIPLE OVERLOADS IN 2017-T3 ALUMINUM ALLOW
Ikuhiko Hayashi, Yuji Suzuki, Eiichi Kusama, and Yasuhiro Majima *In* Society of Materials Science Proc. of the 27th Japan Congr. on Mater. Res. Mar. 1984 p 99-104 refs Previously announced in IAA as A85-23467 (For primary document see N85-34180 23-23)
Avail: NTIS HC A14/MF A01

N85-34197# Toshiba Corp., Fuchu (Japan). Heavy Apparatus Engineering Lab.
SAFETY AND RELIABILITY OF STEEL STRUCTURAL MATERIALS UNDER RANDOM SERVICE IMPACT LOADS
Nagatoshi Okabe, Toshiyuki Yano, and Tadao Mori *In* Society of Materials Science Proc. of the 27th Japan Congr. on Mater. Res. Mar. 1984 p 105-110 refs (For primary document see N85-34180 23-23)
Avail: NTIS HC A14/MF A01

N85-34199# Tokyo Inst. of Tech. (Japan).
ANTI WEAR PROPERTY OF TWO PHASIC METAL COMPOSITE
Susumu Norose, Tadashi Sasada, and Keiichi Maruyama (Fuji Heavy Industry Ltd.) *In* Society of Materials Science Proc. of the 27th Japan Congr. on Mater. Res. Mar. 1984 p 119-124 refs (For primary document see N85-34180 23-23)
Avail: NTIS HC A14/MF A01

N85-34200# Tokyo Inst. of Tech. (Japan).
THREE BODY ABRASIVE WEAR IN VARIOUS METAL COMBINATIONS
Tadashi Sasada, Noibuhiko Emori (Komatsu Ltd.), and Mamoru Oike (National Aerospace Lab., Kakuda) *In* Society of Materials Science Proc. of the 27th Japan Congr. on Mater. Res. Mar. 1984 p 125-130 refs (For primary document see N85-34180 23-23)
Avail: NTIS HC A14/MF A01

N85-34202# Meidensha Electric Mfg. Co. Ltd., Todyo (Japan).
X-RAY RESIDUAL STRESS ANALYSIS ON THE COARSE GRAIN OF COPPER AND ITS APPLICATION TO THE BRAZED COPPER
Masaki Koga, Hidemitsi Takebuchi, and Katsuaki Senba *In* Society of Materials Science Proc. of the 27th Japan Congr. on Mater. Res. Mar. 1984 p 135-140 refs (For primary document see N85-34180 23-23)
Avail: NTIS HC A14/MF A01

N85-34203# Bunka Women's Univ. (Japan). Dept. of Domestic Science.
STUDY ON THE CORRELATION BETWEEN GRINDING CONDITIONS AND RESIDUAL STRESSES IN GROUND SURFACE OF STEEL BY THE X-RAY METHOD
Shigeo Zaima and Hideyuki Mitzutani (Chubu Inst. of Technology) *In* Society of Materials Science Proc. of the 27th Japan Congr. on Mater. Res. Mar. 1984 p 141-146 refs (For primary document see N85-34180 23-23)
Avail: NTIS HC A14/MF A01

N85-34205# Niihama Technical Coll. (Japan).
X-RAY MEASUREMENT OF THERMAL STRESSES IN TUNGSTEN FIBER-COPPER COMPOSITES
Yasukazu Keuchi and Haruo Fujiwara (Tokushima Univ.) *In* Society of Materials Sciences Proc. of the 27th Japan Congr. on Mater. Res. Mar. 1984 p 153-158 refs (For primary document see N85-34180 23-23)
Avail: NTIS HC A14/MF A01

N85-34206# Waseda Univ., Tokyo (Japan). Castings Research Lab.
EVALUATION METHODS OF CERAMIC FIBER REINFORCED METAL MATRIX COMPOSITE
Yutaka Kagawa and Eiichi Nakata *In* Society of Materials Science Proc. of the 27th Japan Congr. on Mater. Res. Mar. 1984 p 159-163 refs Previously announced in IAA as A85-23469 (For primary document see N85-34180 23-23)
Avail: NTIS HC A14/MF A01

27 NONMETALLIC MATERIALS

Includes physical, chemical, and mechanical properties of plastics, elastomers, lubricants, polymers, textiles, adhesives, and ceramic materials.

N85-34280* National Aeronautics and Space Administration. Ames Research Center, Moffett Field, Calif.
FIRE-RESISTANT PHOSPHORUS CONTAINING POLYIMIDES AND COPOLYIMIDES Patent
John A. Mikroyannidis, inventor (to NASA) (National Academy of Sciences - National Research Council, Washington, D.C.) Issued 20 Aug. 1985 12 p Filed 16 Aug. 1984 Supersedes N85-21363 (23 - 12, p 1812) Continuation-in-part of US-Patent-Appl-SN-522629, 12 Aug. 1983
(NASA-Case-ARC-11522-2; US-Patent-4,536,565; US-Patent-Appl-SN-641143; US-Patent-Class-528-352; US-Patent-Class-528-168; US-Patent-Class-528-229; US-Patent-Class-528-353) Avail: US Patent and Trademark Office CSCL 11C

Phosphorus-containing polyimides and copolyimides are synthesized in a two-step polycondensation reaction from 1-[(diorganooxyphosphonl)methly] 2,4- and 2,6-diaminobenzenes and tetracarboxylic anhydride. The diorgano position of the diorganooxyphosphonyl group includes alkyl, such as ethyl, substituted

alkyl, such as 2-chloroethyl, and aryl such as phenyl. The tetracarboxylic anhydries include compounds such as pyrometallitic dianhydride and benzophenone tetracarboxylic dianhydride. The glass transition temperature (Tg) of the polyimides is reduced by incorporation of the (dialkoxyphosphonyl)methyl groups. The phosphorus-containing copolyimides show a considerably higher degree of fire-resistance as compared to that of the corresponding common polyimides.

Official Gazette of the U.S. Patent and Trademark Office

N85-34281* National Aeronautics and Space Administration. Ames Research Center, Moffett Field, Calif.

METAL (2) 4,4',4',4'' PHTHALOCYANINE TETRAAMINES AS CURING AGENTS FOR EPOXY RESINS Patent

Bappalige N. Achar (National Academy of Sciences - National Research Council, Washington, D.C.), George M. Fohlen (National Academy of Sciences - National Research Council, Washington, D.C.), and John A. Parker, inventors (to NASA) (National Academy of Sciences - National Research Council, Washington, D.C.) Issued 27 Aug. 1985 7 p Filed 11 Apr. 1984 Supersedes N85-21361 (23 - 12, p 1811) Continuation-in-part of US-Patent-4,499,260; US-Patent-Appl-SN-440656, 10 Nov. 1982

(NASA-Case-ARC-11424-1; US-Patent-4,537,834; US-Patent-Appl-SN-598777; US-Patent-Class-428-413; US-Patent-Class-428-260; US-Patent-Class-428-408; US-Patent-Class-525-107; US-Patent-Class-525-113; US-Patent-Class-525-229; US-Patent-Class-525-119; US-Patent-Class-525-186; US-Patent-Class-528-94; US-Patent-Class-528-113; US-Patent-Class-528-117; US-Patent-Class-528-407) Avail: US Patent and Trademark Office CSCL 11G

Metal, preferably divalent copper, cobalt or nickel, phthalocyanine tetraamines are used as curing agents for epoxides. The resulting copolymers have high thermal and chemical resistance and are homogeneous. They are useful as binders for laminates, e.g., graphite cloth laminate.

Official Gazette of the U.S. Patent and Trademark Office

N85-34282* National Aeronautics and Space Administration. Langley Research Center, Hampton, Va.

PROCESS FOR IMPROVING MOISTURE RESISTANCE OF EPOXY RESINS BY ADDITION OF CHROMIUM IONS Patent

Anne K. St.Clair, Diane M. Stoakley, Terry L. St.Clair, and Jag J. Singh, inventors (to NASA) Issued 9 Apr. 1985 7 p Filed 3 Nov. 1983 Supersedes N84-20700 (22 - 11, p 1636)

(NASA-Case-LAR-13226-1; US-Patent-4,510,277; US-Patent-Appl-SN-548583; US-Patent-Class-523-454; US-Patent-Class-523-458; US-Patent-Class-528-92; US-Patent-Class-528-106; US-Patent-Class-528-229; US-Patent-Class-528-407) Avail: US Patent and Trademark Office CSCL 11G

A process for improving the moisture resistance properties of epoxidized TGMDA and DGEBA resin system by chemically incorporating chromium ions is described. The addition of chromium ions is believed to prevent the absorption of water molecules.

Official Gazette of the U.S. Patent and Trademark Office

N85-34283 British Library Lending Div., Boston Spa (England).

FEATURES OF BEHAVIOR OF GAS BUBBLES IN MOLTEN OXIDE FILMS DURING ENAMELLING: COMMUNICATION 2

V. A. Deryabin, S. I. Popel, and A. A. Perminov 14 Aug. 1984 10 p refs Transl. into ENGLISH from Izv. Vysshikh Uchebn. Zavedenii, Chernaya Met. (Moscow), no. 12, 1983 p 1-5 (BLL-M-35781-(5828.4)) Avail: British Library Lending Div., Boston Spa, Engl.

The formation of the macrostructure of the enamel layer during enamelling is investigated. The dependence of surface tension of the enamel melt on the content of iron oxides in it, which largely determines the possibility of liberation and distribution of gas bubbles in the enamel layer, is established. The influence of Archimedes' and capillary forces and the orientation and size of the gaseous inclusions on the rate of movement of bubbles is discussed. The passage of bubbles through the base coating/cover-coat enamel boundary is examined. Author

N85-34284*# National Aeronautics and Space Administration. Lewis Research Center, Cleveland, Ohio.

RELIABILITY OF TWO SINTERED SILICON NITRIDE MATERIALS

Diane M. Mieskowski, William A. Sanders, and Laurie A. Pierce Aug. 1985 15 p refs

(NASA-TM-87092; E-2325-1; NAS 1.15:87092) Avail: NTIS HC A02/MF A01 CSCL 11B

Two types of sintered silicon nitride were evaluated in terms of reliability: an experimental high pressure nitrogen sintered material and a commercial material. The results show wide variations in strength for both materials. The Weibull moduli were 5.5, 8.9, and 11 for the experimental material at room temperature, 1200, and 1370 C, respectively. The commercial material showed Weibull moduli of 9.0, 8.6, and 8.9 at these respective temperatures. No correlation between strength and flaw size was noted for the experimental material. The applicability of the Weibull and Griffith theories to processing defects on the order of 100 microns or less in size are discussed. E.A.K.

N85-34285*# National Aeronautics and Space Administration, Washington, D. C.

THE EFFECT OF LIQUID-LIQUID PHASE SEPARATION OF GLASS ON THE PROPERTIES AND CRYSTALLIZATION BEHAVIOR

Jia Zhi Li Sep. 1985 28 p refs Transl. into ENGLISH from J. of the Chinese Silicate Soc. (China), v. 6, no. 4, 1978 p 279-289 Transl. by Scientific Translation Service, Santa Barbara, Calif. Original document prepared by Coll. of Science, Silicates Research Center, Shanghai

(Contract NASw-4004)

(NASA-TM-77890; NAS 1.15:77890) Avail: NTIS HC A03/MF A01 CSCL 11B

A theoretical discussion is given of the phase separation mechanism of amorphous materials. This includes nucleus growth, spinoidal decomposition, and nuclei agglomeration and coarsening. Various types of glass are analyzed. Author

N85-34286# Department of Energy, Washington, D. C.

RIGID ZEOLITE CONTAINING POLYURETHANE FOAMS Patent Application

C. B. Frost, inventor (to DOE) Filed 18 May 1984 23 p

(Contract DE-AC04-76DP-00789)

(DE85-006406; US-Patent-Appl-SN-611772) Avail: NTIS HC A02/MF A01

A closed cell rigid polyurethane form has been prepared which contains up to about 60% by weight of molecular sieves capable of sorbing molecules with effective critical diameters of up to about 10 A. The molecular sieve component of the foam can be preloaded with catalysts or with reative compounds that can be released upon activation of the foam to control and complete crosslinking after the form is formed. The foam can also be loaded with water or other flame-retarding agents after completion. Up to about 50% of the weight of the isocyanate component of the foam can be replaced by polyimide resin precursors for incorporation into the final polymeric network. DOE

N85-34287# Department of Energy, Washington, D. C.

METHOD FOR REMOVING OXIDE CONTAMINATION FROM SILICON CARBIDE POWDERS Patent Application

J. Brynestad (ORNL) and C. E. Bamberger, inventors (to DOE) (ORNL) Filed 1 Aug. 1984 10 p

(Contract DE-AC05-84OR-21400)

(DE85-011648; US-Patent-Appl-SN-636658) Avail: NTIS HC A02/MF A01

The described invention is directed to a method for removing oxide contamination in the form of oxygen containing compounds such as SiO2 and B2O3 from a charge of finely divided silicon carbide. The silicon carbide charge is contacted with a stream of hydrogen fluoride mixed with an inert gas carrier such as argon at

a temperature in the range of about 200 to 650 C. The oxides in the charge react with the heated hydrogen fluoride to form volatile gaseous fluorides such as SiF4 and BF3 which pass through the charge along with unreacted hydrogen fluoride and the carrier gas. Any residual gaseous reaction products and hydrogen fluoride remaining in the charge are removed by contacting the charge with the stream of inert gas which also cools the powder to room temperature. The removal of the oxygen contamination by practicing the present method provides silicon carbide powders with desirable pressing and sintering characteristics. DOE

N85-34288# UOP, Inc., San Diego, Calif. Fluid Systems Div.
DEVELOPMENT AND DEMONSTRATION OF A SPIRAL-WOUND THIN-FILM COMPOSITE MEMBRANE SYSTEM FOR THE ECONOMICAL PRODUCTION OF OXYGEN-ENRICHED AIR, PHASE 4 Final Report, 1 Jan. 1983 - 31 Dec. 1984
D. G. Haesloop, R. J. Swedo, and L. J. Burnett 15 Jan. 1985 146 p Prepared in cooperation with UOP, Inc., Des Plaines, Ill.
(Contract DE-AC01-79CS-40294)
(DE85-012380; DOE/CS-40294/1) Avail: NTIS HC A07/MF A01

Literature searches identified poly (vinyl isobutyl ether) as the most promising candidate barrier material for oxygen enrichment membranes. A membrane with an oxygen/nitrogen selectivity of 6.2 and a stability at 60 C was developed. However, this membrane is fragile. Membranes using poly (2-hexyne) and poly (6-methyl-2-heptyne) were also made. DOE

N85-34289# Washington Univ., Seattle. Dept. of Materials Science and Engineering.
HIGH RESOLUTION ELECTRON MICROSCOPIC CHARACTERIZATION OF INTERFACES IN CERAMICS
M. Sarikaya, I. A. Askay, and G. Thomas (California Univ., Berkeley, Lawrence Berkeley Lab.) Aug. 1984 15 p refs Presented at the Advan. in Mater. Characterization 2 Conf., Alfred, N.Y., 29 Jul. 1984
(Contract DE-AC03-76SF-00098)
(DE85-011207; LBL-19396; CONF-8407123-1) Avail: NTIS HC A02/MF A01

High resolution electron microscopy (HREM) is useful in bringing out the microstructural variations, such as structural details at grain boundaries, at very high resolutions, even at atomic levels. An important aspect is the examination of the surface irregularities at the boundary regions which provide information on the transformation characteristics of the phases. In this paper, we present data on the microstructural characteristics of some high temperature ceramics (silicon nitride, mullite, and a luminum nitride) with particular emphasis on the detection of grain boundary amorphous phases. The HREM technique is also reevaluated with reference to other techniques. DOE

N85-34290# Department of Energy, Washington, D. C.
HIGH TEMPERATURE POLYMER CONCRETE Patent Application
J. J. Fontana and W. Reams, inventors (to DOE) Filed 29 May 1984 15 p
(Contract DE-AC02-76CH-00016)
(DE85-005756; US-Patent-Appl-SN-614508) Avail: NTIS HC A02/MF A01

A polymer concrete composition, which is a two component composition useful with many bases including metal is described. Component A, the aggregate composition, is broadly composed of silica, silica flour, portland cement, and acrylamide, whereas component B, which is primarily vinyl and acrylyl reactive monomers, is a liquid system. DOE

N85-34291# Department of Energy, Washington, D. C.
HIGH TEMPERATURE STRUCTURAL INSULATING MATERIAL Patent Application
W. Y. Chen, inventor (to DOE) Filed 27 Jul. 1984 11 p
(Contract W-31-109-eng-38)
(DE85-006361; US-Patent-Appl-SN-625324) Avail: NTIS HC A02/MF A01

A high temperature structural insulating material is described which is useful as a liner for cylinders of high temperature engines through the favorable combination of high service temperature (above about 800 C), and high compressive strength (above about 250 psi). The insulating material is produced by selecting hollow ceramic beads with a softening temperature above about 800 C, a diameter within the range of 20-200 micro m, and a wall thickness in the range of about 2 to 4 micro m; compacting the beads and a compatible silicate binder composition under pressure and sintering conditions to provide the desired structural form with the structure have a closed-cell, compact array of bonded beads. DOE

N85-34292# Department of Energy, Washington, D. C.
METHOD FOR MAKING A LOW DENSITY POLYETHYLENE WASTE FORM FOR SAFE DISPOSAL OF LOW LEVEL RADIOACTIVE MATERIAL Patent Application
P. Colombo and P. D. Kalb, inventors (to DOE) Filed 5 Jun. 1984 35 p
(Contract DE-AC02-76CH-00016)
(DE85-006401; US-Patent-Appl-SN-617660) Avail: NTIS HC A03/MF A01

A method is described of making a low density polyethylene waste form for safe disposal of low level radioactive material. The mixture is fed through a screw-type extruder that melts the low density polyethylene under a predetermined pressure and temperature. The solid waste forms are adapted to be safely handled, stored for a short time, and safty disposed of in approved depositories. DOE

N85-34293# Department of Energy, Washington, D. C.
CONDUCTOR-POLYMER COMPOSITE ELECTRODE MATERIALS Patent Application
D. S. Ginley, S. R. Kurtz, W. H. Smyrl, and J. M. Zeigler, inventors (to DOE) Filed 13 Jun. 1984 19 p
(Contract DE-AC04-76DP-00789)
(DE85-005766; US-Patent-Appl-SN-620306) Avail: NTIS HC A02/MF A01

A conductive composite material useful as an electrode, comprises a conductor and an organic polymer which is reversibly electrochemically dopable to change its electrical conductivity. Said polymer continuously surrounds the conductor in intimate electrical contact therewith and is prepared by electrochemical growth on said conductor or by reaction of its corresponding monomer(s) on said conductor which has been pre-impregnated or pre-coated with an activator for said polymerization. Amount of the conductor is sufficient to render the resultant composite electrically conductive even when the polymer is in an undoped insulating state. DOE

N85-34294# Enka A.G., Wuppeptal (West Germany). Inst. Technische Garne.
SUBSTITUTION OF ASBESTOS BY ARAMID FIBERS AND FIBER BLENDS IN INDUSTRIAL TEXTILES AND COMPOSITES WITH ORGANIC BINDERS Final Report, Dec. 1982
Karlheinz Hillermeier, Werner Damerau, Joachim Granal, Hubert Roehrens, Udo Schwartzkopff, Ulrich Stoecker, and Wolfgang Wirtz Bonn Bundesministerium fuer Forschung und Technologie Jan. 1985 282 p refs In GERMAN; ENGLISH summary Sponsored by Bundesministerium fuer Forschung und Technologie
(BMFT-FB-T-85-006; ISSN-0340-7608) Avail: NTIS HC A13/MF A01; Fachinformationszentrum, Karlsruhe, West Germany DM 44.50

High-tenacity aramid fibers ability to replace asbestos in applications such as friction material, seals, and heat-protective clothing was assessed. In spite of the higher production costs, the cost/benefit relation is often better than with asbestos. Friction materials may be made with high-tenacity aramid as the reinforcing fiber material. The fiber share in friction compounds can be reduced. Substitution of asbestos can be engineered within wide limits. In many cases the new formulation gives better performance than the old. The same applies to sheet gaskets. With aramid in the place of asbestos and in blends with other fibrous materials the admixture can be notably reduced. Aramid packings can be used instead of asbestos up to operating temperatures of 300 C. In

base fabrics for soft wear compensator arrangements aramid is well capable of replacing asbestos. Heavy heat-protective clothing made of asbestos can for a large part be made of aramid as well. Author (ESA)

N85-34201# Nihon Univ., Tokyo (Japan). Coll. of Science and Technology.
ELECTROLYTIC SYNTHESIS OF COLORED ETA ALUMINA FILM
Midori Yamada and Ikuo Mita (Tokyo Metropolitan Industrial Technology Center) *In* Society of Materials Science Proc. of the 27th Japan Congr. on Mater. Res. Mar. 1984 p 131-134 refs Sponsored in part by The Light Metal Educational Foundation Inc. (For primary document see N85-34180 23-23)
Avail: NTIS HC A14/MF A01

N85-34209# Hokkaido Industrial Research Inst. (Japan).
POLY-FUNCTIONAL BUILDING MATERIAL FROM FIBERGLASS (ITS FABRICATION AND PROPERTIES)
Keiichi Katsuse, Nobuhiro Naano, Toshihiko Maruyama, Toru Hirano, and Takuya Koga (Iwakura-Gumi Lumber Co., Ltd.) *In* Society of Materials Science Proc. of the 27th Japan Congr. on Mater. Res. Mar. 1984 p 253-256 ref (For primary document see N85-34180 23-23)
Avail: NTIS HC A14/MF A01

N85-34212# Kyoto Univ. (Japan). Industrial Arts and Textile Fibers.
STRENGTH PROPERTIES OF GLASSFIBER REINFORCED THERMOPLASTICS
Zenichiro Maekawa, Taichi Fujii (Osaka City Univ.), Teruaki Ikeda (Idemitsu Petrochemical Co.), and Toshio Yamada (Nippon Sheet Glass Co.) *In* Society of Materials Science Proc. of the 27th Japan Congr. on Mater. Res. Mar. 1984 p 269-273 refs (For primary document see N85-34180 23-23)
Avail: NTIS HC A14/MF A01

N85-34215# Waseda Univ., Tokyo (Japan). School of Science and Engineering.
IMPACT FRACTURE MECHANISM OF POLYMER PLATES CONTAINING A HEAVY INNER MATERIAL
Ikuhiko Hayashi, Hisashi Ishikawa, Keishi Takahashi, and Katsumi Kirao *In* Society of Materials Science Proc. of the 27th Japan Congr. on Mater. Res. Mar. 1984 p 289-294 refs (For primary document see N85-34180 23-23)
Avail: NTIS HC A14/MF A01

28 PROPELLANTS AND FUELS

Includes rocket propellants, igniters, and oxidizers; storage and handling; and aircraft fuels.

For related information see also *07 Aircraft Propulsion and Power, 20 Spacecraft Propulsion and Power,* and *44 Energy Production and Conversion.*

N85-34295*# Akron Univ., Ohio. Dept. of Chemical Engineering.
MEASUREMENT AND CORRELATION OF JET FUEL VISCOSITIES AT LOW TEMPERATURES Final Report
Dale L. Schruben Aug. 1985 31 p refs
(Grant NAG3-488)
(NASA-CR-174911; NAS 1.26:174911) Avail: NTIS HC A03/MF A01 CSCL 21D

Apparatus and procedures were developed to measure jet fuel viscosity for eight current and future jet fuels at temperatures from ambient to near -60 C by shear viscometry. Viscosity data showed good reproducibility even at temperatures a few degrees below the measured freezing point. The viscosity-temperature relationship could be correlated by two linear segments when plotted as a standard log-log type representation (ASTM D 341). At high temperatures, the viscosity-temperature slope is low. At low temperatures, where wax precipitation is significant, the slope is higher. The breakpoint between temperature regions is the filter flow temperature, a fuel characteristic approximated by the freezing point. A generalization of the representation for the eight experimental fuels provided a predictive correlation for low-temperature viscosity, considered sufficiently accurate for many design or performance calculations. E.A.K.

N85-34296# Los Alamos Scientific Lab., N. Mex.
INTERMOLECULAR EXPLOSIVES
I. B. Akst 1985 11 p refs Presented at the 8th Intern. Symp. on Detonation, Albuquerque, N. Mex., 15 Jul. 1985
(Contract W-7405-eng-36)
(DE85-009609; LA-UR-85-1130; CONF-850706-10) Avail: NTIS HC A02/MF A01

The steady-state detonation characteristics of a few intermolecular explosives are examined along with results of wedge experiments on initiation and reaction growth in one system (EAK), toward a better understanding of this class of explosives. The importance of factors such as products and their states, and temperature, to performance of these systems and explosives in general is discussed. Hydrogen compounds may be superior enough to carbon and its compounds as fuels and products for quick metal-accelerating explosives that the effect of the generally lower density is offset. High temperatures and condensation of solid products are probably the main causes of late appearance of energy in metal motion. The unusual shock sensitiveness and explosiveness of EAK are indicated by wedge results including pseudo-Pop-plots of overtaking waves, and by plots of shock velocity versus transit distance in the wedges. E.A.K.

N85-34297# Sandia Labs., Albuquerque, N. Mex.
TIME-RESOLVED SPECTROSCOPIC STUDIES OF DETONATING HETEROGENEOUS EXPLOSIVES
W. M. Trott and A. M. Renlund 1985 30 p refs Presented at the 8th Intern. Symp. on Detonation, Albuquerque, N. Mex., 15 Jul. 1985
(Contract DE-AC04-76DP-00789)
(DE85-009760; SAND-84-1741C; CONF-850706-14) Avail: NTIS HC A03/MF A01

Emission spectroscopy and pulsed laser excited Raman scattering methods are applied to the study of detonating heterogeneous explosives, including PETN, HMX and HNS. Time resolved spectra of emission from detonating HNS show the evolution of features due to electronically excited radical species. For HNS, the CN(B-X) system near 388 n has been studied at a wavelength resolution of 0.5 A. Boltzmann vibrational temperatures have been calculated by comparing the experimental data with computer simulated spectra. These temperatures are consistent with the expected trend of detonation temperature as a function of charge density. Using 532 nm laser excitation, single pulse Raman scattering measurements have been made at the free surface of detonating HMX and PETN samples. Monotonic attenuation of Raman scattering intensity over a 100 ns interval is observed after detonation front arrival at the free surface. Depletion of the Raman signal occurs prior to significant loss of the scattered laser light. The significance of the Raman measurements as a possible probe of reaction zone length in detonating explosives is discussed. DOE

N85-34298# Sandia Labs., Albuquerque, N. Mex.
PRESSURE-SHEAR LOADING OF PBX-9404
I. C. Chhabildas and M. E. Kipp 1985 19 p refs Presented at the 8th Intern. Symp. on Detonation, Albuquerque, N. Mex., 15 Jul. 1985
(Contract DE-AC04-76DP-00789)
(DE85-009982; SAND-84-1825C; CONF-850706-15) Avail: NTIS HC A02/MF A01

Pressure shear loading techniques have been used to obtain estimates of dynamic shear strength of PBX-9404 over the stress range of 0.3 to 1.0 GPa. One dimensional pressure shear waves were generated with a single stage compressed gas gun. The gun was used to obtain normal impact of a projectile on a Y cut quartz crystal with an explosive sample bonded to its rear surface.

The anisotropic nature of the Y cut quartz results in a two wave structure having particle velocities in both the longitudinal and transverse directions. Results of these experiments indicate that a maximum shear stress of 0.04 GPa is obtained over the stress range studied. The pulse amplitude and the sample thickness in the present experiments are not optimal to investigate the reaction sensitivity to shear loading. Numerical simulations of these experiments based on an existing thermomechanical model and an elastic, perfectly plastic model, are also reported. DOE

N85-34299# Los Alamos Scientific Lab., N. Mex.
DETONATION IN TUNGSTEN-LOADED HMX
S. Goldstein and C. L. Mader 1985 7 p refs Presented at the 8th Intern. Symp. on Detonation, Albuquerque, N. Mex., 15 Jul. 1985
(Contract W-7405-eng-36)
(DE85-009606; LA-UR-85-1122; CONF-850706-7) Avail: NTIS HC A02/MF A01

The detonation behavior of X-0233, a heavily tungsten-loaded HMX explosive, is studied using failure diameter measurements, plate dents, and aquarium tests. A model with features resembling those of a weak detonation describe the experimental results. DOE

N85-34300# Los Alamos Scientific Lab., N. Mex.
MODELING HETEROGENEOUS HIGH EXPLOSIVE BURN WITH AN EXPLICIT HOT-SPOT PROCESS
P. K. Tang, J. N. Johnson, and C. A. Forest 1985 11 p refs Presented at the 8th Intern. Symp. on Detonation, Albuquerque, N. Mex., 15 Jul. 1985
(Contract W-7405-eng-36)
(DE85-009593; LA-UR-85-769; CONF-850706-5) Avail: NTIS HC A02/MF A01

A method of treating high explosive burn with a multi-step process which includes the hot spot excitation, decomposition, and the propagation of reaction into the region outside the hot spots is presented. The basic features of this model are the separation of the thermal mechanical and chemical processes, and the partition of the explosive into hot spots and the region exclusive of the hot spots. The thermal mechanical aspect are formulated in a way similar to the chemical process. The combined processes lead to a set of rate equations for the mass fractions of reactants, intermediate states, and final products. The rates are expressed initially in terms of general characteristic times, but with specific phenomenological correlations introduced in the final model. Computational examples are given of simulated flyer plate impacts, short-shock initiation, corner turning, and shock desensitization. DOE

N85-34301# Los Alamos National Lab., N. Mex.
THREE-DIMENSIONAL HYDRODYNAMIC HOT-SPOT MODEL
C. L. Mader and J. D. Kershner 1985 10 p refs Presented at the 8th Intern. Symp. on Detonation, Albuquerque, N. Mex., 15 Jul. 1985
(Contract W-7405-eng-36)
(DE85-009587; LA-UR-85-742; CONF-850706-6) Avail: NTIS HC A02/MF A01

The interaction of a shock wave with a single air hole and a matrix of air holes in PETN, HMX, and TATB is numerically modeled. The hot spot formation, interaction, and the resulting buildup toward detonation are computed using three dimensional numerical Eulerian hydrodynamics with Arrhenius chemical reaction and accurate equations of state according to the hydrodynamic hot spot model. The basic differences between shock sensitive explosives (PETN, HMX) and shock insensitive explosives (TATB, NQ) may be described using the hydrodynamic hot spot model. The reactive hydrodynamics of desensitization of heterogeneous explosives by a weak preshock is numerically modeled. The preshock desensitizes the heterogeneous explosive by closing the air holes and making it more homogeneous. A higher pressure second shock has a lower temperature in the multiple shocked explosive than in single shocked explosives. The multiple shock temperature may be low enough to cause a detonation wave to fail to propagate through the preshocked explosive. DOE

N85-34302# Los Alamos National Lab., N. Mex.
EFFECT OF PRECIPITATION VARIABLES ON THE SPECIFIC SURFACE AND EXPLOSION CHARACTERISTICS OF PENTAERYTHRITOL TETRANITRATE
R. H. Dinegar 1985 11 p refs Presented at the Intern. Pyrotech. Soc. Symp., Karlsruhe, West Germany, 3 Jul. 1985
(Contract W-7405-eng-36)
(DE85-009620; LA-UR-85-1023; CONF-850742-1) Avail: NTIS HC A02/MF A01

The particle size, shape, and texture of the crystals of pentaerythritol tetranitrate (PETN) precipitated from acetone solutions by the addition of water depend upon many crystallization factors. Among the most important of these are: (1) the concentration of PETN in the acetone, (2) both the volume of water and the rate at which the nonsolvent is added, and (3) the amount of agitation of the solution during the precipitation process. Fortunately, all of these conditions can be controlled easily because the explosion characteristics of PETN are strong functions of the crystal description. This paper quantitatively describes the effect of precipitation conditions on the type of PETN crystals obtained and the variation of both explosive sensitivity and explosion time with one important quantitative measure of crystal description: the area per unit mass or specific surface. DOE

N85-34303# Los Alamos Scientific Lab., N. Mex.
REAL TIME ANALYSIS OF PETN DETONATION PRODUCTS
N. C. Blais and J. J. Valentini 1985 8 p refs Presented at the 8th Intern. Symp. on Detonation, Albuquerque, N. Mex., 15 Jul. 1985
(Contract W-7405-eng-36)
(DE85-009581; LA-UR-85-860; CONF-850706-8) Avail: NTIS HC A02/MF A01

The freely expanding gases from the detonation of pentaerythritol tetranitrate (PETN) pellet were analyzed as rapidly as the molecules arrived at the mass spectrometer detector. It was found that all of the products arriving at the detector earliest, irrespective of mass, had the same velocity, 11 km/s and peaked at 5 km/s. The width of the time distributions varied from one species to another. Mass and velocity spectra of the important products were obtained and the most intense signals were found to be H20, CO, and CO2, but H2O was by far the largest. Smaller signals arising from O, HCN, HCO, and NO2 were also found. Comparisons of the spectrum with other experiments are discussed. DOE

N85-34304# California Univ., Livermore. Lawrence Livermore Lab.
COMPARISON OF EXPERIMENTAL DATA ON DETONATION VELOCITY AND CHAPMAN-JOUGET PRESSURE VS INITIAL HE DENSITY WITH PREDICTIONS FROM REE'S MODEL EQUATION OF STATE
D. J. Steinberg Feb. 1985 11 p refs Presented at the 8th Intern. Symp. on Detonation, Albuquerque, N. Mex., 15 Jul. 1985
(Contract W-7405-eng-48)
(DE85-007266; UCRL-92102; CONF-850706-2) Avail: NTIS HC A02/MF A01

Data on the change of detonation velocity and Chapman-Jouget pressure vs initial HE density for RDX and HMX are compared with the theoretical predictions of Ree for PEX 9404. Ree's model predicts breaks or changes in the slope of these curves due to the solidification of carbon and the formation of a separate, nitrogen rich phase. There is good evidence for the solidification of carbon at rho0 about 1.15 g/cc, but the evidence for the nitrogen phase separation at rho0 about 1.56 g/cc is conflicting. DOE

N85-34305# Department of Energy, Washington, D. C.
PREPARATION OF ETHYLENEDIAMINE DINITRATE Patent Application
K. Lee, inventor (to DOE) Filed 17 May 1984 10 p
(Contract W-7405-eng-36)

(DE85-006423; US-Patent-Appl-SN-611558) Avail: NTIS HC A02/MF A01

Method for the preparation of ethylenediamine dinitrate is described. Ethylenediamine dinitrate, a useful explosive, is readily prepared by solvent extraction of nitrate ion from an acidic agueous solution thereof using a high-molecular-weight, water-insoluble amine dissolved in an organic solvent, and reacting the resulting organic solution with ethylenediamine. The process of the instant invention avoids the use of concentrated nitric acid, as is currently practiced, resulting in a synthesis which is far less hazardous, especially for large quantities of the explosive, and more efficient. DOE

N85-34306# Department of Energy, Washington, D. C.
ETHYLENEDIAMINE SALT OF 5-NITROTETRAZOLE AND PREPARATION Patent Application
K. Lee and M. D. Coburn, inventors (to DOE) Filed 17 May 1984 16 p
(Contract W-7405-eng-36)
(DE85-005738; US-Patent-Appl-SN-611557) Avail: NTIS HC A02/MF A01

The ethylenediamine salt of 5-nitrotetrazole was found to be useful as an explosive alone and in eutectic mixtures with ammonium nitrate and/or other explosive compounds. Its eutectic with ammonium nitrate was demonstrated to behave in a similar manner to a monomolecular explosive such as TNT, and is less sensitive than the pure salt. Moreover, this eutectic mixture, which contains 87.8 mol% of ammonium nitrate, is close to the CO2-balanced composition of 90 mol%, and has a relatively low melting point of 110.5 C making it readily castable. The ternary eutectic system containing the ethylenediamine salt of 5-nitrotetrazole, ammonium nitrate and ethylenediamine dinitrate has a eutectic temperature of 89.5 C and gives a measured detonation pressure of 24.8 GPa, which is 97.6% of the calculated value. Both the pure ethylenediamine salt and its known eutectic compounds behave in substantially ideal manner. Methods for the preparation of the salt are described. DOE

N85-34307# Institut Franco-Allemand de Recherches, St. Louis (France).
DETONATION OF CONDENSED EXPLOSIVES: EVOLUTION OF KNOWLEDGE IN THE LAST 40 YEARS [LA DETONATION DES EXPLOSIFS CONDENSES: EVOLUTION DES ETUDES ET CONNAISSANCES AU COURS DES QUARANTE DERNIERES ANNEES]
C. Fauquignon 31 Aug. 1985 35 p refs In FRENCH
(ISL-CO-228/84) Avail: NTIS HC A03

Ideal detonation waves; Viriel and BKW state equations; two dimensional steady detonations; direct and indirect diagnosis methods; nonsteady detonations; detonation models; and future trends in condensed explosives are discussed. Author (ESA)

31 ENGINEERING (GENERAL)

Includes vacuum technology; control engineering; display engineering; and cryogenics.

N85-34308# Vonier (Thomas) Associates, Inc., Washington, D.C.
MONITORING BUILDING ENERGY PERFORMANCE: AN INFORMAL REVIEW AND CHARACTERIZATION OF RESEARCH IN PROGRESS
Mar. 1984 79 p refs Prepared for Brookhaven National Lab.
(Contract DE-AC02-76CH-00016)
(BNL-51765) Avail: NTIS HC A05/MF A01

The U.S. Department of Energy (DOE) and Brookhaven National Laboratory (BNL) have had a longstanding interest in the actual performance of energy conservation features in whole buildings. BNL, as part of its work for DOE, has concentrated on detailed understanding of the full-scale performance of innovative components and subsystems interacting within whole buildings over extended time periods. This work has resulted in the publication of several case study reports on the actual energy performance of a variety of innovative residential buildings. To help the federal government and others keep abreast of developments in the field of whole building energy performance monitoring, DOE asked BNL to undertake a limited review of work under way throughout the United States, and to assemble the results of the review in a manner that would provide a resource to policymakers, researchers and others interested in whole building performance monitoring. DOE

N85-34309# Cranfield Inst. of Tech., Bedford (England).
PROCEEDINGS OF THE MECHANISMS CONFERENCE, VOLUME 1
1984 135 p refs Conf. held in Cranfield, England, Jul. 1984 2 Vol.
Avail: NTIS HC A07/MF A01

Proceedings of the mechanisms conference are presented. Topics discussed include: redesigning a mechanism for higher speed, cam mechanism design, problems in high speed gearing, balancing of complex mechanisms, computerized diagnostics, high powered epicyclic gears, use of ultrasound to monitor incipient failure of rolling element bearings, finite elements, inertial stresses and deformation in mechanisms, optimization of computer aided design, conjugated symmetrical coupler curves produced by 4-bar linkages with the same transmission angles, intermittent motion, and software for mechanism design. For individual titles, see N85-34310 through N85-34317.

N85-34310# North Staffordshire Polytechnic, Stafford (England). Dept. of Mechanical Engineering.
RE-DESIGNING A MECHANISM FOR HIGHER SPEED: A CASE HISTORY FROM TEXTILE MACHINERY
S. S. Douglas and G. T. Rooney (Liverpool Polytechnic) *In* Cranfield Inst. of Tech. Proc. of the Mech. Conf., Vol. 1 1984 10 p refs 2 Vol. (For primary document see N85-34309 23-31)
Avail: NTIS HC A07/MF A01

The generation of general mechanism design software which is the formulation of suitable objective functions is discussed. There is a consistent drive towards higher speeds in the development of industrial sewing machines. This led to experimental analyses of dynamic performance and to a search for improved design methods. The experimental work highlighted the need for 'smoothness' of motion at high speed, component inertias, and frame structural stiffness. Smoothness is associated with transmission properties and harmonic analysis. These are added to other design requirements of synchronization, mechanism size, and function. Some of the mechanism trains in overedte sewing machines are shown. All these trains are designed by digital optimization. The design software combines analysis of the sewing machine mechanisms, formulation of objectives in numerical terms, and suitable mathematical optimization techniques. Author

N85-34311# Surrey Univ., Guildford (England). Dept. of Mechanical Engineering.
A RATIONAL APPROACH TO CAM DESIGN **c37**
Gerald Druce *In* Cranfield Inst. of Tech. Proc. of the Mech. Conf., Vol. 1 1984 24 p refs 2 Vol. (For primary document see N85-34309 23-31)
Avail: NTIS HC A07/MF A01

Mechanism design which involves satisfying interacting limiting conditions which are functions of independent parameters are discussed. A flow chart defines the sequence for designing a disc cam to drive a translating roller follower. Subjects for additional design data are identified. E.A.K.

N85-34312# Cranfield Inst. of Tech., Bedford (England). Coll. of Aeronautics.
SOME PROBLEMS IN HIGH SPEED GEARS AND GEARING **c37**
J. H. Webb *In its* Proc. of the Mech. Conf., Vol. 1 1984 10 p refs 2 Vol. (For primary document see N85-34309 23-31)
Avail: NTIS HC A07/MF A01

Some of the causes of noise in high speed gears are consid-

ered. Analytical approaches aimed at the prediction and reduction of noise levels, and work conducted on these matters are discussed. Much of the work is taken from helicopter research, however the methods described are relevant to the process and other industries. E.A.K.

N85-34313# Newcastle-upon-Tyne Univ. (England). Dept. of Mechanical Engineering.
THE BALANCING OF COMPLEX LINKAGE MECHANISMS
M. R. Smith *In* Cranfield Inst. of Tech. Proc. of the Mech. Conf., Vol. 1 1984 21 p refs 2 Vol. (For primary document see N85-34309 23-31)
Avail: NTIS HC A07/MF A01

The development of linkage mechanism balancing is outlined. Methods originally applied to the four bar linkage with in-line and off-set couplers are described together with their application to more complicated mechanisms. Recent investigation of the six-bar linkage which yielded new results leading to the ability to obtain force balance in hitherto unbalancable mechanims is reported. The concept of mass flow which aides are understanding of the necessary procedures is introduced. E.A.K.

N85-34314# Loughborough Univ. of Technology (England). Mechanical Engineering Dept.
A VERSATILE COMPUTER PACKAGE FOR MECHANISM ANALYSIS
Trevor Davies *In* Cranfield Inst. of Tech. Proc. of the Mech. Conf., Vol. 1 1984 18 p refs 2 Vol. (For primary document see N85-34309 23-31)
Avail: NTIS HC A07/MF A01

Features of a multi purpose suite of computer subroutines are described and some of its capabilities are illustrated with the aid of examples based on a mechanism proposed for a textile machine. Finite difference methods are used to estimate velocities and accelerations. These methods are recommended and the package is well suited for adaption to microcomputers. Dynamic analysis and balancing are also described. E.A.K.

N85-34315# Loughborough Univ. of Technology (England). Mechanical Engineering Dept.
A VERSATILE COMPUTER PACKAGE FOR MECHANISM ANALYSIS, PART 2: DYNAMICS AND BALANCE
Trevor Davies *In* Cranfield Inst. of Tech. Proc. of the Mech. Conf., Vol. 1 1984 18 p refs 2 Vol. (For primary document see N85-34309 23-31)
Avail: NTIS HC A07/MF A01

The algorithms required for the shaking force components, the shaking moment about the crankshaft axis, and the input torque and bearing load components are discussed using the textile machine as a focus for the discussion. The example is also used to provide illustrations of the output for options on the hodograph of the shaking force vector. This provides estimates of the optimum contrarotating masses and their locations for a generalized primary Lanchester balancer. The suitability of generalized Lanchester balancers particularly for textile machinery, and the overall strategy used during the development of the package are outlined. E.A.K.

N85-34316# Cranfield Inst. of Tech., Bedford (England).
HIGH POWERED EPICYCLIC GEARS: SOME RECENT DEVELOPMENT **c37**
D. E. Yates *In* Cranfield Inst. of Tech. Proc. of the Mech. Conf., Vol. 1 1984 19 p refs 2 Vol. (For primary document see N85-34309 23-31)
Avail: NTIS HC A07/MF A01

The development of marine and industrial epicyclic gearing is reviewed. Some of the features which are specific to the design and manufacture of this tpe of gearing are illustrated. The development of a new design of annulus system using the basic stoeckicht principle of annulus flexibility is discussed. E.A.K.

N85-34317# Cranfield Inst. of Tech., Bedford (England).
THE USE OF ULTRASOUND TO MONITOR INCIPIENT FAILURE OF ROLLING ELEMENT BEARINGS **c38**
R. H. Bannister *In* Cranfield Inst. of Tech. Proc. of the Mech. Conf., Vol. 1 1984 12 p 2 Vol. (For primary document see N85-34309 23-31)
Avail: NTIS HC A07/MF A01

The design of a microminiature ultrasonic transducer, and its application for detecting failure of rolling element bearings is discussed. The development of a low cost surveillance system is reported. E.A.K.

N85-34318# Cranfield Inst. of Tech., Bedford (England).
PROCEEDINGS OF THE MECHANISMS CONFERENCE, VOLUME 2
1984 89 p refs Conf. held in Cranfield, England, Jul. 1984 2 Vol.
Avail: NTIS HC A05/MF A01

Proceedings of the conference of mechanisms are presented. Topics include: finite element method, internal stresses and deformations, computer aided design, conjugated symmetrical coupler curves produced by 4-bar linkages waving the same transmission angles, intermittent motion, and software for mechanism design. For individual titles, see N85-34319 through N85-34324.

N85-34319# Cranfield Inst. of Tech., Bedford (England).
AN INTRODUCTION TO FINITE ELEMENTS **c64**
P. M. Wheeler (PAFEC, Ltd.) *In* Cranfield Inst. of Tech. Proc. of the Mech. Conf., Vol. 2 1984 20 p 2 Vol. (For primary document see N85-34318 23-31)
Avail: NTIS HC A05/MF A01

Methods for engineering problems are presented. The most often employed methods are: strength of materials, theory of elasticity experimental work, finite difference method, and finite elements. It is concluded that only experiment or finite element can answer all the mechanical questions, and probably only one is economical enough to be considered. E.A.K.

N85-34320# Cranfield Inst. of Tech., Bedford (England). Mechanism Design Unit.
INERTIAL STRESSES AND DEFORMATIONS IN MECHANISMS **c39**
J. N. Hammar *In* Cranfield Inst. of Tech. Proc. of the Mech. Conf., Vol. 2 1984 16 p ref 2 Vol. (For primary document see N85-34318 23-31)
Avail: NTIS HC A05/MF A01

A method was developed to analyze two dimensional stresses and deformations in mechanism links. The thematical predictions must be evidenced and further extended to analyze three dimensional situations. This requires application of a suitable finite element type and an appropriate mass matrix. E.A.K.

N85-34321# Cranfield Inst. of Tech., Bedford (England). Dept. of Applied Computing and Mathematics.
OPTIMISATION IN THE COMPUTER AIDED DESIGN OF MECHANISMS **c61**
M. J. Pratt *In* Cranfield Inst. of Tech. Proc. of the Mech. Conf., Vol. 2 1984 16 p refs 2 Vol. (For primary document see N85-34318 23-31)
Avail: NTIS HC A05/MF A01

Computer aided optimization is discussed. The process has two steps: objective function and stationary points. An optimal solution was sought which is subject to the constraints that all the variables are position. Optimization routines are chosen to cover a range of commonly objective function types and problems of constrained and nonconstrained types. The general approaches are outlined. The computer aided design systems allow parts and assemblies of parts to be designed parametrically. Techniques of symbolic manipulation allow the equations of motion of mechanisms to be generated automatically by computer. E.A.K.

N85-34322# Technische Hogeschool, Eindhoven (Netherlands). Dept. of Mechanical Engineering.
CONJUGATED SYMMETRICAL COUPLER CURVES, PRODUCED

BY 4-BAR LINKAGES HAVING THE SAME TRANSMISSION ANGLES
Evert A. Dijksman *In* Cranfield Inst. of Tech. Proc. of the Mech. Conf., Vol. 2 1984 12 p refs 2 Vol. (For primary document see N85-34318 23-31)
Avail: NTIS HC A05/MF A01

The focal properties of the 4-hour linkage are shown to be at the base of a family relationship between each time of four symmetrical coupler curves. Four-bars producing these related curves are conjugated. It appears that two such conjugate four-bars always form an overconstrained linkage mechanism through the admission of two particular chosen, binary links. It is shown that the four conjugated four-bar linkages develop the same diagonal function and have the same extreme transmission angles that occur in the frame aligned position of their crank. E.A.K.

N85-34323# Liverpool Polytechnic (England).
INTERMITTENT MOTION
J. Rees Jones *In* Cranfield Inst. of Tech. Proc. of the Mech. Conf., Vol. 2 1984 7 p refs 2 Vol. (For primary document see N85-34318 23-31)
Avail: NTIS HC A05/MF A01

Intermittent motions and the machine arrangements intended to produce them are beset with discontinuities and load distortions that are the prime cause of dynamic malfunctions and vibration in high-speed applications. These phenomena are discussed in the context of both fixed and programmable automation and some of the measures that can be taken to offset the undesirable effects are suggested. E.A.K.

N85-34324# Cranfield Inst. of Tech., Bedford (England).
SOFTWARE FOR MECHANISM DESIGN **c61**
S. Molian *In* Cranfield Inst. of Tech. Proc. of the Mech. Conf., Vol. 2 1984 17 p refs 2 Vol. (For primary document see N85-34318 23-31)
Avail: NTIS HC A05/MF A01

The usefulness of various types of mechanism design software for the practicing engineer is discussed. The software should be capable of handling the design problems that are most likely to occur in practice, its cost should be moderate and learning how to use it should be quick and easy. A software package with those characteristics is described. E.A.K.

N85-34325# National Bureau of Standards, Gaithersburg, Md. National Engineering Laboratory.
THE APPLICATION OF MODELS TO THE ASSESSMENT OF FIRE HAZARD FROM CONSUMER PRODUCTS
Richard W. Bukowski Aug. 1985 31 p refs
(NBSIR-85-3219) Avail: NTIS HC A03/MF A01

The differences among models of fire, fire hazard, and fire risk are described. The use of field, zone, and network models for fire hazard assessment is discussed. A number of available single and multiple compartment models are described. Key considerations with respect to the use of the current models by the Consumer Product Safety Commission for hazard assessment from upholstered furniture and mattress fires is presented. Modifications necessary to improve the capability of these models for hazard assessments are identified. Model validation, output presentation, and data sources are discussed. Recommendations on specific models for the sponsor to consider for further study and use are provided. Author

N85-34326# Department of Energy, Washington, D. C.
COMBINED COLD COMPRESSOR/EJECTOR HELIUM REFRIGERATOR Patent Application
D. P. Brown, inventor (to DOE) Filed 5 Jun. 1984 18 p
(Contract DE-AC02-76CH-00016)
(DE85-006408; US-Patent-Appl-SN-617656) Avail: NTIS HC A02/MF A01

A refrigeration apparatus having an ejector operatively connected with a cold compressor to form a two stage pumping system is described. This pumping system is used to lower the pressure, and thereby the temperature of a bath of boiling refrigerant (helium). The apparatus as thus arranged and operated has substantially improved operating efficiency when compared to other processes or arrangements for achieving a similar low pressure. DOE

N85-34582# Victoria Univ. (British Columbia). Dept. of Computer Science.
GENERATIVE DESIGN IN ARCHITECTURE USING AN EXPERT SYSTEM
Eric Gullichsen and Ernest Chang *In* Canadian Information Processing Society Graphics Interface 1985 1985 p 425-433 (For primary document see N85-34523 23-61)
Avail: NTIS HC A19/MF A01

32 COMMUNICATIONS

Includes land and global communications; communications theory; and optical communications.

For related information see also *04 Aircraft Communications and Navigation* and *17 Spacecraft Communications, Command and Tracking.*

N85-34327* National Aeronautics and Space Administration. Pasadena Office, Calif.
METHOD AND APPARATUS FOR DELTA KAPPA SYNTHETIC APERTURE RADAR MEASUREMENT OF OCEAN CURRENT Patent
Atul Jain, inventor (to NASA) (JPL, Pasadena, Calif.) Issued 2 Apr. 1985 8 p Filed 18 Mar. 1982 Supersedes N82-28502 (20 - 19, p 2673)
(NASA-Case-NPO-15704-1; US-Patent-4,509,048; US-Patent-Appl-SN-359382; US-Patent-Class-343-5-CM; US-Patent-Class-343-5-W; US-Patent-Class-343-17.2-PC) Avail: US Patent and Trademark Office CSCL 17I

A synthetic aperture radar (SAR) employed for delta k measurement of ocean current from a spacecraft without the need for a narrow beam and long observation times. The SAR signal is compressed to provide image data for different sections of the chirp band width, equivalent to frequencies and a common area for the separate image fields is selected. The image for the selected area at each frequency is deconvolved to obtain the image signals for the different frequencies and the same area. A product of pairs of signals is formed, Fourier transformed and squared. The spectrum thus obtained from different areas for the same pair of frequencies are added to provide an improved signal to noise ratio. The shift of the peak from the center of the spectrum is measured and compared to the expected shift due to the phase velocity of the Bragg scattering wave. Any difference is a measure of current velocity v sub o (delta k).
Official Gazette of the U.S. Patent and Trademark Office

N85-34328 British Broadcasting Corp., Kingswood (England). Engineering Div.
THE IMPROVED DISPLAY OF 625-LINE TELEVISION PICTURES: ADAPTIVE INTERPOLATION
A. Roberts May 1985 8 p refs
(BBC-RD-1985/5) Avail: BBC, Kingswood Warren, Tadworth, Surrey, Engl.

Some of the defects of a conventional 625-line television scanning system can be reduced, or even eliminated by signal processing in the receiver. The processing need not be very complicated, and most scanning system defects can be treated merely by raising the display scanning rate by standards conversion, or example to a sequential structure of 625-lines at 100 pictures per second, or an interlaced structure of 1250 lines at 100 fields per second. Although such structures do not suffer from the defects of the conventional 625-line system, other effects can arise if unsuitable conversion algorithms are used. Specifically, it is possible to define two algorithms, one best suited to the portrayal of motion, the other to vertical detail, and no compromise is suited to both. This report describes an adaptive

solution to the problem, involving varying the algorithm according to the output of a motion detector such that the appropriate algorithm was used for each pixel. The work was not completely successful in that the motion detector could not be adjusted to give completely acceptable results, although for non-critical test material the results were encouraging. B.W.

N85-34329*# Ohio State Univ., Columbus. Dept. of Electrical Engineering.
ADAPTIVE ANTENNA ARRAYS FOR SATELLITE COMMUNICATIONS: DESIGN AND TESTING
Inder J. Gupta, William G. Swarner, and Eric K. Walton Sep. 1985 116 p refs
(Grant NAG3-536)
(NASA-CR-176162; NAS 1.26:176162; ESL-716111-3) Avail: NTIS HC A06/MF A01 CSCL 20N

When two separate antennas are used with each feedback loop to decorrelate noise, the antennas should be located such that the phase of the interfering signal in the two antennas is the same while the noise in them is uncorrelated. Thus, the antenna patterns and spatial distribution of the auxiliary antennas are quite important and should be carefully selected. The selection and spatial distribution of auxiliary elements is discussed when the main antenna is a center fed reflector antenna. It is shown that offset feeds of the reflector antenna can be used as auxiliary elements of an adaptive array to suppress weak interfering signals. An experimental system is designed to verify the theoretical analysis. The details of the experimental systems are presented. Author

N85-34330# Sandia Labs., Albuquerque, N. Mex. Microwave Physics Div.
NEW DIRECTIONAL COUPLERS FOR MULTIMODE CIRCULAR WAVEGUIDES APPLIED TO INTENSE PULSED MICROWAVE SYSTEMS
L. M. Earley, W. P. Ballard, and C. B. Wharton (Cornell Univ., Ithaca, N.Y.) 1985 4 p Presented at the Particle Accelerator Conf., Vancouver, British Columbia, 13 May 1985
(Contract DE-AC04-76DP-00789)
(DE85-011753; SAND-85-0039C; CONF-850504-27) Avail: NTIS HC A02/MF A01

Three new types of directional couplers are described for use in overmoded circular waveguide operating in the TM01 mode. The types are: (1) circular/rectangular waveguide multihole couplers, (2) circular waveguide/coaxial multihole couplers, and (3) circular waveguide loop couplers. These directional couplers are designed to diagnose intense pulsed microwave systems in the frequency range 3 to 18 GHz. Coupling coefficients vary between 50 dB and 70 dB with directivities between 13 dB and 20 dB. These devices have been used to measure the output powers of relativistic magnetrons and backward wave oscillators (BWOS) in the power range 100 MW to 300 MW. DOE

N85-34331# Ecole Nationale Superieure des Telecommunications, Paris (France). Dept. Informatique.
TELECOMMUNICATION MARKET RESEARCH PROCESSING Ph.D. Thesis - Rennes Univ. [TRAITEMENT D'ENQUETES POUR LES TELECOMMUNICATIONS]
Jean-Francois Dupont 9 Jun. 1983 208 p refs In FRENCH
(ENST-83E018; ISSN-0751-1353) Avail: NTIS HC A10

The data processing in two telecommunication market investigations is described. One of the studies concerns the office applications of communication and the other the experiences with a videotex terminal. Statistical factorial analysis was performed on a large mass of data. A comparison between utilization intentions and effective utilization is made. Extensive rewriting of statistical analysis computer programs was required. Author (ESA)

N85-34332# Forschungsinstitut der Deutschen Bundespost, Darmstadt (West Germany).
THEORETICAL PRINCIPLES OF VERTICAL SUBSAMPLING OF COLOR DIFFERENCE SIGNALS AT HALF THE SAMPLING RATE
Klaus Merzenich Mar. 1985 21 p refs In GERMAN; ENGLISH summary
(FI-447-TBr-18) Avail: NTIS HC A02/MF A01

The consequences of the sampling theorem for the vertical subsampling of color difference signals at half the sampling rate are discussed. The reduction of the bit rate of vision signals consists in a decrease of the sampling rate. The consequences are illustrated with a 4:2 system. Subsampling in the vertical dimension involves special features caused by interlaced scanning. Vertical subsampling only allows an optimal utilization of the theoretically possible resolution if the television signal is frame scanned. Therefore it is meaningful to frame code the signal in the studio and at the transmission, involving the requirement of an image storage for each receiver or decoder. Author (ESA)

33 ELECTRONICS AND ELECTRICAL ENGINEERING

Includes test equipment and maintainability; components, e.g., tunnel diodes and transistors; microminiaturization; and integrated circuitry.

For related information see also *60 Computer Operations and Hardware* and *76 Solid-State Physics.*

N85-34333* National Aeronautics and Space Administration. Pasadena Office, Calif.
METHOD AND APPARATUS FOR TRANSFER FUNCTION SIMULATOR FOR TESTING COMPLEX SYSTEMS Patent
Michael J. Kavaya, inventor (to NASA) (JPL, Pasadena, Calif.) Issued 2 Apr. 1985 13 p Filed 11 Jun. 1982 Supersedes N82-28619 (20 - 19, p 2690)
(NASA-Case-NPO-15696-1; US-Patent-4,509,132;
US-Patent-Appl-SN-387647; US-Patent-Class-364-571;
US-Patent-Class-364-578; US-Patent-Class-372-32) Avail: US Patent and Trademark Office CSCL 09C

A method and apparatus for testing the operation of a complex stabilization circuit in a closed loop system is presented. The method is comprised of a programmed analog or digital computing system for implementing the transfer function of a load thereby providing a predictable load. The digital computing system employs a table stored in a microprocessor in which precomputed values of the load transfer function are stored for values of input signal from the stabilization circuit over the range of interest. This technique may be used not only for isolating faults in the stabilization circuit, but also for analyzing a fault in a faulty load by so varying parameters of the computing system as to simulate operation of the actual load with the fault.
Official Gazette of the U.S. Patent and Trademark Office

N85-34334*# Missouri Univ., Columbia. Dept. of Electrical and Computer Engineering.
EVALUATION OF HALF WAVE INDUCTION MOTOR DRIVE FOR USE IN PASSENGER VEHICLES Final Report
R. G. Hoft, A. Kawamura, A. Goodarzi, G. Q. Yang, and C. L. Erickson 1 May 1985 243 p Prepared in cooperation with JPL, Pasadena, Calif.
(Contract DE-AI01-78CS-54209)
(NASA-CR-176119; JPL-9950-1039; NAS 1.26:176119;
DOE/CS-54209/28) Avail: NTIS HC A11/MF A01 CSCL 09C

Research performed at the University of Missouri-Columbia to devise and design a lower cost inverter induction motor drive for electrical propulsion of passenger vehicles is described. A two phase inverter motor system is recommended. The new design is predicted to provide comparable vehicle performance, improved reliability and a cost advantage for a high production vehicle, decreased total rating of the power semiconductor switches, and a somewhat simpler control hardware compared to the conventional three phase bridge inverter motor drive system. The major disadvantages of the two phase inverter motor drive are that it is larger and more expensive than a three phase machine, the design of snubbers for the power leakage inductances produce higher

transient voltages, and the torque pulsations are relatively large because of the necessity to limit the inverter switching frequency to achieve high efficiency. Author

N85-34335*# Virginia Polytechnic Inst. and State Univ., Blacksburg. Dept. of Electrical Engineering.
EVALUATION OF SEMICONDUCTOR DEVICES FOR ELECTRIC AND HYBRID VEHICLE (EHV) ac-DRIVE APPLICATIONS, VOLUME 1 Final Report
F. C. Lee, D. Y. Chen, M. Jovanovic, and D. C. Hopkins 1 May 1985 241 p refs Prepared in cooperation with JPL, Pasadena, Calif.
(Contract NAS7-100)
(NASA-CR-176118; JPL-9950-1038; NAS 1.26:176118; DOE/CS-54209/27) Avail: NTIS HC A11/MF A01 CSCL 09C

The results of evaluation of power semiconductor devices for electric hybrid vehicle ac drive applications are summarized. Three types of power devices are evaluated in the effort: high power bipolar or Darlington transistors, power MOSFETs, and asymmetric silicon control rectifiers (ASCR). The Bipolar transistors, including discrete device and Darlington devices, range from 100 A to 400 A and from 400 V to 900 V. These devices are currently used as key switching elements inverters for ac motor drive applications. Power MOSFETs, on the other hand, are much smaller in current rating. For the 400 V device, the current rating is limited to 25 A. For the main drive of an electric vehicle, device paralleling is normally needed to achieve practical power level. For other electric vehicle (EV) related applications such as battery charger circuit, however, MOSFET is advantageous to other devices because of drive circuit simplicity and high frequency capability. Asymmetrical SCR is basically a SCR device and needs commutation circuit for turn off. However, the device poses several advantages, i.e., low conduction drop and low cost. Author

N85-34336# Illinois Univ. Observatory, Urbana. Coordinated Science Lab.
JOINT SERVICES ELECTRONICS PROGRAM Progress Report, 1 Jul. 1984 - 31 Mar. 1985
T. N. Trick 30 Mar. 1985 89 p
(Contract N00014-84-C-0149)
(AD-A154748) Avail: NTIS HC A05/MF A01 CSCL 09/5

The July 1984 to March 1985 progress report of the Joint Services Electronics Program lists the following topics: in semiconductor research - molecular beam epitaxy, heterostructure electronic devices by metallorganic chemical vapor deposition, transport phenomena in semiconductors, crystal growth of semiconductor alloys from the vapor phase and controlled doping (ion-surface interactions), an investigation of the plasma and chemistry processes in cylindrical magnetron reactive ion etching discharges, acoustic charge transport, vapor phase growth and characterization of InGaAs and InGaAsP heterostructures and devices; in surface studies - direct examination of the metal semiconductor interface; quantum electronics - quantum dymanics of charge-density waves, excited state chemistry in gases; in electromagnetic communication - electromagnetic radiation and scattering, millimeter and submillimeter wave integrated circutis; in digital communication - multiple-terminal digital communication systems, digital detection and estimation; and, in analog and digital circuits - hierarchical simulation and design verification of VLSI circuits and systems. F.M.R.

N85-34337# Department of the Air Force, Washington, D.C.
WIDE-BAND PHASE LOCKED LOOP AMPLIFIER APPARATUS Patent Application
Hopwood, inventor (to Air Force) Filed 18 Apr. 1985 16 p
(AD-D011720; US-Patent-Appl-SN-724714) Avail: NTIS HC A02/MF A01 CSCL 09/5

A wide-band amplifier apparatus utilizes a low frequency and a high frequency phase lock loop to achieve low phase delay at the loop bandwidth. The bandwidth products of the low and high frequency loops are combined and applied to the voltage controlled oscillator to minimize phase delay and to achieve a more stable loop. Author (GRA)

N85-34338# Department of the Air Force, Washington, D.C.
LOW NOISE POLYCRYSTALLINE SEMICONDUCTOR RESISTORS BY HYDROGEN PASSIVATION Patent Application
Lee, inventor (to Air Force) Filed 24 Apr. 1985 13 p
(AD-D011721; US-Patent-Appl-SN-726558) Avail: NTIS HC A02/MF A01 CSCL 20/12

Low noise polycrystalline silicon resistors are fabricated in the following sequence: (1) deposit an appropriate thickness of polysilicon (e.g., 400nm) on top of an oxidized wafer, (2) resistor doping by ion implantation (e.g., phosphorous), (3) heavy doping of the end-contact regions of the polysilicon resistor by high-dose ion implantation, (4) patterning the polysilicon resistor, (5) oxidation/annealing the polysilicon resistor, (6) open contacts to the polysilicon resistor, (7) aluminum metallization to form ohmic contacts, and (8) a long (e.g., 3 hours) low temperature (e.g., at 375 deg) pure hydrogen annealing to passivate the interface states in the polysilicon resistor. Polyresistors processed this way have a noise figure that is about a factor of three lower than samples processed otherwise. The low temperature post metallization annealing in pure hydrogen passivates the interfaces of polyresistors, reducing the 1/f noise normally generated therein. GRA

N85-34339# Department of the Air Force, Washington, D.C.
REDUCING GRATING LOBES DUE TO SUBARRAY AMPLITUDE TAPERING Patent Application
R. L. Haupt, inventor (to Air Force) Filed 7 May 1985 71 p
(AD-D011723; US-Patent-Appl-SN-731646) Avail: NTIS HC A04/MF A01 CSCL 20/14

Subarray amplitude tapering is a simple, lower cost method of generating low sidelobes in an antenna's far field pattern. Unfortunately, this simple technique also generates unwanted grating lobes. Placing the exact amplitude taper at the element outputs produces the desired far field pattern, but the architecture is complicated and expensive. An alternative to these two techniques is a design process that entails placing amplitude tapering at subarray outputs and element amplitude tapers that are identical between corresponding elements in groups of identical subarrays. In this way, the amplitude taper approximates the desired taper much better than subarray tapering alone, yet groups of subarrays are identical so that the design remains very simple. Author (GRA)

N85-34340# Department of the Air Force, Washington, D.C.
BRUSH AND COMMUTATOR SEGMENT TORQUER MOTOR Patent Application
J. W. Becker, inventor (to Air Force) Filed 11 Apr. 1985 11 p
(AD-D011726; US-Patent-Appl-SN-721836) Avail: NTIS HC A02/MF A01 CSCL 09/3

This patent application discloses a non-continuous brush and commutator segment torquer motor having a single radial air gap. The motor can be placed on the opposite side of the gimbal center line of a payload. This arrangement minimizes torquer mass, as well as providing greater clearance for the gimbal payload to travel through larger angular excursions. Hence, all payloads which are gimbal mounted, such as radar antennas, can be located closer to the gimbal center and can be driven through larger look angles. GRA

N85-34341# Edgerton, Germeshausen and Grier, Inc., Idaho Falls, Idaho.
TEST PLAN FOR PERFORMANCE TESTING OF THE EATON AC-3 ELECTRIC VEHICLE
R. I. Crumley and H. W. Heiselmann Apr. 1985 34 p
(Contract DE-AC07-76ID-01570)
(DE85-011954; EGG-SE-6764) Avail: NTIS HC A03/MF A01

An alternating current (ac) propulsion system for an electric vehicle was developed and tested. The test bed vehicle is a modified 1981 Mercury Lynx. The test plan was prepared specifically for the third modification to this test bed and identified as the Eaton AC-3. The scope of the testing done on the Eaton AC-3 includes coastdown and dynamometer tests but does not include environmental, on-road, or track testing. Coastdown testing is performed in accordance with SAE J-1263 (SAE Recommended

Practice for Road Load Measurement and Dynamometer Simulation Using Coastdown Techniques). DOE

N85-34342# Department of Energy, Washington, D. C.
SERIES-COUNTERPULSE REPETITIVE-PULSE INDUCTIVE STORAGE CIRCUIT Patent Application
E. M. Honig, inventors (to DOE) Filed 5 Jun. 1984 14 p
(Contract W-7405-eng-36)
(DE85-006438; US-Patent-Appl-SN-617658) Avail: NTIS HC A02/MF A01

A high-power series-counterpulse repetitive-pulse inductive energy storage and transfer circuit includes an opening switch, a main energy storage coil, and a counterpulse capacitor. The local pulse is initiated simultaneously with the initiation of the counterpulse used to turn the opening switch off. There is no delay from command to output pulse. During the load pulse, the counterpulse capacitor is automatically charged with sufficient energy to accomplish the load counterpulse which terminates the load pulse and turns the load switch off. When the main opening switch is reclosed to terminate the load pulse, the counterpulse capacitor discharges through the load, causing a rapid, sharp cutoff of the load pulse as well as recovering any energy remaining in the load inductance. The counterpulse capacitor is recharged to its original condition by the main energy storage coil after the load pulse is over, not before it begins. DOE

N85-34343# Department of Energy, Washington, D. C.
FAST SHUTTER APPARATUS Patent Application
E. L. Zimmermann and D. R. Kania, inventors (to DOE) Filed 27 Jun. 1984 10 p
(Contract W-7405-eng-36)
(DE85-006501; US-Patent-Appl-SN-625322) Avail: NTIS HC A02/MF A01

An apparatus for protecting diagnostic equipment from blast damage by rapidly interposing a shuttler between the equipment and the blast area is proposed. The apparatus comprised a sensor for sensing a trigger signal associated with the blast and for converting it into a voltage pulse. The voltage pulse is received by the first end of a firing pin. A pressure chamber holds the gas under pressure. The second end of the firing pin is located inside the pressure chamber and is located above a foil member covering an orifice. When the voltage pulse reaches the second end, point-to-plane discharge ruptures the foil, allowing the gas to enter a drive housing and quickly move a drive piston away from the foil. A drive rod connects the drive piston to a shutter and as the drive piston is moved down, the shutter moves into a closed position, protecting the equipment from debris. DOE

N85-34344# Department of Energy, Washington, D. C.
REVERSING-COUNTERPULSE REPETITIVE-PULSE INDUCTIVE STORAGE CIRCUIT Patent Application
E. M. Honig, inventor (to DOE) Filed 5 Jun. 1984 23 p refs
(Contract W-7405-eng-36)
(DE85-006409; US-Patent-Appl-SN-617653) Avail: NTIS HC A02/MF A01

A high power reversing-counterpulse repetitive-pulse inductive storage and transfer circuit is described which includes an opening swith, a main energy storage coil, a counterpulse capacitor and a small inductor. After counterpulsing the opening switch off, the counterpulse capacitor is recharged by the main energy storage coil before the load pulse is initiated. This gives the counterpulse capacitor sufficient energy for the next counterpulse operation, although the polarity of the capacitor's voltage must be reversed before that can occur. By using a current-zero switch as the counterpulse start switch, the capacitor is disconnected from the circuit (with a full charge) when the load pulse is initiated, preventing the capacitor from depleting its energy store by discharging through the load. After the load pulse is terminated by reclosing the main opening switch, the polarity of the counterpulse capacitor voltage is reversed by discharging the capacitor through a small inductor and interrupting the discharge current oscillation at zero current and peak reversed voltage. DOE

N85-34345# Department of Energy, Washington, D. C.
APPARATUS FOR UNILATERAL GENERATION OF A HOMOGENEOUS MAGNETIC FIELD Patent Application
E. Fukushima and A. R. Rath, inventors (to DOE) Filed 1 May 1984 19 p
(Contract W-7405-eng-36)
(DE85-006001; US-Patent-Appl-SN-605950) Avail: NTIS HC A02/MF A01

An apparatus for unilaterally producing a substantially homogeneous magnetic field is proposed. The apparatus includes two circular electromagnet coils, a small coil and a large coil, which are coaxial with one another and which are separated by a distance equal to one-half the difference in the radius of the two coils. By appropriate selection of electrical currents, which are passed through the coils in opposite directions, a region of homogeneous magnetic field is formed. This region is centered on the common axis of the two coils, at a point on the axis which is at a distance from the small coil equal to one-half the radius of the small coil, and which is on the opposite side of the small coil from the large coil. The apparatus has particular application in the field of diagnostic medical NMR and other NMR applications. DOE

N85-34346# Centre National d'Etudes Spatiales, Toulouse (France). Centre Spatial.
REALIZATION AND LINEARIZATION OF A HYPERFREQUENCY POWER AMPLIFIER IMPLEMENTED WITH BIPOLAR TRANSISTORS IN CLASS C POLARIZATION [REALISATION ET LINEARISATION D'UN AMPLIFICATEUR DE PUISSANCE HYPERFREQUENCE A TRANSISTORS BIPOLAIRES POLARISES EN CLASSE C]
Yves Durand Jan. 1985 106 p refs In FRENCH; ENGLISH summary Report will also be announced as translation (ESA-TT-927) Prepared in cooperation with Technische Hogeschool Twente, Enschede (Netherlands)
(CNES-NT-114) Avail: NTIS HC A06/MF A01

The design of a 10 W amplifier at 2.5 GHz and that of a power characteristic linearization device are discussed. The amplifier consists of 3 stages of transistors on a common base circuit with an MSC 3000 at the output. The linearization is obtained by an emitter polarization voltage related to the incident high frequency power. The circuit that elaborates the control signal is described. The results show the need to separate the stages.
Author (ESA)

N85-34541# ENSIEG, Saint Martin d'Heres (France). Lab. d'Automatique.
RECOGNITION AND CLEAR REPRESENTATION OF HAND-WRITTEN ELECTRONIC DIAGRAMS [RECONNAISSANCE ET MISE AU NET DE SCHEMAS ELECTRONIQUES MANUSCRITS]
Martine Silbermann and Pierre Deschizeaux *In* Canadian Information Processing Society Graphics Interface 1985 1985 p 133-138 refs In FRENCH; ENGLISH summary (For primary document see N85-34523 23-61)
Avail: NTIS HC A19/MF A01

N85-34966*# California Inst. of Tech., Pasadena.
BALLOON-BORNE VIDEO CASSETTE RECORDERS FOR DIGITAL DATA STORAGE
W. E. Althouse and W. R. Cook *In* NASA. Goddard Space Flight Center 19th Intern. Cosmic Ray Conf., Vol. 3 Aug. 1985 p 395-397 refs (For primary document see N85-34862 23-93)
(Grant NGR-05-002-160)
(OG-9.3-11) Avail: NTIS HC as boxed set only $200/MF A01 per volume or E99 per entire set CSCL 09C

34 FLUID MECHANICS AND HEAT TRANSFER

Includes boundary layers; hydrodynamics; fluidics; mass transfer; and ablation cooling.

For related information see also *02 Aerodynamics* and *77 Thermodynamics and Statistical Physics.*

N85-34347 British Library Lending Div., Boston Spa (England).
FINDING THE ROOTS OF THE TRANSCENDENTAL EQUATIONS IN PROBLEMS IN DETERMINING THE THERMAL CONDUCTIVITY OF SPHERES WITH HETEROGENEOUS BOUNDARY CONDITIONS
A. D. Gorbunov and E. M. Goldfarb 24 Sep. 1984 9 p Transl. into ENGLISH from Izv. Vyssh. Ucheb. Zaved Chern. Met. (USSR), no. 2, 1984 p 79-83
(BLL-M-35878-(5828.4)) Avail: British Library Lending Div., Boston Spa, Engl.

The mathematics by which quite simple and effective approximate and accurate equations for finding any of the roots of the characteristic equation for calculating the thermal fields in spherical bodies heated by direct flow or counterflow is presented. Examples of the use of the equations are given. They will also make it easier to determine the thermal and physical properties of substances. Author

N85-34348 British Library Lending Div., Boston Spa (England).
CALCULATION OF FLOW KINETICS OF COMPOSITE MEDIA
B. V. Kucheryaev and P. I. Polukhin 4 Sep. 1984 7 p refs Transl. into ENGLISH from Izv. Vysshikh Uchebn. Zavedenii, Chernaya Met. (Moscow), no. 1, 1984 p 57-59
(BLL-M-35819-(5828.4)) Avail: British Library Lending Div., Boston Spa, Engl.

It is demonstrated that, where continuous composite media flow with a monotonic change in the density of the surrounding body, the pattern of three-dimensional change in the density of the surrounded body is independent of time. Formulae are obtained for calculating the kinematic parameters in the flow zone of continuous composite media. Author

N85-34349 British Library Lending Div., Boston Spa (England).
CALCULATION OF ROOTS OF TRANSCENDENTAL EQUATIONS IN PROBLEMS OF DETERMINING THERMAL CONDUCTIVITY OF CYLINDER WITH NON-UNIFORM BOUNDARY CONDITIONS
A. D. Gorbunov and E. M. Goldfarb 14 Aug. 1984 9 p refs Transl. into ENGLISH from Izv. Vysshikh Uchebn. Zavedenii, Chernaya Met. (Moscow), no. 12, 1983 p 94-97
(BLL-M-35788-(5828.4)) Avail: British Library Lending Div., Boston Spa, Engl.

A procedure was developed for solving transcendental equations containing Bessel functions. Formulae were obtained for determining the roots of the characteristic equation with using tables for Bessel functions. These formulae can be used to calculate the temperature fields during heating of cylinders in parallel-current flow and countercurrent flow with non-uniform boundary conditions. Author

N85-34350*# National Aeronautics and Space Administration. Langley Research Center, Hampton, Va.
A REVIEW OF SPECTRAL METHODS Final Report
Liviu Lustman Dec. 1984 28 p refs
(Contract NAS1-17070)
(NASA-CR-172502; ICASE-84-59; NAS 1.26:172502) Avail: NTIS HC A03/MF A01 CSCL 20D

An outline for spectral methods for partial differential equations is presented. The basic spectral algorithm is defined, collocation are emphasized and the main advantage of the method, the infinite order of accuracy in problems with smooth solutions are discussed. Examples of theoretical numerical analysis of spectral calculations are presented. An application of spectral methods to transonic flow is presented. The full potential transonic equation is among the best understood among nonlinear equations. E.A.K.

N85-34351*# National Aeronautics and Space Administration. Langley Research Center, Hampton, Va.
EXPERIMENTAL AERODYNAMIC HEATING TO SIMULATED SPACE SHUTTLE TILES IN LAMINAR AND TURBULENT BOUNDARY LAYERS WITH VARIABLE FLOW ANGLES AT A NOMINAL MACH NUMBER OF 7 M.S. Thesis - George Washington Univ., Nov. 1983
Don E. Avery Aug. 1985 50 p refs Original contains color illustrations
(NASA-TP-2307; L-15781; NAS 1.60:2307) Avail: NTIS HC A03/MF A01 CSCL 20D

The heat transfer to simulated shuttle thermal protection system tiles was investigated experimentally by using a highly instrumented metallic thin wall tile arranged with other metal tiles in a staggered tile array. Cold wall heating rate data for laminar and turbulent flow were obtained in the Langley 8 foot high Temperature Tunnel at a nominal Mach number of 7, a nominal total temperature of 3300R, a free stream unit Reynolds number from 3.4 x 10 sup 5 to 2.2 10 sup 6 per foot, and a free stream dynamic pressure from 2.1 to 9.0 psia. Experimental data are presented to illustrate the effects of flow angularity and gap width on both local peak heating and overall heating loads. For the conditions of the present study, the results show that localized and total heating are sensitive to changes in flow angle only for the test conditions of turbulent boundary layer flow with high kinetic energy and that a flow angle from 30 deg to 50 deg will minimize the local heating. NASA

N85-34352*# Texas A&M Univ., College Station.
A THEORETICAL STUDY OF NON-ADIABATIC SURFACE EFFECTS FOR A MODEL IN THE NTF CRYOGENIC WIND TUNNEL Contractor Report, 1 Oct. 1983 - 31 Jan. 1985
J. Michael Macha, L. A. Pare, and D. B. Landrum Washington NASA 1985 59 p refs
(Grant NAG1-417)
(NASA-CR-3924; NAS 1.26:3924; TR-83-4975-02) Avail: NTIS HC A04/MF A01 CSCL 20D

A theoretical analysis was made of the severity and effect of nonadiabatic surface conditions for a model in the NTF cryogenic wind tunnel. The nonadiabatic condition arises from heaters that are used to maintain a constant thermal environment for instrumentation internal to the model. The analysis was made for several axi-symmetric representations of a fuselage cavity, using a finite element heat conduction code. Potential flow and boundary layer codes were used to calculate the convection condition for the exterior surface of the model. The results of the steady state analysis show that it is possible to maintain the surface temperature very near the adiabatic value, with the judicious use of insulating material. Even for the most severe nonadiabatic condition studied, the effects on skin friction drag and displacement thickness were only marginally significant. The thermal analysis also provided an estimate of the power required to maintain a specified cavity temperature. Author

N85-34353*# Wisconsin Univ., Milwaukee. Dept. of Mechanical Engineering.
A STUDY OF THE SECOND AND THIRD ORDER CLOSURE MODELS OF TURBULENCE FOR PREDICTION OF SEPARATED SHEAR FLOWS
R. S. Amano Aug. 1985 38 p refs
(Grant NAG3-546)
(NASA-CR-176127; NAS 1.26:176127) Avail: NTIS HC A03/MF A01 CSCL 20D

The hybrid model of the Reynolds-stress turbulence closure is tested for the computation of the flows over a step and disk. Here it is attempted to improve the redistributive action of the turbulence energy among the Reynolds stresses. By evaluating the existing models for the pressure-strain correlation, better coefficients are obtained for the prediction of separating shear flows. Furthermore, the diffusion rate of the Reynolds stresses is

reevaluated adopting several algebraic correlations for the triple-velocity products. The models of Cormack et al., Daly-Harlow, Hanjalic-Launder, and Shir were tested for the reattaching shear flows. It was generally observed that all these algebraic models give considerably low values of the triple-velocity products. This is attributed to the fact that none of the algebraic models can take the convective effect of the triple-velocity products into account in the separating shear flows, thus resulting in much lower diffusion rate than Reynolds stresses. In order to improve the evaluation of these quantities correction factors are introduced based on the comparison with some experimental data. R.J.F.

N85-34354*# Syracuse Univ., N. Y. Dept. of Mechanical and Aerospace Engineering.

UNSTEADY TRANSONIC HEAT TRANSFER IN A TRANSIENT FACILITY Semiannual Progress Report

J. E. LaGraff 1 Sep. 1985 8 p

(Grant NAG3-621)

(NASA-CR-176145; NAS 1.26:176145) Avail: NTIS HC A02/MF A01 CSCL 20D

A facility for making heat transfer measurements on solid surfaces using transient techniques is constructed. The facility being constructed is a Ludweig tube with isentropic compression heating (LICH tube). The work completed is detailed as is the work remaining in order to complete the facility and make useful heat transfer measurements. The scope of the project is briefly discussed along with an overall appraisal of the progress. Author

N85-34355*# National Aeronautics and Space Administration. Langley Research Center, Hampton, Va.

NOZZLE WALL ROUGHNESS EFFECTS ON FREE-STREAM NOISE AND TRANSITION IN THE PILOT LOW-DISTURBANCE TUNNEL

Theodore R. Creel, Jr., Ivan E. Beckwith, and Fang-Jenq Chen (High Technology Corp.) Sep. 1985 34 p refs Original contains color illustrations

(NASA-TM-86389; L-15903; NAS 1.15:86389) Avail: NTIS HC A03/MF A01 CSCL 20D

An investigation at Mach 3.5 into the effects of nozzle wall roughness on free stream pressure fluctuations and cone transition Reynolds numbers was conducted in the pilot low disturbance tunnel at the Langley Research Center. Nozzle wall roughness caused by either particle deposits or imperfections in surface finish increased free stream noise levels and reduced the transition Reynolds numbers on a cone mounted in the test rhombus.

Author

N85-34356*# National Aeronautics and Space Administration. Lewis Research Center, Cleveland, Ohio.

REFRIGERATED DYNAMIC SEAL TO 6.9 MPa (1000 PSI)

R. C. Hendricks, R. L. Mullen (Case Western Reserve Univ.), and M. J. Braun (Akron Univ.) 1985 17 p refs Presented at the Cryogenic Eng. Conf. and Internal Cryogenic Mater. Conf., Cambridge, Mass., 12-16 Aug. 1985; sponsored by CEC/ICMC and NBS

(NASA-TM-87108; E-2708; NAS 1.15:87108) Avail: NTIS HC A02/MF A01 CSCL 11A

The self sealing, high shear flow passage approach which was extended to large pressure differences was studied. In a refrigerated seal the fluid to be sealed flows through a refrigerated housing or constriction. The fluid can be frozen to the housing during the transient phase. Under steady state conditions the refrigerated seal proves to be a dynamic low leakage seal. The concept is extended to pressure differences of 6.9 MPa. E.A.K.

N85-34357*# National Aeronautics and Space Administration. Lewis Research Center, Cleveland, Ohio.

SURFACE TEMPERATURE DISTRIBUTION ALONG A THIN LIQUID LAYER DUE TO THERMOCAPILLARY CONVECTION

Chun-Liang Lai (NAS-NRC) and An-Ti Chai 1985 14 p refs Proposed for presentation at the 36th Intern. Astronautical Congr., Stockholm, 7-12 Oct. 1985; sponsored by the International Astronautical Federation

(NASA-TM-87115; E-2715; NAS 1.15:87115; IAG-85-282) Avail: NTIS HC A02/MF A01 CSCL 20D

The surface temperature distributions due to thermocapillary convections in a thin liquid layer with heat fluxes imposed on the free surface were investigated. The nondimensional analysis predicts that, when convection is important, the characteristics length scale in the flow direction L, and the characteristic temperature difference delta T sub o can be represented by L and delta T sub o approx. (A2Ma)/1/4 delta T sub R, respectively, where L sub R and delta sub R are the reference scales used in the conduction dominant situations with A denoting the aspect ratio and Ma the Marangoni number. Having L and delta sub o defined, the global surface temperature gradient delta sub o/L, the global thermocapillary driving force, and other interesting features can be determined. Numerical calculations involving a Gaussian heat flux distribution are presented to justify these two relations. E.A.K.

N85-34358*# National Aeronautics and Space Administration. Ames Research Center, Moffett Field, Calif.

A THREE-DIMENSIONAL TURBULENT BOUNDARY LAYER UNDERGOING TRANSVERSE STRAIN AND STREAMWISE PRESSURE GRADIENT

Sheshagiri K. Hebbar and David M. Driver Aug. 1985 41 p refs (NASA-TM-86768; Rept-85323; NAS 1.15:86768) Avail: NTIS HC A03/MF A01 CSCL 20D

Results from an experimental investigation designed to provide data on both mean and turbulence quantities in the axisymmetric, swirling boundary layer (with and without pressure gradient) flowing over a stationary cylinder downstreams of a spinning cylindrical section are presented. The pressure gradient was introduced into the flow field by a 25.4 mm-high, forward-facing, circular step mounted on the stationary cylinder, the step height being nearly equal to the thickness of the approaching boundary layer. All the measurements were made at a nominal upstream reference Reynolds number of 2.4 x 10 to the 6th power/m (corresponding to an upstream reference velocity of 36 to 37 m/sec) with the rotation of the spinner set to make its peripheral speed equal the reference velocity. The data reported included measurements of surface pressure and the mean surface shear-stress vector taken with a miniature, directional, surface-fence gage. These measurements were supplemented by oil-flow visualization studies of the stationary cylinder. The data indicates that the streamwise pressure gradient controls the development of the streamwise component of wall shear, but leaves the peripheral component of wall shear practically unaffected. B.W.

N85-34359# Sandia Labs., Albuquerque, N. Mex.

TECHNICAL ASSESSMENT OF THERMAL-HYDRAULICS FOR HIGH HEAT FLUX FUSION COMPONENTS

R. D. Boyd, C. P. C. Wong (GA Technologies, Inc.), and Y. S. Cha (Argonne National Lab., Argonne, Ill.) Jan. 1985 77 p refs (Contract DE-AC04-76DP-00789)

(DE85-013178; SAND-84-0159) Avail: NTIS HC A05/MF A01

A technical assessment of three possible thermal-hydraulic high heat flux (HHF) heat removal techniques which will result in adequate heat removal from fusion components with minimum penalty is presented. The heat removal alternatives discussed are: (1) subcooled flow boiling (SFB) with water; (2) high velocity helium gas convection (HGC); and (3) liquid metal (LM) heat transfer in the presence of a transverse magnetic field (TM). Each heat removal technique is examined for a case study applicable to near-term fusion components such as limiters and divertors. The results can be used, along with other fusion component performance constraints, to determine the research and development direction of generic problems such as HHF removal from fusion components in both near-term or existing fusion reactors and long-term or proposed reactors. Specifically, comparisons are made for the selected case study of heat removal from a 1.5 m long, 1.0 cm diameter (inside) coolant channel which is subjected to a uniform steady-state heat flux of 0.5 kW/cm(2). The results show that SFB has the greatest heat removal capability, with the lowest

coolant channel wall temperature and pumping power, followed by HGC and LMTM. DOE

N85-34360# Sandia Labs., Albuquerque, N. Mex.
PRELIMINARY SPR THERMAL MODEL DESCRIPTION AND RESULTS FOR WH-11 AND BM-4
D. Tomasko May 1985 41 p refs
(Contract DE-AC04-76DP-00789)
(DE85-013171; SAND-84-1957) Avail: NTIS HC A03/MF A01

Fluid temperatures within the Strategic Petroleum Reserve caverns are calculated using a modified one-dimensional, time-dependent Rahm-Walin equation coupled to a two-dimensional, time-dependent heat conduction equation in the salt massif. Comparisons of model results with experimental data from West Hackberry Cavern 11 and Bryan Mound Cavern 4 are very good for up to eight years of cavern life. DOE

N85-34361# California Univ., Livermore. Lawrence Livermore Lab.
COMPRESSIBLE TWO-PHASE FLOW INSTABILITIES SIMULATED WITH A HYBRID LAGRANGE-EULER PSEUDOSPECTRAL METHOD
A. C. Buckingham 29 Mar. 1985 13 p Presented at 4th Intern. Conf. on Numerical Methods in Laminar and Turbulent Flow, Swansea, Wales, 8 Jul. 1985
(Contract W-7405-eng-48)
(DE85-009904; UCRL-91617; CONF-850745-6) Avail: NTIS HC A02/MF A01

A pseudospectral collocation procedure has been developed specifically for studying unsteady, compressible flow instability growth and subsequent random flow states signaling turbulence onset. A mass centered Lagrange moving mesh is used for resolving compressibility and material interfaces. The Lagrange mesh is combined with a fixed Eulerian mesh over which spanwise components are resolved with a special transform method. Time evolution is approximated by means of a conventional third-order Runge Kutta procedure. A Rayleigh-Taylor unstable liquid propellant gas vapor interface situation is simulated during the initial growth phase of the perturbation. The influence of super-imposed pressure oscillations on the fuel sheet breakup is examined. DOE

N85-34362# Michigan State Univ., East Lansing.
SEQUENTIAL REGULARIZATION SOLUTION OF THE INVERSE HEAT CONDUCTION PROBLEM
J. V. Beck, B. F. Blackwell (Sandia National Labs., Albuquerque, N. Mex.), and C. R. St.Clair, Jr. 1985 12 p refs Presented at the 4th Intern. Conf. on Numerical Methods in Laminar and Turbulent Flow, Swansea, England, 8 Jul. 1985
(Contract DE-AC04-76DP-00789)
(DE85-010657; SAND-84-2272C; CONF-850745-4) Avail: NTIS HC A02/MF A01

The Inverse Heat Conduction Problem (IHCP) is defined and a sequential regularization solution is presented. Although the algorithm is developed specifically for the first-order regularization procedure, it can be extended to any order. Example calculations are presented for both the whole domain and sequential methods; similar results can be obtained for both methods. The impact of random temperature errors is also investigated. The conclusion is that the sequential procedure is much more computationally efficient and yields nearly as accurate results as the whole domain procedure. DOE

N85-34363# Argonne National Lab., Ill.
BLOCK-IMPLICIT CALCULATIONS OF THREE-DIMENSIONAL LAMINAR FLOW IN STRONGLY CURVED DUCTS
S. P. Vanka 1985 11 p refs Presented at the 21st AIAA/ASME/SAE Joint Propulsion Conf., Monterey, Calif., 8 Jul. 1985
(Contract W-7405-eng-38)
(DE85-003047; CONF-850712-2) Avail: NTIS HC A02/MF A01

The understanding of flow development in ducts with longitudinal curvature is of interest in the design of aircraft intakes, turbomachinery passages, and heat exchange equipment. The numerical solution of the elliptic partial differential equations governing three dimensional fluid flow in strongly curved rectangular ducts by the use of a fully coupled block implicit solution algorithm is described. Calculations were made for the configuration of Humphrey et al. It is observed that the coupled solution of the momentum and continuity equation converges rapidly and reduces the required computing time by a factor of two and a half over a decoupled solution such as that by Humphrey et al. The flowfield calculated here is in good agreement with the experimental data and with previous calculations. The flow separation on the outer side wall is well predicted, in conformity with earlier observations. DOE

N85-34364# New York Univ., New York. Mathematics and Computing Lab.
STABILITY OF TWO-DIMENSIONAL IMMISCIBLE FLOW TO VISCOUS FINGERING
M. J. King, W. B. Lindquist, and L. Reyna Mar. 1985 41 p
(Contract DE-AC02-76ER-03077)
(DE85-011403; DOE/ER-03077/244) Avail: NTIS HC A03/MF A01

The stability of incompressible, gravity free, immiscible two phase flow to viscous fingering is studied numerically. In contrast to numerical studies in the literature, but in good qualitative agreement with laboratory studies, a large parameter regime for which the displacement is strongly unstable is found. The parameter space examined includes mobility ratio, capillary pressure strength, size of perturbation, and heterogeneity of the medium. DOE

N85-34365# Rockefeller Univ., New York. Lab. for Laser Energetics.
THERMAL TRANSPORT MEASUREMENTS OF UV LASER IRRADIATED SPHERICAL TARGETS
P. A. Jaanimagi, J. Delletrez, B. L. Henke, and M. C. Richardson [1985] 36 p refs
(Contracts DE-FC08-85DP-40200; DE-AS08-82DP-40175)
(DE85-011038; DOE/DP-40200/T1) Avail: NTIS HC A03/MF A01

New measurements are presented of thermal transport in spherical geometry using time-resolved X-ray spectroscopy. The time dependence of the mass ablation rate m(dot) was determined by following the progress of the ablation surface through thin layers of material embedded at various depths below the surface of the target. These measurements made with 6 and 12 UV (351 nm) beams from OMEGA are compared to previous thermal transport data and are in qualitative agreement with detailed LILAC hydrodynamic code simulations which predict a sharp decrease in m(dot) after the peak of the laser pulse. Non-uniform laser irradiation of the target results in the anomalously high values of m(dot) measured in these experiments. DOE

N85-34366# Los Alamos Scientific Lab., N. Mex.
VAPOR PHASE HEAT TRANSPORT CONCEPTS
D. A. Neeper and J. C. Hedstrom 1985 8 p refs Presented at the Solar Bldgs.: Realities for Today - Trends for Tomorrow, Washington, D.C., 18 Mar. 1985
(Contract W-7405-eng-36)
(DE85-009550; LA-UR-85-887; CONF-850388-4) Avail: NTIS HC A02/MF A01

The evolution of the vapor transport concept is briefly discussed. Some of the previous vapor transport designs are presented and include: a vertical collector operating in the percolating mode, a heat pipe, and a self pumping system. The importance of the heat transfer from the accumulation is considered. Two accumulators are used in conjunction with a solar collector and a condenser in the new vapor system. This new system requires no external cooling and a schematic diagram of the system is provided. DOE

N85-34367# California Univ., Livermore. Lawrence Livermore Lab.
NEW SEMI-IMPLICIT METHOD FOR SOLVING THE TIME-DEPENDENT CONSERVATION EQUATIONS FOR INCOMPRESSIBLE FLOW

P. M. Gresho and S. T. Chan Apr. 1985 21 p refs Presented at the 4th Intern. Conf. on Numerical Methods in Laminar and Turbulent Flow, Swansea, England, 8 Jul. 1985
(Contract W-7405-eng-48)
(DE85-010926; UCRL-92505; CONF-850745-5) Avail: NTIS HC A02/MF A01

A semiimplicit time integration scheme for the advection diffusion equation, in which the advection terms are stepped forward in time using explicit Euler and the diffusion terms, which include a truncation error correction term, are integrated via the trapezoid rule, is described and demonstrated. In the extension to the Navier-Stokes and Boussinesq equations, all additional terms are integrated via explicit Euler. DOE

N85-34368# California Univ., Berkeley. Lawrence Berkeley Lab.
DETAILED VALIDATION OF A LIQUID AND HEAT FLOW CODE AGAINST FIELD PERFORMANCE
C. F. Tsang and C. Doughty Feb. 1985 21 p refs Presented at the 8th SPE Symp. on Reservoir Simulation, Dallas, 10 Feb. 1985
(Contract DE-AC03-76SF-00098)
(DE85-009901; LBL-18833; CONF-850270-1) Avail: NTIS HC A02/MF A01

The numerical code PT, which calculated liquid and heat flow in a saturated porous or fractured porous medium, was validated against a series of field experiments involving the injection and subsequent production of hot water into a confined aquifer. The layered structure of the aquifer and strong buoyancy effects, indicating highly coupled liquid and heat flows, provide a stringent test of the code's ability to model the real world. DOE

N85-34369# Argonne National Lab., Ill.
MATHEMATICAL MODELING OF ULTIMATE HEAT SINK COOLING PONDS
A. J. Policastro, M. Wastag, W. E. Dunn, J. Leylak, F. Gavin, and R. A. Carhart Mar. 1985 274 p refs Prepared in cooperation with Illinois Univ., Urbana
(Contract NRC-FIN-A-2238)
(TI85-009747; NUREG/CR-4120) Avail: NTIS HC A12/MF A01

A general treatment of ultimate heat sink (UHS) cooling pond thermal performance is proposed through the application of a three-dimensional grid model. Validation of the model has been shown through comparisons of predictions with data from a field and laboratory pond. The advantage of the model lies in its ability to determine the detailed character of the flow field whether it be one, two, or three dimensional. Existing models require a priori knowledge of the character and dimensionality of the flow field in such ponds. Application of the model to a prototype UHS pond revealed that the balance of physical mechanisms involved in the thermal hydraulics of these ponds is quite different than for ponds used in normal cooling. The small, heavily-loaded, irregularly-shaped nature of the UHS pond should, in many cases, lead to a vertically mixed pond with only a one-dimensional (longitudinal) variation in pond temperature. DOE

N85-34370# California Inst. of Tech., Pasadena. Graduate Aeronautical Labs.
EFFECTS OF AMBIENT PRESSURE ON THE INSTABILITY OF A LIQUID BOILING EXPLOSIVELY AT THE SUPERHEAT LIMIT
B. Sturtevant and D. Frost 1984 10 p refs Presented at the Session on Fundamentals of Phase Change: Boiling and Condensation of the ASME Winter Ann. Meeting, 9-14 Dec. 1984 Submitted for publication
(Contract DE-AT03-80ER-10634)
(DE85-009476; CONF-841201-32-App) Avail: NTIS HC A02/MF A01

The effect of ambient pressure on the intrinsic instability of rapid vaporization in single droplets boiling explosively at the limit of superheat has been studied experimentally and theoretically. In a series of experiments with pentane, isopentane and ethyl ether in a bubble-column apparatus it has been shown that the baroclinic interfacial instability may be suppressed by increasing the ambient pressure. High-speed microphotography shows that, while at atmospheric pressure bubble boundaries are rough and opaque, at elevated pressure the liquid-vapor interface is smooth and transparent. Pressure measurements show that the radiated pressure field is two orders of magnitude smaller from stabilized bubbles than from unstable. At intermediate pressures bubble growth occurs in two stages, first stable then unstable. The transitional regime between unstable and stable vaporization provides convenient conditions or exhibiting many features of unstable vaporization. DOE

N85-34371# Edgerton, Germeshausen and Grier, Inc., Idaho Falls, Idaho.
FORCED CONVECTIVE, NONEQUILIBRIUM, POST-CHF HEAT TRANSFER EXPERIMENT DATA AND CORRELATION COMPARISON REPORT
Richard C. Gottula, Keith G. Condie, Ramu K. Sundaram (Yankee Atomic Electric Co.), Sudhakar Neti (Lehigh Univ.), John C. Chen (Lehigh Univ.), and Ralph A. Nelson Mar. 1985 551 p refs
(Contracts DE-AC07-76ID-01570; NRC-FIN-A-6043)
(TI85-009331; NUREG/CR-3193; EGG-2245) Avail: NTIS HC A24/MF A01

Forced convective, postcritical heat flux heat transfer experiments with water flowing upward in a vertical tube have been conducted at the Idaho National Engineering Laboratory. Thermodynamic nonequilibrium in the form of superheated vapor temperatures was measured at a maximum of three different axial levels. Steady state experiments were conducted at pressures of 0.2 to 0.7 MPa, mass fluxes of 12 to 24 kg/sq ms, heat fluxes of 7.7 to 27.5 kW/sq m, and test section inlet qualities of 38 to 64%. Quasi-steady state (slow moving quench front) experiments were conducted at pressures of 0.4 to 7 MPa, mass fluxes of 12 to 70 kg/sq/s heat fluxes of 8 to 225 kW/sq m, and test section inlet qualities of -7 to 47%. The multiple probe data and the data taken above 0.4 MPa are new data in parameter ranges not previously obtained. Comparison of the data with current vapor generation models and wall heat transfer models yielded unsatisfactory results. This is attributed to the effects of nonequilibrium, quench front quality, and distance from the quench front, which are factors not included in the current models compared. DOE

N85-34372# Oak Ridge National Lab., Tenn.
ADVANCED HEAT PUMP RESEARCH AND DEVELOPMENT
Michael A. Kuliasha 1985 11 p refs Presented at the Energy Technol. Conf. and Exposition, Washington, D.C., 25-27 Mar. 1985
(Contract DE-AC05-84OR-21400)
(DE85-009540; CONF-850301-3) Avail: NTIS HC A02/MF A01

The Office of Building Energy Research and Development of the U.S. Department of Energy (DOE), has been funding R&D in advanced heat pumps and appliances since 1976. Much of that research has been managed for DOE by the Oak Ridge National Laboratory (ORNL). The objective of the Building Equipment Research (BER) program at ORNL has been to generate new concepts and develop a technology base for improving the energy efficiency and load characteristics of energy conversion equipment used in residential and commercial buildings. The research being pursued to achieve these objectives falls under three general areas: thermally activated heat pumps (TAHP), refrigeration systems, and building equipment systems. The TAHP work is concentrated on three technologies: (1) absorption heat pumps; (2) Stirling engine-driven heat pumps; and (3) internal combustion (IC) engine-driven heat pumps. Major project areas in refrigeration systems research include electric heat pumps, ground-coupled heat pumps, and refigerant mixtures. In the building equipment systems areas, project areas include advanced distribution systems, advanced insulation for appliances, and commercial building equipment. DOE

N85-34679# Tokyo Univ. (Japan).
SIMULATION OF INSTABILITY OF CYLINDRICALLY CONVERGING SHOCK WAVES
Toshiaki Itoh and Kanji Abe *In* Nagoya Univ. Workshop Rept. on Simulation Tech. for Shock Wave Phenomena and Characteristics of Plasma in Inertial Confinement Fusion Mar. 1985 p 115-119

refs (For primary document see N85-34670 23-75)
Avail: NTIS HC A11/MF A01

35 INSTRUMENTATION AND PHOTOGRAPHY

Includes remote sensors; measuring instruments and gages; detectors; cameras and photographic supplies; and holography.

For aerial photography see *43 Earth Resources.* For related information see also *06 Aircraft Instrumentation,* and *19 Spacecraft Instrumentation.*

N85-34373* National Aeronautics and Space Administration. Pasadena Office, Calif.
INSTRUMENTATION FOR SENSING MOISTURE CONTENT OF MATERIAL USING A TRANSIENT THERMAL PULSE Patent
Lien C. Yang, inventor (to NASA) (JPL, Pasadena, Calif.) Issued 6 Aug. 1985 8 p Continuation of abandoned US-Patent-Appl-SN-325885 filed 30 Nov. 1981
(NASA-Case-NPO-15493-2; US-Patent-4,532,797;
US-Patent-Appl-SN-563890; US-Patent-Class-73-75;
US-Patent-Class-324-65-P; NAS 1.71:NPO-15493-2) Avail: US Patent and Trademark Office CSCL 14B

Instrumentation for sensing moisture content of material using a transient thermal pulse is comprised of a sensing probe having a sensing element in the form of a ribbon excited by a constant current pulse from a source to increase the temperature and therefore the resistance of the ribbon linearly. Moisture in web material will limit the increase of temperature during the pulse in proportion to the moisture content. This increase in temperature produces a proportional increase in resistivity which is measured with a wheatstone bridge as a change in voltage displayed by a measurement display unit. The probe is glued in a shallow groove of a Lucite bar and connected to copper pins embedded in the bar. Official Gazette of the U.S. Patent and Trademark Office

N85-34374* National Aeronautics and Space Administration. Ames Research Center, Moffett Field, Calif.
MODULATED VOLTAGE METASTABLE IONIZATION DETECTOR Patent
Glenn C. Carle, Daniel R. Kojiro, and Donald E. Humphrey, inventors (to NASA) Issued 27 Aug. 1985 10 p Filed 22 Feb. 1984 Supersedes N84-23093 (22 - 13, p 2019)
(NASA-Case-ARC-11503-1; US-Patent-4,538,066;
US-Patent-Appl-SN-582643; US-Patent-Class-250-374;
US-Patent-Class-250-379) Avail: US Patent and Trademark Office CSCL 14B

The output current from a metastable ionization detector (MID) is applied to a modulation voltage circuit. An adjustment is made to balance out the background current, and an output current, above background, is applied to an input of a strip chart recorder. For low level concentrations, i.e., low detected output current, the ionization potential will be at a maximum and the metastable ionization detector will operate at its most sensitive level. When the detected current from the metastable ionization detector increases above a predetermined threshold level, a voltage control circuit is activated which turns on a high voltage transistor which acts to reduce the ionization potential. The ionization potential applied to the metastable ionization detector is then varied so as to maintain the detected signal level constant. The variation in ionization potential is now related to the concentration of the constituent and a representative amplitude is applied to another input of said strip chart recorder.
Official Gazette of the U.S. Patent and Trademark Office

N85-34375* National Aeronautics and Space Administration. Langley Research Center, Hampton, Va.
TENSILE TESTING APPARATUS Patent
Linda B. Blackburn and John R. Ellingsworth, inventors (to NASA) Issued 20 Aug. 1985 10 p Filed 19 Mar. 1984 Supersedes N84-20804 (22 - 11, p 1656)
(NASA-Case-LAR-13243-1; US-Patent-4,535,636;
US-Patent-Appl-SN-590923; US-Patent-Class-73-831;
US-Patent-Class-73-856) Avail: US Patent and Trademark Office CSCL 14B

An improved mechanical extensometer is described for use with a constant load creep test machine. The dead weight of the extensometer is counterbalanced by two pairs of weights connected through a pulley system and to rod extension and leading into the furnace where the test sample is undergoing elevated temperature (above 500 F.) tensile testing. Novel gripper surfaces, conical tip and flat surface are provided in each sampling engaging platens to reduce the grip pressure normally required for attachment of the extensometer to the specimen and reduce initial specimen bending normally associated with foil-gage metal testing.
Official Gazette of the U.S. Patent and Trademark Office

N85-34376*# KMS Fusion, Inc., Ann Arbor, Mich.
MODULAR DIGITAL HOLOGRAPHIC FRINGE DATA PROCESSING SYSTEM Final Report
James G. Downward, Pamela C. Vavra, Frederick S. Schebor, and Charles M. Vest (Michigan Univ.) Jun. 1985 53 p refs
(Contract NAS1-17945)
(NASA-CR-177952; NAS 1.26:177952) Avail: NTIS HC A04/MF A01 CSCL 14E

A software architecture suitable for reducing holographic fringe data into useful engineering data is developed and tested. The results, along with a detailed description of the proposed architecture for a Modular Digital Fringe Analysis System, are presented.
Author

N85-34377*# Allied Bendix Aerospace, Mishawaka, Ind. Guidance Systems Div.
HARDWARE TEST PROGRAM FOR EVALUATION OF BASELINE RANGE-RANGE RATE SENSOR CONCEPT
E. R. Feagler Aug. 1985 119 p
(Contract NAS8-36144)
(NASA-CR-176143; NAS 1.26:176143; BGSD-MO-7035) Avail: NTIS HC A06/MF A01 CSCL 14B

During the past two and one-half years Bendix has been working with Marshall Space Flight Center (MSFC) on the conceptual design of an on-board sensor for application with the Orbital Maneuvering Vehicle (OMV). The proposed Range and Range Rate (R/R) sensor would aid the OMV in performing rendezvous and docking maneuvers by providing independent measurements of range, range rate, and bearing to a designated spacecraft target. The hardware Test Program was proposed as one of the steps of a development program which has the objective of providing the space qualified sensor required for this application. Through a series of analyses, to establish systems requirements and design definition, hardware modifications of Bendix brassboard radars to appropriate test bed configuration, and hardware testing, the program is designed to reduce technical risks associated with the R/R sensor design concept. A one-third scale model of the Hubble Space Telescope will be used as the target for these tests. Data generated by this signature measurements program will be utilized in formulating tracking algorithms for the extended target signature characteristic. R.J.F.

N85-34378*# National Aeronautics and Space Administration. Ames Research Center, Moffett Field, Calif.
PRACTICAL ASPECTS OF LASER HOLOGRAPHIC INTERFEROMETRY IN WIND TUNNELS
Joseph Licursi and George Lee Sep. 1985 13 p refs
(NASA-TM-86788; Rept-85365; NAS 1.15:86788) Avail: NTIS HC A02/MF A01 CSCL 14B

Practical aspects of using laser holographic interferometry in some NASA Ames wind tunnels are presented. These aspects include the development of techniques for dual-plate interferometry, optics alignment, and laser alignment. In addition, methods to alleviate problems associated with vibration, photographic processing, photographic drying, and photographic reconstruction are discussed. Author

N85-34379*# National Aeronautics and Space Administration. Ames Research Center, Moffett Field, Calif.
NONSIMULTANEOUS COUPLED LASER VELOCIMETER MEASUREMENT TECHNIQUE: ERROR PREDICTION FOR SPATIALLY NONCOINCIDENT MEASUREMENTS
Michael S. Reinath Aug. 1985 47 p refs
(NASA-TM-86718; Rept-85217; NAS 1.15:86718) Avail: NTIS HC A03/MF A01 CSCL 14B

A technique for obtaining orthogonal velocity components from nonorthogonal measurements using the NASA Ames Research Center Long-Range Laser Velocimeter (LRLV) is briefly discussed. A description is then presented of the error that occurs when these nonorthogonal measurements are spatially noncoincident because of positioning inaccuracies, and equations are developed for predicting this error. Sample data are presented and a prediction of the expected error for two typical applications is made. To cover other cases in general, a parametric study is conducted and the results are presented in a tabular format.
Author

N85-34380# Yale Univ., New Haven, Conn. Applied Physics Section.
RESEARCH ON GYROTRONS Final Report
J. L. Hirshfield 15 Apr. 1985 265 p refs
(Contract N00014-80-C-0075; NR Proj. 632-001)
(AD-A154032) Avail: NTIS HC A12/MF A01 CSCL 09/1

A summary is given of research on gyrotron-like mechanisms for amplifying or generating electromagnetic radiation. These mechanisms include slow-wave cyclotron-wave amplification in a dielectrically-loaded waveguide, cyclotron harmonic oscillations in a quasi-optical millimeter-wave structure, a quasi-optical gyroklystron, and cyclotron harmonic amplification in irregular cross section waveguides. Both linearized theory and experimental observations are described.
DOE

N85-34381# Department of the Air Force, Washington, D.C.
ROTOR BLADE TEST APPARATUS Patent Application
E. C. Taschner, inventor (to Air Force) Filed 24 May 1985 13 p
(AD-D011725; US-Patent-Appl-SN-737377) Avail: NTIS HC A02/MF A01 CSCL 14/2

This patent application discloses a rotor blade test apparatus having a striking solenoid to strike a rotor blade to generate an audio signal. A microphone receives the audio signal and applies it to a spectrum analyzer wherein the predominant natural frequencies of the rotor blade are determined.
GRA

N85-34382# Oak Ridge National Lab., Tenn.
THE 1983 INTERNATIONAL INTERCOMPARISON OF NUCLEAR ACCIDENT DOSIMETRY SYSTEMS AT OAK RIDGE NATIONAL LABORATORY
R. E. Swaja, R. T. Greene, and C. S. Sims Apr. 1985 42 p
(Contract DE-AC05-84CR-21400)
(DE85-011303; ORNL-6164) Avail: NTIS HC A03/MF A01

An international intercomparison of nuclear accident dosimetry systems was conducted during September 12 to 16, 1983, at Oak Ridge National Laboratory (ORNL) using the Health Physics Research Reactor operated in the pulse mode to simulate criticality accidents. Participants measured neutron and gamma doses at area monitoring stations and on phantoms for three different shield conditions. Results indicate that foil activation techniques are the most popular and accurate method of determining accident level neutron doses at area monitoring stations. For personnel monitoring, foil activation, blood sodium activation, and thermoluminescent (TL) methods are all capable of providing accurate dose estimates in a variety of radiation fields. All participants used TLD's to determine gamma doses with very good results. Chemical dosimeters were also shown to be capable of yielding accurate estimates of total neutron plus gamma doses in a variety of radiation fields. While 83% of all neutron measurements satisfied regulatory standards relative to reference values, only 39% of all gamma results satisfied corresponding guidelines for gamma measurements. Results indicate that continued improvement in accident dosimetry evaluation and measurement techniques is needed.
DOE

N85-34383# Advanced Research and Applications Corp., Sunnyvale, Calif.
NOVETTE DIAGNOSTIC SUPPORT Final Report
R. Cirigliano, E. Franco, I. Koppel, B. Rodrigues, and J. Smith Feb. 1985 193 p
(Contract W-7405-eng-48)
(DE85-012937; UCRL-15672) Avail: NTIS HC A09/MF A01

The primary research areas were the following: (1) contribute X-ray diagnostic, experimental, and data reduction and analysis support for the Novette DANTE X-ray spectrometer experiments. This effort was expanded to improve the overall quality of the Novette data base; (2) experimental and calculational characterization of the X-ray imaging properties of an ellipsoidal X-ray collection optic serving as a sensitivity enhancing component of the Transmission Grating Streak Spectrometer; (3) performance simulation of the X-ray dispersion properties of candidate X-ray laser cavity, normal incidence end mirror optics; (4) contribute X-ray diagnostic, experimental, and data reduction and analysis support for the Novette Henway crystal spectrometer and the MCPIGS microchannel plate intensified grazing incident spectrometer experiments; and (5) perform a technical performance vs cost evaluation of commercially available hardware required to perform the NOVA neutron time of flight experiments.
DOE

N85-34384# State Univ. of New York, Stony Brook. Dept. of Physics.
APPLICATIONS OF HOLOGRAPHY TO X-RAY IMAGING
M. Howells (LBL), M. Iarocci (Brookhaven National Lab.), J. Kenney, H. Rarback (Brookhaven National Lab.), R. Rosser, and W. Yun Mar. 1985 10 p Presented at the Soc. Photo-Opt. Instr. Engr. Symp., Los Angeles, 21 Jan. 1985
(Contracts DE-AC02-76CH-00016; DE-AC03-76SF-00098)
(DE85-010984; LBL-19319; CONF-850137-3) Avail: NTIS HC A02/MF A01

Various applications of holographic techniques to the problem of soft X-ray imaging are considered. Special attention is given to imaging biological material using X-rays in the wavelength range 24 to 45A. Some experiments on formation and reconstruction of X-ray holograms are described and ways in which holographic techniques might contribute to the difficult problem of fabricating optical elements for use in the soft X-ray region are proposed.
DOE

N85-34385# TRW, Inc., Redondo Beach, Calif. Applied Technology Div.
INVESTIGATION OF NON-INTRUSIVE RADIOMETERS FOR ENTRAINED GASIFIER TEMPERATURE MEASUREMENT, REVISION 3 Quarterly Report, 1 Aug. - 31 Oct. 1984
N. Gat 11 Mar. 1985 14 p refs
(Contract DE-AC21-83MC-20468)
(DE85-011795; TRW-SN-39146-Rev-3; QR-4) Avail: NTIS HC A02/MF A01

A nonintrusive radiometer for entrained bed gasifier/combustor temperature measurements was developed and tested. The design, fabrication and testing of radiometers is presented.
DOE

N85-34386# Goodyear Atomic Corp., Piketon, Ohio.
UPGRADING AUXILIARY FACILITY OUTLEAKAGE AND COMBUSTION DETECTION Final Project Report
R. R. Sandman 20 Dec. 1984 11 p
(Contract DE-AC05-76OR-00001)
(DE85-012796; GAT-T-3297) Avail: NTIS HC A02/MF A01

A new GAT preventive maintenance method, IMG-104, patterned after a similar successful procedure in use at the Oak Ridge Gaseous Diffusion Plant, was issued to improve the performance of the specially modified Pyrotronics HF/F2 detectors used in the X-342-A HF vaporizer bay and X-344-C HF storage facilities. Detector thermal protection was added/improved to increase cold weather sensitivity and reduce moisture absorption by the detectors' dibutylamine reagent. Other moisture problems

previously experienced by the X-342-A feed vaporization facility UF6 outleakage/combustion unmodified detectors were eliminated following replacement of the twelve open steam chests with two totally enclosed autoclaves, and installation of a new outleakage/combustion detection system. Practical alternate methods of detecting UF6 outleakage and combustion by-products are discussed, as is substitution of the reagent used in the HF/F2 detectors; however, no changes were recommended. DOE

N85-34387# Department of Energy, Washington, D. C.
APPARATUS AND METHOD FOR THE SPECTROCHEMICAL ANALYSIS OF LIQUIDS USING THE LASER SPARK Patent Application
D. A. Cremers, L. J. Radziemski, inventors (to DOE), and T. R. Loree Filed 1 May 1984 24 p
(DE85-005749; US-Patent-Appl-SN-606037) Avail: NTIS HC A02/MF A01

A method and apparatus are disclosed for the qualitative and quantitative spectroscopic investigation of elements present in a liquid sample using the laser spark. A series of temporally closely spaced spark pairs is induced in the liquid sample utilizing pulsed electromagnetic radiation from a pair of lasers. The light pulses are not significantly absorbed by the sample so that the sparks occur inside of the liquid. The emitted light from the breakdown events is spectrally and temporally resolved, and the time period between the two laser pulses in each spark pair is adjusted to maximize the signal-to-noise ratio of the emitted signals. In comparison with the single pulse technique, a substantial reduction in the limits of detectability for many elements has been demonstrated. Narrowing of spectral features results in improved discrimination against interfering species. DOE

N85-34388# Department of Energy, Washington, D. C.
MULTIPLE-STAGE INTEGRATING ACCELEROMETER Patent Application
H. F. Devaney, inventor (to DOE) Filed 27 Jun. 1984 32 p
(Contract DE-AC04-76DP-00785)
(DE85-006505; US-Patent-Appl-SN-625326) Avail: NTIS HC A03/MF A01

An accelerometer assembly is provided for use in activating a switch in response to multiple acceleration pulses in series. The accelerometer includes a housing forming a chamber. An inertial mass or piston is slidably disposed in the chamber and spring biased toward a first or reset position. A damping system is also provided to damp piston movement in response to first and subsequent acceleration pulses. Additionally, a cam, including a Z-shaped slot, and cooperating follower pin slidably received therein are mounted to the piston and the housing. The middle or cross-over leg of the Z-shaped slot cooperates with the follower pin to block or limit piston movement and prevent switch activation in response to a lone acceleration pulse. The switch of the assembly is only activated after two or more separate acceleration pulses are sensed and the piston reaches the end of the chamber opposite the reset position. DOE

N85-34389# Department of Energy, Washington, D. C.
METHOD FOR DETERMINING DEPTH AND SHAPE OF A SUB-SURFACE CONDUCTIVE OBJECT Patent Application
D. O. Lee, P. C. Montoya, and J. R. Wayland, Jr., inventors (to DOE) Filed 27 Jun. 1984 20 p
(Contract DE-AC04-76DP-00789)
(DE85-006502; US-Patent-Appl-SN-625321) Avail: NTIS HC A02/MF A01

The depth to and size of an underground object may be determined by sweeping a controlled source audio magnetotelluric (CSAMT) signal and locating a peak response when the receiver spans the edge of the object. The depth of the object is one quarter wavelength in the subsurface media of the frequency of the peak. DOE

N85-34390# Department of Energy, Washington, D. C.
IMPROVED FLOW CYTOMETER MEASUREMENT OF BINDING ASSAYS Patent Application
G. C. Saunders, inventor (to DOE) Filed 30 May 1984 21 p
(Contract W-7405-eng-36)
(DE85-006407; US-Patent-Appl-SN-615486) Avail: NTIS HC A02/MF A01

A method of measuring binding assays is carried out with different size particles wherein the binding assay sample is run through a flow cytometer without separating the sample from the marking agent. The amount of a binding reactant present in a sample is determined by providing particles with a coating of binder and also known quantity of smaller particles with a coating of binder reactant. The smaller particles also contain a fluorescent chemical. The particles are combined with the sample and the binding reaction is allowed to occur for a set length of time followed by combining the smaller particles with the mixture of the particles and the sample produced and allowing the binding reactions to proceed to equilibrium. The fluorescence and light scatter of the combined mixture is then measured as the combined mixture passes through a flow cytometer equipped with a laser to bring about fluorescence, and the number of fluorescent events are compared. A similar method is also provided for determining the amount of antigen present in the sample by providing spheres with an antibody coating and some smaller spheres with an antigen coating. DOE

N85-34391# Department of Energy, Washington, D. C.
ACOUSTIC CROSS-CORRELATION FLOWMETER FOR SOLID-GAS FLOW Patent Application
S. H. Sheen and A. C. Raptis, inventors (to DOE) Filed 14 May 1984 14 p
(Contract W-31-109-eng-38)
(DE85-005988; US-Patent-Appl-SN-609685) Avail: NTIS HC A02/MF A01

An apparatus for measuring particle velocity in a solid-gas flow within a pipe is described. It includes: first and second transmitting transducers for transmitting first and second ultrasonic signals into the pipe at first and second locations, respectively, along the pipe; an acoustic decoupler, positioned between said first and second transmitting transducers, for acoustically isolating said first and second signals from one another; first and second detecting transducers for detecting said first and second signals and for generating first and second detected signals; and means for cross-correlating said first and second output signals. DOE

N85-34392# Department of Energy, Washington, D. C.
OXYGEN ANALYZER Patent Application
W. H. Benner, inventor (to DOE) Filed 8 May 1984 19 p
(Contract DE-AC03-76SF-00098)
(DE85-006002; US-Patent-Appl-SN-608282) Avail: NTIS HC A02/MF A01

An oxygen analyzer is described which identifies and classifies microgram quantities of oxygen in ambient particulate matter and for quantitating organic oxygen in solvent extracts of ambient particulate matter. A sample is pyrolyzed in oxygen-free nitrogen gas (N2), and the resulting oxygen quantitatively converted to carbon monoxide (CO) by contact with hot granular carbon (C). Two analysis modes are made possible: (1) rapid determination of total pyrolyzable obtained by decomposing the sample at 1135 C, or (2) temperature-programmed oxygen thermal analysis obtained by heating the sample from room temperature to 1135 C as a function of time. The analyzer basically comprises a pyrolysis tube containing a bed of granular carbon under N2, ovens used to heat the carbon and/or decompose the sample, and a non-dispersive infrared CO detector coupled to a mini-computer to quantitate oxygen in the decomposition products and control oven heating. DOE

N85-34393# Department of Energy, Washington, D. C.
ELECTRONIC IMAGING SYSTEM AND TECHNIQUE Patent Application
J. O. Bolstad, inventor (to DOE) Filed 12 Jun. 1984 17 p refs
(Contract DE-AC07-76ID-01570)
(DE85-005740; US-Patent-Appl-SN-619759) Avail: NTIS HC A02/MF A01

A method and system for viewing objects obscured by intense plasmas or flames (such as a welding arc) includes a pulsed light source to illuminate the object, the peak brightness of the light reflected from the object being greater than the brightness of the intense plasma or flame; an electronic image sensor for detecting a pulsed image of the illuminated object, the sensor being operated as a high-speed shutter; and electronic means for synchronizing the shutter operation with the pulsed light source. DOE

N85-34394# Systems Designers Ltd., Farnsborough (England).
AMI CALIBRATION STUDY. VOLUME 1: SAR CALIBRATION. VOLUME 2: GROUND TARGETS. VOLUME 3: SCATTEROMETER CALIBRATION Final Report
D. G. Corr, K. Keen, and S. G. Blacker Paris ESA 1 Oct. 1985 771 p refs
(Contract ESA-5276/82)
(C2248/4/4-Vol-1; C2248/4/5-Vol-1; C2685/4/2-Vol-1; ESA-CR(P)-2009-Vol-1; C2248/4/4-Vol-2; C2248/4/5-Vol-2; C2685/4/2-Vol-2; ESA-CR(P)-2009-Vol-2; C2248/4/4-Vol-3; C2248/4/5-Vol-3; C2685/4/2-Vol-3; ESA-CR(P)-2009-C-Vol-3) Avail: NTIS HC A99/MF A01

A calibration strategy for the ERS-1 Active Microwave Instrument in wind scatterometer, imaging, and wave modes was developed. Synthetic aperture radar ground targets were studied. Author (ESA)

N85-34395# Institut Franco-Allemand de Recherches, St. Louis (France).
THE USE OF OPTICAL FIBERS IN PULSED LASER HOLOGRAPHY
F. Albe and H. Fagot 6 Sep. 1984 9 p refs In FRENCH; ENGLISH summary Presented at 16th Congr. Intern. de Photograph. Rapide et de Photonique, Strasbourg, 27-31 Aug. 1984
(Contract DRET-83-1160)
(ISL-CO-226/84) Avail: NTIS HC A02

Holograms of small objects were recorded through multimode and monomode fibers with ruby and YAG lasers. In each case single and double exposure holograms were recorded. The experimental set-up is described. The utilization of monomode fibers for the reference is also discussed. Typical results are presented. Author (ESA)

N85-34396# Institut Franco-Allemand de Recherches, St. Louis (France).
FLASH X-RAY DIFFRACTION
F. Jamet 31 Aug. 1984 10 p refs In FRENCH; ENGLISH summary Presented at 16th Congr. Intern. de Photograph. Rapide et de Photonique, Strasbourg, 27-31 Aug. 1984
(ISL-CO-227/84) Avail: NTIS HC A02

Flash and classic X-ray diffraction are compared. Improvements in the equipment for flash X-ray diffraction are discussed. Applications examined include exploding layers, shock waves, and fast deformations. Author (ESA)

N85-34552# Regina Univ. (Saskatchewan). Dept. of Computer Science.
HOLOGRAM-LIKE TRANSMISSION OF PICTURES
Przemyslaw Prusinkiewicz and Mark Christopher *In* Canadian Information Processing Society Graphics Interface 1985 1985 p 213-219 refs (For primary document see N85-34523 23-61) Avail: NTIS HC A19/MF A01

N85-34965*# National Aeronautics and Space Administration. Goddard Space Flight Center, Greenbelt, Md.
A STAR CAMERA ASPECT SYSTEM SUITABLE FOR USE IN BALLOON EXPERIMENTS
S. D. Hunter and R. G. Baker *In its* 19th Intern. Cosmic Ray Conf., Vol. 3 Aug. 1985 p 391-394 refs (For primary document see N85-34862 23-93)
(OG-9.3-10) Avail: NTIS HC as boxed set only $200/MF A01 per volume or E99 per entire set CSCL 14C

36 LASERS AND MASERS

Includes parametric amplifiers.

N85-34397*# Illinois Univ., Urbana-Champaign. Electrooptics Systems Lab.
THEORETICAL AND EXPERIMENTAL ANALYSES OF THE PERFORMANCE OF TWO-COLOR LASER RANGING SYSTEMS
Kwaifong E. Im and C. S. Gardner Aug. 1985 259 p refs
(Grant NsG-5049)
(NASA-CR-176159; NAS 1.26:176159; EOSL-85-006) Avail: NTIS HC A12/MF A01 CSCL 20E

The statistical properties of the signals reflected from the retroreflector equipped satellites were studied. It is found that coherence interference between pulse reflections from retroreflectors of different ranges on the array platform is the primary cause of signal fluctuations. The performance of a cross-correlation technique to estimate the differential propagation time is analyzed by considering both shot noise and speckle. For the retroreflector arrays, timing performance is dominated by interference induced speckle, and the differential propagation time cannot be resolved to better than the pulse widths of the received signals. The differential timing measurements obtained over a horizontal path are analyzed. The ocean-reflected pulse measurements obtained from the airborne two-color laser altimeter experiment are presented. E.A.K.

N85-34398# California Univ., Livermore. Lawrence Livermore Lab.
INDEX OF LASER PROGRAM PUBLICATIONS AND RELATED REPORTS, CALENDAR YEAR 1984
May 1985 48 p
(Contract W-7405-eng-48)
(DE85-011863; UCRL-53541-84) Avail: NTIS HC A03/MF A01

This document provides a listing of titles and authors of publications from the LLNL Laser program during calendar year 1984. It is presented as an aid for researchers in the field who may not otherwise have access to a full listing of laser related work done at LLNL. The intent is to provide a brief and concise listing. Publications are classified by subject, but cross references are not supplied and those documents that logically fall in more than one category may not appear to be in the obvious location. DOE

N85-34399# Rochester Univ., N. Y.
PHOTOIONIZATION-PUMPED, Ne 2, X-RAY LASER STUDIES PROJECT Final Report
M. C. Richardson, P. L. Hagelstein (California Univ., Livermore, Lawrence Livermore Lab.), M. J. Eckart (California Univ., Livermore, Lawrence Livermore Lab.), J. M. Forsyth, M. Gerrassimenko (California Univ., Livermore, Lawrence Livermore Lab.), and J. M. Soures 1984 77 p refs
(Contract W-7405-eng-48)
(DE85-012973; UCRL-15668) Avail: NTIS HC A05/MF A01

The energetics of this pumping scheme are shown. Short pulse (50 to 100 ps) laser irradiation of an appropriate X-ray flashlamp medium generates broadband emission in the range of 300 to 800 eV which preferentially photoionizes Ne to the (2)S state of Ne 2 creating an inversion at approximately 27 eV. Although this approach does not depend on precise spectral overlap between the X-ray pump radiation and the medium to be pumped, it does require that the X-ray medium remain un-ionized prior to photoionization by the soft X-ray emission. Well controlled focus conditions are required to ensure that the X-ray medium is not subjected to electron or X-ray preheat prior to irradiation by the soft X-ray source. The magnitude of the population inversion is predicted to be critically dependent upon rapid photoionization of the two states; therefore, ultra short pulse irradiation of the laser flashlamps is required. DOE

N85-34400# Institut Franco-Allemand de Recherches, St. Louis (France).
CHEMICAL LASERS [CHEMISCHE LASER]

M. Hugenschmidt and J. Wey 30 May 1985 47 p refs In GERMAN Original contains color illustrations
(ISL-R-107/84) Avail: NTIS HC A03

Fundamental properties of chemical lasers are presented and principal systems described in the nonclassified literature are reviewed. The fundamentals of the production of inversion in molecular gases by chemical processes are discussed. Iodine, HF, and DF lasers are described. The chemical reaction in the pulsed chemical HF and DF lasers is introduced by a transverse electrical discharge. In spite of the high dissociation energy and the electronegative properties which are unfavorable for a stable discharge regime, SF6 is used as fluorine source for safety reasons. The pulse energies reach 26 J in agreement with estimated values. The advantage of the present system is that is can also operate as CO2 laser in the TEA mode. The radiation of DF lasers is particularly interesting for military near-Earth applications because of its good transmission properties in the atmosphere. Author (ESA)

37 MECHANICAL ENGINEERING

Includes auxiliary systems (non-power); machine elements and processes; and mechanical equipment.

N85-34401* National Aeronautics and Space Administration. Marshall Space Flight Center, Huntsville, Ala.
VARIABLE LENGTH STRUT WITH LONGITUDINAL COMPLIANCE AND LOCKING CAPABILITY Patent
Robert R. Belew, inventor (to NASA) Issued 20 Aug. 1985 8 p Filed 1 Jul. 1983 Supersedes N83-31019 (21 - 19, p 3145)
(NASA-Case-MFS-25907-1; US-Patent-4,536,114;
US-Patent-Appl-SN-510137; US-Patent-Class-410-156;
US-Patent-Class-244-118.1; US-Patent-Class-244-158R;
US-Patent-Class-248-550; US-Patent-Class-267-8R;
US-Patent-Class-267-150) Avail: US Patent and Trademark Office CSCL 12I

A variable length strut device is illustrated for connecting two associated structures which includes an outer load bearing shell, a drive assembly, a length varying compliance assembly positioned by drive assembly, and a strut rod locking assembly. The load bearing shell includes a connecting part adapted for connection to a first associated structure. A strut connection rod has a connecting part adapted for connection to a second associated structure and a distal end having a piston driver slidably carried in a housing of compliance assembly. Two compliance pistons act in opposing directions on the piston driver to provide longitudinal compliance in a compliance mode of operation. Locking assembly includes locking balls which are urged in a locking ring as locking bolt is urged to the left by fluid pressure. Microswitches sense the displacement of pistons away from the internal ring to bring the pistons to a neutral position wherein the pistons are in contact with the internal ring when it is desired to do so as affected by a control source.
Official Gazette of the U.S. Patent and Trademark Office

N85-34402* National Aeronautics and Space Administration. Lewis Research Center, Cleveland, Ohio.
OXIDIZING SEAL FOR A TURBINE TIP GAS PATH Patent
James D. Cawley, inventor (to NASA) Issued 10 Sep. 1985 7 p Filed 19 Apr. 1984 Supersedes N84-22935 (22 - 13, p 1993)
(NASA-Case-LEW-14053-1; US-Patent-4,540,336;
US-Patent-Appl-SN-602050; US-Patent-Class-415-174;
US-Patent-Class-415-170-R; US-Patent-Class-415-196;
US-Patent-Class-415-200; US-Patent-Class-416-174) Avail: US Patent and Trademark Office CSCL 11A

The sealing of the gas path in a gas turbine engine at the blade tips is improved by maintaining a minimum clearance between the rotor blade tips and the gas path seal. This is accomplished by taking advantage of an increase in volume during controlled oxidation of certain intermetallic compounds which have high melting points. The increase in volume closes the clearance subsequent to a rub between the blades and the seal. Thus, these compounds re-form the tip seal surface to assure continued engine efficiency.
Official Gazette of the U.S. Patent and Trademark Office

N85-34403* National Aeronautics and Space Administration. Johnson (Lyndon B.) Space Center,
REACTANT PRESSURE DIFFERENTIAL CONTROL FOR FUEL CELL GASES Patent
Albert P. Grasso, inventor (to NASA) (United Technologies Corp., South Windsor, Conn.) Issued 9 Apr. 1985 5 p Continuation of abandoned US-Patent-Appl-SN-394344 filed 1 Jul. 1982
(NASA-Case-MSC-20127-2; US-Patent-4,509,548;
US-Patent-Appl-SN-646044; US-Patent-Class-137-99;
US-Patent-Class-137-116.3) Avail: US Patent and Trademark Office CSCL 13K

A pair of spool valves are described which are balanced between pressures of reactant gases supplied to a fuel cell power plant. The pressure differences are controlled between the gases so as to maintain those pressures substantially in the proportions necessary for operation of the fuel cell.
Official Gazette of the U.S. Patent and Trademark Office

N85-34404*# Ohio State Univ., Columbus. Dept. of Mechanical Engineering.
THE DESIGN AND ANALYSIS OF SINGLE FLANK TRANSMISSION ERROR TESTOR FOR LOADED GEARS Final Report, Apr. 1984 - Jul. 1985
Donald R. Houser and Duane Edward Bassett Sep. 1985 141 p refs
(Grant NAG3-541)
(NASA-CR-176163; NAS 1.26:176163; MPN-764038; ESL-716109) Avail: NTIS HC A07/MF A01 CSCL 13I

Due to geometrical imperfections in gears and finite tooth stiffnesses, the motion transmitted from an input gear shaft to an output gear shaft will not have conjugate action. In order to strengthen the understanding of transmission error and to verify mathematical models of gear transmission error, a test stand that will measure the transmission error of a gear pair at operating loads, but at reduced speeds would be desirable. This document describes the design and development of a loaded transmission error tester. For a gear box with a gear ratio of one, few tooth meshing combinations will occur during a single test. In order to observe the effects of different tooth mesh combinations and to increase the ability to load test gear pairs with higher gear ratios, the system was designed around a gear box with a gear ratio of two. B.W.

N85-34405*# National Aeronautics and Space Administration. Lewis Research Center, Cleveland, Ohio.
GENERATED SPIRAL BEVEL GEARS: OPTIMAL MACHINE-TOOL SETTINGS AND TOOTH CONTACT ANALYSIS
Faydor L. Litvin (Illinois Univ., Chicago), Wei-Jiung Tsung (Illinois Univ., Chicago), John J. Coy, and Charles Heine (Dana Corp.) 1985 14 p refs Presented at the 1985 Off-Highway and Power Plant Congr. and Exposition, Milwaukee, 9-12 Sep. 1985; sponsored by the Society of Automotive Engineers Prepared in cooperation with Army Research and Technology Labs.
(Grant NsG3-48)
(NASA-TM-87075; E-2648; NAS 1.15:87075;
USAAVSCOM-TR-85-C-9) Avail: NTIS HC A02/MF A01 CSCL 13I

Geometry and kinematic errors were studied for Gleason generated spiral bevel gears. A new method was devised for choosing optimal machine settings. These settings provide zero kinematic errors and an improved bearing contact. The kinematic errors are a major source of noise and vibration in spiral bevel gears. The improved bearing contact gives improved conditions for lubrication. A computer program for tooth contact analysis was developed, and thereby the new generation process was confirmed. The new process is governed by the requirement that during the generation process there is directional constancy of the common

normal of the contacting surfaces for generator and generated surfaces of pinion and gear. E.A.K.

N85-34406*# National Aeronautics and Space Administration. Lewis Research Center, Cleveland, Ohio.
THERMAL STRESS ANALYSIS OF A NEW TURBINE SHROUD SEAL CONCEPT
Robert F. Handschuh Aug. 1985 16 p refs Prepared in cooperation with Army Aviation Research and Development Command, Cleveland
(NASA-TM-87082; E-2666; NAS 1.15:87082; USAAVSCOM-TR-85-C-16) Avail: NTIS HC A02/MF A01 CSCL 13I

The thermal stress field of a two piece turbine shroud seal concept was analyzed and results compared to one piece designs by finite element analysis. The two piece seal has independently formed structure (substrate) and ceramic components that are assembled at ambient conditions. The boundary conditions used for analysis were hot gas surface temperatures of 1370 and 1650 C (2500 and 3000 F) and cooled surface temperature of 700 C (1285 F). The resulting thermal stress field, of the two piece seal when compared to the one piece seals in the region of all ceramic material, was reduced substantially. Author

N85-34407*# National Aeronautics and Space Administration. Lewis Research Center, Cleveland, Ohio.
LUBRICATION AND COOLING FOR HIGH SPEED GEARS
Dennis P. Townsend 1985 24 p refs Presented at the Lubrication Session of the Original Equipment Manuf. Design Conf., Philadelphia, 9-11 Sep. 1985
(NASA-TM-87096; E-2660; NAS 1.15:87096) Avail: NTIS HC A02/MF A01 CSCL 13I

The problems and failures occurring with the operation of high speed gears are discussed. The gearing losses associated with high speed gearing such as tooth mesh friction, bearing friction, churning, and windage are discussed with various ways shown to help reduce these losses and thereby improve efficiency. Several different methods of oil jet lubrication for high speed gearing are given such as into mesh, out of mesh, and radial jet lubrication. The experiments and analytical results for the various methods of oil jet lubrication are shown with the strengths and weaknesses of each method discussed. The analytical and experimental results of gear lubrication and cooling at various test conditions are presented. These results show the very definite need of improved methods of gear cooling at high speed and high load conditions. Author

N85-34408*# National Aeronautics and Space Administration. Lewis Research Center, Cleveland, Ohio.
ELASTOHYDRODYNAMIC LUBRICATION CALCULATIONS USED AS A TOOL TO STUDY SCUFFING
L. G. Houpert and B. J. Hamrock 1985 20 p refs Presented at the 12th Leeds-Lyon Symp. on Tribology, Lyon, 3-6 Sep. 1985
(NASA-TM-87097; E-2658; NAS 1.15:87097) Avail: NTIS HC A02/MF A01 CSCL 11H

A new Reynolds equation was developed that takes into account the nonlinear viscous behavior of the fluid. The new Reynolds equation considers the nonlinear viscous fluid model of Eyring, the equilibrium equation, the constant mass flow, and the kinematic boundary condition. The new Reynolds equation and the elasticity equation are solved simultaneously by using a system approach and a Newton-Raphson technique. Comparisons are made with results obtained from the classical Reynolds equation. The effects of sliding speed and introducing a bump or a groove within the conjunction are studied. Results are shown for both moderate and heavy loads. E.A.K.

N85-34409*# National Aeronautics and Space Administration. Lewis Research Center, Cleveland, Ohio.
DESIGN AND LUBRICATION OF HIGH-SPEED ROLLING-ELEMENT BEARINGS
Erwin V. Zaretsky 1985 19 p refs Presented at the Original Equipment Manuf. Design Conf., Philadelphia, 9-11 Sep. 1985
(NASA-TM-87107; E-2670; NAS 1.15:87107) Avail: NTIS HC A02/MF A01 CSCL 13I

The speed capability of rolling element bearings has increased from speeds of less than two million DN to speeds of three million DN. The life and reliability of these bearings also increased where they are equal to, or greater than, those of bearings with limited speed capability. Design parameters must be carefully chosen and optimized based upon sophisticated bearing computer programs. Material and lubricant selection must be integrated into the bearing design. Bearing thermal management must be implemented through proper lubrication and cooling. Parameters which can be used to design, specify, and lubricate high speed bearings are discussed. E.A.K.

N85-34410# Department of the Air Force, Washington, D.C.
HERMETIC CHIP CARRIER COMPLIANT SOLDERING PADS Patent Application
Hemler, inventor (to Air Force) Filed 1 May 1985 11 p
(AD-D011722; US-Patent-Appl-SN-729389) Avail: NTIS HC A02/MF A01 CSCL 09/5

Compliant soldering pads allow for expansion and contraction between hermetic chip carriers (HCC) and printed wiring boards (PWB) due to coefficient of thermal expansion mismatch and prevent solder cracking which in turn causes electrical discontinuities. The pads allow for flexing in three axes. Author (GRA)

N85-34411# Department of Energy, Washington, D. C.
EVACUATE AND BACKFILL APPARATUS AND METHOD Patent Application
D. J. Oakley and O. J. Groves, inventors (to NASA) Filed 27 Jun. 1984 19 p
(Contract DE-AC06-76FF-02170)
(DE85-006018; US-Patent-Appl-SN-625325) Avail: NTIS HC A02/MF A01

An apparatus and method is described for treatment of hollow articles by evacuating existing gas or gases therefrom and purging or backfilling the articles with a second gas such as helium. The apparatus includes a sealed enclosure having an article storage drum mounted therein. A multiplicity of such articles are fed singly into the enclosure and loaded into radial slots formed in the drum. The enclosure is successively evacuated and purged with helium to replace the existing gas in the articles with helium. The purged articles are then discharged singly from the drum and transported out of the enclosure. DOE

N85-34412# Department of Energy, Washington, D. C.
APPARATUS PRODUCING CONSTANT CABLE TENSION FOR INTERMITTENT DEMAND Patent Application
T. Lauritzen, inventor (to NASA) Filed 23 May 1984 26 p
(Contract DE-AC03-76SF-00098)
(DE85-006434; US-Patent-Appl-SN-612955) Avail: NTIS HC A03/MF A01

This invention relates to apparatus for producing constant tension in cable or the like when it is unreeled and reeled from a drum or spool under conditions of intermittent demand. The invention is particularly applicable to the handling of superconductive cable, but the invention is also applicable to the unreeling and reeling of other strands, such as electrical cable, wire, cord, other cables, fish line, wrapping paper and numerous other materials. DOE

N85-34413# Allied Bendix Aerospace, Kansas City, Mo. Technical Communications.
LASER WELDING OF 6Al-4V TITANIUM ALLOY Final Report
E. Jimenez May 1985 30 p refs
(Contract DE-AC04-76DP-00613)
(DE85-012019; BDX-613-3115) Avail: NTIS HC A03/MF A01

Gas laser welding of 6Al-4V titanium alloy as tested. The 6Al-4V-Ti welds were compared with gas tungsten arc and electron beam weld for porosity, ductility, and contamination. It is shown that laser welding is suitable for 6Al-4V titanium alloy and that sound welds can be made over a wide range of welding conditions. DOE

N85-34414# Department of Energy, Washington, D. C.
FEEDBACK REGULATED INDUCTION HEATER FOR A FLOWING FLUID Patent Application
A. Migliori and G. W. Swift, inventors (to DOE) Filed 13 Jun. 1984 15 p
(Contract W-7405-eng-36)
(DE85-006508; US-Patent-Appl-SN-620287) Avail: NTIS HC A02/MF A01

A regulated induction heater for heating a stream of flowing fluid to a predetermined desired temperature is discussed. The heater includes a radiofrequency induction coil which surrounds a glass tube through which the fluid flows. A heating element consisting of a bundle of approximately 200 stainless steel capillary tubes located within the glass tube couples the output of the induction coil to the fluid. The temperature of the fluid downstream from the heating element is sensed with a platinum resistance thermometer, the output of which is applied to an adjustable proportional and integral feedback control circuit which regulates the power applied to the induction coil. The heater regulates the fluid temperature to within 0.005 C at a flow rate of 50 cm(3)/sec with a response time of less than 0.1 second, and can accommodate changes in heat load up to 1500 watts. DOE

N85-34415# Department of Energy, Washington, D. C.
ELECTRICALLY CONDUCTIVE CONTAINMENT VESSEL FOR MOLTEN ALUMINUM Patent Application
C. E. Holcombe and D. G. Scott, inventors (to DOE) Filed 25 Jun. 1984 8 p
(Contract DE-AC05-84CR-21400)
(DE85-006518; US-Patent-Appl-SN-623875) Avail: NTIS HC A02/MF A01

The present invention is directed to a containment vessel which is particularly useful in melting aluminum. The vessel of the present invention is a multilayered vessel characterized by being electrically conductive, essentially nonwettable by and nonreactive with molten aluminum. The vessel of the present invention is a multilayered vessel characterized by being electrically conductive, essentially nonwettable by and nonreactive with molten aluminum. The vessel is formed by coating a tantalum substrate of a suitable configuration with a mixture of yttria and particulate metal borides. The yttria in the coating inhibits the wetting of the coating while the boride particulate material provides the electrical conductivity through the vessel. The vessel of the present invention is particularly suitable for use in melting aluminum by ion bombardment. DOE

N85-34416# Department of Energy, Washington, D. C.
GAS SHIELDING APPARATUS Patent Application
D. Brandt, inventor (to DOE) Filed 5 Jun. 1984 11 p
(Contract W-7405-eng-36)
(DE85-005992; US-Patent-Appl-SN-617652) Avail: NTIS HC A02/MF A01

An apparatus is proposed for preventing oxidation by uniformly distributing inert shielding gas over the weld area of workpieces such as pipes being welded together. The apparatus comprises a chamber and a gas introduction element. The chamber has an annular top wall, an annular bottom wall, an inner side wall and an outer side wall connecting the top and bottom walls. One side wall is a screen and the other has a portion defining an orifice. The gas introduction element has a portion which encloses the orifice and can be one or more pipes. The gas introduction element is in fluid communication with the chamber and introduces inert shielding gas into the chamber. The inert gas leaves the chamber through the screen side wall and is dispersed evenly over the weld area. DOE

N85-34417# Department of Energy, Washington, D. C.
CONTROL SYSTEM FOR FLUID HEATED STEAM GENERATOR Patent Application
J. F. Holand and J. F. Koenig, inventors (to DOE) Filed 29 May 1984 17 p
(Contract W-31-109-eng-38)
(DE85-005734; US-Patent-Appl-SN-614507) Avail: NTIS HC A02/MF A01

A control system for controlling the location of the nucleate-boiling region in a fluid heated steam generator is discussed. It comprises means for measuring the temperature gradient (change in temperature per unit length) of the heating fluid along the steam generator; means for determining a control variable in accordance with a predetermined function of temperature gradients and for generating a control signal in response thereto; and means for adjusting the feedwater flow rate in accordance with the control signal. DOE

N85-34418# Oak Ridge National Lab., Tenn. Engineering Technology Div.
EFFECT OF STAINLESS STEEL WELD OVERLAY CLADDING ON THE STRUCTURAL INTEGRITY OF FLAWED STEEL PLATES IN BENDING, SERIES 1
W. R. Corwin, G. C. Robinson, R. K. Nanstad, J. G. Merkle, R. G. Berggren, G. M. Goodwin, R. L. Swain, and T. D. Owinga Apr. 1985 100 p refs
(Contracts DE-AC05-84OR-21400; NRC-FIN-B-0119)
(TI85-010349; NUREG/CR-4015-Ser-1) Avail: NTIS HC A05/MF A01

The Heavy-Section Steel Technology (HSST) Stainless Steel Cladding Evaluation were undertaken to study the interaction of stainless steel cladding on the inside surface of a reactor pressure vessel with flaws initiating and propagating in base metal. From the light-water reactor vessel designer's viewpoint, stainless steel cladding is primarily a means of preventing contamination of the coolant by corrosion products. Except for the effect of cladding on fatigue in thermal transients, its effect on structural integrity has previously been largely disregarded. With the more recent focus on safety studies on overcooling type transients, for which the behavior of small flaws is important, it has become evident that stainless steel cladding may have a key role in controlling the propagation and/or arrest of propagating flaws. A complicating factor in understanding the role of stainless steel cladding in this setting is the scarcity of data on its fracture toughness as a function of radiation dose and the fabrication process. The initial phase of the HSST evaluation is reported here and addresses this question by testing the response of 51 mm-thick flawed plates clad with single-wire, submerged-arc weld overlays of different toughness levels. DOE

N85-34311# Surrey Univ., Guildford (England). Dept. of Mechanical Engineering.
A RATIONAL APPROACH TO CAM DESIGN
Gerald Druce *In* Cranfield Inst. of Tech. Proc. of the Mech. Conf., Vol. 1 1984 24 p refs 2 Vol. (For primary document see N85-34309 23-31)
Avail: NTIS HC A07/MF A01

N85-34312# Cranfield Inst. of Tech., Bedford (England). Coll. of Aeronautics.
SOME PROBLEMS IN HIGH SPEED GEARS AND GEARING
J. H. Webb *In its* Proc. of the Mech. Conf., Vol. 1 1984 10 p refs 2 Vol. (For primary document see N85-34309 23-31)
Avail: NTIS HC A07/MF A01

N85-34316# Cranfield Inst. of Tech., Bedford (England).
HIGH POWERED EPICYCLIC GEARS: SOME RECENT DEVELOPMENT
D. E. Yates *In* Cranfield Inst. of Tech. Proc. of the Mech. Conf., Vol. 1 1984 19 p refs 2 Vol. (For primary document see N85-34309 23-31)
Avail: NTIS HC A07/MF A01

N85-34556# Ecole Polytechnique, Montreal (Quebec).
A GEOMETRIC MODELLER FOR TURBOMACHINERY APPLICATIONS
B. Ozell and R. Camarero *In* Canadian Information Processing Society Graphics Interface 1985 1985 p 237-244 refs (For primary document see N85-34523 23-61)
Avail: NTIS HC A19/MF A01

38 QUALITY ASSURANCE AND RELIABILITY

Includes product sampling procedures and techniques; and quality control.

N85-34419# United Kingdom Atomic Energy Authority, Harwell (England). Theoretical Physics Div.
CALCULATIONS ON THE FEASIBILITY OF ULTRASONIC INSPECTION OF STEAM GENERATOR TUBING IN PRESSURIZED WATER REACTORS
J. A. G. Temple Apr. 1985 36 p refs
(AERE-R-10960) Avail: NTIS HC A03/MF A01

Calculations have been made to test whether it is feasible to use ultrasound to detect and to size the extent of intergranular attack in steam generator tubes. It is concluded that two methods are possible: a method employing the time differences of short pulses could be used, or one in which longer pulses are used with the amplitude of the reflection related to the amount of intergranular attack present. In the first method, compression waves of 20 MHz at 60 to 70 deg to the normal to the surface are recommended. In the second, either 20 MHz compression waves at 65 deg or 20 MHz shear waves at 30 deg are recommended.
Author

N85-34420# Sandia Labs., Albuquerque, N. Mex.
DEGRADATION MECHANISMS AND ACCELERATED AGING TEST DESIGN
R. L. Cough and K. T. Gillen 1985 10 p refs Sponsored in part by Nuclear Regulatory Commission
(Contracts DOE-40-550-70; NRC-FIN-A-1051)
(TI85-003251; SAND-84-2115C) Avail: NTIS HC A02/MF A01

The fundamental mechanisms underlying the chemical degradation of polymers can change as a function of environmental stress level. When this occurs, it greatly complicates any attempt to use accelerated tests for predicting long-term material degradation behaviors. Understanding how degradation mechanisms can change at different stress levels facilitates both the design and the interpretation of aging tests. Oxidative degradation is a predominant mechanism for many polymers exposed to a variety of different environments in the presence of air, and there are two mechanistic considerations which are widely applicable to material oxidation. One involves a physical process, oxygen diffusion, as a rate-limiting step. This mechanism can predominate at high stress levels. The second is a chemical process, the time-dependent decomposition of peroxide species. This leads to chain branching and can become a rate-controlling factor at lower stress levels involving time-scales applicable to use environments. Methods for identifying the operation of these mechanisms and illustrate the dramatic influence they can have on the degradation behaviors of a number of polymer types are described. Several commonly used approaches to accelerated aging tests are discussed in light of the behaviors which result from changes in degradation mechanisms.
DOE

N85-34421# Rolls-Royce Ltd., Derby (England). Product Assurance Supply Group.
TOWARDS THE YEAR 2000: DEVELOPMENTS IN INSPECTION AND PRODUCT ASSURANCE TO BE ANTICIPATED DURING THE NEXT 15 YEARS
T. Broughton and A. J. S. Pratt 7 Feb. 1985 8 p Proposed for presentation at Assoc. Aeron. et Astronautique de France and Assoc. Franc. pour le Controle et la Qualite
(PNR-90258) Avail: NTIS HC A02/MF A01

Trends in aircraft engine inspection technology, including dimensional inspection; visual inspection; and nondestructive testing, including ultrasonics, X-rays, surface integrity, and functional testing are discussed. The role of the computer, and the Rolls-Royce product assurance philosophy are outlined.
Author (ESA)

N85-34317# Cranfield Inst. of Tech., Bedford (England).
THE USE OF ULTRASOUND TO MONITOR INCIPIENT FAILURE OF ROLLING ELEMENT BEARINGS
R. H. Bannister *In* Cranfield Inst. of Tech. Proc. of the Mech. Conf., Vol. 1 1984 12 p 2 Vol. (For primary document see N85-34309 23-31)
Avail: NTIS HC A07/MF A01

39 STRUCTURAL MECHANICS

Includes structural element design and weight analysis; fatigue; and thermal stress.

For applications see *05 Aircraft Design, Testing and Performance* and *18 Spacecraft Design, Testing and Performance.*

N85-34422 British Library Lending Div., Boston Spa (England).
ALGORITHM FOR CALCULATION OF STRAIN STATE FROM MEASUREMENTS OF NODE COORDINATES OF ARBITRARY CURVILINEAR GRID
B. N. Berezovskii and A. V. Pakalo [1985] 8 p refs Transl. into ENGLISH from Izv. Vyssh. Ucheb. Zaved., Chernaya Met. (USSR), no. 12, 1984 p 63-68
(BLL-M-36304) Avail: British Library Lending Div., Boston Spa, Engl.

A procedure is presented for calculating the strain state in processes of mechanical working of metals from measurements of Cartesian coordinates of the nodes of a plane curvilinear grid of arbitrary shape. The algorithm does not require the introduction of a cylindrical system of coordinates for investigation of processes of axisymmetrical deformation and can be used both for processes of plane deformation and for the planes of symmetry of processes of volume deformation. The strain state in the wall of a forging produced by blind piercing of an ingot is examined to illustrate the use of the described procedure and computer algorithm.
E.A.K.

N85-34423 Imperial Coll. of Science and Technology, London (England). Dept. of Aeronautics.
THREE-DIMENSIONAL FINITE ELEMENT FAILURE MODEL FOR PREDICTING FAILURE IN FIBRE REINFORCED BOLTED JOINTS
F. L. Matthews and H. P. Taank Oct. 1983 77 p refs
(Contract MIN-DEF-2037/0218/XR/STR)
(BR94778) Avail: NTIS HC A05/MF A01

Criteria used in predicting failure in fiber reinforced composites were reviewed, and a three-dimensional finite element failure model which uses failure criteria was developed to analyze layered fiber reinforced laminates. The model can calculate detailed stress distribution, identify the damage zone, analyze damage accumulation, and determine ultimate strength. It also has an option of comparing failure with five failure criteria and identifying the failure mode for one of these criteria. The method was tested for simple structures (e.g., beams) only, not for the bolted joint problem.
Author (ESA)

N85-34424 Admiralty Marine Technology Establishment, Dunfermline (Scotland).
DESIGN OF TRANSVERSELY STIFFENEND FRP PANELS UNDER COMPRESSIVE LOAD
C. S. Smith Dec. 1984 43 p refs
(AMTE(S)-R-84104; BR94017) Copyright. Avail: Issuing Activity

Buckling failure in fiber-reinforced plastic panels having stiffeners of that section under compressive load acting across the line of the stiffeners is reviewed. The problem is related to the design of FRP ships. Analysis methods are discussed, including use of approximate data curves and folded-plate analysis to determine initial buckling behaviour, together with nonlinear finite element analysis referring to imperfection effects and post-buckling behavior. Experimental results and test data are correlated with

theoretical analysis as a basis for design recommendations.
Author (ESA)

N85-34425*# Kaman Aerospace Corp., Bloomfield, Conn.
AUTOMATED DYNAMIC ANALYTICAL MODEL IMPROVEMENT FOR DAMPED STRUCTURES
Jon-Shen Fuh and Alex Berman Sep. 1985 35 p refs
(Contract NAS1-15805)
(NASA-CR-177945; NAS 1.26:177945; R-1810) Avail: NTIS HC A03/MF A01 CSCL 20K

A method is described to improve a linear nonproportionally damped analytical model of a structure. The procedure finds the smallest changes in the analytical model such that the improved model matches the measured modal parameters. Features of the method are: (1) ability to properly treat complex valued modal parameters of a damped system; (2) applicability to realistically large structural models; and (3) computationally efficiency without involving eigensolutions and inversion of a large matrix. E.A.K.

N85-34426*# National Aeronautics and Space Administration. Langley Research Center, Hampton, Va.
NONLINEAR ADHESIVE BEHAVIOR EFFECTS IN A CRACKED ORTHOTROPIC SHEET STIFFENED BY A SEMI-INFINITE ORTHOTROPIC SHEET
C. A. Bigelow Aug. 1985 35 p refs
(NASA-TM-87584; NAS 1.15:87584) Avail: NTIS HC A03/MF A01 CSCL 20K

The stress-intensity factors are determined for a cracked orthotropic sheet adhesively bonded to an orthotropic stringer where the adhesive layer is modeled with a nonlinear stress-strain curve. By the use of Green's functions and the complex variable theory of orthotropic elasticity, a set of integral equations is obtained. The integral equations are replaced by an equivalent set of algebraic equations, which are solved to obtain the shear stress distribution in the adhesive layer, with which the crack-tip stress-intensity factors are found. When the adhesive was modeled with a nonlinear stress-strain curve, the peak shear stresses in the adhesive were considerably reduced in comparison to the solution for the linear elastic adhesive. This resulted in increases in the stress-intensity factors for the nonlinear adhesive solution compared to the linear adhesive solution. The nonlinear adhesive has no significant effect on the stress-intensity factor unless the near crack tip is beneath the stringer. It is assumed that the adhesive bond remains intact and it is predicted that onset of adhesive failure occurs at decreasing levels of applied stress as the crack propagates beneath the stringer. E.A.K.

N85-34427*# National Aeronautics and Space Administration. Lewis Research Center, Cleveland, Ohio.
NONLINEAR FLAP-LAG-EXTENSIONAL VIBRATIONS OF ROTATING, PRETWISTED, PRECONED BEAMS INCLUDING CORIOLIS EFFECTS
K. B. Subrahmanyam (NBKR Inst. of Science and Tech.) and K. R. V. Kaza 1985 35 p refs Presented at the 19th Midwestern Mech. Conf., Columbus, Ohio, 9-11 Sep. 1985; sponsored by the Ohio State Univ.
(NASA-TM-87102; E-2598; NAS 1.15:87102) Avail: NTIS HC A03/MF A01 CSCL 20K

The effects of pretwist, precone, setting angle, Coriolis forces and second degree geometric nonlinearities on the natural frequencies, steady state deflections and mode shapes of rotating, torsionally rigid, cantilevered beams were studied. The governing coupled equations of flap lag extensional motion are derived including the effects of large precone and retaining geometric nonlinearities up to second degree. The Galerkin method, with nonrotating normal modes, is used for the solution of both steady state nonlinear equations and linear perturbation equations. Parametric indicating the individual and collective effects of pretwist, precone, Coriolis forces and second degree geometric nonlinearities on the steady state deflection, natural frequencies and mode shapes of rotating blades are presented. It is indicated that the second degree geometric nonlinear terms, which vanish for zero precone, can produce frequency changes of engineering significance. Further confirmation of the validity of including those generated by MSC NASTRAN. It is indicated that the linear and nonlinear Coriolis effects must be included in analyzing thick blades. The Coriolis effects are significant on the first flatwise and the first edgewise modes. E.A.K.

N85-34428# National Research Council of Canada, Ottawa (Ontario). Div. of Building Research.
SHORT-TIME CREEP OF ICE
Yu. K. Zaretskii and B. D. Chumichev 1985 188 p refs Transl. into ENGLISH of "Kratkovremennaya Polzuchest Lda" Novosibirsk, Nauka Press, 1982 p 1-117
(NRC/CNR-TT-2111; ISSN-0077-5606; Rept-255) Avail: NTIS HC A09/MF A01

Results of theoretical and experimental studies on failure of ice during short-time creep are reported in this work. Deformation and failure of ice under applied load are treated as a stochastic process composed of discrete events of the occurrence and development of microdefects in the crystal structure of ice. Models of ice deformation have been developed in which the magnitude and duration of stresses and the dependence on temperature have been taken into account. The functional relation between the microprocess of the accumulation of brittle structural defects and the macroprocess of ice deformation has been confirmed.
B.W.

N85-34429# Aeronautical Research Labs., Melbourne (Australia).
STRESSES AND STRAINS IN A PLATE RESULTING FROM TWO CLOSELY-SPACED INTERFERENCE-FIT FASTENERS
R. P. Carey and M. Heller May 1985 29 p refs
(ARL-Struc-TM-409; AR-004-018) Avail: NTIS HC A03/MF A01

Electric resistance gauges were used to investigate the strains induced around a pair of closely-spaced interference-fit fasteners (nominal center distance equalling two hole diameters) in a D6ac steel plate. A finite element analysis was performed for the same geometry using the penalty element method. Measured strains show broad agreement with the results of the finite element analysis and it is indicated that the peak stress level in the plate at the hole circumference would be 1.14 times the level for a single similar interference-fit fastener in an infinite plate. E.A.K.

N85-34430# Oak Ridge National Lab., Tenn.
CHARACTERIZATION OF MODIFIED 9 Cr Mo STEEL EXTRUDED PIPE
V. K. Sikka and M. D. Hart Apr. 1985 30 p
(Contract DE-AC05-84OR-21400)
(DE85-012056; ORNL-6154) Avail: NTIS HC A03/MF A01

The fabrication of hot extruded pipe of modified 9 Cr-1 Mo steel is described. Also dealt with the tempering response; tensile, Charpy impact, and creep properties; and microstructure of the hot extruded pipe. The tensile properties of the pipe are compared with the average and average -1.65 standard error of estimate curves for various product forms of several commercial heats of this alloy. The creep rupture properties are compared with the average curve for various product forms of the commercial heats.
DOE

N85-34431# California Univ., Berkeley. Lawrence Berkeley Lab.
NEAR-THRESHOLD FATIGUE: AN OVERVIEW OF THE ROLE OF MICROSTRUCTURE AND ENVIRONMENT
R. O. Ritchie Sep. 1984 64 p refs Presented at the 2nd Intern. Conf. on Fatigue Thresholds - Fatigue 84, Birmingham, England, 3 Sep. 1984
(Contract DE-AC03-76SF-00098)
(DE85-009903; LBL-18457; CONF-8409121-2) Avail: NTIS HC A04/MF A01

An overview is presented of the salient micro mechanisms, primarily involving crack closure, which can influence the growth of fatigue cracks at near threshold levels. Examples are drawn from recent work on crack propagation in dual phase and low alloy steels and in under/peak/overaged aluminum alloys. Factors such as duplex microstructures, variations in slip mode, high pressure hydrogen environments and compression overloads are

shown to modify changes in near threshold crack growth behavior. DOE

N85-34432# Sandia Labs., Albuquerque, N. Mex.
SHOCK AND RELEASE EQUATION OF STATE OF CALCITE
D. E. Grady and R. L. Moody May 1985 26 p refs
(Contract DE-AC04-76DP-00789)
(DE85-013151; SAND-85-0947) Avail: NTIS HC A03/MF A01

Studies were initiated to investigate the unloading response of carbonate minerals from high-pressure Hugoniot states between 10 to 100 GPa. A two-stage gun facility was used. Several impact experiments are reported on crystallite calcite for shock pressure below 10 GPa. Results are compared with other Hugoniot data on various calcium carbonate rocks and minerals. DOE

N85-34433# Rolls-Royce Ltd., Derby (England).
THE STRESS PATTERN ANALYSIS OF COARSE GRAIN TITANIUM SPECIMENS
D. W. Copley 1 Feb. 1985 3 p
(PNR-90250) Avail: NTIS HC A02/MF A01

The SPATE technique was used to study localized strain variations in titanium alloys utilized in aircraft engines. A 1 cm sq uniaxial test specimen was installed in a 100kN tensile testing machine and subjected to a static loads of 15kN. A sinusoidal dynamic load of 10kN was then superimposed at a frequency of 10 Hz. The SPATE scans were carried out, centered on all four faces, with additional scans being performed centered on the corners, to check for continuity. Scans were performed at an intermediate/fine resolution, to identify the face that displayed the greatest structure in the strain distribution, which was then subjected to detailed study. Comparison with strain gages indicates that for load levels up to 30kN the SPATE output for a given principal strain sum is not a constant within the limits of experimental error. Discrepancy may arise from mispositioning of the strain gages, though it is more likely that the orthotropic material properties ensure that thermoelastic heat generation is not directly proportional to the principal strain sum. Author (ESA)

N85-34182# Kobe Univ. (Japan). Faculty of Engineering.
BEHAVIORS OF STRESS WAVES IN A CONICAL BAR
Noritoshi Nakagawa, Yasuo Fujiwara (Kobe Steel Ltd.), and Ryoji Kawai *In* Society of Materials Science Proc. of the 27th Japan Congr. on Mater. Res. Mar. 1984 p 7-12 refs (For primary document see N85-34180 23-23)
Avail: NTIS HC A14/MF A01

N85-34183# Kyushu Univ., Fukuoka (Japan). Faculty of Engineering.
NEGATIVE FLEXURAL BEHAVIOR OF PRECASE COMPOSITE SLABS WITH STEEL JOINT
Toshiaki Ohta, Shinichi Hino (Yamaguchi Univ.), Yutaka Yamamoto (Ishikawajima Kenzai Cogyo Co., Ltd.), Saburo Tomisawa (Ishikawajima Kenzai Cogyo Co., Ltd.), and Takayuki Nose *In* Society of Materials Science Proc. of the 27th Japan Congr. on Mater. Res. Mar. 1984 p 13-18 refs (For primary document see N85-34180 23-23)
Avail: NTIS HC A14/MF A01

N85-34184# Hiroshima Univ. (Japan). Faculty of Engineering.
MECHANICAL RATCHETING BEHAVIORS OF A STEEL PIPE UNDER COMBINED CYCLIC AXIAL LOAD AND INTERNAL PRESSURE
Fusahito Yoshida, Yoichi Obataya (Fukui Univ.), and Eiryo Shiratori (Saitama Univ.) *In* Society of Materials Science Proc. of the 27th Japan Congr. on Mater. Res. Mar. 1984 p 13-24 refs (For primary document see N85-34180 23-23)
Avail: NTIS HC A14/MF A01

N85-34185# Musashi Inst. of Tech., Tokyo (Japan). Dept. of Civil Engineering.
MONOTONOUS STRESS-STRAIN PROPERTIES OF STRUCTURAL STEEL SUBJECTED TO NONSTATIONARY REPETITIVE PRE-LOADING
Masaru Minagawa, Takeo Nishiwaki, and Nobutoshi Masuda *In* Society of Materials Science Proc. of the 27th Japan Congr. on Mater. Res. Mar. 1984 p 25-31 refs Sponsored by the Ministry of Education, Science and Culture (For primary document see N85-34180 23-23)
Avail: NTIS HC A14/MF A01

N85-34186# Osaka Univ. (Japan). Dept. of Mechanical Engineering.
EXPERIMENTAL STUDY OF COLLAPSE OF THICK-WALLED TUBE UNDER EXTERNAL PRESSURE AND AXIAL FORCE
Hiroshi Kitagawa, Yasunori Tanizawa (Sumitomo Metal Industries, Ltd.), and Masaya Okamoto *In* Society of Materials Science Proc. of the 27th Japan Congr. on Mater. Res. Mar. 1984 p 33-37 refs Sponsored in part by the Ministry of Education of Japan (For primary document see N85-34180 23-23)
Avail: NTIS HC A14/MF A01

N85-34187# General Dynamics International Corp., Tokyo (Japan).
ON HIGH STRAIN RATE FRAGMENTATION OF A CLOSED VESSEL
Jiro Yamamasu and Hiroshi Miyamoto (Science Univ. of Tokyo) *In* Society of Materials Science Proc. of the 27th Japan Congr. on Mater. Res. Mar. 1984 p 39-45 refs (For primary document see N85-34180 23-23)
Avail: NTIS HC A14/MF A01

N85-34189# Nagasaki Univ. (Japan). Faculty of Engineering.
ON THE METHODS TO DETERMINE THE STRESS INTENSITY FACTORS IN BOUNDARY ELEMENT METHOD
Hiroyuki Kisu, Ryoji Yuuki (Inst. of Industrial Science), and Hideo Kitagawa (Yokohame National Univ.) *In* Society of Materials Sciences Proc. of the 27th Japan Congr. on Mater. Res. Mar. 1984 p 53-56 refs Previously announced in IAA as A85-23464 (For primary document see N85-34180 23-23)
Avail: NTIS HC A14/MF A01

N85-34193# Aoyamagakuin Univ., Tokyo (Japan). Dept. of Mechanical Engineering.
EXPERIMENTAL STUDY ON TIME AND TEMPERATURE DEPENDENT BEHAVIOR OF CRACK GROWTH IN VISCOELASTIC STRIP
Hidekazu Ohtsuka and Masahisa Takashi *In* Society of Materials Science Proc. of the 27th Japan Congr. on Mater. Res. Mar. 1984 p 79-83 refs (For primary document see N85-34180 23-23)
Avail: NTIS HC A14/MF A01

N85-34198# Kanazawa Inst. of Tech. (Japan). Material System Research Lab.
STATISTICAL POOLING METHOD OF FATIGUE DATA FOR RELIABILITY DESIGN
Hidetoshi Nakayasu and Tadashi Umerhara *In* Society of Materials Science Proc. of the 27th Japan Congr. on Mater. Res. Mar. 1984 p 111-117 refs Previously announced in IAA as A85-23468 (For primary document see N85-34180 23-23)
Avail: NTIS HC A14/MF A01

N85-34204# Musashi Inst. of Tech., Tokyo (Japan).
MULTIAXIAL STRESS ANALYSIS TAKING ACCOUNT OF PENETRATION DEPTH OF X-RAYS. A SOLUTION BY MEANS OF POLYNOMIAL APPROXIMATION
Yasuo Yoshioka, Toshihiko Sasaki, and Makoto Kuramoto (Inst. of Vocational Training) *In* Society of Materials Science Proc. of the 27th Japan Congr. on Mater. Res. Mar. 1984 p 147-152 refs (For primary document see N85-34180 23-23)
Avail: NTIS HC A14/MF A01

N85-34210# Osaka City Univ. (Japan). Faculty of Engineering.
STRESS DISTRIBUTION OF FIBERGLASS REINFORCED PLASTIC BEAM WITH A DELAMINATION UNDER THREE-POINT BENDING
Taichi Fujii and Qian Sun (Beijing FRP Research Inst.) *In* Society of Materials Science Proc. of the 27th Japan Congr. on Mater. Res. Mar. 1984 p 257-261 refs Previously announced in IAA as A85-23472 (For primary document see N85-34180 23-23)
Avail: NTIS HC A14/MF A01

N85-34320# Cranfield Inst. of Tech., Bedford (England). Mechanism Design Unit.
INERTIAL STRESSES AND DEFORMATIONS IN MECHANISMS
J. N. Hammar *In* Cranfield Inst. of Tech. Proc. of the Mech. Conf., Vol. 2 1984 16 p ref 2 Vol. (For primary document see N85-34318 23-31)
Avail: NTIS HC A05/MF A01

42 GEOSCIENCES (GENERAL)

No abstracts in this category.

43 EARTH RESOURCES

Includes remote sensing of earth resources by aircraft and spacecraft; photogrammetry; and aerial photography.

For instrumentation see *35 Instrumentation and Photography.*

N85-34434 National Physical Lab., Teddington (England). Div. of Mechanical and Optical Metrology.
PRODUCTION OF INITIAL ESTIMATES OF PHOTOGRAMMETRIC VARIABLES
R. A. Hunt Sep. 1983 47 p refs
(NPL-MOM-66; ISSN-0309-3069) Copyright. Avail: Issuing Activity

Production of initial estimates required to linearize the equations giving the image coordinates in photogrammetry is discussed. A method of finding the perspective centers (choice of initial points, determination of distances, intersection of three spheres, choice of the best solution, iterative refinement of the perspective center X0); a method of finding the rotation (R) matrix (initial determination of the R matrix, iterative refinement of R); an intersection method to find the unknown points; and simultaneous adjustment of R and X0 (treatment of camera aberrations, forming the derivatives, inclusion of constraints on the solution, the final solution) are outlined. Author (ESA)

N85-34435*# National Aeronautics and Space Administration, Washington, D. C.
SNOW COVER IN THE SIBERIAN FOREST-STEPPE
I. V. Zykov Jul. 1985 20 p Transl. into ENGLISH freom Zemlevedeniye, Moskov. O-va Ispytat. Prirody (USSR), v. 2, no. 42, 1948 p 375-387 Transl. by Scientific Translation Service, Santa Barbara, Calif.
(Contract NASw-4004)
(NASA-TM-77914; NAS 1.15:77914) Avail: NTIS HC A02/MF A01 CSCL 08L

A study is made of the snow cover on an experimental agricultural station in Mariinsk in the winter of 1945 to 1946. Conditions of snow cover formation, and types and indicators of snow cover are discussed. Snow cover structure and conditions and nature of thawing are described. Author

N85-34436# Geological Survey, Laramie, Wyo.
GEOTHERMAL RESOURCES OF THE LARAMIE, HANNA AND SHIRLEY BASINS, WYOMING
B. S. Hinkley and H. P. Heasler 1984 55 p refs
(Contract DE-FC07-79ID-12026)
(DE85-005005; Investigations-26; DOE/ID-12026/T9) Avail: NTIS HC A04/MF A01

This introduction contains: (1) a general discussion of how geothermal resources occur, (2) a discussion of the temperatures, distribution, and possible applications of geothermal resources in Wyoming and a general description of the state's thermal setting, and (3) a discussion of the methods used in assessing the geothermal resources. This introduction is followed by a description of the geothermal resources of the Laramie, Hanna, and Shirley Basins of southeastern Wyoming. The discussion of geothermal resources of the area includes sections on heat flow and conductive gradients, stratigraphy and hydrology, structure and water movement, measured temperatures and gradients, areas of anomalous gradient (including discussion of the warm spring systems at Alcova and Saratoga), temperatures of the Cloverly Formation, and summary and conclusions. DOE

N85-34437# Stanford Univ., Calif. Geothermal Program.
DEPLETION MODELING OF LIQUID DOMINATED GEOTHERMAL RESERVOIRS
G. Olsen Jun. 1984 144 p refs
(Contract DE-AT03-80SF-11459)
(DE85-009923; SGP-TR-80) Avail: NTIS HC A07/MF A01

Depletion models for liquid-dominated geothermal reservoirs are derived and presented. The depletion models are divided into two categories: confined and unconfined. For both cases depletion models with no recharge (or influx), and depletion models including recharge, are used to match field data from the Svartsengi high temperature geothermal field in Iceland. The influx models included with the mass and energy balances are adopted from the petroleum engineering literature. The match to production data from Svartsengi is improved when influx was included. The Schilthuis steady-state influx gives a satisfactory match. The finite aquifer method of Fetkovitch, and the unsteady state method of Hurst gave reasonable answers, but not as good. The best match is obtained using Hurst simplified solution when lambda = 1.3 x 10 to the minus 4 mm. From the match the cross-sectional area of the aquifer was calculated as 3.6 sq km. The drawdown was predicted using the Hurst simplified method, and compared with predicted drawdown from a boiling model and an empirical log-log model. A large difference between the models was obtained. DOE

N85-34438# Utah Geological and Mineralogical Survey, Salt Lake City.
EVALUATION OF LOW-TEMPERATURE GEOTHERMAL POTENTIAL IN UTAH AND GOSHEN VALLEYS AND ADJACENT AREAS, UTAH. PART 2: WATER TEMPERATURE AND CHEMISTRY
R. H. Klauk and D. A. Davis Dec. 1984 75 p refs
(Contract DE-AS07-77ET-28393)
(DE85-009344; DOE/ET-28393/T7-Pt-2) Avail: NTIS HC A04/MF A01

Geothermal reconnaissance techniques have identified five areas in Utah County warranting further investigation for low-temperature geothermal resources. One area in northern Utah Valley is along Utah fault zone and includes Saratoga Hot Springs. Water temperatures within this area range from 21 to 43 (0)C. Common ion analyses as well as B and Li concentrations indicate waters sampled in this area are anomalous when compared to other samples from the same aquifer. Two other areas in southern Utah Valley also coincide with the Utah Lake fault zone. Common ion analyses, trace element concentrations, and C1/HCO3 ratios distinguish these areas from all other waters in this valley. Temperatures within these southern areas range from 21 to 32(0)C. The Castilla Hot Springs area has been expanded by this study to include a spring located 3 mi further up Spanish Fork Canyon near the Thistle earthflow. A temperature of 50(0)C was recorded for this spring and chemistry is similar to Castilla. In Goshen Valley, the fifth geothermal area identified, measured temperatures range from 20 to 27(0)C for some wells and springs. DOE

N85-34439# California Univ., Berkeley. Lawrence Berkeley Lab.
MODELING OF GEOTHERMAL SYSTEMS
G. S. Bodvarsson, K. Pruess, and M. J. Lippmann 25 Mar. 1985 23 p refs Presented at the SPE Ann. Calif. Reg. Meeting, Bakersfield, Calif., 25 Mar. 1985
(Contract DE-AC03-76SF-00098)
(DE85-012553; LBL-18268; CONF-850312-2) Avail: NTIS

HC A02/MF A01

During the last decade the use of numerical modeling for geothermal resource evaluation has grown significantly, and new modeling approaches have been developed. A summary of the present status in numerical modeling of geothermal systems is presented. Recent developments are emphasized. Different modeling approaches are described and their applicability discussed. The various modeling tasks, including natural state, exploitation, injection, multicomponent and subsidence modeling, are illustrated with geothermal field examples. DOE

N85-34440# Stottler, Stagg and Associates, Inc., San Antonio, Tex.
HYDROLOGY Hydraulic Engineering Circular no. 19, Oct. 1983 - Oct. 1984
F. D. Masch Oct. 1984 367 p refs
(Contract DTFH61-83-C-00118)
(PB85-182954; FHWA/IP-84/15) Avail: NTIS HC A16/MF A01 CSCL 08H

A synthesis of practical hydrologic methods and techniques to assist the highway engineer in the analysis and design of highway drainage structures is provided. A discussion of descriptive hydrology, the surface runoff process and hydrologic data with emphasis given to the highway stream-crossing problem follows. USGS regional regression equations and other methods for peak flow determinations in ungaged watersheds and in basins with insufficient data are presented with examples. Methods for developing unit hydrographs from stream-flow data and by the Snyder and SCS synthetic procedures for ungaged sites are described in detail. Techniques for developing design storms and design hydrographs are given for basins with and without data. GRA

N85-34547# Perception Computing, Inc., Downsview (Ontario).
THE SCIENTIFIC AND TECHNICAL ISSUES IN INTEGRATING REMOTELY SENSED IMAGERY WITH GEOCODED DATA BASES
W. Murray Strome and Berne Grush *In* Canadian Information Processing Society Graphics Interface 1985 1985 p 171-177 refs (For primary document see N85-34523 23-61)
Avail: NTIS HC A19/MF A01

N85-34561# Rensselaer Polytechnic Inst., Troy, N. Y.
THE AUTOMATIC LABELING OF GEOGRAPHIC MAPS: A PROBLEM IN COMPUTER AESTHETICS
Herbert Freeman *In* Canadian Information Processing Society Graphics Interface 1985 1985 p 273-281 refs (For primary document see N85-34523 23-61)
Avail: NTIS HC A19/MF A01

N85-34562# Nippon Electric Co. Ltd., Kawasaki (Japan). Systems Research Labs.
HOW MAP DESIGNERS CAN REPRESENT THEIR IDEAS IN THEMATIC MAPS: EFFECTIVE USER INTERFACES FOR THEMATIC MAP DESIGN
Takuya Yamahira, Yutaka Kasahara, and Tateyuki Tsurutani *In* Canadian Information Processing Society Graphics Interface 1985 1985 p 283-290 refs (For primary document see N85-34523 23-61)
Avail: NTIS HC A19/MF A01

44 ENERGY PRODUCTION AND CONVERSION

Includes specific energy conversion systems, e.g., fuel cells and batteries; global sources of energy; fossil fuels; geophysical conversion; hydroelectric power; and wind power.

For related information see also *07 Aircraft Propulsion and Power, 20 Spacecraft Propulsion and Power, 28 Propellants and Fuels,* and *85 Urban Technology and Transportation.*

N85-34441* National Aeronautics and Space Administration. Lewis Research Center, Cleveland, Ohio.
THERMIONIC PHOTOVOLTAIC ENERGY CONVERTER Patent
Donald L. Chubb, inventor (to NASA) Issued 9 Jul. 1985 7 p Filed 15 Feb. 1984 Supersedes N84-20918 (22 - 11, p 1673)
(NASA-Case-LEW-14077-1; US-Patent-4,528,417;
US-Patent-Appl-SN-580573; US-Patent-Class-136-253) Avail: US Patent and Trademark Office CSCL 10A

A thermionic photovoltaic energy conversion device comprises a thermionic diode mounted within a hollow tubular photovoltaic converter. The thermionic diode maintains a cesium discharge for producing excited atoms that emit line radiation in the wavelength region of 850 nm to 890 nm. The photovoltaic converter is a silicon or gallium arsenide photovoltaic cell having bandgap energies in this same wavelength region for optimum cell efficiency. Official Gazette of the U.S. Patent and Trademark Office

N85-34442*# Astro Aerospace Corp., Carpinteria, Calif.
STACBEAM 2 Final Report
Louis R. Adams and Angelika vonRoos 23 Apr. 1985 61 p refs Prepared in cooperation with JPL, Pasadena, Calif.
(NASA-CR-176126; JPL-9950-1159; NAS 1.26:176126;
AAC-TN-1134) Avail: NTIS HC A04/MF A01 CSCL 10B

An investigation being conducted by Astro Aerospace Corporation (Astro) for Jet Propulsion Laboratory in which efficient structures for geosynchronous spacecraft solar arrays are being developed is discussed. Recent developments in solar blanket technology, including the introduction of ultrathin (50 micrometer) silicon solar cells with conversion efficiencies approaching 15 percent, have resulted in a significant increase in blanket specific power. System specific power depends not only on blanket mass but also on the masses of the support structure and deployment mechanism. These masses must clearly be reduced, not only to minimize launch weight, but also to increase array natural frequency. The solar array system natural frequency should be kept high in order to reduce the demands on the attitude control system. This goal is approached by decreasing system mass, by increasing structural stiffness, and by partitioning the blanket. As a result of this work, a highly efficient structure for deploying a solar array was developed. R.F.J.

N85-34443*# National Aeronautics and Space Administration. Lewis Research Center, Cleveland, Ohio.
EVALUATION OF DEVELOPMENTAL MEMBRANES FOR THE MIXED REACTANT IRON-CHROMIUM REDOX SYSTEM
Jerri S. Ling 1984 13 p refs Presented at the 166th Meeting of the Electrochem. Soc., New Orleans, 7-12 Oct. 1984
(Contract DE-AI04-80AL-12726)
(NASA-TM-87074; E-2646; DOE/NASA/12726-26; NAS 1.15:87074) Avail: NTIS HC A02/MF A01 CSCL 10C.

The operation of the redox storage system at 65 C with premixed ion has changed chromium reactant solutions membrane requirements. These new conditions allow the use of low resistivity membranes with relatively poor selectivity compared to membranes developed for system operation with separate reactants at 25 C. The results of in cell evaluations of developmental membranes for the new conditions are presented. Data include diffusion rate, area resistivity, and coulombic and energy efficiencies over a wide range of current densities. Use of these membranes

results in peak round trip energy efficiencies greater than 80% at current densities as high as 80 mA/sq cm. E.A.K.

N85-34444*# National Aeronautics and Space Administration. Lewis Research Center, Cleveland, Ohio.
REFLECTION PLANE TESTS OF A WIND TURBINE BLADE TIP SECTION WITH AILERONS Final Report
J. M. Savino, T. W. Nyland, A. G. Birchenough, F. L. Jordan (NASA, Langley Research Center), and N. K. Campbell (NASA, Langley Research Center) Aug. 1985 57 p refs
(Contract DE-AI01-79ET-20320)
(NASA-TM-87018; E-2564; DOE/NASA/20320-65; NAS 1.15:87018) Avail: NTIS HC A04/MF A01 CSCL 10A

Tests were conducted in the NASA Langley 30 by 60 foot Wind Tunnel on a full scale 7.31 m (24 ft) long tip section of a wind turbine rotor blade. The blade tip section was built with ailerons on the trailing edge. The ailerons, which spanned a length of 6.1 m (20 ft), were designed so that two types could be evaluated: the plain and the balanced. The ailerons were hinged on the suction surface at the 0.62 X chord station behind the leading edge. The purpose of the tests was to measure the aerodynamic characteristics of the blade section for: an angle of attack range from 0 deg to 90 deg aileron deflections from 0 deg to -90 deg, and Reynolds numbers of 0.79 and 1.5 x 10 to the 6th power. These data were then used to determine which aileron configuration had the most desirable rotor control and aerodynamic braking characteristics. Tests were also run to determine the effects of vortex generators, leading edge roughness, and the gaps between the aileron sections on the lift, drag, and chordwise force coefficients of the blade tip section. Author

N85-34445*# Westinghouse Electric Corp., Pittsburgh, Pa. Advanced Energy Systems Div.
FLAT-PLATE SOLAR ARRAY PROJECT PROCESS DEVELOPMENT AREA PROCESS RESEARCH OF NON-CZ SILICON MATERIAL Quarterly Report, 1 Apr. - 30 Jun. 1985
Jul. 1985 22 p Sponsored by NASA Prepared in cooperation with JPL, Pasadena, Calif.
(NASA-CR-176117; JPL-995C 1161; NAS 1.26:176117; DOE/JPL-956616-85/5; DRL-206; DRD-SE-5; QR-5) Avail: NTIS HC A02/MF A01 CSCL 10B

Three sets of samples were laser processed and then cell processed. The laser processing was carried out on P-type and N-type web at laser power levels from 0.5 joule/sq cm to 2.5 joule/sq cm. Six different liquid dopants were tested (3 phosphorus dopants, 2 boron dopants, 1 aluminum dopant). The laser processed web strips were fabricated into solar cells immediately after laser processing and after various annealing cycles. Spreading resistance measurements made on a number of these samples indicate that the N(+)P (phosphorus doped) junction is approx. 0.2 micrometers deep and suitable for solar cells. However, the P(+)N (or P(+)P) junction is very shallow (< 0.1 micrometers) with a low surface concentration and resulting high resistance. Due to this effect, the fabricated cells are of low efficiency. The maximum efficiency attained was 9.6% on P-type web after a 700 C anneal. The main reason for the low efficiency was a high series resistance in the cell due to a high resistance back contact. Author

N85-34446*# Springborn Labs., Inc., Enfield, Conn.
INVESTIGATION OF TEST METHODS, MATERIAL PROPERTIES, AND PROCESSES FOR SOLAR CELL ENCAPSULANTS Annual Report, 1984
1984 104 p refs Sponsored by NASA Prepared in cooperation with JPL, Pasadena, Calif.
(NASA-CR-176132; JPL-9950-1151; NAS 1.26:176132; DOE/JPL-954527-84/27; AR-8) Avail: NTIS HC A06/MF A01 CSCL 11A

Photovoltaic (PV) modules consist of a string of electrically interconnected silicon solar cells capable of producing practical quantities of electrical power when exposed to sunlight. To insure high reliability and long term performance, the functional components of the solar cell module must be adequately protected from the environment by some encapsulation technique. The encapsulation system must provide mechanical support for the cells and corrosion protection for the electrical components. The goal of the program is to identify and develop encapsulation systems consistent with the PV module operating requirements of 30 year life and a target cost of $0.70 per peak watt ($70 per square meter) (1980 dollars). Assuming a module efficiency of ten percent, which is equivalent to a power output of 100 watts per square meter in midday sunlight, the capital cost of the modules may be calculated to be $70.00 per square meter. Out of this cost goal, only 20 percent is available for encapsulation due to the high cost of the cells, interconnects, and other related components. The encapsulation cost allocation may then be stated as $14. 00 per square meter, included all coatings, pottant and mechanical supports for the cells. R.J.F.

N85-34447*# Spectrolab, Inc., Sylmar, Calif.
DEVELOPMENT OF METALLIZATION PROCESS: FSA PROJECT, CELLA AND MODULE FORMATION RESEARCH AREA Final Report
Alexander Garcia, III May 1985 98 p Prepared for JPL, Pasadena, Calif. Sponsored in cooperation with DOE
(Contract JPL-956205; JPL Proj. 9950-1152)
(NASA-CR-176136; NAS 1.26:176136; DOE/JPL-956205-85/9; Rept-6329-29) Avail: NTIS HC A05/MF A01 CSCL 10B

The optimization, evaluation, and demonstration of a novel metallization applied by a screen printing process is examined. Based on previous results of High Resolution, Low Cost Solar Cell Contact Development, a paste consisting of molybdenum, tin, and titanium hydride was selected as the promising composition. No satisfactory cells were made using any of the molybdenum/tin pastes used as a complete replacement for conventional silver pastes. The major problem is the inability to form a bond between the pastes and silicon that withstands soldering. E.R.

N85-34448# Collier Engineering, Cave Creek, Ariz.
DETERMINATION OF PROPERTIES OF ZEOLITE/REFRIGERANT COMBINATIONS FOR SOLAR REFRIGERATION SYSTEMS Final Report
[1985] 47 p refs
(Contract DE-AC03-83SF-11919)
(DE85-012009; DOE/SF-11919/T2) Avail: NTIS HC A03/MF A01

The determination of properties of zeolite/refrigerant combinations of solar refrigeration systems are reviewed in this final report. The US DOE has funded several studies aimed at identifying potential rerigerant/absorption pairs for solar cooling applications. In the case of this report, the absorbent was already chosen (natural zeolite), but criteria of toxicity and heat of vaporization were common among projects. There were three very important criteria studied in this report which were not involved in the other studies. First, a lower evaporator temperature is used in this study than is typical of space cooling applications; second, the effects of molecule size on the system; and third, is the effect of the weight loading differential per unit mass of absorbent. DOE

N85-34449# Conservation and Renewable Energy Inquiry and Referral Service, Silver Spring, Md.
SOLAR THERMAL TECHNOLOGIES PROGRAM SUMMARY
May 1985 3 p refs
(DE85-012253; DOE/CE-0110; FS-196) Avail: NTIS HC A02/MF A01

The primary applications being developed in solar thermal technology are the production of electricity and industrial process heat. Additional applications, such as the production of a transportable fuel, are also being studied to determine their feasibility. Two collector concepts are being examined; central receiver and distributed receiver. Some significant achievements are briefly described, as well as program goals and strategies. The research plan for the 1984 fiscal year is also briefly discussed, including a summary of the budget. DOE

N85-34450# Hawaii Univ., Honolulu. Natural Energy Inst.
WIND ENERGY BATTERY STORAGE, PHASE 2 Final Report
G. D. Curtis, B. H. Auker, and P. K. Takahashi Feb. 1985 167 p
(Contract DE-AC04-76DP-00789)
(DE85-009753; SAND-85-7164) Avail: NTIS HC A08/MF A01

The wind energy battery storage (WEBS) project performed by the Hawaii Natural Energy Institute (HNEI) is a research and development effort funded by the US Department of Energy (USDOE) through the Sandia National Laboratories at Albuquerque (SNLA) battery storage program. The three phase project is intended to design and construct a battery storage system that will be used in conjunction with wind power generating systems for connective to a utility grid serving a small community (Molokai Island). In Phase 2, major efforts included expanding and improving the computer model to include interaction with the utility, collection of additional wind and load data, updating our information on WEBS components, final design of a battery storage facility, and application of the simulation of various configurations and operating strategies. DOE

N85-34451# Brookhaven National Lab., Upton, N. Y.
DUAL-CHAMBER PLASMA DEPOSITION OF A-Si:H SOLAR CELLS AT HIGH RATES USING DISILANE
G. Rajeswaran, P. E. Vanier, R. R. Corderman, and F. J. Kampas 1985 7 p refs Presented at the 2nd Spring Meeting of the Mater. Res. Soc., San Francisco, 15 Apr. 1985
(Contract DE-AC02-76CH-00016)
(DE85-011828; BNL-36369; CONF-850421-6) Avail: NTIS HC A02/MF A01

The use of a separated chamber deposition system for the fabrication of a Si:H solar cells from disilane at high deposition rates results in a substantial improvement in short circuit current compared to that obtained from a single chamber system. The spectral responses of cells fabricated in the dual-chamber mode are compared to those made in the single chamber mode. The results are interpreted by assuming that the rate of removal of boron contaminants from the chamber is independent of deposition rate. DOE

N85-34452# New York State Dept. of Education, Albany. Solar Energy Project.
SOLAR ENERGY EDUCATION. RENEWABLE ENERGY: A BACKGROUND TEXT
[1985] 208 p refs
(Contract DE-AC01-77CS-34039)
(DE85-010365; DOE/CS-34039/T9) Avail: NTIS HC A10/MF A01

Some of the most common forms of renewable energy are presented. The topics include solar energy, wind power hydroelectric power, biomass ocean thermal energy, and tidal and geothermal energy. The main emphasis of the text is on the Sun and the solar energy that it yields. Discussions on the Sun's composition and the relationship between the Earth, Sun and atmosphere are provided. Insolation, active and passive solar systems, and solar collectors are the subtopics included under solar energy. DOE

N85-34453# Viking Engineering, Garretson, S. Dak.
[SOLAR HEAT PUMP] Final Report
R. Hermanson [1985] 18 p
(Contract DE-FG48-81R8-06041)
(DE85-011323; DOE/R8-06041/T1) Avail: NTIS HC A02/MF A01

Brief discussions of the major components of a solar powered, chemical ground source heat pump are presented. The components discussed are the solar collectors and the chemical heat storage battery. Sodium sulfide is the medium used for heat storage. Catalog information which provides a description of all of the heat pump systems is included. DOE

N85-34454# Rocky Mountain Bilogical Lab., Crested Butte, Colo.
SMALL HYDROELECTRIC POWER PLAN DEMONSTRATION PROJECT Final Technical Report
[1985] 6 p
(Contract DE-FG48-79R8-00434)
(DE85-011343; DOE/R8-00434/T1) Avail: NTIS HC A02/MF A01

The Rocky Mountain Biological Laboratory has completed construction of a small scale hydroelectric power plant. The plant utilizes water from the Laboratory's domestic water supply, can generate a maximum of 7.5 kW, and supplies electricity to the Laboratory's dining hall for space heat, cooking, and hot water. DOE

N85-34455# State Univ. of New York, Albany.
SOLAR ENERGY EDUCATION: RENEWABLE ENERGY ACTIVITIES FOR CHEMISTRY AND PHYSICS
[1985] 67 p refs
(Contract DE-AC01-77CS-34039)
(DE85-010371; DOE/CS-34039/T6) Avail: NTIS HC A04/MF A01

Information on renewable energy sources is provided for students in this teachers' guide. With the chemistry and physics student in mind, solar energy topics such as absorber plate coatings for solar collectors and energy collection and storage methods are studied. DOE

N85-34456# Meridian Corp., Falls Church, Va.
OCEAN THERMAL ENERGY CONVERSION Annual Report, Fiscal Year 1984
Mar. 1985 54 p
(Contract W-31-109-eng-38)
(DE85-012291; ANL/OTEC-TM-4) Avail: NTIS HC A04/MF A01

Activities are reported in the area of heat-exchanger development, including designs for aluminum-based heat exchangers, performance/cost models for waterside enhancements and techniques for low-cost manufacture. Specific objectives of the experimental verification and testing program element include experimentally verifying predicted thermohydraulic performance of heat exchangers and determining the biofouling and corrosion rates of various heat exchanger materials and the effects of heat-exchanger manufacturing processes on seawater corrosion. Progress on system performance/cost modelling is also reported. DOE

N85-34457# Department of Energy, Washington, D. C.
NONSATURABLE MICRODRYER Patent Application
T. B. Hirschfeld, inventor (to DOE) Filed 23 May 1984 21 p
(Contract W-7405-eng-48)
(DE85-005760; US-Patent-Appl-SN-612954) Avail: NTIS HC A02/MF A01

A nonsaturable microdryer is provided for electrolytically removing moisture from sealed containers, particularly electronic equipment. An electrode/electrolyte assembly is disposed within a channel between the interior and exterior of a sealed container. A catalytic barrier disposed between the interior of the sealed container and the electrode/electrolyte assembly prevents the buildup of explosive concentrations of hydrogen by converting back diffusing hydrogen and oxygen back into water, which is then recycled. A semipermeable membrane disposed between the exterior of the sealed container and the electrode/electrolyte assembly allows selective removal of hydrogen and prevents intake of water. DOE

N85-34458# Department of Energy, Washington, D. C.
SOLAR SYSTEM FAULT DETECTION Patent Application
R. B. Farrington and J. C. Pruett, Jr., inventors (to DOE) Filed 14 May 1984 29 p
(Contract DE-AC02-83CH-10093)
(DE85-005987; US-Patent-Appl-SN-609686) Avail: NTIS HC A03/MF A01

A fault detecting apparatus and method are provided for use with an active solar system. The apparatus provides an indication as to whether one or more predetermined faults have occurred in the solar system. The apparatus includes a plurality of sensors, each sensor being used in determining whether a predetermined condition is present. The outputs of the sensors are combined in

a pre-established manner in accordance with the kind of predetermined faults to be detected. Indicators communicate with the outputs generated by combing the sensor outputs to give the user of the solar system and the apparatus an indication as to whether a predetermined fault has occurred. Upon detection and indication of any predetermined fault, the user can take appropriate corrective action so that the overall reliability and efficiency of the active solar system are increased. DOE

N85-34459# Department of Energy, Washington, D. C.
FUEL CELL SEPARATOR PLATE WITH BELLOWS-TYPE SEALING FLANGES Patent Application
G. A. Louis, inventor (to DOE) Filed 29 May 1984 15 p
(Contract DE-AC21-79FT-15440)
(DE85-005991; US-Patent-Appl-SN-814505) Avail: NTIS HC A02/MF A01

A fuel cell separator includes a rectangular flat plate having two unitary upper sealing flanges respectively comprising opposite marginal edges of the plate folded upwardly and back on themselves and two lower sealing flanges respectively comprising the other two marginal edges of the plate folded downwardly and back on themselves. Each of the sealing flanges includes a flat wall spaced from the plate and substantially parallel thereto and two accordion pleated side walls, one of which interconnects the flat wall with the plate and the other of which steps just short of the plate, these side walls affording resilient compressibility to the sealing flange in a direction generally normal to the plane of the plate. Four corner members close the ends of the sealing flanges. An additional resiliently compressible reinforcing member may be inserted in the passage formed by each of the sealing flanges with the plate. DOE

N85-34460# Department of Energy, Washington, D. C.
ELECTROLYTE RESEVOIR FOR CARBONATE FUEL CELLS Patent Application
C. D. Iacovangelo and D. A. Shores, inventors (to DOE) Filed 23 May 1984 13 p refs
(Contract DE-AC02-80ET-17019)
(DE85-005736; US-Patent-Appl-SN-612951) Avail: NTIS HC A02/MF A01

An electrode for a carbonate fuel cell and method to make fuel cells are described. A substantially uniform mixture of an electrode-active powder and porous ceramic particles suitable for a carbonate fuel cell are formed into an electrode with the porous ceramic particles with pores in the range of about 1 micron to about 3 microns, and a carbonate electrolyte is in the pores of the ceramic particles. E.A.K.

45 ENVIRONMENT POLLUTION

Includes air, noise, thermal and water pollution; environment monitoring; and contamination control.

N85-34461# Pechan (E. H.) and Associates, Inc., Springfield, Va.
FORECASTING FUTURE INDUSTRIAL SO2 AND NC/SUB x/ EMISSIONS, REVISED
K. Graves, E. Pechan, B. Briggs (DOE, Washington, D.C.), and D. Turner 1984 16 p refs Presented at the Air Pollution Control Assoc. Ann. Meeting, San Francisco, 25 Jun. 1984
(Contract DE-AI01-83PE-70494)
Avail: NTIS HC A02/MF A01

Future emissions from various economic source sectors were estimated with a focus on those emissions associated with industrial activities. The estimates were obtained from the Environmental Trends Analysis Model (ETAM). The projections are based on energy and economic projections and on data inputs from different sources and models. In sulfur dioxide and nitrogen oxide emission trends to the year 2010 from the industrial sector within the context of total anthropogenic emission are reviewed. DOE

N85-34462# California Univ., Livermore. Lawrence Livermore Lab.
MARINE SAMPLE EXPLOITATION PROJECT: ESTIMATES REGARDING THE SENSITIVITY AND TECHNOLOGY FOR THE DETECTION OF NUCLEAR EXPLOSION DEBRIS IN THE MARINE ENVIRONMENT
K. V. Marsh and R. W. Buddemeier 4 Jun. 1985 11 p refs
(Contract W-7405-eng-48)
(DE85-013176; UCID-20381) Avail: NTIS HC A02/MF A01

The possibility of detecting a small nuclear explosion in which most of the fission products are released to the ocean is discussed. The use of marine plankton as bioaccumulators is proposed to deal with the problem of dilution. DOE

N85-34463# Oak Ridge National Lab., Tenn.
EFFECTS OF ACID RAIN ON FOREST NUTRIENT STATUS Final Report
D. W. Johnson and D. W. Cole Apr. 1985 45 p refs Sponsored by EPRI
(Contract DE-AC05-84OR-21400; EPRI Proj. 1813)
(DE85-012486; DOE/OR-21400/T123) Avail: NTIS HC A03/MF A01

In five forest sites (three in eastern Tennessee and two in western Washington) the effect of natural carbonic acid production on soil leaching was equaled or exceeded by that of atmospheric acid inputs. In a nitrogen-fixing red alder site in Washington, however, internal leaching by nitrification and nitric acid formation far exceeded atmospheric H(+) inputs at any site. All other sites retained NO3(-), and soil SO4(2-) adsorption reduced the effectiveness of atmospheric H2SO4 inputs on soil leaching in two of the Tennessee sites and in the Washington red alder site. Atmospheric sulfur inputs exceeded the forest sulfur requirement in all five sites. Decomposer invertebrates appeared to be affected negatively by unrealistically large applications of SO4(2-), either as KHSO4 or K2SO4. Forest floor buffering prevented large changes in pH with acid SO4(2-) treatments. Results indicate that effects of acid deposition on decomposer invertebrates are unlikely except at input levels much higher than ambient. DOE

N85-34464# State Univ. of New York, Albany. Atmospheric Sciences Research Center.
THROUGHFALL RATE AND CHEMISTRY STUDIES: WHITEFACE MOUNTAIN
J. A. Kadlecek and B. Mossl [1985] 30 p ref
(Contract DE-AC02-76EV-02986)
(DE85-012407; DOE/EV-02986/T1) Avail: NTIS HC A03/MF A01

Ranges of site dependent variability in precipitation quantity and chemical composition were studied with the following recommendations. At the 2000 ft level, the distribution of collected volumes is event dependent and normalization by open collection does not help. Averages based on approximately 5 to 10,000 cm(2) collection area should give results commensutrate with uncertainties normally found in precipitation sampling. Troughs and buckets of equivalent areas give similar results. Wet precipitation is the primary mechanism for dominant inorganic ion deposition. However, near summit level, additional collection area will be required to reduce the sampling uncertainties. Throughfall deposition was enriched in this study, relative to rain, by a factor of about 6 for SO4(2-) and 4 for H(+). The uncertainty in these values is large, but enrichment does occur. It is postulated that cloud capture is the primary source. DOE

N85-34465# California Univ., Livermore. Lawrence Livermore Lab.
EVALUATION OF SOURCE STRENGTH AND DISPERSION MODEL PREDICATIONS WITH DATA FROM LARGE NITROGEN TETROXIDE FIELD EXPERIMENTS
T. G. McRae Apr. 1985 23 p refs Presented at the 15th Intern. Tech. Meeting on Air Pollution Modeling and its Appl., St. Louis, 15 Apr. 1985
(Contract W-7405-eng-48)
(DE85-011855; UCRL-91402; CONF-8504135-1) Avail: NTIS

HC A02/MF A01

A series of large scale nitrogen tetroxide spill tests are conducted to determine the source strength characteristics and heavy-gas dispersion aspects of large N2O4 spills. The source strength and downwind dispersion results of two of the spills are used to evaluate several source strength and Gaussian dispersion models. It is concluded that: the internal energy heat source is a major contributor to the source strength; source strength models need improvement; formation of a dense HNO3 mist may account for much of the downwind mass transport of large N2O4 spills; and all models evaluated underpredict downwind gas concentrations. DOE

46 GEOPHYSICS

Includes aeronomy; upper and lower atmosphere studies; ionospheric and magnetospheric physics; and geomagnetism.

For space radiation see *93 Space Radiation*.

N85-34466 Institut d'Aeronomie Spatiale de Belgique, Brussels.
AGENTS AND EFFECTS OF OZONE TRENDS IN THE ATMOSPHERE
G. Brasseur and A. deRudder 1984 46 p refs Presented at NATO Workshop on Impact of Solar Untraviolet Radiation upon Terrestrial Ecosystems. 1: Agr. Systems, Bad Windsheim, West Germany, 27-30 Sep. 1983 Submitted for publication
(Contract CMA-82-396)
(Aeronomica-Acta-A-287-1984) Avail: Issuing Activity

Ozone depletion due to human activity is discussed. Results from an interactive chemical/radiative/dynamic one-dimensional model with several coupled perturbation scenarios are presented. Man-made chlorofluorocarbons should reduce the ozone amount by a few percent if the present release into the atmosphere continues. However, an increase of carbon dioxide should cool the upper stratosphere and consequently increase the ozone concentration. Author (ESA)

N85-34467*# Lamont-Doherty Geological Inst., Palisades, N. Y.
SCALING DIFFERENCES BETWEEN LARGE INTERPLATE AND INTRAPLATE EARTHQUAKES
C. H. Scholz, C. A. Aviles, and S. G. Wesnousky 1985 16 p refs
(Grant NAG5-446)
(NASA-CR-176149; NAS 1.26:176149) Avail: NTIS HC A02/MF A01 CSCL 80K

A study of large intraplate earthquakes with well determined source parameters shows that these earthquakes obey a scaling law similar to large interplate earthquakes, in which M sub o varies as L sup 2 or u = alpha L where L is rupture length and u is slip. In contrast to interplate earthquakes, for which alpha approximately equals 1 x .00001, for the intraplate events alpha approximately equals 6 x .0001, which implies that these earthquakes have stress-drops about 6 times higher than interplate events. This result is independent of focal mechanism type. This implies that intraplate faults have a higher frictional strength than plate boundaries, and hence, that faults are velocity or slip weakening in their behavior. This factor may be important in producing the concentrated deformation that creates and maintains plate boundaries. Author

N85-34468# Geological Survey, Washington, D.C.
THE UNITED STATES GEOLOGICAL SURVEY IN ALASKA: ACCOMPLISHMENTS DURING 1983
Susan Bartsch-Winkler, ed. and Katherine M. Reed, ed. 1985 118 p refs
(USGS-Circ-945) Avail: NTIS HC A06/MF A01

Geologic studies carried out in Alaska during 1983 are reported. Various geological aspects of the onshore and offshore areas of Alaska are investigated. Topics cover a wide range in scientific and economic interest. E.A.K.

N85-34469# Argonne National Lab., Ill.
GEOLOGY AND PETROLEUM RESOURCES OF BASINS IN WESTERN CHINA
G. Ulmishek Nov. 1984 137 p refs
(Contract W-31-109-eng-38)
(DE85-013038; ANL/ES-146) Avail: NTIS HC A07/MF A01

Western China contains 11 recognized petroliferous or potentially petroliferous basins. Despite their great difference in size, these basins have important common features: (1) their Mesozoic-Cenozoic sedimentary sequences are composed of rocks of essentially terrestrial orgin; and (2) they experienced predominantly compressional stress during the late stages of their geologic history. The topics discussed for each basin include the stratigraphic and lithologic composition of the sedimentary cover, the major stages of tectonic development and the present-day structural framework, known oil and gas fields, probable source rocks, reservoir rocks, traps and seals, and potentially important exploration plays. The basins occupy 800,000 sq km of land and contain over 4,000,000 cubic km of prospective sedimentary rocks. The most probable amounts of undiscovered petroleum resources in all these basins are estimated at 19.5 billion barrels of oil and 78 trillion cubic feet of gas. The Tarim, Zhungaer, and Chaidamu basins possess the great majority of these resources. DOE

N85-34470# Amoco Production Co., Chicago, Ill.
COMPREHENSIVE FRACTURE DIAGNOSTICS EXPERIMENT. PART 2: COMPARISON OF SEVEN FRACTURE AZIMUTH MEASUREMENTS
M. B. Smith, N. K. Ren (Dowell Schlumberger), G. G. Sorrells (Teledyne Geotech, Dallas), and L. W. Teufel (Sandia National Labs., Albuquerque, N. Mex.) 1985 16 p refs Presented at the SPE/DOE Symp. on Low Permeability Reservoirs, Denver, 19 May 1985
(Contract DE-AC04-76DP-00789)
(DE85-011707; SAND-85-0990C-Pt-2; CONF-8505115-5-Pt-2; SPE-13894-Pt-2) Avail: NTIS HC A02/MF A01

Geophysical techniques for measuring the hydraulic fracture azimuth were explored. A comparison of seven different measurements used to determine the azimuth in a sandstone formation at a depth of 1000 ft is discussed. The azimuth was determined as N95E, but significant differences existed between some of the results. This is importance since in developing new measurements, the limits of these must be found and honored. The results from microseismic monitoring are examined. The lack of results suggests that remote monitoring for seismic events may be impractical for normal, sedimentary, hydrocarbon-bearing formations. DOE

N85-34471# Geological Survey, Denver, Colo.
URANIUM, THORIUM ISOTOPIC ANALYSES AND URANIUM-SERIES AGES OF CALCITE AND OPAL AND STABLE ISOTOPIC COMPOSITIONS OF CALCITE FROM DRILL CORES UE25a NO. 1, USR G-2 AND USW G-3/GU-3, YUCCA MOUNTAIN, NEVADA
B. J. Szabo and T. K. Kyser 1985 29 p
(Contract DE-AI08-78ET-44802)
(DE85-013039; USGS-OFR-85-224) Avail: NTIS HC A03/MF A01

Fracture and cavity filling calcite and opal in the unsaturated zone of three drill cores at Yucca Mountain were analyzed for uranium and stable isotope contents, and were dated by the uranium-series method. Stable isotope data indicate that the water from which the calcite precipitated was meteoric in origin. The decrease in O-18 and increase in C-13 with depth are interpreted as being due to the increase in temperature in drill holes corresponding to an estimated maximum geothermal gradient of 43 deg per km. Of the eighteen calcite and opal deposits dated, four of the calcite and all four of the opal deposits yield dates older than 400,000 years and ten of the remaining calcite deposits yield dates between 26,000 and 310,000 years. The stable isotope and uranium data together with the finite uranium-series dates of precipitation suggest a complex history of fluid movements, rock

and water interactions, and episodes of fracture filling during the last 310,000 years. DOE

N85-34472# Los Alamos Scientific Lab., N. Mex.
WORKSHOP ON RECENT RESEARCH IN THE VALLES CALDERA
G. Heiken, comp. Feb. 1985 71 p refs Workshop held in Los Alamos, N. Mex., 15 Oct. 1984
(Contract W-7405-eng-36)
(DE85-010569; LA-10339-C-; CONF-8410265-Summs) Avail: NTIS HC A04/MF A01

Over the last 5 years, there has been increased interest in the geology of the Jemez Mountains volcanic field, New Mexico. Of special interest is the Toledo-Valles caldera complex, which is targeted for research coring as part of the Continental Scientific Drilling Program. The general topics covered in this workshop were: (1) hydrothermal systems and rock-water interactions; (2) volcanology and structural framework of the Jemez volcanic field; (3) determining the presence or absence of melt below the Valles caldera; and (4) deep coring and drilling technology. Separate abstracts were prepared for each presentation. DOE

N85-34473# California Univ., Berkeley. Lawrence Berkeley Lab.
STUDIES IN THERMO-HYDRO-CHEMICAL TRANSPORT IN POROUS AND FRACTURED MEDIA
C. F. Tsang May 1984 12 p refs Presented at the Intern. Groundwater Symp., Montreal, 21 May 1984
(Contract DE-AC03-76SF-00098)
(DE85-012555; LBL-17473; CONF-8405144-4) Avail: NTIS HC A02/MF A01

Recent interest in the transport of toxic chemicals or radionuclides in subsurface formation raise the question of the role of processes involving the interplay of fluid flow, chemical interaction, and thermal effects. Three examples of recent studies at Lawrence Berkeley Laboratory in this area, based on numerical modeling with a code called CPT are reviewed. It is a three dimensional chemical parcel model with a fully coupled heat and mass transport formulation for porous fractured media with complex geometries. The three examples are: (1) injection and production of a denser cold fluid into a geothermal reservoir; (2) solute transport in a two layered aquifer; and (3) solute transport in an aquifer with a horizontal fractured zone. DOE

N85-34474# South Dakota School of Mines and Technology, Rapid City.
THERMALLY INDUCED CHEMICAL MIGRATION: A NATURAL ANALOG APPROACH Progress Report, Sep. 1984 - Sep. 1985
J. J. Papike 26 Apr. 1985 51 p refs
(Contract DE-FG01-84ER-13259)
(DE85-012308; DOE/ER-13259/T1) Avail: NTIS HC A04/MF A01

The extent and mechanisms of chemical migration in the broadest sense is studied, i.e., over a range of temperatures and in diverse geologic media. Pegmatites are genetic links between normal granites and hydrothermal systems. At some stage in their crystallization history with falling temperature (and sometimes pressure) an aqueous fluid phase exsolves and coexists with a silicate melt. Little is known about the composition of these fluids, the element partitioning behavior between fluid and silicate melt, and how these fluids interact with previously crystallized granite. It is these fluids that leak out of the pegmatites and form the dispersion halos that are studied. Research progress is reported in the following areas: (1) fluid evolution in metamorphic aureole; (2) tourmaline as a recorder of pegmatite evolution; (3) feldspar as a recorder of pegmatite evolution; (4) the distribution of boron among pegmatite minerals and the mass balance of boron in granitic pegmatite systems; and (5) crystal chemical aspects of Li, Pb, and Cs partitioning between coexisting muscovite and biotite. DOE

N85-34475# Purdue Univ., Lafayette, Ind. Dept. of Geosciences.
GEOPHYSICAL-GEOLOGICAL STUDIES OF POSSIBLE EXTENSIONS OF THE NEW MADRID FAULT ZONE Annual Report, 1983
W. J. Hinze, L. W. Braile, G. R. Keller (Texas Univ., El Paso), and E. G. Lidiak (Pittsburgh Univ.) Apr. 1985 58 p refs
(Contracts NRC-04-81-196-01; NRC-FIN-B-8077)
(TI85-901341; M85901341; NUREG/CR-3174-Vol-2) Avail: NTIS HC A04/MF A01

Recent geophysical investigations have shown that the seismicity of the New Madrid, Missouri seismoganic region is correlative with an ancient rift complex suggesting that the anomalous seismicity is the result of the localization of the regional compressive stress pattern by basement structures. Preliminary evidence indicates that this inferred basement rift complex extends beyond the immediate realm of the intense New Madrid region microseismicity. An integrated geophysical/geological research program is being conducted to evaluate the rift complex hypothesis as an explanation for the earthquake activity in the New Madrid area and its extensions, to refine our knowledge of the structure and physical properties of the rift complex, and to investigate the possible northern extensions of the New Madrid fault zone, especially the possible northeastern connection to the Anna, Ohio seismic region. Investigation of the northeast extension of the New Madrid Rift Complex into eastern Indians, north of 39 Deg N latitude, has focused upon the acquisition and preparation of arrays of gravity and magnetic anomaly data sets. DOE

N85-34476# Cologne Univ. (West Germany). Inst. fuer Geophysik und Meteorologie.
THE TRANSIENT ELECTROMAGNETIC DEPTH SOUNDING TECHNIQUE APPLIED TO HYDROCARBONS AND GEOTHERMAL EXPLORATION [DAS TRANSIENT-ELEKTROMAGNETISCHE TIEFENSONDIERUNGSVERFAHREN ANGEWANDT AUF DIE KOHLENWASSERSTOFF- UND GEOTHERMIE-EXPLORATION]
Kurt-Martin Strack 1985 190 p refs In GERMAN
(Mitt-42; ISSN-0069-5882) Avail: NTIS HC A09

The technical application of the broadband time-domain electromagnetic depth sounding method (TDEM) was tested in field measurements. A field apparatus was designed and built for this purpose. Hardware, data processing, interpretation methods, and computer simulation of field measurements are presented. Geological calibration measurements were performed in the oil producing part of the Denver basin; the field data agree with a geoelectric model within 3%. The gradual resistivity changes and the layer structure of the Imperial Valley in California are determined with the same apparatus. Test measurements in the Australian Sydney Basin give consistent inversion results as well as a good correlation between the seismic interpretation of the Australian Bureau of Mineral Resources and the electromagnetic interpretation. Author (ESA)

N85-34477# New Hampshire Univ., Durham. Marine Systems Engineering Lab.
MAGNETIC SEARCH SYSTEM
Sep. 1984 179 p refs Prepared in cooperation with Shenandoah Systems Co., Vienna, Va.
(Grant NA81AA-D-00035)
(PB85-185108; UNH-MP-TR-SG-84-9) Avail: NTIS HC A09/MF A01 CSCL 17F

The Magnetic Search System (MSS) is virtually the only effective means of detecting and localizing buried ferrous objects such as pipelines, wrecks, mines, etc. It is also effective in the confirmation of the ferrous content of objects located by sonar. In spite of the importance of the magnetometer, as a search and classification sensor, it has not received the research and development emphasis accorded other sensor systems. An objective of this study program to improve MSS performance through the application of intelligent system concepts and the use of modern microprocessors. This document addresses the initial phase of this program, an in depth analysis of the system currently in use by the Explosive Ordnance Disposal Technology Center (EODTC). GRA

47 METEOROLOGY AND CLIMATOLOGY

Includes weather forecasting and modification.

N85-34478 Deutscher Wetterdienst, Offenbach am Main (West Germany).
REPORTS FROM THE GERMAN METEOROLOGICAL SERVICE. NO. 166: THE OPTIMAL SPECTRAL DENSITY OF CLIMATOLOGICAL STATION NETWORKS [BERICHTE DES DEUTSCHEN WETTERDIENSTES. NR. 166: DIE OPTIMALE RAEUMLICHE DICHTE VON KLIMATOLOGISCHEN MESSNETZEN]
E. Grimm-Luczak and H. Luczak 1984 23 p refs In GERMAN; ENGLISH summary
(ISBN-3-88148-214-8; ISSN-0072-4130) Copyright. Avail: Issuing Activity

Based on the theory of linear and optimum interpolation, a method to determine the interrelation between interpolation errors and distances between the stations used in this interpolation was developed. Homogeneous and isotropic measuring values are assumed. With a given tolerable uncertainty for interpolation, the necessary and sufficient density of the station network is derived for total area coverage of the measured values. Results of a test with daily means of temperature illustrate the method.
Author (ESA)

N85-34479 Deutscher Wetterdienst, Offenbach am Main (West Germany).
REPORTS FROM THE GERMAN METEOROLOGICAL SERVICE. NO. 167: RESULTS OF AEROLOGICAL SOUNDINGS IN THE MODEL AREA UPPER RHINE: HEAT RELEASE PROJECT UPPER RHINE AREA, PART 3 [BERICHTE DES DEUTSCHEN WETTERDIENSTES NR. 167: ERGEBNISSE KLEINAEROLOGISCHER AUFSTIEGE MODELLGEBIET OBERRHEINGRABEN ABWAERMEPROJEKT OBERRHEINGEBEIT TEIL 3]
U. Maier, G. Suessenguth, G. Jurksch, and H. Bartels 1984 71 p In GERMAN; ENGLISH summary
(ISBN-3-88148-216-4; ISSN-0072-4130) Copyright. Avail: Issuing Activity

By means of nearly synchronized aerological soundings in the planetary boundary layer carried out at localities which form profiles by their spatial distribution, regional and local differences in vertical distribution of air temperature, relative humidity, wind velocity and wind direction were studied. The measurements were made on days when weather types on a synoptic scale were characterized by weak atmospheric pressure gradient and poor vertical exchange. The data were used to illustrate regional patterns of heat release, and to explain the temporal and spatial development of temperature inversions on the atmosphere of the planetary boundary layer.
Author (ESA)

N85-34480# Colorado Univ., Boulder. Cooperative Inst. for Research in Environmental Sciences.
LAKE ICE OCCURENCE AS A POSSIBLE DETECTOR OF ATMOSPHERIC CO2 EFFECTS ON CLIMATE Annual Progress Report, 1 Dec. 1983 - 31 May 1985
R. G. Barry May 1985 54 p
(Contract DE-AC02-83ER-60106)
(DE85-012987; DOE/ER-60106/2; APR-2) Avail: NTIS HC A04/MF A01

A study has been made of the temporal and spatial patterns of the freeze up and break up of lakes in the subarctic and middle latitudes of the Northern Hemisphere, in an attempt to identify the potential effects of warming due to CO2 and other greenhouse effects. Lake ice is a prime candidate for first effects detection of CO2 induced warming because: (1) it shows a high degree of sensitivity to a single meteorological variable (temperature); (2) it has a short response time to temperature anomalies; (3) a single (in most cases), readily identifiable event (i.e., freeze up/break up) is the response to some integral of seasonal temperature conditions; (4) historical records are available to establish lake ice temperature relationships; (5) freeze up/break up of lakes is recorded at a wide network of sites and, in addition, it can be readily monitored by operational satellite data. DOE

N85-34481# InterAmerica Research Associates, Rosslyn, Va.
CLIMATE MODELING: A RETROSPECTIVE-PROSPECTIVE VIEW WITH CONSIDERATION FOR THE ATMOSPHERIC CARBON DIOXIDE-CLIMATE ISSUE
C. A. Sandahl and S. J. Shieh 29 Jun. 1984 121 p
(Contract DE-AC01-82ER-60081)
(DE85-011532; DOE/ER-60081/T2) Avail: NTIS HC A06/MF A01

This paper provides a retrospective prospective view of scientific and technological developments that led to our present capability to predict climate, with particular emphasis on the potential impact of increased atmospheric carbon dioxide, through the use of computer models of the Earth atmosphere system. This view is illustrated by means of a technology tree that traces out the history of key developments. The trunk of the tree represents present competence; the limbs and branches represent antecedent work and interrelationships therein. The technology tree provides a perspective of overall progress, shows where events have come together to provide substantial advancements, exposes areas where progress may be slower than desired, and indicates profitable directions for future work. DOE

N85-34482# Institut National Polytechnique, Toulouse (France).
TUNISIAN CLIMATE SEEN THROUGH A MARKOV PROCESS
C. Thirriot and Z. Kebaili-Bergaoui (Ecole Nationale d'Ingenieurs, Tunis) Sep. 1983 15 p refs In FRENCH; ENGLISH summary
Presented at Soc. Hydrotech. de France Conf. Intern. le Climat Mediterraneen et les Ressources en Eau, Marseille, 6-8 Sep. 1983
(CT-585) Avail: NTIS HC A02/MF A01

Daily rainfall in Tunis is described by discrete Markov chains. A transition matrix is built in stationary form for year or seasonal variations for 2 classes (dry and humid) or many classes (up to 23). Improvements obtained by second order Markov chains are also considered. A simulation study is carried out. The results show that such a model conveniently describes the observation data. Its predictive value is limited. Author (ESA)

48 OCEANOGRAPHY

Includes biological, dynamic and physical oceanography; and marine resources.

N85-34483# Oak Ridge National Lab., Tenn. Chemistry Div.
TWO DIMENSIONAL CO2-OCEAN MODEL INCLUDING THE BIOLOGICAL PROCESSES
C. F. Baes, Jr. and G. G. Killough May 1985 38 p refs
(Contract DE-AC05-84OR-21400)
(DE85-012341; DOE/NBB-0070) Avail: NTIS HC A03/MF A01

A two dimensional (latitude X depth) multibox model of the ocean has been developed and used to predict the distribution of carbon dioxide between the ocean and the atmosphere. The model simulates the chemical and biological processes in the ocean that affect this distribution (i.e., ocean atmosphere exchange of CO2, photosynthesis and decay, calcium carbonate production and dissolution) by means of linear functions. The boxes are arranged to simulate isothermal regions in an idealized world ocean and the numerous flows are adjusted by means of three diffusivity parameters. In steady state calculations, the concentrations of the various forms of carbon, dissolved oxygen, nutrient, alkalinity, and (14)C in each box are determined by matrix methods with three boundary conditions specified, namely, the partial pressure of CO2 in the atmosphere and the nutrient concentration and alkalinity in one box. DOE

N85-34484# Oregon State Univ., Corvallis.
INCREASE OF TOTAL CO2 IN THE WORLD OCEAN Final Technical Report
C. T. A. Chen 1984 8 p refs
(Contract DE-AT06-81EV-10611)
(DE85-007756; DOE/EV-10611/T1) Avail: NTIS

HC A02/MF A01

Accomplishments achieved include the development of a digital potentiometric oxygen titration system, design of an Apple-IIe controlled automatic CO2 titration system, and new data sets of pH, alkalinity, and CO2 from the Weddell Sea, the Bering Sea, the Pacific Ocean between Alaska and Hawaii and between Kwajalein and Seattle, and from the equatorial Pacific, the Drake Passage, and the Red Sea. DOE

51 LIFE SCIENCES (GENERAL)

Includes genetics.

N85-34485# Midwest Research Inst., Golden, Colo. Solar Energy Research Inst.

RESOURCE EVALUATION AND SITE SELECTION FOR MICROALGAE PRODUCTION SYSTEMS

E. L. Maxwell, A. G. Folger, and S. E. Hogg May 1985 98 p refs

(Contract DE-AC02-83CH-10093)

(DE85-008807; SERI/TR-215-2484) Avail: NTIS HC A05/MF A01

Climate, land, and water resource requirements of microalgae production systems (MPS) were examined relative to construction costs, operating costs, and biomass productivity. The objective was the stratification of the southwestern United States into zones of relative suitability for MPS. Maps of climate (insolation, freeze free period, precipitation, evaporation, thunderstorm days), land (use/cover, ownership, slope), and water (saline groundwater) resource parameters were obtained. These maps were transformed into digital overlays permitting the cell by cell compositing of selected resource parameters to form maps representing relative productivity, make up water, climate suitability, land suitability, water suitability, and overall suitability. The Southwest was selected for this study because of its high levels of insolation, saline water resources, and large areas of relatively low valued land. The stratification maps cannot be used for the selection of specific sites because of their low resolution (12,455 acre cells). DOE

N85-34486# Brookhaven National Lab., Upton, N. Y.

ANAEROBIC MICROBIAL TRANSFORMATIONS IN SUBSURFACE ENVIRONMENTS: PROJECT DESCRIPTION

A. J. Francis Apr. 1985 39 p

(Contract DE-AC02-76CH-00016)

(DE85-012789; DOE/CH-00016/T6) Avail: NTIS HC A03/MF A01

Both laboratory and field investigations were conducted to understand the basic biochemical processes involved in the anaerobic transformation of trace metals and selected organic compounds. Controlled laboratory experiments consist of dissolution of trace metals such as As, Cd, Cr, Hg, Mn, Ni, and Pb from model substrate. The effects of the environmental variables such as temperature, pH, O2 tension, moisture, carbon, nitrogen and alternate electron acceptors that may accelerate or reduce biochemical processes in subsurface environments are being investigated. In concert with laboratory research, field studies in the Appalachian region consist of water leachate and soil/waste core sample collection, and physical, chemical and biological characterizations to develop an improved understanding of anaerobic microbial processes. Laboratory observations and processes will be verified and experimental designs will be modified, using information obtained under actual field conditions. The results generated from this basic scientific study will increase our understanding of the biochemical transformations of toxic substances in subsurface environments. DOE

N85-34487# Edgerton, Germeshausen and Grier, Inc., Goleta, Calif.

THE 1984 BIOTIC STUDIES OF YUCCA MOUNTAIN, NEVADA TEST SITE, NYE COUNTY, NEVADA

E. Collins and T. P. OFarrell Feb. 1985 35 p refs

(Contract DE-AC08-83NV-10282)

(DE85-011715; EGG/10282-2057) Avail: NTIS HC A03/MF A01

A portion of Yucca Mountain on and adjacent to the US Department of Energy's Nevada Test Site, Nye County, Nevada, is considered as a possible location for radioactive waste repository. The geologic and environmental characteristics of the site are investigated to determine suitability. Goals of biotic studies are to identify species of concern, describe major floral and faunal associations, determine exposure levels of external background radiation, and assess possible impacts. The species composition of dominant small mammals inhabiting major vegetation associations in 1984 varied little compared with results of similar surveys conducted in 1982 and 1983. Total captures were lower and reproduction was apparently curtailed. Merriam's kangaroo rat and the long tailed pocket mouse continued to be the most abundant species. The composition and relative abundance of associated species was more variable. Western harvest mice were trapped for the first time, but pinyon mice, which were present in prior years, were not trapped. Five desert tortoises were observed during surveys of possible sites for repository surface facilities. DOE

N85-34488# Alabama A & M Univ., Normal.

SCREENING AND CHARACTERIZING OLEAGINOUS MICROALGAL SPECIES FROM THE SOUTHEASTERN UNITED STATES Final Subcontract Report

M. G. Tadros Mar. 1985 37 p refs

(Contract DE-AC02-83CH-10093)

(DE85-008787; SERI/STR-231-2657) Avail: NTIS HC A03/MF A01

Promising algal species which tolerate high light intensities, temperature variations and accumulate lipids were selected and characterized. Samples were collected from freshwater and saltwater locations in the State of Alabama and intertidal regions of the Gulf of Mexico. Samples were screened through a multi-step process. Selected species: Cyclotella, Nitzschia, Chlorella, Scenedesmus and Ankistrodesmus, were examined for growth requirements. Approximate cellular composition of these species was determined. Over sixty strains were isolated, and of these six were ranked as good growers. Two diatoms were isolated that are of particular interest because of their ability to accumulate high lipids. Cyclotella tolerates high temperatures (30 C to 35 C), grows at moderate salinities (15 to 25 parts per thousand), and with nitrogen stress accumulates 42% of its dry weight as lipid. Hantzschia is a large diatom that also grows well at elevated temperatures and full strength seawater. Hantzschia can accumulate as much as 66% of its dry weight as lipid. DOE

N85-34489# Joint Publications Research Service, Arlington, Va.

USSR REPORT: LIFE SCIENCES. BIOMEDICAL AND BEHAVIORAL SCIENCES

20 Aug. 1985 89 p refs Transl. into ENGLISH from various Russian articles

(JPRS-UBB-85-021) Avail: NTIS HC A05/MF A01

Advances on life science, biomedical, and behavioral sciences research in the U.S.S.R. are reported. Topics discussed include: aerospace medicine, biochemistry, bionics, biophysics, biotechnology, epidemiology, food technology, genetics, laser effects, microbiology, molecular biology, nonionizing electromagnetic radiation effects, pharmacology, physiology, and veterinary medicine. For individual titles, see N85-34490 through N85-34490.

N85-34490# Joint Publications Research Service, Arlington, Va.

MICROORGANISMS IN SPACE FLIGHT Abstract Only

K. M. Sytnik, ed. *In its* USSR Rept.: Life Sci. Biomed. and Behavioral Sci. (JPRS-UBB-85-021) 20 Aug. 1985 p 30-31 Transl. into ENGLISH from Mikrobiol. (Moscow), v. 54, no. 1, Jan. - Feb. 1985 p 169-172 (For primary document see N85-34489 23-51) Avail: NTIS HC A08/MF A01

The results of experiments involving developing cultures yielding new information on the influence of extremal factors on living cells are development of space microbiology; (2) specifics of preparation and performance of experiments in space microbiology; (3) influence of space flight factors on the growth,

development and mobility of P. vulgaris; (4) ultra structural organization of cells as an indicator of the influence of space flight factors on living systems; (5) ultra structure of proteus vulgaris cells with various methods of cultivation under space flight conditions; (6) microbiological study of various strains of chlorella grown under space flight conditions; (7) ultra structure of chlorella cells grown under space flight conditions; and (8) basics of restructuring of eukaryotic cell in space flight. Author

N85-34505# Joint Publications Research Service, Arlington, Va.
EFFECT OF SEEDS OF HEAVY CHARGED PARTICLES OF GALACTIC COSMIC RADIATION
Ye. N. Maksimova *In its* USSR Rept.: Space Biol. and Aerospace Med. (JPRS-USB-85-005) 14 Aug. 1985 p 103-107 refs Transl. into ENGLISH from Kosmicheskaya Biol. I Aviakosmicheskaya Meditsina (Moscow), v. 19, no. 3, May - Jun. 1985 p 71-74 (For primary document see N85-34494 23-52)
Avail: NTIS HC A08

52 AEROSPACE MEDICINE

Includes physiological factors; biological effects of radiation; and weightlessness.

N85-34491* National Aeronautics and Space Administration, Washington, D. C.
AEROSPACE MEDICINE AND BIOLOGY: A CONTINUING BIBLIOGRAPHY WITH INDEXES (SUPPLEMENT 274)
Aug. 1985 53 p
(NASA-SP-7011(274); NAS 1.21:7011(274)) Avail: NTIS HC A04 CSCL 06E

This bibliography lists 128 reports, articles, and other documents introduced into the NASA scientific and technical information system in July 1985. Author

N85-34492# Radiation Monitoring Devices, Inc., Watertown, Mass.
APPLICATIONS OF CdTe TO NUCLEAR MEDICINE Final Report
G. Entine 7 May 1985 16 p
(Contract DE-AC02-76EV-02541)
(DE85-011877; DOE/EV-02541/T2) Avail: NTIS HC A02/MF A01

Uses of cadmium telluride (CdTe) nuclear detectors in medicine are briefly described. They include surgical probes and a system for measuring cerebral blood flow in the intensive care unit. Other uses include nuclear dentistry, X-ray exposure control, cardiology, diabetes, and the testing of new pharmaceuticals. DOE

N85-34493# Argonne National Lab., Ill.
ESTIMATING RISKS OF LEAD-INDUCED HEMOGLOBIN DECREMENTS UNDER CONDITIONS OF UNCERTAINTY: METHODOLOGY, PILOT JUDGMENTS AND ILLUSTRATIVE CALCULATIONS
R. G. Whitfield and T. S. Wallsten Sep. 1984 66 p refs
(Contract W-31-109-eng-38)
(DE85-012293; ANL/EES-TM-276) Avail: NTIS HC A04/MF A01

Probabilistic judgements about dose-response relationships between lead exposure and subsequent hemoglobin decrements are made. A method for obtaining the judgements, representing them mathematically, and combining them with a measure of lead exposure to estimate health risks is described. A study was performed to test a protocol for obtaining probabilistic judgements from health experts. Judgements of two pilot subjects were encoded to determine the subjects' judgemental dose-response functions for lead-induced hemoglobin decrements. Their judgements were represented mathematically (with the normal-on-log-odds function) and combined with blood-lead data (a measure of exposure to lead) from the National Health and Nutrition Examination Survey II to illustrate the estimation of health risks for US children aged 0 to 3 years. The report also discusses ways to summarize large amounts of complex risk assessment data and calculations and present them in a form understandable by and useful to decision makers. DOE

N85-34494# Joint Publications Research Service, Arlington, Va.
USSR REPORT: SPACE BIOLOGY AND AEROSPACE MEDICINE, VOL. 19, NO. 3, MAY - JUNE 1985
14 Aug. 1985 156 p refs Transl. into ENGLISH of Kosmich. Biol. i Aviakosmich. Med. (Moscow), v. 19, no. 3, May - Jun. 1985 (JPRS-USB-85-005) Avail: NTIS HC A08

Advancements in space biology and aerospace medicine are reported. Topics include: aerospace environments; spacecraft environments, biochemistry, physiological effects, cosmonaut performance, effects of hypokinesia, neurological and sensorimotor effects, musculoskeletal system, data processing in psychology, human behavior, and group dynamics. For individual titles, see N85-34495 through N85-34509.

N85-34495# Joint Publications Research Service, Arlington, Va.
FLUID-ELECTROLYTE METABOLISM AND RENAL FUNCTION IN COSMONAUTS FOLLOWING 185-DAY SPACEFLIGHT
A. I. Grigoryev, B. R. Dorokhova, V. Yu. Semenov, B. V. Morukov, E. O. Baychorov, I. S. Skukina, and B. V. Afonin *In its* USSR Rept.: Space Biol. and Aerospace Med. (JPRS-USB-85-005) 14 Aug. 1985 p 27-34 refs Transl. into ENGLISH from Kosmicheskaya Biol. I Aviakosmicheskaya Meditsina (Moscow), v. 19, no. 3, May - Jun. 1985 p 21-27 (For primary document see N85-34494 23-52)
Avail: NTIS HC A08

Fluid electrolyte metabolism (FEM) and renal function of the crewmembers of the 185 day spaceflight were examined. Changes in fluid electrolyte metabolism and its regulation were noted. Fluid and sodium retention and higher than preflight sodium excretion in the urine was observed. Postflight a higher excretion of bivalent ions was shown. The higher excretion of calcium was accompanied by a lower concentration of total and ionized calcium in the serum and by a lower concentration of PTH and calcitonin. Variations in potassium metabolism that occurred during flight are assessed including the inability of tissues to retain potassium due to atrophic processes which develop in the weightless state and are due to the unloading of the musculoskeletal system. E.A.K.

N85-34496# Joint Publications Research Service, Arlington, Va.
TOLERANCE TO +Gz AND +Gx ACCELERATIONS OF INDIVIDUALS IN OLDER AGE GROUPS IN GOOD HEALTH AND WITH EARLY SIGNS OF ARTERIOSCLEROSIS
A. R. Kotovskaya, D. G. Dimitrov, V. Yu. Lukyanyuk, I. F. Vil-Vilyams, O. L. Golovkina, V. G. Andreyeva, N. P. Artamonova, and M. P. Kuzmin *In its* USSR Rept.: Space Biol. and Aerospace Med. (JPRS-USB-85-005) 14 Aug. 1985 p 35-41 refs Transl. into ENGLISH from Kosmicheskaya Biol. I Aviakomicheskaya Meditsina (Moscow), v. 19, no. 3, May - Jun. 1985 p 27-31 (For primary document see N85-34494 23-52)
Avail: NTIS HC A08

Tolerance to +Gz and +Gx accelerations of healthy and arteriosclerotic subjects, aged 40 to 49, was investigated during 256 centrifugation tests. As compared to the healthy people, the arteriosclerotic subjects showed a lower tolerance: when exposed to 7 +Gz the tolerance threshold decreased from 5.93 + or - 0.57 g to 5.7 + or - 0.44. Visual disorders and loss of consciousness were recorded. When exposed to 5 +Gz and 6 +Gx no subjects displayed visual disorders or loss of consciousness. However, lower tolerance of 5 +Gz due to cardiac arrhythmias was observed in 4.8% arteriosclerotic patients and in none healthy subjects. Lower tolerance to 6 +Gx associated with cardiac arrhythmias was recorded in 23.8% arteriosclerotic versus 11.8% healthy subject. In both healthy and arteriosclerotic subjects acceleration tolerance was good. It is indicated that individual assessment of acceleration tolerance is of great importance for people older than 40 years with health abnormalities. E.A.K.

N85-34497# Joint Publications Research Service, Arlington, Va.
EFFECT OF HYPOKINESIA AND +Gz ACCELERATIONS ON TRANSPORT FUNCTION OF HUMAN BLOOD

N. V. Khapilov, V. S. Panchenko, N. N. Kotov, and B. F. Asyamolov *In its* USSR Rept.: Space Biol. and Aerospace Med. (JPRS-USB-85-005) 14 Aug. 1985 p 42-45 refs Transl. into ENGLISH from Kosmicheskaya Biol. I Aviakosmicheskaya Meditsina (Moscow), v. 19, no. 3, May - Jun. 1985 p 31-33 (For primary document see N85-34494 23-52)
Avail: NTIS HC A08

The results of 44 studies of circulation parameters and blood transport function of 14 test subjects exposed to 7 day bed rest and acceleration of 4.5 Gz demonstrated that the blood transport carriers and their actively binding centers from working structures in the adaptive reactions. As compared to the pretest level, the distribution ratio of C-14 adenine between two immiscible phases varies from -12 to 14% on bed rest day 3 to +32 to 40% on bed rest day 7; it increases by 145 to 150% after exposure to +4.5 Gz acceleration. The parameters of the blood transport function give a quantitative description of its adaptive reactions to environmental effects. E.A.K.

N85-34498# Joint Publications Research Service, Arlington, Va.
OXYGENATION AND REGIONAL CIRCULATION IN GINGIVAL MUCOSA DURING EXPOSURE TO LOWER BODY NEGATIVE PRESSURE
S. I. Volvach, Ye. A. Kovalenko, S. I. Ponomarev, V. K. Gabyshev, V. I. Nikiforov, A. P. Kulev, and V. V. Arkhipov *In its* USSR Rept.: Space Biol. and Aerospace Med. (JPRS-USB-85-005) 14 Aug. 1985 p 46-50 refs Transl. into ENGLISH from Kosmicheskaya Biol. I Aviakosmicheskaya Meditsina (Moscow), v. 19, no. 3, May - Jun. 1985 p 33-37 (For primary document see N85-34494 23-52)
Avail: NTIS HC A08

Five subjects were exposed to lower body negative pressure (LBNP). During exposure their regional circulation and oxygen balance of the gingival mucosa were measured and electrocardiography and kinetocardiography were performed to calculate parameters of the left heart function. A distinct correlation between LBNP tolerance and the level of compensatory reactions of the gingival mucosa blood flow and the cardiovascular system as a whole are shown. The subjects with a high LBNP tolerance shows well pronounced regional compensatory reactions of the gingival mucosa that were not accompanied by significant changes in the left heart function. The subjects with a moderate tolerance exhibited either weak or no regional compensatory reactions of the gingival mucosa and significant changes in the left heart function. E.A.K.

N85-34499# Joint Publications Research Service, Arlington, Va.
EFFECT OF WATER IMMERSION OF PARAMETERS OF CENTRAL HEMODYNAMICS IN INDIVIDUALS OVER 45 YEARS OLD
I. O. Fomin, V. N. Orlov, A. E. Radzevich, and G. S. Leskin *In its* USSR Rept.: Space Biol. and Aerospace Med. (JPRS-USB-85-005) 14 Aug. 1985 p 51-56 refs Transl. into ENGLISH from Kosmicheskaya Biol. I Aviakosmicheskaya Meditsina (Moscow), v. 19, no. 3, May - Jun. 1985 p 37-40 (For primary document see N85-34494 23-52)
Avail: NTIS HC A08

The effect of 7 day dry immersion on central hemodynamics of four test subjects, aged 46, with boundary arterial hypertension was investigated. Central hemodynamics was examined by integrated rheography. Variations in blood pressure, central venous pressure, stroke and cardiac indexes, heart rate and total peripheral resistance were measured. The control subjects showed a decrease of blood pressure during exposure. Two of the test subjects with a short history of boundary arterial hypertension displayed similar variations, whereas two others showed an increase of blood pressure during the immersion period. The test and control subjects did not exhibit significant differences in the stroke and cardiac indexes, heart rate, central venous pressure or total peripheral resistance: stroke and cardiac indexes decreased while central venous pressure and total peripheral resistance increased, and heart rate remained unchanged. E.A.K.

N85-34500# Joint Publications Research Service, Arlington, Va.
LIPID HYDROLYSIS IN MAN DURING ANTIORTHOSTATIC HYPOKINESIA
I. L. Medkova, N. M. Nikolayeva, and O. V. Zhiznevskaya *In its* USSR Rept.: Space Biol. and Aerospace Med. (JPRS-USB-85-005) 14 Aug. 1985 p 57-62 refs Transl. into ENGLISH from Kosmicheskaya I Aviakosmicheskaya Meditsina (Moscow), v. 19, no. 3, May - Jun. 1985 p 40-44 (For primary document see N85-34494 23-52)
Avail: NTIS HC A08

The activity of pancreatic lipase in the serum and duodenal juice, the activity of monoglyceride lipase in the duodenal juice, the concentration of lipoproteins in the bile, the activity of intestinal enzymes and the concentration of lipid fractions in the feces were measured. These parameters were determined in six test subjects who were exposed to head down tilt for 120 days. It is suggested that bed rest decreases lipolytic enzymes in the duodenal juice and increases pancreatic lipase in the serum. The exposure also leads to a decrease of lipoproteins in the bile, rearrangement of the lipolytic enzymes in the intestine, and to an increase of mono, di and triglycerides in the feces. Changes in the pancreatic function and in lipid hydrolysis and absorption are indicated which are interpreted as compensatory adaptive processes of the digestive organs. E.A.K.

N85-34501# Joint Publications Research Service, Arlington, Va.
DISSOCIATION OF AUTONOMIC AND SENSORY VESTIBULAR REACTIONS
Yu. V. Krylov, O. A. Vorobyev, and V. V. Zaritskiy *In its* USSR Rept.: Space Biol. and Aerospace Med. (JPRS-USB-85-005) 14 Aug. 1985 p 63-69 refs Transl. into ENGLISH from Kosmicheskaya Biol. I Aviakosmichheskaya Meditsina (Moscow), v. 19, no. 3, May - Jun. 1985 p 44-48 (For primary document see N85-34494 23-52)
Avail: NTIS HC A08

The studies of healthy people and test subjects with vestibular reception disorders yielded data about relative independence of the vestibulo-autonomic and vestibulo sensory reactions during routine vestibulometric and tilt tests. The subjects with a changed labyrinthine function showed a higher vestibulo autonomic stability as compared to those with normal hearing. In both groups the sensory component of vestibular reactions did not differ significantly. Hemodynamic changes were found to modify some parameters of the nystagmic reactions. E.A.K.

N85-34502# Joint Publications Research Service, Arlington, Va.
RAT SKELETAL MUSCLES WITH SIMULATION OF PHYSIOLOGICAL EFFECTS OF WEIGHTLESSNESS (MORPHOLOGICAL STUDY)
Ye. I. Ilina-Kakuyeva and V. Ye. Novikov *In its* USSR Rept.: Space Biol. and Aerospace Med. (JPRS-USB-85-005) 14 Aug. 1985 p 81-92 refs Transl. into ENGLISH from Kosmicheskaya Biol. Aviakosmicheskaya Meditsina (Moscow), v. 19, No. 3, May - Jun. 1985 p 56-60 (For primary document see N85-34494 23-52)
Avail: NTIS HC A08

Rats were suspended in the head down position for 21 days. The effect of this exposure on skeletal muscles of their fore and hindlimbs were studied by morphological and histochemical method. Changes in the hindlimbs were similar to those seen in real weightlessness of similar duration. The two antigravitational muscles, soleus and gastrochemius muscles, showed greatest changes. The changes in the biceps brachit muscle are assumed to be associated with hemodynamic disorders. It is recognized that the method of rat suspension is adequate for the study of morphological effects of weightlessness on hindlimbs and is inacceptable for that of forelimbs where the exposure induces microcirculation disorders. E.A.K.

N85-34503# Joint Publications Research Service, Arlington, Va.
EFFECT OF ACUTE HYPOXIA ON CORONARY AND SYSTEMIC HEMODYNAMICS
V. S. Bednenko, V. N. Polyakov, M. V. Dvornikov, V. K. Stepanov, and A. N. Kozlov *In its* USSR Rept.: Space Biol. and Aerospace Med. (JPRS-USB-85-005) 14 Aug. 1985 p 93-98 refs Transl. into ENGLISH from Kosmicheskaya Biol. I Aviakosmicheskaya

Meditsina (Moscow), v. 19, no. 3, May - Jun. 1985 p 64-68 (For primary document see N85-34494 23-52)
Avail: NTIS HC A08

Variations in coronary circulation, cardiac output and heart rate were examined by dopplerography in 14 test subjects kept in an altitude chamber. It is found that during acute hypoxia the effective coronary blood flow decreases distinctly prior to general circulatory disorders. It is recommended to monitor coronary circulation during altitude exposures. E.A.K.

N85-34504# Joint Publications Research Service, Arlington, Va.
EFFECT OF DIBAZOL ON PARAMETERS OF NONSPECIFIC RESISTANCE OF SUBJECTS IN PRESSURIZED CABINS
V. S. Novikov and V. N. Bortnovskiy *In its* USSR Rept.: Space Biol. and Aerospace Med. (JPRS-USB-85-005) 14 Aug. 1985 p 99-102 refs Transl. into ENGLISH from Kosmicheskaya I Aviakosmicheskaya Meditsina (Moscow), v. 19, no. 3, May - Jun. 1985 p 68-71 (For primary document see N85-34494 23-52)
Avail: NTIS HC A08

Prophylactic administration of dibazol prevents a decrease of nonspecific resistance and ensures stable variations of adaptation processes in men working in enclosures for a long time. The positive effect of the drug occurs 10 to 15 days after the administration and involves a combined action on phagocytosis, blood homeostasis, and skin antiomicrobial resistance. The interated parameters of nonspecific protection of the test subjects who took dibazol are close or even better than the pretest level. Dibazol also has a beneficial effect on the adaptive process and morbidity rate of the subjects. It is suggested that dibazol affects favorably the nonspecific resistance of the human body and it is recommended as a stimulating and training agent. E.A.K.

N85-34505# Joint Publications Research Service, Arlington, Va.
EFFECT OF SEEDS OF HEAVY CHARGED PARTICLES OF GALACTIC COSMIC RADIATION **c51**
Ye. N. Maksimova *In its* USSR Rept.: Space Biol. and Aerospace Med. (JPRS-USB-85-005) 14 Aug. 1985 p 103-107 refs Transl. into ENGLISH from Kosmicheskaya Biol. I Aviakosmicheskaya Meditsina (Moscow), v. 19, no. 3, May - Jun. 1985 p 71-74 (For primary document see N85-34494 23-52)
Avail: NTIS HC A08

The experiments were carried out on Lactuca sativa seeds exposed for 20, 66, 123 and 308 days in a biostack also containing physical detectors of heavy charged particles. The yield of aberrant cells and its dependence on the exposure time and the site where particles hit the object were measured. The cytogenetic examination demonstrated a significant difference between the seeds that were or were not hit by heavy charged particles. A significant contribution of galactic cosmic radiation to the radiobiological effect is indicated. The yield of aberrant cells as a function of the localization of heavy charged particles in the seed is established. The most sensitive target is the root meristem. E.A.K.

N85-34506# Joint Publications Research Service, Arlington, Va.
MONITORING DOSAGE OF VOLATILE COMPOUNDS IN TESTS AT LOW BAROMETRIC PRESSURE
A. V. Sedov and V. I. Akimov *In its* USSR Rept.: Space Biol. and Aerospace Med. (JPRS-USB-85-005) 14 Aug. 1985 p 108-110 refs Transl. into ENGLISH from Kosmicheskaya Biol. I Aviakosmicheskaya Meditsina (Moscow), v. 19, no. 3, May - Jun. 1985 p 74-76 (For primary document see N85-34494 23-52)
Avail: NTIS HC A08

Working airtight spaces, including insulated protective gear exposes man to the combined effect of such specific factors as low barometric pressure and hyperoxic gas atmosphere. These factors, aggravate the toxic effect of chemicals contained in the gas atmosphere of pressurized areas. The presence of volatile compounds in the artificial atmosphere of pressurized areas, the monitoring of which is an important medical and engineering problem in the presence of low barometric pressure and breathing hyperoxic gas mixtures is discussed. A dynamic gas-mixing unit to control dosage of mixtures of carbon monoxide, methane and dimethylamine with oxygen is the most suitable for this purpose. E.A.K.

N85-34507# Joint Publications Research Service, Arlington, Va.
DETERMINATION OF INDIVIDUAL TOLERANCE IN HYPERBARIC OXYGEN
G. L. Zaltsman, G. A. Kuchuk, and A. N. Rovnyy *In its* USSR Rept.: Space Biol. and Aerospace Med. (JPRS-USB-85-005) 14 Aug. 1985 p 111-113 refs Transl. into ENGLISH from Kosmiceskaya Biol. I Aviakosmicheskaya Meditsina (Moscow), v. 19, no. 3, May - Jun. 1985 p 76-77 (For primary document see N85-34494 23-52)
Avail: NTIS HC A08

A hyperbaric gas and water environment, is characterized by the presence of many extreme factors. Under such conditions, human labor is particularly heavy, dangerous and deleterious. Screening individuals with tolerance to extreme factors of a hyperbaric environment is of paramount significance to improve the safety and efficiency of underwater work. Among the most important extreme factors of a hyperbaric environment is the effect on man of high partial pressure of oxygen and neutral gases, nitrogen and helium. These factors, limit the depth of submersion and exposure time, whereas for individual with high predisposition they could be threatening even in the range that is accepted for work. Appearance of early manifestations of pathological reactions is used to determine individual tolerance to the above extreme hyperbaric factors. E.A.K.

N85-34508# Joint Publications Research Service, Arlington, Va.
LIPOGENESIS IN RAT LIVER AFTER FLIGHT ABOARD COSMOS-1129 BIOSATELLITE
L. Macho, R. A. Tigranyan, N. Skottova, and M. Palkovic *In its* USSR Rept.: Space Biol. and Aerospace Med. (JPRS-USB-85-005) 14 Aug. 1985 p 126-128 refs Transl. into ENGLISH from Kosmicheskaya Biol. I Aviakosmicheskaya Meditsina (Moscow), v. 19, no. 3, May - Jun. 1985 p 84-85 (For primary document see N85-34494 23-52)
Avail: NTIS HC A08

Tests conducted aboard biosatellites revealed that long-term exposure of rats to weightlessness is associated with changes in lipid metabolism. The experiment aboard Cosmos-782 revealed considerable decrease in activity of the main lipogenetic enzymes, malic enzyme and ATP-citrate lyase, in the rat liver immediately after the flight. Activity of these enzymes did not differ from the control 26 days after the flight. A decline in activity of liver malic enzyme and ATP citrate lyase was also demonstrated immediately after the flight in rats flown aboard Cosmos-936 in weightlessness, whereas those exposed to artificial gravity aboard the biosatellite showed no difference from the control in activity of these enzymes. Enzyme activity did not differ from the levels in the vivarium control 25 days after landing. The activity of one of the key lipogenetic enzymes, malic enzyme, in the liver of rats flowing aboard Cosmos-1129 are investigated, and the rate of repair of previously found changes when the recovery period was shortened is determined and the effect of recurrent stress in the recovery period on changes in enzyme activity is examined. E.A.K.

N85-34509# Joint Publications Research Service, Arlington, Va.
PROBLEMS OF AVIATION AND SPACE MEDICINE AND PSYCHOLOGY DISCUSSED AT 14TH GAGARIN LECTURES
In its USSR Rept.: Space Biol. and Aerospace Med. (JPRS-USB-85-005) 14 Aug. 1985 p 136-144 refs Transl. into ENGLISH from Kosmicheskaya Biol. I Aviakosmicheskaya Meditsina (Moscow), v. 19, no. 3, May - Jun. 1985 p 89-93 Also presented at 14th Gagarin Sci. Lectures Zvezdnyy, USSR, 5-9 Apr. 1984 (For primary document see N85-34494 23-52)
Avail: NTIS HC A08

Problems of Aviation and Space Medicine and Psychology were discussed. The following problems that are the most pressing are presented: physiological effects of weightlessness, accelerations and altitude; space biology; clinical aerospace medicine; screening and training of flight personnel. E.A.K.

53 BEHAVIORAL SCIENCES

Includes psychological factors; individual and group behavior; crew training and evaluation; and psychiatric research.

No abstracts in this category.

54 MAN/SYSTEM TECHNOLOGY AND LIFE SUPPORT

Includes human engineering; biotechnology; and space suits and protective clothing.

No abstracts in this category.

55 PLANETARY BIOLOGY

Includes exobiology; and extraterrestrial life.

No abstracts in this category.

59 MATHEMATICAL AND COMPUTER SCIENCES (GENERAL)

N85-34510*# National Aeronautics and Space Administration. Ames Research Center, Moffett Field, Calif.
THE IMPACT OF SUPERCOMPUTERS ON EXPERIMENTATION: A VIEW FROM A NATIONAL LABORATORY
Victor L. Peterson and James O. Arnold Aug. 1985 16 p refs (NASA-TM-86822; Rept-85377; NAS 1.15:86822) Avail: NTIS HC A02/MF A01 CSCL 09B

The relative roles of large scale scientific computers and physical experiments in several science and engineering disciplines are discussed. Increasing dependence on computers is shown to be motivated both by the rapid growth in computer speed and memory, which permits accurate numerical simulation of complex physical phenomena, and by the rapid reduction in the cost of performing a calculation, which makes computation an increasingly attractive complement to experimentation. Computer speed and memory requirements are presented for selected areas of such disciplines as fluid dynamics, aerodynamics, aerothermodynamics, chemistry, atmospheric sciences, astronomy, and astrophysics, together with some examples of the complementary nature of computation and experiment. Finally, the impact of the emerging role of computers in the technical disciplines is discussed in terms of both the requirements for experimentation and the attainment of previously inaccessible information on physical processes. Author

60 COMPUTER OPERATIONS AND HARDWARE

Includes computer graphics and data processing.

For components see *33 Electronics and Electrical Engineering.*

N85-34511*# National Aeronautics and Space Administration. Marshall Space Flight Center, Huntsville, Ala.
HARDWARE MATH FOR THE 6502 MICROPROCESSOR
Ralph Kissel and James Currie Jul. 1985 18 p refs (NASA-TM-86517; NAS 1.15:86517) Avail: NTIS HC A02/MF A01 CSCL 09B

A floating-point arithmetic unit is described which is being used in the Ground Facility of Large Space Structures Control Verification (GF/LSSCV). The experiment uses two complete inertial measurement units and a set of three gimbal torquers in a closed loop to control the structural vibrations in a flexible test article (beam). A 6502 (8-bit) microprocessor controls four AMD 9511A floating-point arithmetic units to do all the computation in 20 milliseconds. Author

N85-34512# Sandia Labs., Albuquerque, N. Mex.
GRAPH-THEORETICAL EXORCISM
G. J. Simmons 1985 11 p refs Presented at the 16th Southeastern Intern. Conf. on Combinatorics, Graph Theory and Computing, Boca Raton, Fla., 11 Feb. 1985
(Contract DE-AC04-76DP-00789)
(DE85-011916; SAND-85-1110C; CONF-850283-1) Avail: NTIS HC A02/MF A01

Given a graph G and an ordering phi of the vertices, V(G), we define a parsimonious proper coloring (PPC) of V(G) under phi to be a proper coloring of V(G) in the order phi, where a new color is introduced only when a vertex cannot be properly colored in its order with any of the colors already used. DOE

N85-34529# Memorial Univ. of Newfoundland, St. Johns. Dept. of Computer Science.
INTERFACING INTERACTIVE CIRCUIT SIMULATION WITH STANDARD GRAPHICS FACILITIES
P. Gillard and W. M. Zuberek *In* Canadian Information Processing Society Graphics Interface 1985 1985 p 37-43 refs (For primary document see N85-34523 23-61)
Avail: NTIS HC A19/MF A01

N85-34543# Toronto Univ. (Ontario). Computer Systems Research Inst.
ISSUES AND TECHNIQUES IN TOUCH-SENSITIVE TABLET INPUT (EXECUTIVE SUMMARY)
W. Buxton, R. Hill, and P. Rowley *In* Canadian Information Processing Society Graphics Interface 1985 1985 p 147-149 refs (For primary document see N85-34523 23-61)
Avail: NTIS HC A19/MF A01

N85-34545# California Univ., Davis. Signal and Image Processing Lab.
A MODEL FOR GRAPHICS INTERFACE TOOL DEVELOPMENT
Kenneth I. Joy *In* Canadian Information Processing Society Graphics Interface 1985 1985 p 159-165 refs (For primary document see N85-34523 23-61)
Avail: NTIS HC A19/MF A01

N85-34553# Toronto Univ. (Ontario). Computer Systems Research Inst.
A MULTI-TOUCH THREE DIMENSIONAL TOUCH-SENSITIVE TABLET (EXECUTIVE SUMMARY)
S. K. Lee, W. Buxton, and K. C. Smith *In* Canadian Information Processing Society Graphics Interface 1985 1985 p 221-222 refs Submitted for publication (For primary document see N85-34523 23-61)
Avail: NTIS HC A19/MF A01

N85-34559# Montreal Univ. (Quebec). Dept. d'Informatique et de Rech. Oper.
DESIGN AND IMPLEMENTATION OF AN INTERACTIVE ROUTE EDITOR
Guy Lapalme and Michel Cormier *In* Canadian Information Processing Society Graphics Interface 1985 1985 p 259-263 refs (For primary document see N85-34523 23-61)
Avail: NTIS HC A19/MF A01

N85-34575# Industrial Technical Services, Montreal (Quebec). Research and Development Group.
NAPGEN: AUTOMATIC NAPLPS PAGE GENERATOR
Michel Plante *In* Canadian Information Processing Society Graphics Interface 1985 1985 p 381-383 ref (For primary document see N85-34523 23-61)
Avail: NTIS HC A19/MF A01

61 COMPUTER PROGRAMMING AND SOFTWARE

Includes computer programs, routines, and algorithms.

N85-34513 National Physical Lab., Teddington (England). Div. of Information Technology and Computing.
A PROTOTYPE PASCAL PROGRAM VALIDATION SYSTEM
B. A. Wichmann, T. P. Wilkinson, G. ONeill, G. Parkin, B. Byrne (International Computers Ltd., Bracknell, England), J. Bouchard (International Computers Ltd., Bracknell, England), M. Wetherfield (International Computers Ltd., Bracknell, England), R. A. Snowdon (International Computers Ltd., Kidsgrove, England), M. Tordoff (International Computers Ltd., Kidsgrove, England), and V. Downes (STC IDEC Ltd., Stevenage, England) Mar. 1985 25 p refs
(NPL-DITC-57/85; ISSN-0262-5369) Copyright. Avail: Issuing Activity

A development project to increase the reliability of programs written in PASCAL was developed to: produce a first generation integrated project support environment subsystem for the validation of PASCAL programs; provide an environment for validation tools utilizing a data base; provide an initial system for independent assessment; and derive a final system for industrial use is outlined. Author (ESA)

N85-34514 Royal Signals and Radar Establishment, Malvern (England).
A DEVICE-INDEPENDENT 2D PLOTTING PACKAGE WRITTEN IN FORTRAN
M. Johnson Oct. 1984 25 p
(RSRE-MEMO-3776; BR95018) Copyright. Avail: NTIS HC A02/MF A01

A FORTRAN-based plotting package which offers unlimited device support and is simple to use was developed. Instruction on the use of the FORTRAN subroutines is given, with examples where necessary, and an outline specification for device drivers is described. Author (ESA)

N85-34515 National Physical Lab., Teddington (England). Div. of Mechanical and Optical Metrology.
EXPERIMENTS AND DISCUSSIONS ON THE ANALYSIS OF INTERFEROGRAMS WITH CLOSED-LOOP FRINGES
Ruixiang Liu and K. G. Birch Mar. 1984 15 p refs
(NPL-MOM-68; ISSN-0309-3069) Copyright. Avail: Issuing Activity

A suite of cumputer programs was written in HPL language for use on an HP 9825 desktop computer, to implement an approach to fringe detection and numbering. The programs were used successfully to process a range of interferograms with closed-loop fringes, as generated in on-axis testing of optical transfer function standard lenses. Author (ESA)

N85-34516# Argonne National Lab., Ill.
DISPL1: A SOFTWARE PACKAGE FOR ONE AND TWO SPATIALLY DIMENSIONED KINETICS-DIFFUSION PROBLEMS
G. K. Leaf and M. Minkoff Sep. 1984 262 p refs
(Contract W-31-109-eng-38)
(ANL-84-56) Avail: NTIS HC A12/MF A01

DISPL1 is a software package for solving some second order nonlinear systems of partial differential equations including parabolic, hyperbolic, and some mixed types such as parabolic-elliptic equations. Fairly general nonlinear boundary conditions are allowed as well as interface conditions for problems in an inhomogeneous media. The spatial domain is one or two dimensional with Cartesian, cylindrical, or spherical (in one dimension only) geometry. The numerical method is based on the use of Galerkin's procedure combined with the use of B-splines in order to reduce the system of PDE's to a system of ODE's. The latter system is then solved with a sophisticated ODE software package. Software features include extensive dump/restart facilities, free format input, moderate printed output capability, dynamic storage allocation, and three graphics packages. Author

N85-34517*# Boeing Commercial Airplane Co., Seattle, Wash.
SYSTEM MAINTENANCE MANUAL FOR MASTER MODELING OF AERODYNAMIC SURFACES BY THREE-DIMENSIONAL EXPLICIT REPRESENTATION Final Report
A. F. Gibson Apr. 1983 124 p refs
(Contract NAS1-15325)
(NASA-CR-178224; NAS 1.26:178224; D6-51089) Avail: NTIS HC A06/MF A01 CSCL 09B

A system of computer programs has been developed to model general three-dimensional surfaces. Surfaces are modeled as sets of parametric bicubic patches. There are also capabilities to transform coordinate to compute mesh/surface intersection normals, and to format input data for a transonic potential flow analysis. A graphical display of surface models and intersection normals is available. There are additional capabilities to regulate point spacing on input curves and to compute surface intersection curves. Internal details of the implementation of this system are explained, and mairttenance procedures are specified. Author

N85-34518*# PRC Kentron, Inc., Hampton, Va.
USER'S OPERATING PROCEDURES. VOLUME 1: SCOUT PROJECT INFORMATION PROGRAMS
Cynthia G. Harris and Danny K. Harris Jul. 1985 272 p
(Contract NAS1-18000)
(NASA-CR-177948; NAS 1.26:177948) Avail: NTIS HC A12/MF A01 CSCL 09B

A review of the user's operating procedures for the Scout Project Automatic Data System, called SPADS is given. SPADS is the result of the past seven years of software development on a Prime minicomputer located at the Scout Project Office. SPADS was developed as a single entry, multiple cross reference data management and information retrieval system for the automation of Project office tasks, including engineering, financial, managerial, and clerical support. The instructions to operate the Scout Project Information programs in data retrieval and file maintenance via the user friendly menu drivers is presented. Author

N85-34519*# PRC Kentron, Inc., Hampton, Va.
USER'S OPERATING PROCEDURES. VOLUME 1: SCOUT PROJECT FINANCIAL ANALYSIS PROGRAM
Cynthia G. Harris and Danny K. Haris Jul. 1985 171 p
(Contract NAS1-18000)
(NASA-CR-177949; NAS 1.26:177949) Avail: NTIS HC A08/MF A01 CSCL 09B

A review is presented of the user's operating procedures for the Scout Project Automatic Data system, called SPADS. SPADS is the result of the past seven years of software development on a Prime mini-computer located at the Scout Project Office, NASA Langley Research Center, Hampton, Virginia. SPADS was developed as a single entry, multiple cross-reference data management and information retrieval system for the automation of Project office tasks, including engineering, financial, managerial, and clerical support. This volume, two (2) of three (3), provides the instructions to operate the Scout Project Financial Analysis program in data retrieval and file maintenance via the user friendly menu drivers. Author

N85-34520*# PRC Kentron, Inc., Hampton, Va.
USER'S OPERATING PROCEDURES. VOLUME 3: PROJECTS DIRECTORATE INFORMATION PROGRAMS
Cynthia G. Haris and Danny K. Harris Jul. 1985 240 p 3 Vol.
(Contract NAS1-18000)
(NASA-CR-177950; NAS 1.26:177950) Avail: NTIS

HC A11/MF A01 CSCL 09B

A review of the user's operating procedures for the scout project automatic data system, called SPADS is presented. SPADS is the results of the past seven years of software development on a prime mini-computer. SPADS was developed as a single entry, multiple cross-reference data management and information retrieval system for the automation of Project office tasks, including engineering, financial, managerial, and clerical support. This volume, three of three, provides the instructions to operate the projects directorate information programs in data retrieval and file maintenance via the user friendly menu drivers. Author

N85-34521*# National Aeronautics and Space Administration. Langley Research Center, Hampton, Va.

THE PARSER GENERATOR AS A GENERAL PURPOSE TOOL Final Report

Robert E. Noonan (Colllege of William and Mary) and W. Robert Collins (Colllege of William and Mary) Jul. 1985 37 p refs (Contract NAS1-17070; Grants NsG-1435; NAG1-534) (NASA-CR-177955; ICASE-85-36; NAS 1.26:177955) Avail: NTIS HC A03/MF A01 CSCL 09B

The parser generator has proven to be an extremely useful, general purpose tool. It can be used effectively by programmers having only a knowledge of grammars and no training at all in the theory of formal parsing. Some of the application areas for which a table-driven parser can be used include interactive, query languages, menu systems, translators, and programming support tools. Each of these is illustrated by an example grammar. Author

N85-34522*# National Aeronautics and Space Administration. Langley Research Center, Hampton, Va.

REORDERING COMPUTATIONS FOR PARALLEL EXECUTION Final Report

Loyce Adams (California Univ., Los Angeles) Jul. 1985 20 p (Contract NAS1-17070; Grant AF-AFOSR-1089-85) (NASA-CR-177961; ICASE-85-35; NAS 1.26:177961) Avail: NTIS HC A02/MF A01 CSCL 09B

The computations are reordered in the SOR algorithm to maintain the same asymptotic rate of convergence as the rowwise ordering to obtain parallelism at different levels. A parallel program is written to illustrate these ideas and actual machines for implementation of this program are discussed. Author

N85-34523# Canadian Information Processing Society, Toronto (Ontario).

GRAPHICS INTERFACE 1985: PROCEEDINGS

1985 435 p refs In ENGLISH and FRENCH Conf. held in Montreal, 27-31 May 1985; sponsored by the Canadian Man-Computer Communications Society, the Computer Graphics Society and Montreal Univ. Previously announced in IAA as A85-40790 Original contains color illustrations (ISSN-0713-5424) Avail: NTIS HC A19/MF A01

Aspects of image synthesis and applications are discussed. Taking into account a theoretical and empirical analysis of coherent ray-tracing, frame buffer algorithms for stochastic models, the specification of stochastic objects in a hierarchical graphics system, an interactive planning work station, computer graphics for multivariate data, interfacing interactive circuit simulation with standard graphics facilities, and a graphics interface for interactive simulation of packet-switched networks are presented. Other subjects studied are related to medical computer graphics, graphical data bases, computer animation, editing and printing systems, user interface, image processing, algorithms, CAD systems, cartography, image perception, geometric modelling, graphic standards, robotics, computer animation and image synthesis, and artificial intelligence. Attention is given to generative design in architecture using an expert system, a low cost geometric modelling system for CAM, the design of a graphics application interface, and the strategic use of business graphics. For individual titles, see N85-34524 through N85-34584.

N85-34524# California Univ., Berkeley. Computer Graphics Lab.

A THEORETICAL AND EMPIRICAL ANALYSIS OF COHERENT RAY-TRACING

L. Richard Speer, Tony D. DeRose, and Brian A. Barsky *In* Canadian Information Processing Society Graphics Interface 1985 1985 p 1-8 refs (For primary document see N85-34523 23-61) (Contract N00030-82-C-0235; Grant NSF ECS-82-04381) Avail: NTIS HC A19/MF A01

The use of coherence has been advocated as a means of reducing the large computational cost of the ray tracing method of image synthesis. The theoretical and empirical performance of a typical coherent ray tracing algorithm, one that exploits the similarity between the intersection trees generated by successive rays was examined. It is shown that despite the large degree of coherence present in a scene, the need to ensure the validity of ray object intersections prevents any significant computational savings. This indicates that other algorithmic methods must be used in order to substantially reduce the computational cost of ray traced imagery. Author

N85-34525# Toronto Univ. (Ontario). Computer Systems Research Inst.

FRAME BUFFER ALGORITHMS FOR STOCHASTIC MODELS

Alain Fournier and Tom Milligan *In* Canadian Information Processing Society Graphics Interface 1985 1985 p 9-16 refs (For primary document see N85-34523 23-61) Avail: NTIS HC A19/MF A01

Stochastic modeling is a technique that allows shifting the complexity of the picture away from the modeling database while rendering a class of natural looking objects. When implementing this technique within traditional rendering systems however, one has to deal with a very large number of geometric and display primitives. A test system where most of the database expansion is done at the display level is presented. A simple display processor acting directly on the frame buffer, receives sparse 3-D geometric data, generates dense 2-D stochastic arrays, and determine their color shade and visibility to write the final image on the frame buffer. The system allowed the exploration of the issues of reentrant stochastic subdivision, priority and visibility determination, quick shading techniques and filtering at the frame buffer level with a bit slice display processor. Examples of the images produced and performance statistics are given for the system. Author

N85-34526# Calgary Univ. (Alberta). Dept. of Computer Science.

SPECIFYING STOCHASTIC OBJECTS IN A HIERARCHICAL GRAPHICS SYSTEM

Brian Wyvill, Craig McPheeters, and Milan Novacek *In* Canadian Information Processing Society Graphics Interface 1985 1985 p 17-20 refs Sponsored by Natural Science and Engineering Research Council of Canada (For primary document see N85-34523 23-61) Avail: NTIS HC A19/MF A01

Many graphics systems allow a user to describe three dimensional objects with polygon meshes or surface patches. However to achieve realistic scenes for making animated film some objects are better described with stochastic techniques. Some examples would be clouds, fire and mountains. A hierarchical graphics system consisting of objects which contain geometrical transformations of other objects or primitives is described. Each object is treated in a consistent fashion whatever the types of primitives that are ultimately called, for example an object may consist of polygon mesh subobjects and stochastic objects. The system has been designed so that it may easily be extended to include new primitive types, so far a subsystem for generating particles (fire, volcanos etc.) and a subsystem for generating fractal polygons have been implemented. Examples are given of the results obtained with this technique. Author

N85-34527# Bell Telephone Labs., Inc., Holmdel, N. J.

THE INTERACTIVE PLANNING WORK STATION: A GRAPHICS-BASED UNIX (TRADEMARK) TOOL FOR APPLICATION USERS AND DEVELOPERS

Richard Bournique, Ronald Candrea, and Don Hartman (MLC, Inc.,

Austin, Tex.) *In* Canadian Information Processing Society Graphics Interface 1985 1985 p 21-28 refs (For primary document see N85-34523 23-61)
Avail: NTIS HC A19/MF A01

The Interactive Planning Work Station (PWS) is a UNIX based system intended to support planning and other complex decision making tasks. IPWS addresses the needs of at least two classes of users: end users of an application (including both basic and sophisticated) and application developers. IPWS software provides for a menu oriented user interface, interactive database management capabilities, and graphical input and output. The work station capabilities, how they support end users, and how they simplify the development of new applications are discussed. Author

N85-34528# Montreal Univ. (Quebec).
COMPUTER GRAPHICS FOR MULTIVARIATE DATA
Robert Cleroux, Yves Lepage, and Normand Ranger *In* Canadian Information Processing Society Graphics Interface 1985 1985 p 29-36 refs (For primary document see N85-34523 23-61)
Avail: NTIS HC A19/MF A01

The exploration of multidimensional data involves the use of a set of empirical techniques which aid in the discovery of interesting avenues to be pursued on later statistical analysis. The availability and power of computers has changed the nature of statistical work and has made the exploration of multidimensional data more accessible. Graphical methods constitute one of the main tools for data exploration, and they are therefore of primary importance. Four graphical representation methods are presented and applied to atmospheric pollution data for the Montreal region. These representations enable the data from each monitoring station to be visualized and grouping may then be formed from observed similarities. Author

N85-34529# Memorial Univ. of Newfoundland, St. Johns. Dept. of Computer Science.
INTERFACING INTERACTIVE CIRCUIT SIMULATION WITH STANDARD GRAPHICS FACILITIES **c60**
P. Gillard and W. M. Zuberek *In* Canadian Information Processing Society Graphics Interface 1985 1985 p 37-43 refs (For primary document see N85-34523 23-61)
Avail: NTIS HC A19/MF A01

One of the most popular and most powerful circuit simulators, the SPICE-2G program from University of California, Berkeley is rather inefficient in interactive applications because of its batch-oriented structure. SPICE-PAC is a package (or a set) of subroutines which is functionally equivalent to the SPICE-2G circuit simulator, i.e., it accepts the same circuit description and performs all the analyses which are available in the SPICE-2G programs, but also provides several extensions, e.g., circuit variables, parameterized subcircuit expansion, and an interface to libraries of standard modules. Two immediate applications of the package are: (1) interactive circuit simulation in which an interactive driver controls the simulation subroutines according to user commands, and (2) circuit optimization in which an optimization package is interfaced with the simulation package by user supplied subroutines that evaluate objective functions, constraints, etc. Recently, the package was extended by an interface to graphics facilities. An implementation of this interface, compatible with both the CORE and GKS systems, is described, and some simple examples are given as an illustration. Author

N85-34530# Geneva Univ. (Switzerland). Cardiology Center.
COMPUTER ANALYSIS TECHNIQUES FOR THE TEMPORAL EVALUATION OF CARDIAC WALL MOTION
Osman Ratib and Alberto Righetti *In* Canadian Information Processing Society Graphics Interface 1985 1985 p 45-49 refs (For primary document see N85-34523 23-61)
Avail: NTIS HC A19/MF A01

Digital image processing is emerging as an increasingly important modality in the evolution of different types of image acquisition and analysis in cardiology. It has become an integral element in the technologies that are being developed and explored. New mathematical concepts in the assessment of cardiac function have been applied to digital images of the heart. Among them, the measurement of temporal changes in regional wall motion of the heart using Fourier analysis led to a significant improvement in the detection of regional alterations in ventricular function. Several imaging modalities can benefit from this approach for the assessment of the temporal sequence of cardiac wall motion. Author

N85-34531# Geneva Univ. (Switzerland). Centre Univ. d'Informatique.
A COMPUTERIZED SYSTEM FOR SPOT DETECTION AND ANALYSIS OF TWO-DIMENSIONAL ELECTROPHORESIS IMAGES
R. Appel, M. Funk, C. Pellegrini, D. Hochstrasser, and A. F. Mueller *In* Canadian Information Processing Society Graphics Interface 1985 1985 p 51-56 refs (For primary document see N85-34523 23-61)
Avail: NTIS HC A19/MF A01

The 2 dimensional electrophoresis technique is very powerful to determine the composition of a biological sample. The complexity of the image produced by this process needs the use of a computerized system. A system, called MELANIE, with which the user can process the image of a 2 dimensional electrophoresis gel, separate and quantify the different proteins and compare semiautomatically two different pictures is described. The algorithms involved in the different steps of the process are discussed. Author

N85-34532# Ecole Polytechnique, Palaiseau (France). Centre de Mathematiques Appliquees.
AN IMAGE MANAGEMENT KERNEL FOR THE DESIGN OF RELATIONAL AND PICTORIAL DATA BASES
Philippe Chassignet *In* Canadian Information Processing Society Graphics Interface 1985 1985 p 61-68 refs In FRENCH; ENGLISH summary (For primary document see N85-34523 23-61)
Avail: NTIS HC A19/MF A01

An original scheme for the realization of an Image Management and Description Kernel is presented. This kernel may be easy implemented on any system built around an Iconographic Machine and a Relational Data Base Management System. Thus, one of the main interests of such a system is to permit the joint management of both iconographic and semantic data. To this end, the wealth of data handling, which characterizes a Relational Data Base Management System, allows the system to finely connect information about the form and substance of pictures and about anything else. Owing to performances, the DBMS does not directly handle images. This task is imparted to a specialized Iconographic Machine that allows the system to modify or combine pictures and thus permits to generate many more from a basic library. Thus, the Iconographic Kernel is intended to connect easier both these systems. Author

N85-34533# Brigham Young Univ., Provo, Utah. Dept. of Computer Science.
SPATIAL TREES: A FAST ACCESS METHOD FOR UNSTRUCTURED GRAPHICAL DATA
Dan R. Olsen, Jr. and Carol N. Cooper (Intel Corp.) *In* Canadian Information Processing Society Graphics Interface 1985 1985 p 69-74 refs (For primary document see N85-34523 23-61)
Avail: NTIS HC A19/MF A01

A spatial tree is a data structure for organizing graphical elements into a tree using their extents so as to optimize geometric queries on the database. Algorithms are presented for insertion and deletion. Queries on 2D spatial trees are modeled as simple rectangles for windowing purposes. Query algorithms for rays and convex polyhedra are presented for 3D spatial trees. It is shown how a least recently used swapping algorithm is highly effective when portions of the tree must reside in secondary storage. Simulation statistics as well as worst case analysis are provided for each algorithm. Author

N85-34534# Montreal Univ. (Quebec). Dept. d'Informatique et Recherche Operationnelle.

GRAPHICS INTERACTION IN DATABASES
C. Frasson and M. Erradi *In* Canadian Information Processing Society Graphics Interface 1985 1985 p 75-81 refs Sponsored by Natural Science and Engineering Research Council of Canada (For primary document see N85-34523 23-61)
Avail: NTIS HC A19/MF A01

The evolution of interaction techniques between users and database systems is highlighted. The evolution of database query languages and the importance of the graphical interface taking in account the availability of new functionalities and the users demand is discussed. Using examples in a medical environment, the characteristics of an interactive graphical language based on icons is presented. Author

N85-34535# Tokyo Univ. (Japan). Dept. of Information Science.
ANIMENGINE: AN ENGINEERING ANIMATION SYSTEM
Tsukasa Noma and Tosiyasu L. Kunii *In* Canadian Information Processing Society Graphics Interface 1985 1985 p 83-90A refs Sponsored by Nippon Gakki Co. Ltd., Ricoh Co. Ltd., and Japan Victor Co. Ltd. Original contains color illustrations (For primary document see N85-34523 23-61)
Avail: NTIS HC A19/MF A01

Animation for engineering is very different from traditional animation for entertainment. We do not require realistic images and we cannot afford the cost, or the time, for their production. At the same time, there are other requirements which must be met. Firstly, it must be possible, in an engineering animation, to identify, unambiguously, each separate, mechanical part in a scene. Secondly, the animation must be produced quickly: ideally, in real-time. As an attempt to satisfy these requirements, a new engineering animation system called ANIMENGINE has been implemented. To achieve clear visual identification of objects, each of them is marked with a unique, characteristic color or texture. For fast production and almost realtime display, a combination of on-line video display and recording is employed. Algorithms have been developed for hidden surface removal with moving objects and a special, geometric model, the template model has been used to facilitate the production of scenes using many similar, common parts. Author

N85-34536# Montreal Univ. (Quebec).
3D COMPUTER ANIMATION: MORE AN EVOLUTION PROBLEM THAN A MOTION PROBLEM
N. Magnenat-Thalmann and D. Thalmann *In* Canadian Information Processing Society Graphics Interface 1985 1985 p 91-96 refs (For primary document see N85-34523 23-61)
Avail: NTIS HC A19/MF A01

Three-D computer animation is too often restricted to very simple motion: e.g., logo rotations or camera motions around a 3D reconstructed object. Enormous effort is devoted to image rendering, but little to the motion itself. In fact, research in computer animation needs to look beyond the mere creation of motion towards the evolution of state variables over time according to appropriate laws. This is called the evolution problem. New evolution laws may be introduced into an animation system. Several examples are discussed: collisions, brownian motions, chaotic attractors and models based on simultaneous differential equations. All examples are presented using the extensible director-oriented animation system MIRANIUM. Author

N85-34537# California Univ., Berkeley. Computer Graphics Lab.
USING DYNAMIC ANALYSIS TO ANIMATE ARTICULATED BODIES SUCH AS HUMANS AND ROBOTS
Jane Wilhelms and Brian A. Barsky *In* Canadian Information Processing Society Graphics Interface 1985 1985 p 97-104 refs (For primary document see N85-34523 23-61)
Avail: NTIS HC A19/MF A01

A method of animating articulated (linked) bodies such as humans, animals and robots using dynamic analysis is presented. Dynamic analysis predicts motion by analyzing the effect of forces and torques on mass; this is different than the usual kinematic method of specifying motion, where positions, velocities, and accelerations are given without considering the forces and torques producing motion. It is difficult to kinematically specify realistic motion, particularly in cases where the body is moving fast, in complex patterns, or with great freedom. In such cases, animation based on dynamic analysis, though more expensive, may be preferable. Animation using dynamic analysis is also useful in the design and control of robots and other mechanical manipulators, and for analyzing the movement of humans and animals in biomechanics and sports. Author

N85-34538# Massachusetts Inst. of Tech., Cambridge. Media Lab.
TOWARDS AN INTEGRATED VIEW OF 3-D COMPUTER CHARACTER ANIMATION
David Zeltzer *In* Canadian Information Processing Society Graphics Interface 1985 1985 p 105-115 refs (For primary document see N85-34523 23-61)
(Grant NSF MCS-83-04185)
Avail: NTIS HC A19/MF A01

To automate character animation and extend it to 3-D we need to create and manipulate three-dimensional models of articulated figures. Abstraction and adaptive motion are key mechanisms for dealing with the degrees of freedom problem, which refers to the sheer volume of control information necessary for coordinating the motion of an articulated figure when the number of links is large. A three level hierarchy of control modes for animation is proposed: guiding, animator-level, and task-level systems. Guiding is best suited for specifying fine details but unsuited for controlling complex motion. Animator-level programming is powerful but difficult. Task-level systems gives facile control over complex motions and tasks by trading off explicit control over the details of motion. The integration of these three control levels is discussed. Author

N85-34539# Brown Univ., Providence, R. I. Dept. of Computer Science.
RESEARCH ISSUES IN GENERATING GRAPHICAL EXPLANATIONS
Steven Feiner *In* Canadian Information Processing Society Graphics Interface 1985 1985 p 117-123 refs (For primary document see N85-34523 23-61)
(Contract N00014-78-C-0306)
Avail: NTIS HC A19/MF A01

Advances in computer graphics have led to the ever-increasing ability to depict objects realistically, while work in expert systems has resulted in the capacity to model objects and their interactions well enough to solve some difficult problems. One application in which the power of both disciplines can be coupled is the generation of graphical explanations that depict the performance of actions on objects. A high-level conceptual architecture for automatically generating presentations is discussed. It serves as an organizing framework in which to examine some of the problems that were encountered in implementing APEX, a test-bed system for creating and laying out pictures that depict actions performed by a problem solver. Author

N85-34540# IBM Italia, Rome.
AN INTEGRATED SYSTEM FOR PRINTING AND PUBLISHING APPLICATIONS c82
S. Cavaliere, M. Fantini, and A. Turtur *In* Canadian Information Processing Society Graphics Interface 1985 1985 p 125-132 refs (For primary document see N85-34523 23-61)
Avail: NTIS HC A19/MF A01

The architecture of a system, providing an integrated approach to the printing process, starting from the input of the basic components (images, texts, and graphics) up to the definition and modification of page layout and finally to driving high resolution output devices is described. The system allows an interactive management of the documents to be printed as well as of their elementary components, i.e., the pages, and at a lower level, the boxes, containing texts, images and graphics. The main peculiarities of the system architecture are interactivity, modularity and

non-procedurality discussed in more details and since of its functions are illustrated by means of some system outputs. Author

N85-34541# ENSIEG, Saint Martin d'Heres (France). Lab. d'Automatique.
RECOGNITION AND CLEAR REPRESENTATION OF HAND-WRITTEN ELECTRONIC DIAGRAMS [RECONNAISSANCE ET MISE AU NET DE SCHEMAS ELECTRONIQUES MANUSCRITS] **c33**
Martine Silbermann and Pierre Deschizeaux *In* Canadian Information Processing Society Graphics Interface 1985 1985 p 133-138 refs In FRENCH; ENGLISH summary (For primary document see N85-34523 23-61)
Avail: NTIS HC A19/MF A01

A recognition system for handwritten electronic diagrams is described. This system will be integrated in another one which performs automatic page-settings. The different steps presented are acquisition, skeletonization, segmentation, text elimination, connections detection, classification and identification of the basic symbols. An interactive phase, at the end of the treatment, allows simultaneous correction the final diagram and introduce the text which was previously eliminated. Author

N85-34542# Brown Univ., Providence, R. I. Dept. of Computer Science.
A MODEL FOR A DOCUMENT MAINTENANCE SYSTEM **c82**
Matthew Kaplan *In* Canadian Information Processing Society Graphics Interface 1985 1985 p 139-146 refs Sponsored in part by IBM Corp. and Online Computer Library Center, Inc. (For primary document see N85-34523 23-61)
Avail: NTIS HC A19/MF A01

The architecture of a system for editing formatted documents is presented. Key among the requirements for this system are support for complex page formats and the ability to incorporate diagrams and other non-textual features. The system is interactive, using an incremental formatter to adjust the text after each change. The model allows for extending the set of supported doucment objects and permits multiple views of these objects. Documents are highly structured, and relationships between structures are maintained by constraints resident in each object. Author

N85-34543# Toronto Univ. (Ontario). Computer Systems Research Inst.
ISSUES AND TECHNIQUES IN TOUCH-SENSITIVE TABLET INPUT (EXECUTIVE SUMMARY) **c60**
W. Buxton, R. Hill, and P. Rowley *In* Canadian Information Processing Society Graphics Interface 1985 1985 p 147-149 refs (For primary document see N85-34523 23-61)
Avail: NTIS HC A19/MF A01

Touch-sensitive tablets and their use in human-computer interaction are discussed. It is shown that in certain contexts such devices have some very important advantages over more common technologies (such as mice and joysticks). The analysis serves two purposes: (1) it sheds light on touch tablets, and (2) it demonstrates how other devices might be approached. Three specific distinctions between touch tablets and traditional devices are drawn. These concern: the signing of events, multiple point sensing and the use of templates. These distinctions are reinforced, and possible uses of touch tablets are illustrated, with a simple example system. Potential enhancements to touch tablets and other input devices are discussed, as are some inherent problems. Author

N85-34544# Colspan, Inc., Boulder, Colo. Dept. of Computer Science.
EFFICIENT RECOVERY AND REVERSAL IN GRAPHICAL USER INTERFACES GENERATED BY THE HIGGENS SYSTEM **c62**
Scott E. Hudson and Roger King *In* Canadian Information Processing Society Graphics Interface 1985 1985 p 151-158 refs (For primary document see N85-34523 23-61)
Avail: NTIS HC A19/MF A01

The performance of user recover and reversal, or undo, within a Higgens generated interface is discussed. A special data model is developed which has unique properties which combine to provide an efficient environment for implementing an undo mechanism. New algorithms based on recent work in incremental attribute evaluation are used to efficiently implement both the generated interfaces as a whole, and the undo mechanism in particular. A formal model of undo is used to evaluate the power of the mechanism to compare it with other undo implementations. E.A.K.

N85-34545# California Univ., Davis. Signal and Image Processing Lab.
A MODEL FOR GRAPHICS INTERFACE TOOL DEVELOPMENT **c60**
Kenneth I. Joy *In* Canadian Information Processing Society Graphics Interface 1985 1985 p 159-165 refs (For primary document see N85-34523 23-61)
Avail: NTIS HC A19/MF A01

A Problem Solving Environment (PSE) is an integrated system that supports the solution of a given problem, or a set of related problems. Paramount in the development of such environments is the design, specification and integration of user interface tools that communicate between the system and the user. The interaction with tool parameters, which in many applications CAD/CAM, Imaging Systems, image Processing, are represented by graphical data. A user-interface tool development system in which both textural and graphical display, and interaction techniques are integrated under a single model which is described allows the user to interact with tool parameters in either graphical or textural modes, and to have the parameters displayed in the manner most relevant to the problem set. E.A.K.

N85-34546# Toronto Univ. (Ontario). Dept. of Computer Science.
USING PERCENT-DONE PROGRAM INDICATORS TO ENHANCE USER INTERFACES
Brad A. Myers *In* Canadian Information Processing Society Graphics Interface 1985 1985 p 167-170 refs (For primary document see N85-34523 23-61)
Avail: NTIS HC A19/MF A01

A percent-done progress indicator is a graphical technique which allows the user to monitor the progress through the processing of a task. Progress indicators can be displayed on almost all types of output devices, and can be used with many different kinds of programs. Practical experience and formal experiments show that progress indicators are an important and useful user interface tool, and that they enhance the attractiveness and effectiveness of programs that incorporate them. Progress indicators including the results of a formal experiment with progress indicators are summarized. It is demonstrated that people prefer to have progress indicators. It was attempted to replicate earlier findings to show that people prefer constant to variable response time in general, and to show that this effect is reversed with progress indicators. E.A.K.

N85-34547# Perception Computing, Inc., Downsview (Ontario).
THE SCIENTIFIC AND TECHNICAL ISSUES IN INTEGRATING REMOTELY SENSED IMAGERY WITH GEOCODED DATA BASES **c43**
W. Murray Strome and Berne Grush *In* Canadian Information Processing Society Graphics Interface 1985 1985 p 171-177 refs (For primary document see N85-34523 23-61)
Avail: NTIS HC A19/MF A01

Digital analysis techniques of remote sensed data are discussed. The decreasing cost of computer equipment, especially both on-line and off-line memory, has led to an explosion in the use of digital mapping techniques. It is recognized that the full potential benefits of satellite remote sensing can not be realized until digital analysis of satellite image data and automated cartography/geocoded information systems are more compatible and integrated. The difficulties associated with this integration are explored. E.A.K.

N85-34548# National Research Council of Canada, Ottawa (Ontario).

SELECTION OF SEGMENT SIMILARITY MEASURES FOR HIERARCHICAL PICTURE SEGMENTATION
Jean-Marie Beaulier and Morris Goldberg (Ottawa Univ.) *In* Canadian Information Processing Society Graphics Interface 1985 1985 p 179-186 refs (For primary document see N85-34523 23-61)
Avail: NTIS HC A19/MF A01

The problem of defining appropriate segments similarity measures for picture segmentation was examined. In agglomerative hierarchical segmentation, two segments are compared and merged if found similar. The approximation error resulting from merging two segments. Similarity measures derived from constant approximations and planar approximations are applied to a LANDSAT picture, and the results are presented. The advantages of combining similarity measures are stressed. Different picture areas require different measures which must be combined to obtain good overall results. In hierarchical segmentation, simple measures are used for the first merging steps, while, at a higher level of the segment hierarchy, more complex measures are employed. E.A.K.

N85-34549# Geneva Univ. (Switzerland).
A GENERAL PURPOSE IMAGE PROCESSING PACKAGE
Michel Caplain, Claudine Metral, and Christian Pelligrini *In* Canadian Information Processing Society Graphics Interface 1985 1985 p 187-194 refs (For primary document see N85-34523 23-61)
Avail: NTIS HC A19/MF A01

Optical image processing provides solution to a limited class of applications. Instead of using optical filters and lenses, it propagates discrete images through massively parallel Cellular Networks. The free choice of cells and connections - which may be endowed with memory - appears sufficient to implement any conceivable function. A sequential simulator is available under UNIX BSD 4.2 to help design and validate such image processing networks. Higher resolution implementation would normally require special hardware. This architectural model is also a candidate for other areas of artificial intelligence. E.A.K.

N85-34550# Alberta Univ., Edmonton. Dept. of Computing Science.
A NEW APPROACH TO LINEAR QUADTREES
Wayne A. Davis and Xiaoning Wang *In* Canadian Information Processing Society Graphics Interface 1985 1985 p 195-202 refs Sponsored in part by the Natural Sciences and Engineering Research Council (For primary document see N85-34523 23-61)
Avail: NTIS HC A19/MF A01

A modified version of the linear quadtree for region representations is introduced. The modified linear quadtree (MLQ) uses only (2n+log n)/3n of the memory space required by the linear quadtree to represent the same region, where n is the resolution parameter of the image, results are presented. An MLQ can be constructed, given the array description of the image, in time proportional to the number of pixels in the imaging. Computing a neighbor node and determining its color can be done in time O(N) and O(log N) respectively, where N is the number of nodes in the MLQ. An O(n N) algorithm is given to generate the background of the region. E.A.K.

N85-34551# California Univ., Berkeley. Computer Graphics Lab.
AN ANALYSIS AND ALGORITHM FOR FILLING PROPAGATION
Kenneth P. Fishkin and Brian A. Barsky *In* Canadian Information Processing Society Graphics Interface 1985 1985 p 203-212 refs Sponsored in part by the Semiconductor Research Corp. and the State of California (For primary document see N85-34523 23-61)
(Grant NSF ECS-82-04381)
Avail: NTIS HC A19/MF A01

Fill algorithms are a common graphics utility used to change the color of regions in the frame buffer. The propagation algorithm is a key component of filling algorithms. The problem of propagation within a fill algorithm is presented and defined, and the difficulties of formalization and comparison are discussed. The previous algorithms are presented and analyzed under a new comparison metric whose validity is confirmed by run-time tests. A new algorithm is developed, and is shown to have better average and worst case behavior than the others. E.A.K.

N85-34552# Regina Univ. (Saskatchewan). Dept. of Computer Science.
HOLOGRAM-LIKE TRANSMISSION OF PICTURES **c35**
Przemyslaw Prusinkiewicz and Mark Christopher *In* Canadian Information Processing Society Graphics Interface 1985 1985 p 213-219 refs (For primary document see N85-34523 23-61)
Avail: NTIS HC A19/MF A01

A new digital representation of pictures is proposed. The main feature of this representation is: given a string of data Z representing a picture with full resolution, various substrings of Z represent the same picture with appropriately lower resolution. This is analogous to a well-known property of holograms. The principle of the new representation is presented, its overhead is analyzed, and examples of picture reconstruction are provided. An application of the hologram-like representation to the transmission of pictures with progressive resolution is indicated. E.A.K.

N85-34553# Toronto Univ. (Ontario). Computer Systems Research Inst.
A MULTI-TOUCH THREE DIMENSIONAL TOUCH-SENSITIVE TABLET (EXECUTIVE SUMMARY) **c60**
S. K. Lee, W. Buxton, and K. C. Smith *In* Canadian Information Processing Society Graphics Interface 1985 1985 p 221-222 refs Submitted for publication (For primary document see N85-34523 23-61)
Avail: NTIS HC A19/MF A01

A touch sensitive tablet transducers was developed. The table, a flat surface that can sense where it is touched by the operator's finger. The table combines two additional features: (1) it can sense the degree of contact in a continuous manner; (2) it can sense the amount and location of a number of simultaneous points of contact. These two features, when combined with touch sensing, are very important. Issues relating to the transducer's implementation are analyzed. Two contributions discussed are the method of scanning the table surface, and the method of maintaining high resolution despite the surface being partitioned into a discrete grid. E.A.K.

N85-34554# Politecnico di Milano (Italy). Diparimento di Meccanica.
THE CADME APPROACH TO THE INTERFACE OF SOLID MODELLERS
Carlo Bizzozero and Umberto Cugini *In* Canadian Information Processing Society Graphics Interface 1985 1985 p 223-229 refs (For primary document see N85-34523 23-61)
Avail: NTIS HC A19/MF A01

The man-machine communications was analyzed. In the field of Computer Aided Design the solution led to the definition and realization of an independent interface placed in front of solid modellers accepting CSG definitions. This system is able to simulate the orthographic projections of the specified part without activating the solid modeller. The illustrated interface is a part of an integrated system called CADME. E.A.K.

N85-34555# California Univ., Los Angeles. Manufacturing Engineering Program.
AN INNOVATIVE USER INTERFACE FOR MICROCOMPUTER-BASED COMPUTER-AIDED DESIGN
Larry Lichten and Ronald Eaton *In* Canadian Information Processing Society Graphics Interface 1985 1985 p 231-235 refs (For primary document see N85-34523 23-61)
Avail: NTIS HC A19/MF A01

An innovative user interface for a general purpose computer-aided design (CAD) system is described. Distributed processing in manufacturing environments were investigated. The system supports three-dimensional design capabilities for execution locally and incorporates model compatibility for communication with main-frame CAD systems. E.A.K.

N85-34556# Ecole Polytechnique, Montreal (Quebec).
A GEOMETRIC MODELLER FOR TURBOMACHINERY APPLICATIONS **c37**
B. Ozell and R. Camarero *In* Canadian Information Processing Society Graphics Interface 1985 1985 p 237-244 refs (For primary document see N85-34523 23-61)
Avail: NTIS HC A19/MF A01

A software package tailored for the geometric modelling of turbines, and for the automatic generation of a body-fitted coordinate grid is described. The package consists of four programs used respectively for: (1) the creation and the modification of a model, the designer can edit the model by commands whose basic entities are points, profiles, blades, the hub and the shroud; (2) the refinement of the model by the distribution of points over each profile defining the blade, and then by the interpolation of new intermediate profiles between the hub and the shroud; (3) the construction of surfaces delimiting the blade-to-blade channel boundaries; (4) the calculation of a body-fitted coordinate system, inside the channel, by the solution of a system of differential equations. E.A.K.

N85-34557# GE-Calma Co., Sunnyvale, Calif.
ARCHITECTURE OF LANGUAGES FOR LARGE CAD SYSTEMS DEVELOPMENT
Clive K. Liu *In* Canadian Information Processing Society Graphics Interface 1985 1985 p 245-251 refs (For primary document see N85-34523 23-61)
Avail: NTIS HC A19/MF A01

Current approaches to designing and implementing the user programming language (UPL) for computer-aided design (CAD) are reviewed. The requirements of the UPL, application programming language (APL) and system programming language (SPL) are summarized. Some alternatives to language architectures for users at different levels are analyzed, and a model is proposed for the next generation of CAD systems. The implementation issues of this architecture are also addressed. E.A.K.

N85-34558# Ecole Polytechnique, Montreal (Quebec).
A GRAPHICS INTERFACE FOR INTERACTIVE SIMULATION OF PACKET-SWITCHED NETWORKS
J. L. Houle and L. Richardson *In* Canadian Information Processing Society Graphics Interface 1985 1985 p 253-258 refs (For primary document see N85-34523 23-61)
Avail: NTIS HC A19/MF A01

A way to design and evaluate a packet-switched network is presented: the interactive simulation of the network using computer graphics to present the network states over a simulated time interval. The concept of a software defined network is implemented, allowing the use of an already existing network for a specific application related to distributed control systems. The package could be used as a real-time network control system. E.A.K.

N85-34559# Montreal Univ. (Quebec). Dept. d'Informatique et de Rech. Oper.
DESIGN AND IMPLEMENTATION OF AN INTERACTIVE ROUTE EDITOR **c60**
Guy Lapalme and Michel Cormier *In* Canadian Information Processing Society Graphics Interface 1985 1985 p 259-263 refs (For primary document see N85-34523 23-61)
Avail: NTIS HC A19/MF A01

An interactive color graphic system designed for pickup and delivery route modification is presented. Three fundamental types of commands are identified and it is shown that they correspond to those of a typical text editor. E.A.K.

N85-34560# Sao Paulo Univ. (Brazil). Electrical Engineering Dept.
PROJECT MANAGEMENT USING GRAPHICS **c81**
Fabio Pettinati *In* Canadian Information Processing Society Graphics Interface 1985 1985 p 265-272 refs (For primary document see N85-34523 23-61)
Avail: NTIS HC A19/MF A01

The problem of lack of visualization most managers face when using computer-based project control systems is addressed. Although highly relevant information is generated, usually no graphical output is produced. A system called UniPert that automatically produces high quality drawings showing all activities present in a project and the relationship between them is presented. The UniPert's major components and algorithms are described and examples of its actual use are presented. The integration of many different techniques and concepts that led to the development of the UniPert system are outlined. E.A.K.

N85-34561# Rensselaer Polytechnic Inst., Troy, N. Y.
THE AUTOMATIC LABELING OF GEOGRAPHIC MAPS: A PROBLEM IN COMPUTER AESTHETICS **c43**
Herbert Freeman *In* Canadian Information Processing Society Graphics Interface 1985 1985 p 273-281 refs (For primary document see N85-34523 23-61)
Avail: NTIS HC A19/MF A01

The current state of a project to develop a system for automatically placing the names of area features, point features, and line features in a map is described. A rule-based system is used which incorporates the body of knowledge employed by cartographers when performing this task. The system aims to achieve a fully annotated map in which: (1) all names are unambiguously associated with the features to which they refer; (2) the necessary cartographic standards are satisifed; and (3) a high overall aesthetic quality is accomplished. E.A.K.

N85-34562# Nippon Electric Co. Ltd., Kawasaki (Japan). Systems Research Labs.
HOW MAP DESIGNERS CAN REPRESENT THEIR IDEAS IN THEMATIC MAPS: EFFECTIVE USER INTERFACES FOR THEMATIC MAP DESIGN **c43**
Takuya Yamahira, Yutaka Kasahara, and Tateyuki Tsurutani *In* Canadian Information Processing Society Graphics Interface 1985 1985 p 283-290 refs (For primary document see N85-34523 23-61)
Avail: NTIS HC A19/MF A01

The problems and developed Histogram Interface effectiveness for designing choropleth maps are described. The results obtained from an actual experiment are included. The concept of how computer graphics designers can incorporate their ideas into resulting pictures is discussed. E.A.K.

N85-34563# Canada Land Data Systems, Ottawa (Ontario). Lands Directorate.
APPLIED COMPUTER GRAPHICS IN A GEOGRAPHIC INFORMATION SYSTEM: PROBLEMS AND SUCCESSES **c82**
C. L. MacDonald and I. K. Crain *In* Canadian Information Processing Society Graphics Interface 1985 1985 p 291-296 refs (For primary document see N85-34523 23-61)
Avail: NTIS HC A19/MF A01

A geographic information system (GIS) reports and displays data which are referenced to geographic locations. As opposed to automated cartography, geographic information systems often have developed graphic output as an afterthought or secondary product. The Canada geographic information system, (CGIS) was designed with no graphic output capability, but now provides a variety of interactive and hard-copy graphics on a day-to-day basis. These graphics are applied to problems in land evaluation, land use monitoring, natural resource planning, wildlife habitat conservation, and so on. Three categories of graphic outputs in map form are required, interactive displays, working diagrams and publication quality diagrams. These were achieved by using remote interactive color and monochrome terminals, ink-jet plotters, vector-based plotting on a high quality drum plotter and the direct production of publication quality color separates on a large format optical scanner with laser plotter capabilities. Author

N85-34564# Grundey (Klaus), Essen (West Germany).
A USER-FRIENDLY COMPUTER-AIDED CONSTRUCTION OF BOUNDARIES
Klaus Grundey, Udo Schweitzer, and Rolf Neuser *In* Canadian Information Processing Society Graphics Interface 1985 1985

p 297-301 refs Prepared in cooperation with Schweitzer (Udo), Essen and Neuser (Rolf), Essen (For primary document see N85-34523 23-61)
Avail: NTIS HC A19/MF A01

To calculate a Digital Terrain Model (DTM) of any set M of measuring points M = [(x(i),y(i),z(i)) and i =1,....n], it is often neccessary to combine some subsets of M. Such subsets may be special point sets e.g., boundaries, slopes, break points, etc. Such point sets are important for calculating the altitudes of DTM grid points, because they influence the election of the correct neighborhood of the grid point in question. We wish to present a fast and user-friendly algorithm to calculate such points sets. Author

N85-34565# New York Univ., New York. The Interactive Telecommunications Program.
IMAGE SYNTHESIS: OPTICAL IDENTITY OR PICTORIAL COMMUNICATION?
Michael I. Mills *In* Canadian Information Processing Society Graphics Interface 1985 1985 p 303-308 refs (For primary document see N85-34523 23-61)
Avail: NTIS HC A19/MF A01

Some ideas from E.H. Gombrich (an art historian) and Julian Hochberg (a perception psychologist) on artists' attempts to simulate reality in pointing are reviewed. These ideas suggest that workers in image synthesis enlarge the scope of their mission. Rather than trying to get computers to make images which are industinguishable from direct perception, they should pay more attention to the use of computer graphics for pictorial communication where departures from objective realism can sometimes lead to more effective displays and where the metal process of image interpretation should itself be a legitimate focus of research and experimentation. Author

N85-34566# Montreal Univ. (Quebec). Ecole des Hautes Etudes Commerciales.
STRATEGIC USE OF BUSINESS GRAPHICS: A STAKEHOLDER APPROACH
Albert Lejeune, Francois Bolduc, and Nadia Magnenat-Thalmann *In* Canadian Information Processing Society Graphics Interface 1985 1985 p 309-312 refs (For primary document see N85-34523 23-61)
Avail: NTIS HC A19/MF A01

The concept of stakeholder is borrowed from the strategic management literature. Our question is, which graphics format will influence, a stakeholder network in the most efficient way? To answer this question are defined: (1) circulation graphics intended to circulate from node to node inside a network and (2) terminal graphics in which the specific use is localized at only one node in a network. With the help of the GRAFEDIT, GRAFANA and CINEDATA software packages, various graphic formats (line charts, pie charts, bar charts, size pictograms, number pictograms and 3D charts) are generated. Finally, an exploratory field experiment is set up to verify the following hypothesis: for a given problem and for a multiple stakeholder network, managers manipulate graphics formats to inform and influence different stakeholders in different ways. Author

N85-34567# Toronto Univ. (Ontario). Dept. of Computer Science.
COLOUR SPACES AND COLOUR CONTRAST c74
Avi Naiman *In* Canadian Information Processing Society Graphics Interface 1985 1985 p 313-320 refs (For primary document see N85-34523 23-61)
Avail: NTIS HC A19/MF A01

With the introduction of low cost color graphics systems come a host of problems specifically concerned with the color aspect of the system. Two of these problems are discussed: the selection and manipulation of colors by (possibly) inexperienced users, and the automatic selection of colors by the system to achieve high contrast effects on the screen. A new color model based on color opponency theory is described. This model is useful both in the user interface and in the automatic selection of high contrast colors. Author

N85-34568# Imperial Coll. of Science and Technology, London (England). Dept. of Management Science.
COLOUR CODING SCALES AND COMPUTER GRAPHICS
A. M. Heath and R. B. Flavell *In* Canadian Information Processing Society Graphics Interface 1985 1985 p 321-328 refs (For primary document see N85-34523 23-61)
Avail: NTIS HC A19/MF A01

Color is a powerful tool when used to code information on a graphics display, and the growth in the number of color displays increases the importance of understanding the potential of color coding. The ways in which color can be used to code information is discussed, and previous guidelines are reviewed. An experiment examining the quantitative, rather than qualitative, use of color in ten different ordinal scales is described. The results generate new guidelines that demonstrate the importance of displaying a reference scale, and show that when applied out of context the previous guidelines can significantly underestimate the power of color coding. Author

N85-34569# Tokyo Univ. (Japan).
A SIMPLE BUT SYSTEMATIC CSG SYSTEM
Tosiyasu L. Kunii and Geoff Wyvill (Otago Univ., New Zealand) *In* Canadian Information Processing Society Graphics Interface 1985 1985 p 329-336 refs (For primary document see N85-34523 23-61)
Avail: NTIS HC A19/MF A01

A simple system is described for computer aided design by constructive solid geometry (CSG). The system allows the design of engineering components by combining basic components which represent shapes produced by standard machining operations. The system has four significant original features: (1) the primitive components are described in an object oriented fashion, data plus procedures; (2) a new kind of octree structure is used to render various displays from descriptions; (3) certain objects can be directly associated with composite components of tool paths; and (4) the system consists of four conceptual modules with well-defined interfaces. R.J.F.

N85-34570# Toronto Univ. (Ontario). Computer Systems Research Inst.
GEOMETRIC CONTINUITY WITH INTERPOLATING BEXIER CURVES
Alain Fournier and Brian A. Barsky (California Univ., Berkeley) *In* Canadian Information Processing Society Graphics Interface 1985 1985 p 337-341 refs (For primary document see N85-34523 23-61)
Avail: NTIS HC A19/MF A01

Techniques are presented to use the Bexier formulation to interpolate the two dimensional points given by a user with cubic piecewise Bexier curves, while maintaining up to G(2) continuity, and to interactively manipulate the bias and tension of each span, with geometric entities clearly related to the curve, while preserving the degree of geometric continuity prescribed by the user. R.J.F.

N85-34571# California Univ., Berkeley. Computer Graphics Lab.
AN INTUITIVE APPROACH TO GEOMETRIC CONTINUITY FOR PARAMETRIC CURVES AND SURFACES c64
Tony D. DeRose and Brian A. Barsky *In* Canadian Information Processing Society Graphics Interface 1985 1985 p 343-351 refs Previously announced as N85-28579 (For primary document see N85-34523 23-31)
Avail: NTIS HC A19/MF A01

The notation of geometric continuity is extended to an abritrary order for curves and surfaces, and an intuitive development of constraints equations is presented that are necessary for it. The constraints result from a direct application of the univariate chain rule for curves, and the bivariant chain rule for surfaces. The constaints provide for the introduction of quantities known as shape parameters. The approach taken is important for several reasons: First, it generalizes geometric continuity to arbitrary order for both curves and surfaces. Second, it shows the fundamental connection between geometric continuity of curves and geometric continuity

of surfaces. Third, due to the chain rule derivation, constraints of any order can be determined more easily than derivations based exclusively on geometric measures. Author

N85-34572# Rensselaer Polytechnic Inst., Troy, N. Y. Dept. of Electrical, Computer, and Systems Engineering.
BUILDING AN OCTREE FROM A SET OF PARALLELEPIPEDS
William Randolph Franklin and Varol Akman *In* Canadian Information Processing Society Graphics Interface 1985 1985 p 353-359 refs (For primary document see N85-34523 23-61)
Avail: NTIS HC A19/MF A01

A novel algorithm for building an octree from a set of parallelepipeds approximating an object is given. This is an important operation in solid modeling systems based on octrees. The algorithm is simple to program and easy to understand. It creates a minimal octree from the given parallelepipeds. It does not lead to an intermediate storage swell. It is well-suited to handle very precisely specified objects which are made of a larger number of parallelepipeds since it can work with linear files which are accessed in an orderly manner to lessen virtual memory page faults. Author

N85-34573# Infolytica Corp., Montreal (Quebec). Software Development.
DEVELOPING GRAPHICAL TOOLS WITH MINIMAL GKS
Robert Sabourin and D. A. Lowther (McGill Univ.) *In* Canadian Information Processing Society Graphics Interface 1985 1985 p 365-372 refs (For primary document see N85-34523 23-61)
Avail: NTIS HC A19/MF A01

The Graphical Kernel System (GKS) is emerging as an important standard for the display and manipulation of two dimensional data. Tools described here were developed for the minimal GKS implementation which has both input and output capabilities. Minimal GKS (level MB) is guaranteed to exist in any GKS implemtation with both input and output capabilities. Minimal GKS provides sufficient power to build complex menu driven applications programs while maintaining independence from the graphical hardware used. Info-Menu is a tool for creating interactive menu driven interfaces. Info-Graph is a library of subroutines which enables users to create line graphs with various display attributes and axis mapping functions. The implementation of both packages will be discussed. Author

N85-34574# Lehigh Univ., Bethlehem, Pa. Dept. of Civil Engineering.
DESIGNING A GRAPHICS APPLICATION INTERFACE
John L. Wilson, Stuart S. Chen, and Steven L. Sadofsky *In* Canadian Information Processing Society Graphics Interface 1985 1985 p 373-380 refs (For primary document see N85-34523 23-61)
Avail: NTIS HC A19/MF A01

A systematic approach that can be followed by developers of educational courseware which contains graduated learning capabilities to accommodate a diverse group of users is discussed. A unified conceptual model of a computer integrated engineering system where graphics plays an important function in the user interface is presented. An overall approach to be taken to interface design and the role graphics can assume. The development of an interface is then examined from both the viewpoint of the user and the courseware implementor. Computer generated displays are included which illustrate the use of the Graphical Kernal System (GKS) in picture generation and modification. The examples are chosen from interactive structural engineering courseware developed by the authors at Lehigh University. Author

N85-34575# Industrial Technical Services, Montreal (Quebec). Research and Development Group.
NAPGEN: AUTOMATIC NAPLPS PAGE GENERATOR **c60**
Michel Plante *In* Canadian Information Processing Society Graphics Interface 1985 1985 p 381-383 ref (For primary document see N85-34523 23-61)
Avail: NTIS HC A19/MF A01

The creation of videotex pages from already encoded information (generally in the form of ASCII or EBCDIC codes) involves most of the time a large amount of work from the people doing it and usually they are bound to simply retype the whole information in the new videotex page using some page creation equipment (hardware and/or software). What is needed then is a simple tool that would automate the process of inserting this information (from an ASCII database) into the final videotex page without having to redo all the encoding by hand. The NAPLPS Page GENerator (NAPGEN), application program that was written specifically to perform the conversion function from ASCII to NAPLPS with the addition of graphics made possible by the NAPLPS videotex standard itself is discussed. R.J.F.

N85-34576# McGill Univ., Montreal (Quebec). Computer Vision and Robotics Lab.
NON-RIGID BODY MOTION
Andreas R. Dill and Martin D. Levine *In* Canadian Information Processing Society Graphics Interface 1985 1985 p 383-389 refs Sponsored by Medical Research Council of Canada and Province of Quebec (For primary document see N85-34523 23-61)
Avail: NTIS HC A19/MF A01

During the last few years motion analysis has developed into a major field of interest in image analysis and understanding. Considerable progress has been made as evidenced by the number of publications. However, most of these have been confined to the study of rigid body motion. Very few have addressed the issue of non-rigid body motion which poses many interesting and difficult problems. A new technique is proposed for analyzing non-rigid body motion of closed boundary shapes that is based on the computation of skeletons at multiple resolutions. This technique is used for analyzing the structural changes in the morphology of locomoting lymphocytes and, in particular of their pseudopods. Author

N85-34577# McGill Univ., Montreal (Quebec). Computer Vision and Robotics Lab.
MULTI-ROBOT ASSEMBLY OF IC'S **c63**
C. Michaud, A. S. Malowany, and Martin D. Levine *In* Canadian Information Processing Society Graphics Interface 1985 1985 p 391-397 refs Sponsored by Natural Sciences and Engineering Research Council of Canada and FCAC (For primary document see N85-34523 23-61)
Avail: NTIS HC A19/MF A01

A multi-robot system which assembles integrated circuits is discussed. The problems addressed are the calibration of the robotic station, the control of several robots working concurrently, and pattern recognition. These problems are discussed in the context of a distributed system. The use of image processing is omnipresent. For instance, vision feedback is used to acknowledge almost every move of the robots and also to calibrate the camera itself. Pattern recognition techniques are employed to detect the exact orientation of the iC die. Several robots are used in order to give more flexibility to the system and allow, the experience which could lead toward a multirobot multitasking system. R.J.F.

N85-34578# Chinese Univ. of Hong Kong, Shatin. Dept. of Computer Science.
LOW COST GEOMETRIC MODELLING SYSTEM FOR CAM
W. B. Ngai and Y. K. Chan *In* Canadian Information Processing Society Graphics Interface 1985 1985 p 399-406 refs (For primary document see N85-34523 23-61)
Avail: NTIS HC A19/MF A01

A geometric modelling system is implemented on a low cost, medium resolution, color graphics workstation. When compared with other CAD/CAM systems for the design and manufacture of engineering components, the proposed system is oriented towards the manufacturing of 3-dimensional geometric model using numerical control machine. The colour graphics capability allows a designer to interactively create simple 3-dimensional geometric shapes as the building blocks for complex 3-dimensional engineering component. By shape operating the building blocks interactively with feedback from the graphical screen, the final design as it appears on the graphical screen can then be manufactured by a

numerical control machine subject to designer specified manufacturing parameters such as numerical control machine cutter size and the degree of surface finishing. Author

N85-34579# Alberta Univ., Edmonton. Dept. of Computing Science.
THE DYNAMICS OF ARTICULATED RIGID BODIES FOR PURPOSES OF ANIMATION
W. W. Armstrong and M. Green *In* Canadian Information Processing Society Graphics Interface 1985 1985 p 407-415 refs (For primary document see N85-34523 23-61)
Avail: NTIS HC A19/MF A01

Curves and surfaces satisfying continuity and smoothness conditions are used in computer graphics to fit spatial data points. In a similar fashion smooth motions of objects should be available to animators in such a way that the dynamics are correct to the degree required for realism. The motion, like a curve of surface shape, should be controllable by easy manipulations of a set of control parameters or by realtime interaction between the animator and a scene generated by dynamic simulation. Here, the objects considered have the form of rigid links joined at hinges to form a tree. This is a reasonable first approximation to human and animal bodies. The equations of motion are formulated with respect to hinge-centered coordinates, and are solved by an efficient technique in time which grows linearly with the number of links. Author

N85-34580# Montreal Univ. (Quebec). Centre de Calcul.
SHADOW VOLUMES FOR NON-PLANAR POLYGONS
Philippe Bergeron *In* Canadian Information Processing Society Graphics Interface 1985 1985 p 417-418 In FRENCH; ENGLISH summary (For primary document see N85-34523 23-61)
Avail: NTIS HC A19/MF A01

Crow has introduced a new class of algorithm for the generation of shadows in computer-generated shaded images. His approach is based on the concept of projected shadow volumes. Here, a new algorithm is described for the casting of shadows using Crow's approach. A polygonal data base is assumed. A major advantage of this new technique is that it works for an unconstrainted environment description. Thus, objects made of convex or concave, open or closed polyhedra with or without holes are allowed, each of which may be composed of convex or concave, planar or non-planar polygons with or without holes. Polygons may have any number of edges. Interpenetration between polygons is allowed. No polygon subdivision is necessary at any stage during the process. Any number of light sources can be defined, anywhere in the 3-D space, including the view volume, and any shadow volume. Author

N85-34581# Open Univ., Milton (England). Academic Computing Service.
COMPUTER ANIMATION IN DISTANCE TEACHING c80
Joel M. Greenberg *In* Canadian Information Processing Society Graphics Interface 1985 1985 p 419-423 (For primary document see N85-34523 23-61)
Avail: NTIS HC A19/MF A01

Television plays an important role in the distance teaching methods of the Open University. The use of computer animation has greatly enhanced the teaching process. Computer images are created using a graphics package based on the SIGGRAPH core system and viewed on a range of color raster terminals. Previewing animation sequences has been simplified by developing an interactive animation system. Completed sequences are recorded direct to videotape using a system developed jointly by the BBC and the Open University. They are subsequently edited into television programs for transmission by the BBC. Author

N85-34582# Victoria Univ. (British Columbia). Dept. of Computer Science.
GENERATIVE DESIGN IN ARCHITECTURE USING AN EXPERT SYSTEM c31
Eric Gullichsen and Ernest Chang *In* Canadian Information Processing Society Graphics Interface 1985 1985 p 425-433 (For primary document see N85-34523 23-61)
Avail: NTIS HC A19/MF A01

The mathematician-architect Christopher Alexander has devised a theory of objective architectural design. He believes that all architectural forms can be described as interacting patterns, all possible relationships of which are governed by generative rules. These form a pattern language' capable of generating forms appropriate for a given environmental context. The complexity of interaction among these rules leads to difficulties in their representation by conventional methods. Here, a Prolog-based expert system is presented which implements Alexander's design methodology to produce perspective views of partially and fully differentiated 3-dimensional architectural forms. Author

N85-34583# Toshiba Corp., Tokyo (Japan). Systems and Software Engineering Div.
KNOWLEDGE ENGINEERING APPLICATION IN IMAGE PROCESSING
Kazuo Mikame, Naomichi Sueda, Akira Hoshi, and Shinichi Honiden *In* Canadian Information Processing Society Graphics Interface 1985 1985 p 435-441 refs (For primary document see N85-34523 23-61)
Avail: NTIS HC A19/MF A01

A method using knowledge engineering for image processing is discussed as well as the effectiveness of the method. To establish the logic and procedure for image processing, a specific software module must be selected from 350 software modules, named SPIDER in Japan, according to vague requirements and the original image. Highly specialized and experimental knowledge is required to select it. By using the knowledge engineering method, the authors verified the selection and execution of these software modules. As a result, satisfactory processing has been made available to even nonexperts for use in image processing. In image processing execution, conventional language FORTRAN is used to obtain high speed image processing and AI language Prolog is used to infer a suitable software module. By applying AI language, a greater number of image processings, covering a wider range are expected. Author

N85-34584# Scholl (Laura) and Associates, San Francisco, Calif.
HEURISTIC RULES FOR VISUALIZATION
Laura Scholl *In* Canadian Information Processing Society Graphics Interface 1985 1985 p 443-446 refs (For primary document see N85-34523 23-61)
Avail: NTIS HC A19/MF A01

Visualization is discussed. The process is not to analyze visual perception as in the areas of pattern recognition and image understanding, but the complimentary process - to synthesize. Rather than dissect, the goal is to create. By using a visualization-system guided by heuristic rules, the artist can visualize the invisible and discover new sets of heuristics for exploring new visual concepts. The basis for a visualization system is described. The information is aimed at two groups of people: computer scientists and engineers who are currently most influential in research in artificial intelligence and computer graphics, so that they may use visual thinking and exploring new mediums (i.e.: computer technology). R.J.F.

N85-34585# Stanford Linear Accelerator Center, Calif.
USING LINE AS AN INTERACTIVE GRAPHICS PACKAGE. INTERFACING LINE AND TOPDRAW IN 43 AND 24 VM
B. LeClaire Apr. 1985 33 p
(Contract DE-AC03-76SF-00515)
(DE85-012007; SU-SLAC-TM-85-3) Avail: NTIS HC A03/MF A01

This report serves to describe interactive graphics with the LINE exec for use with any Topdraw file. In particular, the operation of LINE for positioning of Topdraw titles is described. DOE

N85-34586# North Carolina State Univ., Raleigh. Dept. of Electrical and Computer Engineering.
ANALYSIS OF TRANSIENT RADIATION UPSET IN A 16K SRAM

L. W. Massengill and S. E. Diehl-Nagle 1985 11 p Presented at the 22nd Ann. Conf. on Nucl. and Space Radiation Effects, Monterey, Calif., 22 Jul. 1985
(Contract DE-AC04-76DP-00789)
(DE85-009442; SAND-85-7183C; CONF-850711-5) Avail: NTIS HC A02/MF A01

Computer simulations of the transient radiation induced rail span collapse effect in the SA3240 16K SRAM are performed. Simulated bit maps of the upset RAMcell locations show the dose-rate level which causes the onset of information upset and the progression of the information loss across the memory array. Comparisons of simulated and experimental dose-rate upset levels for several radiation pulse widths show good agreement. DOE

N85-34587# California Univ., Livermore. Lawrence Livermore Lab.
USER'S GUIDE TO THE MATHEW/ADPIC MODELS
D. J. Rodriguez, G. D. Greenly, P. M. Gresho, R. Lange, B. S. Lawver, L. A. Lawson, and H. Walker Mar. 1985 165 p refs Prepared in cooperation with NUS Corp.
(Contract W-7405-eng-48)
(DE85-012952; UCID-20415) Avail: NTIS HC A08/MF A01

This user's guide provides both an operational and theoretical summary of the MATHEW/ADPIC transport and diffusion models and supplemental codes needed to execute these models. These models calculate air concentration and ground deposition on a regional scale (up to 200 km) from continuous or instantaneous point sources. MATHEW is a three dimensional meteorological data adjustment model which supplies ADPIC with mean wind fields that are mass consistent, three dimensional, and representative of the available meteorological measurements (surface, tower, and upper air soundings). The bottom boundary in this model is determined by grid cell estimates of the actual topographic features of a given site and its environs, which can play a very important role in defining or modeling regional scale patterns. ADPIC is a three dimensional, particle in cell transport and diffusion code capable of calculating the time dependent dispersion of inert or radioactive air pollutants. In addition to MATHEW/ADPIC, three supplemental codes are required to provide input/output support. These codes, which are also discussed in this user's guide, are TOPOG, MEDIC, and PLOTOCONTR. DOE

N85-34588# North Carolina State Univ., Raleigh. Dept. of Electrical and Computer Engineering.
CIRCUIT APPROACHES TO INCREASING SRAM PERFORMANCE IN TOTAL DOSE ENVIRONMENTS
B. L. Bhuva and S. E. Diehl-Nagle 1985 6 p refs Presented at the 22nd Ann. Conf. on Nucl. and Space Radiation Effects, Monterey, Calif., 22 Jun. 1985
(Contract DE-AC04-76DP-00789)
(DE85-009441; SAND-85-7182C; CONF-850711-6) Avail: NTIS HC A02/MF A01

Performance degradation of CMOS SRAM circuits in total dose environments has been studied by computer simulations. Different failure modes are discussed and new approaches for performance improvements are presented. DOE

N85-34589# Edgerton, Germeshausen and Grier, Inc., Goleta, Calif.
REAL-TIME MULTIPARAMETER PULSE PROCESSING WITH DECISION TABLES
K. Hull and H. Griffin (Michigan Univ., Ann Arbor) 1985 13 p refs Presented at the 6th Symp. on X- and Gamma-Ray Sources and Appl., Ann Arbor, Mich., 21 May 1985
(Contract DE-AC08-83NV-10282)
(DE85-011683; EGG-10282-2056; CONF-850533-6) Avail: NTIS HC A02/MF A01

The basic idea of using decision tables is presented. Through their use, the number of steps necessary to determine the correct processing procedures has been reduced to nearly one for the two parameter case. For applications of more than two parameters, the method expands easily as n - 1 decision table for n-parameter. An example of a three parameter experiment, using decision tables was implemented for the case of a delayed coincidence experiment. For these n-parameters cases, the steps required for the decision then approaches n - 1. Also, it was shown that the decision table process is relatively easy to implement in most languages. In assembly language it only requires a few basic instructions found on any common processor, making it relatively easy to transport. A large variety of applications can be implemented using this technique; the range is limited only by the user's creativity. All of these features make decision tables a viable choice in solving a variety of collection problems where the complexity of processing makes the serial process too slow or cumbersome and may make new techniques possible. DOE

N85-34590# California Univ., Livermore. Lawrence Livermore Lab.
USER'S MANUAL FOR THE FLORA EQUILIBRIUM AND STABILITY CODE
R. P. Freis and B. I. Cohen 1 Apr. 1985 22 p
(Contract W-7405-eng-48)
(DE85-013182; UCID-20400) Avail: NTIS HC A02/MF A01

A user's guide to the content and use of the two dimensional axisymmetric equilibrium and stability code FLORA is presented. FLORA addresses the low frequency MHD stability of long thin axisymmetric tandem mirror systems with finite pressure and finite Larmor radius effects. FLORA solves an initial value problem for interchange, potential, and ballooning stability. DOE

N85-34591# Clarkson Coll. of Technology, Potsdam, N.Y.
MULTI-SOLUTE SUBSURFACE TRANSFER MODELING FOR ENERGY SOLID WASTES: HIGHLIGHTS FY 1984
T. L. Theis, D. J. Kirkner (Notre Dame Univ.), and A. A. Jennings (Notre Dame Univ.) Jan. 1985 8 p
(DE85-012788; DOE/ER-0222) Avail: NTIS HC A02/MF A01

At the present time a general multisolute model, FIESTA, has been developed which combines the chemical processes of ion exchange, adsorption and complex formation, and the physical factors of convection and dispersion. Present research, highlighted in this report, is aimed at incorporating solubility reactions and a general kinetic, rather than equilibrium, approach to the chemical interactions. DOE

N85-34592# Battelle Columbus Labs., Ohio.
MATADOR (METHODS FOR THE ANALYSIS OF TRANSPORT AND DEPOSITION OF RADIONUCLIDES) CODE DESCRIPTION AND USER'S MANUAL
H. I. Avci, S. Raghuram, and P. Baybutt Apr. 1985 76 p refs
(TI85-901402; NUREG/CR-4211; BMI-2126) Avail: NTIS HC A05/MF A01

A new computer code called MATADOR (Methods for the Analysis of Transport And Deposition Of Radionuclides) has been developed to replace the CORRAL computer code which was written for the Reactor Safety Study. MATADOR is intended for use in system risk studies to analyze radionuclide transport and deposition in reactor containments. The principal output of the code is information on the timing and magnitude of radionuclide releases to the environment as a result of severely degraded core accidents. MATADOR considers the transport of radionuclides through the containment and their removal by natural deposition and by engineered safety systems such as sprays. The code requires input data on the source terms into the containment, the geometry of the containment, and thermal hydraulic conditions in the containment. Author

N85-34321# Cranfield Inst. of Tech., Bedford (England). Dept. of Applied Computing and Mathematics.
OPTIMISATION IN THE COMPUTER AIDED DESIGN OF MECHANISMS
M. J. Pratt *In* Cranfield Inst. of Tech. Proc. of the Mech. Conf., Vol. 2 1984 16 p refs 2 Vol. (For primary document see N85-34318 23-31)
Avail: NTIS HC A05/MF A01

N85-34324# Cranfield Inst. of Tech., Bedford (England).
SOFTWARE FOR MECHANISM DESIGN
S. Molian *In* Cranfield Inst. of Tech. Proc. of the Mech. Conf., Vol. 2 1984 17 p refs 2 Vol. (For primary document see N85-34318 23-31)
Avail: NTIS HC A05/MF A01

62 COMPUTER SYSTEMS

Includes computer networks.

N85-34593*# Kent State Univ., Ohio. Dept. of Mathematical Sciences.
ROBOT ENVIRONMENT EXPERT SYSTEM Final Report, Jan. 1983 - May 1984
Jerry L. Potter Washington NASA Aug. 1985 61 p refs
(Grant NAG1-341)
(NASA-CR-3915; NAS 1.26:3915) Avail: NTIS HC A04/MF A01 CSCL 09B

The Robot Environment Expert System uses a hexidecimal tree data structure to model a complex robot environment where not only the robot arm moves, but also the robot itself and other objects may move. The hextree model allows dynamic updating, collision avoidance and path planning over time, to avoid moving objects. Author

N85-34594# Department of the Air Force, Washington, D.C.
MAINTENANCE PORT SYSTEM Patent Application
D. J. Grone, inventor (to Air Force) Filed 14 May 1985 114 p (AD-D011724; US-Patent-Appl-SN-733991) Avail: NTIS HC A06/MF A01 CSCL 09/2

The maintenance port system comprises a maintenance unit, user prom, an available CRT terminal, and a prom software development package. This system accepts parametric definitions for an automatic panel as defined by the designer, and formats the panel data for display and modifications on a CRT (cathode ray tube) terminal. Because the system controls the formats, standard display and modification procedures are then used for transmitting and receiving parameters and are the same from panel to panel. GRA

N85-34595# California Univ., Livermore. Lawrence Livermore Lab.
PARALLEL PROCESSING ON THE LIVERMORE VAX 11/780-4 PARALLEL PROCESSOR SYSTEM WITH COMPATABILITY TO CRAY RESEARCH, INC. (CRI) MULTITASKING, VERSION 1
N. E. Werner and S. W. VanMatre May 1985 48 p Presented at the Spring DECUS Symp., New Orleans, 27 May 1985
(Contract W-7405-eng-48)
(DE85-011856; UCRL-92624; CONF-8505131-3) Avail: NTIS HC A03/MF A01

This manual describes the Cray Research, Inc. (CRI) Subroutine and Utility Package. The CRI library provides Cray multitasking functionality on the four processor shared memory VAX 11/780-4. Additional functionality has been added for more flexibility. A discussion of the library, utilities, error messages, and example programs is provided. DOE

N85-34544# Colspan, Inc., Boulder, Colo. Dept. of Computer Science.
EFFICIENT RECOVERY AND REVERSAL IN GRAPHICAL USER INTERFACES GENERATED BY THE HIGGENS SYSTEM
Scott E. Hudson and Roger King *In* Canadian Information Processing Society Graphics Interface 1985 1985 p 151-158 refs (For primary document see N85-34523 23-61)
Avail: NTIS HC A19/MF A01

63 CYBERNETICS

Includes feedback and control theory.
For related information see also *54 Man/System Technology and Life Support.*

N85-34596 Societe Francaise d'Instruments de Mesure, Massy (France).
IMPLICATIONS OF ARTIFICIAL INTELLIGENCE ON THE DESIGN OF FUTURE ONBOARD SYSTEMS Final Report [IMPLICATIONS DE L'INTELLIGENCE ARTIFICIELLE SUR LA CONCEPTION DES SYSTEMES EMBARQUES FUTURS]
Thierry Billoir Dec. 1984 80 p refs In FRENCH
(Contract DRET-83-1423)
(SFENA-DPS/C/S3/84252A) Avail: Issuing Activity

The applicability of artificial intelligence to aircraft or spacecraft design is discussed. A progress report on the research and development of the AMES airborne maintenance expert system is included. Author (ESA)

N85-34577# McGill Univ., Montreal (Quebec). Computer Vision and Robotics Lab.
MULTI-ROBOT ASSEMBLY OF IC'S
C. Michaud, A. S. Malowany, and Martin D. Levine *In* Canadian Information Processing Society Graphics Interface 1985 1985 p 391-397 refs Sponsored by Natural Sciences and Engineering Research Council of Canada and FCAC (For primary document see N85-34523 23-61)
Avail: NTIS HC A19/MF A01

64 NUMERICAL ANALYSIS

Includes iteration, difference equations, and numerical approximation.

N85-34597# Sandia Labs., Albuquerque, N. Mex. Simulation Theory Div.
COUPLED ELECTRON-PHOTON TRANSPORT CALCULATIONS USING THE METHOD OF DISCRETE ORDINATES
L. J. Lorence, Jr., W. E. Nelson (Science and Engineering Associates, Albuquerque, N. Mex.), and J. E. Morel (LANL) 1985 6 p Presented at the 22nd Ann. Conf. on Nucl. and Space Radiation Effects, Monterey, Calif., 22 Jul. 1985
(Contract DE-AC04-76DP-00789)
(DE85-009444; SAND-85-0564C; CONF-850711-4) Avail: NTIS HC A02/MF A01

A new discrete ordinates method for coupled electron photon transport is presented and applied to space shielding calculations. It is found that the discrete ordinates method is as accurate as the standard Monte Carlo method, but is much more efficient. DOE

N85-34319# Cranfield Inst. of Tech., Bedford (England).
AN INTRODUCTION TO FINITE ELEMENTS
P. M. Wheeler (PAFEC, Ltd.) *In* Cranfield Inst. of Tech. Proc. of the Mech. Conf., Vol. 2 1984 20 p 2 Vol. (For primary document see N85-34318 23-31)
Avail: NTIS HC A05/MF A01

N85-34571# California Univ., Berkeley. Computer Graphics Lab.
AN INTUITIVE APPROACH TO GEOMETRIC CONTINUITY FOR PARAMETRIC CURVES AND SURFACES
Tony D. DeRose and Brian A. Barsky *In* Canadian Information Processing Society Graphics Interface 1985 1985 p 343-351 refs Previously announced as N85-28579 (For primary document see N85-34523 23-31)
Avail: NTIS HC A19/MF A01

N85-34671# Nihon Univ., Shinei (Japan). Atomic Energy Research Inst.

FEMALE: FINITE ELEMENT METHOD FOR ARBITRARY LAGRANGIAN AND EULERIAN ELEMENTS
M. Aizawa and I. Kawakami *In* Nagoya Univ. Workshop Rept. on Simulation Tech. for Shock Wave Phenomena and Characteristics of Plasma in Inertial Confinement Fusion Mar. 1985 p 2-10 (For primary document see N85-34670 23-75)
Avail: NTIS HC A11/MF A01

N85-34672# Kyoto Inst. of Tech. (Japan). Dept. of Mechanical Engineering.
NUMERICAL SOLUTIONS OF THE VLASOV EQUATION
Nobuyuki Satofuka, Koji Morinishi, and Hidetoshi Nishida *In* Nagoya Univ. Workshop Rept. on Simulation Tech. for Shock Wave Phenomena and Characteristics of Plasma in inertial Confinement Fusion Mar. 1985 p 11-24 refs (For primary document see N85-34670 23-75)
Avail: NTIS HC A11/MF A01

N85-34673# Osaka Univ., Suita (Japan). Inst. of Laser Engineering.
CUBIC INTERPOLATED PSEUDO-PARTICLE METHOD (CIP) FOR SOLVING HYPERBOLIC-TYPE EQUATION
H. Takewaki, A. Nishiguchi, and T. Yabe *In* Nagoya Univ. Workshop Rept. on Simulation Tech. for Shock Wave Phenomena and Characteristics of Plasma in Inertial Confinement Fusion Mar. 1985 p 25-48 refs (For primary document see N85-34670 23-75)
Avail: NTIS HC A11/MF A01

N85-34676# National Chemical Lab. for Industry, Tsukuba (Japan).
NUMERICAL CALCULATIONS ON SHOCK LOADED MATERIALS
Katsumi Tanaka *In* Nagoya Univ. Workshop Rept. on Simulation Tech. for Shock Wave Phenomena and Characteristics of Plasma in Inertial Confinement Fusion Mar. 1985 p 74-85 refs (For primary document see N85-34670 23-75)
Avail: NTIS HC A11/MF A01

65 STATISTICS AND PROBABILITY

Includes data sampling and smoothing; Monte Carlo method; and stochastic processes.

N85-34598# Oak Ridge National Lab., Tenn.
MONTE CARLO TECHNIQUES FOR ANALYZING DEEP PENETRATION PROBLEMS
S. N. Cramer, J. Gonnord (Commissariat a l'Energie Atomique, Gif-sur-Yvette, France), and J. S. Hendricks (LASL) 1985 16 p refs Presented at the Intern. Meeting on Advan. in Nucl. Eng. Computational Methods, Knoxville, Tenn., 9 Apr. 1985
(Contract DE-AC05-84OR-21400)
(DE85-011426; CONF-850411-12) Avail: NTIS HC A02/MF A01

A review of current methods and difficulties in Monte Carlo deep-penetration calculations is presented. Statistical uncertainty is discussed, and recent adjoint optimization of splitting, Russian roulette, and exponential transformation biasing is reviewed. Other aspects of the random walk and estimation processes are covered, including the relatively new DXANG angular biasing technique. Specific items summarized are albedo scattering, Monte Carlo coupling techniques with discrete ordinates and other methods, adjoint solutions, and multi-group Monte Carlo. The topic of code-generated biasing parameters is presented, including the creation of adjoint importance functions from forward calculations. Finally, current and future work in the area of computer learning and artificial intelligence is discussed in connection with Monte Carlo applications. DOE

66 SYSTEMS ANALYSIS

Includes mathematical modeling; network analysis; and operations research.

No abstracts in this category.

67 THEORETICAL MATHEMATICS

Includes topology and number theory.

No abstracts in this category.

70 PHYSICS (GENERAL)

For geophysics see *46 Geophysics.* For astrophysics see *90 Astrophysics.* For solar physics see *92 Solar physics.*

No abstracts in this category.

71 ACOUSTICS

Includes sound generation, transmission and attenuation. For noise pollution see *45 Environment Pollution.*

N85-34599# National Research Council of Canada, Ottawa (Ontario). Div. of Building Research.
ACOUSTICAL ABSORPTION COEFFICIENT IN A DIFFUSE FIELD OF A PLANE, RECTANGULAR MATERIAL OF FINITE DIMENSIONS PLACED ON AN INFINITE PERFECTLY REFLECTING SURFACE
J. F. Hamet 1985 29 p refs Transl. into ENGLISH from Rev. D'Acoustique (France), v. 17, no. 71, 1984 p 204-210
(NRC/CNR-TT-2113; ISSN-0077-5606; Rept-257) Avail: NTIS HC A03/MF A01

This study deals with the evaluation of the acoustic absorption coefficient of a rectangular surface of known impedance, placed on an otherwise perfectly reflecting area. The incident acoustic field is supposed diffuse. This problem corresponds to the measurement of the absorption coefficient in a reverberation room. An analytic expression (approximation) is given for the evaluation of the absorption coefficient. From this expression, valid for the case of a rectangular surface of finite dimensions, results are derived and given in the literature for the case of an absorbing strip (surface of finite width and infinite length). The numerical values obtained in the case of a rectangular surface of finite dimensions are greater than those obtained in the case of a surface of infinite dimensions. Values superior to unity can be observed. This corresponds to what is sometimes measured in a reverberant room. Author

N85-34600# Argonne National Lab., Ill. Materials Science and Technology Div.
ANALYTICAL ULTRASONICS FOR STRUCTURAL MATERIALS
David S. Kupperman Nov. 1985 14 p refs Presented at the Anal. Ultrasonics Conf., Cleveland, 13-14 Nov. 1984 Sponsored in part by Nuclear Regulatory Commission and DOE
(TI85-006132; CONF-8411148-1) Avail: NTIS HC A02/MF A01

The application of ultrasonic velocity and attenuation measurements to characterize the microstructure of structural materials is discussed. Velocity measurements in cast stainless steel are correlated with microstructural variations ranging from equiaxed (elastically isotropic) to columnar (elastically anisotropic) grain

structure. The effect of the anisotropic grain structure on the deviation of ultrasonic waves in cast stainless steel is also reported. Field implementable techniques for distinguishing equiaxed from columnar grain structures in cast stainless steel structural members are presented. The application of ultrasonic velocity measurements to characterize structural ceramics in the green state is also discussed. DOE

72 ATOMIC AND MOLECULAR PHYSICS

Includes atomic structure and molecular spectra.

N85-34601# Los Alamos National Lab., N. Mex. ESS Div.
CYLTRAN CALCULATIONS OF ELECTRON EFFECTS ON XD DETECTORS
Stuart Mayer (State Univ. of New York, Stony Brook), George J. Berzins, and Marge Wilson, ed. Oct. 1984 14 p refs
(Contract W-7405-eng-36)
(LA-10264-MS) Avail: NTIS HC A02/MF A01

Coupled electron-photon Monte Carlo calculations were performed with the CYLTRAN code on a typical channel in a detector that was flown aboard several spacecraft. The response of this channel was examined as a function of incident electron energy over a range representative of background electrons in orbit. It is shown that the signal arises from three separate regions whose relative importance change with electron energy. Approximations used to cast the real problem into a format compatible with CYLTRAN are described. E.A.K.

N85-34602# Argonne National Lab., Ill.
PHYSICS DIVISION ANNUAL REVIEW, 1 APRIL 1983 - 31 MARCH 1984 Annual Report
Aug. 1984 289 p refs
(Contract W-31-108-eng-38)
(ANL-84-24) Avail: NTIS HC A13/MF A01

The superconducting linear accelerator for heavy ions is discussed. The superconducting linac is expanded into a larger facility, the ATLAS. The research program, uses the unique properties of the present linac. Experiments are carried out on the importance of quasielastic and particularly neutron-transfer reactions as a dominant feature of near-Coulomb-barrier heavy-ion reactions. Nuclear properties at high angular momentum, heavy-ion fusion reactions, systematics of fission are studied by using the unique properties of the accelerator. The technology of radiofrequency superconductivity as applied to particle acceleration is developed. A new type of quarter-wave structure is constructed out of niobium and the feasibility of accelerating structures for very low-velocity particles is investigated. E.A.K.

N85-34603# Los Alamos Scientific Lab., N. Mex.
ELECTRON DENSITY DISTRIBUTION ANALYSIS FOR NITROGUANIDINE
J. P. Ritchie, D. T. Cromer, R. F. Stewart (Carnegie-Mellon Univ.), H. J. Wasserman, and R. R. Ryan 1985 10 p refs Presented at the 8th Intern. Symp. on Detonation, Albuquerque, N. Mex., 15 Jul. 1985
(Contract W-7405-eng-36)
(DE85-009598; LA-UR-85-1088; CONF-850706-4) Avail: NTIS HC A02/MF A01

The electron density distribution of nitroguanidine was analyzed with both experimental and theoretical techniques to determine how well these methods would work for an explosive molecule. Explosives present special problems with these methods because many atoms are usually involved, which can cause the calculations to become intractable, and because the molecules have many polar bonds. It was found that, although the polar character of the space group made the experimental analysis difficult, the two techniques yielded results very much in harmony. Specifically, electrostatic potentials, which play a large role in determining crystal geometry, were in very good agreement. A discrepancy, however, was observed between the theoretically optimized geometry and the observed geometry. This discrepancy appears to be the result of crystal packing forces which are not present in the theoretical calculations. Some similarities between the hydrogen bond network in NQ and that in TATB were also observed. DOE

N85-34604# Department of Energy, Washington, D. C.
NEUTRAL PARTICLE BEAM INTENSITY CONTROLLER Patent Application
W. K. Dagenhart, inventor (to DOE) Filed 29 May 1984 12 p
(Contract DE-AC05-84OR-21400)
(DE85-006411; US-Patent-Appl-SN-617197) Avail: NTIS HC A02/MF A01

The neutral beam intensity controller is based on selected magnetic defocusing of the ion beam prior to neutralization. The defocused portion of the beam is dumped onto a beam dump disposed perpendicular to the beam axis. Selective defocusing is occomplished by means of a magnetic field generator disposed about the neutralizer so that the field is transverse to the beam axis. The magnetic field intensity is varied to provide the selected partial beam defocusing of the ions prior to neutralization. The desired focused neutral beam portion passes along the beam path through a defining aperture in the beam dump, thereby controlling the desired fraction of neutral particles transmitted to a utilization device without altering the kinetic energy level of the desired neutral particle fraction. By proper selection of the magnetic field intensity, virtually zero through 100 intensity control of the neutral beam is achieved. DOE

73 NUCLEAR AND HIGH-ENERGY PHYSICS

Includes elementary and nuclear particles; and reactor theory.

For space radiation see *93 Space Radiation.*

N85-34605# California Univ., Berkeley. Lawrence Berkeley Lab. Accelerator and Fusion Research Div.
SUMMARY OF ACTIVITIES, 1983
1983 76 p refs
(Contract DE-AC03-76SF-00098)
(LBL-18500) Avail: NTIS HC A05/MF A01

The activities of the Accelerator and Fusion Research Division are described. Technologically advanced techniques for the production, acceleration, or transport of high-energy beams are explored. The beams may be the heavy ions of interest in nuclear science, medical research, and heavy-ion inertial-confinement fusion; they may be beams of deuterium and hydrogen atoms, used to heat and confine plasma in magnetic fusion experiments they may be ultrahigh energy protons for the next high energy hadron collider; or they may be high-brillance, highly coherent picosecond pulses of synchrotron radiation. Topics discussed include: accelerator or operations, high energy physics, magnetic fusion energy, heavy-ion fusion, X-ray optics, and sources of XUV radiation. E.A.K.

N85-34606# Los Alamos National Lab., N. Mex.
GENERAL-PURPOSE HEAT SOURCE DEVELOPMENT: SAFETY TEST PROGRAM. POSTIMPACT EVALUATION, DESIGN ITERATION TEST Status Report
F. W. Schonfeld and T. G. George Jul. 1984 45 p refs
(Contract W-7405-eng-36)
(LA-10034-SR; DIT-3) Avail: NTIS HC A03/MF A01

The general-purpose heat source (GPHS) provides power for space missions by transmitting the heat of 238PuO2 decay to thermoelectric elements. The Design Iteration Test (DIT) is an ongoing test program. The 30 deg impact orientation used in DIT-3 was considerably less severe than the flat on impact utilized in DIT-2. The four capsules used in DIT-1 survived, while two of the capsules used in DIT-2 breached; a small quantity of 238-PuO2 was released from the capsules breached in the DIT-2 impact. All of the capsules used in DIT-1 and DIT-2 were severely

deformed and contained large internal cracks. Postimpact analysis of the DIT-3 test components are described with emphasis on weld structure and the behavior of defects identified by SRP nondestructive testing. E.A.K.

N85-34607# Department of Energy, Washington, D. C.
LIQUID URANIUM ALLOY-HELIUM FISSION REACTOR Patent Application
V. Minkov, inventor (to NASA) Filed 13 Jun. 1984 16 p
(Contract W-31-109-eng-38)
(DE85-006511; US-Patent-Appl-SN-620308) Avail: NTIS HC A02/MF A01

This invention describes a nuclear fission reactor which has a core vessel and at least one tandem heat exchanger vessel coupled therewith across upper and lower passages to define a closed flow loop. Nuclear fuel such as a uranium alloy in its liquid phase fills these vessels and flow passages. Solid control elements in the reactor core vessle are adapted to be adjusted relative to one another to control fission reaction of the liquid fuel therein. Moderator elements in the other vessel and flow passages preclude fission reaction therein. An inert gas such as helium is bubbled upwardly through the heat exchanger vessel operable to move the liquid fuel upwardly therein and unidirectionally round the closed loop and downwardly through the core vessel. This helium gas is further directed to heat conversion means outside of the reactor vessels to utilize the heat from the fission reaction to generate useful output. The nuclear fuel operates in the 1200 to 1800 C range, and even higher to 2500 C. DOE

N85-34608# Los Alamos Scientific Lab., N. Mex.
OBSERVATIONS ON (3)He NEUTRON SPECTROMETRY
A. E. Evans 1985 5 p refs Presented at the Intern. Conf. on Nucl. Data for Basic and Appl. Sci., Santa Fe, N. Mex., 13 May 1985
(Contract W-7405-eng-36)
(DE85-010731; LA-UR-85-1476; CONF-850507-3) Avail: NTIS HC A02/MF A01

The energy resolution of a (3)He ionization chamber, which varies from 13 keV FWHM at 0 keV to approximately 30 keV at 1 MeV, allows observation of false peaks due to the presence of scattering or absorbing materials and due to accidental near coincidences of the rather long risetime detector pulses. Pulse risetime distributions depend on the neutron beam's angle of incidence to the detector axis; ability to separate (3)He recoil pulses from full energy (3)He(n,p) pulses diminishes for neutrons of energy greater than 1.5 MeV and incident normal to the detector axis. When high energy neutrons are present, measurement at a grazing angle is recommended. DOE

N85-34609# Sandia Labs., Albuquerque, N. Mex.
RAPID ANNEALING OF TEMPERATURE-COMPENSATED, PRECISION VOLTAGE REFERENCES FOLLOWING FAST-NEUTRON IRRADIATION
T. A. Fischer and R. A. Williams 1985 8 p Presented at the 22nd Ann. Conf. on Nucl. and Space Radiation Effects, Monterey, Calif., 22 Jul. 1985
(Contract DE-AC04-76DP-00789)
(DE85-009821; SAND-85-0821C; CONF-850711-8) Avail: NTIS HC A02/MF A01

Substantial, short-term voltage variations have been observed during the rapid annealing of twin-junction, temperature-compensated, precision voltage references (TC PVRs) immediately following exposure to fast-neutron bursts of up to 4 x 10 to the 14th n/sq cm. The short term recovery has been found to be dominated by minority carrier lifetime reduction in the forward biased junction of this composite junction device. The shape of the annealing curve has been obtained and found to be roughly independent of neutron fluence in the range from (1 to 4) x 10 to the 14th n/sq cm. DOE

N85-34610# Department of Energy, New York. Environmental Measurements Lab.
EML PULSE IONIZATION CHAMBER SYSTEMS FOR (222)Rn MEASUREMENTS
I. M. Fisenne and H. W. Keller Mar. 1985 28 p refs
(DE85-012320; EML-437) Avail: NTIS HC A03/MF A01

Radon measurements have been performed with pulse ionization chambers at the Environmental Measurements Laboratory (EML) for over 35 years. The evolution of radon measurement systems, with emphasis on the continuous quality control efforts at EML are discussed. DOE

N85-34611# Childrens Hospital Medical Center, Boston, Mass. Dept. of Radiology.
DEVELOPMENT OF THE OSMIUM-191 YIELDS IRIDIUM-191m RADIONUCLIDE GENERATOR Annual Report
S. Treves and A. B. Packard 30 Apr. 1985 44 p refs
(Contract DE-AC02-82ER-60084)
(DE85-011185; DOE/ER-60084/4) Avail: NTIS HC A03/MF A01

The use of Ir-191m in radionuclide angiography has been the subject of increasing interest in recent years. The Os-191-Ir-191m generator that has been used for these studies suffers, however, from Ir-191m yield (10%/ml) and higher than desirable Os-191 breakthrough (5 x 10 to the -3%). Ir generator has been developed that has higher yield (25 to 30%/ml) and lower breakthrough (< x 10 to the -4 power %) when eluted with an eluent (0.001 M oxalic acid/0.9% saline that does not require buffering prior to injection. Studies within the last year have shown the eluate of this generator to be nontoxic at up to 100 times the expected human dose and work is in progress to obtain approval for human use of this system. While a significant improvement over past generator designs, the yield of this generator is still modest and the evaluation of new osmium complexes for use on the generator has continued. Clinical studies involving the use of Ir-191m for first pass angiography in adults and children have continued. DOE

N85-34612# Oak Ridge National Lab., Tenn.
CAPTURE IN THE 1.15-keV IRON RESONANCE
L. W. Weston and J. H. Todd 1985 3 p refs Presented at the Intern. Conf. on Nucl. Data for Basic and Appl. Sci., Santa Fe, N. Mex., 13 May 1985
(Contract DE-AC05-84OR-21400)
(DE85-011913; CONF-850507-10) Avail: NTIS HC A02/MF A01

The 1.15 keV resonance in iron is important to reactors in that a major part of the iron capture integral is due to this one resonance. This resonance is also good test case for capture gamma-ray detectors, which are meant to have an efficiency independent of gamma-ray energy spectra, because this resonance has an unusually hard spectrum and other iron resonances do not. There have been severe discrepancies among different groups who have measured the capture area and transmission of this resonance. A new measurement, employing C6F6 liquid scintillators and pulse-height weighting to effect total energy detection, has been made of the ratio of the capture area of the 22.8 keV resonance relative to that of the 1.15 keV resonance. The 22.8 keV resonance has a relatively soft gamma-ray spectrum and there is agreement on the capture area. The results (2.91 + or - 0.17) agree well with transmission measurements and confirm the applicability of total energy detectors for use on capture resonances with very hard capture gamma-ray spectra. DOE

N85-34613# Brookhaven National Lab., Upton, N. Y.
IMPROVED METHOD FOR THE STABILIZATION OF NaI-PHOTOMULTIPLIER GAMMA DETECTORS AGAINST THERMAL AND OTHER DRIFT
M. S. Zucker 1985 19 p refs Presented at the 6th Symp. on X- and Gamma-Ray Sources and Appl., Ann Arbor, Mich., 21 May 1985
(Contract DE-AC02-76CH-00016)
(DE85-011830; BNL-36395; CONF-850533-7) Avail: NTIS HC A02/MF A01

Alpha peaks are used as part of servo systems to stabilize NaI-photomultiplier gamma detectors against drift. However alpha peaks shift with temperature change differently than do gamma peaks, thus spoiling what would otherwise be a workable scheme

for stabilizing against probably the most serious source of NaI-p.m. detector drift, namely thermal effects. It was found possible to accurately compensate for the difference in the shift with temperature versus gamma peaks using the signal derived from a thermistor in thermal contact with the NaI crystal to control the bias of a discriminator in the servo circuit. The servo circuit utilizing this principle are used in commercial multichannel analyzers of the type intended for field use under adverse ambient conditions. DOE

N85-34614# Childrens Hospital Medical Center, Boston, Mass.
CURRENT STATUS OF THE Os-191 YIELDS Ir-191m GENERATOR
A. B. Packard, G. M. OBrien, and S. Treves 1985 20 p refs
(Contract DE-AC02-82ER-60084)
(DE85-008306; DOE/ER-60084/T2) Avail: NTIS HC A02/MF A01

The advantages of ultrashort lived radionuclides for angiography have been well documented in recent years. Although several isotopes are potentially useful in this application (e.g., Au-195m, Ag-109m, Ir-191m), Ir-191m offers several advantages. Among these advantages are a parent isotope (Os-191) with a sufficiently long half life (15.4 d) to allow production of a generator with a reasonable shelf life, high photon yield (129 keV, 26%; 66 keV, 55%), and ease of production of the parent isotope (i.e., neutron irradiation of Os-190). Ir-191m has not, however, been widely used for radionuclide angiocardiography because of a less than optimal generator design and the assumption that the half life of Ir-191m (4.96 s) was too short to permit visualization of the left ventricle in adult patients. A generator has been developed with higher Ir-191m yield (25 to 30%/ml), lower Os-191 breakthrough (< 5 x 10 to the minus 4 power %) that is easier to assemble. In addition, the eluate of this new generator (0.001M oxalic acid/0.9% saline) does not require buffering prior to injection. It is also demonstrated that adequate studies of the left ventricle can be obtained in adults when sufficient quantities of isotope are injected. DOE

N85-34615# Department of Energy, Washington, D. C.
SPECIFICITY OF (71)Ga(p,N) (71)Ge AT 35 MeV FOR GAMOW-TELLER STRENGTH
A. J. Baltz, J. Weneser (Brookhaven National Lab.), B. A. Brown (Michigan State Univ., East Lansing), and J. Rapaport (Ohio Univ., Athens) 1985 7 p Presented at the Conf. on Antinucleon and Nucleon-Nucleus Interactions, Telluride, Colo., 18 Mar. 1985
(Contract DE-AC02-76CH-00016)
(DE85-011837; BNL-36439; CONF-850315-3) Avail: NTIS HC A02/MF A01

The motivation for considering the 71Ga(p,n)71Ge reaction is to help determine the properties of 71Ga as a detector of solar neutrinos. The proposed solar neutrino experiment, 71Ga(nu,e(-)) 71Ge, has a threshold of only .236 MeV, and is thus sensitive to neutrinos produced in the basic burning process in the Sun p + p (YIELDS) 2H + e(+) nu, which has a .420 MeV endpoint. The excitation of the 5/2(-) state at .175 MeV in 71Ge could be important, however. Were the Gamow-Teller (G-T) transition to the 175 keV state equal in strength to the ground state transition there would be approx. 25% added to the detector signal, the greater part of this coming from the (7)Be neutrinos; the desired sensitivity to the p-p neutrinos would then be less. DOE

N85-34616# Oak Ridge National Lab., Tenn.
CALCULATION OF MIXED DEPTH FOR SOME METAL-Si SYSTEMS
D. B. Poker 1985 11 p Presented at the Workshop on Ion Mixing and Surface Alloying 2, Pasadena, Calif., 19 Apr. 1985
(Contract DE-AC05-84OR-21400)
(DE85-011907; CONF-8504116-2) Avail: NTIS HC A02/MF A01

Results for several metals in Si indicate that the moment method is usually the preferred method for determining mixed depth, due to its insensitivity to detector resolution and lack of an initial offset. DOE

N85-34617# Argonne National Lab., Ill.
DOWNSTREAM BEHAVIOR OF VOLATILE FISSION PRODUCT SPECIES
M. Farahat, J. Settle, I. Johnson, and C. E. Johnson 1985 11 p Presented at the Intern. Symp. and Workshop on Particulate and Multi-Phase Processes and the 16th Ann. Meeting of the Fine Particle Soc., Miami Beach, Fla., 22 Apr. 1985
(Contract W-31-109-eng-38)
(DE85-012124; CONF-850406-10) Avail: NTIS HC A02/MF A01

An experimental facility was constructed to study the behavior of volatile fission product (VFP) species in a flowing steam environment. Experiments were conducted using CsI as the VFP. An aqueous solution of CsI was injected into 1000 C superheated steam flowing into a horizontal pipe, 3.7 m long, under a controlled temperature gradient. The distribution of CsI deposits along the pipe wall was determined. Scanning electron microscopy was used for inspecting the deposits. Vapor condensation patterns and aerosol particles were identified. Comparison of the experimental results with predictions of the reactor aerosol formation and transport (RAFT) computer code was made. DOE

N85-34618# Virginia Univ., Charlottesville. Dept. of Physics.
DUALITY OF TWO-POINT FUNCTIONS FOR CONFINED NON-RELATIVISTIC QUARK-ANTIQUARK SYSTEMS
P. M. Fishbane, S. G. Gasiorowicz (Minnesota Univ., Minneapolis), and P. Kaus (California Univ., Riverside) [1985] 28 p refs
(Contract DE-AC02-83EB-40105)
(DE85-012334; DOE/ER-40105/462) Avail: NTIS HC A03/MF A01

An analog to the scattering matrix describes the spectrum and high energy behavior of confined systems. For nonrelativistic systems this S-matrix is identical to a two point function which transparently describes the bound states for all angular momenta. Confined systems can thus be described in a dual fashion. This result makes it possible to study the modification of linear trajectories (originating in a long range confining potential) due to short range forces which are unknown except for the way in which they modify the asymptotic behavior of the two point function. A type of effective range expansion is one way to calculate the energy shifts. DOE

N85-34619# Oak Ridge National Lab., Tenn.
NEGATIVE ION SOURCES EQUIPPED WITH CONTINUOUS ANNULAR AND SPHERICAL GEOMETRY SURFACE IONIZERS
G. D. Alton and G. D. Mills 1985 5 p refs Presented at the Particle Accelerator Conf., Vancouver, British Columbia, 13 May 1985
(Contract DE-AC05-84OR-21400)
(DE85-011939; CONF-850504-36) Avail: NTIS HC A02/MF A01

Axial geometry negative ion sources have been designed, developed, and evaluated for use in conjunction with tandem accelerator applications. These sources utilize continuous surface solid tungsten ionizers in either annular or spherical geometries to effect ionization of cesium vapor, which in turn is used to sputter a negatively biased probe containing the material of interest. The annular ionizer geometry source has been incorporated as an on-line source for routine operation of the Holifield Heavy Ion Research Facility (HHIRF) tandem accelerator. Both test stand and tandem accelerator operational experience indicate that such sources are reliable, long lived, stably operating and prolific producers of a wide spectrum of negative ions. To date these sources have been used to produce more than 18 negative ion species. Details of the mechanical design features and computational techniques utilized in arriving at the final electrode configuration are presented. Examples of data pertinent to source operation, the dependence of negative ion yields on certain source operational parameters and of intensities typical of a particular negative ion source are also given. DOE

N85-34620# Oak Ridge National Lab., Tenn.
PAIRING CORRECTION OF PARTICLE-HOLE STATE DENSITIES FOR TWO KINDS OF FERMIONS
C. Y. Fu 1985 5 p refs Presented at the Intern. Conf. on Nucl.

Data for Basic and Appl. Sci., Santa Fe, N. Mex., 13 May 1985
(Contract DE-AC05-84OR-21400)
(DE85-011549; CONF-850507-7) Avail: NTIS HC A02/MF A01

Pairing corrections in particle-hole (exciton) state-density formulas used in precompound nuclear reaction theories are, strictly speaking, dependent on the nuclear excitation energy U and the exciton number n. A general formula for (U,n)-dependent pairing corrections has been derived in an earlier paper for exciton state-density formulas for one kind of fermion. A similar derivation is made for two kinds of fermions. It is shown that the constant-pairing-energy correction used in standard level-density formulas, such as U0 in Gilbert and Cameron, is a limiting case of the present general (U,n)-dependent results. DOE

N85-34621# Naval Research Lab., Washington, D. C.
THEORETICAL AND COMPUTATIONAL RESEARCH ON THE FOCUSED TRANSPORT OF INTENSE CHARGED PARTICLE BEAMS Annual Report, Aug. 1983 - Sep. 1984
I. Haber 1984 16 p refs
(Contract DE-AI05-83ER-40112)
(DE85-012980; DOE/ER-40112/T1) Avail: NTIS HC A02/MF A01

Computer calculations were used to investigate the behavior of a periodic solenoidal thin lens focusing system with 90(0) phase advance. Despite strong similarities in the behavior predicted by the linear theory, a 90(0) solenoidal system does not appear to exhibit the emittance growth characteristic of the similar 90(0) alternate gradient system. In other ways, however, behavior is observed which is similar to the analagous alternate gradient system. DOE

N85-34622# Oak Ridge National Lab., Tenn.
ELECTRON IMPACT IONIZATION OF MULTICHARGED IONS AT ORNL: 1980-1984
D. C. Gregory, D. H. Crandall, R. A. Phaneuf, A. M. Howald, G. H. Dunn, R. A. Falk, D. W. Meuller, and T. J. Morgan May 1985 97 p
(Contract DE-AC05-84OR-21400)
(DE85-013104; ORNL/TM-9501) Avail: NTIS HC A05/MF A01

Experimental electron-impact ionization cross sections for thirty-seven target ions are presented, summarizing measurements made at Oak Ridge National Lab., during the period from 1980 through early 1984. Target ions range in atomic number from Z = 5 (boron) to Z = 73 (tantalum), with charge states ranging from +2 through +6 and energies ranging from below the ionization threshold to 1500 eV in most cases. All data are presented in both tables and graphs. Maxwellian ionization rate coefficients are tabulated over the equivalent temperature range 10 to 3000 eV, and fitting parameters are given to allow the calculation of rates at intermediate electron temperatures or for inclusion in computer programs for plasma modeling. DOE

N85-34623# California Univ., Berkeley. Lawrence Berkeley Lab.
FORMATION OF AMORPHOUS SILICON BY LIGHT ION DAMAGE
Y. Shih, J. Washburn, E. R. Weber, and R. Gronsky Apr. 1985 10 p refs Presented at the 2nd Spring Meeting of the Mater. Res. Soc., San Francisco, 15 Apr. 1985
(Contract DE-AC03-76SF-00098)
(DE85-012605; LBL-19466; CONF-850421-8) Avail: NTIS HC A02/MF A01

A model for formation of amorphous silicon by light ion implantation is proposed. It is suggested that accumulation of point defects and/or complexes is required at the initial stage of the amorphization process. Amorphous zone can only form at the end of incoming light ion tracks when the pre-accumulated concentration of point defects reaches a critical value. Depending on the uniformity of point defect distribution, two possibilities for the second stage of amorphization are suggested for the ion implantation at different temperature. Silicon wafers implanted with Boron ions at various temperatures with below and above the critical amorphization dose have been investigated using cross section specimens in high resolution TEM. The amorphization process has as well been studied by Electron Paramagnetic Resonance of the same samples investigated by transmission electron microscopy (TEM), allowing the identification of dangling bonds in amorphous zones and point defect clusters. (113), 1/3(111) extrinsic and other smaller distortion 1/x(111) stacking faults were also found during the amorphization process. Liquid nitrogen temperature and/or high beam current were found to be necessary to amorphizate Silicon by Boron ion implantation. DOE

N85-34624# Texas A&M Univ., College Station.
APPLICATION OF EVALUATED FISSION-PRODUCT DELAYED-NEUTRON PRECURSOR DATA IN REACTOR KINETICS CALCULATIONS
R. T. Perry, W. B. Wilson (LASL), T. R. England (LASL), and M. C. Brady 1985 5 p refs Presented at the Intern. Conf. on Nucl. Data for Basic and Appl. Sci., Santa Fe, N. Mex., 13 May 1985
(Contract W-7405-eng-36)
(DE85-012728; LA-UR-85-1730; CONF-850507-17) Avail: NTIS HC A02/MF A01

Evaluated fission-product yield and decay data have been used to describe 105 delayed neutron precursors explicitly in point reactor kinetics calculations. Results calculated for (235)U thermal fission show that rod-drop reactivity values obtained from kinetics calculations with 6-group precursor data are considerably higher than those calculated with explicit delayed-neutron precursor data. The calculated kinetics associated with positive reactivity steps are significantly different. DOE

N85-34625# GA Technologies, Inc., San Diego, Calif.
SP-100 THERMIONIC TECHNOLOGY PROGRAM Annual Integrated Technical Progress Report, period ending 30 Sep. 1984
J. W. Holland, ed. Nov. 1984 228 p
(Contracts DE-AC03-84SF-11906; DE-AC03-84SF-12192; DE-AC03-84SF-12193)
(DE85-012311; GA-A-17773) Avail: NTIS HC A11/MF A01

The thermionic technology program addresses the feasibility issues of a seven-year-life thermionic fuel element (TFE) for the SP-100 Thermionic Reactor Space Power System. These issues relate to the extension of TFE lifetime from three to seven years, one of the SP-100 requirements. The technology to support three-year lifetimes was demonstrated in the earlier TFE development program conducted in the late-1960s and 1970s. Primary life-limiting factors were recognized to be thermionic emitter dimensional increases due to swelling of the nuclear fuel and electrical structural damage from fast neutrons. The 1984 to 1985 technology program is investigating the fueled emitter and insulator lifetime issues, both experimentally and analytically. The goal is to analytically project the lifetime of the fueled emitter and insulator and to experimentally verify these projection methods. In 1984, the efforts were largely devoted to the design and building of fueled emitters for irradiation in 1985, validation of fuel-emitter models, development of irradiation-resistant metal-ceramic seal and sheath insulator, modeling of insulator lifetime, and development of wide-spread, high-performance thermionic converters. DOE

N85-34626# Department of Energy, Washington, D. C.
CONTAINER FOR RADIOACTIVE MATERIALS Patent Application
S. R. Fields, inventor (to DOE) Filed 30 May 1984 21 p
(Contract DE-AC06-76FF-02170)
(DE85-005757; US-Patent-Appl-SN-615210) Avail: NTIS HC A02/MF A01

A container is claimed for housing a plurality of canister assemblies are stacked in a longitudinally spaced relation within a carrier to form a payload concentrically mounted within the container. The payload package includes a spacer for each canister assembly, said spacer comprising a base member longitudinally spacing adjacent canister assemblies from each other and sleeve surrounding the associated canister assembly for centering the same and conducting heat from the radioactive material in a desired flow path. DOE

N85-34627# Department of Energy, Washington, D. C.
SEPARATION OF URANIUM FROM TECHNETIUM IN RECOVERY OF SPENT NUCLEAR FUEL Patent Application
H. A. Friedman, inventor (to DOE) Filed 13 Jun. 1984 8 p
(Contract DE-AC05-84OR-21400)
(DE85-006499; US-Patent-Appl-SN-559501) Avail: NTIS HC A02/MF A01

A method for decontaminating uranium product from the Purex 5 process is described. Hydrazine is added to the product uranyl nitrate stream from the Purex process, which contains hexavalent (UO2(2+)) uranium and heptavalent technetius (TcO4-). Technetium in the product stream is reduced and then complexed by the addition of oxalic acid (H2O2O4), and the Tc-oxalate complex is readily separated from the 10 uranium by solvent extraction with 30 vol % tributyl phosphate in n-dodecane. DOE

N85-34628# Institute of Oceanographic Sciences, Wormley (England).
RESEARCH AT THE INSTITUTE OF OCEANOGRAPHIC SCIENCES RELATED TO THE POSSIBLE DISPOSAL OF RADIOACTIVE WASTE ON OR BENEATH THE SEAFLOOR Status Report, Apr. 1979 - Mar.1984
B. Booty, ed. 1985 330 p refs Sponsored by UK Department of Environment
(IOS-204; DoE/RW/85/003; DGR-481/176; DGR-481/177; DGR-481/178; DGR-481/179; PECD7/9/023) Avail: NTIS HC A15/MF A01

The suitability for radioactive waste disposal of the Great Meteor East, Kings Trough Flank, Nares Abyssal Plain, and Cape Verde Abyssal Plain regions of the Atlantic Ocean was studied. Benthic boundary layer processes; dispersion in the deep ocean; biological processes; chemical processes; temperature, conductivity, and heat flow; and particulates were investigated.
Author (ESA)

74 OPTICS

Includes light phenomena.

N85-34629* National Aeronautics and Space Administration. Pasadena Office, Calif.
RANGING SYSTEM WHICH COMPARES AN OBJECT REFLECTED COMPONENT OF A LIGHT BEAM TO A REFERENCE COMPONENT OF THE LIGHT BEAM Patent
John M. McLauchlan (JPL, Pasadena, Calif.), John AuYeung (JPL, Pasadena, Calif.), Eldred F. Tubbs (JPL, Pasadena, Calif.), Willis C. Goss (JPL, Pasadena, Calif.), and Demetri Psaltis, inventors (to NASA) (JPL, Pasadena, Calif.) Issued 6 Aug. 1985 8 p Filed 28 Sep. 1982 Supersedes N83-12991 (21 - 03, p 0455)
(NASA-Case-NPO-15865-1; US-Patent-4,533,242; US-Patent-Appl-SN-425202; US-Patent-Class-356-5; US-Patent-Class-343-13-R) Avail: US Patent and Trademark Office CSCL 20F

A system is described for measuring the distance to an object by comparing a first component of a light pulse that is reflected off the object with a second component of the light pulse that passes along a reference path of known length, which provides great accuracy with a relatively simple and rugged design. The reference path can be changed in precise steps so that it has an equivalent length approximately equal to the path length of the light pulse component that is reflected from the object. The resulting small difference in path lengths can be precisely determined by directing the light pulse components into opposite ends of a detector formed of a material that emits a second harmonic light output at the locations where the opposite going pulses past simultaneously across one another.
Official Gazette of the U.S. Patent and Trademark Office

N85-34630 National Physical Lab., Teddington (England). Div. of Mechanical and Optical Metrology.
POLARISATION INSENSITIVE ACHROMATIC CUBE BEAM-SPLITTER
K. W. Raine and W. H. McGivern Jan. 1985 16 p refs
(NPL-MOM-72; ISSN-0309-3069) Copyright. Avail: Issuing Activity

A cemented cube thin film beam splitter design which is achromatic over the wavelength range 450 nm to 650 nm and insensitive to the polarization of the incident light is described. This performance is obtained from a 3 layer metal/dielectric thin film assembly in which the absorptances are $< 15\%$. The most critical feature is the silver film, which is sensitive to the deposition rate and substrate temperature. Deposition conditions for reproducible and acceptable results are described. Author (ESA)

N85-34631*# National Aeronautics and Space Administration. Lewis Research Center, Cleveland, Ohio.
DIAMONDLIKE CARBON PROTECTIVE COATINGS FOR IR MATERIALS
Michael J. Mirtich, Dan Nir, Diane M. Swec, and Bruce A. Banks 1985 18 p refs Presented at the 12th Intern. Conf. on Met. Coatings, Los Angeles, 15-19 Apr. 1985; sponsored by the American Vacuum Society
(NASA-TM-87083; E-2506; NAS 1.15:87083) Avail: NTIS HC A02/MF A01 CSCL 20F

Diamondlike carbon (DLC) films have the potential to protect optical windows in applications where it is important to maintain the integrity of the specular transmittance of these films on ZnS and ZnSe infrared transmitting windows. The films must be adherent and durable such that they protect the windows from rain and particle erosion as well as chemical attack. In order to optimize the performance of these films, 0.1 micro m thick diamondlike carbon films were deposited on fused silica and silicon wafers, using three different methods of ion beam deposition. One method was sputter deposition from a carbon target using an 8 cm ion source. The merits of hydrogen addition were experimentally evaluated in conjunction with this method. The second method used a 30 cm hollow cathode ion source with hydrocarbon/Argon gases to deposit diamondlike carbon films from the primary beam at 90 to 250 eV. The third method used a dual beam system employing a hydrocarbon/Argon 30 cm ion source and an 8 cm ion source. Films were evaluated for adherence, intrinsic stress, infrared transmittance between 2.5 and 50 micro m, and protection from particle erosion. An erosion test using a sandblaster was used to give quantitative values of the protection afforded to the fused silica by the diamondlike carbon films. The fused silica surfaces protected by diamondlike carbon films were exposed to 100 micro m diameter SiO particles at 60 mi/hr (26.8/sec) in the sandblaster. B.W.

N85-34632# Department of the Air Force, Washington, D.C.
DIFFERENTIATING SPATIAL LIGHT MODULATOR Patent Application
Armitage, inventor (to Air Force) Filed 11 Apr. 1985 16 p
(AD-D011727; US-Patent-Appl-SN-721977) Avail: NTIS HC A02/MF A01 CSCL 20/6

A differentiating spatial light modulator device in which a photoreceptor and an electro-optic crystal are isolated by a dielectric mirror is discussed. The electro-optic crystal is configured to have low or zero longitudinal response, yet is sensitive to transverse electric fields. The fringe field generated by the photoreceptor (photodiode) modulates the crystal birefringence. Readout via a polarizing beamsplitter gives an output light related to the spatial gradient of the input light. In a liquid crystal embodiment of the invention, reversal of the applied voltage gives a driven off state which speeds the erasure. Storage is possible in the smectic liquid crystal phase. Author (GRA)

N85-34633# Department of Energy, Washington, D. C.
FIBER OPTICS INTERFACE FOR A DYE LASER OSCILLATOR AND METHOD Patent Application
S. A. Johnson and L. G. Seppala, inventors (to DOE) Filed 13 Jun. 1984 20 p
(Contract W-7405-eng-48)
(DE85-005765; US-Patent-Appl-SN-620305) Avail: NTIS

HC A02/MF A01

A dye laser oscillator in which one light beam is used to pump a continuous stream of dye within a cooperating dye chamber for producing a second, different beam is generally disclosed along with a specific arrnagement including an optical fiber and a fibre optics interface for directing the pumping beam into the dye chamber. The specific fiber optics interface illustrated includes three cooperating lenses which together image one particular dimension of the pumping beam into the dye chamber from the output end of the optical fiber in order to insure that the dye chamber is properly illuminated by the pumping beam. DOE

N85-34634# Institut Franco-Allemand de Recherches, St. Louis (France). Arbeitsgruppe Endballistik.
OMEGA: OPTOELECTRONIC MEASUREMENT OF THE INCIDENCE ANGLE OF A PROJECTILE [OMEGA: OPTOELEKTRONISCHE MESSUNG DES GESCHOSSANSTELLWINKELS]
K. Sterzelmeier 31 Aug. 1985 10 p In GERMAN Presented at 16th Intern. Kongr. Ueber Geschwindigkeitsphotograph. und Photonik, Strasbourg, 27-31 Aug. 1984
(ISL-CO-223/84) Avail: NTIS HC A02

An optoelectronic measuring method for the contactless and interaction-free determination of the spatial position of a free flight body in the form of a rod, e.g., a projectile, is described. A laser beam is expanded to a thin optical pattern that is preferably directed perpendicularly to the flight direction. If the body crosses this plane of present position, a light spot can be observed at its surface traveling more or less strongly depending on the incidence and precession angle. An image of this motion is formed on two uniaxial position sensitive photodiodes. The produced photocurrents are registered via a four channel transient recorder linked to an electronic calculator in which the data are evaluated. Velocity, incidence angle, and precession angle of the flying object are determined from the discrete absolute values of the photocurrents and their time functions. The first measurement results confirm a 0.1 deg arc angular resolution. Author (ESA)

N85-34567# Toronto Univ. (Ontario). Dept. of Computer Science.
COLOUR SPACES AND COLOUR CONTRAST
Avi Naiman *In* Canadian Information Processing Society Graphics Interface 1985 1985 p 313-320 refs (For primary document see N85-34523 23-61)
Avail: NTIS HC A19/MF A01

75 PLASMA PHYSICS

Includes magnetohydrodynamics and plasma fusion.

For ionospheric plasmas see *46 Geophysics*. For space plasmas see *90 Astrophysics*.

N85-34635# Nagoya Univ. (Japan). Inst. of Plasma Physics.
COLLISIONAL RELAXATION OF ELECTRON TAIL DISTRIBUTION
Mitsuru Yamagiwa and Masao Okamoto Apr. 1985 25 p refs
(IPPJ-729) Avail: NTIS HC A02/MF A01

Relaxation due to the Coulomb collisions of the electron velocity distribution function with a high energy tail is investigated in detail. In the course of the relaxation, a saddle point can be created in velocity space owing to Upsilon to the -3 dependence of the deflection rate and a positive slope or a dip appears in the tail direction. The time evolution of the electron tail is studied analytically. A comparison is made with numerical results by using a Fokker-Planck code. Also discussed is the kinetic instability concerned with the positive slope during the relaxation. Author

N85-34636# Nagoya Univ. (Japan). Inst. of Plama Physics.
NONLOCAL AND NONADIABATIC EXPRESSION FOR THE PONDEROMOTIVE FORCE NEAR CYCLOTRON RESONANCE
Heiji Sanuki and Tadatsugu Hatori Jun. 1985 31 p refs
(IPPJ-736) Avail: NTIS HC A03/MF A01

A noniocal and nonadabatic expression for the ponderomotive force near gyroresonance are presented in a case of uniform magnetic field. Due to nonlocality with an arbitrary RHO sub i/delta and nonadiabticity with an intermediate value of X sub i/delta where RHO sub i is the ion Lamor radius, X 1 sub i is the ion excursion length, and delta is the radial scale length of RF electric field, the ponderomotive force is found to be small rather than infinite near gyroresonance. Comparison between the present results and the adiabatic results are made in detail. Author

N85-34637# Nagoya Univ. (Japan). Inst. of Plasma Physics.
SOME PHYSICAL DIFFERENCES BETWEEN SHEET PLASMA AND MULTICUSP PLASMA AS VOLUME PRODUCED H- OR D- ION SOURCES
Joshin Uramoto Apr. 1985 21 p refs
(IPPJ-728) Avail: NTIS HC A02/MF A01

The H- ion volume production by means of a sheet plasma, the extracted H- ion current increases towards the outside across the magnetic field. This fact means that H- ions are produced outside of the sheet plasma, and is in contrast with the act that H- ions in the multicusp plasma are produced almost in the center region without magnetic field. Furthermore, in the optimum condition for extracting H- ions from the sheet plasma, the potential of the first extraction electrode is biased more negatively than that of the discharge anode or the plasma potential, while, in the optimum condition for the multicusp plasma, it is biased more positively. These physical differences between the two plasmas are related with confinement regions of electrons and ambipolar diffusions of plasma without magnetic field or across magnetic field. Author

N85-34638# Nagoya Univ. (Japan). Inst. of Plasma Physics.
MEASURING METHOD AND CONFIRMATION OF H- (D-) ION CURRENT BY SHEET PLASMA 1
Joshin Uramoto May 1985 16 p refs
(IPPJ-730) Avail: NTIS HC A02/MF A01

It is very difficult to separate an electron current from H- and D- ion current under volume production, because both electrons and H- or D- ions are extracted from a discharge plasma in H2 or D2 gas. However, H- or D- ion current by volume production in the sheet plasma can be easily separated from electron current by using the weak magnetic field applied to the sheet plasma itself. Then, if the H- or D- ion current is compared with positive ion (mainly H+3 or D+3) current which is extracted by changing sign of the acceleration voltage from plus (for H- or D- ion) to minus, the H- or D- ion current can be confirmed more exactly. Author

N85-34639# Nagoya Univ. (Japan). Inst. of Plasma Physics.
SIZE EFFECTS OF VACUUM CHAMBER FOR H- (D-) ION VOLUME PRODUCTION BY SHEET PLASMA 1
Joshin Uramoto May 1985 18 p refs
(IPPJ-731) Avail: NTIS HC A02/MF A01

In order to produce H- (D-) ions effectively by volume production in the sheet plasma, effects of vacuum chamber are studied by using two sizes of metal vacuum chamber and by changing their bias voltages for the plasma potential of the sheet plasma. Then, we find the H- (D-) ion current increases abruptly with distance between the sheet plasma surface and the chamber wall perpendicular to the magnetic field, while it takes a maximum near a floating potential of the chamber (negative for the plasma potential outside of the sheet plasma). These effects are related with a size of space where the plasma potential is higher than those of boundaries parallel and perpendicular to the magnetic field. That is, the H- (D-) ion current increases with the spatial size which H- (D-) ions are confined and hydrogen (deuteron) positive ions are lost rapidly along the magnetic field. Author

N85-34640# Tokyo Univ. (Japan). Inst. of Plasma Physics.
MAGNETOHYDRODYNAMIC EQUILIBRIUM AND STABILITY OF SPHEROMAK WITH SPHEROIDAL PLASMA-VACUUM INTERFACE
Shobu Kaneko, Atsushi Kamitani, and Akio Takimoto Nagoya, Japan Nagoya Univ. May 1985 33 p refs
(IPPJ-732) Avail: NTIS HC A03/MF A01

The analytic solutions to the Grad-Shafranov equation are obtained for a prolate and an oblate spheroidal plasma by using Hill's vortex model. Effects of a toroidal magnetic field B sub ph1 on the magnetohydrodynamic (MHD) equilibrium configurations are investigated by using these analytic solutions. When B sub ph1 is larger than that of the force free configuration, the spheroidal plasmas in a vacuum magnetic field are shown to be unable in the MHD equilibrium. The several physical quantities on the equilibrium configuration are evaluated. The spheromak plasma is proved to be unstable if the derivative of p with respect to psi is not = 0 and the second derivative of V w.r.t. psi is = or > 0 on the magnetic axis. Here p is the pressure and V(psi) the volume surrounded by a magnetic surface of psi = const. The equilibrium configurations of the spheroidal plasmas by using Hill's vortex model are shown to satisfy the above conditions, i.e., to be unstable. Author

N85-34641# Kyoto Univ. (Japan). Dept. of Electronics.
COMPUTATIONAL STUDY ON EXCITATION, PROPAGATION AND 3 OMEGA -HEATING DUE TO THE ION BERNSTEIN WAVE
H. Okada (Kyoto Univ., Japan), H. Abe (Kyoto Univ., Japan), R. Itatani (Kyoto Univ., Japan), and M. Ono (Princeton Univ.) Nagoya, Japan Nagoya Univ. May 1985 62 p refs
(IPPJ-733) Avail: NTIS HC A04/MF A01

External excitation, propagation, and ion heating on the ion Bernstein wave (IBW) are studied for the single ion and two ion species plasmas, using the particle simulation. It is found that the value of omega/(cap)omega sub i near the antenna position influences the excitation characteristics of the IBW. The wavelength and the group velocity of the propagating IBW agree well with those calculated from the linear dispersion relation. Corresponding to the experiment done at JIPP T-IIU, 3 (cap) omega sub d heating process in the plasma composed of deuterium like and hydrogen like ions is investigated. The wave energy is deposited into the bulk and tail of the deuterium like ions due to the third harmonic cyclotron resonance and the bulk of the hydrogen like ions is investigated. The wave energy is deposited into the bulk and tail of the deuterium like ions due to the third harmonic cyclotron resonance and the bulk of the hydrogen like ions due to the 3/z (cap) omega sub h cyclotron subharmonic resonance, respectively. It is also discussed on the possibility that the heating efficiency may not depend on the concentration of the deuterium like ion in the 3 (cap) omega sub d heating in the actual tokamak experiment. Author

N85-34642# Nagoya Univ. (Japan). Inst. of Plasma Physics.
A CURVILINEAR COORDINATE METHOD FOR THE SOLUTIONS OF INITIAL VALUE PROBLEMS USING THE THIRD-ORDER UPWIND DIFFERENCING SCHEME
Yukimasa Takemoto, Yoshiaki Nakamura, Haruo Yamabe (Nagoya Inst. of Tech., Japan), Hiroshi Naitou, and Yoshihiko Abe May 1985 37 p refs
(IPPJ-734) Avail: NTIS HC A03/MF A01

A calculation procedure to solve highly unsteady incompressible Navier-Stokes equations in arbitrary shapes is presented. The boundary-fitted curvilinear coordinate system is used to generate a coordinate surface coincident with the boundary contours in the physical plane. A second-order forward difference approximation is used for the time derivative and a third-order upwind differencing method for the convective terms which suppress the instabilities is used. The third-order method for the space derivatives is based on the quadratic upstream interpolation for convective kinematics (QUICK) algorithm. The solutions for a time-marching square cavity flow and a channel flow with a bump at the Reynolds number of 10 to the 4th are obtained. Author

N85-34643# Nagoya Univ. (Japan). Inst. of Plasma Physics.
RESONANT ION ACCELERATION BY OBLIQUE MAGNETOSONIC SHOCK WAVE IN A COLLISIONLESS PLASMA
Yukiharu Ohsawa Jun. 1985 41 p refs
(IPPJ-735) Avail: NTIS HC A03/MF A01

Magnetosonic shock wave propagating obliquely to a magnetic field is studied by theory and simulation, with particular attention to the resonant ion acceleration (the V sub p cross B acceleration) by the shock. Theoretical analysis based on a two fluid model shows that, in the laminar shock, the electric field strength in the direction of the wave normal is about (M sub i/M sub e) to the 1/2 times larger for the quasi-perpendicular shock than that for the quasi-parallel shock, which is a reflection of the fact that the width of the quasi-perpendicular shock is much smaller than that of the quasi-parallel shock. Time evolution of a totally self-consistent magnetosonic shock wave is studied by using a 2-1/2 dimensional fully relativistic, fully electromagnetic particle simulation with full ion and electron dynamics. Even the low Mach number shock wave can significantly accelerate some ions by the V sub p cross B acceleration. The resonant ion acceleration occurs more strongly in the quasi-perpendicular shock, because the magnitude of this acceleration is proportional to the electric field strength. Author

N85-34644# Nagoya Univ. (Japan). Inst. of Plasma Physics.
PROCEEDINGS OF THE US-JAPAN WORKSHOP ON TRANSPORT IN OPEN-ENDED SYSTEMS
Mar. 1985 127 p refs Workshop held in Nagoya, Japan, 30 Jul. - 3 Aug. 1984
(IPPJ-727) Avail: NTIS HC A07/MF A01

The United States fusion program includes ongoing analytic and computational efforts in the theory of transport in tandem mirrors as well as other nonaxisymmetric devices (stellarator, bumpy tórus). At the time this workshop was being organized, it was apparent that similar problems were being addressed by the groups working on these various machines. Transport phenomena associated with nonaxisymmetry were being observed on several experiments (TMX, TMX-Upgrade, EBT). In addition, some results from TMX-U and Phaedrus suggested a deleterious effect of RF on confinement. In Japan, the theoretical effort in transport is at present much smaller. There have been studies of particle orbits, some analytic modeling of RF effects, and Monte Carlo studies of transport coefficients. There has been no work on a transport code for tandem mirrors, but a code by D. Hastings has been implemented at Nagoya to study transport in the Nagoya Bumpy Torus (NBT). Experimentally, many interesting results have recently become available on assymmetries induced by ICRH and ECRH (in RFC-XX and gamma-10), on potential profiles in NBT, and on the effect of potential control plates in gamma-10. For individual titles, see N85-34645 through N85-34667.

N85-34645# Science Applications, Inc., Boulder, Colo.
POTENTIAL EFFECT IN TRANSPORT DUE TO NON-AXISYMMETRIC CONFINING FIELD DC Section Summary Report
Peter J. Catto, Jiro Todoroki (Nagoya Univ.), and Masahiro Wakatani (Kyoto Univ.) *In* Nagoya Univ. Proc. of the US-Japan Workshop on Transport in Open-Ended Systems Mar. 1985 p 11-19 (For primary document see N85-34644 23-75)
Avail: NTIS HC A07/MF A01

The following five neoclassical transport property topics were discussed: (1) multiple ambipolar roots; (2) non-Maxwellian distributions; (3) potential control; (4) large azimuthal precessions in tandem transition regions; and (5) azimuthal electric field dependence along the magnetic field. G.L.C.

N85-34646# GA Technologies, Inc., San Diego, Calif.
[ACTIVITIES OF THE RF SECTION] Summary Report
Paul B. Parks, T. Hatori, and Tsuguhiro Watanabe (Hiroshima Univ.) *In* Nagoya Univ. Proc. of the US-Japan Workshop on Transport in Open-Ended Systems Mar. 1985 p 20-27 (For primary document see N85-34644 23-75)
Avail: NTIS HC A07/MF A01

The emphasis was to address the problem of how radial transport in axisymmetric systems is induced by azimuthally non-uniform RF heating. Axisymmetric systems were chosen for two reasons. First, and most obvious, is that all of the existing ICRF codes used to model the RF field structure in the plasma use axisymmetric magnetic field geometry (1-D cylindrical geometry.

The codes need to be compared with each other and should be checked with key experimental observations e.g., density build-up as function of initial broadness of density profile and RF trapping efficiency as a function of resonance surface location (RFC-XX,). The development of future 2-D codes to include the axial variation of the field was deemed important because of its relevance to radial transport discussion in the following. Secondly, axisymmetric systems allow for the breaking of azimuthal symmetry by RF mechanisms from symmetry breaking by non-axisymmetric magnetic field configuration. In their context further experiments on RFC-XX concerning azimuthal asymmetries will prove very valuable for comparison with theory. G.L.C.

N85-34647# California Univ., Livermore. Lawrence Livermore Lab.
RADIAL TRANSPORT PHENOMENA FOR TMX-UPGRADE
Ronald H. Cohen *In* Nagoya Univ. Proc. of the US-Japan Workshop on Transport in Open-Ended Systems Mar. 1985 p 29-31 ref (For primary document see N85-34644 23-75)
Avail: NTIS HC A07/MF A01

An overview of resonant transport, some non-resonant, finite collisionality effects, some transport reduction techniques, recent results on transport from the TMX-Upgrade experiment, the important role of azimuthal electric fields, and a model calculation for the generation of azimuthal electric fields by asymmetric electron-cyclotron resonance heating (ECRH) in the plug region of a thermal barrier tandem mirror are presented. Resonant transport arises due to the combination of collisions and the radial drifts produced by the quadrupole fields at either end of a tandem-mirror machine. The term resonant refers to the fact that the radial displacements on successive bounces are in phase when the azimuthal drift per bounce is an odd multiple of p1/2. Resonant transport coefficients can be calculated by various techniques. One particlar approach, solution of linearized mapping equations, was reviewed. G.L.C.

N85-34648# Tsukuba Univ. (Japan). Plasma Research Center.
PLUG AND THERMAL BARRIER POTENTIAL FORMATION IN GAMMA 10
Isao Katanuma *In* Nagoya Univ. Proc. of the US-Japan Workshop on Transport in Open-Ended Systems Mar. 1985 p 32-42 (For primary document see N85-34644 23-75)
Avail: NTIS HC A07/MF A01

Tandem mirror Gamma-10 employs thermal barrier to insulate the electrons in the end plugs from those in the central cell. Generation of thermal barrier in Gamma-10 requires the creation of a hot mirror trapped electron population, heated by electron cyclotron resonance heating. The creation of hot electron population when only second harmonic electron cyclotron resonance heating is included in the thermal barrier region was calculated. The plug and thermal barrier potential formation when fundamental electron heating and neutral beam injections are added, were calculated by using our bounce averaged Fokker-Planck code. G.L.C.

N85-34649# Hiroshima Univ. (Japan). Faculty of Science.
RF INDUCED RADIAL DIFFUSION IN TANDEM MIRRORS
Hitoshi Hojo and M. Shigeta (Sharp Corp.) *In* Nagoya Univ. Proc. of the US-Japan Workshop on Transport in Open-Ended Systems Mar. 1985 p 43-46 (For primary document see N85-34644 23-75)
Avail: NTIS HC A07/MF A01

Anomalous radial diffusion due to rf electric field fluctuations in tandem mirrors were studied. The analysis is based on a mapping for (r, psi) [r and psi being the radial position and azimuthal angle in the midplane, respectively], which is derived from the integration of the standard guiding center drift equation for ions. The axial bounce motion is described by the square-well model (the straight orbit approximation). A radial ambipolar field is assumed proportional to r cubed and fluctuations are described by only the azimuthal component of a RF electric field (mode number m, frequency omega) localized in the plug cells when a TMX-type tandem mirror is considered. G.L.C.

N85-34650# Science Applications, Inc., Boulder, Colo.
INDUCED AZIMUTHAL ELECTRIC FIELD EFFECTS ON TANDEM TRANSPORT AND AMBIPOLARITY Abstract Only
Peter J. Catto *In* Nagoya Univ. Proc. of the US-Japan Workshop on Transport in Open-Ended Systems Mar. 1985 p 47-48 (For primary document see N85-34644 23-75)
Avail: NTIS HC A07/MF A01

Because magnetic drifts depend on the sign of the change and normally result in ions making larger steps per bounce than electrons, azimuthal electric fields are normally generated by the quadrupole fields in a tandem mirror. Unlike a tokamak, a tandem mirror can exhibit an interesting and potentially important dielectric response in some situations. In particular, when the azimuthal ExB drift frequency omega times the characteristic wavelength or period of the magnetically driven charge separation is comparable to the ion thermal speed V sub i, the dielectric shielding of the plasma becomes small when omega is approximately equal to the electron diamagnetic drift frequency omega. In this situation the induced azimuthal electric field in a tandem can cause large modifications to the ion diffusion coefficients. These modifications result in the possibility of additional ambipolar solutions of the transport and end loss equations describing tandem mirror transport. G.L.C.

N85-34651# Tsukuba Univ. (Japan). Plasma Research Center.
RECENT EXPERIMENTS IN GAMMA-10
Masaki Inutake *In* Nagoya Univ. Proc. of the US-Japan Workshop on Transport in Open-Ended Systems Mar. 1985 p 49-52 (For primary document see N85-34644 23-75)
Avail: NTIS HC A07/MF A01

Recent experimental results are presented on thermal barrier/plug potential formation and end plugging in an axisymmetrized tandem mirror gamma-10. The gamma-10 device is a minimum-B anchored tandem mirror with outboard thermal barrier. Plug and barrier are produced in the axisymmetric mirror. Ramp coils set at both ends of the central cell throttle the fraction of passing particles through the min-B anchors and into the plug/barrier cells. The min-B mirror is designed to be symmetric w.r.t. the midplane in order to cancel the geodesic curvature through each anchor/transition region. This results in zero average net drift from a flux surface for particles passing through the non-axisymmetric region and zero net parallel current flowing into the central cell, when azimuthal particle drift caused by radial electric field is dept small in the anchor/transition region. G.L.C.

N85-34652# Nihon Univ., Tokyo (Japan). Atomic Energy Research Inst.
RADIAL TRANSPORT CAUSED BY COLLISION
Masamitsu Aizawa *In* Nagoya Univ. Proc. of the US-Japan Workshop on Transport in Open-Ended Systems Mar. 1985 p 53-55 refs (For primary document see N85-34644 23-75)
Avail: NTIS HC A07/MF A01

The particles drift orbits in the magnetic field of the tandem mirror were studied to investigated the radial transport caused by collision. The tandem mirror model is like the original TMX type. The para-axial approximation was used to calculate the drift orbits. An appropriate magnetic field line near the magnet axis is taken and its behavior examined in the exact field, so that the property of the field can be known within this approximation. G.L.C.

N85-34653# Wisconsin Univ., Madison. Nuclear Engineering Dept.
TRANSPORT ISSUES IN PHAEDRUS-TYPE PLASMAS Abstract Only
James D. Callen *In* Nagoya Univ. Proc. of the US-Japan Workshop on Transport in Open-Ended Systems Mar. 1985 p 56-57 ref (For primary document see N85-34644 23-75)
Avail: NTIS HC A07/MF A01

The research program on the Phaedrus tandem mirror experiment emphasizes the use of ion cyclotron radio frequency (ICRF) waves for heating and pumping of particles in velocity or real space, and provision of macroscopic stability through the radial pondermotive force effect. Also, electron cyclotron resonance and

second harmonic heating are utilized. The various RF waves in the central cell and end plug regions affect plasma transport in real and velocity space both directly (as in RF heating) and indirectly (through spatial asymmetries in the RF wave effects). As part of theoretical efforts to model transport processes in Phaedrus type plasmas. The following three issues are discussed: (1) the moment equation approach to transport in tandem mirrors; (2) ion cyclotron radio frequency (ICRF) pumping of electrons in Phaedrus; and (3) second harmonic electron cyclotron heating. G.L.C.

N85-34654# Hiroshima Univ. (Japan). Inst. for Fusion Theory.
POSSIBILITY OF POTENTIAL GENERATION BY LOWER HYBRID WAVE
Tsuguhiro Watanabe and Mitsuhiro Kamei *In* Nagoya Univ. Proc. of the US-Japan Workshop on Transport in Open-Ended Systems Mar. 1985 p 58-60 (For primary document see N85-34644 23-75)
Avail: NTIS HC A07/MF A01

It is important for the tandem mirror systems to establish a method for the potential generation in high density plasma. The possibility of tandem potential generation by lower hybrid wave (LHW) is considered. LHW has suceeded in current drive in tokamak plasma. For current drive, it is necessary to accelerate electrons in one direction. For potential generation, on the other hand, it is necessary to pump out electrons from potential well. Both processes are, however, very similar. Acceleration of electrons by resonant wave particle interaction plays essential role for current drive and potential generation. An advantage of LHW is the applicability for high density plasma. Furthermore, LHW propagate along resonance cone, the wave can be controlled form in a plasma. According to the numerical simulations, the wave form of LHW is relevant to the efficiency of the acceleration of slow velocity electrons. G.L.C.

N85-34655# Himeji Inst. of Tech. (Japan). Dept. of Electrical Engineering.
BOUNCE RESONANCE HEATING AND RADIAL TRANSPORT OF ELECTRONS
Kunihiro Sato and Tadatsugu Hatori (Nagoya Univ.) *In* Nagoya Univ. Proc. of the US-Japan Workshop on Transport in Open-Ended Systems Mar. 1985 p 61-66 refs (For primary document see N85-34644 23-75)
Avail: NTIS HC A07/MF A01

High-level fluctuation in the ion-cyclotron frequency range, which is difficult to be suppressed completely, were observed in experiments of 2XIB and TMX. Although only low-level fluctuation was measured in low-density operation of TMX-U, whether the micro-instabilities in high-density operation can be suppressed or not, still remains a serious problem. Since the bounce frequency of electrons in magnetic mirrors is usually of the order of the ion-cyclotron frequency, electrons can be heated in the direction of the field line and the radial transport associated with the heating can be induced by the fluctuation. The power transfer is calculated from the DCLC or the AIC mode to electrons through the bounce resonance, considering axial variation of the magnetic field strength and the ambipolar potential. The radial transport induced by the waves is also calculated. G.L.C.

N85-34656# Nihon Univ., Tokyo (Japan). Dept. of Physics.
ELECTRON DYNAMICS AND TRANSPORT IN A MIRROR FIELD
Haruyuki Irie and Tadatsugu Hatori (Nagoya Univ.) *In* Nagoya Univ. Proc. of the US-Japan Workshop on Transport in Open-Ended Systems Mar. 1985 p 67-72 refs (For primary document see N85-34644 23-75)
Avail: NTIS HC A07/MF A01

The nonlinear dynamics and the radial transport of an electron in a magnetic mirror field are considered in the presence of an electrostatic monochromatic wave. It is found that a stochastic heating and a stochastic radial diffusion of electrons can simultaneously occur due to the nonlinear interaction between two motions, one is the bounce motion in the mirror and the other is the motion by the monochromatic wave. Three types of dependence of the diffusion coefficient on the wave amplitude are obtained which are different from that derived by the quasilinear theory. Author

N85-34657# Niigata Univ. (Japan). Dept. of Physics.
LOW FREQUENCY INSTABILITY IN A MIRROR FIELD
Akio Ishida *In* Nagoya Univ. Proc. of the US-Japan Workshop on Transport in Open-Ended Systems Mar. 1985 p 73-78 refs (For primary document see N85-34644 23-75)
Avail: NTIS HC A07/MF A01

The low frequency l=1 mode was observed in the central cell of the tandem mirror machines and enhances the radial diffusion. Here l is the azimuthal mode number. Although the l=1 flute mode seems to be the most important candidate for this mode, the identification of the mode is not clear. Experimentally the bounce frequency of the ions between the mirrors is larger than the apparent frequency of the mode. The effects of the finite length of the central cell or the bounce motion of the particles along the magnetic field will be studied theoretically. G.L.C.

N85-34658# GA Technologies, Inc., San Diego, Calif.
MODEL OF AZIMUTHAL NON-UNIFORMITIES INDUCED BY RF HEATING IN RFC-XXM
Paul B. Parks *In* Nagoya Univ. Proc. of the US-Japan Workshop on Transport in Open-Ended Systems Mar. 1985 p 79-81 refs (For primary document see N85-34644 23-75)
Avail: NTIS HC A07/MF A01

Measured azimuthal profiles of the floating potential and radial loss flux in the center cell of RFC-XXM using segmented limiters have revealed stationary azimuthal asymmetries. The asymmetries are believed to be caused by azimuthally nonuniform ICRF and ICRH injection. A study was undertaken to isolate one effect of the RF, namely its role as a heat source and how, in this manner it leads to azimuthally varying ambipolar plasma potential. These calculations have bearing on the problem of ion radial diffusion since the transport is sensitive to the magnitude and azimuthal mode number of the stationary azimuthal electric fields. The existence of ion diffusive transport cross flux surfaces requires an axial variation of the ambipolar potential as well, in order to decorrelate the radial step size from the azimuthal E x B twist angle through the action of the ion bouncing motion. Axially uniform potential can only lead to plasma radial convection not serious unless the plasma is radially convected to material obstructions located just outside the plasma periphery. G.L.C.

N85-34659# Nagoya Univ. (Japan). Inst. of Plasma Physics.
AZIMUTHAL UNIFORMITY AND CURRENT BALANCE STUDY OF ICRH-PRODUCED PLASMA IN RFC-XXM
Shoichi Okamura et al *In its* Proc. of the US-Japan Workshop on Transport in Open-Ended Systems Mar. 1985 p 82-85 (For primary document see N85-34644 23-75)
Avail: NTIS HC A07/MF A01

As the axial confinement of the open ended systems was improved people have become more concerned about the problems of radial transport. At present the problems may be divided into two kinds. One is the general transport problems which might exist in any kind of configuration and another is a rather special problem due to the nonaxisymmetry of the configuration (magnetic field, heating etc.). A series of experiments was undertaken to study such problems on RFC-XX-C. This machine has the unique characteristics in the magnetic field configuration, axisymmetry, which might be great help for such a study because separation or neglect of one problem due to the non-axisymmetry of magnetic field configuration from others is possible. G.L.C.

N85-34660# Nagoya Univ. (Japan). Inst. of Plasma Physics.
BREAKDOWN OF INTRINSIC AMBIPOLARITY FOR THE RADIAL DIFFUSION DUE TO A ROTATING RF FIELD
Tadatsugu Hatori and Hitoshi Hojo (Hiroshima Univ.) *In its* Proc. of the US-Japan Workshop on Transport in Open-Ended Systems Mar. 1985 p 86-92 ref (For primary document see N85-34644 23-75)
Avail: NTIS HC A07/MF A01

In the straight section of RFC device, an RF gas-ionization

experiment is performed with use of a Rotating type III coil. Remarkable contrast is obtained between the two profiles of plasma density produced by left-hand (m=-1) and right-band (m=1) rotation of the rf magnetic field which is applied perpendicularly to the static field. For the case of m=-1, the shape is almost flat, but in the case of m=1 a sharp peak is observed near the axis. This result cannot be explained by the simple balance between the gas source and the end-loss process. The RF-induced radial transport is essential to the phenomena. Author

N85-34661# Nagoya Univ. (Japan).
EFFECT OF ECH AND ICH ON AMBIPOLAR POTENTIAL IN NBT-1M
Tatsuo Shoji *In its* Proc. of the US-Japan Workshop on Transport in Open-Ended Systems Mar. 1985 p 93-103 refs (For primary document see N85-34644 23-75)
Avail: NTIS HC A07/MF A01

In a nonaxisymmetric device like the bumpy torus, the diffusion coefficient of ions and electrons is not automatically equal, so that an ambipolar field develops to maintain charge neutrality. The transport coefficient is strongly influenced by such an ambipolar field, resulting in an E x B drift motion of the plasma. The effect of the ambipolar potential, especially on ion transport is studied experimentally in the wide range of T sub i/T sub e by introducing the addition electron cyclotron heating (ECH) and induction conduction heating (ICH) power to the plasma in an NBT-1M device. Author

N85-34662# Nagoya Univ. (Japan). Inst. of Plasma Physics.
TRANSPORTS STUDIES OF ECH AND ICRH-HEATED BUMPY TORUS PLASMA IN NBT-1M
Tetsuo Kamimura and Daniel E. Hastings (Oak Ridge National Lab.) *In its* Proc. of the US-Japan Workshop on Transport in Open-Ended Systems Mar. 1985 p 104-106 refs (For primary document see N85-34644 23-75)
Avail: NTIS HC A07/MF A01

The 1 1/2 dimensional radial transport equations are solved for a ECH and ICRH-heated bumpy torus core plasma with parameters corresponding to NBT-1M. The radial electric field is determined self consistent by the constraint that the radial ion and electron fluxes be equal. The density and temperature equations are evolved to steady-state for a fixed volume averaged density, volume averaged electron temperature and volume averaged ion temperature. Author

N85-34663# Nagoya Univ. (Japan). Inst. of Plasma Physics.
GUIDING CENTER DISTRIBUTION FUNCTION AND LONGITUDINAL INVARIANT
Jiro Todoroki *In its* Proc. of the US-Japan Workshop on Transport in Open-Ended Systems Mar. 1985 p 107-111 ref (For primary document see N85-34644 23-75)
Avail: NTIS HC A07/MF A01

Guiding center approximation (or drift approximation) is a well known and powerful method to describe charge particle motion in a strong magnetic field. But when the drift kinetic equation is used to describe the collective motion of a plama, paradoxes or confusion arise. In some cases the results obtained by using drift equation do not agree with those obtained by using the Vlasov equation. To solve these paradoxes the relation between the moments of real particle distribution and that of drift approximation is considered. Using the same technique for deriving the drift equation, the bounce averaged equation of motion is considered, and the deviation of the drift orbit from J (parallel) surface is calculated in the first order. Author

N85-34664# Nagoya Univ. (Japan). Inst. of Plasma Physics.
SIMULATION STUDIES ON STABILITY OF HOT ELECTRON PLASMA
Yukiharu Ohsawa *In its* Proc. of the US-Japan Workshop on Transport in Open-Ended Systems Mar. 1985 p 112-117 refs (For primary document see N85-34644 23-75)
Avail: NTIS HC A07/MF A01

Stability of a hot electron plasma in a NBT(EBT)-like geometry is studied, using a 2-1/2 dimensional relativistic, electromagnetic particle code. In the simulation model, spatial variation is allowed only in the x- and y- directions, with the z-direction being an ignorable coordinate, although the particles have three velocity components (u sub x, v sub y, v sub z). The system is periodic in the y-direction and is bounded in the x-direction with total grid size L sub x xL sub y=128d x 128d, where d is the grid spacing. The external magnetic field B sub 0 is formed by an external current J sub 0 which is rigid and not influenced by the plasma. The external magnetic field B sub 0 points in the z-direction, and its strength decreases with x as 1/(x-Lx-2+R), where the constant R is a measure of the magnetic field gradient. The initial plasma density also decreases with x. All quantities are constant in the y-direction in the equilibrium state. Because both the external magnetic field and the plasma density (pressure) decreases with x, the plasma can be interchange unstable if there is no hot electron layer. Author

N85-34665# Oak Ridge National Lab., Tenn.
ANALYTIC AND NUMERICAL CALCULATIONS OF THE AMBIPOLAR ELECTRIC FIELD IN A STELLARATOR
Daniel E. Hastings *In* Nagoya Univ. Proc. of the US-Japan Workshop on Transport in Open-Ended Systems Mar. 1985 p 118-120 (For primary document see N85-34644 23-75)
Avail: NTIS HC A07/MF A01

The formula for calculating the radial electric field in a stellarator is usually the steady state ambipolarity relationship. This equation is local in space and when solved with the density rate equations, results in several different electric field solutions. This raises a number of questions: how does the plasma choose the electric field solution, can two spatially close points be on different roots and what limits how fast the plasma can change solution? The time dependent version of the ambipolarity relationship is analyzed in terms of the theory of nonlinear differential equations. It is also shown that the width of the zone over which the solution changes is limited by the orbit deviation from the flux surface. Finally, the equations are solved numerically to illustrate some of these physical concepts. Author

N85-34666# Kyoto Univ. (Japan). Plasma Physics Lab.
BEHAVIOR OF HELICALLY-TRAPPED FAST ION ORBITS IN HELIOTRON E
Kiyoshi Hanatani, Y. Nakashima (Tsukuba Univ.), H. Zushi, F. Sano, O. Motojima, Masahiro Wakatani, T. Obiki, A. Iiyoshi, and K. Uo *In* Nagoya Univ. Proc. of the US-Japan Workshop on Transport in Open-Ended Systems Mar. 1985 p 121-124 refs (For primary document see N85-34644 23-75)
Avail: NTIS HC A07/MF A01

Helically trapped particles play key roles in non-axisymmetric magnetic traps such as the stellarator and heliotron. They are called localized particles and are believed to escape most easily from the plasma. The possibility of perpendicular NBI into heliotron E using a guiding-center drift orbit calculation with classical slowing-down process of fast ions was predicted. The effectiveness of the perpendicular injection is demonstrated in a series of NBI experiments from the view point of the heating efficiency. The theoretically predicted confinement of the localized fast ions is verified by using a neutral-particle diagnostic and a Monte-Carlo beam orbit Fokker-Planck code. Author

N85-34667# Kyoto Univ. (Japan). Plasma Physics Lab.
NEOCLASSICAL DIFFUSION INCLUDING ELLIPTICITY IN A HELIOTRON-LIKE CONFIGURATION
Masahiro Wakatani *In* Nagoya Univ. Proc. of the US-Japan Workshop on Transport in Open-Ended Systems Mar. 1985 p 125-130 refs (For primary document see N85-34644 23-75)
Avail: NTIS HC A07/MF A01

Neoclassical transport in an l=2 high-shear helical system is described which is similar to the Heliotron-E device with a large helical ripple epsilon sub h (bar-a) approx. 0.3, compared to the toroidal ripple, epsilon sub t (bar-a) approx. 0.1. It has an average minor radius of bar-a=20 cm, an aspect radio of R/bar-a=10 and a helical magnetic field of about 20 KG. It is well known that

the l=2 helical system has elliptic magnetic surfaces. The effect of ellipticity on neoclassical transport has, however, not yet been studied. Our concern is in the neoclassical diffusion for both the 1/nu regime and the plateau regime, where nu is electron-ion collision frequency. Author

N85-34668# Nagoya Univ. (Japan). Inst. of Plasma Physics.
OBSERVATION OF MODE-CONVERTED BY ION BERNSTEIN WAVE BY AN HCN LASER SCATTERING
Tsutomu Tetsuka, Kazuo Kawahata, Shigeki Okajima (Chubu Univ.), Akimitsu Nishizawa, Tetsuo Watari, Ritoku Ando, Shuugo Tanahashi, Kazuo Toi, and Junji Fujita Mar. 1985 22 p refs
(IPPJ-724) Avail: NTIS HC A02/MF A01

An HCN laser scattering technique is employed for detecting an electrotatic wave excited by ion-cyclotron (ICRF) on the Japanese Institute of Plasma Physics (JIPP) T-IIU tokamak. The measured wave is consistent with the theoertically estimated wave dispersion of the ion Berstein wave which is mode-converted from the fast wave near the ion-ion hydrid resonance layer. he ion Bernstein wave is found to be strongly absorbed and damped at least by 30db as propagating a half round of the torus (2.9m in toroidal direction). The influence of magnetohydrodynamics (MHD) activity on the mode-converted ion Bernstein was is examined. When the MHD activity grows and the plasma becomes unstable due to high power ICRF heating, the scattered signal from the ion Bernstein wave decreases, being accompanied with large fluctuations. Author

N85-34669# Nagoya Univ. (Japan). Inst. of Plasma Physics.
FOKKER-PLANCK CALCULATION OF HOT ELECTRON FORMATION IN THE THERMAL BARRIER REGION OF TANDEM MIRROR GAMMA-10
I. Katanuma, Y. Kiwamoto, K. Sawada, and S. Miyoshi Apr. 1984 40 p refs
(IPPJ-726) Avail: NTIS HC A03/MF A01

The hot electron build-up by the second harmonic electron cyclotron resonance heating in the thermal barrier region of tandem mirror gahma-10 has been studied by using a Fokker-Planck code with self-consistent potential profile taken into account. Two phases have been found in the evolution of hot electron population and the potential profile. In the first phase, where RF diffusion is dominant, quick increase of the hot electron density and that of the mean energy are observed. The potential is the deepest during the first phase. The second phase starts in the mean-free-time of the pitch angle scattering of hot electrons on cold electrons and ions. In this phase the hot electron population increases at the rate of the pitch angle scattering. The potential dip shallows due to the accumulation of pitch angle scattering oassubg uibs, This observation indicates the necessity for ion pumping to maintain the negative potential at the thermal barrier. Author

N85-34670# Nagoya Univ. (Japan). Inst. of Plasma Physics.
WORKSHOP REPORT ON SIMULATION TECHNIQUES FOR SHOCK WAVE PHENOMENA AND CHARACTERISTICS OF PLASMAS IN INERTIAL CONFINEMENT FUSION
Mar. 1985 231 p refs Workshop held in Nagoya, Japan, 15-16 Nov. 1984
(IPPJ-725) Avail: NTIS HC A11/MF A01

This report of the Institute of Plasma Physics of Nagoya (Japan) University is based on a workshop which took place there on Nov. 15-17, 1984. The twin themes of the workshop were 'Simulation Techniques for Shock Wave Phenomena' and 'Characteristics of Plasmas in Inertial Confinement Fusion (ICF)'. Topics discussed were numerical techniques to solve hyperbolic type equations, applications of the simulation code to ICF research and physics intrinsic to ICF, such as implosion stability, electron transport, ion transport, and X-ray characteristics. For individual titles, see N85-34671 through N85-34688.

N85-34671# Nihon Univ., Shinei (Japan). Atomic Energy Research Inst.
FEMALE: FINITE ELEMENT METHOD FOR ARBITRARY LAGRANGIAN AND EULERIAN ELEMENTS c64
M. Aizawa and I. Kawakami *In* Nagoya Univ. Workshop Rept. on Simulation Tech. for Shock Wave Phenomena and Characteristics of Plasma in Inertial Confinement Fusion Mar. 1985 p 2-10 (For primary document see N85-34670 23-75)
Avail: NTIS HC A11/MF A01

A hyperbolic system of nonlinear partial differential equations includes the solutions which have discontinuities as in the Riemann problem. It is well known that the numerical oscillation occurs when the finite difference method like the two step Lax-Wendroff method is applied to this problem. To suppress this type of oscillation, numerical diffusion was introduced which is contained in the numerical scheme implicitly, or the artificial viscosity. However, the discontinuities disappear because of numerical diffusion introduced, and then an accuracy of computation becomes poor. The FEMALE method based on the finite method with no numerical diffusion was proposed to solve the hyperbolic equations with no physical diffusion. The outline of FEMALE method, the optimum decision of nodal velocity and the extention to the parabolic equations are described. G.L.C.

N85-34672# Kyoto Inst. of Tech. (Japan). Dept. of Mechanical Engineering.
NUMERICAL SOLUTIONS OF THE VLASOV EQUATION c64
Nobuyuki Satofuka, Koji Morinishi, and Hidetoshi Nishida *In* Nagoya Univ. Workshop Rept. on Simulation Tech. for Shock Wave Phenomena and Characteristics of Plasma in inertial Confinement Fusion Mar. 1985 p 11-24 refs (For primary document see N85-34670 23-75)
Avail: NTIS HC A11/MF A01

A numerical procedure is derived for the solutions of the one and two dimensional Vlasov-Poisson system equations. This numerical procedure consists of the phase space discretization and the integration of the resulting set of ordinary differential equations. In the phase space discretization, derivatives with respect to the phase space variable are approximated by a weighted sum of the values of the distribution function at properly chosen neighboring points. Then, the resulting set of ordinary differential equations is solved by using an appropriate time integration scheme. The results for linear Landau damping, nonlinear Landau damping and counter streaming plasmas are investigated and compared with those of the splitting scheme. The proposed method is found to be very accurate and efficient. Author

N85-34673# Osaka Univ., Suita (Japan). Inst. of Laser Engineering.
CUBIC INTERPOLATED PSEUDO-PARTICLE METHOD (CIP) FOR SOLVING HYPERBOLIC-TYPE EQUATION c64
H. Takewaki, A. Nishiguchi, and T. Yabe *In* Nagoya Univ. Workshop Rept. on Simulation Tech. for Shock Wave Phenomena and Characteristics of Plasma in Inertial Confinement Fusion Mar. 1985 p 25-48 refs (For primary document see N85-34670 23-75)
Avail: NTIS HC A11/MF A01

A cubic interpolated pseudoparticle (CIP) method is presented to solve the hyperbolic type equations. The method takes a similar way to the finite element method (FEM) the boundary element method (BEM) and the particle scheme, and is interpreted to be an extension of a one particle version of the soap scheme. Accordingly the scheme makes a bridge between the FEM and the particle scheme. G.L.C.

N85-34674# Kyoto Univ. (Japan). Dept. of Physics.
NUMERICAL SIMULATION IN ASTROPHYSICS: SMOOTHED PARTICLE METHODS c90
Shoken M. Miyama *In* Nagoya Univ. Workshop Rept. on Simulation Tech. for Shock Wave Phenomena and Characteristics of Plasma in Inertial Connement Fusion refs (For primary document see N85-34670 23-75)
Avail: NTIS HC A11/MF A01

There are many numerical simulations of hydrodynamical problems in astrophysics. Processes of star formation, supernova explosion and formation of neutron stars and general relativistic collapse of star to form black hole were simulated by various

numerical codes. These codes are made to be suitable for computating such problems which have their own characteristic.
G.L.C.

N85-34675# Tokyo Inst. of Tech. (Japan). Dept. of Energy Sciences.
MOVING FINITE ELEMENT METHOD FOR ICF TARGET IMPLOSION
Junichi Furuta, Shigeo Kawata, and Keishiro Niu *In* Nagoya Univ. Workshop Rept. on Simulation Tech. for Shock Wave Phenomena and Characteristics of Plasma in Inertial Confinement Fusion Mar. 1985 p 66-73 ref (For primary document see N85-34670 23-75)
Avail: NTIS HC A11/MF A01

One dimensional hydrodynamic codes for the analysis of internal confinement fusion (ICF) target implosion which include various effects were developed, but most of them utilize the artificial viscosity (e.g., Von Neumann's viscosity) which cannot reveal accurately the shock waves. A gain of ICF target implosion is much due to the dissipation at the shock fronts, so it is necessary to express correctly the shock waves which are affected by the viscosity. The width of the shock waves is usually a few times as large as the length of mean free path, therefore the meshes for the shock waves must be set to about 10 to the 4th to 10 to the 5th power. It is a serious problem because of the computational memories or CPU time. In the moving finite element (MPE) method, both nodal amplitudes and nodal positions move continuously with time in such a way as to satisfy simultaneous ordinary differential equations (OPDs) which minimize partial differential equation (PDE) residuals. Author

N85-34676# National Chemical Lab. for Industry, Tsukuba (Japan).
NUMERICAL CALCULATIONS ON SHOCK LOADED MATERIALS c64
Katsumi Tanaka *In* Nagoya Univ. Workshop Rept. on Simulation Tech. for Shock Wave Phenomena and Characteristics of Plasma in Inertial Confinement Fusion Mar. 1985 p 74-85 refs (For primary document see N85-34670 23-75)
Avail: NTIS HC A11/MF A01

The numerical technique for the analysis of shock waves in condensed materials by using the finite difference method of Lagrangian hydrodynamics is briefly described. Examples of the Lagrangian calculations for the flyer plate acceleration and implosion of D-T fuel by light ion beam are presented. Author

N85-34677# Institute of Physical and Chemical Research, Saitama (Japan).
DISSIPATION TERMS IN ONE-DIMENSIONAL HYDRODYNAMIC CODE FOR ICF TARGET
Moritake Tamba and Keishiro Niu (Tokyo Inst. of Tech., Yokahama) *In* Nagoya Univ. Workshop Rept. on Simulation Tech. for Shock Wave Phenomena and Characteristics of Plasma in Inertial Confinement Fusion Mar. 1985 p 86-98 (For primary document see N85-34670 23-75)
Avail: NTIS HC A11/MF A01

The one dimensional hydrodynamic code so far used for the simulation of the target implosion in ICF, the artificial viscosity has been employed as the dissipation terms. This artificial viscosity depends on the mesh width of the space using in the simulation and is much large in comparison with the real viscosity. It is shown that this artificial viscosity leads to the unreasonable fusion parameters depending on the used mesh width of the space. Several methods to modify the dissipation term are given in this paper. Author

N85-34678# Tokyo Inst. of Tech., Yokahama (Japan). Dept. of Energy Sciences.
TWO-DIMENSIONAL SIMULATION OF LIB TARGET IMPLOSION
Isho Yamaguchi, Shigeo Kawata, and Keishiro Niu *In* Nagoya Univ. Workshop Rept. on Simulation Tech. for Shock Wave Phenomena and Characteristics of Plasma in Inertial Confinement Fusion Mar. 1985 p 99-114 refs (For primary document see N85-34670 23-75)
Avail: NTIS HC A11/MF A01

The behavior of the imploding deuterium-tritium (DT) shell, subjected to nonuniformly distributed external pressure, is investigated numerically. This analysis is performed by using two dimensional hydrodynamic code developed in our laboratory. Mixed Eulerian-Lagrangian Method is adopted in this code to avoid the disadvantages of pure Eulerian and pure Lagrangian Method. Results are shown for several cases and it is shown that the fluctuation of the pressure applied to DT fuel layer must be kept under a few percent. Author

N85-34679# Tokyo Univ. (Japan).
SIMULATION OF INSTABILITY OF CYLINDRICALLY CONVERGING SHOCK WAVES c34
Toshiaki Itoh and Kanji Abe *In* Nagoya Univ. Workshop Rept. on Simulation Tech. for Shock Wave Phenomena and Characteristics of Plasma in Inertial Confinement Fusion Mar. 1985 p 115-119 refs (For primary document see N85-34670 23-75)
Avail: NTIS HC A11/MF A01

Motions of cylindrically converging shock waves are simulated numerically. Spatially two dimensional fluid dynamic equations, which contain the azimuthal angle theta as well as the radius r as independent variables, are solved. A cylindrical shock tube problem is examined. The shape of the converging shock wave is always stable and has a tendency to become circular. The flow behind the shock wave, however, is unstable. The instability growth rate of perturbation increases with wave length of the perturbation. The results of simulation are compared to those of experiment.
Author

N85-34680# Osaka Univ., Suita (Japan). Inst. of Laser Engineering.
STABILITY OF IMPLOSION DYNAMICS
H. Takabe, F. Hattori, and K. Mima *In* Nagoya Univ. Workshop Rept. on Simulation Tech. for Shock Wave Phenomena and Characteristics of Plasma in Inertial Confinement Fusion Mar. 1985 p 120-135 refs (For primary document see N85-34670 23-75)
Avail: NTIS HC A11/MF A01

For the achievement of inertial confinement fusion, a hollow shell filled with the fuel has to be symmetrically imploded so that the fuel may be compressed up to 1000 to 10,000 times the solid density with temperature about 5 keV. When the ablative implosion scheme is adopted for this purpose, potential degradation of the implosion appears to be unavoidable because of its hydrodynamical stability and uniformity. G.L.C.

N85-34681# Tokyo Univ. (Japan).
STABILITY OF ION DISTRIBUTION IN STRONG ION SHOCK STRUCTURE
Kanji Abe and Gyo Sakaguchi (Metropolitan Coll. of Tech.) *In* Nagoya Univ. Workshop Rept. on Simulation Tech. for Shock Wave Phenomena and Characteristics of Plasma in Inertial Confinement Fusion Mar. 1985 p 136-150 refs (For primary document see N85-34670 23-75)
Avail: NTIS HC A11/MF A01

The structure of strong ion shock wave propagating in fully ionized plasma is analyzed. Two methods are available for the analysis. One is the continuum approach employing, for example, the Navier-Stokes equation. The other is the microscopic approach employing the Fokker-Planck equation. The continuum approach is based on the approximation that the distribution in the shock structure maintains always the form of near local equilibrium distribution. In the strong shock structure, the above approximation can not be expected to be valid. The Fokker-Planck equation is employed in the analysis of the ion shock structure. G.L.C.

N85-34682# Keio Univ., Yokahama (Japan). Faculty of Science and Technology.
ON THE HEAT FLUX DERIVED BY THE MOMENT METHOD IN LORENTZIAN PLASMA BETWEEN HOT AND COLD WALLS
Masatada Ogasawara and Azusa Fukano *In* Nagoya Univ. Workshop Rept. on Simulation Tech. for Shock Wave Phenomena

and Characteristics of Plasma in Inertial Confinement Fusion Mar. 1985 p 151-157 refs (For primary document see N85-34670 23-75)
Avail: NTIS HC A11/MF A01

Reasons for disagreement are considered for two expressions of heat fluxes. One is the expression obtained by taking special limit of a general expression for the heat flux, which holds for arbitrary values of collisionality parameter L/lambda, lambda being the mean free path, derived by the moment method in the Lorentzian plasma between hot and cold walls (heat baths) separated by the distance L. The special limit is the collisional limit L/lambda approaches infinity and I sub c/t sub h approaches the temperatures of cold and hot walls. The other is the one derived by Landshoff, which is exact for the Lorentzian plasma in the linear theory. The differences comes from the nonlocal nature of the former heat flux, while Landshoff's one is based on the local nature. G.L.C.

N85-34683# Osaka Univ. (Japan). Inst. of Laser Engineering.
INTEGRAL REPRESENTATION FOR NONLINEAR HEAT TRANSPORT
Y. Kishimoto, K. Mima, and M. G. Haines (Imperial Coll.) *In* Nagoya Univ. Workshop Rept. on Simulation Tech. for Shock Wave Phenomena and Characteristics of Plasma in Inertial Confinement Fusion Mar. 1985 p 158-185 refs (For primary document see N85-34670 23-75)
Avail: NTIS HC A11/MF A01

It is widely recognized that the classical Spitzer-Harm (S-H) theory of thermal transport breaks down at relatively gentle temperature gradients such as lambda sub e (T)/L > .002. Here, lambda sub e (T) is the electron mean free path for 90 deg scattering by electron ion collision and L=T/(VT) is the temperature scale length. A steep temperature gradient is, for example, known to be easily realized near the critical point in high power laser produced plasmas. G.L.C.

N85-34684# Waseda Univ., Tokyo (Japan). School of Engineering and Science.
PULSE EFFECT IN A LIGHT ION BEAM PROPAGATION THROUGH A Z-DISCHARGE PLASMA CHANNEL
Tomokazu Kato *In* Nagoya Univ. Workshop Rept. on Simulation Tech. for Shock Wave Phenomena and Characteristics of Plasma in Inertial Confinement Fusion Mar. 1985 p 186-191 refs (For primary document see N85-34670 23-75)
Avail: NTIS HC A11/MF A01

The modulation of wave form of an intense ion current pulse propagating through a z discharge plasma channel is investigated using the Fourier series. The ion electron collisions are taken into account by the aid of Krook type collision term, while the ion ion collisions are neglected. Author

N85-34685# Science Univ. of Tokyo (Japan). Dept. of Electrical Engineering.
ELECTRON LOSS PROCESS AND CROSS SECTION OF MULTIPLY CHARGED IONS BY NEUTRAL ATOMS
S. Karashima and T. Watanabe (Inst. of Physical and Chemical Research) *In* Nagoya Univ. Workshop Rept. on Simulation Tech. for Shock Wave Phenomena and Characteristics of Plasma in Inertial Confinement Fusion Mar. 1985 p 192-198 refs (For primary document see N85-34670 23-75)
Avail: NTIS HC A11/MF A01

The significance of experimental and theoretical electron loss and capture of ions in matter has come to play an important role in the charge equilibrium problems of fusion plasma physics and of accelerator physics. Electron stripping cross section is calculated using the binary encounter approximation (BEA). The electron loss process of multiply charged ion A sup q+ (atomic number Z sub 1 by the collision with a neutral atom B (atomic number Z sub 2 is expressed as A sup q+ + B yields A sup (q+1) + e + B(sigma). After an electron is stripped from the ions, the charge of the ions becomes (q+1) and B goes to neutral or ionized states, i.e., B (sigma) means all electronic states of the atom including ionized states. The treatment of electron loss processes is based on BEA, in which the nucleus of B screened by the surrounding electrons collides with electrons in the A sup q+. Author

N85-34686# Tokyo Univ. (Japan). Dept. of Earth Science and Astronomy.
X-RAY SPECTRA OF BURSTING NEUTRON STARS **c90**
Toshikazu Ebisuzaki and Kenich Nomoto *In* Nagoya Univ. Workshop Rept. on Simulation Tech. for Shock Wave Phenomena and Characteristics of Plasma in Inertial Confinement Fusion Mar. 1985 p 199-209 refs (For primary document see N85-34670 23-75)
Avail: NTIS HC A11/MF A01

The global properties of Type I X-ray bursts can be successfully accounted for by the thermonuclear shell flash model of accreting neutron stars. According to this model, the luminosity of a relatively large burst approaches the Eddington luminosity. Near the peak of a large X-ray burst density in the neutron star atmosphere is so low that electron scattering opacity dominates over absorptive opacity. In such a situation, the X-ray spectrum emitted by the neutron star surface is performed from Planck spectrum by Compton scattering. The atmospheric structure and the photon energy spectrum of the X-ray bursting neutron star is calculated taking into account such Comptonization. From the X-ray spectrum, theoretical color temperature luminosity diagram (analog of the Hertzsprung-Russell diagram) is obtained. Comparing the theoretical diagram with observations the mass radius relationships of neutron stars and their distances to the galactic center can be estimated. Author

N85-34687# Osaka Univ., Suita (Japan). Inst. of Laser Engineering.
MULTIPLE INNER SHELL VACANCIES IN LASER-IRRADIATED Au PLASMA
S. Kiyokawa, T. Yabe, N. Miyanaga, K. Okada, H. Hasegawa, T. Mochizuki, T. Yamanaka, C. Yamanaka, and T. Kagawa (Nara Women's Univ.) *In* Nagoya Univ. Workshop Rept. on Simulation Tech. for Shock Wave Phenomena and Characteristics of Plasma in Inertial Confinement Fusion Mar. 1985 p 210-221 refs (For primary document see N85-34670 23-75)
Avail: NTIS HC A11/MF A01

The 14 line spectra of 3 approx. 4 keV from laser irradiated gold plasma are identified by the relativistic Hartree-Frock-Slater method, and are found to originate from the multiple inner shell vacancies produced via the Auger process. Furthermore, the relativistic effect, the spin orbit reaction, has been proven to appear in the spectra. From a diagnostic point of view, x-ray line spectra emitted by ions immersed in plasmas include much information on the plasmas and are a useful tool. For example, the existence of very highly charged ions (Gd36+, W45+, Mo13+, Xe25+, etc.), in laser produced and tokamak plasmas have been confirmed from the detailed analysis of the emitted x-ray spectra by Cu- and Zn-line ions, where the relativistic Hartree-Fock calculations have been carried out to identify the transition energies observed. F.M.R.

N85-34688# Osaka Univ., Suita (Japan). Inst. of Laser Engineering.
VECTOR CALCULATION OF PARTICLE CODE
A. Nishiguchi, S. Orii (Fujitsu Limited), and T. Yabe *In* Nagoya Univ. Workshop Rept. on Simulation Tech. for Shock Wave Phenomena and Characteristics of Plasma in Inertial Confinement Fusion Mar. 1985 p 222-226 refs (For primary document see N85-34670 23-75)
Avail: NTIS HC A11/MF A01

The development of a vector calculation for the particle code requires modification of the algorithm. Like many such algorithms, the particle code is an example of one which has suffered damage when fed into a supercomputer due to the danger of recurrent data processing. An algorithm is proposed which will liberate the particle code from recurrent calculations. It should be noted that the method may depend on the architecture of the supercomputer, i.e., it works well on the FACOM VP-100 and VP-200 computers,

i.e., the indirect data accessing must be vectorized and the speed should be fast. Author

N85-34689# Nagoya Univ. (Japan). Inst. of Plasma Physics.
DATA ON THE BACKSCATTERING COEFFICIENTS ON LIGHT IONS FROM SOLIDS: A REVISION
R. Ito, T. Tabata, N. Itoh, K. Morita, T. Kato, and H. Tawara Jun. 1985 153 p
(IPPJ-AM-41-Rev) Avail: NTIS HC A08/MF A01

Experimental data on the number-backscattering coefficient R sub N the energy-backscattering coefficient R sub E, and the mean fractional energy r sub e of backscattered particles are tabulated for H, D, He3, and He-4 ions normally incident on elemental solids. References through 1984 are covered. The dependence of R sub N and R sub E on incident energy is shown graphically for energies from 10 eV to 100 keV by plotting the experimental data, computer-simulation data, and new empirical formulas. Graphs are provided for the projectiles of H, D, T, He-3, and He4 ions incident on 40 elemental targets of atomic numbers from 3 to 92, and for H and He-4 ions incident on compound targets. The listings of the computer program to evaluate the empirical formulas are also given. The programs can be used for elemental and compound targets and for arbitrary angles of incidence. Author

N85-34690# Nagoya Univ. (Japan). Inst. of Plasma Physics.
LOW-ENERGY SPUTTERINGS WITH THE MONTE CARLO PROGRAM ACAT
Y. Yamamura and Y. Mizuno May 1985 61 p refs
(IPPJ-AM-40) Avail: NTIS HC A04/MF A01

The Monte Carlo program ACAT was developed to determine the total sputtering yields and angular distributions of sputtered atoms in physical processes. From computer results of the incident-energy dependent sputterings for various ion-target combinations the mass-ratio dependence and the bombarding-angle dependence of sputtering thresholds was obtained with the help of the Matsunami empirical formula for sputtering yields. The mass-ratio dependence of sputtering thresholds is in good agreement with recent theoretical results. The threshold energy of light-ion sputtering is a slightly increasing function of angle of incidence, while that of heavy-ion sputtering has a minimum value near theta = 60 deg. The angular distributions of sputtered atoms are also calculated for heavy ions, medium ions, and light ions, and reasonable agreements between calculated angular distributions and experimental results are obtained. Author

N85-34691# Sandia Labs., Albuquerque, N. Mex.
RADLAC TECHNOLGY REVIEW
R. B. Miller 1985 10 p refs Presented at Particle Accelerator Conf., Vancouver, British Columbia, 13 May 1985
(Contract DE-AC04-76DP-00789)
(DE85-011995; SAND-85-1133C; CONF-850504-32) Avail: NTIS HC A02/MF A01

The technology development associated with the RADLAC program is reviewed. A basic description of the pulsed transmission line approach for constructing high power electron linacs is given, and two examples, RADLAC I and RIIM, are described in some detail. Important problems associated with the design of the high current beam transport line are also discussed. A recirculating linac concept based on the use of closed accelerating cavities and ionization channel beam transport is described. DOE

N85-34692# Oak Ridge National Lab., Tenn.
COMPACT DT FUSION SPHERICAL TORI AT MODEST FIELD
M. Peng, S. K. Borowski, G. R. Dalton, G. E. Gorker, W. R. Hamilton, M. H. Kunselman, V. D. Lee, E. C. Selcow, and N. A. Uckan 1985 19 p Presented at the 6th Topical Meeting on the Technol. of Fusion Energy, San Francisco, 3 Mar. 1985
(Contract DE-AC05-84CR-21400)
(DE85-011568; CONF-850310-100) Avail: NTIS HC A02/MF A01

A spherical torus is obtained by retaining only the indispensable components on the inboard side of a tokamak plasma. It features an exceptionally small aspect ratio (around 1.5), a naturally elongated, D-shaped plasma cross section (2 to 1 elongation), and ramp-up and maintenance of the plasma current primarily by advanced methods. It takes on the spherical shape with a modest hole through the center, suggesting the name. DOE

N85-34693# Sandia Labs., Albuquerque, N. Mex.
REPETITIVE PULSE ACCELERATOR TECHNOLOGY FOR LIGHT ION INERTIAL CONFINEMENT FUSION
M. T. Buttram 1985 25 p refs Presented at the Particle Accelerator Conf., Vancouver, Canada, 13 May 1985
(Contract DE-AC04-76DP-00789)
(DE85-012030; SAND-85-0040C; CONF-850504-39) Avail: NTIS HC A02/MF A01

This paper will overview the technologies being studied for a repetitively pulsed ICF accelerator. As presently conceived, power is supplied by rotating machinery providing 16 MJ in 1 ms. The generator output is transformed to 3 MV, then switched into a pulse compression system using laser triggered spark gaps. These must be synchronized to about 1 ns. Pulse compression is performed with saturable inductor switches, the output being 40 ns, 1.5 MV pulses. These are transformed to 30 MV in a self-magnetically insulated cavity adder structure. Space charge limited ion beams are drawn from anode plasmas with electron counter streaming being magnetically inhibited. The ions are ballistically focused into the entrances of guiding discharge channels for transport to the pellet. The status of component development from the prime power to the ion sources will be reviewed. DOE

N85-34694# Oak Ridge National Lab., Tenn.
EXPERIMENTAL MEASUREMENTS OF THE ION CYCLOTRON ANTENNAS' COUPLING AND RF CHARACTERISTICS
D. J. Hoffman, F. W. Baity, W. R. Becraft, J. B. O. Caughman, and T. L. Owens 1985 26 p Presented at the 6th Topical Meeting on the Technol. of Fusion Energy, San Francisco, 3 Mar. 1985
(Contract DE-AC05-84OR-21400)
(DE85-011569; CONF-850310-98) Avail: NTIS HC A03/MF A01

The RF coupling capabilities and characteristics of various antennas have been measured. The tested antenna configurations include the simple loop antenna operated at resonant lengths as used on Alcator-C, the cavity antenna proposed for Doublet III-D and the resonant double loop, asymmetric resonant double loop, and U-slot antennas. Models of the voltage, magnetic fields outside the structure, and current have been correlated with the measurements made on these antennas. From these measurements and from typical observations of ICRH coupling in tokamaks, we are studying power and frequency limitations on each antenna and the causes of the limitations. A comparison of the echnology, performance, and power limitations of each type of antenna is presented. DOE

N85-34695# Oak Ridge National Lab., Tenn.
SHIELD DESIGN FOR NEXT-GENERATION, LOW-NEUTRON-FLUENCE, SUPERCONDUCTING TOKAMAKS
V. D. Lee and Y. Gohar (Argonne National Lab.) 1985 6 p refs Presented at the 6th Topical Meeting on the Technol. of Fusion Energy, San Francisco, 3 Mar. 1985
(Contract DE-AC05-84OR-21400)
(DE85-011409; CONF-850310-92) Avail: NTIS HC A02/MF A01

A shield design using stainless steel (SST), water, boron carbide, lead, and concrete materials was developed for the next-generation tokamak device with superconducting toroidal field (TF) coils and low neutron fluence. A device such as the Tokamak Fusion Core Experiment (TFCX) is representative of the tokamak design which could use this shield design. The unique feature of this reference design is that a majority of the bulk steel in the shield is in the form of spherical balls with two small, flat spots. The balls are purchased from ball-bearing manufacturers and are added as bulk shielding to the void areas of built-up, structural steel shells which form the torus cavity of the plasma chamber. This paper describes the design configuration of the shielding components. DOE

N85-34696# Los Alamos Scientific Lab., N. Mex.
SYNTHESIS OF ULTRAFINE CERAMIC AND METALLIC POWDERS IN A THERMAL ARGON rf PLASMA
G. J. Vogt, R. S. Vigil, L. R. Newkirk, and M. Trkula 1985 7 p refs Presented at the Symp. on Plasma Chem., Eindhoven, Netherlands, 1 Jul. 1985
(Contract W-7405-eng-36)
(DE85-009634; LA-UR-85-981; CONF-850714-1) Avail: NTIS HC A02/MF A01

Ultrafine powders of SiC, Si3N4, Ni, and Al2O3 were prepared in a rf plasma reactor, utilizing an induction plasma tube designed at Los Alamos. The primary particle size of the ceramic powders ranges from 5 to 50 nm. Silicon carbide and alumina are ultrapure crystalline powders, while silicon nitride is amorphous for surface areas greater than 100 m (2)/g. Plasma nickel powder will sinter to full density at 1073 K. DOE

N85-34697# Oak Ridge National Lab., Tenn.
LANGMUIR PROBE ON ISX-B
A. J. Wootton, K. E. Yokoyama, and P. H. Edmonds May 1985 23 p
(Contract DE-AC05-84OR-21400)
(DE85-012066; ORNL/TM-8938) Avail: NTIS HC A02/MF A01

The procedures used to derive temperature and density with a floating probe are documented. The accuracy of a Fourier analysis with restricted terms and the importance of various correction terms in calculating the density from the saturation current are discussed. Methods of reducing errors introduced by circuit resistance and fluctuations are presented. DOE

N85-34698# Sandia Labs., Albuquerque, N. Mex.
MEASUREMENT AND INTERPRETATION OF ELECTRON ANGLE AT MABE BEAM STOP
T. W. L. Sanford, P. D. Coleman, and J. W. Poukey 1985 4 p Presented at the Particle Accelerator Conf., Vancouver, British Columbia, 13 May 1985
(Contract DE-AC04-76DP-00789)
(DE85-011918; SAND-84-2421C; CONF-850504-37) Avail: NTIS HC A02/MF A01

Radiation measurements combined with a sophisticated simulation provides a simple but powerful tool for estimating beam temperature in intense pulsed annular electron beam accelerators. Specifically, the mean angle of incidence of a 60 kA, 7 MeV annular electron beam at the beam stop of the MABE accelerator and the transverse beam temperature are determined. The angle is extracted by comparing dose profiles measured downstream of the stop with that expected from a simulation of the electron/photon transport in the stop. By calculating and removing the effect on the trajectories due to the change in electric field near the stop, the beam temperature is determined. Such measurements help give insight to beam generation and propagation within the accelerator. DOE

N85-34699# Oak Ridge National Lab., Tenn.
ADVANCED TOROIDAL FACILITY (ATF)
P. B. Thompson 1985 6 p Presented at the 6th Topical Meeting on the Technol. of Fusion Energy, San Francisco, 3 Mar. 1985
(Contract DE-AC05-84OR-21400)
(DE85-011567; CONF-850310-99) Avail: NTIS HC A02/MF A01

The Advanced Toroidal Facility (ATF) is a new magnetic plasma confinement device, under construction at Oak Ridge National Laboratory (ORNL), which will lead to improvements in toroidal magnetic fusion reactors. ATF is a type of stellarator known as a torsatron which theoretically has the capability at greater than or equal to 8% beta in steady state. The ATF plasma has a major radius of 2.1 m, an average minor radius of 0.3 m, and a field of 2 T for a 5-s duration or 1 T steady state. The ATF device consists of a helical field (HF) coil set, a set of poloidal field (PF) coils, an exterior shell structure to support the coils, and a thin helically contoured vacuum vessel inside the coils. The ATF replaces the ISX-B tokamak at ORNL and will use the ISX-B auxiliary systems including 4 MW of neutral injection heating and 0.2 MW of electron cyclotron heating. ATF device is scheduled to start operation in the fall of 1986. An overview of the ATF device is presented including details of the construction process envisioned. DOE

N85-34700# California Univ., Livermore. Lawrence Livermore Lab.
TECHNOLOGY OF MAGNETICALLY DRIVEN ACCELERATORS
D. L. Birx, S. A. Hawkins, S. E. Poor, L. L. Reginato, D. Rogers, Jr., and M. W. Smith 26 Mar. 1985 21 p Presented at the Particle Accelerator Conf., Vancouver, British Columbia, 13 May 1985
(Contract W-7405-eng-48)
(DE85-011857; UCRL-91936; CONF-850504-33) Avail: NTIS HC A02/MF A01

The marriage of Induction Linac technology with Nonlinar Magnetic Modulators has produced some unique capabilities. It appears possible to produce electron beams with average currents measured in amperes, at gradients exceeding 1 MeV/meter, and with power efficiencies approaching 50%. A 2 MeV, 5 kA electron accelerator has been constructed at the Lawrence Livermore National Laboratory (LLNL) to demonstrate these concepts and to provide a test facility for high brightness sources. The pulse drive for the accelerator is based on magnetic pulse compressors with very high peak power capability, repetition rates exceeding a kilohertz and excellent reliability. DOE

N85-34701# Oak Ridge National Lab., Tenn. Fusion Energy Div.
MULTIPLE-FREQUENCY ELECTRON CYCLOTRON HEATING OF HOT ELECTRON RINGS IN EBT-1
D. A. Rasmussen, T. S. Bigelow, D. B. Batchelor, D. L. Hillis, G. R. Haste, B. H. Quon, and O. B. Hankins May 1985 22 p
(Contract DE-AC05-84OR-21400)
(DE85-011302; ORNL/TM-9372) Avail: NTIS HC A02/MF A01

The use of multiple-frequency microwave power for electron cyclotron heating (MFECH) significantly increased the ring stored energy in the SM-1 simple mirror device. MFECH was used on ELMO Bumpy Torus (EBT) in an effort to increase its hot electron beta. No substantial improvement in the ring parameters was observed in a series of two-frequency ECH experiments, with frequency separations up to 90 MHz, in contrast to the dramatic improvement found in the axisymmetric SM-1 experiment. The absence of superadiabatic behavior by the energetic electrons, combined with the effects of reduced heating efficiency and the additional ring losses introduced by the canting of the EBT mirror sectors, appears to limit the hot electron ring beta. DOE

N85-34702# Sandia Labs., Albuquerque, N. Mex.
LIGHT ION SOURCES FOR ICF
R. A. Gerber, K. W. Bieg, E. J. T. Burns, P. L. Dreike, J. Maenchen, T. A. Mehlhorn, J. N. Olden, A. L. Pregenzer, J. K. Rice, M. A. Sweeney et al 1985 11 p Presented at the Particle Accelerator Conf., Vancouver, British Columbia, 13 May 1985
(Contract DE-Ac04-76DP-00789)
(DE85-011544; SAND-85-0945C; CONF-850504-26) Avail: NTIS HC A02/MF A01

PBFA II, Sandia National Laboratories' (SNLA) advanced light-ion acclerator (now under construction), will deliver a 30-MV, 5 MA lithium ion experiments have been performed with proton beams, lithium ions were selected for PBFA II for several reasons. The use of lithium enables a large anode-cathode spacing, resulting in less impedance change during the pulse. Lithium ions have less magnetic deflection in the diode, so they can be focused for a longer period of time. Also, since the ionization potential of Li(+) is low, while that of L(++) is very large, a Li(+) source should be achievable without significant contamination from Li(++). Ions heavier than Li(+) would require operating voltages greater than 30 MV, or the ions would have to be accelerated in a multiple charged state. DOE

N85-34703# Wisconsin Univ., Madison. Dept. of Physics.
OBSERVATION OF HELICAL SAWTOOTH OSCILLATIONS IN A TOKAMAK

N. S. Brickhouse, T. H. Osborne, R. N. Dexter, and S. C. Prager Feb. 1985 11 p refs
(Contract DE-AC02-76ET-53051)
(DE85-012062; DOE/ET-53051/79) Avail: NTIS HC A02/MF A01

In the Tokapole II tokamak the three-dimensional structure of the rapid sawtooth crach which accompanies internal disruptions was observed. The sawtooth crach is helical, i.e., the decrease in soft X-ray intensity occurs along a q = 1 helical contour, in accord with the standard reconnection model. The poloidally asymmetric radial expansion of the crash inward from the q = 1 surface, provides a measure of the reconnection time consistent with single helicity reconnection from a growing, non-rotating magnetic island. DOE

N85-34704# Oak Ridge National Lab., Tenn.
STELLARATOR APPROACH TO FUSION PLASMA CONFINEMENT
J. H. Harris 1985 13 p refs Presented at the 12th Ann. Energy Technol. Conf. and Exposition, Washington, D.C., 25 Mar. 1985
(Contract DE-AC05-84CR-21400)
(DE85-011420; CONF-850301-7) Avail: NTIS HC A02/MF A01

The stellarator is a toroidal fusion plasma confinement device with nested magnetic flux surfaces. The required twist of the field lines is produced by external helical coils rather than by plasma current, as in a tokamak. Stellarator devices are attractive fusion reactor candidate precisely because they offer the prospect of steady-state operation without plasma current. In the last few years the excellent results achieved with currentless stellarator plasmas of modest minor radius (10 to 20 cm) at Kyoto University (Japan) and the Max Planck Institute (West Germany) have made the stellarator second only to the tokamak in its progress toward fusion breakeven, with temperatures T sub e, T sub i approx. 1 KeV, Lawson products n tau approx. 2 to 5 x 10 to the 12th power/cu cm/s, and volume-averaged beta values approx. = 2%. The Advanced Toroidal Facility (ATF), now under construction at Oak Ridge National Laboratory (ORNL) and scheduled to operate in 1986, represents a significant advance in stellarator research. DOE

N85-34705# Oak Ridge National Lab., Tenn.
ASSESSMENT OF MAGNETIC FIELD ASYMMETRIES IN ELMO BUMPY SQUARE
T. Uckan and N. A. Uckan 1985 8 p Presented at the 6th Topical Meeting on the Technol. of Fusion Energy, San Francisco, 3 Mar. 1985
(Contract DE-AC05-84OR-21400)
(DE85-011559; CONF-850310-97) Avail: NTIS HC A02/MF A01

There exist two separate and independent magnetic field asymmetries in the ELMO Bumpy Square (EBS). One is associated with the small perturbations in the magnetic field, known as the field errors, caused by coil misalignments during installation, imperfection in coil winding, etc. The second source of asymmetry is the magnetic field ripple in the high field toroidal solenoids (corners) produced by the finiteness of the number of coils. In general, these two sources of asymmetry introduce enhanced transport losses (in addition to other effects) to the system, although they affect different classes of particles. Toroidally passing (circulating) particles are influenced by the field errors, whereas trapped particles in the corners are influenced by the field ripple. In this paper we discuss these two effects separately and calculate the allowable magnitudes of the field error and field ripple in EBS, both for an experimental size device and for a reactor. DOE

N85-34706# California Univ., Livermore. Lawrence Livermore Lab.
PERSPECTIVE ON THE NEXT TEN YEARS IN PLASMA PHYSICS
John Killeen Apr. 1985 11 p refs Presented at the Workshop on Orbital Dyn. and Appl. to Accelerators, Berkeley, Calif., 7-12 Mar. 1985 Submitted for publication
(Contract W-7405-eng-48)
(DE85-011849; UCRL-92532; CONF-8503105-2) Avail: NTIS HC A02/MF A01

A brief survey of developments in the plasma physics of magnetic fusion research is presented. The major experimental facilities of the next decade are listed. Eight fusion physics issues are identified which must be addressed as a complete plasma system in order to reach the goal of a fusion reactor. In order to resolve the physics issues the results from these new experimental facilities must be augmented by an extensive program of computer modeling. The use of computer models of a magnetically confined plasma and the implemenation of these models on the new supercomputers of the next decade are the main topics. DOE

N85-34707# California Univ., Los Angeles. Center for Plasma Physics and Fusion Engineering.
ECH TOKAMAK
M. A. Firestone, T. K. Mau, and R. W. Conn Apr. 1985 13 p refs
(Contract DE-AT03-80ER-52061)
(DE85-012074; UCLA/PPG-860) Avail: NTIS HC A02/MF A01

A small steady-state tokamak capable of producing power in the 100 to 300 MWe range and relying on electron cyclotron RF heating (ECH) for both heating and current drive is described. Working in the first magnetohydrodynamic (MHD) stability regime for tokamaks, the approach adheres to the recently discovered maximum beta limit. An appropriate figure of merit is the ratio of the fusion power to absorbed RF power. Efficient devices are feasible at both small and large values of fusion power, thereby pointing to a development path for an attractive commercial fusion reactor. DOE

N85-34708# Oak Ridge National Lab., Tenn.
INSTRUMENT TO SYNCHRONIZE THOMSON SCATTERING DIAGNOSTIC MEASUREMENTS WITH MHD ACTIVITY IN A TOKAMAK
A. L. Wintenberg Apr. 1985 139 p
(Contract DE-AC05-84OR-21400)
(DE85-012082; ORNL/TM-9397) Avail: NTIS HC A07/MF A01

An instrument to synchronize the firing of a ruby laser for a Thomson scattering diagnostic with plasma oscillations was designed, developed, and evaluated. The instrument will fire the laser at a user-selected phase of an input sine or sawtooth wave with an accuracy of plus or minus 15(0). Allowable frequencies range from 20 to 500 Hz for a sawtooth and from 1 to 30 kHz for a sine wave. The instrument also allows synchronization with a sine wave to be enabled by a presented sawtooth phase. The instrument uses analog signal processing circuits to separate the signal components, remove unwanted components, and produce zero-phase synchronizating pulses. The instrument measures the period between zero-phase pulses in order to produce phase synchronization pulses delayed a fraction of the period from the zero-phase pulses. The laser is fired by the phase synchronization pulse. Unwanted signal components are attenuated by handpass filters. A digitally controlled self-adjusting bandpass filter for sine processing. The instrument was used to investigate the variation of the electron temperature profile with the phase of the x-ray signal from an Impurity Studies Experiment (ISX-B) plasma exhibiting magnetohydrodynamic (MHD) activity. DOE

N85-34709# Oak Ridge National Lab., Tenn.
CONFINEMENT EXPERIMENTS ON ISX-B
A. J. Wootton [1985] 35 p
(Contract DE-AC05-84OR-21400)
(DE85-012346; DOE/OR-21400/T125) Avail: NTIS HC A03/MF A01

The following topics are discussed: (1) direction of the experimental program, (2) status as of November 1982, (3) how to improve confinement, and implications for scaling of electron thermal diffusivity, (4) balanced beam injection, and (5) electric fields. DOE

N85-34710# Department of Energy, Washington, D. C.
METHOD OF PRECISELY MODIFYING PREDETERMINED SURFACE LAYERS OF A WORKPIECE BY CLUSTER ION

IMPACT THEREWITH Patent Application
L. Friedman, R. J. Beuhler, M. W. Matthew, and M. Ledbetter, inventors (to DOE) Filed 25 Jun. 1984 49 p
(Contract DE-AC02-76CH-00016)
(DE85-006519; US-Patent-Appl-SN-623874) Avail: NTIS HC A03/MF A01

A method is described of precisely modifying a selected area of a workpiece by producing a beam of charged cluster ions that is narrowly mass selected to a predetermined mean size of cluster ions within a range of 25 to 10 to the 6th power atoms per cluster ion, and accelerated in a beam to a critical velocity. The accelerated beam is used to impact a selected area of an outer surface of the workpiece at a preselected rate of impacts of cluster ions/sq cm/sec in order to effect a precise modification in that selected area of the workpiece. DOE

76 SOLID-STATE PHYSICS

Includes superconductivity.

For related information, see also *33 Electronics and Electrical Engineering* and *36 Lasers and Masers.*

N85-34711 British Library Lending Div., Boston Spa (England).
ON THE POTENTIAL LINK EQUATION OF A SPOT CENTRE WITH RELATIVE DEFORMATION FOR A SEMI-INFINITE MOLECULAR CRYSTAL
V. P. Konyshev and Yu. M. Laperdin 14 Aug. 1984 4 p refs Transl. into ENGLISH from Izv. Vysshikh Uchebn. Zavedenii, Chernaya Met. (Moscow), no. 12, 1983 p 134
(BLL-M-35795-(5828.4)) Avail: British Library Lending Div., Boston Spa, Engl.

An equation is proposed for the definition of equilibrium in molecular crystal lattices. A comparative analysis of the results shows. The possibility, in principle of creating an analytical method for the deformation characteristics of finite lattices with weak links. Author

N85-34712# Argonne National Lab., Ill.
MAGNITUDE AND RANGE OF THE RKKY INTERACTION IN SmRh4B4
B. D. Terris, K. E. Gray, and B. D. Dunlap Apr. 1985 10 p refs Presented at the Mater. and Mech. of Superconductivity Conf., Ames, Iowa, 29 May 1985
(Contract W-31-109-eng-38)
(DE85-012284; CONF-8505138-2) Avail: NTIS HC A02/MF A01

The superconductive and magnetic transition temperatures taken together are shown to provide a unique probe which separately determines both the magnitude and range of the RKKY interaction in the RERh4B4 magnetic-superconductors (RE = Er, Sm). Experimentally, an unexpected peak is found in the antiferromagnetic ordering temperature of SmRh4B4 vs. electron mean free path, while for ErRh4B4 the ferromagnetic ordering temperature decreases monotonically. These qualitative features, as well as the quanitative differences between SmRh4B4 and ErRh4B4, are in excellent agreement with calculations using a mean free path dependent RKKY interaction. DOE

N85-34713# Oak Ridge National Lab., Tenn.
FLUX-LINE LATTICE ANISOTROPY IN V3Si: OBSERVATION AND INTERPRETATION
D. K. Christen, H. R. Kerchner, S. T. Sekula, and Y. K. Chang Apr. 1985 16 p refs Presented at the Mater. and Mech. of Superconductivity Conf., Ames, Iowa, 29 May 1985
(Contract DE-AC05-84OR-21400)
(DE85-011935; CONF-8505138-1) Avail: NTIS HC A02/MF A01

The high T sub C A15 compound V2Si belongs to a small class of intrinsically high kappa, clean, type II superconductors. For such a material in the low field mixed state, the interflux line forces are dominated by the microscopic field interaction. Manifestations of anisotropic flux line (FL) interactions were observed directly by means of small angle neutron scattering (SANS) from the flux line lattice (FLL) in a high quality single crystal of V3Si. Pronounced correlations were found between the FLL morphology (orientation and symmetry) and the symmetry of the real crystal (CL) axis parallel to the applied field. Moreover, for a fixed sample orientation in the field, changes in the FLL symmetry with flux density B. The data were observed in terms of weak nonlocality in the electrodynamic response, and anisotropy in the Fermi surface and electron phonon interaction of the cubic material. A reciprocal space power series expansion for the mixed state free energy is obtained and fitted to the observed FLL morphology. The results are compared with those of previously measured H sub c2 and gap anisotropy. DOE

N85-34714# Oak Ridge National Lab., Tenn.
SURVEY OF MIXING IN METAL/INSULATOR SYSTEMS
B. B. Appleton 1985 10 p refs Presennted at the Workshop on Ion Mixing and Surface Alloyiny 2, Pasadena, Calif., 19 Apr. 1985
(Contract DE-AC05-84OR-21400)
(DE85-011938; CONF-8504116-3) Avail: NTIS HC A02/MF A01

The conclusions from this survey are: Ion beam mixing (and pulsed laser mixing) are valuable methods to induce interface interactions at low temperatures. In many cases one can control and tailor stoichiometries of mixing. In some cases ion beam (and pulsed laser) mixing can initiate reactions not possible by thermal processing. Nevertheless, equilibrium thermodynamic or chemical considerations have much greater influence in dictating materials interactions (phase formation) than any nonequilibrium aspects of ion bombardment. DOE

N85-34715# Pennsylvania State Univ., University Park.
GRAIN BOUNDARY AND SURFACE DIFFUSION IN OXIDE SYSTEMS Final Report, 1 Sep. 1978 - 30 Nov. 1984
V. S. Stubican Feb. 1985 32 p refs
(Contract DE-AC02-78ER-04998)
(DE85-007291; DOE/ER-04998/T5) Avail: NTIS HC A03/MF A01

Study of transport phenomena in refractory oxides is important to explain sintering, grain growth, mechanical, thermal and electrical properties of these materials. Volume, grain boundary and surface diffusion of CR-51 isotope in magnesia, alumina and spinel was studied. Mechanism of volume diffusion was found to be extrinsic and activation energy for the undoped crystals represents the activation energy for motion of an associated impurity. From the measurements of volume diffusion of CR-51 Cr-doped MgO crystals the energy of association of a Cr-vacancy pair was calculated to be 0.88 + or - 0.3 eV. No anisotropy of the volume diffusion was observed for the diffusion of Cr-51 in alumina crystals. A strong anisotropy in the grain boundary diffusion was observed. Mechanism of diffusion in grain boundaries of oxides is a dislocation pipe mechanism. Point defects play an important role in grain boundary diffusion and the grain boundary diffusion is influenced by the stoichiometry. Surface diffusion of Cr-51 on MgO, Al2O3 and MgAl2O4 surfaces are studied using an edge source technique. DOE

N85-34716# Washington Univ., Seattle. Dept. of Physics.
GAUGE INVARIANCE AND FRACTIONAL QUANTIZED HALL EFFECT
R. Tao and Yong-Shi Wu 1984 9 p refs
(Contract DE-AC06-81ER-40048; NSF DMR-79-20735)
(DE85-007832; DOE/ER-40048/10-P4) Avail: NTIS HC A02/MF A01

It is shown that gauge invariance arguments imply the possibility of fractional quantized Hall effect; the Hall conductance is accurately quantized to a rational value. The ground state of a system showing the fractional quantized Hall effect must be degenerate, the non-degenerate ground state can only produce the integral quantized Hall effect. DOE

N85-34717# Rolls-Royce Ltd., Derby (England). Materials Engineering Group.
COST EFFECTIVE SINGLE CRYSTALS: THE ROLLS ROYCE

APPROACH
M. J. Goulette, P. D. Spilling, and R. P. Arthey 1 Nov. 1984 11 p refs Presented at 5th Intern. Symp. on Superalloys, Seven Springs, England, 1984
(PNR-90262) Avail: NTIS HC A02/MF A01

The development of a cost effective single crystal technology, including single crystal casting technique, alloy development, and orientation measurement, is described. The first aspect led to the adoption of the technically more difficult seeding technique as a result of its greater flexibility. The second resulted in the development of a series of three alloys to meet specific turbine applications. The third requirement is met by the development of a rapid and accurate orientation measurement technique suitable for the production environment. Author (ESA)

77 THERMODYNAMICS AND STATISTICAL PHYSICS

Includes quantum mechanics; and Bose and Fermi statistics.

For related information see also *25 Inorganic and Physical Chemistry* and *34 Fluid Mechanics and Heat Transfer.*

No abstracts in this category.

80 SOCIAL SCIENCES (GENERAL)

Includes educational matters.

N85-34581# Open Univ., Milton (England). Academic Computing Service.
COMPUTER ANIMATION IN DISTANCE TEACHING
Joel M. Greenberg *In* Canadian Information Processing Society Graphics Interface 1985 1985 p 419-423 (For primary document see N85-34523 23-61)
Avail: NTIS HC A19/MF A01

81 ADMINISTRATION AND MANAGEMENT

Includes management planning and research.

N85-34718# Department of Energy, Washington, D. C. Office of Project and Facilities Management.
ANALYZING PERFORMANCE OF SMALL PROJECTS USING URS AND PMAS, INFORMATION PAMPHLET
Mar. 1985 64 p
(DE85-011964; DOE/MA-0184) Avail: NTIS HC A04/MF A01

Some basic tools used in the analysis of small project performance, the Uniform Reporting System (URS) and the Performance Measurement Analysis System (PMAS) are addressed. The flexibility inherent in the URS allows DOE project managers the latitude to negotiate with contractors several key elements in contract performance measurement. Through reviews of management systems documentation, analysis of reports, orientation briefings, and site visits, the project team can obtain a good understanding of how the contractor plans and controls work. This knowledge assists them in performing data analysis by understanding how the data is put together. The key performance measurement data, which are taken or calculated from the cost and schedule report, quantifies the overall effect of the small problems that the project manager frequently deals with. The PMAS easily permits management to periodically focus on contract performance trends and forecast contract cost at completion by using simple graphic displays and supporting reports. DOE

N85-34560# Sao Paulo Univ. (Brazil). Electrical Engineering Dept.
PROJECT MANAGEMENT USING GRAPHICS
Fabio Pettinati *In* Canadian Information Processing Society Graphics Interface 1985 1985 p 265-272 refs (For primary document see N85-34523 23-61)
Avail: NTIS HC A19/MF A01

N85-34719# Rolls-Royce Ltd., Derby (England). Operational Research Group.
DISCRETE SIMULATION MODELS - THEIR ROLE IN THE DESIGN, DEVELOPMENT AND MANAGEMENT OF INVENTORY CONTROL SYSTEMS
Tony Cooper 24 Jan. 1985 13 p Presented at BPICS Seminar, 24 Jan. 1985
(PNR-90249) Avail: NTIS HC A02/MF A01

Discrete event simulation models were used as testbeds for the design, development and management of computer-based inventory control/scheduling systems. Inventory management at Rolls-Royce, and a case study are described. Author (ESA)

N85-35145*# National Aeronautics and Space Administration, Washington, D. C.
MANAGEMENT OF LARGE-SCALE TECHNOLOGY
Arnold S. Levine *In its* A Spacefaring People 1985 p 39-53 refs (For primary document see N85-35142 23-99)
Avail: NTIS HC A08/MF A01; also available SOD HC $3.50 as 033-000-009-33-0 CSCL 05A

82 DOCUMENTATION AND INFORMATION SCIENCE

Includes information storage and retrieval technology; micrography; and library science.

For computer documentation see *61 Computer Programming and Software.*

N85-34540# IBM Italia, Rome.
AN INTEGRATED SYSTEM FOR PRINTING AND PUBLISHING APPLICATIONS
S. Cavaliere, M. Fantini, and A. Turtur *In* Canadian Information Processing Society Graphics Interface 1985 1985 p 125-132 refs (For primary document see N85-34523 23-61)
Avail: NTIS HC A19/MF A01

N85-34542# Brown Univ., Providence, R. I. Dept. of Computer Science.
A MODEL FOR A DOCUMENT MAINTENANCE SYSTEM
Matthew Kaplan *In* Canadian Information Processing Society Graphics Interface 1985 1985 p 139-146 refs Sponsored in part by IBM Corp. and Online Computer Library Center, Inc. (For primary document see N85-34523 23-61)
Avail: NTIS HC A19/MF A01

N85-34563# Canada Land Data Systems, Ottawa (Ontario). Lands Directorate.
APPLIED COMPUTER GRAPHICS IN A GEOGRAPHIC INFORMATION SYSTEM: PROBLEMS AND SUCCESSES
C. L. MacDonald and I. K. Crain *In* Canadian Information Processing Society Graphics Interface 1985 1985 p 291-296 refs (For primary document see N85-34523 23-61)
Avail: NTIS HC A19/MF A01

83 ECONOMICS AND COST ANALYSIS

Includes cost effectiveness studies.

No abstracts in this category.

84 LAW AND POLITICAL SCIENCE

Includes space law; international law; international cooperation; and patent policy.

N85-34720# Committee on Appropriations (U. S. Senate).
DEPARTMENT OF HOUSING AND URBAN DEVELOPMENT INDEPENDENT AGENCIES APPROPRIATION BILL, 1986
Washington GPO 1985 117 p Rept. to accompany H.R. 3038 presented by the Comm. on Appropriations to the 99th Congr., 1st Sess., 16 Jul. 1985
(S-Rept-99-129) Avail: US Capitol, Senate Document Room

The Department of Housing and Urban Development-Independent Agencies Appropriations Bill, 1986 is discussed. Various amendments are presented and an explaination of the contents of the bill is given. NASA programs, Antarctic research, environment protection, and construction projects are discussed. For individual title, see N85-34721.

N85-34721# Committee on Appropriations (U. S. Senate).
NATIONAL AERONAUTICS AND SPACE ADMINISTRATION RESEARCH AND DEVELOPMENT: PROGRAM DESCRIPTION
In its Dept. of Housing and Urban Develop. Independent Agencies Appropriation Bill, 1986 1985 p 62-71 (For primary document see N85-34720 23-84)
Avail: US Capitol, Senate Document Room

Appropriations for various NASA research programs are discussed. Space science and applications, space shuttles, space stations, the Hubble space elescope, and spacecraft tracking are among the topics discussed. Funding recommendations of the Committee are given. R.J.F.

N85-35144*# Pennsylvania Univ., Philadelphia.
SATELLITES AND POLITICS: WEATHER, COMMUNICATIONS, AND EARTH RESOURCES
Pamela Mack *In* NASA, Washington A Spacefaring People 1985 p 32-38 refs (For primary document see N85-35142 23-99)
Avail: NTIS HC A08/MF A01; also available SOD HC $3.50 as 033-000-009-33-0 CSCL 05D

85 URBAN TECHNOLOGY AND TRANSPORTATION

Includes applications of space technology to urban problems; technology transfer; technology assessment; and surface and mass transportation.

For related information see *03 Air Transportation and Safety, 16 Space Transportation,* and *44 Energy Production and Conversion.*

N85-34722* National Aeronautics and Space Administration. Pasadena Office, Calif.
SHUTTLE CAR LOADING SYSTEM Patent
Earl R. Collins, Jr., inventor (to NASA) (JPL, Pasadena, Calif.) Issued 27 Aug. 1985 8 p Filed 14 Jan. 1983 Supersedes N83-20155 (21 - 10, p 1526)
(NASA-Case-NPO-15949-1; US-Patent-4,537,554; US-Patent-Appl-SN-457990; US-Patent-Class-414-328; US-Patent-Class-414-288; US-Patent-Class-414-373; US-Patent-Class-414-786) Avail: US Patent and Trademark Office CSCL 13F

A system is described for loading newly mined material such as coal, into a shuttle car, at a location near the mine face where there is only a limited height available for a loading system. The system includes a storage bin having several telescoping bin sections and a shuttle car having a bottom wall that can move under the bin. With the bin in an extended position and filled with coal the bin sections can be telescoped to allow the coal to drop out of the bin sections and into the shuttle car, to quickly load the car. The bin sections can then be extended, so they can be slowly filled with more while waiting another shuttle car.
Official Gazette of the U.S. Patent and Trademark Office

88 SPACE SCIENCES (GENERAL)

No abstracts in this category.

89 ASTRONOMY

Includes radio and gamma-ray astronomy; celestial mechanics; and astrometry.

N85-34723*# Illinois Univ., Urbana-Champaign. Dept. of Physics.
QUASIPERIODIC OSCILLATIONS IN BRIGHT GALACTIC-BULGE X-RAY SOURCES
F. K. Lamb, N. Shibazaki, M. A. Alpar, and J. Shaham 10 Sep. 1985 32 p refs Submitted for publication
(Grants NsG-7653; NAGw-567; NAG8-497; NSF PHY-80-25605) (NASA-CR-176138; NAS 1.26:176138; P/85/8/132) Avail: NTIS HC A03/MF A01 CSCL 03A

Quasiperiodic oscillations with frequencies in the range 5-50 Hz have recently been discovered in X-rays from two bright galactic-bulge sources and Sco X-1. These sources are weakly magnetic neutron stars accreting from disks which the plasma is clumped. The interaction of the magnetosphere with clumps in the inner disk causes oscillations in the X-ray flux with many of the properties observed. Author

N85-34724*# National Radio Astronomy Observatory, Charlottesville, Va.
THE EXTENT OF THE LOCAL HI HALO
Felix J. Lockman, L. M. Hobbs (Yerkes Observatory), and J. Michael Shull (Joint Inst. for Lab. Astrophysics) 28 Aug. 1985 44 p refs Sponsored in part by NSF
(Grant NAG5-255)
(NASA-CR-176115; NAS 1.26:176115) Avail: NTIS HC A03/MF A01 CSCL 03A

Forty-five high-latitude, OB stars have been observed in the Ly alpha and 21 cm lines of HI in an effort to map out the vertical distribution and extent of the local HI halo. The 25 stars for which a reliable HI colum density can be obtained from Ly alpha lie between 60 and 3100 pc from the plane. The principal result is that the total column density of HI at $z > 1$ kpc is, on the average, 5 + or - 3 x 10 the 19th power/sq cm, or 15% of the total sub HI. At relatively low z the data toward some stars suggest a low effective scale height and fairly high average foreground density, while toward others the effective scale height is large and the average density is low. This can be understood as the result of irregularities in the interstellar medium. A model with half of the HI mass in clouds having radii of a few pc and a Gaussian vertical distribution with sigma sub 2 = 135 pc, and half of the mass in an exponential component with a scale height of 500 pc, gives a satisfactory fit to the data. The technique of comparing Ly alpha and 21 cm column densities is also used to discuss the problem of estimating the distance to several possibly subluminous stars. Author

90 ASTROPHYSICS

Includes cosmology; and interstellar and interplanetary gases and dust.

N85-34725*# Lowell Observatory, Flagstaff, Ariz.
THE 13 NOVEMBER 1984 OCCULTATION OF BD +08 DEG

0471 BY (1) CERES
L. H. Wasserman, R. L. Millis, O. G. Franz, M. F. AHearn (Maryland Univ., College Park), W. Osborn (Central Michigan Univ.), and A. Klemola (California Univ., Santa Cruz) 3 Sep. 1985 5 p refs
(Grant NSg-7603)
(NASA-CR-176106; NAS 1.26:176106) Avail: NTIS HC A02/MF A01 CSCL 03B

The 13 November 1984 occultation of BD +08 deg 0471 was discovered during a photographic search carried out with the 0.5 meter Carnegie Double Astrograph at Lick Observatory and the Lowell Observatory PDS microdensitometer. Such a search was stimulated by the curious fact that few favorably located occultations of AGK3 or SAO catalog starts by Ceres will occur during the 1980s. The occultation on 13 November, however, is a particularly good event. The star is 1000 cubic M in V, yielding a predicted drop at occultation of about 10%. Such a drop can be detected by small telescopes equipped with photoelectric photometers, but is too small to be seen visually. The track was predicted to cross the Caribbean, Florida, southern Texas, and Mexico. Based on this prediction, preparations were made to observe the event in Mexico using four portable occultation data systems. G.L.C.

N85-34726*# Missouri Univ., St. Louis. Dept. of Physics.
LOW-EXCITATION HERBIG-HARO OBJECTS AND INTERSTELLAR EXTINCTION Final Technical Report, 1 Aug. 1984 - 31 Jul. 1985
Richard D. Schwartz 31 Jul. 1985 2 p refs
(Grant NAG5-461)
(NASA-CR-176142; NAS 1.26:176142) Avail: NTIS HC A02/MF A01 CSCL 03B

Previous work on low-excitation Herbig-Haro (HH) objects has confirmed the existence of a strongly-enhanced hydrogen two-photon continuum which is produced by low-velocity shocks in neutral material. The theoretical two-photon energy distribution was compared with that observed for HH 43. With the addition of optical (3300 < lambda < 7000A) data to the ultraviolet (1200 < lambda < 3100A) data obtained with the I.U.E, the wavelength dependence of interstellar extinction toward HH 43 has been determined. G.L.C.

N85-34727*# National Aeronautics and Space Administration. Goddard Space Flight Center, Greenbelt, Md.
THE INTERNATIONAL COMETARY EXPLORER (ICE) WALLSHEET TEACHER'S GUIDE
Stephen P. Maran, ed. Jul. 1985 12 p refs
(NASA-TM-87498; TG-101/9-85; NAS 1.15:87498) Avail: NTIS HC A02/MF A01 CSCL 03B

On September 11, 1985, the veteran NASA spacecraft ISEE-3 which has been renamed the International Cometary Explorer (ICE) will make the first visit of a spacecraft to a comet. A teachers' guide to the NASA wallsheet on the ICE and its mission is presented. This circumstance of course results from the current interest in the return of Halley's Comet. This teacher's guide will be helpful in understanding scientists strong interest in sending the ICE spacecraft to investigate the tail of a much less famous object Comet Giacobin-Zinner. G.L.C.

N85-34674# Kyoto Univ. (Japan). Dept. of Physics.
NUMERICAL SIMULATION IN ASTROPHYSICS: SMOOTHED PARTICLE METHODS
Shoken M. Miyama *In* Nagoya Univ. Workshop Rept. on Simulation Tech. for Shock Wave Phenomena and Characteristics of Plasma in Inertial Connement Fusion refs (For primary document see N85-34670 23-75)
Avail: NTIS HC A11/MF A01

N85-34686# Tokyo Univ. (Japan). Dept. of Earth Science and Astronomy.
X-RAY SPECTRA OF BURSTING NEUTRON STARS
Toshikazu Ebisuzaki and Kenich Nomoto *In* Nagoya Univ. Workshop Rept. on Simulation Tech. for Shock Wave Phenomena and Characteristics of Plasma in Inertial Confinement Fusion Mar. 1985 p 199-209 refs (For primary document see N85-34670 23-75)
Avail: NTIS HC A11/MF A01

N85-34772*# Applied Physics Lab., Johns Hopkins Univ., Laurel, Md.
ENERGETIC ION ACCELERATION AT COLLISIONLESS SHOCKS
R. B. Decker and L. Vlahos *In* NASA. Goddard Space Flight Center 19th Intern. Cosmic Ray Conf., Vol. 4 Aug. 1985 p 166-169 refs (For primary document see N85-34729 23-92)
(Contract N00024-83-C-5301; NSF ATM-83-05537)
(SH-1.5-3) Avail: NTIS HC as boxed set only $200/MF A01 per volume or E99 per entire set CSCL 03B

N85-34773*# Applied Physics Lab., Johns Hopkins Univ., Laurel, Md.
ACCELERATION OF IONS AND ELECTRONS TO NEAR-COSMIC RAY ENERGIES IN A PERPENDICULAR SHOCK: THE JANUARY 6, 1978 EVENT
S. M. Krimigis and E. T. Sarris (Thrace Univ., Xanthi, Greece) *In* NASA. Goddard Space Flight Center 19th Intern. Cosmic Ray Conf., Vol. 4 Aug. 1985 p 170-173 refs (For primary document see N85-34729 23-92)
(Contract N00024-83-E-5301)
(SH-1.5-4) Avail: NTIS HC as boxed set only $200/MF A01 per volume or E99 per entire set CSCL 03B

N85-34774*# Kansas Univ., Lawrence.
PARTICLE ACCELERATION DUE TO SHOCKS IN THE INTERPLANETARY FIELD: HIGH TIME RESOLUTION DATA AND SIMULATION RESULTS
R. L. Kessel, T. P. Armstrong, R. Nuber, and J. Bandle *In* NASA. Goddard Space Flight Center 19th Intern. Cosmic Ray Conf., Vol. 4 Aug. 1985 p 174-177 refs (For primary document see N85-34729 23-92)
(Grant NSF ATM-79-25987)
(SH-1.5-5) Avail: NTIS HC as boxed set only $200/MF A01 per volume or E99 per entire set CSCL 03B

N85-34775*# Imperial Coll. of Science and Technology, London (England). Dept. of Physics.
PITCH ANGLE DISTRIBUTIONS OF 35-1000 keV PROTONS AT QUASI-PERPENDICULAR INTERPLANETARY SHOCKS
A. Balogh and G. Erdoes (Central Research Inst. for Physics) *In* NASA. Goddard Space Flight Center 19th Intern. Cosmic Ray Conf., Vol. 4 Aug. 1985 p 178-181 refs (For primary document see N85-34729 23-92)
(SH-1.5-6) Avail: NTIS HC as boxed set only $200/MF A01 per volume or E99 per entire set CSCL 03B

N85-34776*# Maryland Univ., College Park. Dept. of Physics and Astronomy.
SPATIAL DEPENDENCE OF THE LOCAL DIFFUSION COEFFICIENT MEASURED UPSTREAM OF THE NOVEMBER 12, 1978 INTERPLANETARY TRAVELING SHOCK
G. Gloeckler, F. M. Ipavich, B. Klecker (Max-Planck-Inst. fuer Extraterrestrische Physik, Garching, West Germany), D. Hovestadt (Max-Planck-Inst. fuer Extraterrestrische Physik, Garching, West Germany), and M. Scholer (Max-Planck-Inst. fuer Extraterrestrische Physik, Garching, West Germany) *In* NASA. Goddard Space Flight Center 19th Intern. Cosmic Ray Conf., Vol. 4 Aug. 1985 p 182-185 refs (For primary document see N85-34729 23-92)
(Contract NAS5-28704; Grants NAGw-101; NGR-21-002-224)
(SH-1.5-12) Avail: NTIS HC as boxed set only $200/MF A01 per volume E99 per entire set CSCL 03B

N85-34777*# Applied Physics Lab., Johns Hopkins Univ., Laurel, Md.
LATITUDE DEPENDENCE OF CO-ROTATING SHOCK ACCELERATION
R. E. Gold, L. J. Lanzerotti (Bell Telephone Lab, Inc., Murray Hill,

N.J.), C. G. Maclennan (Bell Telephone Lab., Inc., Murray Hill, N.J.), and S. M. Krimigis *In* NASA. Goddard Space Flight Center 19th Intern. Cosmic Ray Conf., Vol. 4 Aug. 1985 p 186-189 refs (For primary document see N85-34729 23-92)
(Contract N00024-83-C-5301)
(SH-1.5-14) Avail: NTIS HC as boxed set only $200/MF A01 per volume or E99 per entire set CSCL 03B

91 LUNAR AND PLANETARY EXPLORATION

Includes planetology; and manned and unmanned flights. For spacecraft design see *18 Spacecraft Design Testing, and Performance.* For space stations see *15 Launch Vehicles and Space Vehicles.*

N85-34728*# National Aeronautics and Space Administration. Goddard Space Flight Center, Greenbelt, Md.
COMPARISONS OF THE NORTH POLAR CAP OF MARS AND THE EARTH'S NORTHERN HEMISPHERE SNOW COVER
J. Foster, M. Owe, and Charles Capen (Solis Lacus Observatory) Feb. 1985 27 p refs
(NASA-TM-86191; NAS 1.15:86191) Avail: NTIS HC A03/MF A01 CSCL 03B

The boundaries of the polar caps of Mars have been measured on more than 3000 photographs since 1905 from the plate collection at the Lowell Observatory. For the Earth the polar caps have been accurately mapped only since the mid 1960's when satellites were first available to synoptically view the polar regions. The polar caps of both planets wax and wane in response to changes in the seasons, and interannual differences in polar cap behavior on Mars as well as Earth are intimately linked to global energy balance. In this study data on the year to year variations in the extent of the polar caps of Mars and Earth were assembled and analyzed together with data on annual variations in solar activity to determine if associations exist between these data. It was found that virtually no correlation exists between measurements of Mars north polar cap and solar variability. An inverse relationship was found between variations in the size of the north polar caps of Mars and Earth, although only 6 years of concurrent data were available for comparison. Author

92 SOLAR PHYSICS

Includes solar activity, solar flares, solar radiation and sunspots.

N85-34729*# National Aeronautics and Space Administration. Goddard Space Flight Center, Greenbelt, Md.
NINETEENTH INTERNATIONAL COSMIC RAY CONFERENCE. SH SESSIONS, VOLUME 4
Frank C. Jones, comp. Washington Aug. 1985 543 p refs Conf. held in La Jolla, Calif., 11-23 Aug. 1985 8 Vol.
(NASA-CP-2376-Vol-4; NAS 1.55:2376-Vol-4) Avail: NTIS HC as boxed set only $200/MF A01 per volume or E99 per entire set CSCL 03B

Papers submitted for presentation at the 19th International Cosmic Ray Conference are compiled. This volume covers solar and heliospheric phenomena, specifically, particle acceleration; cosmic ray compsotion, spectra, and anisotropy; propagation of solar and interplanetary energetic particles; solar-cycle modulation; and propagation of galactic particles in the heliosphere. For individual titles, see N85-34730 through N85-34861.

N85-34730*# New Hampshire Univ., Durham. Space Science Center.
THE PROPAGATION OF SOLAR FLARE PARTICLES IN A TURBULENT CORONAL LOOP
J. M. Ryan *In* NASA. Goddard Space Flight Center 19th Intern. Cosmic Ray Conf., Vol. 4 Aug. 1985 p 1 (For primary document see N85-34729 23-92)
(SH-1.1-3) Avail: NTIS HC as boxed set only $200/MF A01 per volume or E99 per entire set CSCL 03B

Energetic solar flare particles, both electrons and protons, must survive the turbulent environment of a flaring loop and propogate to the lower corona or chromosphere in order to produce hard X-ray and gamma ray bursts. This plasma turbulence, often observed in soft X-ray line widths to be in excess of 100 km/s, is presumably capable of efficiently scattering the fast flare particles. This prevents to some degree the free streaming of accelerated particles and depending on the amplitude of the turbulence, restricts the particles to diffusive propagation along the length of the loop to the target chromosphere. In addition this turbulence is capable of performing additional acceleration of the fast particles by the second order Fermi mechanism. For compact flares with rise times < 10s, the acceleration effect is small and the propagation of the particles is governed by spatial diffusion and energy loss in the ambient medium. The solution of the time dependent diffusion equation with velocity dependent diffusion and energy loss coefficients yields for the case of nonrelativistic protons particle precipitation rates which are necessary for calculating thick target gamma ray emission and also yields the total thin target emissivity. R.J.F.

N85-34731*# Max-Planck-Inst. fuer Radioastronomie, Bonn (West Germany).
STOCHASTIC PARTICLE ACCELERATION IN SOLAR FLARES
W. Droege and R. Schlickeiser *In* NASA. Goddard Space Flight Center 19th Intern. Cosmic Ray Conf., Vol. 4 Aug. 1985 p 2-5 refs (For primary document see N85-34729 23-92)
(SH-1.1-4) Avail: NTIS HC as boxed set only $200/MF A01 per volume or E99 per entire set CSCL 03B

It is proposed that particles during the second phase of solar flares are accelerated by stochastic resonant scattering off hydromagnetic waves and first order Fermi acceleration in shock waves generated in the impulsive phase of the flare. Solutions allow arbitrary power law momentum dependences of the momentum diffusion coefficient as well as the momentum diffusion coefficient as well as the momentum loss time. The acceleration time scale to a characteristic energy approximately 100 keV for protons can be as short as 5s. The resulting electron spectra show a characteristic double power law with a transition around 200 keV and are correlated to the proton spectra evaluated under equal boundary conditions, indicating that electrons and protons are accelerated by the same mechanism. The correlation between the different spectral indices in the electron double power law and between electron and proton spectra are governed by the ratio of first to second order acceleration and therefore allow a determination of the Alfven Mach number of the shock wave. Author

N85-34732*# National Aeronautics and Space Administration. Goddard Space Flight Center, Greenbelt, Md.
FIRST-ORDER SHOCK ACCELERATION IN SOLAR FLARES
Donald C. Ellison (Maryland Univ., College Park) and Reuven Ramaty *In its* 19th Intern. Cosmic Ray Conf., Vol. 4 Aug. 1985 p 6-9 refs (For primary document see N85-34729 23-92)
(SH-1.1-5) Avail: NTIS HC as boxed set only $200/MF A01 per volume or E99 per entire set CSCL 03B

The first order Fermi shock acceleration model is compared with specific observations where electron, proton, and alpha particle spectra are available. In all events, it is found that a single shock with a compression ratio as inferred from the low energy proton spectra can reasonably produce the full proton, electron, and alpha particle spectra. The model predicts that the acceleration time to a given energy will be approximately equal for electrons and protons and, for reasonable solar parameters, can be less than 1 sec to 100 MeV. V.L. (IAA)

N85-34733*# Applied Physics Lab., Johns Hopkins Univ., Laurel, Md. Applied Physics Lab.
PROMPT ACCELERATION OF IONS BY OBLIQUE TURBULENT

SHOCKS IN SOLAR FLARES

R. B. Decker and L. Vlahos *In* NASA. Goddard Space Flight Center 19th Intern. Cosmic Ray Conf., Vol. 4 Aug. 1985 p 10-13 refs (For primary document see N85-34729 23-92)

(SH-1.1-6) Avail: NTIS HC as boxed set only $200/MF A01 per volume or E99 per entire set CSCL 03B

Solar flares often accelerate ions and electrons to relativistic energies. The details of the acceleration process are not well understood, but until recently the main trend was to divide the acceleration process into two phases. During the first phase elctrons and ions are heated and accelerated up to several hundreds of keV simultaneously with the energy release. These mildly relativistic electrons interact with the ambient plasma and magnetic fields and generate hard X-ray and radio radiation. The second phase, usually delayed from the first by several minutes, is responsible for accelerating ions and electrons to relativistic energies. Relativistic electrons and ions interact with the solar atmosphere or escape from the Sun and generate gamma ray continuum, gamma ray line emission, neutron emission or are detected in space by spacecraft. In several flares the second phase is coincident with the start of a type 2 radio burst that is believed to be the signature of a shock wave. Observations from the Solar Maximum Mission spacecraft have shown, for the first time, that several flares accelerate particles to all energies nearly simultaneously. These results posed a new theoretical problem: How fast are shocks and magnetohydrodynamic turbulence formed and how quickly can they accelerate ions to 50 MeV in the lower corona? This problem is discussed. R.J.F.

N85-34734*# National Aeronautics and Space Administration. Goddard Space Flight Center, Greenbelt, Md.

FAST DRIFT KILOMETRIC RADIO BURSTS AND SOLAR PROTON EVENTS

E. W. Cliver (Air Force Geophysics Lab.), S. W. Kahler (Emmanuel Coll.), H. V. Cane, R. E. McGuire, T. T. vonRosenvinge, and R. G. Stone *In* NASA. Goddard Space Flight Center 19th Intern. Cosmic Ray Conf., Vol. 4 Aug. 1985 p 14-17 refs (For primary document see N85-34729 23-92)

(SH-1.1-7) Avail: NTIS HC as boxed set only $200/MF A01 per volume or E99 per enitre set CSCL 03B

Initial results of a comparative study of major fast drift kilometric bursts and solar proton events from Sep. 1978 to Feb. 1983 are presented. It was found that only about half of all intense, long duration (> 40 min above 500 sfu) 1 MHz bursts can be associated with F > 20 MeV proton events. However, for the subset of such fast drift bursts accompanied by metric Type 2 and/or 4 activity (approximately 40% of the total), the degree of association with > 20 MeV events is 80%. For the reverse association, it was found that proton events with J(> 20 MeV) 0.01 1 pr cm(-2)s(-1)sr(-1)MeV(-1) were typically (approximately 80% of the time) preceded by intense 1 MHz bursts that exceeded the 500 sfu level for times > 20 min (median duration approximately 35 min). Author

N85-34735*# Universidad Nacional Autonoma de Mexico, Mexico City. Inst. de Geofisica.

STUDY OF PHOTON EMISSION BY ELECTRON CAPTURE DURING SOLAR NUCLEI ACCELERATION, 1: TEMPERATURE-DEPENDENT CROSS SECTION FOR CHARGE CHANGING PROCESSES

J. Perez-Peraza, M. Alvarez, A. Laville (Inst. Nacional de Astrofisica, Optica y Electronica), and A. Gallegos (UPICSA) *In* NASA. Goddard Space Flight Center 19th Intern. Cosmic Ray Conf., Vol. 4 Aug. 1985 p 18-21 refs (For primary document see N85-34729 23-92)

(SH-1.1-8) Avail: NTIS HC as boxed set only $200/MF A01 per volume or E99 per entire set CSCL 03B

The study of charge changing cross sections of fast ions colliding with matter provides the fundamental basis for the analysis of the charge states produced in such interactions. Given the high degree of complexity of the phenomena, there is no theoretical treatment able to give a comprehensive description. In fact, the involved processes are very dependent on the basic parameters of the projectile, such as velocity charge state, and atomic number, and on the target parameters, the physical state (molecular, atomic or ionized matter) and density. The target velocity, may have also incidence on the process, through the temperature of the traversed medium. In addition, multiple electron transfer in single collisions intrincates more the phenomena. Though, in simplified cases, such as protons moving through atomic hydrogen, considerable agreement has been obtained between theory and experiments However, in general the available theoretical approaches have only limited validity in restricted regions of the basic parameters. Since most measurements of charge changing cross sections are performed in atomic matter at ambient temperature, models are commonly based on the assumption of targets at rest, however at Astrophysical scales, temperature displays a wide range in atomic and ionized matter. Therefore, due to the lack of experimental data , an attempt is made here to quantify temperature dependent cross sections on basis to somewhat arbitrary, but physically reasonable assumptions. R.J.F.

N85-34736*# Universidad Nacional Autonoma de Mexico, Mexico City. Inst. de Geofisica.

STUDY OF PHOTON EMISSION BY ELECTRON CAPTURE DURING SOLAR NUCLEI ACCELERATION. 2: DELIMITATION OF CONDITIONS FOR CHARGE TRANSFERT ESTABLISHMENT

J. Perez-Peraza, M. Alvarez, and A. Gallegos (UPICSA) *In* NASA. Goddard Space Flight Center 19th Intern. Cosmic Ray Conf., Vol. 4 Aug. 1985 p 22-25 refs (For primary document see N85-34729 23-92)

(SH-1.1-9) Avail: NTIS HC as boxed set only $200/MF A01 per volume or E99 per entire set CSCL 03B

The conditions for establishment of charge transfer during acceleration of nuclei up to Fe, for typical conditions of solar flare regions T = 5 x 10 to the 3rd power to 2.5 x 10 to the 8th power degrees K were explored. Results show that such conditions are widely assorted, depending on the acceleration mechanism, the kind of projections and their velocity, the target elements, the source temperature and consequently on the degree of ionization of matter and the local charge state of the accelerated ions. Nevertheless, in spite of that assorted behavior, there are some general tendencies that can be summarized as follows. In atomic H electron capture is systematically established from thermal energies up to high energies, whatever the element and for both acceleration process. For a given element and fixed temperature (T), the probability and energy domain of electron capture and loss with Fermi are higher than with Betatron acceleration. For a given acceleration process the heavier the ion the higher the probability and the wider the energy range for electron capture and loss. For given acceleration mechanism and fixed element the importance and energy domain of capture and loss increase with T: for those reasons, the energy range of charge equilibrium (illustrated with solid lines on the next figs.) is wider with Fermi and increases with temperature and atomic number of projectiles. For the same reasons, electron loss is smaller while the lighter the element, the lower the temperature and the Betatron process, such that there are conditions for which electron loss is not allowed at low energies, but only electron capture is established. R.J.F.

N85-34737*# Universidad Nacional Autonoma de Mexico, Mexico City. Inst. de Geofisica.

STUDY OF PHOTON EMISSION BY ELECTRON CAPTURE DURING SOLAR NUCLEI ACCELERATION. 3: PHOTON PRODUCTION EVALUATIONS

J. Perez-Peraza, M. Alvarez, and A. Gallegos (UPICSA) *In* NASA. Goddard Space Flight Center 19th Intern. Cosmic Ray Conf., Vol. 4 Aug. 1985 p 26-29 refs (For primary document see N85-34729 23-92)

(SH-1.1-10) Avail: NTIS HC as boxed set only $200/MF A01 per volume or E99 per entire set CSCL 03B

Lower limits of photon fluxes were evaluated from electron capture during acceleration in solar flares, because the arbitrary q sub c asterisk assumed in this work evolves very slow with velocity, probably much more slowly than the physical actual situation: in

fact, more emission is expected toward the IR region. Nevertheless the authors claim to show that the factibility of sounding acceleration processes, charge evolution processes and physical parameters of the source itself, by the observational analysis of this kind of emissions. For instance, it would be interesting to search observationally, for the predicted flux and energy drift of F sub e ions interacting with the atomic 0 and F sub e of the source matter, or, even more feasible for the X-ray lines at 4.2 keV and 2.624 + 0.003 KeV from Fe and S ions in ionized Fe at T = 10 to the 7th power K respectively, the 418 + or - 2 eV and 20 + or - 4 eV lines of Fe and S in ionized Fe at 5 x 10 to the 6th power K, which are predicted from Fermi acceleration. R.J.F.

N85-34738*# Universidad Nacional Autonoma de Mexico, Mexico City. Inst. de Geofisica.
STUDY OF NON-THERMAL PHOTON PRODUCTION UNDER DIFFERENT SCENARIOS IN SOLAR FLARES. 1: SCENARIOS AND FORMULATIONS
J. Perez-Peraza, M. Alvarez, and A. Gallegos (UPICSA) *In* NASA. Goddard Space Flight Center 19th Intern. Cosmic Ray Conf., Vol. 4 Aug. 1985 p 30-33 refs (For primary document see N85-34729 23-92)
(SH-1.2-2) Avail: NTIS HC as boxed set only $200/MF A01 per volume or E99 per entire set CSCL 03B

In order to study the overall phenomenology involved in solar flares, it is necessary to understand their individual manifestation before building a corresponding description of the global phenomenon. Here the concern is with the production of X and gamma rays in solar flares. Flares are initiated very often within the closed magnetic field configurations of active centers. According (2) when beta = kinetic energy density/magnetic energy density approximately < 0.2, the magnetic trap configuration is destructed within the time scale of the impulsive phase of flares (< 100 s). A first particle acceleration stage occurs during this phase as indicated by impulsive microwave and hard X-rays bursts. In some flare events, when the field strength beta is very high, the broken field lines may close again, such that later, in the course of the flash and main phases more hot plasma of very high conductivity is created, and so, the field and frozen plasma expand outward, as the kinetic pressure inside the closed loops increases. The magnetically trapped particles excite strong Alfven wave turbulence of small transverse scale. R.J.F.

N85-34739*# Universidad Nacional Autonoma de Mexico, Mexico City. Inst. de Geofisica.
STUDY OF NON-THERMAL PHOTON PRODUCTION UNDER DIFFERENT SCENARIOS IN SOLAR FLARES. 2: THE COMPTON INVERSE AND BREMSSTRAHLUNG MODELS AND FITTINGS
J. Perez-Peraza, M. Alvarez, A. Laville (Inst. Nacional de Astrofisica, Optica y Electronica), and A. Gallegos (UPICSA) *In* NASA. Goddard Space Flight Center 19th Intern. Cosmic Ray Conf., Vol. 4 Aug. 1985 p 34-37 refs (For primary document see N85-34729 23-92)
(SH-1.2-3) Avail: NTIS HC as boxed set only $200/MF A01 per volume or E99 per entire set CSCL 03B

Energy spectra of photons emitted from Bremsstrahlung (BR) of energetic electrons with matter, is obtained from the deconvolution of the electron energy spectra. It can be inferred that the scenario for the production of X-rays and gamma rays in solar flares may vary from event to event. However, it is possible in many cases to associated low energy events to impulsive acceleration, and the high energy phase of some events to stochastic acceleration. In both cases, flare particles seem to be strongly modulated by local energy losses. Electric field acceleration, associated to neutral current sheets is a suitable candidate for impulsive acceleration. Finally, that the predominant radiation process of this radiation is the inverse Compton effect due to the local flare photon field. R.J.F.

N85-34740*# National Aeronautics and Space Administration. Goddard Space Flight Center, Greenbelt, Md.
SPECTRAL AND SPATIAL PROPERTIES OF SOLAR MICROFLARES
G. M. Simnett (Birmingham Univ.) and B. R. Dennis *In its* 19th Intern. Cosmic Ray Conf., Vol. 4 Aug. 1985 p 38-41 refs (For primary document see N85-34729 23-92)
(SH-1.2-4) Avail: NTIS HC as boxed set only $200/MF A01 per volume or E99 per entire set CSCL 03B

Solar microflares are studied using both hard (> 28 keV) and soft (3.5 to 8.0 keV) X-ray observations. The soft X-ray events have durations > 3 m at 0.1x maximum intensity, and typically have similar rise and decay times. The fastest decay observed was > 15 s (1/e). Soft and hard X-ray intensities are uncorrelated. The events are very compact, consistent with a projected area approximately > 8 x 8 inches. They are normally not associated with H alpha or type 3 emissions and their time profiles suggest a thermal origin at the top of the chromosphere. If the primary energy release site is in the corona, an energy transfer agent consistent with the observations is a non-thermal proton beam. Author

N85-34741*# Observatoire de Paris-Meudon (France). Section d'Astrophysique.
TEMPORAL EVOLUTION OF AN ENERGETIC ELECTRON POPULATION IN AN INHOMOGENEOUS MEDIUM: APPLICATION TO SOLAR HARD X-RAY BURSTS
N. Vilmer, A. L. MacKinnon (Glasgow Univ.), and G. Trottet *In* NASA. Goddard Space Flight Center 19th Intern. Cosmic Ray Conf., Vol. 4 Aug. 1985 p 42-45 refs (For primary document see N85-34729 23-92)
(SH-1.2-6) Avail: NTIS HC as boxed set only $200/MF A01 per volume or E99 per entire set CSCL 03B

Energetic electrons accelerated during solar flares can be studied through the hard X-ray emission they produce when interacting with the solar ambient atmosphere. In the case of the non thermal hard X-ray emission, the instanteous X-ray flux emitted at one point of the atmosphere is related to the instantaneous fast electron spectrum at that point. A hard X-ray source model then requires the understanding of the evolution in space and time of the fast particle distribution. The physical processes involved here are energy losses due to Coulomb collisions and pitch angle scattering due to both collisions and magnetic field gradients. Author

N85-34742*# Observatoire de Paris-Meudon (France). Section d'Astrophysique.
QUANTITATIVE ANALYSIS OF FLARE ACCELERATED ELECTRONS THROUGH THEIR HARD X-RAY AND MICROWAVE RADIATION
K.-L. Klein and G. Trottet *In* NASA. Goddard Space Flight Center 19th Intern. Cosmic Ray Conf., Vol. 4 Aug. 1985 p 46-49 refs (For primary document see N85-34729 23-92)
(SH-1.2-7) Avail: NTIS HC as boxed set only $200/MF A01 per volume or E99 per entire set CSCL 03B

Hard X-ray and microwave modelling that takes into account the temporal evolution of the electron spectrum as well as the inhomogeneity of the magnetic field and the ambient medium in the radio source is presented. This method is illustrated for the June 29 1980 10:41 UT event. The implication on the process of acceleration/injection is discussed. R.J.F.

N85-34743*# California Univ., San Diego, La Jolla. Center for Astrophysics and Space Sciences.
AN EXTENDED SUPERHOT SOLAR FLARE X-RAY SOURCE
Hugh S. Hudson, K.-I. Ohki (Tokyo Astronomical Observatory), and S. Tsuneta (Inst. for Space and Astronautical Science, Tokyo) *In* NASA. Goddard Space Flight Center 19th Intern. Cosmic Ray Conf., Vol. 4 Aug. 1985 p 50-53 refs (For primary document see N85-34729 23-92)
(SH-1.2-8) Avail: NTIS HC as boxed set only $200/MF A01 per volume or E99 per entire set CSCL 03B

A superhot hard X-ray source in a solar flare occulted by the solar limb was identified. Its hard X-ray image was found to show great horizontal extent but little vertical extent. An H alpha brightening at the same limb position about an hour later suggests a multi-component loop prominence system, so that it appears

that a superhot source can evolve in the same manner as a normal solar soft X-ray source. The assignment of plausiable values to physical parameters in the source suggests (from the simplest form of classical thermal-conduction theory) that either new physics will be required to suppress conduction, or else that gradual energy release well after the impulsive phase of the flare must occur. In this respect too, the superhot source appears to resemble ordinary soft X-ray sources, except of course that its temperature is higher. R.J.F.

N85-34744*# Rikkyo Univ., Tokyo (Japan). Dept. of Physics
OBSERVATIONS OF SOLAR FLARE PHOTON ENERGY SPECTRA FROM 20 keV TO 7 MeV
M. Yoshimori, H. Watanabe, and N. Nitta (Tokyo Astronomical Observatory) *In* NASA. Goddard Space Flight Center 19th Intern. Cosmic Ray Conf., Vol. 4 Aug. 1985 p 54-57 refs (For primary document see N85-34729 23-92)
(SH-1.2-9) Avail: NTIS HC as boxed set only $200/MF A01 per volume or E99 per entire set CSCL 03B

Solar flare photon energy spectra in the 20 keV to 7 MeV range are derived from the Apr. 1, Apr. 4, apr. 27 and May 13, 1981 flares. The flares were observed with a hard X-ray and a gamma-ray spectrometers on board the Hinotori satellite. The results show that the spectral shape varies from flare to flare and the spectra harden in energies above about 400 keV. Effects of nuclear line emission on the continuum and of higher energy electron bremsstrahlung are considered to explain the spectral hardening. Author

N85-34745*# California Univ., San Diego, La Jolla. Center for Astrophysics and Space Sciences.
ION ENERGY STORAGE FOR POST-FLARE LOOPS
Hugh S. Hudson *In* NASA. Goddard Space Flight Center 19th Intern. Cosmic Ray Conf., Vol. 4 Aug. 1985 p 58-61 refs (For primary document see N85-34729 23-92)
(SH-1.2-10) Avail: NTIS HC as boxed set only $200/MF A01 per volume or E99 per entire set CSCL 03B

Low-energy non-thermal protons may have long lifetimes in coronal loops with low density and high temperature. If energy were stored in such protons in the initial phases of a solar flare, it could be released slowly during the later phases. Within the present observational limits for post-flare loops, this mechanism should be considered in addition to a field-line reconnection theory of the Kopp and Pneuman type. The thin-target gamma ray emission from the trapped protons is below present limits, but more sensitive observations can test the hypothesis. Author

N85-34746*# Moscow State Univ. (USSR). Inst. of Nuclear Physics.
TWO TYPES OF ELECTRON EVENTS IN SOLAR FLARES
E. I. Daibog, V. G. Kurt, Yu. I. Logachev, and V. G. Stolpovsky *In* NASA. Goddard Space Flight Center 19th Intern. Cosmic Ray Conf., Vol. 4 Aug. 1985 p 62-65 refs (For primary document see N85-34729 23-92)
(SH-1.2-11) Avail: NTIS HC as boxed set only $200/MF A01 per volume or E99 per entire set CSCL 03B

The fluxes and spectra of the flare electrons measured on board Venera-I3 and I4 space probes are compared with the parameters of the hard (E sub x approximately $>$ 55 keV) and thermal X-ray bursts. The electron flux amplitude has been found to correlate with flare importance in the thermal X-ray range (r approximately 0.8). The following two types of flare events have been found in the electron component of SCR. The electron flux increase is accompanied by a hard X-ray burst and the electron spectrum index in the approximately 25 to 200 keV energy range is gamma approximately 2 to 3. The electron flux increase is not accompanied by a hard X-ray burst and the electron spectrum is softer (Delta gamma approximately 0.7 to 1.0). Author

N85-34747*# National Aeronautics and Space Administration. Goddard Space Flight Center, Greenbelt, Md.
TWO CLASSES OF SOLAR ENERGETIC PARTICLE EVENTS ASSOCIATED WITH IMPULSIVE AND LONG DURATION SOFT X-RAY FLARES
H. V. Cane, R. E. McGuire, and T. T. vonRosenvinge *In its* 19th Intern. Cosmic Ray Conf., Vol. 4 Aug. 1985 p 66-69 refs (For primary document see N85-34729 23-92)
(SH-1.2-12) Avail: NTIS HC as boxed set only $200/MF A01 per volume or E99 per entire set CSCL 03B

Solar energetic particle events observed in space have different properties depending on the class of associated flare. Impulsive flares, which occur low in the corona in regions of high energy density, are associated with particle events which are deficient in protons. These events are rarely associated with coronal mass ejections and interplanetary shocks. The vast majority of large, high energy proton events are associated with long duration flares, many of which are also associated with fast coronal mass ejections and strong interplanetary shocks. Such flare events originate relatively high in the corona. Author

N85-34748*# Birmingham Univ. (England). Dept. of Space Research.
A DOMINANT ROLE FOR PROTONS AT THE ONSET OF SOLAR FLARES
G. M. Simnett *In* NASA. Goddard Space Flight Center 19th Intern. Cosmic Ray Conf., Vol. 4 Aug. 1985 p 70-73 refs (For primary document see N85-34729 23-92)
(SH-1.2-13) Avail: NTIS HC as boxed set only $200/MF A01 per volume or E99 per entire set CSCL 03B

It is suggested that recent observations have cast considerable doubt on the generally accepted explanation that non-thermal electron beams transfer most of the flare energy during the onset of solar flares. It is argued that non-thermal protons in the energy region 100 to 1000 keV are a more probable energy transfer mechanism. An important consequence of this hypothesis is that the hard X-ray burst must be thermal. Author

N85-34749*# Franklin Inst., Newark, Del.
THE ENERGY SPECTRA OF SOLAR FLARE ELECTRONS
Paul A. Evenson, Dietrich Hovestadt (Max-Planck Inst. for Extraterrestrial Physics), Peter Meyer (Chicago Univ.), and Dan Moses (Chicago Univ.) *In* NASA. Goddard Space Flight Center 19th Intern. Cosmic Ray Conf., Vol. 4 Aug. 1985 p 74-77 refs (For primary document see N85-34729 23-92)
(Contract NAS5-26680; Grant NGL-14-001-005)
(SH-1.2-14) Avail: NTIS HC as boxed set only $200/MF A01 per volume or E99 per entire set CSCL 03B

A survey of 50 electron energy spectra from .1 to 100 MeV originating from solar flares was made by the combination of data from two spectrometers onboard the International Sun Earth Explorer-3 spacecraft. The observed spectral shapes of flare events can be divided into two classes through the criteria of fit to an acceleration model. This standard two step acceleration model, which fits the spectral shape of the first class of flares, involves an impulsive step that accelerates particles up to 100 keV and a second step that further accelerates these particles up to 100 MeV by a single shock. This fit fails for the second class of flares that can be characterized as having excessively hard spectra above 1 MeV relative to the predictions of the model. Correlations with soft X-ray and meter radio observations imply that the acceleration of the high energy particles in the second class of flares is dominated by the impulsive phase of the flares. Author

N85-34750*# Universidad Nacional Autonoma de Mexico, Mexico City. Inst. de Geofisica.
ONSET OF SOLAR FLARES AS PREDICTED BY TWO-DIMENSIONAL MHD-MODELS OF QUIESCENT PROMINENCES
J. GalindoTrejo *In* NASA. Goddard Space Flight Center 19th Intern. Cosmic Ray Conf., Vol. 4 Aug. 1985 p 78-81 refs (For primary document see N85-34729 23-92)
(SH-1.3-1) Avail: NTIS HC as boxed set only $200/MF A01 per volume or E99 per entire set CSCL 03B

The close connection between the sudden disapperance (disparition brusque) of the quiescent prominences and the two-ribbon flares are well known. During this dynamic phase the prominence ascends rapidly (typically with a velocity about 100 Km/sec) and disappears. In another later stage is observed

material falling back into the chromosphere. The impact of this downfalling matter on the chromosphere produces the H brightening, which shows the symmetric double pattern. The occurence of the disparition brusque is thought to be a consequence of a plasma instability of magnetohydrostatic (MHD) structures. By means of the MHD-energy principle, the stability properties of four prominence models are analyzed. It is shown that all considered models undergo instabilities for parameters outside of the observed range at quiescent prominences. The possibility that such instabilities in the flare parameter range may indicate just the onset of a flare is considered. R.J.F.

N85-34751*# Birmingham Univ. (England). Dept. of Space Research.

THE STARTING CONDITIONS FOR AN OPTICALLY SMALL SOLAR GAMMA RAY FLARE

G. M. Simnett and J. M. Ryan (New Hampshire Univ.) *In* NASA. Goddard Space Flight Center 19th Intern. Cosmic Ray Conf., Vol. 4 Aug. 1985 p 82-85 refs (For primary document see N85-34729 23-92)

(SH-1.3-2) Avail: NTIS HC as boxed set only $200/MF A01 per volume or E99 per entire set CSCL 03B

It is suggested that optically small gamma-ray flares result from gradual pre-flare acceleration of protons over approximately 1,000 s by a series of magnetohydrodynamic shocks in the low corona. A fraction of the accelerated protons are trapped in the corona where they form a seed population for future acceleration. If the shock acceleration is sufficiently rapid proton energies may exceed the gamma-ray production threshold and trigger gamma-ray emission. This occurs without the total flare energy being necessarily large. Magnetic field geometry is an important parameter. Author

N85-34752*# California Univ., San Diego, La Jolla. Center for Astrophysics and Space Sciences.

ON THE DETECTABILITY OF KEY-MeV SOLAR PROTONS THROUGH THEIR NONTHERMAL LYMAN-ALPHA EMISSION

Richard C. Canfield and Ching-Ray Chang *In* NASA. Goddard Space Flight Center 19th Intern. Cosmic Ray Conf., Vol. 4 Aug. 1985 p 86-89 refs (For primary document see N85-34729 23-92)

(SH-1.3-5) Avail: NTIS HC as boxed set only $200/MF A01 per volume or E99 per entire set CSCL 03B

The intensity and timescale of nonthermal Doppler-shifted hydrogen L alpha photon emission as diagnostics of 10 keV to 10 MeV protons bombarding the solar chromosphere during flares are investigated. The steady-state excitation and ionization balance of the proton beam are determined, taking into account all important atomic interactions with the ambient chromosphere. For a proton energy flux comparable to the electron energy flux commonly inferred for large flares, L alpha wing intensities orders of magnitude larger than observed nonflaring values were found. Investigation of timescales for ionization and charge exchange leads researchers to conclude that over a wide range of values of mean proton energy and beam parameters, Doppler-shifted nonthermal L alpha emission is a useful observational diagnostic of the presence of 10 keV to 10 MeV superthermal proton beams in the solar flare chromosphere. Author

N85-34753*# Rikkyo Univ., Tokyo (Japan). Dept. of Physics.

OBSERVATIONS OF SOLAR FLARE GAMMA-RAYS AND PROTONS

M. Yoshimori and H. Watanabe *In* NASA. Goddard Space Flight Center 19th Intern. Cosmic Ray Conf., Vol. 4 Aug. 1985 p 90-93 refs (For primary document see N85-34729 23-92)

(SH-1.3-6) Avail: NTIS HC as boxed set only $200/MF A01 per volume or E99 per entire set CSCL 03B

Solar flare gamma-rays (4 to 7 MeV) and protons (8 to 500 MeV) were simultaneously observed from six flares on 1 Apr., 4 Apr., 27, Apr. 13, May 1981, 1 Feb. and 6 June 1982 by the Hinotori and GMS satellites. The relationship between 4 to 7 MeV gamma-ray fluences and peak 16 to 34 MeV proton fluxes for these flares are analyzed. It does not reveal an apparent correlation between these two parameters. The present result implies that the protons producing gamma-rays and the protons observed near the Earth do not always belong to the same population. Author

N85-34754*# National Aeronautics and Space Administration. Goddard Space Flight Center, Greenbelt, Md.

ENERGETIC PROTONS FROM A DISAPPEARING SOLAR FILAMENT

S. W. Kahler (Emmanuel College), E. W. Cliver (Air Force Geophysics Lab.), H. V. Cane, R. E. McGuire, R. G. Stone, and N. R. Sheeley, Jr. (NRL, Washington, D.C.) *In its* 19th Intern. Cosmic Ray Conf., Vol. 4 Aug. 1985 p 94-97 refs (For primary document see N85-34729 23-92)

(SH-1.3-7) Avail: NTIS HC as boxed set only $200/MF A01 per volume or E99 per entire set CSCL 03B

A solar energetic (E > 50 MeV) particle (SEP) event observed at 1 AU began about 15000 UT on 1981 December 5. This event was associated with a fast coronal mass ejection observed with the Solwind coronagraph on the P78-1 satellite. No metric type 2 or type 4 burst was observed, but a weak interplanetary type 2 burst was observed with the low frequency radio experiment on the International Sun-Earth Explorer-3 satellite. The mass ejection was associated with the eruption of a large solar quiescent filament which lay well away from any active regions. The eruption resulted in an H alpha double ribbon structure which straddled the magnetic inversion line. No impulsive phase was obvious in either the H alpha or the microwave observations. This event indicates that neither a detectable impulsive phase nor a strong or complex magnetic field is necessary for the production of energetic ions. Author

N85-34755*# National Aeronautics and Space Administration. Goddard Space Flight Center, Greenbelt, Md.

HELIOS 1 ENERGETIC PARTICLE OBSERVATIONS OF THE SOLAR GAMMA RAY FLARE EVENTS OF 7, 21 JUNE 1980 AND 3 JUNE 1982

Frank B. McDonald (NASA, Washington), M. A. I. VanHollebeke (Musee National des Sciences, Technique et Industrie, Paris), and James H. Trainor *In its* 19th Intern. Cosmic Ray Conf., Vol. 4 Aug. 1985 p 98-101 refs (For primary document see N85-34729 23-92)

(SH-1.3-8) Avail: NTIS HC as boxed set only $200/MF A01 per volume or E99 per entire set CSCL 03B

The observed characteristics of the energetic particles associated with the solar gamma-ray events of 3, 21 June 1980 and 3 June 1982 differ in several important aspects from the typical solar particle increases. They have flat energy spectra, are electron rich and have small precursors increases that begin some hours before the impulsive flare increase. Author

N85-34756*# Kiel Univ. (West Germany). Inst. fuer Reine und Angewandte Kernsphysik.

INJECTION OF ENERGETIC PARTICLES FOLLOWING THE GAMMA-RAY FLARES ON JUNE 7, 1980, AS OBSERVED ON HELIOS 1

H.-H. Neustock, G. Wibberenz, and B. Iwers *In* NASA. Goddard Space Flight Center 19th Intern. Cosmic Ray Conf., Vol. 4 Aug. 1985 p 102-105 refs (For primary document see N85-34729 23-92)

(SH-1.3-9) Avail: NTIS HC as boxed set only $200/MF A01 per volume or E99 per entire set CSCL 03B

On June 7, 1980, two flares with impulsive gamma-ray emission were observed at 0117 Ut and 0312 UT. Measurements of the University of Kiel cosmic-ray experiment on HELIOS-1 are presented. The first approx. 0.5 MeV electrons escaped from the Sun to interplanetary space simultaneously with the hard X-ray burst. For the 0312 UT flare the protons and alpha-particle in the 3 - 20 MeV/nucleon range were injected from the Sun with a delay of approx. 40 min, followed by two subsequent new emissions. Author

N85-34757*# Academy of Sciences (USSR), Leningrad. Physico-Technical Inst.

ULTRARELATIVISTIC ELECTRONS AND SOLAR FLARE GAM-

GAMMA-RADIATION

P. E. Semukhin and G. A. Kovaltsov *In* NASA. Goddard Space Flight Center 19th Intern. Cosmic Ray Conf., Vol. 4 Aug. 1985 p 106-109 refs (For primary document see N85-34729 23-92)
(SH-1.3-11) Avail: NTIS HC as boxed set only $200/MF A01 per volume or E99 per entire set CSCL 03B

Ten solar flares with gamma radiation in excess of 10 MeV were observed. Almost all took place within a heliolatitude greater than 60 deg, close to the solar limb, an indication of the essential anistropy of high-energy gamma radiation. This high-energy solar flare gamma radiation can be explained by the specific features of the bremsstrahlung of ultrarelativistic electrons trapped within the magnetic arc of the solar atmosphere, even if the acceleration of the electrons is anisotropic. F.M.R.

N85-34758*# Universidad Nacional Autonoma de Mexico, Mexico City. Inst. de Geofisica.

SOURCE ENERGY SPECTRA FROM DEMODULATION OF SOLAR PARTICLE DATA BY INTERPLANETARY AND CORONAL TRANSPORT

J. Perez-Peraza, M. Alvarez-Madrigal, F. Rivero, and L. I. Miroshnichenko (Academy of Sciences, USSR, Troitsk) *In* NASA. Goddard Space Flight Center 19th Intern. Cosmic Ray Conf., Vol. 4 Aug. 1985 p 110-113 refs (For primary document see N85-34729 23-92)
(SH-1.3-13) Avail: NTIS HC as boxed set only $200/MF A01 per volume or E99 per entire set CSCL 03B

The data on source energy spectra of solar cosmic rays (SCR), i.e. the data on the spectrum form and on the absolute SCR are of interest for three reasons: (1) the SCR contain the energy comparable to the total energy of electromagnetic flare radiation (less than or equal to 10 to the 32nd power ergs); (2) the source spectrum form indicates a possible acceleration mechanism (or mechanism); and (3) the accelerated particles are efficiently involved in nuclear electromagnetic and plasma processes in the solar atmosphere. Therefore, the data on SCR source spectra are necessary for a theoretical description of the processes mentioned and for the formulation of the consistent flare model. Below it is attempted to sound solar particle sources by means of SCR energy spectrum obtained near the Sun, at the level of the roots of the interplanetary field lines in the upper solar corona. Data from approx. 60 solar proton events (SPE) between 1956-1981. These data were obtained mainly by the interplanetary demodulation of observed fluxes near the Earth. Further, a model of coronal azimuthal transport is used to demodulate those spectra, and to obtain the source energy spectra. Author

N85-34759*# Potchefstroom Univ. for Christian Higher Education (South Africa). Dept. of Physics.

SPECTRA OF SOLAR PROTON GROUND LEVEL EVENTS USING NEUTRON MONITOR AND NEUTRON MODERATED DETECTOR RECORDINGS

P. H. Stoker *In* NASA. Goddard Space Flight Center 19th Intern. Cosmic Ray Conf., Vol. 4 Aug. 1985 p 114-117 refs (For primary document see N85-34729 23-92)
(SH-1.3-14) Avail: NTIS HC as boxed set only $200/MF A01 per volume or E99 per entire set CSCL 03B

Recordings on relativistic solar flare protons observed at Sanae, Antarctic, show that the percentage increase in counting rates of the neutron moderated detector (4NMD) is larger than the percentage increase in counting rates of the 3NM64 neutron monitor. These relative increases are described by solar proton differential spectra j sub s(P) = AP(beta). The power beta is determined for each event and the hardnesses of the temporal variations of beta, found for the ground level events (GLE) of 7 May, 1978 and 22 November, 1977. Author

N85-34760*# Academy of Sciences (USSR), Troitsk. Inst. of Terrestrial Magnetism.

GROUND INCREASE OF COSMIC RAY INTENSITY ON FEBRUARY 16, 1984

A. V. Belov, Ya. L. Blokh, E. A. Broshenko, V. N. Ishkov, and V. G. Yanke *In* NASA. Goddard Space Flight Center 19th Intern. Cosmic Ray Conf., Vol. 4 Aug. 1985 p 118-121 refs (For primary document see N85-34729 23-92)
(SH-1.3-15) Avail: NTIS HC as boxed set only $200/MF A01 per volume or E99 per entire set CSCL 03B

The event of February 16, 1984 is one of the two largest ground increases of solar cosmic rays (CR) in the last two cycles of solar activity. This event happended at a decrease of the 21-st cycle against a quiet background. Although at the beginning of 1984 the observed indices of solar activity were higher than those at the end of 1983, the day of February 16 16 may be characterized as very quiet. On that day the geomagnetic perturbance (Sigma F sub p = 14, A sub p = 7) was the lowest in February. After a small Forbush decrease due to the magnetic storm of February 12-13, the CR intensity almost completely recovered by February 16. Thus, the solar particles that came to the Earth on February 16 got into a practically unperturbed magnetosphere, and the variations of secondary CR induced by these particles were not superimposed on any other substantial variations of extraterrestrial or magnetospheric origin. G.L.C.

N85-34761*# Academy of Sciences (USSR), Irkutsk. Siberian Inst. of Terrestrial Magnetism, Ionosphere and Radio Wave Propagation.

THE SCR FLARE OF 16 FEBRUARY 1984 AS RECORDED BY THE SAYAN SPECTROGRAPH

S. A. Koslov, N. I. Pakhomov, L. A. Shapovalova, and A. L. Yanchukovsky *In* NASA. Goddard Space Flight Center 19th Intern. Cosmic Ray Conf., Vol. 4 Aug. 1985 p 122-125 refs (For primary document see N85-34729 23-92)
(SH-1.3-17) Avail: NTIS HC as boxed set only $200/MF A01 per volume or E99 per entire set CSCL 03B

The Sayan cosmic ray (CR) spectrograph recorded an SCR flare that occurred on 16 February 1984. Data from both 1-hour and 110-minute duration measurements in 10 channels with different energy sensitivity (of neutron monitors HM-64 located at different depths in the atmosphere, and of a neutron, multiple neutron and rigid mumeson component lead-less detector) is presented. The parameters of the SCR variation spectrum are evaluated and it is shown that the recording of multiple neutrons at the same geographic point and at the same level in the atmosphere provides information similar to that from a spectrographic complex of instruments. Author

N85-34762*# New Hampshire Univ., Durham.

TIME EXTENDED PRODUCTION OF NEUTRONS DURING A SOLAR FLARE

E. L. Chupp, D. J. Forrest, W. T. Vestrand, H. Dubrunner (Bern Univ.), E. O. Flueckiger (Bern Univ.), J. F. Cooper (Max-Planck-Inst. fuer Extraterrestriche Physik, Garching, West Germany), G. Kanbach (Mac-Planck-Inst. fuer Extraterrestriche Physik, Garching, West Germany), C. Reppin (Max-Planck-Inst. fuer Extraterrestriche Physik, Garching, West Germany), and G. H. Share (Naval Research Lab., Washington, D.C.) *In* NASA. Goddard Space Flight Center 19th Intern. Cosmic Ray Conf., Vol. 4 Aug. 1985 p 126-129 refs Sponsored in part by the Swiss National Science Foundation (For primary document see N85-34729 23-92)
(Contract NAS5-28609; NASA Order S-70926-A)
(SH-1.4-1) Avail: NTIS HC as boxed set only $200/MF A01 per volume or E99 per entire set CSCL 03B

The most energetic neutral emissions expected from solar flares are gamma rays (>10 MeV) from relativistic primary and secondary electron bremsstrahlung, from approx. 0 meson decay and from neutrons (> 50 MeV). Bremsstrahlung photon energies extend to that of the highest energy electron present, but the shape of the pi sup 0 gamma ray spectrum, peaking at 69 MeV, does not depend strongly on the proton spectrum above threshold, which is approx 292 MeV for meson production on protons. The highest energy neutrons observed indicate directly the highest energy ions which interact at the Sun, and the presence or absence of anergy cutoff in the acceleration process. The high-energy proton spectrum shape can be determined from the neutron spectrum. G.L.C.

N85-34763*# Franklin Inst., Newark, Del.
FURTHER OBSERVATIONS OF PROTONS RESULTING FROM THE DECAY OF NEUTRONS EJECTED BY SOLAR FLARES
Paul A. Evenson, Richard Kroeger (Chicago Univ.), and Peter Meyer (Chicago Univ.) *In* NASA. Goddard Space Flight Center 19th Intern. Cosmic Ray Conf., Vol. 4 Aug. 1985 p 130-133 refs (For primary document see N85-34729 23-92)
(Contract NAS5-26680; Grant NGL-14-001-005)
(SH-1.4-2) Avail: NTIS HC as boxed set only $200/MF A01 per volume or E99 per entire set CSCL 03B

The solar flare of 1984 April 24 produced a large gamma ray fluence with energy > 2MeV. The time profile of the interplanetary flux from this flare indicates the presence of decaying solar neutrons. This makes a total of three neutron flares so far observed by this method. The three flares are used to place constraints on the fluence and spectra of neutrons emitted by the Sun. Author

N85-34764*# Consiglio Nazionale delle Ricerche, Rome (Italy). Dept. di Fisica.
SUGGESTIONS FOR IMPROVING THE EFFICIENCY OF GROUND-BASED NEUTRON MONITORS FOR DETECTING SOLAR NEUTRONS
N. Iucci, M. Parisi, C. Signorini, M. Storini, and G. Villoresi *In* NASA. Goddard Space Flight Center 19th Intern. Cosmic Ray Conf., Vol. 4 Aug. 1985 p 134-137 refs (For primary document see N85-34729 23-92)
(SH-1.4-3) Avail: NTIS HC as boxed set only $200/MF A01 per volume or E99 per entire set CSCL 03B

On the occasion of the June 3, 1982 intense gamma-ray solar flare a significant increase in counting rate due to solar neutrons was observed by the neutron monitors of Junsfraujoch and Lomnicky Stit located at middle latitudes and high altitudes. In spite of a larger detector employed and of the smaller solar zenith angle, the ampliitude of the same event observed at Rome was much smaller and the statistical fluctuations of the salactic cosmic ray background higher than the ones registered at the two mountain stations, because of the greater atmospheric depth at which the Rome monitor is located. The effeciency for detecting a solar neutron event by a NM-64 monitor as a function of the Sun zenith angle, atmospheric depth and threshold rigidity of the station was studied. G.L.C.

N85-34765*# San Andres Univ., La Paz (Bolivia). Cosmic Ray Lab.
SEARCH FOR SOLAR NEUTRONS USING NM-64 EQUIPMENT
N. J. Martinic, A. Reguerin, E. Palenque, M. A. Taquichiri, M. Wada (Inst. of Physical and Chemical Research, Tokyo), A. Inoue (Inst. of Physical and Chemical Research, Tokyo), and K. Takahashi (Inst. of Physical and Chemical Research, Tokyo) *In* NASA. Goddard Space Flight Center 19th Intern. Cosmic Ray Conf., Vol. 4 Aug. 1985 p 138-141 refs (For primary document see N85-34729 23-92)
(SH-1.4-5) Avail: NTIS HC as boxed set only $200/MF A01 per volume or E99 per entire set CSCL 03B

Two years (1980 to 1982) neutron monitor data from the Chacaltaya (geographic coordinates: N16.32 deg W68. 15 deg; cutoff rigidity: 13.1 GV; altitude: 5,300 m a.s.l.) station has been scanned; the sampling time of the 12NM-64 neutron monitor is 5 min. The nucleonic component increases have been correlated with 66 hard X-, gamma rays satellite data from solar origin, as reported by several groups. Typical neutron monitor time profiles of the events are presented. Chree-analysis was performed discriminating the events according to its solar coordinates. Ground data from solar limb locii are more enhanced at the time of the onset than other geometrically visible flares. Chree histograms of neutron monitor output profiles are also presented from geometrically invisible events from the Chacaltaya station. B.W.

N85-34766*# Aerospace Corp., El Segundo, Calif. Space Sciences Lab.
A SEARCH FOR SOLAR NEUTRONS ON A LONG DURATION BALLOON FLIGHT
R. Koga, G. M. Frye, Jr. (Case Western Reserve Univ.), A. Owens (Case Western Reserve Univ.), B. V. Denehy (Melbourne Univ., Parkville, Australia), O. Mace (Melbourne Univ. Parkville, Australia), and J. Thomas (Melbourne Univ., Parkville, Australia) *In* NASA. Goddard Space Flight Center 19th Intern. Cosmic Ray Conf., Vol. 4 Aug. 1985 p 142-145 refs Sponsored in part by the Royal Australian AF, and by Australian Research Grants Committee (For primary document see N85-34729 23-92)
(Grant NSF ATM-82-06044)
(SH-1.4-6) Avail: NTIS HC as boxed set only $200/MF A01 per volume or E99 per entire set CSCL 03B

The EOSCOR 3 detector, designed to measure the flux of solar neutrons, was flown on a long duration RACOON balloon flight from Australia during Jan. through Feb, 1983. The Circumglobal flight lasted 22 days. No major solar activity occurred during the flight and thus only an upper limit to the solar flare neutrons flux is given. The atmospheric neutron response is compared with that obtained on earlier flights from Palestine, Texas. Author

N85-34767*# New Hampshire Univ., Durham.
NEUTRAL PION PRODUCTION IN SOLAR FLARES
D. J. Forrest, W. T. Vestrand, E. L. Chupp, E. Rieger (Max-Planck-Inst. fuer Extraterrestriche Physik, Garching, West Germany), J. F. Cooper (Max-Planck-Inst. fuer Extraterrestriche Physik, Garching, West Germany), and G. Share (Naval Research Lab.) *In* NASA. Goddard Space Flight Center 19th Intern. Cosmic Ray Conf., Vol. 4 Aug. 1985 p 146-149 refs Sponsored in part by Swiss National Science Foundation (For primary document see N85-34729 23-92)
(Contract NAS5-28609; NASA Order S-70926-A)
(SH-1.4-7) Avail: NTIS HC as boxed set only $200/MF A01 per volume or E99 per entire set CSCL 03B

The Gamma-Ray Spectrometer (GRS) on SMM has detected more than 130 flares with emission approx 300 keV. More than 10 of these flares were detected at photon energies > 10 MeV. Although the majority of the emission at 10 MeV must be from electron bremsstrahlung, at least two of the flares have spectral properties > 40 MeV that require gamma rays from the decay of neutral pions. It is found that pion production can occur early in the impulsive phase as defined by hard X-rays near 100 keV. It is also found in one of these flares that a significant portion of this high-energy emission is produced well after the impulsive phase. This extended production phase, most clearly observed at high energies, may be a signature of the acceleration process which produces solar energetic particles (SEP's) in space. Author

N85-34768*# Academy of Sciences (USSR), Leningrad. Ioffe Physico-Tecnical Inst.
HIGH ENERGY NEUTRON AND GAMMA-RADIATION GENERATED DURING THE SOLAR FLARES
G. E. Kocharov and N. Z. Mandzhavidze *In* NASA. Goddard Space Flight Center 19th Intern. Cosmic Ray Conf., Vol. 4 Aug. 1985 p 150-153 refs (For primary document see N85-34729 23-92)
(SH-1.4-8) Avail: NTIS HC as boxed set only $200/MF A01 per volume or E99 per entire set CSCL 03B

The problem of high energy neutrons and gamma rays generation in the solar conditions is considered. It is shown that due to a peculiarity of generation and propagation of neutrons corresponding solar flares should be localized at high heliolongitudes. Author

N85-34769*# Academy of Sciences (USSR), Leningrad. Ioffe Physico-Technical Inst.
ON THE ANGULAR AND ENERGY DISTRIBUTION OF SOLAR NEUTRONS GENERATED IN P-P REACTIONS
Yu. E. Efimov and G. E. Kocharov *In* NASA. Goddard Space Flight Center 19th Intern. Cosmic Ray Conf., Vol. 4 Aug. 1985 p 154-157 refs (For primary document see N85-34729 23-92)
(SH-1.4-9) Avail: NTIS HC as boxed set only $200/MF A01 per volume or E99 per entire set CSCL 03B

The problem of high energy neutron generation in P-P reactions in the solar atmosphere is reconsidered. It is shown that the angular distribution of emitted neutrons is anisotropic and the energy

spectrum of neutrons depends on the angle of neutron emission. Author

N85-34770*# Max-Planck-Inst. fuer Aeronomie, Katlenburg-Lindau (West Germany).

POSSIBLE DETECTION OF FLARE-GENERATED POSITRONS BY HELIOS 1 ON 3 JUN 1982

E. Kirsch, E. Keppler, and K. Richter *In* NASA. Goddard Space Flight Center 19th Intern. Cosmic Ray Conf., Vol. 4 Aug. 1985 p 158-161 refs (For primary document see N85-34729 23-92)
(SH-1.4-10) Avail: NTIS HC as boxed set only $200/MF A01 per volume or E99 per entire set CSCL 03B

The production of neutrons and gamma-ray lines by solar particles in the photosphere has been studied. The principal positron emiters which lead to the 0.51 MeV gamma-line are C-11 0-14, 0-15, N-13, Ne-19. The energies of the positrons form radioactive nuclei are of the order of few hundred keV. Positrons resulting from the pi(+) decay have energies of approx 10-100 MeV and cannot be measured by the MPAe-detector. Most of the positrons annihilate in the photosphere. A fraction however should be able to escape into the interplanetary space. Proton, electron and , for the first time, positron measurements (E = 152-546 keV) obtained by the MPAe-particle detector on board of Helios 1 are presented. B.W.

N85-34771*# Universidad Nacional Autonoma de Mexico, Villa Obregon. Inst. de Geofisica.

SHOCK AND STATISTICAL ACCELERATION OF ENERGETIC PARTICLES IN THE INTERPLANETARY MEDIUM

J. F. Valdes-Galicia, X. Moussas (Athens Univ.), J. J. Quenby (Imperial Coll.), F. Neubauer (Cologne Univ.), and R. Schwenn (Max-Planck Inst. fuer Aeronomie, Katlenburg-Lindau, West Germany) *In* NASA. Goddard Space Flight Center 19th Intern. Cosmic Ray Conf., Vol. 4 Aug. 1985 p 162-165 refs (For primary document see N85-34729 23-92)
(SH-1.5-1) Avail: NTIS HC as boxed set only $200/MF A01 per volume or E99 per entire set CSCL 03B

Definite evidence for particle acceleration in the solar wind came around a decade ago. Two likely sources are known to exist: particles may be accelerated by the turbulence resulting from the superposition of Alfven and Magnetosonic waves (Statistical Acceleration) or they may be accelerated directly at shock fronts formed by the interaction of fast and slow solar wind (CIR's) or by traveling shocks due to sporadic coronal mass ejections. Naurally both mechanisms may be operative. In this work the acceleration problem was tackled numerically using Helios 1 and 2 data to create a realistic representation of the Heliospheric plasma. Two 24 hour samples were used: one where there are only wave like fluctuations of the field (Day 90 Helios 1) and another with a shock present in it (Day 92 of Helios 2) both in 1976 during the STIP 2 interval. Transport coefficients in energy space have been calculated for particles injected in each sample and the effect of the shock studied in detail. B.W.

N85-34772*# Applied Physics Lab., Johns Hopkins Univ., Laurel, Md.

ENERGETIC ION ACCELERATION AT COLLISIONLESS SHOCKS **c90**

R. B. Decker and L. Vlahos *In* NASA. Goddard Space Flight Center 19th Intern. Cosmic Ray Conf., Vol. 4 Aug. 1985 p 166-169 refs (For primary document see N85-34729 23-92)
(Contract N00024-83-C-5301; NSF ATM-83-05537)
(SH-1.5-3) Avail: NTIS HC as boxed set only $200/MF A01 per volume or E99 per entire set CSCL 03B

An example is presented from a test particle simulation designed to study ion acceleration at oblique turbulent shocks. For conditions appropriate at interplanetary shocks near 1 AU, it is found that a shock with theta sub B n = 60 deg is capable of producing an energy spectrum extending from 10 keV to approx. 1 MeV in approx. 1 hour. In this case total energy gains result primarily from several separate episodes of shock drift acceleration, each of which occurs when particles are scattered back to the shock by magnetic fluctuations in the shock vicinity. B.W.

N85-34773*# Applied Physics Lab., Johns Hopkins Univ., Laurel, Md.

ACCELERATION OF IONS AND ELECTRONS TO NEAR-COSMIC RAY ENERGIES IN A PERPENDICULAR SHOCK: THE JANUARY 6, 1978 EVENT **c90**

S. M. Krimigis and E. T. Sarris (Thrace Univ., Xanthi, Greece) *In* NASA. Goddard Space Flight Center 19th Intern. Cosmic Ray Conf., Vol. 4 Aug. 1985 p 170-173 refs (For primary document see N85-34729 23-92)
(Contract N00024-83-E-5301)
(SH-1.5-4) Avail: NTIS HC as boxed set only $200/MF A01 per volume or E99 per entire set CSCL 03B

Acceleration of energetic ions to approx 200 MeV and electrons to approx 2 MeV were detected by the Low Energy Charged Particle (LECP) instrument on Voyager 2 in association with a quasiperpendicular shock of theta sub Bn - 87.5 deg at 1.9 AU. The measurments, obtained at a time resolution of approx. 1.2 sec, reveal structure of the energetic particle intensity enhancements down to a scale of the order of the particle gyroradius, and suggest that acceleration takes place within a gyrodiameter of the shock. The observations are consistent with the prediction of the shock drift acceleration (SDA) mechanism. The absence of any fluctuations in the magnetic field during the shock passage suggest that turbulence is not essential to the shock acceleration process in the interplanetary medium. Author

N85-34774*# Kansas Univ., Lawrence.

PARTICLE ACCELERATION DUE TO SHOCKS IN THE INTERPLANETARY FIELD: HIGH TIME RESOLUTION DATA AND SIMULATION RESULTS **c90**

R. L. Kessel, T. P. Armstrong, R. Nuber, and J. Bandle *In* NASA. Goddard Space Flight Center 19th Intern. Cosmic Ray Conf., Vol. 4 Aug. 1985 p 174-177 refs (For primary document see N85-34729 23-92)
(Grant NSF ATM-79-25987)
(SH-1.5-5) Avail: NTIS HC as boxed set only $200/MF A01 per volume or E99 per entire set CSCL 03B

Data were examined from two experiments aboard the Explorer 50 (IMP 8) spacecraft. The Johns Hopkins University/Applied Lab Charged Particle Measurement Experiment (CPME) provides 10.12 second resolution ion and electron count rates as well as 5.5 minute or longer averages of the same, with data sampled in the ecliptic plane. The high time resolution of the data allows for an explicit, point by point, merging of the magnetic field and particle data and thus a close examination of the pre- and post-shock conditions and particle fluxes associated with large angle oblique shocks in the interplanetary field. A computer simulation has been developed wherein sample particle trajectories, taken from observed fluxes, are allowed to interact with a planar shock either forward or backward in time. One event, the 1974 Day 312 shock, is examined in detail. B.W.

N85-34775*# Imperial Coll. of Science and Technology, London (England). Dept. of Physics.

PITCH ANGLE DISTRIBUTIONS OF 35-1000 keV PROTONS AT QUASI-PERPENDICULAR INTERPLANETARY SHOCKS **c90**

A. Balogh and G. Erdoes (Central Research Inst. for Physics) *In* NASA. Goddard Space Flight Center 19th Intern. Cosmic Ray Conf., Vol. 4 Aug. 1985 p 178-181 refs (For primary document see N85-34729 23-92)
(SH-1.5-6) Avail: NTIS HC as boxed set only $200/MF A01 per volume or E99 per entire set CSCL 03B

The characteristic features of the scatter-free acceleration process near perpendicular shocks are examined in the upstream and downstream pitch angle distributions of 35 to 1000 keV protons. Reasonable quantitative agreement is found between theoretical predictions and observations. The role played by bottle geometries, leading to enhanced acceleration, is highlighted. Author

N85-34776*# Maryland Univ., College Park. Dept. of Physics and Astronomy.

SPATIAL DEPENDENCE OF THE LOCAL DIFFUSION COEFFICIENT MEASURED UPSTREAM OF THE NOVEMBER 12, 1978

INTERPLANETARY TRAVELING SHOCK c90

G. Gloeckler, F. M. Ipavich, B. Klecker (Max-Planck-Inst. fuer Extraterrestrische Physik, Garching, West Germany), D. Hovestadt (Max-Planck-Inst. fuer Extraterrestrische Physik, Garching, West Germany), and M. Scholer (Max-Planck-Inst. fuer Extraterrestrische Physik, Garching, West Germany) *In* NASA. Goddard Space Flight Center 19th Intern. Cosmic Ray Conf., Vol. 4 Aug. 1985 p 182-185 refs (For primary document see N85-34729 23-92)

(Contract NAS5-28704; Grants NAGw-101; NGR-21-002-224)

(SH-1.5-12) Avail: NTIS HC as boxed set only $200/MF A01 per volume E99 per entire set CSCL 03B

Characteristics of wuprathermal particles accelerated by quasi-parallel interplanetary traveling shocks have been generally explained in terms of a first order Fermi mechanism. Such models require diffusive scattering of particles upstream of the shock. This scattering is characterized by a local diffusion coefficient, kappa, which is determined by the local power density of waves in the upstream region. The dependence of the diffusion coefficient of suprathermal upstream protons on distance from the November 12, 1978 interplanetary traveling shock using a different approach is studied. Unlike previous studies this method, which is based on measurements of particle streaming and intensity gradients, does not rely on predictions. The local spatial variations of Kappa upstream of the November 12, 1978 shock have been chosen for study because the characteristics of this quasi-parallel shock have been extensively studied, and also because of its favorable geometry (i.e. B field nearly radial). Author

N85-34777*# Applied Physics Lab., Johns Hopkins Univ., Laurel, Md.

LATITUDE DEPENDENCE OF CO-ROTATING SHOCK ACCELERATION c90

R. E. Gold, L. J. Lanzerotti (Bell Telephone Lab, Inc., Murray Hill, N.J.), C. G. Maclennan (Bell Telephone Lab., Inc., Murray Hill, N.J.), and S. M. Krimigis *In* NASA. Goddard Space Flight Center 19th Intern. Cosmic Ray Conf., Vol. 4 Aug. 1985 p 186-189 refs (For primary document see N85-34729 23-92)

(Contract N00024-83-C-5301)

(SH-1.5-14) Avail: NTIS HC as boxed set only $200/MF A01 per volume or E99 per entire set CSCL 03B

Energetic particle observations in the outer heliosphere (approx> 12 A. U.) by the LECP instruments on the Voyager 1 and Voyager 2 spacecraft are discussed that show a definite latitude dependence of the number and intensity of particle enhancements produced by corotating interplanetary regions during an interval when no solar energetic particle events were observed. The particle enhancements are fewer in number and less intense at higher (approx 20 deg.) heliolatitudes. However, the similar spectral shapes of the accelerated particles at the two spacecraft indicate that the acceleration process is the same at the two latitudes, but less intense at the higher latitude. Author

N85-34778*# National Aeronautics and Space Administration. Goddard Space Flight Center, Greenbelt, Md.

ELEMENTAL ABUNDANCES IN COROTATING EVENTS

T. T. vonRosenvinge and R. E. McGuire *In its* 19th Intern. Cosmic Ray Conf., Vol. 4 Aug. 1985 p 190 (For primary document see N85-34729 23-92)

(SH-1.5-15) Avail: NTIS HC as boxed set only $200/MF A01 per volume or E99 per entire set CSCL 03B

Large, persistent solar-wind streams in 1973 and 1974 produced corotating interaction regions which accelerated particles to energies of a few MeV/nucleon. The proton to helium ratio (H/He) was remarkably constant at a value (22 + or 5) equal to that in the solar wind (21 + or - 3), suggesting that particles were being accelerated directly out of the solar wind. Preliminary results were presented from a similar study approximately 11 years (i.e., one solar cycle) later. Corotating events have been identified by surveying the solar wind data, energetic particle time-histories and anisotropies. This data was all obtained from the ISEE-3/ICE spacecraft. These events also show H/He ratios similar to that in the solar wind. It is flund that in these cases there is evidence for H/He ratios which are significantly different from that of the solar wind but which are consistent with the range of values found in solar flare events. B.W.

N85-34779*# Kansas Univ., Lawrence.

SOLAR AND INTERPLANETARY PARTICLES AT 2 TO 4 MEV DURING SOLAR CYCLES 21, SOLAR CYCLE VARIATIONS OF EVENT SIZES, AND COMPOSITIONS

T. P. Armstrong, J. C. Shields, P. R. Briggs, and S. Eckes *In* NASA. Goddard Space Flight Center 19th Intern. Cosmic Ray Conf., Vol. 4 Aug. 1985 p 192-195 refs (For primary document see N85-34729 23-92)

(Grant NSF ATM-83-05537)

(SH-1.5-16) Avail: NTIS HC as boxed set only $200/MF A01 per volume or E99 per entire set CSCL 03B

In This paper 2 to 4 MeV/nucleon protons, alpha particles, and medium (CNO) nuclei in the near-Earth interplanetary medium during the years 1974 to 1981 are studied. This period contains both the solar activity minimum in 1976, and the very active onset phase of Solar Cycle 21. Characteristic compositional differences between the solar minimum and solar maximum ion populations have been investigated. Previous studies of interplanetary composition at these energies have concentrated on well-defined samples of the heliospheric medium. During flare particle events, the ambient plasma is dominated by ions accelerated in specific regions of the solar atmosphere; observation of the proton/alpha and alpha/medium ratios for flare events shows that there is marked compositional variability both during an event and from event to event suggesting the complicated nature of flare particle production and transport. B.W.

N85-34780*# Academy of Sciences (USSR), Yakutsk.

COSMIC RAY ACCELERATION BY STELLAR WIND. SIMULATION FOR HELIOSPHERE

S. I. Petukhov, A. A. Turpanov, and V. S. Nikolaev *In* NASA. Goddard Space Flight Center 19th Intern. Cosmic Ray Conf., Vol. 4 Aug. 1985 p 196-199 refs (For primary document see N85-34729 23-92)

(SH-1.5-17) Avail: NTIS HC as boxed set only $200/MF A01 per volume or E99 per entire set CSCL 03B

The solar wind deceleration by the interstellar medium may result in the existence of the solar wind terminal shock. In this case a certain fraction of thermal particles after being heated at the shock would obtain enough energy to be injected to the regular acceleration process. An analytical solution for the spectrum in the frame of a simplified model that includes particle acceleration at the shock front and adiabatic cooling inside the stellar wind cavity has been derived. It is shown that the acceleration of the solar wind particles at the solar wind terminal shock is capable of providing the total flux, spectrum and radial gradients of the low-energy protons close to one observed in the interplanetary space. B.W.

N85-34781*# California Inst. of Tech., Pasadena.

THE ENERGY SPECTRUM OF JOVIAN ELECTRONS IN INTERPLANETARY SPACE

S. P. Christon, A. C. Cummings, E. C. Stone, and W. R. Webber (New Hampshire Univ.) *In* NASA. Goddard Space Flight Center 19th Intern. Cosmic Ray Conf., Vol. 4 Aug. 1985 p 200 refs (For primary document see N85-34729 23-93)

(Contract NAS7-918; Grant NGR-05-002-160)

(SH-1.5-18) Avail: NTIS HC as boxed set only $200/MF A01 per volume or E99 per entire set CSCL 03B

The energy spectrum of electrons with energies approx 10 to approx 180 MeV measured with the electron telescope on the Voyager 1 and 2 spacecraft in interplanetary space from 1978 to 1983 is studied. The kinetic energy of electrons is determined by double dE/dx measurements from the first two detectors (D sub 1, D sub 2) of a stack of eight solid state detectors and by the range of particle penetration into the remaining six detectors (D sub 3 to D sub 8) which are interleaved with tungsten absorbers. From 1978 to 1983 (radial range approx 2 to approx 12 AU) electrons of Jovian origin were clearly observable for electrons stopping in D sub 3(e> or MeV) and in D sub 4 (E> or = 8

MeV). . For electrons stopping in D sub 5 (E> or = 12 MeV), the jovian flux dominated the galactic electron flux for a period of approximately one year near the encounter with Jupiter. Jovian electrons were also observed in D sub 6(E> or = 21 Mev) 1 MeV but not in D sub 7(E> 28 MeV). A detailed interpretation of the electron variations in all energy channels depends on an accurate subtraction of background induced by energetic protons of a few 100 MeV. This substraction is facilitated by laboratory calibration results at several energies. Further results on the differential energy spectrum of Jovian electrons and limits on the maximum detected energies will be reported. Author

N85-34782*# Franklin Inst., Newark, Del.
THE JOVIAN ELECTRON SPECTRUM: 1978-1984
Paul A. Evenson, Peter Meyer (Chicago Univ.), and Dan Moses (Chicago Univ.) *In* NASA. Goddard Space Flight Center 19th Intern. Cosmic Ray Conf., Vol. 4 Aug. 1985 p 201-204 refs (For primary document see N85-34729 23-93)
(Contract NAS5-26680; Grant NGL-14-01-005)
(SH-1.5-19) Avail: NTIS HC as boxed set only $200/MF A01 per volume or E99 per entire set CSCL 03B

Observations of Jovian electrons through six consecutive 13-month Jovian synodic periods from 1978 to 1984 have been made by the University of Chicago electron spectrometer onboard the ISEE-3 (ICE) spacecraft. The Jovian electron spectrum was determined from 5 to 30 Mev and was found to have a shape which is not a power law in kinetic energy, but cuts off at approximately 30 MeV. The average shape of the spectrum over each of the six intervals of best magnetic connection remains the same for all intervals within uncertainties. Author

N85-34783*# Moscow State Univ. (USSR). Inst. of Nuclear Physics.
OBSERVATION OF THE FLUXES OF NUCLEI WITH ENERGIES 10-20 MEV PER NUCLEON DURING THE SOLAR FLARE OF APRIL 26, 1984
V. V. Bobrovskaya, N. L. Grigorov, D. A. Zhuravlev, M. A. Kondratyeva, R. A. Nymmik, Ch. A. Tretyakova, N. V. Alekseev, P. V. Vakulov, and V. P. Sechinov *In* NASA. Goddard Flight Center 19th Intern. Cosmic Ray Conf., Vol. 4 Aug. 1985 p 205-208 refs (For primary document see N85-34729 23-92)
(SH-2.1-1) Avail: NTIS HC as boxed set only $200/MF A01 per volume or E99 per entire set CSCL 03B

Observations of the fluxes of low energy nuclei in the Earth's magnetosphere are reported. The energy distribution and the composition of the nuclear component of cosmic rays observed during the solar flare of April 26, 1984 are presented. Author

N85-34784*# National Aeronautics and Space Administration. Goddard Space Flight Center, Greenbelt, Md.
ENERGETIC PARTICLE OBSERVATIONS OF THE SOLAR-GAMMA RAY/NEUTRON FLARE EVENTS OF 3 JUN 1982 AND 21 JUNE 1980 ISOTOPIC AND CHEMICAL COMPOSITION
M. A. I. vanHollebeke (Musee National des Sciences), Frank B. McDonald (NASA, Washington), and James H. Trainor *In its* 19th Intern. Cosmic Ray Conf., Vol. 4 Aug. 1985 p 209-212 refs (For primary document see N85-34729 23-92)
(SH-2.1-3) Avail: NTIS HC as boxed set only $200/MF A01 per volume or E99 per entire set CSCL 03B

Studies of the charge composition of two solar gamma ray/neutron-flare events reveal a striking enrichment of iron relative to oxygen with a smaller enrichment of intermediate nuclei. He/O is also enhanced and moderate amounts of He-3 are detected but there is no evidence for H-2 or H-3. Author

N85-34785*# California Inst. of Tech., Pasadena.
PRECISION MEASUREMENTS OF SOLAR ENERGETIC PARTICLE ELEMENTAL COMPOSITION
H. Breneman and E. C. Stone *In* NASA. Goddard Space Flight Center 19th Intern. Cosmic Ray Conf., Vol. 4 Aug. 1985 p 215-216 refs (For primary document see N85-34729 23-92)
(Contract NAS7-918; Grant NGR-05-002-160)
(SH-2.1-4) Avail: NTIS HC as boxed set only $200/MF A01 per volume or E99 per entire set CSCL 03B

Data from the Cosmic Ray Subsystem (CRS) aboard the Voyager 1 and 2 spacecraft were used to determined, solar energetic particle abundances or upper limits for all elements with $< Z < 30$ from a combined set of 10 solar flares during the 1977 to 1982 time period. Statistically meaningful abundances were determined for several rare elements including P, C1, K, Ti and Mn, while the precision of the mean abundances for the more abundant elements was proved. When compared to solar photospheric spectroscopic abundances, these new SEP abundances more clearly exhibit the step-function dependence on first ionization potential previously reported. E.A.K.

N85-34786*# California Inst. of Tech., Pasadena.
SOLAR CORONAL AND PHOTOSPHERIC ABUNDANCES FROM SOLAR ENERGETIC PARTICLE MEASUREMENTS
H. Breneman and E. C. Stone *In* NASA. Goddard Space Flight Center 19th Intern. Cosmic Ray Conf., Vol. 4 Aug. 1985 p 217-220 refs (For primary document see N85-34729 23-92)
(Contract NAS7-918; Grant NGR-05-002-160)
(SH-2.1-5) Avail: NTIS HC as boxed set only $200/MF A01 per volume or E99 per entire set CSCL 03B

Solar energetic particle (SEP) elemental abundance data from the cosmic ray subsystem (CRS) aboard the Voyager 1 and 2 spacecraft are used to derive unfractionated coronal and photospheric abundances for elements with $3 < Z <$ or $= 30$. It is found that the ionic charge-to-mass ratio (Q/M) is the principal organizing parameter for the fractionation of SEPs by acceleration and propagation processes and for flare-to-flare variability, making possible a single-parameter Q/M-dependent correction to the average SEP abundances to obtain unfractionated coronal abundances. A further correction based on first ionization potential allows the determination of unfractionated photospheric abundances. E.A.K.

N85-34787*# Tata Inst. of Fundamental Research, Bombay (India).
SILICON TO IRON ABUNDANCES IN SOLAR COSMIC RAYS AND IN THE SUN
M. N. Vahia, S. Biswas, and N. Durgaprasad *In* NASA. Goddard Space Flight Center 19th Intern. Cosmic Ray Conf., Vol. 4 Aug. 1985 p 221-224 refs (For primary document see N85-34729 23-92)
(SH-2.1-6) Avail: NTIS HC as boxed set only $200/MF A01 per volume or E99 per entire set CSCL 03B

Differential spectra of even charged nuclei between Si and Fe in the August 4, 1972 event were made in the energy region of 10 to 40 MeV/n-1 using rocket borne plastic detectors. The resulting relative abundances of elements and low energy enhancements are obtained and compared with spectroscopically determined photospheric abundances. The implications of the relative abundances on the acceleration mechanisms is discussed. E.A.K.

N85-34788*# National Aeronautics and Space Administration. Goddard Space Flight Center, Greenbelt, Md.
VARIATIONS IN ELEMENTAL COMPOSITION OF SEVERAL MEV/NUCLEON IONS OBSERVED IN INTERPLANETARY SPACE
R. E. McGuire, T. T. vonRosenvinge, and D. V. Reames *In its* 19th Intern. Cosmic Ray Conf., Vol. 4 Aug. 1985 p 225-228 refs (For primary document see N85-34729 23-92)
(Grant NGR-21-002-316)
(SH-2.1-7) Avail: NTIS HC as boxed set only $200/MF A01 per volume or E99 per entire set CSCL 03B

Six years of accumulated ISEE-3 and IMP-8 data to study. variations in elemental relative abundances among the different populations of energetic ions seen in interplanetary space are surveyed. Evidence suggesting that heavy ion enrichments may be organized by a rigidity scaling factor A/Z over the range H to Fe is presented. Data to support the hypothesis that shock-associated particles are probably accelerated from ambient energetic fluxes are shown. E.A.K.

N85-34789*# Moscow State Univ. (USSR). Inst. of Nuclear Physics.
ON THE RETENTION OF HIGH-ENERGY PROTONS AND NUCLEI WITH CHARGES Z < OR EQUAL TO 2 IN LARGE SOLAR FLARES AFTER THE PROCESS OF THEIR ACCELERATION
N. N. Volodichev, B. M. Kuzhevsky, O. Yu. Nechaev, and I. A. Savenko *In* NASA. Goddard Space Flight Center 19th Intern. Cosmic Ray Conf., Vol. 4 Aug. 1985 p 229-232 refs (For primary document see N85-34729 23-92)
(SH-2.1-8) Avail: NTIS HC as boxed set only $200/MF A01 per volume or E99 per entire set CSCL 03B

Data which suggest that the protons with energies of up to several GeV should be retained on the Sun after the process of their acceleration are presented. The protons are on the average retained for 15 min, irrespectively of the solar flare heliolatitude and of the accelerated particle energy ranging from 100 MeV to several GeV. It is suggested that the particles are retained in a magnetic trap formed in a solar active region. No Z > or = 2 nuclei of solar origin during large solar flares. The absence of the > 500 MeV/nucleon nuclei with Z > or = 2 may be due to their retention in the magnetic trap which also retains the high-energy protons. During the trapping time the approx. > 500 MeV/nucleon nuclei with Z > or = 2 may escape due to nuclear interactions and ionization loss. E.A.K.

N85-34790*# Observatoire du Pic-du-Midi, Bagneres de Bigorre (France).
DIFFUSION IN THE CHROMOSPHERE AND THE COMPOSITION OF THE SOLAR CORONA AND ENERGETIC PARTICLES
Sylvie Vauclair and Jean-Paul Meyer (Centre d'Etudes Nucleaires de Saclay) *In* NASA. Goddard Space Flight Center 19th Intern. Cosmic Ray Conf., Vol. 4 Aug. 1985 p 233-236 refs (For primary document see N85-34729 23-92)
(SH-2.1-9) Avail: NTIS HC as boxed set only $200/MF A01 per volume or E99 per entire set CSCL 03B

Composition observations, in the solar photosphere, and in the upper transition region (TR) and corona imply a change of composition of the solar atmosphere somewhere between the photosphere and the upper TR. Heavy elements with first ionization potential (FIP) > 9 eV (high-FIP element) are approx. 4 times less abundant in the TR and corona than in the photosphere, as compared to both hydrogen and heavy elements with lower low-FIP elements. A separation is suggested between neutral and ionized elements in a region where the high-FIP elements are mostly neutral, and the low-FIP elements ionized. This occurs in the chromosphere at altitudes above 600 km and below 2000 km above photosphere. Whether the diffusion processes can explain the observed change in composition is investigated. E.A.K.

N85-34791*# Franklin Inst., Newark, Del.
ANOMALOUS ABUNDANCES OF SOLAR ENERGETIC PARTICLES AND CORONAL GAS: COULOMB EFFECTS AND FIRST IONIZATION POTENTIAL (FIP) ORDERING
D. J. Mullan *In* NASA. Goddard Space Flight Center 19th Intern. Cosmic Ray Conf., Vol. 4 Aug. 1985 p 237-240 refs (For primary document see N85-34729 23-92)
(SH-2.1-10) Avail: NTIS HC as boxed set only $200/MF A01 per volume or E99 per entire set CSCL 03B

The first ionization potential (FIP) ordering of elemental abundances in solar energetic particles and in the corona which can both be explained Coulomb effects is discussed. Solar energetic particles (SEP) and coronal gas have anomalous abundances relative to the photosphere. The anomalies are similar in both cases: which led to the conclusion that SEP acceleration is not selective, but merely preserves the source abundances. It is argued that SEP acceleration can be selective, because identical selectivity operates to determine the coronal abundances. The abundance anomalies are ordered by first ionization potential (FIP). E.A.K.

N85-34792*# Max-Planck-Inst. fuer Extraterrestrische Physik, Garching (West Germany).
THE MEAN IONIC CHARGES OF N, NE, MG, SI AND S IN SOLAR ENERGETIC PARTICLE EVENTS
A. Luhn, D. Hovestadt, B. Klecker, M. Scholer, G. Gloeckler (Maryland Univ., College Park), F. M. Ipavich (Maryland Univ., College Park), A. B. Galvin (Maryland Univ., College Park), C. Y. Fan (Arizona Univ., Tucson), and L. A. Fisk (New Hampshire Univ.) *In* NASA. Goddard Space Flight Center 19th Intern. Cosmic Ray Conf., Vol. 4 Aug. 1985 p 241-244 refs (For primary document see N85-34729 23-92)
(SH-2.1-11) Avail: NTIS HC as boxed set only $200/MF A01 per volume or E99 per entire set CSCL 03B

The mean ionic charges of nitrogen, neon, magnesium, silicon, and sulfur in solar flare particle events were determined for 12 flares during the time interval from September 1978 to September 1979. The observations were carried out with the MPI/UoMd ULEZEQ Sensor on the ISEE-3 satellite comparing the results with mean charge states established in a hot coronal plasma under equilibrium conditions, different temperatures for different elements are discussed. These range from approx. 2 million K to 7 million K in a single flare. From flare to flare the variation in temperature for each element is less than the variation between different ion species. E.A.K.

N85-34793*# Max-Planck-Inst. fuer Extraterrestrische Physik, Garching (West Germany).
CALCULATIONS OF HEAVY ION CHARGE STATE DISTRIBUTIONS FOR NONEQUILIBRIUM CONDITIONS
A. Luhn and D. Hovestadt *In* NASA. Goddard Sace Flight Center 19th Intern. Cosmic Ray Conf., Vol. 4 Aug. 1985 p 245-248 refs (For primary document see N85-34729 23-92)
(SH-2.1-12) Avail: NTIS HC as boxed set only $200/MF A01 per volume or E99 per entire set CSCL 03B

Numerical calculations of the charge state distributions of test ions in a hot plasma under nonequilibrium conditions are presented. The mean ionic charges of heavy ions for finite residence times in an instantaneously heated plasma and for a non-Maxwellian electron distribution function are derived. The results are compared with measurements of the charge states of solar energetic particles, and it is found that neither of the two simple cases considered can explain the observations. E.A.K.

N85-34794*# National Aeronautics and Space Administration. Goddard Space Flight Center, Greenbelt, Md.
ABUNDANCES FROM SOLAR-FLARE GAMMA-RAY LINE SPECTROSCOPY
R. J. Murphy (Maryland Univ., College Park), R. Ramaty, D. J. Forrest (New Hampshire Univ.), and B. Kozlovsky (Tel Aviv Univ.) *In its* 19th Intern. Cosmic Ray Conf., Vol. 4 Aug. 1985 p 249-252 refs (For primary document see N85-34729 23-92)
(Contract NAS5-28609)
(SH-2.1-13) Avail: NTIS HC as boxed set only $200/MF A01 per volume or E99 per entire set CSCL 03B

Elemental abundances of the ambient gas at the site of gamma ray line production inthe solar atmosphere are deduced using gamma ray line observations from a solar flare. The resultant abundances are different from local galactic abundances which are thought to be similar to photospheric abundances. E.A.K.

N85-34795*# National Aeronautics and Space Administration. Goddard Space Flight Center, Greenbelt, Md.
SOLAR FLARE GAMMA-RAY LINE SPECTROSCOPY
R. J. Murphy (Maryland Univ., College Park), D. J. Forrest, R. Ramaty (New Hampshire Univ.), and B. Kozlovsky (Tel Aviv Univ.) *In its* 19th Intern. Cosmic Ray Conf., Vol. 4 Aug. 1985 p 253-256 refs (For primary document see N85-34729 23-92)
(Contract NAS5-28609)
(SH-2.1-14) Avail: NTIS HC as boxed set only $200/MF A01 per volume or E99 per entire set CSCL 03B

The techniques and the results of solar elemental abundance determinations using observations of gamma ray lines from the April 27 1981 olar flare were outlined. The techniques are elaborated on and observed and the best-fitting theoretical spectra are presented. Numerical values for the photon fluences and the

total number of protons involved in the thick-target production of these gamma rays are derived. E.A.K.

N85-34796*# Universidad Nacional Autonoma de Mexico, Villa Obregon. Inst. de Geoffsica.
ISOTOPIC OVERABUNDANCES AND THE ENERGETIC PARTICLE MODEL OF SOLAR FLARES
R. Perez-Enriquez and S. Bravo *In* NASA. Goddard Space Flight Center 19th Intern. Cosmic Ray Conf., Vol. 4 Aug. 1985 p 257-260 refs (For primary document see N85-34729 23-92)
(SH-2.2-1) Avail: NTIS HC as boxed set only $200/MF A01 per volume or E99 per entire set CSCL 03B

According to the energetic particle model of solar flares particles are efficiently accelerated in the magnetic field loop of an active region (AR) by hydromagnetic turbulence. It is demonstrated that the isotopic overabundances observed in some flares are not a consequence of the flare itself but are characteristic of the plasma in the AR. Only when a flare releases the plasma into the interplanetary space it is possible to observe this anomalous composition at spacecraft locations. E.A.K.

N85-34797*# Yunnan Univ., Kunming (China). Dept. of Physics.
NUCLEOSYNTHESIS IN THE TERRESTRIAL AND SOLAR ATMOSPHERES
Chuanzan Yu, Renming Zhou, and Shijie Zhan *In* NASA. Goddard Space Flight Center 19th Intern. Cosmic Ray Conf., Vol. 4 Aug. 1985 p 261-264 refs (For primary document see N85-34729 23-92)
(SH-2.2-2) Avail: NTIS HC as boxed set only $200/MF A01 per volume or E99 per entire set CSCL 03B

Variations of Delta D, delta C-13, Delta C-14 and Delta O-18 with time were measured by a lot of experiments. Many abnormalities of isotope abundances in cosmic rays were found by balloons and satellites. It is suggested that these abnormalities are related to nuclearsynthesis in the terrestrial and solar atmospheres and are closely related to solar activities. E.A.K.

N85-34798*# National Aeronautics and Space Administration. Goddard Space Flight Center, Greenbelt, Md.
TYPE 3 SOLAR RADIO BURSTS AND 3HE-RICH EVENTS
D. V. Reames and R. G. Stone *In its* 19th Intern. Cosmic Ray Conf., Vol. 4 Aug. 1985 p 265-268 refs (For primary document see N85-34729 23-92)
(SH-2.2-3) Avail: NTIS HC as boxed set only $200/MF A01 per volume or E99 per entire set CSCL 03B

The kilometric radio data for 3He-rich events during the 1979 to 82 time period were investigated. Type 3 bursts are present for each event as expected from the prevous electron 3He-event association. A list of identified solar events is presented. E.A.K.

N85-34799*# National Aeronautics and Space Administration. Goddard Space Flight Center, Greenbelt, Md.
SOLAR SOURCE REGIONS OF 3HE-RICH PARTICLE EVENTS
S. W. Kahler, R. P. Lin (Emmanuel Coll.), D. V. Reames (California Univ., Berkeley), R. G. Stone, and M. Liggett (California Inst. of Tech., Pasadena) *In its* 19th Intern. Cosmic Ray Conf., Vol. 4 Aug. 1985 p 269-272 refs (For primary document see N85-34729 23-92)
(SH-2.2-4) Avail: NTIS HC as boxed set only $200/MF A01 per volume or E99 per entire set CSCL 03B

Hydrogen alpha X-ray, and metric and kilometric radio data to examine the solar sources of energetic 3He-rich particle events observed near earth in association with impulsive 2 to 100 keV electron events were applied. Each 3He/electron event is associated with a kilometric type 3 burst belonging to a family of such bursts characterized by similar interplanetary propagation paths from the same solar active region. The 3He/electron events correlate very well with the interplanetary low frequency radio brightnesses of these events, but progressively worse with signatures from regions closer to the Sun. When H alpha brightnings can be associated with 3He/electron events, they have onsets coinciding to within 1 min of that of the associated metric type 3 burst but are often too small to be reported. The data are consistent with the earlier idea that many type 3 bursts, the 3He/electron events, are due to particle acceleration in the corona, well above the associated H alpha and X-ray flares. E.A.K.

N85-34800*# National Aeronautics and Space Administration. Goddard Space Flight Center, Greenbelt, Md.
THE 3HE IN SOLAR NON-RELATIVISTIC ELECTRON EVENTS
D. V. Reames and R. P. Lin (California Univ., Berkeley) *In its* 19th Intern. Cosmic Ray Conf., Vol. 4 Aug. 1985 p 273-276 ref (For primary document see N85-34729 23-92)
(SH-2.2-5) Avail: NTIS HC as boxed set only $200/MF A01 per volume or E99 per entire set CSCL 03B

The presence of 3He in 187 solar electron events observed on the ISEE-3 spacecraft during a 9-month period beginning in Aug. 1978 is reported. The 3He is present in over half of the events and in 2/3 of events with 19 keV electrons. It is suggested that 3He would be found in all electron events if these was a greater collection efficiency. E.A.K.

N85-34801*# Chicago Univ., Ill.
ELEMENTAL ABUNDANCE DIFFERENCES BETWEEN NUCLEI ACCLERATED IN CIR SHOCKS AND SOLAR FLARES
W. F. Dietrich and J. A. Simpson *In* NASA. Goddard Space Flight Center 19th Intern. Cosmic Ray Conf., Vol. 4 Aug. 1985 p 277-280 refs (For primary document see N85-34729 23-92)
(SH-2.2-6) Avail: NTIS HC as boxed set only $200/MF A01 per volume or E99 per entire set CSCL 03B

Measurement of the ratios of nuclear abundances H/He, CNO/Fe-group and the Fe-group/HE for 51 passages of Corotating Interaction Regions (CIRs) at 1 AU, and measurement of these ratios from 620 solar flares in the energy range 0.6 to 4 MeV per nucleon, show that CIR shock acceleration alone does not change significantly these ratios from the values they have for solar system abundances or the solar wind. The solar flare ratios continue to reflect strong biases in the abundances, consistent with requirements for multistage acceleration rpocesses at the Sun. E.A.K.

N85-34802*# National Aeronautics and Space Administration. Goddard Space Flight Center, Greenbelt, Md.
THE HEAVY ION COMPOSITION IN 3HE-RICH SOLAR FLARES
G. M. Mason (Maryland Univ., College Park), D. V. Reames, D. Hovestadt (Max-Planck-Inst. fuer Extraterrestrische Physik, Garching), and T. T. vonRosenvinge *In its* 19th Intern. Cosmic Ray Conf., Vol. 4 Aug. 1985 p 281-284 refs (For primary document see N85-34729 23-92)
(Contract NAS5-28704; Grants NAGw-101; NGR-21-002-224; NGR-21-002-316; NSF ATM-84-07546)
(SH-2.2-7) Avail: NTIS HC as boxed set only $200/MF A01 per volume or E99 per entire set CSCL 03B

The 3He-rich flares show a tendency to be enriched in heavy ions, and that this enrichment covers the charge range through Fe. The discovery of this association was responsible, in part, for the discarding of 3He enrichment models which involved spallation or thermonuclear reactions, since such models were unable to produce heavy nuclei enhancement. Results of a survey of heavy nucleus abundances observed in 66 3He-rich flares which occurred over the period October 1978 to June 1982 are presented. E.A.K.

N85-34803*# Max-Planck-Inst. fuer Extraterrestrische Physik, Garching (West Germany).
THE MEAN IONIC CHARGE OF SILICON IN 3HE-RICH SOLAR FLARES
A. Luhn, B. Klecker, E. Hovestadt, and E. Moebius *In* NASA. Goddard Space Flight Center 19th Intern. Cosmic Ray Conf., Vol. 4 Aug. 1985 p 285-288 refs (For primary document see N85-34729 23-92)
(SH-2.2-8) Avail: NTIS HC as boxed set only $200/MF A01 per volume or E99 per entire set CSCL 03B

Mean ionic charge of iron in 3He-rich solar flares and the average mean charge of Silicon for 23 #He-rich periods during

the time interval from September 1978 to October 1979 were determined. It is indicated that the value of the mean charge state of Silicon is higher than the normal flare average by approximately 3 units and in perticular it is higher then the value predicted by resonant heating models for 3He-rich solar flares. E.A.K.

N85-34804*# Kalinin (M. I.) Polytechnical Inst., Leningrad (USSR).
ON THE CONNECTION BETWEEN THE 3HE-ENRICHMENT AND SPECTRAL INDEX OF SOLAR ENERGETIC PARTICLES
L. G. Kocharov and Ya. V. Dvoryanchikov (Ioffe Physico-Technical Inst., Leningrad) *In* NASA. Goddard Space Flight Center 19th Intern. Cosmic Ray Conf., Vol. 4 Aug. 1985 p 289-292 refs (For primary document see N85-34729 23-92)
(SH-2.2-9) Avail: NTIS HC as boxed set only $200/MF A01 per volume or E99 per entire set CSCL 03B

A model is presented which explains the observed tendency of events with large 3He/4He ratios to have steeper spectra. In this model preferential injection of 3He, acceleration by Alfven waves and Coulomb deceleration of ions are considered simultaneously. The observed tendency may be obtained as a result of competition between injection and acceleration processes. E.A.K.

N85-34805*# Kalinin (M. I.) Polytechnical Inst., Leningrad (USSR).
THE PLASMA MECHANISM FOR PREFERENTIAL ACCELERATION OF HEAVY IONS
L. G. Kocharov and A. V. Orishchenko (Ioffe Physico-Technical Inst., Leningrad) *In* NASA. Goddard Space Flight Center 19th Intern. Cosmic Ray Conf., Vol. 4 Aug. 1985 p 293-296 refs (For primary document see N85-34729 23-92)
(SH-2.2-10) Avail: NTIS HC as boxed set only $200/MF A01 per volume or E99 per entire set CSCL 03B

The induced scattering of ion-acoustic waves on ions is considered for preferential preacceleration of heavy elements. The reconsidered diffusion coefficient in velocity space is used. If the threshold velocity for the main acceleration is linear in charge-to-mass ratio, the induced scattering can account for the observed heavy element abundances in solar cosmic rays. Author

N85-34806*# Waseda Univ., Tokyo (Japan). Science and Engineering Research Lab.
OBSERVATIONS OF SOLAR ENERGETIC PARTICLES AT A SYNCHRONOUS ORBIT
T. Takenaka, Y. Ohi (Rikkyo Univ., Tokyo), T. Yanagimachi (Rikkyo Univ., Tokyo), K. Ito (Rikkyo Univ., Tokyo), T. Kohno (Inst. of Physical and Chemical Research, Tokyo), and K. Sakurai (Kanagawa Univ.) *In* NASA. Goddard Space Flight Center 19th Intern. Cosmic Ray Conf., Vol. 4 Aug. 1985 p 297-300 refs (For primary document see N85-34729 23-92)
(SH-3.1-1) Avail: NTIS HC as boxed set only $200/MF A01 per volume or E99 per entire set CSCL 03B

The Space Environment Monitors (SEM) on board the Japanese geostationary meteorological satellites (GMS-1 and GMS-2) observed energetic protons, alpha particles and electrons continuously for February 1978 to September 1984. The satellites were at 6.6 Earth radii above 140 deg E equator. G.L.C.

N85-34807*# Institute of Physical and Chemical Research, Tokyo (Japan).
CORONAL PROPAGATION OF SOLAR FLARE PARTICLES OBSERVED BY SATELLITE
Tsuyoshi Kohno, Nariaki Nitta, Masami Wada, and Tomoshige Suda (Meteorological Research Inst.) *In* NASA. Goddard Space Flight Center 19th Intern. Cosmic Ray Conf., Vol. 4 Aug. 1985 p 301-304 refs (For primary document see N85-34729 23-92)
(SH-3.1-2) Avail: NTIS HC as boxed set only $200/MF A01 per volume or E99 per entire set CSCL 03B

Propagation of solar flare particles in corona was studied using the satellite data at the geostationary orbit. by selecting very fast rise time events only, the interplanetary propagation were assumed to be scatter free arrival. The results show that the propagation in corona does not depend on particle energy in 4 to 500 MeV protons, and the time delays from optical flare do not depend on the distance between the flare site and the base of the interplanetary magnetic field which connects to the Earth. Author

N85-34808*# Kiel Univ. (West Germany). Inst. fuer Reine und Angewandte Kernphysik.
CORONAL PROPAGATION OF FLARE ASSOCIATED ELECTRONS AND PROTONS
G. Schellert, G. Wibberenz, and H. Kunow *In* NASA. Goddard Space Flight Center 19th Intern. Cosmic Ray Conf., Vol. 4 Aug. 1985 p 305-308 refs (For primary document see N85-34729 23-92)
(SH-3.1-3) Avail: NTIS HC as boxed set only $200/MF A01 per volume or E99 per entire set CSCL 03B

A statistical study of characteristic times and intensities of 36 solar particle events observed between 1977 and 1979 by the Kiel Cosmic Ray Experiment on board HELIOS-1 and -2 has been carried out. For approx. 0.5 MeV electrons we order the times of maximum and the absolute intensities with respect to angular distance from the parent flare. Discussion of coronal parameters in terms of Reid's model leads to typical time constants for coronal diffusion and escape. Author

N85-34809*# Franklin Inst., Newark, Del.
GEOMETRY OF THE DIFFUSIVE PROPAGATION REGION IN THE AUGUST 14, 1982 SOLAR ELECTRON EVENT
Paul A. Evenson *In* NASA. Goddard Space Flight Center 19th Intern. Cosmic Ray Conf., Vol. 4 Aug. 1985 p 309-312 refs (For primary document see N85-34729 23-92)
(SH-3.1-5) Avail: NTIS HC as boxed set only $200/MF A01 per volume or E99 per entire set CSCL 03B

On August 14, 1982, relativistic electrons arrived promptly after an impulsive gamma ray flare, indicating that very little scattering was taking place in interplanetary space. By ignoring anisotropy data the time profile of the event is well described by interplanetary diffusion except for the derived particle injection time. This discrepancy provides independent evidence that the particles are diffusing in a volume close to the Sun rather than in interplanetary space. The flux at maximum method of determining the number of particles produced is still a good approximation when appropriately applied. Author

N85-34810*# Academy of Sciences (USSR), Moscow. Space Research Inst.
PECULIARITIES OF PROPAGATION OF CHARGED PARTICLES IN SOLAR CORONA
E. I. Morozova, N. F. Pisarenko, N. A. Mikryukova, V. V. Klimenko (Inst. of Cosmophysical Research and Astronomy), V. E. Timofeev (Inst. of Cosmophysical Research and Astronomy), and Yu. G. Shafer (Inst. of Cosmophysical Research and Astronomy) *In* NASA. Goddard Space Flight Center 19th Intern. Cosmic Ray Conf., Vol. 4 Aug. 1985 p 313-316 refs (For primary document see N85-34729 23-92)
(SH-3.1-6) Avail: NTIS HC as boxed set only $200/MF A01 per volume or E99 per entire set CSCL 03B

The influence of boundaries of the large scale unipolar magnetic regions (UMR) on the Sun upon the charged particle propagation in the solar corona and interplanetary space is investigated. Increases of the charged particle fluxes from solar flares on November 4 and 20, 1978 detected by Venera-11 and Prognoz-1 and on December 7, 1982 by Venera-13 and 'GMS-2' were analyzed. Author

N85-34811*# National Aeronautics and Space Administration. Goddard Space Flight Center, Greenbelt, Md.
SOME CHARACTERISTICS OF THE SOLAR FLARE EVENT OF FEBRUARY 16, 1984
H. Debrunner (Bern Univ.), E. O. Flueckiger (New Hampshire Univ.), J. A. Lockwood, and R. E. McGuire *In its* 19th Intern. Cosmic Ray Conf., Vol. 4 Aug. 1985 p 317-320 refs (For primary document see N85-34729 23-92)
(SH-3.1-7) Avail: NTIS HC as boxed set only $200/MF A01 per volume or E99 per entire set CSCL 03B

In the morning of February 16, 1984 a solar cosmic ray event

(GLE) was recorded by the world wide network of neutron monitors (NM). The counting rate vs. time profile of the Goose Bay NM (geog. lat. = 53.3 deg. N, deog. long. = 299.6 deg E) where the increase is expressed as percent of the counting rate of an equatorial sea level NM is presented. The Goose Bay NM was observed to have the maximum response to the solar particles. Its counting rate vs. time profile exhibits a rapid increase to maximum, has a large amplitude (approx. 170%) and decays rapidly to background in approx. 90 min. In Fig. 1 we also show the counting rate vs. time profile for the Tixie Bay NM (71.6 deg, 128.9 deg) which recorded an increase of only a few percent. Since the NMs at Goose Bay and Tixie Bay have asymptotic viewing directions approx. 180 deg apart in longitude, the anisotropy of the solar particle flux at Earth from these stations. G.L.C.

N85-34812*# Maryland Univ., College Park. Dept. of Physics and Astronomy.

CONSTRAINTS OF SOLAR FLARE PARTICLE TRANSPORT MODELS FROM ANISOTROPY OBSERVATIONS AT VOYAGER 1 Abstract Only

D. C. Hamilton, G. M. Mason, and G. Gloeckler *In* NASA. Goddard Space Flight Center 19th Intern. Cosmic Ray Conf., Vol. 4 Aug. 1985 p 321 ref (For primary document see N85-34729 23-92)
(Contract NAS5-28704)
(SH-3.1-8) Avail: NTIS HC as boxed set only $200/MF A01 per volume or E99 per entire set CSCL 03B

In general a particle transport model for energetic solar flare particles contains a number of free parameters which are determined by fitting various features of observed particle events. Frequently the parameter values are not uniquely determined. In order to place tighter constraints on the models, the anisotropy of 1 and 25 MeV/nuc protons and helium nuclei were examined during the 22 November 1977 solar particle event using data from the LECP experiment on Voyager 1 at 1.6 AU. These observations were combined with the time intensity profiles at Voyager 1 and at 1 AU from ISEE-1 and IMP-8 to determine the magnitude and radial dependence of the interplanetary diffusion coefficient and the required injection duration at the sun. The first order anisotropy amplitudes for both 1 MeV and 25 MeV protons are observed to decrease from maximum values (approx. 1) during the event onset at Voyager 1 to values consistent with convection in the solar wind at about 3 days into the event decay phase. The intensity and anisotropy profiles at 1.6 AU are consistent with predictions of diffusive transport with a modest mean free path (lambda = approx. 0.1 AU). Author

N85-34813*# Jet Propulsion Lab., California Inst. of Tech., Pasadena.

LOW ENERGY PROTON BIDIRECTIONAL ANISOTROPIES AND THEIR RELATION TO TRANSIENT INTERPLANETARY MAGNETIC STRUCTURES: ISEE-3 OBSERVATIONS

R. G. Marsden (ESA, Noordwijk), T. R. Sanderson (ESA, Noordwijk), K.-P. Wenzel (ESA, Noordwijk), and E. J. Smith *In* NASA. Goddard Space Flight Center 19th Intern. Cosmic Ray Conf., Vol. 4 Aug. 1985 p 322-325 refs (For primary document see N85-34729 23-92)
(SH-3.1-9) Avail: NTIS HC as boxed set only $200/MF A01 per volume or E99 per entire set CSCL 03B

It is known that the interplanetary medium in the period approaching solar maximum is characterized by an enhancement in the occurrence of transient solar wind streams and shocks and that such systems are often associated with looplike magnetic structures or clouds. There is observational evidence that bidirectional, field aligned flows of low energy particles could be a signature of such looplike structures, although detailed models for the magnetic field configuration and injection mechanisms do not exist at the current time. Preliminary results of a survey of low energy proton bidirectional anisotropies measured on ISEE-3 in the interplanetary medium between August 1978 and May 1982, together with magnetic field data from the same spacecraft are presented. G.L.C.

N85-34814*# Malaya Univ., Kuala-Lumpur. Dept. of Mathematics.

SECOND-ORDER COMPTON-GETTING EFFECT ON ARBITRARY INTENSITY DISTRIBUTION c93

C. K. Ng *In* NASA. Goddard Space Flight Center 19th Intern. Cosmic Ray Conf., Vol. 4 Aug. 1985 p 326-329 refs (For primary document see N85-34729 23-92)
(SH-3.1-10) Avail: NTIS HC as boxed set only $200/MF A01 per volume or E99 per entire set CSCL 03B

Theoretical studies of energetic particles in space are often referred to a special frame of reference. To compare theory with experiment, one has to transform the particle distribution from the special frame to the observer's frame, or vice versa. Various methods have been derived to obtain the directional distribution in the comoving frame from the directional fluxes measured on a spacecraft. These methods have become progressively complicated as increasingly detailed directional particle data become available. A set of 2nd order correct formulae for the transformation of an arbitrary differential intensity distribution, expressed as a series of spherical harmonics, between any two frames in constant relative motion is presented. These formulae greatly simplify the complicated procedures currently in use for the determination of the differential intensity distribution in a comoving frame. G.L.C.

N85-34815*# Malaya Univ., Kuala-Lumpur. Dept. of Mathematics.

DETERMINATION OF THE PITCH-ANGLE DISTRIBUTION AND TRANSVERSE ANISOTROPY OF INTERPLANETARY PARTICLES

C. K. Ng *In* NASA. Goddard Space Flight Center 19th Intern. Cosmic Ray Conf., Vol. 4 Aug. 1985 p 330-333 refs (For primary document see N85-34729 23-92)
(SH-3.1-11) Avail: NTIS HC as boxed set only $200/MF A01 per volume or E99 per entire set CSCL 03B

A method to determine the directional differential intensity (d.d.i.), expressed in terms of spherical harmonics, from sectored particle data, concurrent interplanetary magnetic field (IMF) and solar wind velocity is presented. G.L.C.

N85-34816*# Kiel Univ. (West Germany). Inst. fuer Reine und Angewandte Kernphysik.

PITCH ANGLE DISTRIBUTIONS OF SOLAR ENERGETIC PARTICLES AND THE LOCAL SCATTERING PROPERTIES OF THE INTERPLANETARY MAGNETIC FIELD Abstract Only

J. Beeck and G. Wibberenz *In* NASA. Goddard Space Flight Center 19th Intern. Cosmic Ray Conf., Vol. 4 Aug. 1985 p 335-338 (For primary document see N85-34729 23-92)
(SH-3.1-13) Avail: NTIS HC as boxed set only $200/MF A01 per volume or E99 per entire set CSCL 03B

An approximate solution of the Fokker-Planck equation containing pitch angle scattering and adiabatic focusing is discussed. For modest focusing effects the omnidirectional density obeys an ordinary diffusion equation with a modified diffusion coefficient. The anisotropic part of the distribution function is properly normalized and split into an even and an odd part. The even part is determined by the ratio between the scattering mean free path and the focusing length and by the degree of polarization of the magnetic field fluctuations. The odd part is determined by the deviation of the pitch angle scattering from isotropic scattering. The method supplies a powerful tool to obtain the local characteristics of pitch angle scattering. It is insensitive to long lasting solar injections and to moderate radial variations of the mean free path. The method is applied to solar particle events observed on Helio-1 and -2. Author

N85-34817*# Franklin Inst., Newark, Del.

EXPONENTIAL ANISOTROPY OF SOLAR COSMIC RAYS

J. W. Bieber, P. A. Evenson, and M. A. Pomerantz *In* NASA. Goddard Space Flight Center 19th Intern. Cosmic Ray Conf., Vol. 4 Aug. 1985 p 335-338 refs (For primary document see N85-34729 23-92)
(Grants NAG5-374; NSF ATM-83-03758; NSF DPP-83-00544)
(Sh-3.2-1) Avail: NTIS HC as boxed set only $200/MF A01 per

volume or E99 per entire set CSCL 03B

On 16 February 1984 a flare on the Sun's invisible disk produced a large, highly anisotropic solar particle event. A technique, in which interplanetary scattering parameters are determined purely from the form of the particle anisotropy, is applied to energetic particle data from neutron monitors and the ICE spacecraft. Author

N85-34818*# Tasmania Univ., Hobart (Australia). Dept. of Physics.

ENERGETIC SOLAR PARTICLE EVENTS

K. B. Fenton, A. G. Fenton, and J. E. Humble *In* NASA. Goddard Space Flight Center 19th Intern. Cosmic Ray Conf., Vol. 4 Aug. 1985 p 339-341 refs Sponsored in part by the Australian research grants scheme (For primary document see N85-34729 23-92)

(SH-3.2-2) Avail: NTIS HC as boxed set only $200/MF A01 per volume or E99 per entire set CSCL 03B

Studies of the arrival directions of energetic solar particles during ground level enhancements (CLE's) observed by neutron monitors have shown that, in general, in the first hour of the event most of the particles arrive with a distribution of pitch angles peaked about the garden hose field direction in the vicinity of Earth. During the first hour some of the particles arrive from the antisolar direction, while in later stages of the event the intensity becomes more nearly isotropic as a result of scattering of particles in interplanetary space. An attempt is made to determine the arrival directions of the particles during the early stages of the GLE of 16 February 1984 using the data currently available from high latitude neutron monitors near sea level where the cut off is essentially atmospheric (approx. LGV). G.L.C.

N85-34819*# California Univ., Berkeley. Space Sciences Lab.

CHANNELED PROPAGATION OF SOLAR PARTICLES

K. A. Anderson and W. M. Dougherty *In* NASA. Goddard Space Flight Center 19th Intern. Cosmic Ray Conf., Vol. 4 Aug. 1985 p 342-345 refs (For primary document see N85-34729 23-92)

(Grant NAG5-376)

(SH-3.2-3) Avail: NTIS HC as boxed set only $200/MF A01 per volume or E99 per entire set CSCL 03B

Bartley (1966) and McCracken and Ness (1966) identified bundles of interplanetary magnetic field (IMF) lines that differed in direction from the interplanetary field lines in which they were imbedded. These bundles, called filaments differed in direction by as much as several tens of degrees from the surrounding field. The filaments werre first noticed due to the large and sudden change in flow direction of highly anisotropic solar flare protons in the energy range 1 to 13 MeV. Passage of the filaments over the spacecraft required a few hours, implying a diameter for the filaments of approximately 3 x 10 to the 6th power km at a distance of 1 AU from the Sun. In 1968, Jakipii and Parker used Leighton's hypothesis of random walk of magnetic field lines associated with granules and supergranules (1964) to develop a picture of an interplanetary medium composed of a tangle of field lines frozen into the solar wind, but whose feet were carried about by the random motions at the solar surface. Jakipii and Parker noted that using a correlation length of 15,000 km - about the radius of a supergranule - the magnetic structure would be 3 x 10 to the 6th power km in size of the filaments as determined by Bartley and McCracken and Ness. These workers did not find changes in the solar particle intensity, anisotropy ratio or energy spectrum as the spacecraft entered the filament. G.L.C.

N85-34820*# National Aeronautics and Space Administration. Goddard Space Flight Center, Greenbelt, Md.

THE PROPAGATION OF SOLAR ENERGETIC PARTICLES IN MAGNETIC CHANNELS Abstract Only

Frank B. McDonald (NASA, Washington) and L. F. Burlaga *In its* 19th Intern. Cosmic Ray Conf., Vol. 4 Aug. 1985 p 345 (For primary document see N85-34729 23-92)

(SH-3.2-4) Avail: NTIS HC as boxed set only $200/MF A01 per volume or E99 per entire set CSCL 03B

The existence of interplanetary flow systems produced by the entrainment of interplanetary transients, consisting of flare produced shocks, high speed solar wind streams and coronal mass ejection, has been established. This entrainment process produces enhanced regions of the interplanetary magnetic field that should be connected back to the solar corona. These compressed regions can provide a preferred magnetic channel for the propagation of solar cosmic rays. The characteristics of these events appear to be different from those previously reported by the NASA/University of New Hampshire team and the University of Chicago in their study of a large number of events in the region beyond 1 AU. These new events have a very flat energy spectra (with gamma = approx. 1.5) that frequently extend to energies above 100 MeV and have a significant enhancement of MeV electrons. Author

N85-34821*# Maryland Univ., College Park. Dept. of Physics and Astronomy.

RADIAL TRANSPORT OF APPROXIMATELY 1 MeV/NUCLEON IONS DURING THE 22 NOVEMBER 1977 SOLAR PARTICLE EVENT

G. M. Mason, D. C. Hamilton, G. Gloeckler, and B. Klecker (Max-Planck-Inst. fuer Exterrestrische Physik, Garching, West Germany) *In* NASA. Goddard Space Flight Center 19th Intern. Cosmic Ray Conf., Vol. 4 Aug. 1985 p 347-350 refs (For primary document see N85-34729 23-92)

(Contract NAS5-28704; Grants NGR-21-002-224; NGR-21-002-316; NAGw-101; NSF ATM-84-07546)

(SH-3.2-5) Avail: NTIS HC as boxed set only $200/MF A01 per volume or E99 per entire set CSCL 03B

Time intensity profiles of solar flare energetic particle events carry information on the particle injection processes at the Sun, as well as the transport of particles in interplanetary space. However, in order to help identify the individual processes of injection versus transport it is necessary to use observations taken at more than one radial location. Results of such a study concerning the 22 November 1977 solar particle event, observed with instruments at 1.0 and 1.55 AU are presented. The observations are for particles of energies near 1 MeV/nucleon, considerably less than the approx. 10 to 20 MeV/nucleon energies typical of previous radial transport studies. Thus, in the present work it is possible to examine the validity of transport models to considerably lower energies than in previous work. G.L.C.

N85-34822*# New Hampshire Univ., Durham. Space Science Center.

ENERGETIC SOLAR PARTICLE FLUXES OUT TO 3 AU DURING THE 7 MAY 1978 FLARE EVENT

J. A. Lockwood and H. Debrunner (Bern Univ.) *In* NASA. Goddard Space Flight Center 19th Intern. Cosmic Ray Conf., Vol. 4 Aug. 1985 p 351-354 refs (For primary document see N85-34729 23-92)

(Grants NSF ATM-83-24486; NSF INT-81-18555)

(SH-3.2-6) Avail: NTIS HC as boxed set only $200/MF A01 per volume or E99 per entire set CSCL 03B

Simultaneous solar proton flux measurements on IMP 7 and by the world wide neutron monitor network during the May 7, 1978 flare event led to conclusions that in the energy range from 50 MeV to 10 GeV: (1) the propagation of the flare particles in the interplanetary magnetic field (IMF) between the Sun and the Earth was nearly scatter free; and (2) therefore, the intensity time (IT) profiles of the solar proton fluxes observed at Earth for about one hour after onset represent the solar injection profiles even to energies as low as 50 MeV. Observations of the IMF at Helios A indicate that the IMF was undisturbed between the Sun and Helios A at the time of the May 7, 1978 flare event; and, therefore, the solar particle propagation was also scatter free from the Sun to Helios A. G.L.C.

N85-34823*# Kiel Univ. (West Germany). Inst. fuer Reine und Angewandte Kernphysik.

THE LOCAL CHARACTERISTIC FUNCTION OF INTERPLANETARY PARTICLE PROPAGATION Abstract Only

G. Green and W. Schlueter *In* NASA. Goddard Space Flight Center 19th Intern. Cosmic Ray Conf., Vol. 4 Aug. 1985 p 355 (For primary document see N85-34729 23-92)

(SH-3.2-8) Avail: NTIS HC as boxed set only $200/MF A01 per volume or E99 per entire set CSCL 03B

An easily measurable intensity function which characterizes the interplanetary propagation of charged solar flare particles is presented. This function is nearly time invariant during a solar event despite the large variations of intensity and anisotropy, but varies from event to event. It characterizes the systematic and stochastic forces of the interplanetary magnetic field which focus and scatter the particles in pitch angle. The model of focused transport shows that this function is essentially determined by the local shape and amplitude of the pitch angle diffusion coefficient kappa (mu) and by the local value of the focusing length. The time profile of the solar particle injection is typically of negligible influence. The local characteristic function may be used as a powerful new tool for a systematic analysis of flare particle angular distributions, Examples are given. Author

N85-34824*# Academy of Sciences (USSR), Alma-Ata.
INVESTIGATION OF COSMIC RAY PROPAGATION IN INTERPLANETARY SPACE **c93**
E. A. Chebakova, E. V. Kolomeets, and V. N. Sevastyanov *In* NASA. Goddard Space Flight Center 19th Intern. Cosmic Ray Conf., Vol. 4 Aug. 1985 p 356-359 refs (For primary document see N85-34729 23-92)
(SH-3.2-9) Avail: NTIS HC as boxed set only $200/MF A01 per volume or E99 per entire set CSCL 03B

It was established experimentally that propagation of solar cosmic rays (scr) in interplanetary space up to 1 AU in most cases was of diffusion character. G.L.C.

N85-34825*# Academia Sinica, Beijing (China). Inst. of Space Physics.
DIFFUSION-CONVECTION FUNCTION OF COSMIC RAYS **c93**
Gongliang Zhang and Guang Yang (New Hampshire Univ., Durham) *In* NASA. Goddard Space Flight Center 19th Intern. Cosmic Ray Conf., Vol. 4 Aug. 1985 p 360-363 refs (For primary document see N85-34729 23-92)
(SH-3.2-10) Avail: NTIS HC as boxed set only $200/MF A01 per volume or E99 per entire set CSCL 03B

The fundamental properties and some numerical results of the solution of the diffusion equation of an impulsive cosmic-ray point source in an uniform, unbounded and spherically symmetrical moving medium is presented. The diffusion-convection(D-C) function is an elementary composite function of the solution of the D-C equation for the particles injected impulsively from a diffusive point source into the medium. It is the analytic solution derived by the dimensional method for the propagation equation of solar cosmic rays in the heliosphere, i.e. the interplanetary space. Because of the introduction of convection effect of solar wind, a nonhomogeneous term appears in the propagation equation, it is difficult to express its solution in terms of the ordinary special functions. The research made so far has led to a solution containing only the first order approximation of the convection effect. Author

N85-34826*# Turku Univ. (Finland). Dept. of Physical Sciences.
MONTE CARLO CALCULATIONS OF RELATIVISTIC SOLAR PROTON PROPAGATION IN INTERPLANETARY SPACE
M. Lumme, J. J. Torsti, E. Vainikka, J. Peltonen, M. Nieminen, E. Valtonen, and H. Arvelta *In* NASA. Goddard Space Flight Center 19th Intern. Cosmic Ray Conf., Vol. 4 Aug. 1985 p 364-367 refs (For primary document see N85-34729 23-92)
(SH-3.2-11) Avail: NTIS HC as boxed set only $200/MF A01 per volume or E99 per entire set CSCL 03B

Particle fluxes and pitch angle distributions of relativistic solar protons at 1 AU were determined by Monte Carlo calculations. The analysis covers two hours after the release of the particles from the Sun and total of eight 100000 particle trajectories were simulated. The pitch angle scattering was assumed to be isotropic ad the scattering mean free path was varied from 0.1 to 4 AU. As an application, the solar injection time and interplanetary scattering mean free path of particles that gave rise to the GLE on May, 1978 were determined. Assuming exponential form, the injection decay time was found to be about 11 minutes. The m.f.p. of pitch angle scattering during the event was about 1 AU. Author

N85-34827*# Academy of Sciences (USSR), Yakutsk. Inst. of Cosmophysical Research and Aeronomy.
ON REFLECTING BOUNDARY BEHIND THE EARTH'S ORBIT AT PROPAGATION OF FAST PARTICLES FROM SOLAR FLARES
A. S. Nishkovskikh and A. T. Filippov *In* NASA. Goddard Space Flight Center 19th Intern. Cosmic Ray Conf., Vol. 4 Aug. 1985 p 368-371 refs (For primary document see N85-34729 23-92)
(SH-3.2-13) Avail: NTIS HC as boxed set only $200/MF A01 per volume or E99 per entire set CSCL 03B

The flares of solar cosmic rays (SCR) associated with the presence of shocks in interplanetary magnetic field and with their propagation at significant heliocentric distances were always of great interest. Some events and problems concerning the peculiarities of propagation of flare CR in the interplanetary medium are considered. The distinguishing feature of such events is the presence of shock front behind the Earth's orbit having formed either directly in the process of shock generation on the Sun or at large heliocentric distances as a result of the interaction of fast and slow quasistationary recurrent solar wind (SW) streams. Based on the experimental material it is shown that the significant nonlinear disturbances in IMF behind the Earth's orbit can yield the occurrence of the additional SCR flux from shock front region as a result of the interaction of flare flux with shock and a partial reflection from it. Author

N85-34828*# Maryland Univ., College Park. Dept. of Physics and Astronomy.
THE DISPERSIVE EVOLUTION OF CHARGED-PARTICLE BUNCHES IN RANDOM MAGNETIC FIELDS **c93**
J. A. Earl *In* NASA. Goddard Space Flight Center 19th Intern. Cosmic Ray Conf., Vol. 4 Aug. 1985 p 372-375 refs (For primary document see N85-34729 23-92)
(Grant NGR-21-002-066)
(SH-4.1-2) Avail: NTIS HC as boxed set only $200/MF A01 per volume or E99 per entire set CSCL 03B

Shortly after a strongly anisotropic beam of charged particles is injected along a guiding magnetic field on which is superimposed a small random conponent, the particle density can be represented by a Gaussian profile whose center moves with the coherent velocity and whose width increases with time at a rate controlled by the coefficient of dispersion. Both parameters depend upon the mean free path, which characterizes scattering by the random fields, and the focusing length, which characterizes spatial variations of the guiding field. These dependencies are known explicitly for the coherent velocity. Formulae for coefficient of dispersion are available only in the limits of very weak and very strong focusing. A new expression for coefficient of dispersion, which spans this gap, is presented. Author

N85-34829*# Maryland Univ., College Park. Dept. of Physics and Astronomy.
NUMERICAL DESCRIPTIONS OF COSMIC-RAY TRANSPORT **c93**
J. A. Earl (Arizona Univ., Tucson) and J. R. Jokipii *In* NASA. Goddard Space Flight Center 19th Intern. Cosmic Ray Conf., Vol. 4 Aug. 1985 p 396-379 refs (For primary document see N85-34729 23-92)
(SH-4.1-3) Avail: NTIS HC as boxed set only $200/MF A01 per volume or E99 per entire set CSCL 03B

The behavior of energetic particles in the solar system is described by a well known Fokker-Planck equation. Although analytic methods yield insight into the nature of its solutions, especially in the diffusion regime, calculations that go beyond diffusion are very complicated. The reliability of these calculations is of concern, because numerical methods are notorious for their errors and artifacts. The well known Milne problem of classical transport theory was analyzed with the aid of three different numerical methods. These are: (1) The method of eigenfunctions

in which the distribution function is approximated by a sum of eigenfunctions of the scattering operator, (2) Numerical solutions of a finite difference aquation; and (3) Direct simulation of the scattering and streaming of individual particles with the aid of Monte Carlo methods. Author

N85-34830*# Maryland Univ., College Park. Dept. of Physics and Astronomy.

NUMERICAL AND ANALYTIC DESCRIPTIONS OF COSMIC-RAY TRANSPORT **c93**

J. A. Earl *In* NASA. Goddard Space Flight Center 19th Intern. Cosmic Ray Conf., Vol. 4 Aug. 1985 p 380-383 refs (For primary document see N85-34729 23-92)

(Grant NGR-21-002-066)

(SH-4.1-4) Avail: NTIS HC as boxed set only $200/MF A01 per volume or E99 per entire set CSCL 03B

It is not trivial to solve the equations that describe charged particle transport with the aid of computers, for instabilities, inaccuracies, and subtle artifacts are well known afflictions of numerical analysis. Two specific points are discussed. First to avoid inaccuracies, pitch angle scattering must be treated with great care. In particular, slightly inappropriate numerical formulations give rise to mean free paths that are in error by large factors. Secondly, A previously unrecognized artifact, numerical dispersion, is very similar to the physical phenomenon of dispersion. To avoid misinterpretations arising from this similarity, the spatial increment of the finite difference grid must be a small fraction of the mean free path. These points are illustrated by calculations based upon finite difference approximations to the transport equation. Author

N85-34831*# Universidad Nacional Autonoma de Mexico, Villa Obregon. Inst. de Geofisica.

THE ROLE OF SHOCK WAVES IN MODULATION OF GALACTIC COSMIC RAYS **c93**

R. Gall, B. T. Thomas (Bristol Univ.), and H. Durand *In* NASA. Goddard Space Flight Center 19th Intern. Cosmic Ray Conf., Vol. 4 Aug. 1985 p 384-387 refs (For primary document see N85-34729 23-92)

(SH-4.1-7) Avail: NTIS HC as boxed set only $200/MF A01 per volume or E99 per entire set CSCL 03B

The understanding of modulation of the galactic cosmic rays has considerably progressed by the exploration by space probes of major heliospheric structures, such as the Corotating Interaction Regions, the neutral sheet, and the compression regions of intense heliospheric magnetic fields. Also relevant in this context were the detections in the outer heliosphere of long lasting Forbush type decreases of cosmic ray intensity. The results of recent theoretical studies on the changes in intensity and energy, at different location from the Sun, induced by the passage of shocks across the heliosphere are presented. In this version of the research, the simplest cases of modulation of uGV and 2GV particles by single or several shocks during periods of positive and negative solar field polarity are reviewed. The results of the theoretical aspects of the search is reported. The comparison of the theoretical predictions with space probe data allows conclusions to be drawn on the role of shocks on the modulation on both the 11 and 22 year galactic cosmic ray cycles in the outer heliosphere and on the plausibility of the models and parameters used. Author

N85-34832*# New Hampshire Univ., Durham. Space Science Center.

THE INTENSITY RECOVERY OF FORBUSH-TYPE DECREASES AS A FUNCTION OF HELIOCENTRIC DISTANCE AND ITS RELATIONSHIP TO THE 11-YEAR VARIATION

J. A. Lockwood, W. R. Webber, and J. R. Jokipii (Arizona Univ.) *In* NASA. Goddard Space Flight Center 19th Intern. Cosmic Ray Conf., Vol. 4 Aug. 1985 p 388-391 refs (For primary document see N85-34729 23-92)

(Contract NAS5-24354; Grants NsG-7101; NSF ATM-83-04486; NSF ATM-83-17701)

(SH-4.1-9) Avail: NTIS HC as boxed set only $200/MF A01 per volume or E99 per entire set CSCL 03B

Recent data indicating that the solar modulation effects are propagated outward in the heliospheric cavity suggest that the 11-year cosmic ray modulation can best be described by a dynamic time dependent model. In this context an understanding of the recovery characteristics of large transient Forbush type decreases is important. This includes the typical recovery time at a fixed energy at 1 AU as well as at large heliocentric radial distances, the energy dependence of the recovery time at 1 Au, and the dependence of the time for the intensity to decrease to the minimum in the transient decreases as a function of distance. These transient decreases are characterized by their asymmetrical decrease and recovery times, generally 1 to 2 days and 3 to 10 days respectively at approx. 1 AU. Near earth these are referred to as Forbush decreases, associated witha shock or blast wave passage. At R equal to or greater than + or - 10 AU, these transient decreases may represent the combined effects of several shock waves that have merged together. Author

N85-34833*# Awadhesh Pratap Singh Univ., Rewa (India). Dept. of Physics.

CUMULATIVE EFFECT OF FORBUSH DECREASES IN THE HELIOSPHERIC MODULATION DURING THE PRESENT SOLAR CYCLE

S. P. Agrawal, B. L. Mishra, and A. K. Jain (Government Engineering Coll., Rewa, India) *In* NASA. Goddard Space Flight Center 19th Intern. Cosmic Ray Conf., Vol. 4 Aug. 1985 p 392-395 refs (For primary document see N85-34729 23-92)

(SH-4.1-10) Avail: NTIS HC as boxed set only $200/MF A01 per volume or E99 per entire set CSCL 03B

A monthly Forbush decrease index (Fd-I) is generated and it is compared with the observed long term chnges in the cosmic ray intensity near earth at energies greater than or equal to 1 Gev over 1976-83. Significant correlation is observed between the two except for 1978. Such an effect is also seen in the correlation plot between the solar flare index (SFI) and Fd-I. Author

N85-34834*# National Aeronautics and Space Administration. Goddard Space Flight Center, Greenbelt, Md.

COSMIC RAY MODULATION AND MERGED INTERACTION REGIONS **c93**

L. F. Burlaga, M. L. Goldstein, and Frank B. McDonald (NASA, Washington) *In its* 19th Intern. Cosmic Ray Conf., Vol. 4 Aug. 1985 p 396-399 refs (For primary document see N85-34729 23-92)

(SH-4.1-11) Avail: NTIS HC as boxed set only $200/MF A01 per volume or E99 per entire set CSCL 03B

Beyond several AU, interactions among shocks and streams give rise to merged interaction regions in which the magnetic field is turbulent. The integral intensity of . 75 MeV/Nuc cosmic rays at Voyager is generally observed to decrease when a merged interaction region moves past the spacecraft and to increase during the passage of a rarefaction region. When the separation between interaction regions is relatively large, the cosmic ray intensity tends to increase on a scale of a few months. This was the case at Voyager 1 from July 1, 1983 to May 1, 1984, when the spacecraft moved from 16.7 to 19.6 AU. Changes in cosmic ray intensity were related to the magnetic field strength in a simple way. It is estimated that the diffusion coefficient in merged interaction regions at this distance is similar to 0.6 x 10 to the 22nd power sq cm/s. Author

N85-34835*# National Aeronautics and Space Administration. Goddard Space Flight Center, Greenbelt, Md.

PROPAGATION OF THE PHASE OF SOLAR MODULATION

Miriam A. Forman (State Univ. of New York, Stony Brook), Frank C. Jones, and John S. Perko *In its* 19th Intern. Cosmic Ray Conf., Vol. 4 Aug. 1985 p 400-403 refs (For primary document see N85-34729 23-92)

(SH-4.1-12) Avail: NTIS HC as boxed set only $200/MF A01 per volume or E99 per entire set CSCL 03B

The phase of the 11 year galactic cosmic ray variation, due to a varying rate of emission of long lived propagating regions of enhanced scattering, travels faster than the scattering regions themselves. The radial speed of the 11 year phase in the

quasi-steady, force field approximation is exactly twice the speed of the individual, episodic decreases. A time dependent, numerical solution for 1 GeV protons at 1 and 30 Au gives a phase speed which is 1.85 times the propagation speed of the individual decreases. Author

N85-34836*# California Inst. of Tech., Pasadena.
LATITUDE VARIATION OF RECURRENT FLUXES IN THE OUTER SOLAR SYSTEM Abstract Only **c93**
S. P. Christon and E. C. Stone *In* NASA. Goddard Space Flight Center 19th Intern. Cosmic Ray Conf., Vol. 4 Aug. 1985 p 404 ref (For primary document see N85-34729 23-92)
(SH-4.1-13) Avail: NTIS HC as boxed set only $200/MF A01 per volume or E99 per entire set CSCL 03B

Recurrent low energy (greater than or = to 0.5 MeV) proton flux enhancements, reliable indicators of corotating plasma interaction regions, were observed on the Voyager 1 and 2 and Pioneer 11 spacecraft in the heliographic latitude range 2 deg S to 23 N and the heliocentric radial range 11 to 20 AU. After a period of rather high correlation between fluxes at different latitudes in early 1983, distinct differences developed in the fluxes during an overall flux decrease. The flux intensities returned to higher levels in early 1984 and differences in both the recurrence frequency and flux intensity persisted into 1985, as Voyager 1 traveled to 23 AU and 25 N latitude. Intercomparison of data from the three spacecraft indicates that the flux differences are most likely due to latitudinal rather than radial or temporal variations. Author

N85-34837*# Applied Physics Lab., Johns Hopkins Univ., Laurel, Md.
LONGITUDINAL DISTRIBUTION OF COSMIC RAYS IN THE HELIOSPHERE **c93**
R. E. Gold and D. Venkatesan (Calgary Univ.) *In* NASA. Goddard Space Flight Center 19th Intern. Cosmic Ray Conf., Vol. 4 Aug. 1985 p 405-408 refs (For primary document see N85-34729 23-92)
(Contract N00024-85-C-5301; Grant NSF-ATM-83-05537)
(SH-4.1-14) Avail: NTIS HC as boxed set only $200/MF A01 per volume or E99 per entire set CSCL 03B

The longitudinal distribution of cosmic ray intensity was examined during the years 1974-1976 when the persistent high speed solar wind stream structures produced a well ordered inner heliosphere. Solar wind velocity is mapped back to the Sun and compared with cosmic ray intensity which is represented relative to the solar rotation average. Low solar wind velocity is observed to be a necessary, but not sufficient, condition for the occurrence of higher cosmic ray intensities at 1 AU. These relative enhancements cover a restricted range of heliographic longitudes and persist for several solar rotations. The observed solar wind and cosmic ray intensity relationships are consistent with a simple model suggested here in which cosmic ray modulation is very weak in the inner heliosphere, sunward of the first shock crossing on each field line and more intense in the outer heliosphere. Author

N85-34838*# Chicago Univ., Ill. Dept. of Physics.
THE 1973-1984 SOLAR MODULATION OF COSMIC RAY NUCLEI
M. Garcia-Munox, K. R. Pyle, and J. A. Simpson *In* NASA. Goddard Space Flight Center 19th Intern. Cosmic Ray Conf., Vol. 4 Aug. 1985 p refs (For primary document see N85-34729 23-92)
(Contract NAS5-28442; Grant NGL-14-001-006)
(SH-4.1-16) Avail: NTIS HC as boxed set only $200/MF A01 per volume or E99 per entire set CSCL 03B

As a continuation of the program of solar modulation studies, new measurements were carried out with the cosmic ray telescope on the Earth satellite IMP-8, of the intensity time variations and the energy spectra of galactic cosmic ray protons, helium, carbon and oxygen from 1980 through 1984 including the recent solar maximum. In order to test the applicability of a steady state model of solar modulation during a period which includes times of rapidly changing modulation, these fluxes were equated with the predictions of a conventional model of solar modulation which assumes equilibrium between modulation mechanisms. It is found that for a reasonable range of variations of the diffusion coefficient the model predictions can be made to agree with the measurements at essentially all times during the studied period. The model can account also for the observed hysteresis effects between cosmic rays of different rigidities. Author

N85-34839*# Academy of Sciences (USSR), Troitsk. Inst. of Terrestrial Magnetism, Ionosphere and Radio Wave Propagation.
COSMIC RAY MODULATION IN A RANDOM ANISOTROPIC MAGNETIC FIELD **c93**
L. I. Dorman, Yu. I. Fedorov (Academy of Sciences (USSR), Kiev), M. I. Katz (Academy of Sciences (USSR), Kiev), S. F. Nosov (Academy of Sciences (USSR), Kiev), and B. A. Shakhov (Academy of Sciences (USSR), Kiev) *In* NASA. Goddard Space Flight Center 19th Intern. Cosmic Ray Conf., Vol. 4 Aug. 1985 p 413-416 refs (For primary document see N85-34729 23-92)
(SH-4.1-20) Avail: NTIS HC as boxed set only $200/MF A01 per volume or E99 per entire set CSCL 03B

Inhomogeneities of the interplanetary magnetic field can be divided into small scale and large scale ones as may be required by the character of the problem of cosmic ray (CR) propagation. CR propagation in stochastic magnetic fields is of diffusion character. The main contribution into the scattering of CR particles is made by their interaction with inhomogeneities of the magnetic field H which have characteristic dimensions 1 of the order of Larmor radius R=cp/eH of particle (p is the absolute value of particle momentum, e is particle charge, c is velocity of light). Scattering of particles on such inhomogeneities leads to their diffusion mostly along a magnetic field with characteristic dimensions of variation in space exceeding the mean free path. Author

N85-34840*# Applied Physics Lab., Johns Hopkins Univ., Laurel, Md.
EVIDENCE FOR REGIONS OF NEGLIGIBLE COSMIC-RAY MODULATION IN THE INNER HELIOSPHERE (> 10 AU) **c93**
E. C. Roelof *In* NASA. Goddard Space Flight Center 19th Intern. Cosmic Ray Conf., Vol. 4 Aug. 1985 p 417-420 refs (For primary document see N85-34729 23-92)
(Contract N00024-85-C-5301)
(SH-4.1-21) Avail: NTIS HC as boxed set only $200/MF A01 per volume or E99 per entire set CSCL 03B

Gold and Venkatesan report observations of periods during 1974-1976 when extended regions of heliolongitude that emitted lower than average solar wind velocities at 1 AU also exhibited higher than average cosmic ray intensities as measured by the E 35 MeV CPME anti-coincidence scintillator (28 sq cm omnidirectional geometric factor) on IMP-8. Their observations reproduced by a simple model, based on the observed steady solar wind structure, wherein there is little modulation of cosmic rays in the inner heliosphere until they reach the shocked plasma beyond the stream interactions in the outer heliosphere (similar to 5 to 10 AU). Beyond the interaction boundary, the intensity exhibits a constant radial gradient (similar to 2%/AU). The model also offers an explanation for the irregular behavior of the rotation averaged radial gradients observed by inside 10 AU, as well as the significant, but often ephemeral, latitude gradients observed by Voyagers 1 and 2 and IMP-8. Author

N85-34841*# Potchefstroom Univ. for Christian Higher Education (South Africa). Dept. of Physics.
NOTES ON DRIFT THEORY **c93**
R. A. Burger, H. Moraal, and G. M. Webb (Arizona Univ., Tucson) *In* NASA. Goddard Space Flight Center 19th Intern. Cosmic Ray Conf., Vol. 4 Aug. 1985 p 421-424 refs (For primary document see N85-34729 23-92)
(SH-4.2-3) Avail: NTIS HC as boxed set only $200/MF A01 per volume or E99 per entire set CSCL 03B

It is shown that there is a simpler way to derive the average guiding center drift of a distribution of particles than via the so-called single particle analysis. Based on this derivation it is shown that the entire drift formalism can be considerably simplified, and that results for low order anisotropies are more generally valid

than is usually appreciated. This drift analysis leads to a natural alternative derivation of the drift velocity along a neutral sheet.
Author

N85-34842*# New Hampshire Univ., Durham. Space Science Center.
DRIFT AND OBSERVATIONS IN COSMIC-RAY MODULATION, 1 **c93**
M. S. Potgieter *In* NASA. Goddard Space Flight Center 19th Intern. Cosmic Ray Conf., Vol. 4 Aug. 1985 p 425-428 refs Sponsored in part by CSIR (For primary document see N85-34729 23-92)
(SH-4.2-4) Avail: NTIS HC as boxed set only $200/MF A01 per volume or E99 per entire set CSCL 03B

It is illustrated that a relative simple drift model can, in contrast with no drift models, simultaneously fit proton and electron spectra observed in 1965-66 and 1977, using a single set of modulation parameters except for a change in the IMF polarity. This result is interpreted together with the observation of Evenson and Meyer that electrons are recovering more rapidly than protons after 1980, in contrast with what Burger and Swanenburg observed in 1968-72, as a charge sign dependent effect due to the occurrence of drift in cosmic ray modulation. The same set of parameters produces a shift in the phase and amplitude of the diurnal anisotropy vector, consistent with observations in 1969-71 and 1980-81.
Author

N85-34843*# New Hampshire Univ., Durham. Space Science Center.
DRIFT AND OBSERVATIONS IN COSMIC-RAY MODULATION, 2 **c93**
M. S. Potgieter *In* NASA. Goddard Space Flight Center 19th Intern. Cosmic Ray Conf., Vol. 4 Aug. 1985 p 429-432 refs Sponsored in part by CSIR (For primary document see N85-34729 23-92)
(SH-4.2-5) Avail: NTIS HC as boxed set only $200/MF A01 per volume or E99 per entire set CSCL 03B

The significant effect of drift on the radial and latitudinal dependence of cosmic rays for consecutive solar minimum periods is illustrated. Compared with the integral radial gradient observed in 1976, the calculated value seems too small. A detailed comparison will however have to await the forthcoming solar minimum. The same applies to the latitudinal gradient which is as yet inconclusive about drift effects. Searching the literature for observations related to the IMF polarity reversal, distinct differences were found in neutron monitor response functions for consecutive solar minimum periods, and also in the annual variations of cosmic rays observed before and after polarity reversals. Whether drift is the predominant effect is however not yet clear. Better correlation was found between variations in the cosmic ray intensity and solar activity parameters over a much wider range of heliolatitude during 1970-80 compared to before this period.
Author

N85-34844*# Franklin Inst., Newark, Del.
COSMIC RAY NORTH-SOUTH ANISOTROPY 1961 - 1983 **c93**
J. W. Bieber and M. A. Pomerantz *In* NASA. Goddard Space Flight Center 19th Intern. Cosmic Ray Conf., Vol. 4 Aug. 1985 p 433-436 refs (For primary document see N85-34729 23-92)
(Grants NSF ATM-83-03758; NSF DPP-83-00544)
(SH-4.2-6) Avail: NTIS HC as boxed set only $200/MF A01 per volume or E99 per entire set CSCL 03B

Measurements from neutron monitors in Thule (Greenland) and McMurdo (Antarctica) were used to determine yearly values of the cosmic ray north-south anisotropy over the period 1961-1983. The results strongly suggest that superposed upon the mean anisotropy of 0.05% is a solar cycle variation of amplitude 0.03%. No evidence for a dependence of the anisotropy upon polarity of the solar poloidal magnetic field is found.
Author

N85-34845*# New Mexico Univ., Albuquerque. Dept. of Physics and Astronomy.
NORTH-SOUTH ASYMMETRY IN ACTIVITY ON THE SUN AND COSMIC RAY DENSITY GRADIENTS
D. B. Swinson, M. A. Shea (AFGL), and J. E. Humble (Tasmania Univ., Hobart) *In* NASA. Goddard Space Flight Center 19th Intern. Cosmic Ray Conf., Vol. 4 Aug. 1985 p 437-440 refs (For primary document see N85-34729 23-92)
(SH-4.2-7) Avail: NTIS HC as boxed set only $200/MF A01 per volume or E99 per entire set CSCL 03B

The marked N-S asymmetry in solar activity (with predominant activity in the Sun's Northern Hemisphere) during the 1960's could certainly account for a S-pointing cosmic ray gradient. It is also clear from the data that the response to this change in solar activity asymmetry, and the related change in the perpendicular cosmic ray density gradient, is different for cosmic ray telescopes in the Earth's Northern and Southern Hemispheres. Northern Hemisphere detectors see a S-pointing gradient in the 60's and a N-pointing gradient after 1971, while Southern Hemisphere telescopes see a S-pointing gradient both before and after the reversal.
Author

N85-34846*# Tohoku Univ., Sendai (Japan). Geophysical Inst.
COSMIC RAY INTENSITY AND THE TILT OF THE NEUTRAL SHEET **c93**
T. Saito and D. B. Swinson (New Mexico Univ., Albuquerque) *In* NASA. Goddard Space Flight Center 19th Intern. Cosmic Ray Conf., Vol. 4 Aug. 1985 p 441-444 refs (For primary document see N85-34729 23-92)
(Grant NSF ATM-83-05098)
(SH-4.2-8) Avail: NTIS HC as boxed set only $200/MF A01 per volume or E99 per entire set CSCL 03B

Recent publications have related long-term variations in cosmic ray intensity at the Earth with long term variations in the tilt of the neutral sheet in the inner heliosphere. The tilt of the neutral sheet from 1971 to 1974 is compared with the cosmic ray intensity at Earth, recorded by the Mt. Washington neutron monitor. The remarkable large decreases in cosmic ray intensity which occurred in 1973 and 1974 correlate well with excursions in the tilt of the neutral sheet which occurred earlier during these same two years.
Author

N85-34847*# National Aeronautics and Space Administration. Goddard Space Flight Center, Greenbelt, Md.
DIFFERENTIAL MEASUREMENT OF COSMIC-RAY GRADIENT WITH RESPECT TO INTERPLANETARY CURRENT SHEET **c93**
S. P. Christon (California Inst. of Tech., Pasadena), A. C. Cummings (California Inst. of Tech., Pasadena), E. C. Stone (California Inst. of Tech., Pasadena), K. W. Behannon, and L. F. Burlaga *In its* 19th Intern. Cosmic Ray Conf., Vol. 4 Aug. 1985 p 445-448 refs (For primary document see N85-34729 23-92)
(SH-4.2-9) Avail: NTIS HC as boxed set only $200/MF A01 per volume or E99 per entire set CSCL 03B

Simultaneous magnetic field and charged particle measurements from the Voyager spacecraft at heliographic latitude separations from 10 deg. to 21 deg. are used to determine the latitude gradient of the galactic cosmic ray flux with respect to the interplanetary current sheet. By comparing the ratio of cosmic ray flux at Voyager 1 to that a Voyager 2 during periods when both spacecraft are first nort and then south of the interplanetary current sheet, we find an estimate of the latitudinal gradient with respect to the current sheet of approximately -0.15 + or 0.05% deg under restricted interplanetary conditions.
Author

N85-34848*# Arizona Univ., Tucson.
SPATIAL VARIATION OF COSMIC RAYS NEAR THE HELIOSPHERIC CURRENT SHEET **c93**
J. R. Jokipii and J. Kota (Central Research Inst. for Physics, Budapest) *In* NASA. Goddard Space Flight Center 19th Intern. Cosmic Ray Conf., Vol. 4 Aug. 1985 p 449-452 refs (For primary document see N85-34729 23-92)
(Grant NsG-7101)
(SH-4.2-10) Avail: NTIS HC as boxed set only $200/MF A01 per volume or E99 per entire set CSCL 03B

A quantitative comparison between theoretical predictions and observations of the intensity of galactic cosmic rays near the

interplanetary current sheet is reported. Comparison of model calculations is made with a statistical analysis of observations of galactic cosmic rays at Earth and the simultaneous position of the current sheet. An ensemble of different current sheet inclinations is used, in order to make the analysis of the computations approximate the method used to analyses the data. Author

N85-34849*# Arizona Univ., Tucson.
EFFECTS OF A WAVY NEUTRAL SHEET ON COSMIC RAY ANISOTROPIES **c93**
J. Kota and J. R. Jokipii *In* NASA. Goddard Space Flight Center 19th Intern. Cosmic Ray Conf., Vol. 4 Aug. 1985 p 453-456 refs (For primary document see N85-34729 23-92)
(Grant NSF INT-84-00591)
(SH-4.2-11) Avail: NTIS HC as boxed set only $200/MF A01 per volume or E99 per entire set CSCL 03B

The first results of a three-dimensional numerical code calculating cosmic ray anisotropies is presented. The code includes diffusion, convection, adiabatic cooling, and drift in an interplanetary magnetic field model containing a wavy neutral sheet. The 3-D model can reproduce all the principal observations for a reasonable set of parameters. Author

N85-34850*# Academy of Sciences (USSR), Alma-Ata.
EFFECTS OF SOLAR MAGNETIC FIELD ON COSMIC RAYS **c93**
G. A. Goncher, E. V. Kolomeets, A. Kh. Lyakhova, N. V. Slyunyaeva, and N. V. Stekolnikov *In* NASA. Goddard Space Flight Center 19th Intern. Cosmic Ray Conf., Vol. 4 Aug. 1985 p 457-460 refs (For primary document see N85-34729 23-92)
(SH-4.2-12) Avail: NTIS HC as boxed set only $200/MF A01 per volume or E99 per entire set CSCL 03B

Aspects of the problem of galactic cosmic ray propagation, including inversion of the solar total magnetic field and an analysis of data related to the heliomagnetic cycle are discussed. It is noted that the global structure of the solar magnetic field results in an additional flux of galactic cosmic rays generated by curvature and gradient drifts. An analysis of heliomagnetic cycle data shows that the latitudinal gradient results in a N-S asymmetry, with the amplitude of the effect growing with depth in the atmosphere. The inversion of the solar total magnetic field, drift effects, and other space distributions are found to contribute to a 22-year cycle of solar activity. F.M.R.

N85-34851*# Aligarh Muslim Univ. (India). Space Science Group.
DETERMINATION OF GALACTIC COSMIC RAY LATITUDINAL GRADIENT USING EARTH BASED DETECTORS **c93**
Badruddin and R. S. Yadav *In* NASA. Goddard Space Flight Center 19th Intern. Cosmic Ray Conf., Vol. 4 Aug. 1985 p 461-464 refs (For primary document see N85-34729 23-92)
(SH-4.2-13) Avail: NTIS HC as boxed set only $200/MF A01 per volume or E99 per entire set CSCL 03B

Using cosmic ray intensity data from the Deep River Neutron monitor and the relation between solar wind velocity and heliomagnetic latitude, an attempt is made to evaluate quantitatively the latitudinal gradient of cosmic ray intensity during the periods dominated by a two sector pattern. Assuming a constant orientation of the heliospheric current sheet on a time scale of the order of a year, a relationship is determined between cosmic ray intensity and heliomagnetic latitude. Author

N85-34852*# Academy of Sciences of the Georgian SSR, Tbilisi (USSR). Inst. of Geophysics.
THE EXPECTED COSMIC RAY DENSITY AND STREAM DISTRIBUTIONS AT THE HELIOLATITUDINAL ASYMMETRY OF SOLAR WIND **c93**
M. V. Alania, R. G. Aslamazashvili, L. I. Dorman, and K. Iskra *In* NASA. Goddard Space Flight Center 19th Intern. Cosmic Ray Conf., Vol. 4 Aug. 1985 p 465-468 refs (For primary document see N85-34729 23-92)
(SH-4.2-14) Avail: NTIS HC as boxed set only $200/MF A01 per volume or E99 per entire set CSCL 03B

The results of the spatial distribution of cosmic ray density, gradients, and anisotropy obtained on the basis of the numerical solution of the anisotropic diffusion equation with an account of solar wind velocity change depending on the latitudinal angle theta of the form U=u sub oe sup alpha theta and the diffusion coefficient depending on the spatial coordinates and the particle rigidity are presented. It is shown that the increase of the solar wind velocity and the diffusion coefficient with heliolatitude leads to gradient distributions that are in accord with experimental data observed in space. The results of the energetic spectrum of 11 and 22-year cosmic ray variations obtained with an account of direction of the general magnetic field of the Sun are presented are given. Author

N85-34853*# National Center for Atmospheric Research, Boulder, Colo.
LATITUDINAL GRADIENTS OF COSMIC RAYS AND THE POLARITY REVERSAL OF THE HELIOSPHERIC MAGNETIC FIELD: A PRELIMINARY EVALUATION **c93**
G. Newkirk, Jr., J. A. Lockwood (New Hampshire Univ., Durham), M. Garcia-Munoz (Chicago Univ.), and J. A. Simpson (Chicago Univ.) *In* NASA. Goddard Space Flight Center 19th Intern. Cosmic Ray Conf., Vol. 4 Aug. 1985 p 469-472 refs (For primary document see N85-34729 23-92)
(Contract NAS5-25731; Grants NSF ATM-83-04486; NSF ATM-82-06418)
(SH-4.2-16) Avail: NTIS HC as boxed set only $200/MF A01 per volume or E99 per entire set CSCL 03B

Within the statistical limits imposed by the currently available data and the noise inherent in the determination of the latitudinal gradient, no evidence for the expected change in the latitudinal gradient from pre-1980 to post-1980 epochs can be found. In addition, the rigidity dependence of the gradient appears to be the same in the two epochs. Thus, no evidence is found for a sensitivity of the latitudinal gradient to the polarity of the largescale heliospheric magnetic field such as has been predicted by models incorporating particle drifts. Author

N85-34854*# Academy of Sciences (USSR), Alma-Ata. Inst. of Ionosphere.
THE INFLUENCE OF NONSTATIONARITY OF THE SOLAR ACTIVITY AND GENERAL SOLAR FIELD ON MODULATION OF COSMIC RAYS
A. G. Zusmanovich, O. N. Kryakunova, L. F. Churunova, and Ya. E. Shvartsman *In* NASA. Goddard Space Flight Center 19th Intern. Cosmic Ray Conf., Vol. 4 Aug. 1985 p 473-476 refs (For primary document see N85-34729 23-92)
(SH-4.2-17) Avail: NTIS HC as boxed set only $200/MF A01 per volume or E99 per entire set CSCL 03B

A numerical model of the propagation of galactic cosmic rays in interplanetary space was constructed for the case when the modulation depth determined by the level of solar activity changed in time. Also the contribution of particle drift in the regular field was calculated, and the agreement with experimental data concerning the ratio of protons and electrons in two solar activity minima is shown. Author

N85-34855*# Academy of Sciences of the Georgian SSR, Tbilisi (USSR). Inst. of Geophysics.
THE EFFECT OF THE NEUTRAL SHEET STRUCTURE OF THE INTERPLANETARY MAGNETIC FIELD ON COSMIC RAY DISTRIBUTION IN SPACE **c93**
M. V. Alania, R. G. Aslamazashvili, T. B. Bochorishvili, T. V. Djapiashvili, and V. S. Tkemaladze *In* NASA. Goddard Space Flight Center 19th Intern. Cosmic Ray Conf., Vol. 4 Aug. 1985 p 477-480 refs (For primary document see N85-34729 23-92)
(SH-4.2-18) Avail: NTIS HC as boxed set only $200/MF A01 per volume or E99 per entire set CSCL 03B

Results of the numerical solution of the anistoropic diffusion equation are presented. The modulation depth of galactic cosmic rays is defined by the degree of curvature of the neutral current sheet in the heliosphere. The effect of the regular interplanetary magnetic field (IMF) on cosmic ray anisotropy in the period of solar activity minimum (in 1976) is analyzed by the data of the

neutron super-monitors of the world network, and the heliolatitudinal gradient and cosmic ray diffusion coefficient are defined. Author

N85-34856*# Academy of Sciences (USSR), Moscow.
ON THE INFLUENCE OF THE HELIOMAGNETOSPHERIC PERIPHERY ON THE GALACTIC COSMIC RAYS **c93**
M. B. Krainev, Yu. I. Stozhkov, and T. N. Charakhchyan (Moscow State Univ.) *In* NASA. Goddard Space Flight Center 19th Intern. Cosmic Ray Conf., Vol. 4 Aug. 1985 p 481-484 refs (For primary document see N85-34729 23-92)
(SH-4.2-19) Avail: NTIS HC as boxed set only $200/MF A01 per volume or E99 per entire set CSCL 03B

The suggestion is substantiated that the periphery of the heliomagnetosphere, the region in which properties depend on both solar wind and interstellar space parameters, plays a much more important role in the solar modulation of galactic cosmic rays than previously believed. Author

N85-34857*# Academy of Sciences of the Georgian SSR, Tbilisi (USSR). Inst. of Geophysics.
SPATIAL DISTRIBUTION OF COSMIC RAYS IN MAGNETIC CYCLES OF THE SUN
M. V. Alania, R. T. Gushchina (Academy of Sciences (USSR), Troitsk), and L. I. Dorman (Academy of Sciences (USSR), Troitsk) *In* NASA. Goddard Space Flight Center 19th Intern. Cosmic Ray Conf., Vol. 4 Aug. 1985 p 485-488 refs (For primary document see N85-34729 23-93)
(SH-4.2-20) Avail: NTIS HC as boxed set only $200/MF A01 per volume or E99 per entire set CSCL 03B

The space-time distribution of cosmic ray (CR) density is determined from the solution of the anisotropic diffusion equation. The boundary problem is solved in a quasistationary axisymmetric case, taking into account the delay of cosmic rays relative to the cyclic variations of solar activity. The specificty of the modulation model is the use of the empirical dependence of the free path of particles for scattering on the observed latitudinal distribution of solar activity. Another specific feature of the model is an account of an additional effect due to the drift of charged particles towards the helio-equator plane or backward, depending on the direction of the total magnetic field of the Sun. Author

N85-34858*# Academy of Sciences (USSR), Yakutsk. Inst. of Cosmophysical Research and Aeronomy.
11- AND 22-YEAR VARIATIONS OF THE COSMIC RAY DENSITY AND OF THE SOLAR WIND SPEED **c93**
N. P. Chirkov *In* NASA. Goddard Space Flight Center 19th Intern. Cosmic Ray Conf., Vol. 4 Aug. 1985 p 489-492 refs (For primary document see N85-34729 23-92)
(SH-4.2-21) Avail: NTIS HC as boxed set only $200/MF A01 per volume or E99 per entire set CSCL 03B

Cosmic ray density variations for 17-21 solar activity cycles and the solar wind speed for 20-21 events are investigated. The 22-year solar wind speed recurrence was found in even and odd cycles. The 22-year variations of cosmic ray density were found to be opposite that of solar wind speed and solar activity. The account of solar wind speed in 11-year variations significantly decreases the modulation region of cosmic rays when E = 10-20 GeV. Author

N85-34859*# Universidad Nacional Autonoma de Mexico, Villa Obregon. Inst. de Geofisica.
DIFFERENCE BETWEEN EVEN AND ODD 11-YEAR CYCLES IN COSMIC RAY INTENSITY **c93**
J. A. Otaola, R. Perez-Enriquez, and J. F. Valdes-Galicia *In* NASA. Goddard Space Flight Center 19th Intern. Cosmic Ray Conf., Vol. 4 Aug. 1985 p 493-496 refs (For primary document see N85-34729 23-92)
(SH-4.2-22) Avail: NTIS HC as boxed set only $200/MF A01 per volume or E99 per entire set CSCL 03B

Cosmic ray data for the period 1946-1984 are used to determine the run of the cosmic ray intensity over three complete solar cycles. The analysis shows a tendency towards a regular alternation of cosmic ray intensity cycles with double and single maxima. Whereas a saddle-like shape is characteristic of even cycles, odd cycles are characterized by a peak-like shape. The importance of this behavior is discussed in terms of different processes influencing cosmic ray transport in the heliosphere. Author

N85-34860*# Chicago Univ., Ill.
THE DEPENDENCE OF SOLAR MODULATION ON THE SIGN OF THE COSMIC RAY PARTICLE CHARGE **c93**
M. Garcia-Munoz, P. Meyer, K. R. Pyle, J. A. Simpson (Delaware Univ., Newark), and P. A. Evenson *In* NASA. Goddard Space Flight Center 19th Intern. Cosmic Ray Conf., Vol. 4 Aug. 1985 p 497-500 refs (For primary document see N85-34729 23-92)
(Contracts NAS5-28442; NAS5-28500; Grants NGL-14-001-005; NGL-14-001-006; NAG5-374; NSF ATM-84-12382; NSF ATM-84-01427)
(SH-4.2-23) Avail: NTIS HC as boxed set only $200/MF A01 per volume or E99 per entire set CSCL 03B

The solar modulation of galactic cosmic ray helium and electrons at 1 AU, within the 600-1000 MV magnetic rigidity interval, are compared for the period from 1965 through 1984. The time-intensity variations during the two solar maxima around 1970 and 1981 show that after 1970 the helium intensity recovers earlier than that of the electrons, whereas after 1981 the electron intensity recovers earlier than that of helium. The flux ratio of helium to electrons (He/e) undergoes a major increases during the 1969-1971 period and a major decrease during 1979-83. These experimental results can be interpreted as due to a dependence of the solar modulation of galactic cosmic rays on the sign of the particle charge, possibly as a consequence of drifts due to gradients and curvatures in the interplanetary magnetic field. However, the comparison of the shapes of the intensity-time curves of helium and electrons in the period 1970-1981 does not support a major specific prediction of the drift model. Author

N85-34861*# Air Force Geophysics Lab., Hanscom AFB, Mass.
AN UPDATE ON THE CORRELATION BETWEEN THE COSMIC RADIATION INTENSITY AND THE GEOMAGNETIC AA INDEX **c93**
M. A. Shea and D. F. Smart *In* NASA. Goddard Space Flight Center 19th Intern. Cosmic Ray Conf., Vol. 4 Aug. 1985 p 501-504 refs (For primary document see N85-34729 23-92)
(SH-4.2-24) Avail: NTIS HC as boxed set only $200/MF A01 per volume or E99 per entire set CSCL 03B

A statistical study between the cosmic ray intensity, as observed by a neutron monitor, and of the geomagnetic aa index, as representative of perturbations in the plasma and interplanetary magnetic field in the heliosphere, has been updated to specifically exclude time periods around the reversal of the solar magnetic field. The results of this study show a strong negative correlation for the period 1960 through 1968 with a correlation coefficient of approximately -0.86. However, there is essentially no correlation between the cosmic ray intensity and the aa index for the period 1972-1979 (i.e. correlation coefficient less than 0.16). These results would appear to support the theory of preferential particle propagation into the heliosphere vis the ecliptic during the period 1960-1968 and via the solar polar regions during 1972-1979. Author

N85-35010*# Consiglio Nazionale delle Ricerche, Bologna (Italy).
A STUDY OF PERIODICITIES AND RECURRENCES IN SOLAR ACTIVITY AND COSMIC RAY MODULATION
M. R. Attolini, S. Cecchini, and M. Galli (Bologna Univ.) *In* NASA. Goddard Space Flight Center 19th Intern. Cosmic Ray Conf., Vol. 5 Aug. 1985 p 67-70 refs (For primary document see N85-34991 23-93)
(SH-4.4-14) Avail: NTIS HC as boxed set only $200/MF A01 per volume or E99 per entire set CSCL 03B

N85-35014*# Academy of Sciences (USSR), Moscow.
THE DIFFERENCE IN THE ENERGY SPECTRA OF GALACTIC COSMIC RAYS AT THE MINIMA OF THE 19TH AND 20TH SOLAR ACTIVITY CYCLES
A. K. Svirzhevskaya, N. S. Svirzhevsky, Yu. I. Stozhkov, and T. N.

Charakhchyan (Moscow State Univ.) *In* NASA. Goddard Space Flight Center 19th Intern. Cosmic Ray Conf., Vol. 5 Aug. 1985 p 79-82 refs (For primary document see N85-34991 23-93)
(SH-4.4-18) Avail: NTIS HC as boxed set only $200/MF A01 per volume or E99 per entire set CSCL 03B

N85-35015*# Academy of Sciences (USSR), Moscow. Physical Inst.
COSMIC RAY VARIATIONS WITH THE PERIOD CLOSE TO 27 DAYS AND THEIR CONNECTION WITH SOLAR ACTIVITY LONGITUDINAL DISTRIBUTION
G. A. Bazilevskaya, M. I. Tyasto (Academy of Sciences, USSR, Leningrad), and E. S. Vernova (Academy of Sciences, USSR, Leningrad) *In* NASA. Goddard Space Flight Center 19th Intern. Cosmic Ray Conf., Vol. 5 Aug. 1985 p 83-86 refs (For primary document see N85-34991 23-93)
(SH-4.4-19) Avail: NTIS HC as boxed set only $200/MF A01 per volume or E99 per entire set CSCL 03B

N85-35016*# Academy of Sciences of the Georgian SSR, Tbilisi (USSR). Inst. of Geophysics.
AZIMUTHAL AND MERIDIONAL ASYMMETRIES OF THE SOLAR WIND AND QUASIPERIODIC VARIATIONS OF INTENSITY OF GALACTIC COSMIC RAYS (GCR)
L. Kh. Shatashvili, T. V. Djapiashvili, B. G. Kavlashvili, B. D. Naskidashvili, O. G. Rogava, and G. V. Shafer *In* NASA. Goddard Space Flight Center 19th Intern. Cosmic Ray Conf., Vol. 5 Aug. 1985 p 87-89 refs (For primary document see N85-34991 23-93)
(SH-4.4-20) Avail: NTIS HC as boxed set only $200/MF A01 per volume or E99 per entire set CSCL 03B

N85-35019*# Nagoya Univ. (Japan). Dept. of Physics.
THE FIRST THREE HARMONICS OF SOLAR DAILY VARIATION CAUSED BY THE DIFFUSIVE PROPAGATION OF GALACTIC COSMIC RAYS THROUGH THE HELIOSPHERE
K. Munakata and K. Nagashima *In* NASA. Goddard Space Flight Center 19th Intern. Cosmic Ray Conf., Vol. 5 Aug. 1985 p 98-101 refs (For primary document see N85-34991 23-93)
(SH-4.5-1) Avail: NTIS HC as boxed set only $200/MF A01 per volume or E99 per entire set CSCL 03B

N85-35020*# Nagoya Univ. (Japan). Dept. of Physics.
FORMULATION OF COSMIC-RAY SOLAR DAILY VARIATION AND ITS SEASONAL VARIATION, PRODUCED FROM GENERALIZED STATIONARY ANISOTROPY OF SOLAR ORIGIN
R. Tatsuoka and K. Nagashima *In* NASA. Goddard Space Flight Center 19th Intern. Cosmic Ray Conf., Vol. 5 Aug. 1985 p 102-105 refs (For primary document see N85-34991 23-93)
(SH-4.5-2) Avail: NTIS HC as boxed set only $200/MF A01 per volume or E99 per entire set CSCL 03B

N85-35021*# Shinshu Univ., Matsumoto (Japan). Dept. of Physics.
SOLAR TRI-DIURNAL VARIATION OF COSMIC RAYS IN A WIDE RANGE OF RIGIDITY
S. Mori, H. Ueno (Nagoya Univ.), Z. Fujii (Nagoya Univ.), I. Morishita (Asahi Univ.), and K. Nagashima (Nagoya Univ.) *In* NASA. Goddard Space Flight Center 19th Intern. Cosmic Ray Conf., Vol. 5 Aug. 1985 p 106-109 refs (For primary document see N85-34991 23-93)
(SH-4.5-3) Avail: NTIS HC as boxed set only $200/MF A01 per volume or E99 per entire set CSCL 03B

N85-35022*# New Mexico Univ., Albuquerque. Dept. of Physics and Astronomy.
UPPER CUT-OFF RIGIDITY FOR COROTATION ANISOTROPY DURING SOLAR ACTIVITY CYCLES 20 AND 21 Abstract Only
H. S. Ahluwalia and J. F. Riker (BDM Corp., Albuquerque, N. Mex.) *In* NASA. Goddard Space Flight Center 19th Intern. Cosmic Ray Conf., Vol. 5 Aug. 1985 p 110 (For primary document see N85-34991 23-93)
(SH-4.5-4) Avail: NTIS HC as boxed set only $200/MF A01 per volume or E99 per entire set CSCL 03B

N85-35025*# New Mexico Univ., Albuquerque. Dept. of Physics and Astronomy.
DIURNAL ANISOTROPY DURING SOLAR ACTIVITY CYCLE TWENTY AND DIFFUSION-CONVECTION MODEL
H. S. Ahluwalia and J. F. Riker (BDM Corp., Albuquerque, N. Mex.) *In* NASA. Goddard Space Flight Center 19th Intern. Cosmic Ray Conf., Vol. 5 Aug. 1985 p 116-119 refs (For primary document see N85-34991 23-93)
(SH-4.5-7) Avail: NTIS HC as boxed set only $200/MF A01 per volume or E99 per entire set CSCL 03B

N85-35035*# Nagoya Univ. (Japan). Cosmic Ray Lab.
ANOMALOUS INCREASE OF SOLAR ANISOTROPY ABOVE 150GV IN 1981-1983
H. Ueno, Z. Fujii (Shinshu Univ.), S. Mori (Gifu College of Dentistry), I. Morishita, and K. Nagashima *In* NASA. Goddard Space Flight Center 19th Intern. Cosmic Ray Conf., Vol. 5 Aug. 1985 p 147-150 refs (For primary document see N85-34991 23-93)
(SH-4.5-18) Avail: NTIS HC as boxed set only $200/MF A01 per volume or E99 per entire set CSCL 03B

N85-35036*# Academy of Sciences (USSR), Irkutsk. Inst. of Terrestrial Magnetism, Ionosphere and Radio Wave Propagation.
DIAGNOSTIC OF ELECTROMAGNETIC CONDITIONS IN SPACE USING COSMIC RAYS
V. M. Dvornikov, V. E. Sdobnov, and A. V. Sergeev *In* NASA. Goddard Space Flight Center 19th Intern. Cosmic Ray Conf., Vol. 5 Aug. 1985 p 151-154 refs (For primary document see N85-34991 23-93)
(SH-4.5-19) Avail: NTIS HC as boxed set only $200/MF A01 per volume or E99 per entire set CSCL 03B

N85-35040*# California Inst. of Tech., Pasadena.
SOLAR CYCLE VARIATIONS OF THE ANOMALOUS COSMIC RAY COMPONENT Abstract Only
R. A. Mewaldt and E. C. Stone *In* NASA. Goddard Space Flight Center 19th Intern. Cosmic Ray Conf., Vol. 5 Aug. 1985 p 167 (For primary document see N85-34991 23-93)
(Contracts NAS5-28441; NAS5-28449; Grant NGR-05-002-160)
(SH-4.6-2) Avail: NTIS HC as boxed set only $200/MF A01 per volume or E99 per entire set CSCL 03B

N85-35041*# Maryland Univ., College Park. Dept. of Physics.
TEMPORAL VARIATIONS OF THE ANOMALOUS OXYGEN COMPONENT, 1977 - 1984
G. M. Mason, B. Klecker (Max-Planck-Inst. fuer Extraterrestrische Physik, Garching, West Germany), A. B. Galvin, D. Hovestadt (Max-Planck-Inst. fuer Extraterrestrische, Garching, West Germany), and F. M. Ipavich *In* NASA. Goddard Space Flight Center 19th Intern. Cosmic Ray Conf., Vol. 5 Aug. 1985 p 168-171 refs (For primary document see N85-34991 23-93)
(SH-4.6-3) Avail: NTIS HC as boxed set only $200/MF A01 per volume or E99 per entire set CSCL 03B

N85-35042*# New Hampshire Univ., Durham.
RADIAL AND LATITUDINAL GRADIENTS OF ANOMALOUS OXYGEN DURING 1977 - 1985
W. R. Webber, A. C. Cummings (California Inst. of Tech., Pasadena), and E. C. Stone *In* NASA. Goddard Space Flight Center 19th Intern. Cosmic Ray Conf., Vol. 5 Aug. 1985 p 172-175 refs (For primary document see N85-34991 23-93)
(Contract NAS7-918; Grant NGR-05-002-160)
(SH-4.6-4) Avail: NTIS HC as boxed set only $200/MF A01 per volume or E99 per entire set CSCL 03B

N85-35049*# California Inst. of Tech., Pasadena.
SOLAR MODULATION AND INTERPLANETARY GRADIENTS OF THE GALACTIC ELECTRONS FLUX, 1977 - 1984
S. P. Christon, A. C. Cummings, E. C. Stone, and W. R. Webber (New Hampshire Univ.) *In* NASA. Goddard Space Flight Center 19th Intern. Cosmic Ray Conf., Vol. 5 Aug. 1985 p 197 refs (For primary document see N85-34991 23-93)
(Contracts NAS7-918; NGR-05-002-160)

(SH-4.7-4) Avail: NTIS HC as boxed set only $200/MF A01 per volume or E99 per entire set CSCL 03B

N85-35052*# Chicago Univ., Ill.
THE RECOVERY OF THE COSMIC RAY FLUX FROM MAXIMUM SOLAR MODULATION AT IMP-8 (1 AU) AND AT PIONEER (R > 30 AU)
R. B. McKibben, K. R. Pyle, and J. A. Simpson *In* NASA. Goddard Space Flight Center 19th Intern. Cosmic Ray Conf., Vol. 5 Aug. 1985 p 206-209 refs (For primary document see N85-34991 23-93)
(SH-4.7-7) Avail: NTIS HC as boxed set only $200/MF A01 per volume or E99 per entire set CSCL 03B

N85-35055*# Academy of Sciences (USSR), Moscow. Inst. of History of Science and Technology.
DIMENSIONS OF THE SOLAR WIND CAVITY AND OF THE REGION OF INTERPLANETARY COSMIC RAY MODULATION
I. V. Dorman *In* NASA. Goddard Space Flight Center 19th Intern. Cosmic Ray Conf., Vol. 5 Aug. 1985 p 218-221 refs (For primary document see N85-34991 23-93)
(SH-4.7-11) Avail: NTIS HC as boxed set only $200/MF A01 per volume or E99 per entire set CSCL 03B

N85-35058*# Consiglio Nazionale delle Ricerche, Rome (Italy). Ist. di Fisica dello Spazio Interplanetario.
THE FLARE ORIGIN OF FORBUSH DECREASES NOT ASSOCIATED WITH SOLAR FLARES ON THE VISIBLE HEMISPHERE OF THE SUN
N. Iucci, M. Parisi, C. Signorini, M. Storini, and G. Villoresi *In* NASA. Goddard Space Flight Center 19th Intern. Cosmic Ray Conf., Vol. 5 Aug. 1985 p 230-233 refs (For primary document see N85-34991 23-93)
(SH-5.1-4) Avail: NTIS HC as boxed set only $200/MF A01 per volume or E99 per entire set CSCL 03B

N85-35059*# Consiglio Nazionale delle Ricerche, Rome (Italy). Ist. di Fisica dello Spazio Interplanetario.
LONGITUDINAL DEPENDENCE OF THE INTERPLANETARY PERTURBATION PRODUCED BY ENERGETIC TYPE 4 SOLAR FLARES AND OF THE ASSOCIATED COSMIC RAY MODULATION
N. Iucci, M. Parisi, M. Storini, G. Villoresi, and S. Pinter (Slovak Academy of Sciences, Hurbanovo, Czechoslovakia) *In* NASA. Goddard Space Flight Center 19th Intern. Cosmic Ray Conf., Vol. 5 Aug. 1985 p 234-237 refs (For primary document see N85-34991 23-93)
(SH-5.1-5) Avail: NTIS HC as boxed set only $200/MF A01 per volume or E99 per entire set CSCL 03B

N85-35066*# Nagoya Univ. (Japan). Cosmic Ray Research Lab.
THE SOLAR WIND EFFECT ON COSMIC RAYS AND SOLAR ACTIVITY
K. Fujimoto, H. Kojima (Fujita Gakuen Health Univ., Japan), and K. Murakami *In* NASA. Goddard Space Flight Center 19th Intern. Cosmic Ray Conf., Vol. 5 Aug. 1985 p 262-265 refs (For primary document see N85-34991 23-93)
(SH-5.1-13) Avail: NTIS HC as boxed set only $200/MF A01 per volume or E99 per entire set CSCL 03B

N85-35075*# Academy of Sciences (USSR), Moscow. Inst. of Terrestrial Magnetism, Ionosphere and Radio Wave Propagation.
SOLAR ACTIVITY BEYOND THE DISK AND VARIATIONS OF THE COSMIC RAY GRADIENT
A. V. Belov, L. I. Dorman, E. A. Eroshenko, V. N. Ishkov, and V. A. Oleneva *In* NASA. Goddard Space Flight Center 19th Intern. Cosmic Ray Conf., Vol. 5 Aug. 1985 p 296-299 refs (For primary document see N85-34991 23-93)
(SH-5.1-23) Avail: NTIS HC as boxed set only $200/MF A01 per volume or E99 per entire set CSCL 03B

N85-35077*# Kochi Univ., Akebono (Japan). Dept. of Physics.
ON THE SOLAR CYCLE VARIATION IN THE BAROMETER COEFFICIENTS OF HIGH LATITUDE NEUTRON MONITORS
M. Kusunose and N. Ogita (Inst. of Physical and Chemical Research) *In* NASA. Goddard Space Flight Center 19th Intern. Cosmic Ray Conf., Vol. 5 Aug. 1985 p 304-407 refs (For primary document see N85-34991 23-93)
(SH-6.1-2) Avail: NTIS HC as boxed set only $200/MF per volume or E99 per entire set CSCL 03B

N85-35088*# Moscow State Univ. (USSR). Inst. of Nuclear Physics.
PENETRATION OF SOLAR PROTONS INTO THE EARTH'S MAGNETOSPHERE ON NOVEMBER 22, 1977
E. V. Gorchakov, V. G. Afanasyev, K. G. Afanasyev, P. P. Ignatyev, V. A. Iozenas, M. V. Ternovskaya, and G. G. Zenchev *In* NASA. Goddard Space Flight Center 19th Intern. Cosmic Ray Conf., Vol. 5 Aug. 1985 p 344-347 refs (For primary document see N85-34991 23-93)
(SH-6.1-15) Avail: NTIS HC as boxed set only $200/MF A01 per volume or E99 per entire set CSCL 03B

N85-35089*# Tashkent V. I. Lenin State Univ., Vuzgorodok (USSR).
DYNAMICS OF THE PENETRATION BOUNDARIES OF SOLAR PROTONS DURING A STRONG MAGNETIC STORM
G. A. Glukhov, Yu. P. Kratenko, and Yu. V. Mineev (Moscow State Univ.) *In* NASA. Goddard Space Flight Center 19th Intern. Cosmic Ray Conf., Vol. 5 Aug. 1985 p 348-351 refs (For primary document see N85-34991 23-93)
(SH-6.1-16) Avail: NTIS HC as boxed set only $200/MF A01 per volume or E99 per entire set CSCL 03B

N85-35093*# Academy of Sciences (USSR), Moscow.
THE INFLUENCE OF THE EARTH'S MAGNETOSPHERE ON THE HIGH-ENERGY SOLAR PROTONS
G. A. Bazilevskaya, V. S. Makhmutov (Industrial Inst. of Roudny), and T. N. Charakhchyan (Moscow State Univ.) *In* NASA. Goddard Space Flight Center 19th Intern. Cosmic Ray Conf., Vol. 5 Aug. 1985 p 363-366 refs (For primary document see N85-34991 23-93)
(SH-6.1-22) Avail: NTIS HC as boxed set only $200/MF A01 per volume or E99 per entire set CSCL 03B

N85-35104*# Kanagawa Univ., Yokahama (Japan). Inst. of Physics.
THE 4He1H RATIOS IN THE CHEMICAL COMPOSITIONS OF SOLAR FLARE PARTICLES AND THE PRIMORDIAL SOLAR NEBULA
Kunitomo Sakurai *In* NASA. Goddard Space Flight Center 19th Intern. Cosmic Ray Conf., Vol. 5 Aug. 1985 p 406-409 refs (For primary document see N85-34991 23-93)
(SH-7.1-12) Avail: NTIS HC as boxed set only $200/MF A01 per volume or E99 per entire set CSCL 03B

N85-35109*# Indore Univ. (India). Dept. of Physics.
CORRELATION BETWEEN SOLAR NEUTRINO FLUX AND OTHER SOLAR PHENOMENA
Siddheshwar Lal and A. Subramanian (Tata Inst. of Fundamental Research) *In* NASA. Goddard Space Flight Center 19th Intern. Cosmic Ray Conf., Vol. 5 Aug. 1985 p 426-429 refs (For primary document see N85-34991 23-93)
Avail: NTIS HC as boxed set only $200/MF A01 per volume or E99 per entire set CSCL 03B

N85-35110*# Kanagawa Univ., Yokahama (Japan). Inst. of Physics.
A POSSIBLE MECHANISM TO CAUSE THE QUASI-BIENNIAL VARIABILITY ON THE SOLAR NEUTRINO FLUX
Kunitomo Sakurai and Mitsuru Hasegawa *In* NASA. Goddard Space Flight Center 19th Intern. Cosmic Ray Conf., Vol. 5 Aug. 1985 p 430-433 refs (For primary document see N85-34991 23-93)
(SH-8.1-5) Avail: NTIS HC as boxed set only $200/MF A01 per volume or E99 per entire set CSCL 03B

N85-35111*# Academy of Sciences, Potsdam (East Germany).
THE CONJECTURE CONCERNING TIME VARIATIONS IN THE SOLAR NEUTRINO FLUX
H. J. Haubold and E. Gerth *In* NASA. Goddard Space Flight Center 19th Intern. Cosmic Ray Conf., Vol. 5 Aug. 1985 p 434-437 refs (For primary document see N85-34991 23-93)
(SH-8.1-6) Avail: NTIS HC as boxed set only $200/MF A01 per volume or E99 per entire set CSCL 03B

N85-35112*# Calcutta Univ. (India). Dept. of Applied Mathematics.
SOLAR NEUTRINO: FLUX, COSMIC RAYS AND THE 11 YEAR SOLAR CYCLE
Probhas Raychaudhuri *In* NASA. Goddard Space Flight Center 19th Intern. Cosmic Ray Conf., Vol. 5 Aug. 1985 p 438-441 refs (For primary document see N85-34991 23-93)
(SH-8.1-7) Avail: NTIS HC as boxed set only $200/MF A01 per volume or E99 per entire set CSCL 03B

N85-35113*# Calcutta Univ. (India). Dept. of Applied Mathematics.
SOLAR NEUTRINOS, SOLAR FLARES, SOLAR ACTIVITY CYCLE AND THE PROTON DECAY
Probhas Raychaudhuri *In* NASA. Goddard Space Flight Center 19th Intern. Cosmic Ray Conf., Vol. 5 Aug. 1985 p 442-445 refs (For primary document see N85-34991 23-93)
(SH-8.1-8) Avail: NTIS HC as boxed set only $200/MF A01 per volume or E99 per entire set CSCL 03B

N85-35114*# Kobe Univ. (Japan). Graduate School of Science and Technology.
NEUTRINO PRODUCTION FROM THE SOLAR ATMOSPHERE
H. Inazawa, K. Kobayakawa, and T. Kitamura (Tokyo Univ., Tanashi) *In* NASA. Goddard Space Flight Center 19th Intern. Cosmic Ray Conf., Vol. 5 Aug. 1985 p 446-449 refs (For primary document see N85-34991 23-93)
(SH-8.1-9) Avail: NTIS HC as boxed set only $200/MF A01 per volume or E99 per entire set CSCL 03B

N85-35115*# Academy of Sciences (USSR), Moscow. Physical Inst.
SOLAR COSMIC RAY BURSTS AND SOLAR NEUTRINO FLUXES
G. A. Basilevakaya, S. I. Nikolsky, Yu. I. Stozhkov, and T. N. Charakhchyan (Moscow State Univ.) *In* NASA. Goddard Space Flight Center 19th Intern. Cosmic Ray Conf., Vol. 5 Aug. 1985 p 450-453 refs (For primary document see N85-34991 23-93)
(SH-8.1-10) Avail: NTIS HC as boxed set only $200/MF A01 per volume or E99 per entire set CSCL 03B

N85-35118*# Instituto Nacional de Tecnica Aeroespacial, Madrid (Spain). Grupos Cientificos CONIE.
A SILICON SURFACE BARRIER TELESCOPE FOR SOLAR PARTICLES IDENTIFICATION
J. Sequeiros and J. Medina *In* NASA. Goddard Space Flight Center 19th Intern. Cosmic Ray Conf., Vol. 5 Aug. 1985 p 462-465 refs Sponsored by Comision Asesora de Investigacion Cientifica y Technica (For primary document see N85-34991 23-93)
(SH-9.1-3) Avail: NTIS HC as boxed set only $200/MF A01 per volume or E99 per entire set CSCL 03B

N85-35123*# Academia Sinica, Beijing (China). Inst. of Space Physics.
RECORDING SYSTEM FOR THE SOLAR NEUTRON MONITORING AT MT. NORIKURA
Shao Hua Yu, M. Kusunose (Kochi Univ.), H. Sasaki (Kochi Univ.), N. Ohmori (Kochi Univ.), K. Takahashi (Inst. of Physical and Chemical Research, Tokyo), and M. Wada (Inst. of Physical and Chemical Research, Tokyo) *In* NASA. Goddard Space Flight Center 19th Intern. Cosmic Ray Conf., Vol. 5 Aug. 1985 p 482-485 refs (For primary document see N85-34991 23-93)
(SH-9.1-8) Avail: NTIS HC as boxed set only $200/MF A01 per volume or E99 per entire set CSCL 03B

N85-35127*# Case Western Reserve Univ., Cleveland, Ohio. Dept. of Physics.
SONTRAC: A SOLAR NEUTRON TRACK CHAMBER DETECTOR
Glenn M. Frye, Jr., Thomas L. Jenkins, and Alan Owens *In* NASA. Goddard Space Flight Center 19th Intern. Cosmic Ray Conf., Vol. 5 Aug. 1985 p 498-501 refs (For primary document see N85-34991 23-93)
(SH-9.1-12) Avail: NTIS HC as boxed set only $200/MF A01 per volume or E99 per entire set CSCL 03B

N85-35139*# Kharkov State Univ. (USSR).
SPORADIC RADIO EMISSION CONNECTED WITH A DEFINITE MANIFESTATION OF SOLAR ACTIVITY IN THE NEAR EARTH SPACE
A. V. Dudnic, I. I. Zaljubovski, V. M. Kartashev, and E. S. Shmatko *In* NASA. Goddard Space Flight Center 19th Intern. Cosmic Ray Conf., Vol. 5 Aug. 1985 p 538-541 (For primary document see N85-34991 23-93)
(SH-10.1-8) Avail: NTIS HC as boxed set only $200/MF A01 per volume or E99 per entire set CSCL 03B

93 SPACE RADIATION

Includes cosmic radiation; and inner and outer Earth's radiation belts.

For biological effects of radiation see *52 Aerospace Medicine*. For theory see *73 Nuclear and High-Energy Physics*.

N85-34862*# National Aeronautics and Space Administration. Goddard Space Flight Center, Greenbelt, Md.
NINETEENTH INTERNATIONAL COSMIC RAY CONFERENCE. OG SESSIONS, VOLUME 3
Frank C. Jones, comp. Washington Aug. 1985 530 p refs Conf. held in La Jolla, Calif., 11-23 Aug. 1985 8 Vol.
(NASA-CP-2376-Vol-3; NAS 1.55:2376-Vol-3) Avail: NTIS HC as boxed set only $200/MF A01 per volume or E99 per entire set CSCL 03B

Papers submitted for presentation at the 19th International Cosmic Ray Conference are compiled. This volume addresses cosmic ray sources and acceleration, interstellar propagation and nuclear interactions, and detection techniques and instrumentation. For individual titles, see N85-34863 through N85-34990.

N85-34863*# Minnesota Univ., Minneapolis. School of Physics and Astronomy.
VARIATIONS IN THE PROPAGATION OF UH-NUCLEI
C. J. Waddington, N. R. Brewster, and M. P. Kertzman *In* NASA. Goddard Space Flight Center 19th Intern. Cosmic Ray Conf., Vol. 3 Aug. 1985 p 1-4 refs (For primary document see N85-34862 23-93)
(OG-7.1-1) Avail: NTIS HC as boxed set only $200/MF A01 per volume or E99 per entire set CSCL 03B

Calculations of the propagation of UH-nuclei were improved by extending the number of individual nuclides considered, and by using more recent evaluations of the rigidity dependence of the escape length, the possible source composition, and altered cross sections. The effects of using different expressions for the dependence of abundances on first ionization potentials (FIP) are outlined. The sensitivity of the calculated elemental abundances to the various changes made in the propagation assumptions are discussed. E.A.K.

N85-34864*# Liege Univ. (Belgium).
GERMANIUM AND LEAD: SIGNIFICANT DIFFERENCES BETWEEN METEORITIC AND PHOTOSPHERIC ABUNDANCES?
Nicolas Grevesse and Jean-Paul Meyer (Commissariat de l'Energie Atomique, Saclay) *In* NASA. Goddard Space Flight Center 19th Intern. Cosmic Ray Conf., Vol. 3 Aug. 1985 p 5-8 refs (For primary document see N85-34862 23-93)
(OG-7.1-2) Avail: NTIS HC as boxed set only $200/MF A01 per

volume or E99 per entire set CSCL 03B

The order of the Galactic cosmic ray source (GCRS) composition in terms of first ionization potential (FIP) was examined. For most elements, the degree of volatility is (positively) correlated with the value of the FIP, so that it is not easy to distinguish a correlation of GCRS abundances anomalies with FIP from a correlation with volatility. Only a few permit to distinguish between the two kinds of ordering: if they are depleted relative to refractory metals, volatility must be relevant, if not, FIP is relevant. Among them Cu and Zn would seem to favor FIP. Among the best indicators are Ge and Pb. The abundance anomalies in GCRS are defined relative to a standard which, for the heavy elements concerned, is commonly taken as C1 Carbonaceous Chondrites. Photospheric abundances are more directly representative of the protosolar nebula, and hence of ordinary local galactic (LG) matter. The Ge and Pb reference abundance determinations in the Photosphere and in C1 meteorites are examined and their relevance to the problem with FIP vs. volatility in GCRs is discussed. E.A.K.

N85-34865*# Tata Inst. of Fundamental Research, Bombay (India).
LEAD AND URANIUM GROUP ABUNDANCES IN COSMIC RAYS
J. S. Yadav and V. P. Perelygin (Joint Inst. for Nuclear Research, Dubna) *In* NASA. Goddard Space Flight Center 19th Intern. Cosmic Ray Conf., Vol. 3 Aug. 1985 p 9-12 refs (For primary document see N85-34862 23-93)
(OG-7.1-3) Avail: NTIS HC as boxed set only $200/MF A01 per volume or E99 per entire set CSCL 03B

The importance of Lead and Uranium group abundances in cosmic rays is discussed in understanding their evolution and propagation. The electronic detectors can provide good charge resolution but poor data statistics. The plastic detectors can provide somewhat better statistics but charge resolution deteriorates. The extraterrestrial crystals can provide good statistics but with poor charge resolution. Recent studies of extraterrestrial crystals regarding their calibration to accelerated uranium ion beam and track etch kinetics are discussed. It is hoped that a charge resolution of two charge units can be achieved provided an additional parameter is taken into account. The prospects to study abundances of Lead group, Uranium group and superheavy element in extraterrestrial crystals are discussed, and usefulness of these studies in the light of studies with electronic and plastic detectors is assessed. E.A.K.

N85-34866*# Washington Univ., St. Louis, Mo.
IMPLICATIONS OF SOURCE ABUNDANCES OF ULTRAHEAVY COSMIC RAYS
W. R. Binns, T. L. Garrard (California Inst. of Tech., Pasadena), M. H. Israel, J. Klarmann, S. H. Margolis, E. C. Stone (California Inst. of Tech., Pasadena), and C. J. Waddington (Minnesota Univ., Minneapolis) *In* NASA. Goddard Space Flight Center 19th Intern. Cosmic Ray Conf., Vol. 3 Aug. 1985 p 13-16 refs (For primary document see N85-34862 23-93)
(OG-7.1-4) Avail: NTIS HC as boxed set only $200/MF A01 per volume or E99 per entire set CSCL 03B

The ratio of cosmic ray source abundance to solar-system abundance was examined for individual elements. Correlations of these ratios with first-ionization potential (FIP) and the expected mass-to-charge ratio (A/Q) of the elements in a million-degree plasma are analyzed. The FIP correlation was examined and it is shown that the correlation is affected by the choice of C2 or C1 chondritic meteorites as the solar-system standard for comparison. An A/Q correlation is suggested as a consequence of the shock acceleration model in the hot interstellar medium. The correlations are presented. E.A.K.

N85-34867*# Lodz Univ. (Poland). Inst. of Physics.
PROPAGATION AND NUCLEOSYNTHESIS OF ULTRAHEAVY COSMIC RAYS
M. Giler and T. Wibig *In* NASA. Goddard Space Flight Center 19th Intern. Cosmic Ray Conf., Vol. 3 Aug. 1985 p 17-20 refs (For primary document see N85-34862 23-93)
(OG-7.1-5) Avail: NTIS HC as boxed set only $200/MF A01 per volume or E99 per entire set CSCL 03B

The observed fluxes of cosmic ray (C.R.) ultraheavy elements depend on their charge and mass spectrum at the sources and on the propagation effects, on the distribution of path lengths traversed by the particles on their way from the sources to the observation point. The effect of different path length distributions (p.l.d.) on the infered source abunances is analyzed. It seems that it is rather difficult to fit a reasonable p.l.d. so that the obtained source spectrum coincides with the Solar System (SS) abundances in more detail. It suggests that the nucleosynthesis conditions for c.r. nuclei may differ from that for SS matter. The nucleosynthesis of ultraheavy elements fitting its parameters to get the c.r. source abundances is calculated. It is shown that it is possible to get a very good agreement between the predicted and the observed source abundance. E.A.K.

N85-34868*# Washington Univ., St. Louis, Mo. Center for the Space Sciences.
SOURCES OF THE ULTRAHEAVY COSMIC RAYS
Steven H. Margolis and J. B. Blake (Aerospace Corp., Los Angeles) *In* NASA. Goddard Space Flight Center 19th Intern. Cosmic Ray Conf., Vol. 3 Aug. 1985 p 21-24 refs (For primary document see N85-34862 23-93)
(OG-7.1-7) Avail: NTIS HC as boxed set only $200/MF A01 per volume or E99 per entire set CSCL 03B

The suggestions that the source abundances of cosmic ray nuclei heavier then Fe differ significantly from Solar System abundances are not well supported by the data without assuming preferential acceleration. The Solar System abundances of Pb and Bi are split into r-, standard s-, and cyclic 8-process components; the apprarent deficiency of Pb seen in the HEAO-3 Heavy Nuclei Experiment data might indicate an absence of Pb from the recycling 8-process. M.G.

N85-34869*# Kanagawa Univ., Yokahama (Japan). Inst. of Physics.
THE COSMIC RAY COMPOSITION AS VIEWED FROM THE CHEMICAL ABUNDANCES OF THE SOLAR SYSTEM
Kunitomo Sakurai *In* NASA. Goddard Space Flight Center 19th Intern. Cosmic Ray Conf., Vol. 3 Aug. 1985 p 25-28 refs (For primary document see N85-34862 23-93)
(OG-7.1-8) Avail: NTIS HC as boxed set only $200/MF A01 per volume or E99 per entire set CSCL 03B

It is shown that the chemical composition of cosmic rays at their sources for the elements up to the atomic number as 80 is quite similar to that of the carbonaceous chondrites, which have been keeping the properties of the protosolar nebula. In particular, the similarity between these two compositions is significant to the elements classified as refractory and siderphile, in addition to the elements, Ca and Al. These results as cited above suggest that cosmic rays, being currently observed near the Earth, may have been accelerated from the matter with the composition similar to that which is found of these chondrites as Allende. Author

N85-34870*# California Univ., Berkeley. Physics Dept.
ELEMENTAL TECHNETIUM AS A COSMIC-RAY CLOCK
J. Drach and M. H. Salamon *In* NASA. Goddard Space Flight Center 19th Intern. Cosmic Ray Conf., Vol. 3 Aug. 1985 p 29-32 refs (For primary document see N85-34862 23-93)
(OG-7.1-9) Avail: NTIS HC as boxed set only $200/MF A01 per volume or E99 per entire set CSCL 03B

Several radioactive isotopes have been proposed as clocks for the study of the mean cosmic ray confinement time, T sub e. Measurements of Be-10 and Al-26 give a value for T sub e of about 10 Myr when one uses a leaky box cosmic ray propagation model. It is important to obtain additional measurements of T sub e from other radioactive isotopes in order to check whether the confinement is the same throughout the periodic table. The possible use of Tc (Z = 43) as a cosmic clock is investigated. Since all isotopes of Tc are radioactive, one might be able to group these isotopes and use the elemental abundance as a whole. The results of the calculations are somewhat inconclusive for two reasons. First, the beta + decay half lives of two of the Tc isotopes relevant

to our calculation are not known. Second, the dependence of the Tc abundance on the mean confinement time is rather weak when one considers the number of events expected in 4 trays of plastic track detectors. However, a future, finite measurement of the Beta + half lives and the possible use of the entire collecting area of the HNC to detect Tc nuclei could make the use of Tc as a cosmic ray clock more attractive. Author

N85-34871*# Severn Communications Corp., Severna Park, Md.
ELECTRON CAPTURE DECAY OF COSMIC RAYS: A MODEL OF THE INHOMOGENEOUS INTERSTELLAR MEDIUM
John R. Letaw, Rein Silberberg (NRL, Washington, D.C.), and C. H. Tsao (NRL, Washington, D.C.) *In* NASA. Goddard Space Flight Center 19th Intern. Cosmic Ray Conf., Vol. 3 Aug. 1985 p 33-36 refs (For primary document see N85-34862 23-93)
(OG-7.1-10) Avail: NTIS HC as boxed set only $200/MF A01 per volume or E99 per entire set CSCL 03B

Traditional analyses of cosmic ray composition seek to identify the sources through a determination of a the isotopic abundances of these nuclei prior to acceleration. At the same time, it is both necessary and interesting to understand the nature of the medium through which cosmic rays pass before arriving at detectors. In fact, only within a model of the interstellar medium (ISM) sampled by cosmic rays can a refined estimate of source composition be made. An elaboration of the traditional model of the ISM used in studying cosmic ray propagation is explored. Inhomogeneity of the ISM is accomodated in this model. Within this model it is found that the abundances of some electron apture isotopes, are very sensitive to density inhomogeneities which might be expected in the ISM. These nuclei therefore measure the penetration of heavy cosmic rays into interstellar clouds. Author

N85-34872*# Yunnan Univ., Kunming (China). Dept. of Physics.
A VERY IMPORTANT PROCESS OF NUCLEOSYNTHESIS IN STARS Abstract Only
Chuanzan Yu, Renming Zhou, and Shijie Zhan *In* NASA. Goddard Space Flight Center 19th Intern. Cosmic Ray Conf., Vol. 3 Aug. 1985 p 37 (For primary document see N85-34862 23-93)
(OG-7.1-11) Avail: NTIS HC as boxed set only $200/MF A01 per volume or E99 per entire set CSCL 03B

When some nuclei are free from strong gravitational field, they are unstable and will become stable nuclei by competitions of following processes: (1) neutron-evaporation; (2) spontaneous fission; and (3) beta prime 3-decay. At the initial stage, (1) and (2) are important and (3) can be ignored. The qualitative results are as follows: (1) it seems that nuclei with $A > 100$ come from the spontaneous fission and beta prime decay of neutron-evaporated nuclei with A similiar to 140-440, which can replace the r-process; (2) the super-heavy elements with $Z = 114$--126 (A similar to 330--360) can be formed. They can be observed in cosmic range if they have the halftime T 10 to the 7th power years; (3) the peak in the rare-earth elements comes from the symmetric fission of super-heavy elements; (4) there are more neutron-rich nuclei in the fragments; and (5) the abundances of $a > 83$ elements in cosmic rays are one order of magnitude higher than that in the solar system. Author

N85-34873*# Washington Univ., St. Louis, Mo. Center for the Space Sciences.
THE MODEL-INDEPENDENCE OF COSMIC RAY SOURCE DETERMINATIONS
Steven H. Margolis *In* NASA. Goddard Space Flight Center 19th Intern. Cosmic Ray Conf., Vol. 3 Aug. 1985 p 38-41 refs (For primary document see N85-34862 23-93)
(OG-7.2-1) Avail: NTIS HC as boxed set only $200/MF A01 per volume or E99 per entire set CSCL 03B

The direct inversion method of Margolis is used to explore the dependence of Z less than or equal to 28 source abundance determinations on the choice of the pathlength distribution. The source abundances do not depend strongly on the form of the truncation used, although some truncation at the lower energies (compared to a leaky box) is necessary. The decrease of mean grammage with increasing energy is required by the observations. The effects of errors and he use of other secondary to primary ratios is discussed. Author

N85-34874*# New Hampshire Univ., Durham. Space Science Center.
THE EFFECTS OF NEWLY MEASURED CROSS SECTIONS IN HYDROGEN ON THE PRODUCTION OF SECONDARY NUCLEI DURING THE PROPAGATION OF COSMIC RAYS THROUGH INTERSTELLAR H
W. R. Webber, M. Gupta, L. Koch-Miramond (Commissariat de l'Energie Atomique, Saclay), and P. Masse (Commissariat de l'Energie Atomique, Saclay) *In* NASA. Goddard Space Flight Center 19th Intern. Cosmic Ray Conf., Vol. 3 Aug. 1985 p 42-45 refs (For primary document see N85-34862 23-93)
(OG-7.2-2) Avail: NTIS HC as boxed set only $200/MF A01 per volume or E99 per entire set CSCL 03B

The cross sections of six important cosmic ray source nuclei in hydrogen at several energies between 300 and 1800 MeV/nuc were measured. Significant differences, sometimes exceeding 50%, exist between these new measurements and the earlier semiempirical predictions, and a new set of semiempirical formulae are being determined that better describe this fragmentation. New cross sections were obtained so that the systematics of their effects on cosmic ray propagation through interstellar hydrogen can be examined. Author

N85-34875*# Severn Communications Corp., Severna Park, Md.
IMPLICATIONS OF CROSS SECTION ERRORS FOR COSMIC RAY PROPAGATION
John R. Letaw, Rein Silberberg (NRL, Washington, D.C.), and C. H. Tsao (NRL, Washington, D.C.) *In* NASA. Goddard Space Flight Center 19th Intern. Cosmic Ray Conf., Vol. 3 Aug. 1985 p 46-49 refs (For primary document see N85-34862 23-93)
(OG-7.2-3) Avail: NTIS HC as boxed set only $200/MF A01 per volume or E99 per entire set CSCL 03B

Errors in nuclear interaction cross sections are the single most important limitation on the analysis of cosmic ray composition data. At the 18th International Cosmic Ray Conference, the potential importance of correlations in cross section errors in determining cosmic ray source abundances was demonstrated. In this paper the magnitude of cross section error correlation is estimated. Analysis suggests that cross section errors are essentially uncorrelated for nuclei with $Z < 29$ and that the actual errors may be less than the nominal 35%. Author

N85-34876*# Max-Planck-Inst. fuer Extraterrestrische Physik, Garching (West Germany).
COSMIC RAY SECONDARY NUCLEI AND THE STRUCTURE OF THE GALAXY
G. E. Morfill, P. Meyer (Chicago Univ.), and R. Luest (ESA, Paris) *In* NASA. Goddard Space Flight Center 19th Intern. Cosmic Ray Conf., Vol. 3 Aug. 1985 p 50-53 refs (For primary document see N85-34862 23-93)
(OG-7.2-4) Avail: NTIS HC as boxed set only $200/MF A01 per volume or E99 per entire set CSCL 03B

The consequencies of diffusive acceleration of cosmic rays in supernova shocks propagation through an inhomogeneous interstellar medium are explored. The acceleration takes place in the hot, tenuous, intercloud gas, while nuclear collisions, leading to the production of cosmic ray secondaries, predominantly occur in those regions where the supernova shocks collide with interstellar clouds. A simple model is used to calculate the interaction of a (cosmic ray + gas) shock with a cloud, and thus determine the gross topology. Extending this to the whole system, using mean cloud sizes and space densities, allows us to calculate the secondary/primary cosmic ray abundance ratios for light and heavy nuclei. Author

N85-34877*# Max-Planck-Inst. fuer Radioastronomie, Bonn (West Germany).
WHY DO LEAKY-BOX MODELS WORK SO FINE?
R. Schlickeiser and I. Lerche (South Carolina Univ., Columbia) *In*

NASA. Goddard Space Flight Center 19th Intern. Cosmic Ray Conf., Vol. 3 Aug. 1985 p 54-57 refs (For primary document see N85-34862 23-93)
(OG-7.2-8) Avail: NTIS HC as boxed set only $200/MF A01 per volume or E99 per entire set CSCL 03B

By introducing the concept of the age distribution of cosmic rays it is possible to decouple spatial from momentum transport, and simple leaky-box type equations result. The influence of spatial inhomogeneities, geometries, and source distributions enters the spatially homogeneous, infinite (i.e., leaky box) problem through appropriate mean lifetimes. A precise prescription of how to obtain these mean lifetimes, i.c., for comparison with data measured in the vicinity of the solar system they have to be calculated from the age distribution at the spatial position of the observer. Author

N85-34878*# Washington Univ., St. Louis, Mo. Center for the Space Sciences.
ALFVEN WAVE SCATTERING AND THE SECONDARY TO PRIMARY RATIO
G. Larry Bretthorst and Steven H. Margolis *In* NASA. Goddard Space Flight Center 19th Intern. Cosmic Ray Conf., Vol. 3 Aug. 1985 p 58-60 refs (For primary document see N85-34862 23-93)
(OG-7.2-9) Avail: NTIS HC as boxed set only $200/MF A01 per volume or E99 per entire set CSCL 03B

The cosmic ray abundances have traditionally been used to determine the elemental and isotopic nature of galactic ray sources and average measures of propagation conditions. Detailed studies of the physics of propagation are usually paired with relatively straightforward estimates of the secondary-to-primary (S/P) ratios. In the work reported here, calculations of elemental abundances are paired with a more careful treatment of the propagation process. It is shown that the physics of propagation does indeed leave specific traces of Galactic structure in cosmic ray abundances.
Author

N85-34879*# Commissariat a l'Energie Atomique, Saclay (France).
ON THE IMPORTANCE OF INTERSTELLAR HELIUM FOR THE PROPAGATION OF HEAVY COSMIC RAYS
P. Ferrando, P. Goret, and A. Soutoul *In* NASA. Goddard Space Flight Center 19th Intern. Cosmic Ray Conf., Vol. 3 Aug. 1985 p 61-62 refs (For primary document see N85-34862 23-93)
(OG-7.2-11) Avail: NTIS HC as boxed set only $200/MF A01 per volume or E99 per entire set CSCL 03B

The influence of interstellar He on the fragmentation of heavy cosmic rays in the interstellar medium (ISM) has long been a controversial subject. While H-induced cross section data are now avialable over broad mass and energy ranges, little data for He-induced fragmentation exists. With the recent reports of accurate measurements of the secondary/primary ratios in cosmic rays and of H-induced cross sections the problem of including interstellar He in propagation calculations becomes even more critical. As is argued the escape lengths lambda e deduced from the B/C+) and Sc-Cr/Fe ratios cannot be reconciled within the frame of a simple leaky box model assuming the ISM composed of pure H. It is quite remarkable that the discrepancy is especially large in the GeV region where (1) secondary/primary ratios measured by several groups agree fairly well and (2) fragmentation cross sections have been recently measured with good accuracy.
Author

N85-34880*# Jet Propulsion Lab., California Inst. of Tech., Pasadena.
INTERSTELLAR TURBULENCE, RANDOM DENSITY VARIATIONS, AND SCINTILLATION MEASUREMENTS
J. C. Higdon *In* NASA. Goddard Space Flight Center 19th Intern. Cosmic Ray Conf., Vol. 3 Aug. 1985 p 63-66 refs (For primary document see N85-34862 23-93)
(OG-7.2-13) Avail: NTIS HC as boxed set only $200/MF A01 per volume or E99 per entire set CSCL 03B

The presence of random electron variations suggests that the ionized interstellar medium is turbulent. In the interstellar plasma the presence of power spectra of such variations extending to spatial scales much less than a Coulomb mean free path, Lambda sub c, is required by analyses of measurements of scintillation and angular broadening of pulsar radio signals. The existence of corresponding variations in magnetic field strength could efficiently scatter cosmic rays and thus constrain cosmic-ray propagation. Unfortunately both the origin of the electron density variations and mechanisms by which these variations couple to fluctuations in magnetic field strength are unknown. It is conjectured that the small-scale density variations are generated by the convective distortion of initially large-scale isobaric entropy structures in the turbulent interstellar plasma. An investigation of the spectra of turbulent entropy structures, velocity, and magnetic fields at small spatial scales is made. The modifier small is employed to characterize length scales much less than the dimension, L, containing the bulk of the turbulent energy.
Author

N85-34881*# Kalinin (M. I.) Polytechnical Inst., Leningrad (USSR).
ON THE COSMIC RAY DIFFUSION IN A VIOLENT INTERSTELLAR MEDIUM
A. M. Bykov and I. N. Toptygin *In* NASA. Goddard Space Flight Center 19th Intern. Cosmic Ray Conf., Vol. 3 Aug. 1985 p 67-70 refs (For primary document see N85-34862 23-93)
(OG-7.2-14) Avail: NTIS HC as boxed set only $200/MF A01 per volume or E99 per entire set CSCL 03B

A variety of the available observational data on the cosmic ray (CR) spectrum, anisotropy and composition are in good agreement with a suggestion on the diffusion propagation of CR with energy below 10(15) eV in the interstellar medium. The magnitude of the CR diffusion coefficient and its energy dependence are determined by interstellar medium (ISM) magnetic field spectra. Direct observational data on magnetic field spectra are still absent. A theoretical model to the turbulence generation in the multiphase ISM is resented. The model is based on the multiple generation of secondary shocks and concomitant large-scale rarefactions due to supernova shock interactions with interstellar clouds. The distribution function for ISM shocks are derived to include supernova statistics, diffuse cloud distribution, and various shock wave propagation regimes. This permits calculation of the ISM magnetic field fluctuation spectrum and CR diffusion coefficient for the hot phase of ISM.
Author

N85-34882*# Academy of Sciences (USSR), Moscow. Physical Inst.
THE ROLE OF COSMIC RAYS IN MAGNETIC HYDRODYNAMICS OF INTERSTELLAR MEDIUM
V. L. Ginzburg *In* NASA. Goddard Space Flight Center 19th Intern. Cosmic Ray Conf., Vol. 3 Aug. 1985 p 71-74 refs (For primary document see N85-34862 23-93)
(OG-7.2-15) Avail: NTIS HC as boxed set only $200/MF A01 per volume or E99 per entire set CSCL 03B

Cosmic ray (CR) propagation in the Galaxy and generally in the cosmic plasma is usually considered in the diffusion approximation. The diffusion is regarded to result from CR scattering due to their interaction with a magnetic and an electric field. In most cases the fields are assumed to be given. Meanwhile, in the Galaxy the CR energy density w sub cr is similar to I eV/cm, i.e., it is comparable with the energy densities of the magnetic field and turbulent motions in the interstellar gas. Therefore, for the Galaxy it becomes necessary to take into account the influence of CR on the gas dynamics and on the magnetic fields in this gas. The simplest way to this is to use the hydrodynamic approximation, but this is possible only on scales greatly exceeding the CR free path lambda before scattering and only for times larger than lambda/v approx. equals lambda/c. One should thus obtain corresponding MHD equations and establish the limits of their applicability.
Author

N85-34883*# Academy of Sciences (USSR), Troitsk. Inst. of Terrestrial Magnetism, Ionosphere and Radio Wave Propagation.
DIFFUSION OF STRONGLY MAGNETIZED COSMIC RAY PARTICLES IN A TURBULENT MEDIUM
V. S. Ptuskin *In* NASA. Goddard Space Flight Center 19th Intern. Cosmic Ray Conf., Vol. 3 Aug. 1985 p 75-78 refs (For primary document see N85-34862 23-93)

(OG-7.2-16) Avail: NTIS HC as boxed set only $200/MF A01 per volume or E99 per entire set CSCL 03B

Cosmic ray (CR) propagation in a turbulent medium is usually considered in the diffusion approximation. Here, the diffusion equation is obtained for strongly magnetized particles in the general form. The influence of a large-scale random magnetic field on CR propagation in interstellar medium is discussed. Cosmic rays are assumed to propagate in a medium with a regular field H and an ensemble of random MHD waves. The energy density of waves on scales smaller than the free path 1 of CR particles is small. The collision integral of the general form which describes interaction between relativistic particles and waves in the quasilinear approximation is used. R.J.F.

N85-34884*# Aerospace Corp., El Segundo, Calif. Space Sciences Lab.

COSMIC-RAY TRANSPORT IN THE GALACTIC MAGNETOSPHERE

Michael Schulz and J. G. Luhmann (California Univ., Los Angeles) *In* NASA. Goddard Space Flight Center 19th Intern. Cosmic Ray Conf., Vol. 3 Aug. 1985 p 79-82 refs (For primary document see N85-34862 23-93)

(OG-7.2-17) Avail: NTIS HC as boxed set only $200/MF A01 per volume or E99 per entire set CSCL 03B

It is advantageous to regard cosmic rays as the constitutent particles of the Galactic radiation belts and cosmic ray energization as a consequence of inward radial diffusion in the quasi-dipolar Galactic magnetosphere. This process occurs in addition to Fermi acceleration. The purpose of this work is to explore a magnetospheric explanation for the elevation of Galactic charged particles to cosmic ray energies. The magnetosphere that is of interest in this context is not a planetary magnetosphere but a galactic magnetosphere entirely analogous to those inferred from radio observations of distant galaxies. It is the magnetosphere of the Milky Way. Cosmic rays are (by this interpretation) the charged particles that constitute the radiation belts of the Galactic magnetosphere. Thus, the mechanism by which charged particles attain cosmic-ray energies is presumable the mechanism by which radiation-belt particles attain high energies in more familiar magnetosphere, i.e., the radial diffusion associated with magnetic disturbances that contain spectral power resonant with the azimuthal drift of the particles. R.J.F.

N85-34885*# Natal Univ., Durban (South Africa).

THE ROLE OF COSMIC RAYS AND ALFVEN WAVES IN THE STRUCTURE OF THE GALACTIC HALO

M. K. Dougherty, J. F. McKenzie, and N. J. Westergaard (Danish Space Research Inst., Lyngby) *In* NASA. Goddard Space Flight Center 19th Intern. Cosmic Ray Conf., Vol. 3 Aug. 1985 p 83-86 refs (For primary document see N85-34862 23-93)

(OG-7.2-18) Avail: NTIS HC as boxed set only $200/MF A01 per volume or E99 per entire set

The effect that cosmic rays and the Alfven waves they generate have on the structure of the plasma distribution perpendicular to the galactic disk is examined. It is shown that the plasma distribution exhibits two length scales and the predicted values of gas density far from the galactic plane indicate that models involving hydrostatic equilibrium should be replaced by those allowing for a galactic wind. Author

N85-34886*# New Hampshire Univ., Durham. Space Science Center.

MEASUREMENTS OF THE FRAGMENTATION OF (40)Ar, (28)Si AND (12)C IN CH2C AND H TARGETS BETWEEN 300 AND 1500 MeV/NUC AT THE BEVALAC

W. R. Webber and J. C. Kish *In* NASA. Goddard Space Flight Center 19th Intern. Cosmic Ray Conf., Vol. 3 Aug. 1985 p 87-90 refs (For primary document see N85-34862 23-93)

(Grants NAG8-451; NGR-30-002-052)

(OG-7.2-19) Avail: NTIS HC as boxed set only $200/MF A01 per volume or E99 per entire set CSCL 03B

Studies of the fragmentation of various nuclei in CH2 and C targets were continued with the objective of obtaining cross sections in hydrogen for use in the cosmic ray propagation problem. New measurements include Fe-56. Measurements were made at 6 energies between 300 and 1700 MeV/nuc. C-12 measurements were made at six energies. Si-28 measurements were made at three energies and measurements were made at two energies. New data on C-12 Si-28 and AR-44 nuclei are given. The data are compared with the earlier semi-empirical predictions. Author

N85-34887*# California Inst. of Tech., Pasadena.

MEASUREMENTS OF Fe AND Ar FRAGMENTATION CROSS SECTIONS

K. H. Lau, R. A. Mewaldt, and E. C. Stone *In* NASA. Goddard Space Flight Center 19th Intern. Cosmic Ray Conf., Vol. 3 Aug. 1985 p 91-94 refs (For primary document see N85-34862 23-93)

(OG-7.2-20) Avail: NTIS HC as boxed set only $200/MF A01 per volume or E99 per entire set CSCL 03B

Measurements are reported of the yields of individual isotopes of Cr to Co($Z = 24$ to 27) resulting from the fragmentation of Fe-56, and the isotopes of Mg to K($Z = 12$ to 19) resulting from the fragmentation of Ar-40. Recent advances in the resolution and collecting power of cosmic ray instrumentation, have led to dramatic improvements in the precision of cosmic ray composition measurements, both elemental and isotopic. The interpretation of these measurements is presently limited by uncertainties in the fragmentation cross-sections needed to correct for nuclear interactions with the interstellar gas. Cosmic ray propagation codes now rely mainly on semi-empirical cross-section formulae developed by Silberberg and Tsao (S&T), which have a typical uncertainty of approximately 25%. Relative isotope yields from the fragmentation of approximately 380 MeV/nucleon Fe-56 e and approximately 210 MeV/nucleon Ar-40 r in CH2 targets, observed during the calibration of two cosmic ray spectrometers at the Lawrence Berkeley Laboratory Bevalac are reported. These are compared with calculated yeilds based on the S&T cross-section formulae. R.J.F.

N85-34888*# Minnesota Univ., Minneapolis. School of Physics and Astronomy.

INTERACTIONS OF HEAVY NUCLEI, Kr, Xe AND Ho, IN LIGHT TARGETS

M. P. Kertzman, J. Klarmann (Washington Univ., St. Louis), B. J. Newport (California Inst. of Tech., Pasadena), E. C. Stone (California Inst. of Tech., Pasadena), C. J. Waddington, W. R. Binns (Washington Univ., St. Louis), T. L. Garrard (California Inst. of Tech., Pasadena), and M. H. Israel (Washington Univ., St. Louis) *In* NASA. Goddard Space Flight Center 19th Intern. Cosmic Ray Conf., Vol. 3 Aug. 1985 p 95-98 refs (For primary document see N85-34862 23-93)

(OG-7.2-21) Avail: NTIS HC as boxed set only $200/MF A01 per volume or E99 per entire set CSCL 03B

Over the past few years, the HEAO-3 measurements of the abundances of ultra-heavy cosmic ray nuclei ($Z > 26$) at earth have been analyzed. In order to interpret these abundances in terms of a source composition, allowance must be made for the propagation of the nuclei in the interstellar medium. Vital to any calculation of the propagation is a knowlege of the total and partial interaction cross sections for these heavy nuclei on hydrogen. Until recently, data on such reactions have been scarce. However, now that relativistic heavy ion beams are available at the LBL Bevalac, some of the cross sections of interest can be measured at energies close to those of the cosmic ray nuclei being observed. During a recent calibration at the Bevalac of an array similar to the HEAO-C3 UH-nuclei detector, targets of raphite (C), polyethylene (CH2), and aluminum were exposed to five heavy ion beams ranging in charge (Z) from 36 to 92. Total and partial charge changing cross sections for the various beam nuclei on hydrogen can be determined from the measured cross sections on C and CH2, and will be applied to the propagation problem. The cross sections on Al can be used to correct the abundances of UH cosmic rays observed in the HEAO C-3 detector for interactions in the detector itself. R.J.F.

N85-34889*# Siegen Univ., (West Germany). Physics Dept.
CROSS SECTIONS FOR THE PRODUCTION OF FRAGMENTS WITH Z GREATER THAN OR EQUAL TO 8 BY FRAGMENTATION OF Z GREATER THAN OR EQUAL TO 9 AND LESS THAN OR EQUAL TO 26 NUCLEI
W. Heinrich, H. Drechsel, C. Brechtmann, and J. Beer *In* NASA. Goddard Space Flight Center 19th Intern. Cosmic Ray Conf., Vol. 3 Aug. 1985 p 99-102 refs (For primary document see N85-34862 23-93)
(OG-7.2-22) Avail: NTIS HC as boxed set only $200/MF A01 per volume or E99 per entire set CSCL 03B

Charge changing nuclear collisions in plastic nuclear track detectors were studied using a new experimental technique of automatic track measurement for etched tracks in plastic detectors. Partial cross sections for the production of fragments of charge Z approximately > 8 were measured for projectile nuclei of charge 9 approximately < Z approximately < 26 in the detector material CR39 and in silver. for this purpose three independent experiments were performed using Bevalac beams. The first one was an exposure of a stack of CR39 plastic plates to 1.8 GeV/nucl. Ar-40 nuclei. The second one was an exposure of another CR39 stack of 1.7 GeV/nucl. Fe-56 projectiles. In the third experiment a mixed stack of CR39 plates and silver foils was irradiated with 1.7 GeV/nucl. Fe-56 nuclei. Thus the measurement of nuclear cross sections in a light target (CR39 = C12H18O7) and as well in a heavy target (silver) was possible. Author

N85-34890*# Naval Research Lab., Washington, D. C. Center for Space Research.
CALCULATION OF IMPROVED SPALLATION CROSS SECTIONS
C. H. Tsao, R. Silberberg, and J. R. Letaw (Severn Communications Corp.) *In* NASA. Goddard Space Flight Center 19th Intern. Cosmic Ray Conf., Vol. 3 Aug. 1985 p 103-106 refs (For primary document see N85-34862 23-93)
(OG-7.2-23) Avail: NTIS HC as boxed set only $200/MF A01 per volume or E99 per entire set CSCL 03B

Several research groups have recently carried out highly precise measurements (to about 10 percent) of high-energy nuclear spallation cross sections. These measurements, above 5 GeV, cover a broad range of elements: V, Fe, Cu, Ag, Ta and Au. Even the small cross sections far off the peak of the isotopic distribution curves have been measured. The semiempirical calculations are compared with the measured values. Preliminary comparisons indicate that the parameters of our spallation relations (Silberberg and Tsao, 1973) for atomic numbers 20 to 83 need modifications, e.g. a reduced slope of the mass yield distribution, broader isotopic distributions, and a shift of the isotopic distribution toward the neutron-deficient side. The required modifications are negligible near Fe and Cu, but increase with increasing target mass. Author

N85-34891*# Arizona Univ., Tucson. Dept. of Planetary Sciences.
THE COSMIC-RAY SHOCK STRUCTURE PROBLEM FOR RELATIVISTIC SHOCKS
G. M. Webb *In* NASA. Goddard Space Flight Center 19th Intern. Cosmic Ray Conf., Vol. 3 Aug. 1985 p 107-110 refs (For primary document see N85-34862 23-93)
(Grant NSF ATM-83-11241)
(OG-8.1-1) Avail: NTIS HC as boxed set only $200/MF A01 per volume or E99 per entire set CSCL 03B

The time asymptotic behaviour of a relativistic (parallel) shock wave significantly modified by the diffusive acceleration of cosmic-rays is investigated by means of relativistic hydrodynamical equations for both the cosmic-rays and thermal gas. The form of the shock structure equation and the dispersion relation for both long and short wavelength waves in the system are obtained. The dependence of the shock acceleration efficiency on the upstream fluid spped, long wavelength Mach number and the ratio N = P sub co/cP sub co+P sub go)(Psub co and P sub go are the upstream cosmic-ray and thermal gas pressures respectively) are studied. Author

N85-34892*# Natal Univ., Durban (South Africa). Dept. of Mathematics and Applied Mathematics.
INSTABILITIES IN DECELERATING SUPERSONIC FLOWS WITH APPLICATIONS TO COSMIC RAY SHOCKS
A. P. Zank and J. F. McKenzie *In* NASA. Goddard Space Flight Center 19th Intern. Cosmic Ray Conf., Vol. 3 Aug. 1985 p 111-114 refs (For primary document see N85-34862 23-93)
(OG-8.1-2) Avail: NTIS HC as boxed set only $200/MF A01 per volume or E99 per entire set CSCL 03B

The nature of instabilities in cosmic ray shocks is investigated by using two distinct models for the shock wave. For wavelengths which are short relative to the thickness of the shock wave, the shock is treated as a smoothly decelerating low, and an appropriate JWKB type expansion is used to describe the perturbations to the flow. In this, the short wavelength regime, the presence of squeezing and an effective g renders strong cosmic ray shocks unstable in a way which is similar to instabilities in other supersonic flows, such as in de Laval nozzle flow or a heat conduction dominated shock wave. In the long wavelength limit, where the shock is treated as a discontinuous transition, a stability function is derived which, if negative, corresponds to unstable disturbances growing exponentially in time. In this case, it was found that if the cosmic ray fluid is relativistic (gamma sub c = 4/3) and the background plasma ideal (gamma = 5/3), then strong shocks are unstable. Author

N85-34893*# Max-Planck-Inst. fuer Kernphysik, Heidelberg (West Germany).
TIME-DEPENDENT NONLINEAR COSMIC RAY SHOCKS CONFIRMING ABSTRACT
E. A. Dorfi *In* NASA. Goddard Space Flight Center 19th Intern. Cosmic Ray Conf., Vol. 3 Aug. 1985 p 115-117 refs (For primary document see N85-34862 23-93)
(OG-8.1-3) Avail: NTIS HC as boxed set only $200/MF A01 per volume or E99 per entire set CSCL 03B

Numerical studies of time dependent cosmic ray shock structures in planar geometry are interesting because analytical time-independent solutions are available which include the nonlinear reactions on the plasma flow. A feature of these time asymptotic solutions is that for higher Mach numbers (M approximately > 5) and for a low cosmic ray upstream pressure the solution is not uniquely determined by the usual conservation laws of mass, momentum and energy. These numerical solutions clearly indicate that much work needs to be done before we understand shock acceleration as a time dependent process. The slowness of the process is possibly due to the fact that there is a diffusive flux into the downstream region in addition to the usual advective losses. Analytic investigations of thie phenomenon are required. R.J.F.

N85-34894*# Max-Planck-Inst. fuer Kernphysik, Heidelberg (West Germany).
SELFSIMILAR TIME DEPENDENT SHOCK STRUCTURES
R. Beck and L. OC. Drury *In* NASA. Goddard Space Flight Center 19th Intern. Cosmic Ray Conf., Vol. 3 Aug. 1985 p 118-120 refs (For primary document see N85-34862 23-93)
(OG-8.1-4) Avail: NTIS HC as boxed set only $200/ MF A01 per volume or E99 per entire set CSCL 03B

Diffusive shock acceleration as an astrophysical mechanism for accelerating charged particles has the advantage of being highly efficient. This means however that the theory is of necessity nonlinear; the reaction of the accelerated particles on the shock structure and the acceleration process must be self-consistently included in any attempt to develop a complete theory of diffusive shock acceleration. Considerable effort has been invested in attempting, at least partially, to do this and it has become clear that in general either the maximum particle energy must be restricted by introducing additional loss processes into the problem or the acceleration must be treated as a time dependent problem (Drury, 1984). It is concluded that stationary modified shock structures can only exist for strong shocks if additional loss processes limit the maximum energy a particle can attain. This is certainly possible and if it occurs the energy loss from the shock

will lead to much greater shock compressions. It is however equally possible that no such processes exist and we must then ask what sort of nonstationary shock structure develops. The ame argument which excludes stationary structures also rules out periodic solutions and indeed any solution where the width of the shock remains bounded. It follows that the width of the shock must increase secularly with time and it is natural to examine the possibility of selfsimilar time dependent solutions. R.J.F.

N85-34895*# Wien Univ. (Austria). Inst. fuer Astronomie.
A COSMIC RAY DRIVEN INSTABILITY
E. A. Dorfi and L. OC. Drury (Max-Planck-Inst. fuer Kernphysik) *In* NASA. Goddard Space Flight Center 19th Intern. Cosmic Ray Conf., Vol. 3 Aug. 1985 p 121-123 (For primary document see N85-34862 23-93)
(OG-8.1-5) Avail: NTIS HC as boxed set only $200/MF A01 per volume or E99 per entire set CSCL 03B

The interaction between energetic charged particles and thermal plasma which forms the basis of diffusive shock acceleration leads also to interesting dynamical phenomena. For a compressional mode propagating in a system with homogeneous energetic particle pressure it is well known that friction with the energetic particles leads to damping. The linear theory of this effect has been analyzed in detail by Ptuskin. Not so obvious is that a non-uniform energetic particle pressure can addition amplify compressional disturbances. If the pressure gradient is sufficiently steep this growth can dominate the frictional damping and lead to an instability. It is important to not that this effect results from the collective nature of the interaction between the energetic particles and the gas and is not connected with the Parker instability, nor with the resonant amplification of Alfven waves. Author

N85-34896*# Maryland Univ., College Park. Astronomy Program.
RELATIVISTIC COSMIC RAY SPECTRA IN THE FULL NONLINEAR THEORY OF SHOCK ACCELERATION
David Eichler and Donald C. Ellison *In* NASA. Goddard Space Flight Center 19th Intern. Cosmic Ray Conf., Vol. 3 Aug. 1985 p 124-127 refs (For primary document see N85-34862 23-93)
(OG-8.1-6) Avail: NTIS HC as boxed set only $200/MF A01 per volume or E99 per entire set CSCL 03B

The non-linear theory of shock acceleration was generalized to include wave dynamics. In the limit of rapid wave damping, it is found that a finite ave velocity tempers the acceleration of high Mach number shocks and limits the maximum compression ratio even when energy loss is important. For a given spectrum, the efficiency of relativistic particle production is essentially independent of v sub Ph. For the three families shown, the percentage of kinetic energy flux going into relativistic particles is (1) 72%, 2) 44%, and (3) 26% (this includes the energy loss at the upper energy cuttoff). Even small v sub ph, typical of the HISM, produce quasi-universal spectra that depend only weakly on the acoustic Mach number. These spectra should be close enough to e(-2) to satisfy cosmic ray source requirements. Author

N85-34897*# National Aeronautics and Space Administration. Goddard Space Flight Center, Greenbelt, Md.
THE CENTRAL ENGINE OF QUASARS AND AGNS: A RELATIVISTIC PROTON RADIATIVE SHOCK
Demosthenes Kazanas and Donald C. Ellison *In its* 19th Intern. Cosmic Ray Conf., Vol. 3 Aug. 1985 p 128-131 refs (For primary document see N85-34862 23-93)
(OG-8.1-7) Avail: NTIS HC as boxed set only $200/MF A01 per volume or E99 per entire set CSCL 03B

Active galactic nuclei (AGNs) and quasars (QSOs) appear to emit roughly equal energy per decade from radio to gamma-ray energies (e.g. Ramaty and Ligenfelter 1982). This argues strongly for a nonthermal radiation mechanism (see Rees 1984). In addition, statistical studies have indicated that the spectra of these objects in the IR-UV and 2 to 50 keV X-ray band, can be fitted very well with power laws of specific indices. These spectral indices do not seem to depend on the luminosity or morphology of the objects (Rothschild et al. 1983; Malkan 1984), and any theory should account for them in a basic and model independent way. If shocks accelerate relativistic protons via the first-order Fermi mechanism (e.g. Axfor 1981), the radiating electrons can be produced as secondaries throughout the source by proton-proton (p-p) collisions and pion decay, thus eliminating Compton losses (Protheroe and Kazanas 1983). As shown by Kazanas (1984), if relativistic electrons are injected at high energies, e+-e- pair production results in a steady state electron distribution that is very similar to that observed in AGNs, independent of the details of injection and the dynamics of the source. The conditions required by this mechanism are met in the shock model of Eichler (1984) and Ellison and Eichler (1984) which allows the self-consistent calculation of the shock acceleration efficiency. Author

N85-34898*# Arizona Univ., Tucson.
A MODEL FOR THE ORIGIN OF HIGH-ENERGY COSMIC RAYS
J. R. Jokipii and G. E. Morfill (Max-Planck-Inst. fuer Physik und Astrophysik) *In* NASA. Goddard Space Flight Center 19th Intern. Cosmic Ray Conf., Vol. 3 Aug. 1985 p 132-135 refs Original language document previously announced as A85-28195 Sponsored in part by NSF (For primary document see N85-34862 23-93)
(Grant NsG-7101)
(OG-8.1-8) Avail: NTIS HC as boxed set only $200/MF A01 per volume or E99 per entire set CSCL 03B

It is suggested that cosmic rays, up to the highest energies observed, originate in the Galaxy and are accelerated in astrophysical shock waves. If there is a galactic wind, in analogy with the solar wind, a hierarchy of shocks ranging from supernova shocks to the galactic wind termination shock is expected. This leads to a consistent model in which most cosmic rays, up to perhaps 10 to the 14th eV energy, are accelerated by supernova shocks, but that particles with energies of 10 to the 15th eV and higher are accelerated at the termination shock of the galactic wind. Intermediate energies may be accelerated by intermediate-scale shocks, and there may be larger scale shocks associated with the Local Group of galaxies. Author (IAA)

N85-34899*# Max-Planck-Inst. fuer Kernphysik, Heidelberg (West Germany).
ACCELERATION OF COSMIC RAYS IN SUPERNOVA-REMNANTS
E. A. Dorfi and L. OC. Drury *In* NASA. Goddard Space Flight Center 19th Intern. Cosmic Ray Conf., Vol. 3 Aug. 1985 p 136-139 refs (For primary document see N85-34862 23-93)
(OG-8.1-9) Avail: NTIS HC as boxed set only $200/MF A01 per volume or E99 per entire set CSCL 03B

It is commonly accepted that supernova-explosions are the dominant source of cosmic rays up to an energy of 10 to the 14th power eV/nucleon. Moreover, these high energy particles provide a major contribution to the energy density of the interstellar medium (ISM) and should therefore be included in calculations of interstellar dynamic phenomena. For the following the first order Fermi mechanism in shock waves are considered to be the main acceleration mechanism. The influence of this process is twofold; first, if the process is efficient (and in fact this is the cas) it will modify the dynamics and evolution of a supernova-remnant (SNR), and secondly, the existence of a significant high energy component changes the overall picture of the ISM. The complexity of the underlying physics prevented detailed investigations of the full non-linear selfconsistent problem. For example, in the context of the energy balance of the ISM it has not been investigated how much energy of a SN-explosion can be transfered to cosmic rays in a time-dependent selfconsistent model. Nevertheless, a lot of progress was made on many aspects of the acceleration mechanism. Author

N85-34900*# Max-Planck-Inst. fuer Kernphysik, Heidelberg (West Germany).
ONION-SHELL MODEL FOR COSMIC RAY ELECTRONS AND RADIO SYNCHROTRON EMISSION IN SUPERNOVA REMNANTS
R. Beck, L. OC. Drury, H. J. Voelk, and T. J. Bogdan (National Center for Atmospheric Research) *In* NASA. Goddard Space

Flight Center 19th Intern. Cosmic Ray Conf., Vol. 3 Aug. 1985 p 140-143 refs Sponsored in part by NSF (For primary document see N85-34862 23-93)
(OG-8.1-10) Avail: NTIS HC as boxed set only $200/MF A01 per volume or E99 per entire set CSCL 03B

The spectrum of cosmic ray electrons, accelerated in the shock front of a supernova remnant (SNR), is calculated in the test-particle approximation using an onion-shell model. Particle diffusion within the evolving remnant is explicity taken into account. The particle spectrum becomes steeper with increasing radius as well as SNR age. Simple models of the magnetic field distribution allow a prediction of the intensity and spectrum of radio synchrotron emission and their radial variation. The agreement with existing observations is satisfactory in several SNR's but fails in other cases. Radiative cooling may be an important effect, especially in SNR's exploding in a dense interstellar medium. Author

N85-34901*# Max-Planck-Inst. fuer Kernphysik, Heidelberg (West Germany).
APPROXIMATE SUPERNOVA REMNANT DYNAMICS WITH COSMIC RAY PRODUCTION
H. J. Voelk, L. OC. Drury, and E. A. Dorfi (Wien Univ.) *In* NASA. Goddard Space Flight Center 19th Intern. Cosmic Ray Conf., Vol. 3 Aug. 1985 p 148-151 refs (For primary document see N85-34862 23-93)
(OG-8.1-12) Avail: NTIS HC as boxed set only $200/MF A01 per volume or E99 per entire set CSCL 03B

Supernova explosions are the most violent and energetic events in the galaxy and have long been considered probably sources of Cosmic Rays. Recent shock acceleration models treating the Cosmic Rays (CR's) as test particles nb a prescribed Supernova Remnant (SNR) evolution, indeed indicate an approximate power law momentum distribution f sub source (p) approximation p(-a) for the particles ultimately injected into the Interstellar Medium (ISM). This spectrum extends almost to the momentum p = 1 million GeV/c, where the break in the observed spectrum occurs. The calculated power law index approximately less than 4.2 agrees with that inferred for the galactic CR sources. The absolute CR intensity can however not be well determined in such a test particle approximation. Author

N85-34902*# Academy of Sciences (USSR), Yakutsk. Inst. of Cosmophysical Research and Astronomy.
EFFICIENCY OF REGULAR ACCELERATION OF PARTICLES BY A SHOCK WAVE AT DIFFERENT INJECTION REGIMES
E. G. Berezhko, V. K. Yelshin, G. F. Krymsky, and A. A. Turpanov *In* NASA. Goddard Space Flight Center 19th Intern. Cosmic Ray Conf., Vol. 3 Aug. 1985 p 152-155 refs (For primary document see N85-34862 23-93)
(OG-8.1-13) Avail: NTIS HC as boxed set only $200/MF A01 per volume or E99 per entire set CSCL 03B

A significant fraction of the inflowing plasma energy in the collisionless shock vicinity might be transferred to the particles accelerated by a regular acceleration mechanism. The accelerated particles back pressure modifies an ininite planar shock structure so that a profile of the plasma flow velocity in the shock frame has two characteristic length scales. Author

N85-34903*# Arizona Univ., Tucson.
A NUMERICAL STUDY OF DIFFUSIVE SHOCK ACCELERATION OF COSMIC RAYS IN SUPERNOVA SHOCKS
C. M. Ko and J. R. Jokipii *In* NASA. Goddard Space Flight Center 19th Intern. Cosmic Ray Conf., Vol. 3 Aug. 1985 p 156-159 refs (For primary document see N85-34862 23-93)
(Grant NsG-7101)
(OG-8.2-2) Avail: NTIS HC as boxed set only $200/MF A01 per volume or E99 per entire set CSCL 03B

The evolution of the energy spectrum of cosmic rays accelerated by the first order Fermi mechanism, by a supernova remnant shock wave, including adiabatic deceleration effects behind the front, is carried out by means of a time-dependent numerical code. The calculations apply to the adiabatic stage (or Sedov stage) of the supernova explosion, and the energetic particle spectrum is calculated in the test particle limit (i.e., the back reaction of the cosmic rays on the flow is not included). The particles are injected mono-energetically at the shock. The radial distribution, The radial distribution, and the spectrum of the accelerated and decelerated particles is shown. Author

N85-34904*# Arizona Univ., Tucson. Dept. of Physics.
SCALING FROM JUPITER TO PULSARS AND THE ACCELERATION OF COSMIC RAY PARTICLES BY PULSARS, 3
C. Y. Fan *In* NASA. Goddard Space Flight Center 19th Intern. Cosmic Ray Conf., Vol. 3 Aug. 1985 p 160-162 (For primary document see N85-34862 23-93)
(OG-8.2-3) Avail: NTIS HC as boxed set only $200/MF A01 per volume or E99 per entire set CSCL 03B

An expression for the rate of energy generation by a pulsar an estimate of contribution from all the pulsars in our galaxy to the observed cosmic ray intensity was presented. The theory was then developed to an expanded version, and observational facts supporting the theory were cited. G.L.C.

N85-34905*# Max-Planck-Inst. fuer Astrophysik, Garching (West Germany).
DO SUPERNOVAE OF TYPE 1 PALY A ROLE IN COSMIC-RAY PRODUCTION?
Maurice M. Shapiro *In* NASA. Goddard Space Flight Center 19th Intern. Cosmic Rar Conf., Vol. 3 Aug. 1985 p 163-166 refs (For primary document see N85-34862 23-93)
(OG-8.2-5) Avail: NTIS HC as boxed set only $200/MF A01 per volume or E99 per entire set CSCL 03B

A model of cosmic-ray origin is suggested which aims to account for some salient features of the composition. Relative to solar abundances, the Galactic cosmic rays (GCR) are deficient in hydrogen and helim (H and He) by an order of magnitude when the two compositions are normalized at iron. Our conjectural model implicates supernovae of Type I (SN-I) as sources of some of the GCR. SN-I occur approximately as often as SN-II, through their genesis is thought to be different. Recent studies of nucleosynthesis in SN-I based on accreting white dwarfs, find that the elements from Si to Fe are produced copiously. On the other hand, SN-I are virtually devoid of hydrogen, and upper limits deduced for He are low. If SN-I contribute significantly to the pool of GCR by injecting energetic particles into the interstellar medium (ISM), then this could explain why the resulting GCR is relatively deficient in H and He. A test of the model is proposed, and difficulties are discussed. Author

N85-34906*# Commissariat a l'Energie Atomique, Saclay (France). Service d'Astrophysique.
NEUTRON-RICH NUCLEI IN COSMIC RAYS AND WOLF-RAYET STARS
N. Prantzos, M. Arnould (Brussels Univ.), J. P. Arcoragi (Montreal Univ.), and M. Casse *In* NASA. Goddard Space Flight Center 19th Intern. Cosmic Ray Conf., Vol. 3 Aug. 1985 p 167-170 refs (For primary document see N85-34862 23-93)
(OG-8.2-6) Avail: NTIS HC as boxed set only $200/MF A01 per volume or E99 per entire set CSCL 03B

Wolf-Rayet stars figure prominently in astrophysical research. As a bonus, they seem to offer, in the recent past, an interesting connection between classical astronomy and high energy astrophysics due to their unusual composition and their huge mechanical power. The material flowing from WC stars (carbon-rich WR stars) contains gas which has been processed through core-helium burning, i.e., considerably enriched into 12C,16O, 22Ne, and 25,26Mg. This composition is reminiscent of the cosmic ray source anomalies. Encouraging agreement is obtained with observation in the mass range $12 < A < 26$ assuming acceleration of wind particles at the shock that delineates the WR cavity, and adequate dilution with normal cosmic rays, but silicon poses. G.L.C.

N85-34907*# Vrije Universiteit, Brussels (Belgium). Astrophysical Inst.
BURSTING STAR FORMATION AND THE OVERABUNDANCE OF WOLF-RAYET STARS

G. Bodigfee and C. deLoore *In* NASA. Goddard Space Flight Center 19th Intern. Cosmic Ray conf., Vol. 3 Aug. 1985 p 171-174 refs (For primary document see N85-34862 23-93)
(OG-8.2-8) Avail: NTIS HC as boxed set only $200/MF A01 per volume or E99 per entire set CSCL 03B

The ratio of the number of WR-stars to their OB progenitors appears to be significantly higher in some extragalactic systems than in our Galaxy. This overabundance of Wolf-Rayet-stars can be explained as a consequence of a recent burst of star formation. It is suggested that this burst is the manifestation of a long period nonlinear oscillation in the star formation process, produced by positive feedback effects between young stars and the interstellar medium. Star burst galaxies with large numbers of WR-stars must generate gamma - fluxes but due to the distance, all of them are beyond the reach of present-day ray detectors, except probably 30 Dor. Author

N85-34908*# Ibaraki Univ., Hitachi (Japan). Dept. of Earth Sciences.
INTERSTELLAR (Ne-22) AS A POSSIBLE SOURCE OF THE EXCESS (Ne-22) IN THE GALACTIC COSMIC RAY
S. Yanagita *In* NASA. Goddard Space Flight Center 19th Intern. Cosmic Ray Conf., Vol. 3 Aug. 1985 p 175-178 refs (For primary document see N85-34862 23-93)
(OG-8.2-12) Avail: NTIS HC as boxed set only $200/MF A01 per volume or E99 per entire set CSCL 03B

A selective injection mechanism of cosmic ray seed nuclei due to nuclear decay effects is proposed. It is shown that 22NA ejected by novae explosion can explain the excess 22Ne in the galactic cosmic ray source by invoking energization and ionization during its beta-decay process in interstellar space. Author

N85-34909*# Beijing Teachers Coll. (China). Dept. of Physics.
ON MAGNETIC PAIR PRODUCTION ABOVE FAST PULSAR POLAR CAPS
Shuyman An *In* NASA. Goddard Space Flight Center 19th Intern. Cosmic Ray Conf., Vol. 3 Aug. 1985 p 179-182 refs (For primary document see N85-34862 23-93)
(OG-8.2-13) Avail: NTIS HC as boxed set only $200/MF A01 per volume or E99 per entire set CSCL 03B

Magnetic pair production is one of high-energy electromagnetic conversion processes important to the development of pair-photon cascades in pulsars. On the basis of current polar cap models, the properties of magnetic pair production in fast pulsars are discussed. Suppose there is a roughly dipole magnetic field at the stellar surface, the author estimate the effects on non-zero curvature of magnetic field lines upon curvature radiation from primary particles and pair production rate near the surface of pulsars. Author

N85-34910*# Stevens Inst. of Tech., Hoboken, N. J.
THE ELECTROMAGNETIC RAM ACTION OF THE PLASMA FOCUS AS A PARADIGM FOR THE GENERATION OF COSMIC RAYS AND THE GIGANTIC JETS IN ACTIVE GALAXIES
W. H. Bostick and V. Nardi *In* NASA. Goddard Space Flight Center 19th Intern. Cosmic Ray Conf. Aug. 1985 p 183-186 refs Sponsored in part by Air Force and Navy (For primary document see N85-34862 23-93)
(OG-8.2-14) Avail: NTIS HC as boxed set only $200/MF A01 per volume or E99 per entire set CSCL 03B

Recent measurements of the energy spectrum of the plasma-focus-generated deuteron beam yield as spectrum of the form N(E)=(approx.) E to the -2.7 for 1MeV < E < 13 MeV. Other measurements show that the beta 1 electron beam which is generated simultaneously with the deuteron beam is interrupted into segments of spacing 25ps and duration approximately 4ps. A stuttering-electro-magnetic-ram (ser) model of the plasma focus in proposed which is similar to Raudorf's electronic ram which produces a similar spectrum for an electron beam for 1Mev <E< 10MeV. It is proposed that the cosmic ray spectrum and the giganic galactic jets are both generated by ser action near the centers of active galaxies. Author

N85-34911*# Michigan Univ., Ann Arbor. Lab. of Physics.
THE ORIGINS OF COSMIC RAYS AND QUANTUM EFFECTS ON GRAVITY
Yuko Tomozawa *In* NASA. Goddard Space Flight Center 19th Intern. Cosmic Ray Conf. Aug. 1985 p 187-190 Submitted for publication (For primary document see N85-34862 23-93)
(OG-8.2-15) Avail: NTIS HC as boxed set only $200/MF A01 per volume or E99 per entire set CSCL 03B

The energy spectrum of primary cosmic rays is explained by particles emitted during a thermal expansion of explosive objects inside and near the galaxy, remnants of which may be supernova and/or active talaxies, or even stars or galaxies that disappeared from our sight after the explosion. A power law energy spectrum for cosmic rays, E to the (-alpha -1, is obtained from an expansion rate T is proportional to R to the alpha. Using the solution of the Einstein equation, we obtain a spectrum which agrees very well with experimental data. The implication of an inflationary early universe on the cosmic ray spectrum is also discussed. It is also suggested that the conflict between this model and the singularity theorem in classical general relativity may be eliminated by quantum effects. Author

N85-34912*# Puerto Rico Univ., Humacao. Dept. of Physics.
EVALUATION OF PARAMETERS FOR PARTICLES ACCELERATION BY THE ZERO-POINT FIELD OF QUANTUM ELECTRODYNAMICS
A. Rueda *In* NASA. Goddard Space Flight Center 19th Intern. Cosmic Ray Conf. Aug. 1985 p 191-194 refs (For primary document see N85-34862 23-93)
(OG-8.2-16) Avail: NTIS HC as boxed set only $200/MF A01 per volume or E99 per entire set CSCL 03B

That particles may be accelerated by vacuum effects in quantum field theory has been repeatedly proposed in the last few years. A natural upshot of this is a mechanism for cosmic rays (CR) primaries acceleration. A mechanism for acceleration by the zero-point field (ZPE) when the ZPE is taken in a realistic sense (in opposition to a virtual field) was considered. Originally the idea was developed within a semiclassical context. The classical Einstein-Hopf model (EHM) was used to show that free isolated electromagnetically interacting particles performed a random walk in phase space and more importantly in momentum space when submitted to the perennial action of the so called classical electromagnetic ZPE. G.L.C.

N85-34913*# Academy of Sciences (USSR), Moscow. Physical Inst.
GIANT MOLECULAR CLOUDS AS REGIONS OF PARTICLE ACCELERATION
V. A. Dogiel, A. V. Gurevich, Ye. N. Istomin, and K. A. Zybin *In* NASA. Goddard Space Flight Center 19th Intern. Cosmic Ray Conf., Vol. 3 Aug. 1985 p 195-198 refs (For primary document see N85-34862 23-93)
Avail: NTIS HC as boxed set only $200/MF A01 per volume or E99 per entire set CSCL 03B

One of the most interesting results of investigations carried out on the satellites SAS-II and COS-B is the discovery of unidentified discrete gamma sources. Possibly a considerable part of them may well be giant molecular clouds. Gamma emission from clouds is caused by the processes with participation of cosmic rays. The estimation of the cosmic ray density in clouds has shown that for the energy E approx. = I GeV their density can 10 to 1000 times exceed the one in intercloud space. We have made an attempt to determine the mechanism which could lead to the increase in the cosmic ray density in clouds. G.L.C.

N85-34914*# Academy of Sciences (USSR), Moscow. Inst. of Geochemistry and Analytical Chemistry.
THE NUCLEOSYNTHESIS OF DETERIUM AND HELIUM-3
A. K. Lavrukhina and R. I. Kuznetsova *In* NASA. Goddard Space Flight Center 19th Intern. Cosmic Ray Conf., Vol. 3 Aug. 1985 p 199-202 refs (For primary document see N85-34862 23-93)
(OG-8.2-18) Avail: NTIS HC as boxed set only $200/MF A01 per volume or E99 per entire set CSCL 03B

A new model of the creation of D and 3He in supernova of the first generation was considered. It is based on the idea that a supernova event leads simultaneously to acceleration of particles in the shock wave front and to their interactions with supernova atmosphere matter. The D, 3He, Li, Be, B and bypassed isotopes are created in these interactions. The cosmic abundances of the bypassed isotopes with A > or = 113 allowed to determine the integral proton flux I sub p (E sub p > 25 MeV) = 5 x 10 to the 21/sq cm the spectral index - gamma = 3. The calculations of the D and 3He yields in various nuclear reactions at these irradiation conditions show that only the 4He(p,d)3He reaction leads to cosmic abundances of these isotopes on the assumption that all matter has been exposed. G.L.C.

N85-34915*# Academy of Sciences (USSR), Moscow. Inst. of Geochemistry and Analytical Chemistry.
NUCLEAR REACTIONS IN SHOCK WAVE FRONT DURING SUPERNOVA EVENTS
A. K. Lavrukhina *In* NASA. Goddard Space Flight Center 19th Intern. Cosmic Ray Conf., Vol. 3 Aug. 1985 p 203-206 refs (For primary document see N85-34862 23-93)
(OG-8.2-19) Avail: NTIS HC as boxed set only $200/MF A01 per volume or E99 per entire set CSCL 03B

The new unique isotopic anomalous coponent of Xe(XeX) was found in the carbonaceous chondrites. It is enriched in light shielded isotopes (124Xe and 126Xe) and in heavy nonshielded isotopes (134Xe and 136Xe. All characteristics of Xe-X can be explained by a model of nucleosynthesis of the Xe isotopes in shock wave front passed through the He envelope during supernova events. The light isotopes are created by p process and the heavy isotopes are created by n process (slow r process). They were captured with high temperature carbon grains condensing by supernova shock waves. Author

N85-34916*# California Univ., San Diego, La Jolla. Dept. of Physics.
BREAKDOWN OF HELIUM NUCLEI IN MATTER PROCESSED NEAR BLACK HOLES
Robert J. Gould *In* NASA. Goddard Space Flight Center 19th Intern. Space Flight Center Aug. 1985 p 207-209 refs (For primary document see N85-34862 23-93)
(Grant NGR-05-005-004)
(OG-8.2-20) Avail: NTIS HC as boxed set only $200/MF A01 per volume or E99 per entire set CSCL 03B

The rate of breakup of helium nuclei by particle induced reactions is computed. It is shown that the rate is determined by the endothermic reaction p + 4He 3He + d, becoming effective at kT approx. > few MeV. It is suggested that matter having been processed to these temperatures will be depleted in helium and in the elements C, N, O, and Ne. Author

N85-34917*# Kiel Univ. (West Germany). Inst. fuer Kernphysik.
PULSARS AS COSMIC RAY PARTICLE ACCELERATORS: PROTON ORBITS
K. O. Thielheim *In* NASA. Goddard Space Flight Center 19th Intern. Cosmic Ray Conf., Vol. 3 Aug. 1985 p 210-213 refs (For primary document see N85-34862 23-93)
(OG-8.2-21) Avail: NTIS HC as boxed set only $200/MF A01 per volume or E99 per entire set CSCL 03B

Proton orbits are calculated in the electromagnetic vacuum field of a magnetic point dipole rotating with its angular velocity omega perpendicular to its dipole moment mu by numerical integration of the Lorentz-Dirac equation. Trajectories are shown and discussed for various initial conditions. A critical surface is shown separating initial positions of protons which finally hit the pulsar in the polar region from those which finally recede to infinity. Author

N85-34918*# Kiel Univ. (West Germany). Inst. fuer Kernphysik.
PULSARS AS COSMIC RAY ACCELERATORS: ENERGY DEVELOPMENT OF PROTONS
K. O. Thielheim *In* NASA. Goddard Space Flight Center 19th Intern. Cosmic Ray Conf., Vol. 3 Aug. 1985 p 214-217 (For primary document see N85-34862 23-93)
(OG-8.2-22) Avail: NTIS HC as boxed set only $200/MF A01 per volume or E99 per entire set CSCL 03B

Results of numerical integrations of the Lorentz-Dirac-equation with Landau approximation for protons in the electromagnetic vacuum field of a magnetic dipole rotating with its angular velocity omega perpendicular to its magnetic moment mu will be discussed with special attention to the energy development of protons. Author

N85-34919*# Kiel Univ. (West Germany). Inst. fuer Kernphysik.
PULSARS AS COSMIC RAY PARTICLE ACCELERATORS: DYNAMICS OF ELECTRONS
K. O. Thielheim *In* NASA. Goddard Space Flight Center 19th Intern. Cosmic Ray Conf., Vol. 3 Aug. 1985 p 218-221 refs (For primary document see N85-34862 23-93)
(OG-8.2-23) Avail: NTIS HC as boxed set only $200/MF A01 per volume or E99 per entire set CSCL 03B

The Lorentz-Dirac-equation with Landau approximation has been solved numerically for electrons in the electromagnetic field of a magnetic dipole rotating with the angular velocity omega perpendicular to its magnetic moment mu. Results are discussed with respect to electron orbits and energy development. Author

N85-34920*# South Carolina Univ., Columbia. Dept. of Geology.
INFLUENCE OF THE SOURCE DISTRIBUTION ON THE AGE DISTRIBUTION OF GALACTIC COSMIC RAYS
I. Lerche and R. Schlickeiser (Max-Planck-Inst. fuer Radioastronomie) *In* NASA. Goddard Space Flight Center 19th Intern. Cosmic Ray Conf., Vol. 3 Aug. 1985 p 222-225 refs (For primary document see N85-34862 23-93)
(OG-8.3-1) Avail: NTIS HC as boxed set only $200/MF A01 per volume or E99 per entire set CSCL 03B

The age distribution of galactic cosmic rays in the diffusion approximation is calculated. The influence of the scale height of the spatial source distribution on the mean age of particles arriving at the solar system is discussed. The broader the source distribution with respect to the galactic plane, the longer the mean age. This result provides a natural explanation for the shorter mean age of secondary cosmic rays compared to primary cosmic rays necessary for the understanding of the observed secondary/primary ratio. Author

N85-34921*# South Carolina Univ., Columbia. Dept. of Geology.
EXPLANATION OF THE SECONDARY TO PRIMARY RATIO WITHIN THE CONTINUOUS FERMI ACCELERATOR MODEL
I. Lerche and R. Schlickeiser (Max-Planck-Inst. fuer Radiastronomie) *In* NASA. Goddard Space Flight Center 19th Intern. Cosmic Ray Conf., Vol. 3 Aug. 1985 p 226-229 refs (For primary document see N85-34862 23-93)
(OG-8.3-2) Avail: NTIS HC as boxed set only $200/MF A01 per volume or E99 per entire set CSCL 03B

The secondary to primary ratio in galactic cosmic radiation at relativistic momenta is calculated in a model, where the primaries are continuously accelerated from the thermal galactic background medium by 1st and 2nd order Fermi acceleration. It is shown that the measured decrease with momentum does not exclude that cosmic rays are accelerated in the interstellar medium as a whole. Once a momentum dependence of the mean lifetime and the different spatial source distributions are adequately taken into account, the measured decreasing ratio can be explained. Author

N85-34922*# Siegen Univ., (West Germany). Dept. of Physics.
PROPAGATION OF INJECTED COSMIC RAYS UNDER DISTRIBUTED REACCELERATION
M. Simon, W. Heinrich, and K. D. Mathis *In* NASA. Goddard Space Flight Center 19th Intern. Cosmic Ray Conf., Vol. 3 Aug. 1985 p 230-233 refs (For primary document see N85-34862 23-93)
(OG-8.3-3) Avail: NTIS HC as boxed set only $200/MF A01 per volume or E99 per entire set CSCL 03B

The cosmic ray acceleration model in which the particles gain

continuously energy from stochastic processes in the interstellar space by encountering shocks leads to a logarithmic increase in the secondary to primary ratios with energy, which is inconsistent with observations. The observed decrease of the secondary to primary ratios may therefore suggest that a considerable part of the acceleration has taken place rapidly at the sources. Astronomical observations on the other hand indicate that shocks from supernovae do exist in the galaxy and observations in the interplanetary space show clear evidence that shock acceleration works. G.L.C.

N85-34923*# Lodz Univ. (Poland). Inst. of Physics.
SECONDARY TO PRIMARY RATIO AND THE CONTINUOUS ACCELERATION
M. Giler, B. Szabelska (Institute of Nuclear Studies, Lodz, Poland), J. Wdowczyk (Institute of Nuclear Studies, Lodz, Poland), and A. W. Wolfendale (Birmingham Univ.) *In* NASA. Goddard Space Flight Center 19th Intern. Cosmic Ray Conf., Vol. 3 Aug. 1985 p 234-237 refs (For primary document see N85-34862 23-93)
(OG-8.3-4) Avail: NTIS HC as boxed set only $200/MF A01 per volume or E99 per entire set CSCL 03B

A general formula for the sec/prim ratio, independently of any details of the propagation and acceleration model is presented. In the limit of equal fragmentation paths for primaries and secondaries, this ratio at a given momentum nucleon is proportional only to the mean path of the observed primaries at that moment. It is shown that it is unlikely to get a decreasing sec/prim ratio with energy if an acceleration process takes place during particle propagation in the interstellar medium (ISM). E.A.K.

N85-34924*# Naval Research Lab., Washington, D. C. Center for Space Research.
PROPAGATION OF COSMIC RAYS AND NEW EVIDENCE FOR DISTRIBUTED ACCELERATION
R. Silberberg, C. H. Tsao, J. R. Letaw, and M. M. Shapiro *In* NASA. Goddard Space Flight Center 19th Intern. Cosmic Ray Conf., Vol. 3 Aug. 1985 p 238-241 refs (For primary document see N85-34862 23-93)
(OG-8.3-5) Avail: NTIS HC as boxed set only $200/MF A01 per volume or E99 per entire set CSCL 03B

The origin and propagation of cosmic rays in terms of conventional and supplementary newer assumptions were explored. Cosmic rays are considered to be accelerated by supernoava shock waves and to traverse clouds in the source region. After rigidity-dependent escape from these clouds into interstellar space, cosmic rays are further accelerated by the weakened shocks of old supernova remnants and then pass through additional material. The distributed acceleration hypothesis is discussed with emphasis on recent data on the abundances of cosmic-ray isotopes of N above 1 GeV/u and of He near 6 GeV/u. E.A.K.

N85-34925*# Tata Inst. of Fundamental Research, Bombay (India).
EXACT SOLUTIONS FOR SPORADIC ACCELERATION OF COSMIC RAYS
R. Cowsik *In* NASA. Goddard Space Flight Center 19th Inter. Cosmic Ray Conf., Vol. 3 Aug. 1985 p 242-245 refs (For primary document see N85-34862 23-93)
(OG-8.3-7) Avail: NTIS HC as boxed set only $200/MF A01 per volume or E99 per entire set CSCL 03B

The steady state spectra of cosmic rays which are subject to a sporadic acceleration process, wherein the gain in energy in each encounter is a finite fraction of the particle energy are discussed. They are derived from a mathematical model which includes the possibility of energy dependent leakage of cosmic rays from the galaxy. Comparison with observations allows limits to be placed on the frequency and efficiency of such encounters. E.A.K.

N85-34926*# Arizona Univ., Tucson. Dept. of Planetary Sciences.
RELATIVISTIC TRANSPORT THEORY FOR COSMIC-RAYS
G. M. Webb *In* NASA. Goddard Space Flight Center 19th Intern. Cosmic Ray Conf., Vol. 3 Aug. 1985 p 246-249 refs (For primary document see N85-34862 23-93)
(Grant NSF ATM-83-11241)
(OG-8.3-8) Avail: NTIS HC as boxed set only $200/MF A01 per volume or E99 per entire set CSCL 03B

Various aspects of the transport of cosmic-rays in a relativistically moving magnetized plasma supporting a spectrum of hydromagnetic waves that scatter the cosmic-rays are presented. A local Lorentz frame moving with the waves or turbulence scattering the cosmic-rays is used to specify the individual particle momentum. The comoving frame is in general a noninertial frame in which the observer's volume element is expanding and shearing, geometric energy change terms appear in the cosmic-ray transport equation which consist of the relativistic generalization of the adiabatic deceleration term and a further term involving the acceleration vector of the scatterers. A relativistic version of the pitch angle evolution equation, including the effects of adiabatic focussing, pitch angle scattering, and energy changes is presented. E.A.K.

N85-34927*# National Center for Atmospheric Research, Boulder, Colo. High Altitude Observatory.
STOCHASTIC PARTICLE ACCELERATION IN FLARING STARS
T. J. Bogdan and R. Schlickeiser (Max-Planck-Inst. fuer Radioastronomie) *In* NASA. Goddard Space Flight Center 19th Intern. Cosmic Ray Conf., Vol. 3 Aug. 1985 p 250-253 refs (For primary document see N85-34862 23-93)
(OG-8.3-9) Avail: NTIS HC as boxed set only $200/MF A01 per volume or E99 per entire set CSCL 03B

The acceleration of electrons by the Fermi-Parker mechanisms in a quasistationary turbulent plasma of dimension l, mean magnetic field strength B, and mean number density n are considered. The electrons suffer radiative and ionization losses and have a scattering mean free path that increases linearly with their momentum. Analytic solutions for the steady-state electron energy spectra are presented. The spectra are characterized by an exponential cutoff above a given momentum determined by the synchrontron or the confinement time, depending on the physical characteristics of the accelerating region. E.A.K.

N85-34928*# National Aeronautics and Space Administration. Goddard Space Flight Center, Greenbelt, Md.
THE DESIGN OF AN EXPERIMENT TO DETECT LOW ENERGY ANTIPROTONS
J. Lloyd-Evans, B. S. Acharya (NAS-NRC), V. K. Balasubrahmanyan, J. F. Ormes, R. E. Streitmatter, and S. A. Stephens *In its* 19th Intern. Cosmic Ray Conf., Vol. 3 Aug. 1985 p 254-257 refs (For primary document see N85-34862 23-93)
(OG-9.1-1) Avail: NTIS HC as boxed set only $200/MF A01 per volume or E99 per entire set CSCL 03B

The techniques to be used in a balloon borne experiment APEX to detect < 220 MeV antiprotons are described, paying particular attention to potential sources of background. Event time history is shown to be very effective in eliminating this background. Results of laboratory tests on the timing resolution which may be achieved are presented. E.A.K.

N85-34929*# California Univ., Berkeley. Dept. of Physics.
AN EXPERIMENT TO MEASURE THE ENERGY SPECTRUM OF COSMIC RAY ANTIPROTONS FROM 100 TO 1000 MeV
M. H. Salamon, P. B. Price, S. W. Barwick, D. M. Lowder, and S. P. Ahlen (Indiana Univ., Bloomington) *In* NASA. Goddard Space Flight Center 19th Intern. Cosmic Ray Conf., Vol. 3 Aug. 1985 p 258-261 refs (For primary document see N85-34862 23-93)
(OG-9.1-3) Avail: NTIS HC as boxed set only $200/MF A01 per volume or E99 per entire set CSCL 03B

Production models were developed and the confirmation of each one had significant astrophysical impact. These include radical modifications of propagation models, cosmic ray antiprotons injection from neighboring domains of antimatter, p production by evaporating primordial black holes, and cosmic ray p's as annihilation products of supersymmetry particles that might make up the dark dynamical mass of the Galaxy. It is that p's originating from supersymmetric parents might have distinct spectral features that

would survive solar modulation; in one model, higgsino annihilation proceeds through the bb quark-antiquark channel, producing a spectral bump at approx. 0.3 GeV in the p spectrum. E.A.K.

N85-34930*# National Aeronautics and Space Administration. Goddard Space Flight Center, Greenbelt, Md.
HIGH RESOLUTION CHERENKOV DETECTORS FOR COSMIC RAY ISOTOPE EXPERIMENT
B. S. Acharya (Tata Inst. of Fundamental Research, Bombay), V. K. Balasubrahmanyan, J. A. Esposito, J. Lloyd-Evans, J. F. Ormes, and R. E. Streitmatter *In* NASA. Goddard Space Flight Center 19th Intern. Cosmic Ray Conf., Vol. 3 Aug. 1985 p 262-265 refs (For primary document see N85-34862 23-93)
(OG-9.1-4) Avail: NTIS HC as boxed set only $200/MF A01 per volume or E99 per entire set CSCL 03B

Cerenkov detectors are used to measure the velocity of particles in configurations designed to study the isotopic composition of galactic cosmic rays. The geometrical properties of the detector are outlined. Monte-Carlo simulations of photon propagation in a diffusive detector were undertaken. The scattering properties of diffusively reflecting white paint and of surface treatments for the radiator material were measured. It is found that the absorption of light in the radiator is an important light loss mechanism. The simulations are used to find optimal mapping techniques and data reduction strategies. The application of these techniques are discussed with respect to the large area isotopic composition experiment (ALICE) Cerenkov detector. E.A.K.

N85-34931*# Chicago Univ., Ill. Fermi Inst.
CERENKOV COUNTERS FOR HIGH ENERGY NUCLEI: SOME NEW DEVELOPMENTS
S. P. Swordy and D. Muller *In* NASA. Goddard Space Flight Center 19th Intern. Cosmic Ray Conf., Vol. 3 Aug. 1985 p 266-267 (For primary document see N85-34862 23-93)
(Grants NGL-14-001-258; NsG-7464)
(OG-9.1-5) Avail: NTIS HC as boxed set only $200/MF A01 per volume or E99 per entire set CSCL 03B

A method to determine with gas Cerenkov counters the Lorentz factor, gamma = E/mc, of cosmic ray nuclei with high accuracy over the range gamma approx. 20 to 100 is discussed. The measurement of the Cerenkov emission angle theta, by use of a suitable imaging system is considered. Imaging counters, the ring imaging Cerenkov counters (RICH), were developed for use on accelerators. The image of off-axis particles to determine the amount of image distortion as a function of the direction of the incoming nucleus is examined and an acceptance solid angle, relative to the optical axis, within which the nucleus produces an image with an acceptable level of distortion is defined. The properties of the image, which becomes elliptical, for off-axis particles are analyzed. E.A.K.

N85-34932*# Commissariat a l'Energie Atomique, Saclay (France).
A HIGH RESOLUTION GAS CERENKOV DETECTOR FOR THE SUPERCONDUCTING MAGNET FACILITY
P. Goret and R. L. Golden (New Mexico State Univ.) *In* NASA. Goddard Space Flight Center 19th Intern. Cosmic Ray Conf., Vol. 3 Aug. 1985 p 268-271 refs (For primary document see N85-34862 23-93)
(OG-9.1-6) Avail: NTIS HC as boxed set only $200/MF A01 per volume or E99 per entire set CSCL 03B

A high resolution gas Cerenkov imaging detector for Cosmic Ray heavy ions is described. The performances of this detector are evaluated in view of its association with a superconducting magnet. E.A.K.

N85-34933*# Washington Univ., St. Louis, Mo. Dept. of Physics.
BEVALAC CALIBRATION OF THE SOFIE RANGE AND HODOSCOPE DETECTORS
W. R. Binns, J. J. Connell, M. H. Israel, and J. Klarmann *In* NASA. Goddard Space Flight Center 19th Intern. Cosmic Ray Conf., Vol. 3 Aug. 1985 p 272-275 refs (For primary document see N85-34862 23-93)
(Contract NAS5-27996; Grants NGR-26-008-001; NAGw-122)
(OG-9.1-7) Avail: NTIS HC as boxed set only $200/MF A01 per volume or E99 per entire set CSCL 03B

The scintillating optical fiber isotope experiment (SOFIE) is a Cerenkov-dE/dx-Range experiment which was developed initially for balloon flight to study the isotopic composition of cosmic rays in the iron region. The electronic range and hodoscope detectors use scintillating optical fibers to image the tracks of stopping charged particles and to determine their trajectory. The particle range is determined and used together with a Cerenkov measurement to determine the mass of the stopping particle. Preliminary results of a Bevalac calibration performed in August, 1984 with a prototype of the balloon flight instrument, to study the measurement precision in range and trajectory which could be attained with this detector are described. E.A.K.

N85-34934*# Chicago Univ., Ill.
THE DEVELOPMENT OF A HIGH ENERGY COSMIC RAY DETECTOR FOR SPACELAB-2
Jacques LHeureux, Peter Meyer, Dietrich Mueller, and Simon P. Swordy *In* NASA. Goddard Space Flight Center 19th Intern. Cosmic Ray Conf., Vol. 3 Aug. 1985 p 276-277 (For primary document see N85-34862 23-93)
(Contract NAS8-32828)
(OG-9.1-8) Avail: NTIS HC as boxed set only $200/MF A01 per volume or E99 per entire set CSCL 03B

A large cosmic ray detector aimed at measurements of the energy spectra and of the elemental abundances of cosmic ray nuclei at very high energies, up to several TeV/nucleon was constructed. The instrument is an electronic counter telescope with a geometric factor of 5 sq ster. It accomplishes measurements of the particle energies through the use of gas Cerenkov counters and of transition radiation detectors. The solutions of a number of technological problems that are encountered when developing such instrumentation for Shuttle missions are discussed. E.A.K.

N85-34935*# National Aeronautics and Space Administration. Goddard Space Flight Center, Greenbelt, Md.
MASS RESOLUTION OPTIMIZATION IN A LARGE ISOTOPIC COMPOSITION EXPERIMENT
J. A. Esposito (Maryland Univ., College Park), B. S. Acharya, V. K. Balasubrahmanyan, B. G. Mauger (Spacecom, Las Cruces, N. Mex.), J. F. Ormes, R. E. Streitmatter, W. Heinrich (Siegen Univ.), M. Henkel (Siegen Univ.), M. Simon (Siegen Univ.), and H. O. Tittel (Siegen Univ.) *In* NASA. Goddard Space Flight Center 19th Intern. Cosmic Ray Conf., Vol. 3 Aug. 1985 p 278-281 refs (For primary document see N85-34862 23-93)
(OG-9.1-9) Avail: NTIS HC as boxed set only $200/MF A01 per volume or E99 per entire set CSCL 03B

A range-energy experiment was built to measure the isotopic composition of galactic cosmic rays. An enrichment of neutron rich isotopes, 22Ne and (25Mg + 26Mg) in particular, when compared to the solar composition is shown. A rich statistics measurement of these and other neutron-rich isotopes in the galactic flux yields information to the source of these particles. A computer simulation of the experiment was used to estimate the instrument resolution. The Cherenkov detector light collection efficiency, was calculated. Absorption of light in the radiator was considered to determine the optimum Cherenkov medium thickness. The experiment will determine the isotopic composition for the elements neon through argon in the energy range 300 to 800 MeV per nucleon. E.A.K.

N85-34936*# Hulburt (E. O.) Center for Space Research, Washington, D.C.
THE HEAVY IONS IN SPACE EXPERIMENT
J. H. Adams, Jr., L. P. Beahm, and B. Stiller (M and B Consulting Co., Washington, D.C.) *In* NASA. Goddard Space Flight Center 19th Intern. Cosmic Ray Conf., Vol. 3 Aug. 1985 p 282-285 refs (For primary document see N85-34862 23-93)
(OG-9.1-10) Avail: NTIS HC as boxed set only $200/MF A01 per volume or E99 per entire set CSCL 03B

The Heavy Ions in Space (HIIS) experiment was developed

and is currently in orbit onboard the long duration facility (LDEF). The HIIS will record relativistic cosmic ray nuclei heavier than magnesium and stopping nuclei down to helium. The experiment uses plastic track detectors that have a charge resolution of 0.15 charge units at krypton and 0.10 charge units, or better, for nuclei lighter than cobalt. The HIIS has a collecting power of 2 square meter steradians and it has already collected more than a year's data. E.A.K.

N85-34937*# Kiel Univ. (West Germany). Inst. fuer Reine und Angewandte Kernphysik.

CHERENKOV-dE/dx-RANGE MEASUREMENTS ON COSMIC RAY IRON GROUP NUCLEI Abstract Only

G. Sermund, G. Siegmon, W. Enge, G. A. Simpson (New Hampshire Univ., Durham), and W. R. Webber (New Hampshire Univ., Durham) *In* NASA. Goddard Space Flight Center 19th Intern. Cosmic Ray Conf., Vol. 3 Aug. 1985 p 286 (For primary document see N85-34862 23-93)

(OG-9.1-12) Avail: NTIS HC as boxed set only $200/MF A01 per volume or E99 per entire set CSCL 03B

A balloon experiment which combined a large area plastic detector unit with electronic dE/dx-C data is presented. The correlation of the electronic data with the range data of the plastic detector stack was achieved by rotating plastic detector disks which provided in this way the passive plastic detector with an incorporated time determination. The constant flux of cosmic ray particles with charge Z greater than two was used to gauge the time resolving system. Stopping cosmic ray iron group nuclei in the energy range 400 to 700 MeV/nuc are identified using their electronic scintillator and Cherenkov signals and their etch conelengths and range data. The precise knowledge of the particle's trajectory proposes refined pathlength corrections to the electronic data. E.A.K.

N85-34938*# California Inst. of Tech., Pasadena.

THE RESPONSE OF IONIZATION CHAMBERS TO RELATIVISTIC HEAVY NUCLEI

B. J. Newport, E. C. Stone, C. J. Waddington (Minnesota Univ., Minneapolis), W. R. Binns (Washington Univ., St. Louis), D. J. Fixsen (Minnesota Univ., Minneapolis), T. L. Garrard, G. Grimm (Washington Univ., St. Louis), M. H. Israel (Washington Univ., St. Louis), and J. Klarmann (Washington Univ., St. Louis) *In* NASA. Goddard Space Flight Center 19th Intern. Cosmic Ray Conf., Vol. 3 Aug. 1985 p 287-290 refs (For primary document see N85-34862 23-93)

(Contract NAS8-27976; NAS8-27977; NAS8-27978; Grants NAG8-498; NAG8-500; NAG8-502; NGR-05-002-160; NGR-24-005-050; NGR-26-008-001)

(OG-9.1-13) Avail: NTIS HC as boxed set only $200/MF A01 per volume or E99 per entire set CSCL 03B

The LBL Bevalac for the Heavy Nuclei Experiment on HEAO-3, compared the response of a set of laboratory ionization chambers to beams of 26Fe, 36Kr, 54Xe, 67 Ho, and 79Au nuclei at maximum energies ranging from 1666 MeV/amu for Fe to 1049 MeV/amu for Au. The response of these chambers shows a significant deviation from the expected energy dependence, but only a slight deviation from Z sq scaling. E.A.K.

N85-34939*# California Inst. of Tech., Pasadena.

THE RESPONSE OF IONIZATION CHAMBERS TO RELATIVISTIC HEAVY NUCLEI

B. J. Newport, E. C. Stone, C. J. Waddington (Minnesota Univ., Minneapolis), W. R. Binns (Washington Univ., St. Louis), D. J. Fixsen (Minnesota Univ., Minneapolis), T. L. Garrard, G. Grimm (Washington Univ., St. Louis), M. H. Israel (Washington Univ., St. Louis), and J. Klarmann (Washington Univ., St. Louis) *In* NASA. Goddard Space Flight Center 19th Intern. Cosmic Ray Conf., Vol. 3 Aug. 1985 p 287-290 refs (For primary document see N85-34862 23-93)

(Contract NAS8-27976; NAS8-27977; NAS8-27978; Grants NAG8-498; NAG8-500; NAG8-502; NGR-05-002-160; NGR-24-005-050; NGR-26-008-001)

(OG-9.1-13) Avail: NTIS HC as boxed set only $200/MF A01 per volume or E99 per entire set CSCL 03B

The development of cosmic ray telescopes to separate individual isotopes of heavy elements using the dE/dx-vs.-E technique depends on the incorporation of precise trajectory sensing elements into these systems. In typical implementations the particle trajectory is derived from a set of position measurements made prior to a particle's entering the first energy loss detector. The use of the trajectory obtained in this way to correct energy loss signals for the actual pathlengths through the detectors depends on the assumption that the particle trajectory is a straight line. In order to resolve iron isotopes the angles of incidence, theta the particle track must be known rather accurately. E.A.K.

N85-34940*# California Inst. of Tech., Pasadena.

HEXAGONAL UNIFORMLY REDUNDANT ARRAYS FOR CODED-APERTURE IMAGING

M. H. Finger and T. A. Prince *In* NASA. Goddard Space Flight Center 19th Intern. Cosmic Ray Conf., Vol. 3 Aug. 1985 p 295-298 refs (For primary document see N85-34862 23-93)

(Grant NGR-05-002-160)

(OG-9.2-1) Avail: NTIS HC as boxed set only $200/MF A01 per volume or E99 per entire set CSCL 03B

Uniformly redundant arrays are used in coded-aperture imaging, a technique for forming images without mirrors or lenses. The URAs constructed on hexagonal lattices, are outlined. Details are presented for the construction of a special class of URAs, the skew-Hadamard URAs, which have the following properties: (1) nearly half open and half closed (2) antisymmetric upon rotation by 180 deg except for the central cell and its repetitions. Some of the skew-Hadamard URAs constructed on a hexagonal lattice have additional symmetries. These special URAs that have a hexagonal unit pattern, and are antisymmetric upon rotation by 60 deg, called hexagonal uniformly redundant arrays (HURAs). The HURAs are particularly suited to gamma-ray imaging in high background situations. In a high background situation the best sensitivity is obtained with a half open and half closed mask. The hexagonal symmetry of an HURA is more appropriate for a round position-sensitive detector or a closed-packed array of detectors than a rectangular symmetry. E.A.K.

N85-34941*# California Inst. of Tech., Pasadena.

A BALLOON-BORNE IMAGING GAMMA-RAY TELESCOPE

W. E. Althouse, W. R. Cook, A. C. Cummings, M. H. Finger, T. A. Prince, S. M. Schindler, C. H. Starr, and E. C. Stone *In* NASA. Goddard Space Flight Center 19th Intern. Cosmic Ray Conf., Vol. 3 Aug. 1985 p 299-302 refs (For primary document see N85-34862 23-93)

(Grant NGR-05-002-160)

(OG-9.2-2) Avail: NTIS HC as boxed set only $200/MF A01 per volume or E99 per entire set CSCL 03B

A balloon-borne coded-aperture gamma-ray telescope for galactic and extragalactic astronomy observations is described. The instrument, called Gamma Ray Imaging Payload (GRIP), is designed for measurements in the energy range from 30 keV to 5 MeV with an angular resolution of 0.6 deg over a 20 deg field of view. Distinguishing characteristics of the telescope are a rotating hexagonal coded-aperture mask and a thick NaI scintillation camera. Rotating hexagonal coded-apertures and the development of thick scintillation cameras are discussed. E.A.K.

N85-34942*# National Aeronautics and Space Administration. Goddard Space Flight Center, Greenbelt, Md.

A CODED APERTURE IMAGING SYSTEM OPTIMIZED FOR HARD X-RAY AND GAMMA RAY ASTRONOMY

N. Gehrels, T. L. Cline, A. F. Huters (Sandia Labs., Albuquerque, N. Mex.), M. Leventhal (Bell Telephone Labs., Murray Hill, N.J.), C. J. MacCallum (Sandia Labs., Albuquerque, N. Mex.), J. D. Reber, P. D. Stang (Sandia Labs., Albuquerque, N. Mex.), B. J. Teegarden, and J. Tueller *In its* 19th Intern. Cosmic Ray Conf., Vol. 3 Aug. 1985 p 303-306 refs (For primary document see N85-34862 23-93)

(OG-9.2-3) Avail: NTIS HC as boxed set only $200/MF A01 per volume or E99 per entire set CSCL 03B

A coded aperture imaging system was designed for the Gamma-Ray imaging spectrometer (GRIS). The system is optimized for imaging 511 keV positron-annihilation photons. For a galactic center 511-keV source strength of 0.001 sq/s, the source location accuracy is expected to be + or - 0.2 deg. E.A.K.

N85-34943*# National Aeronautics and Space Administration. Goddard Space Flight Center, Greenbelt, Md.
THE GAMMA-RAY IMAGING SPECTROMETER (GRIS): A NEW BALLOON-BORNE EXPERIMENT FOR GAMMA-RAY LINE ASTRONOMY
B. J. Teegarden, T. L. Cline, N. Gehrels, G. Porreca, J. Tueller, Marvin Leventhal (Bell Telephone Labs.), A. F. Huters (Sandia Labs., Albuquerque, N. Mex.), C. J. MacCallum (Sandia Labs., Albuquerque, N. Mex.), and P. D. Stang (Sandia Labs., Albuquerque, N. Mex.) *In its* 19th Intern. Cosmic Ray Conf., Vol. 3 Aug. 1985 p 307-310 refs (For primary document see N85-34862 23-93)
(OG-9.2-4) Avail: NTIS HC as boxed set only $200/MF A01 per volume or E99 per entire set CSCL 03B

High resolution gamma-ray spectroscopy is a relatively new field that holds great promise for further understanding of high energy astrophysical processes. When the high resolution gamma-ray spectrometer (GRSE) was removed from the GRO payload, a balloon program was initiated to permit continued development and improvement of instrumentation in this field, as well as continued scientific observations. The Gamma-Ray Imaging Spectrometer (GRIS) is one of the experiments selected as part of this program. The instrument contains a number of new and innovative features that are expected to produce a significant improvement in source location accuracy and sensitivity over previous balloon and satellite experiments. B.W.

N85-34944*# Case Western Reserve Univ., Cleveland, Ohio.
MODELING A HIGH ENERGY GAMMA-RAY TELESCOPE
T. L. Jenkins, G. M. Frye, Jr., C. J. Hall, A. Owens, G. N. Pendleton, J. N. Carter (Southampton Univ.), D. Ramsden (Southampton Univ.), and B. Agrinier (CEA, Gif-sur-Yvette, France) *In* NASA. Goddard Space Flight Center 19th Intern. Cosmic Ray Conf., Vol. 3 Aug. 1985 p 311-313 ref (For primary document see N85-34862 23-93)
(Grant NAGw-451)
(OG-9.2-5) Avail: NTIS HC as boxed set only $200/MF A01 per volume or E99 per entire set CSCL 03B

A Monte Carlo program was developed to simulate a high energy gamma-ray telescope using a coded aperture mask (CAMTRAC). The ultimate purpose of the calculation will be to determine the optimum design parameters for such an instrument. The model can also used to ascertain under what conditions CAMTRAC performance is superior to that of conventional telescopes which employ electron-positron pair direction as the sole means of determining gamma ray direction. Author

N85-34945*# Case Western Reserve Univ., Cleveland, Ohio.
SECONDARY GAMMA-RAY PRODUCTION IN A CODED APERTURE MASK
A. Owens, G. M. Frye, Jr., C. J. Hall, T. L. Jenkins, G. N. Pendleton, J. N. Carter (Southampton Univ.), D. Ramsden (Southampton Univ.), B. Agrinier (CEA, Saclay, France), E. Bonfand (CEA, Saclay, France), C. Gouiffes (CEA, Saclay, France) et al *In* NASA. Goddard Space Flight Center 19th Intern. Cosmic Ray Conf., Vol. 3 Aug. 1985 p 314-317 refs (For primary document see N85-34862 23-93)
(Grant NAGw-451)
(OG-9.2-6) Avail: NTIS HC as boxed set only $200/MF A01 per volume or E99 per entire set CSCL 03B

The application of the coded aperture mask to high energy gamma-ray astronomy will provide the capability of locating a cosmic gamma-ray point source with a precision of a few arc-minutes above 20 MeV. Recent tests using a mask in conjunction with drift chamber detectors have shown that the expected point spread function is achieved over an acceptance cone of 25 deg. A telescope employing this technique differs from a conventional telescope only in that the presence of the mask modifies the radiation field in the vicinity of the detection plane. In addition to reducing the primary photon flux incident on the detector by absorption in the mask elements, the mask will also be a secondary radiator of gamma-rays. The various background components in a CAMTRAC (Coded Aperture Mask Track Chamber) telescope are considered. Monte-Carlo calculations are compared with recent measurements obtained using a prototype instrument in a tagged photon beam line. B.W.

N85-34946*# Case Western Reserve Univ., Cleveland, Ohio.
OPERATING CHARACTERISTICS OF A PROTOTYPE HIGH ENERGY GAMMA-RAY TELESCOPE
T. L. Jenkins, G. M. Frye, Jr., C. J. Hall, G. N. Owens, G. N. Pendleton, J. N. Carter (Southampton Univ.), D. Ramsden (Southampton Univ.), B. Agrinier (CEA, Gif-sur-Yvette, France), E. Bonfand (CEA, Gif-sur-Yvette, France), and A. Refloch (Gif-sur-Yvette, France) *In* NASA. Goddard Space Flight Center 19th Intern. Cosmic Ray Conf., Vol. 3 Aug. 1985 p 318-321 refs Sponsored in part by United Kingdom Science and Engineering Research Council (For primary document see N85-34862 23-93)
(Grant NAGw-451)
(OG-9.2-7) Avail: NTIS HC as boxed set only $200/MF A01 per volume or E99 per entire set CSCL 03B

The field of gamma-ray astronomy in the energy range from ten to several hundred MeV is severely limited by the angular resolution that can be achieved by present instruments. The identification of some of the point sources found by the COS-B mission and the resolution of detailed structure existing in those sources may depend on the development of a new class of instrument. The coded aperture mask telescope, used successfully at X-ray energies hold the promise of being such an instrument. A prototype coded aperture telescope was operated in a tagged photon beam ranging in energy from 23 to 123 MeV. The purpose of the experiment was to demonstrate the feasibility of operating a coded aperture mask telescope in this energy region. Some preliminary results and conclusions drawn from some of the data resulting from this experiment are presented. B.W.

N85-34947*# Consiglio Nazionale delle Ricerche, Bologna (Italy).
AN EXPERIMENTAL ASSESSMENT OF THE IMAGING QUALITY OF THE LOW ENERGY GAMMA-RAY TELESCOPE ZEBRA
R. C. Butler, E. Caroli, G. DiCocco, L. Natalucci, G. Spada, A. Spizzichino, J. B. Stephen, J. N. Carter (Southampton Univ.), P. M. Charalambous (Southampton Univ.), A. J. Dean et al *In* NASA. Goddard Space Flight Center 19th Intern. Cosmic Ray Conf., Vol. 3 Aug. 1985 p 322-325 refs (For primary document see N85-34862 23-93)
(OG-9.2-8) Avail: NTIS HC as boxed set only $200/MF A01 per volume or E99 per entire set CSCL 03B

One gamma-ray detection plane of the ZEBRA telescope, consisting of nine position sensitive scintillation crystal bars designed to operate over the spectral range 0.2 to 10 MeV, has been constructed in the laboratory. A series of experimental images has been generated using a scaled down flight pattern mask in conjunction with a diverging gamma-ray beam. Point and extended sources have been imaged in order to assess quantitatively the performance of the system. Author

N85-34948*# California Univ., San Diego, La Jolla.
ADVANCED TECHNIQUES FOR HIGH RESOLUTION SPECTROSCOPIC OBSERVATIONS OF COSMIC GAMMA-RAY SOURCES
J. L. Matteson, M. R. Pelling, L. E. Peterson, R. P. Lin (California Univ., Berkeley), K. A. Anderson (California Univ., Berkeley), R. H. Pehl (California Univ. Lawrence Berkeley Lab.), K. C. Hurley (Centre d'Etude Spatiale des Rayonnements), G. Vedrenne (Centre d'Etude Spatiale des Rayonnements), M. SNiel (Centre d'Etude Spatiale des Rayonnements), and Ph. Durouchoux (CEA, Gif-sur-Yvette, France) *In* NASA. Goddard Space Flight Center 19th Intern. Cosmic Ray Conf., Vol. 3 Aug. 1985 p 326-329 refs (For primary document see N85-34862 23-93)
(OG-9.2-9) Avail: NTIS HC as boxed set only $200/MF A01 per volume or E99 per entire set CSCL 03B

An advanced gamma-ray spectrometer that is currently in development is described. It will obtain a sensitivity of < 0.0001

ph/sq cm./sec in a 6 hour balloon observation and uses innovative techniques for background reduction and source imaging. Author

N85-34949*# Academy of Sciences (USSR), Moscow. Inst. for Cosmic Research.

THE GAMMA-RAY TELESCOPE GAMMA-1

V. V. Akimov, V. E. Nesterov, L. F. Kalinkin, V. M. Balibanov, O. F. Prilutsky, V. G. Rodin, N. G. Leikov, A. S. Bielaoussov, L. B. Dobrian, V. P. Poluektov et al *In* NASA. Goddard Space Flight Center 19th Intern. Cosmic Ray Conf., Vol. 3 Aug. 1985 p 330-333 refs (For primary document see N85-34862 23-93)

(OG-9.2-10) Avail: NTIS HC as boxed set only $200/MF A01 per volume or E99 per entire set CSCL 03B

French and Soviet specialists have designed and built the gamma-ray telescope GAMMA-1 to detect cosmic gamma rays above 50 MeV. The sensitive area of the detector is 1400 sq cm, energy resolution is 30% at 300 MeV, and angular resolution 1.2 deg at 300 MeV (and less than 20' arc when a coded aperture mask is used). Results on calibration of the qualification model and Monte-Carlo calculations are presented. Author

N85-34950*# Consiglio Nazionale delle Ricerche, Palermo (Italy). Ist. de Fisica Cosmica e Informatica.

THE FIGARO EXPERIMENT FOR THE OBSERVATION OF TIME MARKED SOURCES IN THE LOW ENERGY GAMMA-RAY RANGE

G. Agnetta, B. Agrinier (CEA, Saclay, France), J. P. Chabaud (Toulouse Univ.), E. Costa (CNR, Frascati, Italy), R. DiRAffaele, P. Frabel (Toulouse Univ.), G. Gerardi, C. Gouiffes (CEA, Saclay, France), M. F. Landrea (Observatoire de Paris-Meudon), P. Mandrou (Toulouse Univ.) et al *In* NASA. Goddard Space Flight Center 19th Intern. Cosmic Ray Conf., Vol. 3 Aug. 1985 p 334-337 refs (For primary document see N85-34862 23-93)

(OG-9.2-11) Avail: NTIS HC as boxed set only $200/MF A01 per volume or E99 per entire set CSCL 03B

The only two firmly identified galactic gamma-ray sources in the second COS B catalogue are the pulsars PSR 0531+21 (Crab) and PSR 0833-45 (Vela). In the region between 100 keV and 10 MeV the detailed shape of the emission is particularly important, since one expects a turn-off which is related to geometry of the source. A marginal evidence of such a turn-off just below 1 MeV has been reported for the Vela pulsar. In order to study sources with a well marked time signature in this energy band, the FIGARO - French Italian Gamma Ray Observatory was designed. The first version was launched in November 1983 from the Sao Manuel base (Brazil), and was destroyed in a free fall following a balloon burst at an altitude of 50 mbar. A brief description is given of the new improved version of the experiment, FIGARO 2, which is nearly completed and whose launch is scheduled before summer 1986. B.W.

N85-34951*# National Aeronautics and Space Administration. Goddard Space Flight Center, Greenbelt, Md.

HIGH ENERGY GAMMA RAY BALLOON INSTRUMENT

D. J. Thompson, R. G. Baker, D. L. Bertsch, J. R. Chesney, S. M. Derdeyn, C. H. Ehrmann, C. E. Fichtel, S. D. Hunter, J. S. Jacques, N. A. Laubenthal et al *In its* 19th Intern. Cosmic Ray Conf., Vol. 3 Aug. 1985 p 338-341 refs (For primary document see N85-34862 23-93)

(OG-9.2-12) Avail: NTIS HC as boxed set only $200/MF A01 per volume or E99 per entire set CSCL 03B

The High Energy Gamma Ray Balloon Instrument was built in part to verify certain subsystems' performance for the Energetic Gamma Ray Experiment Telescope (EGRET) instrument, the high energy telescope to be carried on the Gamma Ray Observatory. This paper describes the instrument, the performance of some subsystems, and some relevant results. Author

N85-34952*# California Univ., Riverside.

MEASURED PERFORMANCE OF THE NEW UNIVERSITY OF CALIFORNIA GAMMA RAY TELESCOPE

A. D. Zych, T. ONeill, W. Sweeney, J. Simone (California State Univ., Los Angeles), O. T. Tuemer, and R. S. White *In* NASA. Goddard Space Flight Center 19th Intern. Cosmic Ray Conf., Vol. 3 Aug. 1985 p 342 refs (For primary document see N85-34862 23-93)

(OG-9.2-13) Avail: NTIS HC as boxed set only $200/MF A01 per volume or E99 per entire set CSCL 03B

The design of the new medium energy balloon-borne gamma ray telescope is discussed. This telescope is sensitive to 1-30 MeV gamma rays. The results of the initial calibration are described. The position and energy resolutions of 32 plastic and NaI(Tl) scintillator bars, each 100 cm long are discussed. The telescope's measured angular and energy resolutions as a function of incident angle are compared with detailed Monte Carlo calculations at 1.37, 2.75 and 6.13 MeV. The expected resolutions are 5 deg FHWM and 8% at 2.75 MeV. The expected area-efficiency is 250 cm. B.W.

N85-34953*# National Aeronautics and Space Administration. Marshall Space Flight Center, Huntsville, Ala.

BURST AND TRANSIENT SOURCE EXPERIMENT (BATSE) FOR THE GAMMA RAY OBSERVATORY (GRO)

G. J. Fishman, C. A. Meegan, T. A. Parnell, R. B. Wilson, W. Paciesas (Alabama Univ., Huntsville), J. L. Mateson (California Univ., San Diego, La Jolla), T. L. Cline (NASA. Goddard Space Flight Center), and B. J. Teegarden (NASA. Goddard Space Flight Center) *In* NASA. Goddard Space Flight Center 19th Intern. Cosmic Ray Conf., Vol. 3 Aug. 1985 p 343-346 refs (For primary document see N85-34862 23-93)

(OG-9.2-14) Avail: NTIS HC as boxed set only $200/MF A01 per volume or E99 per entire set CSCL 03B

The Burst and Transient Source Experiment (BATSE) on the Gamma Ray Observatory (GRO) is expected to provide new and better observational data on bursts to test current and future models of burst sources. These data will include: (1) the celestial distribution of hundreds of burst sources over the life of the mission, (2) burst locations within several degrees, within 2 days after their occurrence, (3) observations of weaker bursts and better observations of short timescale fluctuations and spectral variations, (4) observations by a single experiment over a much larger energy range than previously available, and (5) more sensitive measurements of the spectral features which have been observed in many bursts. This paper briefly describes the GRO mission, the BATSE instrumentation and the burst observational capabilities. Author

N85-34954*# National Aeronautics and Space Administration. Marshall Space Flight Center, Huntsville, Ala.

GAMMA-RAY BURST SPECTROSCOPY CAPABILITIES OF THE BATSE/GRO EXPERIMENT

J. L. Matteson (California Univ., San Diego, La Jolla), G. J. Fishman, C. A. Meegan, T. A. Parnell, R. B. Wilson, W. Paciesas (Alabama Univ., Huntsville), T. L. Cline (NASA. Goddard Space Flight Center), and B. J. Teegarden (NASA. Goddard Space Flight Center) *In* NASA. Goddard Space Flight Center 19th Intern. Cosmic Ray Conf., Vol. 3 Aug. 1985 p 347-350 refs (For primary document see N85-34862 23-93)

(OG-9.2-15) Avail: NTIS HC as boxed set only $200/MF A01 per volume or E99 per entire set CSCL 03B

A scintillation spectrometer is included in each of the eight BATSE/GRO detector modules, resulting in all-sky coverage for gamma-ray bursts. The scientific motivation, design and capabilities of these spectrometers for performing spectral observations over a wide range of gamma-ray energies and burst intensities are described. Author

N85-34955*# National Aeronautics and Space Administration. Marshall Space Flight Center, Huntsville, Ala.

CAPABILITIES OF THE GRO/BATSE FOR MONITORING OF DISCRETE SOURCES

R. B. Wilson, G. J. Fishman, and C. A. Meegan *In* NASA. Goddard Space Flight Center 19th Intern. Cosmic Ray Conf., Vol. 3 Aug. 1985 p 351-354 refs (For primary document see N85-34862 23-93)

(OG-9.2-16) Avail: NTIS HC as boxed set only $200/MF A01 per volume or E99 per entire set CSCL 03B

Although the Burst and Transient Source Experiment (BATSE) to be flown on the Gamma Ray Observatory has as its primary objective the detection of gamma ray bursts, its uncollimated design will enable it to serve a unique function as an all-sky monitor for bright hard X-ray and low-energy gamma ray sources. Pulsating sources may be detected by conventional techniques such as summed-epoch and Fourier analyses. The BATSE will, in addition, be able to use Earth occultation in an unprecedented way to monitor sufficiently bright sources as often as several times per day over approx. 85% of the sky. Estimates of the expected BATSE sensitivity using both of these techniques are presented. Author

N85-34956*# Consiglio Nazionale delle Ricerche, Bologna (Italy).
LAPEX: A PHOSWICH BALLOON EXPERIMENT FOR HARD X-RAY ASTRONOMY
F. Frontera, A. Basin, D. DalFiume, T. Franceschini, G. Landini, E. Morelli, J. M. Poulsen, A. Rubini, S. Silvestri, and E. Costa (CNR, Frascati, Italy) *In* NASA. Goddard Space Flight Center 19th Intern. Cosmic Ray Conf., Vol. 3 Aug. 1985 p 355-358 refs (For primary document see N85-34862 23-93)
(OG-9.3-1) Avail: NTIS HC as boxed set only $200/MF A01 per volume or E99 per entire set CSCL 03B

Satellite and balloon observations have shown that several classes of celestial objects are hard (> 15 keV) energy band with a sensitivity of approx 10 mCrab has been performed with the UCSD/MIT instrument (A4) on board the HEAO 1 satellite. About 70 X-ray sources were detected, including galactic and extragalactic objects. Hard X-ray emission has been detected in the Galaxy from X-ray pulsars. Extragalactic sources of hard X-ray emission include clusters of galaxies, QSOs, BL Lac objects, Seyfert galaxies. The essential characteristics of the Large Area Phoswich Experiment (LAPEX) for crowded sky field observations are described. It has: (1) a broad energy band of operation (20-300 keV); (2) a 3 sigma sensitivity of about 1 mCrab in 10,000 s of live observing time; and (3) imaging capabilities with an angular resolution of about 20'. B.W.

N85-34957*# Centre d'Etude Spatiale des Rayonnements, Toulouse (France).
AN IMPROVED TIME OF FLIGHT GAMMA-RAY TELESCOPE TO MONITOR DIFFUSE GAMMA-RAY IN THE ENERGY RANGE 5 MeV - 50 MeV
A. DaCostaFereiraNeri, A. Bui-Van, J. M. Lavigne, C. Sabaud, G. Vedrenne, B. Agrinier (CEA, Saclay, France), and C. Gouiffes (CEA, Saclay, France) *In* NASA. Goddard Space Flight Center 19th Intern. Cosmic Ray Conf., Vol. 3 Aug. 1985 p 359-362 refs (For primary document see N85-34862 23-93)
(OG-9.3-2) Avail: NTIS HC as boxed set only $200/MF A01 per volume or E99 per entire set CSCL 03B

A time of flight measuring device is the basic triggering system of most of medium and high energy gamma-ray telescopes. A simple gamma-ray telescope has been built in order to check in flight conditions the functioning of an advanced time of flight system. The technical ratings of the system are described. This telescope has been flown twice with stratospheric balloons, its axis being oriented at various Zenital directions. Flight results are presented for diffuse gamma-rays, atmospheric secondaries, and various causes of noise in the 5 MeV-50 MeV energy range. B.W.

N85-34958*# Smithsonian Astrophysical Observatory, Cambridge, Mass.
RESULTS OF A STUDY TO BUILD A GAMMA-RAY TELESCOPE IN AN EXTERNAL TANK
David Koch *In* NASA. Goddard Space Flight Center 19th Intern. Cosmic Ray Conf., Vol. 3 Aug. 1985 p 363-366 refs (For primary document see N85-34862 23-93)
(OG-9.3-3) Avail: NTIS HC as boxed set only $200/MF A01 per volume or E99 per entire set CSCL 03B

In response to the ever-present need for a very large gamma-ray detector for energies greater than 100 MeV, a concept to build a telescope of 250,000 sq cm sensitive area using a Space Shuttle External Tank (ET) is presented. In the Space Station era, for the first time, large detectors can be constructed on-orbit which would otherwise be limited in size by the launch vehicle. The ET will serve both as the spacecraft and the Cherenkov pressure vessel. The significant feature is that the sensitive area will be forty times that of the high energy detector on GRO and will be able to locate even the faintest sources from the GRO survey to a few arc minutes. The detection technique is based upon that originally proposed by Greisen. Author

N85-34959*# University Coll., Dublin (Ireland). Dept. of Physics.
GeV GAMMA-RAY ASTRONOMY TELESCOPES WITH HIGH ANGULAR RESOLUTION
B. McBreen *In* NASA. Goddard Space Flight Center 19th Intern. Cosmic Ray Conf., Vol. 3 Aug. 1985 p 367-370 refs Previously announced in IAA as A85-24785 (For primary document see N85-34862 23-93)
(OG-9.3-4) Avail: NTIS HC as boxed set only $200/MF A01 per volume or E99 per entire set CSCL 03B

Gamma-ray telescopes flown on satellites have poor angular resolution with typical point source error circles of a few square degrees. It is shown that a major improvement in angular resolution for the detection of gamma-rays in the GeV region can be obtained with a single crystal as converter. The electron produced by a gamma ray incident at a small angle to a major crystal axis or plane is captured into channeling and radiates gamma rays. The channeling radiation and the electron-positron pair can be detected and yield point source locations with a precision of 5 arcseconds at 10 GeV. This is an improvement of three orders of magnitude on the angular precision of telescopes sensitive to gamma-rays above 50 MeV flown on Satellites. Author (IAA)

N85-34960*# Academia Sinica, Beijing (China). Inst. of High Energy Physics.
AN APPROACH OF REDUCING THE BACKGROUND INDUCED BY NEUTRONS
Changquan Shen, Yidong Gu, Yangfang Sun, Yuqian Ma, Changjiang Dai, and Zhenzi Fan *In* NASA. Goddard Space Flight Center 19th Intern. Cosmic Ray Conf., Vol. 3 Aug. 1985 p 371-374 refs (For primary document see N85-34862 23-93)
(OG-9.3-5) Avail: NTIS HC as boxed set only $200/MF A01 per volume or E99 per entire set CSCL 03B

The background induced by interactions of neutrons with detector material (and shield material) is difficult to be rejected. It is one of the most important factors to affect the sensitivity of a balloon-borne gamma-ray astronomical telescope. The main component of neutron flux at the major detector of the telescope is incident neutrons, that consists of atmospheric neutrons and neutrons locally produced in the balloon platform. Therefore, shielding the detector from incident neutrons is a possible way to reduce the background. NaI (T1) crystal is very widely used in gamma-ray astronomical telescopes. Through balloon-borne experiment it is shown that up 6 LiF shield is effective to reduce the background in NaI crystal. B.W.

N85-34961*# California Univ., Riverside.
NEUTRON-INDUCED 2.2 MeV BACKGROUND IN GAMMA RAY TELESCOPES
E. M. Zanrosso (Xerox Corp., Pasadena, Calif.), J. L. Long (Hughes Aircraft Co., Los Angeles), A. D. Zych, and R. S. White *In* NASA. Goddard Space Flight Center 19th Intern. Cosmic Ray Conf., Vol. 3 Aug. 1985 p 375-378 refs (For primary document see N85-34862 23-93)
(Grant NGR-05-008-022)
(OG-9.3-6) Avail: NTIS HC as boxed set only $200/MF A01 per volume or E99 per entire set CSCL 03B

Neutron-induced gamma ray production is an important source of background in Compton scatter gamma ray telescopes where organic scintillator material is used. Most important is deuteron formation when atmospheric albedo and locally produced neutrons are thermalized and subsequently absorbed in the hydrogenous material. The resulting 2.2 MeV gamma ray line radiation essentially represents a continuous isotropic source within the scintillator itself. Interestingly, using a scintillator material with a high

hydrogen-to-carbon ratio to minimize the scintillator material with a high hydrogen-to-carbon ratio to minimize the neutron-induced 4.4 MeV carbon line favors the np reaction. The full problem of neutron-induced background in Compton scatter telescopes has been previously discussed. Results are presented of observations with the University of California balloon-borne Compton scatter telescope where the 2.2 MeV induced line emission is prominently seen. B.W.

N85-34962*# Southampton Univ. (England).
A COMPARISON OF CALCULATED AND MEASURED BACKGROUND NOISE RATES IN HARD X-RAY TELESCOPES AT BALLOON ALTITUDE
A. J. Dean, N. A. Dipper, R. A. Lewis, and F. Perotti (Ist. di Fisica Cosmica, Milan) *In* NASA. Goddard Space Flight Center 19th Intern. Cosmic Ray Conf., Vol. 3 Aug. 1985 p 379-382 refs (For primary document see N85-34862 23-93)
(OG-9.3-7) Avail: NTIS HC as boxed set only $200/MF A01 per volume or E99 per entire set CSCL 03B

An actively shielded hard X-ray astronomical telescope has been flown on stratospheric balloons. An attempt is made to compare the measured spectral distribution of the background noise counting rates over the energy loss range 20-300 keV with the contributions estimated from a series of Monte Carlo and other computations. The relative contributions of individual particle interactions are assessed. Author

N85-34963*# Max-Planck-Inst. fuer Physik und Astrophysik, Garching (West Germany).
THE FINAL COS-B DATABASE NOW PUBLICLY AVAILABLE
H. A. Mayer-Hasselwander, K. Bennett (ESA, Noordwijk, Netherlands), G. F. Bignami (CNR, Milano), J. B. G. M. Bloemen (Lab. for Space Research, Leiden), R. Buccheri (CNR, Palermo, Italy), P. A. Caraveo (CNR. Milano), W. Hermsen (Lab. for Space Research, Leiden), G. Kanbach, F. Lebrun (Centre dEtudes Nucleaires, Saclay, France), J. A. Paul (Centre dEtudes Nucleaires, Saclay, France) et al *In* NASA. Goddard Space Flight Center 19th Intern. Cosmic Ray Conf., Vol. 3 Aug. 1985 p 383-386 refs (For primary document see N85-34862 23-93)
(OG-9.3-8) Avail: NTIS HC as boxed set only $200/MF A01 per volume or E99 per entire set CSCL 03B

The data obtained by the gamma ray satellite COS-B was processed, condensed and integrated together with the relevant mission and experiment parameters into the Final COS-B Database. The database contents and the access programs available with the database are outlined. The final sky coverage and a presentation of the large scale distribution of the observed Milky Way emission are given. The database is announced to be available through the European Space Agency. Author

N85-34964*# Max-Planck-Inst. fuer Physik und Astrophysik, Garching (West Germany). Inst. fuer Extraterrestrische Physik.
THE FINAL COS-B DATABASE: IN-FLIGHT CALIBRATION OF INSTRUMENTAL PARAMETERS
A. W. Strong, J. B. G. M. Bloemen (Lab. for Space Research, Leiden), R. Buccheri (CNR, Palermo, Italy), W. Hermsen (Lab. for Space Research, Leiden), F. Lebrun (Centre dEtudes Nucleaires, Saclay, France), and H. A. Mayer-Hasselwander *In* NASA. Goddard Space Flight Center 19th Intern. Cosmic Ray Conf., Vol. 3 Aug. 1985 p 387-390 ref (For primary document see N85-34862 23-93)
(OG-9.3-9) Avail: NTIS HC as boxed set only $200/MF A01 per volume or E99 per entire set CSCL 03B

A method for the determination of temporal variation of sensitivity is designed to find a set of parameters which lead to maximum consistency between the intensities derived from different observation periods. This method is briefly described and the resulting sensitivity and background variations presented. Author

N85-34965*# National Aeronautics and Space Administration. Goddard Space Flight Center, Greenbelt, Md.
A STAR CAMERA ASPECT SYSTEM SUITABLE FOR USE IN BALLOON EXPERIMENTS **c35**
S. D. Hunter and R. G. Baker *In its* 19th Intern. Cosmic Ray Conf., Vol. 3 Aug. 1985 p 391-394 refs (For primary document see N85-34862 23-93)
(OG-9.3-10) Avail: NTIS HC as boxed set only $200/MF A01 per volume or E99 per entire set CSCL 14C

A balloon-borne experiment containing a star camera aspect system was designed, built, and flown. This system was designed to provide offset corrections to the magnetometer and inclinometer readings used to control an azimuth and elevation pointed experiment. The camera is controlled by a microprocessor, including commendable exposure and noise rejection threshold, as well as formatting the data for telemetry to the ground. As a background program, the microprocessor runs the aspect program to analyze a fraction of the pictures taken so that aspect information and offset corrections are available to the experiment in near real time. The analysis consists of pattern recognition of the star field with a star catalog in ROM memory and a least squares calculation. The performance of this system in ground based tests is described. It is part of the NASA/GSFC High Energy Gamma-Ray Balloon Instrument (2). Author

N85-34966*# California Inst. of Tech., Pasadena.
BALLOON-BORNE VIDEO CASSETTE RECORDERS FOR DIGITAL DATA STORAGE **c33**
W. E. Althouse and W. R. Cook *In* NASA. Goddard Space Flight Center 19th Intern. Cosmic Ray Conf., Vol. 3 Aug. 1985 p 395-397 refs (For primary document see N85-34862 23-93)
(Grant NGR-05-002-160)
(OG-9.3-11) Avail: NTIS HC as boxed set only $200/MF A01 per volume or E99 per entire set CSCL 09C

A high speed, high capacity digital data storage system was developed for a new balloon-borne gamma-ray telescope. The system incorporates economical consumer products: the portable video cassette recorder (VCR) and a relatively newer item - the digital audio processor. The in-flight recording system employs eight VCRs and will provide a continuous data storage rate of 1.4 megabits/sec throughout a 40 hour balloon flight. Data storage capacity is 25 gigabytes and power consumption is only 10 watts. Author

N85-34967*# Southampton Univ. (England). Dept. of Physics.
A POSITION SENSITIVE PHOSWICH HARD X-RAY DETECTOR SYSTEM
A. J. Dean, C. G. Hanson, C. J. Hopkins, R. A. Lewis, and J. Fraser-Mitchell *In* NASA. Goddard Space Flight Center 19th Intern. Cosmic Ray Conf., Vol. 3 Aug. 1985 p 398-401 refs (For primary document see N85-34862 23-93)
(OG-9.3-12) Avail: NTIS HC as boxed set only $200/MF A01 per volume or E99 per entire set CSCL 03B

A prototype position sensitive phoswich hard X-ray detector, designed for eventual astronomical usage, was tested in the laboratory. The scintillation crystal geometry was designed on the basis of a Monte Carlo simulation of the internal optics and includes a 3mm thick NaI(T1) primary X-ray detector which is actively shielded by a 20 mm thick CsI(T1) scintillation crystal. This phoswich arrangement is viewed by a number two inch photomultipliers. Measured values of the positional and spectral resolution of incident X-ray photons are compared with calculation. Author

N85-34968*# Commissariat a l'Energie Atomique, Saclay (France).
A CERENKOV IMAGING TELESCOPE FOR HIGH ENERGY GAMMA RAYS
P. Ferrando and P. Goret *In* NASA. Goddard Space Flight Center 19th Intern. Cosmic Ray Conf., Vol. 3 Aug. 1985 p 402-405 refs (For primary document see N85-34862 23-93)
(OG-9.3-13) Avail: NTIS HC as boxed set only $200/MF A01 per volume or E99 per entire set CSCL 03B

A large area gamma ray telescope based on the gas Cerenkov imaging technique is presented. The performances of the instrument for the observation of high energy gamma ray point sources are discussed. Author

N85-34969*# Durham Univ. (England). Dept. of Physics.
THE UNIVERSITY OF DURHAM MARK 3 VERY HIGH ENERGY GAMMA RAY TELESCOPE
P. M. Chadwick, N. A. Dipper, J. C. Dowthwaite, I. W. Kirkman, T. J. McComb, K. J. Orford, and K. E. Turver *In* NASA. Goddard Space Flight Center 19th Intern. Cosmic Ray Conf., Vol. 3 Aug. 1985 p 406-409 refs Sponsored by Science and Engineering Research Council (For primary document see N85-34862 23-93)
(OG-9.4-2) Avail: NTIS HC as boxed set only $200/MF A01 per volume or E99 per entire set CSCL 03B

A new very high energy gamma-ray telescope employing the atmospheric Cerenkov light technique and currently nearing completion is described. The telescope is designed to have capability as both a wide angle instrument (4 degree field of view) for sky survey work and as a narrow field of view instrument (1.35 degrees) for conventional drift-scanning and tracking modes of operation. The telescope consists of two 10 sq. m. mirrors operated in fast coincidence with multiple phototube assemblies at the prime focus of each mirror. The design philosophy of the instrument is discussed and comparisons of its performance with our previous telescopes are made. Author

N85-34970*# Osaka City Univ. (Japan). Inst. for Cosmic Rays.
A NEW ULTRA HIGH ENERGY GAMMA RAY TELESCOPE AT OHYA MINE
T. Aoki, S. Higashi, Y. Kamiya, T. Kitamura, S. Matsuno, K. Mizutani, K. Mitsui, Y. Muraki, A. Okada, and Y. Ohashi *In* NASA. Goddard Space Flight Center 19th Intern. Cosmic Ray Conf., Vol. 3 Aug. 1985 p 410-413 refs (For primary document see N85-34862 23-93)
(OG-9.4-3) Avail: NTIS HC as boxed set only $200/MF A01 per volume or E99 per entire set CSCL 03B

The search for ultra high energy gamma rays coming from point sources is one of the main experimental aims. A fast air shower timing system was constructed at ICRR for the study of the angular resolution of the system and operated approximately half a year. The characteristics of the surface array of Ohya air shower telescope is described. Author

N85-34971*# Adelaide Univ. (Australia). Dept. of Physics.
THE BUCKLAND PARK AIR SHOWER ARRAY
R. W. Clay, C. L. Corani, J. R. Patterson, B. R. Dawson, P. G. Edwards, A. G. Gregory, J. R. Prescott, S. D. Elton, and D. Clampa *In* NASA. Goddard Space Flight Center 19th Intern. Cosmic Ray Conf., Vol. 3 Aug. 1985 p 414-417 refs (For primary document see N85-34862 23-93)
(OG-9.4-4) Avail: NTIS HC as boxed set only $200/MF A01 per volume or E99 per entire set CSCL 03B

The new Buckland Park Air Shower Array has been producing analyzed shower data since July 1984. The array is described and some preliminary performance figures are presented. Author

N85-34972*# Kiel Univ. (West Germany). Inst. fuer Reime and Angewandte Kernphysik.
AN EAS EXPERIMENT AT MOUNTAIN ALTITUDE FOR THE DETECTION OF GAMMA-RAY SOURCES
O. C. Allkofer, M. Samorski, and W. Stamm *In* NASA. Goddard Space Flight Center 19th Intern. Cosmic Ray Conf., Vol. 3 Aug. 1985 p 418-421 refs (For primary document see N85-34862 23-93)
(OG-9.4-5) Avail: NTIS HC as boxed set only $200/MF A01 per volume or E99 per entire set CSCL 03B

The plan of an extensive air shower experiment 2.200 m above sea level for the detection of 10 to the 14th power eV to 10 to the 17th power eV gamma rays from sources in the declination band 0 deg to + 60 deg is described. The site selection, detector array and electronic layout are detailed. Author

N85-34973*# Harvard-Smithsonian Center for Astrophysics, Cambridge, Mass.
AN OBSERVATORY TO STUDY 10 (10) TO 10 (17) BY EV GAMMA RAYS
Trevor C. Weekes *In* NASA. Goddard Space Flight Center 19th Intern. Cosmic Ray Conf., Vol. 3 Aug. 1985 p 422-425 refs (For primary document see N85-34862 23-93)
(OG-9.4-6) Avail: NTIS HC as boxed set only $200/MF A01 per volume or E99 per entire set CSCL 03B

A facility is described which incorporates many of the best features of existing gamma ray telescopes at a single site. In addition to reducing the flux sensitivity in some energy ranges, it permits the measurements of the energy spectrum over seven decades of energy. Author

N85-34974*# Leeds Univ. (England). Dept. of Physics.
A NEW ARRAY FOR THE STUDY OF ULTRA HIGH ENERGY GAMMA-RAY SOURCES
G. Brooke, A. Lambert, P. A. Ogden, M. Patel, J. C. Ferrett, R. J. O. Reid, A. A. Watson, and A. A. West *In* NASA. Goddard Space Flight Center 19th Intern. Cosmic Ray Conf., Vol. 3 Aug. 1985 p 426-429 refs Sponsored by Science and Engineering Research Council (For primary document see N85-34862 23-93)
(OG-9.4-7) Avail: NTIS HC as boxed set only $200/MF A01 per volume or E99 per entire set CSCL 03B

The design and operation of a 32 x 1 10 to the 15th power sq m array of scintillation detectors for the detection of 10 to the 15th power eV cosmic rays is described with an expected angular resolution of < 1 deg, thus improving the present signal/background ratio for gamma ray sources. Data are recorded on a hybrid CAMAC, an in-house system which uses a laser and Pockel-Cell arrangement to routinely calibrate the timing stability of the detectors. Author

N85-34975*# Tokyo Univ. (Japan). Inst. for Cosmic Ray Research.
AKENO 20 km (2) AIR SHOWER ARRAY (AKENO BRANCH)
M. Teshima (Kyoto Univ.), H. Ohoka, Y. Matsubara (Kyoto Univ.), T. Hara, Y. Hatano, N. Hayashida, C. X. He (Academia Sinica, Beijing), M. Honda, F. Ishikawa, K. Kamata et al *In* NASA. Goddard Space Flight Center 19th intern. Cosmic Ray Conf., Vol. 3 Aug. 1985 p 430-433 refs (For primary document see N85-34862 23-93)
(OG-9.4-8) Avail: NTIS HC as boxed set only $200/MF A01 per volume or E99 per entire set CSCL 03B

As the first stage of the future huge array, the Akeno air shower array was expanded to about 20 sq. km. by adding 19 scintillation detectors of 2.25 sq m area outside the present 1 sq. km. Akeno array with a new data collection system. These detectors are spaced about 1km from each other and connected by two optical fiber cables. This array has been in partial operation from 8th, Sep. 1984 and full operation from 20th, Dec. 1984. 20 sq m muon stations are planned to be set with 2km separation and one of them is now under construction. The origin of the highest energy cosmic rays is studied. Author

N85-34976*# New Mexico Univ., Albuquerque. Dept. of Physics and Astronomy.
MINI AND SUPER MINI ARRAYS FOR THE STUDY OF HIGHEST ENERGY COSMIC RAYS
John Linsley *In* NASA. Goddard Space Flight Center 19th Intern. Cosmic Ray Conf., Vol. 3 Aug. 1985 p 434-437 refs (For primary document see N85-34862 23-93)
(OG-9.4-9) Avail: NTIS HC as boxed set only $200/MF A01 per volume or E99 per entire set CSCL 03B

The chief difficulty in studying the highest energy cosmic rays is the extremely low intensity, only approximately 5 particles per sq km sr century above 10 to the 20th power eV. Instead of attacking the problem by assembling all of the available resources in one place, as has been done in the past, a way that the task can be performed at much less cost per unit sensitive area is suggested, by using numerous inexpensive mini arrays operating independently of each other. In addition to the quantities usually observed, each mini array will record shower particle arrival time distributions. At 10 to the 20th power eV the saving in cost per primary particle is estimated to be a factor of 10 or better, compared to methods now in use, even for mini arrays newly built from scratch for just this purpose. Author

N85-34977*# New Mexico Univ., Albuquerque. Dept. of PHysics and Astronomy.
DETECTION OF 10 (1) GeV COSMIC NEUTRINOS WITH A SPACE STATION
John Linsley *In* NASA. Goddard Space Flight Center 19th Intern. Cosmic Ray Conf., Vol. 3 Aug. 1985 p 438-441 refs (For primary document see N85-34862 23-93)
(OG-9.4-10) Avail: NTIS HC as boxed set only $200/MF A01 per volume or E99 per entire set CSCL 03B

The potential value of SOCRAS (Space Observatory of Cosmic Ray Air Showers) for studying the highest energy cosmic rays, including the neutrinos produced in collisions of cosmic ray protons with photons of the 3 deg background radiation is examined. This instrument would look down at the atmosphere from a space station orbiting the Earth at an altitude of 500 to 600 km. During the night portion of each orbit, air showers would be imaged in the fluorescent light they produce. Progress toward the eventual realization of this scheme is described, including a suggestion by Torii for improving the vertical resolution, measurements of the terrestrial background light by Halverson, and especially an application of the LPM effect, expected to increase the sensitivity for upward moving neutrinos by several orders of magnitude. Author

N85-34978*# Adelaide Univ. (Australia). Dept. of Physics.
THE LONGITUDINAL THICKNESS OF AIR-SHOWER FRONTS
R. W. Clay, R. J. V. Brissenden, S. D. Elton, and N. R. Wild *In* NASA. Goddard Space Flight Center 19th Intern. Cosmic Ray Conf., Vol. 3 Aug. 1985 p 442-444 refs Sponsored by Australian Research Grants Scheme (For primary document see N85-34862 23-93)
(OG-9.5-1) Avail: NTIS HC as boxed set only $200/MF A01 per volume or E99 per entire set CSCL 03B

Linsely (1983) has proposed a technique for the detection and analysis of air showers at large distances from the shower axis based on a measurement of the shower front thickness and the assumption that this thickness is closely related to the core distance. Some of the problems involved with realizing such a technique were investigated, and some related observations are reported. The practical problems of how consistent the measurements of the shower front would be, how one would use the measurement, and how the rate of triggered events would depend on the minimum pulse width required are studied. Author

N85-34979*# Leeds Univ. (England). Dept. of Physics.
CERENKOV LIGHT IMAGES OF EAS PRODUCED BY PRIMARY GAMMA
A. M. Hillas *In* NASA. Goddard Space Flight Center 19th Intern. Cosmic Ray Conf., Vol. 3 Aug. 1985 p 445-448 refs (For primary document see N85-34862 23-93)
(OG-9.5-3) Avail: NTIS HC as boxed set only $200/MF A01 per volume or E99 per entire set CSCL 03B

It is shown that it should be possible to distinguish very effectively between background hadronic showers and TeV gamma ray showers from a point source on the basis of the width, length and orientation of the Cerenkov light images of the shower, seen in the focal plane of a focusing mirror, even with a relatively coarse pixel size such as employed in the Mt. Hopkins detector. Predictions of the response of this system to air showers are presented. Author

N85-34980*# Leeds Univ. (England). Dept. of Physics.
SHOWER DISC SAMPLING AND THE ANGULAR RESOLUTION OF GAMMA-RAY SHOWER DETECTORS
A. Lambert and J. Lloyd-Evans *In* NASA. Goddard Space Flight Center 19th Intern. Cosmic Ray Conf., Vol. 3 Aug. 1985 p 449-452 refs Sponsored by Science and Engineering Research Council. (For primary document see N85-34862 23-93)
(OG-9.5-2) Avail: NTIS HC as boxed set only $200/MF A01 per volume or E99 per entire set CSCL 03B

As part of the design study for the new UHE gamma ray detector being constsructed at Haverah Park, a series of experiments using scintillators operated side-by-side in > 10 to the 15th power eV air showers are undertaken. Investigation of the rms sampling fluctuations in the shower disc arrival time yields an upper limit to the intrinsic sampling uncertainty, sigma sub rms = (1.1 + or - 0.1)ns, implying an angular resolution capability < 1 deg for an inter-detector spacing of approximately 25 m. Author

N85-34981*# University Coll., Dublin (Ireland). Dept. of Physics.
APPLICATION OF IMAGING TO THE ATMOSPHERIC CHERENKOV TECHNIQUE
M. F. Cawley, D. J. Fegan, K. Gibbs (Harvard-Smithsonian Center for Astrophysics), P. W. Gorham (Hawaii Univ.), A. M. Hillas (Leeds Univ., England), R. C. Lamb (Iowa State Univ.), D. F. Liebing (Iowa State Univ.), P. K. MacKeown (Hong Kong Univ.), N. A. Porter, V. J. Stenger (Hawaii Univ.) et al *In* NASA. Goddard Space Flight Center 19th Intern. Cosmic Ray Conf., Vol. 3 Aug. 1985 p 453-456 refs Sponsored in part by DOE, Smithsonian Scholarly Studies Fund and by National Board of Science and Technology of Ireland (For primary document see N85-34862 23-93)
(OG-9.5-4) Avail: NTIS HC as boxed set only $200/MF A01 per volume or E99 per entire set CSCL 03B

Turver and Weekes proposed using a system of phototubes in the focal plane of a large reflector to give an air Cherenkov camera for gamma ray astronomy. Preliminary results with a 19 element camera have been reported previously. In 1983 the camera was increased to 37 pixels; it has now been routinely operated for two years. A brief physical description of the camera, its mode of operation, and the data reduction procedures are presented. The Monte Carlo simultations on which these are based on also reviewed. Author

N85-34982*# Utah Univ., Salt Lake City. Dept. of Physics.
A METHOD TO IMPROVE OBSERVATIONS OF GAMMA-RAY SOURCES NEAR 10 (15) eV
P. Sommers and J. W. Elbert *In* NASA. Goddard Space Flight Center 19th Intern. Cosmic Ray Conf., Vol. 3 Aug. 1985 p 457-460 refs (For primary document see N85-34862 23-93)
(Grant NSF PHY-84-15294)
(OG-9.5-5) Avail: NTIS HC as boxed set only $200/MF A01 per volume or E99 per entire set CSCL 03B

Now that sources of gamma rays near 10 to the 15th power eV have been identified, there is a need for telescopes which can study in detail the high energy gamma ray emissions from these sources. The capabilities of a Cerenkov detector which can track a source at large zenith angle (small elevation angle) are analyzed. Because the observed showers must then develop far from the detector, the effective detection area is very large. During a single half-hour hot phase of Cygnus X-3, for example, it may be possible to detect 45 signal showers compared with 10 background showers. Time structure within the hot phase may then be discernible. The precise capabilities of the detector depend on its mirror size, angular acceptance, electronic speed, coincidence properties, etc. Calculations are presented for one feasible design using mirrors of an improved Fly's Eye type. Author

N85-34983*# New Mexico Univ., Albuquerque. Dept. of Physics and Astronomy.
ANGULAR RESOLUTION OF AIR-SHOWER ARRAY-TELESCOPES
John Linsley *In* NASA. Goddard Space Flight Center 19th Intern. Cosmic Ray Conf., Vol. 3 Aug. 1985 p 461-464 refs (For primary document see N85-34862 23-93)
(OG-9.5-6) Avail: NTIS HC as boxed set only $200/MF A01 per volume or E99 per entire set CSCL 03B

A fundamental limit on the angular resolution of air shower array-telescopes is set by the finite number of shower particles coupled with the finite thickness of the particle swarm. Consequently the angular resolution which can be achieved in practice depends in a determinant manner on the size and number of detectors in an array-telescope, as well as on the detector separation and the timing resolution. It is also necessary to examine the meaning of particle density in whatever type of detector is used. Results are given which can be used to predict the angular

resolution of a given instrument for showers of various sizes, and to compare different instruments. Author

N85-34984*# New Mexico Univ., Albuquerque. Dept. of Physics and Astronomy.
ASTROPHYSICAL APPLICATIONS OF HIGH ANGULAR RESOLUTION ARRAY-TELESCOPES
John Linsley *In* NASA. Goddard Space Flight Center 19th Intern. Cosmic Ray Conf., Vol. 3 Aug. 1985 p 465-468 refs (For primary document see N85-34862 23-93)
(OG-9.5-7) Avail: NTIS HC as boxed set only $200/MF A01 per volume or E99 per entire set CSCL 03B

The air shower array-telescopes which are currently being used to search for and study point sources of UHE gamma-rays have angular resolution similar to 1 deg, limited by either the small total area of particle detectors or poor timing resolution. As the signal to noise ratio depends sensitively on the angular resolution, it seems certain that this figure will quickly be surpassed when second generation instruments come into operation. Since the trajectories of galactic cosmic rays with E > 100,000 GeV are practically straight lines on scales of 1 A.U. or less, these new instruments will be able to observe a shadow cast by the Moon (angular diameter 0.5 deg). Although the angular diameter of the Sun is practically the same, its shadow will be more complex because of its magnetic field. Thus, high angular resolution observations of the Sun afford a means of investigating the solar magnetic field, and also the charge composition of cosmic rays, including the ratio of antiprotons to protons. Author

N85-34985*# Tata Inst. of Fundamental Research, Bombay (India).
ANGULAR RESOLUTION OF AN EAS ARRAY FOR GAMMA RAY ASTRONOMY ENERGIES < 5 X 10 (13) eV
A. R. Apte, N. V. Gopalakrishnan, S. C. Tonwar, and V. Uma *In* NASA. Goddard Space Flight Center 19th Intern. Cosmic Ray Conf., Vol. 3 Aug. 1985 p 469-472 refs (For primary document see N85-34862 23-93)
(OG-9.5-8) Avail: NTIS HC as boxed set only $200/MF A01 per volume or E99 per entire set CSCL 03B

A 24 detector extensive air shower array is being operated at Ootacamund (2300 m altitude, 11.4 deg N latitude) in southern India for a study of arrival directions of showers of energies greater than 5 x 10 to the 13th power eV. Various configurations of the array of detectors have been used to estimate the accuracy in determination of arrival angle of showers with such an array. These studies show that it is possible to achieve an angular resolution of better than 2 deg with the Ooty array for search for point sources of Cosmic gamma rays at energies above 5 x 10 to the 13th power eV. Author

N85-34986*# Tokyo Univ., Tanashi (Japan). Inst. for Cosmic-Ray Research.
NOTE ON THE DETECTION OF HIGH ENERGY PRIMARY COSMIC GAMMA RAYS BY AIR SHOWER OBSERVATION
K. Kasahara, S. Torii (Kanagawa Univ.), and T. Yuda *In* NASA. Goddard Space Flight Center 19th Intern. Cosmic Ray Conf., Vol. 3 Aug. 1985 p 473-476 refs (For primary document see N85-34862 23-93)
(OG-9.5-9) Avail: NTIS HC as boxed set only $200/MF A01 per volume or E99 per entire set CSCL 03B

A mountain altitude experiment is planned at Mt. Norikura in Japan to search for point sources of astrophysical high-energy gamma rays in the > 10 to the 15th power eV range. The advantages of mountain level observation of IR showers is stressed, especially in the case of high-energy gamma primaries from Cygnus X3 and other similar point sources. F.M.R.

N85-34987*# Tuebingen Univ. (West Germany). Astronomisches Inst.
ON THE STATISTICAL SIGNIFICANCE OF EXCESS EVENTS: REMARKS OF CAUTION AND THE NEED FOR A STANDARD METHOD OF CALCULATION
R. Staubert *In* NASA. Goddard Space Flight Center 19th Intern. Cosmic Ray Conf., Vol. 3 Aug. 1985 p 477-480 refs (For primary document see N85-34862 23-93)
(OG-9.5-10) Avail: NTIS HC as boxed set only $200/MF A01 per volume or E99 per entire set CSCL 03B

Methods for calculating the statistical significance of excess events and the interpretation of the formally derived values are discussed. It is argued that a simple formula for a conservative estimate should generally be used in order to provide a common understanding of quoted values. Author

N85-34988*# Council for Scientific and Industrial Research, Pretoria (South Africa). Cosmic Ray Research Unit.
A NEW APPROACH TO EVALUATE GAMMA-RAY MEASUREMENTS
O. C. DeJager, J. W. H. Swanepoel, B. C. Raubenheimer, and D. J. vanderValt *In* NASA. Goddard Space Flight Center 19th Intern. Cosmic Ray Conf., Vol. 3 Aug. 1985 p 481-484 refs (For primary document see N85-34862 23-93)
(OG-9.5-11) Avail: NTIS HC as boxed set only $200/MF A01 per volume or E99 per entire set CSCL 03B

Misunderstandings about the term random samples its implications may easily arise. Conditions under which the phases, obtained from arrival times, do not form a random sample and the dangers involved are discussed. Watson's U sup 2 test for uniformity is recommended for light curves with duty cycles larger than 10%. Under certain conditions, non-parametric density estimation may be used to determine estimates of the true light curve and its parameters. Author

N85-34989*# Adelaide Univ. (Australia). Dept. of Physics.
A NEW STATISTIC FOR THE ANALYSIS OF CIRCULAR DATA IN GAMMA-RAY ASTRONOMY
R. J. Protheroe *In* NASA. Goddard Space Flight Center 19th Intern. Cosmic Ray Conf., Vol. 3 Aug. 1985 p 485-488 refs Sponsored in part by Queen Elizabeth II Fellowship, and Australian Research Grants Scheme (For primary document see N85-34862 23-93)
(OG-9.5-13) Avail: NTIS HC as boxed set only $200/MF A01 per volume or E99 per entire set CSCL 03B

A new statistic is proposed for the analysis of circular data. The statistic is designed specifically for situations where a test of uniformity is required which is powerful against alternatives in which a small fraction of the observations is grouped in a small range of directions, or phases. F.M.R.

N85-34990*# Consiglio Nazionale delle Ricerche, Turin (Italy). Ist. di Comogeofisica.
THE ANGULAR RESOLUTION OF AIR SHOWER GAMMA RAY TELESCOPES
C. Morello, G. Navarra (Turin Univ.), L. Periale, and P. Vallania *In* NASA. Goddard Space Flight Center 19th Intern. Cosmic Ray Conf., Vol. 3 Aug. 1985 p 489-491 refs (For primary document see N85-34862 23-93)
(OG-9.5-14) Avail: NTIS HC as boxed set only $200/MF A01 per volume or E99 per entire set CSCL 03B

A crucial charactristic of air shower arrays in the field of high energy gamma-ray astronomy is their angular resolving power, the arrival directions being obtained by the time of flight measurements. A small air shower array-telescope is used to study the resolution in the definition of the shower front as a function of the shower size. Author

N85-34991*# National Aeronautics and Space Administration. Goddard Space Flight Center, Greenbelt, Md.
NINETEENTH INTERNATIONAL COSMIC RAY CONFERENCE. SH SESSIONS, VOLUME 5
Frank C. Jones, comp. Washington Aug. 1985 589 p refs Conf. held in La Jolla, Calif., 11-23 Aug. 1985 8 Vol.
(NASA-CP-2376-Vol-5; NAS 1.55:2376-Vol-5) Avail: NTIS HC as boxed set only $200/MF A01 per volume or E99 per entire set CSCL 03B

Papers submitted for presentation at the 19th International Cosmic Ray Conference are compiled. This volume contains papers addressing cosmic ray gradients in the heliosphere; siderial, diurnal,

and long term modulations; geomagnetic and atmospheric effects; cosmogenic nuclides; solar neutrinos; and detection techniques. For individual titles, see N85-34992 through N85-35140.

N85-34992*# Jet Propulsion Lab., California Inst. of Tech., Pasadena.
GRADIENTS AND ANISOTROPIES OF HIGH ENERGY COSMIC RAYS IN THE OUTER HELIOSPHERE
Walker Fillius (California Univ., San Diego, La Jolla), E. C. Roelof (Johns Hopkins Univ., Laurel, Md.), Edward J. Smith, David Wood (California Univ., San Diego, La Jolla), and Wing-Huen Ip (Max-Planck Inst. fuer Aeronomie) *In* NASA. Goddard Space Flight Center 19th Intern. Cosmic Ray Conf., Vol. 5 Aug. 1985 p 1-4 refs (For primary document see N85-34991 23-93)
(Contract NAS2-153; Grant NGL-05-005-007; Contract N00024-85-C-5301)
(SH-4.3-7) Avail: NTIS HC as boxed set only $200/MF A01 per volume or E99 per entire set CSCL 03B

Previous studies at lower energies have shown that the cosmic ray density gradients vary in space and time, and many authors currently are suggesting that the radial gradient associated with solar cycle modulation is supported largely by narrow barriers which encircle the Sun and propagate outward with the solar wind. If so, the anisotropy is a desirable way to detect spatial gradients, because it can be associated with the local solar wind and magnetic field conditions. With this in mind, the anisotropy measurements made by the UCSD Cerenkov detectors on Pioneers 10 and 11 are studied. It is shown that the local anisotropy varies greatly, but that the long term average is consistent with the global radial gradient measured between two spacecraft over a baseline of many AU. R.J.F.

N85-34993*# Tasmania Univ., Hobart (Australia). Antarctic Div.
ISOTROPIC INTENSITY WAVES AND FEATURES OF THEIR OCCURRENCE
M. L. Duldig, R. M. Jacklyn, and M. A. Pomerantz (Delaware Univ., Newark) *In* NASA. Goddard Space Flight Center 19th Intern. Cosmic Ray Conf., Vol. 5 Aug. 1985 p 5-8 refs (For primary document see N85-34991 23-93)
(SH-4.3-8) Avail: NTIS HC as boxed set only $200/MF A01 per volume or E99 per entire set CSCL 03B

Waves of daily average cosmic ray intensity, dependent on interplanetary magnetic fields (IMF) polarity, have been observed in 1982 (Jacklyn and Pomerantz, 1983) and again in 1983 and 1984. These waves at first appeared to be due to the North-South anisotropy. Further investigation revealed that the waves comprise two components, a large isotropic and a smaller anisotropic component. The anisotropic part is attributed to the North-South anisotropy and is in phase with the larger isotropic component in the Southern Hemisphere. Unlike the North-South anisotropy which is a permanent feature of cosmic ray modulation, the isotropic phenomenon appears to be episodic in character. When present, it is clearly dependent on IMF polarity but does not correlate well with IMF field strength. It is conjectured that the phenomenon might indicate some difference between the intensity regimes above and below the neutral sheet. Author

N85-34994*# Nagoya Univ. (Japan). Cosmic Ray Research Lab.
IMF-SENSE-DEPENDENT COSMIC RAY ANISOTROPY PRODUCED FROM DIFFUSION-CONVECTION IN HELIOSPHERE
K. Nagashima, K. Munakata, and R. Tatsuoka *In* NASA. Goddard Space Flight Center 19th Intern. Cosmic Ray Conf., Vol. 5 Aug. 1985 p 9-12 refs (For primary document see N85-34991 23-93)
(SH-4.3-9) Avail: NTIS HC as boxed set only $200/MF A01 per volume or E99 per entire set CSCL 03B

It was demonstrated that an interplanetary magnetic field (IMF) sense dependent 2nd order anisotropy is produced by the diffusion convection of cosmic rays in the heliomagnetosphere. The result implies that the anisotropy cannot be expressed only by the pitch angle with respect to the IMF axis. R.J.F.

N85-34995*# Chubu Univ., Kasugai (Japan). College of Engineering.
INFLUENCE OF THE NEUTRAL SHEET ON THE SWINSON'S TYPE NORTH-SOUTH ANISOTROPY OF COSMIC RAYS
Y. Munakata, S. Shibata (Nagoya Univ.), and K. Hakamada *In* NASA. Goddard Space Flight Center 19th Intern. Cosmic Ray Conf., Vol. 5 Aug. 1985 p 13-14 (For primary document see N85-34991 23-93)
(SH-4.3-10) Avail: NTIS HC as boxed set only $200/MF A01 per volume or E99 per entire set CSCL 03B

The relations between the north-south anisotropy of cosmic rays and/or nucleonic intensity variation and the latitudinal angular distance (lambda) of the Earth from the neutral sheet is examined using the data in the period from Apr. 1976 to Aug. 1977 at the solar minimum. It is found that the nucleonic intensity variation of the cosmic rays has no correlation with sin lambda in this period as shown in a correlation diagram; but the amplitude of the north-south anisotropy is fairly correlated with sin lambda as shown in another diagram. Author

N85-34996*# Iwate Univ., Morioka (Japan). Dept. of Physics.
CHARACTERISTICS OF COSMIC RAY POLE-EQUATOR ANISOTROPY DERIVED FROM SPHERICAL HARMONIC ANALYSIS OF NEUTRON MONITOR DATA
H. Takahashi and N. Yahagi *In* NASA. Goddard Space Flight Center 19th Intern. Cosmic Ray Conf., Vol. 5 Aug. 1985 p 15-18 (For primary document see N85-34991 23-93)
(SH-4.3-12) Avail: NTIS HC as boxed set only $200/MF A01 per volume or E99 per entire set CSCL 03B

The spherical harmonic analysis of cosmic ray neutron data from the worldwide network neutron monitor stations during the years, 1966 to 1969 was carried out. The second zonal harmonic component obtained from the analysis corresponds to the Pole-Equator anisotropy of the cosmic ray neutron intensity. Such an anisotropy makes a semiannual variation. In addition to this, it is shown that the Pole-Equator anisotropy makes a variation depending on the interplanetary magnetic field (IMF) sector polarities around the passages of the IMF sector boundary. A mechanism to interpret these results is also discussed. Author

N85-34997*# Iwate Univ., Morioka (Japan). Dept. of Physics.
FIRST ZONAL HARMONIC COMPONENT OF COSMIC RAY NEUTRON INTENSITY
H. Takahashi, N. Yahagi, and T. Chiba *In* NASA. Goddard Space Flight Center 19th Intern. Cosmic Ray Conf., Vol. 5 Aug. 1985 p 19-22 refs (For primary document see N85-34991 23-93)
(SH-4.3-13) Avail: NTIS HC as boxed set only $200/MF A01 per volume or E99 per entire set CSCL 03B

Cosmic ray neutron data from the cosmic ray stations from the worldwide network in 1966, 1967 and 1969 are analyzed by means of the three dimensional analysis method by Nagashima. The variations of the north-south anisotropy, which is the first zonal harmonic component obtained from the analysis are studied. The result obtained confirms earlier findings. Relationship of the anisotropy to the interplanetary magnetic field sector polarity is also studied. Author

N85-34998*# Awadhesh Pratap Singh Univ., Rewa (India). Physics Dept.
COSMIC RAY INTENSITY DISTRIBUTION PERPENDICULAR TO SOLAR EQUATORIAL PLANE AT 1 A.U. DURING 1978-83
S. P. Pathak, S. P. Agrawal, P. K. Shrivastava, and R. S. Yadav (Aligarh Muslim Univ.) *In* NASA. Goddard Space Flight Center 19th Intern. Cosmic Ray Conf., Vol. 5 Aug. 1985 p 23-26 refs (For primary document see N85-34991 23-93)
(SH-4.3-14) Avail: NTIS HC as boxed set only $200/MF A01 per volume or E99 per entire set CSCL 03B

The distribution of cosmic ray intensity perpendicular to solar equatorial plane, was investigated by using its yearly variation with respect to the heliolatitudinal position of the Earth, for the two intervals 1978 to 1980 and 1981 to 1983. The monthly mean values of two high latitude stations along with the solar and geomagnetic indices are used to derive the cosmic ray intensity

distribution free from the changes due to variation in solar activity. The correction is found to be significant only during the interval 1976 to 1980. The results indicate a significant linear increase in cosmic ray intensity from north to south of solar equator, contrary to that observed during 1973 to 1975. No symmetrical gradients are found during the period of study, in agreement with earlier results. Author

N85-34999*# Academia Sinica, Beijing (China). Inst. of Space Physics.
THE COROTATING VARIATION OF THE NORTH-SOUTH ANISOTROPY OF COSMIC RAYS
Shunsheng Xue, Gongliang Zhang, and Shaoyu Xao *In* NASA. Goddard Space Flight Center 19th Intern. Cosmic Ray Conf., Vol. 5 Aug. 1985 p 27-30 refs (For primary document see N85-34991 23-93)
(SH-4.3-15) Avail: NTIS HC as boxed set only $200/MF A01 per volume or E99 per entire set CSCL 03B

Correlation analysis on the relation of the north-south (N-S) anisotropy of cosmic rays, observed by the Nagoya multidirectional meson telescope, with the interplanetary magnetic field (IMP) as well the solar wind velocity within solar Carrington rotation for the period 1971 to 1976 is discussed. It is found that the N-S anisotropy of cosmic rays correlates quite well with the Bx component of the IMF. The correlation coefficient is nearly equal to 0.8. Author

N85-35000*# Fukushima Univ. (Japan). Dept. of Physics.
COSMIC RAY SIDEREAL DIURNAL VARIATION OF GALACTIC ORIGIN OBSERVED BY NEUTRON MONITORS
Y. Ishida, K. Nagashima (Nagoya Univ.), S. Mori (Shinshu Univ.), and I. Morishita (Gifu College of Dentistry) *In* NASA. Goddard Space Flight Center 19th Intern. Cosmic Ray Conf., Vol. 5 Aug. 1985 p 31-34 refs (For primary document see N85-34991 23-93)
(SH-4.4-2) Avail: NTIS HC as boxed set only $200/MF A01 per volume or E99 per entire set CSCL 03B

Cosmic ray sidereal diurnal variations observed by neutron monitors are analyzed for the period 1961 to 1978, by adding 134 station years data to the previous paper (Nagashima, et al., 1983). Also the dependence of the sidereal variations on Sun's polar magnetic field polarity is examined for two periods; the period of negative polarity in the northern region, 1961 to 1969 and the period of positive polarity, 1970 to 1978. It is obtained that for the former period, the amplitude A=0.0203 + or 0.0020% and the phase phi=6.1 + or - 0.4 h LST and for the latter period, 0.0020% and phi=8.6 + or - 4 h LST, respectively. Author

N85-35001*# Nagoya Univ. (Japan). Cosmic Ray Research Lab.
SIDEREAL ANISOTROPIES IN THE MEDIAN RIGIDITY RANGE 60-600GV IN 1978-1983
H. Ueno, Z. Fujii (Shinshu Univ.), S. Mori (Shinshu Univ.), S. Yasue, and K. Nagashima *In* NASA. Goddard Space Flight Center 19th Intern. Cosmic Ray Conf., Vol. 5 Aug. 1985 p 35-38 refs (For primary document see N85-34991 23-93)
(SH-4.4-3) Avail: NTIS HC as boxed set only $200/MF A01 per volume or E99 per entire set CSCL 03B

Observed sidereal variations are corrected for the influence of spurious variation by a method using the antisidereal diurnal variations produced from the same 2nd order anisotropy (Nagashima, et al., 1983). It is demonstrated that the corrected variations are a resultant product of two constituents of galactic origin: one is north-south (N-S) symmetric and the other is N-S asymmetric. R.J.F.

N85-35002*# Tasmania Univ., Hobart (Australia). Physics Dept.
SIDEREAL VARIATIONS DEEP UNDERGROUND IN TASMANIA
J. E. Humble, A. G. Fenton, and K. B. Fenton *In* NASA. Goddard Space Flight Center 19th Intern. Cosmic Ray Conf., Vol. 5 Aug. 1985 p 39-41 refs Sponsored in part by Australian Research Grants Scheme (For primary document see N85-34991 23-93)
(SH-4.4-4) Avail: NTIS HC as boxed set only $200/MF A01 per volume or E99 per entire set CSCL 03B

Data from the deep underground vertically directed muon telescopes at Poatina, Tasmania, have been used since 1972 for a number of investigations, including the daily intensity variations, atmospheric influences, and checking for possible effects due to the interplanetary magnetic field. These telescopes have a total sensitive area of only 3 square meters, with the result that the counting rate is low (about 1680 events per hour) and the statistical errors on the results are rather large. Consequently, it was decided several years ago to construct larger detectors for this station. The first of these telescopes has been in operation for two complete years, and the results from it are presented. Results from the new, more stable equipment at Poatina appear to confirm the existence of a first harmonic in the daily variations in sidereal time reported earlier, and are consistent with small or non-existent first harmonics in solar and anti-sidereal time. All the second harmonics appear to be small, if not zero at these energies. R.J.F.

N85-35003*# Tasmania Univ., Hobart (Australia). Physics Dept.
THE EFFECT OF THE INTERPLANETARY MAGNETIC FIELD ON SIDEREAL VARIATIONS OBSERVED AT MEDIUM DEPTH UNDERGROUND DETECTORS
J. E. Humble and A. G. Fenton *In* NASA. Goddard Space Flight Center 19th Intern. Cosmic Ray Conf., Vol. 5 Aug. 1985 p 42-43 refs Sponsored in part by Australian Research Grants Scheme (For primary document see N85-34991 23-93)
(SH-4.4-5) Avail: NTIS HC as boxed set only $200/MF A01 per volume or E99 per entire set CSCL 03B

It has been known for some years that the intensity variations in sidereal time observed by muon detectors at moderate underground depths are sensitive to the polarity of the interplanetary magnetic field (ipmf) near the Earth. There are differences in the response to these anisotropies as observed in the Northern and Southern Hemispheres. When fully understood, the nature of the anisotropy seems likely to provide information on the 3-dimensional structure of the heliomagnetosphere, its time variations, and its linking with the local interstellar field. The summation harmonic dials for the sidereal diurnal variation during 1958 to 1982 show that there is a strong dependence on whether the ipmf near the Earth is directed outwards from the Sun or inwards it. R.J.F.

N85-35004*# Tasmania Univ., Hobart (Australia). Dept. of Science.
THE SIDEREAL SEMI-DIURNAL VARIATION OBSERVED AT HIGH ZENITH ANGLES AT MAWSON, 1968-1984, AND THE POLARITY OF THE SOLAR MAIN FIELD
R. M. Jacklyn and M. L. Duldig *In* NASA. Goddard Space Flight Center 19th Intern. Cosmic Ray Conf., Vol. 5 Aug. 1985 p 44-47 refs (For primary document see N85-34991 23-93)
(SH-4.4-6) Avail: NTIS HC as boxed set only $200/MF A01 per volume or E99 per entire set CSCL 03B

High zenith-angle North/South telescopes viewing equatorially and at midlatitudes through 40 MWE of atmosphere have been operating at Mawson since early 1968. It is evident that a sidereal semi-diurnal component of galactic origin has been observed, over and above a possible spurious component proposed by Nagashima, arising from a bi-directional component of the solar anisotropy. Although a very pronounced reduction in the semi-diurnal galactic response followed the reversal of polarity of the solar main field during 1969 to 1971, so far the observations indicate that there has been no recurrence of a larger galactic response following the reversal of polarity around 1981. The possible role of the latitudinal extent lambda omicron of the wavy neutral sheet is discussed. Author

N85-35005*# New Mexico Univ., Albuquerque. Dept. of Physics and Astronomy.
CORRECTED SIDEREAL ANISOTROPY FOR UNDERGROUND MOONS
D. B. Swinson and K. Nagashima (Nagoya Univ.) *In* NASA. Goddard Space Flight Center 19th Intern. Cosmic Ray Conf., Vol. 5 Aug. 1985 p 48-51 refs (For primary document see N85-34991 23-93)
(Grant NSF ATM-83-05098)

(SH-4.4-7) Avail: NTIS HC as boxed set only $200/MF A01 per volume or E99 per entire set CSCL 03B

Data from underground muon telescopes in New Mexico and Bolivia are analyzed in sidereal time and anti-sidereal time in the rigidity range 20 GV to a few 100's of GV. Using both vertical and north- and south-pointing telescopes in both hemispheres, a latitude range of 70 N to 50 S is covered. It is shown that there is an anti-sidereal variation of the P 1 over 2 type, having opposite phase in the Northern and Southern Hemispheres, and maximum amplitude at mid latitudes. The anti-sidereal data are used to correct the sidereal data, using the Nagashima method (Nagashima, 1984); the resulting corrected sidereal vectors for Northern Hemisphere telescopes have their sidereal maxima close to 3h sidereal time, in reasonable agreement with sidereal data at higher energies from small air showers. The Nagashima correction also eliminates effects due to the reversal of the Sun's polar magnetic field which show up in the uncorrected sidereal data. Author

N85-35006*# Yakutsk State Univ. (USSR).
SIDEREAL ANISOTROPY OF COSMIC RAYS
A. I. Kuzmin, P. A. Krivoshapkin, G. V. Skripin, and G. V. Shafer *In* NASA. Goddard Space Flight Center 19th Intern. Cosmic Ray Conf., Vol. 5 Aug. 1985 p 52-55 refs (For primary document see N85-34991 23-93)
(SH-4.4-8) Avail: NTIS HC as boxed set only $200/MF A01 per volume or E99 per entire set CSCL 03B

The data of the ionization chamber in Yakutsk for 1954 to 1984 are analyzed. A false sidereal variation caused by the second spherical harmonic in cosmic ray distribution was found and it has the amplitude 0.020 plus or minus 0.002%. The sidereal anisotropy with a very small amplitude (not more than 0.005%) was observed to exist. Author

N85-35007*# Shinshu Univ., Matsumoto (Japan). Dept. of Physics.
COSMIC RAY INTENSITY VARIATIONS OBSERVED AT MATSUSHIRO (220 M.W.E. IN DEPTH)
S. Yasue, S. Mori, and S. Sagisaka *In* NASA. Goddard Space Flight Center 19th Intern. Cosmic Ray Conf., Vol. 5 Aug. 1985 p 56-59 refs (For primary document see N85-34991 23-93)
(SH-4.4-9) Avail: NTIS HC as boxed set only $200/MF A01 per volume or E99 per entire set CSCL 03B

Cosmic ray data from Matsushiro underground station were analyzed for four years (1981 to 84). It is found that a marked semi-annual intensity variation has been observed in this period. Solar diurnal and semi-diurnal variations have also been observed. After correcting for the spurious sidereal diurnal variation arising from the anisotropy responsible for the solar semi-diurnal variation (Nagashima et al., 1983), it is found that the corrected sidereal diurnal variation is consistent with those so far reported. Author

N85-35008*# Tasmania Univ., Hobart (Australia). Physics Dept.
LONG-TERM MODULATION OF COSMIC RAYS DURING SOLAR CYCLE 21
A. G. Fenton, K. B. Fenton, and J. E. Humble *In* NASA. Goddard Space Flight Center 19th Intern. Cosmic Ray Conf., Vol. 5 Aug. 1985 p 60-62 refs (For primary document see N85-34991 23-93)
(SH-4.4-10) Avail: NTIS HC as boxed set only $200/MF A01 per volume or E99 per entire set CSCL 03B

A preliminary result concerning the rigidity dependence of the longer-term solar cycle modulation is reported. The long-term modulation, using monthly mean intensities and referred to November 1977 as a normalizing level, appear to be in accordance with the exponent gamma = 1, provided only Brisbane and Hobart data are used. Darwin data do not conform to this pattern except perhaps during the early years of the cycle until about the end of 1980, since when the Darwin long-term intensity has been largely steady, apart from Forbush-type decreases and the as yet unidentified vector from the observed SI vector. The true SI vector of galactic origin can be obtained. The resultant vector has the amplitude of 0.031% and the phase of 2.3h. The present result seems to be consistent with those so far reported. R.J.F.

N85-35009*# Awadhesh Pratap Singh Univ., Rewa (India). Space Physics Centre.
ROLE OF SOLAR FLARE INDEX IN LONG TERM MODULATION OF COSMIC RAY INTENSITY
P. K. Pandey, A. K. Jain, P. K. Shrivastava, S. P. Pathak, and S. P. Agrawal *In* NASA. Goddard Space Flight Center 19th Intern. Cosmic Ray Conf., Vol. 5 Aug. 1985 p 63-66 refs (For primary document see N85-34991 23-93)
(SH-4.4-12) Avail: NTIS HC as boxed set only $200/MF A01 per volume or E99 per entire set CSCL 03B

Recently, the importance of the occurrence of solar flares in the long-term modulation of cosmic ray intensity has been re-emphasized. For this purpose, the data of solar flares have been used from various publications, such as Solar Geophysical Data books, U.A.G. reports and Quarterly Bulletin Of Solar Activity. Research very clearly reveals that even the periodic changes in the solar flare observations, obtained from the four different data sources, for the same interval, differ significantly from one another; this is evidenced even on an average basis. Hence, in any study using solar flares, the importance of selecting a single compilation of the solar-flare data for the entire period of investigation is stressed. Author

N85-35010*# Consiglio Nazionale delle Ricerche, Bologna (Italy).
A STUDY OF PERIODICITIES AND RECURRENCES IN SOLAR ACTIVITY AND COSMIC RAY MODULATION c92
M. R. Attolini, S. Cecchini, and M. Galli (Bologna Univ.) *In* NASA. Goddard Space Flight Center 19th Intern. Cosmic Ray Conf., Vol. 5 Aug. 1985 p 67-70 refs (For primary document see N85-34991 23-93)
(SH-4.4-14) Avail: NTIS HC as boxed set only $200/MF A01 per volume or E99 per entire set CSCL 03B

The 154d periodicity was found in the cosmic ray intensity (RE) vs Flares, and some other peaks of coherency in the RC vs aa sub I, that when interpreted as aliased values, might correspond to recurring interplanetary magnetic field structures and solar wind streams. It cannot be excluded, however, that some of the correspondence with aa are of terrestrial origin. This study cannot be considered exhaustive due to the fact that other solar variables, such as polar hole size, are possibly correlated to cosmic ray intensities. However, the number of observations is small so that the interpretation of the results is very difficult. R.J.F.

N85-35011*# Consiglio Nazionale delle Ricerche, Bologna (Italy).
COSMIC RAY BIANNUAL VARIATION Abstract Only
M. R. Attolini, S. Cecchini, G. CiniCastagnoli (Turin Univ.), and M. Galli (Bologna Univ.) *In* NASA. Goddard Space Flight Center 19th Intern. Cosmic Ray Conf., Vol. 5 Aug. 1985 p 71 (For primary document see N85-34991 23-93)
(SH-4.4-15) Avail: NTIS HC as boxed set only $200/MF A01 per volume or E99 per entire set CSCL 03B

The study of the cosmic ray (CR) power spectrum has revealed a significant variation with a period around 2 yr that cannot be explained as a high order harmonic of the 11 yr solar cycle. Comparative study of the correlation on different time scales between CR intensity and Rz, aa, high speed streams and polar hole size has put in evidence that a high degree of coherency exists between each couple of variables at 1.58 to 1.64 yr, except between CR and Rz. On the other hand cyclic variation on a short time scale, around 26 months, has been claimed to be present in the neutrino flux. Critical tests of this hypothesis are considered and a preliminary result seems to indicate that the hypothesis of the existence of a 1.6 yr periodicity in the neutrino data during the measurement time interval, has a significance > or = 99.9%. The possible origin of this variation as due to a contribution either of CR interactions in the upper atmosphere or to the solar dynamics, are discussed. Author.

N85-35012*# Awadhesh Pratap Singh Univ., Rewa (India). Space Physics Centre.
COSMIC RAY POWER SPECTRAL VARIATIONS. 3: SOLAR ROTATION PERIODICITIES
S. P. Agrawal *In* NASA. Goddard Space Flight Center 19th

Intern. Cosmic Ray Conf., Vol. 5 Aug. 1985 p 72-74 refs (For primary document see N85-34991 23-93)
(SH-4.4-16) Avail: NTIS HC as boxed set only $200/MF A01 per volume or E99 per entire set CSCL 03B

Earlier studies of the periodic changes in cosmic ray intensity by power spectral analysis provided some understanding of the daily variation in terms of ambient power. The solar rotation periodicities are investigated, using daily means of calgary neutron monitor data during 1965 to 1976. Significant peaks with periods of 27 and 13.5 days with varying magnitudes are observed. Author

N85-35013*# Moscow State Univ. (USSR). Inst. of Nuclear Physics.
VARIATIONS OF THE COSMIC RAY GENERAL COMPONENT IN ANTARCTICA
T. N. Charakhchyan, A. F. Krasotkin, A. I. Kurguzova, and N. S. Svirzhevsky (Academy of Sciences, USSR, Moscow) *In* NASA. Goddard Space Flight Center 19th Intern. Cosmic Ray Conf., Vol. 5 Aug. 1985 p 75-78 refs (For primary document see N85-34991 23-93)
(SH-4.4-17) Avail: NTIS HC as boxed set only $200/MF A01 per volume or E99 per entire set CSCL 03B

A cosmic ray variations, zonal cosmic ray modulation, was found in the lower atmosphere from the sonde measurement results. The variations give rise to anomalies in the latitude distributions of the cosmic ray charged component and the anomalous north-south asymmetry. To find the nature of the variations, the cosmic ray general component was measured with the same detectors as in the sonde measurements gas discharge counters and the counter telescopes with 7-mm Al filters detecting the electrons of energy above 200 keV and 5 MeV. The measurement data obtained in Antarctica in the years 1978 to 1983 are presented and discussed. Author

N85-35014*# Academy of Sciences (USSR), Moscow.
THE DIFFERENCE IN THE ENERGY SPECTRA OF GALACTIC COSMIC RAYS AT THE MINIMA OF THE 19TH AND 20TH SOLAR ACTIVITY CYCLES **c92**
A. K. Svirzhevskaya, N. S. Svirzhevsky, Yu. I. Stozhkov, and T. N. Charakhchyan (Moscow State Univ.) *In* NASA. Goddard Space Flight Center 19th Intern. Cosmic Ray Conf., Vol. 5 Aug. 1985 p 79-82 refs (For primary document see N85-34991 23-93)
(SH-4.4-18) Avail: NTIS HC as boxed set only $200/MF A01 per volume or E99 per entire set CSCL 03B

The absorption curves of the cosmic ray charged component for solar minima in 1965 and 1975 to 1977 are analyzed on the basis of daily stratospheric measurements in Murmansk, Moscow, Alma-Ata and Mirny (Antarctic). Two distinct features in the energy spectra of galactic cosmic rays are revealed during these periods. At the 20th solar activity minimum there was the additional short range component of cosmic rays. Additional fluxes in the stratosphere at high latitudes caused by this component are probably protons and He nuclei with the energy 100 to 500 MeV/n. The fluxes are estimates as Approx. 300 sq m/s/sr. At the minimum in 1975 to 1977 the proton intensity in the energy range 1 to 15 GeV is 10 to 15% lower than that in the 1965 solar activity minimum. Author

N85-35015*# Academy of Sciences (USSR), Moscow. Physical Inst.
COSMIC RAY VARIATIONS WITH THE PERIOD CLOSE TO 27 DAYS AND THEIR CONNECTION WITH SOLAR ACTIVITY LONGITUDINAL DISTRIBUTION **c92**
G. A. Bazilevskaya, M. I. Tyasto (Academy of Sciences, USSR, Leningrad), and E. S. Vernova (Academy of Sciences, USSR, Leningrad) *In* NASA. Goddard Space Flight Center 19th Intern. Cosmic Ray Conf., Vol. 5 Aug. 1985 p 83-86 refs (For primary document see N85-34991 23-93)
(SH-4.4-19) Avail: NTIS HC as boxed set only $200/MF A01 per volume or E99 per entire set CSCL 03B

The amplitude and phase changes of the 27 day cosmic ray variation from 1958 to 1975 are studied. The comparison between cosmic ray intensity characteristics and longitudinal distribution of solar activity ones for different stages of the solar cycle are made. Author

N85-35016*# Academy of Sciences of the Georgian SSR, Tbilisi (USSR). Inst. of Geophysics.
AZIMUTHAL AND MERIDIONAL ASYMMETRIES OF THE SOLAR WIND AND QUASIPERIODIC VARIATIONS OF INTENSITY OF GALACTIC COSMIC RAYS (GCR) **c92**
L. Kh. Shatashvili, T. V. Djapiashvili, B. G. Kavlashvili, B. D. Naskidashvili, O. G. Rogava, and G. V. Shafer *In* NASA. Goddard Space Flight Center 19th Intern. Cosmic Ray Conf., Vol. 5 Aug. 1985 p 87-89 refs (For primary document see N85-34991 23-93)
(SH-4.4-20) Avail: NTIS HC as boxed set only $200/MF A01 per volume or E99 per entire set CSCL 03B

The results of analysis of 27 day, annual and quasi-two year variation of galactic cosmic rays (GCR) are presented. The dependence of the periods of 27 day GCR variation on the energy of initial radiation is discovered, according to the data during 1980 of the World network of station in sufficiently wide range of the observed threshold energy. The dependence of the annual variation of GCR is established, according to the data of the Huancayo station in conforming with the change of the polarity of the General Magnetic Field of the Sun (GMFS). Author

N85-35017*# Moscow State Univ. (USSR). Inst. of Nuclear Physics.
DYNAMICS OF TWO-YEAR COSMIC RAY VARIATIONS INFERRED FROM THE DATA OF SPACECRAFT AND STRATOSPHERIC MEASUREMENTS AND FROM THE NEUTRON MONITOR DATA IN 1959-1981
T. N. Charakhchyan, E. V. Gorchakov, V. P. Okhlopkov, L. S. Okhlopkova, and M. V. Ternovskaya *In* NASA. Goddard Space Flight Center 19th Intern. Cosmic Ray Conf., Vol. 5 Aug. 1985 p 90-93 refs (For primary document see N85-34991 23-93)
(SH-4.4-21) Avail: NTIS HC as boxed set only $200/MF A01 per volume or E99 per entire set CSCL 03B

The two year cosmic ray variations are studied using the spacecraft measurements of 1967 to 1976, the sonde measurements at high latitudes in the stratosphere (Murmansk, Mirny), and the neutron monitor data of 1959 to 1981. The two year variations are most pronounced from 1967 to 1975. An anticorrelation is observed between the two year variations in cosmic rays and in geomagnetic activity. Author

N85-35018*# Academy of Sciences (USSR), Yakutsk. Inst. of Cosmophysical Research and Aeronomy.
LONG-TERM MODULATION OF GALACTIC COSMIC RAYS IN HIGH-ENERGY REGION
P. A. Krivoshapkin, A. N. Prikhodko, G. V. Skripin, I. A. Transky, and G. V. Shafer *In* NASA. Goddard Space Flight Center 19th Intern. Cosmic Ray Conf., Vol. 5 Aug. 1985 p 94-97 refs (For primary document see N85-34991 23-93)
(SH-4.4-22) Avail: NTIS HC as boxed set only $200/MF A01 per volume or E99 per entire set CSCL 03B

The results of continuous registration of the cosmic ray muon intensity on the ground and underground at 7, 20 and 60 m w.e. depths in Yakutsk for 1957 to 1983 are presented. In years of the solar activity maximum in cosmic ray density were found two minima or two-stepped decrease. The second intensity minimum appears to be not the result of the inversion of the general magnetic field of the Sun but caused by the increase of the solar wind speed. Author

N85-35019*# Nagoya Univ. (Japan). Dept. of Physics.
THE FIRST THREE HARMONICS OF SOLAR DAILY VARIATION CAUSED BY THE DIFFUSIVE PROPAGATION OF GALACTIC COSMIC RAYS THROUGH THE HELIOSPHERE **c92**
K. Munakata and K. Nagashima *In* NASA. Goddard Space Flight Center 19th Intern. Cosmic Ray Conf., Vol. 5 Aug. 1985 p 98-101 refs (For primary document see N85-34991 23-93)
(SH-4.5-1) Avail: NTIS HC as boxed set only $200/MF A01 per volume or E99 per entire set CSCL 03B

Some results for the first three harmonics derived from the

simulation of diffusion convection of galactic cosmic rays is presented. Also, some dependences of the results to the modulation parameters are presented. The results are discussed in comparison with observations and with the former studies of higher order anisotropy. In addition to this, the existence is suggested of the IMF-sense-dependent anisotropy of higher order. Author

N85-35020*# Nagoya Univ. (Japan). Dept. of Physics.
FORMULATION OF COSMIC-RAY SOLAR DAILY VARIATION AND ITS SEASONAL VARIATION, PRODUCED FROM GENERALIZED STATIONARY ANISOTROPY OF SOLAR ORIGIN c92
R. Tatsuoka and K. Nagashima *In* NASA. Goddard Space Flight Center 19th Intern. Cosmic Ray Conf., Vol. 5 Aug. 1985 p 102-105 refs (For primary document see N85-34991 23-93)
(SH-4.5-2) Avail: NTIS HC as boxed set only $200/MF A01 per volume or E99 per entire set CSCL 03B

In previous papers, a formulation was presented of cosmic ray daily variations produced from solar anisotropies stationary through a year, and also of their annual (or seasonal) modulation caused by the annual variation of the rotation axis of the Earth relative to that of the Sun. These anisotropies are symmetric for an arbitrary rotation around an axis. From observations of the tri-diurnal variation, it has been suggested that solar anisotropies also contain some axis-asymmetric term of the third order with respect to the IMF-axis. This suggestion has recently found support in a theoretical study by Munakata and Nagashima. According to their results, the terms of axis-asymmetry with respect to IMF-axis appear also in the 2nd order anisotropy, together with some different kinds of axis-symmetric terms. The contribution of these anisotropies to the daily variation is different from that of those discussed previously. The above mentioned formulation is extended to a case of a generalized anisotropy. Author

N85-35021*# Shinshu Univ., Matsumoto (Japan). Dept. of Physics.
SOLAR TRI-DIURNAL VARIATION OF COSMIC RAYS IN A WIDE RANGE OF RIGIDITY c92
S. Mori, H. Ueno (Nagoya Univ.), Z. Fujii (Nagoya Univ.), I. Morishita (Asahi Univ.), and K. Nagashima (Nagoya Univ.) *In* NASA. Goddard Space Flight Center 19th Intern. Cosmic Ray Conf., Vol. 5 Aug. 1985 p 106-109 refs (For primary document see N85-34991 23-93)
(SH-4.5-3) Avail: NTIS HC as boxed set only $200/MF A01 per volume or E99 per entire set CSCL 03B

Solar tri-diurnal variations of cosmic rays have been analyzed in a wide range of rigidity, using data from neutron monitors, and the surface and underground muon telescopes for the period 1978-1983. The rigidity spectrum of the anisotropy in space is assumed to be of power-exponential type as (P/gamma P sub o) to the gamma exp (gamma-P/P sub o). By means of the best-fit method between the observed and the expected variations, it is obtained that the spectrum has a peak at P (=gamma P sub o) approx = 90 GV, where gamma=approx 3.0 and P sub o approx. 30 GV. The phase in space of the tri-diurnal variation is also obtained as 7.0 hr (15 hr and 23 hr LT), which is quite different from that of approx. 1 hr. arising from the axisymmetric distribution of cosmic rays with respect to the IMF. Author

N85-35022*# New Mexico Univ., Albuquerque. Dept. of Physics and Astronomy.
UPPER CUT-OFF RIGIDITY FOR COROTATION ANISOTROPY DURING SOLAR ACTIVITY CYCLES 20 AND 21 Abstract Only c92
H. S. Ahluwalia and J. F. Riker (BDM Corp., Albuquerque, N. Mex.) *In* NASA. Goddard Space Flight Center 19th Intern. Cosmic Ray Conf., Vol. 5 Aug. 1985 p 110 (For primary document see N85-34991 23-93)
(SH-4.5-4) Avail: NTIS HC as boxed set only $200/MF A01 per volume or E99 per entire set CSCL 03B

At the Eleventh International Conference on Cosmic Rays in 1969, the results of a study of the solar diurnal variations of solar rays observed during the ascending phase of solar activity cycle twenty was discussed. The diurnal variation, observed underground during 1965-68 period, and results from an extraterrestrial anisotropy having a continuously increasing upper cut-off rigidity R sub c were reported. However, the coupling functions applicable to underground telescopes were controversial then. This situation has improved now. Those results wsere re-examined and extended to cover the period 1965-78. The coupling functions given by Murakami et al. for underground muons and those given by Lockwood and Weber for neutron monitors were used showed that a great deal of care should be exercised in the value of R sub c was calculated. Although numerical values of R sub c are a little different, the trend for 1965-68 period remains unchanged. Highest value of R sub c occur in 1970 and the lowest value occurs in 1976. Author

N85-35023*# Central Research Inst. for Physics, Budapest (Hungary).
TWENTY-TWO-YEAR CYCLE OF THE UPPER LIMITING RIGIDITY OF DALY WAVES
G. Erdos, J. Kota, and E. Merenyi *In* NASA. Goddard Space Flight Center 19th Intern. Cosmic Ray Conf., Vol. 5 Aug. 1985 p 111-114 refs (For primary document see N85-34991 23-93)
(SH-4.5-5) Avail: NTIS HC as boxed set only $200/MF A01 per volume or E99 per entire set CSCL 03B

The method of calculating energy losses along regular particle trajectories is applied to obtain the predicted cosmic ray anisotropies from 200 to 500 GV. The tilt angle of the interplanetary neutral sheet varies to simulate a 22-year cycle magnetic cycle. The calculated values of solar diurnal and semidiurnal, and sidereal diurnal intensity waves are compared with observations. Author

N85-35024*# New Mexico Univ., Albuquerque. Dept. of Physics and Astronomy.
SOLAR WIND VELOCITY AND DAILY VARIATION OF COSMIC RAYS Abstract Only
H. S. Ahluwalia and J. F. Riker (BDM Corp., Albuquerque, N. Mex.) *In* NASA. Goddard Space Flight Center 19th Intern. Cosmic Ray Conf., Vol. 5 Aug. 1985 p 115 (For primary document see N85-34991 23-93)
(SH-4.5-6) Avail: NTIS HC as boxed set only $200/MF A01 per volume or E99 per entire set CSCL 03B

Recently parameters applicable to the solar wind and the interplanetary magnetic field (IMF) have become much better defined. Superior quality of data bases that are now available, particularly for post-1971 period, make it possible to believe the long-term trends in the data. These data are correlated with the secular changes observed in the diurnal variation parameters obtained from neutron monitor data at Deep River and underground muon telescope data at Embudo (30 MEW) and Socorro (82 MWE). The annual mean amplitudes appear to have large values during the epochs of high speed solar wind streams. Results are discussed. Author

N85-35025*# New Mexico Univ., Albuquerque. Dept. of Physics and Astronomy.
DIURNAL ANISOTROPY DURING SOLAR ACTIVITY CYCLE TWENTY AND DIFFUSION-CONVECTION MODEL c92
H. S. Ahluwalia and J. F. Riker (BDM Corp., Albuquerque, N. Mex.) *In* NASA. Goddard Space Flight Center 19th Intern. Cosmic Ray Conf., Vol. 5 Aug. 1985 p 116-119 refs (For primary document see N85-34991 23-93)
(SH-4.5-7) Avail: NTIS HC as boxed set only $200/MF A01 per volume or E99 per entire set CSCL 03B

Underground muon telescope data obtained at Embudo and Neutron monitor data obtained at Deep River are divided into two sets; one covers the ascending phase of the cycle (1965-70) and the other covers the descending phase (1971-76). The amplitude of diurnal anisotropy calculated from the data does not agree with the value predicted by the simplified version of the Diffusion-Convection Model (DCM); the discrepancy is worse for neutron data. Author

N85-35026*# Academy of Sciences of the Armenian SSR, Erivan (USSR).
DIURNAL EFFECT IN COSMIC RAYS AT MIDDLE LATITUDES ACCORDING TO STRATOSPHERIC MEASUREMENTS
G. A. Asatryan, V. Kh. Babayan, and Yu. I. Stozhkov (Academy of Sciences, USSR, Moscow) *In* NASA. Goddard Space Flight Center 19th Intern. Cosmic Ray Conf., Vol. 5 Aug. 1985 p 120-123 refs (For primary document see N85-34991 23-93)
(SH-4.5-8) Avail: NTIS HC as boxed set only $200/MF A01 per volume or E99 per entire set CSCL 03B

Results of measurements of the diurnal wave of the cosmic ray (CR) intensity in stratosphere at the latitude with the geomagnetic cutoff rigidity R sub c = 7.6 GV are presented. Measurements of diurnal variation of the CR intensity were carried by means of radiosondes: by a detector composed of a gas discharge counter CTC-6 and a telescope containing two counters with a 7 mm aluminum filter between them. Author

N85-35027*# Rani Durgavati Univ., Jabalpur (India).
COMPARATIVE STUDY OF THE PHASE OF DIURNAL ANISOTROPY ON QUIET AND DISTURBED DAYS ON A LONG TERM BASIS UP TO RECENT PERIOD Abstract Only
Santosh Kumar *In* NASA. Goddard Space Flight Center 19th Intern. Cosmic Ray Conf., Vol. 5 Aug. 1985 p 124 (For primary document see N85-34991 23-93)
(SH-4.5-9) Avail: NTIS HC as boxed set only $200/MF A01 per volume or E99 per entire set CSCL 03B

The data from the world wide grid of neutron monitoring stations was analyzed for a comparative study of the phase of diurnal anisotropy on quiet and disturbed days on a long term basis up to recent period. It has been observed that the phase of the diurnal anisotropy on disturbed days where the value of the Ap-index is higher, is found to shift towards earlier hours in comparison to the phase of the diurnal anisotropy on quiet days where the value of Ap-index is lower on all the stations from 1965 to 71. Such a trend is not observable for the later period. This affect is found to be more pronounced on equatorial stations, in particular, in comparison to high latitude stations. It was derived from these observational facts that the relationship between Ap-index and the phase of the diurnal anisotropy is not invariant throughout the period of consideration. Furthermore, the exact cause of such a drastic change is not known, but it demonstrates very clearly that the interplanetary conditions which are responsible for both, diurnal anisotropy of cosmic ray intensity and the geomagnetic Ap-index variation, have drastically changed during the period 1971 and onwards. Author

N85-35028*# Rani Durgavati Univ., Jabalpur (India).
STUDY OF SPECTRAL EXPONENT ON QUIET AND DISTURBED DAYS Abstract Only
Santosh Kumar *In* NASA. Goddard Space Flight Center 19th Intern. Cosmic Ray Conf., Vol. 5 Aug. 1985 p 125 (For primary document see N85-34991 23-93)
(SH-4.5-10) Avail: NTIS HC as boxed set only $200/MF A01 per volume or E99 per entire set CSCL 03B

The spectral exponents of the diurnal and semidiurnal anisotropies are studied on quiet and disturbed days for a period from 1964 to 75. It has been observed for the diurnal anisotropy that the spectral exponent for quiet days is 0.0 from 1964 to 70, however during 1971 and onwards its value is found different from zero and is -0.4; for disturbed days the spectral exponent is observed to be 0.0 from 1964 to 75 with an exception of the year 1966. Further, it has been observed for the semi-diurnal anisotropy that the best value for the spectral exponent on quiet days being + 0.6 from 1964 to 74; however on disturbed days the value of spectral exponent is sometimes negative or positive but different from zero. It was derived from the present investigation that superimposed on the corotational anisotropy, expected from a balance between outward radial convection and inward field aligned diffusion, there is an additional component operating during the period under consideration. Author

N85-35029*# Rani Durgavati Univ., Jabalpur (India). Dept. of Postgraduate Studies and Research in Physics.
DIURNAL VARIATION OF GALACTIC COSMIC RAY INTENSITY ON QUIET DAYS
Santosh Kumar and S. C. Datt *In* NASA. Goddard Space Flight Center 19th Intern. Cosmic Ray Conf., Vol. 5 Aug. 1985 p 126-129 refs (For primary document see N85-34991 23-93)
(SH-4.5-11) Avail: NTIS HC as boxed set only $200/MF A01 per volume or E99 per entire set CSCL 03B

A detailed study of the diurnal variation on long term basis was performed on geomagnetically quiet days using the experimental data of the cosmic ray intensity from the worldwide neutron monitoring stations. During the period when the polarity of the solar magnetic field in the Northern Hemisphere of the Sun is negative the phase and amplitude of the diurnal anisotropy on quiet days was observed to remain almost constant. When the polarity of solar magnetic field in the Northern Hemisphere changes from negative to positive, a shift in the phase of the diurnal anisotropy on quiet days towards earlier hours is observed and the shift is found to be maximum during minimum solar activity periods 1953-54 and 1975-76. When the polarity of solar magnetic field changes from positive to negative in the Northern Hemisphere of the Sun the phase of the diurnal anisotropy on quiet days recovers to its usual direction of corotational anisotropy and is observed to remain almost constant till the polarity of the solar magnetic field does not change. Author

N85-35030*# Institute of Physical and Chemical Research, Tokyo (Japan).
DIURNAL VARIATIONS FROM MUON DATA AT TAKEYAMA UNDERGROUND STATION
K. Takahashi, K. Imai, T. Imai, S. Kudo, and M. Wada *In* NASA. Goddard Space Flight Center 19th Intern. Cosmic Ray Conf., Vol. 5 Aug. 1985 p 130-133 refs (For primary document see N85-34991 23-93)
(SH-4.5-13) Avail: NTIS HC as boxed set only $200/MF A01 per volume or E99 per entire set CSCL 03B

An underground station, Takeyama, is introduced, and some results of the solar diurnal and semi-diurnal variations for the period between 1967 and 1984 are presented. There are clear tendencies of double and single solar cycle variations in the daily variations which are in good accord with those detected by other underground and neutron monitor observations. Author

N85-35031*# Chinese Univ. of Hong Kong, Shatin. Dept. of Physics.
LONG TERM CHANGES IN COSMIC RAY DIURNAL VARIATIONS OBSERVED BY ION CHAMBERS IN HONG KONG AND JAPAN
L. S. Chuang, M. Kusunose (Kochi Univ.), and M. Wada (Inst. of Physical and Chemical Research, Tokyo) *In* NASA. Goddard Space Flight Center 19th Intern. Cosmic Ray Conf., Vol. 5 Aug. 1985 p 134-137 refs (For primary document see N85-34991 23-93)
(SH-4.5-14) Avail: NTIS HC as boxed set only $200/MF A01 per volume or E99 per entire set CSCL 03B

Yearly average solar diurnal variations of cosmic ray ion chamber data are inspected from a view point of the eleven and the 22 year solar activity cycle modulations. Ion chamber data and neutron data from various stations are added. From an inspection of observed data, a simple approximation that the 11 year and the 22 year variations of the solar diurnal variation are along 18-hour and 12-hour axes, respectively is proposed. The 18-hour component of diurnal variation in the 11 year cycle increases toward the solar active years. The 12-hour component is enhanced when the solar general magnetic field is parallel to the rotation vector, and is almost zero for the other state. The transition occurs when the amplitude of the 18-hour component is greater owing to the transition of the field during the maximum phase of solar activity. The 22 year shift is consistent with the drift modulation model in heliosphere. Author

N85-35032*# Agriculture-Teacher Univ., Siedlce (Poland). Physics and Biophysics Dept.
THE MODULATION FEATURES OF THE LONG-PERIOD COSMIC RAY VARIATIONS IN CONNECTION WITH THE SIGN CHANGE OF THE GENERAL MAGNETIC FIELD OF THE SUN Abstract Only
K. Iskra *In* NASA. Goddard Space Flight Center 19th Intern. Cosmic Ray Conf., Vol. 5 Aug. 1985 p 138 (For primary document see N85-34991 23-93)
(SH-4.5-15) Avail: NTIS HC as boxed set only $200/MF A01 per volume or E99 per entire set CSCL 03B

On the basis of the model and experimental investigations, the spatial distribution of cosmic ray anisotropy for the different epochs of solar activity is studied. A solution is offered to the anisotropic diffusion equation with regard to the electromagnetic conditions for the periods of minimum and maximum solar activity and cosmic ray particle drift in a regular interplanetary magnetic field. It is shown that the long period changes amplitude and phase of the diurnal variations of cosmic rays is limited not only by convection and diffusion of particles but also by the drift effect before and after the sing change of the general magnetic field of the Sun. The calculated model is compared with the results obtained on the basis of an analysis of the experimental data from the neutron super monitor station, and it is shown that for the periods when the lines of magnetic force of the Sun come from the Northern Hemisphere the phase of the first harmonic diurnal variation is shifted forwards to an earlier time. Author

N85-35033*# Bulgarian Academy of Science, Sofia. Inst. for Nuclear Research and Nuclear Energy.
THE COSMIC RAY DIFFERENTIAL DIURNAL VARIATION DEPENDENCES ON THE ZENITH ANGLE AND THE GEOMAGNETIC DISTURBANCE
S. Kavlakov and L. Georgiev *In* NASA. Goddard Space Flight Center 19th Intern. Cosmic Ray Conf., Vol. 5 Aug. 1985 p 139-142 refs (For primary document see N85-34991 23-93)
(SH-4.5-16) Avail: NTIS HC as boxed set only $200/MF A01 per volume or E99 per entire set CSCL 03B

Simultaneous and continuous muon measurements in two opposite azimuthal directions under equal zenith angles demonstrated the importance of this method for cosmic ray diurnal variation investigations. Lately these measurements were extended by means of improved telescopes. The obtained cosmic ray diurnal variations were presented as intensity differential curves. Theoretical investigations connected the properties of these curves with some interplanetary spece parameters. The harmonics of these curves were interpreted physically. Some order difference curves were introduced. In earlier works some dependences between the parameters characterizing the first and the second harmonics of the differential intensity curves and the geomagnetic activity were found. Then all measurements were carried out under only one zenith angle. The results of investigations of similar dependences using data of simultaneous measurements under three different zenith angles are presented. Author

N85-35034*# Aligarh Muslim Univ. (India). Space Science Group.
COSMIC RAY DENSITY GRADIENT AND ITS DEPENDENCE ON THE NORTH-SOUTH ASYMMETRY IN SOLAR ACTIVITY
Badruddin, R. S. Yadav, and N. R. Yadav *In* NASA. Goddard Space Flight Center 19th Intern. Cosmic Ray Conf., Vol. 5 Aug. 1985 p 143-146 refs (For primary document see N85-34991 23-93)
(SH-4.5-17) Avail: NTIS HC as boxed set only $200/MF A01 per volume or E99 per entire set CSCL 03B

An analysis of the diurnal anisotropy on geomagnetically quiet days was performed using neutron monitor data at Deep River, Leeds, Rome and Tokyo, well distributed in latitude and longitude for the period 1964-79. The days were separated according to the polarity of IMF on that day. A significant difference in the amplitude and phase was found on towards and away polarity days, particularly during the years of high solar activity and large north-south asymmetry. These results (particularly time of maximum) on geomagnetically quiet days show some better relationship to the expected results as compared to the results obtained using all the days in a year. Author

N85-35035*# Nagoya Univ. (Japan). Cosmic Ray Lab.
ANOMALOUS INCREASE OF SOLAR ANISOTROPY ABOVE 150GV IN 1981-1983 **c92**
H. Ueno, Z. Fujii (Shinshu Univ.), S. Mori (Gifu College of Dentistry), I. Morishita, and K. Nagashima *In* NASA. Goddard Space Flight Center 19th Intern. Cosmic Ray Conf., Vol. 5 Aug. 1985 p 147-150 refs (For primary document see N85-34991 23-93)
(SH-4.5-18) Avail: NTIS HC as boxed set only $200/MF A01 per volume or E99 per entire set CSCL 03B

An analysis was carried out of the observed data with Nagoya (surface). Misato (34mwe) and Sakashita (80mwe) multidirectional muon telescope, for the solar activity maximum period of 1978-1983. These data respond to primaries extending over the median rigidity range 60GV to 600GV. The observed amplitude at Sakashita station in 1981-1983 increased, especially in 1982; the amplitude is twice as large as that in 1978-1980, when those at Nagoya and Misato stations are nearly the same as those in 1978-1980. Uni-directional anisotropy is derived by the best fit method by assuming the flat rigidity spectrum with the upper cutoff rigidity Pu. The value of Pu obtained is 270GV in 1981-1983 and 150GV in 1978-1980. Author

N85-35036*# Academy of Sciences (USSR), Irkutsk. Inst. of Terrestrial Magnetism, Ionosphere and Radio Wave Propagation.
DIAGNOSTIC OF ELECTROMAGNETIC CONDITIONS IN SPACE USING COSMIC RAYS **c92**
V. M. Dvornikov, V. E. Sdobnov, and A. V. Sergeev *In* NASA. Goddard Space Flight Center 19th Intern. Cosmic Ray Conf., Vol. 5 Aug. 1985 p 151-154 refs (For primary document see N85-34991 23-93)
(SH-4.5-19) Avail: NTIS HC as boxed set only $200/MF A01 per volume or E99 per entire set CSCL 03B

The method of spectrographic global survey was used to study the time variations in parameters of cosmic ray (CR) pitch angle anisotropy and their relationship with the variations of some solar wind characteristics under different electromagnetic conditions in interplanetary space. A classification is made of the conditions that are accompanied by the increase in CR anisotropy. Author

N85-35037*# Academy of Sciences (USSR), Yakutsk. Inst. of Cosmophysical Research and Aeronomy.
CHANGE OF COSMIC RAY ANISOTROPY WITH SOLAR ACTIVITY
N. G. Kravtsov, P. A. Krivoshapkin, A. I. Kuzmin, G. V. Skripin, I. A. Transky, and G. V. Shafer *In* NASA. Goddard Space Flight Center 19th Intern. Cosmic Ray Conf., Vol. 5 Aug. 1985 p 155-158 refs (For primary document see N85-34991 23-93)
(SH-4.5-20) Avail: NTIS HC as boxed set only $200/MF A01 per volume or E99 per entire set CSCL 03B

Muon telescope data at various depths underground in Yakutsk within energy range 10 to 300 GeV for 1957 to 1984 are analyzed. The 22-year variation of the interplanetary magnetic field aligned component is found. The variation is caused by interaction of heliomagnetosphere with the local galactic field and interstellar wind. Author

N85-35038*# Franklin Inst., Newark, Del.
MAGNETIC FLUCTUATION AND COSMIC RAY DIURNAL VARIATIONS
J. W. Bieber and M. A. Pomerantz *In* NASA. Goddard Space Flight Center 19th Intern. Cosmic Ray Conf., Vol. 5 Aug. 1985 p 159-162 refs (For primary document see N85-34991 23-93)
(Grant NSF ATM-83-03758)
(SH-4.5-21) Avail: NTIS HC as boxed set only $200/MF A01 per volume or E99 per entire set CSCL 03B

A unified theory of cosmic ray diurnal variations has been proposed in which the first 3 harmonics of the cosmic ray daily variation all results from a single anisotropy produced by the

combined effects of adiabatic focusing and anisotropic pitch angle scattering. The theoretical description of steady state cosmic ray anisotropies are simplified and improved. Preliminary results of a study of correlations between cosmic ray diurnal variations and the fluctuation characteristics of the interplanetary magnetic field are presented and discussed in light of the theory. Author

N85-35039*# California Inst. of Tech., Pasadena.
CHANGES IN THE ENERGY SPECTRUM OF ANOMALOUS OXYGEN AND HELIUM DURING 1977-1985
A. C. Cummings, E. C. Stone, and W. R. Webber (New Hampshire Univ.) *In* NASA. Goddard Space Flight Center 19th Intern. Cosmic Ray Conf., Vol. 5 Aug. 1985 p 163-166 refs (For primary document see N85-34991 23-93)
(Contract NAS7-918; Grant NGR-05-002-160)
(SH-4.6-1) Avail: NTIS HC as boxed set only $200/MF A01 per volume or E99 per entire set CSCL 03B

Data was used from the cosmic ray experiment on the Voyager spacecraft to measure the energy spectrum of anomalous O and He during the period 1977 to 1985. These spectra are found to change dramatically after the middle of 1980, with the peak of plateau region of the differential spectrum shifting to a higher energy. This change appears to be related to the reversal of the solar magnetic field and could imply that particle drifts are important to the acceleration of propagation of these particles. Author

N85-35040*# California Inst. of Tech., Pasadena.
SOLAR CYCLE VARIATIONS OF THE ANOMALOUS COSMIC RAY COMPONENT Abstract Only **c92**
R. A. Mewaldt and E. C. Stone *In* NASA. Goddard Space Flight Center 19th Intern. Cosmic Ray Conf., Vol. 5 Aug. 1985 p 167 (For primary document see N85-34991 23-93)
(Contracts NAS5-28441; NAS5-28449; Grant NGR-05-002-160)
(SH-4.6-2) Avail: NTIS HC as boxed set only $200/MF A01 per volume or E99 per entire set CSCL 03B

The intensity of the anomalous cosmic ray component, consisting of He, N, O, and Ne, has long been known to be especially sensitive to the effects of solar modulation. Following its discovery in 1972, this component dominated the quiet time flux of cosmic ray nuclei below approx. 30 MeV/nucleon during the 1972 to 1978 solar minimum, but then became essentially unobservable at 1 AU with the approach of solar maximum conditions. One recent theoretical model predicts substantial differences in the intensity of the anomalous fluxes from one solar minimum period to the next because of the reversal of the solar magnetic field. Using data from the Caltech experiments on IMP-8 and ICE (ISEE-3), the intensity of anomalous O and He at 1 AU during the years 1972 to 1985 is reported in particular. Whether the anomalous fluxes will return to their 1972-1978 levels, as predicted by spherically symmetric modulation models, or whether they will fail to return to 1 AU, as suggested by modulation models in which gradient and curvature drifts dominate are to be determined. The preliminary analysis of data from 1984 shows that the intensity of 8 to 27 MeV/nucleon O is still more than an order of magnitude below its 1972 to 1978 levels, while the intensity of 25 to 43 MeV/nucleon He is a factor of Approx. 8 below its maximum level in 1977. Author

N85-35041*# Maryland Univ., College Park. Dept. of Physics.
TEMPORAL VARIATIONS OF THE ANOMALOUS OXYGEN COMPONENT, 1977 - 1984 **c92**
G. M. Mason, B. Klecker (Max-Planck-Inst. fuer Extraterrestrische Physik, Garching, West Germany), A. B. Galvin, D. Hovestadt (Max-Planck-Inst. fuer Extraterrestrische, Garching, West Germany), and F. M. Ipavich *In* NASA. Goddard Space Flight Center 19th Intern. Cosmic Ray Conf., Vol. 5 Aug. 1985 p 168-171 refs (For primary document see N85-34991 23-93)
(SH-4.6-3) Avail: NTIS HC as boxed set only $200/MF A01 per volume or E99 per entire set CSCL 03B

A survey is of the long term temporal variations of 6.6 to 12 MeV/nucleon anomalous oxygen at 1 AU covering the period 1977 to 1984. This time interval included the recent solar maximum, with the recovery at neutron monitor energies beginning in 1982. During this time interval, 6.6 to 12 MeV/nucleon O fluxes decreased by at least a factor of 50, and indeed remained below the instrumental detection threshold after 1979. By late 1984, neutron monitors had recovered to roughly 1979 levels from the 1982 solar maximum, and anomalous O still remained below the detection threshold. Author

N85-35042*# New Hampshire Univ., Durham.
RADIAL AND LATITUDINAL GRADIENTS OF ANOMALOUS OXYGEN DURING 1977 - 1985 **c92**
W. R. Webber, A. C. Cummings (California Inst. of Tech., Pasadena), and E. C. Stone *In* NASA. Goddard Space Flight Center 19th Intern. Cosmic Ray Conf., Vol. 5 Aug. 1985 p 172-175 refs (For primary document see N85-34991 23-93)
(Contract NAS7-918; Grant NGR-05-002-160)
(SH-4.6-4) Avail: NTIS HC as boxed set only $200/MF A01 per volume or E99 per entire set CSCL 03B

It is found that the radial gradient of anomalous O remains during 1977 to 1985 at approx. 10% to 15%/AU although the intensity changes by more than a factor of 100. These results can be used to deduce that most of the modulation of the intensities of these particles is occurring beyond 27 AU. Evidence is also found for a latitudinal gradient of approx. +3%/degree at low energies (7.1 to 10.6 MeV/nuc). Author

N85-35043*# Max-Planck-Inst. fuer Extraterrestrische Physik, Garching (West Germany).
OBSERVATION OF PICK-UP IONS IN THE SOLAR WIND: EVIDENCE FOR THE SOURCE OF THE ANOMALOUS COSMIC RAY COMPONENT?
D. Hovestadt, E. Moebius, B. Klecker, M. Scholer, G. Gloeckler (Maryland Univ., College Park), and F. M. Ipavich (Maryland Univ., College Park) *In* NASA. Goddard Space Flight Center 19th Intern. Cosmic Ray Conf., Vol. 5 Aug. 1985 p 176-179 refs (For primary document see N85-34991 23-93)
(SH-4.6-5) Avail: NTIS HC as boxed set only $200/MF A01 per volume or E99 per entire set CSCL 03B

Singly ionized energetic helium has been observed in the solar wind by using the time of flight spectrometer SULEICA on the AMPTE/IRM satellite between September and December, 1984. The energy density spectrum shows a sharp cut off which is strongly correlated with the four fold solar wind bulk energy. The absolute flux of the He(+)ions of about 10000 ion/sq cm.s is present independent of the IPL magnetic field orientation. The most likely source is the neutral helium of the interstellar wind which is ionized by solar UV radiation. It is suggested that these particles represent the source of the anomalous cosmic ray component. Author

N85-35044*# New Hampshire Univ., Durham. Space Science Center.
ON THE ANOMALOUS COMPONENT
M. S. Potgieter, L. A. Fisk, and M. A. Lee *In* NASA. Goddard Space Flight Center 19th Intern. Cosmic Ray Conf., Vol. 5 Aug. 1985 p 180-183 refs (For primary document see N85-34991 23-93)
(SH-4.6-6) Avail: NTIS HC as boxed set only $200/MF A01 per volume or E99 per entire set CSCL 03B

The so-called anomalous cosmic ray component, which occurs at energies of about 10 MeV/nucleon and consists only of He, N, O, and Ne, has been a subject of interest for more than a decade. The origin of this component is generally considered to be interstellar neutral gas that is ionized and accelerated in the solar wind. The mechanism and the location for the acceleration, however, remains an unsolved problem. A model is used which includes the effects of gradient and curvature drifts and considers the implications of observed spatial gradients of the anomalous component for the location of the acceleration region. It is concluded that if drifts are important the acceleration region cannot lie at the solar poles. It is also concluded that there is no single region for the acceleration which can account for both the observed intensities and gradients in models which include drift effects. Author

N85-35045*# Tata Inst. of Fundamental Research, Bombay (India).
POSSIBLE ORIGIN OF THE ANOMALOUS COMPONENT OF COSMIC RAYS Abstract Only
S. Biswas, N. Durgaprasad, R. K. Singh, M. N. Vahia, and J. S. Yadav *In* NASA. Goddard Space Flight Center 19th Intern. Cosmic Ray Conf., Vol. 5 Aug. 1985 p 184 (For primary document see N85-34991 23-93)
(SH-4.6-7) Avail: NTIS HC as boxed set only $200/MF A01 per volume or E99 per entire set CSCL 03B

The possible origin of the anomalous cosmic rays (ACR) are studied in terms of stellar wind injection from O type stars and their acceleration in shock fronts of SNR's. It is assumed that a fraction of heavy ions will encounter interstellar shock fronts of SNR's and these are accelerated to about 5 to 100 MeV/N and give rise to ACR's. Typically these ions would travel a distance of the order of a few 1000 pc. Therefore it is estimated that O type stars in a volume of radius of a few Kpc around the solar system are contributing to the intensity of ACR in the local ISM. From observational data, the intensity of ACR in the local ISM is estimated. It is suggested that these ACR ions enter the solar system along the solar dipole field lines connected to the interplanetary magnetic field lines. Author

N85-35046*# New Hampshire Univ., Durham. Space Science Center.
THE COSMIC RAY INTERPLANETARY RADIAL GRADIENT FROM 1972 - 1985
W. R. Webber and J. A. Lockwood *In* NASA. Goddard Space Flight Center 19th Intern. Cosmic Ray Conf., Vol. 5 Aug. 1985 p 185-188 refs (For primary document see N85-34991 23-93)
(Contract NAS2-4354; Grant NSF ATM-83-04486)
(SH-4.7-1) Avail: NTIS HC as boxed set only $200/MF A01 per volume or E99 per entire set CSCL 03B

It is now established that the solar modulation of cosmic rays is produced by turbulent magnetic fields propagated outward by the solar wind. Changes in cosmic ray intensity are not simultaneous throughout the modulation region, thus requiring time dependent theories for the cosmic ray modulation. Fundamental to an overall understanding of this observed time dependent cosmic ray modulation is the behavior of the radial intensity gradient with time and heliocentric distance over the course of a solar modulation cycle. The period from 1977 to 1985 when data are available from the cosmic ray telescopes on Pioneer (P) 10, Voyager (V) 1 and 2, and IMP 8 spacecraft is studied. Additional data from P10 and other IMP satellites for 1972 to 1977 can be used to determine the gradient at the minimum in the solar modulation cycle and as a function of heliocentric distance. All of these telescopes have thresholds for protons and helium nuclei of E > 60 MeV/nucleon. Author

N85-35047*# California Univ., San Diego, La Jolla.
TIME AND ENERGY DEPENDENCE OF THE COSMIC RAY GRADIENT IN THE OUTER HELIOSPHERE
Walker Fillius, Ian Axford (Victoria Univ., Wellington, New Zealand), and David Wood *In* NASA. Goddard Space Flight Center 19th Intern. Cosmic Ray Conf., Vol. 5 Aug. 1985 p 189-192 (For primary document see N85-34991 23-93)
(SH-4.7-2) Avail: NTIS HC as boxed set only $200/MF A01 per volume or E99 per entire set CSCL 03B

Pioneers 10 and 11, now 35 and 18 AU from the Sun, continue to extend our knowledge of the spatial dependence of cosmic ray intensities in the heliosphere. Radial gradients measured from these spacecraft by UCSD detectors which have integral energy responses above thresholds of 80 and 500 MeV/nucleon are reported. An average gradient of 2%/AU typifies the data set as a whole, but there are time and energy dependences that deviate from this value. With operating lifetimes of 13 and 12 years, respectively, for the two spacecraft, the time dependence was followed for over a solar cycle. The higher energy channel shows less modulation on all time scales. At the start of the present cycle, the gradient is lower than the average value during the last solar cycle. Author

N85-35048*# National Aeronautics and Space Administration, Washington, D. C.
THE LARGE SCALE DYNAMICS OF THE OUTER HELIOSPHERE AND THE LONG-TERM MODULATION OF GALACTIC COSMIC RAYS
Frank B. McDonald, T. T. vonRosenvinge (NASA. Goddard Space Flight Center), N. Lal (NASA. Goddard Space Flight Center), P. Schuster (NASA. Goddard Space Flight Center), J. Trainor (NASA. Goddard Space Flight Center), and M. A. I. VanHollebeke (Musee National des Sciences, Paris, France) *In* NASA. Goddard Space Flight Center 19th Intern. Cosmic Ray Conf., Vol. 5 Aug. 1985 p 193-196 refs (For primary document see N85-34991 23-93)
(SH-4.7-3) Avail: NTIS HC as boxed set only $200/MF A01 per volume or E99 per entire set CSCL 03B

The network of cosmic ray observatories reaching across the heliosphere has given new insight into the process of solar modulation, establishing that the decreases occur principally in the outer heliosphere and are produced by interplanetary flow systems; that the hysteresis effects appear to be produced by changes in the rigidity dependence of the diffusion coefficient and that the predicted effects on the cosmic ray gradients associated with the reversal of the solar magnetic field polarity are not observed. Author

N85-35049*# California Inst. of Tech., Pasadena.
SOLAR MODULATION AND INTERPLANETARY GRADIENTS OF THE GALACTIC ELECTRONS FLUX, 1977 - 1984 **c92**
S. P. Christon, A. C. Cummings, E. C. Stone, and W. R. Webber (New Hampshire Univ.) *In* NASA. Goddard Space Flight Center 19th Intern. Cosmic Ray Conf., Vol. 5 Aug. 1985 p 197 refs (For primary document see N85-34991 23-93)
(Contracts NAS7-918; NGR-05-002-160)
(SH-4.7-4) Avail: NTIS HC as boxed set only $200/MF A01 per volume or E99 per entire set CSCL 03B

The flux of electrons with energy from approx. 10 to 180 MeV measured with the electron telescope on the Voyager 1 and 2 spacecraft in the heliocentric radial range 1 - 22 AU between 1977 and 1984 is reported. Jovian electrons were clearly observable between 1978 and 1983 (radial range 2 - 12 AU) at energies below approx. 50 MeV. Above approx. 50 MeV the electron intensity exhibited temporal variations generally related to the 11 year modulation of protons > 75 MeV. The overall magnitude of the electron intensity changes between the maximum intensity observed in 1977 and the minimum intensity in 1981 was a factor approx. 2, also comparable to that observed for > 75 MeV protons. By early 1985 the electron intensity had apparently recovered to the level observed in 1977 whereas the proton intensity was still about 20% lower. A detailed interpretation of these electron variations in all energy channels depends on an accurate subtraction of background induced by energetic protons of a few 100 MeV. This subtraction is facilitated by calibration results at several energies. G.L.C.

N85-35050*# Chicago Univ., Ill.
GALACTIC COSMIC RAY RADIAL GRADIENTS AND THE ANOMALOUS He COMPONENT NEAR MAXIMUM SOLAR MODULATION AND TO RADII BEYOND 34 AU FROM THE SUN
R. B. McKibben, K. R. Pyle, and J. A. Simpson *In* NASA. Goddard Space Flight Center 19th Intern. Cosmic Ray Conf., Vol. 5 Aug. 1985 p 198-201 refs (For primary document see N85-34991 23-93)
(Contracts NAS2-11126; NAS5-28442)
(SH-4.7-5) Avail: NTIS HC as boxed set only $200/MF A01 per volume or E99 per entire set CSCL 03B

Radial gradients for relativistic galactic cosmic rays (E > 70 MeV) remained nearly constant at approx. 2.5%/AU from 1978-84, which includes the period of maximum solar modulation in 1981-82. For energies 30-70 MeV/n, gradients decreased at solar maximum to values of 1%/AU (protons) and 4%/AU (helium), and appear to be increasing again in 1983-84 toward the values found for solar minimum. The anomalous helium component has not reappeared, either at 1 AU or at Pioneer 10 at R > 34 AU.
Author

N85-35051*# Applied Physics Lab., Johns Hopkins Univ., Laurel, Md.
VOYAGER 1 AND 2 MEASUREMENTS OF RADIAL AND LATITUDINAL COSMIC RAY GRADIENTS DURING 1981 - 1984
D. Venkatesan, R. B. Decker, and S. M. Krimigis *In* NASA. Goddard Space Flight Center 19th Intern. Cosmic Ray Conf., Vol. 5 Aug. 1985 p 202-205 refs (For primary document see N85-34991 23-93)
(Contract N00024-78-C-5384; Grant NSF ATM-83-05537)
(SH-4.7-6) Avail: NTIS HC as boxed set only $200/MF A01 per volume or E99 per entire set CSCL 03B

The cosmic ray radial gradient was determined during 1981-84 using data from very similar detectors onboard spacecraft Voyagers 1 and 2 (radial separation approx. 6 AU, heliolatitude separation approx. 25 deg.) and from the Earth-orbiting satellite IMP 8. The principal result is that the radial gradient over this period decreased at the rate approx. 2.0%/AU between 1 and 16 AU and approx. 0.6%/AU between approx. 16 and 22 AU.
Author

N85-35052*# Chicago Univ., Ill.
THE RECOVERY OF THE COSMIC RAY FLUX FROM MAXIMUM SOLAR MODULATION AT IMP-8 (1 AU) AND AT PIONEER (R > 30 AU) **c92**
R. B. McKibben, K. R. Pyle, and J. A. Simpson *In* NASA. Goddard Space Flight Center 19th Intern. Cosmic Ray Conf., Vol. 5 Aug. 1985 p 206-209 refs (For primary document see N85-34991 23-93)
(SH-4.7-7) Avail: NTIS HC as boxed set only $200/MF A01 per volume or E99 per entire set CSCL 03B

In the period 1980-84, observations of relativistic and low energy ($30 < E < 70$ MeV/n) cosmic ray nuclei from Pioneer 10 in the outer heliosphere and from IMP-8 at AU show that increases as well as decreases in intensity propagate outward at velocities equal to or greater than the average solar wind velocity.
Author

N85-35053*# Chicago Univ., Ill.
THE LARGE-SCALE MODULATION OF COSMIC RAYS IN MID-1982: ITS DEPENDENCE ON HELIOSPHERIC LONGITUDE AND RADIUS
K. R. Pyle and J. A. Simpson *In* NASA. Goddard Space Flight Center 19th Intern. Cosmic Ray Conf., Vol. 5 Aug. 1985 p 210-213 refs (For primary document see N85-34991 23-93)
(SH-4.7-9) Avail: NTIS HC as boxed set only $200/MF A01 per volume or E99 per entire set CSCL 03B

Near solar maximum, a series of large radial solar wind shocks in June and July 1982 provided a unique opportunity to study the solar modulation of galactic cosmic rays with an array of spacecraft widely separated both in heliocentric radius and longitude. By eliminating hysteresis effects it is possible to begin to separate radial and azimuthal effects in the outer heliosphere. On the large scale, changes in modulation (both the increasing and recovery phases) propagate outward at close to the solar wind velocity, except for the near-term effects of solar wind shocks, which may propagate at a significantly higher velocity. In the outer heliosphere, azimuthal effects are small in comparison with radial effects for large-scale modulation at solar maximum.
Author

N85-35054*# Academy of Sciences of the Armenian SSR, Erivan (USSR).
NONSTATIONARY MODULATION OF GALACTIC COSMIC RAYS IN A NONLINEAR MODEL
V. KH. Babayan and M. B. Bagdasarian *In* NASA. Goddard Space Flight Center 19th Intern. Cosmic Ray Conf., Vol. 5 Aug. 1985 p 214-217 refs (For primary document see N85-34991 23-93)
(SH-4.7-10) Avail: NTIS HC as boxed set only $200/MF A01 per volume or E99 per entire set CSCL 03B

An automdel equation for the solar wind velocity is obtained in the self-consistent model. The solution of the convection-diffusion equation is obtained for the density of galactic cosmic rays at a definite dependence of the diffusion coefficient and solar wind velocity on the rigidity and distance.
Author

N85-35055*# Academy of Sciences (USSR), Moscow. Inst. of History of Science and Technology.
DIMENSIONS OF THE SOLAR WIND CAVITY AND OF THE REGION OF INTERPLANETARY COSMIC RAY MODULATION **c92**
I. V. Dorman *In* NASA. Goddard Space Flight Center 19th Intern. Cosmic Ray Conf., Vol. 5 Aug. 1985 p 218-221 refs (For primary document see N85-34991 23-93)
(SH-4.7-11) Avail: NTIS HC as boxed set only $200/MF A01 per volume or E99 per entire set CSCL 03B

The problem of determining effective dimensions of the region of global galactic cosmic ray modulation from the data on 11 year cosmic ray variations and the data on the parameters of the solar activity and the solar wind is discussed.
Author

N85-35056*# Potchefstroom Univ. for Christian Higher Education (South Africa). Dept. of Physics.
DRIFT AND FORBUSH DECREASES
H. Moraal and M. S. Mulder *In* NASA. Goddard Space Flight Center 19th Intern. Cosmic Ray Conf., Vol. 5 Aug. 1985 p 222-225 refs (For primary document see N85-34991 23-93)
(SH-5.1-2) Avail: NTIS HC as boxed set only $200/MF A01 per volume or E99 per entire set CSCL 03B

Evidence is presented that the drift effect on the modulation of galactic cosmic rays can be seen on Forbush decreases observed by the Deep River and Hermanus neutron monitors.
Author

N85-35057*# Consiglio Nazionale delle Ricerche, Rome (Italy). Ist. di Fisica dello Spazio Interplanetario.
ANOMALOUS SHORT-TERM INCREASES IN THE GALACTIC COSMIC RAY INTENSITY: ARE THEY RELATED TO THE INTERPLANETARY MAGNETIC CLOUD-LIKE STRUCTURES?
N. Iucci, M. Parisi, C. Signorini, M. Storini, and G. Villoresi *In* NASA. Goddard Space Flight Center 19th Intern. Cosmic Ray Conf., Vol. 5 Aug. 1985 p 226-229 refs (For primary document see N85-34991 23-93)
(SH-5.1-3) Avail: NTIS HC as boxed set only $200/MF A01 per volume or E99 per entire set CSCL 03B

Thirty-one short-term increases (time duration < 24 hours and amplitude up to 5%) in the galactic cosmic ray intensity, occurring inside Forbush decreases events, have been identified over the period 1966 - 1977. These increases are highly anisotropic and occur after the compression region following the shock; the interplanetary medium is characterized by intense (> 10 nT) and higly fluctuating magnetic field B, high velocity, low density and temperature (flare ejecta piston?). These B-fluctuations seem to be ordered variations which could be representative of magnetic clouds. Also the large cosmic ray increase occurring on 17-18 September 1979, belongs to this category of events.
G.L.C.

N85-35058*# Consiglio Nazionale delle Ricerche, Rome (Italy). Ist. di Fisica dello Spazio Interplanetario.
THE FLARE ORIGIN OF FORBUSH DECREASES NOT ASSOCIATED WITH SOLAR FLARES ON THE VISIBLE HEMISPHERE OF THE SUN **c92**
N. Iucci, M. Parisi, C. Signorini, M. Storini, and G. Villoresi *In* NASA. Goddard Space Flight Center 19th Intern. Cosmic Ray Conf., Vol. 5 Aug. 1985 p 230-233 refs (For primary document see N85-34991 23-93)
(SH-5.1-4) Avail: NTIS HC as boxed set only $200/MF A01 per volume or E99 per entire set CSCL 03B

Investigations have shown that Forbush decreases (Fds) are produced by the propagation into the interplanetary space of a strong perturbation originating from a solar flare (Sf) accompanied by Type IV radioemission. As the front of the perturbation propagates into the interplanetary space, the region in which the galactic cosmic rays are modulated (Fd-modulated region) rotates westward with the Sun and is generally included between two boundary streams; therefore the Fds not associated with observed

type IV Sfs (N.Ass.Fds) are likely to be produced by type IV Sfs occurred on the Sun's backside: these vents can be observed when the Earth crosses the corotating Western boundary of the modulated region. G.L.C.

N85-35059*# Consiglio Nazionale delle Ricerche, Rome (Italy). Ist. di Fisica dello Spazio Interplanetario.

LONGITUDINAL DEPENDENCE OF THE INTERPLANETARY PERTURBATION PRODUCED BY ENERGETIC TYPE 4 SOLAR FLARES AND OF THE ASSOCIATED COSMIC RAY MODULATION **c92**

N. Iucci, M. Parisi, M. Storini, G. Villoresi, and S. Pinter (Slovak Academy of Sciences, Hurbanovo, Czechoslovakia) *In* NASA. Goddard Space Flight Center 19th Intern. Cosmic Ray Conf., Vol. 5 Aug. 1985 p 234-237 refs (For primary document see N85-34991 23-93)

(SH-5.1-5) Avail: NTIS HC as boxed set only $200/MF A01 per volume or E99 per entire set CSCL 03B

One of the most significant features of the flare-associated Forbush decreases (Fds) in the galatctic cosmic ray (c.r.) is the so-called East-West asymmetry: the solar flares (Sfs) observed in the Eastern or central region of the solar disk exhibit a higher probability to cause large Fds than the Sfs occurring in the Western portion of the disk. In particular the interplanetary perturbations generated by Type IV Sfs depress the c.r. intensity in a vast spiral cone-like region (modulated region) which extends along the interplanetary magnetic field from the neighborhood of the active region to the advancing perturbation, and that, immediately after the flare-generated perturbation, the maximum c.r. modulation is observed between 0 and 40 deg. W of the meridian plane crossings the flare site at time of flare (flare's meridian plane). G.L.C.

N85-35060*# Nagoya Univ. (Japan). Cosmic Ray Research Lab.

RIGIDITY SPECTRUM OF FORBUSH DECREASE

S. Sakakibara, K. Munakata, and K. Nagashima *In* NASA. Goddard Space Flight Center 19th Intern. Cosmic Ray Conf., Vol. 5 Aug. 1985 p 238-241 refs (For primary document see N85-34991 23-93)

(SH-5.1-6) Avail: NTIS HC as boxed set only $200/MF A01 per volume or E99 per entire set CSCL 03B

Using data from neutron monitors and muon telescopes at surface and underground stations, the average rigidity spectrum of Forbush decreases (Fds) during the period of 1978-1982 were obtained. Thirty-eight Ed-events are classified into two groups Hard Fd and Soft Fd according to size of Fd at Sakashita station. It is found that a spectral form of fractional-power type (P to the-gamma sub 1 (P+P sub c) to the -gamma sub2) is more suitable for the present purpose than that of power-exponential type or of power type with an upper limiting rigidity. The best fitted spectrum of fractional-power type is expressed by gamma sub1 = 0.37, gamma sub2 = 0.89 and P subc = 10 GV for Hard Fd and gamma sub1 = 0.77, gamma sub2 = 1.02 and P sub c - 14GV for Soft Fd. Author

N85-35061*# Turku Univ. (Finland). Dept. of Physical Sciences.

SPECTRAL ANALYSIS OF THE FORBUSH DECREASE OF 13 JULY 1982

E. Vainikka, J. J. Torsti, E. Valtonen, M. Lumme, M. Nieminen, J. Peltonen, and H. Arvela *In* NASA. Goddard Space Sciences 19th Intern. Cosmic Ray Conf., Vol. 5 Aug. 1985 p 242-245 refs (For primary document see N85-34991 23-93)

(SH-5.1-7) Avail: NTIS HC as boxed set only $200/MF A01 per volume or E99 per entire set CSCL 03B

The maximum entropy method has been applied in the spectral analysis of high-energy cosmic-ray intensity during the large Forbush event of July 13, 1982. An oscillation with period of about 2 hours and amplitude of 1 to 3% was found to be present during the decrease phase. This oscillation can be related to a similar periodicity in the magnetospheric field. However, the variation was not observed at all neutron monitor stations. In the beginning of the recovery phase, the intensity oscillated with a period of about 10 hours and amplitude of < 3%. Author

N85-35062*# Institute of Physical and Chemical Research, Tokyo (Japan). Cosmic Ray Lab.

TRANSIENT COSMIC RAY INCREASE ASSOCIATED WITH A GEOMAGNETIC STORM

S. Kudo, M. Wada, P. Tanskanen (Oulu Univ.), and M. Kodama (Yamanashi Medical Coll., Japan) *In* NASA. Goddard Space Flight Center 19th Intern. Cosmic Ray Conf., Vol. 5 Aug. 1985 p 246-249 refs (For primary document see N85-34991 23-93)

(SH-5.1-8) Avail: NTIS HC as boxed set only $200/MF A01 per volume or E99 per entire set CSCL 03B

On the basis of worldwide network data of cosmic ray nucleonic components, the transient cosmic ray increase due to the depression of cosmic ray cutoff rigidity during a severe geomagnetic storm was investigated in terms of the longitudinal dependence. Multiple correlation analysis among isotropic and diurnal terms of cosmic ray intensity variations and Dst term of the geomagnetic field is applied to each of various station's data. It is shown that the amplitude of the transient cosmic ray increase associated with Dst depends on the local time of the station, and that its maximum phase is found in the evening sector. This fact is consistent with the theoretical estimation based on the azimuthally asymmetric ring current model for the magnetic DS field. Author

N85-35063*# Yakutsk State Univ. (USSR).

GALACTIC COSMIC RAY CURRENTS AND MAGNETIC FIELD IRREGULARITY DEGREE IN HIGH-SPEED SOLAR WIND STREAMS

A. I. Kuzmin, I. S. Samsonov (Academy of Sciences, Yakutsk, USSR), and Z. N. Samsonova (Academy of Sciences, Yakutsk, USSR) *In* NASA. Goddard Space Flight Center 19th Intern. Cosmic Ray Conf., Vol. 5 Aug. 1985 p 250-253 refs (For primary document see N85-34991 23-93)

(SH-5.1-9) Avail: NTIS HC as boxed set only $200/MF A01 per volume or E99 per entire set CSCL 03B

Currents of galactic cosmic rays (GCR) obtained by global survey method are analyzed. The cases of almost total disappearance of GCR currents are compared with the results of direct measurements of the solar wind parameters. The conclusion is made on a restricted application of the convective-diffusive mechanism of the GCR modulation by the solar wind during the occurrence of stationary and regular magnetic fields in the interplanetary medium. Author

N85-35064*# Government Engineering Coll., Rewa (India).

STUDY OF DOMINATING PARAMETERS OF HIGH SPEED SOLAR PLASMA STREAMS IN RELATION TO COSMIC RAY AND GEOMAGNETIC STORMS

B. L. Mishra and S. P. Agrawal (Awadhesh Pratap Sing Univ.) *In* NASA. Goddard Space Flight Research Center 19th Intern. Cosmic Ray Conf., Vol. 5 Aug. 1985 p 254-257 refs (For primary document see N85-34991 23-93)

(SH-5.1-11) Avail: NTIS HC as boxed set only $200/MF A01 per volume or E99 per entire set CSCL 03B

The high speed solar wind streams observed near Earth are generally associated with the solar features, such as solar flares and coronal holes. Past studies of these streams from the two sources have revealed distinctly different effects on cosmic ray intensity, whereas the effect is similar for geomagnetic disturbances. Moreover, the effect of the magnitude of the high speed streams (V) and its rate of increase (dv/dt) has also been a subject of investigation to understand their relative contribution in producing geomagnetic disturbances. From the analysis of some of the fast streams presented here, it is difficult to predict, which one of the two (V, dv/dt) is more effective in producing geomagnetic disturbances. Further, in most of the cases, no substantial decrease in cosmic ray intensity is observed. Author

N85-35065*# Aligarh Muslim Univ. (India). Space Science Group.

INFLUENCE OF MAGNETIC CLOUDS ON COSMIC RAY INTENSITY VARIATIONS

Badruddin, R. S. Yadav, N. R. Yadav, and S. P. Agrawal (Awadhesh Pratap Sing Univ.) *In* NASA. Goddard Space Flight Center 19th Intern. Cosmic Ray Conf., Vol. 5 Aug. 1985 p 258-261 refs (For primary document see N85-34991 23-93)

(SH-5.1-12) Avail: NTIS HC as boxed set only $200/MF A01 per volume or E99 per entire set CSCL 03B

Neutron monitor data has been analyzed to study the nature of galactic cosmic ray transient modulation associated with three types of interplanetary magnetic clouds - clouds associated with shocks, stream interfaces and cold magnetic enhancements. Author

N85-35066*# Nagoya Univ. (Japan). Cosmic Ray Research Lab.

THE SOLAR WIND EFFECT ON COSMIC RAYS AND SOLAR ACTIVITY c92

K. Fujimoto, H. Kojima (Fujita Gakuen Health Univ., Japan), and K. Murakami *In* NASA. Goddard Space Flight Center 19th Intern. Cosmic Ray Conf., Vol. 5 Aug. 1985 p 262-265 refs (For primary document see N85-34991 23-93)

(SH-5.1-13) Avail: NTIS HC as boxed set only $200/MF A01 per volume or E99 per entire set CSCL 03B

The relation of cosmic ray intensity to solar wind velocity is investigated, using neutron monitor data from Kiel and Deep River. The analysis shows that the regression coefficient of the average intensity for a time interval to the corresponding average velocity is negative and that the absolute effect increases monotonously with the interval of averaging, tau, that is, from -0.5% per 100km/s for tau = 1 day to -1.1% per 100km/s for tau = 27 days. For tau > 27 days the coefficient becomes almost constant independently of the value of tau. The analysis also shows that this tau-dependence of the regression coefficiently is varying with the solar activity. Author

N85-35067*# Nihon Univ., Shinei (Japan). Physical Science Lab.

A RELATION BETWEEN THE SHORT TIME VARIATIONS OF COSMIC RAYS AND GEOMAGNETIC FIELD CHANGE

Takasuke Saki and Masahito Kato *In* NASA. Goddard Space Flight Center 19th Intern. Cosmic Ray Conf., Vol. 5 Aug. 1985 p 266-269 refs (For primary document see N85-34991 23-93)

(SH-5.1-14) Avail: NTIS HC as boxed set only $200/MF A01 per volume or E99 per entire set CSCL 03B

An event is reported of approx. 37 min periodicity in cosmic ray intensity observed at Akeno(38 deg 47 N, 138 deg 30 E. 900m above s.l., cutoff 10.4 GV) during 1300 approx. 1900 UT on April 25th, 1984, just a day before Forbush decrease of April 26th. This event seemed to be followed by the periodic variations of the geomagnetic field observed at Kakioka (36 deg 23 N, 140 deg 18 E). The regression coefficient between them was obtained approx. 0.07%/10nT. It is shown that in general the power spectral density of cosmic rays in the frequency of 0.0001 approx. 0.001Hz correlates positively with the fluctuations of geomagnetic field (Dst field) around approx. 1.2x0.0001Hz. From the analysis of 47 days data (April 14th to June 13th, 1984) the regression curve was obtained as y=0.275x sup 0.343 with the correlation coefficient of 0.48, where x and y mean Fourier components of Dst field summed over 1.04 approx. 1.39x0.001Hz and cosmic ray power spectral density averaged over 0.0001 approx. 0.001Hz. B.W.

N85-35068*# Awadhesh Pratap Singh Univ., Rewa (India). Space Physics Centre.

ANOMALOUS LOW LEVEL OF COSMIC RAY INTENSITY DECREASES OBSERVED DURING 1980

A. K. Jain, P. K. Pandey, and S. P. Agrawal *In* NASA. Goddard Space Flight Center 19th Intern. Cosmic Ray Conf., Vol. 5 Aug. 1985 p 270-273 refs (For primary document see N85-34991 23-93)

(SH-5.1-15) Avail: NTIS HC as boxed set only $200/MF A01 per volume or E99 per entire set CSCL 03B

Past studies have revealed solar cycle changes in the sunspot activity, as well as in many other solar parameters, such as, solar flares and solar coronal holes. These solar features in turn produce the observed cyclic variations in the interplanetary plasma and fields. Both the cosmic ray intensity as well as the intensity of geomagnetic disturbances are affected by the interplanetary changes and produce 11/22 year periodicity. An anomalous situation has been noticed during the year 1980 (period of high sunspot activity), when both the geomagnetic disturbance index Ap, as well as the magnitude and number of Forbush decreases as small. Such an anomaly occurs, in spite of the fact that both the sunspot numbers and the energetic solar flares are almost maximum during the present solar cycle. B.W.

N85-35069*# Turku Univ. (Finland). Physics Lab.

OBSERVATIONS OF COSMIC-RAY MODULATIONS IN THE FALL, 1984

J. J. Torsti, M. Nieminen, E. Valtonen, H. Arvela, M. Lumme, J. Peltonen, and E. Vainikka *In* NASA. Goddard Space Flight Center 19th Intern. Cosmic Ray Conf., Vol. 5 Aug. 1985 p 274-277 refs (For primary document see N85-34991 23-93)

(SH-5.1-16) Avail: NTIS HC as boxed set only $200/MF A01 per volume or E99 per entire set CSCL 03B

Modulation of cosmic-ray energy spectrum was studied by using the Turku double neutron monitor. The multiplicity region of detected neutrons produced by cosmic ray hadrons in the monitor was divided into seven categories corresponding to mean energies 0.1, 0.3, 1.0, 3.2, 8.6, 21, and 94 GeV of hadrons at sea level. Based on 24-hour frequencies, a statistical analysis showed that modulation of the intensity in all categories occurred during several periods in the fall 1984. The magnitude of the variation was a few per cent. Author

N85-35070*# Academy of Sciences (USSR), Alma-Ata. Inst. of Ionosphere.

FREQUENCY SPECTRA OF SHORT-PERIOD VARIATIONS OF COSMIC RAY

V. P. Antonova and A. G. Zusmanovich *In* NASA. Goddard Space Flight Center 19th Intern. Cosmic Ray Conf., Vol. 5 Aug. 1985 p 278-280 refs (For primary document see N85-34991 23-93)

(SH-5.1-17) Avail: NTIS HC as boxed set only $200/MF A01 per volume or E99 per entire set CSCL 03B

Frequency spectra for different periods of solar activity were calculated by 5-minutes data of a neutron super-monitor, (altitude 3340 m, cutoff rigidity is 6, 7 GV, counting rate is about 4.5.10 per hour). It was shown that shifting of the spectrum power from low-frequency range to high-frequency range takes place from minimum to maximum of the solar activity. It was reliably distinguished the peak with 160-minutes period coincided with the period of the Sun's atmosphere oscillation and some types of geomagnetic pulsation by the method of accumulation of the frequency spectra. It was conducted the comparison of cosmic ray spectra with spectra of geomagnetic field for the same point of the registration and at the same period. Author

N85-35071*# Academy of Sciences (USSR), Moscow. Inst. of Terrestrial Magnetism.

STUDY OF COSMIC RAY SCINTILLATIONS FROM 5-MINUTE DATA OF THE SCINTILLATIONS TELESCOPE IZMRAN AND WORLD-WIDE NETWORK STATIONS

O. V. Gulinsky, L. I. Dorman, I. Ya. Libin, R. E. Prilutsky, and K. F. Yudakhin *In* NASA. Goddard Space Flight Center 19th Intern. Cosmic Ray Conf., Vol. 5 Aug. 1985 p 281-284 refs (For primary document see N85-34991 23-93)

(SH-5.1-18) Avail: NTIS HC as boxed set only $200/MF A01 per volume or E99 per entire set CSCL 03B

During cosmic ray propagation in interplanetary space there appear characteristic cosmic-ray intensity scintillations which are due to charged particle scattering on random inhomogeneities of the interplanetary magnetic field. The power spectra of cosmic ray scintillations on the Earth during some intervals from 1977 to 1982 (for quiet periods, for solar flares and Forbush decreases

due to power shock waves) have been calculated from five-minute, one and two-hour values of the cosmic-ray intensity measured by the scintillator supertelescope IZMIRAN. The spectra were estimated by the methods of spectral analysis and by autoregressive methods which mutually control each other and make it possible not only to analyze scintillation powers at distinguished frequencies, but also to determine the behavior of spectrum slopes in some frequency ranges. B.W.

N85-35072*# Academy of Sciences of the Georgian SSR, Tbilisi (USSR). Inst. of Geophysics.
THE THEORETICAL AND EXPERIMENTAL INVESTIGATION OF COSMIC RAY FORBUSH-EFFECTS
M. V. Alania, T. S. Bakradze, T. V. Bochorishvili, D. P. Bochikashvili, M. A. Despotashvili, and N. A. Nachkebia *In* NASA. Goddard Space Flight Center 19th Intern. Cosmic Ray Conf., Vol. 5 Aug. 1985 p 285-288 refs (For primary document see N85-34991 23-93)
(SH-5.1-20) Avail: NTIS HC as boxed set only $200/MF A01 per volume or E99 per entire set CSCL 03B

The theoretical results of analysis of the expected spatial distributions of density, gradients and anisotropy of cosmic rays, obtained on the basis of the numerical solution of anisotropic diffusion equation in the presence of the disturbances of shock wave type in the interplanetary space are presented. The theoretical calculations on the definition of the energy spectrum and anisotropy of galactic cosmic rays during Forbush effect are compared with the experimental data. Author

N85-35073*# Academy of Sciences of the Georgian SSR, Tbilisi (USSR). Inst. of Geophysics.
PECULIARITIES OF GALACTIC COSMIC RAY (GCR) ANISOTROPY VARIATION IN CONNECTION WITH THE RECURRENT AND SPORADIC FORBUSH EFFECTS
B. D. Naskidashvili, N. A. Nachkebia, G. L. Tsereteli, and L. Kh. Shatashvili *In* NASA. Goddard Space Flight Center 19th Intern. Cosmic Ray Conf., Vol. 5 Aug. 1985 p 289-292 refs (For primary document see N85-34991 23-93)
(SH-5.1-21) Avail: NTIS HC as boxed set only $200/MF A01 per volume or E99 per entire set CSCL 03B

It has been established, that the beginning of the change of vector of Solar-diurnal anisotropy of Galactic Cosmic Rays (GCR) preceeds due to disturbed region (DR) of Solar wind existing time of which is Tau > or = 8 days. The meridional gradient delta theta eta of density during the recurrent FD is valued. Author

N85-35074*# Academy of Sciences (USSR), Moscow. Inst. of Terrestrial Magnetism, Ionosphere and Radio Wave Propagation.
COSMIC RAY MODULATION BY HIGH-SPEED SOLAR WIND FLUXES
L. I. Dorman, N. S. Kaminer, A. E. Kuzmicheva (Uralsk Pedagogical Inst.), and N. V. Mymrina (Uralsk Pedagogical Inst.) *In* NASA. Goddard Space Flight Center 19th Intern. Cosmic Ray Conf., Vol. 5 Aug. 1985 p 293-295 (For primary document see N85-34991 23-93)
(SH-5.1-22) Avail: NTIS HC as boxed set only $200/MF A01 per volume or E99 per entire set CSCL 03B

Cosmic ray intensity variations connected with recurrent high-speed fluxes (HSF) of solar wind are investigated. The increase of intensity before the Earth gets into a HSF, north-south anisotropy and diurnal variation of cosmic rays inside a HSF as well as the characteristics of Forbush decreases are considered. Author

N85-35075*# Academy of Sciences (USSR), Moscow. Inst. of Terrestrial Magnetism, Ionosphere and Radio Wave Propagation.
SOLAR ACTIVITY BEYOND THE DISK AND VARIATIONS OF THE COSMIC RAY GRADIENT **c92**
A. V. Belov, L. I. Dorman, E. A. Eroshenko, V. N. Ishkov, and V. A. Oleneva *In* NASA. Goddard Space Flight Center 19th Intern. Cosmic Ray Conf., Vol. 5 Aug. 1985 p 296-299 refs (For primary document see N85-34991 23-93)
(SH-5.1-23) Avail: NTIS HC as boxed set only $200/MF A01 per volume or E99 per entire set CSCL 03B

Part of galactic cosmic rays (CR) observed near the Earth and on the Earth come from beyond-disk regions of circumsolar space. But CR of those energies which undergo substantial modulation cover too large a path across the lines of force of the interplanetary magnetic field (IMF) in order that they could provide an effective transfer of information about beyond-disk solar activity. And if it is still possible, the most probable channel for transferring such information must be a neutral layer of heliomagnetosphere in which the transverse CR transport is facilitated by their drift in an inhomogeneous magnetic field. A simple diffusion model for an expected CR variation in a neutral layer near the Earth is discussed. It is of importance that variations of the CR gradient are not at all always accompanied by considerable variations of IMF and solar wind velocity at the point of observation. B.W.

N85-35076*# Academy of Sciences (USSR), Moscow. Inst. of Terrestrial Magnetism, Ionosphere and Radio Wave Propagation.
COUPLING FUNCTIONS FOR LEAD AND LEAD-FREE NEUTRON MONITORS FROM THE LATITUDINAL MEASUREMENTS PERFORMED IN 1982 IN THE RESEARCH STATION ACADEMICIAN KURCHATOV
T. M. Alekanyan, L. I. Dorman, V. G. Yanke, and V. K. Korotkov (SVKNII) *In* NASA. Goddard Space Flight Center 19th Intern. Cosmic Ray Conf., Vol. 5 Aug. 1985 p 300-303 refs (For primary document see N85-34991 23-93)
(SH-6.1-1) Avail: NTIS HC as boxed set only $200/MF A01 per volume or E99 per entire set CSCL 03B

The latitudinal behavior of intensities and multiplicities was registered by the neutron monitor 2 NM and the lead-free neutron monitor 3 SND (slow-neuron detector) in the equator-Kaliningrad line in the Atlantic Ocean. Coupling coefficients for 3 SND show the sensitivity of this detector to primary particles of cosmic rays of energies on the average lower than for 2 NM. As multiplicities increase, the coupling coefficients shift towards higher energies. Author

N85-35077*# Kochi Univ., Akebono (Japan). Dept. of Physics.
ON THE SOLAR CYCLE VARIATION IN THE BAROMETER COEFFICIENTS OF HIGH LATITUDE NEUTRON MONITORS **c92**
M. Kusunose and N. Ogita (Inst. of Physical and Chemical Research) *In* NASA. Goddard Space Flight Center 19th Intern. Cosmic Ray Conf., Vol. 5 Aug. 1985 p 304-307 refs (For primary document see N85-34991 23-93)
(SH-6.1-2) Avail: NTIS HC as boxed set only $200/MF per volume or E99 per entire set CSCL 03B

Evaluation of barometer coefficients of neutron monitors located at high latitudes has been performed by using the results of the spherical harmonic analysis based on the records from around twenty stations for twelve years from January 1966 to December 1977. The average of data at eight stations, where continuous records are available for twelve years, show that the absolute value of barometer coefficient is in positive correlation with the cosmic ray neutron intensity. The variation rate of the barometer coefficient to the cosmic ray neutron intensity is influenced by the changes in the cutoff rigidity and in the primary spectrum. Author

N85-35078*# Tasmania Univ., Hobart (Australia). Dept. of Physics.
ATMOSPHERIC EFFECTS ON THE UNDERGROUND MUON INTENSITY
A. G. Fenton, K. B. Fenton, J. E. Humble, and G. B. Hyland *In* NASA. Goddard Space Flight Center 19th Intern. Cosmic Ray Conf., Vol. 5 Aug. 1985 p 308 ref Sponsored in part by the Australian Research Grants Scheme (For primary document see N85-34991 23-93)
(SH-6.1-3) Avail: NTIS HC as boxed set only $200/MF A01 per volume or E99 per entire set CSCL 03B

It has previously been reported that the barometric pressure coefficient observed for muons at Poatina (vertical absorber depth 357 hg/sq cm) appears to be appreciably higher than would be expected from atmospheric absorption alone. There is a possibility

that the effect is due to an upper atmospheric temperature effect arising from an inverse correlation of surface pressure with stratospheric temperature. A new proportional telescope is discussed which has been operating at Poatina since about the beginning of 83 and which has a long term stability suitable for studying variations of atmospheric origin. B.W.

N85-35079*# Institute of Physical and Chemical Research, Tokyo (Japan).
ALTITUDE VARIATIONS OF COSMIC-RAY SOFT AND HARD COMPONENTS OBSERVED BY AIRBORNE DETECTORS
K. Takahashi, A. Inoue, M. Wada, K. Nishi, and K. Murakami (Nagoya Univ.) *In* NASA. Goddard Space Flight Center 19th Intern. Cosmic Ray Conf., Vol. 5 Aug. 1985 p 309-311 refs (For primary document see N85-34991 23-93)
(SH-6.1-5) Avail: NTIS HC as boxed set only $200/MF A01 per volume or E99 per entire set CSCL 03B

The altitude variations of cosmic-ray total and hard components were measured up to 12,000 m on board a jet liner over Japan island on December, 1981. Observed results together with soft component are presented comparing with the model calculations through the atmosphere by applying the hadronic cascade. Author

N85-35080*# Kazan State Univ. (USSR).
ADDITIONAL FLUX OF PARTICLES AND ALBEDO-ELECTRONS IN UPPER ATMOSPHERE
F. B. Aitbaev, B. M. Dyuisembaev, and E. V. Kolomeets *In* NASA. Goddard Space Flight Center 19th Intern. Cosmic Ray Conf., Vol. 5 Aug. 1985 p 312-315 refs (For primary document see N85-34991 23-93)
(SH-6.1-6) Avail: NTIS HC as boxed set only $200/MF A01 per volume or E99 per entire set CSCL 03B

The results are presented of the Monte Carlo simulation of albedo flux from the dense layers of the Earth's atmosphere and the dependence of angular distribution on the rigidity of geomagnetic cut off and additional flux of particles at the depth in the atmosphere 15-20 g/sq sm. Influence of geomagnetic field on the propagation of charged particles was not taken into account. Author

N85-35081*# Gujarat Univ., Ahmedabad (India). Dept. of Physics.
OBSERVATION OF ENERGY SPECTRUM OF ELECTRON ALBEDO IN LOW LATITUDE REGION AT HYDERABAD, INDIA
S. D. Verma and S. P. Bhatnagar *In* NASA. Goddard Space Flight Center 19th Intern. Cosmic Ray Conf., Vol. 5 Aug. 1985 p 316-319 refs (For primary document see N85-34991 23-93)
(SH-6.1-7) Avail: NTIS HC as boxed set only $200/MF A01 per volume or E99 per entire set CSCL 03B

The preliminary results are presented of the measurement of the energy spectrum of low energy (5-24 MeV) albedo electrons, moving upward as well as downwards, at about 37 km (-4 mb) altitude, over Hyderabad, India, in low latitude region. The flux and energy spectrum was observed by a bi-directional, multidetector charged particle telescope which was flown in a high altitude balloon on 8th December 1984. Results based on a quick look data acquisition and analysis system are presented here. Author

N85-35082*# Gujarat Univ., Ahmedabad (India). Dept. of Physics.
PROTON ALBEDO SPECTRUM OBSERVATION IN LOW LATITUDE REGION AT HYDERABAD, INDIA
S. D. Verma and S. K. Kothari *In* NASA. Goddard Space Flight Center 19th Intern. Cosmic Ray Conf., Vol. 5 Aug. 1985 p 320-323 refs (For primary document see N85-34991 23-93)
(SH-6.1-8) Avail: NTIS HC as boxed set only $200/MF A01 per volume or E99 per entire set CSCL 03B

The flux and the energy spectrum of low energy (30-100 MeV) proton albedos, have been observed for the first time in a low latitude region, over Hyderabad, India. The preliminary results, based on the quick look data acquisition and display system are presented. A charged particle telescope, capable of distinguishing singly charged particles such as electrons, muons, protons in low energy region, records the data of both upward as well as downward moving particles. Thus spectra of splash and re-entrant albedo protons have been recorded simultaneously in a high altitude Balloon flight carried out on 8th December, 1985, over Hyderabad, India. Balloon floated at an latitude of approx. 37 km (4 mb). Author

N85-35083*# Academy of Sciences (USSR), Leningrad.
THE INFLUENCE OF QUIET ASYMMETRIC MAGNETOSPHERE ON THE CUTOFF RIGIDITIES OF THE MAIN CONE
M. I. Tyasto and O. A. Danilova *In* NASA. Goddard Space Flight Center 19th Intern. Cosmic Ray Conf., Vol. 5 Aug. 1985 p 324-327 refs (For primary document see N85-34991 23-93)
(SH-6.1-10) Avail: NTIS HC as boxed set only $200/MF A01 per volume or E99 per entire set CSCL 03B

Some earlier studies show that cutoff rigidities of cosmic-ray particles in the model magnetospheric fields of internal and external sources have daily variations caused by asymmetry of the magnetic field due to the currents induced at the magnetopause and tail currents. Cutoff rigidities of the charged particles coming down at the middle latitudes are examined in this paper. The mathematical model of the magnetospheric field is based on the merged IMP-HEOS experimental data set and includes all known at the present time current systems of the magnetosphere: magnetopause, ring, and magnetotail currents. B.W.

N85-35084*# Utah Univ., Salt Lake City. Dept. of Physics.
RE-EVALUATION OF COSMIC RAY CUTOFF TERMINOLOGY
D. J. Cooke, J. E. Humble (Tasmania Univ.), M. A. Shea (AFGL), D. F. Smart (AFGL), N. Lund (Danish Space Research Inst.), I. L. Rasmussen (Danish Space Research Inst.), B. Byrnak (Danish Space Research Inst.), P. Goret (Centre d'Etudes Nucleaires de Saclay), and N. Petrou (Centre d'Etudes Nucleaires de Saclay) *In* NASA. Goddard Space Flight Center 19th Intern. Cosmic Ray Conf., Vol. 5 Aug. 1985 p 328-331 refs (For primary document see N85-34991 23-93)
(Contract F19628-81-K-0020)
(SH-6.1-11) Avail: NTIS HC as boxed set only $200/MF A01 per volume or E99 per entire set CSCL 03B

The study of cosmic ray access to locations inside the geomagnetic field has evolved in a manner that has led to some misunderstanding and misapplication of the terminology originally developed to describe particle access. This paper presents what is believed to be a useful set of definitions for cosmic ray cutoff terminology for use in theoretical and experimental cosmic ray studies. Author

N85-35085*# Air Force Geophysics Lab., Hanscom AFB, Mass.
THE USE OF THE MCILWAIN L-PARAMETER TO ESTIMATE COSMIC RAY VERTICAL CUTOFF RIGIDITIES FOR DIFFERENT EPOCHS OF THE GEOMAGNETIC FIELD
M. A. Shea, D. F. Smart, and L. C. Gentile (Emmanuel Coll.) *In* NASA. Goddard Space Flight Center 19th Intern. Cosmic Ray Conf., Vol. 5 Aug. 1985 p 332-335 refs (For primary document see N85-34991 23-93)
(Contract F19628-82-K-0039)
(SH-6.1-12) Avail: NTIS HC as boxed set only $200/MF A01 per volume or E99 per entire set CSCL 03B

Secular changes in the geomagnetic field between 1955 and 1980 have been large enough to produce significant differences in both the vertical cutoff rigidities and in the L-value for a specified position. A useful relationship employing the McIlwain L-parameter to estimate vertical cutoff rigidities has been derived for the twenty-five year period. B.W.

N85-35086*# Bern Univ. (Switzerland). Physikalisches Inst.
ESTIMATING THE CHANGE IN ASYMPTOTIC DIRECTION DUE TO SECULAR CHANGES IN THE GEOMAGNETIC FIELD
E. O. Fluecklger, D. F. Smart (AFGL), M. A. Shea (AFGL), L. C. Gentile (Emmanuel Coll.), and A. A. Bathurat (Emmanuel Coll.) *In* NASA. Goddard Space Flight Center 19th Intern. Cosmic Ray Conf., Vol. 5 Aug. 1985 p 336-339 refs (For primary document see N85-34991 23-93)

(Contract F19628-82-K-0039)
(SH-6.1-13) Avail: NTIS HC as boxed set only $200/MF A01 per volume or E99 per entire set CSCL 03B

The concept of geomagnetic optics, as described by the asymptotic directions of approach, is extremely useful in the analysis of cosmic radiation data. However, when changes in cutoff occur as a result of evolution in the geomagnetic field, there are corresponding changes in the asymptotic cones of acceptance. A method is introduced of estimating the change in the asymptotic direction of approach for vertically incident cosmic ray particles from a reference set of directions at a specific epoch by considering the change in the geomagnetic cutoff. Author

N85-35087*# Turku Univ. (Finland). Dept. of Physics.
EMPIRICAL MODEL FOR THE EARTH'S COSMIC RAY SHADOW AT 400 KM: PROHIBITED COSMIC RAY ACCESS
J. E. Humble, D. F. Smart (AFGL), and M. A. Shea (AFGL) *In* NASA. Goddard Space Flight Center 19th Intern. Cosmic Ray Conf., Vol. 5 Aug. 1985 p 340-343 refs (For primary document see N85-34991 23-93)
(SH-6.1-14) Avail: NTIS HC as boxed set only $200/MF A01 per volume or E99 per entire set CSCL 03B

The possibility to construct a unit sphere of access that describes the cosmic radiation allowed to an Earth-orbiting spacecraft is discussed. It is found that it is possible to model the occluded portion of the cosmic ray sphere of access as a circular projection with a diameter bounded by the satellite-Earth horizon. Maintaining tangency at the eastern edge of the spacecraft-Earth horizon, this optically occluded area is projected downward by an angle beta which is a function of the magnetic field inclination and cosmic ray arrival direction. This projected plane, corresponding to the forbidden area of cosmic ray access, is bounded by the spacecraft-Earth horizon in easterly directions, and is rotated around the vertical axis by an angle alpha from the eastern direction, where the angle alpha is a function of the offset dipole latitude of the spacecraft. E.A.K.

N85-35088*# Moscow State Univ. (USSR). Inst. of Nuclear Physics.
PENETRATION OF SOLAR PROTONS INTO THE EARTH'S MAGNETOSPHERE ON NOVEMBER 22, 1977 **c92**
E. V. Gorchakov, V. G. Afanasyev, K. G. Afanasyev, P. P. Ignatyev, V. A. Iozenas, M. V. Ternovskaya, and G. G. Zenchev *In* NASA. Goddard Space Flight Center 19th Intern. Cosmic Ray Conf., Vol. 5 Aug. 1985 p 344-347 refs (For primary document see N85-34991 23-93)
(SH-6.1-15) Avail: NTIS HC as boxed set only $200/MF A01 per volume or E99 per entire set CSCL 03B

The low polar-orbiting Cosmos-900 satellite carried a large geometric factor Cerenkov counter to study the particle anisotropy and spectrum near the proton increase peak in solar cosmic rays. The data help understand different temporal behavior of the increases detected at the stations because the whole set of data showed that the angular distribution of solar cosmic ray particles in interplanetary space was narrow throughout the observation time, resulting in a rapid variation of particle intensity near the poles. The power-law index of the solar cosmic ray integral spectrum varied from -2.4 to -5.2 in the 1 to 4 GV rigidity range from 10.31 to 11.25 UT on November 22, 1977. The flare-time data from all orbits indicate an increased radiation intensity on L=3.5 to 4.0. E.A.K.

N85-35089*# Tashkent V. I. Lenin State Univ., Vuzgorodok (USSR).
DYNAMICS OF THE PENETRATION BOUNDARIES OF SOLAR PROTONS DURING A STRONG MAGNETIC STORM **c92**
G. A. Glukhov, Yu. P. Kratenko, and Yu. V. Mineev (Moscow State Univ.) *In* NASA. Goddard Space Flight Center 19th Intern. Cosmic Ray Conf., Vol. 5 Aug. 1985 p 348-351 refs (For primary document see N85-34991 23-93)
(SH-6.1-16) Avail: NTIS HC as boxed set only $200/MF A01 per volume or E99 per entire set CSCL 03B

The variations in the equatorial penetration boundary of solar protons with E sub p = 0.9 to 8.0 MeV during a strong magnetic storm of April 3 to 5, were analyzed. The dynamics of this boundary is compared with the dynamics of the outer trapping boundary of electrons with E sub e = - 0.3 to 0.6 MeV. The solar-proton penetration and the structure of the real magnetic field are studied. The unique data on the thin structure of development of a magnetospheric substorm were obtained for the first time. E.A.K.

N85-35090*# Academy of Sciences (USSR), Moscow. Inst. for Nuclear Research.
SHORT PERTURBATIONS OF COSMIC RAY INTENSITY AND ELECTRIC FIELD IN ATMOSPHERE
V. V. Alexeyenko, A. E. Chudakov, V. G. Sborshikov, and V. A. Tizengauzen *In* NASA. Goddard Space Flight Center 19th Intern. Cosmic Ray Conf., Vol. 5 Aug. 1985 p 352-355 refs (For primary document see N85-34991 23-93)
(SH-6.1-18) Avail: NTIS HC as boxed set only $200/MF A01 per volume or E99 per entire set CSCL 03B

Short perturbations of cosmic ray intensity were found to be a common phenomenon. Its meteorological origin and correlation with electric field is established. The phenomenon can be explained by the electric field if the strength of this field at high altitudes is much bigger than the measured one at surface. E.A.K.

N85-35091*# Academy of Sciences (USSR), Moscow. Inst. of Terrestrial Magnetism, Ionosphere and Radio Wave Propagation.
LONG-PERIOD COSMIC RAY VARIATIONS AND THEIR ALTITUDE DEPENDENCE
A. V. Belov, R. T. Gushchina, L. I. Dorman, and I. V. Sirotina *In* NASA. Goddard Space Flight Center 19th Intern. Cosmic Ray Conf., Vol. 5 Aug. 1985 p 356-358 refs (For primary document see N85-34991 23-93)
(SH-6.1-19) Avail: NTIS HC as boxed set only $200/MF A01 per volume or E99 per entire set CSCL 03B

Long-period variations were studied from the data of ground-based cosmic ray (CR) observations. In spite of a large value of an 2-year variation, it is more difficult to obtain its spectrum than the spectrum of a solar diurnal variation. Serious obstacles are caused by changes in individual detectors and in the whole world wide network of CR detectors, by the absence of continuity and uniformity of data series, by various apparatus variations. In discrimination and investigation of long-period variations an important and determining point is preparation and preliminary analysis of data. E.A.K.

N85-35092*# Academy of Sciences (USSR), Irkutsk.
DIURNAL VARIATIONS OF COSMIC RAY GEOMAGNETIC CUT-OFF THRESHOLD RIGIDITIES
V. M. Dvornikov, V. E. Sdobnov, A. V. Sergeev, O. A. Danilova (Academy of Science, Leningrad), and M. I. Tyasto (Academy of Science, Leningrad) *In* NASA. Goddard Space Flight Center 19th Intern. Cosmic Ray Conf., Vol. 5 Aug. 1985 p 359-362 refs (For primary document see N85-34991 23-93)
(SH-6.1-21) Avail: NTIS HC as boxed set only $200/MF A01 per volume or E99 per entire set CSCL 03B

The spectrographic global survey method was used to investigate the rigidity variations Rc of geomagnetic cut-off as a function of local time and the level of geomagnetic disturbance for a number of stations of the world wide network. It is shown that geomagnetic cut-off threshold rigidities undergo diurnal variations. The diurnal wave amplitude decreases with increasing threshold rigidity Rc, and the wave maximum occurs at 2 to 4 hr LT. The amplitude of diurnal variations increases with increasing geomagnetic activity. The results agree with those from trajectory calculations made for an asymmetric model of the magnetosphere during different geomagnetic disturbance conditions. E.A.K.

N85-35093*# Academy of Sciences (USSR), Moscow.
THE INFLUENCE OF THE EARTH'S MAGNETOSPHERE ON THE HIGH-ENERGY SOLAR PROTONS **c92**
G. A. Bazilevskaya, V. S. Makhmutov (Industrial Inst. of Roudny), and T. N. Charakhchyan (Moscow State Univ.) *In* NASA. Goddard Space Flight Center 19th Intern. Cosmic Ray Conf., Vol. 5 Aug.

1985 p 363-366 refs (For primary document see N85-34991 23-93)
(SH-6.1-22) Avail: NTIS HC as boxed set only $200/MF A01 per volume or E99 per entire set CSCL 03B

In the Earth's polar regions the intensity of the solar protons with the energy above the critical energy of geomagnetic cutoff is the same as in the interplanetary space. The penumbra in the polar regions is small and the East-West effect is also small. However the geomagnetic cutoff rigidity R sub c in polar regions is difficult to calculate because it is not sufficient to include only the internal sources of the geomagnetic field. During the magneto-quiescent periods the real value of R sub c can be less by 0.1 GV than the calculated value because of the external sources. During the geomagnetic storms the real value of R sub c is still lower. E.A.K.

N85-35094*# Consiglio Nazionale delle Ricerche, Bologna (Italy). Istituto TESRE.
COSMIC RAYS 10Be BIENNAL DATA AND THEIR RELATIONSHIP TO AURORAE AND SUNSPOTS
M. R. Attolini, S. Cecchini, G. Cini. Castagnoli (Torino Univ.), M. Galli (Bologna Univ.), and T. Nanni *In* NASA. Goddard Space Flight Center 19th Intern. Cosmic Ray Conf., Vol. 5 Aug. 1985 p 367-370 refs (For primary document see N85-34991 23-93)
(SH-7.1-1) Avail: NTIS HC as boxed set only $200/MF A01 per volume or E99 per entire set CSCL 03B

The galactic cosmic ray (C.R.) variations which should give information on three dimensional aspects of the heliospheric magnetic fields and on the solar wind, which modulate their influx into the Solar System were studied. In order to decode the information from the C.R. series it is necessary to know the mechanisms through which the modulation is produced. It it clear that a balance of effects with sources at different heliospheric latitudes results in the modulated C.R. intensity. It is found that the modulation of 10Be in polar ice may be due to at least two main contributions: (1) negative and in phase with the Solar flare activity modulating the cosmic ray flux in Forbush-type decreases, and (2) positive in phase with the appearance of large wind streams situated at both polar coronal holes. It is found that the high heliolatitude activity is related to a stable periodicity of 11.1y whereas the low heliolatitude activity contributes to the wondering of the solar cycles. E.A.K.

N85-35095*# Arizona Univ., Tucson. Dept. of Physics.
SOLAR MODULATION OF COSMIC RAY INTENSITY AND SOLAR FLARE EVENTS INFERRED FROM (14)C CONTENTS IN DATED TREE RINGS
C. Y. Fan, T. M. Chen (Peking Univ.), S. X. Yun (Peking Univ.), and K. M. Dai (Nanjing Univ.) *In* NASA. Goddard Space Flight Center 19th Intern. Cosmic Ray Conf., Vol. 5 Aug. 1985 p 371-374 refs (For primary document see N85-34991 23-93)
(SH-7.1-2) Avail: NTIS HC as boxed set only $200/MF A01 per volume or E99 per entire set CSCL 03B

The delta 14C values in 42 rings of a white spruce grown in Mackenzie Delta was measured as a continuing effort of tracing the history of solar modulation of cosmic ray intensity. The delta 14C values in six rings were measured, in search of a 14C increase due to two large solar flares that occurred in 1942. The results are presented. E.A.K.

N85-35096*# Consiglio Nazionale delle Ricerche, Turin (Italy). Istituto TESRE.
COSMIC RAY SECULAR VARIATIONS IN TERRESTRIAL RECORDS AND AURORAE
M. R. Attolini, G. Cini Castagnoli (Torino Univ.), G. Bonino (Torino Univ.), M. Galli (Bologna Univ.), and T. Nanni *In* NASA. Goddard Space Flight Center 19th Intern. Cosmic Ray Conf., Vol. 5 Aug. 1985 p 375-378 refs (For primary document see N85-34991 23-93)
(SH-7.1-3) Avail: NTIS HC as boxed set only $200/MF A01 per volume or E99 per entire set CSCL 03B

The rediscovery that the Sun and the solar wind can undergo important changes on historical time scales has brought into question the stability of the cyclic behavior of past time series of solar and solar-terrestrial origin. It was found by Vector Fourier analysis that the solar 11 year cycle is present in the series of 10Be, delta 180, in ice cores and of thermoluminescence (TL) in sea sediments during the last Millennia with a frequency modulation, related to the Sun behavior, as tested by comparison with the Sunspot number R sub z series. It was shown that the cyclogram of the series of yearly Aurorae from 1721 to 1979 linear-regression-corrected-for-R sub z is straight for the periodicity zeta=11,1y, which indicates that such periodicity is constant in time corresponding to the only line present in the 11y band. The maxima of this component appear at the same time together with the high speed solar wind streams taking place in coronal holes situated in high heliolatitudes. It is evidenced that the 11 year cycle has undergone frequency oscillations on a time scale of two centuries, although it is very difficult to determine the periodicities with high accuracy. E.A.K.

N85-35097*# California Univ., San Diego, La Jolla. Dept. of Chemistry.
WHEN DID THE AVERAGE COSMIC RAY FLUX INCREASE?
K. Nishiizumi, S. V. S. Murty, K. Marti, and J. R. Arnold *In* NASA. Goddard Space Flight Center 19th Intern. Cosmic Ray Conf., Vol. 5 Aug. 1985 p 379-381 refs (For primary document see N85-34991 23-93)
(Grants NAG9-33; NAG9-41)
(SH-7.1-4) Avail: NTIS HC as boxed set only $200/MF A01 per volume or E99 per entire set CSCL 03B

A new 129 to 129 Xe method to obtain cosmic ray exposure ages and to study the average cosmic ray flux on a 10 to the 7th power to 10 to the 8th power year time-scale was developed. The method is based on secondary neutron reactions on Te in troilite and the subsequent decay of 129I, the reaction product to stable 129 Xe. The first measurements of 129 I and 129 Xe in aliquot samples of a Cape York troilite sample are reported.E.A.K.

N85-35098*# Los Alamos Scientific Lab., N. Mex. Nuclear Chemistry Group.
COSMOGENIC-NUCLIDE PRODUCTION BY PRIMARY COSMIC-RAY PROTONS
Robert C. Reedy *In* NASA. Goddard Space Flight Center 19th Intern. Cosmic Ray Conf., Vol. 5 Aug. 1985 p 382-385 refs Sponsored in part by DOE (For primary document see N85-34991 23-93)
(NASA Order W-14084)
(SH-7.1-6) Avail: NTIS HC as boxed set only $200/MF A01 per volume or E99 per entire set CSCL 03B

The production rates of cosmogenic nuclides were calculated for the primary protons in the galactic and solar cosmic rays. At 1 AU, the long-term average fluxes of solar protons usually produce many more atoms of cosmogenic nuclide than the primary protons in the galactic cosmic rays (GCR). Because the particle fluxes inside meteorites and other large objects in space include many secondary neutrons, the production rates and ratios inside large objects are often very different from those by just the primary GCR protons. It is possible to determine if a small object, was small in space or broken from a meteorite. Because heliospherical modulation and other interactions change the GCR particle spectrum, the production of cosmogenic nuclides by the GCR particles outside the heliosphere will be different from that by modulated GCR primaries. E.A.K.

N85-35099*# Los Alamos Scientific Lab., N. Mex. Nuclear Chemistry Group.
COSMIC-RAY EXPOSURE RECORDS AND ORIGINS OF METEORITES
Robert C. Reedy *In* NASA. Goddard Space Flight Center 19th Intern. Cosmic Ray Conf., Vol. 5 Aug. 1985 p 386-389 refs Sponsored in part by DOE (For primary document see N85-34991 23-93)
(NASA Order W-14084)
(SH-7.1-7) Avail: NTIS HC as boxed set only $200/MF A01 per volume or E99 per entire set CSCL 03B

The cosmic-ray records of meteorites are used to infer much about their origins and recent histories. The methods used to interpret meteorites' cosmic-ray records, especially identifying simple or complex exposure histories, often are inadequate. Spallogenic radionuclides, stable nuclides, and measurements of products that have location-sensitive production rates, such as the tracks of heavy cosmic-ray nuclei or neutron-capture nuclides, are very useful in accurately determining a meteorite's history. Samples from different, known locations of a meteorite help in studying the cosmic-ray record. Such extensive sets of meteorite measurements, plus theoretical modeling of complex histories, improves the ability to predict the production of cosmogenic nuclides in meteorites, to distinguish simple and complex exposure histories, and to better determine exposure ages. E.A.K.

N85-35100*# Cologne Univ. (West Germany). Dept. of Nuclear Chemistry.

ACCELERATOR EXPERIMENTS ON THE CONTRIBUTION OF SECONDARY PARTICLES TO THE PRODUCTION OF COSMOGENIC NUCLIDES IN METEORITES

P. Dragovitsch and P. Englert *In* NASA. Goddard Space Flight Center 19th Intern. Cosmic Ray Conf., Vol. 5 Aug. 1985 p 390-393 refs Sponsored in part by DFG (For primary document see N85-34991 23-93)

(SH-7.1-8) Avail: NTIS HC as boxed set only $200/MF A01 per volume or E99 per entire set CSCL 03B

Through the interaction of galactic cosmic particle radiation (GCR) a wide variety of cosmogenic nuclides is produced in meteorites. They provide historical information about the cosmic radiation and the bombarded meteorites. An important way to understand the production mechanisms of cosmogenic nuclides in meteorites is to gather information about the depth and size dependence of the build-up of Galactic Rays Cosmic-secondary particles within meteorites of different sizes and chemical compositions. Simulation experiments with meteorite models offer an alternative to direct observation providing a data basis to describe the development and action of the secondary cascade induced by the GCR in meteorites. E.A.K.

N85-35101*# Cologne Univ. (West Germany). Dept. of Nuclear Chemistry.

DEPTH AND SIZE EFFECTS ON COSMOGENIC NUCLIDE PRODUCTION IN METEORITES

P. Englert *In* NASA. Goddard Space Flight Center 19th Intern. Cosmic Ray Conf., Vol. 5 Aug. 1985 p 394-397 refs (For primary document see N85-34991 23-93)

(SH-7.1-9) Avail: NTIS HC as boxed set only $200/MF A01 per volume or E99 per entire set CSCL 03B

The galactic cosmic particle radiation (GCR) can cause changes in condensed extraterrestrial matter in different ways. It can lose energy via ionization processes of induced nuclear reactions which lead to a wide variety of stable and radioactive cosmogenic nuclides. Heavy particles incur radiation damage in minerals such as olivine and pyroxene. Light particles predominantly tend to induce nuclear reactions, causing the development of a secondary particle cascade of neutrons, protons, pions and gamma-rays and the production of cosmogenic nuclides. Such processes are described by various models, which predict the depth and size dependent production of cosmogenic nuclides. E.A.K.

N85-35102*# Centre National de la Recherche Scientifique, Paris (France). Inst. d'Astrophysique.

SPALLOGENIC ORIGIN OF NUCLEI IN METEORITES

B. Zanda and J. Audouze (Lab. Rene Bernas) *In* NASA. Goddard Space Flight Center 19th Intern. Cosmic Ray Conf., Vol. 5 Aug. 1985 p 398-401 refs (For primary document see N85-34991 23-93)

(SH-7.1-10) Avail: NTIS HC as boxed set only $200/MF A01 per volume or E99 per entire set CSCL 03B

Results obtained from a model built to evaluate the different interactions between cosmic rays and meteorites are presented. The model, computes, fluxes as a function of depth inside the meteorite, taking into account energy losses by ionization and spallation reactions which induce both particle destruction and production. This procedure, in which particle fluxes and cross sections are treated independently from each other, differs significantly from the thick target approach based on the measurement of spallation products generated in accelerator experiments. E.A.K.

N85-35103*# California Univ., San Diego, La Jolla.

CLUSTERS AND CYCLES IN THE COSMIC RAY AGE DISTRIBUTIONS OF METEORITES

Martin F. Woodard and K. Marti *In* NASA. Goddard Space Flight Center 19th Intern. Cosmic Ray Conf., Vol. 5 Aug. 1985 p 402-405 refs (For primary document see N85-34991 23-93)

(SH-7.1-11) Avail: NTIS HC as boxed set only $200/MF A01 per volume or E99 per entire set CSCL 03B

Statistically significant clusters in the cosmic ray exposure age distributions of some groups of iron and stone meteorites were observed, suggesting epochs of enhanced collision and breakups. Fourier analyses of the age distributions of chondrites reveal no significant periods, nor does the same analysis when applied to iron meteorite clusters. E.A.K.

N85-35104*# Kanagawa Univ., Yokahama (Japan). Inst. of Physics.

THE 4He1H RATIOS IN THE CHEMICAL COMPOSITIONS OF SOLAR FLARE PARTICLES AND THE PRIMORDIAL SOLAR NEBULA **c92**

Kunitomo Sakurai *In* NASA. Goddard Space Flight Center 19th Intern. Cosmic Ray Conf., Vol. 5 Aug. 1985 p 406-409 refs (For primary document see N85-34991 23-93)

(SH-7.1-12) Avail: NTIS HC as boxed set only $200/MF A01 per volume or E99 per entire set CSCL 03B

The chemical abundances of solar flare particles are similar to those of galactic cosmic rays at their sources. In order to infer the 4He/1H ratio in the solar atmosphere, this ratio as observed in the interstellar gases was considered in addition to those which were contained of galactic cosmic rays and the stars classified as the early types. Since it is clear that the most of these ratios ever deduced for both of the Sun and solar flare particles are lower than those for the interstellar gases, this ratio suggests that hydrogens are relatively overabundant in the chemical abundances of the Sun and the primordial solar nebula as compared to those of the interstellar gases currently observed. E.A.K.

N85-35105*# Academy of Sciences (USSR), Leningrad. Physico-Technical Inst.

HIGH PRECISE MEASUREMENTS OF COSMOGENIC RADIOCARBON ABUNDANCE BY COMPLEX OF SCINTILLATION EQUIPMENTS

G. E. Kocharov, R. Ya. Metskvarishvili (Tbilisi State Univ.), and S. L. Tsereteli (Tbilisi State Univ.) *In* NASA. Goddard Space Flight Center 19th Intern. Cosmic Ray Conf., Vol. 5 Aug. 1985 p 410-413 refs (For primary document see N85-34991 23-93)

(SH-7.1-14) Avail: NTIS HC as boxed set only $200/MF A01 per volume or E99 per entire set CSCL 03B

The main characteristics of scintillation equipments which enable the measurements of radiocarbon content with high accuracy of 0.2 to 0.3% were considered. The complex of scintillation devices operated very well for the last 15 years and allowed the investigation of the temporal variation of solar activity and intensity of cosmic rays for the last 300 years. E.A.K.

N85-35106*# Academy of Sciences (USSR), Leningrad. Physico-Technical Inst.

RADIOCARBON CONTENT IN THE ANNUAL TREE RINGS DURING LAST 150 YEARS AND TIME VARIATION OF COSMIC RAYS

G. E. Kocharov, R. Ya. Metskvarishvili (Tbilisi State Univ.), and S. L. Tsereteli (Tbilisi State Univ.) *In* NASA. Goddard Space Flight Center 19th Intern. Cosmic Ray Conf., Vol. 5 Aug. 1985 p 414-417 refs (For primary document see N85-34991 23-93)

(SH-7.1-15) Avail: NTIS HC as boxed set only $200/MF A01 per volume or E99 per entire set CSCL 03B

The results of the high accuracy measurements of radiocarbon abundance in precisely dated tree rings in the interval 1800 to 1950 yrs are discussed. Radiocarbon content caused by solar activity is established. The temporal dependence of cosmic rays is constructed, by use of radio abundance data. E.A.K.

N85-35107*# Academy of Sciences (USSR), Moscow. Inst. of Geochemistry and Analytical Chemistry.
COSMOGENIC Mn-53 IN METEORITES
V. A. Alexeev and A. K. Lavrukhina *In* NASA. Goddard Space Flight Center 19th Intern. Cosmic Ray Conf., Vol. 5 Aug. 1985 p 418-421 refs (For primary document see N85-34991 23-93)
(SH-7.1-17) Avail: NTIS HC as boxed set only $200/MF A01 per volume or E99 per entire set CSCL 03B

The distributions of the Mn-53 contents in 106 nonantarctic and 112 antarctic chondrites were analyzed. A correlation analysis of these distributions showed that the correlation coefficient is a maximum r sub max = 0.75 plus or minus 0.03) when the histogram for antarctic chondrites is displaced by 40 plus or minus 8 dpm kg-1Fe towards lower Mn-53 contents. The distribution of Mn-53 saturated contents in nonantarctic ordinary chondrites was investigated as a function of their radiation age (T). It is found that the Mn-53 average content is higher by (21 plus or minus 9)% in H-chondrites with radiation age T approximately 12 Myr than in thse with T > 12 Myr. This effect can be attributed to the fact that a considerable proportion of H-chondrites with T < 12 Myr originates from a comet or from the objects of Chiron like, with the orbits more inclined to the ecliptic plane and/or more extended, which caused their irradiation by cosmic rays of higher intensity. R.J.F.

N85-35108*# Max-Planck-Inst. fuer Kernphysik, Heidelberg (West Germany).
RESULTS OF ULTRA-LOW LEVEL 71Ge COUNTING FOR APPLICATION IN THE GALLEX-SOLAR NEUTRINO EXPERIMENT AT THE GRAN SASSO UNDERGROUND PHYSICS LABORATORY
W. Hampel, G. Heusser, M. Huebner, J. Kiko, T. Kirsten, K. Schneider, and R. Schlotz *In* NASA. Goddard Space Flight Center 19th Intern. Cosmic Ray Conf., Vol. 5 Aug. 1985 p 422-425 refs (For primary document see N85-34991 23-93)
(SH-8.1-2) Avail: NTIS HC as boxed set only $200/MF A01 per volume or E99 per entire set CSCL 03B

It has been experimentally verified that the Ultra-Low-Level Counting System for the Gallex solar neutrino experiment is capable of measuring the expected solar up silon-flux to plus or minus 12% during two years of operation. Author

N85-35109*# Indore Univ. (India). Dept. of Physics.
CORRELATION BETWEEN SOLAR NEUTRINO FLUX AND OTHER SOLAR PHENOMENA **c92**
Siddheshwar Lal and A. Subramanian (Tata Inst. of Fundamental Research) *In* NASA. Goddard Space Flight Center 19th Intern. Cosmic Ray Conf., Vol. 5 Aug. 1985 p 426-429 refs (For primary document see N85-34991 23-93)
Avail: NTIS HC as boxed set only $200/MF A01 per volume or E99 per entire set CSCL 03B

A study was made of the solar neutrino data with a tank of CC14 located 4800 mwe underground for the period 1970 to 83. These observations are on the production rates of Ar37 atoms via the reaction upsilon sub e + Cl37 yields Ar37 plus e(-) in the tank caused presumably by a flux of neutrinos from the Sun. The idea of possible time variations in the data shown is discussed and an attempt is made to correlate the variations to two other phenomena of solar origin—the sunspot number and the geomagnetic Ap index. R.J.F.

N85-35110*# Kanagawa Univ., Yokahama (Japan). Inst. of Physics.
A POSSIBLE MECHANISM TO CAUSE THE QUASI-BIENNIAL VARIABILITY ON THE SOLAR NEUTRINO FLUX **c92**
Kunitomo Sakurai and Mitsuru Hasegawa *In* NASA. Goddard Space Flight Center 19th Intern. Cosmic Ray Conf., Vol. 5 Aug. 1985 p 430-433 refs (For primary document see N85-34991 23-93)
(SH-8.1-5) Avail: NTIS HC as boxed set only $200/MF A01 per volume or E99 per entire set CSCL 03B

It is suggested that the quasi-biennial change in the observed flux of the solar neutrinos is causally related to some non-linear process at the central core of the Sun, being associated with the charge in the central temperature. This process seems to be responsible for the physical adjustment of the internal structure of the Sun. Numerical simulation on this process is able to reproduce the quasi-biennial change in the flux of these neutrinos. Author

N85-35111*# Academy of Sciences, Potsdam (East Germany).
THE CONJECTURE CONCERNING TIME VARIATIONS IN THE SOLAR NEUTRINO FLUX **c92**
H. J. Haubold and E. Gerth *In* NASA. Goddard Space Flight Center 19th Intern. Cosmic Ray Conf., Vol. 5 Aug. 1985 p 434-437 refs (For primary document see N85-34991 23-93)
(SH-8.1-6) Avail: NTIS HC as boxed set only $200/MF A01 per volume or E99 per entire set CSCL 03B

The results of the Fourier transformation of the unequally-spaced time series of the recorded Ar-37 production rate of the solar neutrino experiment (runs 18 to 80, 1970 to 1983) are reviewed. Significance criteria for every period discovered by the harmonic analysis are determined. A Fourier synthesis of certain discovered harmonics are performed. It seems that the solar neutrino flux increases shock-like with a period of approximately 8.3 years and after that breaks down. Possible connections between the periods found by the harmonic analysis and several observed phenomena on the solar surface are indicated. R.J.F.

N85-35112*# Calcutta Univ. (India). Dept. of Applied Mathematics.
SOLAR NEUTRINO: FLUX, COSMIC RAYS AND THE 11 YEAR SOLAR CYCLE **c92**
Probhas Raychaudhuri *In* NASA. Goddard Space Flight Center 19th Intern. Cosmic Ray Conf., Vol. 5 Aug. 1985 p 438-441 refs (For primary document see N85-34991 23-93)
(SH-8.1-7) Avail: NTIS HC as boxed set only $200/MF A01 per volume or E99 per entire set CSCL 03B

It is shown that the results of maximum likelihood treatment of Monte Carlo simulation with constant production rate of 7.6 SNU and 1.Epsilon SNU are consistent with the constant production rate when the tests of hypotheses (e.g., t-test, sigma squared-test, Wilcoxon-Mann-Whitney test, run test, etc.) are applied to the two groups of data formed from sunspot minimum range and sunspot maximum range, whereas the real data pulsates with the solar activity cycle. It is shown that SN flux-change is in opposition phase to the solar activity cycle and lags behind the latter by about one year. A correlation between SN flux and the cosmic rays is suggested. Author

N85-35113*# Calcutta Univ. (India). Dept. of Applied Mathematics.
SOLAR NEUTRINOS, SOLAR FLARES, SOLAR ACTIVITY CYCLE AND THE PROTON DECAY **c92**
Probhas Raychaudhuri *In* NASA. Goddard Space Flight Center 19th Intern. Cosmic Ray Conf., Vol. 5 Aug. 1985 p 442-445 refs (For primary document see N85-34991 23-93)
(SH-8.1-8) Avail: NTIS HC as boxed set only $200/MF A01 per volume or E99 per entire set CSCL 03B

It is shown that there may be a correlation between the galactic cosmic rays and the solar neutrino data, but it appears that the neutrino flux which may be generated during the large solar cosmic ray events cannot in any way effect the solar neutrino data in Davis experiment. Only initial stage of mixing between the solar core and solar outer layers after the sunspot maximum in the solar activity cycle can explain the higher (run number 27 and 71) of solar neutrino data in Davis experiment. But solar flare induced atmospheric neutrino flux may have effect in the nucleon decay detector on the underground. The neutrino flux from solar cosmic rays may be a useful guide to understand the background

of nucleon decay, magnetic monopole search, and the detection of neutrino flux in sea water experiment. Author

N85-35114*# Kobe Univ. (Japan). Graduate School of Science and Technology.

NEUTRINO PRODUCTION FROM THE SOLAR ATMOSPHERE **c92**

H. Inazawa, K. Kobayakawa, and T. Kitamura (Tokyo Univ., Tanashi) *In* NASA. Goddard Space Flight Center 19th Intern. Cosmic Ray Conf., Vol. 5 Aug. 1985 p 446-449 refs (For primary document see N85-34991 23-93)

(SH-8.1-9) Avail: NTIS HC as boxed set only $200/MF A01 per volume or E99 per entire set CSCL 03B

When the high energy primary cosmic rays enter near the solar surface, they pass through a thick matter but having a low density. If the density and path length satisfy an appropriate condition, the primaries collide with the constituents near the solar sphere (almost protons) and produce pions and kaons, most of which decay into mu plus nu sub mu without successive hadron collisions. Muons also decay into NU sub mu and NU sub e before reaching the Earth. The neutrino flux of which the producer is matter near the solar surface is computed by solving cascade diffusion equations. The calculated differential flux of muon neutrino at 1 TeV is 1 X 10 to the minus 13 power (GeV. cm square centimeters 2.s.ster)(-1) which is rather difficult to be observed in the present apparatuses or DUMAND. Author

N85-35115*# Academy of Sciences (USSR), Moscow. Physical Inst.

SOLAR COSMIC RAY BURSTS AND SOLAR NEUTRINO FLUXES **c92**

G. A. Basilevakaya, S. I. Nikolsky, Yu. I. Stozhkov, and T. N. Charakhchyan (Moscow State Univ.) *In* NASA. Goddard Space Flight Center 19th Intern. Cosmic Ray Conf., Vol. 5 Aug. 1985 p 450-453 refs (For primary document see N85-34991 23-93)

(SH-8.1-10) Avail: NTIS HC as boxed set only $200/MF A01 per volume or E99 per entire set CSCL 03B

The neutrino flux detected in the C1-Ar experiment seems to respond to the powerful solar cosmic ray bursts. The ground-based detectors, the balloons and the satellites detect about 50% of the bursts of soalr cosmic ray generated on the Sun's visible side. As a rule, such bursts originate from the Western side of the visible solar disk. Since the solar cosmic ray bursts are in opposite phase withthe 11-year galactic cosmic ray cycle which also seems to be reflected by neutrino experiment. The neutrino generation in the bursts will flatten the possible 11-year behavior of the AR-37 production rate, Q, in the Cl-Ar experiment. The detection of solar-flare-generated gamma-quanta with energies above tens of Mev is indicative of the generation of high-energy particles which in turn may produce neutrinos. Thus, the increased Q during the runs, when the flare-generated high energy gamma-quanta have been registered, may be regarded as additional evidence for neutrino geneation in the solar flare processes. Author

N85-35116*# Pennsylvania Univ., Philadelphia. Dept. of Physics.

THREE DIMENSIONAL CALCULATION OF FLUX OF LOW ENERGY ATMOSPHERIC NEUTRINOS

H. Lee and S. A. Bludman *In* NASA. Goddard Space Flight Center 19th Intern. Cosmic Ray Conf., Vol. 5 Aug. 1985 p 454-457 refs Sponsored in part by DOE (For primary document see N85-34991 23-93)

(SH-8.1-11) Avail: NTIS HC as boxed set only $200/MF A01 per volume or E99 per entire set CSCL 03B

Results of three-dimensional Monte Carlo calculation of low energy flux of atmospheric neutrinos are presented and compared with earlier one-dimensional calculations [1,2] valid at higher neutrino energies. These low energy neutrinos are the atmospheric background in searching for neutrinos from astrophysical sources. Primary cosmic rays produce the neutrino flux peaking at near E sub=40 MeV and neutrino intensity peaking near E sub v=100 MeV. Because such neutrinos typically deviate by 20 approximately 30 from the primary cosmic ray direction, three-dimensional effects are important for the search of atmospheric neutrinos. Nevertheless, the background of these atmospheric neutrinos is negligible for the detection of solar and supernova neutrinos. Author

N85-35117*# Tata Inst. of Fundamental Research, Bombay (India).

DETECTOR CALIBRATION OF THE INDIAN COSMIC RAY EXPERIMENT (IONS) IN SPACE-SHUTTLE SPACELAB-13

J. S. Yadav, S. Biswas, and N. Durgaprasad *In* NASA. Goddard Space Flight Center 19th Intern. Cosmic Ray Conf., Vol. 5 Aug. 1985 p 458-461 refs (For primary document see N85-34991 23-93)

(SH-9.1-2) Avail: NTIS HC as boxed set only $200/MF A01 per volume or E99 per entire set CSCL 03B

In the Indian cosmic ray experiment (IONS) in Spacelab-3 the intention is to study nuclei up to iron in low energy cosmic rays, using CR-39 (DOP) detectors. CR-39 (DOP) was exposed to He4, C12, O16, Ne20, Si28, Ar40, Cr52 and Fe56 accelerated beams from various accelerator facilities available around the world. Different beam energies and exposure angles were used. From these exposures, the charge resolution and energy resolution for the detector in the region of interest were studied. The effect of pre-annealing and depth on the response of our detector was studied. For isotopic resolution, exposed the detector samples were exposed to Ne2O and Ne22 accelerated beams. Samples of CR-39 (DOP) exposed to different accelerated heavy ions were kept in the detector module to take into account the effect of ambient conditions on detector response during the flight. Author

N85-35118*# Instituto Nacional de Tecnica Aeroespacial, Madrid (Spain). Grupos Cientificos CONIE.

A SILICON SURFACE BARRIER TELESCOPE FOR SOLAR PARTICLES IDENTIFICATION **c92**

J. Sequeiros and J. Medina *In* NASA. Goddard Space Flight Center 19th Intern. Cosmic Ray Conf., Vol. 5 Aug. 1985 p 462-465 refs Sponsored by Comision Asesora de Investigacion Cientifica y Technica (For primary document see N85-34991 23-93)

(SH-9.1-3) Avail: NTIS HC as boxed set only $200/MF A01 per volume or E99 per entire set CSCL 03B

From the results three conclusions can be made: (1) the detector system described and tested is capable of good charge resolution from He to Al although beyond Ne the statistic is very poor; (2) in the high gain mode, isotopic resolution has been achieved for Li-6/Li-7 Be-7/Be-9; (3) the much higher yield of He over He and of Be-9 over Be-10 in these types of nuclear reactions prevents obtaining experimental evidence of those isotopes, although it is believed that, at least He-3/He-4 can be resolved under other more favorable conditions (i.e., solar He-3-rich events). R.J.F.

N85-35119*# Gujarat Univ., Ahmedabad (India). Dept. of Physics.

A BI-DIRECTIONAL CHARGED PARTICLE TELESCOPE TO OBSERVE FLUX, ENERGY SPECTRUM AND ANGULAR DISTRIBUTION OF RELATIVISTIC AND NON-RELATIVISTIC PARTICLES

S. D. Verma, S. P. Bhatnagar, and S. K. Kothari *In* NASA. Goddard Space Flight Center 19th Intern. Cosmic Ray Conf., Vol. 5 Aug. 1985 p 466-469 refs Sponsored by the Indian Space Research Organization (For primary document see N85-34991 23-93)

(SH-9.1-4) Avail: NTIS HC as boxed set only $200/MF A01 per volume or E99 per entire set CSCL 03B

A Charged Particle Telescope (CPT) was designed, fabricated and calibrated to make the following observations: (1) discrimination between various singly charged particles, e.g., electrons, muons and protons, in about 5 to 100 MeV energy range; (2) measurement of the flux and the energy of the charged particles incident to the telescope from two opposite directions and stopping in the telescope, thus obtaining flux and energy spectrum of downward and upward moving charged particles; and (3) measurement of the broad angular distribution of selected particles as a function of azimuthal angle. This telescope can be used to study low energy electron, muon and proton energy spectra. The experiment was

flown in a high altitude balloon from Hyderabad, India, in December 1984. This same equipment is also useful in ground level electron, muon spectrum study. Author

N85-35120*# California Univ., San Diego, La Jolla.
PHOTOMETRIC AND SPECTROSCOPIC GAMMA-RAY OBSERVATIONS OF SOLAR TRANSIENT PHENOMENA USING LONG DURATION BALLOONS
M. R. Pelling, F. Duttweiler, R. F. Lin (California Univ., Berkeley), W. K. Levedahl (California Univ., Berkeley), H. Primbach (California Univ., Berkeley), D. W. Curtis (California Univ., Berkeley), and K. C. Burley (Centre dEtude Spatiales des Rayonnements) *In* NASA. Goddard Space Flight Center 19th Intern. Cosmic Ray Conf., Vol. 5 Aug. 1985 p 470-473 refs (For primary document see N85-34991 23-93)
(SH-9.1-5) Avail: NTIS HC as boxed set only $200/MF A01 per volume or E99 per entire set CSCL 03B

A program currently in progress to conduct extended duration spectroscopic and photometric observation of solar X-ray phenomena from balloons is described. High photometric sensitivity to weak hard X-ray bursts is attained using a 600 sq cm array of phoswich scintillators. High spectral resolution for stronger bursts is available from an array of planar germanium detectors. These instruments are carried in a novel balloon gondola designed for the 15 to 20 day float durations available through using conventional zero pressure balloons in the radiation controlled (RACOON) mode. Author

N85-35121*# Max-Planck-Inst. fuer Extraterrestrische Physik, Garching (West Germany).
MONTE CARLO CALIBRATION OF THE SMM GAMMA RAY SPECTROMETER FOR HIGH ENERGY GAMMA RAYS AND NEUTRONS
J. F. Cooper, C. Reppin, D. J. Forrest (New Hampshire Univ.), E. L. Chupp (New Hampshire Univ.), G. H. Share (NRL, Washington), and R. L. Kinzer (NRL, Washington) *In* NASA. Goddard Space Flight Center 19th Intern. Cosmic Ray Conf., Vol. 5 Aug. 1985 p 474-477 refs (For primary document see N85-34991 23-93)
(Contract NAS5-23761; NASA Order S-70926-A)
(SH-9.1-6) Avail: NTIS HC as boxed set only $200/MF A01 per volume or E99 per entire set CSCL 03B

The Gamma Ray Spectrometer (GRS) on the Solar Maximum Mission spacecraft was primarily designed and calibrated for nuclear gamma ray line measurements, but also has a high energy mode which allows the detection of gamma rays at energies above 10 MeV and solar neutrons above 20 MeV. The GRS response has been extrapolated until now for high energy gamma rays from an early design study employing Monte Carlo calculations. The response to 50 to 600 MeV solar neutrons was estimated from a simple model which did not consider secondary charged particles escaping into the veto shields. In view of numerous detections by the GRS of solar flares emitting high energy gamma rays, including at least two emitting directly detectable neutrons, the calibration of the high energy mode in the flight model has been recalculated by the use of more sophisticated Monte Carlo computer codes. New results presented show that the GRS response to gamma rays above 20 MeV and to neutrons above 100 MeV is significantly lower than the earlier estimates. Author

N85-35122*# Kunsan National Univ., Miryoun-dong, Kunsan-City (South Korea). Dept. of Physics.
COMPARISONS OF MONTHLY MEAN COSMIC RAY COUNTING RATES OBSERVES FROM WORLDWIDE NETWORK OF NEUTRON MONITORS
Jai Young Ryu and Masami Wada (Inst. of Physical and Chemical Research, Tokyo) *In* NASA. Goddard Space Flight Center 19th Intern. Cosmic Ray Conf., Vol. 5 Aug. 1985 p 478-481 refs (For primary document see N85-34991 23-93)
(SH-9.1-7) Avail: NTIS HC as boxed set only $200/MF A01 per volume or E99 per entire set CSCL 03B

In order to examine the stability of neutron monitor observation, each of the monthly average counting rates of a neutron monitors is correlated to those of Kiel neutron monitor. The regression coefficients thus obtained are compared with the coupling coefficients of isotropic intensity radiation. The results of the comparisons for five year periods during 1963 to 1982, and for whole period are given. The variation spectrum with a single power law with an exponent of -0.75 up to 50 GV is not so unsatisfactory one. More than one half of the stations show correlations with the coefficient greater than 0.9. Some stations have shifted the level of mean counting rates by changing the instrumental characteristics which can be adjusted. Author

N85-35123*# Academia Sinica, Beijing (China). Inst. of Space Physics.
RECORDING SYSTEM FOR THE SOLAR NEUTRON MONITORING AT MT. NORIKURA **c92**
Shao Hua Yu, M. Kusunose (Kochi Univ.), H. Sasaki (Kochi Univ.), N. Ohmori (Kochi Univ.), K. Takahashi (Inst. of Physical and Chemical Research, Tokyo), and M. Wada (Inst. of Physical and Chemical Research, Tokyo) *In* NASA. Goddard Space Flight Center 19th Intern. Cosmic Ray Conf., Vol. 5 Aug. 1985 p 482-485 refs (For primary document see N85-34991 23-93)
(SH-9.1-8) Avail: NTIS HC as boxed set only $200/MF A01 per volume or E99 per entire set CSCL 03B

To monitor solar neutron events, a new recording system will be installed at Mt. Norikura Cosmic Ray Observatory. The recording system is composed of a pulse counter with clock and a microcomputer with minifloppy disk. The counter and the microcomputer are connected through the General Purpose Interface Bus line. The one minute total count of the neutron monitor is recorded on the minifloppy disk. Author

N85-35124*# Kochi Univ., Akebono (Japan). Dept. of Physics.
BURST SIZE DISTRIBUTIONS IN THE DIGITIZED DATA OF THE ION CHAMBERS T MT. NORIKURA AND SEA LEVEL STATIONS
M. Kusunose, M. Wada (Inst. of Physical and Chemical Research, Tokyo), S. Kudo (Inst. of Physical and Chemical Research, Tokyo), and L. S. Chuang (Chinese Univ. of Hong Kong) *In* NASA. Goddard Space Flight Center 19th Intern. Cosmic Ray Conf., Vol. 5 Aug. 1985 p 486-489 refs (For primary document see N85-34991 23-93)
(SH-9.1-9) Avail: NTIS HC as boxed set only $200/MF A01 per volume or E99 per entire set CSCL 03B

A practical and simple method for burst rejection is applied to the digitized data of cosmic ray ion chambers at Mt. Norikura, Tokyo and Kochi. As a result of burst rejection, the burst size frequency distributions in the digitized data at mountain altitude and sea level ion chambers is obtained. Results show that there are no significant differences between the digital and analog data processing in burst rejection. Author

N85-35125*# Academy of Sciences (USSR), Moscow. Inst. of Terrestrial Magnetism.
SENSITIVITY OF SINGLE AND MULTIPLE COSMIC RAY NEUTRONS TO THE SURROUNDING MEDIUM IN A LEAD-FREE MONITOR
I. V. Dorman, L. T. Dorman, T. Ya. Libin, and V. K. Korotkov (SVKNII) *In* NASA. Goddard Space Flight Center 19th Intern. Cosmic Ray Conf., Vol. 5 Aug. 1985 p 490-493 refs (For primary document see N85-34991 23-93)
(SH-9.1-10) Avail: NTIS HC as boxed set only $200/MF A01 per volume or E99 per entire set CSCL 03B

In 1981-1985 the neutron component of cosmic rays was recorded, the effect of cosmic ray multiplication in lead being disregarded. The recording device consisted of neutron counters placed in a polyethylene retarder (polyethylene tubes with wall thickness of 2 cm). The device registered neutrons formed directly on the surface or not deep underground; the intensity of neutrons depended on the chemical composition of the substance. The neutron component was also measured in the Moscow Canal, Belomor-Baltic Canal, and in the Atlantic Ocean. The time variation of 5 minute data of the intensity obtained in the Belomor-Baltic Canal and in the Atlantic Ocean relative to the mean value in the open sea (in %) is presented. Author

N85-35126*# Chinese Univ. of Hong Kong, Shatin. Dept. of Physics.

PLASTIC SCINTILLATORS IN COINCIDENCE FOR THE STUDY OF MULTI-PARTICLE PRODUCTION OF SEA LEVEL COSMIC RAYS IN DENSE MEDIUM

L. S. Chuang, K. W. Chan, and M. Wada (Inst. of Physical and Chemical Research, Tokyo) *In* NASA. Goddard Space Flight Center 19th Intern. Cosmic Ray Conf., Vol. 5 Aug. 1985 p 494-497 refs (For primary document see N85-34991 23-93)

(SH-9.1-11) Avail: NTIS HC as boxed set only $200/MF A01 per volume or E99 per entire set CSCL 03B

Cosmic ray particles at sea level penetrate a thick layer of dense medium without appreciable interaction. These penetrating particles are identified with muons. The only appreciable interaction of muons are by knock on processes. A muon may have single, double or any number of knock on with atoms of the material so that one, two, three or more particles will come out from the medium in which the knock on processes occur. The probability of multiparticle production is expected to decrease with the increase of multiplicity. Measurements of the single, double, and triple particles generated in a dense medium (Fe and Al) by sea level cosmic rays at 22.42 N. Lat. and 114.20 E. Long. (Hong Kong) are presented using a detector composed of two plastic scintillators connected in coincidence. Author

N85-35127*# Case Western Reserve Univ., Cleveland, Ohio. Dept. of Physics.

SONTRAC: A SOLAR NEUTRON TRACK CHAMBER DETECTOR **c92**

Glenn M. Frye, Jr., Thomas L. Jenkins, and Alan Owens *In* NASA. Goddard Space Flight Center 19th Intern. Cosmic Ray Conf., Vol. 5 Aug. 1985 p 498-501 refs (For primary document see N85-34991 23-93)

(SH-9.1-12) Avail: NTIS HC as boxed set only $200/MF A01 per volume or E99 per entire set CSCL 03B

The recent detection on the solar maximum mission (SMM) satellite of high energy neutrons emitted during large solar flares has provided renewed incentive to design a neutron detector which has the sensitivity, energy resolution, and time resolution to measure the neutron time and energy spectra with sufficient precision to improve our understanding of the basic flare processes. Over the past two decades a variety of neutron detectors has been flown to measure the atmospheric neutron intensity above 10 MeV and to search for solar neutrons. The SONTRAC (Solar Neutron Track Chamber) detector, a new type of neutron detector which utilizes n-p scattering and has a sensitivity 1-3 orders of magnitude greater than previous instruments in the 20-200 MeV range is described. The energy resolution is 1% for neutron kinetic energy, T sub n $>$ 50 MeV. When used with a coded aperture mask at 50 m (as would be possible on the space station) an angular resolution of approx. 4 arc sec could be achieved, thereby locating the sites of high energy nuclear interactions with an angular precision comparable to the existing X-ray experiments on SMM. The scintillation chamber is investigated as a track chamber for high energy physics, either by using arrays of scintillating optical fibers or by optical imaging of particle trajectories in a block of scintillator. Author

N85-35128*# Potchefstroom Univ. for Christian Higher Education (South Africa). Dept. of Physics.

THE NEUTRON MODERATED DETECTOR AND GROUNDBASED COSMIC RAY MODULATION STUDIES

P. H. Stoker and B. C. Raubenheimer *In* NASA. Goddard Space Flight Center 19th Intern. Cosmic Ray Conf., Vol. 5 Aug. 1985 p 502-505 refs (For primary document see N85-34991 23-93)

(SH-9.1-13) Avail: NTIS HC as boxed set only $200/MF A01 per volume or E99 per entire set CSCL 03B

Reports appear on modulation studies with the neutron monitor without lead. Some of these studies cast doubt on the reliability of this detector. The stability of the neutron moderated detector (NMD) at Sanae, Antarctic is discussed. The barometric coeficient of the 4NMD for epoch 1976 appears not to differ statistically from the 0.73%/mb of the 3NM64. The monthly averaged hourly counting rate of our 4NMD and 3NM64 correlates very well (correlation coefficient: 98%) over the years from 1974-1984, with the 4NMD showing a 8% larger long term modulation effect than the 3NM64, indicating a difference in sensitivities of the two detectors. From this difference in sensitivities spectra of ground level solar proton events and modulation functions of Forbush decreases are deduced. Author

N85-35129*# Shinshu Univ., Matsumoto (Japan). Dept. of Physics.

NEW MATSUSHIRO UNDERGROUND COSMIC RAY STATION (220 M.W.E. IN DEPTH)

S. Mori, S. Yasue, S. Sagisaka, K. Chino, S. Akahane, T. Higuchi, M. Ozaki, and M. Ichinose *In* NASA. Goddard Space Flight Center 19th Intern. Cosmic Ray Conf., Vol. 5 Aug. 1985 p 506-509 refs (For primary document see N85-34991 23-93)

(SH-9.1-14) Avail: NTIS HC as boxed set only $200/MF A01 per volume or E99 per entire set CSCL 03B

A new underground cosmic ray station has been opened at Matsushiro, Japan, and a multidirectional (17 directional channels) muon telescope has been installed at an effective vertical depth of 220 m.w.e. The counting rates are; 8.7 x 10,000/hr for the wide vertical component and 2.0 x 10,000/hr for the vertical component. Continuous observation has been performed since March 22,1984. Some details of the telescope and preliminary analyzed results of the data are presented. Author

N85-35130*# Air Force Geophysics Lab., Hanscom AFB, Mass.

A SUGGESTED STANDARDIZED FORMAT FOR COSMIC RAY GROUND-LEVEL EVENT DATA

M. A. Shea, D. F. Smart, M. Wada (Inst. of Physical and Chemical Research, Tokyo), and A. Inoue (Inst. of Physical and Chemical Research, Tokyo) *In* NASA. Goddard Space Flight Center 19th Intern. Cosmic Ray Conf., Vol. 5 Aug. 1985 p 510-513 ref (For primary document see N85-34991 23-93)

(SH-9.1-15) Avail: NTIS HC as boxed set only $200/MF A01 per volume or E99 per entire set CSCL 03B

A standardized format is suggested for the archival storage and exchange of neutron monitor data obtained during solar flare initiated ground level cosmic ray events. Using the data for the 7 May 1978 ground level event, a format has been developed that incorporates hourly data preceding and following the event and small time interval data immediately before and during the event. Provision has been made for the inclusion of uncorrected and corrected data as well as the atmospheric pressure. The cosmic ray intensity data are then reduced to a standard counting rate of counts per second facilitating the graphing and comparison of these data for various analyses. Author

N85-35131*# Okayama Univ. of Science (Japan).

THE READ-OUT SYSTEM OF SPATIAL DISTRIBUTION OF THERMOLUMINESCENCE IN METEORITES

Kiyotaka Ninagawa, Isac Yamamoto, Yasumasa Takano, Tomonori Wada, Yoshihiko Yamashita, and Nobuo Takaoka *In* NASA. Goddard Space Flight Center 19th Intern. Cosmic Ray Conf., Vol. 5 Aug. 1985 p 514-517 refs (For primary document see N85-34991 23-93)

(SH-9.1-16) Avail: NTIS HC as boxed set only $200/MF A01 per volume or E99 per entire set CSCL 03B

The thermoluminescence (TL) technique used for dating the terrestrial age of meteorites is based on the TL fading of interior samples. The depth dependence of the TL for Antarctic meteorites with fusion crust is measured. Usually, meteorites are powdered and their TL measured under a photomultiplier. In this case, a TL spatial distribution of a cross section of antarctic meteorites is measured using a read out system of spatial distribution of TL, since a meteorite is made up of inhomogeneous material. Antarctic meteorites MET-78028(L6) and ALH-77278(L13) are used. Author

N85-35132*# Academy of Sciences (USSR), Moscow. Inst. of Terrestrial Magnetism, Ionosphere and Radio Wave Propagation.

METHODS AND SOFTWARE FOR COSMIC RAY SCINTILLA-

TION STUDIES
O. V. Gulinsky, L. I. Dorman, and R. E. Prilutsky *In* NASA. Goddard Space Flight Center 19th Intern. Cosmic Ray Conf., Vol. 5 Aug. 1985 p 518-520 refs (For primary document see N85-34991 23-93)
(SH-9.1-17) Avail: NTIS HC as boxed set only $200/MF A01 per volume or E99 per entire set CSCL 03B

The principal instrument used in cosmic ray scintillation studies is the spectra constructed from intensive observation. This method has its drawbacks in that the statistical characteristics of the process undergo essential reconstruction, i.e., the process becomes nonstationary from the viewpoint of such phenomena as Forbush decrease and during solar flares. The software used to process the above includes the direct Fourier transform and its modifications, autoregressive processes, and instantaneous spectrum methods. Used in various combinations, they prove helpful in handling the time series. Author

N85-35133*# Academia Sinica, Beijing (China). Inst. of Space Physics.
THE INFLUENCES OF THE GALACTIC COSMIC RAY ON THE ATMOSPHERIC OZONE
Zonghai Ye, Shunsheng Xue, and Lianying Wang *In* NASA. Goddard Space Flight Center 19th Intern. Cosmic Ray Conf., Vol. 5 Aug. 1985 p 521-524 refs (For primary document see N85-34991 23-93)
(SH-10.1-1) Avail: NTIS HC as boxed set only $200/MF A01 per volume or E99 per entire set CSCL 03B

The relationship between the yearly variations of cosmic ray intensity and ozone in the atmosphere, and the ozone disturbance initiated by the Forbush decrease of 1965-1976 is analyzed. The data on cosmic ray intensity were selected from the records of the super neutron monitor at Deep River station and the ionization chamber at Beijing station. Ozone data were taken from Resolute (Canada), Bismark (N. Dakota, USA), Kagoshima (Japan), and Kodaikanal (India). The statistical results show that ozone is prominently modulated and disturbed by the 11 year variation and the Forbush decrease in the galactic cosmic ray. F.M.R.

N85-35134*# Hubei Research Inst. of Environmental Protection, Wuhan (China).
USING THE INFORMATION OF COSMIC RAYS TO PREDICT INFLUENCE EPIDEMIC
Zhen-dong Yu *In* NASA. Goddard Space Flight Center 19th Intern. Cosmic Ray Conf., Vol. 5 Aug. 1985 p 525-528 refs (For primary document see N85-34991 23-93)
(SH-10.1-2) Avail: NTIS HC as boxed set only $200/MF A01 per volume or E99 per entire set CSCL 03B

A correlation between the incidence of influenza pandemics and increased cosmic ray activity is made. A correlation is also made between the occurrence of these pandemics and the appearance of bright novae, e.g., Nova Eta Car. Four indices based on increased cosmic ray activity and novae are proposed to predict future influenza pandemics and viral antigenic shifts. F.M.R.

N85-35135*# Hubei Research Inst. of Environmental Protection, Wuhan (China).
STRONG EARTHQUAKES, NOVAE AND COSMIC RAY ENVIRONMENT
Zeng-dong Yu *In* NASA. Goddard Space Flight Center 19th Intern. Cosmic Ray Conf., Vol. 5 Aug. 1985 p 529-532 refs (For primary document see N85-34991 23-93)
(SH-10.1-3) Avail: NTIS HC as boxed set only $200/MF A01 per volume or E99 per entire set CSCL 03B

Observations about the relationship between seismic activity and astronomical phenomena are discussed. First, after investigating the seismic data (magnitude 7.0 and over) with the method of superposed epochs it is found that world seismicity evidently increased after the occurring of novae with apparent magnitude brighter than 2.2. Second, a great many earthquakes of magnitude 7.0 and over occurred in the 13th month after two of the largest ground level solar cosmic ray events (GLEs). The causes of three high level phenomena of global seismic activity in 1918-1965 can be related to these, and it is suggested that according to the information of large GLE or bright nova predictions of the times of global intense seismic activity can be made. Author

N85-35136*# Moscow State Univ. (USSR). Inst. of Nuclear Physics.
OBSERVATION OF NUCLEI WITH ENERGIES 8-30 MeV PER NUCLEON IN THE EARTH'S MAGNETOSPHERE AT THE ALTITUDES 350 KM
V. V. Bobrovskaya, N. L. Grigorov, Yu. P. Gorleev, D. A. Zhuravlev, R. A. Nymmik, A. V. Podgurskaya, L. G. Smolenski, Ch. A. Tretyakova, I. V. Gordeev, V. I. Iyagushin et al *In* NASA. Goddard Space Flight Center 19th Intern. Cosmic Ray Conf., Vol. 5 Aug. 1985 p 533-535 refs (For primary document see N85-34991 23-93)
(SH-10.1-5) Avail: NTIS HC as boxed set only $200/MF A01 per volume or E99 per entire set CSCL 03B

Observations of the flux of nuclei with an energy of IO MeV per nucleon on the Salyut-7 Station in September 1984 are presented. The observed flux is smaller by a factor of 50 than the flux detected in May, 1981. Author

N85-35137*# Kiel Univ. (West Germany). Inst. fuer Reine und Angewandte Kernphysik.
MEASUREMENT OF LOW ENERGY COSMIC RAYS ABOARD SPACELAB-1 Abstract Only
R. Beaujean, K. Oschlies, and W. Enge *In* NASA. Goddard Space Flight Center 19th Intern. Cosmic Ray Conf., Vol. 5 Aug. 1985 p 536 (For primary document see N85-34991 23-93)
(SH-10.1-6) Avail: NTIS HC as boxed set only $200/MF A01 per volume or E99 per entire set CSCL 03B

In December 1983 the first Spacelab mission was launched for a duration of 10 days. Aboard was the Kiel experiment Isotopic Stack designed for measurement of heavy cosmic ray nuclei with nuclear charge equal to or greater than 3 and energies up to some 100MeV/nuc. One part of the stack was rotated in well defined steps registered by an angle encoder to receive information on impact times of the nuclei. Using this time resolving system geomagnetically forbidden particles can be detected. The chemical composition and energy spectra of mainly CNO particles are examined using a rotated 300 microns m thick CR-39 foil beneath a fixed 100 microns m thick Kodak-Cellulose Nitrate foil. About 600 sq cm have been scanned yielding nearly 100 nuclear tracks within an energy range of approximately 8 to 30 MeV/nuc. The calibration is done by means of a postflight irradiation with 410 MeV/nuc Fe-56 at Berkeley Laboratory, California, USA. Relative abundances and energy spectra are presented. Author

N85-35138*# Kiel Univ. (West Germany). Inst. fuer Reine under Angeswandte Kernphysik.
HEAVY COSMIC RAY MEASUREMENT ABOARD SPACELAB-1 Abstract Only
R. Beaujean, J. Krause, E. Fischer, and W. Enge *In* NASA. Goddard Space Flight Center 19th Intern. Cosmic Ray Conf., Vol. 5 Aug. 1985 p 537 (For primary document see N85-34991 23-93)
(SH-10.1-7) Avail: NTIS HC as boxed set only $200/MF A01 per volume oe E99 per entire set CSCL 03B

A stack of CR-39 plastic track detectors was exposed to cosmic radiation during the 10 days mission aboard Spacelab-1. A part of the stack was rotated one revolution within 7 days. The impact time of most of the particles was correlated with the orbit position of the shuttle and thus with geomagnetic field parameters. The analysis of heavy particles with charge Z 6 in the energy range 50-150 MeV per nucleon with special emphasis on geomagnetically forbidden particles is reported. Author

N85-35139*# Kharkov State Univ. (USSR).
SPORADIC RADIO EMISSION CONNECTED WITH A DEFINITE MANIFESTATION OF SOLAR ACTIVITY IN THE NEAR EARTH SPACE c92
A. V. Dudnic, I. I. Zaljubovski, V. M. Kartashev, and E. S. Shmatko *In* NASA. Goddard Space Flight Center 19th Intern. Cosmic Ray Conf., Vol. 5 Aug. 1985 p 538-541 (For primary document see

N85-34991 23-93)
(SH-10.1-8) Avail: NTIS HC as boxed set only $200/MF A01 per volume or E99 per entire set CSCL 03B

Sporadic radio emission of near Earth space at the frequency of 38 MHz is shown to appear in the event of a rapid development of instabilities in the ionospheric plasma. The instabilities are generated due to primary ionospheric disturbances occurring under the influence of solar chromospheric flares. Author

N85-35140*# Kharkov State Univ. (USSR).
NEAR EARTH SPACE SPORADIC RADIO EMISSION BUSTS OCCURRING DURING SUNRISE
A. V. Dudnik, I. I. Zaljubovsky, V. M. Kartashev, A. V. Lasarev, and E. S. Shmatko *In* NASA. Goddard Space Flight Center 19th Intern. Cosmic Ray Conf., Vol. 5 Aug. 1985 p 542-545 (For primary document see N85-34991 23-93)
(SH-10.1-9) Avail: NTIS HC as boxed set only $200/MF A01 per volume or E99 per entire set CSCL 03B

During the period of low solar activity at sunrise the effect of sporadic high frequency near Earth space radio emission was experimentally discovered at middle latitudes. The possible mechanism of its origin is discussed. Author

N85-35141*# Smithsonian Astrophysical Observatory, Cambridge, Mass.
RESEARCH OF ADVANCED TECHNIQUES FOR X-RAY DETECTORS AND TELESCOPES WITH APPLICATIONS TO ROCKETS AND THE LAMAR FACILITY Semiannual Report, 1 Jul. 1984 - 30 Jun. 1985
Paul Gorenstein Aug. 1985 18 p
(Grant NsG5-138)
(NASA-CR-176161; NAS 1.26:176161; SAR-16; SAR-17) Avail: NTIS HC A02/MF A01 CSCL 03B

A program for the development of high throughput instrumentation for X-ray astronomy based upon focusing optics is being carried out by the Smithsonian Astrophysical Observatory. The instrumentation is applicable to investigations requiring large area focusing optics for direct imaging or dispersive spectroscopy. The long range goals of this program are the development of telescopes and gratings for future major X-ray astronomy facilities, including additions to the LAMAR OSS-2/SHEAL experiment after the initial flights. Tests of the devices and their more immediate utilization in scientific investigations can be carried out with SPARTAN payloads deployed and retrieved by the Space Shuttle. However, the present backlog of approved SPARTAN missions is longer than the three-year duration of the program described in this program. Laboratory studies and breadboarding of instrumentation are discussed. B.W.

N85-34781*# California Inst. of Tech., Pasadena.
THE ENERGY SPECTRUM OF JOVIAN ELECTRONS IN INTERPLANETARY SPACE
S. P. Christon, A. C. Cummings, E. C. Stone, and W. R. Webber (New Hampshire Univ.) *In* NASA. Goddard Space Flight Center 19th Intern. Cosmic Ray Conf., Vol. 4 Aug. 1985 p 200 refs (For primary document see N85-34729 23-93)
(Contract NAS7-918; Grant NGR-05-002-160)
(SH-1.5-18) Avail: NTIS HC as boxed set only $200/MF A01 per volume or E99 per entire set CSCL 03B

N85-34782*# Franklin Inst., Newark, Del.
THE JOVIAN ELECTRON SPECTRUM: 1978-1984
Paul A. Evenson, Peter Meyer (Chicago Univ.), and Dan Moses (Chicago Univ.) *In* NASA. Goddard Space Flight Center 19th Intern. Cosmic Ray Conf., Vol. 4 Aug. 1985 p 201-204 refs (For primary document see N85-34729 23-93)
(Contract NAS5-26680; Grant NGL-14-01-005)
(SH-1.5-19) Avail: NTIS HC as boxed set only $200/MF A01 per volume or E99 per entire set CSCL 03B

N85-32814*# Malaya Univ., Kuala-Lumpur. Dept. of Mathematics.
SECOND-ORDER COMPTON-GETTING EFFECT ON ARBITRARY INTENSITY DISTRIBUTION
C. K. Ng *In* NASA. Goddard Space Flight Center 19th Intern. Cosmic Ray Conf., Vol. 4 Aug. 1985 p 326-329 refs (For primary document see N85-34729 23-92)
(SH-3.1-10) Avail: NTIS HC as boxed set only $200/MF A01 per volume or E99 per entire set CSCL 03B

N85-34824*# Academy of Sciences (USSR), Alma-Ata.
INVESTIGATION OF COSMIC RAY PROPAGATION IN INTERPLANETARY SPACE
E. A. Chebakova, E. V. Kolomeets, and V. N. Sevastyanov *In* NASA. Goddard Space Flight Center 19th Intern. Cosmic Ray Conf., Vol. 4 Aug. 1985 p 356-359 refs (For primary document see N85-34729 23-92)
(SH-3.2-9) Avail: NTIS HC as boxed set only $200/MF A01 per volumeor E99 per entire set CSCL 03B

N85-34825*# Academia Sinica, Beijing (China). Inst. of Space Physics.
DIFFUSION-CONVECTION FUNCTION OF COSMIC RAYS
Gongliang Zhang and Guang Yang (New Hampshire Univ., Durham) *In* NASA. Goddard Space Flight Center 19th Intern. Cosmic Ray Conf., Vol. 4 Aug. 1985 p 360-363 refs (For primary document see N85-34729 23-92)
(SH-3.2-10) Avail: NTIS HC as boxed set only $200/MF A01 per volume or E99 per entire set CSCL 03B

N85-34828*# Maryland Univ., College Park. Dept. of Physics and Astronomy.
THE DISPERSIVE EVOLUTION OF CHARGED-PARTICLE BUNCHES IN RANDOM MAGNETIC FIELDS
J. A. Earl *In* NASA. Goddard Space Flight Center 19th Intern. Cosmic Ray Conf., Vol. 4 Aug. 1985 p 372-375 refs (For primary document see N85-34729 23-92)
(Grant NGR-21-002-066)
(SH-4.1-2) Avail: NTIS HC as boxed set only $200/MF A01 per volume or E99 per entire set CSCL 03B

N85-34829*# Maryland Univ., College Park. Dept. of Physics and Astronomy.
NUMERICAL DESCRIPTIONS OF COSMIC-RAY TRANSPORT
J. A. Earl (Arizona Univ., Tucson) and J. R. Jokipii *In* NASA. Goddard Space Flight Center 19th Intern. Cosmic Ray Conf., Vol. 4 Aug. 1985 p 396-379 refs (For primary document see N85-34729 23-92)
(SH-4.1-3) Avail: NTIS HC as boxed set only $200/MF A01 per volume or E99 per entire set CSCL 03B

N85-34830*# Maryland Univ., College Park. Dept. of Physics and Astronomy.
NUMERICAL AND ANALYTIC DESCRIPTIONS OF COSMIC-RAY TRANSPORT
J. A. Earl *In* NASA. Goddard Space Flight Center 19th Intern. Cosmic Ray Conf., Vol. 4 Aug. 1985 p 380-383 refs (For primary document see N85-34729 23-92)
(Grant NGR-21-002-066)
(SH-4.1-4) Avail: NTIS HC as boxed set only $200/MF A01 per volume or E99 per entire set CSCL 03B

N85-34831*# Universidad Nacional Autonoma de Mexico, Villa Obregon. Inst. de Geofisica.
THE ROLE OF SHOCK WAVES IN MODULATION OF GALACTIC COSMIC RAYS
R. Gall, B. T. Thomas (Bristol Univ.), and H. Durand *In* NASA. Goddard Space Flight Center 19th Intern. Cosmic Ray Conf., Vol. 4 Aug. 1985 p 384-387 refs (For primary document see N85-34729 23-92)
(SH-4.1-7) Avail: NTIS HC as boxed set only $200/MF A01 per volume or E99 per entire set CSCL 03B

N85-34834*# National Aeronautics and Space Administration. Goddard Space Flight Center, Greenbelt, Md.
COSMIC RAY MODULATION AND MERGED INTERACTION REGIONS

L. F. Burlaga, M. L. Goldstein, and Frank B. McDonald (NASA, Washington) *In its* 19th Intern. Cosmic Ray Conf., Vol. 4 Aug. 1985 p 396-399 refs (For primary document see N85-34729 23-92)
(SH-4.1-11) Avail: NTIS HC as boxed set only $200/MF A01 per volume or E99 per entire set CSCL 03B

N85-34836*# California Inst. of Tech., Pasadena.
LATITUDE VARIATION OF RECURRENT FLUXES IN THE OUTER SOLAR SYSTEM Abstract Only
S. P. Christon and E. C. Stone *In* NASA. Goddard Space Flight Center 19th Intern. Cosmic Ray Conf., Vol. 4 Aug. 1985 p 404 ref (For primary document see N85-34729 23-92)
(SH-4.1-13) Avail: NTIS HC as boxed set only $200/MF A01 per volume or E99 per entire set CSCL 03B

N85-34837*# Applied Physics Lab., Johns Hopkins Univ., Laurel, Md.
LONGITUDINAL DISTRIBUTION OF COSMIC RAYS IN THE HELIOSPHERE
R. E. Gold and D. Venkatesan (Calgary Univ.) *In* NASA. Goddard Space Flight Center 19th Intern. Cosmic Ray Conf., Vol. 4 Aug. 1985 p 405-408 refs (For primary document see N85-34729 23-92)
(Contract N00024-85-C-5301; Grant NSF-ATM-83-05537)
(SH-4.1-14) Avail: NTIS HC as boxed set only $200/MF A01 per volume or E99 per entire set CSCL 03B

N85-34839*# Academy of Sciences (USSR), Troitsk. Inst. of Terrestrial Magnetism, Ionosphere and Radio Wave Propagation.
COSMIC RAY MODULATION IN A RANDOM ANISOTROPIC MAGNETIC FIELD
L. I. Dorman, Yu. I. Fedorov (Academy of Sciences (USSR), Kiev), M. I. Katz (Academy of Sciences (USSR), Kiev), S. F. Nosov (Academy of Sciences (USSR), Kiev), and B. A. Shakhov (Academy of Sciences (USSR), Kiev) *In* NASA. Goddard Space Flight Center 19th Intern. Cosmic Ray Conf., Vol. 4 Aug. 1985 p 413-416 refs (For primary document see N85-34729 23-92)
(SH-4.1-20) Avail: NTIS HC as boxed set only $200/MF A01 per volume or E99 per entire set CSCL 03B

N85-34840*# Applied Physics Lab., Johns Hopkins Univ., Laurel, Md.
EVIDENCE FOR REGIONS OF NEGLIGIBLE COSMIC-RAY MODULATION IN THE INNER HELIOSPHERE (> 10 AU)
E. C. Roelof *In* NASA. Goddard Space Flight Center 19th Intern. Cosmic Ray Conf., Vol. 4 Aug. 1985 p 417-420 refs (For primary document see N85-34729 23-92)
(Contract N00024-85-C-5301)
(SH-4.1-21) Avail: NTIS HC as boxed set only $200/MF A01 per volume or E99 per entire set CSCL 03B

N85-34841*# Potchefstroom Univ. for Christian Higher Education (South Africa). Dept. of Physics.
NOTES ON DRIFT THEORY
R. A. Burger, H. Moraal, and G. M. Webb (Arizona Univ., Tucson) *In* NASA. Goddard Space Flight Center 19th Intern. Cosmic Ray Conf., Vol. 4 Aug. 1985 p 421-424 refs (For primary document see N85-34729 23-92)
(SH-4.2-3) Avail: NTIS HC as boxed set only $200/MF A01 per volume or E99 per entire set CSCL 03B

N85-34842*# New Hampshire Univ., Durham. Space Science Center.
DRIFT AND OBSERVATIONS IN COSMIC-RAY MODULATION, 1
M. S. Potgieter *In* NASA. Goddard Space Flight Center 19th Intern. Cosmic Ray Conf., Vol. 4 Aug. 1985 p 425-428 refs Sponsored in part by CSIR (For primary document see N85-34729 23-92)
(SH-4.2-4) Avail: NTIS HC as boxed set only $200/MF A01 per volume or E99 per entire set CSCL 03B

N85-34843*# New Hampshire Univ., Durham. Space Science Center.
DRIFT AND OBSERVATIONS IN COSMIC-RAY MODULATION, 2
M. S. Potgieter *In* NASA. Goddard Space Flight Center 19th Intern. Cosmic Ray Conf., Vol. 4 Aug. 1985 p 429-432 refs Sponsored in part by CSIR (For primary document see N85-34729 23-92)
(SH-4.2-5) Avail: NTIS HC as boxed set only $200/MF A01 per volume or E99 per entire set CSCL 03B

N85-34844*# Franklin Ir.st., Newark, Del.
COSMIC RAY NORTH-SOUTH ANISOTROPY 1961 - 1983
J. W. Bieber and M. A. Pomerantz *In* NASA. Goddard Space Flight Center 19th Intern. Cosmic Ray Conf., Vol. 4 Aug. 1985 p 433-436 refs (For primary document see N85-34729 23-92)
(Grants NSF ATM-83-03758; NSF DPP-83-00544)
(SH-4.2-6) Avail: NTIS HC as boxed set only $200/MF A01 per volume or E99 per entire set CSCL 03B

N85-34846*# Tohoku Univ., Sendai (Japan). Geophysical Inst.
COSMIC RAY INTENSITY AND THE TILT OF THE NEUTRAL SHEET
T. Saito and D. B. Swinson (New Mexico Univ., Albuquerque) *In* NASA. Goddard Space Flight Center 19th Intern. Cosmic Ray Conf., Vol. 4 Aug. 1985 p 441-444 refs (For primary document see N85-34729 23-92)
(Grant NSF ATM-83-05098)
(SH-4.2-8) Avail: NTIS HC as boxed set only $200/MF A01 per volume or E99 per entire set CSCL 03B

N85-34847*# National Aeronautics and Space Administration. Goddard Space Flight Center, Greenbelt, Md.
DIFFERENTIAL MEASUREMENT OF COSMIC-RAY GRADIENT WITH RESPECT TO INTERPLANETARY CURRENT SHEET
S. P. Christon (California Inst. of Tech., Pasadena), A. C. cummings (California Inst. of Tech., Pasadena), E. C. Stone (California Inst. of Tech., Pasadena), K. W. Behannon, and L. F. Burlaga *In its* 19th Intern. Cosmic Ray Conf., Vol. 4 Aug. 1985 p 445-448 refs (For primary document see N85-34729 23-92)
(SH-4.2-9) Avail: NTIS HC as boxed set only $200/MF A01 per volume or E99 per entire set CSCL 03B

N85-34848*# Arizona Univ., Tucson.
SPATIAL VARIATION OF COSMIC RAYS NEAR THE HELIOSPHERIC CURRENT SHEET
J. R. Jokipii and J. Kota (Central Research Inst. for Physics, Budapest) *In* NASA. Goddard Space Flight Center 19th Intern. Cosmic Ray Conf., Vol. 4 Aug. 1985 p 449-452 refs (For primary document see N85-34729 23-92)
(Grant NsG-7101)
(SH-4.2-10) Avail: NTIS HC as boxed set only $200/MF A01 per volume or E99 per entire set CSCL 03B

N85-34849*# Arizona Univ., Tucson.
EFFECTS OF A WAVY NEUTRAL SHEET ON COSMIC RAY ANISOTROPIES
J. Kota and J. R. Jokipii *In* NASA. Goddard Space Flight Center 19th Intern. Cosmic Ray Conf., Vol. 4 Aug. 1985 p 453-456 refs (For primary document see N85-34729 23-92)
(Grant NSF INT-84-00591)
(SH-4.2-11) Avail: NTIS HC as boxed set only $200/MF A01 per volume or E99 per entire set CSCL 03B

N85-34850*# Academy of Sciences (USSR), Alma-Ata.
EFFECTS OF SOLAR MAGNETIC FIELD ON COSMIC RAYS
G. A. Goncher, E. V. Kolomeets, A. Kh. Lyakhova, N. V. Slyunyaeva, and N. V. Stekolnikov *In* NASA. Goddard Space Flight Center 19th Intern. Cosmic Ray Conf., Vol. 4 Aug. 1985 p 457-460 refs (For primary document see N85-34729 23-92)
(SH-4.2-12) Avail: NTIS HC as boxed set only $200/MF A01 per volume or E99 per entire set CSCL 03B

N85-34851*# Aligarh Muslim Univ. (India). Space Science Group.
DETERMINATION OF GALACTIC COSMIC RAY LATITUDINAL GRADIENT USING EARTH BASED DETECTORS
Badruddin and R. S. Yadav *In* NASA. Goddard Space Flight Center 19th Intern. Cosmic Ray Conf., Vol. 4 Aug. 1985 p 461-464 refs (For primary document see N85-34729 23-92)
(SH-4.2-13) Avail: NTIS HC as boxed set only $200/MF A01 per volume or E99 per entire set CSCL 03B

N85-34852*# Academy of Sciences of the Georgian SSR, Tbilisi (USSR). Inst. of Geophysics.
THE EXPECTED COSMIC RAY DENSITY AND STREAM DISTRIBUTIONS AT THE HELIOLATITUDINAL ASYMMETRY OF SOLAR WIND
M. V. Alania, R. G. Aslamazashvili, L. I. Dorman, and K. Iskra *In* NASA. Goddard Space Flight Center 19th Intern. Cosmic Ray Conf., Vol. 4 Aug. 1985 p 465-468 refs (For primary document see N85-34729 23-92)
(SH-4.2-14) Avail: NTIS HC as boxed set only $200/MF A01 per volume or E99 per entire set CSCL 03B

N85-34853*# National Center for Atmospheric Research, Boulder, Colo.
LATITUDINAL GRADIENTS OF COSMIC RAYS AND THE POLARITY REVERSAL OF THE HELIOSPHERIC MAGNETIC FIELD: A PRELIMINARY EVALUATION
G. Newkirk, Jr., J. A. Lockwood (New Hampshire Univ., Durham), M. Garcia-Munoz (Chicago Univ.), and J. A. Simpson (Chicago Univ.) *In* NASA. Goddard Space Flight Center 19th Intern. Cosmic Ray Conf., Vol. 4 Aug. 1985 p 469-472 refs (For primary document see N85-34729 23-92)
(Contract NAS5-25731; Grants NSF ATM-83-04486; NSF ATM-82-06418)
(SH-4.2-16) Avail: NTIS HC as boxed set only $200/MF A01 per volume or E99 per entire set CSCL 03B

N85-34855*# Academy of Sciences of the Georgian SSR, Tbilisi (USSR). Inst. of Geophysics.
THE EFFECT OF THE NEUTRAL SHEET STRUCTURE OF THE INTERPLANETARY MAGNETIC FIELD ON COSMIC RAY DISTRIBUTION IN SPACE
M. V. Alania, R. G. Aslamazashvili, T. B. Bochorishvili, T. V. Djapiashvili, and V. S. Tkemaladze *In* NASA. Goddard Space Flight Center 19th Intern. Cosmic Ray Conf., Vol. 4 Aug. 1985 p 477-480 refs (For primary document see N85-34729 23-92)
(SH-4.2-18) Avail: NTIS HC as boxed set only $200/MF A01 per volume or E99 per entire set CSCL 03B

N85-34856*# Academy of Sciences (USSR), Moscow.
ON THE INFLUENCE OF THE HELIOMAGNETOSPHERIC PERIPHERY ON THE GALACTIC COSMIC RAYS
M. B. Krainev, Yu. I. Stozhkov, and T. N. Charakhchyan (Moscow State Univ.) *In* NASA. Goddard Space Flight Center 19th Intern. Cosmic Ray Conf., Vol. 4 Aug. 1985 p 481-484 refs (For primary document see N85-34729 23-92)
(SH-4.2-19) Avail: NTIS HC as boxed set only $200/MF A01 per volume or E99 per entire set CSCL 03B

N85-34857*# Academy of Sciences of the Georgian SSR, Tbilisi (USSR). Inst. of Geophysics.
SPATIAL DISTRIBUTION OF COSMIC RAYS IN MAGNETIC CYCLES OF THE SUN
M. V. Alania, R. T. Gushchina (Academy of Sciences (USSR), Troitsk), and L. I. Dorman (Academy of Sciences (USSR), Troitsk) *In* NASA. Goddard Space Flight Center 19th Intern. Cosmic Ray Conf., Vol. 4 Aug. 1985 p 485-488 refs (For primary document see N85-34729 23-93)
(SH-4.2-20) Avail: NTIS HC as boxed set only $200/MF A01 per volume or E99 per entire set CSCL 03B

N85-34858*# Academy of Sciences (USSR), Yakutsk. Inst. of Cosmophysical Research and Aeronomy.
11- AND 22-YEAR VARIATIONS OF THE COSMIC RAY DENSITY AND OF THE SOLAR WIND SPEED
N. P. Chirkov *In* NASA. Goddard Space Flight Center 19th Intern. Cosmic Ray Conf., Vol. 4 Aug. 1985 p 489-492 refs (For primary document see N85-34729 23-92)
(SH-4.2-21) Avail: NTIS HC as boxed set only $200/MF A01 per volume or E99 per entire set CSCL 03B

N85-34859*# Universidad Nacional Autonoma de Mexico, Villa Obregon. Inst. de Geofisica.
DIFFERENCE BETWEEN EVEN AND ODD 11-YEAR CYCLES IN COSMIC RAY INTENSITY
J. A. Otaola, R. Perez-Enriquez, and J. F. Valdes-Galicia *In* NASA. Goddard Space Flight Center 19th Intern. Cosmic Ray Conf., Vol. 4 Aug. 1985 p 493-496 refs (For primary document see N85-34729 23-92)
(SH-4.2-22) Avail: NTIS HC as boxed set only $200/MF A01 per volume or E99 per entire set CSCL 03B

N85-34860*# Chicago Univ., Ill.
THE DEPENDENCE OF SOLAR MODULATION ON THE SIGN OF THE COSMIC RAY PARTICLE CHARGE
M. Garcia-Munoz, P. Meyer, K. R. Pyle, J. A. Simpson (Delaware Univ., Newark), and P. A. Evenson *In* NASA. Goddard Space Flight Center 19th Intern. Cosmic Ray Conf., Vol. 4 Aug. 1985 p 497-500 refs (For primary document see N85-34729 23-92)
(Contracts NAS5-28442; NAS5-28500; Grants NGL-14-001-005; NGL-14-001-006; NAG5-374; NSF ATM-84-12382; NSF ATM-84-01427)
(SH-4.2-23) Avail: NTIS HC as boxed set only $200/MF A01 per volume or E99 per entire set CSCL 03B

N85-34861*# Air Force Geophysics Lab., Hanscom AFB, Mass.
AN UPDATE ON THE CORRELATION BETWEEN THE COSMIC RADIATION INTENSITY AND THE GEOMAGNETIC AA INDEX
M. A. Shea and D. F. Smart *In* NASA. Goddard Space Flight Center 19th Intern. Cosmic Ray Conf., Vol. 4 Aug. 1985 p 501-504 refs (For primary document see N85-34729 23-92)
(SH-4.2-24) Avail: NTIS HC as boxed set only $200/MF A01 per volume or E99 per entire set CSCL 03B

99 GENERAL

N85-35142*# National Aeronautics and Space Administration, Washington, D. C.
A SPACEFARING PEOPLE: PERSPECTIVES ON EARLY SPACEFLIGHT
Alex Roland 1985 158 p refs Proc. of a Conf. on the History of Space Activity, New Haven, Conn., 6-7 Feb. 1981 *Its* the NASA History Series
(NASA-SP-4405; NAS 1.12/6:4405; LC-84-979) Avail: NTIS HC A08/MF A01; also available SOD HC $3.50 as 033-000-009-33-0 CSCL 22A

The early years of space flight are discussed. An historical perspective is offered. Satellites and politics, management of large scale technology, the state of the literature of space, the domestic and international ramifications of space activity, and rationales for space exploration are discussed. For individual titles, see N85-35143 through N85-35150.

N85-35143*# Chicago Univ., Ill.
SPACE SCIENCE AND EXPLORATION: A HISTORICAL PERSPECTIVE **c12**
John A. Simpson *In* NASA, Washington A Spacefaring People 1985 p 3-31 refs (For primary document see N85-35142 23-99)
(Grant NGL-14-001-006)
Avail: NTIS HC A08/MF A01; also available SOD HC $3.50 as 033-000-009-33-0 CSCL 22A

Major achievements in space sciences and exploration are briefly reviewed. Artificial satellites, space missions, planetology and space law are among the topics discussed. R.J.F.

N85-35144*# Pennsylvania Univ., Phiiadelphia.
SATELLITES AND POLITICS: WEATHER, COMMUNICATIONS, AND EARTH RESOURCES c84
Pamela Mack *In* NASA, Washington A Spacefaring People 1985 p 32-38 refs (For primary document see N85-35142 23-99)
Avail: NTIS HC A08/MF A01; also available SOD HC $3.50 as 033-000-009-33-0 CSCL 05D

Political problems surrounding the development of weather, communications, and Earth resources satellites are discussed. Tiros satellites, LANDSAT satellites, and Nimbus satellites are discussed. R.J.F.

N85-35145*# National Aeronautics and Space Administration, Washington, D. C.
MANAGEMENT OF LARGE-SCALE TECHNOLOGY c81
Arnold S. Levine *In its* A Spacefaring People 1985 p 39-53 refs (For primary document see N85-35142 23-99)
Avail: NTIS HC A08/MF A01; also available SOD HC $3.50 as 033-000-009-33-0 CSCL 05A

Two major themes are addressed in this assessment of the management of large-scale NASA programs: (1) how a high technology agency was a decade marked by a rapid expansion of funds and manpower in the first half and almost as rapid contraction in the second; and (2) how NASA combined central planning and control with decentralized project execution. R.J.F.

N85-35146*# Air Force Flight Test Center, Edwards AFB, Calif.
THE NEXT ASSIGNMENT: THE STATE OF THE LITERATURE ON SPACE
Richard P. Hallion *In* NASA, Washington A Spacefaring People 1985 p 61-67 (For primary document see N85-35142 23-99)
Avail: NTIS HC A08/MF A01; also available SOD HC $3.50 as 033-000-009-33-0 CSCL 05B

Several books dealing with space programs are reviewed. Problems facing historians of space and technology are discussed. R.J.F.

N85-35147*# George Washington Univ., Washington, D.C.
OPPORTUNITIES FOR POLICY HISTORIANS: THE EVOLUTION OF THE US CIVILIAN SPACE PROGRAM
John Logsdon *In* NASA, Washington A Spacefaring People 1985 p 81-107 refs (For primary document see N85-35142 23-99)
Avail: NTIS HC A08/MF A01; also available SOD HC $3.50 as 033-000-009-33-0 CSCL 05A

The evolution of U.S. civilian space policy and the institutional framework through which that policy was implemented are discussed. Space policy principles the governed decision making between 1957 and 1962 are identified. The government/industry relations regarding space related research and development are discussed. R.J.F.

N85-35148*# California Univ., Berkeley.
SPACE-AGE EUROPE, 1957-1980
Walter A. McDougall *In* NASA, Washington A Spacefaring People 1985 p 108-117 refs (For primary document see N85-35142 23-99)
Avail: NTIS HC A08/MF A01; also available SOD HC $3.50 as 033-000-009-33-0 CSCL 05B

European space related research and development from the launch of Sputnik in 1957 to 1980 in discussed. The political response to Sputnik is analyzed in the context of cold war. The development of the European Space Agency is traced. R.J.F.

N85-35149*# National Aeronautics and Space Administration. Johnson (Lyndon B.) Space Center,
SPACE ACTIVITIES IN THE SOVIET UNION, JAPAN, AND THE PEOPLE'S REPUBLIC OF CHINA
Edward C. Ezell *In* NASA, Washington A Spacefaring People 1985 p 118-130 refs (For primary document see N85-35142 23-99)
Avail: NTIS HC A08/MF A01; also available SOD HC $3.50 as 033-000-009-33-0 CSCL 05B

The space programs of the Soviet Union, Japan, and China are discussed. The types of launch vehicles they used and the classes of spacecraft they launched are examined. The political motivations of these nations are analyzed. R.J.F.

N85-35150*# Massachusetts Inst. of Tech., Cambridge.
THE IDEA OF SPACE EXPLORATION
Bruce Mazlish *In* NASA, Washington A Spacefaring People 1985 p 137-143 refs (For primary document see N85-35142 23-99)
Avail: NTIS HC A08/MF A01; also available SOD HC $3.50 as 033-000-009-33-0 CSCL 05B

Public reactions to the space program, especially to the 1969 Moon landing are discussed. Space exploration is compared to explorations during the Age of Discovery. It is argued that space exploration has failed to capture the public's imagination, that it has had few economic or social consequences of any importance, and that it has had a minimum impact on national prestige. R.J.F.

N85-35151*# National Aeronautics and Space Administration. Langley Research Center, Hampton, Va.
LANGLEY AERONAUTICS AND SPACE TEST HIGHLIGHTS, 1984
1984 89 p refs
(NASA-TM-87585; NAS 1.15:87585) Avail: NTIS HC A05/MF A01 CSCL 05D

The role of the Langley Research Center is to perform basic and applied research necessary for the advancement of aeronautics and space flight, to generate new and advanced concepts for the accomplishment of related national goals, and to provide research advice, technological support, and assistance to other NASA installations, other government agencies, and industry. Some of the significant tests which were performed during calendar year 1984 in Langley test facilities are highlighted. The broad range of the research and technology activities at the Langley Research Center and the contributions of this work toward maintaining United States leadership in aeronautics and space research are illustrated. R.J.F.

SUBJECT INDEX

Typical Subject Index Listing

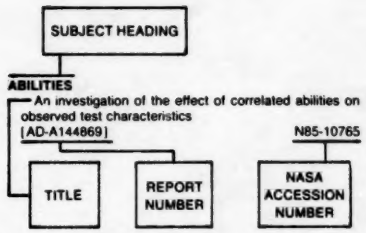

The subject heading is the key to the subject content of the document. Titles, report numbers, and accession numbers of pertinent documents are provided under each subject heading. When the title is insufficiently descriptive of the document content, a title extension has been added, separated from the title by three hyphens. The report number helps to indicate the type of document cited (e.g., NASA report, NASA translation, NASA contractor report). The NASA accession number is the number by which the document abstracts are arranged in this journal and by which the document is sold or requested. The titles, with title extensions if present, are arranged under each subject heading in ascending accession number order. The subject headings have been selected from the latest revision of the *NASA Thesaurus* (NASA SP-7051).

A

ABLATION
Thermal transport measurements of UV laser irradiated spherical targets
[DE85-011038] N85-34365
ABLATIVE MATERIALS
Thermal protection systems for reentry vehicles
[CNES-NT-113] N85-34157
ABRASION
Three body abrasive wear in various metal combinations N85-34200
ABSORPTION SPECTRA
Time-resolved and infrared spectroscopy of excitons
[DE85-011879] N85-34235
ABSORPTIVITY
Aluminum work function: Effect of oxidation, mechanical scraping and ion bombardment
[NASA-TM-87079] N85-34265
Acoustical absorption coefficient in a diffuse field of a plane, rectangular material of finite dimensions placed on an infinite perfectly reflecting surface
[NRC/CNR-TT-2113] N85-34599
X-ray spectra of bursting neutron stars N85-34686
ABSTRACTS
Monitoring building energy performance: An informal review and characterization of research in progress
[BNL-51765] N85-34308
ABUNDANCE
Solar Coronal and photospheric abundances from solar energetic particle measurements
[SH-2.1-5] N85-34786
Variations in elemental composition of several MEV/nucleon ions observed in interplanetary space
[SH-2.1-7] N85-34788
Anomalous abundances of solar energetic particles and coronal gas: Coulomb effects and First Ionization Potential (FIP) ordering
[SH-2.1-10] N85-34791
Abundances from solar-flare gamma-ray line spectroscopy
[SH-2.1-13] N85-34794
Solar flare gamma-ray line spectroscopy
[SH-2.1-14] N85-34795
Elemental abundance differences between nuclei accelerated in CIR shocks and solar flares
[SH-2.2-6] N85-34801
The heavy ion composition in 3HE-rich solar flares
[SH-2.2-7] N85-34802
Germanium and lead: Significant differences between meteoritic and photospheric abundances?
[OG-7.1-2] N85-34864
Lead and uranium group abundances in cosmic rays
[OG-7.1-3] N85-34865
Implications of source abundances of ultraheavy cosmic rays
[OG-7.1-4] N85-34866
Alfven wave scattering and the secondary to primary ratio
[OG-7.2-9] N85-34878
Do supernovae of type 1 paly a role in cosmic-ray production?
[OG-8.2-5] N85-34905
Bursting star formation and the overabundance of Wolf-Rayet stars
[OG-8.2-8] N85-34907
Measurement of low energy cosmic rays aboard Spacelab-1
[SH-10.1-6] N85-35137
ACCELERATED LIFE TESTS
Degradation mechanisms and accelerated aging test design
[TI85-003251] N85-34420
ACCELERATION
Accelerator experiments on the contribution of secondary particles to the production of cosmogenic nuclides in meteorites
[SH-7.1-8] N85-35100
ACCELERATION (PHYSICS)
Injection of energetic particles following the gamma-ray flares on June 7, 1980, as observed on Helios 1
[SH-1.3-9] N85-34756
The cosmic-ray shock structure problem for relativistic shocks
[OG-8.1-1] N85-34891
Time-dependent nonlinear cosmic ray shocks confirming abstract
[OG-8.1-3] N85-34893
Relativistic cosmic ray spectra in the full non-linear theory of shock acceleration
[OG-8.1-6] N85-34896
Acceleration of cosmic rays in supernova-remnants
[OG-8.1-9] N85-34899
Evaluation of parameters for particles acceleration by the zero-point field of quantum electrodynamics
[OG-8.2-16] N85-34912
ACCELERATION STRESSES (PHYSIOLOGY)
Oxygenation and regional circulation in gingival mucosa during exposure to lower body negative pressure N85-34498
ACCELERATION TOLERANCE
Tolerance to +Gz and +Gx accelerations of individuals in older age groups in good health and with early signs of arteriosclerosis N85-34496
Effect of hypokinesia and +Gz accelerations on transport function of human blood N85-34497
ACCELEROMETERS
Multiple-stage integrating accelerometer
[DE85-006505] N85-34388
ACCEPTABILITY
Atmospheric modeling of organics for risk assessment: A Chemist's view
[DE85-009770] N85-34217
ACCIDENTS
The 1983 international intercomparison of nuclear accident dosimetry systems at Oak Ridge National Laboratory
[DE85-011303] N85-34382
ACCUMULATORS
Vapor phase heat transport concepts
[DE85-009550] N85-34366
ACEE PROGRAM
Energy efficient engine. Fan and quarter-stage component performance report
[NASA-CR-168070] N85-34141
ACETYLENE
Metal alkoxides: Models for metal oxides. Alkoxide ligands in early transition metal organometallic chemistry
[DE85-011368] N85-34269
ACID RAIN
Effects of acid rain on forest nutrient status
[DE85-012486] N85-34483
Throughfall rate and chemistry studies: Whiteface Mountain
[DE85-012407] N85-34484
ACIDS
Method for extracting lanthanides and actinides from acid solutions by modification of Purex solvent
[DE85-005763] N85-34220
ACOUSTIC ATTENUATION
Acoustical absorption coefficient in a diffuse field of a plane, rectangular material of finite dimensions placed on an infinite perfectly reflecting surface
[NRC/CNR-TT-2113] N85-34599
ACOUSTIC EMISSION
Acoustic emission during transformation of austenite in 38KhN3MF steel
[BLL-M-35825-(5828.4)] N85-34256
ACOUSTIC MEASUREMENT
Acoustic cross-correlation flowmeter for solid-gas flow
[DE85-005986] N85-34391
Acoustical absorption coefficient in a diffuse field of a plane, rectangular material of finite dimensions placed on an infinite perfectly reflecting surface
[NRC/CNR-TT-2113] N85-34599
ACTINIDE SERIES COMPOUNDS
Method for extracting lanthanides and actinides from acid solutions by modification of Purex solvent
[DE85-005763] N85-34220
ACTIVATED CARBON
Radiocarbon content in the annual tree rings during last 150 years and time variation of cosmic rays
[SH-7.1-15] N85-35106
ACTIVATION ENERGY
Three-dimensional hydrodynamic hot-spot model
[DE85-009587] N85-34301
Grain boundary and surface diffusion in oxide systems
[DE85-007291] N85-34715
ACTUATORS
Intelligent redundant actuation system requirements and preliminary system design
[NASA-CR-177366] N85-34136
ADAPTATION
Effect of hypokinesia and +Gz accelerations on transport function of human blood N85-34497
Lipid hydrolysis in man during antiorthostatic hypokinesia N85-34500
ADHESIVE BONDING
Nonlinear adhesive behavior effects in a cracked orthotropic sheet stiffened by a semi-infinite orthotropic sheet
[NASA-TM-87584] N85-34426
ADIABATIC CONDITIONS
A theoretical study of non-adiabatic surface effects for a model in the NTF cryogenic wind tunnel
[NASA-CR-3924] N85-34352
Why do leaky-box models work so fine?
[OG-7.2-8] N85-34877
Relativistic transport theory for cosmic-rays
[OG-8.3-8] N85-34926
ADJOINTS
Monte Carlo techniques for analyzing deep penetration problems
[DE85-011426] N85-34598
ADMIXTURES
High temperature polymer concrete
[DE85-005756] N85-34290
ADVECTION
New semi-implicit method for solving the time-dependent conservation equations for incompressible flow
[DE85-010926] N85-34367

AERODYNAMIC CHARACTERISTICS
The aerodynamic characteristics of a GU25-5(11)8 aerofoil for low Reynolds numbers
[GU-AERO-8410] N85-34121
AERODYNAMIC HEAT TRANSFER
Unsteady transonic heat transfer in a transient facility
[NASA-CR-176145] N85-34354
AERODYNAMIC NOISE
Nozzle wall roughness effects on free-stream noise and transition in the pilot low-disturbance tunnel
[NASA-TM-86389] N85-34355
AERODYNAMIC STALLING
A design procedure to modify the trailing edge upper surface pressure gradient of a given aerofoil
[GU-AERO-8408] N85-34120
An investigation into the three-dimensional stall development on a modified NACA 23012 aerofoil
[GU-AERO-8414] N85-34124
Comments on the prediction of dynamic stall
[GU-AERO-8501] N85-34125
AEROELASTICITY
Aeroelastic constraints for a wing weight minimization procedure
[FFA-TN-1985-4] N85-34126
AEROLOGY
Reports from the German Meteorological Service. No. 167: Results of aerological soundings in the model area upper Rhine: Heat release project upper Rhine area, part 3
[ISBN-3-88148-216-4] N85-34479
AEROSOLS
Evaluation of source strength and dispersion model predications with data from large nitrogen tetroxide field experiments
[DE85-011855] N85-34465
MATADOR (Methods for the Analysis of Transport And Deposition Of Radionuclides) code description and user's manual
[TI85-901402] N85-34592
Downstream behavior of volatile fission product species
[DE85-012124] N85-34617
AEROSPACE ENVIRONMENTS
Microorganisms in space flight N85-34490
Effect of seeds of heavy charged particles of galactic cosmic radiation N85-34505
Problems of aviation and space medicine and psychology discussed at 14th Gagarin lectures N85-34509
AEROSPACE MEDICINE
Aerospace Medicine and Biology: A continuing bibliography with indexes (supplement 274)
[NASA-SP-7011(274)] N85-34491
USSR report: Space Biology and Aerospace Medicine, vol. 19, no. 3, May - June 1985
[JPRS-USB-85-005] N85-34494
Problems of aviation and space medicine and psychology discussed at 14th Gagarin lectures N85-34509
AEROSPACE SYSTEMS
A spacefaring people: Perspectives on early spaceflight
[NASA-SP-4405] N85-35142
Space science and exploration: A historical perspective N85-35143
The next assignment: The state of the literature on space N85-35146
AEROSPACE TECHNOLOGY TRANSFER
Product definition: Technical specification of needs
[SNIAS-851-430-104] N85-34228
AGGREGATES
High temperature polymer concrete
[DE85-005756] N85-34290
AGING (BIOLOGY)
Tolerance to +Gz and +Gx accelerations of individuals in older age groups in good health and with early signs of arteriosclerosis N85-34496
AGING (MATERIALS)
Near-threshold fatigue: An overview of the role of microstructure and environment
[DE85-009903] N85-34431
AGRICULTURE
Snow cover in the Siberian forest-steppe
[NASA-TM-77914] N85-34435
AILERONS
Reflection plane tests of a wind turbine blade tip section with ailerons
[NASA-TM-87018] N85-34444
AIR
Influence of technology of atomization of naturally alloyed iron on grain-size characteristics of powder material
[BLL-M-35810-(5828.4)] N85-34257
AIR POLLUTION
Atmospheric modeling of organics for risk assessment: A Chemist's view
[DE85-009770] N85-34217
Description of a test site for large-scale heavy gas dispersion and combustion experiments
[DE85-004987] N85-34231
Forecasting future industrial SO2 and NC/sub x/ emissions, revised N85-34461
User's guide to the MATHEW/ADPIC models
[DE85-012952] N85-34587
AIR TRAFFIC CONTROL
Effect of interference on the performance of a minimum TCAS 2
[FAA/PM-84/33] N85-34131
AIRBORNE EQUIPMENT
Altitude variations of cosmic-ray soft and hard components observed by airborne detectors
[SH-6.1-5] N85-35079
AIRCRAFT COMPARTMENTS
Aviation safety (aircraft passenger survivability and cabin safety)
[GPO-39-847] N85-34130
AIRCRAFT CONFIGURATIONS
Flight testing the fixed-wing configuration of the Rotor Systems Research Aircraft (RSRA)
[NASA-TM-86762] N85-34135
AIRCRAFT ENGINES
Performance improvements from surfacing in aero engine components
[PNR-90257] N85-34142
Directionally solidified gas turbine alloys
[PNR-90264] N85-34279
Towards the year 2000: Developments in inspection and product assurance to be anticipated during the next 15 years — aircraft engines
[PNR-90258] N85-34421
Cost effective single crystals: The Rolls Royce approach — gas turbine components
[PNR-90262] N85-34717
AIRCRAFT INSTRUMENTS
Determination of instrument errors by compatibility checking: Results from dynamic flight test data
[ARL-AERO-R-162] N85-34137
AIRCRAFT MAINTENANCE
Implications of artificial intelligence on the design of future onboard systems
[SFENA-DPS/C/S3/84252A] N85-34596
AIRCRAFT NOISE
Langley aeronautics and space test highlights, 1984
[NASA-TM-87585] N85-35151
AIRCRAFT SAFETY
Aviation safety (aircraft passenger survivability and cabin safety)
[GPO-39-847] N85-34130
AIRCRAFT STRUCTURES
Flight service evaluation of composite helicopter components
[NASA-CR-172562] N85-34222
AIRFOIL PROFILES
An investigation into the three-dimensional stall development on a modified NACA 23012 aerofoil
[GU-AERO-8414] N85-34124
AIRFOILS
An evaluation of three helicopter rotor sections
[NASA-TM-86719] N85-34115
A design procedure to modify the trailing edge upper surface pressure gradient of a given aerofoil
[GU-AERO-8408] N85-34120
Modelling of unsteady, incompressible separation on an aerofoil using an inviscid flow algorithm
[GU-AERO-8412] N85-34122
The collected data for ramp function tests on a NACA 23012 aerofoil. Volume 1: Description and pressure data
[GU-AERO-8413-VOL-1] N85-34123
A comparison of laser Doppler anemometry and probe measurements within the boundary layer of an airfoil at subsonic flow
[ISL-CO-219/84] N85-34127
AIRGLOW
Atmospheric Emission Photometric Imaging (AEPI) N85-34170
ALASKA
The United States Geological Survey in Alaska: Accomplishments during 1983
[USGS-CIRC-945] N85-34468
ALBEDO
Monte Carlo techniques for analyzing deep penetration problems
[DE85-011426] N85-34598
Additional flux of particles and albedo-electrons in upper atmosphere
[SH-6.1-6] N85-35080
Observation of energy spectrum of electron albedo in low latitude region at Hyderabad, India
[SH-6.1-7] N85-35081
Proton albedo spectrum observation in low latitude region at Hyderabad, India
[SH-6.1-8] N85-35082
ALCOHOLS
Metal alkoxides: Models for metal oxides. Alkoxide ligands in early transition metal organometallic chemistry
[DE85-011368] N85-34269
ALGAE
Resource evaluation and site selection for microalgae production systems
[DE85-008807] N85-34485
Screening and characterizing oleaginous microalgal species from the southeastern United States
[DE85-008787] N85-34488
ALGEBRA
A study of the second and third order closure models of turbulence for prediction of separated shear flows
[NASA-CR-176127] N85-34353
ALGORITHMS
Modelling of unsteady, incompressible separation on an aerofoil using an inviscid flow algorithm
[GU-AERO-8412] N85-34122
A versatile computer package for mechanism analysis, part 2: Dynamics and balance N85-34315
The improved display of 625-line television pictures: Adaptive interpolation
[BBC-RD-1985/5] N85-34328
Sequential regularization solution of the inverse heat conduction problem
[DE85-010657] N85-34362
Algorithm for calculation of strain state from measurements of node coordinates of arbitrary curvilinear grid
[BLL-M-36304] N85-34422
Short-time creep of ice
[NRC/CNR-TT-2111] N85-34428
Reordering computations for parallel execution
[NASA-CR-177961] N85-34522
A theoretical and empirical analysis of coherent ray-tracing N85-34524
Computer analysis techniques for the temporal evaluation of cardiac wall motion N85-34530
An analysis and algorithm for filling propagation N85-34551
A curvilinear coordinate method for the solutions of initial value problems using the third-order upwind differencing scheme
[IPPJ-734] N85-34642
Cubic interpolated pseudo-particle method (CIP) for solving hyperbolic-type equation N85-34673
Numerical simulation in astrophysics: Smoothed particle methods N85-34674
Vector calculation of particle code N85-34688
ALKALI METALS
Infrared studies of the influence of alkali metals on the C-O bond in chemisorbed carbon monoxide
[DE85-005306] N85-34232
Metal alkoxides: Models for metal oxides. Alkoxide ligands in early transition metal organometallic chemistry
[DE85-011368] N85-34269
ALLOYS
The study of the effect of residual microimpurities on the fatigue strength of 55S2 steel
[BLL-M-36317-(5828.4)] N85-34246
ALPHA PARTICLES
Injection of energetic particles following the gamma-ray flares on June 7, 1980, as observed on Helios 1
[SH-1.3-9] N85-34756
Observations of solar energetic particles at a synchronous orbit
[SH-3.1-1] N85-34806
ALTITUDE
Altitude variations of cosmic-ray soft and hard components observed by airborne detectors
[SH-6.1-5] N85-35079
Long-period cosmic ray variations and their altitude dependence
[SH-6.1-19] N85-35091
ALTITUDE ACCLIMATIZATION
Effect of dibazol on parameters of nonspecific resistance of subjects in pressurized cabins N85-34504
ALTITUDE TOLERANCE
Effect of acute hypoxia on coronary and systemic hemodynamics N85-34503
ALUMINUM
Fracture behavior of aluminum composites reinforced with fiber N85-34207
Enthalpies of formation of liquid Fe-Ce-Si and Fe-Ce-Al three-component alloys
[BLL-M-36296-(5828.4)] N85-34247
The properties of VSt3sp inoculated steel
[BLL-M-35894-(5828.4)] N85-34263

Aluminum work function: Effect of oxidation, mechanical scraping and ion bombardment
[NASA-TM-87079] N85-34265
Electrically conductive containment vessel for molten aluminum
[DE85-006518] N85-34415
ALUMINUM ALLOYS
Mechanical properties of plasma arc cut steel N85-34188
The influence of temperature on static and dynamic SCC crack growth behavior in aluminum alloy N85-34190
A fractographic study on mode 2 and mode 3 SCC crack growth in an Al-Zn-Mg alloy N85-34191
Fatigue crack retardation phenomenon caused by single-multiple overloads in 2017-T3 aluminum allow N85-34196
Method for preparing high purity vanadium
[DE85-006412] N85-34242
Influence of particle erosion on the microstructural changes in metals and alloys
[TI85-901384] N85-34276
ALUMINUM OXIDES
Electrolytic synthesis of colored eta alumina film N85-34201
Rotating bending fatigue strength of silicon carbide and alumina-fiber reinforced aluminum N85-34208
Grain boundary and surface diffusion in oxide systems
[DE85-007291] N85-34715
AMBIENT TEMPERATURE
Lake ice occurence as a possible detector of atmospheric CO2 effects on climate
[DE85-012987] N85-34480
AMBIPOLAR DIFFUSION
Breakdown of intrinsic ambipolarity for the radial diffusion due to a rotating RF field N85-34660
Effect of ECH and ICH on ambipolar potential in NBT-1M N85-34661
Analytic and numerical calculations of the ambipolar electric field in a stellarator N85-34665
AMINES
Metal (2) 4,4',4',4'' phthalocyanine tetraamines as curing agents for epoxy resins
[NASA-CASE-ARC-11424-1] N85-34281
AMMONIA
Metal alkoxides: Models for metal oxides. Alkoxide ligands in early transition metal organometallic chemistry
[DE85-011368] N85-34269
Determination of properties of zeolite/refrigerant combinations for solar refrigeration systems
[DE85-012009] N85-34448
AMMONIUM COMPOUNDS
Throughfall rate and chemistry studies: Whiteface Mountain
[DE85-012407] N85-34464
AMORPHOUS MATERIALS
The effect of liquid-liquid phase separation of glass on the properties and crystallization behavior
[NASA-TM-77890] N85-34285
AMORPHOUS SEMICONDUCTORS
Formation of amorphous silicon by light ion damage
[DE85-012605] N85-34623
AMPLIFIERS
Wide-band phase locked loop amplifier apparatus
[AD-D011720] N85-34337
AMPLITUDE DISTRIBUTION ANALYSIS
Cosmic ray variations with the period close to 27 days and their connection with solar activity longitudinal distribution
[SH-4.4-19] N85-35015
AMPLITUDES
Reducing grating lobes due to subarray amplitude tapering
[AD-D011723] N85-34339
ANALYSIS (MATHEMATICS)
Stability of two-dimensional immiscible flow to viscous fingering
[DE85-011403] N85-34364
Analytic and numerical calculations of the ambipolar electric field in a stellarator N85-34665
ANGLES (GEOMETRY)
Comprehensive fracture diagnostics experiement. Part 2: Comparison of seven fracture azimuth measurements
[DE85-011707] N85-34470
OMEGA: Optoelectronic measurement of the incidence angle of a projectile
[ISL-CO-223/84] N85-34634
The response of ionization chambers to relativistic heavy nuclei
[OG-9.1-13] N85-34939
ANGULAR DISTRIBUTION
Low-energy sputterings with the Monte Carlo Program ACAT
[IPPJ-AM-40] N85-34690
On the angular and energy distribution of solar neutrons generated in P-P reactions
[SH-1.4-9] N85-34769
Additional flux of particles and albedo-electrons in upper atmosphere
[SH-6.1-6] N85-35080
ANGULAR MOMENTUM
Duality of two-point functions for confined non-relativistic quark-antiquark systems
[DE85-012334] N85-34618
ANGULAR RESOLUTION
The gamma-ray telescope Gamma-1
[OG-9.2-10] N85-34949
Lapex: A Phoswich balloon experiment for hard X-ray astronomy
[OG-9.3-1] N85-34956
A new ultra high energy gamma ray telescope at Ohya mine
[OG-9.4-3] N85-34970
An EAS experiment at mountain altitude for the detection of gamma-ray sources
[OG-9.4-5] N85-34972
A new array for the study of ultra high energy gamma-ray sources
[OG-9.4-7] N85-34974
Shower disc sampling and the angular resolution of gamma-ray shower detectors
[OG-9.5-2] N85-34980
A method to improve observations of gamma-ray sources near 10 (15) eV
[OG-9.5-5] N85-34982
Angular resolution of air-shower array-telescopes
[OG-9.5-6] N85-34983
Astrophysical applications of high angular resolution array-telescopes
[OG-9.5-7] N85-34984
Angular resolution of an EAS array for gamma ray astronomy energies 5 x 10 (13) eV
[OG-9.5-8] N85-34985
Note on the detection of high energy primary cosmic gamma rays by air shower observation
[OG-9.5-9] N85-34986
The angular resolution of air shower gamma ray telescopes
[OG-9.5-14] N85-34990
Measurement of low energy cosmic rays aboard Spacelab-1
[SH-10.1-6] N85-35137
ANIMALS
The 1984 biotic studies of Yucca Mountain, Nevada test site, Nye County, Nevada
[DE85-011715] N85-34487
ANIONS
Electron photoejection in carbanions
[DE85-011747] N85-34230
Electron photoejection in carbanions
[DE85-011748] N85-34237
Throughfall rate and chemistry studies: Whiteface Mountain
[DE85-012407] N85-34464
ANISOTROPY
Flux-line lattice anisotropy in V3Si: Observation and interpretation
[DE85-011935] N85-34713
Helios 1 energetic particle observations of the solar gamma ray flare events of 7, 21 June 1980 and 3 June 1982
[SH-1.3-8] N85-34755
Ultrarelativistic electrons and solar flare gamma-radiation
[SH-1.3-11] N85-34757
Cosmic ray north-south anisotropy 1961 - 1983
[SH-4.2-6] N85-34844
Effects of a wavy neutral sheet on cosmic ray anisotropies
[SH-4.2-11] N85-34849
The expected cosmic ray density and stream distributions at the heliolatitudinal asymmetry of solar wind
[SH-4.2-14] N85-34852
The effect of the neutral sheet structure of the interplanetary magnetic field on cosmic ray distribution in space
[SH-4.2-18] N85-34855
On the cosmic ray diffusion in a violent interstellar medium
[OG-7.2-14] N85-34881
Gradients and anisotropies of high energy cosmic rays in the outer heliosphere
[SH-4.3-7] N85-34992
IMF-sense-dependent cosmic ray anisotropy produced from diffusion-convection in heliosphere
[SH-4.3-9] N85-34994
Influence of the neutral sheet on the Swinson's type north-south anisotropy of cosmic rays
[SH-4.3-10] N85-34995
Characteristics of cosmic ray pole-equator anisotropy derived from spherical harmonic analysis of neutron monitor data
[SH-4.3-12] N85-34996
First zonal harmonic component of cosmic ray neutron intensity
[SH-4.3-13] N85-34997
The corotating variation of the north-south anisotropy of cosmic rays
[SH-4.3-15] N85-34999
Sidereal anisotropies in the median rigidity range 60-600GV in 1978-1983
[SH-4.4-3] N85-35001
The effect of the interplanetary magnetic field on sidereal variations observed at medium depth underground detectors
[SH-4.4-5] N85-35003
The sidereal semi-diurnal variation observed at high zenith angles at Mawson, 1968-1984, and the polarity of the solar main field
[SH-4.4-6] N85-35004
Sidereal anisotropy of cosmic rays
[SH-4.4-8] N85-35006
Formulation of cosmic-ray solar daily variation and its seasonal variation, produced from generalized stationary anisotropy of solar origin
[SH-4.5-2] N85-35020
Solar tri-diurnal variation of cosmic rays in a wide range of rigidity
[SH-4.5-3] N85-35021
Upper cut-off rigidity for corotation anisotropy during solar activity cycles 20 and 21
[SH-4.5-4] N85-35022
Diurnal anisotropy during solar activity cycle twenty and diffusion-convection model
[SH-4.5-7] N85-35025
Comparative study of the phase of diurnal anisotropy on quiet and disturbed days on a long term basis up to recent period
[SH-4.5-9] N85-35027
Study of spectral exponent on quiet and disturbed days
[SH-4.5-10] N85-35028
The modulation features of the long-period cosmic ray variations in connection with the sign change of the general magnetic field of the Sun
[SH-4.5-15] N85-35032
Cosmic ray density gradient and its dependence on the north-south asymmetry in solar activity
[SH-4.5-17] N85-35034
Anomalous increase of solar anisotropy above 150GV in 1981-1983
[SH-4.5-18] N85-35035
Diagnostic of electromagnetic conditions in space using cosmic rays
[SH-4.5-19] N85-35036
Change of cosmic ray anisotropy with solar activity
[SH-4.5-20] N85-35037
Magnetic fluctuation and cosmic ray diurnal variations
[SH-4.5-21] N85-35038
The theoretical and experimental investigation of cosmic ray Forbush-effects
[SH-5.1-20] N85-35072
Peculiarities of Galactic Cosmic Ray (GCR) anisotropy variation in connection with the recurrent and sporadic Forbush effects
[SH-5.1-21] N85-35073
ANNEALING
Ultra-trace analysis of sinter tantalum with SIMS
[BLL-RARDE-TR-1220-(7291.7965)] N85-34245
Changes in lattice cell parameter of film intermetallic compounds RT2
[BLL-M-35874-(5828.4)] N85-34261
An X-ray diffraction study of titanium oxidation
[NASA-CR-176263] N85-34264
Rapid annealing of temperature-compensated, precision voltage references following fast-neutron irradiation
[DE85-009821] N85-34609
ANNUAL VARIATIONS
Comparisons of the North Polar Cap of Mars and the Earth's Northern Hemisphere snow cover
[NASA-TM-86191] N85-34728
Characteristics of cosmic ray pole-equator anisotropy derived from spherical harmonic analysis of neutron monitor data
[SH-4.3-12] N85-34996
Cosmic ray intensity distribution perpendicular to solar equatorial plane at 1 A.U. during 1978-83
[SH-4.3-14] N85-34998
The corotating variation of the north-south anisotropy of cosmic rays
[SH-4.3-15] N85-34999
Cosmic ray intensity variations observed at Matsushiro (220 M.W.E. in depth)
[SH-4.4-9] N85-35007

Cosmic ray biannual variation
[SH-4.4-15] N85-35011
Cosmic ray modulation by high-speed solar wind fluxes
[SH-5.1-22] N85-35074
The influence of quiet asymmetric magnetosphere on the cutoff rigidities of the main cone
[SH-6.1-10] N85-35083
A possible mechanism to cause the quasi-biennial variability on the solar neutrino flux
[SH-8.1-5] N85-35110

ANODIZING
Electrolytic synthesis of colored eta alumina film
N85-34201

ANOMALIES
Anomalous abundances of solar energetic particles and coronal gas: Coulomb effects and First Ionization Potential (FIP) ordering
[SH-2.1-10] N85-34791

ANTENNA ARRAYS
Adaptive antenna arrays for satellite communications: Design and testing
[NASA-CR-176162] N85-34329

ANTENNA RADIATION PATTERNS
Box truss analysis and technology development. Task 1: Mesh analysis and control
[NASA-CR-172570] N85-34156
Adaptive antenna arrays for satellite communications: Design and testing
[NASA-CR-176162] N85-34329

ANTENNAS
Reducing grating lobes due to subarray amplitude tapering
[AD-D011723] N85-34339

ANTIPROTONS
The design of an experiment to detect low energy antiprotons
[OG-9.1-1] N85-34928
An experiment to measure the energy spectrum of cosmic ray antiprotons from 100 to 1000 MeV
[OG-9.1-3] N85-34929

APERTURES
Method of precisely modifying predetermined surface layers of a workpiece by cluster ion impact therewith
[DE85-006519] N85-34710
Hexagonal uniformly redundant arrays for coded-aperture imaging
[OG-9.2-1] N85-34940
SONTRAC: A solar neutron track chamber detector
[SH-9.1-12] N85-35127

APPROACH
Ground-based and in-flight simulator studies of flight characteristics of a twin-fuselage passenger transport airplane during approach and landing
[NASA-TP-2451] N85-34144

APPROACH CONTROL
Guidelines for the evaluation of visual approach slope indicators
[ARL-SYS-R-32] N85-34132

APPROPRIATIONS
Department of Housing and Urban Development Independent Agencies Appropriation Bill, 1986
[S-REPT-99-129] N85-34720
National Aeronautics and Space Administration research and development: Program description N85-34721

APPROXIMATION
Multiaxial stress analysis taking account of penetration depth of X-rays. A solution by means of polynomial approximation N85-34204
Building an octree from a set of parallelepipeds N85-34572
Guiding center distribution function and longitudinal invariant N85-34663
The role of cosmic rays in magnetic hydrodynamics of interstellar medium
[OG-7.2-15] N85-34882

AQUEOUS SOLUTIONS
Experimental evaluation of the thermodynamic properties of concentrated aqueous potassium hydroxide solutions
[DE85-010628] N85-34238

AQUIFERS
Detailed validation of a liquid and heat flow code against field performance
[DE85-009901] N85-34368
Depletion modeling of liquid dominated geothermal reservoirs
[DE85-009923] N85-34437

ARC DISCHARGES
Hollow cathodes in high pressure arc discharges
[NASA-TM-87098] N85-34179

ARC JET ENGINES
Electrode erosion in arc discharges at atmospheric pressure
[NASA-TM-87087] N85-34178
Hollow cathodes in high pressure arc discharges
[NASA-TM-87098] N85-34179

ARC WELDING
Chromium-base powder alloys for welding cladding layer of bimetal
[BLL-M-35776-(5828.4)] N85-34260
Electronic imaging system and technique
[DE85-005740] N85-34393

ARCHITECTURE
Generative design in architecture using an expert system N85-34582

ARCHITECTURE (COMPUTERS)
Modular digital holographic fringe data processing system
[NASA-CR-177952] N85-34376
The parser generator as a general purpose tool
[NASA-CR-177955] N85-34521
Architecture of languages for large CAD systems development N85-34557

ARGON ISOTOPES
Measurements of the fragmentation of (40)Ar, (28)Si and (12)C in CH2C and H targets between 300 and 1500 MeV/nuc at the Bevalac
[OG-7.2-19] N85-34886
Measurements of Fe and Ar fragmentation cross sections
[OG-7.2-20] N85-34887
Correlation between solar neutrino flux and other solar phenomena N85-35109
The conjecture concerning time variations in the solar neutrino flux
[SH-8.1-6] N85-35111

ARGON PLASMA
Synthesis of ultrafine ceramic and metallic powders in a thermal argon rf plasma
[DE85-009634] N85-34696

ARID LANDS
Resource evaluation and site selection for microalgae production systems
[DE85-008807] N85-34485

ARRAYS
Hexagonal uniformly redundant arrays for coded-aperture imaging
[OG-9.2-1] N85-34940
Mini and super mini arrays for the study of highest energy cosmic rays
[OG-9.4-9] N85-34976
Angular resolution of air-shower array-telescopes
[OG-9.5-6] N85-34983
Astrophysical applications of high angular resolution array-telescopes
[OG-9.5-7] N85-34984
Angular resolution of an EAS array for gamma ray astronomy energies 5 x 10 (13) eV
[OG-9.5-8] N85-34985

ARTERIOSCLEROSIS
Tolerance to +Gz and +Gx accelerations of individuals in older age groups in good health and with early signs of arteriosclerosis N85-34496

ARTIFICIAL INTELLIGENCE
Knowledge engineering application in image processing N85-34583
Heuristic rules for visualization N85-34584
Robot environment expert system
[NASA-CR-3915] N85-34593
Implications of artificial intelligence on the design of future onboard systems
[SFENA-DPS/C/S3/84252A] N85-34596
Monte Carlo techniques for analyzing deep penetration problems
[DE85-011426] N85-34598

ARTIFICIAL SATELLITES
Magnetospheric multiprobes: MMP/CHEMSAT N85-34171

ASBESTOS
Substitution of asbestos by aramid fibers and fiber blends in industrial textiles and composites with organic binders
[BMFT-FB-T-85-006] N85-34294

ASPECT RATIO
Neoclassical diffusion including ellipticity in a heliotron-like configuration N85-34667

ASSAYING
Improved flow cytometer measurement of binding assays
[DE85-006407] N85-34390

ASSEMBLING
Multi-robot assembly of IC's N85-34577

ASSESSMENTS
Description of a test site for large-scale heavy gas dispersion and combustion experiments
[DE85-004987] N85-34231

ASSURANCE
Towards the year 2000: Developments in inspection and product assurance to be anticipated during the next 15 years — aircraft engines
[PNR-90258] N85-34421

ASTEROIDS
The 13 November 1984 occultation of BD +08 deg 0471 by (1) Ceres
[NASA-CR-176106] N85-34725

ASTRONOMICAL MODELS
First-order shock acceleration in solar flares
[SH-1.1-5] N85-34732
Variations in the propagation of UH-nuclei
[OG-7.1-1] N85-34863
An experiment to measure the energy spectrum of cosmic ray antiprotons from 100 to 1000 MeV
[OG-9.1-3] N85-34929

ASTRONOMICAL OBSERVATORIES
Research of advanced techniques for X-ray detectors and telescopes with applications to rockets and the LAMAR facility
[NASA-CR-176161] N85-35141

ASTRONOMICAL PHOTOGRAPHY
A star camera aspect system suitable for use in balloon experiments
[OG-9.3-10] N85-34965

ASTRONOMY
The 13 November 1984 occultation of BD +08 deg 0471 by (1) Ceres
[NASA-CR-176106] N85-34725

ASTROPHYSICS
Numerical simulation in astrophysics: Smoothed particle methods N85-34674
Research of advanced techniques for X-ray detectors and telescopes with applications to rockets and the LAMAR facility
[NASA-CR-176161] N85-35141

ASYMMETRY
Model of azimuthal non-uniformities induced by RF heating in RFC-XXM N85-34658
Assessment of magnetic field asymmetries in ELMO Bumpy square
[DE85-011559] N85-34705
North-south asymmetry in activity on the Sun and cosmic ray density gradients
[SH-4.2-7] N85-34845
The expected cosmic ray density and stream distributions at the heliolatitudinal asymmetry of solar wind
[SH-4.2-14] N85-34852
The influence of quiet asymmetric magnetosphere on the cutoff rigidities of the main cone
[SH-6.1-10] N85-35083
New Matsushiro underground cosmic ray station (220 M.W.E. in depth)
[SH-9.1-14] N85-35129

ATLANTIC OCEAN
Research at the Institute of Oceanographic Sciences related to the possible disposal of radioactive waste on or beneath the seafloor
[IOS-204] N85-34628

ATMOSPHERES
On the angular and energy distribution of solar neutrons generated in P-P reactions
[SH-1.4-9] N85-34769

ATMOSPHERIC COMPOSITION
Potential spin-offs of the carbon dioxide observational platform system (CO-OPS) for remote sensing opportunities
[NASA-TP-2510] N85-34149
Agents and effects of ozone trends in the atmosphere
[AERONOMICA-ACTA-A-287-1984] N85-34466
Climate modeling: A retrospective-prospective view with consideration for the atmospheric carbon dioxide-climate issue
[DE85-011532] N85-34481

ATMOSPHERIC DIFFUSION
The first three harmonics of solar daily variation caused by the diffusive propagation of galactic cosmic rays through the heliosphere
[SH-4.5-1] N85-35019

ATMOSPHERIC EFFECTS
Lake ice occurence as a possible detector of atmospheric CO2 effects on climate
[DE85-012987] N85-34480
Atmospheric effects on the underground muon intensity
[SH-6.1-3] N85-35078

ATMOSPHERIC MODELS
Atmospheric modeling of organics for risk assessment: A Chemist's view
[DE85-009770] N85-34217
User's guide to the MATHEW/ADPIC models
[DE85-012952] N85-34587

ATMOSPHERIC MOISTURE
Throughfall rate and chemistry studies: Whiteface Mountain
[DE85-012407] N85-34464

ATMOSPHERIC PRESSURE
Electrode erosion in arc discharges at atmospheric pressure
[NASA-TM-87087] N85-34178
Monitoring dosage of volatile compounds in tests at low barometric pressure N85-34506
Comparative study of the phase of diurnal anisotropy on quiet and disturbed days on a long term basis up to recent period
[SH-4.5-9] N85-35027
Atmospheric effects on the underground muon intensity
[SH-6.1-3] N85-35078
The neutron moderated detector and groundbased cosmic ray modulation studies
[SH-9.1-13] N85-35128
ATMOSPHERIC RADIATION
Application of imaging to the atmospheric Cherenkov technique
[OG-9.5-4] N85-34981
Three dimensional calculation of flux of low energy atmospheric neutrinos
[SH-8.1-11] N85-35116
ATMOSPHERIC TEMPERATURE
Reports from the German Meteorological Service. No. 167: Results of aerological soundings in the model area upper Rhine: Heat release project upper Rhine area, part 3
[ISBN-3-88148-216-4] N85-34479
Variations of the cosmic ray general component in Antarctica
[SH-4.4-17] N85-35013
ATOM CONCENTRATION
The influence of temperature on the composition density of the transition metals
[BLL-M-35896-(5826.4)] N85-34262
ATOMIC CLOCKS
Elemental technetium as a cosmic-ray clock
[OG-7.1-9] N85-34870
ATOMIC EXCITATIONS
Pairing correction of particle-hole state densities for two kinds of fermions
[DE85-011549] N85-34620
ATOMIZING
Influence of technology of atomization of naturally alloyed iron on grain-size characteristics of powder material
[BLL-M-35810-(5828.4)] N85-34257
ATTITUDE (INCLINATION)
Cosmic ray intensity and the tilt of the neutral sheet
[SH-4.2-8] N85-34846
AUDITORY PERCEPTION
Dissociation of autonomic and sensory vestibular reactions N85-34501
AUDITORY SIGNALS
Rotor blade test apparatus
[AD-D011725] N85-34381
AUGER EFFECT
Multiple inner shell vacancies in laser-irradiated Au plasma N85-34687
AURORAS
Atmospheric Emission Photometric Imaging (AEPI) N85-34170
Vehicle Charging And Potential (VCAP) N85-34173
Cosmic rays 10Be biennal data and their relationship to aurorae and sunspots
[SH-7.1-1] N85-35094
Cosmic ray secular variations in terrestrial records and aurorae
[SH-7.1-3] N85-35096
AUSTENITE
Effects of hot deformation on the kinetics of the pearlite transformation in eutectoid steel
[BLL-M-35844-(5828.4)] N85-34250
Acoustic emission during transformation of austenite in 38KhN3MF steel
[BLL-M-35825-(5828.4)] N85-34256
AUSTENITIC STAINLESS STEELS
Phase transformations taking place in austenitic steel during deformation at different rates
[BLL-M-35875-(5828.4)] N85-34254
The effect of pre-heating on the structure and properties of chromiun-molybdenum steels
[BLL-M-35897-(5828.4)] N85-34255
Acoustic emission during transformation of austenite in 38KhN3MF steel
[BLL-M-35825-(5828.4)] N85-34256
AUTOMATA THEORY
Intermittent motion N85-34323
AUTOMATIC CONTROL
Centralized surveillance of flexible workshops for the manufacturing of composite materials
[SNIAS-851-430-103] N85-34227
Multi-robot assembly of IC's N85-34577
Maintenance port system
[AD-D011724] N85-34594
AUTONOMIC NERVOUS SYSTEM
Dissociation of autonomic and sensory vestibular reactions N85-34501
AUTOREGRESSIVE PROCESSES
Methods and software for cosmic ray scintillation studies
[SH-9.1-17] N85-35132
AXIAL COMPRESSION LOADS
Mechanical ratcheting behaviors of a steel pipe under combined cyclic axial load and internal pressure N85-34184
Monotonous stress-strain properties of structural steel subjected to nonstationary repetitive pre-loading N85-34185
AXIAL LOADS
Experimental study of collapse of thick-walled tube under external pressure and axial force N85-34186
AXIAL STRESS
Multiaxial stress analysis taking account of penetration depth of X-rays. A solution by means of polynomial approximation N85-34204
AZIMUTH
Comprehensive fracture diagnostics experiement. Part 2: Comparison of seven fracture azimuth measurements
[DE85-011707] N85-34470
A star camera aspect system suitable for use in balloon experiments
[OG-9.3-10] N85-34965
Azimuthal and meridional asymmetries of the solar wind and quasiperiodic variations of intensity of Galactic Cosmic Rays (GCR)
[SH-4.4-20] N85-35016
AZOLES
Ethylenediamine salt of 5-nitrotetrazole and preparation
[DE85-005738] N85-34306

B

BACKGROUND NOISE
A comparison of calculated and measured background noise rates in hard X-ray telescopes at balloon altitude
[OG-9.3-7] N85-34962
BACKGROUND RADIATION
The 1984 biotic studies of Yucca Mountain, Nevada test site, Nye County, Nevada
[DE85-011715] N85-34487
CYLTRAN calculations of electron effects on XD detectors
[LA-10264-MS] N85-34601
The design of an experiment to detect low energy antiprotons
[OG-9.1-1] N85-34928
Neutron-induced 2.2 MeV background in gamma ray telescopes
[OG-9.3-6] N85-34961
Three dimensional calculation of flux of low energy atmospheric neutrinos
[SH-8.1-11] N85-35116
BACKSCATTERING
Data on the backscattering coefficients on light ions from solids: A revision
[IPPJ-AM-41-REV] N85-34689
BALANCING
The balancing of complex linkage mechanisms N85-34313
A versatile computer package for mechanism analysis, part 2: Dynamics and balance N85-34315
BALL BEARINGS
Special features of the fracture of ball-bearing steel close to non-metallic inclusion eutectics
[BLL-M-35809-(5828.4)] N85-34258
BALLISTIC TRAJECTORIES
OMEGA: Optoelectronic measurement of the incidence angle of a projectile
[ISL-CO-223/84] N85-34634
BALLOON SOUNDING
The dependence of solar modulation on the sign of the cosmic ray particle charge
[SH-4.2-23] N85-34860
BALLOON-BORNE INSTRUMENTS
A search for solar neutrons on a long duration balloon flight
[SH-1.4-6] N85-34766
The design of an experiment to detect low energy antiprotons
[OG-9.1-1] N85-34928
Cherenkov-dE/dx-range measurements on cosmic ray iron group nuclei
[OG-9.1-12] N85-34937
A balloon-borne imaging gamma-ray telescope
[OG-9.2-2] N85-34941
The Gamma-Ray Imaging Spectrometer (GRIS): A new balloon-borne experiment for gamma-ray line astronomy
[OG-9.2-4] N85-34943
An experimental assessment of the imaging quality of the low energy gamma-ray telescope ZEBRA
[OG-9.2-8] N85-34947
High energy gamma ray balloon instrument
[OG-9.2-12] N85-34951
Measured performance of the new University of California gamma ray telescope
[OG-9.2-13] N85-34952
An improved time of flight gamma-ray telescope to monitor diffuse gamma-ray in the energy range 5 MeV - 50 MeV
[OG-9.3-2] N85-34957
An approach of reducing the background induced by neutrons
[OG-9.3-5] N85-34960
A star camera aspect system suitable for use in balloon experiments
[OG-9.3-10] N85-34965
Balloon-borne video cassette recorders for digital data storage
[OG-9.3-11] N85-34966
Photometric and spectroscopic gamma-ray observations of solar transient phenomena using long duration balloons
[SH-9.1-5] N85-35120
BALLOONS
Lapex: A Phoswich balloon experiment for hard X-ray astronomy
[OG-9.3-1] N85-34956
A comparison of calculated and measured background noise rates in hard X-ray telescopes at balloon altitude
[OG-9.3-7] N85-34962
BAROMETERS
On the solar cycle variation in the barometer coefficients of high latitude neutron monitors
[SH-6.1-2] N85-35077
The neutron moderated detector and groundbased cosmic ray modulation studies
[SH-9.1-13] N85-35128
BARRELS (CONTAINERS)
Container for radioactive materials
[DE85-005757] N85-34626
BARS
Behaviors of stress waves in a conical bar N85-34182
BEAM CURRENTS
RADLAC technolgy review
[DE85-011995] N85-34691
Technology of magnetically driven accelerators
[DE85-011857] N85-34700
BEAM SPLITTERS
Applications of holography to X-ray imaging
[DE85-010984] N85-34384
Polarisation insensitive achromatic cube beamsplitter — binocular microscopes
[NPL-MOM-72] N85-34630
Differentiating spatial light modulator
[AD-D011727] N85-34632
BEAMS (SUPPORTS)
Stress distribution of fiberglass reinforced plastic beam with a delamination under three-point bending N85-34210
BEARING (DIRECTION)
Angular resolution of air-shower array-telescopes
[OG-9.5-6] N85-34983
BENDING
Stress distribution of fiberglass reinforced plastic beam with a delamination under three-point bending N85-34210
BENDING FATIGUE
Rotating bending fatigue strength of silicon carbide and alumina-fiber reinforced aluminum N85-34208
BENDING MOMENTS
Negative flexural behavior of precase composite slabs with steel joint N85-34183
Nonlinear flap-lag-extensional vibrations of rotating, pretwisted, preconed beams including Coriolis effects
[NASA-TM-87102] N85-34427
BERYLLIUM 10
Cosmic rays 10Be biennal data and their relationship to aurorae and sunspots
[SH-7.1-1] N85-35094
BESSEL FUNCTIONS
Calculation of roots of transcendental equations in problems of determining thermal conductivity of cylinder with non-uniform boundary conditions
[BLL-M-35788-(5828.4)] N85-34349
BETA FACTOR
Simulation studies on stability of hot electron plasma N85-34684
BIBLIOGRAPHIES
Index of laser program publications and related reports, calendar year 1984
[DE85-011863] N85-34398

Aerospace Medicine and Biology: A continuing bibliography with indexes (supplement 274) [NASA-SP-7011(274)] N85-34491
The next assignment: The state of the literature on space N85-35146

BIMETALS
Chromium-base powder alloys for welding cladding layer of bimetal [BLL-M-35776-(5828.4)] N85-34260

BINARY ALLOYS
Anti wear property of two phasic metal composite N85-34199
Enthalpies of formation of liquid Fe-Ce-Si and Fe-Ce-Al three-component alloys [BLL-M-36296-(5828.4)] N85-34247
Calculation of activities of components in liquid alloys of iron with yttrium [BLL-M-35868-(5828.4)] N85-34253

BINDING
Improved flow cytometer measurement of binding assays [DE85-006407] N85-34390

BIOASSAY
Applications of holography to X-ray imaging [DE85-010984] N85-34384

BIOASTRONAUTICS
USSR report: Space Biology and Aerospace Medicine, vol. 19, no. 3, May - June 1985 [JPRS-USB-85-005] N85-34494

BIOCHEMISTRY
Improved flow cytometer measurement of binding assays [DE85-006407] N85-34390
Anaerobic microbial transformations in subsurface environments: Project description [DE85-012789] N85-34486
USSR report: Space Biology and Aerospace Medicine, vol. 19, no. 3, May - June 1985 [JPRS-USB-85-005] N85-34494

BIODEGRADATION
Two dimensional CO2-ocean model including the biological processes [DE85-012341] N85-34483

BIODYNAMICS
USSR report: Space Biology and Aerospace Medicine, vol. 19, no. 3, May - June 1985 [JPRS-USB-85-005] N85-34494
Using dynamic analysis to animate articulated bodies such as humans and robots N85-34537

BIOLOGICAL EFFECTS
Ocean thermal energy conversion [DE85-012291] N85-34456
Aerospace Medicine and Biology: A continuing bibliography with indexes (supplement 274) [NASA-SP-7011(274)] N85-34491
Effect of seeds of heavy charged particles of galactic cosmic radiation N85-34505

BIOMEDICAL DATA
USSR report: Life sciences. Biomedical and behavioral sciences [JPRS-UBB-85-021] N85-34489

BIPOLAR TRANSISTORS
Realization and linearization of a hyperfrequency power amplifier implemented with bipolar transistors in class C polarization --- microwave amplifiers [CNES-NT-114] N85-34346

BLACK HOLES (ASTRONOMY)
Breakdown of helium nuclei in matter processed near black holes [OG-8.2-20] N85-34916

BLADE TIPS
Oxidizing seal for a turbine tip gas path [NASA-CASE-LEW-14053-1] N85-34402

BLOOD CIRCULATION
Effect of hypokinesia and +Gz accelerations on transport function of human blood N85-34497
Oxygenation and regional circulation in gingival mucosa during exposure to lower body negative pressure N85-34498

BLOOD PRESSURE
Effect of water immersion of parameters of central hemodynamics in individuals over 45 years old N85-34499

BLOOD VESSELS
Development of the osmium-191 yields iridium-191m radionuclide generator [DE85-011165] N85-34611

BODY FLUIDS
Fluid-electrolyte metabolism and renal function in cosmonauts following 185-day spaceflight N85-34495

BODY KINEMATICS
The dynamics of articulated rigid bodies for purposes of animation N85-34579

BOILERS
Control system for fluid heated steam generator [DE85-005734] N85-34417
Calculations on the feasibility of ultrasonic inspection of steam generator tubing in pressurized water reactors [AERE-R-10960] N85-34419

BOILING
Effects of ambient pressure on the instability of a liquid boiling explosively at the superheat limit [DE85-009476] N85-34370

BOILING WATER REACTORS
Technical assessment of thermal-hydraulics for high heat flux fusion components [DE85-013178] N85-34359

BOLTS
Three-dimensional finite element failure model for predicting failure in fibre reinforced bolted joints [BR94778] N85-34423
Stresses and strains in a plate resulting from two closely-spaced interference-fit fasteners [ARL-STRUC-TM-409] N85-34429

BOLTZMANN DISTRIBUTION
Time-resolved spectroscopic studies of detonating heterogeneous explosives [DE85-009760] N85-34297

BOOLEAN FUNCTIONS
An analysis and algorithm for filling propagation N85-34551

BOREHOLES
Iron and manganese in oxide minerals and in glasses: Preliminary consideration of Eh buffering potential at Yucca Mountain, Nevada [DE85-011892] N85-34271

BORIDES
Magnitude and range of the RKKy interaction in SmRh4B4 [DE85-012284] N85-34712

BORON
Evaluation of low-temperature geothermal potential in Utah and Goshen Valleys and adjacent areas, Utah. Part 2: Water temperature and chemistry [DE85-009344] N85-34438

BORON CARBIDES
Shield design for next-generation, low-neutron-fluence, superconducting tokamaks [DE85-011409] N85-34695

BORON OXIDES
Method for removing oxide contamination from silicon carbide powders [DE85-011648] N85-34287

BOUNDARIES
Scaling differences between large interplate and intraplate earthquakes [NASA-CR-176149] N85-34467
A user-friendly computer-aided construction of boundaries N85-34564
Dynamics of the penetration boundaries of solar protons during a strong magnetic storm [SH-6.1-16] N85-35089

BOUNDARY ELEMENT METHOD
On the methods to determine the stress intensity factors in boundary element method N85-34189

BOUNDARY LAYER FLOW
A comparison of laser Doppler anemometry and probe measurements within the boundary layer of an airfoil at subsonic flow [ISL-CO-219/84] N85-34127

BOUNDARY LAYER SEPARATION
Modelling of unsteady, incompressible separation on an aerofoil using an inviscid flow algorithm [GU-AERO-8412] N85-34122
Study of boundary layer separation on a supercritical profile with a spoiler by means of a laser Doppler velocimeter [ISL-CO-225/84] N85-34128

BOUNDARY LAYER TRANSITION
Nozzle wall roughness effects on free-stream noise and transition in the pilot low-disturbance tunnel [NASA-TM-86389] N85-34355

BOUNDARY LAYERS
Evaluation of source strength and dispersion model predications with data from large nitrogen tetroxide field experiments [DE85-011855] N85-34465

BRAZING
X-ray residual stress analysis on the coarse grain of copper and its application to the brazed copper N85-34202

BREMSSTRAHLUNG
Study of non-thermal photon production under different scenarios in solar flares. 2: The Compton inverse and Bremsstrahlung models and fittings [SH-1.2-3] N85-34739
Burst size distributions in the digitized data of the ion chambers t Mt. Norikura and sea level stations [SH-9.1-9] N85-35124

BRIGHTNESS DISTRIBUTION
Clusters and cycles in the cosmic ray age distributions of meteorites [SH-7.1-11] N85-35103

BRUSH (BOTANY)
Determination of low chloride values in Rocky Flats scrub alloy solutions and other complex matrices [DE85-011506] N85-34234

BRUSHES (ELECTRICAL CONTACTS)
Brush and commutator segment torquer motor [AD-D011726] N85-34340

BUBBLES
Features of behavior of gas bubbles in molten oxide films during enamelling: Communication 2 [BLL-M-35781-(5828.4)] N85-34283

BUFFERS (CHEMISTRY)
Iron and manganese in oxide minerals and in glasses: Preliminary consideration of Eh buffering potential at Yucca Mountain, Nevada [DE85-011892] N85-34271

BUMPY TORUSES
Proceedings of the US-Japan Workshop on Transport in Open-Ended Systems [IPPJ-727] N85-34644
Compact DT fusion spherical tori at modest field [DE85-011568] N85-34692
Multiple-frequency electron cyclotron heating of hot electron rings in EBT-1 [DE85-011302] N85-34701
Assessment of magnetic field asymmetries in ELMO Bumpy square [DE85-011559] N85-34705

BURNING RATE
Investigation of the flame speeds of propane/methanol gas mixtures [DE85-012817] N85-34239
Modeling heterogeneous high explosive burn with an explicit hot-spot process [DE85-009593] N85-34300

BURSTS
X-ray spectra of bursting neutron stars N85-34686

BYPASS RATIO
Energy efficient engine. Fan and quarter-stage component performance report [NASA-CR-168070] N85-34141

C

CABLES (ROPES)
Apparatus producing constant cable tension for intermittent demand [DE85-006434] N85-34412

CADMIUM
Towards the development of technological processes for the preparation of cadmium plated steel articles [BLL-M-36315-(5828.4)] N85-34248

CADMIUM TELLURIDES
Applications of CdTe to nuclear medicine [DE85-011877] N85-34492

CALCITE
Shock and release equation of state of calcite [DE85-013151] N85-34432
Uranium, thorium isotopic analyses and uranium-series ages of calcite and opal and stable isotopic compositions of calcite from drill cores UE25a no. 1, USR G-2 and USW G-3/GU-3, Yucca Mountain, Nevada [DE85-013039] N85-34471

CALCIUM
Effects of acid rain on forest nutrient status [DE85-012486] N85-34463

CALCIUM CARBONATES
Two dimensional CO2-ocean model including the biological processes [DE85-012341] N85-34483

CALDERAS
Workshop on Recent Research in the Valles Caldera [DE85-010569] N85-34472

CALIBRATING
AMI calibration study. Volume 1: SAR calibration. Volume 2: Ground Targets. Volume 3: Scatterometer calibration --- Active Microwave Instrument (AMI) ERS-1 [C2248/4/4-VOL-1] N85-34394
Multi-robot assembly of IC's N85-34577
Measured performance of the new University of California gamma ray telescope [OG-9.2-13] N85-34952
The final COS-B database: In-flight calibration of instrumental parameters [OG-9.3-9] N85-34964
Detector calibration of the Indian cosmic ray experiment (IONS) in Space-Shuttle Spacelab-13 [SH-9.1-2] N85-35117

CAMERA SHUTTERS
Electronic imaging system and technique [DE85-005740] N85-34393

CAMERAS
A star camera aspect system suitable for use in balloon experiments
[OG-9.3-10] N85-34965
CAMS
A rational approach to cam design N85-34311
CANARD CONFIGURATIONS
The aerodynamic characteristics of a GU25-5(11)8 aerofoil for low Reynolds numbers
[GU-AERO-8410] N85-34121
CANTILEVER BEAMS
Nonlinear flap-lag-extensional vibrations of rotating, pretwisted, preconed beams including Coriolis effects
[NASA-TM-87102] N85-34427
CAPACITORS
Reversing-counterpulse repetitive-pulse inductive storage circuit
[DE85-006409] N85-34344
CAPTURE EFFECT
Capture in the 1.15-keV iron resonance
[DE85-011913] N85-34612
Electron loss process and cross section of multiply charged ions by neutral atoms N85-34685
CARBON
Electron photoejection in carbanions
[DE85-011747] N85-34230
Electron photoejection in carbanions
[DE85-011748] N85-34237
Diamondlike carbon protective coatings for IR materials
[NASA-TM-87083] N85-34631
CARBON CYCLE
Two dimensional CO2-ocean model including the biological processes
[DE85-012341] N85-34483
CARBON DIOXIDE
Potential spin-offs of the carbon dioxide observational platform system (CO-OPS) for remote sensing opportunities
[NASA-TP-2510] N85-34149
Separation of gas mixtures by supported complexes
[DE85-011996] N85-34236
Climate modeling: A retrospective-prospective view with consideration for the atmospheric carbon dioxide-climate issue
[DE85-011532] N85-34481
Increase of total CO2 in the World ocean
[DE85-007756] N85-34484
Solar modulation of cosmic ray intensity and solar flare events inferred from (14)C contents in dated tree rings
[SH-7.1-2] N85-35095
CARBON DIOXIDE CONCENTRATION
Potential spin-offs of the carbon dioxide observational platform system (CO-OPS) for remote sensing opportunities
[NASA-TP-2510] N85-34149
CARBON ISOTOPES
Nucleosynthesis in the terrestrial and solar atmospheres
[SH-2.2-2] N85-34797
Measurements of the fragmentation of (40)Ar, (28)Si and (12)C in CH2C and H targets between 300 and 1500 MeV/nuc at the Bevalac
[OG-7.2-19] N85-34886
CARBON MONOXIDE
Infrared studies of the influence of alkali metals on the C-O bond in chemisorbed carbon monoxide
[DE85-005306] N85-34232
Separation of gas mixtures by supported complexes
[DE85-011996] N85-34236
Oxygen analyzer
[DE85-006002] N85-34392
CARBON STARS
Neutron-rich nuclei in cosmic rays and Wolf-Rayet stars
[OG-8.2-6] N85-34906
CARBON STEELS
Corrosion fatigue strength and crack growth in prestrained 0.16% C carbon steel N85-34192
CARBON 14
Solar modulation of cosmic ray intensity and solar flare events inferred from (14)C contents in dated tree rings
[SH-7.1-2] N85-35095
High precise measurements of cosmogenic radiocarbon abundance by complex of scintillation equipments
[SH-7.1-14] N85-35105
CARBON-CARBON COMPOSITES
Carbon/carbon combustor external insulation
[AD-D011719] N85-34224
CARBONACEOUS MATERIALS
Method of distributing liquefaction catalysts in solid carbonaceous material
[DE85-005759] N85-34218
CARBONATES
Electrolyte resevoir for carbonate fuel cells
[DE85-005736] N85-34460
CARDIOGRAPHY
Current status of the Os-191 yields Ir-191m generator
[DE85-008306] N85-34614
CARDIOVASCULAR SYSTEM
Effect of acute hypoxia on coronary and systemic hemodynamics N85-34503
CARTESIAN COORDINATES
Algorithm for calculation of strain state from measurements of node coordinates of arbitrary curvilinear grid
[BLL-M-36304] N85-34422
CASES (CONTAINERS)
Electrically conductive containment vessel for molten aluminum
[DE85-006518] N85-34415
CATALYSIS
Rigid zeolite containing polyurethane foams
[DE85-006406] N85-34286
CATALYSTS
Method of distributing liquefaction catalysts in solid carbonaceous material
[DE85-005759] N85-34218
CATHODE RAY TUBES
Maintenance port system
[AD-D011724] N85-34594
CATHODES
Electrode erosion in arc discharges at atmospheric pressure
[NASA-TM-87087] N85-34178
CATIONS
Throughfall rate and chemistry studies: Whiteface Mountain
[DE85-012407] N85-34464
CAVITIES
Method of precisely modifying predetermined surface layers of a workpiece by cluster ion impact therewith
[DE85-006519] N85-34710
CAVITY RESONATORS
New directional couplers for multimode circular waveguides applied to intense pulsed microwave systems
[DE85-011753] N85-34330
CELLS (BIOLOGY)
Microorganisms in space flight N85-34490
CEMENTS
High temperature polymer concrete
[DE85-005756] N85-34290
CENTRIFUGES
Method for controlling the viscosity of siloxane oils
[DE85-011586] N85-34221
CERAMIC MATRIX COMPOSITES
Evaluation methods of ceramic fiber reinforced metal matrix composite N85-34208
CERAMICS
Thermal protection systems for reentry vehicles
[CNES-NT-113] N85-34157
X-ray residual stress analysis on the coarse grain of copper and its application to the brazed copper N85-34202
High resolution electron microscopic characterization of interfaces in ceramics
[DE85-011207] N85-34289
High temperature structural insulating material
[DE85-006361] N85-34291
Synthesis of ultrafine ceramic and metallic powders in a thermal argon rf plasma
[DE85-009634] N85-34696
CERENKOV COUNTERS
High resolution Cherenkov detectors for cosmic ray isotope experiment
[OG-9.1-4] N85-34930
Cerenkov counters for high energy nuclei: Some new developments
[OG-9.1-5] N85-34931
A high resolution gas Cerenkov detector for the superconducting magnet facility
[OG-9.1-6] N85-34932
Bevalac calibration of the SOFIE range and hodoscope detectors
[OG-9.1-7] N85-34933
The development of a high energy cosmic ray detector for Spacelab-2
[OG-9.1-8] N85-34934
Mass resolution optimization in a large isotopic composition experiment
[OG-9.1-9] N85-34935
Cherenkov-dE/dx-range measurements on cosmic ray iron group nuclei
[OG-9.1-12] N85-34937
Application of imaging to the atmospheric Cherenkov technique
[OG-9.5-4] N85-34981
A method to improve observations of gamma-ray sources near 10 (15) eV
[OG-9.5-5] N85-34982
CERENKOV RADIATION
A high resolution gas Cerenkov detector for the superconducting magnet facility
[OG-9.1-6] N85-34932
A Cerenkov imaging telescope for high energy gamma rays
[OG-9.3-13] N85-34968
The University of Durham Mark 3 very high energy gamma ray telescope
[OG-9.4-2] N85-34969
Cerenkov light images of EAS produced by primary gamma
[OG-9.5-3] N85-34979
Angular resolution of an EAS array for gamma ray astronomy energies 5 x 10 (13) eV
[OG-9.5-8] N85-34985
CERIUM
Enthalpies of formation of liquid Fe-Ce-Si and Fe-Ce-Al three-component alloys
[BLL-M-36296-(5828.4)] N85-34247
CESIUM IODIDES
Downstream behavior of volatile fission product species
[DE85-012124] N85-34617
CHARGE CARRIERS
Hermetic chip carrier compliant soldering pads
[AD-D011722] N85-34410
CHARGE DISTRIBUTION
Electron photoejection in carbanions
[DE85-011747] N85-34230
Electron photoejection in carbanions
[DE85-011748] N85-34237
Calculations of heavy ion charge state distributions for nonequilibrium conditions
[SH-2.1-12] N85-34793
On the influence of the heliomagnetospheric periphery on the galactic cosmic rays
[SH-4.2-19] N85-34856
CHARGED PARTICLES
Effect of seeds of heavy charged particles of galactic cosmic radiation N85-34505
Theoretical and computational research on the focused transport of intense charged particle beams
[DE85-012980] N85-34621
Guiding center distribution function and longitudinal invariant N85-34663
Acceleration of ions and electrons to near-cosmic ray energies in a perpendicular shock: The January 6, 1978 event
[SH-1.5-4] N85-34773
The Jovian electron spectrum: 1978-1984
[SH-1.5-19] N85-34782
Silicon to iron abundances in solar cosmic rays and in the sun
[SH-2.1-6] N85-34787
The mean ionic charges of N, Ne, MG, SI and S in solar energetic particle events
[SH-2.1-11] N85-34792
On the connection between the 3HE-enrichment and spectral index of solar energetic particles
[SH-2.2-9] N85-34804
The dispersive evolution of charged-particle bunches in random magnetic fields
[SH-4.1-2] N85-34828
Spatial distribution of cosmic rays in magnetic cycles of the Sun
[SH-4.2-20] N85-34857
The dependence of solar modulation on the sign of the cosmic ray particle charge
[SH-4.2-23] N85-34860
Observation of energy spectrum of electron albedo in low latitude region at Hyderabad, India
[SH-6.1-7] N85-35081
The influence of quiet asymmetric magnetosphere on the cutoff rigidities of the main cone
[SH-6.1-10] N85-35083
A bi-directional charged particle telescope to observe flux, energy spectrum and angular distribution of relativistic and non-relativistic particles
[SH-9.1-4] N85-35119
Burst size distributions in the digitized data of the ion chambers t Mt. Norikura and sea level stations
[SH-9.1-9] N85-35124
Plastic scintillators in coincidence for the study of multi-particle production of sea level cosmic rays in dense medium
[SH-9.1-11] N85-35126
Observation of nuclei with energies 8-30 MeV per nucleon in the Earth's magnetosphere at the altitudes 350 KM
[SH-10.1-5] N85-35136
CHEMICAL ANALYSIS
A manual of methods for the continuous flow determination of ammonia, nitrate-nitrite, phosphate and silicate in seawater
[IOS-177] N85-34243

Uranium, thorium isotopic analyses and uranium-series ages of calcite and opal and stable isotopic compositions of calcite from drill cores UE25a no. 1, USR G-2 and USW G-3/GU-3, Yucca Mountain, Nevada
[DE85-013039] N85-34471

CHEMICAL BONDS

Infrared studies of the influence of alkali metals on the C-O bond in chemisorbed carbon monoxide
[DE85-005306] N85-34232
Separation of gas mixtures by supported complexes
[DE85-011996] N85-34236

CHEMICAL COMPOSITION

Determination of low chloride values in Rocky Flats scrub alloy solutions and other complex matrices
[DE85-011506] N85-34234
The influence of temperature on the composition density of the transition metals
[BLL-M-35896-(5826.4)] N85-34262
Throughfall rate and chemistry studies: Whiteface Mountain
[DE85-012407] N85-34464
Thermally induced chemical migration: A natural analog approach
[DE85-012308] N85-34474
Energetic particle observations of the solar-gamma ray/neutron flare events of 3 Jun 1982 and 21 June 1980 isotopic and chemical composition
[SH-2.1-3] N85-34784
Precision measurements of solar energetic particle elemental composition
[SH-2.1-4] N85-34785
Variations in elemental composition of several MEV/nucleon ions observed in interplanetary space
[SH-2.1-7] N85-34788
The cosmic ray composition as viewed from the chemical abundances of the solar system
[OG-7.1-8] N85-34869
The 4He1H ratios in the chemical compositions of solar flare particles and the primordial solar nebula
[SH-7.1-12] N85-35104
Measurement of low energy cosmic rays aboard Spacelab-1
[SH-10.1-6] N85-35137

CHEMICAL ELEMENTS

The cosmic ray composition as viewed from the chemical abundances of the solar system
[OG-7.1-8] N85-34869

CHEMICAL ENERGY

Modeling heterogeneous high explosive burn with an explicit hot-spot process
[DE85-009593] N85-34300

CHEMICAL EQUILIBRIUM

Comparison of experimental data on detonation velocity and Chapman-Jouget pressure vs initial HE density with predictions from Ree's model equation of state
[DE85-007266] N85-34304

CHEMICAL EXPLOSIONS

Time-resolved spectroscopic studies of detonating heterogeneous explosives
[DE85-009760] N85-34297
Pressure-shear loading of PBX-9404
[DE85-009982] N85-34296
Modeling heterogeneous high explosive burn with an explicit hot-spot process
[DE85-009593] N85-34300
Three-dimensional hydrodynamic hot-spot model
[DE85-009587] N85-34301
Effect of precipitation variables on the specific surface and explosion characteristics of pentaerythritol tetranitrate
[DE85-009620] N85-34302
Comparison of experimental data on detonation velocity and Chapman-Jouget pressure vs initial HE density with predictions from Ree's model equation of state
[DE85-007266] N85-34304

CHEMICAL LASERS

Chemical lasers
[ISL-R-107/84] N85-34400

CHEMICAL PROPERTIES

The effect of liquid-liquid phase separation of glass on the properties and crystallization behavior
[NASA-TM-77890] N85-34285
Chemical lasers
[ISL-R-107/84] N85-34400

CHEMICAL REACTIONS

Separation of gas mixtures by supported complexes
[DE85-011996] N85-34236
Experimental evaluation of the thermodynamic properties of concentrated aqueous potassium hydroxide solutions
[DE85-010628] N85-34238
Metal alkoxides: Models for metal oxides. Alkoxide ligands in early transition metal organometallic chemistry
[DE85-011368] N85-34269
Fire-resistant phosphorus containing polyimides and copolyimides
[NASA-CASE-ARC-11522-2] N85-34280
Real time analysis of PETN detonation products
[DE85-009581] N85-34303
Chemical lasers
[ISL-R-107/84] N85-34400
Studies in thermo-hydro-chemical transport in porous and fractured media
[DE85-012555] N85-34473
Thermally induced chemical migration: A natural analog approach
[DE85-012308] N85-34474
Multi-solute subsurface transfer modeling for energy solid wastes: Highlights FY 1984
[DE85-012788] N85-34591

CHEMISORPTION

Infrared studies of the influence of alkali metals on the C-O bond in chemisorbed carbon monoxide
[DE85-005306] N85-34232

CHEMISTRY

Solar energy education: Renewable energy activities for chemistry and physics
[DE85-010371] N85-34455

CHINA

Geology and petroleum resources of basins in western China
[DE85-013038] N85-34469
Space activities in the Soviet Union, Japan, and the People's Republic of China N85-35149

CHIPS (ELECTRONICS)

Hermetic chip carrier compliant soldering pads
[AD-D011722] N85-34410

CHLORINATION

The development of titanium production in the USSR
[BLL-OA-TRANS-3226-(6196.3)] N85-34244

CHLORINE

Results of ultra-low level 71ge counting for application in the Gallex-solar neutrino experiment at the Gran Sasso Underground Physics Laboratory
[SH-8.1-2] N85-35108
Correlation between solar neutrino flux and other solar phenomena N85-35109

CHLORINE COMPOUNDS

Throughfall rate and chemistry studies: Whiteface Mountain
[DE85-012407] N85-34464

CHONDRITES

The cosmic ray composition as viewed from the chemical abundances of the solar system
[OG-7.1-8] N85-34869
Cosmogenic Mn-53 in meteorites
[SH-7.1-17] N85-35107

CHROMATOGRAPHY

Modulated voltage metastable ionization detector
[NASA-CASE-ARC-11503-1] N85-34374

CHROMIUM

The effect of pre-heating on the structure and properties of chromiun-molybdenum steels
[BLL-M-35897-(5828.4)] N85-34255
Special features of the fracture of ball-bearing steel close to non-metallic inclusion eutectics
[BLL-M-35809-(5828.4)] N85-34258
Process for improving moisture resistance of epoxy resins by addition of chromium ions
[NASA-CASE-LAR-13226-1] N85-34282

CHROMIUM ALLOYS

Dynamics of the melting of chromium-manganese alloys in molten steel
[BLL-M-35850-(5828.4)] N85-34252
Chromium-base powder alloys for welding cladding layer of bimetal
[BLL-M-35776-(5828.4)] N85-34260

CHROMIUM STEELS

Characterization of modified 9 Cr Mo steel extruded pipe
[DE85-012056] N85-34430

CHROMOSPHERE

Study of photon emission by electron capture during solar nuclei acceleration. 3: Photon production evaluations
[SH-1.1-10] N85-34737
Onset of solar flares as predicted by two-dimensional MHD-models of quiescent prominences
[SH-1.3-1] N85-34750
On the detectability of key-MeV solar protons through their nonthermal Lyman-alpha emission
[SH-1.3-5] N85-34752
Diffusion in the chromosphere and the composition of the solar corona and energetic particles
[SH-2.1-9] N85-34790
Sporadic radio emission connected with a definite manifestation of solar activity in the near Earth space
[SH-10.1-8] N85-35139
Near Earth space sporadic radio emission busts occurring during sunrise
[SH-10.1-9] N85-35140

CHRONIC CONDITIONS

Estimating risks of lead-induced hemoglobin decrements under conditions of uncertainty: Methodology, pilot judgments and illustrative calculations
[DE85-012293] N85-34493

CHRONOLOGY

Why do leaky-box models work so fine?
[OG-7.2-8] N85-34877

CIRCUIT DIAGRAMS

Recognition and clear representation of handwritten electronic diagrams N85-34541

CIRCUITS

Method and apparatus for transfer function simulator for testing complex systems
[NASA-CASE-NPO-15696-1] N85-34333
Interfacing interactive circuit simulation with standard graphics fucilities N85-34529

CIRCULAR WAVEGUIDES

New directional couplers for multimode circular waveguides applied to intense pulsed microwave systems
[DE85-011753] N85-34330

CITIES

Department of Housing and Urban Development Independent Agencies Appropriation Bill, 1986
[S-REPT-99-129] N85-34720

CLADDING

Chromium-base powder alloys for welding cladding layer of bimetal
[BLL-M-35776-(5828.4)] N85-34260
Manufacturing process to reduce large grain growth in zirconium alloys
[DE85-011649] N85-34267
Effect of stainless steel weld overlay cladding on the structural integrity of flawed steel plates in bending, series 1
[TI85-010349] N85-34418

CLIMATOLOGY

Reports from the German Meteorological Service. No. 166: The optimal spectral density of climatological station networks
[ISBN-3-88148-214-8] N85-34478
Lake ice occurence as a possible detector of atmospheric CO2 effects on climate
[DE85-012987] N85-34480

CLINICAL MEDICINE

USSR report: Life sciences. Biomedical and behavioral sciences
[JPRS-UBB-85-021] N85-34489
Effect of water immersion of parameters of central hemodynamics in individuals over 45 years old N85-34499
Effect of dibazol on parameters of nonspecific resistance of subjects in pressurized cabins N85-34504

CLOCKS

Recording system for the solar neutron monitoring at Mt. Norikura
[SH-9.1-8] N85-35123

CLOSURE LAW

A study of the second and third order closure models of turbulence for prediction of separated shear flows
[NASA-CR-176127] N85-34353

CLUMPS

Clusters and cycles in the cosmic ray age distributions of meteorites
[SH-7.1-11] N85-35103

COAL

Shuttle car loading system
[NASA-CASE-NPO-15949-1] N85-34722

COAL LIQUEFACTION

Method of distributing liquefaction catalysts in solid carbonaceous material
[DE85-005759] N85-34218

COARSENESS

X-ray residual stress analysis on the coarse grain of copper and its application to the brazed copper N85-34202

COATINGS

Electrically conductive containment vessel for molten aluminum
[DE85-006518] N85-34415

COBALT

Metal (2) 4,4',4',4'' phthalocyanine tetraamines as curing agents for epoxy resins
[NASA-CASE-ARC-11424-1] N85-34281

CODING

Colour coding scales and computer graphics N85-34568
Hexagonal uniformly redundant arrays for coded-aperture imaging
[OG-9.2-1] N85-34940

A coded aperture imaging system optimized for hard X-ray and gamma ray astronomy
[OG-9.2-3] N85-34942
SONTRAC: A solar neutron track chamber detector
[SH-9.1-12] N85-35127

COHERENT RADIATION
A theoretical and empirical analysis of coherent ray-tracing N85-34524

COHERENT SCATTERING
Numerical and analytic descriptions of cosmic-ray transport
[SH-4.1-4] N85-34830

COLD SURFACES
Experimental aerodynamic heating to simulated space shuttle tiles in laminar and turbulent boundary layers with variable flow angles at a nominal Mach number of 7
[NASA-TP-2307] N85-34351

COLLAPSE
Experimental study of collapse of thick-walled tube under external pressure and axial force N85-34186

COLLISION PARAMETERS
Fokker-Planck calculation of hot electron formation in the thermal barrier region of tandem mirror Gamma-10
[IPPJ-726] N85-34669
Electron loss process and cross section of multiply charged ions by neutral atoms N85-34685

COLLISION RATES
Breakdown of intrinsic ambipolarity for the radial diffusion due to a rotating RF field N85-34660

COLLISIONLESS PLASMAS
Resonant ion acceleration by oblique magnetosonic shock wave in a collisionless plasma
[IPPJ-735] N85-34643
Numerical solutions of the Vlasov equation N85-34672

COLOR
Electrolytic synthesis of colored eta alumina film N85-34201
Theoretical and experimental analyses of the performance of two-color laser ranging systems
[NASA-CR-176159] N85-34397
Graph-theoretical exorcism
[DE85-011916] N85-34512
An analysis and algorithm for filling propagation N85-34551
Design and implementation of an interactive route editor N85-34559
Colour spaces and colour contrast N85-34567
Colour coding scales and computer graphics N85-34568
Low cost geometric modelling system for CAM N85-34578

COLOR TELEVISION
Theoretical principles of vertical subsampling of color difference signals at half the sampling rate — television
[FI-447-TBR-18] N85-34332

COLOR VISION
Theoretical principles of vertical subsampling of color difference signals at half the sampling rate — television
[FI-447-TBR-18] N85-34332

COLORIMETRY
A manual of methods for the continuous flow determination of ammonia, nitrate-nitrite, phosphate and silicate in seawater
[IOS-177] N85-34243

COMBUSTION
Description of a test site for large-scale heavy gas dispersion and combustion experiments
[DE85-004987] N85-34231
The application of models to the assessment of fire hazard from consumer products
[NBSIR-85-3219] N85-34325
Upgrading auxiliary facility outleakage and combustion detection
[DE85-012796] N85-34386

COMBUSTION CHAMBERS
Carbon/carbon combustor external insulation
[AD-D011719] N85-34224
Numerical model of a pulse combustor
[DE85-011717] N85-34240
Investigation of non-intrusive radiometers for entrained gasifier temperature measurement, revision 3
[DE85-011795] N85-34385

COMBUSTION EFFICIENCY
Effect of precipitation variables on the specific surface and explosion characteristics of pentaerythritol tetranitrate
[DE85-009620] N85-34302

COMMUNICATION NETWORKS
Performance interface document for the S-band diplexer for space users of NASA networks
[NASA-TM-86224] N85-34155
A graphics interface for interactive simulation of packet-switched networks N85-34558

COMMUNICATION SATELLITES
Telecommunications forecast for ITU Region 2 to the year 1995
[NASA-TM-87077] N85-34150
Spacecraft (Mobile Satellite) configuration design study
[NASA-CR-176153] N85-34152
Satellites and politics: Weather, communications, and earth resources N85-35144

COMMUTATORS
Brush and commutator segment torquer motor
[AD-D011726] N85-34340

COMPARISON
Comparison of experimental data on detonation velocity and Chapman-Jouget pressure vs initial HE density with predictions from Ree's model equation of state
[DE85-007266] N85-34304

COMPATIBILITY
Determination of instrument errors by compatibility checking: Results from dynamic flight test data
[ARL-AERO-R-162] N85-34137
Parallel processing on the Livermore VAX 11/780-4 parallel processor system with compatability to Cray Research, Inc. (CRI) multitasking, version 1
[DE85-011856] N85-34595

COMPILERS
The parser generator as a general purpose tool
[NASA-CR-177955] N85-34521

COMPLEXITY
Determination of low chloride values in Rocky Flats scrub alloy solutions and other complex matrices
[DE85-011506] N85-34234

COMPONENT RELIABILITY
High pressure compressor component performance report
[NASA-CR-168245] N85-34138

COMPOSITE MATERIALS
Proceedings of the Twentyseventh Japan Congress on Materials Research
[ISSN-0368-3141] N85-34180
Negative flexural behavior of precase composite slabs with steel joint N85-34183
Composite desiccant structure
[DE85-006400] N85-34226
Centralized surveillance of flexible workshops for the manufacturing of composite materials
[SNIAS-851-430-103] N85-34227
Product definition: Technical specification of needs
[SNIAS-851-430-104] N85-34228
Process for improving moisture resistance of epoxy resins by addition of chromium ions
[NASA-CASE-LAR-13226-1] N85-34282
Development and demonstration of a spiral-wound thin-film composite membrane system for the economical production of oxygen-enriched air, phase 4
[DE85-012380] N85-34288

COMPOSITION (PROPERTY)
Uranium, thorium isotopic analyses and uranium-series ages of calcite and opal and stable isotopic compositions of calcite from drill cores UE25a no. 1, USR G-2 and USW G-3/GU-3, Yucca Mountain, Nevada
[DE85-013039] N85-34471
Screening and characterizing oleaginous microalgal species from the southeastern United States
[DE85-008787] N85-34488

COMPRESSIBLE FLOW
Scalar/Vector potential formulation for compressible viscous unsteady flows
[NASA-CR-3921] N85-34113
Compressible two-phase flow instabilities simulated with a hybrid Lagrange-Euler pseudospectral method
[DE85-009904] N85-34361

COMPRESSION LOADS
Design of transversely stiffenend FRP panels under compressive load — fiber reinforced plastic (FRP) ships
[AMTE(S)-R-84104] N85-34424

COMPRESSOR BLADES
Design, development and operation of a high simultaneous capacity digital telemetry system — turbomachine blade flutter
[PNR-90261] N85-34151

COMPRESSORS
High pressure compressor component performance report
[NASA-CR-168245] N85-34138
Combined cold compressor/ejector helium refrigerator
[DE85-006408] N85-34326

COMPTON EFFECT
X-ray spectra of bursting neutron stars N85-34686
Study of non-thermal photon production under different scenarios in solar flares. 2: The Compton inverse and Bremsstrahlung models and fittings
[SH-1.2-3] N85-34739
Solar flare gamma-ray line spectroscopy
[SH-2.1-14] N85-34795

COMPUTATION
Reordering computations for parallel execution
[NASA-CR-177961] N85-34522
On the statistical significance of excess events: Remarks of caution and the need for a standard method of calculation
[OG-9.5-10] N85-34987

COMPUTATIONAL FLUID DYNAMICS
Tabular and graphical solutions of regular and Mach reflections in pseudo-stationary frozen and vibrational-equilibrium flows, part 1
[UTIAS-283-PT-1] N85-34117
Tabular and graphical solutions of regular and Mach reflections in pseudo-stationary frozen and vibrational-equilibrium flows, part 2
[UTIAS-283-PT-2] N85-34118
A study of the second and third order closure models of turbulence for prediction of separated shear flows
[NASA-CR-176127] N85-34353

COMPUTATIONAL GRIDS
Use of a hyperbolic grid generation scheme in simulating supersonic viscous flow about three-dimensional winged configuration
[NASA-TM-85344] N85-34116
Box truss analysis and technology development. Task 1: Mesh analysis and control
[NASA-CR-172570] N85-34156

COMPUTER AIDED DESIGN
Proceedings of the Mechanisms Conference, volume 1 N85-34309
Proceedings of the Mechanisms Conference, volume 2 N85-34318
Optimisation in the computer aided design of mechanisms N85-34321
Design and lubrication of high-speed rolling-element bearings
[NASA-TM-87107] N85-34409
A model for graphics interface tool development N85-34545
An analysis and algorithm for filling propagation N85-34551
The CADME approach to the interface of solid modellers N85-34554
An innovative user interface for microcomputer-based computer-aided design N85-34555
A geometric modeller for turbomachinery applications N85-34556
Architecture of languages for large CAD systems development N85-34557
Design and implementation of an interactive route editor N85-34559
A user-friendly computer-aided construction of boundaries N85-34564
A simple but systematic CSG system N85-34569
Geometric continuity with interpolating Bezier curves N85-34570
An intuitive approach to geometric continuity for parametric curves and surfaces N85-34571
Developing graphical tools with minimal GKS N85-34573
Designing a graphics application interface N85-34574
Low cost geometric modelling system for CAM N85-34578
Computer animation in distance teaching N85-34581
Generative design in architecture using an expert system N85-34582

COMPUTER AIDED MANUFACTURING
Low cost geometric modelling system for CAM N85-34578

COMPUTER AIDED MAPPING
A model for graphics interface tool development N85-34545
The scientific and technical issues in integrating remotely sensed imagery with geocoded data bases N85-34547
A new approach to linear quadtrees N85-34550
The automatic labeling of geographic maps: A problem in computer aesthetics N85-34561
How map designers can represent their ideas in thematic maps: Effective user interfaces for thematic map design N85-34562
Applied computer graphics in a geographic information system: Problems and successes N85-34563

COMPUTER ASSISTED INSTRUCTION
Designing a graphics application interface N85-34574

COMPUTER GRAPHICS
An introduction to finite elements N85-34319
A device-independent 2D plotting package written in FORTRAN
[RSRE-MEMO-3776] N85-34514
Graphics Interface 1985: Proceedings
[ISSN-0713-5424] N85-34523
A theoretical and empirical analysis of coherent ray-tracing N85-34524

Frame buffer algorithms for stochastic models N85-34525
Specifying stochastic objects in a hierarchical graphics system N85-34526
The interactive planning work station: A graphics-based UNIX (trademark) tool for application users and developers N85-34527
Computer graphics for multivariate data N85-34528
Interfacing interactive circuit simulation with standard graphics facilities N85-34529
Computer analysis techniques for the temporal evaluation of cardiac wall motion N85-34530
A computerized system for spot detection and analysis of two-dimensional electrophoresis images N85-34531
An image management kernel for the design of relational and pictorial data bases N85-34532
Spatial trees: A fast access method for unstructured graphical data N85-34533
Graphics Interaction in databases N85-34534
Animengine: An engineering animation system N85-34535
3D computer animation: More an evolution problem than a motion problem N85-34536
Using dynamic analysis to animate articulated bodies such as humans and robots N85-34537
Towards an integrated view of 3-D computer character animation N85-34538
Research issues in generating graphical explanations N85-34539
An integrated system for printing and publishing applications N85-34540
Recognition and clear representation of handwritten electronic diagrams N85-34541
A model for a document maintenance system N85-34542
Efficient recovery and reversal in graphical user interfaces generated by the Higgens system N85-34544
A model for graphics interface tool development N85-34545
Using percent-done program indicators to enhance user interfaces N85-34546
Selection of segment similarity measures for hierarchical picture segmentation N85-34548
A general purpose image processing package N85-34549
A new approach to linear quadtrees N85-34550
An analysis and algorithm for filling propagation N85-34551
The CADME approach to the interface of solid modellers N85-34554
A graphics interface for interactive simulation of packet-switched networks N85-34558
Design and implementation of an interactive route editor N85-34559
Project management using graphics N85-34560
The automatic labeling of geographic maps: A problem in computer aesthetics N85-34561
How map designers can represent their ideas in thematic maps: Effective user interfaces for thematic map design N85-34562
Applied computer graphics in a geographic information system: Problems and successes N85-34563
Image synthesis: Optical identity or pictorial communication? N85-34565
Strategic use of business graphics: A stakeholder approach N85-34566
Colour spaces and colour contrast N85-34567
Colour coding scales and computer graphics N85-34568
Geometric continuity with interpolating Bezier curves N85-34570
An intuitive approach to geometric continuity for parametric curves and surfaces N85-34571
Building an octree from a set of parallelepipeds N85-34572
Developing graphical tools with minimal GKS N85-34573
Designing a graphics application interface N85-34574
NAPGEN: Automatic NAPLPS page generator N85-34575
Low cost geometric modelling system for CAM N85-34578
The dynamics of articulated rigid bodies for purposes of animation N85-34579
Shadow volumes for non-planar polygons N85-34580
Computer animation in distance teaching N85-34581
Generative design in architecture using an expert system N85-34582
Heuristic rules for visualization N85-34584
Using LINE as an interactive °graphics package. Interfacing line and Topdraw in 43 and 24 VM [DE85-012007] N85-34585

COMPUTER NETWORKS
An innovative user interface for microcomputer-based computer-aided design N85-34555

COMPUTER PROGRAMMING
The interactive planning work station: A graphics-based UNIX (trademark) tool for application users and developers N85-34527
Graphics Interaction in databases N85-34534
Parallel processing on the Livermore VAX 11/780-4 parallel processor system with compatability to Cray Research, Inc. (CRI) multitasking, version 1 [DE85-011856] N85-34595

COMPUTER PROGRAMS
Component-specific modeling [NASA-CR-174765] N85-34140
Box truss analysis and technology development. Task 1: Mesh analysis and control [NASA-CR-172570] N85-34156
An introduction to finite elements N85-34319
Detailed validation of a liquid and heat flow code against field performance [DE85-009901] N85-34368
Modular digital holographic fringe data processing system [NASA-CR-177952] N85-34376
Hardware math for the 6502 microprocessor [NASA-TM-86517] N85-34511
DiSPL1: A software package for one and two spatially dimensioned kinetics-diffusion problems [ANL-84-56] N85-34516
User's operating procedures. Volume 3: Projects directorate information programs [NASA-CR-177950] N85-34520
Computer graphics for multivariate data N85-34528
Interfacing interactive circuit simulation with standard graphics facilities N85-34529
Research issues in generating graphical explanations N85-34539
An integrated system for printing and publishing applications N85-34540
Using percent-done program indicators to enhance user interfaces N85-34546
Knowledge engineering application in image processing N85-34583
Using LINE as an interactive graphics package. Interfacing line and Topdraw in 43 and 24 VM [DE85-012007] N85-34585
Analysis of transient radiation upset in a 16K SRAM [DE85-009442] N85-34586
Real-time multiparameter pulse processing with decision tables [DE85-011683] N85-34589
User's manual for the FLORA equilibrium and stability code [DE85-013182] N85-34590
Maintenance port system [AD-D011724] N85-34594
CYLTRAN calculations of electron effects on XD detectors [LA-10264-MS] N85-34601
Modeling a high energy gamma-ray telescope [OG-9.2-5] N85-34944
The final COS-B database now publicly available [OG-9.3-8] N85-34963

COMPUTER STORAGE DEVICES
Spatial trees: A fast access method for unstructured graphical data N85-34533

COMPUTER SYSTEMS DESIGN
Re-designing a mechanism for higher speed: A case history from textile machinery N85-34310
An integrated system for printing and publishing applications N85-34540
Efficient recovery and reversal in graphical user interfaces generated by the Higgens system N85-34544
A model for graphics interface tool development N85-34545
Using percent-done program indicators to enhance user interfaces N85-34546
Selection of segment similarity measures for hierarchical picture segmentation N85-34548
A graphics interface for interactive simulation of packet-switched networks N85-34558

COMPUTER SYSTEMS PROGRAMS
Proceedings of the Mechanisms Conference, volume 1 N85-34309
A versatile computer package for mechanism analysis, part 2: Dynamics and balance N85-34315
Proceedings of the Mechanisms Conference, volume 2 N85-34318
Software for mechanism design N85-34324
An innovative user interface for microcomputer-based computer-aided design N85-34555
A geometric modeller for turbomachinery applications N85-34556
Architecture of languages for large CAD systems development N85-34557
The automatic labeling of geographic maps: A problem in computer aesthetics N85-34561

COMPUTER TECHNIQUES
Proceedings of the Mechanisms Conference, volume 1 N85-34309
A versatile computer package for mechanism analysis N85-34314
A versatile computer package for mechanism analysis, part 2: Dynamics and balance N85-34315
Optimisation in the computer aided design of mechanisms N85-34321
Method and apparatus for transfer function simulator for testing complex systems [NASA-CASE-NPO-15696-1] N85-34333
Animengine: An engineering animation system N85-34535
Efficient recovery and reversal in graphical user interfaces generated by the Higgens system N85-34544
Numerical and analytic descriptions of cosmic-ray transport [SH-4.1-4] N85-34830

COMPUTERIZED SIMULATION
Time-resolved spectroscopic studies of detonating heterogeneous explosives [DE85-009760] N85-34297
Method and apparatus for transfer function simulator for testing complex systems [NASA-CASE-NPO-15696-1] N85-34333
Compressible two-phase flow instabilities simulated with a hybrid Lagrange-Euler pseudospectral method [DE85-009904] N85-34361
The impact of supercomputers on experimentation: A view from a national laboratory [NASA-TM-86822] N85-34510
System maintenance manual for master modeling of aerodynamic surfaces by three-dimensional explicit representation [NASA-CR-178224] N85-34517
Frame buffer algorithms for stochastic models N85-34525
Specifying stochastic objects in a hierarchical graphics system N85-34526
Interfacing interactive circuit simulation with standard graphics facilities N85-34529
A computerized system for spot detection and analysis of two-dimensional electrophoresis images N85-34531
Animengine: An engineering animation system N85-34535
3D computer animation: More an evolution problem than a motion problem N85-34536
Using dynamic analysis to animate articulated bodies such as humans and robots N85-34537
Towards an integrated view of 3-D computer character animation N85-34538
The CADME approach to the interface of solid modellers N85-34554
An innovative user interface for microcomputer-based computer-aided design N85-34555
Analysis of transient radiation upset in a 16K SRAM [DE85-009442] N85-34586
Circuit approaches to increasing SRAM performance in total dose environments [DE85-009441] N85-34588
Workshop report on Simulation Techniques for Shock Wave Phenomena and Characteristics of Plasmas in Inertial Confinement Fusion [IPPJ-725] N85-34670
Vector calculation of particle code N85-34688
Data on the backscattering coefficients on light ions from solids: A revision [IPPJ-AM-41-REV] N85-34689
Perspective on the next ten years in plasma physics [DE85-011849] N85-34706
Acceleration of ions and electrons to near-cosmic ray energies in a perpendicular shock: The January 6, 1978 event [SH-1.5-4] N85-34773
Particle acceleration due to shocks in the interplanetary field: High time resolution data and simulation results [SH-1.5-5] N85-34774

COMPUTERS
Issues and techniques in touch-sensitive tablet input (executive summary) N85-34543
Ranging system which compares an object reflected component of a light beam to a reference component of the light beam [NASA-CASE-NPO-15865-1] N85-34629

CONCENTRATION (COMPOSITION)
The heavy ion composition in 3HE-rich solar flares [SH-2.2-7] N85-34802

CONCRETE STRUCTURES
Negative flexural behavior of precase composite slabs with steel joint N85-34183

CONCRETES
High temperature polymer concrete
[DE85-005756] N85-34290
CONDITIONS
Estimating risks of lead-induced hemoglobin decrements under conditions of uncertainty: Methodology, pilot judgments and illustrative calculations
[DE85-012293] N85-34493
CONDUCTIVE HEAT TRANSFER
Sequential regularization solution of the inverse heat conduction problem
[DE85-010657] N85-34362
CONDUCTORS
Method for determining depth and shape of a sub-surface conductive object
[DE85-006502] N85-34389
CONFERENCES
Space Station Engineering and Technology Development: Proceedings of the Panel on In-Space Engineering Research and Technology Development
[NASA-CR-176110] N85-34153
Coordinated study of solar-terrestrial payloads on space station
[NASA-CR-176160] N85-34158
Proceedings of the Twentyseventh Japan Congress on Materials Research
[ISSN-0368-3141] N85-34180
Proceedings of the Mechanisms Conference, volume 1 N85-34309
Proceedings of the Mechanisms Conference, volume 2 N85-34318
Problems of aviation and space medicine and psychology discussed at 14th Gagarin lectures N85-34509
Graphics Interface 1985: Proceedings
[ISSN-0713-5424] N85-34523
Ninteenth International Cosmic Ray Conference. SH sessions, volume 4
[NASA-CP-2376-VOL-4] N85-34729
Ninteenth International Cosmic Ray Conference. OG sessions, volume 3
[NASA-CP-2376-VOL-3] N85-34862
Ninteenth International Cosmic Ray Conference. SH sessions, volume 5
[NASA-CP-2376-VOL-5] N85-34991
CONGRESSIONAL REPORTS
Aviation safety (aircraft passenger survivability and cabin safety)
[GPO-39-847] N85-34130
Department of Housing and Urban Development Independent Agencies Appropriation Bill, 1986
[S-REPT-99-129] N85-34720
National Aeronautics and Space Administration research and development: Program description N85-34721
CONICAL BODIES
Behaviors of stress waves in a conical bar N85-34182
CONICAL NOZZLES
Nozzle wall roughness effects on free-stream noise and transition in the pilot low-disturbance tunnel
[NASA-TM-86389] N85-34355
CONJUGATE POINTS
Conjugated symmetrical coupler curves, produced by 4-bar linkages having the same transmission angles N85-34322
CONSERVATION LAWS
New semi-implicit method for solving the time-dependent conservation equations for incompressible flow
[DE85-010926] N85-34367
CONSTRUCTION
Space Station Engineering and Technology Development: Proceedings of the Panel on In-Space Engineering Research and Technology Development
[NASA-CR-176110] N85-34153
Small Hydroelectric Power Plan Demonstration Project
[DE85-011343] N85-34454
CONSUMABLES (SPACECREW SUPPLIES)
A life-saving device for ships
[NASA-TM-77670] N85-34129
CONTAINMENT
MATADOR (Methods for the Analysis of Transport And Deposition Of Radionuclides) code description and user's manual
[TI85-901402] N85-34592
CONTAMINANTS
Atmospheric modeling of organics for risk assessment: A Chemist's view
[DE85-009770] N85-34217
CONTAMINATION
Method for removing oxide contamination from silicon carbide powders
[DE85-011648] N85-34287
CONTINUUMS
Low-excitation Herbig-Haro objects and interstellar extinction
[NASA-CR-176142] N85-34726
CONTOURS
Block-implicit calculations of three-dimensional laminar flow in strongly curved ducts
[DE85-003047] N85-34363
CONTRACT MANAGEMENT
Analyzing performance of small projects using URS and PMAS, information pamphlet
[DE85-011964] N85-34718
CONTROL EQUIPMENT
Method for controlling the viscosity of siloxane oils
[DE85-011586] N85-34221
CONTROL SYSTEMS DESIGN
Reactant pressure differential control for fuel cell gases
[NASA-CASE-MSC-20127-2] N85-34403
Robot environment expert system
[NASA-CR-3915] N85-34593
Discrete simulation models - their role in the design, development and management of inventory control systems
[PNR-90249] N85-34719
CONTROLLABILITY
Ground-based and in-flight simulator studies of flight characteristics of a twin-fuselage passenger transport airplane during approach and landing
[NASA-TP-2451] N85-34144
CONTROLLERS
Feedback regulated induction heater for a flowing fluid
[DE85-006508] N85-34414
Neutral particle beam intensity controller
[DE85-006411] N85-34604
CONVECTION
Forced convective, nonequilibrium, post-CHF heat transfer experiment data and correlation comparison report
[TI85-009331] N85-34371
Diffusion-convection function of cosmic rays
[SH-3.2-10] N85-34825
IMF-sense-dependent cosmic ray anisotropy produced from diffusion-convection in heliosphere
[SH-4.3-9] N85-34994
Diurnal anisotropy during solar activity cycle twenty and diffusion-convection model
[SH-4.5-7] N85-35025
CONVECTIVE FLOW
Effects of solar magnetic field on cosmic rays
[SH-4.2-12] N85-34850
Difference between even and odd 11-year cycles in cosmic ray intensity
[SH-4.2-22] N85-34859
CONVERGENCE
Reordering computations for parallel execution
[NASA-CR-177961] N85-34522
CONVEYORS
Shuttle car loading system
[NASA-CASE-NPO-15949-1] N85-34722
COOLING
Design and lubrication of high-speed rolling-element bearings
[NASA-TM-87107] N85-34409
COOLING SYSTEMS
Mathematical modeling of ultimate heat sink cooling ponds
[TI85-009747] N85-34369
COORDINATE TRANSFORMATIONS
Second-order Compton-Getting effect on arbitrary intensity distribution
[SH-3.1-10] N85-34814
COORDINATES
Production of initial estimates of photogrammetric variables
[NPL-MOM-66] N85-34434
Second-order Compton-Getting effect on arbitrary intensity distribution
[SH-3.1-10] N85-34814
COPPER
X-ray residual stress analysis on the coarse grain of copper and its application to the brazed copper N85-34202
Metal (2) 4,4',4',4" phthalocyanine tetraamines as curing agents for epoxy resins
[NASA-CASE-ARC-11424-1] N85-34281
COPPER OXIDES
Time-resolved and infrared spectroscopy of excitons
[DE85-011879] N85-34235
CORE FLOW
Transports studies of ECH and ICRH-heated bumpy torus plasma in NBT-1M N85-34662
Simulation studies on stability of hot electron plasma N85-34664
CORE SAMPLING
Uranium, thorium isotopic analyses and uranium-series ages of calcite and opal and stable isotopic compositions of calcite from drill cores UE25a no. 1, USR G-2 and USW G-3/GU-3, Yucca Mountain, Nevada
[DE85-013039] N85-34471
CORIOLIS EFFECT
Nonlinear flap-lag-extensional vibrations of rotating, pretwisted, preconed beams including Coriolis effects
[NASA-TM-87102] N85-34427
CORONAL HOLES
White Light Coronograph (WLC) and Ultra-Violet Coronal Spectrometer (UVCS) N85-34161
The expected cosmic ray density and stream distributions at the heliolatitudinal asymmetry of solar wind
[SH-4.2-14] N85-34852
Study of dominating parameters of high speed solar plasma streams in relation to cosmic ray and geomagnetic storms
[SH-5.1-11] N85-35064
CORONAL LOOPS
The propagation of solar flare particles in a turbulent coronal loop
[SH-1.1-3] N85-34730
Ion energy storage for post-flare loops
[SH-1.2-10] N85-34745
Helios 1 energetic particle observations of the solar gamma ray flare events of 7, 21 June 1980 and 3 June 1982
[SH-1.3-8] N85-34755
CORONARY CIRCULATION
Effect of acute hypoxia on coronary and systemic hemodynamics N85-34503
CORONAS
Helios 1 energetic particle observations of the solar gamma ray flare events of 7, 21 June 1980 and 3 June 1982
[SH-1.3-8] N85-34755
Source energy spectra from demodulation of solar particle data by interplanetary and coronal transport
[SH-1.3-13] N85-34758
CORRELATION
Comparison of experimental data on detonation velocity and Chapman-Jouget pressure vs initial HE density with predictions from Ree's model equation of state
[DE85-007266] N85-34304
An update on the correlation between the cosmic radiation intensity and the geomagnetic AA index
[SH-4.2-24] N85-34861
Implications of source abundances of ultraheavy cosmic rays
[OG-7.1-4] N85-34866
On the solar cycle variation in the barometer coefficients of high latitude neutron monitors
[SH-6.1-2] N85-35077
Correlation between solar neutrino flux and other solar phenomena N85-35109
CORRELATION COEFFICIENTS
The corotating variation of the north-south anisotropy of cosmic rays
[SH-4.3-15] N85-34999
CORROSION
Ocean thermal energy conversion
[DE85-012291] N85-34456
CORROSION RESISTANCE
Nitriding of super alloys for enhancing physical properties
[DE85-005762] N85-34275
The development and evaluation of the creep and corrosion resistant alloy IN6201
[PNR-90253] N85-34278
Electrically conductive containment vessel for molten aluminum
[DE85-006518] N85-34415
CORROSION TESTS
Corrosion fatigue strength and crack growth in prestrained 0.18% C carbon steel N85-34192
COSMIC GASES
Breakdown of helium nuclei in matter processed near black holes
[OG-8.2-20] N85-34916
COSMIC PLASMA
Interstellar turbulence, random density variations, and scintillation measurements
[OG-7.2-13] N85-34880
The role of cosmic rays in magnetic hydrodynamics of interstellar medium
[OG-7.2-15] N85-34882
COSMIC RAY SHOWERS
Injection of energetic particles following the gamma-ray flares on June 7, 1980, as observed on Helios 1
[SH-1.3-9] N85-34756
Spectra of solar proton ground level events using neutron monitor and neutron moderated detector recordings
[SH-1.3-14] N85-34759
Ground increase of cosmic ray intensity on February 16, 1984
[SH-1.3-15] N85-34760

The SCR flare of 16 February 1984 as recorded by the Sayan spectrograph
[SH-1.3-17] N85-34761
Energetic solar particle events
[SH-3.2-2] N85-34818
Cosmic ray intensity and the tilt of the neutral sheet
[SH-4.2-8] N85-34846
Differential measurement of cosmic-ray gradient with respect to interplanetary current sheet
[SH-4.2-9] N85-34847
Effects of a wavy neutral sheet on cosmic ray anisotropies
[SH-4.2-11] N85-34849
Implications of cross section errors for cosmic ray propagation
[OG-7.2-3] N85-34875
Cosmic ray secondary nuclei and the structure of the galaxy
[OG-7.2-4] N85-34876
Why do leaky-box models work so fine?
[OG-7.2-8] N85-34877
Alfven wave scattering and the secondary to primary ratio
[OG-7.2-9] N85-34878
On the cosmic ray diffusion in a violent interstellar medium
[OG-7.2-14] N85-34881
The role of cosmic rays in magnetic hydrodynamics of interstellar medium
[OG-7.2-15] N85-34882
A new ultra high energy gamma ray telescope at Ohya mine
[OG-9.4-3] N85-34970
The Buckland Park air shower array
[OG-9.4-4] N85-34971
An EAS experiment at mountain altitude for the detection of gamma-ray sources
[OG-9.4-5] N85-34972
An observatory to study 10 (10) to 10 (17) by EV gamma rays
[OG-9.4-6] N85-34973
A new array for the study of ultra high energy gamma-ray sources
[OG-9.4-7] N85-34974
Akeno 20 km (2) air shower array (Akeno Branch)
[OG-9.4-8] N85-34975
Mini and super mini arrays for the study of highest energy cosmic rays
[OG-9.4-9] N85-34976
Detection of 10 (1) GeV cosmic neutrinos with a space station
[OG-9.4-10] N85-34977
The longitudinal thickness of air-shower fronts
[OG-9.5-1] N85-34978
Cerenkov light images of EAS produced by primary gamma
[OG-9.5-3] N85-34979
Shower disc sampling and the angular resolution of gamma-ray shower detectors
[OG-9.5-2] N85-34980
A method to improve observations of gamma-ray sources near 10 (15) eV
[OG-9.5-5] N85-34982
Angular resolution of air-shower array-telescopes
[OG-9.5-6] N85-34983
Astrophysical applications of high angular resolution array-telescopes
[OG-9.5-7] N85-34984
Angular resolution of an EAS array for gamma ray astronomy energies 5 x 10 (13) eV
[OG-9.5-8] N85-34985
Note on the detection of high energy primary cosmic gamma rays by air shower observation
[OG-9.5-9] N85-34986
On the statistical significance of excess events: Remarks of caution and the need for a standard method of calculation
[OG-9.5-10] N85-34987
A new statistic for the analysis of circular data in gamma-ray astronomy
[OG-9.5-13] N85-34989
The angular resolution of air shower gamma ray telescopes
[OG-9.5-14] N85-34990
Accelerator experiments on the contribution of secondary particles to the production of cosmogenic nuclides in meteorites
[SH-7.1-8] N85-35100
Depth and size effects on cosmogenic nuclide production in meteorites
[SH-7.1-9] N85-35101
A suggested standardized format for cosmic ray ground-level event data
[SH-9.1-15] N85-35130
Using the information of cosmic rays to predict influence epidemic
[SH-10.1-2] N85-35134
Strong earthquakes, novae and cosmic ray environment
[SH-10.1-3] N85-35135

COSMIC RAYS

Effect of seeds of heavy charged particles of galactic cosmic radiation N85-34505
Nineteenth International Cosmic Ray Conference. SH sessions, volume 4
[NASA-CP-2376-VOL-4] N85-34729
Acceleration of ions and electrons to near-cosmic ray energies in a perpendicular shock: The January 6, 1978 event
[SH-1.5-4] N85-34773
Cosmic ray acceleration by stellar wind. Simulation for heliosphere
[SH-1.5-17] N85-34780
The energy spectrum of Jovian electrons in interplanetary space
[SH-1.5-18] N85-34781
Observation of the fluxes of nuclei with energies 10-20 MEV per nucleon during the solar flare of April 26, 1984
[SH-2.1-1] N85-34783
On the retention of high-energy protons and nuclei with charges Z or equal to 2 in large solar flares after the process of their acceleration
[SH-2.1-8] N85-34789
Type 3 solar radio bursts and 3HE-rich events
[SH-2.2-3] N85-34798
Numerical descriptions of cosmic-ray transport
[SH-4.1-3] N85-34829
Numerical and analytic descriptions of cosmic-ray transport
[SH-4.1-4] N85-34830
the role of shock waves in modulation of galactic cosmic rays
[SH-4.1-7] N85-34831
The intensity recovery of Forbush-type decreases as a function of heliocentric distance and its relationship to the 11-year variation
[SH-4.1-9] N85-34832
Cumulative effect of Forbush decreases in the heliospheric modulation during the present solar cycle
[SH-4.1-10] N85-34833
Cosmic ray modulatin and merged interaction regions
[SH-4.1-11] N85-34834
Longitudinal distribution of cosmic rays in the heliosphere
[SH-4.1-14] N85-34837
The 1973-1984 solar modulation of cosmic ray nuclei
[SH-4.1-16] N85-34838
Cosmic ray modulation in a random anisotropic magnetic field
[SH-4.1-20] N85-34839
Evidence for regions of negligible cosmic-ray modulation in the inner heliosphere (10 AU)
[SH-4.1-21] N85-34840
Notes on drift theory
[SH-4.2-3] N85-34841
Drift and observations in cosmic-ray modulation, 1
[SH-4.2-4] N85-34842
Drift and observations in cosmic-ray modulation, 2
[SH-4.2-5] N85-34843
Cosmic ray north-south anisotropy 1961 - 1983
[SH-4.2-6] N85-34844
Ninteenth International Cosmic Ray Conference. OG sessions, volume 3
[NASA-CP-2376-VOL-3] N85-34862
Germanium and lead: Significant differences between meteoritic and photospheric abundances?
[OG-7.1-2] N85-34864
Lead and uranium group abundances in cosmic rays
[OG-7.1-3] N85-34865
Implications of source abundances of ultraheavy cosmic rays
[OG-7.1-4] N85-34866
Propagation and nucleosynthesis of ultraheavy cosmic rays
[OG-7.1-5] N85-34867
Sources of the ultraheavy cosmic rays
[OG-7.1-7] N85-34868
The cosmic ray composition as viewed from the chemical abundances of the solar system
[OG-7.1-8] N85-34869
Elemental technetium as a cosmic-ray clock
[OG-7.1-9] N85-34870
Electron capture decay of cosmic rays: A model of the inhomogeneous interstellar medium
[OG-7.1-10] N85-34871
The model-independence of cosmic ray source determinations
[OG-7.2-1] N85-34873
Interstellar turbulence, random density variations, and scintillation measurements
[OG-7.2-13] N85-34880
Diffusion of strongly magnetized cosmic ray particles in a turbulent medium
[OG-7.2-16] N85-34883
Cosmic-ray transport in the galactic magnetosphere
[OG-7.2-17] N85-34884
The role of cosmic rays and Alfven waves in the structure of the galactic halo
[OG-7.2-18] N85-34885
Measurements of Fe and Ar fragmentation cross sections
[OG-7.2-20] N85-34887
Interactions of heavy nuclei, Kr, Xe and Ho, in light targets
[OG-7.2-21] N85-34888
The cosmic-ray shock structure problem for relativistic shocks
[OG-8.1-1] N85-34891
Instabilities in decelerating supersonic flows with applications to cosmic ray shocks
[OG-8.1-2] N85-34892
Time-dependent nonlinear cosmic ray shocks confirming abstract
[OG-8.1-3] N85-34893
A cosmic ray driven instability
[OG-8.1-5] N85-34895
Relativistic cosmic ray spectra in the full non-linear theory of shock acceleration
[OG-8.1-6] N85-34896
Acceleration of cosmic rays in supernova-remnants
[OG-8.1-9] N85-34899
Onion-shell model for cosmic ray electrons and radio synchrotron emission in supernova remnants
[OG-8.1-10] N85-34900
Approximate supernova remnant dynamics with cosmic ray production
[OG-8.1-12] N85-34901
A numerical study of diffusive shock acceleration of cosmic rays in supernova shocks
[OG-8.2-2] N85-34903
Scaling from Jupiter to pulsars and the acceleration of cosmic ray particles by pulsars, 3
[OG-8.2-3] N85-34904
Do supernovae of type 1 paly a role in cosmic-ray production?
[OG-8.2-5] N85-34905
Neutron-rich nuclei in cosmic rays and Wolf-Rayet stars
[OG-8.2-6] N85-34906
Interstellar (Na-22) as a possible source of the excess (Ne-22) in the galactic cosmic ray
[OG-8.2-12] N85-34908
The electromagnetic ram action of the plasma focus as a paradigm for the generation of cosmic rays and the gigantic jets in active galaxies
[OG-8.2-14] N85-34910
The origins of cosmic rays and quantum effects on gravity
[OG-8.2-15] N85-34911
Evaluation of parameters for particles acceleration by the zero-point field of quantum electrodynamics
[OG-8.2-16] N85-34912
Giant molecular clouds as regions of particle acceleration N85-34913
The nucleosynthesis of deterium and helium-3
[OG-8.2-18] N85-34914
Pulsars as cosmic ray particle accelerators: Proton orbits
[OG-8.2-21] N85-34917
Pulsars as cosmic ray accelerators: Energy development of protons
[OG-8.2-22] N85-34918
Pulsars as cosmic ray particle accelerators: Dynamics of electrons
[OG-8.2-23] N85-34919
Propagation of injected cosmic rays under distributed reacceleration
[OG-8.3-3] N85-34922
Propagation of cosmic rays and new evidence for distributed acceleration
[OG-8.3-5] N85-34924
Exact solutions for sporadic acceleration of cosmic rays
[OG-8.3-7] N85-34925
Relativistic transport theory for cosmic-rays
[OG-8.3-8] N85-34926
The design of an experiment to detect low energy antiprotons
[OG-9.1-1] N85-34928
An experiment to measure the energy spectrum of cosmic ray antiprotons from 100 to 1000 MeV
[OG-9.1-3] N85-34929

High resolution Cherenkov detectors for cosmic ray isotope experiment
[OG-9.1-4] N85-34930
A high resolution gas Cerenkov detector for the superconducting magnet facility
[OG-9.1-6] N85-34932
Bevalac calibration of the SOFIE range and hodoscope detectors
[OG-9.1-7] N85-34933
The development of a high energy cosmic ray detector for Spacelab-2
[OG-9.1-8] N85-34934
Mass resolution optimization in a large isotopic composition experiment
[OG-9.1-9] N85-34935
The heavy ions in space experiment
[OG-9.1-10] N85-34936
Cherenkov-dE/dx-range measurements on cosmic ray iron group nuclei
[OG-9.1-12] N85-34937
The response of ionization chambers to relativistic heavy nuclei
[OG-9.1-13] N85-34939
A balloon-borne imaging gamma-ray telescope
[OG-9.2-2] N85-34941
A coded aperture imaging system optimized for hard X-ray and gamma ray astronomy
[OG-9.2-3] N85-34942
The final COS-B database: In-flight calibration of instrumental parameters
[OG-9.3-9] N85-34964
Ninteenth International Cosmic Ray Conference. SH sessions, volume 5
[NASA-CP-2376-VOL-5] N85-34991
Isotropic intensity waves and features of their occurrence
[SH-4.3-8] N85-34993
Cosmic ray sidereal diurnal variation of galactic origin observed by neutron monitors
[SH-4.4-2] N85-35000
Sidereal anisotropies in the median rigidity range 60-600GV in 1978-1983
[SH-4.4-3] N85-35001
Sidereal variations deep underground in Tasmania
[SH-4.4-4] N85-35002
The effect of the interplanetary magnetic field on sidereal variations observed at medium depth underground detectors
[SH-4.4-5] N85-35003
Corrected sidereal anisotropy for underground muons
[SH-4.4-7] N85-35005
A study of periodicities and recurrences in solar activity and cosmic ray modulation
[SH-4.4-14] N85-35010
Cosmic ray biannual variation
[SH-4.4-15] N85-35011
Cosmic ray power spectral variations. 3: Solar rotation periodicities
[SH-4.4-16] N85-35012
Variations of the cosmic ray general component in Antarctica
[SH-4.4-17] N85-35013
The difference in the energy spectra of galactic cosmic rays at the minima of the 19th and 20th solar activity cycles
[SH-4.4-18] N85-35014
Cosmic ray variations with the period close to 27 days and their connection with solar activity longitudinal distribution
[SH-4.4-19] N85-35015
Long-term modulation of galactic cosmic rays in high-energy region
[SH-4.4-22] N85-35018
The first three harmonics of solar daily variation caused by the diffusive propagation of galactic cosmic rays through the heliosphere
[SH-4.5-1] N85-35019
Formulation of cosmic-ray solar daily variation and its seasonal variation, produced from generalized stationary anisotropy of solar origin
[SH-4.5-2] N85-35020
Diurnal effect in cosmic rays at middle latitudes according to stratospheric measurements
[SH-4.5-8] N85-35026
Comparative study of the phase of diurnal anisotropy on quiet and disturbed days on a long term basis up to recent period
[SH-4.5-9] N85-35027
Study of spectral exponent on quiet and disturbed days
[SH-4.5-10] N85-35028
Diurnal variation of galactic cosmic ray intensity on quiet days
[SH-4.5-11] N85-35029
Diurnal variations from muon data at Takeyama underground station
[SH-4.5-13] N85-35030
Long term changes in cosmic ray diurnal variations observed by ion chambers in Hong Kong and Japan
[SH-4.5-14] N85-35031
The modulation features of the long-period cosmic ray variations in connection with the sign change of the general magnetic field of the Sun
[SH-4.5-15] N85-35032
The cosmic ray differential diurnal variation dependences on the zenith angle and the geomagnetic disturbance
[SH-4.5-16] N85-35033
Cosmic ray density gradient and its dependence on the north-south asymmetry in solar activity
[SH-4.5-17] N85-35034
Anomalous increase of solar anisotropy above 150GV in 1981-1983
[SH-4.5-18] N85-35035
Diagnostic of electromagnetic conditions in space using cosmic rays
[SH-4.5-19] N85-35036
Change of cosmic ray anisotropy with solar activity
[SH-4.5-20] N85-35037
Magnetic fluctuation and cosmic ray diurnal variations
[SH-4.5-21] N85-35038
Changes in the energy spectrum of anomalous oxygen and helium during 1977-1985
[SH-4.6-1] N85-35039
Solar cycle variations of the anaomalous cosmic ray component
[SH-4.6-2] N85-35040
Radial and latitudinal gradients of anomalous oxygen during 1977 - 1985
[SH-4.6-4] N85-35042
Observation of pick-up ions in the solar wind: Evidence for the source of the anomalous cosmic ray component?
[SH-4.6-5] N85-35043
On the anomalous component
[SH-4.6-6] N85-35044
Possible origin of the anomalous component of cosmic rays
[SH-4.6-7] N85-35045
The cosmic ray interplanetary radial gradient from 1972 - 1985
[SH-4.7-1] N85-35046
The large scale dynamics of the outer heliosphere and the long-term modulation of galactic cosmic rays
[SH-4.7-3] N85-35048
Solar modulation and interplanetary gradients of the galactic electrons flux, 1977 - 1984
[SH-4.7-4] N85-35049
Galactic cosmic ray radial gradients and the anomalous He component near maximum solar modulation and to radii beyond 34 AU from the Sun
[SH-4.7-5] N85-35050
Voyager 1 and 2 measurements of radial and latitudinal cosmic ray gradients during 1981 - 1984
[SH-4.7-6] N85-35051
The recovery of the cosmic ray flux from maximum solar modulation at IMP-8 (1 AU) and at Pioneer (R 30 AU)
[SH-4.7-7] N85-35052
The large-scale modulation of cosmic rays in mid-1982: Its dependence on heliospheric longitude and radius
[SH-4.7-9] N85-35053
Nonstationary modulation of galactic cosmic rays in a nonlinear model
[SH-4.7-10] N85-35054
Dimensions of the solar wind cavity and of the region of interplanetary cosmic ray modulation
[SH-4.7-11] N85-35055
Drift and Forbush decreases
[SH-5.1-2] N85-35056
Anomalous short-term increases in the galactic cosmic ray intensity: Are they related to the interplanetary magnetic cloud-like structures?
[SH-5.1-3] N85-35057
The flare origin of Forbush decreases not associated with solar flares on the visible hemisphere of the Sun
[SH-5.1-4] N85-35058
Longitudinal dependence of the interplanetary perturbation produced by energetic type 4 solar flares and of the associated cosmic ray modulation
[SH-5.1-5] N85-35059
Rigidity spectrum of Forbush decrease
[SH-5.1-6] N85-35060
Spectral analysis of the Forbush decrease of 13 July 1982
[SH-5.1-7] N85-35061
Transient cosmic ray increase associated with a geomagnetic storm
[SH-5.1-8] N85-35062
Galactic cosmic ray currents and magnetic field irregularity degree in high-speed solar wind streams
[SH-5.1-9] N85-35063
Study of dominating parameters of high speed solar plasma streams in relation to cosmic ray and geomagnetic storms
[SH-5.1-11] N85-35064
Influence of magnetic clouds on cosmic ray intensity variations
[SH-5.1-12] N85-35065
The solar wind effect on cosmic rays and solar activity
[SH-5.1-13] N85-35066
A relation between the short time variations of cosmic rays and geomagnetic field change
[SH-5.1-14] N85-35067
Anomalous low level of cosmic ray intensity decreases observed during 1980
[SH-5.1-15] N85-35068
Observations of cosmic-ray modulations in the fall, 1984
[SH-5.1-16] N85-35069
Study of cosmic ray scintillations from 5-minute data of the scintillations telescope Izmran and world-wide network stations
[SH-5.1-18] N85-35071
The theoretical and experimental investigation of cosmic ray Forbush-effects
[SH-5.1-20] N85-35072
Peculiarities of Galactic Cosmic Ray (GCR) anisotropy variation in connection with the recurrent and sporadic Forbush effects
[SH-5.1-21] N85-35073
Cosmic ray modulation by high-speed solar wind fluxes
[SH-5.1-22] N85-35074
Solar activity beyond the disk and variations of the cosmic ray gradient
[SH-5.1-23] N85-35075
Coupling functions for lead and lead-free neutron monitors from the latitudinal measurements performed in 1982 in the research station Academician Kurchatov
[SH-6.1-1] N85-35076
On the solar cycle variation in the barometer coefficients of high latitude neutron monitors
[SH-6.1-2] N85-35077
Altitude variations of cosmic-ray soft and hard components observed by airborne detectors
[SH-6.1-5] N85-35079
Additional flux of particles and albedo-electrons in upper atmosphere
[SH-6.1-6] N85-35080
Observation of energy spectrum of electron albedo in low latitude region at Hyderabad, India
[SH-6.1-7] N85-35081
Proton albedo spectrum observation in low latitude region at Hyderabad, India
[SH-6.1-8] N85-35082
The influence of quiet asymmetric magnetosphere on the cutoff rigidities of the main cone
[SH-6.1-10] N85-35083
Re-evaluation of cosmic ray cutoff terminology
[SH-6.1-11] N85-35084
The use of the McIlwain L-parameter to estimate cosmic ray vertical cutoff rigidities for different epochs of the geomagnetic field
[SH-6.1-12] N85-35085
Estimating the change in asymptotic direction due to secular changes in the geomagnetic field
[SH-6.1-13] N85-35086
Short perturbations of cosmic ray intensity and electric field in atmosphere
[SH-6.1-18] N85-35090
Long-period cosmic ray variations and their altitude dependence
[SH-6.1-19] N85-35091
Diurnal variations of cosmic ray geomagnetic cut-off threshold rigidities
[SH-6.1-21] N85-35092
The influence of the Earth's magnetosphere on the high-energy solar protons
[SH-6.1-22] N85-35093
Cosmic rays 10Be biennal data and their relationship to aurorae and sunspots
[SH-7.1-1] N85-35094
Solar modulation of cosmic ray intensity and solar flare events inferred from (14)C contents in dated tree rings
[SH-7.1-2] N85-35095
Cosmic ray secular variations in terrestrial records and aurorae
[SH-7.1-3] N85-35096
When did the average cosmic ray flux increase?
[SH-7.1-4] N85-35097
Cosmic-ray exposure records and origins of meteorites
[SH-7.1-7] N85-35099
Accelerator experiments on the contribution of secondary particles to the production of cosmogenic nuclides in meteorites
[SH-7.1-8] N85-35100

Depth and size effects on cosmogenic nuclide production in meteorites
[SH-7.1-9] N85-35101
Spallogenic origin of nuclei in meteorites
[SH-7.1-10] N85-35102
Clusters and cycles in the cosmic ray age distributions of meteorites
[SH-7.1-11] N85-35103
High precise measurements of cosmogenic radiocarbon abundance by complex of scintillation equipments
[SH-7.1-14] N85-35105
Radiocarbon content in the annual tree rings during last 150 years and time variation of cosmic rays
[SH-7.1-15] N85-35106
Cosmogenic Mn-53 in meteorites
[SH-7.1-17] N85-35107
Solar neutrinos, solar flares, solar activity cycle and the proton decay
[SH-8.1-8] N85-35113
Neutrino production from the solar atmosphere
[SH-8.1-9] N85-35114
Three dimensional calculation of flux of low energy atmospheric neutrinos
[SH-8.1-11] N85-35116
Detector calibration of the Indian cosmic ray experiment (IONS) in Space-Shuttle Spacelab-13
[SH-9.1-2] N85-35117

COSMOCHEMISTRY
The cosmic ray composition as viewed from the chemical abundances of the solar system
[OG-7.1-8] N85-34869

COSMOLOGY
Cosmogenic-nuclide production by primary cosmic-ray protons
[SH-7.1-6] N85-35098

COSMOS 1129 SATELLITE
Lipogenesis in rat liver after flight aboard Cosmos-1129 biosatellite N85-34508

COST ANALYSIS
Spacecraft (Mobile Satellite) configuration design study
[NASA-CR-176153] N85-34152

COST EFFECTIVENESS
Cost effective single crystals: The Rolls Royce approach — gas turbine components
[PNR-90262] N85-34717

COULOMB COLLISIONS
Collisional relaxation of electron tail distribution
[IPPJ-729] N85-34635

COULOMB POTENTIAL
Electron loss process and cross section of multiply charged ions by neutral atoms N85-34685
Anomalous abundances of solar energetic particles and coronal gas: Coulomb effects and First Ionization Potential (FIP) ordering
[SH-2.1-10] N85-34791

COUNTERS
Observations on (3)He neutron spectrometry
[DE85-010731] N85-34608

COUPLED MODES
Mechanical ratcheting behaviors of a steel pipe under combined cyclic axial load and internal pressure N85-34184
Nonlinear flap-lag-extensional vibrations of rotating, pretwisted, preconed beams including Coriolis effects
[NASA-TM-87102] N85-34427

COUPLERS
Conjugated symmetrical coupler curves, produced by 4-bar linkages having the same transmission angles N85-34322

COUPLING
Experimental measurements of the ion cyclotron antennas' coupling and RF characteristics
[DE85-011569] N85-34694

COUPLINGS
Mechanical ratcheting behaviors of a steel pipe under combined cyclic axial load and internal pressure N85-34184
The balancing of complex linkage mechanisms N85-34313

CRACK CLOSURE
Fatigue crack retardation phenomenon caused by single-multiple overloads in 2017-T3 aluminum allow N85-34196

CRACK INITIATION
Short-time creep of ice
[NRC/CNR-TT-2111] N85-34428

CRACK PROPAGATION
The influence of temperature on static and dynamic SCC crack growth behavior in aluminum alloy N85-34190
A fractographic study on mode 2 and mode 3 SCC crack growth in an Al-Zn-Mg alloy N85-34191
Corrosion fatigue strength and crack growth in prestrained 0.16% C carbon steel N85-34192
Experimental study on time and temperature dependent behavior of crack growth in viscoelastic strip N85-34193
Fractographic analysis for nonpropagating conditions of fatigue crack at high stress ratios in mild steel N85-34194
Crystallographic orientation dependence of fatigue crack propagation in extremely low carbon steel N85-34195
Influence of cyclic thermal loading on internal stress in casted epoxy resin N85-34211
Near-threshold fatigue: An overview of the role of microstructure and environment
[DE85-009903] N85-34431

CRACKING (FRACTURING)
Study on fracture behavior of epoxy resin N85-34216

CRASH INJURIES
Design and testing of an energy-absorbing crewseat for the F/FB-111 aircraft. Volume 3: Data from crew module testing
[NASA-CR-3918] N85-34134

CRASHWORTHINESS
Aviation safety (aircraft passenger survivability and cabin safety)
[GPO-39-847] N85-34130
Design and testing of an energy-absorbing crewseat for the F/FB-111 aircraft. Volume 3: Data from crew module testing
[NASA-CR-3918] N85-34134

CRAY COMPUTERS
Parallel processing on the Livermore VAX 11/780-4 parallel processor system with compatability to Cray Research, Inc. (CRI) multitasking, version 1
[DE85-011856] N85-34595

CREEP PROPERTIES
Short-time creep of ice
[NRC/CNR-TT-2111] N85-34428

CREEP STRENGTH
The development and evaluation of the creep and corrosion resistant alloy IN6201
[PNR-90253] N85-34278

CREEP TESTS
Tensile testing apparatus
[NASA-CASE-LAR-13243-1] N85-34375

CREWS
Design and testing of an energy-absorbing crewseat for the F/FB-111 aircraft. Volume 3: Data from crew module testing
[NASA-CR-3918] N85-34134

CRITICAL MASS
A very important process of nucleosynthesis in stars
[OG-7.1-11] N85-34872

CROSS SECTIONS
On the importance of interstellar helium for the propagation of heavy cosmic rays
[OG-7.2-11] N85-34879

CROSSED FIELDS
Improved negative ion source
[DE85-006445] N85-34241

CRUDE OIL
Preliminary SPR thermal model description and results for WH-11 and BM-4
[DE85-013171] N85-34360
Geology and petroleum resources of basins in western China
[DE85-013038] N85-34469

CRYOGENIC WIND TUNNELS
A theoretical study of non-adiabatic surface effects for a model in the NTF cryogenic wind tunnel
[NASA-CR-3924] N85-34352

CRYOGENICS
Separation of gas mixtures by supported complexes
[DE85-011996] N85-34236

CRYSTAL GROWTH
Manufacturing process to reduce large grain growth in zirconium alloys
[DE85-011649] N85-34267

CRYSTAL LATTICES
On the potential link equation of a spot centre with relative deformation for a semi-infinite molecular crystal
[BLL-M-35795-(5828.4)] N85-34711
Flux-line lattice anisotropy in V3Si: Observation and interpretation
[DE85-011935] N85-34713

CRYSTAL STRUCTURE
Electrolytic synthesis of colored eta alumina film N85-34201
High resolution electron microscopic characterization of interfaces in ceramics
[DE85-011207] N85-34289
On the potential link equation of a spot centre with relative deformation for a semi-infinite molecular crystal
[BLL-M-35795-(5828.4)] N85-34711

CRYSTALLIZATION
The effect of liquid-liquid phase separation of glass on the properties and crystallization behavior
[NASA-TM-77890] N85-34285

CRYSTALLOGRAPHY
Crystallographic orientation dependence of fatigue crack propagation in extremely low carbon steel N85-34195

CRYSTALS
Lead and uranium group abundances in cosmic rays
[OG-7.1-3] N85-34865

CURING
Metal (2) 4,4',4',4'' phthalocyanine tetraamines as curing agents for epoxy resins
[NASA-CASE-ARC-11424-1] N85-34281

CURRENT SHEETS
Cosmic ray intensity and the tilt of the neutral sheet
[SH-4.2-8] N85-34846
Differential measurement of cosmic-ray gradient with respect to interplanetary current sheet
[SH-4.2-9] N85-34847
Spatial variation of cosmic rays near the heliospheric current sheet
[SH-4.2-10] N85-34848
Determination of galactic cosmic ray latitudinal gradient using Earth based detectors
[SH-4.2-13] N85-34851
Latitudinal gradients of cosmic rays and the polarity reversal of the heliospheric magnetic field: A preliminary evaluation
[SH-4.2-16] N85-34853
The effect of the neutral sheet structure of the interplanetary magnetic field on cosmic ray distribution in space
[SH-4.2-18] N85-34855
Difference between even and odd 11-year cycles in cosmic ray intensity
[SH-4.2-22] N85-34859
The dependence of solar modulation on the sign of the cosmic ray particle charge
[SH-4.2-23] N85-34860

CURVATURE
Effects of solar magnetic field on cosmic rays
[SH-4.2-12] N85-34850
The effect of the neutral sheet structure of the interplanetary magnetic field on cosmic ray distribution in space
[SH-4.2-18] N85-34855
The dependence of solar modulation on the sign of the cosmic ray particle charge
[SH-4.2-23] N85-34860

CURVES (GEOMETRY)
Conjugated symmetrical coupler curves, produced by 4-bar linkages having the same transmission angles N85-34322
Geometric continuity with interpolating Bezier curves N85-34570
An intuitive approach to geometric continuity for parametric curves and surfaces N85-34571
The dynamics of articulated rigid bodies for purposes of animation N85-34579

CUTTERS
Properties of tungsten-free steel for cutting tools
[BLL-M-35808-(5828.4)] N85-34259

CYCLIC LOADS
Influence of cyclic thermal loading on internal stress in casted epoxy resin N85-34211

CYCLOTRON RADIATION
Research on gyrotrons
[AD-A154032] N85-34380
Multiple-frequency electron cyclotron heating of hot electron rings in EBT-1
[DE85-011302] N85-34701

CYCLOTRON RESONANCE
Transport issues in Phaedrus-type plasmas N85-34653

CYCLOTRON RESONANCE DEVICES
Research on gyrotrons
[AD-A154032] N85-34380

CYCLOTRONS
Experimental measurements of the ion cyclotron antennas' coupling and RF characteristics
[DE85-011569] N85-34694

CYLINDRICAL BODIES
Calculation of roots of transcendental equations in problems of determining thermal conductivity of cylinder with non-uniform boundary conditions
[BLL-M-35788-(5828.4)] N85-34349

CYTOLOGY
Improved flow cytometer measurement of binding assays
[DE85-006407] N85-34390

D

DATA ACQUISITION
Determination of instrument errors by compatibility checking: Results from dynamic flight test data
[ARL-AERO-R-162] N85-34137

Separation of gas mixtures by supported complexes [DE85-011996] N85-34236
Throughfall rate and chemistry studies: Whiteface Mountain [DE85-012407] N85-34464
The 1984 biotic studies of Yucca Mountain, Nevada test site, Nye County, Nevada [DE85-011715] N85-34487
Akeno 20 km (2) air shower array (Akeno Branch) [OG-9.4-8] N85-34975

DATA BASE MANAGEMENT SYSTEMS
User's operating procedures. Volume 1: Scout project financial analysis program [NASA-CR-177949] N85-34519
The interactive planning work station: A graphics-based UNIX (trademark) tool for application users and developers N85-34527
An image management kernel for the design of relational and pictorial data bases N85-34532

DATA BASES
Novette diagnostic support [DE85-012937] N85-34383
User's operating procedures. Volume 3: Projects directorate information programs [NASA-CR-177950] N85-34520
Graphics Interaction in databases N85-34534
NAPGEN: Automatic NAPLPS page generator N85-34575
The final COS-B database now publicly available [OG-9.3-8] N85-34963
The final COS-B database: In-flight calibration of instrumental parameters [OG-9.3-9] N85-34964

DATA CORRELATION
A suggested standardized format for cosmic ray ground-level event data [SH-9.1-15] N85-35130

DATA LINKS
Performance interface document for the S-band diplexer for space users of NASA networks [NASA-TM-86224] N85-34155

DATA PROCESSING
Comparison of experimental data on detonation velocity and Chapman-Jouget pressure vs initial HE density with predictions from Ree's model equation of state [DE85-007266] N85-34304
Modular digital holographic fringe data processing system [NASA-CR-177952] N85-34376
Evaluation of low-temperature geothermal potential in Utah and Goshen Valleys and adjacent areas, Utah. Part 2: Water temperature and chemistry [DE85-009344] N85-34438
Real-time multiparameter pulse processing with decision tables [DE85-011683] N85-34589
Vector calculation of particle code N85-34688
On the statistical significance of excess events: Remarks of caution and the need for a standard method of calculation [OG-9.5-10] N85-34987

DATA RECORDERS
Balloon-borne video cassette recorders for digital data storage [OG-9.3-11] N85-34966
Mini and super mini arrays for the study of highest energy cosmic rays [OG-9.4-9] N85-34976

DATA REDUCTION
Time-resolved spectroscopic studies of detonating heterogeneous explosives [DE85-009760] N85-34297
Computer graphics for multivariate data N85-34528
An image management kernel for the design of relational and pictorial data bases N85-34532
Spatial trees: A fast access method for unstructured graphical data N85-34533
New Matsushiro underground cosmic ray station (220 M.W.E. in depth) [SH-9.1-14] N85-35129
A suggested standardized format for cosmic ray ground-level event data [SH-9.1-15] N85-35130

DATA RETRIEVAL
NAPGEN: Automatic NAPLPS page generator N85-34575

DATA SAMPLING
Theoretical principles of vertical subsampling of color difference signals at half the sampling rate — television [FI-447-TBR-18] N85-34332

DATA STORAGE
The automatic labeling of geographic maps: A problem in computer aesthetics N85-34561
Building an octree from a set of parallelepipeds N85-34572
Balloon-borne video cassette recorders for digital data storage [OG-9.3-11] N85-34966
A suggested standardized format for cosmic ray ground-level event data [SH-9.1-15] N85-35130

DEBRIS
Marine Sample Exploitation Project: Estimates regarding the sensitivity and technology for the detection of nuclear explosion debris in the marine environment [DE85-013176] N85-34462

DECAY
Application of evaluated fission-product delayed-neutron precursor data in reactor kinetics calculations [DE85-012728] N85-34624

DECELERATION
Why do leaky-box models work so fine? [OG-7.2-8] N85-34877
Instabilities in decelerating supersonic flows with applications to cosmic ray shocks [OG-8.1-2] N85-34892

DECISION MAKING
Real-time multiparameter pulse processing with decision tables [DE85-011683] N85-34589
Opportunities for policy historians: The evolution of the US civilian space program N85-35147

DECISION THEORY
Strategic use of business graphics: A stakeholder approach N85-34566

DEFORMATION
Effects of hot deformation on the kinetics of the pearlite transformation in eutectoid steel [BLL-M-35844-(5828.4)] N85-34250
Phase transformations taking place in austenitic steel during deformation at different rates [BLL-M-35875-(5828.4)] N85-34254
Inertial stresses and deformations in mechanisms N85-34320
Scaling differences between large interplate and intraplate earthquakes [NASA-CR-176149] N85-34467
On the potential link equation of a spot centre with relative deformation for a semi-infinite molecular crystal [BLL-M-35795-(5828.4)] N85-34711

DEGASSING
Evacuate and backfill apparatus and method [DE85-006018] N85-34411

DEGRADATION
Solar maximum: Solar array degradation [NASA-TM-86194] N85-34175
Degradation mechanisms and accelerated aging test design [TI85-003251] N85-34420

DEGREES OF FREEDOM
Ground-based and in-flight simulator studies of flight characteristics of a twin-fuselage passenger transport airplane during approach and landing [NASA-TP-2451] N85-34144

DELAMINATING
Stress distribution of fiberglass reinforced plastic beam with a delamination under three-point bending N85-34210

DEMODULATION
Source energy spectra from demodulation of solar particle data by interplanetary and coronal transport [SH-1.3-13] N85-34758

DENDROCHRONOLOGY
Solar modulation of cosmic ray intensity and solar flare events inferred from (14)C contents in dated tree rings [SH-7.1-2] N85-35095
High precise measurements of cosmogenic radiocarbon abundance by complex of scintillation equipments [SH-7.1-14] N85-35105
Radiocarbon content in the annual tree rings during last 150 years and time variation of cosmic rays [SH-7.1-15] N85-35106

DENSITY (MASS/VOLUME)
The influence of temperature on the composition density of the transition metals [BLL-M-35896-(5826.4)] N85-34262
Comparison of experimental data on detonation velocity and Chapman-Jouget pressure vs initial HE density with predictions from Ree's model equation of state [DE85-007266] N85-34304
Transports studies of ECH and ICRH-heated bumpy torus plasma in NBT-1M N85-34662

DENSITY (NUMBER/VOLUME)
Solar flare gamma-ray line spectroscopy [SH-2.1-14] N85-34795
Gradients and anisotropies of high energy cosmic rays in the outer heliosphere [SH-4.3-7] N85-34992

DENSITY DISTRIBUTION
Electron density distribution analysis for nitroguanidine [DE85-009598] N85-34603
Breakdown of intrinsic ambipolarity for the radial diffusion due to a rotating RF field N85-34660
Transports studies of ECH and ICRH-heated bumpy torus plasma in NBT-1M N85-34662
Guiding center distribution function and longitudinal invariant N85-34663
Cosmic ray density gradient and its dependence on the north-south asymmetry in solar activity [SH-4.5-17] N85-35034
Observation of pick-up ions in the solar wind: Evidence for the source of the anomalous cosmic ray component? [SH-4.6-5] N85-35043

DENSITY MEASUREMENT
Calculation of flow kinetics of composite media [BLL-M-35819-(5828.4)] N85-34348

DENTISTRY
Applications of CdTe to nuclear medicine [DE85-011877] N85-34492

DEPLETION
Depletion modeling of liquid dominated geothermal reservoirs [DE85-009923] N85-34437

DEPOSITION
Dual-chamber plasma deposition of A-Si:H solar cells at high rates using disilane [DE85-011828] N85-34451
Throughfall rate and chemistry studies: Whiteface Mountain [DE85-012407] N85-34464
User's guide to the MATHEW/ADPIC models [DE85-012952] N85-34587
MATADOR (Methods for the Analysis of Transport And Deposition Of Radionuclides) code description and user's manual [TI85-901402] N85-34592
Diamondlike carbon protective coatings for IR materials [NASA-TM-87083] N85-34631

DEPTH
Altitude variations of cosmic-ray soft and hard components observed by airborne detectors [SH-6.1-5] N85-35079

DEPTH MEASUREMENT
Method for determining depth and shape of a sub-surface conductive object [DE85-006502] N85-34389
The transient electromagnetic depth sounding technique applied to hydrocarbons and geothermal exploration [MITT-42] N85-34476

DESENSITIZING
Manufacturing process to reduce large grain growth in zirconium alloys [DE85-011649] N85-34267

DESICCANTS
Rigid zeolite containing polyurethane foams [DE85-006406] N85-34286

DESIGN ANALYSIS
Optimisation in the computer aided design of mechanisms N85-34321
Realization and linearization of a hyperfrequency power amplifier implemented with bipolar transistors in class C polarization --- microwave amplifiers [CNES-NT-114] N85-34346

DETECTION
Direct determination of metals in organic matrices by Inductively Coupled Plasma-Atomic Emission Spectrometry (ICP-AES) [DE85-012015] N85-34233
Instrumentation for sensing moisture content of material using a transient thermal pulse [NASA-CASE-NPO-15493-2] N85-34373
Modulated voltage metastable ionization detector [NASA-CASE-ARC-11503-1] N85-34374
Upgrading auxiliary facility outleakage and combustion detection [DE85-012796] N85-34386
Solar system fault detection [DE85-005987] N85-34458
Marine Sample Exploitation Project: Estimates regarding the sensitivity and technology for the detection of nuclear explosion debris in the marine environment [DE85-013176] N85-34462
Magnetic search system [PB85-185108] N85-34477
Applications of CdTe to nuclear medicine [DE85-011877] N85-34492
Issues and techniques in touch-sensitive tablet input (executive summary) N85-34543
On the detectability of key-MeV solar protons through their nonthermal Lyman-alpha emission [SH-1.3-5] N85-34752
Measurement of low energy cosmic rays aboard Spacelab-1 [SH-10.1-6] N85-35137
Heavy cosmic ray measurement aboard Spacelab-1 [SH-10.1-7] N85-35138

DETONATION
A model of hypersonic two-dimensional oblique detonation wave ramjet
[UTIAS-TN-257] N85-34139
Intermolecular explosives
[DE85-009609] N85-34296
Time-resolved spectroscopic studies of detonating heterogeneous explosives
[DE85-009760] N85-34297
Pressure-shear loading of PBX-9404
[DE85-009982] N85-34298
Detonation in tungsten-loaded HMX
[DE85-009606] N85-34299
Modeling heterogeneous high explosive burn with an explicit hot-spot process
[DE85-009593] N85-34300
Three-dimensional hydrodynamic hot-spot model
[DE85-009587] N85-34301
Real time analysis of PETN detonation products
[DE85-009581] N85-34303
Comparison of experimental data on detonation velocity and Chapman-Jouget pressure vs initial HE density with predictions from Ree's model equation of state
[DE85-007266] N85-34304
Detonation of condensed explosives: Evolution of knowledge in the last 40 years
[ISL-CO-226/84] N85-34307

DETONATION WAVES
A model of hypersonic two-dimensional oblique detonation wave ramjet
[UTIAS-TN-257] N85-34139

DEUTERIUM
Measuring method and confirmation of H- (D-) ion current by sheet plasma 1
[IPPJ-730] N85-34638
Size effects of vacuum chamber for H- (D-) ion volume production by sheet plasma 1
[IPPJ-731] N85-34639
Data on the backscattering coefficients on light ions from solids: A revision
[IPPJ-AM-41-REV] N85-34689

DEUTERIUM PLASMA
Measuring method and confirmation of H- (D-) ion current by sheet plasma 1
[IPPJ-730] N85-34638

DEUTERONS
The electromagnetic ram action of the plasma focus as a paradigm for the generation of cosmic rays and the gigantic jets in active galaxies
[OG-8.2-14] N85-34910

DEW POINT
Instrumentation for sensing moisture content of material using a transient thermal pulse
[NASA-CASE-NPO-15493-2] N85-34373

DF LASERS
Chemical lasers
[ISL-R-107/84] N85-34400

DIAGNOSIS
Applications of CdTe to nuclear medicine
[DE85-011877] N85-34492

DIAGRAMS
A model for a document maintenance system N85-34542

DIAMINES
Preparation of ethylenediamine dinitrate
[DE85-006423] N85-34305

DIFFERENTIAL EQUATIONS
Nonlinear flap-lag-extensional vibrations of rotating, pretwisted, precone beams including Coriolis effects
[NASA-TM-87102] N85-34427
DISPL1: A software package for one and two spatially dimensioned kinetics-diffusion problems
[ANL-84-56] N85-34516
A geometric modeller for turbomachinery applications N85-34556
Second-order Compton-Getting effect on arbitrary intensity distribution
[SH-3.1-10] N85-34814

DIFFERENTIATION
Differentiating spatial light modulator
[AD-D011727] N85-34632

DIFFUSION
New semi-implicit method for solving the time-dependent conservation equations for incompressible flow
[DE85-010926] N85-34367
Evaluation of source strength and dispersion model predications with data from large nitrogen tetroxide field experiments
[DE85-011855] N85-34465
User's guide to the MATHEW/ADPIC models
[DE85-012952] N85-34587
Grain boundary and surface diffusion in oxide systems
[DE85-007291] N85-34715
The model-independence of cosmic ray source determinations
[OG-7.2-1] N85-34873
The role of cosmic rays in magnetic hydrodynamics of interstellar medium
[OG-7.2-15] N85-34882
IMF-sense-dependent cosmic ray anisotropy produced from diffusion-convection in heliosphere
[SH-4.3-9] N85-34994
Diurnal anisotropy during solar activity cycle twenty and diffusion-convection model
[SH-4.5-7] N85-35025

DIFFUSION COEFFICIENT
Breakdown of intrinsic ambipolarity for the radial diffusion due to a rotating RF field N85-34660
Effect of ECH and ICH on ambipolar potential in NBT-1M N85-34661
Neoclassical diffusion including ellipticity in a heliotron-like configuration N85-34667
Spatial dependence of the local diffusion coefficient measured upstream of the November 12, 1978 interplanetary traveling shock
[SH-1.5-12] N85-34776
The Jovian electron spectrum: 1978-1984
[SH-1.5-19] N85-34782
Cosmic ray modulatin and merged interaction regions
[SH-4.1-11] N85-34834
Cosmic ray modulation in a random anisotropic magnetic field
[SH-4.1-20] N85-34839
Spatial variation of cosmic rays near the heliospheric current sheet
[SH-4.2-10] N85-34848
Effects of a wavy neutral sheet on cosmic ray anisotropies
[SH-4.2-11] N85-34849
Effects of solar magnetic field on cosmic rays
[SH-4.2-12] N85-34850
The expected cosmic ray density and stream distributions at the heliolatitudinal asymmetry of solar wind
[SH-4.2-14] N85-34852
The influence of nonstationarity of the solar activity and general solar field on modulation of cosmic rays
[SH-4.2-17] N85-34854
The effect of the neutral sheet structure of the interplanetary magnetic field on cosmic ray distribution in space
[SH-4.2-18] N85-34855
Spatial distribution of cosmic rays in magnetic cycles of the Sun
[SH-4.2-20] N85-34857
Difference between even and odd 11-year cycles in cosmic ray intensity
[SH-4.2-22] N85-34859
Nonstationary modulation of galactic cosmic rays in a nonlinear model
[SH-4.7-10] N85-35054

DIGESTING
Lipid hydrolysis in man during antiorthostatic hypokinesia N85-34500

DIGITAL COMPUTERS
Re-designing a mechanism for higher speed: A case history from textile machinery N85-34310
Method and apparatus for transfer function simulator for testing complex systems
[NASA-CASE-NPO-15696-1] N85-34333

DIGITAL SYSTEMS
Modular digital holographic fringe data processing system
[NASA-CR-177952] N85-34376
Balloon-borne video cassette recorders for digital data storage
[OG-9.3-11] N85-34966
Burst size distributions in the digitized data of the ion chambers t Mt. Norikura and sea level stations
[SH-9.1-9] N85-35124

DIGITAL TECHNIQUES
Design, development and operation of a high simultaneous capacity digital telemetry system --- turbomachine blade flutter
[PNR-90261] N85-34151
Computer analysis techniques for the temporal evaluation of cardiac wall motion N85-34530
The scientific and technical issues in integrating remotely sensed imagery with geocoded data bases N85-34547
A general purpose image processing package N85-34549
Hologram-like transmission of pictures N85-34552

DIMENSIONAL ANALYSIS
Diffusion-convection function of cosmic rays
[SH-3.2-10] N85-34825

DINITRATES
Preparation of ethylenediamine dinitrate
[DE85-006423] N85-34305

DIPLEXERS
Performance interface document for the S-band diplexer for space users of NASA networks
[NASA-TM-86224] N85-34155

DIRECTIONAL CONTROL
New Matsushiro underground cosmic ray station (220 M.W.E. in depth)
[SH-9.1-14] N85-35129

DIRECTIONAL COUPLERS
New directional couplers for multimode circular waveguides applied to intense pulsed microwave systems
[DE85-011753] N85-34330

DIRECTIONAL SOLIDIFICATION (CRYSTALS)
Directionally solidified gas turbine alloys
[PNR-90264] N85-34279

DIRECTIVITY
Study on the correlation between grinding conditions and residual stresses in ground surface of steel by the X-ray method N85-34203

DISCRETE FUNCTIONS
Monte Carlo techniques for analyzing deep penetration problems
[DE85-011426] N85-34598

DISK GALAXIES
Solar activity beyond the disk and variations of the cosmic ray gradient
[SH-5.1-23] N85-35075

DISLOCATIONS (MATERIALS)
Hydrogen embrittlement testing
[DE85-007352] N85-34273

DISPERSION
Evaluation of source strength and dispersion model predications with data from large nitrogen tetroxide field experiments
[DE85-011855] N85-34465

DISPLACEMENT
The collected data for ramp function tests on a NACA 23012 aerofoil. Volume 1: Description and pressure data
[GU-AERO-8413-VOL-1] N85-34123

DISPLAY DEVICES
The improved display of 625-line television pictures: Adaptive interpolation
[BBC-RD-1985/5] N85-34328
Instrumentation for sensing moisture content of material using a transient thermal pulse
[NASA-CASE-NPO-15493-2] N85-34373
An integrated system for printing and publishing applications N85-34540
Colour coding scales and computer graphics N85-34568
Developing graphical tools with minimal GKS N85-34573
NAPGEN: Automatic NAPLPS page generator N85-34575
Using LINE as an interactive graphics package. Interfacing line and Topdraw in 43 and 24 VM
[DE85-012007] N85-34585
Maintenance port system
[AD-D011724] N85-34594

DISTRIBUTION (PROPERTY)
Pitch angle distributions of solar energetic particles and the local scattering properties of the interplanetary magnetic field
[SH-3.1-13] N85-34816
Cosmic ray intensity distribution perpendicular to solar equatorial plane at 1 A.U. during 1978-83
[SH-4.3-14] N85-34998
Cosmogenic Mn-53 in meteorites
[SH-7.1-17] N85-35107

DISTRIBUTION FUNCTIONS
A graphics interface for interactive simulation of packet-switched networks N85-34558
Numerical solutions of the Vlasov equation N85-34672
Pitch angle distributions of 35-1000 keV protons at quasi-perpendicular interplanetary shocks
[SH-1.5-6] N85-34775
The dispersive evolution of charged-particle bunches in random magnetic fields
[SH-4.1-2] N85-34828

DIURNAL VARIATIONS
Drift and observations in cosmic-ray modulation, 2
[SH-4.2-5] N85-34843
Cosmic ray sidereal diurnal variation of galactic origin observed by neutron monitors
[SH-4.4-2] N85-35000
Sidereal anisotropies in the median rigidity range 60-600GV in 1978-1983
[SH-4.4-3] N85-35001
The sidereal semi-diurnal variation observed at high zenith angles at Mawson, 1968-1984, and the polarity of the solar main field
[SH-4.4-6] N85-35004
Cosmic ray intensity variations observed at Matsushiro (220 M.W.E. in depth)
[SH-4.4-9] N85-35007

Solar tri-diurnal variation of cosmic rays in a wide range of rigidity
[SH-4.5-3] N85-35021
Upper cut-off rigidity for corotation anisotropy during solar activity cycles 20 and 21
[SH-4.5-4] N85-35022
Twenty-two-year cycle of the upper limiting rigidity of Daly waves
[SH-4.5-5] N85-35023
Solar wind velocity and daily variation of cosmic rays
[SH-4.5-6] N85-35024
Diurnal anisotropy during solar activity cycle twenty and diffusion-convection model
[SH-4.5-7] N85-35025
Diurnal effect in cosmic rays at middle latitudes according to stratospheric measurements
[SH-4.5-8] N85-35026
Comparative study of the phase of diurnal anisotropy on quiet and disturbed days on a long term basis up to recent period
[SH-4.5-9] N85-35027
Study of spectral exponent on quiet and disturbed days
[SH-4.5-10] N85-35028
Diurnal variation of galactic cosmic ray intensity on quiet days
[SH-4.5-11] N85-35029
Diurnal variations from muon data at Takeyama underground station
[SH-4.5-13] N85-35030
Long term changes in cosmic ray diurnal variations observed by ion chambers in Hong Kong and Japan
[SH-4.5-14] N85-35031
The cosmic ray differential diurnal variation dependences on the zenith angle and the geomagnetic disturbance
[SH-4.5-16] N85-35033
Anomalous increase of solar anisotropy above 150GV in 1981-1983
[SH-4.5-18] N85-35035
Magnetic fluctuation and cosmic ray diurnal variations
[SH-4.5-21] N85-35038
Transient cosmic ray increase associated with a geomagnetic storm
[SH-5.1-8] N85-35062
Long-period cosmic ray variations and their altitude dependence
[SH-6.1-19] N85-35091
Diurnal variations of cosmic ray geomagnetic cut-off threshold rigidities
[SH-6.1-21] N85-35092

DOCUMENTS
Recognition and clear representation of handwritten electronic diagrams N85-34541
A model for a document maintenance system N85-34542

DOMES (GEOLOGY)
Preliminary SPR thermal model description and results for WH-11 and BM-4
[DE85-013171] N85-34360

DOPES
Flat-plate solar array project process development area process research of non-CZ silicon material
[NASA-CR-176117] N85-34445

DOPPLER EFFECT
Wide Angle Michelson Doppler Imaging Interferometer (WAMDII) N85-34172
On the detectability of key-MeV solar protons through their nonthermal Lyman-alpha emission
[SH-1.3-5] N85-34752

DOSAGE
The 1983 international intercomparison of nuclear accident dosimetry systems at Oak Ridge National Laboratory
[DE85-011303] N85-34382
The 1984 biotic studies of Yucca Mountain, Nevada test site, Nye County, Nevada
[DE85-011715] N85-34487
Estimating risks of lead-induced hemoglobin decrements under conditions of uncertainty: Methodology, pilot judgments and illustrative calculations
[DE85-012293] N85-34493
Analysis of transient radiation upset in a 16K SRAM
[DE85-009442] N85-34586

DOSIMETERS
The 1983 international intercomparison of nuclear accident dosimetry systems at Oak Ridge National Laboratory
[DE85-011303] N85-34382

DRAINAGE
Hydrology
[PB85-182954] N85-34440

DRIFT (INSTRUMENTATION)
Improved method for the stabilization of NaI-photomultiplier gamma detectors against thermal and other drift
[DE85-011830] N85-34613

DRIFT RATE
Guiding center distribution function and longitudinal invariant N85-34663
Notes on drift theory
[SH-4.2-3] N85-34841
Drift and observations in cosmic-ray modulation, 1
[SH-4.2-4] N85-34842
Drift and observations in cosmic-ray modulation, 2
[SH-4.2-5] N85-34843
The influence of nonstationarity of the solar activity and general solar field on modulation of cosmic rays
[SH-4.2-17] N85-34854
Changes in the energy spectrum of anomalous oxygen and helium during 1977-1985
[SH-4.6-1] N85-35039
On the anomalous component
[SH-4.6-6] N85-35044

DRUGS
Effect of dibazol on parameters of nonspecific resistance of subjects in pressurized cabins N85-34504

DRYING
Composite desiccant structure
[DE85-006400] N85-34226
Nonsaturable microdryer
[DE85-005760] N85-34457

DUCTS
Block-implicit calculations of three-dimensional laminar flow in strongly curved ducts
[DE85-003047] N85-34363

DYE LASERS
Fiber optics interface for a dye laser oscillator and method
[DE85-005765] N85-34633

DYNAMIC LOADS
Shock and release equation of state of calcite
[DE85-013151] N85-34432

DYNAMIC PRESSURE
Pressure-shear loading of PBX-9404
[DE85-009982] N85-34298

DYNAMIC RESPONSE
Automated dynamic analytical model improvement for damped structures
[NASA-CR-177945] N85-34425
A multi-touch three dimensional touch-sensitive tablet (executive summary) N85-34553

DYNAMIC STRUCTURAL ANALYSIS
Negative flexural behavior of precase composite slabs with steel joint N85-34183
Mechanical ratcheting behaviors of a steel pipe under combined cyclic axial load and internal pressure N85-34184
Automated dynamic analytical model improvement for damped structures
[NASA-CR-177945] N85-34425

E

EARTH (PLANET)
Comparisons of the North Polar Cap of Mars and the Earth's Northern Hemisphere snow cover
[NASA-TM-86191] N85-34728

EARTH ATMOSPHERE
Imaging Spectrometric Observatory (ISO) N85-34169
Evaluation of source strength and dispersion model predications with data from large nitrogen tetroxide field experiments
[DE85-011855] N85-34485
Nucleosynthesis in the terrestrial and solar atmospheres
[SH-2.2-2] N85-34797
The influences of the galactic cosmic ray on the atmospheric ozone
[SH-10.1-1] N85-35133

EARTH RESOURCES
Geology and petroleum resources of basins in western China
[DE85-013038] N85-34469
The scientific and technical issues in integrating remotely sensed imagery with geocoded data bases N85-34547
Selection of segment similarity measures for hierarchical picture segmentation N85-34548
Satellites and politics: Weather, communications, and earth resources N85-35144

EARTHQUAKES
Scaling differences between large interplate and intraplate earthquakes
[NASA-CR-176149] N85-34467
Geophysical-geological studies of possible extensions of the New Madrid fault zone
[TI85-901341] N85-34475

ECLIPTIC
An update on the correlation between the cosmic radiation intensity and the geomagnetic AA index
[SH-4.2-24] N85-34861

ECOLOGY
Climate modeling: A retrospective-prospective view with consideration for the atmospheric carbon dioxide-climate issue
[DE85-011532] N85-34481
The 1984 biotic studies of Yucca Mountain, Nevada test site, Nye County, Nevada
[DE85-011715] N85-34487

EDDINGTON APPROXIMATION
X-ray spectra of bursting neutron stars N85-34686

EDGE DISLOCATIONS
Crystallographic orientation dependence of fatigue crack propagation in extremely low carbon steel N85-34195

EDGES
Mechanical properties of plasma arc cut steel N85-34188
Anti wear property of two phasic metal composite N85-34199

EDITING
An integrated system for printing and publishing applications N85-34540
A model for a document maintenance system N85-34542

EDITING ROUTINES (COMPUTERS)
Design and implementation of an interactive route editor N85-34559

EDUCATION
Solar energy education. Renewable energy: A background text
[DE85-010365] N85-34452

EFFICIENCY
Lubrication and cooling for high speed gears
[NASA-TM-87096] N85-34407

EIGENVALUES
Finding the roots of the transcendental equations in problems in determining the thermal conductivity of spheres with heterogeneous boundary conditions
[BLL-M-35878-(5828.4)] N85-34347

EJECTORS
Combined cold compressor/ejector helium refrigerator
[DE85-006408] N85-34326

ELASTIC PROPERTIES
Viscoelastic behavior of short-fiber composite materials
[DE85-011233] N85-34225
The study of the effect of residual microimpurities on the fatigue strength of 55S2 steel
[BLL-M-36317-(5828.4)] N85-34246
An introduction to finite elements N85-34319
Stresses and strains in a plate resulting from two closely-spaced interference-fit fasteners
[ARL-STRUC-TM-409] N85-34429

ELECTRIC AUTOMOBILES
Test plan for performance testing of the Eaton AC-3 electric vehicle
[DE85-011954] N85-34341

ELECTRIC BATTERIES
Test plan for performance testing of the Eaton AC-3 electric vehicle
[DE85-011954] N85-34341
Wind energy battery storage, phase 2
[DE85-009753] N85-34450

ELECTRIC FIELDS
Theoretical and Experimental Beam Plasma Physics (TEBPP) N85-34166
Improved negative ion source
[DE85-006445] N85-34241
Negative ion sources equipped with continuous annular and spherical geometry surface ionizers
[DE85-011939] N85-34619
Potential effect in transport due to non-axisymmetric confining field N85-34645
Activities of the RF Section N85-34646
Radial transport phenomena for TMX-upgrade N85-34647
RF induced radial diffusion in tandem mirrors N85-34649
Induced azimuthal electric field effects on tandem transport and ambipolarity N85-34650
Breakdown of intrinsic ambipolarity for the radial diffusion due to a rotating RF field N85-34660
Transports studies of ECH and ICRH-heated bumpy torus plasma in NBT-1M N85-34662
Guiding center distribution function and longitudinal invariant N85-34663
Analytic and numerical calculations of the ambipolar electric field in a stellarator N85-34665
Confinement experiments on ISX-B
[DE85-012346] N85-34709
The role of cosmic rays in magnetic hydrodynamics of interstellar medium
[OG-7.2-15] N85-34882

Short perturbations of cosmic ray intensity and electric field in atmosphere
[SH-6.1-18] N85-35090

ELECTRIC HYBRID VEHICLES
Evaluation of semiconductor devices for Electric and Hybrid Vehicle (EHV) ac-drive applications, volume 1
[NASA-CR-176118] N85-34335

ELECTRIC MOTOR VEHICLES
Evaluation of half wave induction motor drive for use in passenger vehicles
[NASA-CR-176119] N85-34334
Evaluation of semiconductor devices for Electric and Hybrid Vehicle (EHV) ac-drive applications, volume 1
[NASA-CR-176118] N85-34335
Test plan for performance testing of the Eaton AC-3 electric vehicle
[DE85-011954] N85-34341

ELECTRIC MOTORS
Evaluation of half wave induction motor drive for use in passenger vehicles
[NASA-CR-176119] N85-34334

ELECTRIC POTENTIAL
Experimental evaluation of the thermodynamic properties of concentrated aqueous potassium hydroxide solutions
[DE85-010628] N85-34238
Reversing-counterpulse repetitive-pulse inductive storage circuit
[DE85-006409] N85-34344
Modulated voltage metastable ionization detector
[NASA-CASE-ARC-11503-1] N85-34374
Rapid annealing of temperature-compensated, precision voltage references following fast-neutron irradiation
[DE85-009821] N85-34609

ELECTRIC SPARKS
Apparatus and method for the spectrochemical analysis of liquids using the laser spark
[DE85-005749] N85-34387

ELECTRICAL ENGINEERING
Joint services electronics program
[AD-A154748] N85-34336

ELECTRICAL FAULTS
Method and apparatus for transfer function simulator for testing complex systems
[NASA-CASE-NPO-15696-1] N85-34333
Solar system fault detection
[DE85-005987] N85-34458

ELECTRICAL PROPERTIES
Grain boundary and surface diffusion in oxide systems
[DE85-007291] N85-34715

ELECTRICAL RESISTANCE
Tensile testing apparatus
[NASA-CASE-LAR-13243-1] N85-34375

ELECTRICAL RESISTIVITY
Electrical resistivity and hysteresis of the equiatomic nickel-titanium alloy near the martensitic transformation temperature N85-34181
Instrumentation for sensing moisture content of material using a transient thermal pulse
[NASA-CASE-NPO-15493-2] N85-34373
Electrically conductive containment vessel for molten aluminum
[DE85-006518] N85-34415

ELECTRO-OPTICAL EFFECT
OMEGA: Optoelectronic measurement of the incidence angle of a projectile
[ISL-CO-223/84] N85-34634

ELECTRO-OPTICS
Differentiating spatial light modulator
[AD-D011727] N85-34632

ELECTROCHEMICAL CELLS
Experimental evaluation of the thermodynamic properties of concentrated aqueous potassium hydroxide solutions
[DE85-010628] N85-34238

ELECTROCHEMICAL CORROSION
Corrosion fatigue strength and crack growth in prestrained 0.16% C carbon steel N85-34192

ELECTRODE MATERIALS
Conductor-polymer composite electrode materials
[DE85-005766] N85-34293

ELECTRODES
Electrode erosion in arc discharges at atmospheric pressure
[NASA-TM-87087] N85-34178
Experimental evaluation of the thermodynamic properties of concentrated aqueous potassium hydroxide solutions
[DE85-010628] N85-34238
Conductor-polymer composite electrode materials
[DE85-005766] N85-34293
Nonsaturable microdryer
[DE85-005760] N85-34457
Negative ion sources equipped with continuous annular and spherical geometry surface ionizers
[DE85-011939] N85-34619

ELECTROHYDRODYNAMICS
Electrodynamic tether N85-34168
Elastohydrodynamic lubrication calculations used as a tool to study scuffing
[NASA-TM-87097] N85-34408

ELECTROLYSIS
Electrolytic synthesis of colored eta alumina film N85-34201

ELECTROLYTE METABOLISM
Fluid-electrolyte metabolism and renal function in cosmonauts following 185-day spaceflight N85-34495

ELECTROLYTES
Nonsaturable microdryer
[DE85-005760] N85-34457

ELECTROMAGNETIC ACCELERATION
Pulsars as cosmic ray accelerators: Energy development of protons
[OG-8.2-22] N85-34918
Pulsars as cosmic ray particle accelerators: Dynamics of electrons
[OG-8.2-23] N85-34919

ELECTROMAGNETIC FIELDS
Pulsars as cosmic ray accelerators: Energy development of protons
[OG-8.2-22] N85-34918

ELECTROMAGNETIC INTERFERENCE
Effect of interference on the performance of a minimum TCAS 2
[FAA/PM-84/33] N85-34131

ELECTROMAGNETIC RADIATION
Recoverable Plasma Diagnostics Package (RPDP) N85-34167
Simulation studies on stability of hot electron plasma N85-34664
Pulse effect in a light ion beam propagation through a Z-discharge plasma channel N85-34684
Source energy spectra from demodulation of solar particle data by interplanetary and coronal transport
[SH-1.3-13] N85-34758
Solar source regions of 3HE-rich particle events
[SH-2.2-4] N85-34799

ELECTROMAGNETIC SPECTRA
A position sensitive phoswich hard X-ray detector system
[OG-9.3-12] N85-34967

ELECTROMAGNETIC WAVE TRANSMISSION
Injection of energetic particles following the gamma-ray flares on June 7, 1980, as observed on Helios 1
[SH-1.3-9] N85-34756

ELECTROMAGNETISM
Diagnostic of electromagnetic conditions in space using cosmic rays
[SH-4.5-19] N85-35036

ELECTRON ACCELERATION
Possibility of potential generation by lower hybrid wave N85-34654

ELECTRON ACCELERATORS
Space Experiments with Particle Accelerators (SEPAC) N85-34165
Vehicle Charging And Potential (VCAP) N85-34173

ELECTRON BEAM WELDING
Laser welding of 6Al-4V titanium alloy
[DE85-012019] N85-34413

ELECTRON BEAMS
Theoretical and Experimental Beam Plasma Physics (TEBPP) N85-34166
RADLAC technolgy review
[DE85-011995] N85-34691
Measurement and interpretation of electron angle at MABE beam stop
[DE85-011918] N85-34698
Technology of magnetically driven accelerators
[DE85-011857] N85-34700
Note on the detection of high energy primary cosmic gamma rays by air shower observation
[OG-9.5-9] N85-34986

ELECTRON BOMBARDMENT
Aluminum work function: Effect of oxidation, mechanical scraping and ion bombardment
[NASA-TM-87079] N85-34265

ELECTRON CAPTURE
Study of photon emission by electron capture during solar nuclei acceleration, 1: Temperature-dependent cross section for charge changing processes
[SH-1.1-8] N85-34735
Study of photon emission by electron capture during solar nuclei acceleration. 2: Delimitation of conditions for charge transfert establishment
[SH-1.1-9] N85-34736
Study of photon emission by electron capture during solar nuclei acceleration. 3: Photon production evaluations
[SH-1.1-10] N85-34737
Electron capture decay of cosmic rays: A model of the inhomogeneous interstellar medium
[OG-7.1-10] N85-34871

ELECTRON CYCLOTRON HEATING
Plug and thermal barrier potential formation in Gamma 10 N85-34648
Effect of ECH and ICH on ambipolar potential in NBT-1M N85-34661
Transports studies of ECH and ICRH-heated bumpy torus plasma in NBT-1M N85-34662
Multiple-frequency electron cyclotron heating of hot electron rings in EBT-1
[DE85-011302] N85-34701
ECH tokamak
[DE85-012074] N85-34707

ELECTRON DENSITY (CONCENTRATION)
Electron density distribution analysis for nitroguanidine
[DE85-009598] N85-34603
Helios 1 energetic particle observations of the solar gamma ray flare events of 7, 21 June 1980 and 3 June 1982
[SH-1.3-8] N85-34755
Akeno 20 km (2) air shower array (Akeno Branch)
[OG-9.4-8] N85-34975

ELECTRON DENSITY PROFILES
Interstellar turbulence, random density variations, and scintillation measurements
[OG-7.2-13] N85-34880

ELECTRON DIFFUSION
Onion-shell model for cosmic ray electrons and radio synchrotron emission in supernova remnants
[OG-8.1-10] N85-34900

ELECTRON DISTRIBUTION
Electron density distribution analysis for nitroguanidine
[DE85-009598] N85-34603

ELECTRON EMISSION
Hollow cathodes in high pressure arc discharges
[NASA-TM-87098] N85-34179
Electron photoejection in carbanions
[DE85-011748] N85-34237
Improved negative ion source
[DE85-006445] N85-34241
Workshop report on Simulation Techniques for Shock Wave Phenomena and Characteristics of Plasmas in Inertial Confinement Fusion
[IPPJ-725] N85-34670

ELECTRON ENERGY
Improved negative ion source
[DE85-006445] N85-34241
Electron impact ionization of multicharged ions at ORNL: 1980-1984
[DE85-013104] N85-34622
Recent experiments in Gamma-10 N85-34651
Bounce resonance heating and radial transport of electrons N85-34655
Transports studies of ECH and ICRH-heated bumpy torus plasma in NBT-1M N85-34662
Stochastic particle acceleration in flaring stars
[OG-8.3-9] N85-34927

ELECTRON GAS
Breakdown of helium nuclei in matter processed near black holes
[OG-8.2-20] N85-34916

ELECTRON IMPACT
Electron impact ionization of multicharged ions at ORNL: 1980-1984
[DE85-013104] N85-34622

ELECTRON MICROSCOPY
Microstructures in rapidly solidified Ni-Mo alloys
[NASA-TM-87100] N85-34266
High resolution electron microscopic characterization of interfaces in ceramics
[DE85-011207] N85-34289
Intermolecular explosives
[DE85-009609] N85-34296

ELECTRON PHOTON CASCADES
Coupled electron-photon transport calculations using the method of discrete ordinates
[DE85-009444] N85-34597

ELECTRON SCATTERING
Electron loss process and cross section of multiply charged ions by neutral atoms N85-34685
X-ray spectra of bursting neutron stars N85-34686
The propagation of solar flare particles in a turbulent coronal loop
[SH-1.1-3] N85-34730

ELECTRON TRANSFER
Electron photoejection in carbanions
[DE85-011747] N85-34230
Electron photoejection in carbanions
[DE85-011748] N85-34237
Study of photon emission by electron capture during solar nuclei acceleration, 1: Temperature-dependent cross section for charge changing processes
[SH-1.1-8] N85-34735

ELECTRON TRANSITIONS
Multiple inner shell vacancies in laser-irradiated Au plasma N85-34687

ELECTRONIC EQUIPMENT
Electronic imaging system and technique
[DE85-005740] N85-34393
ELECTRONS
Atmospheric Emission Photometric Imaging (AEPI)
N85-34170
Measuring method and confirmation of H- (D-) ion current by sheet plasma 1
[IPPJ-730] N85-34638
Electron dynamics and transport in a mirror field
N85-34656
Model of azimuthal non-uniformities induced by RF heating in RFC-XXM N85-34658
The propagation of solar flare particles in a turbulent coronal loop
[SH-1.1-3] N85-34730
Stochastic particle acceleration in solar flares
[SH-1.1-4] N85-34731
Study of non-thermal photon production under different scenarios in solar flares. 2: The Compton inverse and Bremsstrahlung models and fittings
[SH-1.2-3] N85-34739
Temporal evolution of an energetic electron population in an inhomogeneous medium: Application to solar hard X-ray bursts
[SH-1.2-6] N85-34741
Quantitative analysis of flare accelerated electrons through their hard X-ray and microwave radiation
[SH-1.2-7] N85-34742
Two types of electron events in solar flares
[SH-1.2-11] N85-34746
The energy spectra of solar flare electrons
[SH-1.2-14] N85-34749
The Jovian electron spectrum: 1978-1984
[SH-1.5-19] N85-34782
Observations of solar energetic particles at a synchronous orbit
[SH-3.1-1] N85-34806
Coronal propagation of flare associated electrons and protons
[SH-3.1-3] N85-34808
Geometry of the diffusive propagation region in the August 14, 1982 solar electron event
[SH-3.1-5] N85-34809
The dependence of solar modulation on the sign of the cosmic ray particle charge
[SH-4.2-23] N85-34860
Onion-shell model for cosmic ray electrons and radio synchrotron emission in supernova remnants
[OG-8.1-10] N85-34900
Pulsars as cosmic ray particle accelerators: Dynamics of electrons
[OG-8.2-23] N85-34919
Solar modulation and interplanetary gradients of the galactic electrons flux, 1977 - 1984
[SH-4.7-4] N85-35049
Additional flux of particles and albedo-electrons in upper atmosphere
[SH-6.1-6] N85-35080
ELECTROPHORESIS
A computerized system for spot detection and analysis of two-dimensional electrophoresis images N85-34531
ELECTROSTATIC PROBES
Recoverable Plasma Diagnostics Package (RPDP)
N85-34167
Langmuir probe on ISX-B
[DE85-012066] N85-34697
ELECTROSTATIC WAVES
Recoverable Plasma Diagnostics Package (RPDP)
N85-34167
Observation of mode-converted by ion Bernstein wave by an HCN laser scattering
[IPPJ-724] N85-34668
ELEMENTARY PARTICLES
Depth and size effects on cosmogenic nuclide production in meteorites
[SH-7.1-9] N85-35101
ELEVATION ANGLE
A star camera aspect system suitable for use in balloon experiments
[OG-9.3-10] N85-34965
ELLIPTICITY
Neoclassical diffusion including ellipticity in a heliotron-like configuration N85-34667
EMERGENCY LIFE SUSTAINING SYSTEMS
A life-saving device for ships
[NASA-TM-77670] N85-34129
EMISSION
Atmospheric Emission Photometric Imaging (AEPI)
N85-34170
Wide Angle Michelson Doppler Imaging Interferometer (WAMDII) N85-34172
EMISSION SPECTRA
Time-resolved spectroscopic studies of detonating heterogeneous explosives
[DE85-009760] N85-34297
Apparatus and method for the spectrochemical analysis of liquids using the laser spark
[DE85-005749] N85-34387
The read-out system of spatial distribution of thermoluminescence in meteorites
[SH-9.1-16] N85-35131
ENAMELS
Features of behavior of gas bubbles in molten oxide films during enamelling: Communication 2
[BLL-M-35781-(5828.4)] N85-34283
ENCAPSULATING
Investigation of test methods, material properties, and processes for solar cell encapsulants
[NASA-CR-176132] N85-34446
ENERGETIC PARTICLES
Two classes of solar energetic particle events associated with impulsive and long duration soft X-ray flares
[SH-1.2-12] N85-34747
Energetic protons from a disappearing solar filament
[SH-1.3-7] N85-34754
Injection of energetic particles following the gamma-ray flares on June 7, 1980, as observed on Helios 1
[SH-1.3-9] N85-34756
Shock and statistical acceleration of energetic particles in the interplanetary medium
[SH-1.5-1] N85-34771
Energetic ion acceleration at collisionless shocks
[SH-1.5-3] N85-34772
Latitude dependence of co-rotating shock acceleration
[SH-1.5-14] N85-34777
Elemental abundances in corotating events
[SH-1.5-15] N85-34778
Solar and interplanetary particles at 2 to 4 MEV during solar cycles 21, solar cycle variations of event sizes, and compositions
[SH-1.5-16] N85-34779
Energetic particle observations of the solar-gamma ray/neutron flare events of 3 Jun 1982 and 21 June 1980 isotopic and chemical composition
[SH-2.1-3] N85-34784
Precision measurements of solar energetic particle elemental composition
[SH-2.1-4] N85-34785
Solar Coronal and photospheric abundances from solar energetic particle measurements
[SH-2.1-5] N85-34786
Variations in elemental composition of several MEV/nucleon ions observed in interplanetary space
[SH-2.1-7] N85-34788
Diffusion in the chromosphere and the composition of the solar corona and energetic particles
[SH-2.1-9] N85-34790
Anomalous abundances of solar energetic particles and coronal gas: Coulomb effects and First Ionization Potential (FIP) ordering
[SH-2.1-10] N85-34791
The mean ionic charges of N, Ne, MG, SI and S in solar energetic particle events
[SH-2.1-11] N85-34792
Calculations of heavy ion charge state distributions for nonequilibrium conditions
[SH-2.1-12] N85-34793
Isotopic overabundances and the energetic particle model of solar flares
[SH-2.2-1] N85-34796
Solar source regions of 3HE-rich particle events
[SH-2.2-4] N85-34799
On the connection between the 3HE-enrichment and spectral index of solar energetic particles
[SH-2.2-9] N85-34804
A cosmic ray driven instability
[OG-8.1-5] N85-34895
Cosmogenic-nuclide production by primary cosmic-ray protons
[SH-7.1-6] N85-35098
A silicon surface barrier telescope for solar particles identification
[SH-9.1-3] N85-35118
ENERGY ABSORPTION
Design and testing of an energy-absorbing crewseat for the F/FB-111 aircraft, volume 1
[NASA-CR-3916] N85-34133
ENERGY CONSERVATION
Monitoring building energy performance: An informal review and characterization of research in progress
[BNL-51765] N85-34308
Advanced heat pump research and development
[DE85-009540] N85-34372
ENERGY CONVERSION EFFICIENCY
Advanced heat pump research and development
[DE85-009540] N85-34372
ENERGY DISSIPATION
Monitoring building energy performance: An informal review and characterization of research in progress
[BNL-51765] N85-34308
Twenty-two-year cycle of the upper limiting rigidity of Daly waves
[SH-4.5-5] N85-35023
Spallogenic origin of nuclei in meteorites
[SH-7.1-10] N85-35102
ENERGY DISTRIBUTION
Variations in elemental composition of several MEV/nucleon ions observed in interplanetary space
[SH-2.1-7] N85-34788
On the retention of high-energy protons and nuclei with charges Z or equal to 2 in large solar flares after the process of their acceleration
[SH-2.1-8] N85-34789
The response of ionization chambers to relativistic heavy nuclei
[OG-9.1-13] N85-34938
Clusters and cycles in the cosmic ray age distributions of meteorites
[SH-7.1-11] N85-35103
ENERGY LEVELS
Capture in the 1.15-keV iron resonance
[DE85-011913] N85-34612
Duality of two-point functions for confined non-relativistic quark-antiquark systems
[DE85-012334] N85-34618
Exact solutions for sporadic acceleration of cosmic rays
[OG-8.3-7] N85-34925
Relativistic transport theory for cosmic-rays
[OG-8.3-8] N85-34926
The design of an experiment to detect low energy antiprotons
[OG-9.1-1] N85-34928
The response of ionization chambers to relativistic heavy nuclei
[OG-9.1-13] N85-34938
ENERGY POLICY
Monitoring building energy performance: An informal review and characterization of research in progress
[BNL-51765] N85-34308
ENERGY SOURCES
Solar source regions of 3HE-rich particle events
[SH-2.2-4] N85-34799
ENERGY SPECTRA
Study of non-thermal photon production under different scenarios in solar flares. 2: The Compton inverse and Bremsstrahlung models and fittings
[SH-1.2-3] N85-34739
Observations of solar flare photon energy spectra from 20 keV to 7 MeV
[SH-1.2-9] N85-34744
The energy spectra of solar flare electrons
[SH-1.2-14] N85-34749
Source energy spectra from demodulation of solar particle data by interplanetary and coronal transport
[SH-1.3-13] N85-34758
High energy neutron and gamma-radiation generated during the solar flares
[SH-1.4-8] N85-34768
On the angular and energy distribution of solar neutrons generated in P-P reactions
[SH-1.4-9] N85-34769
Acceleration of ions and electrons to near-cosmic ray energies in a perpendicular shock: The January 6, 1978 event
[SH-1.5-4] N85-34773
The energy spectrum of Jovian electrons in interplanetary space
[SH-1.5-18] N85-34781
Observation of the fluxes of nuclei with energies 10-20 MEV per nucleon during the solar flare of April 26, 1984
[SH-2.1-1] N85-34783
Silicon to iron abundances in solar cosmic rays and in the sun
[SH-2.1-6] N85-34787
The 1973-1984 solar modulation of cosmic ray nuclei
[SH-4.1-16] N85-34838
A numerical study of diffusive shock acceleration of cosmic rays in supernova shocks
[OG-8.2-2] N85-34903
The origins of cosmic rays and quantum effects on gravity
[OG-8.2-15] N85-34911
Stochastic particle acceleration in flaring stars
[OG-8.3-9] N85-34927
An experiment to measure the energy spectrum of cosmic ray antiprotons from 100 to 1000 MeV
[OG-9.1-3] N85-34929
The development of a high energy cosmic ray detector for Spacelab-2
[OG-9.1-8] N85-34934
An observatory to study 10 (10) to 10 (17) by EV gamma rays
[OG-9.4-6] N85-34973

Mini and super mini arrays for the study of highest energy cosmic rays
[OG-9.4-9] N85-34976
Detection of 10 (1) GeV cosmic neutrinos with a space station
[OG-9.4-10] N85-34977
The difference in the energy spectra of galactic cosmic rays at the minima of the 19th and 20th solar activity cycles
[SH-4.4-18] N85-35014
Solar tri-diurnal variation of cosmic rays in a wide range of rigidity
[SH-4.5-3] N85-35021
Upper cut-off rigidity for corotation anisotropy during solar activity cycles 20 and 21
[SH-4.5-4] N85-35022
Change of cosmic ray anisotropy with solar activity
[SH-4.5-20] N85-35037
Changes in the energy spectrum of anomalous oxygen and helium during 1977-1985
[SH-4.6-1] N85-35039
Radial and latitudinal gradients of anomalous oxygen during 1977 - 1985
[SH-4.6-4] N85-35042
Observation of pick-up ions in the solar wind: Evidence for the source of the anomalous cosmic ray component?
[SH-4.6-5] N85-35043
On the anomalous component
[SH-4.6-6] N85-35044
Time and energy dependence of the cosmic ray gradient in the outer heliosphere
[SH-4.7-2] N85-35047
Galactic cosmic ray radial gradients and the anomalous He component near maximum solar modulation and to radii beyond 34 AU from the Sun
[SH-4.7-5] N85-35050
Rigidity spectrum of Forbush decrease
[SH-5.1-6] N85-35060
Observations of cosmic-ray modulations in the fall, 1984
[SH-5.1-16] N85-35069
Observation of energy spectrum of electron albedo in low latitude region at Hyderabad, India
[SH-6.1-7] N85-35081
A bi-directional charged particle telescope to observe flux, energy spectrum and angular distribution of relativistic and non-relativistic particles
[SH-9.1-4] N85-35119
A suggested standardized format for cosmic ray ground-level event data
[SH-9.1-15] N85-35130
Measurement of low energy cosmic rays aboard Spacelab-1
[SH-10.1-6] N85-35137

ENERGY STORAGE
Series-counterpulse repetitive-pulse inductive storage circuit
[DE85-006438] N85-34342
Reversing-counterpulse repetitive-pulse inductive storage circuit
[DE85-006409] N85-34344
Evaluation of developmental membranes for the mixed reactant iron-chromium redox system
[NASA-TM-87074] N85-34443
Wind energy battery storage, phase 2
[DE85-009753] N85-34450
Solar heat pump
[DE85-011323] N85-34453
Ion energy storage for post-flare loops
[SH-1.2-10] N85-34745

ENERGY TECHNOLOGY
Monitoring building energy performance: An informal review and characterization of research in progress
[BNL-51765] N85-34308

ENERGY TRANSFER
A dominant role for protons at the onset of solar flares
[SH-1.2-13] N85-34748

ENGINE DESIGN
Energy efficient engine. Fan and quarter-stage component performance report
[NASA-CR-168070] N85-34141
Shroud segments for unshrouded blade turbines
[PNR-90260] N85-34143

ENGINE MONITORING INSTRUMENTS
Design, development and operation of a high simultaneous capacity digital telemetry system --- turbomachine blade flutter
[PNR-90261] N85-34151

ENGINE TESTS
Energy efficient engine. Fan and quarter-stage component performance report
[NASA-CR-168070] N85-34141

ENGINEERING DRAWINGS
A rational approach to cam design N85-34311

ENGINES
High temperature structural insulating material
[DE85-006361] N85-34291

ENRICHMENT
Development and demonstration of a spiral-wound thin-film composite membrane system for the economical production of oxygen-enriched air, phase 4
[DE85-012380] N85-34288

ENTHALPY
Enthalpies of formation of liquid Fe-Ce-Si and Fe-Ce-Al three-component alloys
[BLL-M-36296-(5828.4)] N85-34247
Dynamics of the melting of chromium-manganese alloys in molten steel
[BLL-M-35850-(5828.4)] N85-34252

ENVIRONMENT EFFECTS
Near-threshold fatigue: An overview of the role of microstructure and environment
[DE85-009903] N85-34431
Effects of acid rain on forest nutrient status
[DE85-012486] N85-34463
Agents and effects of ozone trends in the atmosphere
[AERONOMICA-ACTA-A-287-1984] N85-34466
Effect of hypokinesia and +Gz accelerations on transport function of human blood N85-34497

ENVIRONMENTAL CONTROL
Evaluation of source strength and dispersion model predications with data from large nitrogen tetroxide field experiments
[DE85-011855] N85-34465

ENVIRONMENTAL ENGINEERING
Recommendations for the design and equipping of engineering metrology laboratories
[NPL-MOM-22] N85-34145

ENVIRONMENTAL MONITORING
Multi-solute subsurface transfer modeling for energy solid wastes: Highlights FY 1984
[DE85-012788] N85-34591

ENVIRONMENTAL TESTS
Flight service evaluation of composite helicopter components
[NASA-CR-172562] N85-34222

ENVIRONMENTS
Anaerobic microbial transformations in subsurface environments: Project description
[DE85-012789] N85-34486
Circuit approaches to increasing SRAM performance in total dose environments
[DE85-009441] N85-34588

ENZYME ACTIVITY
Lipid hydrolysis in man during antiorthostatic hypokinesia N85-34500
Lipogenesis in rat liver after flight aboard Cosmos-1129 biosatellite N85-34508

EPICYCLOIDS
High powered epicyclic gears: Some recent development N85-34316

EPIDEMIOLOGY
Using the information of cosmic rays to predict influence epidemic
[SH-10.1-2] N85-35134

EPOXY COMPOUNDS
Impact fracture mechanism of polymer plates containing a heavy inner material N85-34215

EPOXY RESINS
Influence of cyclic thermal loading on internal stress in casted epoxy resin N85-34211
Time and temperature dependence of fracture surface in soft epoxy resin N85-34213
Study on fracture behavior of epoxy resin N85-34216
Metal (2) 4,4',4',4'' phthalocyanine tetraamines as curing agents for epoxy resins
[NASA-CASE-ARC-11424-1] N85-34281
Process for improving moisture resistance of epoxy resins by addition of chromium ions
[NASA-CASE-LAR-13226-1] N85-34282

EQUATIONS OF MOTION
Space station rotational equations of motion
[NASA-TP-2511] N85-34148
Optimisation in the computer aided design of mechanisms N85-34321
Conjugated symmetrical coupler curves, produced by 4-bar linkages having the same transmission angles N85-34322
Intermittent motion N85-34323
The dynamics of articulated rigid bodies for purposes of animation N85-34579
The model-independence of cosmic ray source determinations
[OG-7.2-1] N85-34873

EQUATIONS OF STATE
Comparison of experimental data on detonation velocity and Chapman-Jouget pressure vs initial HE density with predictions from Ree's model equation of state
[DE85-007266] N85-34304
Detonation of condensed explosives: Evolution of knowledge in the last 40 years
[ISL-CO-228/84] N85-34307
Shock and release equation of state of calcite
[DE85-013151] N85-34432
Calculations of heavy ion charge state distributions for nonequilibrium conditions
[SH-2.1-12] N85-34793

EQUILIBRIUM FLOW
Elastohydrodynamic lubrication calculations used as a tool to study scuffing
[NASA-TM-87097] N85-34408

ERBIUM COMPOUNDS
Magnitude and range of the RKKy interaction in SmRh4B4
[DE85-012284] N85-34712

EROSION
Electrode erosion in arc discharges at atmospheric pressure
[NASA-TM-87087] N85-34178
Influence of particle erosion on the microstructural changes in metals and alloys
[TI85-901384] N85-34276

ERROR ANALYSIS
Implications of cross section errors for cosmic ray propagation
[OG-7.2-3] N85-34875

ERRORS
Nonsimultaneous coupled laser velocimeter measurement technique: Error prediction for spatially noncoincident measurements
[NASA-TM-86718] N85-34379

ERS-1 (ESA SATELLITE)
AMI calibration study. Volume 1: SAR calibration. Volume 2: Ground Targets. Volume 3: Scatterometer calibration --- Active Microwave Instrument (AMI) ERS-1
[C2248/4/4-VOL-1] N85-34394

ESCAPE SYSTEMS
Design and testing of an energy-absorbing crewseat for the F/FB-111 aircraft, volume 1
[NASA-CR-3916] N85-34133

ESTIMATES
Estimating the change in asymptotic direction due to secular changes in the geomagnetic field
[SH-6.1-13] N85-35086

ESTIMATING
Monte Carlo techniques for analyzing deep penetration problems
[DE85-011426] N85-34598

ETHYLENE
Preparation of ethylenediamine dinitrate
[DE85-006423] N85-34305

ETHYLENEDIAMINE
Ethylenediamine salt of 5-nitrotetrazole and preparation
[DE85-005738] N85-34306

EULER EQUATIONS OF MOTION
Three-dimensional hydrodynamic hot-spot model
[DE85-009587] N85-34301
Compressible two-phase flow instabilities simulated with a hybrid Lagrange-Euler pseudospectral method
[DE85-009904] N85-34361

EULER-LAGRANGE EQUATION
FEMALE: Finite Element Method for Arbitrary Lagrangian and Eulerian elements N85-34671
Two-dimensional simulation of LIB target implosion N85-34678

EUROPE
Space-age Europe, 1957-1980 N85-35148

EUROPEAN SPACE AGENCY
Space-age Europe, 1957-1980 N85-35148

EUROPEAN SPACE PROGRAMS
Thermal protection systems for reentry vehicles
[CNES-NT-113] N85-34157

EVACUATING (VACUUM)
Evacuate and backfill apparatus and method
[DE85-006018] N85-34411

EVALUATION
Effect of interference on the performance of a minimum TCAS 2
[FAA/PM-84/33] N85-34131
Evaluation of low-temperature geothermal potential in Utah and Goshen Valleys and adjacent areas, Utah. Part 2: Water temperature and chemistry
[DE85-009344] N85-34438

EVAPORATION
Evaluation of source strength and dispersion model predications with data from large nitrogen tetroxide field experiments
[DE85-011855] N85-34465

EXCIMER LASERS
Flat-plate solar array project process development area process research of non-CZ silicon material
[NASA-CR-176117] N85-34445

EXCITATION
Electron photoejection in carbanions
[DE85-011748] N85-34237
EXCITONS
Time-resolved and infrared spectroscopy of excitons
[DE85-011879] N85-34235
Pairing correction of particle-hole state densities for two kinds of fermions
[DE85-011549] N85-34620
EXOBIOLOGY
Aerospace Medicine and Biology: A continuing bibliography with indexes (supplement 274)
[NASA-SP-7011(274)] N85-34491
EXPERIMENT DESIGN
Apparatus for unilateral generation of a homogeneous magnetic field
[DE85-006001] N85-34345
EXPERIMENTATION
Separation of gas mixtures by supported complexes
[DE85-011996] N85-34236
Evaluation of low-temperature geothermal potential in Utah and Goshen Valleys and adjacent areas, Utah. Part 2: Water temperature and chemistry
[DE85-009344] N85-34438
Throughfall rate and chemistry studies: Whiteface Mountain
[DE85-012407] N85-34464
The 1984 biotic studies of Yucca Mountain, Nevada test site, Nye County, Nevada
[DE85-011715] N85-34487
The impact of supercomputers on experimentation: A view from a national laboratory
[NASA-TM-86822] N85-34510
Analysis of transient radiation upset in a 16K SRAM
[DE85-009442] N85-34586
EXPERT SYSTEMS
Research issues in generating graphical explanations N85-34539
Generative design in architecture using an expert system N85-34582
Knowledge engineering application in image processing N85-34583
Robot environment expert system
[NASA-CR-3915] N85-34593
Implications of artificial intelligence on the design of future onboard systems
[SFENA-DPS/C/S3/84252A] N85-34596
EXPLOITATION
Marine Sample Exploitation Project: Estimates regarding the sensitivity and technology for the detection of nuclear explosion debris in the marine environment
[DE85-013176] N85-34462
EXPLOSIVES
Intermolecular explosives
[DE85-009609] N85-34296
Pressure-shear loading of PBX-9404
[DE85-009982] N85-34298
Modeling heterogeneous high explosive burn with an explicit hot-spot process
[DE85-009593] N85-34300
Detonation of condensed explosives: Evolution of knowledge in the last 40 years
[ISL-CO-228/84] N85-34307
EXPOSURE
Estimating risks of lead-induced hemoglobin decrements under conditions of uncertainty: Methodology, pilot judgments and illustrative calculations
[DE85-012293] N85-34493
EXTENSOMETERS
Tensile testing apparatus
[NASA-CASE-LAR-13243-1] N85-34375
EXTERNAL TANKS
Results of a study to build a gamma-ray telescope in an external tank
[OG-9.3-3] N85-34958
EXTRAGALACTIC RADIO SOURCES
Propagation of cosmic rays and new evidence for distributed acceleration
[OG-8.3-5] N85-34924
EXTRAPOLATION
Changes in lattice cell parameter of film intermetallic compounds RT2
[BLL-M-35874-(5828.4)] N85-34261
EXTRATERRESTRIAL MATTER
Lead and uranium group abundances in cosmic rays
[OG-7.1-3] N85-34865
EXTRUDING
Characterization of modified 9 Cr Mo steel extruded pipe
[DE85-012056] N85-34430

F

F-111 AIRCRAFT
Design and testing of an energy-absorbing crewseat for the F/FB-111 aircraft. Volume 3: Data from crew module testing
[NASA-CR-3918] N85-34134
FABRICATION
Poly-functional building material from fiberglass (its fabrication and properties) N85-34209
Evacuate and backfill apparatus and method
[DE85-006018] N85-34411
Electrolyte resevoir for carbonate fuel cells
[DE85-005736] N85-34460
FACTOR ANALYSIS
Telecommunication market research processing
[ENST-83E018] N85-34331
FAILURE ANALYSIS
Detonation in tungsten-loaded HMX
[DE85-009606] N85-34299
The use of ultrasound to monitor incipient failure of rolling element bearings N85-34317
Method and apparatus for transfer function simulator for testing complex systems
[NASA-CASE-NPO-15696-1] N85-34333
Short-time creep of ice
[NRC/CNR-TT-2111] N85-34428
FAILURE MODES
Circuit approaches to increasing SRAM performance in total dose environments
[DE85-009441] N85-34588
FAR FIELDS
Reducing grating lobes due to subarray amplitude tapering
[AD-D011723] N85-34339
FATIGUE (MATERIALS)
Near-threshold fatigue: An overview of the role of microstructure and environment
[DE85-009903] N85-34431
FATIGUE LIFE
Corrosion fatigue strength and crack growth in prestrained 0.16% C carbon steel N85-34192
Statistical pooling method of fatigue data for reliability design N85-34198
FATIGUE TESTS
Rotating bending fatigue strength of silicon carbide and alumina-fiber reinforced aluminum N85-34208
FEASIBILITY ANALYSIS
Thermal protection systems for reentry vehicles
[CNES-NT-113] N85-34157
Calculations on the feasibility of ultrasonic inspection of steam generator tubing in pressurized water reactors
[AERE-R-10960] N85-34419
SP-100 Thermionic Technology Program
[DE85-012311] N85-34625
FEDERAL BUDGETS
Department of Housing and Urban Development Independent Agencies Appropriation Bill, 1986
[S-REPT-99-129] N85-34720
National Aeronautics and Space Administration research and development: Program description N85-34721
FEEDBACK CONTROL
Method and apparatus for transfer function simulator for testing complex systems
[NASA-CASE-NPO-15696-1] N85-34333
Feedback regulated induction heater for a flowing fluid
[DE85-006508] N85-34414
FERMI-DIRAC STATISTICS
First-order shock acceleration in solar flares
[SH-1.1-5] N85-34732
FERMIONS
Pairing correction of particle-hole state densities for two kinds of fermions
[DE85-011549] N85-34620
FERROMAGNETIC MATERIALS
Magnetic search system
[PB85-185108] N85-34477
FIBER COMPOSITES
Substitution of asbestos by aramid fibers and fiber blends in industrial textiles and composites with organic binders
[BMFT-FB-T-85-006] N85-34294
FIBER OPTICS
The use of optical fibers in pulsed laser holography
[ISL-CO-226/84] N85-34395
Fiber optics interface for a dye laser oscillator and method
[DE85-005765] N85-34633
Bevalac calibration of the SOFIE range and hodoscope detectors
[OG-9.1-7] N85-34933
Akeno 20 km (2) air shower array (Akeno Branch)
[OG-9.4-8] N85-34975
FIBER ORIENTATION
Strength properties of glassfiber reinforced thermoplastics N85-34212
FIBER REINFORCED COMPOSITES
X-ray measurement of thermal stresses in tungsten fiber-copper composites N85-34205
Evaluation methods of ceramic fiber reinforced metal matrix composite N85-34206
Fracture behavior of aluminum composites reinforced with fiber N85-34207
Rotating bending fatigue strength of silicon carbide and alumina-fiber reinforced aluminum N85-34208
Mechanical properties of SiC fiber-reinforced reaction-bonded Si3N4 composites
[NASA-TM-87085] N85-34223
Viscoelastic behavior of short-fiber composite materials
[DE85-011233] N85-34225
Three-dimensional finite element failure model for predicting failure in fibre reinforced bolted joints
[BR94778] N85-34423
FIELD STRENGTH
Short perturbations of cosmic ray intensity and electric field in atmosphere
[SH-6.1-18] N85-35090
FILE MAINTENANCE (COMPUTERS)
User's operating procedures. Volume 1: Scout project information programs
[NASA-CR-177948] N85-34518
Using LINE as an interactive graphics package. Interfacing line and Topdraw in 43 and 24 VM
[DE85-012007] N85-34585
FILLING
An analysis and algorithm for filling propagation N85-34551
FINANCIAL MANAGEMENT
User's operating procedures. Volume 1: Scout project financial analysis program
[NASA-CR-177949] N85-34519
FINITE DIFFERENCE THEORY
Use of a hyperbolic grid generation scheme in simulating supersonic viscous flow about three-dimensional winged configuration
[NASA-TM-85344] N85-34116
A versatile computer package for mechanism analysis N85-34314
Block-implicit calculations of three-dimensional laminar flow in strongly curved ducts
[DE85-003047] N85-34363
Numerical and analytic descriptions of cosmic-ray transport
[SH-4.1-4] N85-34830
FINITE ELEMENT METHOD
Behaviors of stress waves in a conical bar N85-34182
Experimental study of collapse of thick-walled tube under external pressure and axial force N85-34186
Proceedings of the Mechanisms Conference, volume 1 N85-34309
Proceedings of the Mechanisms Conference, volume 2 N85-34318
An introduction to finite elements N85-34319
Inertial stresses and deformations in mechanisms N85-34320
Thermal stress analysis of a new turbine shroud seal concept
[NASA-TM-87082] N85-34406
Three-dimensional finite element failure model for predicting failure in fibre reinforced bolted joints
[BR94778] N85-34423
Stresses and strains in a plate resulting from two closely-spaced interference-fit fasteners
[ARL-STRUC-TM-409] N85-34429
FEMALE: Finite Element Method for Arbitrary Lagrangian and Eulerian elements N85-34671
FIRE PREVENTION
Scaling parameters of flashover
[NBS-GCR-85-497] N85-34229
Review of zirconium-zircaloy pyrophoricity
[DE85-011169] N85-34270
FIREBREAKS
Scaling parameters of flashover
[NBS-GCR-85-497] N85-34229
FIREPROOFING
Aviation safety (aircraft passenger survivability and cabin safety)
[GPO-39-847] N85-34130
FIRES
Aviation safety (aircraft passenger survivability and cabin safety)
[GPO-39-847] N85-34130
The application of models to the assessment of fire hazard from consumer products
[NBSIR-85-3219] N85-34325
FISSION PRODUCTS
Marine Sample Exploitation Project: Estimates regarding the sensitivity and technology for the detection of nuclear explosion debris in the marine environment
[DE85-013176] N85-34462

Downstream behavior of volatile fission product species
[DE85-012124] N85-34617
Application of evaluated fission-product delayed-neutron precursor data in reactor kinetics calculations
[DE85-012728] N85-34624

FIXED WINGS
Flight testing the fixed-wing configuration of the Rotor Systems Research Aircraft (RSRA)
[NASA-TM-86762] N85-34135

FLAME PROPAGATION
Investigation of the flame speeds of propane/methanol gas mixtures
[DE85-012817] N85-34239

FLAMES
Effects of ambient pressure on the instability of a liquid boiling explosively at the superheat limit
[DE85-009476] N85-34370
Electronic imaging system and technique
[DE85-005740] N85-34393

FLAMMABILITY
Review of zirconium-zircaloy pyrophoricity
[DE85-011169] N85-34270

FLAMMABLE GASES
Investigation of the flame speeds of propane/methanol gas mixtures
[DE85-012817] N85-34239

FLANGES
Fuel cell separator plate with bellows-type sealing flanges
[DE85-005991] N85-34459

FLARE STARS
Stochastic particle acceleration in flaring stars
[OG-8.3-9] N85-34927

FLASHOVER
Scaling parameters of flashover
[NBS-GCR-85-497] N85-34229

FLAT PLATES
Fuel cell separator plate with bellows-type sealing flanges
[DE85-005991] N85-34459

FLEXIBILITY
Strength properties of glassfiber reinforced thermoplastics N85-34212

FLEXIBLE BODIES
Non-rigid body motion N85-34576

FLEXING
Reliability of two sintered silicon nitride materials
[NASA-TM-87092] N85-34284

FLIGHT CHARACTERISTICS
Ground-based and in-flight simulator studies of flight characteristics of a twin-fuselage passenger transport airplane during approach and landing
[NASA-TP-2451] N85-34144

FLIGHT CONTROL
Intelligent redundant actuation system requirements and preliminary system design
[NASA-CR-177366] N85-34136

FLIGHT PATHS
Guidelines for the evaluation of visual approach slope indicators
[ARL-SYS-R-32] N85-34132
Determination of instrument errors by compatibility checking: Results from dynamic flight test data
[ARL-AERO-R-162] N85-34137

FLIGHT SIMULATORS
Langley aeronautics and space test highlights, 1984
[NASA-TM-87585] N85-35151

FLIGHT STRESS (BIOLOGY)
Microorganisms in space flight N85-34490

FLIGHT TESTS
Flight testing the fixed-wing configuration of the Rotor Systems Research Aircraft (RSRA)
[NASA-TM-86762] N85-34135
Determination of instrument errors by compatibility checking: Results from dynamic flight test data
[ARL-AERO-R-162] N85-34137

FLOATING POINT ARITHMETIC
Hardware math for the 6502 microprocessor
[NASA-TM-86517] N85-34511

FLOW CHARACTERISTICS
Compressible two-phase flow instabilities simulated with a hybrid Lagrange-Euler pseudospectral method
[DE85-009904] N85-34361

FLOW CHARTS
A rational approach to cam design N85-34311

FLOW DISTRIBUTION
A three-dimensional viscous flow analysis for the helicopter tip vortex generation problem
[NASA-CR-3906] N85-34114
A comparison of laser Doppler anemometry and probe measurements within the boundary layer of an airfoil at subsonic flow
[ISL-CO-219/84] N85-34127
Prediction of the flow-field interference induced by the long-range laser velocimeter in the Ames 40- by 80-foot and the 80- by 120-foot wind tunnels
[NASA-TM-86763] N85-34146
A three-dimensional turbulent boundary layer undergoing transverse strain and streamwise pressure gradient
[NASA-TM-86768] N85-34358
Block-implicit calculations of three-dimensional laminar flow in strongly curved ducts
[DE85-003047] N85-34363
Mathematical modeling of ultimate heat sink cooling ponds
[TI85-009747] N85-34369

FLOW EQUATIONS
Tabular and graphical solutions of regular and Mach reflections in pseudo-stationary frozen and vibrational-equilibrium flows, part 1
[UTIAS-283-PT-1] N85-34117
Tabular and graphical solutions of regular and Mach reflections in pseudo-stationary frozen and vibrational-equilibrium flows, part 2
[UTIAS-283-PT-2] N85-34118

FLOW MEASUREMENT
Improved flow cytometer measurement of binding assays
[DE85-006407] N85-34390

FLOW STABILITY
Stability of implosion dynamics N85-34680

FLOW THEORY
A curvilinear coordinate method for the solutions of initial value problems using the third-order upwind differencing scheme
[IPPJ-734] N85-34642

FLOW VELOCITY
A comparison of laser Doppler anemometry and probe measurements within the boundary layer of an airfoil at subsonic flow
[ISL-CO-219/84] N85-34127

FLOWMETERS
Acoustic cross-correlation flowmeter for solid-gas flow
[DE85-005988] N85-34391

FLUENCE
Solar flare gamma-ray line spectroscopy
[SH-2.1-14] N85-34795

FLUID DYNAMICS
Simulation of instability of cylindrically converging shock waves N85-34679

FLUID FLOW
The application of models to the assessment of fire hazard from consumer products
[NBSIR-85-3219] N85-34325
Refrigerated dynamic seal to 6.9 MPa (1000 psi)
[NASA-TM-87108] N85-34356
Feedback regulated induction heater for a flowing fluid
[DE85-006508] N85-34414
Studies in thermo-hydro-chemical transport in porous and fractured media
[DE85-012555] N85-34473

FLUTTER ANALYSIS
Design, development and operation of a high simultaneous capacity digital telemetry system — turbomachine blade flutter
[PNR-90261] N85-34151

FLUX (RATE)
A search for solar neutrons on a long duration balloon flight
[SH-1.4-6] N85-34766
Observation of the fluxes of nuclei with energies 10-20 MEV per nucleon during the solar flare of April 26, 1984
[SH-2.1-1] N85-34783
The 3HE in solar non-relativistic electron events
[SH-2.2-5] N85-34800
The dependence of solar modulation on the sign of the cosmic ray particle charge
[SH-4.2-23] N85-34860
Scaling from Jupiter to pulsars and the acceleration of cosmic ray particles by pulsars, 3
[OG-8.2-3] N85-34904
The design of an experiment to detect low energy antiprotons
[OG-9.1-1] N85-34928
Cosmic ray modulation by high-speed solar wind fluxes
[SH-5.1-22] N85-35074
Additional flux of particles and albedo-electrons in upper atmosphere
[SH-6.1-6] N85-35080
Empirical model for the Earth's cosmic ray shadow at 400 KM: Prohibited cosmic ray access
[SH-6.1-14] N85-35087

FLUX DENSITY
Analytic and numerical calculations of the ambipolar electric field in a stellarator N85-34665
Spectral analysis of the Forbush decrease of 13 July 1982
[SH-5.1-7] N85-35061
Transient cosmic ray increase associated with a geomagnetic storm
[SH-5.1-8] N85-35062
Short perturbations of cosmic ray intensity and electric field in atmosphere
[SH-6.1-18] N85-35090
Diurnal variations of cosmic ray geomagnetic cut-off threshold rigidities
[SH-6.1-21] N85-35092
The influence of the Earth's magnetosphere on the high-energy solar protons
[SH-6.1-22] N85-35093
Observation of nuclei with energies 8-30 MeV per nucleon in the Earth's magnetosphere at the altitudes 350 KM
[SH-10.1-5] N85-35136

FOCUSING
Theoretical and computational research on the focused transport of intense charged particle beams
[DE85-012980] N85-34621

FOILS (MATERIALS)
Fast shutter apparatus
[DE85-006501] N85-34343

FOKKER-PLANCK EQUATION
Fokker-Planck calculation of hot electron formation in the thermal barrier region of tandem mirror Gamma-10
[IPPJ-726] N85-34669
Pitch angle distributions of solar energetic particles and the local scattering properties of the interplanetary magnetic field
[SH-3.1-13] N85-34816
Numerical descriptions of cosmic-ray transport
[SH-4.1-3] N85-34829

FOLIAGE
Throughfall rate and chemistry studies: Whiteface Mountain
[DE85-012407] N85-34464

FORBUSH DECREASES
the role of shock waves in modulation of galactic cosmic rays
[SH-4.1-7] N85-34831
The intensity recovery of Forbush-type decreases as a function of heliocentric distance and its relationship to the 11-year variation
[SH-4.1-9] N85-34832
Cumulative effect of Forbush decreases in the heliospheric modulation during the present solar cycle
[SH-4.1-10] N85-34833
Drift and Forbush decreases
[SH-5.1-2] N85-35056
Anomalous short-term increases in the galactic cosmic ray intensity: Are they related to the interplanetary magnetic cloud-like structures?
[SH-5.1-3] N85-35057
The flare origin of Forbush decreases not associated with solar flares on the visible hemisphere of the Sun
[SH-5.1-4] N85-35058
Longitudinal dependence of the interplanetary perturbation produced by energetic type 4 solar flares and of the associated cosmic ray modulation
[SH-5.1-5] N85-35059
Rigidity spectrum of Forbush decrease
[SH-5.1-6] N85-35060
Spectral analysis of the Forbush decrease of 13 July 1982
[SH-5.1-7] N85-35061
The theoretical and experimental investigation of cosmic ray Forbush-effects
[SH-5.1-20] N85-35072
Peculiarities of Galactic Cosmic Ray (GCR) anisotropy variation in connection with the recurrent and sporadic Forbush effects
[SH-5.1-21] N85-35073
Cosmic ray modulation by high-speed solar wind fluxes
[SH-5.1-22] N85-35074
The neutron moderated detector and groundbased cosmic ray modulation studies
[SH-9.1-13] N85-35128
The influences of the galactic cosmic ray on the atmospheric ozone
[SH-10.1-1] N85-35133

FORCE DISTRIBUTION
On high strain rate fragmentation of a closed vessel N85-34187

FORECASTING
Study to encourage and facilitate industrial investment and involvement in space
[NASA-CR-176152] N85-34147

FORESTS
Snow cover in the Siberian forest-steppe
[NASA-TM-77914] N85-34435

Effects of acid rain on forest nutrient status
[DE85-012486] N85-34463

FORMAT
A model for a document maintenance system
N85-34542

FORTRAN
A device-independent 2D plotting package written in FORTRAN
[RSRE-MEMO-3776] N85-34514

FOULING
Ocean thermal energy conversion
[DE85-012291] N85-34456

FOURIER ANALYSIS
Clusters and cycles in the cosmic ray age distributions of meteorites
[SH-7.1-11] N85-35103

FOURIER TRANSFORMATION
Pulse effect in a light ion beam propagation through a Z-discharge plasma channel N85-34684
The conjecture concerning time variations in the solar neutrino flux
[SH-8.1-6] N85-35111
Methods and software for cosmic ray scintillation studies
[SH-9.1-17] N85-35132

FRACTOGRAPHY
A fractographic study on mode 2 and mode 3 SCC crack growth in an Al-Zn-Mg alloy N85-34191
Fractographic analysis for nonpropagating conditions of fatigue crack at high stress ratios in mild steel
N85-34194

FRACTURE MECHANICS
Proceedings of the Twentyseventh Japan Congress on Materials Research
[ISSN-0368-3141] N85-34180
On the methods to determine the stress intensity factors in boundary element method N85-34189
Experimental study on time and temperature dependent behavior of crack growth in viscoelastic strip
N85-34193
Fatigue crack retardation phenomenon caused by single-multiple overloads in 2017-T3 aluminum allow
N85-34196
Fracture behavior of aluminum composites reinforced with fiber N85-34207
Time and temperature dependence of fracture surface in soft epoxy resin N85-34213
Impact fracture mechanism of polymer plates containing a heavy inner material N85-34215
Study on fracture behavior of epoxy resin N85-34216

FRACTURE STRENGTH
On high strain rate fragmentation of a closed vessel
N85-34187
Study on fracture behavior of epoxy resin N85-34216

FRACTURES (MATERIALS)
Special features of the fracture of ball-bearing steel close to non-metallic inclusion eutectics
[BLL-M-35809-(5828.4)] N85-34258

FRACTURING
Comprehensive fracture diagnostics experiement. Part 2: Comparison of seven fracture azimuth measurements
[DE85-011707] N85-34470

FRAGMENTATION
On high strain rate fragmentation of a closed vessel
N85-34187
On the importance of interstellar helium for the propagation of heavy cosmic rays
[OG-7.2-11] N85-34879
Measurements of the fragmentation of (40)Ar, (28)Si and (12)C in CH2C and H targets between 300 and 1500 MeV/nuc at the Bevalac
[OG-7.2-19] N85-34886
Measurements of Fe and Ar fragmentation cross sections
[OG-7.2-20] N85-34887
Cross sections for the production of fragments with Z greater than or equal to 8 by fragmentation of Z greater than or equal to 9 and less than or equal to 26 nuclei
[OG-7.2-22] N85-34889

FREE CONVECTION
Surface temperature distribution along a thin liquid layer due to thermocapillary convection
[NASA-TM-87115] N85-34357

FREE FLOW
Nozzle wall roughness effects on free-stream noise and transition in the pilot low-disturbance tunnel
[NASA-TM-86389] N85-34355

FREEZING
Refrigerated dynamic seal to 6.9 MPa (1000 psi)
[NASA-TM-87108] N85-34356
Lake ice occurence as a possible detector of atmospheric CO2 effects on climate
[DE85-012987] N85-34480

FREQUENCY ANALYZERS
Rotor blade test apparatus
[AD-D011725] N85-34381

FREQUENCY DISTRIBUTION
Burst size distributions in the digitized data of the ion chambers t Mt. Norikura and sea level stations
[SH-9.1-9] N85-35124

FRICTION
Three body abrasive wear in various metal combinations N85-34200
Lubrication and cooling for high speed gears
[NASA-TM-87096] N85-34407

FROZEN EQUILIBRIUM FLOW
Tabular and graphical solutions of regular and Mach reflections in pseudo-stationary frozen and vibrational-equilibrium flows, part 1
[UTIAS-283-PT-1] N85-34117
Tabular and graphical solutions of regular and Mach reflections in pseudo-stationary frozen and vibrational-equilibrium flows, part 2
[UTIAS-283-PT-2] N85-34118

FUEL CAPSULES
Evacuate and backfill apparatus and method
[DE85-006018] N85-34411

FUEL CELL POWER PLANTS
Reactant pressure differential control for fuel cell gases
[NASA-CASE-MSC-20127-2] N85-34403

FUEL CELLS
Reactant pressure differential control for fuel cell gases
[NASA-CASE-MSC-20127-2] N85-34403
Evaluation of developmental membranes for the mixed reactant iron-chromium redox system
[NASA-TM-87074] N85-34443
Fuel cell separator plate with bellows-type sealing flanges
[DE85-005991] N85-34459
Electrolyte resevoir for carbonate fuel cells
[DE85-005736] N85-34460

FUNCTIONAL DESIGN SPECIFICATIONS
Product definition: Technical specification of needs
[SNIAS-851-430-104] N85-34228

FUSELAGES
Ground-based and in-flight simulator studies of flight characteristics of a twin-fuselage passenger transport airplane during approach and landing
[NASA-TP-2451] N85-34144

FUSION (MELTING)
Summary of activities, 1983
[LBL-18500] N85-34605

FUSION REACTORS
Data on the backscattering coefficients on light ions from solids: A revision
[IPPJ-AM-41-REV] N85-34689
Advanced Toroidal Facility (ATF)
[DE85-011567] N85-34699
Perspective on the next ten years in plasma physics
[DE85-011849] N85-34706
ECH tokamak
[DE85-012074] N85-34707

G

GALACTIC COSMIC RAYS
Cosmic ray intensity and the tilt of the neutral sheet
[SH-4.2-8] N85-34846
Differential measurement of cosmic-ray gradient with respect to interplanetary current sheet
[SH-4.2-9] N85-34847
Spatial variation of cosmic rays near the heliospheric current sheet
[SH-4.2-10] N85-34848
Effects of a wavy neutral sheet on cosmic ray anisotropies
[SH-4.2-11] N85-34849
Effects of solar magnetic field on cosmic rays
[SH-4.2-12] N85-34850
Determination of galactic cosmic ray latitudinal gradient using Earth based detectors
[SH-4.2-13] N85-34851
The expected cosmic ray density and stream distributions at the heliolatitudinal asymmetry of solar wind
[SH-4.2-14] N85-34852
Latitudinal gradients of cosmic rays and the polarity reversal of the heliospheric magnetic field: A preliminary evaluation
[SH-4.2-16] N85-34853
The influence of nonstationarity of the solar activity and general solar field on modulation of cosmic rays
[SH-4.2-17] N85-34854
The effect of the neutral sheet structure of the interplanetary magnetic field on cosmic ray distribution in space
[SH-4.2-18] N85-34855
On the influence of the heliomagnetospheric periphery on the galactic cosmic rays
[SH-4.2-19] N85-34856
Spatial distribution of cosmic rays in magnetic cycles of the Sun
[SH-4.2-20] N85-34857
11- and 22-year variations of the cosmic ray density and of the solar wind speed
[SH-4.2-21] N85-34858
Difference between even and odd 11-year cycles in cosmic ray intensity
[SH-4.2-22] N85-34859
The dependence of solar modulation on the sign of the cosmic ray particle charge
[SH-4.2-23] N85-34860
An update on the correlation between the cosmic radiation intensity and the geomagnetic AA index
[SH-4.2-24] N85-34861
Cosmic ray secondary nuclei and the structure of the galaxy
[OG-7.2-4] N85-34875
Why do leaky-box models work so fine?
[OG-7.2-8] N85-34877
On the importance of interstellar helium for the propagation of heavy cosmic rays
[OG-7.2-11] N85-34879
A model for the origin of high-energy cosmic rays
[OG-8.1-8] N85-34896
Astrophysical applications of high angular resolution array-telescopes
[OG-9.5-7] N85-34984
Recording system for the solar neutron monitoring at Mt. Norikura
[SH-9.1-8] N85-35123
Burst size distributions in the digitized data of the ion chambers t Mt. Norikura and sea level stations
[SH-9.1-9] N85-35124
Sensitivity of single and multiple cosmic ray neutrons to the surrounding medium in a lead-free monitor
[SH-9.1-10] N85-35125
Plastic scintillators in coincidence for the study of multi-particle production of sea level cosmic rays in dense medium
[SH-9.1-11] N85-35126
The neutron moderated detector and groundbased cosmic ray modulation studies
[SH-9.1-13] N85-35128
New Matsushiro underground cosmic ray station (220 M.W.E. in depth)
[SH-9.1-14] N85-35129
Methods and software for cosmic ray scintillation studies
[SH-9.1-17] N85-35132
The influences of the galactic cosmic ray on the atmospheric ozone
[SH-10.1-1] N85-35133
Observation of nuclei with energies 8-30 MeV per nucleon in the Earth's magnetosphere at the altitudes 350 KM
[SH-10.1-5] N85-35136
Measurement of low energy cosmic rays aboard Spacelab-1
[SH-10.1-6] N85-35137
Heavy cosmic ray measurement aboard Spacelab-1
[SH-10.1-7] N85-35138

GALACTIC EVOLUTION
Why do leaky-box models work so fine?
[OG-7.2-8] N85-34877
Cosmic-ray exposure records and origins of meteorites
[SH-7.1-7] N85-35099

GALACTIC NUCLEI
The 1973-1984 solar modulation of cosmic ray nuclei
[SH-4.1-16] N85-34838
The effects of newly measured cross sections in hydrogen on the production of secondary nuclei during the propagation of cosmic rays through interstellar H
[OG-7.2-2] N85-34874
The central engine of quasars and AGNs: A relativistic proton radiative shock
[OG-8.1-7] N85-34897
Cerenkov light images of EAS produced by primary gamma
[OG-9.5-3] N85-34979

GALACTIC RADIATION
Effect of seeds of heavy charged particles of galactic cosmic radiation N85-34505
Abundances from solar-flare gamma-ray line spectroscopy
[SH-2.1-13] N85-34794
Type 3 solar radio bursts and 3HE-rich events
[SH-2.2-3] N85-34798
the role of shock waves in modulation of galactic cosmic rays
[SH-4.1-7] N85-34831

Propagation of the phase of solar modulation
[SH-4.1-12] N85-34835
Germanium and lead: Significant differences between meteoritic and photospheric abundances?
[OG-7.1-2] N85-34864
Implications of source abundances of ultraheavy cosmic rays
[OG-7.1-4] N85-34866
Propagation and nucleosynthesis of ultraheavy cosmic rays
[OG-7.1-5] N85-34867
On the importance of interstellar helium for the propagation of heavy cosmic rays
[OG-7.2-11] N85-34879
Cosmic-ray transport in the galactic magnetosphere
[OG-7.2-17] N85-34884
The role of cosmic rays and Alfven waves in the structure of the galactic halo
[OG-7.2-18] N85-34885
Do supernovae of type 1 paly a role in cosmic-ray production?
[OG-8.2-5] N85-34905
Neutron-rich nuclei in cosmic rays and Wolf-Rayet stars
[OG-8.2-6] N85-34906
Bursting star formation and the overabundance of Wolf-Rayet stars
[OG-8.2-8] N85-34907
Interstellar (Na-22) as a possible source of the excess (Ne-22) in the galactic cosmic ray
[OG-8.2-12] N85-34908
The electromagnetic ram action of the plasma focus as a paradigm for the generation of cosmic rays and the gigantic jets in active galaxies
[OG-8.2-14] N85-34910
The origins of cosmic rays and quantum effects on gravity
[OG-8.2-15] N85-34911
Influence of the source distribution on the age distribution of galactic cosmic rays
[OG-8.3-1] N85-34920
Explanation of the secondary to primary ratio within the continuous Fermi accelerator model
[OG-8.3-2] N85-34921
Propagation of cosmic rays and new evidence for distributed acceleration
[OG-8.3-5] N85-34924
High resolution Cherenkov detectors for cosmic ray isotope experiment
[OG-9.1-4] N85-34930
A high resolution gas Cerenkov detector for the superconducting magnet facility
[OG-9.1-6] N85-34932
Mass resolution optimization in a large isotopic composition experiment
[OG-9.1-9] N85-34935
The difference in the energy spectra of galactic cosmic rays at the minima of the 19th and 20th solar activity cycles
[SH-4.4-18] N85-35014
Azimuthal and meridional asymmetries of the solar wind and quasiperiodic variations of intensity of Galactic Cosmic Rays (GCR)
[SH-4.4-20] N85-35016
Long-term modulation of galactic cosmic rays in high-energy region
[SH-4.4-22] N85-35018
The first three harmonics of solar daily variation caused by the diffusive propagation of galactic cosmic rays through the heliosphere
[SH-4.5-1] N85-35019
Diurnal variation of galactic cosmic ray intensity on quiet days
[SH-4.5-11] N85-35029
Solar modulation and interplanetary gradients of the galactic electrons flux, 1977 - 1984
[SH-4.7-4] N85-35049
Galactic cosmic ray radial gradients and the anomalous He component near maximum solar modulation and to radii beyond 34 AU from the Sun
[SH-4.7-5] N85-35050
Voyager 1 and 2 measurements of radial and latitudinal cosmic ray gradients during 1981 - 1984
[SH-4.7-6] N85-35051
The large-scale modulation of cosmic rays in mid-1982: Its dependence on heliospheric longitude and radius
[SH-4.7-9] N85-35053
Nonstationary modulation of galactic cosmic rays in a nonlinear model
[SH-4.7-10] N85-35054
Dimensions of the solar wind cavity and of the region of interplanetary cosmic ray modulation
[SH-4.7-11] N85-35055
Drift and Forbush decreases
[SH-5.1-2] N85-35056
Anomalous short-term increases in the galactic cosmic ray intensity: Are they related to the interplanetary magnetic cloud-like structures?
[SH-5.1-3] N85-35057
Longitudinal dependence of the interplanetary perturbation produced by energetic type 4 solar flares and of the associated cosmic ray modulation
[SH-5.1-5] N85-35059
Galactic cosmic ray currents and magnetic field irregularity degree in high-speed solar wind streams
[SH-5.1-9] N85-35063
Influence of magnetic clouds on cosmic ray intensity variations
[SH-5.1-12] N85-35065
Cosmic rays 10Be biennal data and their relationship to aurorae and sunspots
[SH-7.1-1] N85-35094
Cosmogenic-nuclide production by primary cosmic-ray protons
[SH-7.1-6] N85-35098
Accelerator experiments on the contribution of secondary particles to the production of cosmogenic nuclides in meteorites
[SH-7.1-8] N85-35100
Depth and size effects on cosmogenic nuclide production in meteorites
[SH-7.1-9] N85-35101

GALACTIC STRUCTURE
Cosmic ray secondary nuclei and the structure of the galaxy
[OG-7.2-4] N85-34876

GALLIUM
Specificity of (71)Ga(p,n) (71)Ge at 35 MeV for Gamow-Teller strength
[DE85-011837] N85-34615

GALLIUM PHOSPHIDES
Time-resolved and infrared spectroscopy of excitons
[DE85-011879] N85-34235

GAMMA RAY ASTRONOMY
A coded aperture imaging system optimized for hard X-ray and gamma ray astronomy
[OG-9.2-3] N85-34942
The Gamma-Ray Imaging Spectrometer (GRIS): A new balloon-borne experiment for gamma-ray line astronomy
[OG-9.2-4] N85-34943
Operating characteristics of a prototype high energy gamma-ray telescope
[OG-9.2-7] N85-34946
The gamma-ray telescope Gamma-1
[OG-9.2-10] N85-34949
The Figaro experiment for the observation of time marked sources in the low energy gamma-ray range
[OG-9.2-11] N85-34950
GeV gamma-ray astronomy telescopes with high angular resolution
[OG-9.3-4] N85-34959
The final COS-B database now publicly available
[OG-9.3-8] N85-34963
The University of Durham Mark 3 very high energy gamma ray telescope
[OG-9.4-2] N85-34969
Application of imaging to the atmospheric Cherenkov technique
[OG-9.5-4] N85-34981
A new statistic for the analysis of circular data in gamma-ray astronomy
[OG-9.5-13] N85-34989

GAMMA RAY BURSTS
The 1983 international intercomparison of nuclear accident dosimetry systems at Oak Ridge National Laboratory
[DE85-011303] N85-34382
Helios 1 energetic particle observations of the solar gamma ray flare events of 7, 21 June 1980 and 3 June 1982
[SH-1.3-8] N85-34755
Injection of energetic particles following the gamma-ray flares on June 7, 1980, as observed on Helios 1
[SH-1.3-9] N85-34756
Ultrarelativistic electrons and solar flare gamma-radiation
[SH-1.3-11] N85-34757
North-south asymmetry in activity on the Sun and cosmic ray density gradients
[SH-4.2-7] N85-34845
Burst and Transient Source Experiment (BATSE) for the Gamma Ray Observatory (GRO)
[OG-9.2-14] N85-34953
Gamma-ray burst spectroscopy capabilities of the BATSE/GRO experiment
[OG-9.2-15] N85-34954
Capabilities of the GRO/BATSE for monitoring of discrete sources
[OG-9.2-16] N85-34955
Astrophysical applications of high angular resolution array-telescopes
[OG-9.5-7] N85-34984
Angular resolution of an EAS array for gamma ray astronomy energies 5 x 10 (13) eV
[OG-9.5-8] N85-34985
Note on the detection of high energy primary cosmic gamma rays by air shower observation
[OG-9.5-9] N85-34986
A new approach to evaluate gamma-ray measurements
[OG-9.5-11] N85-34988
A new statistic for the analysis of circular data in gamma-ray astronomy
[OG-9.5-13] N85-34989

GAMMA RAY OBSERVATORY
The Figaro experiment for the observation of time marked sources in the low energy gamma-ray range
[OG-9.2-11] N85-34950
High energy gamma ray balloon instrument
[OG-9.2-12] N85-34951
Burst and Transient Source Experiment (BATSE) for the Gamma Ray Observatory (GRO)
[OG-9.2-14] N85-34953
Gamma-ray burst spectroscopy capabilities of the BATSE/GRO experiment
[OG-9.2-15] N85-34954
An observatory to study 10 (10) to 10 (17) by EV gamma rays
[OG-9.4-6] N85-34972

GAMMA RAY SPECTRA
Capture in the 1.15-keV iron resonance
[DE85-011913] N85-34612
Abundances from solar-flare gamma-ray line spectroscopy
[SH-2.1-13] N85-34794
Solar flare gamma-ray line spectroscopy
[SH-2.1-14] N85-34795
The Gamma-Ray Imaging Spectrometer (GRIS): A new balloon-borne experiment for gamma-ray line astronomy
[OG-9.2-4] N85-34943
Modeling a high energy gamma-ray telescope
[OG-9.2-5] N85-34944
Secondary gamma-ray production in a coded aperture mask
[OG-9.2-6] N85-34945
An experimental assessment of the imaging quality of the low energy gamma-ray telescope ZEBRA
[OG-9.2-8] N85-34947
Advanced techniques for high resolution spectroscopic observations of cosmic gamma-ray sources
[OG-9.2-9] N85-34948
The gamma-ray telescope Gamma-1
[OG-9.2-10] N85-34949
The Figaro experiment for the observation of time marked sources in the low energy gamma-ray range
[OG-9.2-11] N85-34950
Measured performance of the new University of California gamma ray telescope
[OG-9.2-13] N85-34952
Burst and Transient Source Experiment (BATSE) for the Gamma Ray Observatory (GRO)
[OG-9.2-14] N85-34953
Gamma-ray burst spectroscopy capabilities of the BATSE/GRO experiment
[OG-9.2-15] N85-34954
An improved time of flight gamma-ray telescope to monitor diffuse gamma-ray in the energy range 5 MeV - 50 MeV
[OG-9.3-2] N85-34957
Neutron-induced 2.2 MeV background in gamma ray telescopes
[OG-9.3-6] N85-34961

GAMMA RAY SPECTROMETERS
Neutral pion production in solar flares
[SH-1.4-7] N85-34767
A coded aperture imaging system optimized for hard X-ray and gamma ray astronomy
[OG-9.2-3] N85-34942
The Gamma-Ray Imaging Spectrometer (GRIS): A new balloon-borne experiment for gamma-ray line astronomy
[OG-9.2-4] N85-34943
Advanced techniques for high resolution spectroscopic observations of cosmic gamma-ray sources
[OG-9.2-9] N85-34948
Gamma-ray burst spectroscopy capabilities of the BATSE/GRO experiment
[OG-9.2-15] N85-34954
Monte Carlo calibration of the SMM gamma ray spectrometer for high energy gamma rays and neutrons
[SH-9.1-6] N85-35121

GAMMA RAY TELESCOPES
North-south asymmetry in activity on the Sun and cosmic ray density gradients
[SH-4.2-7] N85-34845

A balloon-borne imaging gamma-ray telescope
[OG-9.2-2] N85-34941
Modeling a high energy gamma-ray telescope
[OG-9.2-5] N85-34944
Operating characteristics of a prototype high energy gamma-ray telescope
[OG-9.2-7] N85-34946
An experimental assessment of the imaging quality of the low energy gamma-ray telescope ZEBRA
[OG-9.2-8] N85-34947
The gamma-ray telescope Gamma-1
[OG-9.2-10] N85-34949
High energy gamma ray balloon instrument
[OG-9.2-12] N85-34951
Measured performance of the new University of California gamma ray telescope
[OG-9.2-13] N85-34952
An improved time of flight gamma-ray telescope to monitor diffuse gamma-ray in the energy range 5 MeV - 50 MeV
[OG-9.3-2] N85-34957
Results of a study to build a gamma-ray telescope in an external tank
[OG-9.3-3] N85-34958
GeV gamma-ray astronomy telescopes with high angular resolution
[OG-9.3-4] N85-34959
An approach of reducing the background induced by neutrons
[OG-9.3-5] N85-34960
A Cerenkov imaging telescope for high energy gamma rays
[OG-9.3-13] N85-34968
The University of Durham Mark 3 very high energy gamma ray telescope
[OG-9.4-2] N85-34969
A new ultra high energy gamma ray telescope at Ohya mine
[OG-9.4-3] N85-34970
An observatory to study 10 (10) to 10 (17) by EV gamma rays
[OG-9.4-6] N85-34973
A method to improve observations of gamma-ray sources near 10 (15) eV
[OG-9.5-5] N85-34982
Angular resolution of an EAS array for gamma ray astronomy energies 5 x 10 (13) eV
[OG-9.5-8] N85-34985
The angular resolution of air shower gamma ray telescopes
[OG-9.5-14] N85-34990

GAMMA RAYS
Improved method for the stabilization of NaI-photomultiplier gamma detectors against thermal and other drift
[DE85-011830] N85-34613
Study of non-thermal photon production under different scenarios in solar flares. 1: Scenarios and formulations
[SH-1.2-2] N85-34738
Study of non-thermal photon production under different scenarios in solar flares. 2: The Compton inverse and Bremsstrahlung models and fittings
[SH-1.2-3] N85-34739
The starting conditions for an optically small solar gamma ray flare
[SH-1.3-2] N85-34751
Observations of solar flare gamma-rays and protons
[SH-1.3-6] N85-34753
Time extended production of neutrons during a solar flare
[SH-1.4-1] N85-34762
Further observations of protons resulting from the decay of neutrons ejected by solar flares
[SH-1.4-2] N85-34763
Suggestions for improving the efficiency of ground-based neutron monitors for detecting solar neutrons
[SH-1.4-3] N85-34764
Search for solar neutrons using NM-64 equipment
[SH-1.4-5] N85-34765
Neutral pion production in solar flares
[SH-1.4-7] N85-34767
High energy neutron and gamma-radiation generated during the solar flares
[SH-1.4-8] N85-34768
Possible detection of flare-generated positrons by Helios 1 on 3 Jun 1982
[SH-1.4-10] N85-34770
Energetic particle observations of the solar-gamma ray/neutron flare events of 3 Jun 1982 and 21 June 1980 isotopic and chemical composition
[SH-2.1-3] N85-34784
Geometry of the diffusive propagation region in the August 14, 1982 solar electron event
[SH-3.1-5] N85-34809
A very important process of nucleosynthesis in stars
[OG-7.1-11] N85-34872
Bursting star formation and the overabundance of Wolf-Rayet stars
[OG-8.2-8] N85-34907
Giant molecular clouds as regions of particle acceleration N85-34913
A balloon-borne imaging gamma-ray telescope
[OG-9.2-2] N85-34941
Secondary gamma-ray production in a coded aperture mask
[OG-9.2-6] N85-34945
The final COS-B database now publicly available
[OG-9.3-8] N85-34963
The Buckland Park air shower array
[OG-9.4-4] N85-34971
An EAS experiment at mountain altitude for the detection of gamma-ray sources
[OG-9.4-5] N85-34972
A new array for the study of ultra high energy gamma-ray sources
[OG-9.4-7] N85-34974
Cerenkov light images of EAS produced by primary gamma
[OG-9.5-3] N85-34979
Shower disc sampling and the angular resolution of gamma-ray shower detectors
[OG-9.5-2] N85-34980
Photometric and spectroscopic gamma-ray observations of solar transient phenomena using long duration balloons
[SH-9.1-5] N85-35120

GAS ANALYSIS
Method for controlling the viscosity of siloxane oils
[DE85-011586] N85-34221
Oxygen analyzer
[DE85-006002] N85-34392

GAS COOLED REACTORS
Technical assessment of thermal-hydraulics for high heat flux fusion components
[DE85-013178] N85-34359
Liquid uranium alloy-helium fission reactor
[DE85-006511] N85-34607

GAS DYNAMICS
Separation of gas mixtures by supported complexes
[DE85-011996] N85-34236
Numerical model of a pulse combustor
[DE85-011717] N85-34240

GAS EXPANSION
Real time analysis of PETN detonation products
[DE85-009581] N85-34303

GAS FLOW
Unsteady transonic heat transfer in a transient facility
[NASA-CR-176145] N85-34354

GAS GUNS
Shock and release equation of state of calcite
[DE85-013151] N85-34432

GAS IONIZATION
Breakdown of intrinsic ambipolarity for the radial diffusion due to a rotating RF field N85-34660

GAS MIXTURES
Separation of gas mixtures by supported complexes
[DE85-011996] N85-34236
Investigation of the flame speeds of propane/methanol gas mixtures
[DE85-012817] N85-34239

GAS PRESSURE
Determination of individual tolerance in hyperbaric oxygen N85-34507

GAS TUNGSTEN ARC WELDING
Laser welding of 6Al-4V titanium alloy
[DE85-012019] N85-34413

GAS TURBINE ENGINES
Shroud segments for unshrouded blade turbines
[PNR-90260] N85-34143
The development and evaluation of the creep and corrosion resistant alloy IN6201
[PNR-90253] N85-34278
Directionally solidified gas turbine alloys
[PNR-90264] N85-34279
Oxidizing seal for a turbine tip gas path
[NASA-CASE-LEW-14053-1] N85-34402
Cost effective single crystals: The Rolls Royce approach --- gas turbine components
[PNR-90262] N85-34717

GAS TURBINES
High powered epicyclic gears: Some recent development N85-34316

GAS-METAL INTERACTIONS
Hydrogen embrittlement testing
[DE85-007352] N85-34273

GASES
Description of a test site for large-scale heavy gas dispersion and combustion experiments
[DE85-004987] N85-34231
Features of behavior of gas bubbles in molten oxide films during enamelling: Communication 2
[BLL-M-35781-(5828.4)] N85-34283
The cosmic-ray shock structure problem for relativistic shocks
[OG-8.1-1] N85-34891

GASTROINTESTINAL SYSTEM
Lipid hydrolysis in man during antiorthostatic hypokinesia N85-34500

GAUGE INVARIANCE
Gauge invariance and fractional quantized Hall effect
[DE85-007832] N85-34716

GAUSS EQUATION
Evaluation of source strength and dispersion model predications with data from large nitrogen tetroxide field experiments
[DE85-011855] N85-34465

GEARS
Some problems in high speed gears and gearing N85-34312
High powered epicyclic gears: Some recent development N85-34316
The design and analysis of single flank transmission error testor for loaded gears
[NASA-CR-176163] N85-34404
Generated spiral bevel gears: Optimal machine-tool settings and tooth contact analysis
[NASA-TM-87075] N85-34405
Lubrication and cooling for high speed gears
[NASA-TM-87096] N85-34407
Elastohydrodynamic lubrication calculations used as a tool to study scuffing
[NASA-TM-87097] N85-34408

GENERATORS
Control system for fluid heated steam generator
[DE85-005734] N85-34417
Development of the osmium-191 yields iridium-191m radionuclide generator
[DE85-011185] N85-34611
Current status of the Os-191 yields Ir-191m generator
[DE85-008306] N85-34614

GEOCHEMISTRY
Thermally induced chemical migration: A natural analog approach
[DE85-012308] N85-34474

GEOCHRONOLOGY
Geology and petroleum resources of basins in western China
[DE85-013038] N85-34469

GEOGRAPHY
Applied computer graphics in a geographic information system: Problems and successes N85-34563

GEOLOGICAL FAULTS
Comprehensive fracture diagnostics experiement. Part 2: Comparison of seven fracture azimuth measurements
[DE85-011707] N85-34470
Studies in thermo-hydro-chemical transport in porous and fractured media
[DE85-012555] N85-34473
Geophysical-geological studies of possible extensions of the New Madrid fault zone
[TI85-901341] N85-34475

GEOLOGICAL SURVEYS
The United States Geological Survey in Alaska: Accomplishments during 1983
[USGS-CIRC-945] N85-34468
The transient electromagnetic depth sounding technique applied to hydrocarbons and geothermal exploration
[MITT-42] N85-34476

GEOLOGY
Geology and petroleum resources of basins in western China
[DE85-013038] N85-34469

GEOMAGNETISM
An update on the correlation between the cosmic radiation intensity and the geomagnetic AA index
[SH-4.2-24] N85-34861
Dynamics of two-year cosmic ray variations inferred from the data of spacecraft and stratospheric measurements and from the neutron monitor data in 1959-1981
[SH-4.4-21] N85-35017
Formulation of cosmic-ray solar daily variation and its seasonal variation, produced from generalized stationary anisotropy of solar origin
[SH-4.5-2] N85-35020
Diurnal variation of galactic cosmic ray intensity on quiet days
[SH-4.5-11] N85-35029
A relation between the short time variations of cosmic rays and geomagnetic field change
[SH-5.1-14] N85-35067
Anomalous low level of cosmic ray intensity decreases observed during 1980
[SH-5.1-15] N85-35068

Frequency spectra of short-period variations of cosmic ray
[SH-5.1-17] N85-35070
Re-evaluation of cosmic ray cutoff terminology
[SH-6.1-11] N85-35084
The use of the McIlwain L-parameter to estimate cosmic ray vertical cutoff rigidities for different epochs of the geomagnetic field
[SH-6.1-12] N85-35085
Estimating the change in asymptotic direction due to secular changes in the geomagnetic field
[SH-6.1-13] N85-35086
Empirical model for the Earth's cosmic ray shadow at 400 KM: Prohibited cosmic ray access
[SH-6.1-14] N85-35087
Diurnal variations of cosmic ray geomagnetic cut-off threshold rigidities
[SH-6.1-21] N85-35092
The influence of the Earth's magnetosphere on the high-energy solar protons
[SH-6.1-22] N85-35093
Correlation between solar neutrino flux and other solar phenomena N85-35109
Heavy cosmic ray measurement aboard Spacelab-1
[SH-10.1-7] N85-35138

GEOMETRY
Thermal transport measurements of UV laser irradiated spherical targets
[DE85-011038] N85-34365
System maintenance manual for master modeling of aerodynamic surfaces by three-dimensional explicit representation
[NASA-CR-178224] N85-34517
A simple but systematic CSG system N85-34569
Low cost geometric modelling system for CAM N85-34578

GEOMORPHOLOGY
The United States Geological Survey in Alaska: Accomplishments during 1983
[USGS-CIRC-945] N85-34468

GEOPHYSICS
Geophysical-geological studies of possible extensions of the New Madrid fault zone
[TI85-901341] N85-34475

GEOTHERMAL ENERGY CONVERSION
Solar energy education. Renewable energy: A background text
[DE85-010365] N85-34452

GEOTHERMAL RESOURCES
Geothermal resources of the Laramie, Hanna and Shirley Basins, Wyoming
[DE85-005005] N85-34436
Depletion modeling of liquid dominated geothermal reservoirs
[DE85-009923] N85-34437
Evaluation of low-temperature geothermal potential in Utah and Goshen Valleys and adjacent areas, Utah. Part 2: Water temperature and chemistry
[DE85-009344] N85-34438
Modeling of geothermal systems
[DE85-012553] N85-34439
Workshop on Recent Research in the Valles Caldera
[DE85-010569] N85-34472

GEOTHERMAL TECHNOLOGY
The transient electromagnetic depth sounding technique applied to hydrocarbons and geothermal exploration
[MITT-42] N85-34476

GERMANIUM
Specificity of (71)Ga(p,n) (71)Ge at 35 MeV for Gamow-Teller strength
[DE85-011837] N85-34615
Germanium and lead: Significant differences between meteoritic and photospheric abundances?
[OG-7.1-2] N85-34864

GERMANIUM ISOTOPES
Results of ultra-low level 71ge counting for application in the Gallex-solar neutrino experiment at the Gran Sasso Underground Physics Laboratory
[SH-8.1-2] N85-35108

GIACOBINI-ZINNER COMET
The International Cometary Explorer (ICE)wallsheet teacher's guide
[NASA-TM-87498] N85-34727

GLASS
Iron and manganese in oxide minerals and in glasses: Preliminary consideration of Eh buffering potential at Yucca Mountain, Nevada
[DE85-011892] N85-34271
The effect of liquid-liquid phase separation of glass on the properties and crystallization behavior
[NASA-TM-77890] N85-34285

GLASS FIBER REINFORCED PLASTICS
Poly-functional building material from fiberglass (its fabrication and properties) N85-34209
Stress distribution of fiberglass reinforced plastic beam with a delamination under three-point bending N85-34210
Strength properties of glassfiber reinforced thermoplastics N85-34212
Effect of strain rate on the initial failure of notched GRP laminates N85-34214
Design of transversely stiffenend FRP panels under compressive load --- fiber reinforced plastic (FRP) ships
[AMTE(S)-R-84104] N85-34424

GOLD
Multiple inner shell vacancies in laser-irradiated Au plasma N85-34687

GRADIENTS
Differential measurement of cosmic-ray gradient with respect to interplanetary current sheet
[SH-4.2-9] N85-34847
Determination of galactic cosmic ray latitudinal gradient using Earth based detectors
[SH-4.2-13] N85-34851
The expected cosmic ray density and stream distributions at the heliolatitudinal asymmetry of solar wind
[SH-4.2-14] N85-34852
Latitudinal gradients of cosmic rays and the polarity reversal of the heliospheric magnetic field: A preliminary evaluation
[SH-4.2-16] N85-34853
The dependence of solar modulation on the sign of the cosmic ray particle charge
[SH-4.2-23] N85-34860
Voyager 1 and 2 measurements of radial and latitudinal cosmic ray gradients during 1981 - 1984
[SH-4.7-6] N85-35051

GRAIN BOUNDARIES
High resolution electron microscopic characterization of interfaces in ceramics
[DE85-011207] N85-34289
Grain boundary and surface diffusion in oxide systems
[DE85-007291] N85-34715

GRAIN SIZE
Influence of technology of atomization of naturally alloyed iron on grain-size characteristics of powder material
[BLL-M-35810-(5828.4)] N85-34257

GRAPH THEORY
Graph-theoretical exorcism
[DE85-011916] N85-34512

GRAPHIC ARTS
Image synthesis: Optical identity or pictorial communication? N85-34565

GRAPHITE-EPOXY COMPOSITES
Flight service evaluation of composite helicopter components
[NASA-CR-172562] N85-34222

GRAVITATIONAL EFFECTS
Tolerance to +Gz and +Gx accelerations of individuals in older age groups in good health and with early signs of arteriosclerosis N85-34496

GROUND TESTS
A suggested standardized format for cosmic ray ground-level event data
[SH-9.1-15] N85-35130

GROUND WATER
Anaerobic microbial transformations in subsurface environments: Project description
[DE85-012789] N85-34486

GROUP DYNAMICS
USSR report: Space Biology and Aerospace Medicine, vol. 19, no. 3, May - June 1985
[JPRS-USB-85-005] N85-34494

GROWTH
Screening and characterizing oleaginous microalgal species from the southeastern United States
[DE85-008787] N85-34488

GYROMAGNETISM
Nonlocal and nonadiabatic expression for the ponderomotive force near cyclotron resonance
[IPPJ-736] N85-34636

H

HADRONS
Observations of cosmic-ray modulations in the fall, 1984
[SH-5.1-16] N85-35069

HALL EFFECT
Gauge invariance and fractional quantized Hall effect
[DE85-007832] N85-34716

HALOGENATION
Process for functionalizing alkanes
[DE85-006420] N85-34219

HALOS
The extent of the local hi halo
[NASA-CR-176115] N85-34724

HARMONIC ANALYSIS
Characteristics of cosmic ray pole-equator anisotropy derived from spherical harmonic analysis of neutron monitor data
[SH-4.3-12] N85-34996
Magnetic fluctuation and cosmic ray diurnal variations
[SH-4.5-21] N85-35038
On the solar cycle variation in the barometer coefficients of high latitude neutron monitors
[SH-6.1-2] N85-35077
The conjecture concerning time variations in the solar neutrino flux
[SH-8.1-6] N85-35111

HARMONIC FUNCTIONS
The first three harmonics of solar daily variation caused by the diffusive propagation of galactic cosmic rays through the heliosphere
[SH-4.5-1] N85-35019

HARMONICS
Sidereal variations deep underground in Tasmania
[SH-4.4-4] N85-35002
The effect of the interplanetary magnetic field on sidereal variations observed at medium depth underground detectors
[SH-4.4-5] N85-35003
Cosmic ray intensity variations observed at Matsushiro (220 M.W.E. in depth)
[SH-4.4-9] N85-35007

HARTREE APPROXIMATION
Multiple inner shell vacancies in laser-irradiated Au plasma N85-34687

HAZARDS
Description of a test site for large-scale heavy gas dispersion and combustion experiments
[DE85-004987] N85-34231
The application of models to the assessment of fire hazard from consumer products
[NBSIR-85-3219] N85-34325
Estimating risks of lead-induced hemoglobin decrements under conditions of uncertainty: Methodology, pilot judgments and illustrative calculations
[DE85-012293] N85-34493

HCN LASERS
Observation of mode-converted by ion Bernstein wave by an HCN laser scattering
[IPPJ-724] N85-34668

HEART
Development of the osmium-191 yields iridium-191m radionuclide generator
[DE85-011185] N85-34611
Current status of the Os-191 yields Ir-191m generator
[DE85-008306] N85-34614

HEART FUNCTION
Oxygenation and regional circulation in gingival mucosa during exposure to lower body negative pressure N85-34498

HEART RATE
Effect of water immersion of parameters of central hemodynamics in individuals over 45 years old N85-34499
Effect of acute hypoxia on coronary and systemic hemodynamics N85-34503

HEAT EXCHANGERS
Ocean thermal energy conversion
[DE85-012291] N85-34456

HEAT FLUX
Technical assessment of thermal-hydraulics for high heat flux fusion components
[DE85-013178] N85-34359
Sequential regularization solution of the inverse heat conduction problem
[DE85-010657] N85-34362
Forced convective, nonequilibrium, post-CHF heat transfer experiment data and correlation comparison report
[TI85-009331] N85-34371
On the heat flux derived by the moment method in Lorentzian plasma between hot and cold walls N85-34682
Integral representation for nonlinear heat transport N85-34683

HEAT GENERATION
Generated spiral bevel gears: Optimal machine-tool settings and tooth contact analysis
[NASA-TM-87075] N85-34405

HEAT PUMPS
Advanced heat pump research and development
[DE85-009540] N85-34372
Solar heat pump
[DE85-011323] N85-34453

HEAT RESISTANT ALLOYS
Nitriding of super alloys for enhancing physical properties
[DE85-005762] N85-34275

The development and evaluation of the creep and corrosion resistant alloy IN6201
[PNR-90253] N85-34278
Directionally solidified gas turbine alloys
[PNR-90264] N85-34279
HEAT SHIELDING
Experimental aerodynamic heating to simulated space shuttle tiles in laminar and turbulent boundary layers with variable flow angles at a nominal Mach number of 7
[NASA-TP-2307] N85-34351
HEAT SINKS
Mathematical modeling of ultimate heat sink cooling ponds
[TI85-009747] N85-34369
HEAT SOURCES
General-purpose heat source development: Safety test program. Postimpact evaluation, design iteration test
[LA-10034-SR] N85-34606
HEAT STORAGE
Solar energy education: Renewable energy activities for chemistry and physics
[DE85-010371] N85-34455
HEAT TRANSFER
Component-specific modeling
[NASA-CR-174765] N85-34140
Numerical model of a pulse combustor
[DE85-011717] N85-34240
The application of models to the assessment of fire hazard from consumer products
[NBSIR-85-3219] N85-34325
Technical assessment of thermal-hydraulics for high heat flux fusion components
[DE85-013178] N85-34359
Preliminary SPR thermal model description and results for WH-11 and BM-4
[DE85-013171] N85-34360
Thermal transport measurements of UV laser irradiated spherical targets
[DE85-011038] N85-34365
Vapor phase heat transport concepts
[DE85-009550] N85-34366
Forced convective, nonequilibrium, post-CHF heat transfer experiment data and correlation comparison report
[TI85-009331] N85-34371
Determination of properties of zeolite/refrigerant combinations for solar refrigeration systems
[DE85-012009] N85-34448
Ocean thermal energy conversion
[DE85-012291] N85-34456
Studies in thermo-hydro-chemical transport in porous and fractured media
[DE85-012555] N85-34473
HEAT TRANSMISSION
Detailed validation of a liquid and heat flow code against field performance
[DE85-009901] N85-34368
HEAT TREATMENT
The study of the effect of residual microimpurities on the fatigue strength of 55S2 steel
[BLL-M-36317-(5828.4)] N85-34246
The effect of pre-heating on the structure and properties of chromium-molybdenum steels
[BLL-M-35897-(5828.4)] N85-34255
Properties of tungsten-free steel for cutting tools
[BLL-M-35808-(5828.4)] N85-34259
Stress corrosion cracking susceptibility of types 316NG and 316 stainless steel in an impurity environment
[TI85-006884] N85-34277
The read-out system of spatial distribution of thermoluminescence in meteorites
[SH-9.1-16] N85-35131
HEATERS
Feedback regulated induction heater for a flowing fluid
[DE85-006508] N85-34414
HEAVY IONS
Physics Division annual review, 1 April 1983 - 31 March 1984
[ANL-84-24] N85-34602
Summary of activities, 1983
[LBL-18500] N85-34605
Low-energy sputterings with the Monte Carlo Program ACAT
[IPPJ-AM-40] N85-34690
Calculations of heavy ion charge state distributions for nonequilibrium conditions
[SH-2.1-12] N85-34793
The heavy ion composition in 3HE-rich solar flares
[SH-2.2-7] N85-34802
The plasma mechanism for preferential acceleration of heavy ions
[SH-2.2-10] N85-34805
A high resolution gas Cerenkov detector for the superconducting magnet facility
[OG-9.1-8] N85-34932
The heavy ions in space experiment
[OG-9.1-10] N85-34936
The response of ionization chambers to relativistic heavy nuclei
[OG-9.1-13] N85-34938
Detector calibration of the Indian cosmic ray experiment (IONS) in Space-Shuttle Spacelab-13
[SH-9.1-2] N85-35117
HEAVY NUCLEI
The heavy ion composition in 3HE-rich solar flares
[SH-2.2-7] N85-34802
Variations in the propagation of UH-nuclei
[OG-7.1-1] N85-34863
Propagation and nucleosynthesis of ultraheavy cosmic rays
[OG-7.1-5] N85-34867
Sources of the ultraheavy cosmic rays
[OG-7.1-7] N85-34868
Interactions of heavy nuclei, Kr, Xe and Ho, in light targets
[OG-7.2-21] N85-34888
The response of ionization chambers to relativistic heavy nuclei
[OG-9.1-13] N85-34938
The response of ionization chambers to relativistic heavy nuclei
[OG-9.1-13] N85-34939
Measurement of low energy cosmic rays aboard Spacelab-1
[SH-10.1-6] N85-35137
Heavy cosmic ray measurement aboard Spacelab-1
[SH-10.1-7] N85-35138
HELICAL FLOW
Behavior of helically-trapped fast ion orbits in heliotron E N85-34666
Neoclassical diffusion including ellipticity in a heliotron-like configuration N85-34667
HELICOPTERS
A three-dimensional viscous flow analysis for the helicopter tip vortex generation problem
[NASA-CR-3906] N85-34114
An evaluation of three helicopter rotor sections
[NASA-TM-86719] N85-34115
Flight service evaluation of composite helicopter components
[NASA-CR-172562] N85-34222
Some problems in high speed gears and gearing N85-34312
HELIOSPHERE
Ninteenth International Cosmic Ray Conference. SH sessions, volume 4
[NASA-CP-2376-VOL-4] N85-34729
Latitude dependence of co-rotating shock acceleration
[SH-1.5-14] N85-34777
The intensity recovery of Forbush-type decreases as a function of heliocentric distance and its relationship to the 11-year variation
[SH-4.1-9] N85-34832
Cumulative effect of Forbush decreases in the heliospheric modulation during the present solar cycle
[SH-4.1-10] N85-34833
Latitude variation of recurrent fluxes in the outer solar system
[SH-4.1-13] N85-34836
Longitudinal distribution of cosmic rays in the heliosphere
[SH-4.1-14] N85-34837
Evidence for regions of negligible cosmic-ray modulation in the inner heliosphere (10 AU)
[SH-4.1-21] N85-34840
Drift and observations in cosmic-ray modulation, 1
[SH-4.2-4] N85-34842
Cosmic ray intensity and the tilt of the neutral sheet
[SH-4.2-8] N85-34846
Spatial variation of cosmic rays near the heliospheric current sheet
[SH-4.2-10] N85-34848
Effects of a wavy neutral sheet on cosmic ray anisotropies
[SH-4.2-11] N85-34849
Determination of galactic cosmic ray latitudinal gradient using Earth based detectors
[SH-4.2-13] N85-34851
Latitudinal gradients of cosmic rays and the polarity reversal of the heliospheric magnetic field: A preliminary evaluation
[SH-4.2-16] N85-34853
The effect of the neutral sheet structure of the interplanetary magnetic field on cosmic ray distribution in space
[SH-4.2-18] N85-34855
On the influence of the heliomagnetospheric periphery on the galactic cosmic rays
[SH-4.2-19] N85-34856
The dependence of solar modulation on the sign of the cosmic ray particle charge
[SH-4.2-23] N85-34860
An update on the correlation between the cosmic radiation intensity and the geomagnetic AA index
[SH-4.2-24] N85-34861
Ninteenth International Cosmic Ray Conference. SH sessions, volume 5
[NASA-CP-2376-VOL-5] N85-34991
Gradients and anisotropies of high energy cosmic rays in the outer heliosphere
[SH-4.3-7] N85-34992
IMF-sense-dependent cosmic ray anisotropy produced from diffusion-convection in heliosphere
[SH-4.3-9] N85-34994
The effect of the interplanetary magnetic field on sidereal variations observed at medium depth underground detectors
[SH-4.4-5] N85-35003
The first three harmonics of solar daily variation caused by the diffusive propagation of galactic cosmic rays through the heliosphere
[SH-4.5-1] N85-35019
Time and energy dependence of the cosmic ray gradient in the outer heliosphere
[SH-4.7-2] N85-35047
The large scale dynamics of the outer heliosphere and the long-term modulation of galactic cosmic rays
[SH-4.7-3] N85-35048
Voyager 1 and 2 measurements of radial and latitudinal cosmic ray gradients during 1981 - 1984
[SH-4.7-6] N85-35051
The recovery of the cosmic ray flux from maximum solar modulation at IMP-8 (1 AU) and at Pioneer (R 30 AU)
[SH-4.7-7] N85-35052
The large-scale modulation of cosmic rays in mid-1982: Its dependence on heliospheric longitude and radius
[SH-4.7-9] N85-35053
Cosmic rays 10Be biennal data and their relationship to aurorae and sunspots
[SH-7.1-1] N85-35094
HELITRONS
Behavior of helically-trapped fast ion orbits in heliotron E N85-34666
Neoclassical diffusion including ellipticity in a heliotron-like configuration N85-34667
HELIUM
Combined cold compressor/ejector helium refrigerator
[DE85-006408] N85-34326
Technical assessment of thermal-hydraulics for high heat flux fusion components
[DE85-013178] N85-34359
Determination of individual tolerance in hyperbaric oxygen N85-34507
Observations on (3)He neutron spectrometry
[DE85-010731] N85-34606
On the importance of interstellar helium for the propagation of heavy cosmic rays
[OG-7.2-11] N85-34879
Changes in the energy spectrum of anomalous oxygen and helium during 1977-1985
[SH-4.8-1] N85-35039
HELIUM IONS
Data on the backscattering coefficients on light ions from solids: A revision
[IPPJ-AM-41-REV] N85-34689
Injection of energetic particles following the gamma-ray flares on June 7, 1980, as observed on Helios 1
[SH-1.3-9] N85-34756
Spectra of solar proton ground level events using neutron monitor and neutron moderated detector recordings
[SH-1.3-14] N85-34759
Observation of pick-up ions in the solar wind: Evidence for the source of the anomalous cosmic ray component?
[SH-4.6-5] N85-35043
HELIUM ISOTOPES
Type 3 solar radio bursts and 3HE-rich events
[SH-2.2-3] N85-34798
Solar source regions of 3HE-rich particle events
[SH-2.2-4] N85-34799
The 3HE in solar non-relativistic electron events
[SH-2.2-5] N85-34800
The heavy ion composition in 3HE-rich solar flares
[SH-2.2-7] N85-34802
The mean ionic charge of silicon in 3HE-rich solar flares
[SH-2.2-8] N85-34803
On the connection between the 3HE-enrichment and spectral index of solar energetic particles
[SH-2.2-9] N85-34804
Breakdown of helium nuclei in matter processed near black holes
[OG-8.2-20] N85-34916

The 4He1H ratios in the chemical compositions of solar flare particles and the primordial solar nebula [SH-7.1-12] N85-35104

HELIUM PLASMA
The dependence of solar modulation on the sign of the cosmic ray particle charge [SH-4.2-23] N85-34860

HEMODYNAMIC RESPONSES
Effect of hypokinesia and +Gz accelerations on transport function of human blood N85-34497
Oxygenation and regional circulation in gingival mucosa during exposure to lower body negative pressure N85-34498
Effect of water immersion of parameters of central hemodynamics in individuals over 45 years old N85-34499
Effect of acute hypoxia on coronary and systemic hemodynamics N85-34503

HEMODYNAMICS
USSR report: Space Biology and Aerospace Medicine, vol. 19, no. 3, May - June 1985 [JPRS-USB-85-005] N85-34494
Effect of dibazol on parameters of nonspecific resistance of subjects in pressurized cabins N85-34504

HEMOGLOBIN
Estimating risks of lead-induced hemoglobin decrements under conditions of uncertainty: Methodology, pilot judgments and illustrative calculations [DE85-012293] N85-34493

HERBIG-HARO OBJECTS
Low-excitation Herbig-Haro objects and interstellar extinction [NASA-CR-176142] N85-34726

HERMETIC SEALS
X-ray residual stress analysis on the coarse grain of copper and its application to the brazed copper N85-34202
Hermetic chip carrier compliant soldering pads [AD-D011722] N85-34410

HERTZSPRUNG-RUSSELL DIAGRAM
X-ray spectra of bursting neutron stars N85-34686

HEURISTIC METHODS
Heuristic rules for visualization N85-34584

HF LASERS
Chemical lasers [ISL-R-107/84] N85-34400

HIERARCHIES
Selection of segment similarity measures for hierarchical picture segmentation N85-34548

HIGH ALTITUDE
An EAS experiment at mountain altitude for the detection of gamma-ray sources [OG-9.4-5] N85-34972
Short perturbations of cosmic ray intensity and electric field in atmosphere [SH-6.1-18] N85-35090

HIGH ALTITUDE TESTS
The design of an experiment to detect low energy antiprotons [OG-9.1-1] N85-34928

HIGH ENERGY ELECTRONS
Collisional relaxation of electron tail distribution [IPPJ-729] N85-34635
On the retention of high-energy protons and nuclei with charges Z or equal to 2 in large solar flares after the process of their acceleration [SH-2.1-8] N85-34789
The influence of the Earth's magnetosphere on the high-energy solar protons [SH-6.1-22] N85-35093

HIGH ENERGY INTERACTIONS
Summary of activities, 1983 [LBL-18500] N85-34605
Calculation of improved spallation cross sections [OG-7.2-23] N85-34890
Cerenkov counters for high energy nuclei: Some new developments [OG-9.1-5] N85-34931
SONTRAC: A solar neutron track chamber detector [SH-9.1-12] N85-35127

HIGH PRESSURE
High pressure compressor component performance report [NASA-CR-168245] N85-34138
Hollow cathodes in high pressure arc discharges [NASA-TM-87098] N85-34179
Determination of individual tolerance in hyperbaric oxygen N85-34507

HIGH RESOLUTION
High resolution electron microscopic characterization of interfaces in ceramics [DE85-011207] N85-34289
Acceleration of ions and electrons to near-cosmic ray energies in a perpendicular shock: The January 6, 1978 event [SH-1.5-4] N85-34773
Advanced techniques for high resolution spectroscopic observations of cosmic gamma-ray sources [OG-9.2-9] N85-34948

HIGH STRENGTH ALLOYS
The influence of temperature on static and dynamic SCC crack growth behavior in aluminum alloy N85-34190

HIGH TEMPERATURE
X-ray measurement of thermal stresses in tungsten fiber-copper composites N85-34205
Dynamics of the melting of chromium-manganese alloys in molten steel [BLL-M-35850-(5828.4)] N85-34252
High temperature structural insulating material [DE85-006361] N85-34291
Depletion modeling of liquid dominated geothermal reservoirs [DE85-009923] N85-34437

HIGH TEMPERATURE PLASMAS
Calculations of heavy ion charge state distributions for nonequilibrium conditions [SH-2.1-12] N85-34793
A cosmic ray driven instability [OG-8.1-5] N85-34895

HILL METHOD
Magnetohydrodynamic equilibrium and stability of spheromak with spheroidal plasma-vacuum interface [IPPJ-732] N85-34640

HISTOGRAMS
How map designers can represent their ideas in thematic maps: Effective user interfaces for thematic map design N85-34562

HISTORIES
A spacefaring people: Perspectives on early spaceflight [NASA-SP-4405] N85-35142
The next assignment: The state of the literature on space N85-35146
Opportunities for policy historians: The evolution of the US civilian space program N85-35147
Space-age Europe, 1957-1980 N85-35148
Space activities in the Soviet Union, Japan, and the People's Republic of China N85-35149
The idea of space exploration N85-35150

HMX
Detonation in tungsten-loaded HMX [DE85-009606] N85-34299

HODOSCOPES
Bevalac calibration of the SOFIE range and hodoscope detectors [OG-9.1-7] N85-34933

HOLLOW CATHODES
Heaterless ignition of inert gas ion thruster hollow cathodes [NASA-TM-87086] N85-34177
Hollow cathodes in high pressure arc discharges [NASA-TM-87098] N85-34179

HOLMIUM
Interactions of heavy nuclei, Kr, Xe and Ho, in light targets [OG-7.2-21] N85-34888

HOLOGRAMMETRY
Hologram-like transmission of pictures N85-34552

HOLOGRAPHIC INTERFEROMETRY
Practical aspects of laser holographic interferometry in wind tunnels [NASA-TM-86788] N85-34378

HOLOGRAPHY
Modular digital holographic fringe data processing system [NASA-CR-177952] N85-34376
Applications of holography to X-ray imaging [DE85-010984] N85-34384
The use of optical fibers in pulsed laser holography [ISL-CO-226/84] N85-34395

HOMEOSTASIS
Effect of dibazol on parameters of nonspecific resistance of subjects in pressurized cabins N85-34504

HOMOGENEITY
Apparatus for unilateral generation of a homogeneous magnetic field [DE85-006001] N85-34345
Why do leaky-box models work so fine? [OG-7.2-8] N85-34877

HOT ELECTRONS
Plug and thermal barrier potential formation in Gamma 10 N85-34648
Effect of ECH and ICH on ambipolar potential in NBT-1M N85-34661
Simulation studies on stability of hot electron plasma N85-34664
Fokker-Planck calculation of hot electron formation in the thermal barrier region of tandem mirror Gamma-10 [IPPJ-726] N85-34669

HOT SURFACES
Component-specific modeling [NASA-CR-174765] N85-34140

HOUSINGS
Refrigerated dynamic seal to 6.9 MPa (1000 psi) [NASA-TM-87108] N85-34356

HUMAN BEHAVIOR
USSR report: Life sciences. Biomedical and behavioral sciences [JPRS-UBB-85-021] N85-34489

HUMAN FACTORS ENGINEERING
Using percent-done program indicators to enhance user interfaces N85-34546

HUMAN TOLERANCES
Determination of individual tolerance in hyperbaric oxygen N85-34507

HYDRAULIC SHOCK
Comprehensive fracture diagnostics experiement. Part 2: Comparison of seven fracture azimuth measurements [DE85-011707] N85-34470

HYDRIDES
Method for preparing hydride configurations and reactive metal surface [DE85-006443] N85-34274

HYDROCARBONS
Process for functionalizing alkanes [DE85-006420] N85-34219

HYDRODYNAMIC EQUATIONS
The cosmic-ray shock structure problem for relativistic shocks [OG-8.1-1] N85-34891

HYDRODYNAMICS
Three-dimensional hydrodynamic hot-spot model [DE85-009587] N85-34301
Numerical simulation in astrophysics: Smoothed particle methods N85-34674
Numerical calculations on shock loaded materials N85-34676
Dissipation terms in one-dimensional hydrodynamic code for ICF target N85-34677
Two-dimensional simulation of LIB target implosion N85-34678
Stability of implosion dynamics N85-34680
Pulse effect in a light ion beam propagation through a Z-discharge plasma channel N85-34684

HYDROELECTRIC POWER STATIONS
Small Hydroelectric Power Plan Demonstration Project [DE85-011343] N85-34454

HYDROELECTRICITY
Solar energy education. Renewable energy: A background text [DE85-010365] N85-34452
Small Hydroelectric Power Plan Demonstration Project [DE85-011343] N85-34454

HYDROGEN
Separation of gas mixtures by supported complexes [DE85-011996] N85-34236
Method for preparing hydride configurations and reactive metal surface [DE85-006443] N85-34274
Low noise polycrystalline semiconductor resistors by hydrogen passivation [AD-D011721] N85-34338
Dual-chamber plasma deposition of A-Si:H solar cells at high rates using disilane [DE85-011828] N85-34451
The extent of the local hi halo [NASA-CR-176115] N85-34724
Low-excitation Herbig-Haro objects and interstellar extinction [NASA-CR-176142] N85-34726
On the detectability of key-MeV solar protons through their nonthermal Lyman-alpha emission [SH-1.3-5] N85-34752
The effects of newly measured cross sections in hydrogen on the production of secondary nuclei during the propagation of cosmic rays through interstellar H [OG-7.2-2] N85-34874
On the importance of interstellar helium for the propagation of heavy cosmic rays [OG-7.2-11] N85-34879
Interactions of heavy nuclei, Kr, Xe and Ho, in light targets [OG-7.2-21] N85-34888

HYDROGEN CLOUDS
Cosmic ray secondary nuclei and the structure of the galaxy [OG-7.2-4] N85-34876

HYDROGEN COMPOUNDS
Intermolecular explosives [DE85-009609] N85-34296

HYDROGEN EMBRITTLEMENT
Hydrogen embrittlement testing [DE85-007352] N85-34273

HYDROGEN IONS
Some physical differences between sheet plasma and multicusp plasma as volume produced H- or D- ion sources [IPPJ-728] N85-34637

Data on the backscattering coefficients on light ions from solids: A revision
[IPPJ-AM-41-REV] N85-34689

HYDROGEN ISOTOPES
The 4He1H ratios in the chemical compositions of solar flare particles and the primordial solar nebula
[SH-7.1-12] N85-35104

HYDROLOGY
Hydrology
[PB85-182954] N85-34440

HYDROLOGY MODELS
Hydrology
[PB85-182954] N85-34440

HYDROLYSIS
Lipid hydrolysis in man during antiorthostatic hypokinesia N85-34500

HYDROTHERMAL SYSTEMS
Workshop on Recent Research in the Valles Caldera
[DE85-010569] N85-34472

HYPERBARIC CHAMBERS
Determination of individual tolerance in hyperbaric oxygen N85-34507

HYPERBOLIC DIFFERENTIAL EQUATIONS
Use of a hyperbolic grid generation scheme in simulating supersonic viscous flow about three-dimensional winged configuration
[NASA-TM-85344] N85-34116
Workshop report on Simulation Techniques for Shock Wave Phenomena and Characteristics of Plasmas in Inertial Confinement Fusion
[IPPJ-725] N85-34670
Cubic interpolated pseudo-particle method (CIP) for solving hyperbolic-type equation N85-34673

HYPERSONIC FLOW
Experimental aerodynamic heating to simulated space shuttle tiles in laminar and turbulent boundary layers with variable flow angles at a nominal Mach number of 7
[NASA-TP-2307] N85-34351

HYPERSONIC VEHICLES
A model of hypersonic two-dimensional oblique detonation wave ramjet
[UTIAS-TN-257] N85-34139

HYPOKINESIA
Effect of hypokinesia and +Gz accelerations on transport function of human blood N85-34497
Lipid hydrolysis in man during antiorthostatic hypokinesia N85-34500
Rat skeletal muscles with simulation of physiological effects of weightlessness (morphological study) N85-34502

HYPOXIA
Effect of acute hypoxia on coronary and systemic hemodynamics N85-34503
Monitoring dosage of volatile compounds in tests at low barometric pressure N85-34506

HYSTERESIS
Electrical resistivity and hysteresis of the equiatomic nickel-titanium alloy near the martensitic transformation temperature N85-34181
Monotonous stress-strain properties of structural steel subjected to nonstationary repetitive pre-loading N85-34185

I

ICE
Short-time creep of ice
[NRC/CNR-TT-2111] N85-34428
Lake ice occurence as a possible detector of atmospheric CO2 effects on climate
[DE85-012987] N85-34480

IGNITION
Scaling parameters of flashover
[NBS-GCR-85-497] N85-34229

IGNITION TEMPERATURE
Review of zirconium-zircaloy pyrophoricity
[DE85-011169] N85-34270

IMAGE ANALYSIS
Experiments and discussions on the analysis of interferograms with closed-loop fringes
[NPL-MOM-68] N85-34515
Non-rigid body motion N85-34576

IMAGE CONTRAST
Colour spaces and colour contrast N85-34567

IMAGE PROCESSING
Electronic imaging system and technique
[DE85-005740] N85-34393
Production of initial estimates of photogrammetric variables
[NPL-MOM-66] N85-34434
A model for graphics interface tool development N85-34545
A general purpose image processing package N85-34549
A new approach to linear quadtrees N85-34550
Image synthesis: Optical identity or pictorial communication? N85-34565
Knowledge engineering application in image processing N85-34583
The read-out system of spatial distribution of thermoluminescence in meteorites
[SH-9.1-16] N85-35131

IMAGE RECONSTRUCTION
Hologram-like transmission of pictures N85-34552

IMAGE RESOLUTION
An analysis and algorithm for filling propagation N85-34551
Hologram-like transmission of pictures N85-34552

IMAGERY
Recognition and clear representation of handwritten electronic diagrams N85-34541

IMAGES
Image synthesis: Optical identity or pictorial communication? N85-34565
Shadow volumes for non-planar polygons N85-34580

IMAGING TECHNIQUES
Method and apparatus for Delta Kappa synthetic aperture radar measurement of ocean current
[NASA-CASE-NPO-15704-1] N85-34327
Applications of holography to X-ray imaging
[DE85-010984] N85-34384
A theoretical and empirical analysis of coherent ray-tracing N85-34524
Frame buffer algorithms for stochastic models N85-34525
Specifying stochastic objects in a hierarchical graphics system N85-34526
Computer analysis techniques for the temporal evaluation of cardiac wall motion N85-34530
A computerized system for spot detection and analysis of two-dimensional electrophoresis images N85-34531
An image management kernel for the design of relational and pictorial data bases N85-34532
Animengine: An engineering animation system N85-34535
3D computer animation: More an evolution problem than a motion problem N85-34536
Towards an integrated view of 3-D computer character animation N85-34538
Research issues in generating graphical explanations N85-34539
The scientific and technical issues in integrating remotely sensed imagery with geocoded data bases N85-34547
Selection of segment similarity measures for hierarchical picture segmentation N85-34548
Hexagonal uniformly redundant arrays for coded-aperture imaging
[OG-9.2-1] N85-34940
A coded aperture imaging system optimized for hard X-ray and gamma ray astronomy
[OG-9.2-3] N85-34942
An experimental assessment of the imaging quality of the low energy gamma-ray telescope ZEBRA
[OG-9.2-8] N85-34947
Advanced techniques for high resolution spectroscopic observations of cosmic gamma-ray sources
[OG-9.2-9] N85-34948
A Cerenkov imaging telescope for high energy gamma rays
[OG-9.3-13] N85-34968
The University of Durham Mark 3 very high energy gamma ray telescope
[OG-9.4-2] N85-34969
Application of imaging to the atmospheric Cherenkov technique
[OG-9.5-4] N85-34981

IMPACT DAMAGE
Design and testing of an energy-absorbing crewseat for the F/FB-111 aircraft, volume 1
[NASA-CR-3916] N85-34133

IMPACT LOADS
Safety and reliability of steel structural materials under random service impact loads N85-34197

IMPACT STRENGTH
Impact fracture mechanism of polymer plates containing a heavy inner material N85-34215

IMPACT TESTS
Design and testing of an energy-absorbing crewseat for the F/FB-111 aircraft, volume 1
[NASA-CR-3916] N85-34133
Design and testing of an energy-absorbing crewseat for the F/FB-111 aircraft. Volume 3: Data from crew module testing
[NASA-CR-3918] N85-34134

IMPINGEMENT
Experimental aerodynamic heating to simulated space shuttle tiles in laminar and turbulent boundary layers with variable flow angles at a nominal Mach number of 7
[NASA-TP-2307] N85-34351

IMPLOSIONS
Workshop report on Simulation Techniques for Shock Wave Phenomena and Characteristics of Plasmas in Inertial Confinement Fusion
[IPPJ-725] N85-34670
Moving finite element method for ICF target implosion N85-34675
Two-dimensional simulation of LIB target implosion N85-34678
Stability of implosion dynamics N85-34680

IMPROVEMENT
The properties of VSt3sp inoculated steel
[BLL-M-35894-(5828.4)] N85-34263

IMPURITIES
The study of the effect of residual microimpurities on the fatigue strength of 55S2 steel
[BLL-M-36317-(5828.4)] N85-34246
Stress corrosion cracking susceptibility of types 316NG and 316 stainless steel in an impurity environment
[TI85-006884] N85-34277

INCIDENCE
OMEGA: Optoelectronic measurement of the incidence angle of a projectile
[ISL-CO-223/84] N85-34634

INCIDENT RADIATION
Formulation of cosmic-ray solar daily variation and its seasonal variation, produced from generalized stationary anisotropy of solar origin
[SH-4.5-2] N85-35020

INCLUSIONS
Viscoelastic behavior of short-fiber composite materials
[DE85-011233] N85-34225
Special features of the fracture of ball-bearing steel close to non-metallic inclusion eutectics
[BLL-M-35809-(5828.4)] N85-34258

INCOMPRESSIBLE FLOW
Modelling of unsteady, incompressible separation on an aerofoil using an inviscid flow algorithm
[GU-AERO-8412] N85-34122
Calculation of flow kinetics of composite media
[BLL-M-35819-(5828.4)] N85-34348
Stability of two-dimensional immiscible flow to viscous fingering
[DE85-011403] N85-34364
New semi-implicit method for solving the time-dependent conservation equations for incompressible flow
[DE85-010926] N85-34367
A curvilinear coordinate method for the solutions of initial value problems using the third-order upwind differencing scheme
[IPPJ-734] N85-34642

INDEXES (DOCUMENTATION)
Index of laser program publications and related reports, calendar year 1984
[DE85-011883] N85-34398
Role of solar flare index in long term modulation of cosmic ray intensity
[SH-4.4-12] N85-35009

INDIA
Observation of energy spectrum of electron albedo in low latitude region at Hyderabad, India
[SH-6.1-7] N85-35081
Proton albedo spectrum observation in low latitude region at Hyderabad, India
[SH-6.1-8] N85-35082

INDUCTION
RADLAC technolgy review
[DE85-011995] N85-34691

INDUCTION HEATING
Feedback regulated induction heater for a flowing fluid
[DE85-006508] N85-34414
Effect of ECH and ICH on ambipolar potential in NBT-1M N85-34661
Transports studies of ECH and ICRH-heated bumpy torus plasma in NBT-1M N85-34662

INDUCTION MOTORS
Evaluation of half wave induction motor drive for use in passenger vehicles
[NASA-CR-176119] N85-34334

INDUSTRIAL PLANTS
Centralized surveillance of flexible workshops for the manufacturing of composite materials
[SNIAS-851-430-103] N85-34227
Solar thermal technologies program summary
[DE85-012253] N85-34449

INDUSTRIES
Forecasting future industrial SO2 and NC/sub x/ emissions, revised N85-34461

INELASTIC STRESS
Monotonous stress-strain properties of structural steel subjected to nonstationary repetitive pre-loading N85-34185

INERTIAL CONFINEMENT FUSION
Workshop report on Simulation Techniques for Shock Wave Phenomena and Characteristics of Plasmas in Inertial Confinement Fusion
[IPPJ-725] N85-34670
Stellarator approach to fusion plasma confinement
[DE85-011420] N85-34704
INFLUENZA
Using the information of cosmic rays to predict influence epidemic
[SH-10.1-2] N85-35134
INFORMATION
Colour coding scales and computer graphics N85-34568
INFORMATION RETRIEVAL
User's operating procedures. Volume 3: Projects directorate information programs
[NASA-CR-177950] N85-34520
NAPGEN: Automatic NAPLPS page generator N85-34575
INFORMATION SYSTEMS
User's operating procedures. Volume 1: Scout project information programs
[NASA-CR-177948] N85-34518
User's operating procedures. Volume 1: Scout project financial analysis program
[NASA-CR-177949] N85-34519
Applied computer graphics in a geographic information system: Problems and successes N85-34563
INFRARED INSTRUMENTS
Instrumentation for sensing moisture content of material using a transient thermal pulse
[NASA-CASE-NPO-15493-2] N85-34373
INFRARED SPECTROSCOPY
Infrared studies of the influence of alkali metals on the C-O bond in chemisorbed carbon monoxide
[DE85-005306] N85-34232
Time-resolved and infrared spectroscopy of excitons
[DE85-011879] N85-34235
INHOMOGENEITY
Cosmic ray secondary nuclei and the structure of the galaxy
[OG-7.2-4] N85-34876
INJECTION
Method for determining depth and shape of a sub-surface conductive object
[DE85-006502] N85-34389
INJURIES
Design and testing of an energy-absorbing crewseat for the F/FB-111 aircraft, volume 1
[NASA-CR-3916] N85-34133
INORGANIC COMPOUNDS
Anaerobic microbial transformations in subsurface environments: Project description
[DE85-012789] N85-34486
INPUT
Issues and techniques in touch-sensitive tablet input (executive summary) N85-34543
INSOLATION
Resource evaluation and site selection for microalgae production systems
[DE85-008807] N85-34485
INSPECTION
Towards the year 2000: Developments in inspection and product assurance to be anticipated during the next 15 years — aircraft engines
[PNR-90258] N85-34421
INSTRUMENT COMPENSATION
The final COS-B database: In-flight calibration of instrumental parameters
[OG-9.3-9] N85-34964
INTEGRAL EQUATIONS
Integral equation formulation for three-dimensional unsteady transonic flow
[ARL-STRUC-R-416] N85-34119
Nonlinear adhesive behavior effects in a cracked orthotropic sheet stiffened by a semi-infinite orthotropic sheet
[NASA-TM-87584] N85-34426
INTEGRATED CIRCUITS
Joint services electronics program
[AD-A154748] N85-34336
Multi-robot assembly of IC's N85-34577
INTERFACE STABILITY
Compressible two-phase flow instabilities simulated with a hybrid Lagrange-Euler pseudospectral method
[DE85-009904] N85-34361
INTERFACES
High resolution electron microscopic characterization of interfaces in ceramics
[DE85-011207] N85-34289
The interactive planning work station: A graphics-based UNIX (trademark) tool for application users and developers N85-34527
An image management kernel for the design of relational and pictorial data bases N85-34532
Graphics interaction in databases N85-34534
Issues and techniques in touch-sensitive tablet input (executive summary) N85-34543
Efficient recovery and reversal in graphical user interfaces generated by the Higgens system N85-34544
A model for graphics interface tool development N85-34545
Using percent-done program indicators to enhance user interfaces N85-34546
The CADME approach to the interface of solid modellers N85-34554
An innovative user interface for microcomputer-based computer-aided design N85-34555
How map designers can represent their ideas in thematic maps: Effective user interfaces for thematic map design N85-34562
INTERFACIAL TENSION
Hydrogen embrittlement testing
[DE85-007352] N85-34273
INTERFERENCE GRATING
Modular digital holographic fringe data processing system
[NASA-CR-177952] N85-34376
INTERFEROMETRY
Ranging system which compares an object reflected component of a light beam to a reference component of the light beam
[NASA-CASE-NPO-15865-1] N85-34629
INTERGALACTIC MEDIA
Interstellar turbulence, random density variations, and scintillation measurements
[OG-7.2-13] N85-34880
INTERMETALLICS
Changes in lattice cell parameter of film intermetallic compounds RT2
[BLL-M-35874-(5828.4)] N85-34261
Oxidizing seal for a turbine tip gas path
[NASA-CASE-LEW-14053-1] N85-34402
INTERMITTENCY
Intermittent motion N85-34323
INTERNAL PRESSURE
Mechanical ratcheting behaviors of a steel pipe under combined cyclic axial load and internal pressure N85-34184
INTERNATIONAL SUN EARTH EXPLORER 3
The International Cometary Explorer (ICE)wallsheet teacher's guide
[NASA-TM-87498] N85-34727
INTERPLANETARY DUST
Elemental abundance differences between nuclei acclerated in CIR shocks and solar flares
[SH-2.2-6] N85-34801
INTERPLANETARY MAGNETIC FIELDS
Determination of the pitch-angle distribution and transverse anisotropy of interplanetary particles
[SH-3.1-11] N85-34815
Pitch angle distributions of solar energetic particles and the local scattering properties of the interplanetary magnetic field
[SH-3.1-13] N85-34816
Channeled propagation of solar particles
[SH-3.2-3] N85-34819
The propagation of solar energetic particles in magnetic channels
[SH-3.2-4] N85-34820
The local characteristic function of interplanetary particle propagation
[SH-3.2-8] N85-34823
On reflecting boundary behind the Earth's orbit at propagation of fast particles from solar flares
[SH-3.2-13] N85-34827
The intensity recovery of Forbush-type decreases as a function of heliocentric distance and its relationship to the 11-year variation
[SH-4.1-9] N85-34832
Cosmic ray modulatin and merged interaction regions
[SH-4.1-11] N85-34834
Cosmic ray modulation in a random anisotropic magnetic field
[SH-4.1-20] N85-34839
Drift and observations in cosmic-ray modulation, 1
[SH-4.2-4] N85-34842
Drift and observations in cosmic-ray modulation, 2
[SH-4.2-5] N85-34843
Cosmic ray north-south anisotropy 1961 - 1983
[SH-4.2-6] N85-34844
Cosmic ray intensity and the tilt of the neutral sheet
[SH-4.2-8] N85-34846
Differential measurement of cosmic-ray gradient with respect to interplanetary current sheet
[SH-4.2-9] N85-34847
Spatial variation of cosmic rays near the heliospheric current sheet
[SH-4.2-10] N85-34848
The effect of the neutral sheet structure of the interplanetary magnetic field on cosmic ray distribution in space
[SH-4.2-18] N85-34855
The dependence of solar modulation on the sign of the cosmic ray particle charge
[SH-4.2-23] N85-34860
An update on the correlation between the cosmic radiation intensity and the geomagnetic AA index
[SH-4.2-24] N85-34861
Isotropic intensity waves and features of their occurrence
[SH-4.3-8] N85-34993
IMF-sense-dependent cosmic ray anisotropy produced from diffusion-convection in heliosphere
[SH-4.3-9] N85-34994
Characteristics of cosmic ray pole-equator anisotropy derived from spherical harmonic analysis of neutron monitor data
[SH-4.3-12] N85-34996
The corotating variation of the north-south anisotropy of cosmic rays
[SH-4.3-15] N85-34999
Sidereal variations deep underground in Tasmania
[SH-4.4-4] N85-35002
The effect of the interplanetary magnetic field on sidereal variations observed at medium depth underground detectors
[SH-4.4-5] N85-35003
Corrected sidereal anisotropy for underground moons
[SH-4.4-7] N85-35005
A study of periodicities and recurrences in solar activity and cosmic ray modulation
[SH-4.4-14] N85-35010
Solar wind velocity and daily variation of cosmic rays
[SH-4.5-6] N85-35024
Magnetic fluctuation and cosmic ray diurnal variations
[SH-4.5-21] N85-35038
Observation of pick-up ions in the solar wind: Evidence for the source of the anomalous cosmic ray component?
[SH-4.6-5] N85-35043
Possible origin of the anomalous component of cosmic rays
[SH-4.6-7] N85-35045
Anomalous short-term increases in the galactic cosmic ray intensity: Are they related to the interplanetary magnetic cloud-like structures?
[SH-5.1-3] N85-35057
Galactic cosmic ray currents and magnetic field irregularity degree in high-speed solar wind streams
[SH-5.1-9] N85-35063
Influence of magnetic clouds on cosmic ray intensity variations
[SH-5.1-12] N85-35065
Solar activity beyond the disk and variations of the cosmic ray gradient
[SH-5.1-23] N85-35075
INTERPLANETARY MEDIUM
Ninteenth International Cosmic Ray Conference. SH sessions, volume 4
[NASA-CP-2376-VOL-4] N85-34729
Source energy spectra from demodulation of solar particle data by interplanetary and coronal transport
[SH-1.3-13] N85-34758
Shock and statistical acceleration of energetic particles in the interplanetary medium
[SH-1.5-1] N85-34771
Energetic ion acceleration at collisionless shocks
[SH-1.5-3] N85-34772
Particle acceleration due to shocks in the interplanetary field: High time resolution data and simulation results
[SH-1.5-5] N85-34774
Pitch angle distributions of 35-1000 keV protons at quasi-perpendicular interplanetary shocks
[SH-1.5-6] N85-34775
Spatial dependence of the local diffusion coefficient measured upstream of the November 12, 1978 interplanetary traveling shock
[SH-1.5-12] N85-34776
Solar and interplanetary particles at 2 to 4 MEV during solar cycles 21, solar cycle variations of event sizes, and compositions
[SH-1.5-16] N85-34779
Cosmic ray acceleration by stellar wind. Simulation for heliosphere
[SH-1.5-17] N85-34780
Low energy proton bidirectional anisotropies and their relation to transient interplanetary magnetic structures: ISEE-3 observations
[SH-3.1-9] N85-34813
Latitudinal gradients of cosmic rays and the polarity reversal of the heliospheric magnetic field: A preliminary evaluation
[SH-4.2-16] N85-34853

Solar modulation and interplanetary gradients of the galactic electrons flux, 1977 - 1984
[SH-4.7-4] N85-35049
Anomalous short-term increases in the galactic cosmic ray intensity: Are they related to the interplanetary magnetic cloud-like structures?
[SH-5.1-3] N85-35057
A suggested standardized format for cosmic ray ground-level event data
[SH-9.1-15] N85-35130

INTERPLANETARY SPACE
Possible detection of flare-generated positrons by Helios 1 on 3 Jun 1982
[SH-1.4-10] N85-34770
Variations in elemental composition of several MEV/nucleon ions observed in interplanetary space
[SH-2.1-7] N85-34788
On the retention of high-energy protons and nuclei with charges Z or equal to 2 in large solar flares after the process of their acceleration
[SH-2.1-8] N85-34789
Isotopic overabundances and the energetic particle model of solar flares
[SH-2.2-1] N85-34796
Radial transport of approximately 1 MeV/nucleon ions during the 22 November 1977 solar particle event
[SH-3.2-5] N85-34821
Investigation of cosmic ray propagation in interplanetary space
[SH-3.2-9] N85-34824
Monte Carlo calculations of relativistic solar proton propagation in interplanetary space
[SH-3.2-11] N85-34826
The influence of nonstationarity of the solar activity and general solar field on modulation of cosmic rays
[SH-4.2-17] N85-34854
The cosmic ray interplanetary radial gradient from 1972 - 1985
[SH-4.7-1] N85-35046
The large scale dynamics of the outer heliosphere and the long-term modulation of galactic cosmic rays
[SH-4.7-3] N85-35048
Study of cosmic ray scintillations from 5-minute data of the scintillations telescope Izmran and world-wide network stations
[SH-5.1-18] N85-35071
The theoretical and experimental investigation of cosmic ray Forbush-effects
[SH-5.1-20] N85-35072
Observation of nuclei with energies 8-30 MeV per nucleon in the Earth's magnetosphere at the altitudes 350 KM
[SH-10.1-5] N85-35136

INTERPOLATION
The improved display of 625-line television pictures: Adaptive interpolation
[BBC-RD-1985/5] N85-34328
Reports from the German Meteorological Service. No. 166: The optimal spectral density of climatological station networks
[ISBN-3-88148-214-8] N85-34478
Geometric continuity with interpolating Bezier curves N85-34570

INTERSTELLAR GAS
The extent of the local hi halo
[NASA-CR-176115] N85-34724
On the influence of the heliomagnetospheric periphery on the galactic cosmic rays
[SH-4.2-19] N85-34856
On the importance of interstellar helium for the propagation of heavy cosmic rays
[OG-7.2-11] N85-34879
The role of cosmic rays in magnetic hydrodynamics of interstellar medium
[OG-7.2-15] N85-34882

INTERSTELLAR MAGNETIC FIELDS
Angular resolution of an EAS array for gamma ray astronomy energies 5 x 10 (13) eV
[OG-9.5-8] N85-34985
Change of cosmic ray anisotropy with solar activity
[SH-4.5-20] N85-35037

INTERSTELLAR MATTER
Variations in the propagation of UH-nuclei
[OG-7.1-1] N85-34863
Electron capture decay of cosmic rays: A model of the inhomogeneous interstellar medium
[OG-7.1-10] N85-34871
The effects of newly measured cross sections in hydrogen on the production of secondary nuclei during the propagation of cosmic rays through interstellar H
[OG-7.2-2] N85-34874
Interstellar turbulence, random density variations, and scintillation measurements
[OG-7.2-13] N85-34880
Interstellar (Na-22) as a possible source of the excess (Ne-22) in the galactic cosmic ray
[OG-8.2-12] N85-34908
Giant molecular clouds as regions of particle acceleration N85-34913
Secondary to primary ratio and the continuous acceleration
[OG-8.3-4] N85-34923
Exact solutions for sporadic acceleration of cosmic rays
[OG-8.3-7] N85-34925

INTERSTELLAR RADIATION
Influence of the source distribution on the age distribution of galactic cosmic rays
[OG-8.3-1] N85-34920

INTERSTELLAR SPACE
On the influence of the heliomagnetospheric periphery on the galactic cosmic rays
[SH-4.2-19] N85-34856
Cosmic ray secondary nuclei and the structure of the galaxy
[OG-7.2-4] N85-34876
On the cosmic ray diffusion in a violent interstellar medium
[OG-7.2-14] N85-34881
The role of cosmic rays in magnetic hydrodynamics of interstellar medium
[OG-7.2-15] N85-34882

INVENTORY CONTROLS
Discrete simulation models - their role in the design, development and management of inventory control systems
[PNR-90249] N85-34719

INVERTEBRATES
Effects of acid rain on forest nutrient status
[DE85-012486] N85-34463

INVERTERS
Evaluation of half wave induction motor drive for use in passenger vehicles
[NASA-CR-176119] N85-34334

INVISCID FLOW
Modelling of unsteady, incompressible separation on an aerofoil using an inviscid flow algorithm
[GU-AERO-8412] N85-34122

ION ACCELERATORS
Energetic ion acceleration at collisionless shocks
[SH-1.5-3] N85-34772

ION BEAMS
Calculation of mixed depth for some metal-Si systems
[DE85-011907] N85-34616
Diamondlike carbon protective coatings for IR materials
[NASA-TM-87083] N85-34631
Numerical calculations on shock loaded materials N85-34676
Dissipation terms in one-dimensional hydrodynamic code for ICF target N85-34677
Pulse effect in a light ion beam propagation through a Z-discharge plasma channel N85-34684
Repetitive pulse accelerator technology for light ion inertial confinement fusion
[DE85-012030] N85-34693
Light ion sources for ICF
[DE85-011544] N85-34702
Method of precisely modifying predetermined surface layers of a workpiece by cluster ion impact therewith
[DE85-006519] N85-34710
Survey of mixing in metal/insulator systems
[DE85-011938] N85-34714
Injection of energetic particles following the gamma-ray flares on June 7, 1980, as observed on Helios 1
[SH-1.3-9] N85-34756

ION CHARGE
The mean ionic charges of N, Ne, MG, SI and S in solar energetic particle events
[SH-2.1-11] N85-34792
The mean ionic charge of silicon in 3HE-rich solar flares
[SH-2.2-8] N85-34803

ION CURRENTS
Some physical differences between sheet plasma and multicusp plasma as volume produced H- or D- ion sources
[IPPJ-728] N85-34637
Measuring method and confirmation of H- (D-) ion current by sheet plasma 1
[IPPJ-730] N85-34638

ION CYCLOTRON RADIATION
Computational study on excitation, propagation and 3 omega -heating due to the ion Bernstein wave
[IPPJ-733] N85-34641
Transport issues in Phaedrus-type plasmas N85-34653
Bounce resonance heating and radial transport of electrons N85-34655
Effect of ECH and ICH on ambipolar potential in NBT-1M N85-34661
Simulation studies on stability of hot electron plasma N85-34664
Observation of mode-converted by ion Bernstein wave by an HCN laser scattering
[IPPJ-724] N85-34668

ION DISTRIBUTION
Stability of ion distribution in strong ion shock structure N85-34681
Solar Coronal and photospheric abundances from solar energetic particle measurements
[SH-2.1-5] N85-34786

ION EMISSION
Workshop report on Simulation Techniques for Shock Wave Phenomena and Characteristics of Plasmas in Inertial Confinement Fusion
[IPPJ-725] N85-34670

ION ENGINES
Heaterless ignition of inert gas ion thruster hollow cathodes
[NASA-TM-87086] N85-34177

ION EXCHANGE MEMBRANE ELECTROLYTES
Evaluation of developmental membranes for the mixed reactant iron-chromium redox system
[NASA-TM-87074] N85-34443

ION EXCHANGING
Multi-solute subsurface transfer modeling for energy solid wastes: Highlights FY 1984
[DE85-012788] N85-34591

ION EXTRACTION
Some physical differences between sheet plasma and multicusp plasma as volume produced H- or D- ion sources
[IPPJ-728] N85-34637

ION IMPACT
Method of precisely modifying predetermined surface layers of a workpiece by cluster ion impact therewith
[DE85-006519] N85-34710

ION IMPLANTATION
Calculation of mixed depth for some metal-Si systems
[DE85-011907] N85-34616
Formation of amorphous silicon by light ion damage
[DE85-012605] N85-34623

ION IRRADIATION
Breakdown of intrinsic ambipolarity for the radial diffusion due to a rotating RF field N85-34660

ION MOTION
Behavior of helically-trapped fast ion orbits in heliotron E N85-34666

ION SCATTERING
Solar flare gamma-ray line spectroscopy
[SH-2.1-14] N85-34795

ION SHEATHS
Some physical differences between sheet plasma and multicusp plasma as volume produced H- or D- ion sources
[IPPJ-728] N85-34637

ION SOURCES
Improved negative ion source
[DE85-006445] N85-34241
Negative ion sources equipped with continuous annular and spherical geometry surface ionizers
[DE85-011939] N85-34619
Light ion sources for ICF
[DE85-011544] N85-34702

ION TEMPERATURE
Transports studies of ECH and ICRH-heated bumpy torus plasma in NBT-1M N85-34662
Langmuir probe on ISX-B
[DE85-012066] N85-34697

IONIC COLLISIONS
Study of photon emission by electron capture during solar nuclei acceleration, 1: Temperature-dependent cross section for charge changing processes
[SH-1.1-8] N85-34735

IONIC DIFFUSION
The plasma mechanism for preferential acceleration of heavy ions
[SH-2.2-10] N85-34805

IONIC WAVES
Resonant ion acceleration by oblique magnetosonic shock wave in a collisionless plasma
[IPPJ-735] N85-34643

IONIZATION
Electron impact ionization of multicharged ions at ORNL: 1980-1984
[DE85-013104] N85-34622
Stability of ion distribution in strong ion shock structure N85-34681
Solar Coronal and photospheric abundances from solar energetic particle measurements
[SH-2.1-5] N85-34786

IONIZATION CHAMBERS
Observations on (3)He neutron spectrometry
[DE85-010731] N85-34608

The response of ionization chambers to relativistic heavy nuclei
[OG-9.1-13] N85-34938
Sidereal anisotropy of cosmic rays
[SH-4.4-8] N85-35006
Long term changes in cosmic ray diurnal variations observed by ion chambers in Hong Kong and Japan
[SH-4.5-14] N85-35031
Burst size distributions in the digitized data of the ion chambers t Mt.' Norikura and sea level stations
[SH-9.1-9] N85-35124
The influences of the galactic cosmic ray on the atmospheric ozone
[SH-10.1-1] N85-35133

IONIZATION CROSS SECTIONS
Electron impact ionization of multicharged ions at ORNL: 1980-1984
[DE85-013104] N85-34622
Electron loss process and cross section of multiply charged ions by neutral atoms N85-34685
On the importance of interstellar helium for the propagation of heavy cosmic rays
[OG-7.2-11] N85-34879

IONIZATION POTENTIALS
Modulated voltage metastable ionization detector
[NASA-CASE-ARC-11503-1] N85-34374
Anomalous abundances of solar energetic particles and coronal gas: Coulomb effects and First Ionization Potential (FIP) ordering
[SH-2.1-10] N85-34791
Variations in the propagation of UH-nuclei
[OG-7.1-1] N85-34863
Germanium and lead: Significant differences between meteoritic and photospheric abundances?
[OG-7.1-2] N85-34864
Implications of source abundances of ultraheavy cosmic rays
[OG-7.1-4] N85-34866

IONIZED GASES
Anomalous abundances of solar energetic particles and coronal gas: Coulomb effects and First Ionization Potential (FIP) ordering
[SH-2.1-10] N85-34791
The mean ionic charges of N, Ne, MG, SI and S in solar energetic particle events
[SH-2.1-11] N85-34792

IONOSPHERE
Waves In Space Plasmas (WISP) N85-34164
Electrodynamic tether N85-34168
Atmospheric Emission Photometric Imaging (AEPI) N85-34170

IONOSPHERIC DISTURBANCES
Vehicle Charging And Potential (VCAP) N85-34173
Sporadic radio emission connected with a definite manifestation of solar activity in the near Earth space
[SH-10.1-8] N85-35139
Near Earth space sporadic radio emission busts occurring during sunrise
[SH-10.1-9] N85-35140

IONOSPHERIC NOISE
Sporadic radio emission connected with a definite manifestation of solar activity in the near Earth space
[SH-10.1-8] N85-35139

IONOSPHERIC PROPAGATION
Waves In Space Plasmas (WISP) N85-34164

IONS
Measuring method and confirmation of H- (D-) ion current by sheet plasma 1
[IPPJ-730] N85-34638
Low frequency instability in a mirror field N85-34657
Model of azimuthal non-uniformities induced by RF heating in RFC-XXM N85-34658
Experimental measurements of the ion cyclotron antennas' coupling and RF characteristics
[DE85-011569] N85-34694
Study of photon emission by electron capture during solar nuclei acceleration, 1: Temperature-dependent cross section for charge changing processes
[SH-1.1-8] N85-34735
Quantitative analysis of flare accelerated electrons through their hard X-ray and microwave radiation
[SH-1.2-7] N85-34742
Ion energy storage for post-flare loops
[SH-1.2-10] N85-34745
Energetic protons from a disappearing solar filament
[SH-1.3-7] N85-34754

IRIDIUM
Development of the osmium-191 yields iridium-191m radionuclide generator
[DE85-011185] N85-34611
Current status of the Os-191 yields Ir-191m generator
[DE85-006306] N85-34614

IRON
Calculation of activities of components in liquid alloys of iron with yttrium
[BLL-M-35868-(5828.4)] N85-34253
Capture in the 1.15-keV iron resonance
[DE85-011913] N85-34612
Silicon to iron abundances in solar cosmic rays and in the sun
[SH-2.1-6] N85-34787

IRON ALLOYS
Enthalpies of formation of liquid Fe-Ce-Si and Fe-Ce-Al three-component alloys
[BLL-M-36296-(5828.4)] N85-34247
Influence of technology of atomization of naturally alloyed iron on grain-size characteristics of powder material
[BLL-M-35810-(5828.4)] N85-34257

IRON ISOTOPES
Measurements of Fe and Ar fragmentation cross sections
[OG-7.2-20] N85-34887
The response of ionization chambers to relativistic heavy nuclei
[OG-9.1-13] N85-34939

IRON OXIDES
Iron and manganese in oxide minerals and in glasses: Preliminary consideration of Eh buffering potential at Yucca Mountain, Nevada
[DE85-011892] N85-34271
Features of behavior of gas bubbles in molten oxide films during enamelling: Communication 2
[BLL-M-35781-(5828.4)] N85-34283

IRRADIANCE
Solar Ultraviolet Spectral Irradiance Monitor (SUSIM) N85-34160
Active Cavity Radiometer (ACR) N85-34163

ISOTOPE EFFECT
Electron photoejection in carbanions
[DE85-011748] N85-34237

ISOTOPES
High resolution Cherenkov detectors for cosmic ray isotope experiment
[OG-9.1-4] N85-34930
Mass resolution optimization in a large isotopic composition experiment
[OG-9.1-9] N85-34935
Measurement of low energy cosmic rays aboard Spacelab-1
[SH-10.1-6] N85-35137

ISOTOPIC ENRICHMENT
On the connection between the 3HE-enrichment and spectral index of solar energetic particles
[SH-2.2-9] N85-34804

ISOTOPIC LABELING
Uranium, thorium isotopic analyses and uranium-series ages of calcite and opal and stable isotopic compositions of calcite from drill cores UE25a no. 1, USR G-2 and USW G-3/GU-3, Yucca Mountain, Nevada
[DE85-013039] N85-34471

J

JAPAN
Cosmic ray intensity variations observed at Matsushiro (220 M.W.E. in depth)
[SH-4.4-9] N85-35007
Space activities in the Soviet Union, Japan, and the People's Republic of China N85-35149

JET ENGINE FUELS
Measurement and correlation of jet fuel viscosities at low temperatures
[NASA-CR-174911] N85-34295

JET ENGINES
Component-specific modeling
[NASA-CR-174765] N85-34140

JOINTS (JUNCTIONS)
Three-dimensional finite element failure model for predicting failure in fibre reinforced bolted joints
[BR94778] N85-34423
Stresses and strains in a plate resulting from two closely-spaced interference-fit fasteners
[ARL-STRUC-TM-409] N85-34429

JUPITER ATMOSPHERE
The Jovian electron spectrum: 1978-1984
[SH-1.5-19] N85-34782

K

KEVLAR (TRADEMARK)
Flight service evaluation of composite helicopter components
[NASA-CR-172562] N85-34222

KINEMATICS
A versatile computer package for mechanism analysis N85-34314
Calculation of flow kinetics of composite media
[BLL-M-35819-(5828.4)] N85-34348
Generated spiral bevel gears: Optimal machine-tool settings and tooth contact analysis
[NASA-TM-87075] N85-34405
Non-rigid body motion N85-34576

KINETIC ENERGY
SONTRAC: A solar neutron track chamber detector
[SH-9.1-12] N85-35127

KINETIC EQUATIONS
Guiding center distribution function and longitudinal invariant N85-34663

KINETIC THEORY
The balancing of complex linkage mechanisms N85-34313

KLYSTRONS
Research on gyrotrons
[AD-A154032] N85-34380

KNOWLEDGE
Knowledge engineering application in image processing N85-34583

KOLMOGOROFF-SMIRNOFF TEST
A new statistic for the analysis of circular data in gamma-ray astronomy
[OG-9.5-13] N85-34989

KRYPTON
Interactions of heavy nuclei, Kr, Xe and Ho, in light targets
[OG-7.2-21] N85-34888

L

LABORATORY EQUIPMENT
Recommendations for the design and equipping of engineering metrology laboratories
[NPL-MOM-22] N85-34145

LABYRINTH
Dissociation of autonomic and sensory vestibular reactions N85-34501

LAGRANGE COORDINATES
Compressible two-phase flow instabilities simulated with a hybrid Lagrange-Euler pseudospectral method
[DE85-009904] N85-34361

LAKES
Lake ice occurence as a possible detector of atmospheric CO2 effects on climate
[DE85-012987] N85-34480

LAMINAR FLOW
Block-implicit calculations of three-dimensional laminar flow in strongly curved ducts
[DE85-003047] N85-34363
Effects of ambient pressure on the instability of a liquid boiling explosively at the superheat limit
[DE85-009476] N85-34370

LAND USE
Resource evaluation and site selection for microalgae production systems
[DE85-008807] N85-34485

LANDING
Ground-based and in-flight simulator studies of flight characteristics of a twin-fuselage passenger transport airplane during approach and landing
[NASA-TP-2451] N85-34144

LANDSAT SATELLITES
Satellites and politics: Weather, communications, and earth resources N85-35144

LARGE SPACE STRUCTURES
Space station rotational equations of motion
[NASA-TP-2511] N85-34148
Space Station Engineering and Technology Development: Proceedings of the Panel on In-Space Engineering Research and Technology Development
[NASA-CR-176110] N85-34153
Box truss analysis and technology development. Task 1: Mesh analysis and control
[NASA-CR-172570] N85-34156

LASER APPLICATIONS
Flat-plate solar array project process development area process research of non-CZ silicon material
[NASA-CR-176117] N85-34445
Observation of mode-converted by ion Bernstein wave by an HCN laser scattering
[IPPJ-724] N85-34668

LASER DOPPLER VELOCIMETERS
A comparison of laser Doppler anemometry and probe measurements within the boundary layer of an airfoil at subsonic flow
[ISL-CO-219/84] N85-34127
Study of boundary layer separation on a supercritical profile with a spoiler by means of a laser Doppler velocimeter
[ISL-CO-225/84] N85-34128
Prediction of the flow-field interference induced by the long-range laser velocimeter in the Ames 40- by 80-foot and the 80- by 120-foot wind tunnels
[NASA-TM-86763] N85-34146

Nonsimultaneous coupled laser velocimeter measurement technique: Error prediction for spatially noncoincident measurements
[NASA-TM-86718] N85-34379

LASER INTERFEROMETRY
Practical aspects of laser holographic interferometry in wind tunnels
[NASA-TM-86788] N85-34378

LASER OUTPUTS
Time-resolved spectroscopic studies of detonating heterogeneous explosives
[DE85-009760] N85-34297
Thermal transport measurements of UV laser irradiated spherical targets
[DE85-011038] N85-34365
Apparatus and method for the spectrochemical analysis of liquids using the laser spark
[DE85-005749] N85-34387
Ranging system which compares an object reflected component of a light beam to a reference component of the light beam
[NASA-CASE-NPO-15865-1] N85-34629

LASER PLASMAS
Multiple inner shell vacancies in laser-irradiated Au plasma N85-34687

LASER PUMPING
Photoionization-pumped, Ne 2, X-ray laser studies project
[DE85-012973] N85-34399

LASER RANGER/TRACKER
Theoretical and experimental analyses of the performance of two-color laser ranging systems
[NASA-CR-176159] N85-34397

LASER SPECTROSCOPY
Apparatus and method for the spectrochemical analysis of liquids using the laser spark
[DE85-005749] N85-34387

LASER TARGETS
Thermal transport measurements of UV laser irradiated spherical targets
[DE85-011038] N85-34365

LASER WELDING
Laser welding of 6Al-4V titanium alloy
[DE85-012019] N85-34413

LASERS
Index of laser program publications and related reports, calendar year 1984
[DE85-011863] N85-34398

LATITUDE
Latitude dependence of co-rotating shock acceleration
[SH-1.5-14] N85-34777
Differential measurement of cosmic-ray gradient with respect to interplanetary current sheet
[SH-4.2-9] N85-34847
Determination of galactic cosmic ray latitudinal gradient using Earth based detectors
[SH-4.2-13] N85-34851
Latitudinal gradients of cosmic rays and the polarity reversal of the heliospheric magnetic field: A preliminary evaluation
[SH-4.2-16] N85-34853
Comparative study of the phase of diurnal anisotropy on quiet and disturbed days on a long term basis up to recent period
[SH-4.5-9] N85-35027
Radial and latitudinal gradients of anomalous oxygen during 1977 - 1985
[SH-4.6-4] N85-35042

LATTICE PARAMETERS
Changes in lattice cell parameter of film intermetallic compounds RT2
[BLL-M-35874-(5828.4)] N85-34261

LEACHING
Effects of acid rain on forest nutrient status
[DE85-012486] N85-34463

LEAD (METAL)
Germanium and lead: Significant differences between meteoritic and photospheric abundances?
[OG-7.1-2] N85-34864
Lead and uranium group abundances in cosmic rays
[OG-7.1-3] N85-34865
Coupling functions for lead and lead-free neutron monitors from the latitudinal measurements performed in 1982 in the research station Academician Kurchatov
[SH-6.1-1] N85-35076
Sensitivity of single and multiple cosmic ray neutrons to the surrounding medium in a lead-free monitor
[SH-9.1-10] N85-35125
The neutron moderated detector and groundbased cosmic ray modulation studies
[SH-9.1-13] N85-35128

LEAD POISONING
Estimating risks of lead-induced hemoglobin decrements under conditions of uncertainty: Methodology, pilot judgments and illustrative calculations
[DE85-012293] N85-34493

LEAKAGE
Refrigerated dynamic seal to 6.9 MPa (1000 psi)
[NASA-TM-87108] N85-34356
Upgrading auxiliary facility outleakage and combustion detection
[DE85-012796] N85-34386

LEARNING
The International Cometary Explorer (ICE)wallsheet teacher's guide
[NASA-TM-87498] N85-34727

LEARNING MACHINES
Monte Carlo techniques for analyzing deep penetration problems
[DE85-011426] N85-34598

LEG (ANATOMY)
Rat skeletal muscles with simulation of physiological effects of weightlessness (morphological study) N85-34502

LENSES
Theoretical and computational research on the focused transport of intense charged particle beams
[DE85-012980] N85-34621

LIFE SCIENCES
USSR report: Life sciences. Biomedical and behavioral sciences
[JPRS-UBB-85-021] N85-34489
Effect of seeds of heavy charged particles of galactic cosmic radiation N85-34505

LIGANDS
Metal alkoxides: Models for metal oxides. Alkoxide ligands in early transition metal organometallic chemistry
[DE85-011368] N85-34269

LIGHT BEAMS
Ranging system which compares an object reflected component of a light beam to a reference component of the light beam
[NASA-CASE-NPO-15865-1] N85-34629

LIGHT CURVE
A new approach to evaluate gamma-ray measurements
[OG-9.5-11] N85-34988

LIGHT IONS
Light ion sources for ICF
[DE85-011544] N85-34702

LIGHT MODULATION
Differentiating spatial light modulator
[AD-D011727] N85-34632

LIGHT SCATTERING
High resolution Cherenkov detectors for cosmic ray isotope experiment
[OG-9.1-4] N85-34930

LIGHT SOURCES
Electronic imaging system and technique
[DE85-005740] N85-34393

LIGHT WATER REACTORS
Effect of stainless steel weld overlay cladding on the structural integrity of flawed steel plates in bending, series 1
[TI85-010349] N85-34418

LINE SPECTRA
Abundances from solar-flare gamma-ray line spectroscopy
[SH-2.1-13] N85-34794
Solar flare gamma-ray line spectroscopy
[SH-2.1-14] N85-34795

LINEAR ACCELERATORS
Physics Division annual review, 1 April 1983 - 31 March 1984
[ANL-84-24] N85-34602
RADLAC technolgy review
[DE85-011995] N85-34691
Technology of magnetically driven accelerators
[DE85-011857] N85-34700

LINEARITY
Instrumentation for sensing moisture content of material using a transient thermal pulse
[NASA-CASE-NPO-15493-2] N85-34373
A new approach to linear quadtrees N85-34550

LINEARIZATION
Realization and linearization of a hyperfrequency power amplifier implemented with bipolar transistors in class C polarization --- microwave amplifiers
[CNES-NT-114] N85-34346
Production of initial estimates of photogrammetric variables
[NPL-MOM-66] N85-34434

LINES (GEOMETRY)
Selection of segment similarity measures for hierarchical picture segmentation N85-34548

LININGS
High temperature structural insulating material
[DE85-006361] N85-34291

LINKAGES
The balancing of complex linkage mechanisms N85-34313
Conjugated symmetrical coupler curves, produced by 4-bar linkages having the same transmission angles N85-34322

LIPID METABOLISM
Lipid hydrolysis in man during antiorthostatic hypokinesia N85-34500
Lipogenesis in rat liver after flight aboard Cosmos-1129 biosatellite N85-34508

LIQUID CRYSTALS
Differentiating spatial light modulator
[AD-D011727] N85-34632

LIQUID FLOW
Detailed validation of a liquid and heat flow code against field performance
[DE85-009901] N85-34368

LIQUID METAL COOLED REACTORS
Technical assessment of thermal-hydraulics for high heat flux fusion components
[DE85-013178] N85-34359

LIQUID METALS
Electrically conductive containment vessel for molten aluminum
[DE85-006518] N85-34415

LIQUID PHASES
The effect of liquid-liquid phase separation of glass on the properties and crystallization behavior
[NASA-TM-77890] N85-34285

LIQUID SURFACES
Surface temperature distribution along a thin liquid layer due to thermocapillary convection
[NASA-TM-87115] N85-34357

LIQUID-SOLID INTERFACES
Approximate determination of the extent of the solid-liquid zone
[BLL-M-35829-(5828.4)] N85-34251

LIQUID-VAPOR INTERFACES
Effects of ambient pressure on the instability of a liquid boiling explosively at the superheat limit
[DE85-009476] N85-34370

LIQUIDS
Apparatus and method for the spectrochemical analysis of liquids using the laser spark
[DE85-005749] N85-34387
Depletion modeling of liquid dominated geothermal reservoirs
[DE85-009923] N85-34437

LITERATURE
The next assignment: The state of the literature on space N85-35146

LITHIUM
Evaluation of low-temperature geothermal potential in Utah and Goshen Valleys and adjacent areas, Utah. Part 2: Water temperature and chemistry
[DE85-009344] N85-34438
Light ion sources for ICF
[DE85-011544] N85-34702

LITHOLOGY
Geology and petroleum resources of basins in western China
[DE85-013038] N85-34469

LIVER
Lipogenesis in rat liver after flight aboard Cosmos-1129 biosatellite N85-34508

LOADING MOMENTS
Intermittent motion N85-34323

LOADING OPERATIONS
Shuttle car loading system
[NASA-CASE-NPO-15949-1] N85-34722

LOADS (FORCES)
Pressure-shear loading of PBX-9404
[DE85-009982] N85-34298
Inertial stresses and deformations in mechanisms N85-34320
Tensile testing apparatus
[NASA-CASE-LAR-13243-1] N85-34375
The design and analysis of single flank transmission error tesior for loaded gears
[NASA-CR-176163] N85-34404

LOCKING
Variable length strut with longitudinal compliance and locking capability
[NASA-CASE-MFS-25907-1] N85-34401

LOCOMOTION
Non-rigid body motion N85-34576

LONG DURATION EXPOSURE FACILITY
The heavy ions in space experiment
[OG-9.1-10] N85-34936

LONG DURATION SPACE FLIGHT
Fluid-electrolyte metabolism and renal function in cosmonauts following 185-day spaceflight N85-34495

LONG TERM EFFECTS
Lipogenesis in rat liver after flight aboard Cosmos-1129 biosatellite N85-34508
Long-period cosmic ray variations and their altitude dependence
[SH-6.1-19] N85-35091

LONG WAVE RADIATION
Sporadic radio emission connected with a definite manifestation of solar activity in the near Earth space
[SH-10.1-8] N85-35139
LONGITUDE
Longitudinal distribution of cosmic rays in the heliosphere
[SH-4.1-14] N85-34837
LONGITUDINAL WAVES
The longitudinal thickness of air-shower fronts
[OG-9.5-1] N85-34978
LOOP ANTENNAS
Experimental measurements of the ion cyclotron antennas' coupling and RF characteristics
[DE85-011569] N85-34694
LOOPS
Wide-band phase locked loop amplifier apparatus
[AD-D011720] N85-34337
LORENTZ FORCE
Cerenkov counters for high energy nuclei: Some new developments
[OG-9.1-5] N85-34931
LOUVERS
Fast shutter apparatus
[DE85-006501] N85-34343
LOW CARBON STEELS
Fractographic analysis for nonpropagating conditions of fatigue crack at high stress ratios in mild steel N85-34194
Crystallographic orientation dependence of fatigue crack propagation in extremely low carbon steel N85-34195
Safety and reliability of steel structural materials under random service impact loads N85-34197
LOW DENSITY MATERIALS
Method for making a low density polyethylene waste form for safe disposal of low level radioactive material
[DE85-006401] N85-34292
LOW NOISE
Low noise polycrystalline semiconductor resistors by hydrogen passivation
[AD-D011721] N85-34338
LOW PRESSURE
Monitoring dosage of volatile compounds in tests at low barometric pressure N85-34506
LOW TEMPERATURE
Measurement and correlation of jet fuel viscosities at low temperatures
[NASA-CR-174911] N85-34295
LOWER BODY NEGATIVE PRESSURE
Oxygenation and regional circulation in gingival mucosa during exposure to lower body negative pressure N85-34498
LUBRICATION
Lubrication and cooling for high speed gears
[NASA-TM-87096] N85-34407
Elastohydrodynamic lubrication calculations used as a tool to study scuffing
[NASA-TM-87097] N85-34408
Design and lubrication of high-speed rolling-element bearings
[NASA-TM-87107] N85-34409
LUMINOSITY
X-ray spectra of bursting neutron stars N85-34686
LYMAN ALPHA RADIATION
The extent of the local hi halo
[NASA-CR-176115] N85-34724
On the detectability of key-MeV solar protons through their nonthermal Lyman-alpha emission
[SH-1.3-5] N85-34752
LYMPHOCYTES
Non-rigid body motion N85-34576

M

M REGION
Isotopic overabundances and the energetic particle model of solar flares
[SH-2.2-1] N85-34796
MACH NUMBER
An evaluation of three helicopter rotor sections
[NASA-TM-86719] N85-34115
MACH REFLECTION
Tabular and graphical solutions of regular and Mach reflections in pseudo-stationary frozen and vibrational-equilibrium flows, part 1
[UTIAS-263-PT-1] N85-34117
Tabular and graphical solutions of regular and Mach reflections in pseudo-stationary frozen and vibrational-equilibrium flows, part 2
[UTIAS-263-PT-2] N85-34118
MACHINE TOOLS
Properties of tungsten-free steel for cutting tools
[BLL-M-35808-(5828.4)] N85-34259
Generated spiral bevel gears: Optimal machine-tool settings and tooth contact analysis
[NASA-TM-87075] N85-34405
MACHINING
Method of precisely modifying predetermined surface layers of a workpiece by cluster ion impact therewith
[DE85-006519] N85-34710
MAGNET COILS
Series-counterpulse repetitive-pulse inductive storage circuit
[DE85-006438] N85-34342
MAGNETIC ANOMALIES
Solar cycle variations of the anaomalous cosmic ray component
[SH-4.6-2] N85-35040
Temporal variations of the anomalous oxygen component, 1977 - 1984
[SH-4.6-3] N85-35041
MAGNETIC COILS
Reversing-counterpulse repetitive-pulse inductive storage circuit
[DE85-006409] N85-34344
Apparatus for unilateral generation of a homogeneous magnetic field
[DE85-006001] N85-34345
Assessment of magnetic field asymmetries in ELMO Bumpy square
[DE85-011559] N85-34705
MAGNETIC DIPOLES
On the influence of the heliomagnetospheric periphery on the galactic cosmic rays
[SH-4.2-19] N85-34856
Pulsars as cosmic ray particle accelerators: Dynamics of electrons
[OG-8.2-23] N85-34919
MAGNETIC DISTURBANCES
Study of spectral exponent on quiet and disturbed days
[SH-4.5-10] N85-35028
The cosmic ray differential diurnal variation dependences on the zenith angle and the geomagnetic disturbance
[SH-4.5-16] N85-35033
MAGNETIC EFFECTS
Summary of activities, 1983
[LBL-18500] N85-34605
Heavy cosmic ray measurement aboard Spacelab-1
[SH-10.1-7] N85-35138
MAGNETIC EQUATOR
Spatial variation of cosmic rays near the heliospheric current sheet
[SH-4.2-10] N85-34848
Effects of a wavy neutral sheet on cosmic ray anisotropies
[SH-4.2-11] N85-34849
Determination of galactic cosmic ray latitudinal gradient using Earth based detectors
[SH-4.2-13] N85-34851
MAGNETIC FIELD CONFIGURATIONS
Potential effect in transport due to non-axisymmetric confining field N85-34645
Activities of the RF Section N85-34646
Radial transport caused by collision N85-34652
Assessment of magnetic field asymmetries in ELMO Bumpy square
[DE85-011559] N85-34705
MAGNETIC FIELD INVERSIONS
Effects of solar magnetic field on cosmic rays
[SH-4.2-12] N85-34850
On the influence of the heliomagnetospheric periphery on the galactic cosmic rays
[SH-4.2-19] N85-34856
An update on the correlation between the cosmic radiation intensity and the geomagnetic AA index
[SH-4.2-24] N85-34861
MAGNETIC FIELDS
Theoretical and Experimental Beam Plasma Physics (TEBPP) N85-34166
Improved negative ion source
[DE85-006445] N85-34241
Apparatus for unilateral generation of a homogeneous magnetic field
[DE85-006001] N85-34345
Some physical differences between sheet plasma and multicusp plasma as volume produced H- or D- ion sources
[IPPJ-728] N85-34637
Size effects of vacuum chamber for H- (D-) ion volume production by sheet plasma 1
[IPPJ-731] N85-34639
Magnetohydrodynamic equilibrium and stability of spheromak with spheroidal plasma-vacuum interface
[IPPJ-732] N85-34640
Radial transport phenomena for TMX-upgrade N85-34647
RF induced radial diffusion in tandem mirrors N85-34649
Induced azimuthal electric field effects on tandem transport and ambipolarity N85-34650
Low frequency instability in a mirror field N85-34657
Azimuthal uniformity and current balance study of ICRH-produced plasma in RFC-XXM N85-34659
Breakdown of intrinsic ambipolarity for the radial diffusion due to a rotating RF field N85-34660
Guiding center distribution function and longitudinal invariant N85-34663
Simulation studies on stability of hot electron plasma N85-34664
Behavior of helically-trapped fast ion orbits in heliotron E N85-34666
Neoclassical diffusion including ellipticity in a heliotron-like configuration N85-34667
Technology of magnetically driven accelerators
[DE85-011857] N85-34700
Acceleration of ions and electrons to near-cosmic ray energies in a perpendicular shock: The January 6, 1978 event
[SH-1.5-4] N85-34773
Isotopic overabundances and the energetic particle model of solar flares
[SH-2.2-1] N85-34796
The dispersive evolution of charged-particle bunches in random magnetic fields
[SH-4.1-2] N85-34828
Numerical descriptions of cosmic-ray transport
[SH-4.1-3] N85-34829
Latitudinal gradients of cosmic rays and the polarity reversal of the heliospheric magnetic field: A preliminary evaluation
[SH-4.2-16] N85-34853
Alfven wave scattering and the secondary to primary ratio
[OG-7.2-9] N85-34878
The role of cosmic rays in magnetic hydrodynamics of interstellar medium
[OG-7.2-15] N85-34882
On magnetic pair production above fast pulsar polar caps
[OG-8.2-13] N85-34909
Cosmic rays 10Be biennal data and their relationship to aurorae and sunspots
[SH-7.1-1] N85-35094
MAGNETIC FILMS
Changes in lattice cell parameter of film intermetallic compounds RT2
[BLL-M-35874-(5828.4)] N85-34261
MAGNETIC FLUX
Neutral particle beam intensity controller
[DE85-006411] N85-34604
Effect of ECH and ICH on ambipolar potential in NBT-1M N85-34661
Stellarator approach to fusion plasma confinement
[DE85-011420] N85-34704
Interstellar turbulence, random density variations, and scintillation measurements
[OG-7.2-13] N85-34880
MAGNETIC MIRRORS
Proceedings of the US-Japan Workshop on Transport in Open-Ended Systems
[IPPJ-727] N85-34644
Electron dynamics and transport in a mirror field N85-34656
MAGNETIC PROPERTIES
Magnitude and range of the RKKy interaction in SmRh4B4
[DE85-012284] N85-34712
MAGNETIC RIGIDITY
Diurnal effect in cosmic rays at middle latitudes according to stratospheric measurements
[SH-4.5-8] N85-35026
Anomalous increase of solar anisotropy above 150GV in 1981-1983
[SH-4.5-18] N85-35035
Re-evaluation of cosmic ray cutoff terminology
[SH-6.1-11] N85-35084
The use of the McIlwain L-parameter to estimate cosmic ray vertical cutoff rigidities for different epochs of the geomagnetic field
[SH-6.1-12] N85-35085
MAGNETIC SPECTROSCOPY
Improved negative ion source
[DE85-006445] N85-34241
MAGNETIC STORMS
Transient cosmic ray increase associated with a geomagnetic storm
[SH-5.1-8] N85-35062
Study of dominating parameters of high speed solar plasma streams in relation to cosmic ray and geomagnetic storms
[SH-5.1-11] N85-35064

Dynamics of the penetration boundaries of solar protons during a strong magnetic storm
[SH-6.1-16] N85-35089

MAGNETIC SURVEYS
Method for determining depth and shape of a sub-surface conductive object
[DE85-006502] N85-34389
Magnetic search system
[PB85-185108] N85-34477

MAGNETIC VARIATIONS
Diurnal variations from muon data at Takeyama underground station
[SH-4.5-13] N85-35030
Long term changes in cosmic ray diurnal variations observed by ion chambers in Hong Kong and Japan
[SH-4.5-14] N85-35031
The modulation features of the long-period cosmic ray variations in connection with the sign change of the general magnetic field of the Sun
[SH-4.5-15] N85-35032
Change of cosmic ray anisotropy with solar activity
[SH-4.5-20] N85-35037
Magnetic fluctuation and cosmic ray diurnal variations
[SH-4.5-21] N85-35038
Solar cycle variations of the anaomalous cosmic ray component
[SH-4.6-2] N85-35040

MAGNETIZATION
Diffusion of strongly magnetized cosmic ray particles in a turbulent medium
[OG-7.2-16] N85-34883

MAGNETOELASTIC WAVES
Resonant ion acceleration by oblique magnetosonic shock wave in a collisionless plasma
[IPPJ-735] N85-34643

MAGNETOHYDRODYNAMIC FLOW
Time-dependent nonlinear cosmic ray shocks confirming abstract
[OG-8.1-3] N85-34893
Efficiency of regular acceleration of particles by a shock wave at different injection regimes
[OG-8.1-13] N85-34902

MAGNETOHYDRODYNAMIC STABILITY
User's manual for the FLORA equilibrium and stability code
[DE85-013182] N85-34590
Magnetohydrodynamic equilibrium and stability of spheromak with spheroidal plasma-vacuum interface
[IPPJ-732] N85-34640
Low frequency instability in a mirror field ECH tokamak N85-34657
[DE85-012074] N85-34707
Onset of solar flares as predicted by two-dimensional MHD-models of quiescent prominences
[SH-1.3-1] N85-34750
A cosmic ray driven instability
[OG-8.1-5] N85-34895

MAGNETOHYDRODYNAMIC TURBULENCE
Prompt acceleration of ions by oblique turbulent shocks in solar flares
[SH-1.1-6] N85-34733
Isotopic overabundances and the energetic particle model of solar flares
[SH-2.2-1] N85-34796
Diffusion of strongly magnetized cosmic ray particles in a turbulent medium
[OG-7.2-16] N85-34883

MAGNETOHYDRODYNAMIC WAVES
Stochastic particle acceleration in solar flares
[SH-1.1-4] N85-34731
Alfven wave scattering and the secondary to primary ratio
[OG-7.2-9] N85-34878
Diffusion of strongly magnetized cosmic ray particles in a turbulent medium
[OG-7.2-16] N85-34883
The role of cosmic rays and Alfven waves in the structure of the galactic halo
[OG-7.2-18] N85-34885
A cosmic ray driven instability
[OG-8.1-5] N85-34895
Relativistic transport theory for cosmic-rays
[OG-8.3-8] N85-34926

MAGNETOHYDRODYNAMICS
Moving finite element method for ICF target implosion N85-34675
Instrument to synchronize Thomson scattering diagnostic measurements with MHD activity in a Tokamak
[DE85-012082] N85-34708
Onset of solar flares as predicted by two-dimensional MHD-models of quiescent prominences
[SH-1.3-1] N85-34750
The role of cosmic rays in magnetic hydrodynamics of interstellar medium
[OG-7.2-15] N85-34882

MAGNETOMETERS
Magnetic search system
[PB85-185108] N85-34477

MAGNETOSPHERE
Waves in Space Plasmas (WISP) N85-34164
Cosmic-ray transport in the galactic magnetosphere
[OG-7.2-17] N85-34884
The influence of quiet asymmetric magnetosphere on the cutoff rigidities of the main cone
[SH-6.1-10] N85-35083
Penetration of solar protons into the Earth's magnetosphere on November 22, 1977
[SH-6.1-15] N85-35088
Dynamics of the penetration boundaries of solar protons during a strong magnetic storm
[SH-6.1-16] N85-35089
The influence of the Earth's magnetosphere on the high-energy solar protons
[SH-6.1-22] N85-35093
A suggested standardized format for cosmic ray ground-level event data
[SH-9.1-15] N85-35130
Observation of nuclei with energies 8-30 MeV per nucleon in the Earth's magnetosphere at the altitudes 350 KM
[SH-10.1-5] N85-35136

MAGNETRONS
Improved negative ion source
[DE85-006445] N85-34241

MAINTENANCE
Upgrading auxiliary facility outleakage and combustion detection
[DE85-012796] N85-34386
Maintenance port system
[AD-D011724] N85-34594

MAN ENVIRONMENT INTERACTIONS
Agents and effects of ozone trends in the atmosphere
[AERONOMICA-ACTA-A-287-1984] N85-34466

MAN MACHINE SYSTEMS
The CADME approach to the interface of solid modellers N85-34554
Designing a graphics application interface N85-34574

MANAGEMENT METHODS
Discrete simulation models - their role in the design, development and management of inventory control systems
[PNR-90249] N85-34719

MANAGEMENT PLANNING
Study to encourage and facilitate industrial investment and involvement in space
[NASA-CR-176152] N85-34147
Analyzing performance of small projects using URS and PMAS, information pamphlet
[DE85-011964] N85-34718

MANGANESE ALLOYS
Dynamics of the melting of chromium-manganese alloys in molten steel
[BLL-M-35850-(5828.4)] N85-34252

MANGANESE ISOTOPES
Cosmogenic Mn-53 in meteorites
[SH-7.1-17] N85-35107

MANGANESE OXIDES
Iron and manganese in oxide minerals and in glasses: Preliminary consideration of Eh buffering potential at Yucca Mountain, Nevada
[DE85-011892] N85-34271

MANUALS
A manual of methods for the continuous flow determination of ammonia, nitrate-nitrite, phosphate and silicate in seawater
[IOS-177] N85-34243

MANUFACTURING
Centralized surveillance of flexible workshops for the manufacturing of composite materials
[SNIAS-851-430-103] N85-34227
Manufacturing process to reduce large grain growth in zirconium alloys
[DE85-011649] N85-34267
A rational approach to cam design N85-34311

MAPPING
Graph-theoretical exorcism
[DE85-011916] N85-34512

MAPS
The automatic labeling of geographic maps: A problem in computer aesthetics N85-34561

MARINE ENVIRONMENTS
The development and evaluation of the creep and corrosion resistant alloy IN6201
[PNR-90253] N85-34278

MARINE TECHNOLOGY
High powered epicyclic gears: Some recent development N85-34316

MARKET RESEARCH
Telecommunication market research processing
[ENST-83E018] N85-34331

MARKOV CHAINS
Tunisian climate seen through a Markov process
[CT-585] N85-34482

MARS (PLANET)
Comparisons of the North Polar Cap of Mars and the Earth's Northern Hemisphere snow cover
[NASA-TM-86191] N85-34728

MARTENSITE
Shape memory effect in uranium-niobium alloys below room temperature
[DE85-012964] N85-34268

MARTENSITIC TRANSFORMATION
Electrical resistivity and hysteresis of the equiatomic nickel-titanium alloy near the martensitic transformation temperature N85-34181

MASKING
SONTRAC: A solar neutron track chamber detector
[SH-9.1-12] N85-35127

MASS FLOW
The balancing of complex linkage mechanisms N85-34313

MASS SPECTRA
Mass resolution optimization in a large isotopic composition experiment
[OG-9.1-9] N85-34935

MASS SPECTROSCOPY
Improved negative ion source
[DE85-006445] N85-34241
Real time analysis of PETN detonation products
[DE85-009581] N85-34303

MASS TRANSFER
Determination of properties of zeolite/refrigerant combinations for solar refrigeration systems
[DE85-012009] N85-34448
Studies in thermo-hydro-chemical transport in porous and fractured media
[DE85-012555] N85-34473

MATERIALS HANDLING
Container for radioactive materials
[DE85-005757] N85-34626

MATERIALS SCIENCE
Proceedings of the Twentyseventh Japan Congress on Materials Research
[ISSN-0368-3141] N85-34180

MATERIALS TESTS
Evaluation methods of ceramic fiber reinforced metal matrix composite N85-34206

MATHEMATICAL MODELS
Component-specific modeling
[NASA-CR-174765] N85-34140
On high strain rate fragmentation of a closed vessel N85-34187
Experimental evaluation of the thermodynamic properties of concentrated aqueous potassium hydroxide solutions
[DE85-010628] N85-34238
Pressure-shear loading of PBX-9404
[DE85-009982] N85-34298
Modeling heterogeneous high explosive burn with an explicit hot-spot process
[DE85-009593] N85-34300
Three-dimensional hydrodynamic hot-spot model
[DE85-009587] N85-34301
Detonation of condensed explosives: Evolution of knowledge in the last 40 years
[ISL-CO-228/84] N85-34307
Finding the roots of the transcendental equations in problems in determining the thermal conductivity of spheres with heterogeneous boundary conditions
[BLL-M-35878-(5828.4)] N85-34347
Preliminary SPR thermal model description and results for WH-11 and BM-4
[DE85-013171] N85-34360
Detailed validation of a liquid and heat flow code against field performance
[DE85-009901] N85-34368
Mathematical modeling of ultimate heat sink cooling ponds
[TI85-009747] N85-34369
Modeling of geothermal systems
[DE85-012553] N85-34439
Ocean thermal energy conversion
[DE85-012291] N85-34456
Evaluation of source strength and dispersion model predications with data from large nitrogen tetroxide field experiments
[DE85-011855] N85-34465
Graph-theoretical exorcism
[DE85-011916] N85-34512
Computer analysis techniques for the temporal evaluation of cardiac wall motion N85-34530
A user-friendly computer-aided construction of boundaries N85-34564
Numerical solutions of the Vlasov equation N85-34672

Cubic interpolated pseudo-particle method (CIP) for solving hyperbolic-type equation N85-34673
Numerical simulation in astrophysics: Smoothed particle methods N85-34674
Moving finite element method for ICF target implosion N85-34675
Dissipation terms in one-dimensional hydrodynamic code for ICF target N85-34677
Simulation of instability of cylindrically converging shock waves N85-34679
On the heat flux derived by the moment method in Lorentzian plasma between hot and cold walls N85-34682
Observation of helical sawtooth oscillations in a tokamak
[DE85-012062] N85-34703
The 1973-1984 solar modulation of cosmic ray nuclei
[SH-4.1-16] N85-34838
Evidence for regions of negligible cosmic-ray modulation in the inner heliosphere (10 AU)
[SH-4.1-21] N85-34840
Drift and observations in cosmic-ray modulation, 2
[SH-4.2-5] N85-34843
Electron capture decay of cosmic rays: A model of the inhomogeneous interstellar medium
[OG-7.1-10] N85-34871
The model-independence of cosmic ray source determinations
[OG-7.2-1] N85-34873
Explanation of the secondary to primary ratio within the continuous Fermi accelerator model
[OG-8.3-2] N85-34921
Empirical model for the Earth's cosmic ray shadow at 400 KM: Prohibited cosmic ray access
[SH-6.1-14] N85-35087

MATHEMATICAL PROGRAMMING
A geometric modeller for turbomachinery applications N85-34556

MATRICES (MATHEMATICS)
Determination of low chloride values in Rocky Flats scrub alloy solutions and other complex matrices
[DE85-011506] N85-34234

MATRIX MATERIALS
Impact fracture mechanism of polymer plates containing a heavy inner material N85-34215
Mechanical properties of SiC fiber-reinforced reaction-bonded Si3N4 composites
[NASA-TM-87085] N85-34223
Viscoelastic behavior of short-fiber composite materials
[DE85-011233] N85-34225

MAXWELL-BOLTZMANN DENSITY FUNCTION
Effect of ECH and ICH on ambipolar potential in NBT-1M N85-34661

MEAN
The mean ionic charge of silicon in 3HE-rich solar flares
[SH-2.2-8] N85-34803

MEAN FREE PATH
Monte Carlo techniques for analyzing deep penetration problems
[DE85-011426] N85-34598

MEASURING INSTRUMENTS
Instrumentation for sensing moisture content of material using a transient thermal pulse
[NASA-CASE-NPO-15493-2] N85-34373
Apparatus and method for the spectrochemical analysis of liquids using the laser spark
[DE85-005749] N85-34387
Improved flow cytometer measurement of binding assays
[DE85-006407] N85-34390
Hydrology
[PB85-182954] N85-34440
Measurement of low energy cosmic rays aboard Spacelab-1
[SH-10.1-6] N85-35137

MECHANICAL DEVICES
The balancing of complex linkage mechanisms N85-34313
A versatile computer package for mechanism analysis N85-34314
A versatile computer package for mechanism analysis, part 2: Dynamics and balance N85-34315

MECHANICAL DRIVES
High powered epicyclic gears: Some recent development N85-34316

MECHANICAL ENGINEERING
Proceedings of the Mechanisms Conference, volume 1 N85-34309
Proceedings of the Mechanisms Conference, volume 2 N85-34318
An introduction to finite elements N85-34319
Inertial stresses and deformations in mechanisms N85-34320
Optimisation in the computer aided design of mechanisms N85-34321

MECHANICAL MEASUREMENT
A versatile computer package for mechanism analysis N85-34314

MECHANICAL OSCILLATORS
Method for controlling the viscosity of siloxane oils
[DE85-011586] N85-34221

MECHANICAL PROPERTIES
Mechanical properties of SiC fiber-reinforced reaction-bonded Si3N4 composites
[NASA-TM-87085] N85-34223
Proceedings of the Mechanisms Conference, volume 1 N85-34309
A versatile computer package for mechanism analysis, part 2: Dynamics and balance N85-34315
Proceedings of the Mechanisms Conference, volume 2 N85-34318
Generated spiral bevel gears: Optimal machine-tool settings and tooth contact analysis
[NASA-TM-87075] N85-34405

MECHANIZATION
Re-designing a mechanism for higher speed: A case history from textile machinery N85-34310

MEDICAL SCIENCE
USSR report: Life sciences. Biomedical and behavioral sciences
[JPRS-UBB-85-021] N85-34489
USSR report: Space Biology and Aerospace Medicine, vol. 19, no. 3, May - June 1985
[JPRS-USB-85-005] N85-34494
Tolerance to +Gz and +Gx accelerations of individuals in older age groups in good health and with early signs of arteriosclerosis N85-34496

MELT SPINNING
Microstructures in rapidly solidified Ni-Mo alloys
[NASA-TM-87100] N85-34266

MELTING POINTS
Measurement and correlation of jet fuel viscosities at low temperatures
[NASA-CR-174911] N85-34295

MEMBRANE STRUCTURES
Evaluation of developmental membranes for the mixed reactant iron-chromium redox system
[NASA-TM-87074] N85-34443

MEMBRANES
Development and demonstration of a spiral-wound thin-film composite membrane system for the economical production of oxygen-enriched air, phase 4
[DE85-012380] N85-34288

MEMORY (COMPUTERS)
Spatial trees: A fast access method for unstructured graphical data N85-34533
Analysis of transient radiation upset in a 16K SRAM
[DE85-009442] N85-34586

MERIDIONAL FLOW
Azimuthal and meridional asymmetries of the solar wind and quasiperiodic variations of intensity of Galactic Cosmic Rays (GCR)
[SH-4.4-20] N85-35016

MESONS
The SCR flare of 16 February 1984 as recorded by the Sayan spectrograph
[SH-1.3-17] N85-34761

METAL COMBUSTION
Review of zirconium-zircaloy pyrophoricity
[DE85-011169] N85-34270

METAL CUTTING
Mechanical properties of plasma arc cut steel N85-34188

METAL FATIGUE
Fractographic analysis for nonpropagating conditions of fatigue crack at high stress ratios in mild steel N85-34194
Crystallographic orientation dependence of fatigue crack propagation in extremely low carbon steel N85-34195
Fatigue crack retardation phenomenon caused by single-multiple overloads in 2017-T3 aluminum allow N85-34196
The stress pattern analysis of coarse grain titanium specimens
[PNR-90250] N85-34433

METAL GRINDING
Study on the correlation between grinding conditions and residual stresses in ground surface of steel by the X-ray method N85-34203

METAL JOINTS
Negative flexural behavior of precase composite slabs with steel joint N85-34183

METAL MATRIX COMPOSITES
Three body abrasive wear in various metal combinations N85-34200
X-ray measurement of thermal stresses in tungsten fiber-copper composites N85-34205
Evaluation methods of ceramic fiber reinforced metal matrix composite N85-34206
Fracture behavior of aluminum composites reinforced with fiber N85-34207
Rotating bending fatigue strength of silicon carbide and alumina-fiber reinforced aluminum N85-34208

METAL OXIDES
Composite desiccant structure
[DE85-006400] N85-34226
Metal alkoxides: Models for metal oxides. Alkoxide ligands in early transition metal organometallic chemistry
[DE85-011368] N85-34269

METAL PLATES
Stresses and strains in a plate resulting from two closely-spaced interference-fit fasteners
[ARL-STRUC-TM-409] N85-34429

METAL POWDER
Influence of technology of atomization of naturally alloyed iron on grain-size characteristics of powder material
[BLL-M-35810-(5828.4)] N85-34257
Chromium-base powder alloys for welding cladding layer of oimetal
[BLL-M-35776-(5828.4)] N85-34260
Synthesis of ultrafine ceramic and metallic powders in a thermal argon rf plasma
[DE85-009634] N85-34696

METAL SURFACES
Study on the correlation between grinding conditions and residual stresses in ground surface of steel by the X-ray method N85-34203
Method for preparing hydride configurations and reactive metal surface
[DE85-006443] N85-34274

METAL WORKING
Study on the correlation between grinding conditions and residual stresses in ground surface of steel by the X-ray method N85-34203
Algorithm for calculation of strain state from measurements of node coordinates of arbitrary curvilinear grid
[BLL-M-36304] N85-34422

METAL-METAL BONDING
Anti wear property of two phasic metal composite N85-34199

METALLIC PLASMAS
Synthesis of ultrafine ceramic and metallic powders in a thermal argon rf plasma
[DE85-009634] N85-34696

METALLIZING
Development of metallization process: FSA project, cells and module formation research area
[NASA-CR-176136] N85-34447

METALLOGRAPHY
Proceedings of the Twentyseventh Japan Congress on Materials Research
[ISSN-0368-3141] N85-34180

METALS
Proceedings of the Twentyseventh Japan Congress on Materials Research
[ISSN-0368-3141] N85-34180
Method for extracting lanthanides and actinides from acid solutions by modification of Purex solvent
[DE85-005763] N85-34220
Direct determination of metals in organic matrices by Inductively Coupled Plasma-Atomic Emission Spectrometry (ICP-AES)
[DE85-012015] N85-34233

METASTABLE STATE
Modulated voltage metastable ionization detector
[NASA-CASE-ARC-11503-1] N85-34374

METEORITES
Cosmic-ray exposure records and origins of meteorites
[SH-7.1-7] N85-35099
Depth and size effects on cosmogenic nuclide production in meteorites
[SH-7.1-9] N85-35101
Clusters and cycles in the cosmic ray age distributions of meteorites
[SH-7.1-11] N85-35103
The read-out system of spatial distribution of thermoluminescence in meteorites
[SH-9.1-16] N85-35131

METEORITIC COMPOSITION
Cosmic-ray exposure records and origins of meteorites
[SH-7.1-7] N85-35099
Accelerator experiments on the contribution of secondary particles to the production of cosmogenic nuclides in meteorites
[SH-7.1-8] N85-35100
Depth and size effects on cosmogenic nuclide production in meteorites
[SH-7.1-9] N85-35101
Spallogenic origin of nuclei in meteorites
[SH-7.1-10] N85-35102

METEOROLOGICAL PARAMETERS
Description of a test site for large-scale heavy gas dispersion and combustion experiments
[DE85-004987] N85-34231
METHANE
Measurements of the fragmentation of (40)Ar, (28)Si and (12)C in CH2C and H targets between 300 and 1500 MeV/nuc at the Bevalac
[OG-7.2-19] N85-34886
METHOD OF MOMENTS
Calculation of mixed depth for some metal-Si systems
[DE85-011907] N85-34616
METHYL ALCOHOLS
Investigation of the flame speeds of propane/methanol gas mixtures
[DE85-012817] N85-34239
METROLOGY
Recommendations for the design and equipping of engineering metrology laboratories
[NPL-MOM-22] N85-34145
MICHELSON INTERFEROMETERS
Wide Angle Michelson Doppler Imaging Interferometer (WAMDII) N85-34172
MICROBIOLOGY
USSR report: Space Biology and Aerospace Medicine, vol. 19, no. 3, May - June 1985
[JPRS-USB-85-005] N85-34494
MICROCOMPUTERS
An innovative user interface for microcomputer-based computer-aided design N85-34555
Recording system for the solar neutron monitoring at Mt. Norikura
[SH-9.1-8] N85-35123
MICROMINIATURIZATION
The use of ultrasound to monitor incipient failure of rolling element bearings N85-34317
MICROORGANISMS
Screening and characterizing oleaginous microalgal species from the southeastern United States
[DE85-006787] N85-34488
Microorganisms in space flight N85-34490
MICROPROCESSORS
Magnetic search system
[PB85-185108] N85-34477
Hardware math for the 6502 microprocessor
[NASA-TM-86517] N85-34511
MICROSTRUCTURE
Manufacturing process to reduce large grain growth in zirconium alloys
[DE85-011649] N85-34267
Experimental attempt to achieve microstructure variations through temperature/time permutations for a nonwrought powder metallurgy uranium-6 niobium alloy
[DE85-013166] N85-34272
Influence of particle erosion on the microstructural changes in metals and alloys
[TI85-901384] N85-34276
High resolution electron microscopic characterization of interfaces in ceramics
[DE85-011207] N85-34289
Near-threshold fatigue: An overview of the role of microstructure and environment
[DE85-009903] N85-34431
Analytical ultrasonics for structural materials
[TI85-006132] N85-34600
MICROWAVE AMPLIFIERS
Realization and linearization of a hyperfrequency power amplifier implemented with bipolar transistors in class C polarization — microwave amplifiers
[CNES-NT-114] N85-34346
MICROWAVE EQUIPMENT
Instrumentation for sensing moisture content of material using a transient thermal pulse
[NASA-CASE-NPO-15493-2] N85-34373
MICROWAVE TRANSMISSION
New directional couplers for multimode circular waveguides applied to intense pulsed microwave systems
[DE85-011753] N85-34330
MICROWAVES
Quantitative analysis of flare accelerated electrons through their hard X-ray and microwave radiation
[SH-1.2-7] N85-34742
MIGRATION
Thermally induced chemical migration: A natural analog approach
[DE85-012308] N85-34474
MILKY WAY GALAXY
Cosmic-ray transport in the galactic magnetosphere
[OG-7.2-17] N85-34884
MILLING (MACHINING)
Re-designing a mechanism for higher speed: A case history from textile machinery N85-34310
MINERAL DEPOSITS
The United States Geological Survey in Alaska: Accomplishments during 1983
[USGS-CIRC-945] N85-34468
MINERAL METABOLISM
Fluid-electrolyte metabolism and renal function in cosmonauts following 185-day spaceflight N85-34495
MINICOMPUTERS
User's operating procedures. Volume 3: Projects directorate information programs
[NASA-CR-177950] N85-34520
MINING
Shuttle car loading system
[NASA-CASE-NPO-15949-1] N85-34722
MIRROR FUSION
Proceedings of the US-Japan Workshop on Transport in Open-Ended Systems
[IPPJ-727] N85-34644
Plug and thermal barrier potential formation in Gamma 10 N85-34648
RF induced radial diffusion in tandem mirrors N85-34649
Induced azimuthal electric field effects on tandem transport and ambipolarity N85-34650
Recent experiments in Gamma-10 N85-34651
Radial transport caused by collision N85-34652
Transport issues in Phaedrus-type plasmas N85-34653
Possibility of potential generation by lower hybrid wave N85-34654
Bounce resonance heating and radial transport of electrons N85-34655
Electron dynamics and transport in a mirror field N85-34656
Low frequency instability in a mirror field N85-34657
Model of azimuthal non-uniformities induced by RF heating in RFC-XXM N85-34658
Azimuthal uniformity and current balance study of ICRH-produced plasma in RFC-XXM N85-34659
Advanced Toroidal Facility (ATF)
[DE85-011567] N85-34699
Perspective on the next ten years in plasma physics
[DE85-011849] N85-34706
MIRRORS
Effect of ECH and ICH on ambipolar potential in NBT-1M N85-34661
Fokker-Planck calculation of hot electron formation in the thermal barrier region of tandem mirror Gamma-10
[IPPJ-726] N85-34669
A method to improve observations of gamma-ray sources near 10 (15) eV
[OG-9.5-5] N85-34982
MISSION PLANNING
Space Station Engineering and Technology Development: Proceedings of the Panel on In-Space Engineering Research and Technology Development
[NASA-CR-176110] N85-34153
MIXING
Survey of mixing in metal/insulator systems
[DE85-011938] N85-34714
MODAL RESPONSE
Automated dynamic analytical model improvement for damped structures
[NASA-CR-177945] N85-34425
MODELS
Detonation in tungsten-loaded HMX
[DE85-009606] N85-34299
Mathematical modeling of ultimate heat sink cooling ponds
[TI85-009747] N85-34369
The impact of supercomputers on experimentation: A view from a national laboratory
[NASA-TM-86822] N85-34510
Spatial trees: A fast access method for unstructured graphical data N85-34533
3D computer animation: More an evolution problem than a motion problem N85-34536
Using dynamic analysis to animate articulated bodies such as humans and robots N85-34537
Simulation studies on stability of hot electron plasma N85-34664
Perspective on the next ten years in plasma physics
[DE85-011849] N85-34706
The influence of nonstationarity of the solar activity and general solar field on modulation of cosmic rays
[SH-4.2-17] N85-34854
Spatial distribution of cosmic rays in magnetic cycles of the Sun
[SH-4.2-20] N85-34857
Diurnal anisotropy during solar activity cycle twenty and diffusion-convection model
[SH-4.5-7] N85-35025
MODULATION
Modulated voltage metastable ionization detector
[NASA-CASE-ARC-11503-1] N85-34374
Longitudinal distribution of cosmic rays in the heliosphere
[SH-4.1-14] N85-34837
Effects of solar magnetic field on cosmic rays
[SH-4.2-12] N85-34850
The influence of nonstationarity of the solar activity and general solar field on modulation of cosmic rays
[SH-4.2-17] N85-34854
The effect of the neutral sheet structure of the interplanetary magnetic field on cosmic ray distribution in space
[SH-4.2-18] N85-34855
On the influence of the heliomagnetospheric periphery on the galactic cosmic rays
[SH-4.2-19] N85-34856
Spatial distribution of cosmic rays in magnetic cycles of the Sun
[SH-4.2-20] N85-34857
11- and 22-year variations of the cosmic ray density and of the solar wind speed
[SH-4.2-21] N85-34858
The dependence of solar modulation on the sign of the cosmic ray particle charge
[SH-4.2-23] N85-34860
An update on the correlation between the cosmic radiation intensity and the geomagnetic AA index
[SH-4.2-24] N85-34861
Long-term modulation of cosmic rays during solar cycle 21
[SH-4.4-10] N85-35008
Role of solar flare index in long term modulation of cosmic ray intensity
[SH-4.4-12] N85-35009
A study of periodicities and recurrences in solar activity and cosmic ray modulation
[SH-4.4-14] N85-35010
MOIRE FRINGES
Modular digital holographic fringe data processing system
[NASA-CR-177952] N85-34376
Experiments and discussions on the analysis of interferograms with closed-loop fringes
[NPL-MOM-68] N85-34515
MOIRE INTERFEROMETRY
Experiments and discussions on the analysis of interferograms with closed-loop fringes
[NPL-MOM-68] N85-34515
MOISTURE
Upgrading auxiliary facility outleakage and combustion detection
[DE85-012796] N85-34386
MOISTURE CONTENT
Instrumentation for sensing moisture content of material using a transient thermal pulse
[NASA-CASE-NPO-15493-2] N85-34373
MOISTURE METERS
Instrumentation for sensing moisture content of material using a transient thermal pulse
[NASA-CASE-NPO-15493-2] N85-34373
MOISTURE RESISTANCE
Process for improving moisture resistance of epoxy resins by addition of chromium ions
[NASA-CASE-LAR-13226-1] N85-34282
MOLECULAR CLOUDS
Cosmic ray secondary nuclei and the structure of the galaxy
[OG-7.2-4] N85-34876
Alfven wave scattering and the secondary to primary ratio
[OG-7.2-9] N85-34878
Giant molecular clouds as regions of particle acceleration N85-34913
MOLECULAR INTERACTIONS
Intermolecular explosives
[DE85-009609] N85-34296
MOLECULAR IONS
Imaging Spectrometric Observatory (ISO) N85-34169
Negative ion sources equipped with continuous annular and spherical geometry surface ionizers
[DE85-011939] N85-34519
MOLECULAR STRUCTURE
On the potential link equation of a spot centre with relative deformation for a semi-infinite molecular crystal
[BLL-M-35795-(5828.4)] N85-34711
MOLECULES
Electron density distribution analysis for nitroguanidine
[DE85-009598] N85-34603
Solar modulation of cosmic ray intensity and solar flare events inferred from (14)C contents in dated tree rings
[SH-7.1-2] N85-35095
MOLTEN SALT ELECTROLYTES
Electrolyte resevoir for carbonate fuel cells
[DE85-005736] N85-34460

MOLYBDENUM
The effect of pre-heating on the structure and properties of chromiun-molybdenum steels
[BLL-M-35897-(5828.4)] N85-34255
Development of metallization process: FSA project, cells and module formation research area
[NASA-CR-176136] N85-34447
MOLYBDENUM ALLOYS
Microstructures in rapidly solidified Ni-Mo alloys
[NASA-TM-87100] N85-34266
Characterization of modified 9 Cr Mo steel extruded pipe
[DE85-012056] N85-34430
MOMENTS OF INERTIA
Inertial stresses and deformations in mechanisms N85-34320
MOMENTUM
Electron loss process and cross section of multiply charged ions by neutral atoms N85-34685
MONITORS
Monitoring dosage of volatile compounds in tests at low barometric pressure N85-34506
MONTE CARLO METHOD
Coupled electron-photon transport calculations using the method of discrete ordinates
[DE85-009444] N85-34597
Monte Carlo techniques for analyzing deep penetration problems
[DE85-011426] N85-34598
CYLTRAN calculations of electron effects on XD detectors
[LA-10264-MS] N85-34601
Low-energy sputterings with the Monte Carlo Program ACAT
[IPPJ-AM-40] N85-34690
Monte Carlo calculations of relativistic solar proton propagation in interplanetary space
[SH-3.2-11] N85-34826
Modeling a high energy gamma-ray telescope
[OG-9.2-5] N85-34944
A position sensitive phoswich hard X-ray detector system
[OG-9.3-12] N85-34967
On the statistical significance of excess events: Remarks of caution and the need for a standard method of calculation
[OG-9.5-10] N85-34987
Additional flux of particles and albedo-electrons in upper atmosphere
[SH-6.1-6] N85-35080
Monte Carlo calibration of the SMM gamma ray spectrometer for high energy gamma rays and neutrons
[SH-9.1-6] N85-35121
MOTION
3D computer animation: More an evolution problem than a motion problem N85-34536
Using dynamic analysis to animate articulated bodies such as humans and robots N85-34537
Towards an integrated view of 3-D computer character animation N85-34538
Research issues in generating graphical explanations N85-34539
MOUNTAINS
The 1984 biotic studies of Yucca Mountain, Nevada test site, Nye County, Nevada
[DE85-011715] N85-34487
MULTIVARIATE STATISTICAL ANALYSIS
Computer graphics for multivariate data N85-34528
MUONS
Corrected sidereal anisotropy for underground muons
[SH-4.4-7] N85-35005
Long-term modulation of galactic cosmic rays in high-energy region
[SH-4.4-22] N85-35018
The cosmic ray differential diurnal variation dependences on the zenith angle and the geomagnetic disturbance
[SH-4.5-16] N85-35033
Anomalous increase of solar anisotropy above 150GV in 1981-1983
[SH-4.5-18] N85-35035
Atmospheric effects on the underground muon intensity
[SH-6.1-3] N85-35078
Burst size distributions in the digitized data of the ion chambers t Mt. Norikura and sea level stations
[SH-9.1-9] N85-35124
Plastic scintillators in coincidence for the study of multi-particle production of sea level cosmic rays in dense medium
[SH-9.1-11] N85-35126
New Matsushiro underground cosmic ray station (220 M.W.E. in depth)
[SH-9.1-14] N85-35129
MUSCULAR STRENGTH
Rat skeletal muscles with simulation of physiological effects of weightlessness (morphological study) N85-34502
MUSCULOSKELETAL SYSTEM
Fluid-electrolyte metabolism and renal function in cosmonauts following 185-day spaceflight N85-34495

N

NAMING
The automatic labeling of geographic maps: A problem in computer aesthetics N85-34561
NASA PROGRAMS
Department of Housing and Urban Development Independent Agencies Appropriation Bill, 1986
[S-REPT-99-129] N85-34720
National Aeronautics and Space Administration research and development: Program description N85-34721
A spacefaring people: Perspectives on early spaceflight
[NASA-SP-4405] N85-35142
Management of large-scale technology N85-35145
NAVIER-STOKES EQUATION
A three-dimensional viscous flow analysis for the helicopter tip vortex generation problem
[NASA-CR-3906] N85-34114
Comments on the prediction of dynamic stall
[GU-AERO-8501] N85-34125
A curvilinear coordinate method for the solutions of initial value problems using the third-order upwind differencing scheme
[IPPJ-734] N85-34642
NEGATIVE IONS
Improved negative ion source
[DE85-006445] N85-34241
Negative ion sources equipped with continuous annular and spherical geometry surface ionizers
[DE85-011939] N85-34619
NEON
Photoionization-pumped, Ne 2, X-ray laser studies project
[DE85-012973] N85-34399
NEUTRAL BEAMS
Recent experiments in Gamma-10 N85-34651
NEUTRAL GASES
On the anomalous component
[SH-4.6-6] N85-35044
NEUTRAL PARTICLES
Neutral particle beam intensity controller
[DE85-006411] N85-34604
Behavior of helically-trapped fast ion orbits in heliotron E N85-34666
Neutral pion production in solar flares
[SH-1.4-7] N85-34767
NEUTRAL SHEETS
Cosmic ray intensity and the tilt of the neutral sheet
[SH-4.2-8] N85-34846
Effects of a wavy neutral sheet on cosmic ray anisotropies
[SH-4.2-11] N85-34849
Difference between even and odd 11-year cycles in cosmic ray intensity
[SH-4.2-22] N85-34859
Influence of the neutral sheet on the Swinson's type north-south anisotropy of cosmic rays
[SH-4.3-10] N85-34995
The sidereal semi-diurnal variation observed at high zenith angles at Mawson, 1968-1984, and the polarity of the solar main field
[SH-4.4-6] N85-35004
NEUTRINOS
Detection of 10 (1) GeV cosmic neutrinos with a space station
[OG-9.4-10] N85-34977
Neutrino production from the solar atmosphere
[SH-8.1-9] N85-35114
Solar cosmic ray bursts and solar neutrino fluxes
[SH-8.1-10] N85-35115
Three dimensional calculation of flux of low energy atmospheric neutrinos
[SH-8.1-11] N85-35116
NEUTRON BEAMS
Cosmic ray north-south anisotropy 1961 - 1983
[SH-4.2-6] N85-34844
NEUTRON COUNTERS
Spectra of solar proton ground level events using neutron monitor and neutron moderated detector recordings
[SH-1.3-14] N85-34759
Determination of galactic cosmic ray latitudinal gradient using Earth based detectors
[SH-4.2-13] N85-34851
An update on the correlation between the cosmic radiation intensity and the geomagnetic AA index
[SH-4.2-24] N85-34861
Cosmic ray sidereal diurnal variation of galactic origin observed by neutron monitors
[SH-4.4-2] N85-35000
Observations of cosmic-ray modulations in the fall, 1984
[SH-5.1-16] N85-35069
Frequency spectra of short-period variations of cosmic ray
[SH-5.1-17] N85-35070
Coupling functions for lead and lead-free neutron monitors from the latitudinal measurements performed in 1982 in the research station Academician Kurchatov
[SH-6.1-1] N85-35076
On the solar cycle variation in the barometer coefficients of high latitude neutron monitors
[SH-6.1-2] N85-35077
Recording system for the solar neutron monitoring at Mt. Norikura
[SH-9.1-8] N85-35123
Sensitivity of single and multiple cosmic ray neutrons to the surrounding medium in a lead-free monitor
[SH-9.1-10] N85-35125
SONTRAC: A solar neutron track chamber detector
[SH-9.1-12] N85-35127
The neutron moderated detector and groundbased cosmic ray modulation studies
[SH-9.1-13] N85-35128
New Matsushiro underground cosmic ray station (220 M.W.E. in depth)
[SH-9.1-14] N85-35129
A suggested standardized format for cosmic ray ground-level event data
[SH-9.1-15] N85-35130
The influences of the galactic cosmic ray on the atmospheric ozone
[SH-10.1-1] N85-35133
NEUTRON CROSS SECTIONS
The effects of newly measured cross sections in hydrogen on the production of secondary nuclei during the propagation of cosmic rays through interstellar H
[OG-7.2-2] N85-34874
NEUTRON DECAY
High energy neutron and gamma-radiation generated during the solar flares
[SH-1.4-8] N85-34768
NEUTRON EMISSION
Helios 1 energetic particle observations of the solar gamma ray flare events of 7, 21 June 1980 and 3 June 1982
[SH-1.3-8] N85-34755
Source energy spectra from demodulation of solar particle data by interplanetary and coronal transport
[SH-1.3-13] N85-34758
On the angular and energy distribution of solar neutrons generated in P-P reactions
[SH-1.4-9] N85-34769
Recording system for the solar neutron monitoring at Mt. Norikura
[SH-9.1-8] N85-35123
Sensitivity of single and multiple cosmic ray neutrons to the surrounding medium in a lead-free monitor
[SH-9.1-10] N85-35125
The neutron moderated detector and groundbased cosmic ray modulation studies
[SH-9.1-13] N85-35128
NEUTRON FLUX DENSITY
Solar modulation of cosmic ray intensity and solar flare events inferred from (14)C contents in dated tree rings
[SH-7.1-2] N85-35095
NEUTRON IRRADIATION
The 1983 international intercomparison of nuclear accident dosimetry systems at Oak Ridge National Laboratory
[DE85-011303] N85-34382
Rapid annealing of temperature-compensated, precision voltage references following fast-neutron irradiation
[DE85-009821] N85-34609
NEUTRON SCATTERING
Capture in the 1.15-keV iron resonance
[DE85-011913] N85-34612
NEUTRON SOURCES
Time extended production of neutrons during a solar flare
[SH-1.4-1] N85-34762
NEUTRON SPECTRA
SONTRAC: A solar neutron track chamber detector
[SH-9.1-12] N85-35127
The neutron moderated detector and groundbased cosmic ray modulation studies
[SH-9.1-13] N85-35128
NEUTRON SPECTROMETERS
Observations on (3)He neutron spectrometry
[DE85-010731] N85-34608

NEUTRON STARS
X-ray spectra of bursting neutron stars N85-34686
Quasiperiodic oscillations in bright galactic-buige X-ray sources
[NASA-CR-176138] N85-34723
A very important process of nucleosynthesis in stars
[OG-7.1-11] N85-34872
NEUTRONS
Novette diagnostic support
[DE85-012937] N85-34383
Application of evaluated fission-product delayed-neutron precursor data in reactor kinetics calculations
[DE85-012728] N85-34624
The SCR flare of 16 February 1984 as recorded by the Sayan spectrograph
[SH-1.3-17] N85-34761
Further observations of protons resulting from the decay of neutrons ejected by solar flares
[SH-1.4-2] N85-34763
Suggestions for improving the efficiency of ground-based neutron monitors for detecting solar neutrons
[SH-1.4-3] N85-34764
Search for solar neutrons using NM-64 equipment
[SH-1.4-5] N85-34765
A search for solar neutrons on a long duration balloon flight
[SH-1.4-6] N85-34766
High energy neutron and gamma-radiation generated during the solar flares
[SH-1.4-8] N85-34768
Energetic particle observations of the solar-gamma ray/neutron flare events of 3 Jun 1982 and 21 June 1980 isotopic and chemical composition
[SH-2.1-3] N85-34784
Exponential anisotropy of solar cosmic rays
[SH-3.2-1] N85-34817
Neutron-rich nuclei in cosmic rays and Wolf-Rayet stars
[OG-8.2-6] N85-34906
An approach of reducing the background induced by neutrons
[OG-9.3-5] N85-34960
Neutron-induced 2.2 MeV background in gamma ray telescopes
[OG-9.3-6] N85-34961
Characteristics of cosmic ray pole-equator anisotropy derived from spherical harmonic analysis of neutron monitor data
[SH-4.3-12] N85-34996
First zonal harmonic component of cosmic ray neutron intensity
[SH-4.3-13] N85-34997
Monte Carlo calibration of the SMM gamma ray spectrometer for high energy gamma rays and neutrons
[SH-9.1-6] N85-35121
Comparisons of monthly mean cosmic ray counting rates observes from worldwide network of neutron monitors
[SH-9.1-7] N85-35122
NEVADA
Iron and manganese in oxide minerals and in glasses: Preliminary consideration of Eh buffering potential at Yucca Mountain, Nevada
[DE85-011892] N85-34271
NEWTON-RAPHSON METHOD
X-ray spectra of bursting neutron stars N85-34686
NICKEL
Calculating the interatomic pair potential allowing for resonance interaction in titanium, nickel and vanadium
[BLL-M-35843-(5828.4)] N85-34249
Metal (2) 4,4',4',4'' phthalocyanine tetraamines as curing agents for epoxy resins
[NASA-CASE-ARC-11424-1] N85-34281
NICKEL ALLOYS
Electrical resistivity and hysteresis of the equiatomic nickel-titanium alloy near the martensitic transformation temperature N85-34181
Microstructures in rapidly solidified Ni-Mo alloys
[NASA-TM-87100] N85-34266
The development and evaluation of the creep and corrosion resistant alloy IN6201
[PNR-90253] N85-34278
NIMBUS SATELLITES
Satellites and politics: Weather, communications, and earth resources N85-35144
NIOBIUM
Shape memory effect in uranium-niobium alloys below room temperature
[DE85-012964] N85-34268
NIOBIUM ALLOYS
Experimental attempt to achieve microstructure variations through temperature/time permutations for a nonwrought powder metallurgy uranium-6 niobium alloy
[DE85-013166] N85-34272
NITRATES
Throughfall rate and chemistry studies: Whiteface Mountain
[DE85-012407] N85-34464
NITRIDING
Nitriding of super alloys for enhancing physical properties
[DE85-005762] N85-34275
NITRO COMPOUNDS
Ethylenediamine salt of 5-nitrotetrazole and preparation
[DE85-005738] N85-34306
NITROGEN
Electrode erosion in arc discharges at atmospheric pressure
[NASA-TM-87087] N85-34178
Oxygen analyzer
[DE85-006002] N85-34392
Determination of individual tolerance in hyperbaric oxygen N85-34507
NITROGEN OXIDES
Forecasting future industrial SO2 and NC/sub x/ emissions, revised N85-34461
NITROGEN TETROXIDE
Evaluation of source strength and dispersion model predications with data from large nitrogen tetroxide field experiments
[DE85-011855] N85-34465
NITROGENATION
Effects of acid rain on forest nutrient status
[DE85-012486] N85-34463
NITROGUANIDINE
Electron density distribution analysis for nitroguanidine
[DE85-009598] N85-34603
NOISE (SOUND)
Some problems in high speed gears and gearing N85-34312
Generated spiral bevel gears: Optimal machine-tool settings and tooth contact analysis
[NASA-TM-87075] N85-34405
NOISE PREDICTION (AIRCRAFT)
Some problems in high speed gears and gearing N85-34312
NOISE PROPAGATION
Some problems in high speed gears and gearing N85-34312
NOISE REDUCTION
Some problems in high speed gears and gearing N85-34312
Langley aeronautics and space test highlights, 1984
[NASA-TM-87585] N85-35151
NOISE SPECTRA
A comparison of calculated and measured background noise rates in hard X-ray telescopes at balloon altitude
[OG-9.3-7] N85-34962
NONADIABATIC THEORY
Nonlocal and nonadiabatic expression for the ponderomotive force near cyclotron resonance
[IPPJ-736] N85-34636
NONDESTRUCTIVE TESTS
Acoustic emission during transformation of austenite in 38KhN3MF steel
[BLL-M-35825-(5828.4)] N85-34256
NONEQUILIBRIUM CONDITIONS
Calculations of heavy ion charge state distributions for nonequilibrium conditions
[SH-2.1-12] N85-34793
NONLINEAR EQUATIONS
Numerical model of a pulse combustor
[DE85-011717] N85-34240
A review of spectral methods
[NASA-CR-172502] N85-34350
Nonlinear flap-lag-extensional vibrations of rotating, pretwisted, preconed beams including Coriolis effects
[NASA-TM-87102] N85-34427
DISPL1: A software package for one and two spatially dimensioned kinetics-diffusion problems
[ANL-84-56] N85-34516
NONLINEARITY
Elastohydrodynamic lubrication calculations used as a tool to study scuffing
[NASA-TM-87097] N85-34408
Nonlinear adhesive behavior effects in a cracked orthotropic sheet stiffened by a semi-infinite orthotropic sheet
[NASA-TM-87584] N85-34426
NONPARAMETRIC STATISTICS
A new approach to evaluate gamma-ray measurements
[OG-9.5-11] N85-34988
NORMAL DENSITY FUNCTIONS
The dispersive evolution of charged-particle bunches in random magnetic fields
[SH-4.1-2] N85-34828
On the statistical significance of excess events: Remarks of caution and the need for a standard method of calculation
[OG-9.5-10] N85-34987
NOTCH TESTS
Effect of strain rate on the initial failure of notched GRP laminates N85-34214
NOVAE
Strong earthquakes, novae and cosmic ray environment
[SH-10.1-3] N85-35135
NOZZLE FLOW
Nozzle wall roughness effects on free-stream noise and transition in the pilot low-disturbance tunnel
[NASA-TM-86389] N85-34355
NUCLEAR EXPLOSIONS
Marine Sample Exploitation Project: Estimates regarding the sensitivity and technology for the detection of nuclear explosion debris in the marine environment
[DE85-013176] N85-34462
NUCLEAR FISSION
Liquid uranium alloy-helium fission reactor
[DE85-006511] N85-34607
A very important process of nucleosynthesis in stars
[OG-7.1-11] N85-34872
NUCLEAR FUEL ELEMENTS
Evacuate and backfill apparatus and method
[DE85-006018] N85-34411
NUCLEAR FUELS
Liquid uranium alloy-helium fission reactor
[DE85-006511] N85-34607
Separation of uranium from technetium in recovery of spent nuclear fuel
[DE85-006499] N85-34627
NUCLEAR FUSION
Numerical solutions of the Vlasov equation N85-34672
Dissipation terms in one-dimensional hydrodynamic code for ICF target N85-34677
Stability of implosion dynamics N85-34680
Nucleosynthesis in the terrestrial and solar atmospheres
[SH-2.2-2] N85-34797
Propagation and nucleosynthesis of ultraheavy cosmic rays
[OG-7.1-5] N85-34867
A very important process of nucleosynthesis in stars
[OG-7.1-11] N85-34872
Results of ultra-low level 71ge counting for application in the Gallex-solar neutrino experiment at the Gran Sasso Underground Physics Laboratory
[SH-8.1-2] N85-35108
NUCLEAR INTERACTIONS
Ninteenth International Cosmic Ray Conference. OG sessions, volume 3
[NASA-CP-2376-VOL-3] N85-34862
Cosmic ray secondary nuclei and the structure of the galaxy
[OG-7.2-4] N85-34876
NUCLEAR MAGNETIC RESONANCE
Apparatus for unilateral generation of a homogeneous magnetic field
[DE85-006001] N85-34345
NUCLEAR MEDICINE
Applications of CdTe to nuclear medicine
[DE85-011877] N85-34492
NUCLEAR PARTICLES
Abundances from solar-flare gamma-ray line spectroscopy
[SH-2.1-13] N85-34794
The heavy ions in space experiment
[OG-9.1-10] N85-34936
Cherenkov-dE/dx-range measurements on cosmic ray iron group nuclei
[OG-9.1-12] N85-34937
The response of ionization chambers to relativistic heavy nuclei
[OG-9.1-13] N85-34938
NUCLEAR PHYSICS
Physics Division annual review, 1 April 1983 - 31 March 1984
[ANL-84-24] N85-34602
NUCLEAR RADIATION
MATADOR (Methods for the Analysis of Transport And Deposition Of Radionuclides) code description and user's manual
[TI85-901402] N85-34592
Abundances from solar-flare gamma-ray line spectroscopy
[SH-2.1-13] N85-34794
NUCLEAR REACTIONS
Pairing correction of particle-hole state densities for two kinds of fermions
[DE85-011549] N85-34620

NUCLEATION
The effect of liquid-liquid phase separation of glass on the properties and crystallization behavior
[NASA-TM-77890] N85-34285

NUCLEI
Breakdown of helium nuclei in matter processed near black holes
[OG-8.2-20] N85-34916

NUCLEI (NUCLEAR PHYSICS)
Study of photon emission by electron capture during solar nuclei acceleration, 1: Temperature-dependent cross section for charge changing processes
[SH-1.1-8] N85-34735
Study of photon emission by electron capture during solar nuclei acceleration. 2: Delimitation of conditions for charge transfert establishment
[SH-1.1-9] N85-34736
Observation of the fluxes of nuclei with energies 10-20 MEV per nucleon during the solar flare of April 26, 1984
[SH-2.1-1] N85-34783
Measurements of the fragmentation of (40)Ar, (28)Si and (12)C in CH2C and H targets between 300 and 1500 MeV/nuc at the Bevalac
[OG-7.2-19] N85-34886
Cross sections for the production of fragments with Z greater than or equal to 8 by fragmentation of Z greater than or equal to 9 and less than or equal to 26 nuclei
[OG-7.2-22] N85-34889
Calculation of improved spallation cross sections
[OG-7.2-23] N85-34890
Cerenkov counters for high energy nuclei: Some new developments
[OG-9.1-5] N85-34931
Detector calibration of the Indian cosmic ray experiment (IONS) in Space-Shuttle Spacelab-13
[SH-9.1-2] N85-35117
Observation of nuclei with energies 8-30 MeV per nucleon in the Earth's magnetosphere at the altitudes 350 KM
[SH-10.1-5] N85-35136

NUCLEONS
Observation of nuclei with energies 8-30 MeV per nucleon in the Earth's magnetosphere at the altitudes 350 KM
[SH-10.1-5] N85-35136
Heavy cosmic ray measurement aboard Spacelab-1
[SH-10.1-7] N85-35138

NUCLIDES
Variations in the propagation of UH-nuclei
[OG-7.1-1] N85-34863
Cosmogenic-nuclide production by primary cosmic-ray protons
[SH-7.1-6] N85-35098

NULL HYPOTHESIS
A new approach to evaluate gamma-ray measurements
[OG-9.5-11] N85-34988

NUMERICAL ANALYSIS
Three-dimensional hydrodynamic hot-spot model
[DE85-009587] N85-34301
Modeling of geothermal systems
[DE85-012553] N85-34439
The impact of supercomputers on experimentation: A view from a national laboratory
[NASA-TM-86822] N85-34510
Analytic and numerical calculations of the ambipolar electric field in a stellarator N85-34665
Numerical simulation in astrophysics: Smoothed particle methods N85-34674
Numerical calculations on shock loaded materials N85-34676
Two-dimensional simulation of LIB target implosion N85-34678
Effects of a wavy neutral sheet on cosmic ray anisotropies
[SH-4.2-11] N85-34849
The influence of nonstationarity of the solar activity and general solar field on modulation of cosmic rays
[SH-4.2-17] N85-34854
Time-dependent nonlinear cosmic ray shocks confirming abstract
[OG-8.1-3] N85-34893

NUMERICAL CONTROL
Project management using graphics N85-34560
The automatic labeling of geographic maps: A problem in computer aesthetics N85-34561

NUTRIENTS
Effects of acid rain on forest nutrient status
[DE85-012486] N85-34463

O

O STARS
Possible origin of the anomalous component of cosmic rays
[SH-4.6-7] N85-35045

OBLIQUE SHOCK WAVES
Tabular and graphical solutions of regular and Mach reflections in pseudo-stationary frozen and vibrational-equilibrium flows, part 1
[UTIAS-283-PT-1] N85-34117
Tabular and graphical solutions of regular and Mach reflections in pseudo-stationary frozen and vibrational-equilibrium flows, part 2
[UTIAS-283-PT-2] N85-34118

OCEAN BOTTOM
Research at the Institute of Oceanographic Sciences related to the possible disposal of radioactive waste on or beneath the seafloor
[IOS-204] N85-34628

OCEAN CURRENTS
Method and apparatus for Delta Kappa synthetic aperture radar measurement of ocean current
[NASA-CASE-NPO-15704-1] N85-34327

OCEAN THERMAL ENERGY CONVERSION
Solar energy education. Renewable energy: A background text
[DE85-010365] N85-34452
Ocean thermal energy conversion
[DE85-012291] N85-34456

OCEANOGRAPHY
Climate modeling: A retrospective-prospective view with consideration for the atmospheric carbon dioxide-climate issue
[DE85-011532] N85-34481

OCEANS
Two dimensional CO2-ocean model including the biological processes
[DE85-012341] N85-34483

OIL EXPLORATION
The transient electromagnetic depth sounding technique applied to hydrocarbons and geothermal exploration
[MITT-42] N85-34476

OILS
Method of distributing liquefaction catalysts in solid carbonaceous material
[DE85-005759] N85-34218
Method for controlling the viscosity of siloxane oils
[DE85-011586] N85-34221

ONBOARD DATA PROCESSING
Implications of artificial intelligence on the design of future onboard systems
[SFENA-DPS/C/S3/84252A] N85-34596

OPACITY
X-ray spectra of bursting neutron stars N85-34686

OPERATING SYSTEMS (COMPUTERS)
User's operating procedures. Volume 1: Scout project information programs
[NASA-CR-177948] N85-34518

OPERATIONS RESEARCH
Design and implementation of an interactive route editor N85-34559

OPERATORS (PERSONNEL)
Robot environment expert system
[NASA-CR-3915] N85-34593

OPTICAL DATA PROCESSING
A general purpose image processing package N85-34549

OPTICAL MICROSCOPES
Polarisation insensitive achromatic cube beamsplitter --- binocular microscopes
[NPL-MOM-72] N85-34630

OPTICAL PROPERTIES
Theoretical and experimental analyses of the performance of two-color laser ranging systems
[NASA-CR-176159] N85-34397

OPTICAL PUMPING
Fiber optics interface for a dye laser oscillator and method
[DE85-005765] N85-34633

OPTICAL SCANNERS
Applied computer graphics in a geographic information system: Problems and successes N85-34563

OPTICS
Summary of activities, 1983
[LBL-18500] N85-34605

OPTIMIZATION
High pressure compressor component performance report
[NASA-CR-168245] N85-34138
Re-designing a mechanism for higher speed: A case history from textile machinery N85-34310
Optimisation in the computer aided design of mechanisms N85-34321
Mass resolution optimization in a large isotopic composition experiment
[OG-9.1-9] N85-34935

ORBITAL MANEUVERING VEHICLES
Hardware test program for evaluation of basline range-range rate sensor concept
[NASA-CR-176143] N85-34377

ORBITS
Estimating the change in asymptotic direction due to secular changes in the geomagnetic field
[SH-6.1-13] N85-35086

ORGANIC COMPOUNDS
Atmospheric modeling of organics for risk assessment: A Chemist's view
[DE85-009770] N85-34217

ORGANOMETALLIC COMPOUNDS
Metal alkoxides: Models for metal oxides. Alkoxide ligands in early transition metal organometallic chemistry
[DE85-011368] N85-34269

ORTHOTROPIC PLATES
Nonlinear adhesive behavior effects in a cracked orthotropic sheet stiffened by a semi-infinite orthotropic sheet
[NASA-TM-87584] N85-34426

OSCILLATORS
Fiber optics interface for a dye laser oscillator and method
[DE85-005765] N85-34633

OSMIUM
Current status of the Os-191 yields Ir-191m generator
[DE85-008306] N85-34614

OXIDATION
Electrolytic synthesis of colored eta alumina film N85-34201
An X-ray diffraction study of titanium oxidation
[NASA-CR-176263] N85-34264
Aluminum work function: Effect of oxidation, mechanical scraping and ion bombardment
[NASA-TM-87079] N85-34265
Gas shielding apparatus
[DE85-005992] N85-34416

OXIDE FILMS
Electrolytic synthesis of colored eta alumina film N85-34201
Features of behavior of gas bubbles in molten oxide films during enamelling: Communication 2
[BLL-M-35781-(5828.4)] N85-34283

OXYGEN
Oxygen analyzer
[DE85-006002] N85-34392
Increase of total CO2 in the World ocean
[DE85-007756] N85-34484
Determination of individual tolerance in hyperbaric oxygen N85-34507
Changes in the energy spectrum of anomalous oxygen and helium during 1977-1985
[SH-4.6-1] N85-35039
Temporal variations of the anomalous oxygen component, 1977 - 1984
[SH-4.6-3] N85-35041
Radial and latitudinal gradients of anomalous oxygen during 1977 - 1985
[SH-4.6-4] N85-35042

OXYGEN IONS
Observation of nuclei with energies 8-30 MeV per nucleon in the Earth's magnetosphere at the altitudes 350 KM
[SH-10.1-5] N85-35136

OXYGEN ISOTOPES
Nucleosynthesis in the terrestrial and solar atmospheres
[SH-2.2-2] N85-34797

OXYGEN PRODUCTION
Development and demonstration of a spiral-wound thin-film composite membrane system for the economical production of oxygen-enriched air, phase 4
[DE85-012380] N85-34288

OXYGENATION
Oxygenation and regional circulation in gingival mucosa during exposure to lower body negative pressure N85-34498

OZONE
Agents and effects of ozone trends in the atmosphere
[AERONOMICA-ACTA-A-287-1984] N85-34466
The influences of the galactic cosmic ray on the atmospheric ozone
[SH-10.1-1] N85-35133

P

PACKET SWITCHING
A graphics interface for interactive simulation of packet-switched networks N85-34558

PAIR PRODUCTION
Calculating the interatomic pair potential allowing for resonance interaction in titanium, nickel and vanadium
[BLL-M-35843-(5828.4)] N85-34249
Neutral pion production in solar flares
[SH-1.4-7] N85-34767
On magnetic pair production above fast pulsar polar caps
[OG-8.2-13] N85-34909
Neutron-induced 2.2 MeV background in gamma ray telescopes
[OG-9.3-6] N85-34961
PANCREAS
Lipid hydrolysis in man during antiorthostatic hypokinesia N85-34500
PARABOLIC DIFFERENTIAL EQUATIONS
FEMALE: Finite Element Method for Arbitrary Lagrangian and Eulerian elements N85-34671
PARABOLIC REFLECTORS
Optical analysis of parabolic dish concentrators for solar dynamic power systems in space
[NASA-TM-87080] N85-34176
PARALLAX
Ranging system which compares an object reflected component of a light beam to a reference component of the light beam
[NASA-CASE-NPO-15865-1] N85-34629
PARALLEL PROCESSING (COMPUTERS)
Parallel processing on the Livermore VAX 11/780-4 parallel processor system with compatability to Cray Research, Inc. (CRI) multitasking, version 1
[DE85-011856] N85-34595
PARALLEL PROGRAMMING
Reordering computations for parallel execution
[NASA-CR-177961] N85-34522
PARALLELEPIPEDS
Building an octree from a set of parallelepipeds N85-34572
PARAMETER IDENTIFICATION
Real-time multiparameter pulse processing with decision tables
[DE85-011683] N85-34589
PARSING ALGORITHMS
Project management using graphics N85-34560
PARTIAL DIFFERENTIAL EQUATIONS
A review of spectral methods
[NASA-CR-172502] N85-34350
PARTICLE ACCELERATION
Physics Division annual review, 1 April 1983 - 31 March 1984
[ANL-84-24] N85-34602
Nineenth International Cosmic Ray Conference. SH sessions, volume 4
[NASA-CP-2376-VOL-4] N85-34729
Stochastic particle acceleration in solar flares
[SH-1.1-4] N85-34731
First-order shock acceleration in solar flares
[SH-1.1-5] N85-34732
Prompt acceleration of ions by oblique turbulent shocks in solar flares
[SH-1.1-6] N85-34733
Study of photon emission by electron capture during solar nuclei acceleration, 1: Temperature-dependent cross section for charge changing processes
[SH-1.1-8] N85-34735
Study of photon emission by electron capture during solar nuclei acceleration. 2: Delimitation of conditions for charge transfert establishment
[SH-1.1-9] N85-34736
Study of non-thermal photon production under different scenarios in solar flares. 2: The Compton inverse and Bremsstrahlung models and fittings
[SH-1.2-3] N85-34739
Quantitative analysis of flare accelerated electrons through their hard X-ray and microwave radiation
[SH-1.2-7] N85-34742
Two classes of solar energetic particle events associated with impulsive and long duration soft X-ray flares
[SH-1.2-12] N85-34747
The energy spectra of solar flare electrons
[SH-1.2-14] N85-34749
The starting conditions for an optically small solar gamma ray flare
[SH-1.3-2] N85-34751
Observations of solar flare gamma-rays and protons
[SH-1.3-6] N85-34753
Energetic protons from a disappearing solar filament
[SH-1.3-7] N85-34754
Helios 1 energetic particle observations of the solar gamma ray flare events of 7, 21 June 1980 and 3 June 1982
[SH-1.3-8] N85-34755
Shock and statistical acceleration of energetic particles in the interplanetary medium
[SH-1.5-1] N85-34771
Particle acceleration due to shocks in the interplanetary field: High time resolution data and simulation results
[SH-1.5-5] N85-34774
Spatial dependence of the local diffusion coefficient measured upstream of the November 12, 1978 interplanetary traveling shock
[SH-1.5-12] N85-34776
Latitude dependence of co-rotating shock acceleration
[SH-1.5-14] N85-34777
Elemental abundances in corotating events
[SH-1.5-15] N85-34778
Cosmic ray acceleration by stellar wind. Simulation for heliosphere
[SH-1.5-17] N85-34780
On the retention of high-energy protons and nuclei with charges Z or equal to 2 in large solar flares after the process of their acceleration
[SH-2.1-8] N85-34789
Type 3 solar radio bursts and 3HE-rich events
[SH-2.2-3] N85-34798
Elemental abundance differences between nuclei acclerated in CIR shocks and solar flares
[SH-2.2-6] N85-34801
On the connection between the 3HE-enrichment and spectral index of solar energetic particles
[SH-2.2-9] N85-34804
The plasma mechanism for preferential acceleration of heavy ions
[SH-2.2-10] N85-34805
Ninteenth International Cosmic Ray Conference. OG sessions, volume 3
[NASA-CP-2376-VOL-3] N85-34862
Sources of the ultraheavy cosmic rays
[OG-7.1-7] N85-34868
Selfsimilar time dependent shock structures
[OG-8.1-4] N85-34894
The central engine of quasars and AGNs: A relativistic proton radiative shock
[OG-8.1-7] N85-34897
A model for the origin of high-energy cosmic rays
[OG-8.1-8] N85-34898
Onion-shell model for cosmic ray electrons and radio synchrotron emission in supernova remnants
[OG-8.1-10] N85-34900
Approximate supernova remnant dynamics with cosmic ray production
[OG-8.1-12] N85-34901
Efficiency of regular acceleration of particles by a shock wave at different injection regimes
[OG-8.1-13] N85-34902
The nucleosynthesis of deterium and helium-3
[OG-8.2-18] N85-34914
Pulsars as cosmic ray particle accelerators: Proton orbits
[OG-8.2-21] N85-34917
Pulsars as cosmic ray accelerators: Energy development of protons
[OG-8.2-22] N85-34918
Propagation of injected cosmic rays under distributed reacceleration
[OG-8.3-3] N85-34922
Secondary to primary ratio and the continuous acceleration
[OG-8.3-4] N85-34923
Propagation of cosmic rays and new evidence for distributed acceleration
[OG-8.3-5] N85-34924
Exact solutions for sporadic acceleration of cosmic rays
[OG-8.3-7] N85-34925
Stochastic particle acceleration in flaring stars
[OG-8.3-9] N85-34927
On the anomalous component
[SH-4.6-6] N85-35044
Possible origin of the anomalous component of cosmic rays
[SH-4.6-7] N85-35045
PARTICLE ACCELERATOR TARGETS
Light ion sources for ICF
[DE85-011544] N85-34702
Interactions of heavy nuclei, Kr, Xe and Ho, in light targets
[OG-7.2-21] N85-34888
PARTICLE ACCELERATORS
Summary of activities, 1983
[LBL-18500] N85-34605
Repetitive pulse accelerator technology for light ion inertial confinement fusion
[DE85-012030] N85-34693
PARTICLE BEAMS
Space Experiments with Particle Accelerators (SEPAC) N85-34165
Recoverable Plasma Diagnostics Package (RPDP) N85-34167
Neutral particle beam intensity controller
[DE85-006411] N85-34604
Theoretical and computational research on the focused transport of intense charged particle beams
[DE85-012980] N85-34621
Depth and size effects on cosmogenic nuclide production in meteorites
[SH-7.1-9] N85-35101
PARTICLE COLLISIONS
Radial transport caused by collision N85-34652
Electron loss process and cross section of multiply charged ions by neutral atoms N85-34685
Low-energy sputterings with the Monte Carlo Program ACAT
[IPPJ-AM-40] N85-34690
Cross sections for the production of fragments with Z greater than or equal to 8 by fragmentation of Z greater than or equal to 9 and less than or equal to 26 nuclei
[OG-7.2-22] N85-34889
The response of ionization chambers to relativistic heavy nuclei
[OG-9.1-13] N85-34939
Plastic scintillators in coincidence for the study of multi-particle production of sea level cosmic rays in dense medium
[SH-9.1-11] N85-35126
PARTICLE DENSITY (CONCENTRATION)
Second-order Compton-Getting effect on arbitrary intensity distribution
[SH-3.1-10] N85-34814
The expected cosmic ray density and stream distributions at the heliolatitudinal asymmetry of solar wind
[SH-4.2-14] N85-34852
Angular resolution of air-shower array-telescopes
[OG-9.5-6] N85-34983
PARTICLE DIFFUSION
Guiding center distribution function and longitudinal invariant N85-34663
Diffusion in the chromosphere and the composition of the solar corona and energetic particles
[SH-2.1-9] N85-34790
Coronal propagation of solar flare particles observed by satellite
[SH-3.1-2] N85-34807
Investigation of cosmic ray propagation in interplanetary space
[SH-3.2-9] N85-34824
Diffusion-convection function of cosmic rays
[SH-3.2-10] N85-34825
Numerical descriptions of cosmic-ray transport
[SH-4.1-3] N85-34829
Numerical and analytic descriptions of cosmic-ray transport
[SH-4.1-4] N85-34830
Diffusion of strongly magnetized cosmic ray particles in a turbulent medium
[OG-7.2-16] N85-34883
PARTICLE EMISSION
Forecasting future industrial SO2 and NC/sub x/ emissions, revised N85-34461
Study of photon emission by electron capture during solar nuclei acceleration, 1: Temperature-dependent cross section for charge changing processes
[SH-1.1-8] N85-34735
Study of photon emission by electron capture during solar nuclei acceleration. 2: Delimitation of conditions for charge transfert establishment
[SH-1.1-9] N85-34736
Study of photon emission by electron capture during solar nuclei acceleration. 3: Photon production evaluations
[SH-1.1-10] N85-34737
Solar neutrinos, solar flares, solar activity cycle and the proton decay
[SH-8.1-8] N85-35113
PARTICLE ENERGY
Source energy spectra from demodulation of solar particle data by interplanetary and coronal transport
[SH-1.3-13] N85-34758
the role of shock waves in modulation of galactic cosmic rays
[SH-4.1-7] N85-34831
SONTRAC: A solar neutron track chamber detector
[SH-9.1-12] N85-35127
PARTICLE FLUX DENSITY
Helios 1 energetic particle observations of the solar gamma ray flare events of 7, 21 June 1980 and 3 June 1982
[SH-1.3-8] N85-34755
The dispersive evolution of charged-particle bunches in random magnetic fields
[SH-4.1-2] N85-34828
Observation of pick-up ions in the solar wind: Evidence for the source of the anomalous cosmic ray component?
[SH-4.6-5] N85-35043

Cosmogenic-nuclide production by primary cosmic-ray protons
[SH-7.1-6] N85-35098
Accelerator experiments on the contribution of secondary particles to the production of cosmogenic nuclides in meteorites
[SH-7.1-8] N85-35100
Spallogenic origin of nuclei in meteorites
[SH-7.1-10] N85-35102
The 4He1H ratios in the chemical compositions of solar flare particles and the primordial solar nebula
[SH-7.1-12] N85-35104

PARTICLE INTERACTIONS
Space Experiments with Particle Accelerators (SEPAC) N85-34165
Electron loss process and cross section of multiply charged ions by neutral atoms N85-34685
Multiple inner shell vacancies in laser-irradiated Au plasma N85-34687
Cosmic ray modulation in a random anisotropic magnetic field
[SH-4.1-20] N85-34839
Interactions of heavy nuclei, Kr, Xe and Ho, in light targets
[OG-7.2-21] N85-34888
A cosmic ray driven instability
[OG-8.1-5] N85-34895
Plastic scintillators in coincidence for the study of multi-particle production of sea level cosmic rays in dense medium
[SH-9.1-11] N85-35126
A suggested standardized format for cosmic ray ground-level event data
[SH-9.1-15] N85-35130

PARTICLE MOTION
Pulsars as cosmic ray particle accelerators: Proton orbits
[OG-8.2-21] N85-34917
Mini and super mini arrays for the study of highest energy cosmic rays
[OG-9.4-9] N85-34976
The cosmic ray differential diurnal variation dependences on the zenith angle and the geomagnetic disturbance
[SH-4.5-16] N85-35033
Changes in the energy spectrum of anomalous oxygen and helium during 1977-1985
[SH-4.6-1] N85-35039

PARTICLE PRECIPITATION
Helios 1 energetic particle observations of the solar gamma ray flare events of 7, 21 June 1980 and 3 June 1982
[SH-1.3-8] N85-34755

PARTICLE PRODUCTION
Study of non-thermal photon production under different scenarios in solar flares. 1: Scenarios and formulations
[SH-1.2-2] N85-34738
Study of non-thermal photon production under different scenarios in solar flares. 2: The Compton inverse and Bremsstrahlung models and fittings
[SH-1.2-3] N85-34739
The starting conditions for an optically small solar gamma ray flare
[SH-1.3-2] N85-34751
Time extended production of neutrons during a solar flare
[SH-1.4-1] N85-34762
Relativistic cosmic ray spectra in the full non-linear theory of shock acceleration
[OG-8.1-6] N85-34896
Secondary gamma-ray production in a coded aperture mask
[OG-9.2-6] N85-34945
Spallogenic origin of nuclei in meteorites
[SH-7.1-10] N85-35102
Neutrino production from the solar atmosphere
[SH-8.1-9] N85-35114
Solar cosmic ray bursts and solar neutrino fluxes
[SH-8.1-10] N85-35115

PARTICLE SIZE DISTRIBUTION
Review of zirconium-zircaloy pyrophoricity
[DE85-011169] N85-34270
Synthesis of ultrafine ceramic and metallic powders in a thermal argon rf plasma
[DE85-009634] N85-34696

PARTICLE TELESCOPES
Secondary gamma-ray production in a coded aperture mask
[OG-9.2-6] N85-34945
Operating characteristics of a prototype high energy gamma-ray telescope
[OG-9.2-7] N85-34946
High energy gamma ray balloon instrument
[OG-9.2-12] N85-34951
Results of a study to build a gamma-ray telescope in an external tank
[OG-9.3-3] N85-34958
An approach of reducing the background induced by neutrons
[OG-9.3-5] N85-34960
Astrophysical applications of high angular resolution array-telescopes
[OG-9.5-7] N85-34984
Sidereal variations deep underground in Tasmania
[SH-4.4-4] N85-35002
Corrected sidereal anisotropy for underground moons
[SH-4.4-7] N85-35005
Cosmic ray intensity variations observed at Matsushiro (220 M.W.E. in depth)
[SH-4.4-9] N85-35007
Study of cosmic ray scintillations from 5-minute data of the scintillations telescope Izmran and world-wide network stations
[SH-5.1-18] N85-35071
Coupling functions for lead and lead-free neutron monitors from the latitudinal measurements performed in 1982 in the research station Academician Kurchatov
[SH-6.1-1] N85-35076
Atmospheric effects on the underground muon intensity
[SH-6.1-3] N85-35078
Observation of energy spectrum of electron albedo in low latitude region at Hyderabad, India
[SH-6.1-7] N85-35081
A silicon surface barrier telescope for solar particles identification
[SH-9.1-3] N85-35118
A bi-directional charged particle telescope to observe flux, energy spectrum and angular distribution of relativistic and non-relativistic particles
[SH-9.1-4] N85-35119

PARTICLE THEORY
Vector calculation of particle code N85-34688
Relativistic cosmic ray spectra in the full non-linear theory of shock acceleration
[OG-8.1-6] N85-34896

PARTICLE TRACKS
Cross sections for the production of fragments with Z greater than or equal to 8 by fragmentation of Z greater than or equal to 9 and less than or equal to 26 nuclei
[OG-7.2-22] N85-34889
SONTRAC: A solar neutron track chamber detector
[SH-9.1-12] N85-35127
Observation of nuclei with energies 8-30 MeV per nucleon in the Earth's magnetosphere at the altitudes 350 KM
[SH-10.1-5] N85-35136
Measurement of low energy cosmic rays aboard Spacelab-1
[SH-10.1-6] N85-35137
Heavy cosmic ray measurement aboard Spacelab-1
[SH-10.1-7] N85-35138

PARTICLE TRAJECTORIES
Pulsars as cosmic ray particle accelerators: Proton orbits
[OG-8.2-21] N85-34917
Bevalac calibration of the SOFIE range and hodoscope detectors
[OG-9.1-7] N85-34933
Cherenkov-dE/dx-range measurements on cosmic ray iron group nuclei
[OG-9.1-12] N85-34937
The response of ionization chambers to relativistic heavy nuclei
[OG-9.1-13] N85-34939
Twenty-two-year cycle of the upper limiting rigidity of Daly waves
[SH-4.5-5] N85-35023
Re-evaluation of cosmic ray cutoff terminology
[SH-6.1-11] N85-35084
Estimating the change in asymptotic direction due to secular changes in the geomagnetic field
[SH-6.1-13] N85-35086

PARTICLES
Influence of particle erosion on the microstructural changes in metals and alloys
[TI85-901384] N85-34276
Acoustic cross-correlation flowmeter for solid-gas flow
[DE85-005988] N85-34391
The influence of nonstationarity of the solar activity and general solar field on modulation of cosmic rays
[SH-4.2-17] N85-34854

PASCAL (PROGRAMMING LANGUAGE)
A prototype PASCAL program validation system
[NPL-DITC-57/85] N85-34513

PASSENGERS
Aviation safety (aircraft passenger survivability and cabin safety)
[GPO-39-847] N85-34130

PASSIVITY
Low noise polycrystalline semiconductor resistors by hydrogen passivation
[AD-D011721] N85-34338

PASTE (CONSISTENCY)
Development of metallization process: FSA project, cells and module formation research area
[NASA-CR-176136] N85-34447

PATTERN RECOGNITION
Recognition and clear representation of handwritten electronic diagrams N85-34541
A star camera aspect system suitable for use in balloon experiments
[OG-9.3-10] N85-34965

PATTERNS
Multi-robot assembly of IC's N85-34577

PAYLOAD DEPLOYMENT & RETRIEVAL SYSTEM
The role of tethers on space station
[NASA-TM-86519] N85-34154

PAYLOADS
Brush and commutator segment torquer motor
[AD-D011726] N85-34340
Research of advanced techniques for X-ray detectors and telescopes with applications to rockets and the LAMAR facility
[NASA-CR-176161] N85-35141

PEARLITE
Effects of hot deformation on the kinetics of the pearlite transformation in eutectoid steel
[BLL-M-35844-(5826.4)] N85-34250

PENETRATION
Multiaxial stress analysis taking account of penetration depth of X-rays. A solution by means of polynomial approximation N85-34204
Monte Carlo techniques for analyzing deep penetration problems
[DE85-011426] N85-34598
Dynamics of the penetration boundaries of solar protons during a strong magnetic storm
[SH-6.1-16] N85-35089

PERFORMANCE TESTS
Effect of interference on the performance of a minimum TCAS 2
[FAA/PM-84/33] N85-34131
Test plan for performance testing of the Eaton AC-3 electric vehicle
[DE85-011954] N85-34341
Circuit approaches to increasing SRAM performance in total dose environments
[DE85-009441] N85-34588

PERIODIC VARIATIONS
Propagation of the phase of solar modulation
[SH-4.1-12] N85-34835
Ninteenth International Cosmic Ray Conference. SH sessions, volume 5
[NASA-CP-2376-VOL-5] N85-34991
Cosmic ray power spectral variations. 3: Solar rotation periodicities
[SH-4.4-16] N85-35012
Variations of the cosmic ray general component in Antarctica
[SH-4.4-17] N85-35013
Cosmic ray variations with the period close to 27 days and their connection with solar activity longitudinal distribution
[SH-4.4-19] N85-35015
Azimuthal and meridional asymmetries of the solar wind and quasiperiodic variations of intensity of Galactic Cosmic Rays (GCR)
[SH-4.4-20] N85-35016
Dynamics of two-year cosmic ray variations inferred from the data of spacecraft and stratospheric measurements and from the neutron monitor data in 1959-1981
[SH-4.4-21] N85-35017
Formulation of cosmic-ray solar daily variation and its seasonal variation, produced from generalized stationary anisotropy of solar origin
[SH-4.5-2] N85-35020
Temporal variations of the anomalous oxygen component, 1977 - 1984
[SH-4.6-3] N85-35041
A relation between the short time variations of cosmic rays and geomagnetic field change
[SH-5.1-14] N85-35067
Observations of cosmic-ray modulations in the fall, 1984
[SH-5.1-16] N85-35069
Frequency spectra of short-period variations of cosmic ray
[SH-5.1-17] N85-35070
Long-period cosmic ray variations and their altitude dependence
[SH-6.1-19] N85-35091
Solar modulation of cosmic ray intensity and solar flare events inferred from (14)C contents in dated tree rings
[SH-7.1-2] N85-35095

When did the average cosmic ray flux increase?
[SH-7.1-4] N85-35097
Radiocarbon content in the annual tree rings during last 150 years and time variation of cosmic rays
[SH-7.1-15] N85-35106
PERTURBATION
Longitudinal dependence of the interplanetary perturbation produced by energetic type 4 solar flares and of the associated cosmic ray modulation
[SH-5.1-5] N85-35059
Short perturbations of cosmic ray intensity and electric field in atmosphere
[SH-6.1-18] N85-35090
PETN
Time-resolved spectroscopic studies of detonating heterogeneous explosives
[DE85-009760] N85-34297
Effect of precipitation variables on the specific surface and explosion characteristics of pentaerythritol tetranitrate
[DE85-009620] N85-34302
Real time analysis of PETN detonation products
[DE85-009581] N85-34303
PH
Increase of total CO2 in the World ocean
[DE85-007756] N85-34484
PH FACTOR
Throughfall rate and chemistry studies: Whiteface Mountain
[DE85-012407] N85-34484
Increase of total CO2 in the World ocean
[DE85-007756] N85-34484
PHARMACOLOGY
Effect of dibazol on parameters of nonspecific resistance of subjects in pressurized cabins N85-34504
PHASE CONTROL
Wide-band phase locked loop amplifier apparatus
[AD-D011720] N85-34337
PHASE LOCKED SYSTEMS
Wide-band phase locked loop amplifier apparatus
[AD-D011720] N85-34337
PHASE TRANSFORMATIONS
Phase transformations taking place in austenitic steel during deformation at different rates
[BLL-M-35875-(5828.4)] N85-34254
Shape memory effect in uranium-niobium alloys below room temperature
[DE85-012964] N85-34268
PHENOLIC RESINS
Poly-functional building material from fiberglass (its fabrication and properties) N85-34209
PHONONS
Calculating the interatomic pair potential allowing for resonance interaction in titanium, nickel and vanadium
[BLL-M-35843-(5828.4)] N85-34249
PHOSPHORUS
Fire-resistant phosphorus containing polyimides and copolyimides
[NASA-CASE-ARC-11522-2] N85-34280
PHOTOCHEMICAL REACTIONS
Process for functionalizing alkanes
[DE85-006420] N85-34219
Electron photoejection in carbanions
[DE85-011747] N85-34230
Electron photoejection in carbanions
[DE85-011748] N85-34237
PHOTOCONDUCTIVE CELLS
A general purpose image processing package N85-34549
PHOTOGRAMMETRY
Production of initial estimates of photogrammetric variables
[NPL-MOM-66] N85-34434
PHOTOIONIZATION
Photoionization-pumped, Ne 2, X-ray laser studies project
[DE85-012973] N85-34399
PHOTOMULTIPLIER TUBES
Improved method for the stabilization of NaI-photomultiplier gamma detectors against thermal and other drift
[DE85-011830] N85-34613
The angular resolution of air shower gamma ray telescopes
[OG-9.5-14] N85-34990
The read-out system of spatial distribution of thermoluminescence in meteorites
[SH-9.1-16] N85-35131
PHOTON BEAMS
X-ray spectra of bursting neutron stars N85-34686
PHOTON-ELECTRON INTERACTION
CYLTRAN calculations of electron effects on XD detectors
[LA-10264-MS] N85-34601
PHOTONS
Low-excitation Herbig-Haro objects and interstellar extinction
[NASA-CR-176142] N85-34726
Study of photon emission by electron capture during solar nuclei acceleration, 1: Temperature-dependent cross section for charge changing processes
[SH-1.1-8] N85-34735
Study of photon emission by electron capture during solar nuclei acceleration. 2: Delimitation of conditions for charge transfert establishment
[SH-1.1-9] N85-34736
Study of photon emission by electron capture during solar nuclei acceleration. 3: Photon production evaluations
[SH-1.1-10] N85-34737
Study of non-thermal photon production under different scenarios in solar flares. 1: Scenarios and formulations
[SH-1.2-2] N85-34738
Study of non-thermal photon production under different scenarios in solar flares. 2: The Compton inverse and Bremsstrahlung models and fittings
[SH-1.2-3] N85-34739
Observations of solar flare photon energy spectra from 20 keV to 7 MeV
[SH-1.2-9] N85-34744
On the detectability of key-MeV solar protons through their nonthermal Lyman-alpha emission
[SH-1.3-5] N85-34752
A coded aperture imaging system optimized for hard X-ray and gamma ray astronomy
[OG-9.2-3] N85-34942
Secondary gamma-ray production in a coded aperture mask
[OG-9.2-6] N85-34945
The final COS-B database now publicly available
[OG-9.3-8] N85-34963
PHOTORECEPTORS
Differentiating spatial light modulator
[AD-D011727] N85-34632
PHOTOSENSITIVITY
Electron photoejection in carbanions
[DE85-011747] N85-34230
Screening and characterizing oleaginous microalgal species from the southeastern United States
[DE85-008787] N85-34488
PHOTOSPHERE
Helios 1 energetic particle observations of the solar gamma ray flare events of 7, 21 June 1980 and 3 June 1982
[SH-1.3-8] N85-34755
Precision measurements of solar energetic particle elemental composition
[SH-2.1-4] N85-34785
Solar Coronal and photospheric abundances from solar energetic particle measurements
[SH-2.1-5] N85-34786
Diffusion in the chromosphere and the composition of the solar corona and energetic particles
[SH-2.1-9] N85-34790
Abundances from solar-flare gamma-ray line spectroscopy
[SH-2.1-13] N85-34794
PHOTOVISCOELASTICITY
Influence of cyclic thermal loading on internal stress in casted epoxy resin N85-34211
PHOTOVOLTAIC CELLS
Thermionic photovoltaic energy converter
[NASA-CASE-LEW-14077-1] N85-34441
PHOTOVOLTAIC EFFECT
Thermionic photovoltaic energy converter
[NASA-CASE-LEW-14077-1] N85-34441
Investigation of test methods, material properties, and processes for solar cell encapsulants
[NASA-CR-176132] N85-34446
PHTHALOCYANIN
Metal (2) 4,4',4',4'' phthalocyanine tetraamines as curing agents for epoxy resins
[NASA-CASE-ARC-11424-1] N85-34281
PHYSICS
Solar energy education: Renewable energy activities for chemistry and physics
[DE85-010371] N85-34455
PHYSIOLOGICAL ACCELERATION
Problems of aviation and space medicine and psychology discussed at 14th Gagarin lectures N85-34509
PHYSIOLOGICAL EFFECTS
Rat skeletal muscles with simulation of physiological effects of weightlessness (morphological study) N85-34502
PINS
Evacuate and backfill apparatus and method
[DE85-006018] N85-34411
PIONS
Neutral pion production in solar flares
[SH-1.4-7] N85-34767
PIPES (TUBES)
Mechanical ratcheting behaviors of a steel pipe under combined cyclic axial load and internal pressure N85-34184
Experimental study of collapse of thick-walled tube under external pressure and axial force N85-34186
Forced convective, nonequilibrium, post-CHF heat transfer experiment data and correlation comparison report
[TI85-009331] N85-34371
Calculations on the feasibility of ultrasonic inspection of steam generator tubing in pressurized water reactors
[AERE-R-10960] N85-34419
Characterization of modified 9 Cr Mo steel extruded pipe
[DE85-012056] N85-34430
PISTONS
Fast shutter apparatus
[DE85-006501] N85-34343
PITCH (INCLINATION)
Fokker-Planck calculation of hot electron formation in the thermal barrier region of tandem mirror Gamma-10
[IPPJ-726] N85-34669
Pitch angle distributions of 35-1000 keV protons at quasi-perpendicular interplanetary shocks
[SH-1.5-6] N85-34775
Diagnostic of electromagnetic conditions in space using cosmic rays
[SH-4.5-19] N85-35036
Magnetic fluctuation and cosmic ray diurnal variations
[SH-4.5-21] N85-35038
PITCHING MOMENTS
An evaluation of three helicopter rotor sections
[NASA-TM-86719] N85-34115
PITOT TUBES
A comparison of laser Doppler anemometry and probe measurements within the boundary layer of an airfoil at subsonic flow
[ISL-CO-219/84] N85-34127
PLANCKS CONSTANT
X-ray spectra of bursting neutron stars N85-34686
PLANETARY BOUNDARY LAYER
Reports from the German Meteorological Service. No. 167: Results of aerological soundings in the model area upper Rhine: Heat release project upper Rhine area, part 3
[ISBN-3-88148-216-4] N85-34479
PLANKTON
Marine Sample Exploitation Project: Estimates regarding the sensitivity and technology for the detection of nuclear explosion debris in the marine environment
[DE85-013176] N85-34462
PLANTS (BOTANY)
The 1984 biotic studies of Yucca Mountain, Nevada test site, Nye County, Nevada
[DE85-011715] N85-34487
PLASMA ACCELERATORS
Space Experiments with Particle Accelerators (SEPAC) N85-34185
PLASMA ARC CUTTING
Mechanical properties of plasma arc cut steel N85-34188
PLASMA CLOUDS
Influence of magnetic clouds on cosmic ray intensity variations
[SH-5.1-12] N85-35085
PLASMA COMPOSITION
Diffusion in the chromosphere and the composition of the solar corona and energetic particles
[SH-2.1-9] N85-34790
PLASMA CONTROL
Collisional relaxation of electron tail distribution
[IPPJ-729] N85-34635
Proceedings of the US-Japan Workshop on Transport in Open-Ended Systems
[IPPJ-727] N85-34644
Potential effect in transport due to non-axisymmetric confining field N85-34645
Activities of the RF Section N85-34646
Radial transport phenomena for TMX-upgrade N85-34647
Plug and thermal barrier potential formation in Gamma 10 N85-34648
Induced azimuthal electric field effects on tandem transport and ambipolarity N85-34650
Recent experiments in Gamma-10 N85-34651
Azimuthal uniformity and current balance study of ICRH-produced plasma in RFC-XXM N85-34659
Moving finite element method for ICF target implosion N85-34675
Stability of implosion dynamics N85-34680

On the heat flux derived by the moment method in Lorentzian plasma between hot and cold walls N85-34682
Integral representation for nonlinear heat transport N85-34683
Advanced Toroidal Facility (ATF) [DE85-011567] N85-34699
Stellarator approach to fusion plasma confinement [DE85-011420] N85-34704

PLASMA CURRENTS
Size effects of vacuum chamber for H- (D-) ion volume production by sheet plasma 1 [IPPJ-731] N85-34639
Langmuir probe on ISX-B [DE85-012066] N85-34697

PLASMA DENSITY
Theoretical and Experimental Beam Plasma Physics (TEBPP) N85-34166
Breakdown of intrinsic ambipolarity for the radial diffusion due to a rotating RF field N85-34660
Simulation studies on stability of hot electron plasma N85-34664

PLASMA DIAGNOSTICS
Space Experiments with Particle Accelerators (SEPAC) N85-34165
Recoverable Plasma Diagnostics Package (RPDP) N85-34167
Magnetospheric multiprobes: MMP/CHEMSAT N85-34171
Novette diagnostic support [DE85-012937] N85-34383
Langmuir probe on ISX-B [DE85-012066] N85-34697
Instrument to synchronize Thomson scattering diagnostic measurements with MHD activity in a Tokamak [DE85-012082] N85-34708

PLASMA DIFFUSION
RF induced radial diffusion in tandem mirrors N85-34649
Guiding center distribution function and longitudinal invariant N85-34663
The plasma mechanism for preferential acceleration of heavy ions [SH-2.2-10] N85-34805

PLASMA DYNAMICS
Workshop report on Simulation Techniques for Shock Wave Phenomena and Characteristics of Plasmas in Inertial Confinement Fusion [IPPJ-725] N85-34670

PLASMA EQUILIBRIUM
User's manual for the FLORA equilibrium and stability code [DE85-013182] N85-34590
Magnetohydrodynamic equilibrium and stability of spheromak with spheroidal plasma-vacuum interface [IPPJ-732] N85-34640

PLASMA FOCUS
The electromagnetic ram action of the plasma focus as a paradigm for the generation of cosmic rays and the gigantic jets in active galaxies [OG-8.2-14] N85-34910

PLASMA FREQUENCIES
Experimental measurements of the ion cyclotron antennas' coupling and RF characteristics [DE85-011569] N85-34694

PLASMA HEATING
Computational study on excitation, propagation and 3 omega -heating due to the ion Bernstein wave [IPPJ-733] N85-34641
On the heat flux derived by the moment method in Lorentzian plasma between hot and cold walls N85-34682
Integral representation for nonlinear heat transport N85-34683

PLASMA INTERACTIONS
Vehicle Charging And Potential (VCAP) N85-34173
Latitude variation of recurrent fluxes in the outer solar system [SH-4.1-13] N85-34836

PLASMA OSCILLATIONS
Instrument to synchronize Thomson scattering diagnostic measurements with MHD activity in a Tokamak [DE85-012082] N85-34708

PLASMA PHYSICS
Waves in Space Plasmas (WISP) N85-34164
Theoretical and Experimental Beam Plasma Physics (TEBPP) N85-34166

PLASMA POTENTIALS
Model of azimuthal non-uniformities induced by RF heating in RFC-XXM N85-34658

PLASMA PROBES
Vehicle Charging And Potential (VCAP) N85-34173

PLASMA PUMPING
Transport issues in Phaedrus-type plasmas N85-34653
Fokker-Planck calculation of hot electron formation in the thermal barrier region of tandem mirror Gamma-10 [IPPJ-726] N85-34669

PLASMA RESONANCE
Nonlocal and nonadiabatic expression for the ponderomotive force near cyclotron resonance [IPPJ-736] N85-34636
Computational study on excitation, propagation and 3 omega -heating due to the ion Bernstein wave [IPPJ-733] N85-34641
Bounce resonance heating and radial transport of electrons N85-34655
The heavy ion composition in 3HE-rich solar flares [SH-2.2-7] N85-34802

PLASMA TEMPERATURE
Theoretical and Experimental Beam Plasma Physics (TEBPP) N85-34166

PLASMA TURBULENCE
The propagation of solar flare particles in a turbulent coronal loop [SH-1.1-3] N85-34730

PLASMA-PARTICLE INTERACTIONS
Selfsimilar time dependent shock structures [OG-8.1-4] N85-34894
A cosmic ray driven instability [OG-8.1-5] N85-34895

PLASMAS (PHYSICS)
Waves in Space Plasmas (WISP) N85-34164
Theoretical and Experimental Beam Plasma Physics (TEBPP) N85-34166
Electrodynamic tether N85-34168
Magnetospheric multiprobes: MMP/CHEMSAT N85-34171
Electronic imaging system and technique [DE85-005740] N85-34393
Some physical differences between sheet plasma and multicusp plasma as volume produced H- or D- ion sources [IPPJ-728] N85-34637
Effect of ECH and ICH on ambipolar potential in NBT-1M N85-34661
Transports studies of ECH and ICRH-heated bumpy torus plasma in NBT-1M N85-34662
Stability of ion distribution in strong ion shock structure N85-34681
On the heat flux derived by the moment method in Lorentzian plasma between hot and cold walls N85-34682
The role of cosmic rays and Alfven waves in the structure of the galactic halo [OG-7.2-18] N85-34885
Stochastic particle acceleration in flaring stars [OG-8.3-9] N85-34927

PLATES (TECTONICS)
Scaling differences between large interplate and intraplate earthquakes [NASA-CR-176149] N85-34467

PLATING
Towards the development of technological processes for the preparation of cadmium plated steel articles [BLL-M-36315-(5828.4)] N85-34248

PLOTTERS
Applied computer graphics in a geographic information system: Problems and successes N85-34563

PLOTTING
A device-independent 2D plotting package written in FORTRAN [RSRE-MEMO-3776] N85-34514

PLUTONIUM ISOTOPES
General-purpose heat source development: Safety test program. Postimpact evaluation, design iteration test [LA-10034-SR] N85-34606

PLUTONIUM OXIDES
General-purpose heat source development: Safety test program. Postimpact evaluation, design iteration test [LA-10034-SR] N85-34606

PNEUMATICS
Acoustic cross-correlation flowmeter for solid-gas flow [DE85-005988] N85-34391

POINT DEFECTS
Formation of amorphous silicon by light ion damage [DE85-012605] N85-34623

POINT SOURCES
Diffusion-convection function of cosmic rays [SH-3.2-10] N85-34825
The cosmic ray composition as viewed from the chemical abundances of the solar system [OG-7.1-8] N85-34869
Electron capture decay of cosmic rays: A model of the inhomogeneous interstellar medium [OG-7.1-10] N85-34871
The model-independence of cosmic ray source determinations [OG-7.2-1] N85-34873
The effects of newly measured cross sections in hydrogen on the production of secondary nuclei during the propagation of cosmic rays through interstellar H [OG-7.2-2] N85-34874
A Cerenkov imaging telescope for high energy gamma rays [OG-9.3-13] N85-34968
A new ultra high energy gamma ray telescope at Ohya mine [OG-9.4-3] N85-34970
The Buckland Park air shower array [OG-9.4-4] N85-34971
An EAS experiment at mountain altitude for the detection of gamma-ray sources [OG-9.4-5] N85-34972
A new array for the study of ultra high energy gamma-ray sources [OG-9.4-7] N85-34974
Cerenkov light images of EAS produced by primary gamma [OG-9.5-3] N85-34979
A method to improve observations of gamma-ray sources near 10 (15) eV [OG-9.5-5] N85-34982
Note on the detection of high energy primary cosmic gamma rays by air shower observation [OG-9.5-9] N85-34986

POISSON DENSITY FUNCTIONS
On the statistical significance of excess events: Remarks of caution and the need for a standard method of calculation [OG-9.5-10] N85-34987

POLAR CAPS
Comparisons of the North Polar Cap of Mars and the Earth's Northern Hemisphere snow cover [NASA-TM-86191] N85-34728
On magnetic pair production above fast pulsar polar caps [OG-8.2-13] N85-34909

POLAR REGIONS
Comparisons of the North Polar Cap of Mars and the Earth's Northern Hemisphere snow cover [NASA-TM-86191] N85-34728
The influence of the Earth's magnetosphere on the high-energy solar protons [SH-6.1-22] N85-35093

POLARITY
Effects of a wavy neutral sheet on cosmic ray anisotropies [SH-4.2-11] N85-34849
Latitudinal gradients of cosmic rays and the polarity reversal of the heliospheric magnetic field: A preliminary evaluation [SH-4.2-16] N85-34853
Isotropic intensity waves and features of their occurrence [SH-4.3-8] N85-34993
Cosmic ray sidereal diurnal variation of galactic origin observed by neutron monitors [SH-4.4-2] N85-35000
The sidereal semi-diurnal variation observed at high zenith angles at Mawson, 1968-1984, and the polarity of the solar main field [SH-4.4-6] N85-35004

POLICIES
Opportunities for policy historians: The evolution of the US civilian space program N85-35147

POLITICS
Satellites and politics: Weather, communications, and earth resources N85-35144

POLLUTION TRANSPORT
Studies in thermo-hydro-chemical transport in porous and fractured media [DE85-012555] N85-34473
User's guide to the MATHEW/ADPIC models [DE85-012952] N85-34587
MATADOR (Methods for the Analysis of Transport And Deposition Of Radionuclides) code description and user's manual [TI85-901402] N85-34592

POLOIDAL FLUX
Observation of helical sawtooth oscillations in a tokamak [DE85-012062] N85-34703

POLYCRYSTALS
Aluminum work function: Effect of oxidation, mechanical scraping and ion bombardment [NASA-TM-87079] N85-34265
Low noise polycrystalline semiconductor resistors by hydrogen passivation [AD-D011721] N85-34338

POLYESTERS
Impact fracture mechanism of polymer plates containing a heavy inner material N85-34215
POLYETHYLENES
Method for making a low density polyethylene waste form for safe disposal of low level radioactive material [DE85-006401] N85-34292
Sensitivity of single and multiple cosmic ray neutrons to the surrounding medium in a lead-free monitor [SH-9.1-10] N85-35125
POLYGONS
Shadow volumes for non-planar polygons N85-34580
POLYIMIDE RESINS
Rigid zeolite containing polyurethane foams [DE85-006406] N85-34286
POLYIMIDES
Fire-resistant phosphorus containing polyimides and copolyimides [NASA-CASE-ARC-11522-2] N85-34280
POLYMER MATRIX COMPOSITES
Conductor-polymer composite electrode materials [DE85-005766] N85-34293
POLYMERIC FILMS
Development and demonstration of a spiral-wound thin-film composite membrane system for the economical production of oxygen-enriched air, phase 4 [DE85-012380] N85-34288
POLYMERS
Process for improving moisture resistance of epoxy resins by addition of chromium ions [NASA-CASE-LAR-13226-1] N85-34282
Degradation mechanisms and accelerated aging test design [TI85-003251] N85-34420
POLYPROPYLENE
Strength properties of glassfiber reinforced thermoplastics N85-34212
POLYURETHANE FOAM
Rigid zeolite containing polyurethane foams [DE85-006406] N85-34286
PONDEROMOTIVE FORCES
Nonlocal and nonadiabatic expression for the ponderomotive force near cyclotron resonance [IPPJ-736] N85-34636
Transport issues in Phaedrus-type plasmas N85-34653
POROUS MATERIALS
Detailed validation of a liquid and heat flow code against field performance [DE85-009901] N85-34368
Studies in thermo-hydro-chemical transport in porous and fractured media [DE85-012555] N85-34473
POSITION (LOCATION)
Initial placement of STO instruments N85-34174
POSITION SENSING
A position sensitive phoswich hard X-ray detector system [OG-9.3-12] N85-34967
POSITRON ANNIHILATION
A coded aperture imaging system optimized for hard X-ray and gamma ray astronomy [OG-9.2-3] N85-34942
POSITRONS
Possible detection of flare-generated positrons by Helios 1 on 3 Jun 1982 [SH-1.4-10] N85-34770
POTASSIUM COMPOUNDS
Throughfall rate and chemistry studies: Whiteface Mountain [DE85-012407] N85-34464
POTASSIUM HYDROXIDES
Experimental evaluation of the thermodynamic properties of concentrated aqueous potassium hydroxide solutions [DE85-010628] N85-34238
POTENTIAL GRADIENTS
Possibility of potential generation by lower hybrid wave N85-34654
Fokker-Planck calculation of hot electron formation in the thermal barrier region of tandem mirror Gamma-10 [IPPJ-726] N85-34669
POWDER (PARTICLES)
Method for removing oxide contamination from silicon carbide powders [DE85-011648] N85-34287
POWDER METALLURGY
Experimental attempt to achieve microstructure variations through temperature/time permutations for a nonwrought powder metallurgy uranium-6 niobium alloy [DE85-013166] N85-34272
The read-out system of spatial distribution of thermoluminescence in meteorites [SH-9.1-16] N85-35131
POWER AMPLIFIERS
Research on gyrotrons [AD-A154032] N85-34380
POWER EFFICIENCY
Technology of magnetically driven accelerators [DE85-011857] N85-34700
POWER SPECTRA
Cosmic ray biannual variation [SH-4.4-15] N85-35011
Cosmic ray power spectral variations. 3: Solar rotation periodicities [SH-4.4-16] N85-35012
A relation between the short time variations of cosmic rays and geomagnetic field change [SH-5.1-14] N85-35067
PRECIPITATION (CHEMISTRY)
Effect of precipitation variables on the specific surface and explosion characteristics of pentaerythritol tetranitrate [DE85-009620] N85-34302
PRECIPITATION (METEOROLOGY)
Throughfall rate and chemistry studies: Whiteface Mountain [DE85-012407] N85-34464
PREDICTION ANALYSIS TECHNIQUES
Comments on the prediction of dynamic stall [GU-AERO-8501] N85-34125
Prediction of the flow-field interference induced by the long-range laser velocimeter in the Ames 40- by 80-foot and the 80- by 120-foot wind tunnels [NASA-TM-86763] N85-34146
Nonsimultaneous coupled laser velocimeter measurement technique: Error prediction for spatially noncoincident measurements [NASA-TM-86718] N85-34379
Lubrication and cooling for high speed gears [NASA-TM-87096] N85-34407
Forecasting future industrial SO2 and NC/sub x/ emissions, revised N85-34461
PREDICTIONS
Comparison of experimental data on detonation velocity and Chapman-Jouget pressure vs initial HE density with predictions from Ree's model equation of state [DE85-007266] N85-34304
Evaluation of source strength and dispersion model predications with data from large nitrogen tetroxide field experiments [DE85-011855] N85-34465
PREFORMS
Negative flexural behavior of precase composite slabs with steel joint N85-34183
PRESSURE DISTRIBUTION
Experimental study of collapse of thick-walled tube under external pressure and axial force N85-34186
PRESSURE EFFECTS
Pressure-shear loading of PBX-9404 [DE85-009982] N85-34298
PRESSURE GRADIENTS
A design procedure to modify the trailing edge upper surface pressure gradient of a given aerofoil [GU-AERO-8408] N85-34120
Refrigerated dynamic seal to 6.9 MPa (1000 psi) [NASA-TM-87108] N85-34356
A three-dimensional turbulent boundary layer undergoing transverse strain and streamwise pressure gradient [NASA-TM-86768] N85-34358
PRESSURE RATIO
High pressure compressor component performance report [NASA-CR-168245] N85-34138
PRESSURE VESSELS
Effect of stainless steel weld overlay cladding on the structural integrity of flawed steel plates in bending, series 1 [TI85-010349] N85-34418
PRESSURIZED CABINS
Effect of dibazol on parameters of nonspecific resistance of subjects in pressurized cabins N85-34504
PRESSURIZED WATER REACTORS
Calculations on the feasibility of ultrasonic inspection of steam generator tubing in pressurized water reactors [AERE-R-10960] N85-34419
PRESTRESSING
Monotonous stress-strain properties of structural steel subjected to nonstationary repetitive pre-loading N85-34185
Corrosion fatigue strength and crack growth in prestrained 0.16% C carbon steel N85-34192
PRIMARY COSMIC RAYS
Variations in the propagation of UH-nuclei [OG-7.1-1] N85-34863
Secondary to primary ratio and the continuous acceleration [OG-8.3-4] N85-34923
The response of ionization chambers to relativistic heavy nuclei [OG-9.1-13] N85-34938
Empirical model for the Earth's cosmic ray shadow at 400 KM: Prohibited cosmic ray access [SH-6.1-14] N85-35087
Cosmogenic-nuclide production by primary cosmic-ray protons [SH-7.1-6] N85-35098
The neutron moderated detector and groundbased cosmic ray modulation studies [SH-9.1-13] N85-35128
Measurement of low energy cosmic rays aboard Spacelab-1 [SH-10.1-6] N85-35137
Heavy cosmic ray measurement aboard Spacelab-1 [SH-10.1-7] N85-35138
PRINTED CIRCUITS
Hermetic chip carrier compliant soldering pads [AD-D011722] N85-34410
PRINTING
Development of metallization process: FSA project, cells and module formation research area [NASA-CR-176136] N85-34447
PROBABILITY DENSITY FUNCTIONS
A new approach to evaluate gamma-ray measurements [OG-9.5-11] N85-34988
PROBABILITY THEORY
The application of models to the assessment of fire hazard from consumer products [NBSIR-85-3219] N85-34325
Estimating risks of lead-induced hemoglobin decrements under conditions of uncertainty: Methodology, pilot judgments and illustrative calculations [DE85-012293] N85-34493
On the statistical significance of excess events: Remarks of caution and the need for a standard method of calculation [OG-9.5-10] N85-34987
PROBLEM SOLVING
DISPL1: A software package for one and two spatially dimensioned kinetics-diffusion problems [ANL-84-56] N85-34516
A model for graphics interface tool development N85-34545
PROCEDURES
Method for controlling the viscosity of siloxane oils [DE85-011586] N85-34221
Method for preparing hydride configurations and reactive metal surface [DE85-006443] N85-34274
PROCESS HEAT
Solar thermal technologies program summary [DE85-012253] N85-34449
PRODUCT DEVELOPMENT
The development and evaluation of the creep and corrosion resistant alloy IN6201 [PNR-90253] N85-34278
A rational approach to cam design N85-34311
Cost effective single crystals: The Rolls Royce approach --- gas turbine components [PNR-90262] N85-34717
PRODUCTION ENGINEERING
Centralized surveillance of flexible workshops for the manufacturing of composite materials [SNIAS-851-430-103] N85-34227
PRODUCTIVITY
Resource evaluation and site selection for microalgae production systems [DE85-008807] N85-34485
PROGRAM VERIFICATION (COMPUTERS)
A prototype PASCAL program validation system [NPL-DITC-57/85] N85-34513
PROGRAMMING LANGUAGES
Graphics interaction in databases N85-34534
Architecture of languages for large CAD systems development N85-34557
PROGRAMS
Index of laser program publications and related reports, calendar year 1984 [DE85-011863] N85-34398
PROGRESS
Confinement experiments on ISX-B [DE85-012346] N85-34709
PROJECT MANAGEMENT
Project management using graphics N85-34560
Analyzing performance of small projects using URS and PMAS, information pamphlet [DE85-011964] N85-34718
Management of large-scale technology N85-35145
PROJECT PLANNING
Management of large-scale technology N85-35145

PROJECTILES
OMEGA: Optoelectronic measurement of the incidence angle of a projectile
[ISL-CO-223/84] N85-34634
PROPAGATION
Exponential anisotropy of solar cosmic rays
[SH-3.2-1] N85-34817
Energetic solar particle events
[SH-3.2-2] N85-34818
Channeled propagation of solar particles
[SH-3.2-3] N85-34819
The local characteristic function of interplanetary particle propagation
[SH-3.2-8] N85-34823
PROPAGATION MODES
The use of optical fibers in pulsed laser holography
[ISL-CO-226/84] N85-34395
PROPAGATION VELOCITY
The recovery of the cosmic ray flux from maximum solar modulation at IMP-8 (1 AU) and at Pioneer (R 30 AU)
[SH-4.7-7] N85-35052
PROPANE
Investigation of the flame speeds of propane/methanol gas mixtures
[DE85-012617] N85-34239
PROTECTION
Fast shutter apparatus
[DE85-006501] N85-34343
PROTECTIVE COATINGS
Towards the development of technological processes for the preparation of cadmium plated steel articles
[BLL-M-36315-(5828.4)] N85-34248
Diamondlike carbon protective coatings for IR materials
[NASA-TM-87083] N85-34631
PROTEINS
A computerized system for spot detection and analysis of two-dimensional electrophoresis images N85-34531
PROTON BEAMS
Injection of energetic particles following the gamma-ray flares on June 7, 1980, as observed on Helios 1
[SH-1.3-9] N85-34756
PROTON FLUX DENSITY
Further observations of protons resulting from the decay of neutrons ejected by solar flares
[SH-1.4-2] N85-34763
Latitude variation of recurrent fluxes in the outer solar system
[SH-4.1-13] N85-34836
PROTON SCATTERING
The propagation of solar flare particles in a turbulent coronal loop
[SH-1.1-3] N85-34730
The neutron moderated detector and groundbased cosmic ray modulation studies
[SH-9.1-13] N85-35128
Observation of nuclei with energies 8-30 MeV per nucleon in the Earth's magnetosphere at the altitudes 350 KM
[SH-10.1-5] N85-35136
PROTONS
Two classes of solar energetic particle events associated with impulsive and long duration soft X-ray flares
[SH-1.2-12] N85-34747
Solar flare gamma-ray line spectroscopy
[SH-2.1-14] N85-34795
The central engine of quasars and AGNs: A relativistic proton radiative shock
[OG-8.1-7] N85-34897
Pulsars as cosmic ray particle accelerators: Proton orbits
[OG-8.2-21] N85-34917
Pulsars as cosmic ray accelerators: Energy development of protons
[OG-8.2-22] N85-34918
Detection of 10 (1) GeV cosmic neutrinos with a space station
[OG-9.4-10] N85-34977
Solar modulation and interplanetary gradients of the galactic electrons flux, 1977 - 1984
[SH-4.7-4] N85-35049
Proton albedo spectrum observation in low latitude region at Hyderabad, India
[SH-6.1-8] N85-35082
PSYCHOLOGICAL EFFECTS
Problems of aviation and space medicine and psychology discussed at 14th Gagarin lectures N85-34509
PULSARS
Scaling from Jupiter to pulsars and the acceleration of cosmic ray particles by pulsars, 3
[OG-8.2-3] N85-34904
On magnetic pair production above fast pulsar polar caps
[OG-8.2-13] N85-34909
Pulsars as cosmic ray particle accelerators: Proton orbits
[OG-8.2-21] N85-34917
Pulsars as cosmic ray accelerators: Energy development of protons
[OG-8.2-22] N85-34918
Pulsars as cosmic ray particle accelerators: Dynamics of electrons
[OG-8.2-23] N85-34919
PULSE AMPLITUDE
Behaviors of stress waves in a conical bar N85-34182
Cosmic ray north-south anisotropy 1961 - 1983
[SH-4.2-6] N85-34844
PULSE COMMUNICATION
New directional couplers for multimode circular waveguides applied to intense pulsed microwave systems
[DE85-011753] N85-34330
Joint services electronics program
[AD-A154748] N85-34336
PULSE COMPRESSION
Repetitive pulse accelerator technology for light ion inertial confinement fusion
[DE85-012030] N85-34693
PULSE DURATION
The longitudinal thickness of air-shower fronts
[OG-9.5-1] N85-34978
PULSE GENERATORS
Series-counterpulse repetitive-pulse inductive storage circuit
[DE85-006438] N85-34342
PULSE MODULATION
Cosmic ray modulatin and merged interaction regions
[SH-4.1-11] N85-34834
Propagation of the phase of solar modulation
[SH-4.1-12] N85-34835
The 1973-1984 solar modulation of cosmic ray nuclei
[SH-4.1-16] N85-34838
Cosmic ray modulation in a random anisotropic magnetic field
[SH-4.1-20] N85-34839
Evidence for regions of negligible cosmic-ray modulation in the inner heliosphere (10 AU)
[SH-4.1-21] N85-34840
Drift and observations in cosmic-ray modulation, 1
[SH-4.2-4] N85-34842
Drift and observations in cosmic-ray modulation, 2
[SH-4.2-5] N85-34843
Variations of the cosmic ray general component in Antarctica
[SH-4.4-17] N85-35013
PULSED LASERS
The use of optical fibers in pulsed laser holography
[ISL-CO-226/84] N85-34395
Theoretical and experimental analyses of the performance of two-color laser ranging systems
[NASA-CR-176159] N85-34397
Ranging system which compares an object reflected component of a light beam to a reference component of the light beam
[NASA-CASE-NPO-15865-1] N85-34629
Survey of mixing in metal/insulator systems
[DE85-011938] N85-34714
PULSED RADIATION
Instrumentation for sensing moisture content of material using a transient thermal pulse
[NASA-CASE-NPO-15493-2] N85-34373
Cosmic ray modulatin and merged interaction regions
[SH-4.1-11] N85-34834
PULSES
Multiple-stage integrating accelerometer
[DE85-006505] N85-34388
Electronic imaging system and technique
[DE85-005740] N85-34393
EML pulse ionization chamber systems for (222)Rn measurements
[DE85-012320] N85-34610
PUMPS
Combined cold compressor/ejector helium refrigerator
[DE85-006408] N85-34326
PURGING
Evacuate and backfill apparatus and method
[DE85-006018] N85-34411
PURIFICATION
Method for removing oxide contamination from silicon carbide powders
[DE85-011648] N85-34287
PURITY
Method for preparing high purity vanadium
[DE85-006412] N85-34242
An X-ray diffraction study of titanium oxidation
[NASA-CR-176263] N85-34264
PYROHELIOMETERS
Active Cavity Radiometer (ACR) N85-34163
PYROLYSIS
Oxygen analyzer
[DE85-006002] N85-34392
PYROMETERS
Investigation of non-intrusive radiometers for entrained gasifier temperature measurement, revision 3
[DE85-011795] N85-34385
PYROPHORIC MATERIALS
Review of zirconium-zircaloy pyrophoricity
[DE85-011169] N85-34270

Q

QUALITATIVE ANALYSIS
Direct determination of metals in organic matrices by Inductively Coupled Plasma-Atomic Emission Spectrometry (ICP-AES)
[DE85-012015] N85-34233
QUALITY CONTROL
EML pulse ionization chamber systems for (222)Rn measurements
[DE85-012320] N85-34610
QUANTITATIVE ANALYSIS
Quantitative analysis of flare accelerated electrons through their hard X-ray and microwave radiation
[SH-1.2-7] N85-34742
QUANTUM CHROMODYNAMICS
Duality of two-point functions for confined non-relativistic quark-antiquark systems
[DE85-012334] N85-34618
QUANTUM ELECTRODYNAMICS
Evaluation of parameters for particles acceleration by the zero-point field of quantum electrodynamics
[OG-8.2-16] N85-34912
QUANTUM ELECTRONICS
Joint services electronics program
[AD-A154748] N85-34336
QUASARS
The central engine of quasars and AGNs: A relativistic proton radiative shock
[OG-8.1-7] N85-34897

R

RADAR SIGNATURES
Hardware test program for evaluation of basline range-range rate sensor concept
[NASA-CR-176143] N85-34377
RADIAL DISTRIBUTION
Breakdown of intrinsic ambipolarity for the radial diffusion due to a rotating RF field N85-34660
Transports studies of ECH and ICRH-heated bumpy torus plasma in NBT-1M N85-34662
Analytic and numerical calculations of the ambipolar electric field in a stellarator N85-34665
Radial and latitudinal gradients of anomalous oxygen during 1977 - 1985
[SH-4.6-4] N85-35042
The cosmic ray interplanetary radial gradient from 1972 - 1985
[SH-4.7-1] N85-35046
RADIANCE
Diurnal variations of cosmic ray geomagnetic cut-off threshold rigidities
[SH-6.1-21] N85-35092
RADIANT FLUX DENSITY
the role of shock waves in modulation of galactic cosmic rays
[SH-4.1-7] N85-34831
Cumulative effect of Forbush decreases in the heliospheric modulation during the present solar cycle
[SH-4.1-10] N85-34833
Cosmic ray modulatin and merged interaction regions
[SH-4.1-11] N85-34834
Propagation of the phase of solar modulation
[SH-4.1-12] N85-34835
Longitudinal distribution of cosmic rays in the heliosphere
[SH-4.1-14] N85-34837
The 1973-1984 solar modulation of cosmic ray nuclei
[SH-4.1-16] N85-34838
Evidence for regions of negligible cosmic-ray modulation in the inner heliosphere (10 AU)
[SH-4.1-21] N85-34840
Notes on drift theory
[SH-4.2-3] N85-34841
Drift and observations in cosmic-ray modulation, 2
[SH-4.2-5] N85-34843
Propagation and nucleosynthesis of ultraheavy cosmic rays
[OG-7.1-5] N85-34867
High resolution Cherenkov detectors for cosmic ray isotope experiment
[OG-9.1-4] N85-34930

The final COS-B database now publicly available
[OG-9.3-8] N85-34963
The final COS-B database: In-flight calibration of instrumental parameters
[OG-9.3-9] N85-34964
An observatory to study 10 (10) to 10 (17) by EV gamma rays
[OG-9.4-6] N85-34973
Mini and super mini arrays for the study of highest energy cosmic rays
[OG-9.4-9] N85-34976
Cosmic ray biannual variation
[SH-4.4-15] N85-35011
Cosmic ray power spectral variations. 3: Solar rotation periodicities
[SH-4.4-16] N85-35012
The difference in the energy spectra of galactic cosmic rays at the minima of the 19th and 20th solar activity cycles
[SH-4.4-18] N85-35014
Cosmic ray variations with the period close to 27 days and their connection with solar activity longitudinal distribution
[SH-4.4-19] N85-35015
Azimuthal and meridional asymmetries of the solar wind and quasiperiodic variations of intensity of Galactic Cosmic Rays (GCR)
[SH-4.4-20] N85-35016
Dynamics of two-year cosmic ray variations inferred from the data of spacecraft and stratospheric measurements and from the neutron monitor data in 1959-1981
[SH-4.4-21] N85-35017
Long-term modulation of galactic cosmic rays in high-energy region
[SH-4.4-22] N85-35018
Diurnal effect in cosmic rays at middle latitudes according to stratospheric measurements
[SH-4.5-8] N85-35026
Diurnal variation of galactic cosmic ray intensity on quiet days
[SH-4.5-11] N85-35029
Diurnal variations from muon data at Takeyama underground station
[SH-4.5-13] N85-35030
Long term changes in cosmic ray diurnal variations observed by ion chambers in Hong Kong and Japan
[SH-4.5-14] N85-35031
Cosmic ray density gradient and its dependence on the north-south asymmetry in solar activity
[SH-4.5-17] N85-35034
Diagnostic of electromagnetic conditions in space using cosmic rays
[SH-4.5-19] N85-35036
Solar cycle variations of the anaomalous cosmic ray component
[SH-4.6-2] N85-35040
Temporal variations of the anomalous oxygen component, 1977 - 1984
[SH-4.6-3] N85-35041
Radial and latitudinal gradients of anomalous oxygen during 1977 - 1985
[SH-4.6-4] N85-35042
The cosmic ray interplanetary radial gradient from 1972 - 1985
[SH-4.7-1] N85-35046
When did the average cosmic ray flux increase?
[SH-7.1-4] N85-35097

RADIATION
Longitudinal distribution of cosmic rays in the heliosphere
[SH-4.1-14] N85-34837

RADIATION ABSORPTION
An approach of reducing the background induced by neutrons
[OG-9.3-5] N85-34960

RADIATION BELTS
Cosmic-ray transport in the galactic magnetosphere
[OG-7.2-17] N85-34884

RADIATION COUNTERS
Solar Ultraviolet Spectral Irradiance Monitor (SUSIM) N85-34160
The response of ionization chambers to relativistic heavy nuclei
[OG-9.1-13] N85-34939
Comparisons of monthly mean cosmic ray counting rates observes from worldwide network of neutron monitors
[SH-9.1-7] N85-35122

RADIATION DAMAGE
The 1983 international intercomparison of nuclear accident dosimetry systems at Oak Ridge National Laboratory
[DE85-011303] N85-34382

RADIATION DETECTORS
CYLTRAN calculations of electron effects on XD detectors
[LA-10264-MS] N85-34601
Improved method for the stabilization of NaI-photomultiplier gamma detectors against thermal and other drift
[DE85-011830] N85-34613
Cross sections for the production of fragments with Z greater than or equal to 8 by fragmentation of Z greater than or equal to 9 and less than or equal to 26 nuclei
[OG-7.2-22] N85-34889
The development of a high energy cosmic ray detector for Spacelab-2
[OG-9.1-8] N85-34934
Cherenkov-dE/dx-range measurements on cosmic ray iron group nuclei
[OG-9.1-12] N85-34937
The response of ionization chambers to relativistic heavy nuclei
[OG-9.1-13] N85-34939
A balloon-borne imaging gamma-ray telescope
[OG-9.2-2] N85-34941
The Figaro experiment for the observation of time marked sources in the low energy gamma-ray range
[OG-9.2-11] N85-34950
A position sensitive phoswich hard X-ray detector system
[OG-9.3-12] N85-34967
The Buckland Park air shower array
[OG-9.4-4] N85-34971
An EAS experiment at mountain altitude for the detection of gamma-ray sources
[OG-9.4-5] N85-34972
Detection of 10 (1) GeV cosmic neutrinos with a space station
[OG-9.4-10] N85-34977
Shower disc sampling and the angular resolution of gamma-ray shower detectors
[OG-9.5-2] N85-34980
Angular resolution of air-shower array-telescopes
[OG-9.5-6] N85-34983
Astrophysical applications of high angular resolution array-telescopes
[OG-9.5-7] N85-34984
Results of ultra-low level 71ge counting for application in the Gallex-solar neutrino experiment at the Gran Sasso Underground Physics Laboratory
[SH-8.1-2] N85-35108
Detector calibration of the Indian cosmic ray experiment (IONS) in Space-Shuttle Spacelab-13
[SH-9.1-2] N85-35117

RADIATION DISTRIBUTION
Longitudinal distribution of cosmic rays in the heliosphere
[SH-4.1-14] N85-34837
Notes on drift theory
[SH-4.2-3] N85-34841
The model-independence of cosmic ray source determinations
[OG-7.2-1] N85-34873

RADIATION DOSAGE
Marine Sample Exploitation Project: Estimates regarding the sensitivity and technology for the detection of nuclear explosion debris in the marine environment
[DE85-013176] N85-34462
Circuit approaches to increasing SRAM performance in total dose environments
[DE85-009441] N85-34588

RADIATION EFFECTS
Analysis of transient radiation upset in a 16K SRAM
[DE85-009442] N85-34586

RADIATION HARDENING
Circuit approaches to increasing SRAM performance in total dose environments
[DE85-009441] N85-34588

RADIATION HAZARDS
MATADOR (Methods for the Analysis of Transport And Deposition Of Radionuclides) code description and user's manual
[TI85-901402] N85-34592

RADIATION INJURIES
The 1983 international intercomparison of nuclear accident dosimetry systems at Oak Ridge National Laboratory
[DE85-011303] N85-34382

RADIATION MEASUREMENT
The 1983 international intercomparison of nuclear accident dosimetry systems at Oak Ridge National Laboratory
[DE85-011303] N85-34382
EML pulse ionization chamber systems for (222)Rn measurements
[DE85-012320] N85-34610
Measurement and interpretation of electron angle at MABE beam stop
[DE85-011918] N85-34696
Solar Coronal and photospheric abundances from solar energetic particle measurements
[SH-2.1-5] N85-34786

RADIATION MEASURING INSTRUMENTS
Search for solar neutrons using NM-64 equipment
[SH-1.4-5] N85-34765

RADIATION SHIELDING
Container for radioactive materials
[DE85-005757] N85-34826
A comparison of calculated and measured background noise rates in hard X-ray telescopes at balloon altitude
[OG-9.3-7] N85-34962

RADIATION SOURCES
Type 3 solar radio bursts and 3HE-rich events
[SH-2.2-3] N85-34798
Germanium and lead: Significant differences between meteoritic and photospheric abundances?
[OG-7.1-2] N85-34864
Implications of source abundances of ultraheavy cosmic rays
[OG-7.1-4] N85-34866
Propagation and nucleosynthesis of ultraheavy cosmic rays
[OG-7.1-5] N85-34867
A model for the origin of high-energy cosmic rays
[OG-8.1-8] N85-34898
Approximate supernova remnant dynamics with cosmic ray production
[OG-8.1-12] N85-34901
Scaling from Jupiter to pulsars and the acceleration of cosmic ray particles by pulsars, 3
[OG-8.2-3] N85-34904

RADIATION SPECTRA
Nucleosynthesis in the terrestrial and solar atmospheres
[SH-2.2-2] N85-34797
Penetration of solar protons into the Earth's magnetosphere on November 22, 1977
[SH-6.1-15] N85-35088

RADIATION TRANSPORT
Coupled electron-photon transport calculations using the method of discrete ordinates
[DE85-009444] N85-34597
Monte Carlo techniques for analyzing deep penetration problems
[DE85-011426] N85-34598
Numerical descriptions of cosmic-ray transport
[SH-4.1-3] N85-34829
Numerical and analytic descriptions of cosmic-ray transport
[SH-4.1-4] N85-34830

RADICALS
Measurements of the fragmentation of (40)Ar, (28)Si and (12)C in CH2C and H targets between 300 and 1500 MeV/nuc at the Bevalac
[OG-7.2-19] N85-34886

RADIO COMMUNICATION
Performance interface document for the S-band diplexer for space users of NASA networks
[NASA-TM-86224] N85-34155

RADIO EMISSION
The final COS-B database now publicly available
[OG-9.3-8] N85-34963
Sporadic radio emission connected with a definite manifestation of solar activity in the near Earth space
[SH-10.1-8] N85-35139
Near Earth space sporadic radio emission busts occurring during sunrise
[SH-10.1-9] N85-35140

RADIO FREQUENCIES
Breakdown of intrinsic ambipolarity for the radial diffusion due to a rotating RF field N85-34660
Synthesis of ultrafine ceramic and metallic powders in a thermal argon rf plasma
[DE85-009634] N85-34696
Sporadic radio emission connected with a definite manifestation of solar activity in the near Earth space
[SH-10.1-8] N85-35139
Near Earth space sporadic radio emission busts occurring during sunrise
[SH-10.1-9] N85-35140

RADIO FREQUENCY DISCHARGE
Fokker-Planck calculation of hot electron formation in the thermal barrier region of tandem mirror Gamma-10
[IPPJ-726] N85-34669

RADIO FREQUENCY HEATING
Activities of the RF Section N85-34646
RF induced radial diffusion in tandem mirrors N85-34649
Model of azimuthal non-uniformities induced by RF heating in RFC-XXM N85-34658

RADIO FREQUENCY INTERFERENCE
Adaptive antenna arrays for satellite communications: Design and testing
[NASA-CR-176162] N85-34329

RADIO RECEIVERS
Waves in Space Plasmas (WISP) N85-34164

RADIO SOURCES (ASTRONOMY)
The extent of the local hi halo
[NASA-CR-176115] N85-34724
Burst and Transient Source Experiment (BATSE) for the Gamma Ray Observatory (GRO)
[OG-9.2-14] N85-34953
Capabilities of the GRO/BATSE for monitoring of discrete sources
[OG-9.2-16] N85-34955
RADIO TRANSMITTERS
Waves in Space Plasmas (WISP) N85-34164
RADIO WAVES
Onion-shell model for cosmic ray electrons and radio synchrotron emission in supernova remnants
[OG-8.1-10] N85-34900
RADIOACTIVE CONTAMINANTS
MATADOR (Methods for the Analysis of Transport And Deposition Of Radionuclides) code description and user's manual
[TI85-901402] N85-34592
RADIOACTIVE DECAY
Electron capture decay of cosmic rays: A model of the inhomogeneous interstellar medium
[OG-7.1-10] N85-34871
RADIOACTIVE ISOTOPES
MATADOR (Methods for the Analysis of Transport And Deposition Of Radionuclides) code description and user's manual
[TI85-901402] N85-34592
Development of the osmium-191 yields iridium-191m radionuclide generator
[DE85-011185] N85-34611
Current status of the Os-191 yields Ir-191m generator
[DE85-008306] N85-34614
Elemental technetium as a cosmic-ray clock
[OG-7.1-9] N85-34870
Bevalac calibration of the SOFIE range and hodoscope detectors
[OG-9.1-7] N85-34933
High precise measurements of cosmogenic radiocarbon abundance by complex of scintillation equipments
[SH-7.1-14] N85-35105
RADIOACTIVE MATERIALS
Container for radioective materials
[DE85-005757] N85-34626
RADIOACTIVE WASTES
Method for extracting lanthanides and actinides from acid solutions by modification of Purex solvent
[DE85-005763] N85-34220
Research at the Institute of Oceanographic Sciences related to the possible disposal of radioactive waste on or beneath the seafloor
[IOS-204] N85-34628
RADIOMETERS
Active Cavity Radiometer (ACR) N85-34163
Investigation of non-intrusive radiometers for entrained gasifier temperature measurement, revision 3
[DE85-011795] N85-34385
RADIOMETRIC RESOLUTION
The 13 November 1984 occultation of BD +08 deg 0471 by (1) Ceres
[NASA-CR-176106] N85-34725
RADON
EML pulse ionization chamber systems for (222)Rn measurements
[DE85-012320] N85-34610
RAIN
Tunisian climate seen through a Markov process
[CT-585] N85-34482
RAMAN SPECTRA
Time-resolved spectroscopic studies of detonating heterogeneous explosives
[DE85-009760] N85-34297
RAMJET ENGINES
A model of hypersonic two-dimensional oblique detonation wave ramjet
[UTIAS-TN-257] N85-34139
RAMP FUNCTIONS
The collected data for ramp function tests on a NACA 23012 aerofoil. Volume 1: Description and pressure data
[GU-AERO-8413-VOL-1] N85-34123
RANDOM LOADS
Safety and reliability of steel structural materials under random service impact loads N85-34197
RANDOM SAMPLING
A new approach to evaluate gamma-ray measurements
[OG-9.5-11] N85-34988
RANDOM WALK
Monte Carlo techniques for analyzing deep penetration problems
[DE85-011426] N85-34598
RANGE FINDERS
Ranging system which compares an object reflected component of a light beam to a reference component of the light beam
[NASA-CASE-NPO-15865-1] N85-34629
RANGEFINDING
Hardware test program for evaluation of basline range-range rate sensor concept
[NASA-CR-176143] N85-34377
RAPID BALLISTICS IDENTIFICATION
Flash X-ray diffraction
[ISL-CO-227/84] N85-34396
RARE EARTH COMPOUNDS
Changes in lattice cell parameter of film intermetallic compounds RT2
[BLL-M-35874-(5828.4)] N85-34261
RARE EARTH ELEMENTS
Method for extracting lanthanides and actinides from acid solutions by modification of Purex solvent
[DE85-005763] N85-34220
RARE GASES
Heaterless ignition of inert gas ion thruster hollow cathodes
[NASA-TM-87086] N85-34177
Gas shielding apparatus
[DE85-005992] N85-34416
The 3HE in solar non-relativistic electron events
[SH-2.2-5] N85-34800
RAREFIED GAS DYNAMICS
Unsteady transonic heat transfer in a transient facility
[NASA-CR-176145] N85-34354
RATES (PER TIME)
Time-resolved spectroscopic studies of detonating heterogeneous explosives
[DE85-009760] N85-34297
Dual-chamber plasma deposition of A-Si:H solar cells at high rates using disilane
[DE85-011828] N85-34451
Analysis of transient radiation upset in a 16K SRAM
[DE85-009442] N85-34586
Ranging system which compares an object reflected component of a light beam to a reference component of the light beam
[NASA-CASE-NPO-15865-1] N85-34629
Injection of energetic particles following the gamma-ray flares on June 7, 1980, as observed on Helios 1
[SH-1.3-9] N85-34756
Angular resolution of air-shower array-telescopes
[OG-9.5-6] N85-34983
The angular resolution of air shower gamma ray telescopes
[OG-9.5-14] N85-34990
Recording system for the solar neutron monitoring at Mt. Norikura
[SH-9.1-8] N85-35123
Burst size distributions in the digitized data of the ion chambers t Mt. Norikura and sea level stations
[SH-9.1-9] N85-35124
Sensitivity of single and multiple cosmic ray neutrons to the surrounding medium in a lead-free monitor
[SH-9.1-10] N85-35125
The neutron moderated detector and groundbased cosmic ray modulation studies
[SH-9.1-13] N85-35128
A suggested standardized format for cosmic ray ground-level event data
[SH-9.1-15] N85-35130
RATIOS
Explanation of the secondary to primary ratio within the continuous Fermi accelerator model
[OG-8.3-2] N85-34921
Propagation of injected cosmic rays under distributed reacceleration
[OG-8.3-3] N85-34922
RATS
The 1984 biotic studies of Yucca Mountain, Nevada test site, Nye County, Nevada
[DE85-011715] N85-34487
Rat skeletal muscles with simulation of physiological effects of weightlessness (morphological study) N85-34502
Lipogenesis in rat liver after flight aboard Cosmos-1129 biosatellite N85-34508
RAY TRACING
A theoretical and empirical analysis of coherent ray-tracing N85-34524
A simple but systematic CSG system N85-34569
RAYLEIGH DISTRIBUTION
A new approach to evaluate gamma-ray measurements
[OG-9.5-11] N85-34988
A new statistic for the analysis of circular data in gamma-ray astronomy
[OG-9.5-13] N85-34989
RAYS
Solar neutrino: Flux, cosmic rays and the 11 year solar cycle
[SH-8.1-7] N85-35112
REACTION KINETICS
Separation of gas mixtures by supported complexes
[DE85-011996] N85-34236
Effects of hot deformation on the kinetics of the pearlite transformation in eutectoid steel
[BLL-M-35844-(5828.4)] N85-34250
Metal alkoxides: Models for metal oxides. Alkoxide ligands in early transition metal organometallic chemistry
[DE85-011368] N85-34269
Thermally induced chemical migration: A natural analog approach
[DE85-012308] N85-34474
Application of evaluated fission-product delayed-neutron precursor data in reactor kinetics calculations
[DE85-012728] N85-34624
Survey of mixing in metal/insulator systems
[DE85-011938] N85-34714
REACTIVITY
Method for preparing hydride configurations and reactive metal surface
[DE85-006443] N85-34274
REACTOR CORES
MATADOR (Methods for the Analysis of Transport And Deposition Of Radionuclides) code description and user's manual
[TI85-901402] N85-34592
Liquid uranium alloy-helium fission reactor
[DE85-006511] N85-34607
REACTOR MATERIALS
Stress corrosion cracking susceptibility of types 316NG and 316 stainless steel in an impurity environment
[TI85-006884] N85-34277
Effect of stainless steel weld overlay cladding on the structural integrity of flawed steel plates in bending, series 1
[TI85-010349] N85-34418
REACTOR SAFETY
MATADOR (Methods for the Analysis of Transport And Deposition Of Radionuclides) code description and user's manual
[TI85-901402] N85-34592
READ-ONLY MEMORY DEVICES
Maintenance port system
[AD-D011724] N85-34594
READOUT
The read-out system of spatial distribution of thermoluminescence in meteorites
[SH-9.1-16] N85-35131
REAL TIME OPERATION
Animengine: An engineering animation system N85-34535
Real-time multiparameter pulse processing with decision tables
[DE85-011683] N85-34589
RECTANGLES
Acoustical absorption coefficient in a diffuse field of a plane, rectangular material of finite dimensions placed on an infinite perfectly reflecting surface
[NRC/CNR-TT-2113] N85-34599
REDOX CELLS
Evaluation of developmental membranes for the mixed reactant iron-chromium redox system
[NASA-TM-87074] N85-34443
REDUCTION (CHEMISTRY)
Electron photoejection in carbanions
[DE85-011748] N85-34237
Method for preparing high purity vanadium
[DE85-006412] N85-34242
REDUNDANCY
Intelligent redundant actuation system requirements and preliminary system design
[NASA-CR-177366] N85-34136
Hexagonal uniformly redundant arrays for coded-aperture imaging
[OG-9.2-1] N85-34940
REDUNDANT COMPONENTS
Intelligent redundant actuation system requirements and preliminary system design
[NASA-CR-177366] N85-34136
REENTRY VEHICLES
Thermal protection systems for reentry vehicles
[CNES-NT-113] N85-34157
REFLECTANCE
Empirical model for the Earth's cosmic ray shadow at 400 KM: Prohibited cosmic ray access
[SH-6.1-14] N85-35087
REFLECTION
Ranging system which compares an object reflected component of a light beam to a reference component of the light beam
[NASA-CASE-NPO-15865-1] N85-34629

REFRACTORY MATERIALS
Thermal protection systems for reentry vehicles
[CNES-NT-113] N85-34157
REFRIGERANTS
Determination of properties of zeolite/refrigerant combinations for solar refrigeration systems
[DE85-012009] N85-34448
REFRIGERATING
Refrigerated dynamic seal to 6.9 MPa (1000 psi)
[NASA-TM-87108] N85-34356
REFRIGERATORS
Combined cold compressor/ejector helium refrigerator
[DE85-006408] N85-34326
REGENERATION (ENGINEERING)
Composite desiccant structure
[DE85-006400] N85-34226
REGIONS
A new approach to linear quadtrees N85-34550
An analysis and algorithm for filling propagation N85-34551
REINFORCED PLATES
Impact fracture mechanism of polymer plates containing a heavy inner material N85-34215
REINFORCING FIBERS
Substitution of asbestos by aramid fibers and fiber blends in industrial textiles and composites with organic binders
[BMFT-FB-T-85-006] N85-34294
RELATIVISTIC ELECTRON BEAMS
Injection of energetic particles following the gamma-ray flares on June 7, 1980, as observed on Helios 1
[SH-1.3-9] N85-34756
Ultrarelativistic electrons and solar flare gamma-radiation
[SH-1.3-11] N85-34757
RELATIVISTIC PARTICLES
Simulation studies on stability of hot electron plasma N85-34664
Multiple inner shell vacancies in laser-irradiated Au plasma N85-34687
Neutron-induced 2.2 MeV background in gamma ray telescopes
[OG-9.3-6] N85-34961
A bi-directional charged particle telescope to observe flux, energy spectrum and angular distribution of relativistic and non-relativistic particles
[SH-9.1-4] N85-35119
RELATIVISTIC PLASMAS
Multiple inner shell vacancies in laser-irradiated Au plasma N85-34687
Monte Carlo calculations of relativistic solar proton propagation in interplanetary space
[SH-3.2-11] N85-34826
Selfsimilar time dependent shock structures
[OG-8.1-4] N85-34894
RELATIVISTIC VELOCITY
Spectra of solar proton ground level events using neutron monitor and neutron moderated detector recordings
[SH-1.3-14] N85-34759
RELIABILITY
Analytical ultrasonics for structural materials
[TI85-006132] N85-34600
RELIABILITY ENGINEERING
Statistical pooling method of fatigue data for reliability design N85-34198
REMOTE SENSING
Potential spin-offs of the carbon dioxide observational platform system (CO-OPS) for remote sensing opportunities
[NASA-TP-2510] N85-34149
The scientific and technical issues in integrating remotely sensed imagery with geocoded data bases N85-34547
Selection of segment similarity measures for hierarchical picture segmentation N85-34548
The International Cometary Explorer (ICE) wallsheet teacher's guide
[NASA-TM-87498] N85-34727
RENAL FUNCTION
Fluid-electrolyte metabolism and renal function in cosmonauts following 185-day spaceflight N85-34495
REPETITION
Vector calculation of particle code N85-34688
REPLACING
Negative flexural behavior of precase composite slabs with steel joint N85-34183
REPORTS
Confinement experiments on ISX-B
[DE85-012346] N85-34709
RESEARCH AND DEVELOPMENT
Electron photoejection in carbanions
[DE85-011747] N85-34230
RESEARCH FACILITIES
Langley aeronautics and space test highlights, 1984
[NASA-TM-87585] N85-35151
RESERVES
Preliminary SPR thermal model description and results for WH-11 and BM-4
[DE85-013171] N85-34360
RESERVOIRS
Comprehensive fracture diagnostics experiement. Part 2: Comparison of seven fracture azimuth measurements
[DE85-011707] N85-34470
Studies in thermo-hydro-chemical transport in porous and fractured media
[DE85-012555] N85-34473
RESIDENTIAL ENERGY
Advanced heat pump research and development
[DE85-009540] N85-34372
RESIDUAL STRESS
X-ray residual stress analysis on the coarse grain of copper and its application to the brazed copper N85-34202
Study on the correlation between grinding conditions and residual stresses in ground surface of steel by the X-ray method N85-34203
Multiaxial stress analysis taking account of penetration depth of X-rays. A solution by means of polynomial approximation N85-34204
Influence of cyclic thermal loading on internal stress in casted epoxy resin N85-34211
RESIN MATRIX COMPOSITES
Effect of strain rate on the initial failure of notched GRP laminates N85-34214
RESISTANCE HEATING
Instrumentation for sensing moisture content of material using a transient thermal pulse
[NASA-CASE-NPO-15493-2] N85-34373
RESISTORS
Low noise polycrystalline semiconductor resistors by hydrogen passivation
[AD-D011721] N85-34338
RESONANCE
Calculating the interatomic pair potential allowing for resonance interaction in titanium, nickel and vanadium
[BLL-M-35843-(5828.4)] N85-34249
Capture in the 1.15-keV iron resonance
[DE85-011913] N85-34612
RESONANCE PROBES
The heavy ion composition in 3HE-rich solar flares
[SH-2.2-7] N85-34802
RESONANT FREQUENCIES
Rotor blade test apparatus
[AD-D011725] N85-34381
RESPONSE TIME (COMPUTERS)
Using percent-done program indicators to enhance user interfaces N85-34546
RETARDERS (DEVICES)
Sensitivity of single and multiple cosmic ray neutrons to the surrounding medium in a lead-free monitor
[SH-9.1-10] N85-35125
REUSABLE HEAT SHIELDING
Thermal protection systems for reentry vehicles
[CNES-NT-113] N85-34157
Experimental aerodynamic heating to simulated space shuttle tiles in laminar and turbulent boundary layers with variable flow angles at a nominal Mach number of 7
[NASA-TP-2307] N85-34351
REVERSING
Latitudinal gradients of cosmic rays and the polarity reversal of the heliospheric magnetic field: A preliminary evaluation
[SH-4.2-16] N85-34853
REYNOLDS NUMBER
The aerodynamic characteristics of a GU25-5(11)8 aerofoil for low Reynolds numbers
[GU-AERO-8410] N85-34121
REYNOLDS STRESS
A study of the second and third order closure models of turbulence for prediction of separated shear flows
[NASA-CR-176127] N85-34353
RHODIUM COMPOUNDS
Magnitude and range of the RKKy interaction in SmRh4B4
[DE85-012284] N85-34712
RIGID STRUCTURES
The dynamics of articulated rigid bodies for purposes of animation N85-34579
RIGID WINGS
The aerodynamic characteristics of a GU25-5(11)8 aerofoil for low Reynolds numbers
[GU-AERO-8410] N85-34121
RIGIDITY
Rigid zeolite containing polyurethane foams
[DE85-006406] N85-34286
Effects of solar magnetic field on cosmic rays
[SH-4.2-12] N85-34850
The expected cosmic ray density and stream distributions at the heliolatitudinal asymmetry of solar wind
[SH-4.2-14] N85-34852
The dependence of solar modulation on the sign of the cosmic ray particle charge
[SH-4.2-23] N85-34860
Observation of nuclei with energies 8-30 MeV per nucleon in the Earth's magnetosphere at the altitudes 350 KM
[SH-10.1-5] N85-35136
RIPPLES
Neoclassical diffusion including ellipticity in a heliotron-like configuration N85-34667
RISK
Description of a test site for large-scale heavy gas dispersion and combustion experiments
[DE85-004987] N85-34231
The application of models to the assessment of fire hazard from consumer products
[NBSIR-85-3219] N85-34325
ROADS
Design and implementation of an interactive route editor N85-34559
ROBOTS
Multi-robot assembly of IC's N85-34577
Robot environment expert system
[NASA-CR-3915] N85-34593
ROCKET THRUST
Heaterless ignition of inert gas ion thruster hollow cathodes
[NASA-TM-87086] N85-34177
ROLLER BEARINGS
The use of ultrasound to monitor incipient failure of rolling element bearings N85-34317
Elastohydrodynamic lubrication calculations used as a tool to study scuffing
[NASA-TM-87097] N85-34408
Design and lubrication of high-speed rolling-element bearings
[NASA-TM-87107] N85-34409
ROOTS OF EQUATIONS
Finding the roots of the transcendental equations in problems in determining the thermal conductivity of spheres with heterogeneous boundary conditions
[BLL-M-35878-(5828.4)] N85-34347
ROTARY WINGS
A three-dimensional viscous flow analysis for the helicopter tip vortex generation problem
[NASA-CR-3906] N85-34114
An evaluation of three helicopter rotor sections
[NASA-TM-86719] N85-34115
ROTATING DISKS
A rational approach to cam design N85-34311
ROTATION
Breakdown of intrinsic ambipolarity for the radial diffusion due to a rotating RF field N85-34660
Measurement of low energy cosmic rays aboard Spacelab-1
[SH-10.1-6] N85-35137
Heavy cosmic ray measurement aboard Spacelab-1
[SH-10.1-7] N85-35138
ROTOR BLADES (TURBOMACHINERY)
Rotor blade test apparatus
[AD-D011725] N85-34381
Reflection plane tests of a wind turbine blade tip section with ailerons
[NASA-TM-87018] N85-34444
ROTOR SYSTEMS RESEARCH AIRCRAFT
Flight testing the fixed-wing configuration of the Rotor Systems Research Aircraft (RSRA)
[NASA-TM-86762] N85-34135
ROUGHNESS
Mechanical properties of plasma arc cut steel N85-34188
RUBY LASERS
Instrument to synchronize Thomson scattering diagnostic measurements with MHD activity in a Tokamak
[DE85-012082] N85-34708
RUNGE-KUTTA METHOD
Compressible two-phase flow instabilities simulated with a hybrid Lagrange-Euler pseudospectral method
[DE85-009904] N85-34361
RUNWAYS
Guidelines for the evaluation of visual approach slope indicators
[ARL-SYS-R-32] N85-34132

S

S MATRIX THEORY
Duality of two-point functions for confined non-relativistic quark-antiquark systems
[DE85-012334] N85-34618
S WAVES
On the cosmic ray diffusion in a violent interstellar medium
[OG-7.2-14] N85-34881

SAFETY DEVICES
Fast shutter apparatus
[DE85-006501] N85-34343
SAFETY FACTORS
Safety and reliability of steel structural materials under random service impact loads N85-34197
General-purpose heat source development: Safety test program. Postimpact evaluation, design iteration test
[LA-10034-SR] N85-34606
SAFETY MANAGEMENT
Description of a test site for large-scale heavy gas dispersion and combustion experiments
[DE85-004987] N85-34231
SALT BEDS
Preliminary SPR thermal model description and results for WH-11 and BM-4
[DE85-013171] N85-34360
SAMARRIUM COMPOUNDS
Magnitude and range of the RKKy interaction in SmRh4B4
[DE85-012284] N85-34712
SAMPLING
Marine Sample Exploitation Project: Estimates regarding the sensitivity and technology for the detection of nuclear explosion debris in the marine environment
[DE85-013176] N85-34462
SATELLITE OBSERVATION
Method and apparatus for Delta Kappa synthetic aperture radar measurement of ocean current
[NASA-CASE-NPO-15704-1] N85-34327
SATELLITE TRANSMISSION
Adaptive antenna arrays for satellite communications: Design and testing
[NASA-CR-176162] N85-34329
SATELLITE-BORNE INSTRUMENTS
SONTRAC: A solar neutron track chamber detector
[SH-9.1-12] N85-35127
Measurement of low energy cosmic rays aboard Spacelab-1
[SH-10.1-6] N85-35137
SCALARS
Scalar/Vector potential formulation for compressible viscous unsteady flows
[NASA-CR-3921] N85-34113
SCALING LAWS
Scaling parameters of flashover
[NBS-GCR-85-497] N85-34229
Scaling differences between large interplate and intraplate earthquakes
[NASA-CR-176149] N85-34467
Confinement experiments on ISX-B
[DE85-012346] N85-34709
SCANNING
Intermolecular explosives
[DE85-009609] N85-34296
SCATTER PROPAGATION
Implications of cross section errors for cosmic ray propagation
[OG-7.2-3] N85-34875
Alfven wave scattering and the secondary to primary ratio
[OG-7.2-9] N85-34878
Interstellar turbulence, random density variations, and scintillation measurements
[OG-7.2-13] N85-34880
Relativistic transport theory for cosmic-rays
[OG-8.3-8] N85-34926
An experiment to measure the energy spectrum of cosmic ray antiprotons from 100 to 1000 MeV
[OG-9.1-3] N85-34929
SCATTERING
Monte Carlo techniques for analyzing deep penetration problems
[DE85-011426] N85-34598
Fokker-Planck calculation of hot electron formation in the thermal barrier region of tandem mirror Gamma-10
[IPPJ-726] N85-34669
Stochastic particle acceleration in solar flares
[SH-1.1-4] N85-34731
Exponential anisotropy of solar cosmic rays
[SH-3.2-1] N85-34817
Energetic solar particle events
[SH-3.2-2] N85-34818
Channeled propagation of solar particles
[SH-3.2-3] N85-34819
The local characteristic function of interplanetary particle propagation
[SH-3.2-8] N85-34823
Spatial distribution of cosmic rays in magnetic cycles of the Sun
[SH-4.2-20] N85-34857
SONTRAC: A solar neutron track chamber detector
[SH-9.1-12] N85-35127
SCATTERING CROSS SECTIONS
Implications of cross section errors for cosmic ray propagation
[OG-7.2-3] N85-34875
On the importance of interstellar helium for the propagation of heavy cosmic rays
[OG-7.2-11] N85-34879
SCATTEROMETERS
AMI calibration study. Volume 1: SAR calibration. Volume 2: Ground Targets. Volume 3: Scatterometer calibration --- Active Microwave Instrument (AMI) ERS-1
[C2248/4/4-VOL-1] N85-34394
SCINTILLATION
Methods and software for cosmic ray scintillation studies
[SH-9.1-17] N85-35132
SCINTILLATION COUNTERS
Specificity of (71)Ga(p,n) (71)Ge at 35 MeV for Gamow-Teller strength
[DE85-011837] N85-34615
A balloon-borne imaging gamma-ray telescope
[OG-9.2-2] N85-34941
Gamma-ray burst spectroscopy capabilities of the BATSE/GRO experiment
[OG-9.2-15] N85-34954
A position sensitive phoswich hard X-ray detector system
[OG-9.3-12] N85-34967
The Buckland Park air shower array
[OG-9.4-4] N85-34971
A new array for the study of ultra high energy gamma-ray sources
[OG-9.4-7] N85-34974
Akeno 20 km (2) air shower array (Akeno Branch)
[OG-9.4-8] N85-34975
The longitudinal thickness of air-shower fronts
[OG-9.5-1] N85-34978
Shower disc sampling and the angular resolution of gamma-ray shower detectors
[OG-9.5-2] N85-34980
Angular resolution of air-shower array-telescopes
[OG-9.5-6] N85-34983
Astrophysical applications of high angular resolution array-telescopes
[OG-9.5-7] N85-34984
The angular resolution of air shower gamma ray telescopes
[OG-9.5-14] N85-34990
Study of cosmic ray scintillations from 5-minute data of the scintillations telescope Izmran and world-wide network stations
[SH-5.1-18] N85-35071
High precise measurements of cosmogenic radiocarbon abundance by complex of scintillation equipments
[SH-7.1-14] N85-35105
Plastic scintillators in coincidence for the study of multi-particle production of sea level cosmic rays in dense medium
[SH-9.1-11] N85-35126
SCOUT PROJECT
User's operating procedures. Volume 1: Scout project information programs
[NASA-CR-177948] N85-34518
User's operating procedures. Volume 1: Scout project financial analysis program
[NASA-CR-177949] N85-34519
SCREENS
Development of metallization process: FSA project, cells and module formation research area
[NASA-CR-176136] N85-34447
SEA LEVEL
Plastic scintillators in coincidence for the study of multi-particle production of sea level cosmic rays in dense medium
[SH-9.1-11] N85-35126
The neutron moderated detector and groundbased cosmic ray modulation studies
[SH-9.1-13] N85-35128
Strong earthquakes, novae and cosmic ray environment
[SH-10.1-3] N85-35135
SEA WATER
A manual of methods for the continuous flow determination of ammonia, nitrate-nitrite, phosphate and silicate in seawater
[IOS-177] N85-34243
SEALERS
Fuel cell separator plate with bellows-type sealing flanges
[DE85-005991] N85-34459
SEALS (STOPPERS)
Refrigerated dynamic seal to 6.9 MPa (1000 psi)
[NASA-TM-87108] N85-34356
Oxidizing seal for a turbine tip gas path
[NASA-CASE-LEW-14053-1] N85-34402
Thermal stress analysis of a new turbine shroud seal concept
[NASA-TM-87082] N85-34406
SEAS
Marine Sample Exploitation Project: Estimates regarding the sensitivity and technology for the detection of nuclear explosion debris in the marine environment
[DE85-013176] N85-34462
SEATS
Design and testing of an energy-absorbing crewseat for the F/FB-111 aircraft, volume 1
[NASA-CR-3916] N85-34133
Design and testing of an energy-absorbing crewseat for the F/FB-111 aircraft. Volume 3: Data from crew module testing
[NASA-CR-3918] N85-34134
SECONDARY COSMIC RAYS
The effects of newly measured cross sections in hydrogen on the production of secondary nuclei during the propagation of cosmic rays through interstellar H
[OG-7.2-2] N85-34874
Cosmic ray secondary nuclei and the structure of the galaxy
[OG-7.2-4] N85-34876
Alfven wave scattering and the secondary to primary ratio
[OG-7.2-9] N85-34878
Influence of the source distribution on the age distribution of galactic cosmic rays
[OG-8.3-1] N85-34920
Explanation of the secondary to primary ratio within the continuous Fermi accelerator model
[OG-8.3-2] N85-34921
Secondary to primary ratio and the continuous acceleration
[OG-8.3-4] N85-34923
SECULAR VARIATIONS
Cosmic ray secular variations in terrestrial records and aurorae
[SH-7.1-3] N85-35096
SEEDS
Effect of seeds of heavy charged particles of galactic cosmic radiation N85-34505
SEGMENTS
Selection of segment similarity measures for hierarchical picture segmentation N85-34548
SEISMOLOGY
Geophysical-geological studies of possible extensions of the New Madrid fault zone
[TI85-901341] N85-34475
Strong earthquakes, novae and cosmic ray environment
[SH-10.1-3] N85-35135
SELECTION
Knowledge engineering application in image processing N85-34583
SELF SEALING
Refrigerated dynamic seal to 6.9 MPa (1000 psi)
[NASA-TM-87108] N85-34356
SEMICONDUCTOR DEVICES
Joint services electronics program
[AD-A154748] N85-34336
Applications of CdTe to nuclear medicine
[DE85-011877] N85-34492
Analysis of transient radiation upset in a 16K SRAM
[DE85-009442] N85-34586
Circuit approaches to increasing SRAM performance in total dose environments
[DE85-009441] N85-34588
SEMICONDUCTOR JUNCTIONS
Flat-plate solar array project process development area process research of non-CZ silicon material
[NASA-CR-176117] N85-34445
Rapid annealing of temperature-compensated, precision voltage references following fast-neutron irradiation
[DE85-009821] N85-34609
SENSITIVITY
A multi-touch three dimensional touch-sensitive tablet (executive summary) N85-34553
The final COS-B database: In-flight calibration of instrumental parameters
[OG-9.3-9] N85-34964
SENSORY PERCEPTION
Dissociation of autonomic and sensory vestibular reactions N85-34501
SEPARATED FLOW
Modelling of unsteady, incompressible separation on an aerofoil using an inviscid flow algorithm
[GU-AERO-8412] N85-34122
A study of the second and third order closure models of turbulence for prediction of separated shear flows
[NASA-CR-176127] N85-34353
Block-implicit calculations of three-dimensional laminar flow in strongly curved ducts
[DE85-003047] N85-34363

SEPARATION
Separation of gas mixtures by supported complexes
[DE85-011996] N85-34236
Separation of uranium from technetium in recovery of spent nuclear fuel
[DE85-006499] N85-34627
SEPARATORS
Fuel cell separator plate with bellows-type sealing flanges
[DE85-005991] N85-34459
SEQUENTIAL ANALYSIS
Sequential regularization solution of the inverse heat conduction problem
[DE85-010657] N85-34362
SERVICE LIFE
Performance improvements from surfacing in aero engine components
[PNR-90257] N85-34142
SEWING
Re-designing a mechanism for higher speed: A case history from textile machinery N85-34310
SHADOWS
Shadow volumes for non-planar polygons N85-34580
Empirical model for the Earth's cosmic ray shadow at 400 KM: Prohibited cosmic ray access
[SH-6.1-14] N85-35087
SHAPE MEMORY ALLOYS
Shape memory effect in uranium-niobium alloys below room temperature
[DE85-012964] N85-34268
SHAPES
Block-implicit calculations of three-dimensional laminar flow in strongly curved ducts
[DE85-003047] N85-34363
A user-friendly computer-aided construction of boundaries N85-34564
Non-rigid body motion N85-34576
SHEAR FLOW
A study of the second and third order closure models of turbulence for prediction of separated shear flows
[NASA-CR-176127] N85-34353
SHEAR PROPERTIES
Pressure-shear loading of PBX-9404
[DE85-009982] N85-34298
SHEAR STRENGTH
Pressure-shear loading of PBX-9404
[DE85-009982] N85-34298
SHEAR STRESS
Pressure-shear loading of PBX-9404
[DE85-009982] N85-34298
SHIELDING
Gas shielding apparatus
[DE85-005992] N85-34416
Coupled electron-photon transport calculations using the method of discrete ordinates
[DE85-009444] N85-34597
Monte Carlo techniques for analyzing deep penetration problems
[DE85-011426] N85-34598
SHIP HULLS
Design of transversely stiffenend FRP panels under compressive load — fiber reinforced plastic (FRP) ships
[AMTE(S)-R-84104] N85-34424
SHIPS
A life-saving device for ships
[NASA-TM-77670] N85-34129
SHOCK FRONTS
Energetic ion acceleration at collisionless shocks
[SH-1.5-3] N85-34772
On reflecting boundary behind the Earth's orbit at propagation of fast particles from solar flares
[SH-3.2-13] N85-34827
The nucleosynthesis of deterium and helium-3
[OG-8.2-18] N85-34914
Nuclear reactions in shock wave front during supernova events
[OG-8.2-19] N85-34915
Propagation of injected cosmic rays under distributed reacceleration
[OG-8.3-3] N85-34922
SHOCK WAVE PROPAGATION
Resonant ion acceleration by oblique magnetosonic shock wave in a collisionless plasma
[IPPJ-735] N85-34643
Workshop report on Simulation Techniques for Shock Wave Phenomena and Characteristics of Plasmas in Inertial Confinement Fusion
[IPPJ-725] N85-34670
Simulation of instability of cylindrically converging shock waves N85-34679
Stability of ion distribution in strong ion shock structure N85-34681
First-order shock acceleration in solar flares
[SH-1.1-5] N85-34732
On reflecting boundary behind the Earth's orbit at propagation of fast particles from solar flares
[SH-3.2-13] N85-34827
The intensity recovery of Forbush-type decreases as a function of heliocentric distance and its relationship to the 11-year variation
[SH-4.1-9] N85-34832
On the cosmic ray diffusion in a violent interstellar medium
[OG-7.2-14] N85-34881
The central engine of quasars and AGNs: A relativistic proton radiative shock
[OG-8.1-7] N85-34897
Propagation of cosmic rays and new evidence for distributed acceleration
[OG-8.3-5] N85-34924
SHOCK WAVES
Detonation in tungsten-loaded HMX
[DE85-009606] N85-34299
Three-dimensional hydrodynamic hot-spot model
[DE85-009587] N85-34301
Shock and release equation of state of calcite
[DE85-013151] N85-34432
Cubic interpolated pseudo-particle method (CIP) for solving hyperbolic-type equation N85-34673
Moving finite element method for ICF target implosion N85-34675
Numerical calculations on shock loaded materials N85-34676
Simulation of instability of cylindrically converging shock waves N85-34679
Stochastic particle acceleration in solar flares
[SH-1.1-4] N85-34731
Prompt acceleration of ions by oblique turbulent shocks in solar flares
[SH-1.1-6] N85-34733
Shock and statistical acceleration of energetic particles in the interplanetary medium
[SH-1.5-1] N85-34771
Energetic ion acceleration at collisionless shocks
[SH-1.5-3] N85-34772
Pitch angle distributions of 35-1000 keV protons at quasi-perpendicular interplanetary shocks
[SH-1.5-6] N85-34775
Spatial dependence of the local diffusion coefficient measured upstream of the November 12, 1978 interplanetary traveling shock
[SH-1.5-12] N85-34776
Latitude dependence of co-rotating shock acceleration
[SH-1.5-14] N85-34777
Cosmic ray acceleration by stellar wind. Simulation for heliosphere
[SH-1.5-17] N85-34780
the role of shock waves in modulation of galactic cosmic rays
[SH-4.1-7] N85-34831
Cosmic ray secondary nuclei and the structure of the galaxy
[OG-7.2-4] N85-34876
On the cosmic ray diffusion in a violent interstellar medium
[OG-7.2-14] N85-34881
The cosmic-ray shock structure problem for relativistic shocks
[OG-8.1-1] N85-34891
Instabilities in decelerating supersonic flows with applications to cosmic ray shocks
[OG-8.1-2] N85-34892
Time-dependent nonlinear cosmic ray shocks confirming abstract
[OG-8.1-3] N85-34893
Selfsimilar time dependent shock structures
[OG-8.1-4] N85-34894
A cosmic ray driven instability
[OG-8.1-5] N85-34895
Relativistic cosmic ray spectra in the full non-linear theory of shock acceleration
[OG-8.1-6] N85-34896
The central engine of quasars and AGNs: A relativistic proton radiative shock
[OG-8.1-7] N85-34897
A model for the origin of high-energy cosmic rays
[OG-8.1-8] N85-34898
Acceleration of cosmic rays in supernova-remnants
[OG-8.1-9] N85-34899
Efficiency of regular acceleration of particles by a shock wave at different injection regimes
[OG-8.1-13] N85-34902
A numerical study of diffusive shock acceleration of cosmic rays in supernova shocks
[OG-8.2-2] N85-34903
Nuclear reactions in shock wave front during supernova events
[OG-8.2-19] N85-34915
The theoretical and experimental investigation of cosmic ray Forbush-effects
[SH-5.1-20] N85-35072
SHROUDED TURBINES
Shroud segments for unshrouded blade turbines
[PNR-90260] N85-34143
Thermal stress analysis of a new turbine shroud seal concept
[NASA-TM-87082] N85-34406
SHROUDS
Snroud segments for unshrouded blade turbines
[PNR-90260] N85-34143
SIBERIA
Snow cover in the Siberian forest-steppe
[NASA-TM-77914] N85-34435
SIDELOBES
Reducing grating lobes due to subarray amplitude tapering
[AD-D011723] N85-34339
SIDEREAL TIME
Cosmic ray sidereal diurnal variation of galactic origin observed by neutron monitors
[SH-4.4-2] N85-35000
Sidereal anisotropies in the median rigidity range 60-600GV in 1978-1983
[SH-4.4-3] N85-35001
Sidereal variations deep underground in Tasmania
[SH-4.4-4] N85-35002
The effect of the interplanetary magnetic field on sidereal variations observed at medium depth underground detectors
[SH-4.4-5] N85-35003
The sidereal semi-diurnal variation observed at high zenith angles at Mawson, 1968-1984, and the polarity of the solar main field
[SH-4.4-6] N85-35004
Corrected sidereal anisotropy for underground moons
[SH-4.4-7] N85-35005
Sidereal anisotropy of cosmic rays
[SH-4.4-8] N85-35006
SIEVES
Rigid zeolite containing polyurethane foams
[DE85-006406] N85-34286
SIGNAL GENERATORS
Rotor blade test apparatus
[AD-D011725] N85-34381
SIGNAL PROCESSING
The improved display of 625-line television pictures: Adaptive interpolation
[BBC-RD-1985/5] N85-34328
A general purpose image processing package N85-34549
SIGNAL REFLECTION
Theoretical and experimental analyses of the performance of two-color laser ranging systems
[NASA-CR-176159] N85-34397
SIGNAL TO NOISE RATIOS
A new array for the study of ultra high energy gamma-ray sources
[OG-9.4-7] N85-34974
Astrophysical applications of high angular resolution array-telescopes
[OG-9.5-7] N85-34984
SIGNATURE ANALYSIS
Hardware test program for evaluation of basline range-range rate sensor concept
[NASA-CR-176143] N85-34377
SILANES
Dual-chamber plasma deposition of A-Si:H solar cells at high rates using disilane
[DE85-011828] N85-34451
SILICIDES
Flux-line lattice anisotropy in V3Si: Observation and interpretation
[DE85-011935] N85-34713
SILICON
Enthalpies of formation of liquid Fe-Ce-Si and Fe-Ce-Al three-component alloys
[BLL-M-36296-(5828.4)] N85-34247
Dual-chamber plasma deposition of A-Si:H solar cells at high rates using disilane
[DE85-011828] N85-34451
Formation of amorphous silicon by light ion damage
[DE85-012605] N85-34623
Silicon to iron abundances in solar cosmic rays and in the sun
[SH-2.1-6] N85-34787
The mean ionic charge of silicon in 3HE-rich solar flares
[SH-2.2-8] N85-34803
A silicon surface barrier telescope for solar particles identification
[SH-9.1-3] N85-35118
SILICON CARBIDES
Rotating bending fatigue strength of silicon carbide and alumina-fiber reinforced aluminum N85-34208

Mechanical properties of SiC fiber-reinforced reaction-bonded Si3N4 composites [NASA-TM-87085] N85-34223
Method for removing oxide contamination from silicon carbide powders [DE85-011648] N85-34287

SILICON COMPOUNDS
Calculation of mixed depth for some metal-Si systems [DE85-011907] N85-34616

SILICON DIOXIDE
Uranium, thorium isotopic analyses and uranium-series ages of calcite and opal and stable isotopic compositions of calcite from drill cores UE25a no. 1, USR G-2 and USW G-3/GU-3, Yucca Mountain, Nevada [DE85-013039] N85-34471

SILICON ISOTOPES
Measurements of the fragmentation of (40)Ar, (28)Si and (12)C in CH2C and H targets between 300 and 1500 MeV/nuc at the Bevalac [OG-7.2-19] N85-34886

SILICON NITRIDES
Mechanical properties of SiC fiber-reinforced reaction-bonded Si3N4 composites [NASA-TM-87085] N85-34223
Reliability of two sintered silicon nitride materials [NASA-TM-87092] N85-34284

SILOXANES
Method for controlling the viscosity of siloxane oils [DE85-011586] N85-34221

SILVER
Polarisation insensitive achromatic cube beamsplitter --- binocular microscopes [NPL-MOM-72] N85-34630

SILVER CHLORIDES
Determination of low chloride values in Rocky Flats scrub alloy solutions and other complex matrices [DE85-011506] N85-34234

SIMILARITY NUMBERS
Selection of segment similarity measures for hierarchical picture segmentation N85-34548

SIMULATION
Effect of interference on the performance of a minimum TCAS 2 [FAA/PM-84/33] N85-34131
The 1983 international intercomparison of nuclear accident dosimetry systems at Oak Ridge National Laboratory [DE85-011303] N85-34382
Image synthesis: Optical identity or pictorial communication? N85-34565
Simulation studies on stability of hot electron plasma N85-34664
Numerical simulation in astrophysics: Smoothed particle methods N85-34674
Simulation of instability of cylindrically converging shock waves N85-34679
A position sensitive phoswich hard X-ray detector system [OG-9.3-12] N85-34967

SINGLE CRYSTALS
Infrared studies of the influence of alkali metals on the C-O bond in chemisorbed carbon monoxide [DE85-005306] N85-34232
Cost effective single crystals: The Rolls Royce approach --- gas turbine components [PNR-90262] N85-34717

SINTERING
Ultra-trace analysis of sinter tantalum with SIMS [BLL-RARDE-TR-1220-(7291.7965)] N85-34245
Reliability of two sintered silicon nitride materials [NASA-TM-87092] N85-34284

SITE SELECTION
Reports from the German Meteorological Service. No. 166: The optimal spectral density of climatological station networks [ISBN-3-88148-214-8] N85-34478
Resource evaluation and site selection for microalgae production systems [DE85-008807] N85-34485
The 1984 biotic studies of Yucca Mountain, Nevada test site, Nye County, Nevada [DE85-011715] N85-34487

SIZE DISTRIBUTION
Burst size distributions in the digitized data of the ion chambers t Mt. Norikura and sea level stations [SH-9.1-9] N85-35124

SKIN FRICTION
A three-dimensional turbulent boundary layer undergoing transverse strain and streamwise pressure gradient [NASA-TM-86768] N85-34358

SLABS
Negative flexural behavior of precase composite slabs with steel joint N85-34183

SLAGS
The development of titanium production in the USSR [BLL-OA-TRANS-3226-(6196.3)] N85-34244

SLICING
The read-out system of spatial distribution of thermoluminescence in meteorites [SH-9.1-16] N85-35131

SLIDING FRICTION
Anti wear property of two phasic metal composite N85-34199

SLOPES
Guidelines for the evaluation of visual approach slope indicators [ARL-SYS-R-32] N85-34132

SLOT ANTENNAS
Experimental measurements of the ion cyclotron antennas' coupling and RF characteristics [DE85-011569] N85-34694

SNOW COVER
Snow cover in the Siberian forest-steppe [NASA-TM-77914] N85-34435
Comparisons of the North Polar Cap of Mars and the Earth's Northern Hemisphere snow cover [NASA-TM-86191] N85-34728

SODIUM IODIDES
Improved method for the stabilization of NaI-photomultiplier gamma detectors against thermal and other drift [DE85-011830] N85-34613

SOFTWARE ENGINEERING
Software for mechanism design N85-34324
A prototype PASCAL program validation system [NPL-DITC-57/85] N85-34513
The parser generator as a general purpose tool [NASA-CR-177955] N85-34521

SOFTWARE TOOLS
The parser generator as a general purpose tool [NASA-CR-177955] N85-34521
Developing graphical tools with minimal GKS N85-34573

SOILS
Effects of acid rain on forest nutrient status [DE85-012486] N85-34463
Multi-solute subsurface transfer modeling for energy solid wastes: Highlights FY 1984 [DE85-012788] N85-34591

SOLAR ACTIVITY
Comparisons of the North Polar Cap of Mars and the Earth's Northern Hemisphere snow cover [NASA-TM-86191] N85-34728
Precision measurements of solar energetic particle elemental composition [SH-2.1-4] N85-34785
Energetic solar particle events [SH-3.2-2] N85-34818
A study of periodicities and recurrences in solar activity and cosmic ray modulation [SH-4.4-14] N85-35010
Variations of the cosmic ray general component in Antarctica [SH-4.4-17] N85-35013
The difference in the energy spectra of galactic cosmic rays at the minima of the 19th and 20th solar activity cycles [SH-4.4-18] N85-35014
Cosmic ray variations with the period close to 27 days and their connection with solar activity longitudinal distribution [SH-4.4-19] N85-35015
Long-term modulation of galactic cosmic rays in high-energy region [SH-4.4-22] N85-35018
Diurnal anisotropy during solar activity cycle twenty and diffusion-convection model [SH-4.5-7] N85-35025
Diurnal variations from muon data at Takeyama underground station [SH-4.5-13] N85-35030
The modulation features of the long-period cosmic ray variations in connection with the sign change of the general magnetic field of the Sun [SH-4.5-15] N85-35032
Cosmic ray density gradient and its dependence on the north-south asymmetry in solar activity [SH-4.5-17] N85-35034
Anomalous increase of solar anisotropy above 150GV in 1981-1983 [SH-4.5-18] N85-35035
Change of cosmic ray anisotropy with solar activity [SH-4.5-20] N85-35037
The large scale dynamics of the outer heliosphere and the long-term modulation of galactic cosmic rays [SH-4.7-3] N85-35048
Galactic cosmic ray radial gradients and the anomalous He component near maximum solar modulation and to radii beyond 34 AU from the Sun [SH-4.7-5] N85-35050
The recovery of the cosmic ray flux from maximum solar modulation at IMP-8 (1 AU) and at Pioneer (R 30 AU) [SH-4.7-7] N85-35052
The solar wind effect on cosmic rays and solar activity [SH-5.1-13] N85-35066
Solar activity beyond the disk and variations of the cosmic ray gradient [SH-5.1-23] N85-35075
Cosmic rays 10Be biennal data and their relationship to aurorae and sunspots [SH-7.1-1] N85-35094

SOLAR ACTIVITY EFFECTS
Search for solar neutrons using NM-64 equipment [SH-1.4-5] N85-34765
A search for solar neutrons on a long duration balloon flight [SH-1.4-6] N85-34766
On the retention of high-energy protons and nuclei with charges Z or equal to 2 in large solar flares after the process of their acceleration [SH-2.1-8] N85-34789
Nucleosynthesis in the terrestrial and solar atmospheres [SH-2.2-2] N85-34797
Type 3 solar radio bursts and 3HE-rich events [SH-2.2-3] N85-34798
Anomalous low level of cosmic ray intensity decreases observed during 1980 [SH-5.1-15] N85-35068
When did the average cosmic ray flux increase? [SH-7.1-4] N85-35097
Cosmic-ray exposure records and origins of meteorites [SH-7.1-7] N85-35099

SOLAR ARRAYS
Solar maximum: Solar array degradation [NASA-TM-86194] N85-34175

SOLAR ATMOSPHERE
Temporal evolution of an energetic electron population in an inhomogeneous medium: Application to solar hard X-ray bursts [SH-1.2-6] N85-34741
Ultrarelativistic electrons and solar flare gamma-radiation [SH-1.3-11] N85-34757
Precision measurements of solar energetic particle elemental composition [SH-2.1-4] N85-34785
Solar Coronal and photospheric abundances from solar energetic particle measurements [SH-2.1-5] N85-34786
Nucleosynthesis in the terrestrial and solar atmospheres [SH-2.2-2] N85-34797
Dynamics of the penetration boundaries of solar protons during a strong magnetic storm [SH-6.1-16] N85-35089
Neutrino production from the solar atmosphere [SH-8.1-9] N85-35114

SOLAR BLANKETS
STACBEAM 2 [NASA-CR-176126] N85-34442

SOLAR CELLS
Solar maximum: Solar array degradation [NASA-TM-86194] N85-34175
Flat-plate solar array project process development area process research of non-CZ silicon material [NASA-CR-176117] N85-34445
Investigation of test methods, material properties, and processes for solar cell encapsulants [NASA-CR-176132] N85-34446
Development of metallization process: FSA project, cells and module formation research area [NASA-CR-176136] N85-34447
Dual-chamber plasma deposition of A-Si:H solar cells at high rates using disilane [DE85-011828] N85-34451

SOLAR COLLECTORS
Optical analysis of parabolic dish concentrators for solar dynamic power systems in space [NASA-TM-87080] N85-34176
Vapor phase heat transport concepts [DE85-009550] N85-34366
Solar thermal technologies program summary [DE85-012253] N85-34449
Solar heat pump [DE85-011323] N85-34453
Solar energy education: Renewable energy activities for chemistry and physics [DE85-010371] N85-34455

SOLAR CORONA
Soft X-Ray Telescope (SXRT) N85-34159

White Light Coronograph (WLC) and Ultra-Violet Coronal Spectrometer (UVCS) N85-34161
Prompt acceleration of ions by oblique turbulent shocks in solar flares
[SH-1.1-6] N85-34733
Study of photon emission by electron capture during solar nuclei acceleration. 3: Photon production evaluations
[SH-1.1-10] N85-34737
Spectral and spatial properties of solar microflares
[SH-1.2-4] N85-34740
Two classes of solar energetic particle events associated with impulsive and long duration soft X-ray flares
[SH-1.2-12] N85-34747
The starting conditions for an optically small solar gamma ray flare
[SH-1.3-2] N85-34751
Energetic protons from a disappearing solar filament
[SH-1.3-7] N85-34754
Solar Coronal and photospheric abundances from solar energetic particle measurements
[SH-2.1-5] N85-34786
Diffusion in the chromosphere and the composition of the solar corona and energetic particles
[SH-2.1-9] N85-34790
Anomalous abundances of solar energetic particles and coronal gas: Coulomb effects and First Ionization Potential (FIP) ordering
[SH-2.1-10] N85-34791
Coronal propagation of solar flare particles observed by satellite
[SH-3.1-2] N85-34807
Coronal propagation of flare associated electrons and protons
[SH-3.1-3] N85-34808
Peculiarities of propagation of charged particles in solar corona
[SH-3.1-6] N85-34810
The propagation of solar energetic particles in magnetic channels
[SH-3.2-4] N85-34820
The flare origin of Forbush decreases not associated with solar flares on the visible hemisphere of the Sun
[SH-5.1-4] N85-35058
The 4He1H ratios in the chemical compositions of solar flare particles and the primordial solar nebula
[SH-7.1-12] N85-35104

SOLAR CORPUSCULAR RADIATION

Ninteenth International Cosmic Ray Conference. SH sessions, volume 4
[NASA-CP-2376-VOL-4] N85-34729
Ninteenth International Cosmic Ray Conference. SH sessions, volume 5
[NASA-CP-2376-VOL-5] N85-34991

SOLAR COSMIC RAYS

Source energy spectra from demodulation of solar particle data by interplanetary and coronal transport
[SH-1.3-13] N85-34758
Ground increase of cosmic ray intensity on February 16, 1984
[SH-1.3-15] N85-34760
The SCR flare of 16 February 1984 as recorded by the Sayan spectrograph
[SH-1.3-17] N85-34761
Time extended production of neutrons during a solar flare
[SH-1.4-1] N85-34762
Further observations of protons resulting from the decay of neutrons ejected by solar flares
[SH-1.4-2] N85-34763
Suggestions for improving the efficiency of ground-based neutron monitors for detecting solar neutrons
[SH-1.4-3] N85-34764
Precision measurements of solar energetic particle elemental composition
[SH-2.1-4] N85-34785
Solar Coronal and photospheric abundances from solar energetic particle measurements
[SH-2.1-5] N85-34786
Silicon to iron abundances in solar cosmic rays and in the sun
[SH-2.1-6] N85-34787
Variations in elemental composition of several MEV/nucleon ions observed in interplanetary space
[SH-2.1-7] N85-34788
The mean ionic charges of N, Ne, MG, SI and S in solar energetic particle events
[SH-2.1-11] N85-34792
Nucleosynthesis in the terrestrial and solar atmospheres
[SH-2.2-2] N85-34797
Solar source regions of 3HE-rich particle events
[SH-2.2-4] N85-34799
The 3HE in solar non-relativistic electron events
[SH-2.2-5] N85-34800
Elemental abundance differences between nuclei acclerated in CIR shocks and solar flares
[SH-2.2-6] N85-34801
The heavy ion composition in 3HE-rich solar flares
[SH-2.2-7] N85-34802
The mean ionic charge of silicon in 3HE-rich solar flares
[SH-2.2-8] N85-34803
On the connection between the 3HE-enrichment and spectral index of solar energetic particles
[SH-2.2-9] N85-34804
The plasma mechanism for preferential acceleration of heavy ions
[SH-2.2-10] N85-34805
Observations of solar energetic particles at a synchronous orbit
[SH-3.1-1] N85-34806
Coronal propagation of solar flare particles observed by satellite
[SH-3.1-2] N85-34807
Coronal propagation of flare associated electrons and protons
[SH-3.1-3] N85-34808
Geometry of the diffusive propagation region in the August 14, 1982 solar electron event
[SH-3.1-5] N85-34809
Some characteristics of the solar flare event of February 16, 1984
[SH-3.1-7] N85-34811
Constraints of solar flare particle transport models from anisotropy observations at Voyager 1
[SH-3.1-8] N85-34812
Determination of the pitch-angle distribution and transverse anisotropy of interplanetary particles
[SH-3.1-11] N85-34815
Pitch angle distributions of solar energetic particles and the local scattering properties of the interplanetary magnetic field
[SH-3.1-13] N85-34816
Exponential anisotropy of solar cosmic rays
[SH-3.2-1] N85-34817
Energetic solar particle events
[SH-3.2-2] N85-34818
Channeled propagation of solar particles
[SH-3.2-3] N85-34819
The propagation of solar energetic particles in magnetic channels
[SH-3.2-4] N85-34820
Radial transport of approximately 1 MeV/nucleon ions during the 22 November 1977 solar particle event
[SH-3.2-5] N85-34821
Energetic solar particle fluxes out to 3 AU during the 7 May 1978 flare event
[SH-3.2-6] N85-34822
The local characteristic function of interplanetary particle propagation
[SH-3.2-8] N85-34823
Investigation of cosmic ray propagation in interplanetary space
[SH-3.2-9] N85-34824
Diffusion-convection function of cosmic rays
[SH-3.2-10] N85-34825
On reflecting boundary behind the Earth's orbit at propagation of fast particles from solar flares
[SH-3.2-13] N85-34827
Propagation of the phase of solar modulation
[SH-4.1-12] N85-34835
North-south asymmetry in activity on the Sun and cosmic ray density gradients
[SH-4.2-7] N85-34845
Gradients and anisotropies of high energy cosmic rays in the outer heliosphere
[SH-4.3-7] N85-34992
IMF-sense-dependent cosmic ray anisotropy produced from diffusion-convection in heliosphere
[SH-4.3-9] N85-34994
Influence of the neutral sheet on the Swinson's type north-south anisotropy of cosmic rays
[SH-4.3-10] N85-34995
Characteristics of cosmic ray pole-equator anisotropy derived from spherical harmonic analysis of neutron monitor data
[SH-4.3-12] N85-34996
First zonal harmonic component of cosmic ray neutron intensity
[SH-4.3-13] N85-34997
Cosmic ray intensity distribution perpendicular to solar equatorial plane at 1 A.U. during 1978-83
[SH-4.3-14] N85-34998
The corotating variation of the north-south anisotropy of cosmic rays
[SH-4.3-15] N85-34999
Sidereal anisotropy of cosmic rays
[SH-4.4-8] N85-35006
Cosmic ray intensity variations observed at Matsushiro (220 M.W.E. in depth)
[SH-4.4-9] N85-35007
Long-term modulation of cosmic rays during solar cycle 21
[SH-4.4-10] N85-35008
Role of solar flare index in long term modulation of cosmic ray intensity
[SH-4.4-12] N85-35009
Azimuthal and meridional asymmetries of the solar wind and quasiperiodic variations of intensity of Galactic Cosmic Rays (GCR)
[SH-4.4-20] N85-35016
Dynamics of two-year cosmic ray variations inferred from the data of spacecraft and stratospheric measurements and from the neutron monitor data in 1959-1981
[SH-4.4-21] N85-35017
Solar tri-diurnal variation of cosmic rays in a wide range of rigidity
[SH-4.5-3] N85-35021
Upper cut-off rigidity for corotation anisotropy during solar activity cycles 20 and 21
[SH-4.5-4] N85-35022
Twenty-two-year cycle of the upper limiting rigidity of Daly waves
[SH-4.5-5] N85-35023
Solar wind velocity and daily variation of cosmic rays
[SH-4.5-6] N85-35024
Time and energy dependence of the cosmic ray gradient in the outer heliosphere
[SH-4.7-2] N85-35047
Frequency spectra of short-period variations of cosmic ray
[SH-5.1-17] N85-35070
Penetration of solar protons into the Earth's magnetosphere on November 22, 1977
[SH-6.1-15] N85-35088
Dynamics of the penetration boundaries of solar protons during a strong magnetic storm
[SH-6.1-16] N85-35089
Solar cosmic ray bursts and solar neutrino fluxes
[SH-8.1-10] N85-35115
A silicon surface barrier telescope for solar particles identification
[SH-9.1-3] N85-35118
Strong earthquakes, novae and cosmic ray environment
[SH-10.1-3] N85-35135

SOLAR CYCLES

Elemental abundances in corotating events
[SH-1.5-15] N85-34778
Solar and interplanetary particles at 2 to 4 MEV during solar cycles 21, solar cycle variations of event sizes, and compositions
[SH-1.5-16] N85-34779
Cumulative effect of Forbush decreases in the heliospheric modulation during the present solar cycle
[SH-4.1-10] N85-34833
Cosmic ray north-south anisotropy 1961 - 1983
[SH-4.2-6] N85-34844
The expected cosmic ray density and stream distributions at the heliolatitudinal asymmetry of solar wind
[SH-4.2-14] N85-34852
The effect of the neutral sheet structure of the interplanetary magnetic field on cosmic ray distribution in space
[SH-4.2-18] N85-34855
Spatial distribution of cosmic rays in magnetic cycles of the Sun
[SH-4.2-20] N85-34857
11- and 22-year variations of the cosmic ray density and of the solar wind speed
[SH-4.2-21] N85-34858
Difference between even and odd 11-year cycles in cosmic ray intensity
[SH-4.2-22] N85-34859
An update on the correlation between the cosmic radiation intensity and the geomagnetic AA index
[SH-4.2-24] N85-34861
Gradients and anisotropies of high energy cosmic rays in the outer heliosphere
[SH-4.3-7] N85-34992
Long-term modulation of cosmic rays during solar cycle 21
[SH-4.4-10] N85-35008
Cosmic ray biannual variation
[SH-4.4-15] N85-35011
The difference in the energy spectra of galactic cosmic rays at the minima of the 19th and 20th solar activity cycles
[SH-4.4-18] N85-35014
Cosmic ray variations with the period close to 27 days and their connection with solar activity longitudinal distribution
[SH-4.4-19] N85-35015

Diurnal anisotropy during solar activity cycle twenty and diffusion-convection model
[SH-4.5-7] N85-35025

Diurnal variations from muon data at Takeyama underground station
[SH-4.5-13] N85-35030

Solar cycle variations of the anaomalous cosmic ray component
[SH-4.6-2] N85-35040

Time and energy dependence of the cosmic ray gradient in the outer heliosphere
[SH-4.7-2] N85-35047

Dimensions of the solar wind cavity and of the region of interplanetary cosmic ray modulation
[SH-4.7-11] N85-35055

The solar wind effect on cosmic rays and solar activity
[SH-5.1-13] N85-35066

On the solar cycle variation in the barometer coefficients of high latitude neutron monitors
[SH-6.1-2] N85-35077

Cosmic ray secular variations in terrestrial records and aurorae
[SH-7.1-3] N85-35096

When did the average cosmic ray flux increase?
[SH-7.1-4] N85-35097

Solar neutrino: Flux, cosmic rays and the 11 year solar cycle
[SH-8.1-7] N85-35112

Solar cosmic ray bursts and solar neutrino fluxes
[SH-8.1-10] N85-35115

The influences of the galactic cosmic ray on the atmospheric ozone
[SH-10.1-1] N85-35133

SOLAR ELECTRONS

The 3HE in solar non-relativistic electron events
[SH-2.2-5] N85-34800

SOLAR ENERGY

Optical analysis of parabolic dish concentrators for solar dynamic power systems in space
[NASA-TM-87080] N85-34176

Solar thermal technologies program summary
[DE85-012253] N85-34449

Solar energy education. Renewable energy: A background text
[DE85-010365] N85-34452

Solar energy education: Renewable energy activities for chemistry and physics
[DE85-010371] N85-34455

Anomalous abundances of solar energetic particles and coronal gas: Coulomb effects and First Ionization Potential (FIP) ordering
[SH-2.1-10] N85-34791

SOLAR ENERGY CONVERSION

Electron photoejection in carbanions
[DE85-011747] N85-34230

Electron photoejection in carbanions
[DE85-011748] N85-34237

SOLAR FLARES

High Resolution Telescope and Spectrograph (HRTS)
N85-34162

Ninteenth International Cosmic Ray Conference. SH sessions, volume 4
[NASA-CP-2376-VOL-4] N85-34729

The propagation of solar flare particles in a turbulent coronal loop
[SH-1.1-3] N85-34730

Stochastic particle acceleration in solar flares
[SH-1.1-4] N85-34731

First-order shock acceleration in solar flares
[SH-1.1-5] N85-34732

Prompt acceleration of ions by oblique turbulent shocks in solar flares
[SH-1.1-6] N85-34733

Fast drift kilometric radio bursts and solar proton events
[SH-1.1-7] N85-34734

Study of photon emission by electron capture during solar nuclei acceleration. 2: Delimitation of conditions for charge transfert establishment
[SH-1.1-9] N85-34736

Study of photon emission by electron capture during solar nuclei acceleration. 3: Photon production evaluations
[SH-1.1-10] N85-34737

Study of non-thermal photon production under different scenarios in solar flares. 1: Scenarios and formulations
[SH-1.2-2] N85-34738

Study of non-thermal photon production under different scenarios in solar flares. 2: The Compton inverse and Bremsstrahlung models and fittings
[SH-1.2-3] N85-34739

Spectral and spatial properties of solar microflares
[SH-1.2-4] N85-34740

Temporal evolution of an energetic electron population in an inhomogeneous medium: Application to solar hard X-ray bursts
[SH-1.2-6] N85-34741

Quantitative analysis of flare accelerated electrons through their hard X-ray and microwave radiation
[SH-1.2-7] N85-34742

An extended superhot solar flare X-ray source
[SH-1.2-8] N85-34743

Observations of solar flare photon energy spectra from 20 keV to 7 MeV
[SH-1.2-9] N85-34744

Ion energy storage for post-flare loops
[SH-1.2-10] N85-34745

Two types of electron events in solar flares
[SH-1.2-11] N85-34746

Two classes of solar energetic particle events associated with impulsive and long duration soft X-ray flares
[SH-1.2-12] N85-34747

A dominant role for protons at the onset of solar flares
[SH-1.2-13] N85-34748

The energy spectra of solar flare electrons
[SH-1.2-14] N85-34749

Onset of solar flares as predicted by two-dimensional MHD-models of quiescent prominences
[SH-1.3-1] N85-34750

The starting conditions for an optically small solar gamma ray flare
[SH-1.3-2] N85-34751

On the detectability of key-MeV solar protons through their nonthermal Lyman-alpha emission
[SH-1.3-5] N85-34752

Observations of solar flare gamma-rays and protons
[SH-1.3-6] N85-34753

Energetic protons from a disappearing solar filament
[SH-1.3-7] N85-34754

Helios 1 energetic particle observations of the solar gamma ray flare events of 7, 21 June 1980 and 3 June 1982
[SH-1.3-8] N85-34755

Injection of energetic particles following the gamma-ray flares on June 7, 1980, as observed on Helios 1
[SH-1.3-9] N85-34756

Ultrarelativistic electrons and solar flare gamma-radiation
[SH-1.3-11] N85-34757

Source energy spectra from demodulation of solar particle data by interplanetary and coronal transport
[SH-1.3-13] N85-34758

Spectra of solar proton ground level events using neutron monitor and neutron moderated detector recordings
[SH-1.3-14] N85-34759

Ground increase of cosmic ray intensity on February 16, 1984
[SH-1.3-15] N85-34760

The SCR flare of 16 February 1984 as recorded by the Sayan spectrograph
[SH-1.3-17] N85-34761

Time extended production of neutrons during a solar flare
[SH-1.4-1] N85-34762

Further observations of protons resulting from the decay of neutrons ejected by solar flares
[SH-1.4-2] N85-34763

Suggestions for improving the efficiency of ground-based neutron monitors for detecting solar neutrons
[SH-1.4-3] N85-34764

Search for solar neutrons using NM-64 equipment
[SH-1.4-5] N85-34765

A search for solar neutrons on a long duration balloon flight
[SH-1.4-6] N85-34766

Neutral pion production in solar flares
[SH-1.4-7] N85-34767

High energy neutron and gamma-radiation generated during the solar flares
[SH-1.4-8] N85-34768

On the angular and energy distribution of solar neutrons generated in P-P reactions
[SH-1.4-9] N85-34769

Possible detection of flare-generated positrons by Helios 1 on 3 Jun 1982
[SH-1.4-10] N85-34770

Elemental abundances in corotating events
[SH-1.5-15] N85-34778

Solar and interplanetary particles at 2 to 4 MEV during solar cycles 21, solar cycle variations of event sizes, and composites
[SH-1.5-16] N85-34779

Observation of the fluxes of nuclei with energies 10-20 MEV per nucleon during the solar flare of April 26, 1984
[SH-2.1-1] N85-34783

Energetic particle observations of the solar-gamma ray/neutron flare events of 3 Jun 1982 and 21 June 1980 isotopic and chemical composition
[SH-2.1-3] N85-34784

Precision measurements of solar energetic particle elemental composition
[SH-2.1-4] N85-34785

On the retention of high-energy protons and nuclei with charges Z or equal to 2 in large solar flares after the process of their acceleration
[SH-2.1-8] N85-34789

The mean ionic charges of N, Ne, MG, SI and S in solar energetic particle events
[SH-2.1-11] N85-34792

Abundances from solar-flare gamma-ray line spectroscopy
[SH-2.1-13] N85-34794

Solar flare gamma-ray line spectroscopy
[SH-2.1-14] N85-34795

Isotopic overabundances and the energetic particle model of solar flares
[SH-2.2-1] N85-34796

Solar source regions of 3HE-rich particle events
[SH-2.2-4] N85-34799

Elemental abundance differences between nuclei acclerated in CIR shocks and solar flares
[SH-2.2-6] N85-34801

The heavy ion composition in 3HE-rich solar flares
[SH-2.2-7] N85-34802

The mean ionic charge of silicon in 3HE-rich solar flares
[SH-2.2-8] N85-34803

Coronal propagation of solar flare particles observed by satellite
[SH-3.1-2] N85-34807

Coronal propagation of flare associated electrons and protons
[SH-3.1-3] N85-34808

Geometry of the diffusive propagation region in the August 14, 1982 solar electron event
[SH-3.1-5] N85-34809

Peculiarities of propagation of charged particles in solar corona
[SH-3.1-6] N85-34810

Some characteristics of the solar flare event of February 16, 1984
[SH-3.1-7] N85-34811

Constraints of solar flare particle transport models from anisotropy observations at Voyager 1
[SH-3.1-8] N85-34812

Exponential anisotropy of solar cosmic rays
[SH-3.2-1] N85-34817

The propagation of solar energetic particles in magnetic channels
[SH-3.2-4] N85-34820

Radial transport of approximately 1 MeV/nucleon ions during the 22 November 1977 solar particle event
[SH-3.2-5] N85-34821

Energetic solar particle fluxes out to 3 AU during the 7 May 1978 flare event
[SH-3.2-6] N85-34822

The local characteristic function of interplanetary particle propagation
[SH-3.2-8] N85-34823

On reflecting boundary behind the Earth's orbit at propagation of fast particles from solar flares
[SH-3.2-13] N85-34827

Cumulative effect of Forbush decreases in the heliospheric modulation during the present solar cycle
[SH-4.1-10] N85-34833

North-south asymmetry in activity on the Sun and cosmic ray density gradients
[SH-4.2-7] N85-34845

Role of solar flare index in long term modulation of cosmic ray intensity
[SH-4.4-12] N85-35009

Drift and Forbush decreases
[SH-5.1-2] N85-35056

The flare origin of Forbush decreases not associated with solar flares on the visible hemisphere of the Sun
[SH-5.1-4] N85-35058

Longitudinal dependence of the interplanetary perturbation produced by energetic type 4 solar flares and of the associated cosmic ray modulation
[SH-5.1-5] N85-35059

Spectral analysis of the Forbush decrease of 13 July 1982
[SH-5.1-7] N85-35061

Study of dominating parameters of high speed solar plasma streams in relation to cosmic ray and geomagnetic storms
[SH-5.1-11] N85-35064

Anomalous low level of cosmic ray intensity decreases observed during 1980
[SH-5.1-15] N85-35068

Peculiarities of Galactic Cosmic Ray (GCR) anisotropy variation in connection with the recurrent and sporadic Forbush effects
[SH-5.1-21] N85-35073
Cosmic ray modulation by high-speed solar wind fluxes
[SH-5.1-22] N85-35074
Penetration of solar protons into the Earth's magnetosphere on November 22, 1977
[SH-6.1-15] N85-35088
Solar modulation of cosmic ray intensity and solar flare events inferred from (14)C contents in dated tree rings
[SH-7.1-2] N85-35095
The 4He1H ratios in the chemical compositions of solar flare particles and the primordial solar nebula
[SH-7.1-12] N85-35104
Solar neutrinos, solar flares, solar activity cycle and the proton decay
[SH-8.1-8] N85-35113
Solar cosmic ray bursts and solar neutrino fluxes
[SH-8.1-10] N85-35115
SONTRAC: A solar neutron track chamber detector
[SH-9.1-12] N85-35127
A suggested standardized format for cosmic ray ground-level event data
[SH-9.1-15] N85-35130
Sporadic radio emission connected with a definite manifestation of solar activity in the near Earth space
[SH-10.1-8] N85-35139
Near Earth space sporadic radio emission busts occurring during sunrise
[SH-10.1-9] N85-35140

SOLAR FLUX

Results of ultra-low level 71ge counting for application in the Gallex-solar neutrino experiment at the Gran Sasso Underground Physics Laboratory
[SH-8.1-2] N85-35108
Correlation between solar neutrino flux and other solar phenomena N85-35109
A possible mechanism to cause the quasi-biennial variability on the solar neutrino flux
[SH-8.1-5] N85-35110
The conjecture concerning time variations in the solar neutrino flux
[SH-8.1-6] N85-35111
Solar neutrino: Flux, cosmic rays and the 11 year solar cycle
[SH-8.1-7] N85-35112
Solar cosmic ray bursts and solar neutrino fluxes
[SH-8.1-10] N85-35115

SOLAR FLUX DENSITY

Peculiarities of propagation of charged particles in solar corona
[SH-3.1-6] N85-34810
Energetic solar particle fluxes out to 3 AU during the 7 May 1978 flare event
[SH-3.2-6] N85-34822

SOLAR HEATING

Solar heat pump
[DE85-011323] N85-34453
Solar system fault detection
[DE85-005987] N85-34458

SOLAR LIMB

An extended superhot solar flare X-ray source
[SH-1.2-8] N85-34743
Ultrarelativistic electrons and solar flare gamma-radiation
[SH-1.3-11] N85-34757
Search for solar neutrons using NM-64 equipment
[SH-1.4-5] N85-34765

SOLAR MAGNETIC FIELD

Ultrarelativistic electrons and solar flare gamma-radiation
[SH-1.3-11] N85-34757
Peculiarities of propagation of charged particles in solar corona
[SH-3.1-6] N85-34810
Some characteristics of the solar flare event of February 16, 1984
[SH-3.1-7] N85-34811
Low energy proton bidirectional anisotropies and their relation to transient interplanetary magnetic structures: ISEE-3 observations
[SH-3.1-9] N85-34813
the role of shock waves in modulation of galactic cosmic rays
[SH-4.1-7] N85-34831
Cosmic ray intensity and the tilt of the neutral sheet
[SH-4.2-8] N85-34846
Differential measurement of cosmic-ray gradient with respect to interplanetary current sheet
[SH-4.2-9] N85-34847
Spatial variation of cosmic rays near the heliospheric current sheet
[SH-4.2-10] N85-34848
Effects of a wavy neutral sheet on cosmic ray anisotropies
[SH-4.2-11] N85-34849
Effects of solar magnetic field on cosmic rays
[SH-4.2-12] N85-34850
Determination of galactic cosmic ray latitudinal gradient using Earth based detectors
[SH-4.2-13] N85-34851
The expected cosmic ray density and stream distributions at the heliolatitudinal asymmetry of solar wind
[SH-4.2-14] N85-34852
Latitudinal gradients of cosmic rays and the polarity reversal of the heliospheric magnetic field: A preliminary evaluation
[SH-4.2-16] N85-34853
The influence of nonstationarity of the solar activity and general solar field on modulation of cosmic rays
[SH-4.2-17] N85-34854
On the influence of the heliomagnetospheric periphery on the galactic cosmic rays
[SH-4.2-19] N85-34856
Spatial distribution of cosmic rays in magnetic cycles of the Sun
[SH-4.2-20] N85-34857
An update on the correlation between the cosmic radiation intensity and the geomagnetic AA index
[SH-4.2-24] N85-34861
Astrophysical applications of high angular resolution array-telescopes
[OG-9.5-7] N85-34984
Gradients and anisotropies of high energy cosmic rays in the outer heliosphere
[SH-4.3-7] N85-34992
Cosmic ray sidereal diurnal variation of galactic origin observed by neutron monitors
[SH-4.4-2] N85-35000
Long-term modulation of galactic cosmic rays in high-energy region
[SH-4.4-22] N85-35018
Diurnal variation of galactic cosmic ray intensity on quiet days
[SH-4.5-11] N85-35029
Long term changes in cosmic ray diurnal variations observed by ion chambers in Hong Kong and Japan
[SH-4.5-14] N85-35031
The modulation features of the long-period cosmic ray variations in connection with the sign change of the general magnetic field of the Sun
[SH-4.5-15] N85-35032
Cosmic ray density gradient and its dependence on the north-south asymmetry in solar activity
[SH-4.5-17] N85-35034
Anomalous increase of solar anisotropy above 150GV in 1981-1983
[SH-4.5-18] N85-35035
Changes in the energy spectrum of anomalous oxygen and helium during 1977-1985
[SH-4.6-1] N85-35039
Radial and latitudinal gradients of anomalous oxygen during 1977 - 1985
[SH-4.6-4] N85-35042
The cosmic ray interplanetary radial gradient from 1972 - 1985
[SH-4.7-1] N85-35046
The large scale dynamics of the outer heliosphere and the long-term modulation of galactic cosmic rays
[SH-4.7-3] N85-35048

SOLAR MAXIMUM MISSION

Solar maximum: Solar array degradation
[NASA-TM-86194] N85-34175
Monte Carlo calibration of the SMM gamma ray spectrometer for high energy gamma rays and neutrons
[SH-9.1-6] N85-35121

SOLAR NEUTRINOS

Specificity of (71)Ga(p,n) (71)Ge at 35 MeV for Gamow-Teller strength
[DE85-011837] N85-34615
Ninteenth International Cosmic Ray Conference. SH sessions, volume 5
[NASA-CP-2376-VOL-5] N85-34991
Results of ultra-low level 71ge counting for application in the Gallex-solar neutrino experiment at the Gran Sasso Underground Physics Laboratory
[SH-8.1-2] N85-35108
Correlation between solar neutrino flux and other solar phenomena N85-35109
A possible mechanism to cause the quasi-biennial variability on the solar neutrino flux
[SH-8.1-5] N85-35110
The conjecture concerning time variations in the solar neutrino flux
[SH-8.1-6] N85-35111
Solar neutrino: Flux, cosmic rays and the 11 year solar cycle
[SH-8.1-7] N85-35112
Solar neutrinos, solar flares, solar activity cycle and the proton decay
[SH-8.1-8] N85-35113

SOLAR OBSERVATORIES

Coordinated study of solar-terrestrial payloads on space station
[NASA-CR-176160] N85-34158
Soft X-Ray Telescope (SXRT) N85-34159
Solar Ultraviolet Spectral Irradiance Monitor (SUSIM) N85-34160
White Light Coronograph (WLC) and Ultra-Violet Coronal Spectrometer (UVCS) N85-34161
High Resolution Telescope and Spectrograph (HRTS) N85-34162
Active Cavity Radiometer (ACR) N85-34163
Waves In Space Plasmas (WISP) N85-34164
Space Experiments with Particle Accelerators (SEPAC) N85-34165
Theoretical and Experimental Beam Plasma Physics (TEBPP) N85-34166
Recoverable Plasma Diagnostics Package (RPDP) N85-34167
Electrodynamic tether N85-34168
Imaging Spectrometric Observatory (ISO) N85-34169
Atmospheric Emission Photometric Imaging (AEPI) N85-34170
Magnetospheric multiprobes: MMP/CHEMSAT N85-34171
Wide Angle Michelson Doppler Imaging Interferometer (WAMDII) N85-34172
Vehicle Charging And Potential (VCAP) N85-34173
Initial placement of STO instruments N85-34174

SOLAR POSITION

Cosmic ray intensity distribution perpendicular to solar equatorial plane at 1 A.U. during 1978-83
[SH-4.3-14] N85-34998

SOLAR PROMINENCES

Onset of solar flares as predicted by two-dimensional MHD-models of quiescent prominences
[SH-1.3-1] N85-34750

SOLAR PROTONS

The propagation of solar flare particles in a turbulent coronal loop
[SH-1.1-3] N85-34730
Stochastic particle acceleration in solar flares
[SH-1.1-4] N85-34731
Fast drift kilometric radio bursts and solar proton events
[SH-1.1-7] N85-34734
Spectral and spatial properties of solar microflares
[SH-1.2-4] N85-34740
Ion energy storage for post-flare loops
[SH-1.2-10] N85-34745
A dominant role for protons at the onset of solar flares
[SH-1.2-13] N85-34748
The starting conditions for an optically small solar gamma ray flare
[SH-1.3-2] N85-34751
On the detectability of key-MeV solar protons through their nonthermal Lyman-alpha emission
[SH-1.3-5] N85-34752
Observations of solar flare gamma-rays and protons
[SH-1.3-6] N85-34753
Energetic protons from a disappearing solar filament
[SH-1.3-7] N85-34754
Spectra of solar proton ground level events using neutron monitor and neutron moderated detector recordings
[SH-1.3-14] N85-34759
On the retention of high-energy protons and nuclei with charges Z or equal to 2 in large solar flares after the process of their acceleration
[SH-2.1-8] N85-34789
Observations of solar energetic particles at a synchronous orbit
[SH-3.1-1] N85-34806
Coronal propagation of flare associated electrons and protons
[SH-3.1-3] N85-34808
Constraints of solar flare particle transport models from anisotropy observations at Voyager 1
[SH-3.1-8] N85-34812
Low energy proton bidirectional anisotropies and their relation to transient interplanetary magnetic structures: ISEE-3 observations
[SH-3.1-9] N85-34813
Determination of the pitch-angle distribution and transverse anisotropy of interplanetary particles
[SH-3.1-11] N85-34815
Channeled propagation of solar particles
[SH-3.2-3] N85-34819
Energetic solar particle fluxes out to 3 AU during the 7 May 1978 flare event
[SH-3.2-6] N85-34822

Monte Carlo calculations of relativistic solar proton propagation in interplanetary space
[SH-3.2-11] N85-34826
Latitude variation of recurrent fluxes in the outer solar system
[SH-4.1-13] N85-34836
Penetration of solar protons into the Earth's magnetosphere on November 22, 1977
[SH-6.1-15] N85-35088
Dynamics of the penetration boundaries of solar protons during a strong magnetic storm
[SH-6.1-16] N85-35089
The influence of the Earth's magnetosphere on the high-energy solar protons
[SH-6.1-22] N85-35093
Solar neutrinos, solar flares, solar activity cycle and the proton decay
[SH-8.1-8] N85-35113

SOLAR RADIATION
Three dimensional calculation of flux of low energy atmospheric neutrinos
[SH-8.1-11] N85-35116
Monte Carlo calibration of the SMM gamma ray spectrometer for high energy gamma rays and neutrons
[SH-9.1-6] N85-35121
Recording system for the solar neutron monitoring at Mt. Norikura
[SH-9.1-8] N85-35123
Using the information of cosmic rays to predict influence epidemic
[SH-10.1-2] N85-35134

SOLAR RADIO BURSTS
Fast drift kilometric radio bursts and solar proton events
[SH-1.1-7] N85-34734
Temporal evolution of an energetic electron population in an inhomogeneous medium: Application to solar hard X-ray bursts
[SH-1.2-6] N85-34741
Two types of electron events in solar flares
[SH-1.2-11] N85-34746
A dominant role for protons at the onset of solar flares
[SH-1.2-13] N85-34748
Ground increase of cosmic ray intensity on February 16, 1984
[SH-1.3-15] N85-34760
Type 3 solar radio bursts and 3HE-rich events
[SH-2.2-3] N85-34798
The 3HE in solar non-relativistic electron events
[SH-2.2-5] N85-34800

SOLAR ROTATION
The corotating variation of the north-south anisotropy of cosmic rays
[SH-4.3-15] N85-34999
Cosmic ray power spectral variations. 3: Solar rotation periodicities
[SH-4.4-16] N85-35012
Study of spectral exponent on quiet and disturbed days
[SH-4.5-10] N85-35028

SOLAR SPECTRA
Source energy spectra from demodulation of solar particle data by interplanetary and coronal transport
[SH-1.3-13] N85-34758
Spectra of solar proton ground level events using neutron monitor and neutron moderated detector recordings
[SH-1.3-14] N85-34759

SOLAR SPECTROMETERS
White Light Coronograph (WLC) and Ultra-Violet Coronal Spectrometer (UVCS) N85-34161
The Jovian electron spectrum: 1978-1984
[SH-1.5-19] N85-34782

SOLAR STORMS
Dynamics of the penetration boundaries of solar protons during a strong magnetic storm
[SH-6.1-16] N85-35089

SOLAR SYSTEM
Implications of source abundances of ultraheavy cosmic rays
[OG-7.1-4] N85-34866

SOLAR WIND
White Light Coronograph (WLC) and Ultra-Violet Coronal Spectrometer (UVCS) N85-34161
Shock and statistical acceleration of energetic particles in the interplanetary medium
[SH-1.5-1] N85-34771
Pitch angle distributions of 35-1000 keV protons at quasi-perpendicular interplanetary shocks
[SH-1.5-6] N85-34775
Elemental abundances in corotating events
[SH-1.5-15] N85-34778
Cosmic ray acceleration by stellar wind. Simulation for heliosphere
[SH-1.5-17] N85-34780
Low energy proton bidirectional anisotropies and their relation to transient interplanetary magnetic structures: ISEE-3 observations
[SH-3.1-9] N85-34813
The propagation of solar energetic particles in magnetic channels
[SH-3.2-4] N85-34820
Effects of a wavy neutral sheet on cosmic ray anisotropies
[SH-4.2-11] N85-34849
On the influence of the heliomagnetospheric periphery on the galactic cosmic rays
[SH-4.2-19] N85-34856
An update on the correlation between the cosmic radiation intensity and the geomagnetic AA index
[SH-4.2-24] N85-34861
Gradients and anisotropies of high energy cosmic rays in the outer heliosphere
[SH-4.3-7] N85-34992
The corotating variation of the north-south anisotropy of cosmic rays
[SH-4.3-15] N85-34999
A study of periodicities and recurrences in solar activity and cosmic ray modulation
[SH-4.4-14] N85-35010
Azimuthal and meridional asymmetries of the solar wind and quasiperiodic variations of intensity of Galactic Cosmic Rays (GCR)
[SH-4.4-20] N85-35016
Diagnostic of electromagnetic conditions in space using cosmic rays
[SH-4.5-19] N85-35036
Observation of pick-up ions in the solar wind: Evidence for the source of the anomalous cosmic ray component?
[SH-4.6-5] N85-35043
On the anomalous component
[SH-4.6-6] N85-35044
The large-scale modulation of cosmic rays in mid-1982: Its dependence on heliospheric longitude and radius
[SH-4.7-9] N85-35053
Dimensions of the solar wind cavity and of the region of interplanetary cosmic ray modulation
[SH-4.7-11] N85-35055
Galactic cosmic ray currents and magnetic field irregularity degree in high-speed solar wind streams
[SH-5.1-9] N85-35063
Influence of magnetic clouds on cosmic ray intensity variations
[SH-5.1-12] N85-35065
Peculiarities of Galactic Cosmic Ray (GCR) anisotropy variation in connection with the recurrent and sporadic Forbush effects
[SH-5.1-21] N85-35073
Cosmic ray modulation by high-speed solar wind fluxes
[SH-5.1-22] N85-35074
Coupling functions for lead and lead-free neutron monitors from the latitudinal measurements performed in 1982 in the research station Academician Kurchatov
[SH-6.1-1] N85-35076
Cosmic rays 10Be biennal data and their relationship to aurorae and sunspots
[SH-7.1-1] N85-35094

SOLAR WIND VELOCITY
Determination of the pitch-angle distribution and transverse anisotropy of interplanetary particles
[SH-3.1-11] N85-34815
Evidence for regions of negligible cosmic-ray modulation in the inner heliosphere (10 AU)
[SH-4.1-21] N85-34840
Determination of galactic cosmic ray latitudinal gradient using Earth based detectors
[SH-4.2-13] N85-34851
The expected cosmic ray density and stream distributions at the heliolatitudinal asymmetry of solar wind
[SH-4.2-14] N85-34852
Latitudinal gradients of cosmic rays and the polarity reversal of the heliospheric magnetic field: A preliminary evaluation
[SH-4.2-16] N85-34853
The effect of the neutral sheet structure of the interplanetary magnetic field on cosmic ray distribution in space
[SH-4.2-18] N85-34855
11- and 22-year variations of the cosmic ray density and of the solar wind speed
[SH-4.2-21] N85-34858
The corotating variation of the north-south anisotropy of cosmic rays
[SH-4.3-15] N85-34999
Long-term modulation of galactic cosmic rays in high-energy region
[SH-4.4-22] N85-35018
Solar wind velocity and daily variation of cosmic rays
[SH-4.5-6] N85-35024
The cosmic ray interplanetary radial gradient from 1972 - 1985
[SH-4.7-1] N85-35046
The recovery of the cosmic ray flux from maximum solar modulation at IMP-8 (1 AU) and at Pioneer (R 30 AU)
[SH-4.7-7] N85-35052
The large-scale modulation of cosmic rays in mid-1982: Its dependence on heliospheric longitude and radius
[SH-4.7-9] N85-35053
Nonstationary modulation of galactic cosmic rays in a nonlinear model
[SH-4.7-10] N85-35054
Study of dominating parameters of high speed solar plasma streams in relation to cosmic ray and geomagnetic storms
[SH-5.1-11] N85-35064
The solar wind effect on cosmic rays and solar activity
[SH-5.1-13] N85-35066

SOLAR X-RAYS
Study of non-thermal photon production under different scenarios in solar flares. 1: Scenarios and formulations
[SH-1.2-2] N85-34738
Study of non-thermal photon production under different scenarios in solar flares. 2: The Compton inverse and Bremsstrahlung models and fittings
[SH-1.2-3] N85-34739
Spectral and spatial properties of solar microflares
[SH-1.2-4] N85-34740
Temporal evolution of an energetic electron population in an inhomogeneous medium: Application to solar hard X-ray bursts
[SH-1.2-6] N85-34741
Quantitative analysis of flare accelerated electrons through their hard X-ray and microwave radiation
[SH-1.2-7] N85-34742
Two types of electron events in solar flares
[SH-1.2-11] N85-34746
Two classes of solar energetic particle events associated with impulsive and long duration soft X-ray flares
[SH-1.2-12] N85-34747
A dominant role for protons at the onset of solar flares
[SH-1.2-13] N85-34748
Photometric and spectroscopic gamma-ray observations of solar transient phenomena using long duration balloons
[SH-9.1-5] N85-35120

SOLDERING
Hermetic chip carrier compliant soldering pads
[AD-D011722] N85-34410

SOLENOIDS
Rotor blade test apparatus
[AD-D011725] N85-34381
Theoretical and computational research on the focused transport of intense charged particle beams
[DE85-012980] N85-34621

SOLID SURFACES
Unsteady transonic heat transfer in a transient facility
[NASA-CR-176145] N85-34354
System maintenance manual for master modeling of aerodynamic surfaces by three-dimensional explicit representation
[NASA-CR-178224] N85-34517
The dynamics of articulated rigid bodies for purposes of animation N85-34579

SOLID WASTES
Multi-solute subsurface transfer modeling for energy solid wastes: Highlights FY 1984
[DE85-012788] N85-34591

SOLIDIFICATION
Approximate determination of the extent of the solid-liquid zone
[BLL-M-35829-(5828.4)] N85-34251
Microstructures in rapidly solidified Ni-Mo alloys
[NASA-TM-87100] N85-34266
Method for making a low density polyethylene waste form for safe disposal of low level radioactive material
[DE85-006401] N85-34292

SOLUBILITY
Stability of two-dimensional immiscible flow to viscous fingering
[DE85-011403] N85-34364

SOLVENT EXTRACTION
Method for extracting lanthanides and actinides from acid solutions by modification of Purex solvent
[DE85-005763] N85-34220
Separation of uranium from technetium in recovery of spent nuclear fuel
[DE85-006499] N85-34627

SONAR
Magnetic search system
[PB85-185108] N85-34477

SOUNDING
The transient electromagnetic depth sounding technique applied to hydrocarbons and geothermal exploration
[MITT-42] N85-34476
SPACE CHARGE
Electron photoejection in carbanions
[DE85-011747] N85-34230
Repetitive pulse accelerator technology for light ion inertial confinement fusion
[DE85-012030] N85-34693
SPACE COMMERCIALIZATION
Study to encourage and facilitate industrial investment and involvement in space
[NASA-CR-176152] N85-34147
SPACE COOLING (BUILDINGS)
Advanced heat pump research and development
[DE85-009540] N85-34372
SPACE EXPLORATION
A spacefaring people: Perspectives on early spaceflight
[NASA-SP-4405] N85-35142
Space science and exploration: A historical perspective N85-35143
The next assignment: The state of the literature on space N85-35146
The idea of space exploration N85-35150
SPACE FLIGHT
Microorganisms in space flight N85-34490
SPACE PLATFORMS
Initial placement of STO instruments N85-34174
SPACE POWER REACTORS
SP-100 Thermionic Technology Program
[DE85-012311] N85-34625
SPACE PROBES
Magnetospheric multiprobes: MMP/CHEMSAT N85-34171
Precision measurements of solar energetic particle elemental composition
[SH-2.1-4] N85-34785
SPACE PROGRAMS
A spacefaring people: Perspectives on early spaceflight
[NASA-SP-4405] N85-35142
Space science and exploration: A historical perspective N85-35143
The next assignment: The state of the literature on space N85-35146
Opportunities for policy historians: The evolution of the US civilian space program N85-35147
Space-age Europe, 1957-1980 N85-35148
Space activities in the Soviet Union, Japan, and the People's Republic of China N85-35149
SPACE RENDEZVOUS
Hardware test program for evaluation of basline range-range rate sensor concept
[NASA-CR-176143] N85-34377
SPACE SHUTTLE ORBITERS
Use of a hyperbolic grid generation scheme in simulating supersonic viscous flow about three-dimensional winged configuration
[NASA-TM-85344] N85-34116
SPACE SHUTTLES
Results of a study to build a gamma-ray telescope in an external tank
[OG-9.3-3] N85-34958
SPACE STATIONS
Study to encourage and facilitate industrial investment and involvement in space
[NASA-CR-176152] N85-34147
Space station rotational equations of motion
[NASA-TP-2511] N85-34148
Space Station Engineering and Technology Development: Proceedings of the Panel on In-Space Engineering Research and Technology Development
[NASA-CR-176110] N85-34153
The role of tethers on space station
[NASA-TM-86519] N85-34154
Coordinated study of solar-terrestrial payloads on space station
[NASA-CR-176160] N85-34158
Soft X-Ray Telescope (SXRT) N85-34159
Solar Ultraviolet Spectral Irradiance Monitor (SUSIM) N85-34160
White Light Coronograph (WLC) and Ultra-Violet Coronal Spectrometer (UVCS) N85-34161
High Resolution Telescope and Spectrograph (HRTS) N85-34162
Active Cavity Radiometer (ACR) N85-34163
Waves in Space Plasmas (WISP) N85-34164
Space Experiments with Particle Accelerators (SEPAC) N85-34165
Theoretical and Experimental Beam Plasma Physics (TEBPP) N85-34166
Recoverable Plasma Diagnostics Package (RPDP) N85-34167
Electrodynamic tether N85-34168
Imaging Spectrometric Observatory (ISO) N85-34169
Atmospheric Emission Photometric Imaging (AEPI) N85-34170
Magnetospheric multiprobes: MMP/CHEMSAT N85-34171
Wide Angle Michelson Doppler Imaging Interferometer (WAMDII) N85-34172
Vehicle Charging And Potential (VCAP) N85-34173
Initial placement of STO instruments N85-34174
Optical analysis of parabolic dish concentrators for solar dynamic power systems in space
[NASA-TM-87080] N85-34176
Detection of 10 (1) GeV cosmic neutrinos with a space station
[OG-9.4-10] N85-34977
SPACEBORNE EXPERIMENTS
The development of a high energy cosmic ray detector for Spacelab-2
[OG-9.1-8] N85-34934
The heavy ions in space experiment
[OG-9.1-10] N85-34936
SPACECRAFT ANTENNAS
Box truss analysis and technology development. Task 1: Mesh analysis and control
[NASA-CR-172570] N85-34156
SPACECRAFT CONFIGURATIONS
Spacecraft (Mobile Satellite) configuration design study
[NASA-CR-176153] N85-34152
SPACECRAFT CONTROL
Space station rotational equations of motion
[NASA-TP-2511] N85-34148
Hardware math for the 6502 microprocessor
[NASA-TM-86517] N85-34511
SPACECRAFT DOCKING
Hardware test program for evaluation of basline range-range rate sensor concept
[NASA-CR-176143] N85-34377
SPACECRAFT ENVIRONMENTS
USSR report: Space Biology and Aerospace Medicine, vol. 19, no. 3, May - June 1985
[JPRS-USB-85-005] N85-34494
SPACECRAFT POWER SUPPLIES
Solar maximum: Solar array degradation
[NASA-TM-86194] N85-34175
Optical analysis of parabolic dish concentrators for solar dynamic power systems in space
[NASA-TM-87080] N85-34176
STACBEAM 2
[NASA-CR-176126] N85-34442
General-purpose heat source development: Safety test program. Postimpact evaluation, design iteration test
[LA-10034-SR] N85-34606
SPACELAB PAYLOADS
Detector calibration of the Indian cosmic ray experiment (IONS) in Space-Shuttle Spacelab-13
[SH-9.1-2] N85-35117
SPALLATION
Calculation of improved spallation cross sections
[OG-7.2-23] N85-34890
Spallogenic origin of nuclei in meteorites
[SH-7.1-10] N85-35102
SPATIAL DEPENDENCIES
Spatial dependence of the local diffusion coefficient measured upstream of the November 12, 1978 interplanetary traveling shock
[SH-1.5-12] N85-34776
SPATIAL DISTRIBUTION
The expected cosmic ray density and stream distributions at the heliolatitudinal asymmetry of solar wind
[SH-4.2-14] N85-34852
Spatial distribution of cosmic rays in magnetic cycles of the Sun
[SH-4.2-20] N85-34857
Influence of the source distribution on the age distribution of galactic cosmic rays
[OG-8.3-1] N85-34920
Explanation of the secondary to primary ratio within the continuous Fermi accelerator model
[OG-8.3-2] N85-34921
The modulation features of the long-period cosmic ray variations in connection with the sign change of the general magnetic field of the Sun
[SH-4.5-15] N85-35032
On the anomalous component
[SH-4.6-6] N85-35044
The read-out system of spatial distribution of thermoluminescence in meteorites
[SH-9.1-16] N85-35131
SPATIAL FILTERING
Theoretical principles of vertical subsampling of color difference signals at half the sampling rate — television
[FI-447-TBR-18] N85-34332
SPECIFIC HEAT
Dynamics of the melting of chromium-manganese alloys in molten steel
[BLL-M-35850-(5828.4)] N85-34252
SPECIFICATIONS
Stellarator approach to fusion plasma confinement
[DE85-011420] N85-34704
SPECTRA
Spectral and spatial properties of solar microflares
[SH-1.2-4] N85-34740
Relativistic cosmic ray spectra in the full non-linear theory of shock acceleration
[OG-8.1-6] N85-34896
SPECTRAL METHODS
A review of spectral methods
[NASA-CR-172502] N85-34350
SPECTRAL RESOLUTION
Mass resolution optimization in a large isotopic composition experiment
[OG-9.1-9] N85-34935
SPECTROHELIOGRAPHS
High Resolution Telescope and Spectrograph (HRTS) N85-34162
SPECTROMETERS
Imaging Spectrometric Observatory (ISO) N85-34169
Investigation of non-intrusive radiometers for entrained gasifier temperature measurement, revision 3
[DE85-011795] N85-34385
Measurements of Fe and Ar fragmentation cross sections
[OG-7.2-20] N85-34887
SPECTROSCOPIC ANALYSIS
Precision measurements of solar energetic particle elemental composition
[SH-2.1-4] N85-34785
SPECTROSCOPY
Direct determination of metals in organic matrices by Inductively Coupled Plasma-Atomic Emission Spectrometry (ICP-AES)
[DE85-012015] N85-34233
Time-resolved spectroscopic studies of detonating heterogeneous explosives
[DE85-009760] N85-34297
Apparatus and method for the spectrochemical analysis of liquids using the laser spark
[DE85-005749] N85-34387
Solar flare gamma-ray line spectroscopy
[SH-2.1-14] N85-34795
Results of ultra-low level 71ge counting for application in the Gallex-solar neutrino experiment at the Gran Sasso Underground Physics Laboratory
[SH-8.1-2] N85-35108
The read-out system of spatial distribution of thermoluminescence in meteorites
[SH-9.1-16] N85-35131
SPECTRUM ANALYSIS
On the cosmic ray diffusion in a violent interstellar medium
[OG-7.2-14] N85-34881
Study of spectral exponent on quiet and disturbed days
[SH-4.5-10] N85-35028
Spectral analysis of the Forbush decrease of 13 July 1982
[SH-5.1-7] N85-35061
Proton albedo spectrum observation in low latitude region at Hyderabad, India
[SH-6.1-8] N85-35082
SPHERES
Thermal transport measurements of UV laser irradiated spherical targets
[DE85-011038] N85-34365
Improved flow cytometer measurement of binding assays
[DE85-006407] N85-34390
SPHERICAL COORDINATES
Algorithm for calculation of strain state from measurements of node coordinates of arbitrary curvilinear grid
[BLL-M-36304] N85-34422
SPHERICAL HARMONICS
Characteristics of cosmic ray pole-equator anisotropy derived from spherical harmonic analysis of neutron monitor data
[SH-4.3-12] N85-34996
Sidereal anisotropy of cosmic rays
[SH-4.4-8] N85-35006
SPHERICAL PLASMAS
Magnetohydrodynamic equilibrium and stability of spheromak with spheroidal plasma-vacuum interface
[IPPJ-732] N85-34640
SPILLING
Description of a test site for large-scale heavy gas dispersion and combustion experiments
[DE85-004987] N85-34231

Evaluation of source strength and dispersion model predications with data from large nitrogen tetroxide field experiments
[DE85-011855] N85-34465
MATADOR (Methods for the Analysis of Transport And Deposition Of Radionuclides) code description and user's manual
[TI85-901402] N85-34592

SPIRAL WRAPPING
Generated spiral bevel gears: Optimal machine-tool settings and tooth contact analysis
[NASA-TM-87075] N85-34405

SPLINE FUNCTIONS
An intuitive approach to geometric continuity for parametric curves and surfaces N85-34571

SPOILERS
Study of boundary layer separation on a supercritical profile with a spoiler by means of a laser Doppler velocimeter
[ISL-CO-225/84] N85-34128

SPRAYING
MATADOR (Methods for the Analysis of Transport And Deposition Of Radionuclides) code description and user's manual
[TI85-901402] N85-34592

SPRINGS (WATER)
Evaluation of low-temperature geothermal potential in Utah and Goshen Valleys and adjacent areas, Utah. Part 2: Water temperature and chemistry
[DE85-009344] N85-34438

SPUTTERING
Low-energy sputterings with the Monte Carlo Program ACAT
[IPPJ-AM-40] N85-34690

STABILITY
Compressible two-phase flow instabilities simulated with a hybrid Lagrange-Euler pseudospectral method
[DE85-009904] N85-34361
Stability of two-dimensional immiscible flow to viscous fingering
[DE85-011403] N85-34364
Simulation studies on stability of hot electron plasma N85-34664
Workshop report on Simulation Techniques for Shock Wave Phenomena and Characteristics of Plasmas in Inertial Confinement Fusion
[IPPJ-725] N85-34670
Instabilities in decelerating supersonic flows with applications to cosmic ray shocks
[OG-8.1-2] N85-34892

STABILIZATION
Electron photoejection in carbanions
[DE85-011747] N85-34230
The balancing of complex linkage mechanisms N85-34313
Method and apparatus for transfer function simulator for testing complex systems
[NASA-CASE-NPO-15696-1] N85-34333
Improved method for the stabilization of NaI-photomultiplier gamma detectors against thermal and other drift
[DE85-011830] N85-34613

STAINLESS STEELS
Mechanical properties of plasma arc cut steel N85-34188
Approximate determination of the extent of the solid-liquid zone
[BLL-M-35829-(5828.4)] N85-34251
Influence of particle erosion on the microstructural changes in metals and alloys
[TI85-901384] N85-34276
Stress corrosion cracking susceptibility of types 316NG and 316 stainless steel in an impurity environment
[TI85-006884] N85-34277
Effect of stainless steel weld overlay cladding on the structural integrity of flawed steel plates in bending, series 1
[TI85-010349] N85-34418
Analytical ultrasonics for structural materials
[TI85-006132] N85-34600
Shield design for next-generation, low-neutron-fluence, superconducting tokamaks
[DE85-011409] N85-34695

STANDARD DEVIATION
On the statistical significance of excess events: Remarks of caution and the need for a standard method of calculation
[OG-9.5-10] N85-34987

STANDARDS
Recommendations for the design and equipping of engineering metrology laboratories
[NPL-MOM-22] N85-34145

STAR DISTRIBUTION
A star camera aspect system suitable for use in balloon experiments
[OG-9.3-10] N85-34965

STATISTICAL ANALYSIS
Statistical pooling method of fatigue data for reliability design N85-34198
Theoretical and experimental analyses of the performance of two-color laser ranging systems
[NASA-CR-176159] N85-34397
On the statistical significance of excess events: Remarks of caution and the need for a standard method of calculation
[OG-9.5-10] N85-34987
A new statistic for the analysis of circular data in gamma-ray astronomy
[OG-9.5-13] N85-34989
Rigidity spectrum of Forbush decrease
[SH-5.1-6] N85-35060
Methods and software for cosmic ray scintillation studies
[SH-9.1-17] N85-35132

STATISTICAL WEATHER FORECASTING
Tunisian climate seen through a Markov process
[CT-585] N85-34482

STEADY STATE
Transports studies of ECH and ICRH-heated bumpy torus plasma in NBT-1M N85-34662
Analytic and numerical calculations of the ambipolar electric field in a stellarator N85-34665
Numerical descriptions of cosmic-ray transport
[SH-4.1-3] N85-34829
The 1973-1984 solar modulation of cosmic ray nuclei
[SH-4.1-16] N85-34838
Exact solutions for sporadic acceleration of cosmic rays
[OG-8.3-7] N85-34925
Stochastic particle acceleration in flaring stars
[OG-8.3-9] N85-34927

STEAM
Method for determining depth and shape of a sub-surface conductive object
[DE85-006502] N85-34389
Control system for fluid heated steam generator
[DE85-005734] N85-34417
Calculations on the feasibility of ultrasonic inspection of steam generator tubing in pressurized water reactors
[AERE-R-10960] N85-34419
Downstream behavior of volatile fission product species
[DE85-012124] N85-34617

STEEL STRUCTURES
Monotonous stress-strain properties of structural steel subjected to nonstationary repetitive pre-loading N85-34185
Safety and reliability of steel structural materials under random service impact loads N85-34197

STEELS
The study of the effect of residual microimpurities on the fatigue strength of 55S2 steel
[BLL-M-36317-(5828.4)] N85-34246
Special features of the fracture of ball-bearing steel close to non-metallic inclusion eutectics
[BLL-M-35809-(5828.4)] N85-34258
Properties of tungsten-free steel for cutting tools
[BLL-M-35808-(5828.4)] N85-34259
Chromium-base powder alloys for welding cladding layer of bimetal
[BLL-M-35776-(5828.4)] N85-34260
The properties of VSt3sp inoculated steel
[BLL-M-35894-(5828.4)] N85-34263
Hydrogen embrittlement testing
[DE85-007352] N85-34273

STELLAR ATMOSPHERES
X-ray spectra of bursting neutron stars N85-34686

STELLAR MASS ACCRETION
X-ray spectra of bursting neutron stars N85-34686

STELLAR OCCULTATION
The 13 November 1984 occultation of BD +08 deg 0471 by (1) Ceres
[NASA-CR-176106] N85-34725

STELLAR OSCILLATIONS
Quasiperiodic oscillations in bright galactic-bulge X-ray sources
[NASA-CR-176138] N85-34723

STELLAR RADIATION
Low-excitation Herbig-Haro objects and interstellar extinction
[NASA-CR-176142] N85-34726

STELLAR SPECTRA
The cosmic ray interplanetary radial gradient from 1972 - 1985
[SH-4.7-1] N85-35046

STELLAR SPECTROPHOTOMETRY
Photometric and spectroscopic gamma-ray observations of solar transient phenomena using long duration balloons
[SH-9.1-5] N85-35120

STELLAR STRUCTURE
A possible mechanism to cause the quasi-biennial variability on the solar neutrino flux
[SH-8.1-5] N85-35110

STELLAR WINDS
Possible origin of the anomalous component of cosmic rays
[SH-4.6-7] N85-35045

STELLARATORS
Proceedings of the US-Japan Workshop on Transport in Open-Ended Systems
[IPPJ-727] N85-34644
Analytic and numerical calculations of the ambipolar electric field in a stellarator N85-34665
Behavior of helically-trapped fast ion orbits in heliotron E N85-34666
Advanced Toroidal Facility (ATF)
[DE85-011567] N85-34699
Stellarator approach to fusion plasma confinement
[DE85-011420] N85-34704

STEPPES
Snow cover in the Siberian forest-steppe
[NASA-TM-77914] N85-34435

STIFFENING
Design of transversely stiffenend FRP panels under compressive load --- fiber reinforced plastic (FRP) ships
[AMTE(S)-R-84104] N85-34424

STIFFNESS
An introduction to finite elements N85-34319

STIFFNESS MATRIX
Automated dynamic analytical model improvement for damped structures
[NASA-CR-177945] N85-34425

STOCHASTIC PROCESSES
Frame buffer algorithms for stochastic models N85-34525
Specifying stochastic objects in a hierarchical graphics system N85-34526
Stochastic particle acceleration in flaring stars
[OG-8.3-9] N85-34927
On the statistical significance of excess events: Remarks of caution and the need for a standard method of calculation
[OG-9.5-10] N85-34987

STOICHIOMETRY
Survey of mixing in metal/insulator systems
[DE85-011938] N85-34714

STORAGE BATTERIES
Solar heat pump
[DE85-011323] N85-34453

STORAGE RINGS (PARTICLE ACCELERATORS)
Multiple-frequency electron cyclotron heating of hot electron rings in EBT-1
[DE85-011302] N85-34701

STORAGE STABILITY
Review of zirconium-zircaloy pyrophoricity
[DE85-011169] N85-34270

STRAIN MEASUREMENT
Algorithm for calculation of strain state from measurements of node coordinates of arbitrary curvilinear grid
[BLL-M-36304] N85-34422

STRAIN RATE
On high strain rate fragmentation of a closed vessel N85-34187
Experimental study on time and temperature dependent behavior of crack growth in viscoelastic strip N85-34193
Effect of strain rate on the initial failure of notched GRP laminates N85-34214

STRATEGIC MATERIALS
Preliminary SPR thermal model description and results for WH-11 and BM-4
[DE85-013171] N85-34360

STRATEGY
Strategic use of business graphics: A stakeholder approach N85-34566

STRATIGRAPHY
Geology and petroleum resources of basins in western China
[DE85-013038] N85-34469

STRATOSPHERE
A comparison of calculated and measured background noise rates in hard X-ray telescopes at balloon altitude
[OG-9.3-7] N85-34962
Dynamics of two-year cosmic ray variations inferred from the data of spacecraft and stratospheric measurements and from the neutron monitor data in 1959-1981
[SH-4.4-21] N85-35017
Diurnal effect in cosmic rays at middle latitudes according to stratospheric measurements
[SH-4.5-8] N85-35026

STREAMS
Hydrology
[PB85-182954] N85-34440

STRESS (PHYSIOLOGY)
Determination of individual tolerance in hyperbaric oxygen N85-34507
STRESS ANALYSIS
Proceedings of the Mechanisms Conference, volume 1 N85-34309
The use of ultrasound to monitor incipient failure of rolling element bearings N85-34317
Inertial stresses and deformations in mechanisms N85-34320
Thermal stress analysis of a new turbine shroud seal concept
[NASA-TM-87082] N85-34406
Design of transversely stiffenend FRP panels under compressive load --- fiber reinforced plastic (FRP) ships
[AMTE(S)-R-84104] N85-34424
The stress pattern analysis of coarse grain titanium specimens
[PNR-90250] N85-34433
STRESS CONCENTRATION
Fractographic analysis for nonpropagating conditions of fatigue crack at high stress ratios in mild steel N85-34194
Multiaxial stress analysis taking account of penetration depth of X-rays. A solution by means of polynomial approximation N85-34204
Stress distribution of fiberglass reinforced plastic beam with a delamination under three-point bending N85-34210
Stresses and strains in a plate resulting from two closely-spaced interference-fit fasteners
[ARL-STRUC-TM-409] N85-34429
The stress pattern analysis of coarse grain titanium specimens
[PNR-90250] N85-34433
Geophysical-geological studies of possible extensions of the New Madrid fault zone
[TI85-901341] N85-34475
STRESS CORROSION CRACKING
The influence of temperature on static and dynamic SCC crack growth behavior in aluminum alloy N85-34190
A fractographic study on mode 2 and mode 3 SCC crack growth in an Al-Zn-Mg alloy N85-34191
Stress corrosion cracking susceptibility of types 316NG and 316 stainless steel in an impurity environment
[TI85-006884] N85-34277
STRESS INTENSITY FACTORS
On the methods to determine the stress intensity factors in boundary element method N85-34189
Time and temperature dependence of fracture surface in soft epoxy resin N85-34213
Nonlinear adhesive behavior effects in a cracked orthotropic sheet stiffened by a semi-infinite orthotropic sheet
[NASA-TM-87584] N85-34426
STRESS RATIO
Fractographic analysis for nonpropagating conditions of fatigue crack at high stress ratios in mild steel N85-34194
STRESS WAVES
Behaviors of stress waves in a conical bar N85-34182
STRESS-STRAIN RELATIONSHIPS
Monotonous stress-strain properties of structural steel subjected to nonstationary repetitive pre-loading N85-34185
STRINGERS
Nonlinear adhesive behavior effects in a cracked orthotropic sheet stiffened by a semi-infinite orthotropic sheet
[NASA-TM-87584] N85-34426
STRUCTURAL ANALYSIS
Intermittent motion N85-34323
Software for mechanism design N85-34324
STRUCTURAL BASINS
Geothermal resources of the Laramie, Hanna and Shirley Basins, Wyoming
[DE85-005005] N85-34436
Hydrology
[PB85-182954] N85-34440
Geology and petroleum resources of basins in western China
[DE85-013038] N85-34469
STRUCTURAL DESIGN
A rational approach to cam design N85-34311
STRUCTURAL DESIGN CRITERIA
Design of transversely stiffenend FRP panels under compressive load --- fiber reinforced plastic (FRP) ships
[AMTE(S)-R-84104] N85-34424
STRUCTURAL ENGINEERING
Designing a graphics application interface N85-34574
STRUCTURAL FAILURE
Safety and reliability of steel structural materials under random service impact loads N85-34197
Effect of strain rate on the initial failure of notched GRP laminates N85-34214
Three-dimensional finite element failure model for predicting failure in fibre reinforced bolted joints
[BR94778] N85-34423
STRUCTURAL MEMBERS
Poly-functional building material from fiberglass (its fabrication and properties) N85-34209
A simple but systematic CSG system N85-34569
Analytical ultrasonics for structural materials
[TI85-006132] N85-34600
STRUCTURAL RELIABILITY
Safety and reliability of steel structural materials under random service impact loads N85-34197
Statistical pooling method of fatigue data for reliability design N85-34198
STRUTS
Variable length strut with longitudinal compliance and locking capability
[NASA-CASE-MFS-25907-1] N85-34401
SUBROUTINES
A versatile computer package for mechanism analysis N85-34314
Software for mechanism design N85-34324
SUBSONIC FLOW
A comparison of laser Doppler anemometry and probe measurements within the boundary layer of an airfoil at subsonic flow
[ISL-CO-219/84] N85-34127
SULFATES
Effects of acid rain on forest nutrient status
[DE85-012486] N85-34463
Throughfall rate and chemistry studies: Whiteface Mountain
[DE85-012407] N85-34464
SULFIDES
Special features of the fracture of ball-bearing steel close to non-metallic inclusion eutectics
[BLL-M-35809-(5828.4)] N85-34258
SULFUR DIOXIDES
Forecasting future industrial SO2 and NC/sub x/ emissions, revised N85-34461
Throughfall rate and chemistry studies: Whiteface Mountain
[DE85-012407] N85-34464
SUN
Coordinated study of solar-terrestrial payloads on space station
[NASA-CR-176160] N85-34158
Soft X-Ray Telescope (SXRT) N85-34159
Solar Ultraviolet Spectral Irradiance Monitor (SUSIM) N85-34160
White Light Coronograph (WLC) and Ultra-Violet Coronal Spectrometer (UVCS) N85-34161
High Resolution Telescope and Spectrograph (HRTS) N85-34162
Active Cavity Radiometer (ACR) N85-34163
Sidereal anisotropies in the median rigidity range 60-600GV in 1978-1983
[SH-4.4-3] N85-35001
The sidereal semi-diurnal variation observed at high zenith angles at Mawson, 1968-1984, and the polarity of the solar main field
[SH-4.4-6] N85-35004
A study of periodicities and recurrences in solar activity and cosmic ray modulation
[SH-4.4-14] N85-35010
Results of ultra-low level 71ge counting for application in the Gallex-solar neutrino experiment at the Gran Sasso Underground Physics Laboratory
[SH-8.1-2] N85-35108
Correlation between solar neutrino flux and other solar phenomena N85-35109
A possible mechanism to cause the quasi-biennial variability on the solar neutrino flux
[SH-8.1-5] N85-35110
The conjecture concerning time variations in the solar neutrino flux
[SH-8.1-6] N85-35111
Solar neutrino: Flux, cosmic rays and the 11 year solar cycle
[SH-8.1-7] N85-35112
Solar neutrinos, solar flares, solar activity cycle and the proton decay
[SH-8.1-8] N85-35113
Neutrino production from the solar atmosphere
[SH-8.1-9] N85-35114
Solar cosmic ray bursts and solar neutrino fluxes
[SH-8.1-10] N85-35115
A silicon surface barrier telescope for solar particles identification
[SH-9.1-3] N85-35118
Photometric and spectroscopic gamma-ray observations of solar transient phenomena using long duration balloons
[SH-9.1-5] N85-35120
Monte Carlo calibration of the SMM gamma ray spectrometer for high energy gamma rays and neutrons
[SH-9.1-6] N85-35121
SUNSPOT CYCLE
Difference between even and odd 11-year cycles in cosmic ray intensity
[SH-4.2-22] N85-34859
An update on the correlation between the cosmic radiation intensity and the geomagnetic AA index
[SH-4.2-24] N85-34861
SUNSPOTS
High Resolution Telescope and Spectrograph (HRTS) N85-34162
Anomalous low level of cosmic ray intensity decreases observed during 1980
[SH-5.1-15] N85-35068
Cosmic rays 10Be biennal data and their relationship to aurorae and sunspots
[SH-7.1-1] N85-35094
Correlation between solar neutrino flux and other solar phenomena N85-35109
Solar neutrino: Flux, cosmic rays and the 11 year solar cycle
[SH-8.1-7] N85-35112
Solar neutrinos, solar flares, solar activity cycle and the proton decay
[SH-8.1-8] N85-35113
Using the information of cosmic rays to predict influence epidemic
[SH-10.1-2] N85-35134
SUPERCOMPUTERS
The impact of supercomputers on experimentation: A view from a national laboratory
[NASA-TM-86822] N85-34510
Vector calculation of particle code N85-34588
SUPERCONDUCTING MAGNETS
Shield design for next-generation, low-neutron-fluence, superconducting tokamaks
[DE85-011409] N85-34695
A high resolution gas Cerenkov detector for the superconducting magnet facility
[OG-9.1-6] N85-34932
SUPERCONDUCTIVITY
Physics Division annual review, 1 April 1983 - 31 March 1984
[ANL-84-24] N85-34602
Magnitude and range of the RKKy interaction in SmRh4B4
[DE85-012284] N85-34712
SUPERCONDUCTORS
Magnitude and range of the RKKy interaction in SmRh4B4
[DE85-012284] N85-34712
Flux-line lattice anisotropy in V3Si: Observation and interpretation
[DE85-011935] N85-34713
SUPERCRITICAL WINGS
Study of boundary layer separation on a supercritical profile with a spoiler by means of a laser Doppler velocimeter
[ISL-CO-225/84] N85-34128
SUPERHEATING
Effects of ambient pressure on the instability of a liquid boiling explosively at the superheat limit
[DE85-009476] N85-34370
SUPERNOVA REMNANTS
Cosmic ray secondary nuclei and the structure of the galaxy
[OG-7.2-4] N85-34876
On the cosmic ray diffusion in a violent interstellar medium
[OG-7.2-14] N85-34881
Acceleration of cosmic rays in supernova-remnants
[OG-8.1-9] N85-34899
Onion-shell model for cosmic ray electrons and radio synchrotron emission in supernova remnants
[OG-8.1-10] N85-34900
Approximate supernova remnant dynamics with cosmic ray production
[OG-8.1-12] N85-34901
Interstellar (Na-22) as a possible source of the excess (Ne-22) in the galactic cosmic ray
[OG-8.2-12] N85-34908
The origins of cosmic rays and quantum effects on gravity
[OG-8.2-15] N85-34911
SUPERNOVAE
A very important process of nucleosynthesis in stars
[OG-7.1-11] N85-34872
A numerical study of diffusive shock acceleration of cosmic rays in supernova shocks
[OG-8.2-2] N85-34903
Do supernovae of type 1 paly a role in cosmic-ray production?
[OG-8.2-5] N85-34905

The nucleosynthesis of deterium and helium-3
[OG-8.2-18] N85-34914
Nuclear reactions in shock wave front during supernova events
[OG-8.2-19] N85-34915
Propagation of injected cosmic rays under distributed reacceleration
[OG-8.3-3] N85-34922
Propagation of cosmic rays and new evidence for distributed acceleration
[OG-8.3-5] N85-34924
SUPERSONIC FLOW
Use of a hyperbolic grid generation scheme in simulating supersonic viscous flow about three-dimensional winged configuration
[NASA-TM-85344] N85-34116
Instabilities in decelerating supersonic flows with applications to cosmic ray shocks
[OG-8.1-2] N85-34892
SUPPORTS
STACBEAM 2
[NASA-CR-176126] N85-34442
SURFACE ENERGY
Effect of precipitation variables on the specific surface and explosion characteristics of pentaerythritol tetranitrate
[DE85-009620] N85-34302
SURFACE FINISHING
Performance improvements from surfacing in aero engine components
[PNR-90257] N85-34142
Towards the development of technological processes for the preparation of cadmium plated steel articles
[BLL-M-36315-(5828.4)] N85-34248
SURFACE LAYERS
Method of precisely modifying predetermined surface layers of a workpiece by cluster ion impact therewith
[DE85-006519] N85-34710
SURFACE PROPERTIES
Anti wear property of two phasic metal composite N85-34199
Infrared studies of the influence of alkali metals on the C-O bond in chemisorbed carbon monoxide
[DE85-005306] N85-34232
Method for preparing hydride configurations and reactive metal surface
[DE85-006443] N85-34274
SURFACE TEMPERATURE
Surface temperature distribution along a thin liquid layer due to thermocapillary convection
[NASA-TM-87115] N85-34357
SURFACE VEHICLES
Evaluation of semiconductor devices for Electric and Hybrid Vehicle (EHV) ac-drive applications, volume 1
[NASA-CR-176118] N85-34335
SURFACE WATER
Hydrology
[PB85-182954] N85-34440
SURFACES
Block-implicit calculations of three-dimensional laminar flow in strongly curved ducts
[DE85-003047] N85-34363
Acoustical absorption coefficient in a diffuse field of a plane, rectangular material of finite dimensions placed on an infinite perfectly reflecting surface
[NRC/CNR-TT-2113] N85-34599
SURGERY
Applications of CdTe to nuclear medicine
[DE85-011877] N85-34492
SURVIVAL
Aviation safety (aircraft passenger survivability and cabin safety)
[GPO-39-847] N85-34130
SWITCHES
Multiple-stage integrating accelerometer
[DE85-006505] N85-34388
SWITCHING CIRCUITS
Series-counterpulse repetitive-pulse inductive storage circuit
[DE85-006438] N85-34342
SYNCHRONIZERS
Instrument to synchronize Thomson scattering diagnostic measurements with MHD activity in a Tokamak
[DE85-012082] N85-34708
SYNCHROTRON RADIATION
Onion-shell model for cosmic ray electrons and radio synchrotron emission in supernova remnants
[OG-8.1-10] N85-34900
SYNTHESIS (CHEMISTRY)
Electrolytic synthesis of colored eta alumina film N85-34201
Fire-resistant phosphorus containing polyimides and copolyimides
[NASA-CASE-ARC-11522-2] N85-34280
Preparation of ethylenediamine dinitrate
[DE85-006423] N85-34305
Ethylenediamine salt of 5-nitrotetrazole and preparation
[DE85-005738] N85-34306
Synthesis of ultrafine ceramic and metallic powders in a thermal argon rf plasma
[DE85-009634] N85-34696
SYNTHETIC APERTURE RADAR
Method and apparatus for Delta Kappa synthetic aperture radar measurement of ocean current
[NASA-CASE-NPO-15704-1] N85-34327
AMI calibration study. Volume 1: SAR calibration. Volume 2: Ground Targets. Volume 3: Scatterometer calibration — Active Microwave Instrument (AMI) ERS-1
[C2248/4/4-VOL-1] N85-34394
SYNTHETIC FIBERS
Substitution of asbestos by aramid fibers and fiber blends in industrial textiles and composites with organic binders
[BMFT-FB-T-85-006] N85-34294
SYSTEMS ENGINEERING
Space Station Engineering and Technology Development: Proceedings of the Panel on In-Space Engineering Research and Technology Development
[NASA-CR-176110] N85-34153
SYSTEMS SIMULATION
Discrete simulation models - their role in the design, development and management of inventory control systems
[PNR-90249] N85-34719

T

TABLETS
A multi-touch three dimensional touch-sensitive tablet (executive summary) N85-34553
TANTALUM
Ultra-trace analysis of sinter tantalum with SIMS
[BLL-RARDE-TR-1220-(7291.7965)] N85-34245
TAPERING
Reducing grating lobes due to subarray amplitude tapering
[AD-D011723] N85-34339
TARGET RECOGNITION
Hardware test program for evaluation of basline range-range rate sensor concept
[NASA-CR-176143] N85-34377
TARGETS
Moving finite element method for ICF target implosion N85-34675
TASMANIA
Sidereal variations deep underground in Tasmania
[SH-4.4-4] N85-35002
TECHNETIUM
Separation of uranium from technetium in recovery of spent nuclear fuel
[DE85-006499] N85-34627
Elemental technetium as a cosmic-ray clock
[OG-7.1-9] N85-34870
TECHNOLOGICAL FORECASTING
Telecommunications forecast for ITU Region 2 to the year 1995
[NASA-TM-87077] N85-34150
Towards the year 2000: Developments in inspection and product assurance to be anticipated during the next 15 years — aircraft engines
[PNR-90258] N85-34421
TECHNOLOGIES
Management of large-scale technology N85-35145
TECHNOLOGY ASSESSMENT
The development of titanium production in the USSR
[BLL-OA-TRANS-3226-(6196.3)] N85-34244
Vapor phase heat transport concepts
[DE85-009550] N85-34366
SP-100 Thermionic Technology Program
[DE85-012311] N85-34625
TECHNOLOGY UTILIZATION
High powered epicyclic gears: Some recent development N85-34316
TECTONICS
Geology and petroleum resources of basins in western China
[DE85-013038] N85-34469
TELECOMMUNICATION
Telecommunication market research processing
[ENST-83E018] N85-34331
TELEMETRY
Design, development and operation of a high simultaneous capacity digital telemetry system — turbomachine blade flutter
[PNR-90261] N85-34151
TELESCOPES
High Resolution Telescope and Spectrograph (HRTS) N85-34162
Angular resolution of air-shower array-telescopes
[OG-9.5-6] N85-34983
New Matsushiro underground cosmic ray station (220 M.W.E. in depth)
[SH-9.1-14] N85-35129
TELEVISION CAMERAS
Electronic imaging system and technique
[DE85-005740] N85-34393
TELEVISION SYSTEMS
Space Experiments with Particle Accelerators (SEPAC) N85-34165
Computer animation in distance teaching N85-34581
TEMPERATURE CONTROL
Feedback regulated induction heater for a flowing fluid
[DE85-006508] N85-34414
TEMPERATURE DEPENDENCE
The influence of temperature on static and dynamic SCC crack growth behavior in aluminum alloy N85-34190
Experimental study on time and temperature dependent behavior of crack growth in viscoelastic strip N85-34193
Time and temperature dependence of fracture surface in soft epoxy resin N85-34213
Shape memory effect in uranium-niobium alloys below room temperature
[DE85-012964] N85-34268
Study of photon emission by electron capture during solar nuclei acceleration, 1: Temperature-dependent cross section for charge changing processes
[SH-1.1-8] N85-34735
TEMPERATURE DISTRIBUTION
Surface temperature distribution along a thin liquid layer due to thermocapillary convection
[NASA-TM-87115] N85-34357
TEMPERATURE EFFECTS
The influence of temperature on the composition density of the transition metals
[BLL-M-35896-(5826.4)] N85-34262
Evaluation of source strength and dispersion model predications with data from large nitrogen tetroxide field experiments
[DE85-011855] N85-34465
Studies in thermo-hydro-chemical transport in porous and fractured media
[DE85-012555] N85-34473
Thermally induced chemical migration: A natural analog approach
[DE85-012308] N85-34474
TEMPERATURE GRADIENTS
Approximate determination of the extent of the solid-liquid zone
[BLL-M-35829-(5828.4)] N85-34251
Control system for fluid heated steam generator
[DE85-005734] N85-34417
Integral representation for nonlinear heat transport N85-34683
TEMPERATURE INVERSIONS
Reports from the German Meteorological Service. No. 167: Results of aerological soundings in the model area upper Rhine: Heat release project upper Rhine area, part 3
[ISBN-3-88148-216-4] N85-34479
TEMPERATURE MEASUREMENT
Measurement and correlation of jet fuel viscosities at low temperatures
[NASA-CR-174911] N85-34295
Preliminary SPR thermal model description and results for WH-11 and BM-4
[DE85-013171] N85-34360
Investigation of non-intrusive radiometers for entrained gasifier temperature measurement, revision 3
[DE85-011795] N85-34385
Control system for fluid heated steam generator
[DE85-005734] N85-34417
Measurement and interpretation of electron angle at MABE beam stop
[DE85-011918] N85-34698
TEMPORAL DISTRIBUTION
Temporal variations of the anomalous oxygen component, 1977 - 1984
[SH-4.6-3] N85-35041
TENSILE PROPERTIES
Fracture behavior of aluminum composites reinforced with fiber N85-34207
Apparatus producing constant cable tension for intermittent demand
[DE85-006434] N85-34412
TENSILE STRENGTH
Strength properties of glassfiber reinforced thermoplastics N85-34212
Study on fracture behavior of epoxy resin N85-34216
TENSILE STRESS
Apparatus producing constant cable tension for intermittent demand
[DE85-006434] N85-34412

TENSILE TESTS
Tensile testing apparatus
[NASA-CASE-LAR-13243-1] N85-34375
TENSORS
Scalar/Vector potential formulation for compressible viscous unsteady flows
[NASA-CR-3921] N85-34113
TERMINATOR LINES
Near Earth space sporadic radio emission busts occurring during sunrise
[SH-10.1-9] N85-35140
TERMINOLOGY
Re-evaluation of cosmic ray cutoff terminology
[SH-6.1-11] N85-35084
TERNARY ALLOYS
A fractographic study on mode 2 and mode 3 SCC crack growth in an Al-Zn-Mg alloy N85-34191
Enthalpies of formation of liquid Fe-Ce-Si and Fe-Ce-Al three-component alloys
[BLL-M-36296-(5828.4)] N85-34247
TERNARY SYSTEMS
Three body abrasive wear in various metal combinations N85-34200
TERRAIN
A user-friendly computer-aided construction of boundaries N85-34564
TERRESTRIAL RADIATION
Empirical model for the Earth's cosmic ray shadow at 400 KM: Prohibited cosmic ray access
[SH-6.1-14] N85-35087
Cosmic ray secular variations in terrestrial records and aurorae
[SH-7.1-3] N85-35096
TEST EQUIPMENT
The design and analysis of single flank transmission error testor for loaded gears
[NASA-CR-176163] N85-34404
TEST FACILITIES
Description of a test site for large-scale heavy gas dispersion and combustion experiments
[DE85-004987] N85-34231
The 1984 biotic studies of Yucca Mountain, Nevada test site, Nye County, Nevada
[DE85-011715] N85-34487
TEST STANDS
The design and analysis of single flank transmission error testor for loaded gears
[NASA-CR-176163] N85-34404
TEST VEHICLES
Test plan for performance testing of the Eaton AC-3 electric vehicle
[DE85-011954] N85-34341
TETHERED SATELLITES
Recoverable Plasma Diagnostics Package (RPDP) N85-34167
Electrodynamic tether N85-34168
TETHERING
The role of tethers on space station
[NASA-TM-86519] N85-34154
TEXTILES
Substitution of asbestos by aramid fibers and fiber blends in industrial textiles and composites with organic binders
[BMFT-FB-T-85-006] N85-34294
Re-designing a mechanism for higher speed: A case history from textile machinery N85-34310
A versatile computer package for mechanism analysis N85-34314
TEXTS
NAPGEN: Automatic NAPLPS page generator N85-34575
THEMATIC MAPPING
How map designers can represent their ideas in thematic maps: Effective user interfaces for thematic map design N85-34562
THERMAL CONDUCTIVITY
Poly-functional building material from fiberglass (its fabrication and properties) N85-34209
Finding the roots of the transcendental equations in problems in determining the thermal conductivity of spheres with heterogeneous boundary conditions
[BLL-M-35878-(5828.4)] N85-34347
Calculation of roots of transcendental equations in problems of determining thermal conductivity of cylinder with non-uniform boundary conditions
[BLL-M-35788-(5828.4)] N85-34349
Sequential regularization solution of the inverse heat conduction problem
[DE85-010657] N85-34362
Confinement experiments on ISX-B
[DE85-012346] N85-34709
THERMAL CYCLING TESTS
Electrical resistivity and hysteresis of the equiatomic nickel-titanium alloy near the martensitic transformation temperature N85-34181
X-ray measurement of thermal stresses in tungsten fiber-copper composites N85-34205
THERMAL EXPANSION
Hermetic chip carrier compliant soldering pads
[AD-D011722] N85-34410
THERMAL INSULATION
Carbon/carbon combustor external insulation
[AD-D011719] N85-34224
High temperature structural insulating material
[DE85-006361] N85-34291
THERMAL MAPPING
Modeling of geothermal systems
[DE85-012553] N85-34439
THERMAL PLASMAS
Integral representation for nonlinear heat transport N85-34683
Synthesis of ultrafine ceramic and metallic powders in a thermal argon rf plasma
[DE85-009634] N85-34696
THERMAL PROTECTION
Experimental aerodynamic heating to simulated space shuttle tiles in laminar and turbulent boundary layers with variable flow angles at a nominal Mach number of 7
[NASA-TP-2307] N85-34351
Upgrading auxiliary facility outleakage and combustion detection
[DE85-012796] N85-34386
THERMAL RADIATION
Instrumentation for sensing moisture content of material using a transient thermal pulse
[NASA-CASE-NPO-15493-2] N85-34373
THERMAL RESOURCES
The United States Geological Survey in Alaska: Accomplishments during 1983
[USGS-CIRC-945] N85-34468
THERMAL STABILITY
Review of zirconium-zircaloy pyrophoricity
[DE85-011169] N85-34270
A theoretical study of non-adiabatic surface effects for a model in the NTF cryogenic wind tunnel
[NASA-CR-3924] N85-34352
THERMAL STRESSES
X-ray measurement of thermal stresses in tungsten fiber-copper composites N85-34205
Influence of cyclic thermal loading on internal stress in casted epoxy resin N85-34211
Thermal stress analysis of a new turbine shroud seal concept
[NASA-TM-87082] N85-34406
THERMIONIC CONVERTERS
SP-100 Thermionic Technology Program
[DE85-012311] N85-34625
THERMIONIC POWER GENERATION
Thermionic photovoltaic energy converter
[NASA-CASE-LEW-14077-1] N85-34441
THERMODYNAMIC COUPLING
Survey of mixing in metal/insulator systems
[DE85-011938] N85-34714
THERMODYNAMIC PROPERTIES
Experimental evaluation of the thermodynamic properties of concentrated aqueous potassium hydroxide solutions
[DE85-010628] N85-34238
Calculation of activities of components in liquid alloys of iron with yttrium
[BLL-M-35868-(5828.4)] N85-34253
Design and lubrication of high-speed rolling-element bearings
[NASA-TM-87107] N85-34409
Determination of properties of zeolite/refrigerant combinations for solar refrigeration systems
[DE85-012009] N85-34448
THERMODYNAMICS
Technical assessment of thermal-hydraulics for high heat flux fusion components
[DE85-013178] N85-34359
THERMOHYDRAULICS
Technical assessment of thermal-hydraulics for high heat flux fusion components
[DE85-013178] N85-34359
Mathematical modeling of ultimate heat sink cooling ponds
[TI85-009747] N85-34369
Ocean thermal energy conversion
[DE85-012291] N85-34456
MATADOR (Methods for the Analysis of Transport And Deposition Of Radionuclides) code description and user's manual
[TI85-901402] N85-34592
THERMOLUMINESCENCE
The read-out system of spatial distribution of thermoluminescence in meteorites
[SH-9.1-16] N85-35131
THERMONUCLEAR POWER GENERATION
Technical assessment of thermal-hydraulics for high heat flux fusion components
[DE85-013178] N85-34359
THERMONUCLEAR REACTIONS
X-ray spectra of bursting neutron stars N85-34686
THERMOPLASTIC RESINS
Strength properties of glassfiber reinforced thermoplastics N85-34212
THICK WALLS
Experimental study of collapse of thick-walled tube under external pressure and axial force N85-34186
THICKNESS
The longitudinal thickness of air-shower fronts
[OG-9.5-1] N85-34978
THIN FILMS
Development and demonstration of a spiral-wound thin-film composite membrane system for the economical production of oxygen-enriched air, phase 4
[DE85-012380] N85-34288
Polarisation insensitive achromatic cube beamsplitter --- binocular microscopes
[NPL-MOM-72] N85-34630
THOMSON SCATTERING
Instrument to synchronize Thomson scattering diagnostic measurements with MHD activity in a Tokamak
[DE85-012082] N85-34708
THORIUM
Uranium, thorium isotopic analyses and uranium-series ages of calcite and opal and stable isotopic compositions of calcite from drill cores UE25a no. 1, USR G-2 and USW G-3/GU-3, Yucca Mountain, Nevada
[DE85-013039] N85-34471
THREE DIMENSIONAL BODIES
Mathematical modeling of ultimate heat sink cooling ponds
[TI85-009747] N85-34369
A simple but systematic CSG system N85-34569
Building an octree from a set of parallelepipeds N85-34572
Low cost geometric modeling system for CAM N85-34578
Generative design in architecture using an expert system N85-34582
THREE DIMENSIONAL FLOW
A three-dimensional viscous flow analysis for the helicopter tip vortex generation problem
[NASA-CR-3906] N85-34114
Integral equation formulation for three-dimensional unsteady transonic flow
[ARL-STRUC-R-416] N85-34119
Block-implicit calculations of three-dimensional laminar flow in strongly curved ducts
[DE85-003047] N85-34363
System maintenance manual for master modeling of aerodynamic surfaces by three-dimensional explicit representation
[NASA-CR-178224] N85-34517
THREE DIMENSIONAL MOTION
Three-dimensional hydrodynamic hot-spot model
[DE85-009587] N85-34301
TILES
Experimental aerodynamic heating to simulated space shuttle tiles in laminar and turbulent boundary layers with variable flow angles at a nominal Mach number of 7
[NASA-TP-2307] N85-34351
TIME DEPENDENCE
Experimental study on time and temperature dependent behavior of crack growth in viscoelastic strip N85-34193
Time and temperature dependence of fracture surface in soft epoxy resin N85-34213
Preliminary SPR thermal model description and results for WH-11 and BM-4
[DE85-013171] N85-34360
Compressible two-phase flow instabilities simulated with a hybrid Lagrange-Euler pseudospectral method
[DE85-009904] N85-34361
Thermal transport measurements of UV laser irradiated spherical targets
[DE85-011038] N85-34365
New semi-implicit method for solving the time-dependent conservation equations for incompressible flow
[DE85-010926] N85-34367
Guiding center distribution function and longitudinal invariant N85-34663
The dependence of solar modulation on the sign of the cosmic ray particle charge
[SH-4.2-23] N85-34860
Time-dependent nonlinear cosmic ray shocks confirming abstract
[OG-8.1-3] N85-34893
Selfsimilar time dependent shock structures
[OG-8.1-4] N85-34894
A new approach to evaluate gamma-ray measurements
[OG-9.5-11] N85-34988

Diagnostic of electromagnetic conditions in space using cosmic rays
[SH-4.5-19] N85-35036
Time and energy dependence of the cosmic ray gradient in the outer heliosphere
[SH-4.7-2] N85-35047

TIME MEASUREMENT
Mini and super mini arrays for the study of highest energy cosmic rays
[OG-9.4-9] N85-34976
Shower disc sampling and the angular resolution of gamma-ray shower detectors
[OG-9.5-2] N85-34980
The use of the McIlwain L-parameter to estimate cosmic ray vertical cutoff rigidities for different epochs of the geomagnetic field
[SH-6.1-12] N85-35085

TIME OF FLIGHT SPECTROMETERS
An improved time of flight gamma-ray telescope to monitor diffuse gamma-ray in the energy range 5 MeV - 50 MeV
[OG-9.3-2] N85-34957

TIME SERIES ANALYSIS
The conjecture concerning time variations in the solar neutrino flux
[SH-8.1-6] N85-35111
Methods and software for cosmic ray scintillation studies
[SH-9.1-17] N85-35132

TIN
Development of metallization process: FSA project, cells and module formation research area
[NASA-CR-176136] N85-34447

TIP SPEED
Energy efficient engine. Fan and quarter-stage component performance report
[NASA-CR-168070] N85-34141

TIROS SATELLITES
Satellites and politics: Weather, communications, and earth resources N85-35144

TITANIUM
The development of titanium production in the USSR
[BLL-OA-TRANS-3226-(6196.3)] N85-34244
Calculating the interatomic pair potential allowing for resonance interaction in titanium, nickel and vanadium
[BLL-M-35843-(5828.4)] N85-34249
The properties of VSt3sp inoculated steel
[BLL-M-35894-(5828.4)] N85-34263
An X-ray diffraction study of titanium oxidation
[NASA-CR-176263] N85-34264

TITANIUM ALLOYS
Electrical resistivity and hysteresis of the equiatomic nickel-titanium alloy near the martensitic transformation temperature N85-34181
Influence of particle erosion on the microstructural changes in metals and alloys
[TI85-901384] N85-34276
Laser welding of 6Al-4V titanium alloy
[DE85-012019] N85-34413
The stress pattern analysis of coarse grain titanium specimens
[PNR-90250] N85-34433

TITANIUM COMPOUNDS
The development of titanium production in the USSR
[BLL-OA-TRANS-3226-(6196.3)] N85-34244
Development of metallization process: FSA project, cells and module formation research area
[NASA-CR-176136] N85-34447

TITRATION
Increase of total CO2 in the World ocean
[DE85-007756] N85-34484

TOKAMAK DEVICES
Possibility of potential generation by lower hybrid wave N85-34654
Observation of mode-converted by ion Bernstein wave by an HCN laser scattering
[IPPJ-724] N85-34668
Compact DT fusion spherical tori at modest field
[DE85-011568] N85-34692
Experimental measurements of the ion cyclotron antennas' coupling and RF characteristics
[DE85-011569] N85-34694
Shield design for next-generation, low-neutron-fluence, superconducting tokamaks
[DE85-011409] N85-34695
Observation of helical sawtooth oscillations in a tokamak
[DE85-012062] N85-34703
ECH tokamak
[DE85-012074] N85-34707

TOLERANCES (PHYSIOLOGY)
Tolerance to +Gz and +Gx accelerations of individuals in older age groups in good health and with early signs of arteriosclerosis N85-34496

TOPOLOGY
Graph-theoretical exorcism
[DE85-011916] N85-34512
Cosmic ray secondary nuclei and the structure of the galaxy
[OG-7.2-4] N85-34876
Alfven wave scattering and the secondary to primary ratio
[OG-7.2-9] N85-34878

TOROIDAL PLASMAS
Compact DT fusion spherical tori at modest field
[DE85-011568] N85-34692
Advanced Toroidal Facility (ATF)
[DE85-011567] N85-34699
Observation of helical sawtooth oscillations in a tokamak
[DE85-012062] N85-34703

TORQUE MOTORS
Brush and commutator segment torquer motor
[AD-D011726] N85-34340

TORUSES
Effect of ECH and ICH on ambipolar potential in NBT-1M N85-34661
Transports studies of ECH and ICRH-heated bumpy torus plasma in NBT-1M N85-34662
Simulation studies on stability of hot electron plasma N85-34664
Behavior of helically-trapped fast ion orbits in heliotron E N85-34666
Observation of mode-converted by ion Bernstein wave by an HCN laser scattering
[IPPJ-724] N85-34668

TOUCH
Issues and techniques in touch-sensitive tablet input (executive summary) N85-34543
A multi-touch three dimensional touch-sensitive tablet (executive summary) N85-34553

TOXICITY
Anaerobic microbial transformations in subsurface environments: Project description
[DE85-012789] N85-34486
Estimating risks of lead-induced hemoglobin decrements under conditions of uncertainty: Methodology, pilot judgments and illustrative calculations
[DE85-012293] N85-34493

TRACE ELEMENTS
Ultra-trace analysis of sinter tantalum with SIMS
[BLL-RARDE-TR-1220-(7291.7965)] N85-34245
Evaluation of low-temperature geothermal potential in Utah and Goshen Valleys and adjacent areas, Utah. Part 2: Water temperature and chemistry
[DE85-009344] N85-34438

TRAILING EDGES
A design procedure to modify the trailing edge upper surface pressure gradient of a given aerofoil
[GU-AERO-8408] N85-34120
Reflection plane tests of a wind turbine blade tip section with ailerons
[NASA-TM-87018] N85-34444

TRANSCENDENTAL FUNCTIONS
Calculation of roots of transcendental equations in problems of determining thermal conductivity of cylinder with non-uniform boundary conditions
[BLL-M-35788-(5828.4)] N85-34349

TRANSDUCERS
Fast shutter apparatus
[DE85-006501] N85-34343
Acoustic cross-correlation flowmeter for solid-gas flow
[DE85-005988] N85-34391
A multi-touch three dimensional touch-sensitive tablet (executive summary) N85-34553

TRANSFER FUNCTIONS
Method and apparatus for transfer function simulator for testing complex systems
[NASA-CASE-NPO-15696-1] N85-34333
A multi-touch three dimensional touch-sensitive tablet (executive summary) N85-34553

TRANSIENT HEATING
Instrumentation for sensing moisture content of material using a transient thermal pulse
[NASA-CASE-NPO-15493-2] N85-34373

TRANSIENT OSCILLATIONS
Analysis of transient radiation upset in a 16K SRAM
[DE85-009442] N85-34586

TRANSIENT RESPONSE
The transient electromagnetic depth sounding technique applied to hydrocarbons and geothermal exploration
[MITT-42] N85-34476

TRANSITION FLOW
Nozzle wall roughness effects on free-stream noise and transition in the pilot low-disturbance tunnel
[NASA-TM-86389] N85-34355

TRANSITION METALS
The influence of temperature on the composition density of the transition metals
[BLL-M-35896-(5826.4)] N85-34262

TRANSMISSION
Conjugated symmetrical coupler curves, produced by 4-bar linkages having the same transmission angles N85-34322
Hologram-like transmission of pictures N85-34552

TRANSMISSIONS (MACHINE ELEMENTS)
The design and analysis of single flank transmission error testor for loaded gears
[NASA-CR-176163] N85-34404

TRANSONIC FLOW
Integral equation formulation for three-dimensional unsteady transonic flow
[ARL-STRUC-R-416] N85-34119
A review of spectral methods
[NASA-CR-172502] N85-34350
Unsteady transonic heat transfer in a transient facility
[NASA-CR-176145] N85-34354
System maintenance manual for master modeling of aerodynamic surfaces by three-dimensional explicit representation
[NASA-CR-178224] N85-34517

TRANSPONDERS
Performance interface document for the S-band diplexer for space users of NASA networks
[NASA-TM-86224] N85-34155

TRANSPORT AIRCRAFT
Guidelines for the evaluation of visual approach slope indicators
[ARL-SYS-R-32] N85-34132
Ground-based and in-flight simulator studies of flight characteristics of a twin-fuselage passenger transport airplane during approach and landing
[NASA-TP-2451] N85-34144

TRANSPORT PROPERTIES
Proceedings of the US-Japan Workshop on Transport in Open-Ended Systems
[IPPJ-727] N85-34644
Potential effect in transport due to non-axisymmetric confining field N85-34645
Radial transport phenomena for TMX-upgrade N85-34647
Induced azimuthal electric field effects on tandem transport and ambipolarity N85-34650
Radial transport caused by collision N85-34652
Bounce resonance heating and radial transport of electrons N85-34655
Electron dynamics and transport in a mirror field N85-34656
Azimuthal uniformity and current balance study of ICRH-produced plasma in RFC-XXM N85-34659
Effect of ECH and ICH on ambipolar potential in NBT-1M N85-34661
Transports studies of ECH and ICRH-heated bumpy torus plasma in NBT-1M N85-34662
Workshop report on Simulation Techniques for Shock Wave Phenomena and Characteristics of Plasmas in Inertial Confinement Fusion
[IPPJ-725] N85-34670
Helios 1 energetic particle observations of the solar gamma ray flare events of 7, 21 June 1980 and 3 June 1982
[SH-1.3-8] N85-34755
Source energy spectra from demodulation of solar particle data by interplanetary and coronal transport
[SH-1.3-13] N85-34758
Constraints of solar flare particle transport models from anisotropy observations at Voyager 1
[SH-3.1-8] N85-34812
Radial transport of approximately 1 MeV/nucleon ions during the 22 November 1977 solar particle event
[SH-3.2-5] N85-34821
Cosmic-ray transport in the galactic magnetosphere
[OG-7.2-17] N85-34884

TRANSPORT THEORY
Theoretical and computational research on the focused transport of intense charged particle beams
[DE85-012980] N85-34621
Why do leaky-box models work so fine?
[OG-7.2-8] N85-34877
Exact solutions for sporadic acceleration of cosmic rays
[OG-8.3-7] N85-34925
Relativistic transport theory for cosmic-rays
[OG-8.3-8] N85-34926

TRANSPORTATION
Shuttle car loading system
[NASA-CASE-NPO-15949-1] N85-34722

TRANSPORTATION NETWORKS
Design and implementation of an interactive route editor N85-34559

TRAPPED PARTICLES
CYLTRAN calculations of electron effects on XD detectors
[LA-10264-MS] N85-34601

TREES (MATHEMATICS)
A theoretical and empirical analysis of coherent ray-tracing N85-34524
A new approach to linear quadtrees N85-34550
TREES (PLANTS)
Effects of acid rain on forest nutrient status [DE85-012486] N85-34463
TRIBOLOGY
Aluminum work function: Effect of oxidation, mechanical scraping and ion bombardment [NASA-TM-87079] N85-34265
TRIGGER CIRCUITS
Fast shutter apparatus [DE85-006501] N85-34343
TRITIUM
Compact DT fusion spherical tori at modest field [DE85-011568] N85-34692
TROPICAL REGIONS
Observation of energy spectrum of electron albedo in low latitude region at Hyderabad, India [SH-6.1-7] N85-35081
Proton albedo spectrum observation in low latitude region at Hyderabad, India [SH-6.1-8] N85-35082
TRUSSES
Box truss analysis and technology development. Task 1: Mesh analysis and control [NASA-CR-172570] N85-34156
TUNGSTEN
Properties of tungsten-free steel for cutting tools [BLL-M-35808-(5828.4)] N85-34259
Detonation in tungsten-loaded HMX [DE85-009606] N85-34299
TUNISIA
Tunisian climate seen through a Markov process [CT-585] N85-34482
TURBIDITY
Determination of low chloride values in Rocky Flats scrub alloy solutions and other complex matrices [DE85-011506] N85-34234
TURBINE BLADES
Design, development and operation of a high simultaneous capacity digital telemetry system — turbomachine blade flutter [PNR-90261] N85-34151
TURBOFANS
Energy efficient engine. Fan and quarter-stage component performance report [NASA-CR-168070] N85-34141
TURBOMACHINE BLADES
Directionally solidified gas turbine alloys [PNR-90264] N85-34279
TURBOMACHINERY
A geometric modeller for turbomachinery applications N85-34556
TURBULENCE
Interstellar turbulence, random density variations, and scintillation measurements [OG-7.2-13] N85-34880
On the cosmic ray diffusion in a violent interstellar medium [OG-7.2-14] N85-34881
The role of cosmic rays in magnetic hydrodynamics of interstellar medium [OG-7.2-15] N85-34882
TURBULENCE EFFECTS
Compressible two-phase flow instabilities simulated with a hybrid Lagrange-Euler pseudospectral method [DE85-009904] N85-34361
TURBULENT BOUNDARY LAYER
Experimental aerodynamic heating to simulated space shuttle tiles in laminar and turbulent boundary layers with variable flow angles at a nominal Mach number of 7 [NASA-TP-2307] N85-34351
A three-dimensional turbulent boundary layer undergoing transverse strain and streamwise pressure gradient [NASA-TM-86768] N85-34358
TURBULENT FLOW
Experimental aerodynamic heating to simulated space shuttle tiles in laminar and turbulent boundary layers with variable flow angles at a nominal Mach number of 7 [NASA-TP-2307] N85-34351
A study of the second and third order closure models of turbulence for prediction of separated shear flows [NASA-CR-176127] N85-34353
TWO PHASE FLOW
Compressible two-phase flow instabilities simulated with a hybrid Lagrange-Euler pseudospectral method [DE85-009904] N85-34361
Stability of two-dimensional immiscible flow to viscous fingering [DE85-011403] N85-34364
TYPE 3 BURSTS
Type 3 solar radio bursts and 3HE-rich events [SH-2.2-3] N85-34798
TYPE 4 BURSTS
The flare origin of Forbush decreases not associated with solar flares on the visible hemisphere of the Sun [SH-5.1-4] N85-35058

U

U.S.S.R.
The development of titanium production in the USSR [BLL-OA-TRANS-3226-(6196.3)] N85-34244
Space activities in the Soviet Union, Japan, and the People's Republic of China N85-35149
ULTRASONIC TESTS
The use of ultrasound to monitor incipient failure of rolling element bearings N85-34317
Calculations on the feasibility of ultrasonic inspection of steam generator tubing in pressurized water reactors [AERE-R-10960] N85-34419
ULTRASONIC WAVE TRANSDUCERS
The use of ultrasound to monitor incipient failure of rolling element bearings N85-34317
ULTRASONICS
Analytical ultrasonics for structural materials [TI85-006132] N85-34600
ULTRAVIOLET LASERS
Thermal transport measurements of UV laser irradiated spherical targets [DE85-011038] N85-34365
ULTRAVIOLET RADIATION
Solar Ultraviolet Spectral Irradiance Monitor (SUSIM) N85-34160
Process for functionalizing alkanes [DE85-006420] N85-34219
Using the information of cosmic rays to predict influence epidemic [SH-10.1-2] N85-35134
ULTRAVIOLET SPECTROMETERS
Solar Ultraviolet Spectral Irradiance Monitor (SUSIM) N85-34160
High Resolution Telescope and Spectrograph (HRTS) N85-34162
UNDERGROUND ACOUSTICS
Sidereal variations deep underground in Tasmania [SH-4.4-4] N85-35002
The effect of the interplanetary magnetic field on sidereal variations observed at medium depth underground detectors [SH-4.4-5] N85-35003
Corrected sidereal anisotropy for underground muons [SH-4.4-7] N85-35005
Cosmic ray intensity variations observed at Matsushiro (220 M.W.E. in depth) [SH-4.4-9] N85-35007
UNDERGROUND STORAGE
Preliminary SPR thermal model description and results for WH-11 and BM-4 [DE85-013171] N85-34360
UNDERGROUND STRUCTURES
Method for determining depth and shape of a sub-surface conductive object [DE85-006502] N85-34389
New Matsushiro underground cosmic ray station (220 M.W.E. in depth) [SH-9.1-14] N85-35129
UNSTEADY FLOW
Scalar/Vector potential formulation for compressible viscous unsteady flows [NASA-CR-3921] N85-34113
Integral equation formulation for three-dimensional unsteady transonic flow [ARL-STRUC-R-416] N85-34119
Modelling of unsteady, incompressible separation on an aerofoil using an inviscid flow algorithm [GU-AERO-8412] N85-34122
Unsteady transonic heat transfer in a transient facility [NASA-CR-176145] N85-34354
UPGRADING
The properties of VSt3sp inoculated steel [BLL-M-35894-(5828.4)] N85-34263
UPPER ATMOSPHERE
Wide Angle Michelson Doppler Imaging Interferometer (WAMDII) N85-34172
Additional flux of particles and albedo-electrons in upper atmosphere [SH-6.1-6] N85-35080
URANIUM
Shape memory effect in uranium-niobium alloys below room temperature [DE85-012964] N85-34268
Method for preparing hydride configurations and reactive metal surface [DE85-006443] N85-34274
Uranium, thorium isotopic analyses and uranium-series ages of calcite and opal and stable isotopic compositions of calcite from drill cores UE25a no. 1, USR G-2 and USW G-3/GU-3, Yucca Mountain, Nevada [DE85-013039] N85-34471
Separation of uranium from technetium in recovery of spent nuclear fuel [DE85-006499] N85-34627
Lead and uranium group abundances in cosmic rays [OG-7.1-3] N85-34865
URANIUM ALLOYS
Experimental attempt to achieve microstructure variations through temperature/time permutations for a nonwrought powder metallurgy uranium-6 niobium alloy [DE85-013166] N85-34272
URANIUM 235
Application of evaluated fission-product delayed-neutron precursor data in reactor kinetics calculations [DE85-012728] N85-34624
USER MANUALS (COMPUTER PROGRAMS)
User's operating procedures. Volume 1: Scout project information programs [NASA-CR-177948] N85-34518
User's operating procedures. Volume 1: Scout project financial analysis program [NASA-CR-177949] N85-34519
User's guide to the MATHEW/ADPIC models [DE85-012952] N85-34587
User's manual for the FLORA equilibrium and stability code [DE85-013182] N85-34590
USER REQUIREMENTS
Product definition: Technical specification of needs [SNIAS-851-430-104] N85-34228
Graphics interaction in databases N85-34534
A model for graphics interface tool development N85-34545
Using percent-done program indicators to enhance user interfaces N85-34546
Architecture of languages for large CAD systems development N85-34557
How map designers can represent their ideas in thematic maps: Effective user interfaces for thematic map design N85-34562
UTILIZATION
Applications of $CdTe$ to nuclear medicine [DE85-011877] N85-34492

V

VACUUM CHAMBERS
Dual-chamber plasma deposition of A-Si:H solar cells at high rates using disilane [DE85-011828] N85-34451
Monitoring dosage of volatile compounds in tests at low barometric pressure N85-34506
Size effects of vacuum chamber for H- (D-) ion volume production by sheet plasma 1 [IPPJ-731] N85-34639
VACUUM DEPOSITION
Polarisation insensitive achromatic cube beamsplitter — binocular microscopes [NPL-MOM-72] N85-34630
VALVES
Reactant pressure differential control for fuel cell gases [NASA-CASE-MSC-20127-2] N85-34403
VANADIUM
Method for preparing high purity vanadium [DE85-006412] N85-34242
Calculating the interatomic pair potential allowing for resonance interaction in titanium, nickel and vanadium [BLL-M-35843-(5828.4)] N85-34249
Flux-line lattice anisotropy in V3Si: Observation and interpretation [DE85-011935] N85-34713
VAPOR PHASES
Vapor phase heat transport concepts [DE85-009550] N85-34366
VAPORIZERS
Forced convective, nonequilibrium, post-CHF heat transfer experiment data and correlation comparison report [TI85-009331] N85-34371
VAPORIZING
Effects of ambient pressure on the instability of a liquid boiling explosively at the superheat limit [DE85-009475] N85-34370
Monitoring dosage of volatile compounds in tests at low barometric pressure N85-34506
VARIABILITY
Effect of precipitation variables on the specific surface and explosion characteristics of pentaerythritol tetranitrate [DE85-009620] N85-34302

VARIATIONS
The final COS-B database: In-flight calibration of instrumental parameters
[OG-9.3-9] N85-34964
The effect of the interplanetary magnetic field on sidereal variations observed at medium depth underground detectors
[SH-4.4-5] N85-35003
Corrected sidereal anisotropy for underground moons
[SH-4.4-7] N85-35005
Sidereal anisotropy of cosmic rays
[SH-4.4-8] N85-35006
A study of periodicities and recurrences in solar activity and cosmic ray modulation
[SH-4.4-14] N85-35010
Altitude variations of cosmic-ray soft and hard components observed by airborne detectors
[SH-6.1-5] N85-35079

VAX-11 SERIES COMPUTERS
Parallel processing on the Livermore VAX 11/780-4 parallel processor system with compatability to Cray Research, Inc. (CRI) multitasking, version 1
[DE85-011856] N85-34595

VECTOR ANALYSIS
Vector calculation of particle code N85-34688

VELOCITY
Detonation in tungsten-loaded HMX
[DE85-009606] N85-34299
Comparison of experimental data on detonation velocity and Chapman-Jouget pressure vs initial HE density with predictions from Ree's model equation of state
[DE85-007266] N85-34304
Design and lubrication of high-speed rolling-element bearings
[NASA-TM-87107] N85-34409

VELOCITY DISTRIBUTION
A comparison of laser Doppler anemometry and probe measurements within the boundary layer of an airfoil at subsonic flow
[ISL-CO-219/84] N85-34127
Real time analysis of PETN detonation products
[DE85-009581] N85-34303
Collisional relaxation of electron tail distribution
[IPPJ-729] N85-34635
Electron loss process and cross section of multiply charged ions by neutral atoms N85-34685
High resolution Cherenkov detectors for cosmic ray isotope experiment
[OG-9.1-4] N85-34930

VELOCITY MEASUREMENT
Nonsimultaneous coupled laser velocimeter measurement technique: Error prediction for spatially noncoincident measurements
[NASA-TM-86718] N85-34379

VERTICAL DISTRIBUTION
Estimating the change in asymptotic direction due to secular changes in the geomagnetic field
[SH-6.1-13] N85-35086

VERTICAL PERCEPTION
Dissociation of autonomic and sensory vestibular reactions N85-34501

VESTIBULAR TESTS
Dissociation of autonomic and sensory vestibular reactions N85-34501

VESTIBULES
Dissociation of autonomic and sensory vestibular reactions N85-34501

VIBRATION
Generated spiral bevel gears: Optimal machine-tool settings and tooth contact analysis
[NASA-TM-87075] N85-34405
Nonlinear flap-lag-extensional vibrations of rotating, pretwisted, preconed beams including Coriolis effects
[NASA-TM-87102] N85-34427

VIBRATIONAL SPECTRA
Time-resolved spectroscopic studies of detonating heterogeneous explosives
[DE85-009760] N85-34297

VIDEO DISKS
Balloon-borne video cassette recorders for digital data storage
[OG-9.3-11] N85-34966

VIDEO EQUIPMENT
Atmospheric Emission Photometric Imaging (AEPI) N85-34170

VINYL POLYMERS
Development and demonstration of a spiral-wound thin-film composite membrane system for the economical production of oxygen-enriched air, phase 4
[DE85-012380] N85-34288
High temperature polymer concrete
[DE85-005756] N85-34290

VIRUSES
Using the information of cosmic rays to predict influence epidemic
[SH-10.1-2] N85-35134

VISCOELASTICITY
Experimental study on time and temperature dependent behavior of crack growth in viscoelastic strip N85-34193
Viscoelastic behavior of short-fiber composite materials
[DE85-011233] N85-34225

VISCOPLASTICITY
Short-time creep of ice
[NRC/CNR-TT-2111] N85-34428

VISCOSITY
Method for controlling the viscosity of siloxane oils
[DE85-011586] N85-34221
Measurement and correlation of jet fuel viscosities at low temperatures
[NASA-CR-174911] N85-34295

VISCOUS FLOW
Scalar/Vector potential formulation for compressible viscous unsteady flows
[NASA-CR-3921] N85-34113
A three-dimensional viscous flow analysis for the helicopter tip vortex generation problem
[NASA-CR-3906] N85-34114
Stability of two-dimensional immiscible flow to viscous fingering
[DE85-011403] N85-34364
Elastohydrodynamic lubrication calculations used as a tool to study scuffing
[NASA-TM-87097] N85-34408

VISION
Heuristic rules for visualization N85-34584

VISUAL CONTROL
Guidelines for the evaluation of visual approach slope indicators
[ARL-SYS-R-32] N85-34132

VISUAL PERCEPTION
Image synthesis: Optical identity or pictorial communication? N85-34565
Heuristic rules for visualization N85-34584

VISUAL PHOTOMETRY
A manual of methods for the continuous flow determination of ammonia, nitrate-nitrite, phosphate and silicate in seawater
[IOS-177] N85-34243

VLASOV EQUATIONS
Guiding center distribution function and longitudinal invariant N85-34663
Numerical solutions of the Vlasov equation N85-34672

VOLATILITY
Monitoring dosage of volatile compounds in tests at low barometric pressure N85-34506

VOLCANOLOGY
Workshop on Recent Research in the Valles Caldera
[DE85-010569] N85-34472

VOLTAGE CONTROLLED OSCILLATORS
Wide-band phase locked loop amplifier apparatus
[AD-D011720] N85-34337

VORTICES
A three-dimensional viscous flow analysis for the helicopter tip vortex generation problem
[NASA-CR-3906] N85-34114
Comments on the prediction of dynamic stall
[GU-AERO-8501] N85-34125

VOYAGER 1 SPACECRAFT
The energy spectrum of Jovian electrons in interplanetary space
[SH-1.5-18] N85-34781

VOYAGER 2 SPACECRAFT
Acceleration of ions and electrons to near-cosmic ray energies in a perpendicular shock: The January 6, 1978 event
[SH-1.5-4] N85-34773
The energy spectrum of Jovian electrons in interplanetary space
[SH-1.5-18] N85-34781

W

WARNING SYSTEMS
Solar system fault detection
[DE85-005987] N85-34458

WASTE DISPOSAL
Review of zirconium-zircaloy pyrophoricity
[DE85-011169] N85-34270
Method for making a low density polyethylene waste form for safe disposal of low level radioactive material
[DE85-006401] N85-34292
Research at the Institute of Oceanographic Sciences related to the possible disposal of radioactive waste on or beneath the seafloor
[IOS-204] N85-34628

WASTE TREATMENT
Method for extracting lanthanides and actinides from acid solutions by modification of Purex solvent
[DE85-005763] N85-34220

WATER
Nonsaturable microdryer
[DE85-005760] N85-34457
Multi-solute subsurface transfer modeling for energy solid wastes: Highlights FY 1984
[DE85-012788] N85-34591

WATER COOLED REACTORS
Technical assessment of thermal-hydraulics for high heat flux fusion components
[DE85-013178] N85-34359

WATER HEATING
Advanced heat pump research and development
[DE85-009540] N85-34372

WATER TEMPERATURE
Evaluation of low-temperature geothermal potential in Utah and Goshen Valleys and adjacent areas, Utah. Part 2: Water temperature and chemistry
[DE85-009344] N85-34438

WATER VAPOR
Potential spin-offs of the carbon dioxide observational platform system (CO-OPS) for remote sensing opportunities
[NASA-TP-2510] N85-34149

WATERSHEDS
Hydrology
[PB85-182954] N85-34440

WAVE DISPERSION
Observation of mode-converted by ion Bernstein wave by an HCN laser scattering
[IPPJ-724] N85-34668

WAVE FRONTS
The longitudinal thickness of air-shower fronts
[OG-9.5-1] N85-34978

WAVE PROPAGATION
Behaviors of stress waves in a conical bar N85-34182
Computational study on excitation, propagation and 3 omega -heating due to the ion Bernstein wave
[IPPJ-733] N85-34641
Cosmic ray modulatin and merged interaction regions
[SH-4.1-11] N85-34834
Propagation of the phase of solar modulation
[SH-4.1-12] N85-34835
Cosmic ray modulation in a random anisotropic magnetic field
[SH-4.1-20] N85-34839
Diffusion of strongly magnetized cosmic ray particles in a turbulent medium
[OG-7.2-16] N85-34883
Measurements of the fragmentation of (40)Ar, (28)Si and (12)C in CH2C and H targets between 300 and 1500 MeV/nuc at the Bevalac
[OG-7.2-19] N85-34886
Interactions of heavy nuclei, Kr, Xe and Ho, in light targets
[OG-7.2-21] N85-34888

WAVE SCATTERING
Method and apparatus for Delta Kappa synthetic aperture radar measurement of ocean current
[NASA-CASE-NPO-15704-1] N85-34327

WEAR
Three body abrasive wear in various metal combinations N85-34200

WEAR INHIBITORS
Anti wear property of two phasic metal composite N85-34199

WEATHER
Satellites and politics: Weather, communications, and earth resources N85-35144

WEATHER STATIONS
Reports from the German Meteorological Service. No. 166: The optimal spectral density of climatological station networks
[ISBN-3-88148-214-8] N85-34478

WEBS (SHEETS)
Instrumentation for sensing moisture content of material using a transient thermal pulse
[NASA-CASE-NPO-15493-2] N85-34373
Flat-plate solar array project process development area process research of non-CZ silicon material
[NASA-CR-176117] N85-34445

WEDGE FLOW
Tabular and graphical solutions of regular and Mach reflections in pseudo-stationary frozen and vibrational-equilibrium flows, part 1
[UTIAS-283-PT-1] N85-34117
Tabular and graphical solutions of regular and Mach reflections in pseudo-stationary frozen and vibrational-equilibrium flows, part 2
[UTIAS-283-PT-2] N85-34118

WEIBULL DENSITY FUNCTIONS
Reliability of two sintered silicon nitride materials
[NASA-TM-87092] N85-34284
WEIGHT (MASS)
On high strain rate fragmentation of a closed vessel N85-34187
WEIGHT REDUCTION
Aeroelastic constraints for a wing weight minimization procedure
[FFA-TN-1985-4] N85-34126
WEIGHTLESSNESS
Fluid-electrolyte metabolism and renal function in cosmonauts following 185-day spaceflight N85-34495
Effect of hypokinesia and +Gz accelerations on transport function of human blood N85-34497
Effect of water immersion of parameters of central hemodynamics in individuals over 45 years old N85-34499
Rat skeletal muscles with simulation of physiological effects of weightlessness (morphological study) N85-34502
Lipogenesis in rat liver after flight aboard Cosmos-1129 biosatellite N85-34508
Problems of aviation and space medicine and psychology discussed at 14th Gagarin lectures N85-34509
WELDED JOINTS
Gas shielding apparatus
[DE85-005992] N85-34416
WELLS
Method for determining depth and shape of a sub-surface conductive object
[DE85-006502] N85-34389
Depletion modeling of liquid dominated geothermal reservoirs
[DE85-009923] N85-34437
WEST GERMANY
Reports from the German Meteorological Service. No. 167: Results of aerological soundings in the model area upper Rhine: Heat release project upper Rhine area, part 3
[ISBN-3-88148-216-4] N85-34479
WHEATSTONE BRIDGES
Instrumentation for sensing moisture content of material using a transient thermal pulse
[NASA-CASE-NPO-15493-2] N85-34373
WIND (METEOROLOGY)
Evaluation of source strength and dispersion model predications with data from large nitrogen tetroxide field experiments
[DE85-011855] N85-34465
WIND PROFILES
User's guide to the MATHEW/ADPIC models
[DE85-012952] N85-34587
WIND TUNNEL TESTS
The collected data for ramp function tests on a NACA 23012 aerofoil. Volume 1: Description and pressure data
[GU-AERO-8413-VOL-1] N85-34123
An investigation into the three-dimensional stall development on a modified NACA 23012 aerofoil
[GU-AERO-8414] N85-34124
Prediction of the flow-field interference induced by the long-range laser velocimeter in the Ames 40- by 80-foot and the 80- by 120-foot wind tunnels
[NASA-TM-86763] N85-34146
Reflection plane tests of a wind turbine blade tip section with ailerons
[NASA-TM-87018] N85-34444
WIND TUNNELS
Practical aspects of laser holographic interferometry in wind tunnels
[NASA-TM-86788] N85-34378
Langley aeronautics and space test highlights, 1984
[NASA-TM-87585] N85-35151
WIND TURBINES
Reflection plane tests of a wind turbine blade tip section with ailerons
[NASA-TM-87018] N85-34444
WINDING
Apparatus producing constant cable tension for intermittent demand
[DE85-006434] N85-34412
WINDOWS (APERTURES)
Diamondlike carbon protective coatings for IR materials
[NASA-TM-87083] N85-34631
WINDPOWER UTILIZATION
Wind energy battery storage, phase 2
[DE85-009753] N85-34450
Solar energy education. Renewable energy: A background text
[DE85-010365] N85-34452
WINGS
Aeroelastic constraints for a wing weight minimization procedure
[FFA-TN-1985-4] N85-34126
WINTER
Snow cover in the Siberian forest-steppe
[NASA-TM-77914] N85-34435
WIRE
Towards the development of technological processes for the preparation of cadmium plated steel articles
[BLL-M-36315-(5828.4)] N85-34248
Apparatus producing constant cable tension for intermittent demand
[DE85-006434] N85-34412
WOLF-RAYET STARS
Neutron-rich nuclei in cosmic rays and Wolf-Rayet stars
[OG-8.2-6] N85-34906
Bursting star formation and the overabundance of Wolf-Rayet stars
[OG-8.2-8] N85-34907
WYOMING
Geothermal resources of the Laramie, Hanna and Shirley Basins, Wyoming
[DE85-005005] N85-34436

X

X RAY ANALYSIS
X-ray residual stress analysis on the coarse grain of copper and its application to the brazed copper N85-34202
Study on the correlation between grinding conditions and residual stresses in ground surface of steel by the X-ray method N85-34203
X-ray measurement of thermal stresses in tungsten fiber-copper composites N85-34205
X RAY APPARATUS
Flash X-ray diffraction
[ISL-CO-227/84] N85-34396
X RAY ASTRONOMY
Quasiperiodic oscillations in bright galactic-bulge X-ray sources
[NASA-CR-176138] N85-34723
Lapex: A Phoswich balloon experiment for hard X-ray astronomy
[OG-9.3-1] N85-34956
Research of advanced techniques for X-ray detectors and telescopes with applications to rockets and the LAMAR facility
[NASA-CR-176161] N85-35141
X RAY DIFFRACTION
An X-ray diffraction study of titanium oxidation
[NASA-CR-176263] N85-34264
Flash X-ray diffraction
[ISL-CO-227/84] N85-34396
X RAY IRRADIATION
Applications of holography to X-ray imaging
[DE85-010984] N85-34384
The read-out system of spatial distribution of thermoluminescence in meteorites
[SH-9.1-16] N85-35131
X RAY LASERS
Novette diagnostic support
[DE85-012937] N85-34383
Photoionization-pumped, Ne 2, X-ray laser studies project
[DE85-012973] N85-34399
Summary of activities, 1983
[LBL-18500] N85-34605
X RAY SOURCES
An extended superhot solar flare X-ray source
[SH-1.2-8] N85-34743
Capabilities of the GRO/BATSE for monitoring of discrete sources
[OG-9.2-16] N85-34955
Lapex: A Phoswich balloon experiment for hard X-ray astronomy
[OG-9.3-1] N85-34956
X RAY SPECTRA
Workshop report on Simulation Techniques for Shock Wave Phenomena and Characteristics of Plasmas in Inertial Confinement Fusion
[IPPJ-725] N85-34670
X-ray spectra of bursting neutron stars N85-34686
Multiple inner shell vacancies in laser-irradiated Au plasma N85-34687
Helios 1 energetic particle observations of the solar gamma ray flare events of 7, 21 June 1980 and 3 June 1982
[SH-1.3-8] N85-34755
Injection of energetic particles following the gamma-ray flares on June 7, 1980, as observed on Helios 1
[SH-1.3-9] N85-34756
X RAY SPECTROSCOPY
Thermal transport measurements of UV laser irradiated spherical targets
[DE85-011038] N85-34365
X RAY STRESS ANALYSIS
Multiaxial stress analysis taking account of penetration depth of X-rays. A solution by means of polynomial approximation N85-34204
X RAY TELESCOPES
Coordinated study of solar-terrestrial payloads on space station
[NASA-CR-176160] N85-34158
Soft X-Ray Telescope (SXRT) N85-34159
A comparison of calculated and measured background noise rates in hard X-ray telescopes at balloon altitude
[OG-9.3-7] N85-34962
X RAYS
Applications of holography to X-ray imaging
[DE85-010984] N85-34384
Quasiperiodic oscillations in bright galactic-bulge X-ray sources
[NASA-CR-176138] N85-34723
A position sensitive phoswich hard X-ray detector system
[OG-9.3-12] N85-34967
XENON
Interactions of heavy nuclei, Kr, Xe and Ho, in light targets
[OG-7.2-21] N85-34888
XENON ISOTOPES
Nuclear reactions in shock wave front during supernova events
[OG-8.2-19] N85-34915
XENON 129
When did the average cosmic ray flux increase?
[SH-7.1-4] N85-35097

Y

YIELD STRENGTH
Mechanical properties of plasma arc cut steel N85-34188
YTTRIUM
Calculation of activities of components in liquid alloys of iron with yttrium
[BLL-M-35868-(5828.4)] N85-34253

Z

ZEOLITES
Rigid zeolite containing polyurethane foams
[DE85-006406] N85-34286
Determination of properties of zeolite/refrigerant combinations for solar refrigeration systems
[DE85-012009] N85-34448
ZERO POINT ENERGY
Evaluation of parameters for particles acceleration by the zero-point field of quantum electrodynamics
[OG-8.2-16] N85-34912
ZIRCONIUM ALLOYS
Manufacturing process to reduce large grain growth in zirconium alloys
[DE85-011649] N85-34267
ZONAL HARMONICS
First zonal harmonic component of cosmic ray neutron intensity
[SH-4.3-13] N85-34997

PERSONAL AUTHOR INDEX

Typical Personal Author Index Listing

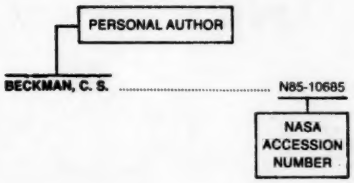

Listings in this index are arranged alphabetically by personal author. The NASA accession number denotes the number by which the citation is identified.

A

ABE, H. N85-34641
ABE, K. N85-34679
N85-34681
ABE, Y. N85-34642
ACHAR, B. N. N85-34281
ACHARYA, B. S. N85-34928
N85-34930
N85-34935
ADAMS, J. H., JR. N85-34936
ADAMS, L. N85-34522
ADAMS, L. R. N85-34442
AFANASYEV, K. G. N85-35088
AFANASYEV, V. G. N85-35088
AFONIN, B. V. N85-34495
AGNETTA, G. N85-34950
AGRAWAL, S. P. N85-34833
N85-34998
N85-35009
N85-35012
N85-35064
N85-35065
N85-35068
AGRINIER, B. N85-34944
N85-34945
N85-34946
N85-34950
N85-34957
AHEARN, M. F. N85-34725
AHLEN, S. P. N85-34929
AHLUWALIA, H. S. N85-35022
N85-35024
N85-35025
AITBAEV, F. B. N85-35080
AIZAWA, M. N85-34652
N85-34671
AKAHANE, S. N85-35129
AKIMENKO, V. B. N85-34257
AKIMOV, V. I. N85-34506
AKIMOV, V. V. N85-34949
AKMAN, V. N85-34572
AKST, I. B. N85-34296
ALANIA, M. V. N85-34852
N85-34855
N85-34857
N85-35072
ALBE, F. N85-34395
ALEKANYAN, T. M. N85-35076
ALEKSEEV, N. V. N85-34783
ALEXANDER-MORRISON, G. M. N85-34272
ALEXEEV, V. A. N85-35107
ALEXEYENKO, V. V. N85-35090
ALIMOV, V. I. N85-34263
ALLKOFER, O. C. N85-34972
ALPAR, M. A. N85-34723
ALTHOUSE, W. E. N85-34941
N85-34966
ALTON, G. D. N85-34619
ALVAREZ-MADRIGAL, M. N85-34758
ALVAREZ, M. N85-34735
N85-34736
N85-34737
N85-34738
N85-34739
AMANO, R. S. N85-34353
AN, S. N85-34909
ANDERSON, K. A. N85-34819
N85-34948
ANDO, R. N85-34668
ANDREYEVA, V. G. N85-34496
ANTONOVA, V. P. N85-35070
AOKI, T. N85-34970
APKHANOV, V. B. N85-34261
APPEL, R. N85-34531
APPLETON, B. B. N85-34714
APTE, A. R. N85-34985
ARCORAGI, J. P. N85-34906
ARKHIPOV, V. V. N85-34498
ARMITAGE, ... N85-34632
ARMSTRONG, T. P. N85-34774
N85-34779
ARMSTRONG, W. W. N85-34579
ARNOLD, J. O. N85-34510
ARNOLD, J. R. N85-35097
ARNOULD, M. N85-34906
ARTAMONOVA, N. P. N85-34496
ARTHEY, R. P. N85-34717
ARVELA, H. N85-35061
N85-35069
ARVELTA, H. N85-34826
ASATRYAN, G. A. N85-35026
ASKAY, I. A. N85-34289
ASLAMAZASHVILI, R. G. N85-34852
N85-34855
ASYAMOLOV, B. F. N85-34497
ATTOLINI, M. R. N85-35010
N85-35011
N85-35094
N85-35096
ATTWOOD, R. S. N85-34143
AUDOUZE, J. N85-35102
AUKER, B. H. N85-34450
AUYEUNG, J. N85-34629
AVCI, H. I. N85-34592
AVERY, D. E. N85-34351
AVILES, C. A. N85-34467
AXFORD, I. N85-35047

B

BABAYAN, V. K. N85-35026
N85-35054
BACHTELL, E. E. N85-34156
BADRUDDIN N85-34851
N85-35034
N85-35065
BAES, C. F., JR. N85-34483
BAGDASARIAN, M. B. N85-35054
BAITY, F. W. N85-34694
BAKER, R. G. N85-34951
N85-34965
BAKRADZE, T. S. N85-35072
BALAKIR, S. E. N85-34249
BALASUBRAHMANYAN, V. K. N85-34928
N85-34930
N85-34935
BALIBANOV, V. M. N85-34949
BALLARD, W. P. N85-34330
BALOGH, A. N85-34775
BALTZ, A. J. N85-34615
BAMBERGER, C. E. N85-34287
BANDLE, J. N85-34774
BANKS, B. A. N85-34631
BANNISTER, R. H. N85-34317
BARRY, R. G. N85-34480
BARSKY, B. A. N85-34524
N85-34537
N85-34551
N85-34570
N85-34571
BARTELS, H. N85-34479
BARTSCH-WINKLER, S. N85-34468
BARWICK, S. W. N85-34929
BASILEVAKAYA, G. A. N85-35115
BASIN, A. N85-34956
BASSETT, D. E. N85-34404
BATCHELOR, D. B. N85-34701
BATHURAT, A. A. N85-35086
BAYBUTT, P. N85-34592
BAYCHOROV, E. O. N85-34495
BAZILEVSKAYA, G. A. N85-35015
N85-35093
BEAHM, L. P. N85-34936
BEAUJEAN, R. N85-35137
N85-35138
BEAULIER, J. M. N85-34548
BECK, J. V. N85-34362
BECK, R. N85-34894
N85-34900
BECKER, J. W. N85-34340
BECKWITH, I. E. N85-34355
BECRAFT, W. R. N85-34694
BEDNENKO, V. S. N85-34503
BEECK, J. N85-34816
BEELEY, P. R. N85-34279
BEER, J. N85-34889
BEHANNON, K. W. N85-34847
BELEW, R. R. N85-34401
BELOV, A. V. N85-34760
N85-35075
N85-35091
BENNER, W. H. N85-34392
BENNETT, K. N85-34963
BEREZHKO, E. G. N85-34902
BEREZOVSKII, B. N. N85-34422
BERGERON, P. N85-34580
BERGGREN, R. G. N85-34418
BERGMAN, R. G. N85-34219
BERMAN, A. N85-34425
BERTSCH, D. L. N85-34951
BERZINS, G. J. N85-34601
BETTADAPUR, S. S. N85-34156
BEUHLER, R. J. N85-34710
BHATNAGAR, S. P. N85-35081
N85-35119
BHATT, R. T. N85-34223
BHUVA, B. L. N85-34588
BIEBER, J. W. N85-34817
N85-34844
N85-35038
BIEG, K. W. N85-34702
BIELAOUSSOV, A. S. N85-34949
BIGELOW, C. A. N85-34426
BIGELOW, T. S. N85-34701
BIGNAMI, G. F. N85-34963
BILLOIR, T. N85-34596
BINNS, W. R. N85-34866
N85-34888
N85-34933
N85-34938
N85-34939
BIRCH, K. G. N85-34515
BIRCHENOUGH, A. G. N85-34444
BIRX, D. L. N85-34700
BISWAS, S. N85-34787
N85-35045
N85-35117
BIZZOZERO, C. N85-34554
BLACKBURN, L. B. N85-34375
BLACKER, S. G. N85-34394
BLACKWELL, B. F. N85-34362
BLAIS, N. C. N85-34303
BLAKE, J. B. N85-34868
BLOEMEN, J. B. G. M. N85-34963
N85-34964
BLOKH, Y. L. N85-34760
BLUDMAN, S. A. N85-35116
BOBKOVA, O. S. N85-34252
BOBROVSKAYA, V. V. N85-34783
N85-35136
BOCHIKASHVILI, D. P. N85-35072
BOCHORISHVILI, T. B. N85-34855
BOCHORISHVILI, T. V. N85-35072
BODIGFEE, G. N85-34907
BODVARSSON, G. S. N85-34439
BOGATOV, A. A. N85-34248

BOGDAN, T. J. N85-34900
N85-34927
BOLDUC, F. N85-34566
BOLSTAD, J. O. N85-34393
BONFAND, E. N85-34945
N85-34946
BONINO, G. N85-35096
BOOTY, B. N85-34628
BOROWSKI, S. K. N85-34692
BORTNOVSKIY, V. N. N85-34504
BOSTICK, W. H. N85-34910
BOUCHARD, J. N85-34513
BOURNIQUE, R. N85-34527
BOYD, R. D. N85-34359
BRADLEY, K. N85-34151
BRADY, M. C. N85-34624
BRAILE, L. W. N85-34475
BRAMLETTE, T. T. N85-34240
BRANDT, D. N85-34416
BRASSEUR, G. N85-34466
BRAUN, M. J. N85-34356
BRAVO, S. N85-34796
BRECHTMANN, C. N85-34889
BRENEMAN, H. N85-34785
N85-34786
BRETTHORST, G. L. N85-34878
BREWSTER, N. R. N85-34863
BRICKHOUSE, N. S. N85-34703
BRIGGS, B. N85-34461
BRIGGS, P. R. N85-34779
BRISSENDEN, R. J. V. N85-34978
BROOKE, G. N85-34974
BROSHENKO, E. A. N85-34760
BROUGHTON, T. N85-34421
BROWN, B. A. N85-34615
BROWN, D. P. N85-34326
BRUNS N85-34224
BRYNESTAD, J. N85-34287
BUCCHERI, R. N85-34963
N85-34964
BUCKINGHAM, A. C. N85-34361
BUDDEMEIER, R. W. N85-34462
BUI-VAN, A. N85-34957
BUKOWSKI, R. W. N85-34325
BULANOV, V. Y. N85-34257
BURCH, J. N85-34171
BURGER, R. A. N85-34841
BURLAGA, L. F. N85-34820
N85-34834
N85-34847
BURLEY, K. C. N85-35120
BURNETT, L. J. N85-34288
BURNS, E. J. T. N85-34702
BUTLER, R. C. N85-34947
BUTTRAM, M. T. N85-34693
BUXTON, W. N85-34543
N85-34553
BYKOV, A. M. N85-34881
BYRNAK, B. N85-35084
BYRNE, B. N85-34513

C

CALLEN, J. D. N85-34653
CAMARERO, R. N85-34556
CAMPBELL, N. K. N85-34444
CANDREA, R. N85-34527
CANE, H. V. N85-34734
N85-34747
N85-34754
CANFIELD, R. C. N85-34752
CAPEN, C. N85-34728
CAPLAIN, M. N85-34549
CAPORUSCIO, F. A. N85-34271
CARAVEO, P. A. N85-34963
CAREY, A. A. N85-34221
CAREY, R. P. N85-34429
CARHART, R. A. N85-34369
CARLE, G. C. N85-34374
CARLSON, O. N. N85-34242
CAROLI, E. N85-34947
CARROLL, S. N. N85-34148
CARTER, J. N. N85-34944
N85-34945
N85-34946
N85-34947
CASSE, M. N85-34906
CASTAGNOLI, G. C. N85-35094
N85-35096
CATTO, P. J. N85-34845
N85-34850
CAUGHMAN, J. B. O. N85-34694
CAVALIERE, S. N85-34540
CAWLEY, J. D. N85-34402
CAWLEY, M. F. N85-34981
CECCHINI, S. N85-35010
N85-35011
N85-35094
CHA, Y. S. N85-34359
CHABAUD, J. P. N85-34950
CHADWICK, P. M. N85-34969
CHAI, A. T. N85-34357
CHAN, K. W. N85-35126
CHAN, S. T. N85-34367
CHAN, Y. K. N85-34578
CHANG, C. R. N85-34752
CHANG, E. N85-34582
CHANG, Y. K. N85-34713
CHARAKHCHYAN, T. N. N85-34856
N85-35013
N85-35014
N85-35017
N85-35093
N85-35115
CHARALAMBOUS, P. M. N85-34947
CHASSIGNET, P. N85-34532
CHAUSSEE, D. S. N85-34116
CHEBAKOVA, E. A. N85-34824
CHEN, C. T. A. N85-34484
CHEN, D. Y. N85-34335
CHEN, F. J. N85-34355
CHEN, J. C. N85-34371
CHEN, S. S. N85-34574
CHEN, T. M. N85-35095
CHEN, W. Y. N85-34291
CHERKASKIN, A. L. N85-34255
CHESNEY, J. R. N85-34951
CHHABILDAS, I. C. N85-34298
CHIBA, T. N85-34997
CHINO, K. N85-35129
CHIRKOV, N. P. N85-34858
CHISHOLM, M. H. N85-34269
CHOU, T. W. N85-34225
CHRISTEN, D. K. N85-34713
CHRISTON, S. P. N85-34781
N85-34836
N85-34847
N85-35049
CHRISTOPHER, M. N85-34552
CHUANG, L. S. N85-35031
N85-35124
N85-35126
CHUBB, D. L. N85-34441
CHUDAKOV, A. E. N85-35090
CHUMICHEV, B. D. N85-34428
CHUPP, E. L. N85-34762
N85-34767
N85-35121
CHURUNOVA, L. F. N85-34854
CINICASTAGNOLI, G. N85-35011
CIRIGLIANO, R. N85-34383
CLAMPA, D. N85-34971
CLAY, R. W. N85-34971
N85-34978
CLEROUX, R. N85-34528
CLINE, S. J. N85-34138
N85-34141
CLINE, T. L. N85-34942
N85-34943
N85-34953
N85-34954
CLIVER, E. W. N85-34734
N85-34754
COBURN, M. D. N85-34306
COHEN, B. I. N85-34590
COHEN, R. H. N85-34647
COLE, D. W. N85-34463
COLEMAN, P. D. N85-34698
COLLINS, E. N85-34487
COLLINS, E. R., JR. N85-34722
COLLINS, L. J. N85-34115
COLLINS, W. R. N85-34521
COLOMBO, P. N85-34292
CONDIE, K. G. N85-34371
CONN, R. W. N85-34707
CONNELL, J. J. N85-34933
CONVERTI, P. N85-34129
COOK, W. R. N85-34941
N85-34966
COOKE, D. J. N85-35084
COOPER, C. N. N85-34533
COOPER, J. F. N85-34762
N85-34767
N85-35121
COOPER, T. N85-34719
COOPER, T. D. N85-34270
COPLEY, D. W. N85-34433
CORANI, C. L. N85-34971
CORDERMAN, R. R. N85-34451
CORMIER, M. N85-34559
CORR, D. G. N85-34394
CORWIN, W. R. N85-34418
COSTA, E. N85-34950
N85-34956
COUGH, R. L. N85-34420
COWSIK, R. N85-34925
COY, J. J. N85-34405
COYNER, J. V. N85-34156
CRAIN, I. K. N85-34563
CRAMER, S. N. N85-34598
CRANDALL, D. H. N85-34622
CREEL, T. R., JR. N85-34355
CREMERS, D. A. N85-34387
CROMER, D. T. N85-34603
CRUMLEY, R. I. N85-34341
CUGINI, U. N85-34554
CUMMINGS, A. C. N85-34781
N85-34847
N85-34941
N85-35039
N85-35042
N55-35049
CURRAN, F. M. N85-34179
CURRIE, J. N85-34511
CURTIS, D. W. N85-35120
CURTIS, G. D. N85-34450
CURYANOV, C. N. N85-34248

D

DACOSTAFEREIRANERI, A. N85-34957
DAGENHART, W. K. N85-34604
DAI, C. N85-34960
DAI, K. M. N85-35095
DAIBOG, E. I. N85-34746
DALFIUME, D. N85-34956
DALTON, G. R. N85-34692
DAMERAU, W. N85-34294
DANILOVA, O. A. N85-35083
N85-35092
DATT, S. C. N85-35029
DAVIES, T. N85-34314
N85-34315
DAVIS, D. A. N85-34438
DAVIS, W. A. N85-34550
DAWSON, B. R. N85-34971
DEAL, P. L. N85-34144
DEAN, A. J. N85-34947
N85-34962
N85-34967
DEBRUNNER, H. N85-34811
N85-34822
DECKER, R. B. N85-34733
N85-34772
N85-35051
DEFEO, P. N85-34136
DEJAGER, O. C. N85-34988
DELLETREZ, J. N85-34365
DELMORE, J. E. N85-34241
DELOORE, C. N85-34907
DENEHY, B. V. N85-34766
DENNIS, B. R. N85-34740
DERDEYN, S. M. N85-34951
DEROSE, T. D. N85-34524
N85-34571
DERUDDER, A. N85-34466
DERYABIN, V. A. N85-34283
DESCHIZEAUX, P. N85-34541
DESLOIRE, M. N85-34157
DESPOTASHVILI, M. A. N85-35072
DEVANEY, H. F. N85-34388
DEXTER, R. N. N85-34703
DICOCCO, G. N85-34947
DIEHL-NAGLE, S. E. N85-34586
N85-34588
DIETRICH, W. F. N85-34801
DIJKSMAN, E. A. N85-34322
DIKUN, V. N. N85-34260
DILL, A. R. N85-34576
DIMITROV, D. G. N85-34496
DINEGAR, R. H. N85-34302
DIPPER, N. A. N85-34962
N85-34969
DIRAFFAELE, R. N85-34950
DJAPIASHVILI, T. V. N85-34855
N85-35016
DOBRIAN, L. B. N85-34949
DOGIEL, V. A. N85-34913
DOHI, S. N85-34181
DOMYSHEV, V. A. N85-34261
DORFI, E. A. N85-34893
N85-34895
N85-34899
N85-34901
DORMAN, I. V. N85-35055
N85-35125

DORMAN, L. I. N85-34839
N85-34852
N85-34857
N85-35071
N85-35074
N85-35075
N85-35076
N85-35091
N85-35132
DORMAN, L. T. N85-35125
DOROKHOVA, B. R. N85-34495
DOUGHERTY, M. K. N85-34885
DOUGHERTY, W. M. N85-34819
DOUGHTY, C. N85-34368
DOUGLAS, S. S. N85-34310
DOWNES, V. N85-34513
DOWNWARD, J. G. N85-34376
DOWTHWAITE, J. C. N85-34969
DRACH, J. N85-34870
DRAGOVITSCH, P. N85-35100
DRECHSEL, H. N85-34889
DREIKE, P. L. N85-34702
DRIVER, D. N85-34279
DRIVER, D. M. N85-34358
DROEGE, W. N85-34731
DRUCE, G. N85-34311
DRURY, L. O. N85-34894
N85-34895
N85-34899
N85-34900
N85-34901
DUBEN, L. V. N85-34260
DUBRUNNER, H. N85-34762
DUDNIC, A. V. N85-35139
DUDNIK, A. V. N85-35140
DULDIG, M. L. N85-34993
N85-35004
DUNLAP, B. D. N85-34712
DUNN, G. H. N85-34622
DUNN, W. E. N85-34369
DUPONT, J. F. N85-34331
DURAND, H. N85-34831
DURAND, Y. N85-34346
DURGAPRASAD, N. N85-34787
N85-35045
N85-35117
DUROUCHOUX, P. N85-34948
DUTTWEILER, F. N85-35120
DVORNIKOV, M. V. N85-34503
DVORNIKOV, V. M. N85-35036
N85-35092
DVORYANCHIKOV, Y. V. N85-34804
DWYER, H. A. N85-34240
DYUISEMBAEV, B. M. N85-35080
DZNELADZE, Z. I. N85-34260

E

EARL, J. A. N85-34828
N85-34829
N85-34830
EARLEY, L. M. N85-34330
EATON, R. N85-34555
EBISUZAKI, T. N85-34686
ECKART, M. J. N85-34399
ECKES, S. N85-34779
EDMONDS, P. H. N85-34697
EDWARDS, P. G. N85-34971
EFIMOV, Y. E. N85-34769
EGOROV, V. A. N85-34261
EHRMANN, C. H. N85-34951
EICHLER, D. N85-34896
ELBERT, J. W. N85-34982
ELLINGSWORTH, J. R. N85-34375
ELLISON, D. C. N85-34732
N85-34896
N85-34897
ELTON, S. D. N85-34971
N85-34978
EMORI, N. N85-34200
ENGE, W. N85-34937
N85-35137
N85-35138
ENGLAND, T. R. N85-34624
ENGLERT, P. N85-35100
N85-35101
ENTINE, G. N85-34492
ERDOES, G. N85-34775
ERDOS, G. N85-35023
ERICKSON, C. L. N85-34334
ERMAKOV, A. P. N85-34247
EROSHENKO, E. A. N85-35075
ERRADI, M. N85-34534
ESIN, Y. O. N85-34247
ESPOSITO, J. A. N85-34930
N85-34935
EVANS, A. E. N85-34608
EVDOKIMENKO, O. A. N85-34262
EVENSON, P. A. N85-34749
N85-34763
N85-34782
N85-34809
N85-34817
N85-34860
EZELL, E. C. N85-35149

F

FAGOT, H. N85-34395
FALK, R. A. N85-34622
FAN, C. Y. N85-34792
N85-34904
N85-35095
FAN, Z. N85-34960
FANTINI, M. N85-34540
FARAHAT, M. N85-34617
FARRINGTON, R. B. N85-34458
FAUQUIGNON, C. N85-34307
FEAGLER, E. R. N85-34377
FEDOROV, Y. I. N85-34839
FEGAN, D. J. N85-34981
FEIK, R. A. N85-34137
FEINER, S. N85-34539
FENTON, A. G. N85-34818
N85-35002
N85-35003
N85-35006
N85-35078
FENTON, K. B. N85-34818
N85-35002
N85-35008
N85-35078
FERRANDO, P. N85-34879
N85-34968
FERRETT, J. C. N85-34974
FESLER, W. N85-34138
FICHTEL, C. E. N85-34951
FIELDS, S. R. N85-34626
FILIMONOV, Y. P. N85-34252
FILIPPOV, A. T. N85-34827
FILLIUS, W. N85-34992
N85-35047
FINGER, M. H. N85-34940
N85-34941
FIRESTONE, M. A. N85-34707
FISCHER, E. N85-35138
FISCHER, T. A. N85-34609
FISENNE, I. M. N85-34610
FISHBANE, P. M. N85-34618
FISHKIN, K. P. N85-34551
FISHMAN, G. J. N85-34953
N85-34954
N85-34955
FISK, L. A. N85-34792
N85-35044
FIXSEN, D. J. N85-34938
N85-34939
FLAVELL, R. B. N85-34568
FLUECKIGER, E. O. N85-34762
N85-34811
N85-35086
FOHLEN, G. M. N85-34281
FOLGER, A. G. N85-34485
FOMIN, I. O. N85-34499
FONTANA, J. J. N85-34290
FOOTE, K. L. N85-34239
FOREST, C. A. N85-34300
FORMAN, M. A. N85-34835
FORREST, D. J. N85-34762
N85-34767
N85-34794
N85-34795
N85-35121
FORSYTH, J. M. N85-34399
FOSTER, J. N85-34728
FOURNIER, A. N85-34570
FRABEL, P. N85-34950
FRAIOLI, A. V. N85-34226
FRANCESCHINI, T. N85-34956
FRANCIS, A. J. N85-34486
FRANCO, E. N85-34383
FRANKLIN, W. R. N85-34572
FRANZ, O. G. N85-34725
FRASER-MITCHELL, J. N85-34967
FRASSON, C. N85-34534
FREELOVE, R. L. N85-34278
FREEMAN, H. N85-34561
FREIS, R. P. N85-34590
FRIEDMAN, H. A. N85-34627
FRIEDMAN, L. N85-34710
FRONTERA, F. N85-34956
FROST, C. B. N85-34286
FROST, D. N85-34370
FRYE, G. M., JR. N85-34766
N85-34944
N85-34945
N85-34946
N85-35127
FU, C. Y. N85-34620
FUH, J. S. N85-34425
FUJII, T. N85-34210
N85-34212
FUJII, Z. N85-35001
N85-35021
N85-35035
FUJIMOTO, K. N85-35066
FUJITA, J. N85-34668
FUJIWARA, H. N85-34205
FUJIWARA, Y. N85-34182
FUKANO, A. N85-34682
FUKUNAGA, H. N85-34208
FUKUSHIMA, E. N85-34345
FUNK, M. N85-34531
FURUTA, J. N85-34675

G

GABYSHEV, V. K. N85-34498
GAFFNEY, J. S. N85-34217
GALBRAITH, R. A. M. N85-34120
N85-34121
N85-34122
N85-34123
N85-34124
N85-34125
GALINDOTREJO, J. N85-34750
GALKIN, A. M. N85-34258
GALL, R. N85-34831
GALLEGOS, A. N85-34735
N85-34736
N85-34737
N85-34738
N85-34739
GALLI, M. N85-35010
N85-35011
N85-35094
N85-35096
GALVIN, A. B. N85-34792
N85-35041
GARCIA-MUNOX, M. N85-34838
GARCIA-MUNOZ, M. N85-34853
N85-34860
GARCIA, A., III N85-34447
GARDNER, C. S. N85-34397
GARRARD, T. L. N85-34866
N85-34888
N85-34938
N85-34939
GASIOROWICZ, S. G. N85-34618
GAT, N. N85-34385
GAVIN, F. N85-34369
GEAR, J. A. N85-34119
GEHRELS, N. N85-34942
N85-34943
GEIGER, L. J. N85-34136
GENTILE, L. C. N85-35085
N85-35086
GEORGE, T. G. N85-34606
GEORGIEV, L. N85-35033
GERARDI, G. N85-34950
GERBER, R. A. N85-34702
GERRASSIMENKO, M. N85-34399
GERTH, E. N85-35111
GIBBS, K. N85-34981
GIBSON, A. F. N85-34517
GILER, M. N85-34867
N85-34923
GILLARD, P. N85-34529
GILLEN, K. T. N85-34420
GINLEY, D. S. N85-34293
GINZBURG, V. L. N85-34882
GLADYSHEV, S. A. N85-34256
GLASGOW, T. K. N85-34266
GLEBOVA, O. D. N85-34261
GLICKSMAN, M. N85-34235
GLOECKLER, G. N85-34776
N85-34792
N85-34812
N85-34821
N85-35043
GLUKHOV, G. A. N85-35089
GODA, K. N85-34208
GOHAR, Y. N85-34695
GOLD, R. E. N85-34777
N85-34837
GOLDBERG, M. N85-34548

GOLDEN, R. L. N85-34932
GOLDFARB, E. M. N85-34347
N85-34349
GOLDSTEIN, M. L. N85-34834
GOLDSTEIN, S. N85-34299
GOLOVKINA, O. L. N85-34496
GONCHER, G. A. N85-34850
GONNORD, J. N85-34598
GOODARZI, A. N85-34334
GOODWIN, G. M. N85-34418
GOPALAKRISHNAN, N. V. N85-34985
GORBUNOV, A. D. N85-34347
N85-34349
GORCHAKOV, E. V. N85-35017
N85-35088
GORDEEV, I. V. N85-35136
GORENSTEIN, P. N85-35141
GORET, P. N85-34879
N85-34932
N85-34968
N85-35084
GORHAM, P. W. N85-34981
GORKER, G. E. N85-34692
GORLEEV, Y. P. N85-35136
GOSS, W. C. N85-34629
GOTTULA, R. C. N85-34371
GOUIFFES, C. N85-34945
N85-34950
N85-34957
GOULD, R. J. N85-34916
GOULETTE, M. J. N85-34717
GOVINDAN, T. R. N85-34114
GRABOVSKII, V. Y. N85-34258
GRADY, D. E. N85-34432
GRAHAM, J. A. S. N85-34142
GRANAL, J. N85-34294
GRANTHAM, W. D. N85-34144
GRASSERBAUER, M. N85-34245
GRASSO, A. P. N85-34403
GRAVES, K. N85-34461
GRAY, K. E. N85-34712
GREEN, G. N85-34823
GREEN, M. N85-34579
GREENBERG, J. M. N85-34581
GREENE, R. T. N85-34382
GREENLY, G. D. N85-34587
GREGORY, A. G. N85-34971
GREGORY, D. C. N85-34622
GRESHO, P. M. N85-34367
N85-34587
GREVESSE, N. N85-34864
GRIFFIN, H. N85-34589
GRIGOROV, N. L. N85-34783
N85-35136
GRIGORYEV, A. I. N85-34495
GRIMM-LUCZAK, E. N85-34478
GRIMM, G. N85-34938
N85-34939
GRONE, D. J. N85-34594
GRONSKY, R. N85-34623
GROVES, O. J. N85-34411
GRUNDEY, K. N85-34564
GRUSH, B. N85-34547
GU, Y. N85-34960
GUBENKO, S. I. N85-34258
GULINSKY, O. V. N85-35071
N85-35132
GULLICHSEN, E. N85-34582
GUPTA, I. J. N85-34329
GUPTA, M. N85-34874
GUREVICH, A. V. N85-34913
GURSKAYA, E. G. N85-34249
GUSHCHINA, R. T. N85-34857
N85-35091

H

HABER, I. N85-34621
HAESLOOP, D. G. N85-34288
HAGELSTEIN, P. L. N85-34399
HAINES, M. G. N85-34683
HAKAMADA, K. N85-34995
HALL, C. J. N85-34944
N85-34945
N85-34946
HALL, G. W. N85-34135
HALLION, R. P. N85-35146
HALTER, P. H. N85-34141
HAMADA, M. N85-34207
HAMET, J. F. N85-34599
HAMILTON, D. C. N85-34812
N85-34821
HAMILTON, W. R. N85-34692
HAMMAR, J. H. N85-34320
HAMPEL, W. N85-35108
HAMROCK, B. J. N85-34408
HANATANI, K. N85-34666
HANDSCHUH, R. F. N85-34406
HANKINS, O. B. N85-34701
HANSON, C. G. N85-34967
HARA, T. N85-34975
HARDY, T. L. N85-34178
N85-34179
HARIS, C. G. N85-34520
HARIS, D. K. N85-34519
HARRIS, C. G. N85-34518
N85-34519
HARRIS, D. K. N85-34518
N85-34520
HARRIS, J. N85-34136
HARRIS, J. H. N85-34704
HART, M. D. N85-34430
HARTMAN, D. N85-34527
HASEGAWA, H. N85-34687
HASEGAWA, M. N85-34207
N85-35110
HASTE, G. R. N85-34701
HASTINGS, D. E. N85-34662
N85-34665
HATANO, Y. N85-34975
HATORI, T. N85-34636
N85-34646
N85-34655
N85-34656
N85-34660
HATTORI, F. N85-34680
HAUBOLD, H. J. N85-35111
HAUPT, R. L. N85-34339
HAWKINS, S. A. N85-34700
HAYASHI, I. N85-34195
N85-34196
N85-34214
N85-34215
HAYASHI, S. N85-34188
HAYASHIDA, N. N85-34975
HE, C. X. N85-34975
HEASLER, H. P. N85-34436
HEATH, A. M. N85-34568
HEBBAR, S. K. N85-34358
HEDMAN, S. G. N85-34126
HEDSTROM, J. C. N85-34366
HEIKEN, G. N85-34472
HEINE, C. N85-34405
HEINRICH, W. N85-34889
N85-34922
N85-34935
HEISELMANN, H. W. N85-34341
HELLER, M. N85-34429
HEMKER, K. J. N85-34266
HEMLER N85-34410
HENDRICKS, J. S. N85-34598
HENDRICKS, R. C. N85-34356
HENKE, B. L. N85-34365
HENKEL, M. N85-34935
HERMANSON, R. N85-34453
HERMSEN, W. N85-34963
N85-34964
HEUSSER, G. N85-35108
HICKS, R. M. N85-34115
HIGASHI, S. N85-34970
HIGDON, J. C. N85-34880
HIGUCHI, T. N85-35129
HILL, R. N85-34543
HILLAS, A. M. N85-34979
N85-34981
HILLERMEIER, K. N85-34294
HILLIS, D. L. N85-34701
HINKLEY, B. S. N85-34436
HINO, S. N85-34183
HINZE, W. J. N85-34475
HIRANO, T. N85-34209
HIRSCHFELD, T. B. N85-34457
HIRSHFIELD, J. L. N85-34380
HOBBS, L. M. N85-34724
HOCHSTRASSER, D. N85-34531
HOEGER, M. N85-34127
HOFFMAN, D. J. N85-34694
HOFT, R. G. N85-34334
HOGG, S. E. N85-34485
HOHEISEL, H. N85-34127
HOJO, H. N85-34649
N85-34660
HOLAND, J. F. N85-34417
HOLCOMB, H. P. N85-34234
HOLCOMBE, C. E. N85-34415
HOLLAND, J. W. N85-34625
HOLLANSWORTH, J. E. N85-34150
HONDA, M. N85-34975
HONIDEN, S. N85-34583
HONIG, E. M. N85-34342
N85-34344
HOOPER, P. R. N85-34278
HOPKINS, C. J. N85-34967
HOPKINS, D. C. N85-34335
HOPWOOD N85-34337
HORWITZ, E. P. N85-34220
HOSHI, A. N85-34583
HOULE, J. L. N85-34558
HOUPERT, L. G. N85-34408
HOUSER, D. R. N85-34404
HOVESTADT, D. N85-34749
N85-34776
N85-34792
N85-34793
N85-34802
N85-35041
N85-35043
HOVESTADT, E. N85-34803
HOWALD, A. M. N85-34622
HOWELLS, M. N85-34384
HU, T. C. J. N85-34117
HUDSON, H. S. N85-34743
N85-34745
HUDSON, S. E. N85-34544
HUEBNER, M. N85-35108
HUFF, E. A. N85-34233
HUGENSCHMIDT, M. N85-34400
HULL, K. N85-34589
HUMBLE, J. E. N85-34818
N85-34845
N85-35002
N85-35003
N85-35008
N85-35078
N85-35084
N85-35087
HUMPHREY, D. E. N85-34374
HUNT, R. A. N85-34434
HUNTER, S. D. N85-34951
N85-34965
HURLEY, K. C. N85-34948
HUTERS, A. F. N85-34942
N85-34943
HYDES, D. J. N85-34243
HYLAND, G. B. N85-35078

I

IACOVANGELO, C. D. N85-34460
IAROCCI, M. N85-34384
ICHIDA, K. N85-34194
ICHINOSE, M. N85-35129
IGNATYEV, P. P. N85-35088
IIYOSHI, A. N85-34666
IKEDA, T. N85-34212
ILINA-KAKUYEVA, Y. I. N85-34502
IM, K. E. N85-34397
IMAI, K. N85-35030
IMAI, T. N85-35030
INAZAWA, H. N85-35114
INOUE, A. N85-34765
N85-35079
N85-35130
INUTAKE, M. N85-34651
IOZENAS, V. A. N85-35088
IP, W. H. N85-34992
IPAVICH, F. M. N85-34776
N85-34792
N85-35041
N85-35043
IRIE, H. N85-34656
ISHIDA, A. N85-34657
ISHIDA, Y. N85-35000
ISHIHARA, S. N85-34192
ISHII, H. N85-34195
ISHIKAWA, F. N85-34975
ISHIKAWA, H. N85-34215
ISHKOV, V. N. N85-34760
N85-35075
ISKRA, K. N85-34852
N85-35032
ISRAEL, M. H. N85-34866
N85-34888
N85-34933
N85-34938
N85-34939
ISTOMIN, Y. N. N85-34913
ISTRATOVA, G. P. N85-34263
ITATANI, R. N85-34641
ITO, K. N85-34806
ITO, R. N85-34689
ITOH, N. N85-34689
ITOH, T. N85-34679
IUCCI, N. N85-34764
N85-35057
N85-35058
N85-35059

IWERS, B. N85-34756
IYAGUSHIN, V. I. N85-35136

J

JAANIMAGI, P. A. N85-34365
JACKLYN, R. M. N85-34993
N85-35004
JACQUES, J. S. N85-34951
JAIN, A. N85-34327
JAIN, A. K. N85-34833
N85-35009
N85-35068
JAMET, F. N85-34396
JANOWICZ, A. H. N85-34219
JAYARAMAN, N. N85-34266
JEFFERIES, K. S. N85-34176
JENKINS, T. L. N85-34944
N85-34945
N85-34946
N85-35127
JENNINGS, A. A. N85-34591
JIMENEZ, E. N85-34413
JOHNSON, C. E. N85-34617
JOHNSON, D. W. N85-34463
JOHNSON, I. N85-34617
JOHNSON, J. N. N85-34300
JOHNSON, M. N85-34514
JOHNSON, S. A. N85-34633
JOHNSON, W. B. N85-34238
JOKIPII, J. R. N85-34829
N85-34832
N85-34848
N85-34849
N85-34898
N85-34903
JONES, F. C. N85-34729
N85-34835
N85-34862
N85-34991
JONES, J. R. N85-34323
JORDAN, F. L. N85-34444
JOVANOVIC, M. N85-34335
JOY, K. I. N85-34545
JURKSCH, G. N85-34479

K

KADLECEK, J. A. N85-34464
KAGAWA, T. N85-34687
KAGAWA, Y. N85-34206
KAHLER, S. W. N85-34734
N85-34754
N85-34799
KALB, P. D. N85-34292
KALINA, D. G. N85-34220
KALINKIN, L. F. N85-34949
KAMATA, K. N85-34975
KAMEI, M. N85-34654
KAMIMURA, T. N85-34662
KAMINER, N. S. N85-35074
KAMITANI, A. N85-34640
KAMIYA, Y. N85-34970
KAMPAS, F. J. N85-34451
KANBACH, G. N85-34762
N85-34963
KANEKO, S. N85-34640
KANIA, D. R. N85-34343
KANURY, A. M. N85-34229
KAPLAN, M. N85-34542
KARASHIMA, S. N85-34685
KARTASHEV, V. M. N85-35139
N85-35140
KASAHARA, K. N85-34986
KASAHARA, Y. N85-34562
KATANUMA, I. N85-34648
N85-34669
KATAOKA, S. N85-34214
KATO, M. N85-35067
KATO, T. N85-34684
N85-34689
KATSUSE, K. N85-34209
KATZ, M. I. N85-34839
KAUS, P. N85-34618
KAVAYA, M. J. N85-34333
KAVLAKOV, S. N85-35033
KAVLASHVILI, B. G. N85-35016
KAWAHATA, K. N85-34668
KAWAI, R. N85-34182
KAWAKAMI, I. N85-34671
KAWAMURA, A. N85-34334
KAWATA, S. N85-34675
N85-34678
KAZA, K. R. V. N85-34427
KAZANAS, D. N85-34897
KEBAILI-BERGAOUI, Z. N85-34482
KEEN, K. N85-34394
KELLER, G. R. N85-34475
KELLER, H. W. N85-34610
KELLER, J. O. N85-34240
KENNEY, J. N85-34384
KEPPLER, E. N85-34770
KERCHNER, H. R. N85-34713
KERSHNER, J. D. N85-34301
KERTZMAN, M. P. N85-34863
N85-34888
KESSEL, R. L. N85-34774
KEUCHI, Y. N85-34205
KHAPILOV, N. V. N85-34497
KHARCHENKO, A. V. N85-34246
KHAZAN, G. L. N85-34257
KHOROSHAILOV, V. G. N85-34254
KIKO, J. N85-35108
KILLEEN, J. N85-34706
KILLOUGH, G. G. N85-34483
KING, M. J. N85-34364
KING, R. N85-34544
KINZER, R. L. N85-35121
KIPP, M. E. N85-34298
KIRAO, K. N85-34215
KIRKMAN, I. W. N85-34969
KIRKNER, D. J. N85-34591
KIRSCH, E. N85-34770
KIRSTEN, T. N85-35108
KISH, J. C. N85-34886
KISHIMOTO, Y. N85-34683
KISSEL, R. N85-34511
KISU, H. N85-34189
KITAEV, E. M. N85-34251
KITAGAWA, H. N85-34186
N85-34189
KITAMURA, T. N85-34970
N85-35114
KIWAMOTO, Y. N85-34669
KIYOKAWA, S. N85-34687
KLARMANN, J. N85-34866
N85-34888
N85-34933
N85-34938
N85-34939
KLAUK, R. H. N85-34438
KLECKER, B. N85-34776
N85-34792
N85-34803
N85-34821
N85-35041
N85-35043
KLEIN, K. L. N85-34742
KLEMOLA, A. N85-34725
KLIMENKO, V. V. N85-34810
KO, C. M. N85-34903
KOBAYAKAWA, K. N85-35114
KOCH-MIRAMOND, L. N85-34874
KOCH, D. N85-34958
KOCHAROV, G. E. N85-34768
N85-34769
N85-35105
N85-35106
KOCHAROV, L. G. N85-34804
N85-34805
KODAMA, M. N85-35062
KOENIG, J. F. N85-34417
KOERBER, G. N85-34127
N85-34128
KOGA, M. N85-34202
N85-34211
N85-34216
KOGA, R. N85-34766
KOGA, T. N85-34209
KOHNO, T. N85-34806
N85-34807
KOIKE, S. N85-34211
N85-34216
KOJIMA, H. N85-35066
KOJIRO, D. R. N85-34374
KOLMOGOROV, V. L. N85-34248
KOLOMEETS, E. V. N85-34824
N85-34850
N85-35080
KOMAI, K. N85-34190
N85-34191
KONDO, H. N85-34214
KONDRATYEVA, M. A. N85-34783
KONYSHEV, V. P. N85-34711
KOOPMAN, R. P. N85-34231
KOPPEL, I. N85-34383
KOROTKOV, V. K. N85-35076
N85-35125
KOSLOV, S. A. N85-34761
KOTA, J. N85-34848
N85-34849
N85-35023
KOTHARI, S. K. N85-35082
N85-35119
KOTOV, N. N. N85-34497
KOTOVSKAYA, A. R. N85-34496
KOVALENKO, Y. A. N85-34498
KOVALTSOV, G. A. N85-34757
KOZLOV, A. N. N85-34503
KOZLOVSKY, B. N85-34794
N85-34795
KRAINEV, M. B. N85-34856
KRASOTKIN, A. F. N85-35013
KRATENKO, Y. P. N85-35089
KRAUSE, J. N85-35138
KRAVTSOV, N. G. N85-35037
KRIMIGIS, S. M. N85-34773
N85-34777
N85-35051
KRIVANDIN, V. A. N85-34252
KRIVOSHAPKIN, P. A. N85-35006
N85-35018
N85-35037
KROEGER, R. N85-34763
KRYAKUNOVA, O. N. N85-34854
KRYLOV, Y. V. N85-34501
KRYMSKY, G. F. N85-34902
KUCHERYAEV, B. V. N85-34348
KUCHUK, G. A. N85-34507
KUDO, S. N85-35030
N85-35062
N85-35124
KULEV, A. P. N85-34498
KULIASHA, M. A. N85-34372
KUMAR, S. N85-35027
N85-35028
N85-35029
KUNII, T. L. N85-34535
N85-34589
KUNOW, H. N85-34808
KUNSELMAN, M. H. N85-34692
KUPPERMAN, D. S. N85-34600
KURAMOTO, M. N85-34204
KURGUZOVA, A. I. N85-35013
KURT, V. G. N85-34746
KURTZ, S. R. N85-34293
KUSAMA, E. N85-34196
KUSUNOSE, M. N85-35031
N85-35077
N85-35123
N85-35124
KUTNEY, J. T., JR. N85-34141
KUZHEVSKY, B. M. N85-34789
KUZMICHEVA, A. E. N85-35074
KUZMIN, A. I. N85-35006
N85-35037
N85-35063
KUZMIN, M. P. N85-34496
KUZNETSOVA, R. I. N85-34914
KYSER, T. K. N85-34471

L

LAGRAFF, J. E. N85-34354
LAI, C. L. N85-34357
LAL, N. N85-35048
LAL, S. N85-35109
LAMB, F. K. N85-34723
LAMB, R. C. N85-34981
LAMBERT, A. N85-34974
N85-34980
LANDINI, G. N85-34956
LANDREA, M. F. N85-34950
LANDRUM, D. B. N85-34352
LANGE, R. N85-34587
LANSKAYA, K. A. N85-34259
LANZEROTTI, L. J. N85-34777
LAPALME, G. N85-34559
LAPERDIN, Y. M. N85-34711
LASAREV, A. V. N85-35140
LAU, K. H. N85-34887
LAUBENTHAL, N. A. N85-34951
LAURITZEN, T. N85-34412
LAVIGNE, J. M. N85-34957
LAVILLE, A. N85-34735
N85-34739
LAVRUKHINA, A. K. N85-34914
N85-34915
N85-35107
LAWSON, L. A. N85-34587
LAWVER, B. S. N85-34587
LEAF, G. K. N85-34516
LEBRUN, F. N85-34963
N85-34964
LECLAIRE, B. N85-34585
LEDBETTER, M. N85-34710

LEE N85-34338
LEE, D. O. N85-34389
LEE, F. C. N85-34335
LEE, G. N85-34378
LEE, H. N85-35116
LEE, K. N85-34305
N85-34306
LEE, M. A. N85-35044
LEE, S. K. N85-34553
LEE, V. D. N85-34692
N85-34695
LEIKOV, N. G. N85-34949
LEIRIKH, I. V. N85-34255
LEJEUNE, A. N85-34566
LEMOGNE, T. N85-34265
LEPAGE, Y. N85-34528
LERCHE, I. N85-34877
N85-34920
N85-34921
LESKIN, G. S. N85-34499
LETAW, J. R. N85-34871
N85-34875
N85-34890
N85-34924
LEUPRECHT, R. N85-34245
LEVEDAHL, W. K. N85-35120
LEVENTHAL, M. N85-34942
N85-34943
LEVINE, A. S. N85-35145
LEVINE, M. D. N85-34576
N85-34577
LEVY, R. N85-34114
LEWIS, R. A. N85-34962
N85-34967
LEYLAK, J. N85-34369
LHEUREUX, J. N85-34934
LI, J. Z. N85-34285
LIBIN, I. Y. N85-35071
LIBIN, T. Y. N85-35125
LICHTEN, L. N85-34555
LICURSI, J. N85-34378
LIDIAK, E. G. N85-34475
LIEBING, D. F. N85-34981
LIGGETT, M. N85-34799
LIN, R. F. N85-35120
LIN, R. P. N85-34799
N85-34800
N85-34948
LIN, S. J. N85-34114
LINDQUIST, W. B. N85-34364
LINE, L. G. N85-34155
LING, J. S. N85-34443
LINSLEY, J. N85-34976
N85-34977
N85-34983
N85-34984
LIPPMANN, M. J. N85-34439
LITVIN, F. L. N85-34405
LIU, C. K. N85-34557
LIU, H. S. N85-34138
LIU, R. N85-34515
LLOYD-EVANS, J. N85-34928
N85-34930
N85-34980
LOCKMAN, F. J. N85-34724
LOCKWOOD, J. A. N85-34811
N85-34822
N85-34832
N85-34853
N85-35046
LOGACHEV, Y. I. N85-34746
LOGSDON, J. N85-35147
LONG, J. L. N85-34961
LOREE, T. R. N85-34387
LORENCE, L. J., JR. N85-34597
LOUIS, G. A. N85-34459
LOVELL, R. C. N85-34138
LOWDER, D. M. N85-34929
LOWRY, D. W. N85-34222
LOWTHER, D. A. N85-34573
LUCZAK, H. N85-34478
LUEST, R. N85-34876
LUHMANN, J. G. N85-34884
LUHN, A. N85-34792
N85-34793
N85-34803
LUKYANYUK, V. Y. N85-34496
LUMME, M. N85-34626
N85-35061
N85-35069
LUND, N. N85-35084
LUSTMAN, L. N85-34350
LYAKHOVA, A. K. N85-34850
LYUBUSHKINA, L. M. N85-34261

M

MA, Y. N85-34960
MACCALLUM, C. J. N85-34942
N85-34943
MACDONALD, C. L. N85-34563
MACDONALD, D. D. N85-34238
MACE, O. N85-34766
MACHA, J. M. N85-34352
MACHKIN, V. I. N85-34246
MACHO, L. N85-34508
MACK, P. N85-35144
MACKEOWN, P. K. N85-34981
MACKINNON, A. L. N85-34741
MACLENNAN, C. G. N85-34777
MADER, C. L. N85-34299
N85-34301
MAEKAWA, I. N85-34192
MAEKAWA, Z. N85-34212
MAENCHEN, J. N85-34702
MAGNENAT-THALMANN, N. N85-34536
N85-34566
MAIER, U. N85-34479
MAIYA, P. S. N85-34277
MAJIMA, Y. N85-34196
MAKHMUTOV, V. S. N85-35093
MAKSIMOVA, Y. N. N85-34505
MALHOTRA, M. K. N85-34238
MALOWANY, A. S. N85-34577
MALYUCHKOV, O. T. N85-34262
MANAKOV, N. A. N85-34261
MANDROU, P. N85-34950
MANDZHAVIDZE, N. Z. N85-34768
MARAN, S. P. N85-34727
MARGOLIS, S. H. N85-34866
N85-34868
N85-34873
N85-34878
MARSDEN, R. G. N85-34813
MARSH, K. V. N85-34462
MARTI, K. N85-35097
N85-35103
MARTINIC, N. J. N85-34765
MARUYAMA, K. N85-34199
MARUYAMA, T. N85-34209
MASCH, F. D. N85-34440
MASON, G. M. N85-34802
N85-34812
N85-34821
N85-35041
MASSE, P. N85-34874
MASSENGILL, L. W. N85-34586
MASUDA, N. N85-34185
MATESON, J. L. N85-34953
MATHIS, K. D. N85-34922
MATSUBARA, Y. N85-34975
MATSUMOTO, H. N85-34181
MATSUNO, S. N85-34970
MATTESON, J. L. N85-34948
N85-34954
MATTHEW, M. W. N85-34710
MATTHEWS, F. L. N85-34423
MAU, T. K. N85-34707
MAUGER, B. G. N85-34935
MAXWELL, E. L. N85-34485
MAYER-HASSELWANDER, H. A. N85-34963
N85-34964
MAYER, S. N85-34601
MAZLISH, B. N85-35150
MCBREEN, B. N85-34959
MCCOMB, T. J. N85-34969
MCDONALD, F. B. N85-34755
N85-34784
N85-34820
N85-34834
N85-35048
MCDOUGALL, W. A. N85-35148
MCGIVERN, W. H. N85-34630
MCGUIRE, R. E. N85-34734
N85-34747
N85-34754
N85-34778
N85-34788
N85-34811
MCKENZIE, J. F. N85-34885
N85-34892
MCKIBBEN, R. B. N85-35050
N85-35052
MCKNIGHT, R. L. N85-34140
MCLAUCHLAN, J. M. N85-34629
MCPHEETERS, C. N85-34526
MCRAE, T. G. N85-34465
MEDINA, J. N85-35118
MEDKOVA, I. L. N85-34500
MEEGAN, C. A. N85-34953
N85-34954
N85-34955
MEHLHORN, T. A. N85-34702
MERENYI, E. N85-35023
MERKLE, J. G. N85-34418
MERZENICH, K. N85-34332
METRAL, C. N85-34549
METSKVARISHVILI, R. Y. N85-35105
N85-35106
MEULLER, D. W. N85-34622
MEWALDT, R. A. N85-34887
N85-35040
MEYER, J. P. N85-34790
N85-34864
MEYER, P. N85-34127
N85-34128
N85-34749
N85-34763
N85-34782
N85-34860
N85-34876
N85-34934
MICHAUD, C. N85-34577
MICHKOVA, E. S. N85-34257
MIESKOWSKI, D. M. N85-34284
MIGLIORI, A. N85-34414
MIKAME, K. N85-34583
MIKROYANNIDIS, J. A. N85-34280
MIKRYUKOVA, N. A. N85-34810
MILLAR, J. N85-34132
MILLER, R. B. N85-34691
MILLER, T. N85-34175
MILLIS, R. L. N85-34725
MILLS, G. D. N85-34619
MILLS, M. I. N85-34565
MIMA, K. N85-34680
N85-34683
MINAGAWA, M. N85-34185
MINEEV, Y. V. N85-35089
MINKOFF, M. N85-34516
MINKOV, V. N85-34607
MINOSHIMA, K. N85-34190
MIROSHNICHENKO, L. I. N85-34758
MIRTICH, M. J. N85-34631
MISHRA, B. L. N85-34833
N85-35064
MITA, I. N85-34201
MITSUI, K. N85-34970
MITZUTANI, H. N85-34203
MIYAMA, S. M. N85-34674
MIYAMOTO, H. N85-34187
MIYANAGA, N. N85-34687
MIYAO, K. N85-34192
MIYOSHI, S. N85-34669
MIZUNO, Y. N85-34690
MIZUTANI, K. N85-34970
MOCHIZUKI, T. N85-34687
MOEBIUS, E. N85-34803
N85-35043
MOLIAN, S. N85-34324
MONTES, H. N85-34265
MONTOYA, P. C. N85-34389
MOODY, R. L. N85-34432
MOORE, R. L. N85-34159
N85-34160
N85-34161
N85-34162
N85-34163
MORAAL, H. N85-34841
N85-35056
MOREL, J. E. N85-34597
MORELLI, E. N85-34956
MORELLO, C. N85-34990
MORFILL, G. E. N85-34876
N85-34898
MORGAN, T. J. N85-34622
MORI, S. N85-35000
N85-35001
N85-35007
N85-35021
N85-35035
N85-35129
MORI, T. N85-34197
MORINISHI, K. N85-34672
MORINO, L. N85-34113
MORISHITA, I. N85-35000
N85-35021
N85-35035
MORITA, K. N85-34689
MOROZOVA, E. I. N85-34810
MORRIS, P. M. N85-34135
MORUKOV, B. V. N85-34495
MOSES, D. N85-34749
N85-34782
MOSSL, B. N85-34464
MOTEFF, J. N85-34276
MOTOJIMA, O. N85-34666

MOUSSAS, X. N85-34771
MUELLER, A. F. N85-34531
MUELLER, D. N85-34934
MULDER, M. S. N85-35056
MULLAN, D. J. N85-34791
MULLEN, R. L. N85-34356
MULLER, D. N85-34931
MUNAKATA, K. N85-34994
N85-35019
N85-35060
MUNAKATA, Y. N85-34995
MURAKAMI, K. N85-35066
N85-35079
MURAKI, Y. N85-34970
MURPHY, R. J. N85-34794
N85-34795
MURTY, S. V. S. N85-35097
MYERS, B. A. N85-34546
MYMRINA, N. V. N85-35074

N

NAANO, N. N85-34209
NACHKEBIA, N. A. N85-35072
N85-35073
NAGAMATSU, T. N85-34188
NAGASHIMA, K. N85-34994
N85-35000
N85-35001
N85-35005
N85-35019
N85-35020
N85-35021
N85-35035
N85-35060
NAIMAN, A. N85-34567
NAITOU, H. N85-34642
NAKAGAWA, N. N85-34182
NAKAMURA, Y. N85-34642
NAKASHIMA, Y. N85-34666
NAKATA, E. N85-34206
NAKAYASU, H. N85-34198
NANNI, T. N85-35094
N85-35096
NANSTAD, R. K. N85-34418
NARDI, V. N85-34910
NASKIDASHVILI, B. D. N85-35016
N85-35073
NATALUCCI, L. N85-34947
NAVARRA, G. N85-34990
NECHAEV, O. Y. N85-34789
NEELY, W. R., JR. N85-34144
NEEPER, D. A. N85-34366
NELSON, R. A. N85-34371
NELSON, W. E. N85-34597
NESTEROV, V. E. N85-34949
NETI, S. N85-34371
NEUBAUER, F. N85-34771
NEUSER, R. N85-34584
NEUSTOCK, H. H. N85-34756
NEWKIRK, G., JR. N85-34853
NEWKIRK, L. R. N85-34696
NEWPORT, B. J. N85-34888
N85-34938
N85-34939
NG, C. K. N85-34814
N85-34815
NGAI, W. B. N85-34578
NIEMINEN, M. N85-34826
N85-35061
N85-35069
NIKIFOROV, V. I. N85-34498
NIKOLAEV, V. S. N85-34780
NIKOLAYEVA, N. M. N85-34500
NIKOLSKY, S. I. N85-35115
NINAGAWA, K. N85-35131
NIR, D. N85-34631
NISHI, K. N85-35079
NISHIDA, H. N85-34672
NISHIGUCHI, A. N85-34673
N85-34688
NISHIIZUMI, K. N85-35097
NISHIWAKI, T. N85-34185
NISHIZAWA, A. N85-34668
NISHKOVSKIKH, A. S. N85-34827
NITTA, N. N85-34744
N85-34807
NIU, K. N85-34675
N85-34677
N85-34678
NIVEN, A. J. N85-34120
N85-34124
NOMA, T. N85-34535
NOMOTO, K. N85-34686
NOMURA, S. N85-34225
NOONAN, R. E. N85-34521
NOROSE, S. N85-34199
NOSE, T. N85-34183
NOSOV, S. F. N85-34839
NOVACEK, M. N85-34526
NOVIKOV, V. S. N85-34504
NOVIKOV, V. Y. N85-34502
NUBER, R. N85-34774
NURMIKKO, A. V. N85-34235
NYLAND, T. W. N85-34444
NYMMIK, R. A. N85-34783
N85-35136

O

OAKLEY, D. J. N85-34411
OBATAYA, Y. N85-34184
OBIKI, T. N85-34666
OBRIEN, G. M. N85-34614
OFARRELL, T. P. N85-34487
OGASAWARA, M. N85-34682
OGAWA, K. N85-34213
OGDEN, P. A. N85-34974
OGITA, N. N85-35077
OHASHI, Y. N85-34970
OHI, Y. N85-34806
OHKI, K. I. N85-34743
OHKOUCHI, T. N85-34194
OHMORI, N. N85-35123
OHOKA, H. N85-34975
OHSAWA, Y. N85-34643
N85-34664
OHTA, T. N85-34183
N85-34214
OHTSUKA, H. N85-34193
OIKE, M. N85-34200
OIYAMA, M. N85-34195
OKABE, N. N85-34197
OKADA, A. N85-34970
OKADA, H. N85-34641
OKADA, K. N85-34687
OKAJIMA, S. N85-34668
OKAMOTO, M. N85-34186
N85-34635
OKAMURA, S. N85-34659
OKHLOPKOV, V. P. N85-35017
OKHLOPKOVA, L. S. N85-35017
OLDEN, J. N. N85-34702
OLENEVA, V. A. N85-35075
OLSEN, D. R., JR. N85-34533
OLSEN, G. N85-34437
ONEILL, G. N85-34513
ONEILL, T. N85-34952
ONISHCHENKO, S. A. N85-34246
ONO, M. N85-34641
ORFORD, K. J. N85-34969
ORII, S. N85-34688
ORISHCHENKO, A. V. N85-34805
ORLOV, V. N. N85-34499
ORMES, J. F. N85-34928
N85-34930
N85-34935
ORTNER, H. M. N85-34245
OSBORN, W. N85-34725
OSBORNE, T. H. N85-34703
OSCHLIES, K. N85-35137
OTAOLA, J. A. N85-34859
OWE, M. N85-34728
OWENS, A. N85-34766
N85-34944
N85-34945
N85-35127
OWENS, G. N. N85-34946
OWENS, T. L. N85-34694
OWINGA, T. D. N85-34418
OZAKI, M. N85-35129
OZELL, B. N85-34556

P

PACIESAS, W. N85-34953
N85-34954
PACKARD, A. B. N85-34611
N85-34614
PAKALO, A. V. N85-34422
PAKHOMOV, N. I. N85-34761
PALENQUE, E. N85-34765
PALKOVIC, M. N85-34508
PANCHENKO, V. S. N85-34497
PANDEY, P. K. N85-35009
N85-35068
PANTELEEVA, N. V. N85-34252
PAPIKE, J. J. N85-34474
PARE, L. A. N85-34352
PARISI, M. N85-34764
N85-35057
N85-35058
N85-35059
PARKER, J. A. N85-34281
PARKIN, G. N85-34513
PARKS, P. B. N85-34646
N85-34658
PARNELL, T. A. N85-34953
N85-34954
PATEL, M. N85-34974
PATHAK, S. P. N85-34996
N85-35009
PATTERSON, J. R. N85-34971
PAUL, J. A. N85-34963
PECHAN, E. N85-34461
PEHL, R. H. N85-34948
PELLEGRINI, C. N85-34531
PELLIGRINI, C. N85-34549
PELLING, M. R. N85-34948
N85-35120
PELTONEN, J. N85-34826
N85-35061
N85-35069
PENDLETON, G. N. N85-34944
N85-34945
N85-34946
PENG, M. N85-34692
PERE, J. F. N85-34227
PERELYGIN, V. P. N85-34865
PEREZ-ENRIQUEZ, R. N85-34796
N85-34859
PEREZ-PERAZA, J. N85-34735
N85-34736
N85-34737
N85-34738
N85-34739
N85-34758
PERIALE, L. N85-34990
PERIANA-PILLAI, R. A. N85-34219
PERKO, J. S. N85-34835
PERMINOV, A. A. N85-34283
PEROTTI, F. N85-34962
PERRY, R. T. N85-34624
PETERSON, L. E. N85-34948
PETERSON, V. L. N85-34510
PETROU, N. N85-35084
PETRUNKO, A. N. N85-34244
PETRUSHEVSKII, M. S. N85-34253
PETTINATI, F. N85-34560
PETUKHOV, S. I. N85-34780
PHAN, A. N85-34228
PHANEUF, R. A. N85-34622
PIERCE, L. A. N85-34284
PIMMINGER, M. N85-34245
PINTER, S. N85-35059
PISARENKO, N. F. N85-34810
PLANTE, M. N85-34575
PLECHEV, V. N. N85-34260
PLETNEVA, E. D. N85-34247
PLOTNIKOV, V. A. N85-34256
PODGURSKAYA, A. V. N85-35136
POKER, D. B. N85-34616
POLICASTRO, A. J. N85-34369
POLUEKTOV, V. P. N85-34949
POLUKHIN, P. I. N85-34348
POLYAKOV, V. N. N85-34503
POMERANTZ, M. A. N85-34817
N85-34844
N85-34993
N85-35038
PONOMAREV, S. I. N85-34498
POOR, S. E. N85-34700
POPEL, S. I. N85-34283
PORRECA, G. N85-34943
PORTER, N. A. N85-34981
POTGIETER, M. S. N85-34842
N85-34843
N85-35044
POTTER, J. L. N85-34593
POUKEY, J. W. N85-34698
POULSEN, J. M. N85-34956
PRAGER, S. C. N85-34703
PRANTZOS, N. N85-34906
PRATT, A. J. S. N85-34421
PRATT, M. J. N85-34321
PREGENZER, A. L. N85-34702
PRESCOTT, J. R. N85-34971
PRICE, P. B. N85-34929
PRIKHODKO, A. N. N85-35018
PRILUTSKY, O. F. N85-34949
PRILUTSKY, R. E. N85-35071
N85-35132
PRIMBACH, H. N85-35120
PRINCE, T. A. N85-34940
N85-34941

PROTHEROE, R. J. N85-34989
PRUESS, K. N85-34439
PRUETT, J. C., JR. N85-34458
PRUSINKIEWICZ, P. N85-34552
PSALTIS, D. N85-34629
PTUSKIN, V. S. N85-34883
PUROHIT, A. N85-34275
PYLE, K. R. N85-34838
N85-34860
N85-35050
N85-35052
N85-35053

Q

QUENBY, J. J. N85-34771
QUON, B. H. N85-34701

R

RADZEVICH, A. E. N85-34499
RADZIEMSKI, L. J. N85-34387
RAGHURAM, S. N85-34592
RAINE, K. W. N85-34630
RAJESWARAN, G. N85-34451
RAMATY, R. N85-34732
N85-34794
N85-34795
RAMLER, J. R. N85-34150
RAMSDEN, D. N85-34944
N85-34945
N85-34946
RANGER, N. N85-34528
RAPAPORT, J. N85-34615
RAPTIS, A. C. N85-34391
RARBACK, H. N85-34384
RASMUSSEN, D. A. N85-34701
RASMUSSEN, I. L. N85-35084
RASPOPOV, N. A. N85-34257
RATH, A. R. N85-34345
RATIB, O. N85-34530
RAUBENHEHEIMER, B. C. N85-35128
RAUBENHEIMER, B. C. N85-34988
RAYCHAUDHURI, P. N85-35112
N85-35113
REAMES, D. V. N85-34788
N85-34798
N85-34799
N85-34800
N85-34802
REAMS, W. N85-34290
REBER, J. D. N85-34942
REED, K. M. N85-34468
REEDY, R. C. N85-35098
N85-35099
REFLOCH, A. N85-34946
REGINATO, L. L. N85-34700
REGUERIN, A. N85-34765
REID, R. J. O. N85-34974
REINATH, M. S. N85-34146
N85-34379
REN, N. K. N85-34470
RENLUND, A. M. N85-34297
REPPIN, C. N85-34762
N85-35121
REYNA, L. N85-34364
RHEINFURTH, M. H. N85-34148
RICE, J. K. N85-34702
RICH, M. J. N85-34222
RICHARDSON, L. N85-34558
RICHARDSON, M. C. N85-34365
N85-34399
RICHTER, K. N85-34770
RIEGER, E. N85-34767
RIGHETTI, A. N85-34530
RIKER, J. F. N85-35022
N85-35024
N85-35025
RITCHIE, J. P. N85-34603
RITCHIE, R. O. N85-34431
RIVERO, F. N85-34758
RIZK, Y. M. N85-34116
ROBERTS, A. N85-34328
ROBERTS, W. T. N85-34165
N85-34166
N85-34167
N85-34168
N85-34169
N85-34170
N85-34172
N85-34173
ROBINSON, G. C. N85-34418
RODIN, V. G. N85-34949
RODRIGUES, B. N85-34383
RODRIGUEZ, D. J. N85-34587
ROEHRENS, H. N85-34294
ROELOF, E. C. N85-34840
N85-34992
ROGAVA, O. G. N85-35016
ROGERS, D., JR. N85-34700
ROLAND, A. N85-35142
ROONEY, G. T. N85-34310
ROSA, E. N85-34276
ROSECRANS, P. M. N85-34267
ROSS, J. C. N85-34146
ROSSER, R. N85-34384
ROVNYY, A. N. N85-34507
ROWLEY, P. N85-34543
RUBINI, A. N85-34956
RUEDA, A. N85-34912
RYAN, J. M. N85-34730
N85-34751
RYAN, R. R. N85-34603
RYU, J. Y. N85-35122

S

SABAUD, C. N85-34957
SABOURIN, R. N85-34573
SADOFSKY, S. L. N85-34574
SAGISAKA, S. N85-35007
N85-35129
SAITO, T. N85-34846
SAKAGUCHI, G. N85-34681
SAKAKIBARA, S. N85-35060
SAKAMAKI, K. N85-34207
SAKI, T. N85-35067
SAKURAI, K. N85-34806
N85-34869
N85-35104
N85-35110
SALAMON, M. H. N85-34870
N85-34929
SALZMAN, J. A. N85-34150
SAMEDOV, O. V. N85-34250
SAMORSKI, M. N85-34972
SAMSONOV, I. S. N85-35063
SAMSONOVA, Z. N. N85-35063
SANDAHL, C. A. N85-34481
SANDERS, B. R. N85-34240
SANDERS, W. A. N85-34284
SANDERSON, T. R. N85-34813
SANDHOLM, R. G. N85-34131
SANDMAN, R. R. N85-34386
SANFORD, T. W. L. N85-34698
SANO, F. N85-34666
SANUKI, H. N85-34636
SARIKAYA, M. N85-34289
SARRIS, E. T. N85-34773
SASADA, T. N85-34199
N85-34200
SASAKI, H. N85-35123
SASAKI, T. N85-34204
SATO, K. N85-34655
SATOFUKA, N. N85-34672
SAUNDERS, G. C. N85-34390
SAVENKO, I. A. N85-34789
SAVINO, J. M. N85-34444
SAWADA, K. N85-34669
SBORSHIKOV, V. G. N85-35090
SCHATZ, M. F. N85-34177
SCHEBOR, F. S. N85-34376
SCHELLERT, G. N85-34808
SCHERTZ, W. W. N85-34226
SCHINDLER, S. M. N85-34941
SCHLICKEISER, R. N85-34731
N85-34877
N85-34920
N85-34921
N85-34927
SCHLOTZ, R. N85-35108
SCHLUETER, W. N85-34823
SCHMIDT, F. N85-34242
SCHNEIDER, K. N85-35108
SCHOLER, M. N85-34776
N85-34792
N85-35043
SCHOLL, I. N85-34584
SCHOLZ, C. H. N85-34467
SCHONFELD, F. W. N85-34606
SCHRUBEN, D. L. N85-34295
SCHULZ, M. N85-34884
SCHUSTER, P. N85-35048
SCHWARTZ, R. D. N85-34726
SCHWARTZKOPFF, U. N85-34294
SCHWEITZER, U. N85-34564
SCHWENN, R. N85-34771
SCOTT, D. G. N85-34415
SDOBNOV, V. E. N85-35036
N85-35092
SECHINOV, V. P. N85-34783
SEDOV, A. V. N85-34506
SEKULA, S. T. N85-34713
SELCOW, E. C. N85-34692
SEMENOV, V. Y. N85-34495
SEMUKHIN, P. E. N85-34757
SENBA, K. N85-34202
SEPPALA, L. G. N85-34633
SEQUEIROS, J. N85-35118
SERGEEV, A. V. N85-35036
N85-35092
SERMUND, G. N85-34937
SETRO, L. Y. N85-34123
SETTLE, J. N85-34617
SEVASTYANOV, V. N. N85-34824
SHACK, W. J. N85-34277
SHAFER, G. V. N85-35006
N85-35016
N85-35018
N85-35037
SHAFER, Y. G. N85-34810
SHAFFER, S. J. N85-34138
SHAHAM, J. N85-34723
SHAKHOV, B. A. N85-34839
SHAMROTH, S. J. N85-34114
SHANE, S. J. N85-34133
N85-34134
SHAPIRO, M. M. N85-34905
N85-34924
SHAPOVALOVA, L. A. N85-34761
SHARE, G. N85-34767
SHARE, G. H. N85-34762
N85-35121
SHATASHVILI, L. K. N85-35016
N85-35073
SHAW, S. N85-34278
SHCHEGOLEVA, R. P. N85-34260
SHEA, M. A. N85-34845
N85-34861
N85-35084
N85-35085
N85-35086
N85-35087
N85-35130
SHEELEY, N. R., JR. N85-34754
SHEEN, S. H. N85-34391
SHEN, C. N85-34960
SHENG, Y. N85-34139
SHIBATA, S. N85-34995
SHIBAZAKI, N. N85-34723
SHIEH, S. J. N85-34481
SHIELDS, J. C. N85-34779
SHIGETA, M. N85-34649
SHIH, Y. N85-34623
SHINKARENKO, E. T. N85-34254
SHIOZAWA, K. N85-34192
SHIRATORI, E. N85-34184
SHIROUZU, M. N85-34117
SHMATKO, E. S. N85-35139
N85-35140
SHOJI, T. N85-34661
SHOR, J. T. N85-34221
SHORES, D. A. N85-34460
SHRIVASTAVA, P. K. N85-34998
N85-35009
SHULL, J. M. N85-34724
SHVARTSMAN, Y. E. N85-34854
SIEGMON, G. N85-34937
SIGNORINI, C. N85-34764
N85-35057
N85-35058
SIKKA, V. K. N85-34430
SILBERBERG, R. N85-34871
N85-34875
N85-34890
N85-34924
SILBERMANN, M. N85-34541
SILVER, G. L. N85-34274
SILVESTRI, S. N85-34956
SIMMONS, G. J. N85-34512
SIMNETT, G. M. N85-34740
N85-34748
N85-34751
SIMON, M. N85-34922
N85-34935
SIMONE, J. N85-34952
SIMPSON, G. A. N85-34937
SIMPSON, J. A. N85-34801
N85-34838
N85-34853
N85-34860
N85-35050
N85-35052
N85-35053
N85-35143
SIMS, C. S. N85-34382

SINGH, J. J. N85-34282
SINGH, R. K. N85-35045
SIROTINA, I. V. N85-35091
SISLIAN, J. P. N85-34139
SKOTTOVA, N. N85-34508
SKRIPIN, G. V. N85-35006
N85-35018
N85-35037
SKUKINA, I. S. N85-34495
SLYUNYAEVA, N. V. N85-34850
SLYUSAREV, V. Y. N85-34255
SMART, D. F. N85-34861
N85-35084
N85-35085
N85-35086
N85-35087
N85-35130
SMITH, C. S. N85-34424
SMITH, E. J. N85-34813
N85-34992
SMITH, J. N85-34383
SMITH, K. C. N85-34553
SMITH, M. B. N85-34470
SMITH, M. R. N85-34313
SMITH, M. W. N85-34700
SMITH, P. M. N85-34144
SMOLENSKI, L. G. N85-35136
SMYRL, W. H. N85-34293
SNIEL, M. N85-34948
SNOWDON, R. A. N85-34513
SOMMERS, P. N85-34982
SORKIN, L. P. N85-34250
SORRELLS, G. G. N85-34470
SOURES, J. M. N85-34399
SOUTOUL, A. N85-34879
SPADA, G. N85-34947
SPEER, L. R. N85-34524
SPILLING, P. D. N85-34717
SPIZZICHINO, A. N85-34947
ST.CLAIR, A. K. N85-34282
ST.CLAIR, C. R., JR. N85-34362
ST.CLAIR, T. L. N85-34282
ST.PIERRE, G. R. N85-34238
STAMM, W. N85-34972
STANG, P. D. N85-34942
N85-34943
STARK, Y. S. N85-34249
STARR, C. H. N85-34941
STAUBERT, R. N85-34987
STEGER, J. L. N85-34116
STEINBERG, D. J. N85-34304
STEKOLNIKOV, N. V. N85-34850
STENGER, V. J. N85-34981
STEPANOV, V. K. N85-34503
STEPHEN, J. B. N85-34947
STEPHENS, J. B. N85-34149
STEPHENS, S. A. N85-34928
STERZELMEIER, K. N85-34634
STEWART, R. F. N85-34603
STILLER, B. N85-34936
STOAKLEY, D. M. N85-34282
STOECKER, U. N85-34294
STOKER, P. H. N85-34759
N85-35128
STOLPOVSKY, V. G. N85-34746
STONE, E. C. N85-34781
N85-34785
N85-34786
N85-34836
N85-34847
N85-34866
N85-34887
N85-34888
N85-34938
N85-34939
N85-34941
N85-35039
N85-35040
N85-35042
N85-35049
STONE, R. G. N85-34734
N85-34754
N85-34798
N85-34799
STORINI, M. N85-34764
N85-35057
N85-35058
N85-35059
STOZHKOV, Y. I. N85-34856
N85-35014
N85-35026
N85-35115
STRACK, K. M. N85-34476
STREITMATTER, R. E. N85-34928
N85-34930
N85-34935
STROME, W. M. N85-34547
STRONG, A. W. N85-34964
STUBICAN, V. S. N85-34715
STURTEVANT, B. N85-34370
SUBRAHMANYAM, K. B. N85-34427
SUBRAMANIAN, A. N85-35109
SUDA, T. N85-34807
SUEDA, N. N85-34583
SUESSENGUTH, G. N85-34479
SULLIVAN, T. J. N85-34141
SUN, Q. N85-34210
SUN, Y. N85-34960
SUNDARAM, R. K. N85-34371
SUZUKI, T. N85-34195
SUZUKI, Y. N85-34196
SVIRZHEVSKAYA, A. K. N85-35014
SVIRZHEVSKY, N. S. N85-35013
N85-35014
SWAIN, R. L. N85-34418
SWAJA, R. E. N85-34382
SWANEPOEL, J. W. H. N85-34988
SWARNER, W. G. N85-34329
SWEC, D. M. N85-34631
SWEDO, R. J. N85-34288
SWEENEY, M. A. N85-34702
SWEENEY, W. N85-34952
SWIFT, G. W. N85-34414
SWINSON, D. B. N85-34845
N85-34846
N85-35005
SWORDY, S. P. N85-34931
N85-34934
SYTNIK, K. M. N85-34490
SZABELSKA, B. N85-34923
SZABO, B. J. N85-34471

T

TAANK, H. P. N85-34423
TABATA, T. N85-34689
TACHIHARA, T. N85-34208
TADROS, M. G. N85-34488
TAKABE, H. N85-34680
TAKAHASHI, H. N85-34214
N85-34996
N85-34997
TAKAHASHI, K. N85-34215
N85-34765
N85-35030
N85-35079
N85-35123
TAKAHASHI, P. K. N85-34450
TAKANO, Y. N85-35131
TAKAOKA, N. N85-35131
TAKASHI, M. N85-34193
N85-34211
N85-34213
N85-34216
TAKEBUCHI, H. N85-34202
TAKEMOTO, Y. N85-34642
TAKENAKA, T. N85-34806
TAKEWAKI, H. N85-34673
TAKIMOTO, A. N85-34640
TAMBA, M. N85-34677
TANAHASHI, S. N85-34668
TANAKA, A. N85-34213
TANAKA, K. N85-34676
TANG, P. K. N85-34300
TANIZAWA, Y. N85-34186
TANSKANEN, P. N85-35062
TAO, R. N85-34716
TAQUICHIRI, M. A. N85-34765
TASCHNER, E. C. N85-34381
TATSUOKA, R. N85-34994
N85-35020
TAWARA, H. N85-34689
TAYLOR, A. N85-34278
TAYLOR, W. W. L. N85-34164
TEEGARDEN, B. J. N85-34942
N85-34943
N85-34953
N85-34954
TEMPLE, J. A. G. N85-34419
TERNOVSKAYA, M. V. N85-35017
N85-35088
TERRIS, B. D. N85-34712
TESHIMA, M. N85-34975
TETSUKA, T. N85-34688
TEUFEL, L. W. N85-34470
TEWARI, S. N. N85-34266
THALMANN, D. N85-34536
THEIS, T. L. N85-34591
THIELHEIM, K. O. N85-34917
N85-34918
N85-34919
THIRRIOT, C. N85-34482
THOMAS, B. T. N85-34831
THOMAS, G. N85-34289
THOMAS, J. N85-34766
THOMPSON, D. N85-34231
THOMPSON, D. J. N85-34951
THOMPSON, P. B. N85-34699
TIGRANYAN, R. A. N85-34508
TIMOFEEV, V. E. N85-34810
TITTEL, H. O. N85-34935
TIZENGAUZEN, V. A. N85-35090
TKEMALADZE, V. S. N85-34855
TODD, J. H. N85-34612
TODOROKI, J. N85-34645
N85-34663
TOI, K. N85-34668
TOLBERT, L. M. N85-34230
N85-34237
TOMASKO, D. N85-34360
TOMISAWA, S. N85-34183
TOMOZAWA, Y. N85-34911
TONWAR, S. C. N85-34985
TOPTYGIN, I. N. N85-34881
TORDOFF, M. N85-34513
TORII, S. N85-34986
TORSTI, J. J. N85-34826
N85-35061
N85-35069
TOWNSEND, D. P. N85-34407
TRAINOR, J. N85-35048
TRAINOR, J. H. N85-34755
N85-34784
TRANSKY, I. A. N85-35018
N85-35037
TRETYAKOVA, C. A. N85-34783
N85-35136
TREVES, S. N85-34611
N85-34614
TRICK, T. N. N85-34336
TRKULA, M. N85-34696
TROTT, W. M. N85-34297
TROTTET, G. N85-34741
N85-34742
TSANG, C. F. N85-34388
N85-34473
TSAO, C. H. N85-34871
N85-34875
N85-34890
N85-34924
TSERETELI, G. L. N85-35073
TSERETELI, S. L. N85-35105
N85-35106
TSUNETA, S. N85-34743
TSUNG, W. J. N85-34405
TSURUTANI, T. N85-34562
TUBBS, E. F. N85-34629
TUELLER, J. N85-34942
N85-34943
TUEMER, O. T. N85-34952
TURNER, D. N85-34461
TURPANOV, A. A. N85-34780
N85-34902
TURTUR, A. N85-34540
TURVER, K. E. N85-34969
TYASTO, M. I. N85-35015
N85-35083
N85-35092

U

UCKAN, N. A. N85-34692
N85-34705
UCKAN, T. N85-34705
UENO, H. N85-35001
N85-35021
N85-35035
ULMISHEK, G. N85-34469
UMA, V. N85-34985
UMERHARA, T. N85-34198
UNNAM, J. N85-34264
UO, K. N85-34666
URAMOTO, J. N85-34637
N85-34638
N85-34639
USUKI, E. N85-34191

V

VAHIA, M. N. N85-34787
N85-35045
VAINIKKA, E. N85-34826
N85-35061
N85-35069
VAKULOV, P. V. N85-34783

VALDES-GALICIA, J. F. N85-34771
N85-34859
VALENTINI, J. J. N85-34303
VALLANIA, P. N85-34990
VALTONEN, E. N85-34826
N85-35061
N85-35069
VALYSHEV, M. G. N85-34247
VANDERMEER, R. A. N85-34268
VANDERVALT, D. J. N85-34988
VANHOLLEBEKE, M. A. I. N85-34755
N85-34784
N85-35048
VANIER, P. E. N85-34451
VANIMAN, D. T. N85-34271
VANKA, S. P. N85-34363
VANMATRE, S. W. N85-34595
VAUCLAIR, S. N85-34790
VAVRA, P. C. N85-34376
VEDREMNE, G. N85-34948
N85-34957
VENKATESAN, D. N85-34837
N85-35051
VERMA, S. D. N85-35081
N85-35082
N85-35119
VERNOVA, E. S. N85-35015
VEST, C. M. N85-34376
VESTRAND, W. T. N85-34762
N85-34767
VEZZA, M. N85-34122
VIGIL, R. S. N85-34696
VIL-VILYAMS, I. F. N85-34496
VILLAREAL, J. N85-34239
VILLORESI, G. N85-34764
N85-35057
N85-35058
N85-35059
VILMER, N. N85-34741
VINET, P. N85-34265
VLAHOS, L. N85-34733
N85-34772
VOELK, H. J. N85-34900
N85-34901
VOGT, G. J. N85-34696
VOLODICHEV, N. N. N85-34789
VOLVACH, S. I. N85-34498
VONROOS, A. N85-34442
VONROSENVINGE, T. T. N85-34734
N85-34747
N85-34778
N85-34788
N85-34802
N85-35048
VONTIESENHAUSEN, G. N85-34154
VOROBYEV, O. A. N85-34501

W

WADA, M. N85-34765
N85-34807
N85-35030
N85-35031
N85-35062
N85-35079
N85-35122
N85-35123
N85-35124
N85-35126
N85-35130
WADA, T. N85-35131
WADDINGTON, C. J. N85-34863
N85-34866
N85-34888
N85-34938
N85-34939
WAKATANI, M. N85-34645
N85-34666
N85-34667
WALKER, H. N85-34587
WALLSTEN, T. S. N85-34493
WALTON, E. K. N85-34329
WANG, L. N85-35133
WANG, X. N85-34550
WASHBURN, J. N85-34623
WASSERMAN, H. J. N85-34603
WASSERMAN, L. H. N85-34725
WASTAG, M. N85-34369
WATANABE, H. N85-34744
N85-34753
WATANABE, T. N85-34646
N85-34654
N85-34685
WATARI, T. N85-34668
WATSON, A. A. N85-34974
WAYLAND, J. R., JR. N85-34389
WDOWCZYK, J. N85-34923
WEBB, G. M. N85-34841
N85-34891
N85-34926
WEBB, J. H. N85-34312
WEBBER, W. R. N85-34781
N85-34832
N85-34874
N85-34886
N85-34937
N85-35039
N85-35042
N85-35046
N85-35049
WEBER, E. R. N85-34623
WEEKES, T. C. N85-34973
WELLER, S. W. N85-34218
WENESER, J. N85-34615
WENZEL, K. P. N85-34813
WERNER, N. E. N85-34595
WESNOUSKY, S. G. N85-34467
WEST, A. A. N85-34974
WESTERGAARD, N. J. N85-34885
WESTON, L. W. N85-34612
WETHERFIELD, M. N85-34513
WEY, J. N85-34400
WHARTON, C. B. N85-34330
WHEELER, P. M. N85-34319
WHITE, R. S. N85-34952
N85-34961
WHITFIELD, R. G. N85-34493
WIBBERENZ, G. N85-34756
N85-34808
N85-34816
WIBIG, T. N85-34867
WICHMANN, B. A. N85-34513
WIEDEMANN, K. E. N85-34264
WILD, N. R. N85-34978
WILHARTITZ, P. N85-34245
WILHELMS, J. N85-34537
WILKINSON, T. P. N85-34513
WILLIAMS, R. A. N85-34609
WILSON, J. E. N85-34147
WILSON, J. L. N85-34574
WILSON, M. N85-34601
WILSON, R. B. N85-34953
N85-34954
N85-34955
WILSON, W. B. N85-34624
WINTENBERG, A. L. N85-34708
WIRTZ, W. N85-34294
WOLFENDALE, A. W. N85-34923
WONG, C. P. C. N85-34359
WOOD, D. N85-34992
N85-35047
WOODARD, M. F. N85-35103
WOOTTON, A. J. N85-34697
N85-34709
WU, S. T. N85-34158
WU, Y. S. N85-34716
WYVILL, B. N85-34526
WYVILL, G. N85-34569

X

XAO, S. N85-34999
XUE, S. N85-34999
N85-35133

Y

YABE, T. N85-34673
N85-34687
N85-34688
YADAV, J. S. N85-34865
N85-35045
N85-35117
YADAV, N. R. N85-35034
N85-35065
YADAV, R. S. N85-34851
N85-34998
N85-35034
N85-35065
YAHAGI, N. N85-34996
N85-34997
YAMABE, H. N85-34642
YAMADA, M. N85-34201
YAMADA, T. N85-34212
YAMAGIWA, M. N85-34635
YAMAGUCHI, I. N85-34678
YAMAHIRA, T. N85-34562
YAMAMASU, J. N85-34187
YAMAMOTO, I. N85-35131
YAMAMOTO, Y. N85-34183
YAMAMURA, Y. N85-34690
YAMANAKA, C. N85-34687
YAMANAKA, T. N85-34687
YAMASHITA, Y. N85-35131
YANAGIMACHI, T. N85-34806
YANAGITA, S. N85-34908
YANCHUKOVSKY, A. L. N85-34761
YANG, G. N85-34825
YANG, G. Q. N85-34334
YANG, L. C. N85-34373
YANKE, V. G. N85-34760
N85-35076
YANO, T. N85-34197
YASTREBOV, L. I. N85-34262
YASUE, S. N85-35001
N85-35007
N85-35129
YATES, D. E. N85-34316
YATES, J. T., JR. N85-34232
YATSENKO, Y. V. N85-34258
YE, Z. N85-35133
YELSHIN, V. K. N85-34902
YENNI, K. R. N85-34144
YOKOYAMA, K. E. N85-34697
YOSHIDA, F. N85-34184
YOSHIMORI, M. N85-34744
N85-34753
YOSHIOKA, Y. N85-34204
YU, C. N85-34797
N85-34872
YU, S. H. N85-35123
YU, Z. D. N85-35134
N85-35135
YUDA, T. N85-34986
YUDAKHIN, K. F. N85-35071
YUKIMACHI, H. N85-34190
YUN, S. X. N85-35095
YUN, W. N85-34384
YUUKI, R. N85-34189

Z

ZAIMA, S. N85-34203
ZALJUBOVSKI, I. I. N85-35139
ZALJUBOVSKY, I. I. N85-35140
ZALTSMAN, G. L. N85-34507
ZANDA, B. N85-35102
ZANK, A. P. N85-34892
ZANROSSO, E. M. N85-34961
ZARETSKII, Y. K. N85-34428
ZARETSKY, E. V. N85-34409
ZARITSKIY, V. V. N85-34501
ZEIGLER, J. M. N85-34293
ZELTZER, D. N85-34538
ZENCHEV, G. G. N85-35088
ZHAN, S. N85-34797
N85-34872
ZHANG, G. N85-34825
N85-34999
ZHIZNEVSKAYA, O. V. N85-34500
ZHOU, R. N85-34797
N85-34872
ZHUK, V. L. N85-34263
ZHURAVLEV, D. A. N85-34783
N85-35136
ZIMMERMANN, E. L. N85-34343
ZUBEREK, W. M. N85-34529
ZUCKER, M. S. N85-34613
ZUSHI, H. N85-34666
ZUSMANOVICH, A. G. N85-34854
N85-35070
ZYBIN, K. A. N85-34913
ZYCH, A. D. N85-34952
N85-34961
ZYKOV, I. V. N85-34435

CORPORATE SOURCE INDEX

Typical Corporate Source Index Listing

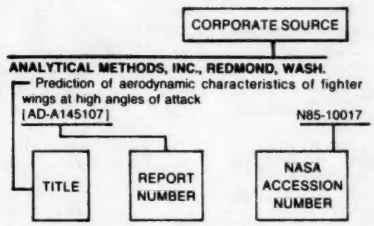

Listings in this index are arranged alphabetically by corporate source. The title of the document provides the user with a brief description of the subject matter. The report number helps to indicate the type of document cited (e.g., NASA report, translation, NASA contractor report). The NASA accession number denotes the number by which the citation is identified. The titles are arranged under each corporate source in ascending accession number order.

A

ACADEMIA SINICA, BEIJING (CHINA).
Diffusion-convection function of cosmic rays
[SH-3.2-10] N85-34825
An approach of reducing the background induced by neutrons
[OG-9.3-5] N85-34960
The corotating variation of the north-south anisotropy of cosmic rays
[SH-4.3-15] N85-34999
Recording system for the solar neutron monitoring at Mt. Norikura
[SH-9.1-8] N85-35123
The influences of the galactic cosmic ray on the atmospheric ozone
[SH-10.1-1] N85-35133

ACADEMY OF SCIENCES, POTSDAM (EAST GERMANY).
The conjecture concerning time variations in the solar neutrino flux
[SH-8.1-6] N85-35111

ACADEMY OF SCIENCES OF THE ARMENIAN SSR, ERIVAN (USSR).
Diurnal effect in cosmic rays at middle latitudes according to stratospheric measurements
[SH-4.5-8] N85-35026
Nonstationary modulation of galactic cosmic rays in a nonlinear model
[SH-4.7-10] N85-35054

ACADEMY OF SCIENCES OF THE GEORGIAN SSR, TBILISI (USSR).
The expected cosmic ray density and stream distributions at the heliolatitudinal asymmetry of solar wind
[SH-4.2-14] N85-34852
The effect of the neutral sheet structure of the interplanetary magnetic field on cosmic ray distribution in space
[SH-4.2-18] N85-34855
Spatial distribution of cosmic rays in magnetic cycles of the Sun
[SH-4.2-20] N85-34857
Azimuthal and meridional asymmetries of the solar wind and quasiperiodic variations of intensity of Galactic Cosmic Rays (GCR)
[SH-4.4-20] N85-35016
The theoretical and experimental investigation of cosmic ray Forbush-effects
[SH-5.1-20] N85-35072
Peculiarities of Galactic Cosmic Ray (GCR) anisotropy variation in connection with the recurrent and sporadic Forbush effects
[SH-5.1-21] N85-35073

ACADEMY OF SCIENCES (USSR), ALMA-ATA.
Investigation of cosmic ray propagation in interplanetary space
[SH-3.2-9] N85-34824
Effects of solar magnetic field on cosmic rays
[SH-4.2-12] N85-34850
The influence of nonstationarity of the solar activity and general solar field on modulation of cosmic rays
[SH-4.2-17] N85-34854
Frequency spectra of short-period variations of cosmic ray
[SH-5.1-17] N85-35070

ACADEMY OF SCIENCES (USSR), IRKUTSK.
The SCR flare of 16 February 1984 as recorded by the Sayan spectrograph
[SH-1.3-17] N85-34761
Diagnostic of electromagnetic conditions in space using cosmic rays
[SH-4.5-19] N85-35036
Diurnal variations of cosmic ray geomagnetic cut-off threshold rigidities
[SH-6.1-21] N85-35092

ACADEMY OF SCIENCES (USSR), LENINGRAD.
Ultrarelativistic electrons and solar flare gamma-radiation
[SH-1.3-11] N85-34757
High energy neutron and gamma-radiation generated during the solar flares
[SH-1.4-8] N85-34763
On the angular and energy distribution of solar neutrons generated in P-P reactions
[SH-1.4-9] N85-34769
The influence of quiet asymmetric magnetosphere on the cutoff rigidities of the main cone
[SH-6.1-10] N85-35083
High precise measurements of cosmogenic radiocarbon abundance by complex of scintillation equipments
[SH-7.1-14] N85-35105
Radiocarbon content in the annual tree rings during last 150 years and time variation of cosmic rays
[SH-7.1-15] N85-35106

ACADEMY OF SCIENCES (USSR), MOSCOW.
Peculiarities of propagation of charged particles in solar corona
[SH-3.1-6] N85-34810
On the influence of the heliomagnetospheric periphery on the galactic cosmic rays
[SH-4.2-19] N85-34856
The role of cosmic rays in magnetic hydrodynamics of interstellar medium
[OG-7.2-15] N85-34882
Giant molecular clouds as regions of particle acceleration N85-34913
The nucleosynthesis of deterium and helium-3
[OG-8.2-18] N85-34914
Nuclear reactions in shock wave front during supernova events
[OG-8.2-19] N85-34915
The gamma-ray telescope Gamma-1
[OG-9.2-10] N85-34949
The difference in the energy spectra of galactic cosmic rays at the minima of the 19th and 20th solar activity cycles
[SH-4.4-18] N85-35014
Cosmic ray variations with the period close to 27 days and their connection with solar activity longitudinal distribution
[SH-4.4-19] N85-35015
Dimensions of the solar wind cavity and of the region of interplanetary cosmic ray modulation
[SH-4.7-11] N85-35055
Study of cosmic ray scintillations from 5-minute data of the scintillations telescope Izmran and world-wide network stations
[SH-5.1-18] N85-35071
Cosmic ray modulation by high-speed solar wind fluxes
[SH-5.1-22] N85-35074
Solar activity beyond the disk and variations of the cosmic ray gradient
[SH-5.1-23] N85-35075
Coupling functions for lead and lead-free neutron monitors from the latitudinal measurements performed in 1982 in the research station Academician Kurchatov
[SH-6.1-1] N85-35076
Short perturbations of cosmic ray intensity and electric field in atmosphere
[SH-6.1-18] N85-35090
Long-period cosmic ray variations and their altitude dependence
[SH-6.1-19] N85-35091
The influence of the Earth's magnetosphere on the high-energy solar protons
[SH-6.1-22] N85-35093
Cosmogenic Mn-53 in meteorites
[SH-7.1-17] N85-35107
Solar cosmic ray bursts and solar neutrino fluxes
[SH-8.1-10] N85-35115
Sensitivity of single and multiple cosmic ray neutrons to the surrounding medium in a lead-free monitor
[SH-9.1-10] N85-35125
Methods and software for cosmic ray scintillation studies
[SH-9.1-17] N85-35132

ACADEMY OF SCIENCES (USSR), TROITSK.
Ground increase of cosmic ray intensity on February 16, 1984
[SH-1.3-15] N85-34760
Cosmic ray modulation in a random anisotropic magnetic field
[SH-4.1-20] N85-34839
Diffusion of strongly magnetized cosmic ray particles in a turbulent medium
[OG-7.2-16] N85-34883

ACADEMY OF SCIENCES (USSR), YAKUTSK.
Cosmic ray acceleration by stellar wind. Simulation for heliosphere
[SH-1.5-17] N85-34780
On reflecting boundary behind the Earth's orbit at propagation of fast particles from solar flares
[SH-3.2-13] N85-34827
11- and 22-year variations of the cosmic ray density and of the solar wind speed
[SH-4.2-21] N85-34858
Efficiency of regular acceleration of particles by a shock wave at different injection regimes
[OG-8.1-13] N85-34902
Long-term modulation of galactic cosmic rays in high-energy region
[SH-4.4-22] N85-35018
Change of cosmic ray anisotropy with solar activity
[SH-4.5-20] N85-35037

ADELAIDE UNIV. (AUSTRALIA).
The Buckland Park air shower array
[OG-9.4-4] N85-34971
The longitudinal thickness of air-shower fronts
[OG-9.5-1] N85-34978
A new statistic for the analysis of circular data in gamma-ray astronomy
[OG-9.5-13] N85-34989

ADMIRALTY MARINE TECHNOLOGY ESTABLISHMENT, DUNFERMLINE (SCOTLAND).
Design of transversely stiffenend FRP panels under compressive load
[AMTE(S)-R-84104] N85-34424

ADVANCED RESEARCH AND APPLICATIONS CORP., SUNNYVALE, CALIF.
Novette diagnostic support
[DE85-012937] N85-34383

AERONAUTICAL RESEARCH INST. OF SWEDEN, STOCKHOLM.
Aeroelastic constraints for a wing weight minimization procedure
[FFA-TN-1985-4] N85-34126

AERONAUTICAL RESEARCH LABS., MELBOURNE (AUSTRALIA).
Integral equation formulation for three-dimensional unsteady transonic flow
[ARL-STRUC-R-416] N85-34119
Guidelines for the evaluation of visual approach slope indicators
[ARL-SYS-R-32] N85-34132

Determination of instrument errors by compatibility checking: Results from dynamic flight test data
[ARL-AERO-R-162] N85-34137
Stresses and strains in a plate resulting from two closely-spaced interference-fit fasteners
[ARL-STRUC-TM-409] N85-34429

AEROSPACE CORP., EL SEGUNDO, CALIF.
A search for solar neutrons on a long duration balloon flight
[SH-1.4-6] N85-34766
Cosmic-ray transport in the galactic magnetosphere
[OG-7.2-17] N85-34884

AGRICULTURE-TEACHER UNIV., SIEDLCE (POLAND).
The modulation features of the long-period cosmic ray variations in connection with the sign change of the general magnetic field of the Sun
[SH-4.5-15] N85-35032

AIR FORCE FLIGHT TEST CENTER, EDWARDS AFB, CALIF.
The next assignment: The state of the literature on space N85-35146

AIR FORCE GEOPHYSICS LAB., HANSCOM AFB, MASS.
An update on the correlation between the cosmic radiation intensity and the geomagnetic AA index
[SH-4.2-24] N85-34861
The use of the McIlwain L-parameter to estimate cosmic ray vertical cutoff rigidities for different epochs of the geomagnetic field
[SH-6.1-12] N85-35085
A suggested standardized format for cosmic ray ground-level event data
[SH-9.1-15] N85-35130

AKRON UNIV., OHIO.
Measurement and correlation of jet fuel viscosities at low temperatures
[NASA-CR-174911] N85-34295

ALABAMA A & M UNIV., NORMAL.
Screening and characterizing oleaginous microalgal species from the southeastern United States
[DE85-008787] N85-34488

ALABAMA UNIV., HUNTSVILLE.
Coordinated study of solar-terrestrial payloads on space station
[NASA-CR-176160] N85-34158

ALBERTA UNIV., EDMONTON.
A new approach to linear quadtrees N85-34550
The dynamics of articulated rigid bodies for purposes of animation N85-34579

ALIGARH MUSLIM UNIV. (INDIA).
Determination of galactic cosmic ray latitudinal gradient using Earth based detectors
[SH-4.2-13] N85-34851
Cosmic ray density gradient and its dependence on the north-south asymmetry in solar activity
[SH-4.5-17] N85-35034
Influence of magnetic clouds on cosmic ray intensity variations
[SH-5.1-12] N85-35065

ALLIED BENDIX AEROSPACE, KANSAS CITY, MO.
Laser welding of 6Al-4V titanium alloy
[DE85-012019] N85-34413

ALLIED BENDIX AEROSPACE, MISHAWAKA, IND.
Hardware test program for evaluation of basline range-range rate sensor concept
[NASA-CR-176143] N85-34377

AMOCO PRODUCTION CO., CHICAGO, ILL.
Comprehensive fracture diagnostics experiement. Part 2: Comparison of seven fracture azimuth measurements
[DE85-011707] N85-34470

ANALYTICAL SERVICES AND MATERIALS, INC., TABB, VA.
An X-ray diffraction study of titanium oxidation
[NASA-CR-176263] N85-34264

AOYAMAGAKUIN UNIV., TOKYO (JAPAN).
Experimental study on time and temperature dependent behavior of crack growth in viscoelastic strip N85-34193
Influence of cyclic thermal loading on internal stress in casted epoxy resin N85-34211
Time and temperature dependence of fracture surface in soft epoxy resin N85-34213

APPLIED PHYSICS LAB., JOHNS HOPKINS UNIV., LAUREL, MD.
Prompt acceleration of ions by oblique turbulent shocks in solar flares
[SH-1.1-6] N85-34733
Energetic ion acceleration at collisionless shocks
[SH-1.5-3] N85-34772
Acceleration of ions and electrons to near-cosmic ray energies in a perpendicular shock: The January 6, 1978 event
[SH-1.5-4] N85-34773
Latitude dependence of co-rotating shock acceleration
[SH-1.5-14] N85-34777
Longitudinal distribution of cosmic rays in the heliosphere
[SH-4.1-14] N85-34837
Evidence for regions of negligible cosmic-ray modulation in the inner heliosphere (10 AU)
[SH-4.1-21] N85-34840
Voyager 1 and 2 measurements of radial and latitudinal cosmic ray gradients during 1981 - 1984
[SH-4.7-6] N85-35051

ARGONNE NATIONAL LAB., ILL.
Direct determination of metals in organic matrices by Inductively Coupled Plasma-Atomic Emission Spectrometry (ICP-AES)
[DE85-012015] N85-34233
Stress corrosion cracking susceptibility of types 316NG and 316 stainless steel in an impurity environment
[TI85-006884] N85-34277
Block-implicit calculations of three-dimensional laminar flow in strongly curved ducts
[DE85-003047] N85-34363
Mathematical modeling of ultimate heat sink cooling ponds
[TI85-009747] N85-34369
Geology and petroleum resources of basins in western China
[DE85-013038] N85-34469
Estimating risks of lead-induced hemoglobin decrements under conditions of uncertainty: Methodology, pilot judgments and illustrative calculations
[DE85-012293] N85-34493
DISPL1: A software package for one and two spatially dimensioned kinetics-diffusion problems
[ANL-84-56] N85-34516
Analytical ultrasonics for structural materials
[TI85-006132] N85-34600
Physics Division annual review, 1 April 1983 - 31 March 1984
[ANL-84-24] N85-34602
Downstream behavior of volatile fission product species
[DE85-012124] N85-34617
Magnitude and range of the RKKy interaction in SmRh4B4
[DE85-012284] N85-34712

ARIZONA UNIV., TUCSON.
Spatial variation of cosmic rays near the heliospheric current sheet
[SH-4.2-10] N85-34848
Effects of a wavy neutral sheet on cosmic ray anisotropies
[SH-4.2-11] N85-34849
The cosmic-ray shock structure problem for relativistic shocks
[OG-8.1-1] N85-34891
A model for the origin of high-energy cosmic rays
[OG-8.1-8] N85-34898
A numerical study of diffusive shock acceleration of cosmic rays in supernova shocks
[OG-8.2-2] N85-34903
Scaling from Jupiter to pulsars and the acceleration of cosmic ray particles by pulsars, 3
[OG-8.2-3] N85-34904
Relativistic transport theory for cosmic-rays
[OG-8.3-8] N85-34926
Solar modulation of cosmic ray intensity and solar flare events inferred from (14)C contents in dated tree rings
[SH-7.1-2] N85-35095

ARMY AVIATION RESEARCH AND DEVELOPMENT COMMAND, CLEVELAND, OHIO.
Mechanical properties of SiC fiber-reinforced reaction-bonded Si3N4 composites
[NASA-TM-87085] N85-34223
Generated spiral bevel gears: Optimal machine-tool settings and tooth contact analysis
[NASA-TM-87075] N85-34405
Thermal stress analysis of a new turbine shroud seal concept
[NASA-TM-87082] N85-34406

ASTRO AEROSPACE CORP., CARPINTERIA, CALIF.
STACBEAM 2
[NASA-CR-176126] N85-34442

AWADHESH PRATAP SINGH UNIV., REWA (INDIA).
Cumulative effect of Forbush decreases in the heliospheric modulation during the present solar cycle
[SH-4.1-10] N85-34833
Cosmic ray intensity distribution perpendicular to solar equatorial plane at 1 A.U. during 1978-83
[SH-4.3-14] N85-34998
Role of solar flare index in long term modulation of cosmic ray intensity
[SH-4.4-12] N85-35009
Cosmic ray power spectral variations. 3: Solar rotation periodicities
[SH-4.4-16] N85-35012
Anomalous low level of cosmic ray intensity decreases observed during 1980
[SH-5.1-15] N85-35068

B

BATTELLE COLUMBUS LABS., OHIO.
MATADOR (Methods for the Analysis of Transport And Deposition Of Radionuclides) code description and user's manual
[TI85-901402] N85-34592

BEIJING TEACHERS COLL. (CHINA).
On magnetic pair production above fast pulsar polar caps
[OG-8.2-13] N85-34909

BELL TELEPHONE LABS., INC., HOLMDEL, N. J.
The interactive planning work station: A graphics-based UNIX (trademark) tool for application users and developers N85-34527

BERN UNIV. (SWITZERLAND).
Estimating the change in asymptotic direction due to secular changes in the geomagnetic field
[SH-6.1-13] N85-35086

BIRMINGHAM UNIV. (ENGLAND).
A dominant role for protons at the onset of solar flares
[SH-1.2-13] N85-34748
The starting conditions for an optically small solar gamma ray flare
[SH-1.3-2] N85-34751

BOEING COMMERCIAL AIRPLANE CO., SEATTLE, WASH.
System maintenance manual for master modeling of aerodynamic surfaces by three-dimensional explicit representation
[NASA-CR-176224] N85-34517

BRIGHAM YOUNG UNIV., PROVO, UTAH.
Spatial trees: A fast access method for unstructured graphical data N85-34533

BRITISH BROADCASTING CORP., KINGSWOOD (ENGLAND).
The improved display of 625-line television pictures: Adaptive interpolation
[BBC-RD-1985/5] N85-34328

BRITISH LIBRARY LENDING DIV., BOSTON SPA (ENGLAND).
Ultra-trace analysis of sinter tantalum with SIMS
[BLL-RARDE-TR-1220-(7291.7965)] N85-34245
The study of the effect of residual microimpurities on the fatigue strength of 55S2 steel
[BLL-M-36317-(5828.4)] N85-34246
Enthalpies of formation of liquid Fe-Ce-Si and Fe-Ce-Al three-component alloys
[BLL-M-36296-(5828.4)] N85-34247
Towards the development of technological processes for the preparation of cadmium plated steel articles
[BLL-M-36315-(5828.4)] N85-34248
Calculating the interatomic pair potential allowing for resonance interaction in titanium, nickel and vanadium
[BLL-M-35843-(5828.4)] N85-34249
Effects of hot deformation on the kinetics of the pearlite transformation in eutectoid steel
[BLL-M-35844-(5828.4)] N85-34250
Approximate determination of the extent of the solid-liquid zone
[BLL-M-35829-(5828.4)] N85-34251
Dynamics of the melting of chromium-manganese alloys in molten steel
[BLL-M-35850-(5828.4)] N85-34252
Calculation of activities of components in liquid alloys of iron with yttrium
[BLL-M-35868-(5828.4)] N85-34253
Phase transformations taking place in austenitic steel during deformation at different rates
[BLL-M-35875-(5828.4)] N85-34254
The effect of pre-heating on the structure and properties of chromium-molybdenum steels
[BLL-M-35897-(5828.4)] N85-34255
Acoustic emission during transformation of austenite in 38KhN3MF steel
[BLL-M-35825-(5828.4)] N85-34256
Influence of technology of atomization of naturally alloyed iron on grain-size characteristics of powder material
[BLL-M-35810-(5828.4)] N85-34257
Special features of the fracture of ball-bearing steel close to non-metallic inclusion eutectics
[BLL-M-35809-(5828.4)] N85-34258
Properties of tungsten-free steel for cutting tools
[BLL-M-35808-(5828.4)] N85-34259
Chromium-base powder alloys for welding cladding layer of bimetal
[BLL-M-35776-(5828.4)] N85-34260

Changes in lattice cell parameter of film intermetallic compounds RT2
[BLL-M-35874-(5828.4)] N85-34261
The influence of temperature on the composition density of the transition metals
[BLL-M-35896-(5826.4)] N85-34262
The properties of VSt3sp inoculated steel
[BLL-M-35894-(5828.4)] N85-34263
Features of behavior of gas bubbles in molten oxide films during enamelling: Communication 2
[BLL-M-35781-(5828.4)] N85-34283
Finding the roots of the transcendental equations in problems in determining the thermal conductivity of spheres with heterogeneous boundary conditions
[BLL-M-35878-(5828.4)] N85-34347
Calculation of flow kinetics of composite media
[BLL-M-35819-(5828.4)] N85-34348
Calculation of roots of transcendental equations in problems of determining thermal conductivity of cylinder with non-uniform boundary conditions
[BLL-M-35788-(5828.4)] N85-34349
Algorithm for calculation of strain state from measurements of node coordinates of arbitrary curvilinear grid
[BLL-M-36304] N85-34422
On the potential link equation of a spot centre with relative deformation for a semi-infinite molecular crystal
[BLL-M-35795-(5828.4)] N85-34711

BROOKHAVEN NATIONAL LAB., UPTON, N. Y.
Atmospheric modeling of organics for risk assessment: A Chemist's view
[DE85-009770] N85-34217
Monitoring building energy performance: An informal review and characterization of research in progress
[BNL-51765] N85-34308
Dual-chamber plasma deposition of A-Si:H solar cells at high rates using disilane
[DE85-011828] N85-34451
Anaerobic microbial transformations in subsurface environments: Project description
[DE85-012789] N85-34486
Improved method for the stabilization of NaI-photomultiplier gamma detectors against thermal and other drift
[DE85-011830] N85-34613

BROWN UNIV., PROVIDENCE, R. I.
Time-resolved and infrared spectroscopy of excitons
[DE85-011879] N85-34235
Research issues in generating graphical explanations N85-34539
A model for a document maintenance system N85-34542

BULGARIAN ACADEMY OF SCIENCE, SOFIA.
The cosmic ray differential diurnal variation dependences on the zenith angle and the geomagnetic disturbance
[SH-4.5-16] N85-35033

BUNKA WOMEN'S UNIV. (JAPAN).
Study on the correlation between grinding conditions and residual stresses in ground surface of steel by the X-ray method N85-34203

C

CALCUTTA UNIV. (INDIA).
Solar neutrino: Flux, cosmic rays and the 11 year solar cycle
[SH-8.1-7] N85-35112
Solar neutrinos, solar flares, solar activity cycle and the proton decay
[SH-8.1-8] N85-35113

CALGARY UNIV. (ALBERTA).
Specifying stochastic objects in a hierarchical graphics system N85-34526

CALIFORNIA INST. OF TECH., PASADENA.
Effects of ambient pressure on the instability of a liquid boiling explosively at the superheat limit
[DE85-009476] N85-34370
The energy spectrum of Jovian electrons in interplanetary space
[SH-1.5-18] N85-34781
Precision measurements of solar energetic particle elemental composition
[SH-2.1-4] N85-34785
Solar Coronal and photospheric abundances from solar energetic particle measurements
[SH-2.1-5] N85-34786
Latitude variation of recurrent fluxes in the outer solar system
[SH-4.1-13] N85-34836
Measurements of Fe and Ar fragmentation cross sections
[OG-7.2-20] N85-34887
The response of ionization chambers to relativistic heavy nuclei
[OG-9.1-13] N85-34938
The response of ionization chambers to relativistic heavy nuclei
[OG-9.1-13] N85-34939
Hexagonal uniformly redundant arrays for coded-aperture imaging
[OG-9.2-1] N85-34940
A balloon-borne imaging gamma-ray telescope
[OG-9.2-2] N85-34941
Balloon-borne video cassette recorders for digital data storage
[OG-9.3-11] N85-34966
Changes in the energy spectrum of anomalous oxygen and helium during 1977-1985
[SH-4.6-1] N85-35039
Solar cycle variations of the anaomalous cosmic ray component
[SH-4.6-2] N85-35040
Solar modulation and interplanetary gradients of the galactic electrons flux, 1977 - 1984
[SH-4.7-4] N85-35049

CALIFORNIA UNIV., BERKELEY.
A theoretical and empirical analysis of coherent ray-tracing N85-34524
Using dynamic analysis to animate articulated bodies such as humans and robots N85-34537
An analysis and algorithm for filling propagation N85-34551
An intuitive approach to geometric continuity for parametric curves and surfaces N85-34571
Channeled propagation of solar particles
[SH-3.2-3] N85-34819
Elemental technetium as a cosmic-ray clock
[OG-7.1-9] N85-34870
An experiment to measure the energy spectrum of cosmic ray antiprotons from 100 to 1000 MeV
[OG-9.1-3] N85-34929
Space-age Europe, 1957-1980 N85-35148

CALIFORNIA UNIV., BERKELEY. LAWRENCE BERKELEY LAB.
Detailed validation of a liquid and heat flow code against field performance
[DE85-009901] N85-34368
Near-threshold fatigue: An overview of the role of microstructure and environment
[DE85-009903] N85-34431
Modeling of geothermal systems
[DE85-012553] N85-34439
Studies in thermo-hydro-chemical transport in porous and fractured media
[DE85-012555] N85-34473
Summary of activities, 1983
[LBL-18500] N85-34605
Formation of amorphous silicon by light ion damage
[DE85-012605] N85-34623

CALIFORNIA UNIV., DAVIS.
A model for graphics interface tool development N85-34545

CALIFORNIA UNIV., LIVERMORE. LAWRENCE LIVERMORE LAB.
Description of a test site for large-scale heavy gas dispersion and combustion experiments
[DE85-004987] N85-34231
Investigation of the flame speeds of propane/methanol gas mixtures
[DE85-012817] N85-34239
Comparison of experimental data on detonation velocity and Chapman-Jouget pressure vs initial HE density with predictions from Ree's model equation of state
[DE85-007266] N85-34304
Compressible two-phase flow instabilities simulated with a hybrid Lagrange-Euler pseudospectral method
[DE85-009904] N85-34361
New semi-implicit method for solving the time-dependent conservation equations for incompressible flow
[DE85-010926] N85-34367
Index of laser program publications and related reports, calendar year 1984
[DE85-011863] N85-34398
Marine Sample Exploitation Project: Estimates regarding the sensitivity and technology for the detection of nuclear explosion debris in the marine environment
[DE85-013176] N85-34462
Evaluation of source strength and dispersion model predications with data from large nitrogen tetroxide field experiments
[DE85-011855] N85-34465
User's guide to the MATHEW/ADPIC models
[DE85-012952] N85-34587
User's manual for the FLORA equilibrium and stability code
[DE85-013182] N85-34590
Parallel processing on the Livermore VAX 11/780-4 parallel processor system with compatability to Cray Research, Inc. (CRI) multitasking, version 1
[DE85-011856] N85-34595
Radial transport phenomena for TMX-upgrade N85-34647
Technology of magnetically driven accelerators
[DE85-011857] N85-34700
Perspective on the next ten years in plasma physics
[DE85-011849] N85-34706

CALIFORNIA UNIV., LOS ANGELES.
An innovative user interface for microcomputer-based computer-aided design N85-34555
ECH tokamak
[DE85-012074] N85-34707

CALIFORNIA UNIV., RIVERSIDE.
Measured performance of the new University of California gamma ray telescope
[OG-9.2-13] N85-34952
Neutron-induced 2.2 MeV background in gamma ray telescopes
[OG-9.3-6] N85-34961

CALIFORNIA UNIV., SAN DIEGO, LA JOLLA.
An extended superhot solar flare X-ray source
[SH-1.2-8] N85-34743
Ion energy storage for post-flare loops
[SH-1.2-10] N85-34745
On the detectability of key-MeV solar protons through their nonthermal Lyman-alpha emission
[SH-1.3-5] N85-34752
Breakdown of helium nuclei in matter processed near black holes
[OG-8.2-20] N85-34916
Advanced techniques for high resolution spectroscopic observations of cosmic gamma-ray sources
[OG-9.2-9] N85-34948
Time and energy dependence of the cosmic ray gradient in the outer heliosphere
[SH-4.7-2] N85-35047
When did the average cosmic ray flux increase?
[SH-7.1-4] N85-35097
Clusters and cycles in the cosmic ray age distributions of meteorites
[SH-7.1-11] N85-35103
Photometric and spectroscopic gamma-ray observations of solar transient phenomena using long duration balloons
[SH-9.1-5] N85-35120

CANADA LAND DATA SYSTEMS, OTTAWA (ONTARIO).
Applied computer graphics in a geographic information system: Problems and successes N85-34563

CANADIAN INFORMATION PROCESSING SOCIETY, TORONTO (ONTARIO).
Graphics Interface 1985: Proceedings
[ISSN-0713-5424] N85-34523

CASE WESTERN RESERVE UNIV., CLEVELAND, OHIO.
Modeling a high energy gamma-ray telescope
[OG-9.2-5] N85-34944
Secondary gamma-ray production in a coded aperture mask
[OG-9.2-6] N85-34945
Operating characteristics of a prototype high energy gamma-ray telescope
[OG-9.2-7] N85-34946
SONTRAC: A solar neutron track chamber detector
[SH-9.1-12] N85-35127

CENTRAL RESEARCH INST. FOR PHYSICS, BUDAPEST (HUNGARY).
Twenty-two-year cycle of the upper limiting rigidity of Daly waves
[SH-4.5-5] N85-35023

CENTRE D'ETUDE SPATIALE DES RAYONNEMENTS, TOULOUSE (FRANCE).
An improved time of flight gamma-ray telescope to monitor diffuse gamma-ray in the energy range 5 MeV - 50 MeV
[OG-9.3-2] N85-34957

CENTRE NATIONAL D'ETUDES SPATIALES, TOULOUSE (FRANCE).
Thermal protection systems for reentry vehicles
[CNES-NT-113] N85-34157
Realization and linearization of a hyperfrequency power amplifier implemented with bipolar transistors in class C polarization
[CNES-NT-114] N85-34348

CENTRE NATIONAL DE LA RECHERCHE SCIENTIFIQUE, PARIS (FRANCE).
Spallogenic origin of nuclei in meteorites
[SH-7.1-10] N85-35102

CHICAGO UNIV., ILL.
Elemental abundance differences between nuclei accelerated in CIR shocks and solar flares
[SH-2.2-6] N85-34801
The 1973-1984 solar modulation of cosmic ray nuclei
[SH-4.1-16] N85-34838

The dependence of solar modulation on the sign of the cosmic ray particle charge
[SH-4.2-23] N85-34860
Cerenkov counters for high energy nuclei: Some new developments
[OG-9.1-5] N85-34931
The development of a high energy cosmic ray detector for Spacelab-2
[OG-9.1-8] N85-34934
Galactic cosmic ray radial gradients and the anomalous He component near maximum solar modulation and to radii beyond 34 AU from the Sun
[SH-4.7-5] N85-35050
The recovery of the cosmic ray flux from maximum solar modulation at IMP-8 (1 AU) and at Pioneer (R 30 AU)
[SH-4.7-7] N85-35052
The large-scale modulation of cosmic rays in mid-1982: Its dependence on heliospheric longitude and radius
[SH-4.7-9] N85-35053
Space science and exploration: A historical perspective N85-35143

CHILDRENS HOSPITAL MEDICAL CENTER, BOSTON, MASS.
Development of the osmium-191 yields iridium-191m radionuclide generator
[DE85-011185] N85-34611
Current status of the Os-191 yields Ir-191m generator
[DE85-008306] N85-34614

CHINESE UNIV. OF HONG KONG, SHATIN.
Low cost geometric modelling system for CAM N85-34578
Long term changes in cosmic ray diurnal variations observed by ion chambers in Hong Kong and Japan
[SH-4.5-14] N85-35031
Plastic scintillators in coincidence for the study of multi-particle production of sea level cosmic rays in dense medium
[SH-9.1-11] N85-35126

CHUBU UNIV., KASUGAI (JAPAN).
Influence of the neutral sheet on the Swinson's type north-south anisotropy of cosmic rays
[SH-4.3-10] N85-34995

CINCINNATI UNIV., OHIO.
Influence of particle erosion on the microstructural changes in metals and alloys
[TI85-901384] N85-34276

CLARKSON COLL. OF TECHNOLOGY, POTSDAM, N.Y.
Multi-solute subsurface transfer modeling for energy solid wastes: Highlights FY 1984
[DE85-012788] N85-34591

COLLIER ENGINEERING, CAVE CREEK, ARIZ.
Determination of properties of zeolite/refrigerant combinations for solar refrigeration systems
[DE85-012009] N85-34448

COLOGNE UNIV. (WEST GERMANY).
The transient electromagnetic depth sounding technique applied to hydrocarbons and geothermal exploration
[MITT-42] N85-34476
Accelerator experiments on the contribution of secondary particles to the production of cosmogenic nuclides in meteorites
[SH-7.1-8] N85-35100
Depth and size effects on cosmogenic nuclide production in meteorites
[SH-7.1-9] N85-35101

COLORADO UNIV., BOULDER.
Lake ice occurence as a possible detector of atmospheric CO2 effects on climate
[DE85-012987] N85-34480

COLSPAN, INC., BOULDER, COLO.
Efficient recovery and reversal in graphical user interfaces generated by the Higgens system N85-34544

COMMISSARIAT A L'ENERGIE ATOMIQUE, SACLAY (FRANCE).
On the importance of interstellar helium for the propagation of heavy cosmic rays
[OG-7.2-11] N85-34879
Neutron-rich nuclei in cosmic rays and Wolf-Rayet stars
[OG-8.2-6] N85-34906
A high resolution gas Cerenkov detector for the superconducting magnet facility
[OG-9.1-6] N85-34932
A Cerenkov imaging telescope for high energy gamma rays
[OG-9.3-13] N85-34968

COMMITTEE ON APPROPRIATIONS (U. S. SENATE).
Department of Housing and Urban Development Independent Agencies Appropriation Bill, 1986
[S-REPT-99-129] N85-34720
National Aeronautics and Space Administration research and development: Program description N85-34721

COMMITTEE ON PUBLIC WORKS AND TRANSPORTATION (U. S. HOUSE).
Aviation safety (aircraft passenger survivability and cabin safety)
[GPO-39-847] N85-34130

CONSERVATION AND RENEWABLE ENERGY INQUIRY AND REFERRAL SERVICE, SILVER SPRING, MD.
Solar thermal technologies program summary
[DE85-012253] N85-34449

CONSIGLIO NAZIONALE DELLE RICERCHE, BOLOGNA (ITALY).
An experimental assessment of the imaging quality of the low energy gamma-ray telescope ZEBRA
[OG-9.2-8] N85-34947
Lapex: A Phoswich balloon experiment for hard X-ray astronomy
[OG-9.3-1] N85-34956
A study of periodicities and recurrences in solar activity and cosmic ray modulation
[SH-4.4-14] N85-35010
Cosmic ray biannual variation
[SH-4.4-15] N85-35011
Cosmic rays 10Be biennal data and their relationship to aurorae and sunspots
[SH-7.1-1] N85-35094

CONSIGLIO NAZIONALE DELLE RICERCHE, PALERMO (ITALY).
The Figaro experiment for the observation of time marked sources in the low energy gamma-ray range
[OG-9.2-11] N85-34950

CONSIGLIO NAZIONALE DELLE RICERCHE, ROME (ITALY).
Suggestions for improving the efficiency of ground-based neutron monitors for detecting solar neutrons
[SH-1.4-3] N85-34764
Anomalous short-term increases in the galactic cosmic ray intensity: Are they related to the interplanetary magnetic cloud-like structures?
[SH-5.1-3] N85-35057
The flare origin of Forbush decreases not associated with solar flares on the visible hemisphere of the Sun
[SH-5.1-4] N85-35058
Longitudinal dependence of the interplanetary perturbation produced by energetic type 4 solar flares and of the associated cosmic ray modulation
[SH-5.1-5] N85-35059

CONSIGLIO NAZIONALE DELLE RICERCHE, TURIN (ITALY).
The angular resolution of air shower gamma ray telescopes
[OG-9.5-14] N85-34990
Cosmic ray secular variations in terrestrial records and aurorae
[SH-7.1-3] N85-35096

COUNCIL FOR SCIENTIFIC AND INDUSTRIAL RESEARCH, PRETORIA (SOUTH AFRICA).
A new approach to evaluate gamma-ray measurements
[OG-9.5-11] N85-34988

CRANFIELD INST. OF TECH., BEDFORD (ENGLAND).
Proceedings of the Mechanisms Conference, volume 1 N85-34309
Some problems in high speed gears and gearing N85-34312
High powered epicyclic gears: Some recent development N85-34316
The use of ultrasound to monitor incipient failure of rolling element bearings N85-34317
Proceedings of the Mechanisms Conference, volume 2 N85-34318
An introduction to finite elements N85-34319
Inertial stresses and deformations in mechanisms N85-34320
Optimisation in the computer aided design of mechanisms N85-34321
Software for mechanism design N85-34324

D

DELAWARE UNIV., NEWARK.
Viscoelastic behavior of short-fiber composite materials
[DE85-011233] N85-34225

DEPARTMENT OF ENERGY, NEW YORK.
EML pulse ionization chamber systems for (222)Rn measurements
[DE85-012320] N85-34610

DEPARTMENT OF ENERGY, WASHINGTON, D. C.
Method of distributing liquefaction catalysts in solid carbonaceous material
[DE85-005759] N85-34218
Process for functionalizing alkanes
[DE85-006420] N85-34219
Method for extracting lanthanides and actinides from acid solutions by modification of Purex solvent
[DE85-005763] N85-34220
Method for controlling the viscosity of siloxane oils
[DE85-011586] N85-34221
Composite desiccant structure
[DE85-006400] N85-34226
Improved negative ion source
[DE85-006445] N85-34241
Method for preparing high purity vanadium
[DE85-006412] N85-34242
Manufacturing process to reduce large grain growth in zirconium alloys
[DE85-011649] N85-34267
Method for preparing hydride configurations and reactive metal surface
[DE85-006443] N85-34274
Nitriding of super alloys for enhancing physical properties
[DE85-005762] N85-34275
Rigid zeolite containing polyurethane foams
[DE85-006406] N85-34286
Method for removing oxide contamination from silicon carbide powders
[DE85-011648] N85-34287
High temperature polymer concrete
[DE85-005756] N85-34290
High temperature structural insulating material
[DE85-006361] N85-34291
Method for making a low density polyethylene waste form for safe disposal of low level radioactive material
[DE85-006401] N85-34292
Conductor-polymer composite electrode materials
[DE85-005766] N85-34293
Preparation of ethylenediamine dinitrate
[DE85-006423] N85-34305
Ethylenediamine salt of 5-nitrotetrazole and preparation
[DE85-005738] N85-34306
Combined cold compressor/ejector helium refrigerator
[DE85-006408] N85-34326
Series-counterpulse repetitive-pulse inductive storage circuit
[DE85-006438] N85-34342
Fast shutter apparatus
[DE85-006501] N85-34343
Reversing-counterpulse repetitive-pulse inductive storage circuit
[DE85-006409] N85-34344
Apparatus for unilateral generation of a homogeneous magnetic field
[DE85-006001] N85-34345
Apparatus and method for the spectrochemical analysis of liquids using the laser spark
[DE85-005749] N85-34387
Multiple-stage integrating accelerometer
[DE85-006505] N85-34388
Method for determining depth and shape of a sub-surface conductive object
[DE85-006502] N85-34389
Improved flow cytometer measurement of binding assays
[DE85-006407] N85-34390
Acoustic cross-correlation flowmeter for solid-gas flow
[DE85-005988] N85-34391
Oxygen analyzer
[DE85-006002] N85-34392
Electronic imaging system and technique
[DE85-005740] N85-34393
Evacuate and backfill apparatus and method
[DE85-006018] N85-34411
Apparatus producing constant cable tension for intermittent demand
[DE85-006434] N85-34412
Feedback regulated induction heater for a flowing fluid
[DE85-006508] N85-34414
Electrically conductive containment vessel for molten aluminum
[DE85-006518] N85-34415
Gas shielding apparatus
[DE85-005992] N85-34416
Control system for fluid heated steam generator
[DE85-005734] N85-34417
Nonsaturable microdryer
[DE85-005760] N85-34457
Solar system fault detection
[DE85-005987] N85-34458
Fuel cell separator plate with bellows-type sealing flanges
[DE85-005991] N85-34459
Electrolyte resevoir for carbonate fuel cells
[DE85-005736] N85-34460
Neutral particle beam intensity controller
[DE85-006411] N85-34604
Liquid uranium alloy-helium fission reactor
[DE85-006511] N85-34607

Specificity of (71)Ga(p,n) (71)Ge at 35 MeV for Gamow-Teller strength
[DE85-011837] N85-34615
Container for radioactive materials
[DE85-005757] N85-34626
Separation of uranium from technetium in recovery of spent nuclear fuel
[DE85-006499] N85-34627
Fiber optics interface for a dye laser oscillator and method
[DE85-005765] N85-34633
Method of precisely modifying predetermined surface layers of a workpiece by cluster ion impact therewith
[DE85-006519] N85-34710
Analyzing performance of small projects using URS and PMAS, information pamphlet
[DE85-011964] N85-34718

DEPARTMENT OF THE AIR FORCE, WASHINGTON, D.C.
Carbon/carbon combustor external insulation
[AD-D011719] N85-34224
Wide-band phase locked loop amplifier apparatus
[AD-D011720] N85-34337
Low noise polycrystalline semiconductor resistors by hydrogen passivation
[AD-D011721] N85-34338
Reducing grating lobes due to subarray amplitude tapering
[AD-D011723] N85-34339
Brush and commutator segment torquer motor
[AD-D011726] N85-34340
Rotor blade test apparatus
[AD-D011725] N85-34381
Hermetic chip carrier compliant soldering pads
[AD-D011722] N85-34410
Maintenance port system
[AD-D011724] N85-34594
Differentiating spatial light modulator
[AD-D011727] N85-34632

DEUTSCHER WETTERDIENST, OFFENBACH AM MAIN (WEST GERMANY).
Reports from the German Meteorological Service. No. 166: The optimal spectral density of climatological station networks
[ISBN-3-88148-214-8] N85-34478
Reports from the German Meteorological Service. No. 167: Results of aerological soundings in the model area upper Rhine: Heat release project upper Rhine area, part 3
[ISBN-3-88148-216-4] N85-34479

DU PONT DE NEMOURS (E. I.) AND CO., AIKEN, S.C.
Determination of low chloride values in Rocky Flats scrub alloy solutions and other complex matrices
[DE85-011506] N85-34234

DURHAM UNIV. (ENGLAND).
The University of Durham Mark 3 very high energy gamma ray telescope
[OG-9.4-2] N85-34969

E

ECOLE NATIONALE SUPERIEURE DES TELECOMMUNICATIONS, PARIS (FRANCE).
Telecommunication market research processing
[ENST-83E018] N85-34331

ECOLE POLYTECHNIQUE, MONTREAL (QUEBEC).
A geometric modeller for turbomachinery applications N85-34556
A graphics interface for interactive simulation of packet-switched networks N85-34558

ECOLE POLYTECHNIQUE, PALAISEAU (FRANCE).
An image management kernel for the design of relational and pictorial data bases N85-34532

EDGERTON, GERMESHAUSEN AND GRIER, INC., GOLETA, CALIF.
The 1984 biotic studies of Yucca Mountain, Nevada test site, Nye County, Nevada
[DE85-011715] N85-34487
Real-time multiparameter pulse processing with decision tables
[DE85-011683] N85-34589

EDGERTON, GERMESHAUSEN AND GRIER, INC., IDAHO FALLS, IDAHO.
Test plan for performance testing of the Eaton AC-3 electric vehicle
[DE85-011954] N85-34341
Forced convective, nonequilibrium, post-CHF heat transfer experiment data and correlation comparison report
[TI85-009331] N85-34371

ELECTRICITY COUNCIL, LONDON (ENGLAND).
The development of titanium production in the USSR
[BLL-OA-TRANS-3226-(6196.3)] N85-34244

ENKA A.G., WUPPEPTAL (WEST GERMANY).
Substitution of asbestos by aramid fibers and fiber blends in industrial textiles and composites with organic binders
[BMFT-FB-T-85-006] N85-34294

ENSIEG, SAINT MARTIN D'HERES (FRANCE).
Recognition and clear representation of handwritten electronic diagrams N85-34541

F

FORSCHUNGSINSTITUT DER DEUTSCHEN BUNDESPOST, DARMSTADT (WEST GERMANY).
Theoretical principles of vertical subsampling of color difference signals at half the sampling rate
[FI-447-TBR-18] N85-34332

FRANKLIN INST., NEWARK, DEL.
The energy spectra of solar flare electrons
[SH-1.2-14] N85-34749
Further observations of protons resulting from the decay of neutrons ejected by solar flares
[SH-1.4-2] N85-34763
The Jovian electron spectrum: 1978-1984
[SH-1.5-19] N85-34782
Anomalous abundances of solar energetic particles and coronal gas: Coulomb effects and First Ionization Potential (FIP) ordering
[SH-2.1-10] N85-34791
Geometry of the diffusive propagation region in the August 14, 1982 solar electron event
[SH-3.1-5] N85-34809
Exponential anisotropy of solar cosmic rays
[SH-3.2-1] N85-34817
Cosmic ray north-south anisotropy 1961 - 1983
[SH-4.2-6] N85-34844
Magnetic fluctuation and cosmic ray diurnal variations
[SH-4.5-21] N85-35038

FUKUSHIMA UNIV. (JAPAN).
Cosmic ray sidereal diurnal variation of galactic origin observed by neutron monitors
[SH-4.4-2] N85-35000

G

GA TECHNOLOGIES, INC., SAN DIEGO, CALIF.
SP-100 Thermionic Technology Program
[DE85-012311] N85-34625
Activities of the RF Section N85-34646
Model of azimuthal non-uniformities induced by RF heating in RFC-XXM N85-34658

GE-CALMA CO., SUNNYVALE, CALIF.
Architecture of languages for large CAD systems development N85-34557

GENERAL DYNAMICS INTERNATIONAL CORP., TOKYO (JAPAN).
On high strain rate fragmentation of a closed vessel N85-34187

GENERAL ELECTRIC CO., CINCINNATI, OHIO.
High pressure compressor component performance report
[NASA-CR-168245] N85-34138
Component-specific modeling
[NASA-CR-174765] N85-34140
Energy efficient engine. Fan and quarter-stage component performance report
[NASA-CR-168070] N85-34141

GENERAL ELECTRIC CO., SCHENECTADY, N. Y.
Manufacturing process to reduce large grain growth in zirconium alloys
[DE85-011649] N85-34267

GENEVA UNIV. (SWITZERLAND).
Computer analysis techniques for the temporal evaluation of cardiac wall motion N85-34530
A computerized system for spot detection and analysis of two-dimensional electrophoresis images N85-34531
A general purpose image processing package N85-34549

GEOLOGICAL SURVEY, DENVER, COLO.
Uranium, thorium isotopic analyses and uranium-series ages of calcite and opal and stable isotopic compositions of calcite from drill cores UE25a no. 1, USR G-2 and USW G-3/GU-3, Yucca Mountain, Nevada
[DE85-013039] N85-34471

GEOLOGICAL SURVEY, LARAMIE, WYO.
Geothermal resources of the Laramie, Hanna and Shirley Basins, Wyoming
[DE85-005005] N85-34436

GEOLOGICAL SURVEY, WASHINGTON, D.C.
The United States Geological Survey in Alaska: Accomplishments during 1983
[USGS-CIRC-945] N85-34468

GEORGE WASHINGTON UNIV., WASHINGTON, D.C.
Opportunities for policy historians: The evolution of the US civilian space program N85-35147

GLASGOW UNIV. (SCOTLAND).
A design procedure to modify the trailing edge upper surface pressure gradient of a given aerofoil
[GU-AERO-8408] N85-34120
The aerodynamic characteristics of a GU25-5(11)8 aerofoil for low Reynolds numbers
[GU-AERO-8410] N85-34121
Modelling of unsteady, incompressible separation on an aerofoil using an inviscid flow algorithm
[GU-AERO-8412] N85-34122
The collected data for ramp function tests on a NACA 23012 aerofoil. Volume 1: Description and pressure data
[GU-AERO-8413-VOL-1] N85-34123
An investigation into the three-dimensional stall development on a modified NACA 23012 aerofoil
[GU-AERO-8414] N85-34124
Comments on the prediction of dynamic stall
[GU-AERO-8501] N85-34125

GOODYEAR ATOMIC CORP., PIKETON, OHIO.
Upgrading auxiliary facility outleakage and combustion detection
[DE85-012796] N85-34386

GOVERNMENT ENGINEERING COLL., REWA (INDIA).
Study of dominating parameters of high speed solar plasma streams in relation to cosmic ray and geomagnetic storms
[SH-5.1-11] N85-35064

GRUNDEY (KLAUS), ESSEN (WEST GERMANY).
A user-friendly computer-aided construction of boundaries N85-34564

GUJARAT UNIV., AHMEDABAD (INDIA).
Observation of energy spectrum of electron albedo in low latitude region at Hyderabad, India
[SH-6.1-7] N85-35081
Proton albedo spectrum observation in low latitude region at Hyderabad, India
[SH-6.1-8] N85-35082
A bi-directional charged particle telescope to observe flux, energy spectrum and angular distribution of relativistic and non-relativistic particles
[SH-9.1-4] N85-35119

H

HARVARD-SMITHSONIAN CENTER FOR ASTROPHYSICS, CAMBRIDGE, MASS.
An observatory to study 10 (10) to 10 (17) by EV gamma rays
[OG-9.4-6] N85-34973

HAWAII UNIV., HONOLULU.
Wind energy battery storage, phase 2
[DE85-009753] N85-34450

HIMEJI INST. OF TECH. (JAPAN).
Bounce resonance heating and radial transport of electrons N85-34655

HIROSHIMA UNIV. (JAPAN).
Mechanical ratcheting behaviors of a steel pipe under combined cyclic axial load and internal pressure N85-34184
Rotating bending fatigue strength of silicon carbide and alumina-fiber reinforced aluminum N85-34208
RF induced radial diffusion in tandem mirrors N85-34649
Possibility of potential generation by lower hybrid wave N85-34654

HOKKAIDO INDUSTRIAL RESEARCH INST. (JAPAN).
Poly-functional building material from fiberglass (its fabrication and properties) N85-34209

HUBEI RESEARCH INST. OF ENVIRONMENTAL PROTECTION, WUHAN (CHINA).
Using the information of cosmic rays to predict influence epidemic
[SH-10.1-2] N85-35134
Strong earthquakes, novae and cosmic ray environment
[SH-10.1-3] N85-35135

HULBURT (E. O.) CENTER FOR SPACE RESEARCH, WASHINGTON, D.C.
The heavy ions in space experiment
[OG-9.1-10] N85-34936

HYDRAULIC RESEARCH TEXTRON, IRVINE, CALIF.
Intelligent redundant actuation system requirements and preliminary system design
[NASA-CR-177366] N85-34136

I

IBARAKI UNIV., HITACHI (JAPAN).
Interstellar (Na-22) as a possible source of the excess (Ne-22) in the galactic cosmic ray
[OG-8.2-12] N85-34908

IBM ITALIA, ROME.
An integrated system for printing and publishing applications N85-34540
ILLINOIS UNIV. OBSERVATORY, URBANA.
Joint services electronics program
[AD-A154748] N85-34336
ILLINOIS UNIV., URBANA.
Mathematical modeling of ultimate heat sink cooling ponds
[TI85-009747] N85-34369
ILLINOIS UNIV., URBANA-CHAMPAIGN.
Theoretical and experimental analyses of the performance of two-color laser ranging systems
[NASA-CR-176159] N85-34397
Quasiperiodic oscillations in bright galactic-bulge X-ray sources
[NASA-CR-176138] N85-34723
IMPERIAL COLL. OF SCIENCE AND TECHNOLOGY, LONDON (ENGLAND).
Three-dimensional finite element failure model for predicting failure in fibre reinforced bolted joints
[BR94778] N85-34423
Colour coding scales and computer graphics N85-34568
Pitch angle distributions of 35-1000 keV protons at quasi-perpendicular interplanetary shocks
[SH-1.5-6] N85-34775
INDIANA UNIV., BLOOMINGTON.
Metal alkoxides: Models for metal oxides. Alkoxide ligands in early transition metal organometallic chemistry
[DE85-011368] N85-34269
INDORE UNIV. (INDIA).
Correlation between solar neutrino flux and other solar phenomena N85-35109
INDUSTRIAL TECHNICAL SERVICES, MONTREAL (QUEBEC).
NAPGEN: Automatic NAPLPS page generator N85-34575
INFOLYTICA CORP., MONTREAL (QUEBEC).
Developing graphical tools with minimal GKS N85-34573
INSTITUT D'AERONOMIE SPATIALE DE BELGIQUE, BRUSSELS.
Agents and effects of ozone trends in the atmosphere
[AERONOMICA-ACTA-A-287-1984] N85-34466
INSTITUT FRANCO-ALLEMAND DE RECHERCHES, ST. LOUIS (FRANCE).
A comparison of laser Doppler anemometry and probe measurements within the boundary layer of an airfoil at subsonic flow
[ISL-CO-219/84] N85-34127
Study of boundary layer separation on a supercritical profile with a spoiler by means of a laser Doppler velocimeter
[ISL-CO-225/84] N85-34128
Detonation of condensed explosives: Evolution of knowledge in the last 40 years
[ISL-CO-228/84] N85-34307
The use of optical fibers in pulsed laser holography
[ISL-CO-226/84] N85-34395
Flash X-ray diffraction
[ISL-CO-227/84] N85-34396
Chemical lasers
[ISL-R-107/84] N85-34400
OMEGA: Optoelectronic measurement of the incidence angle of a projectile
[ISL-CO-223/84] N85-34634
INSTITUT NATIONAL POLYTECHNIQUE, TOULOUSE (FRANCE).
Tunisian climate seen through a Markov process
[CT-585] N85-34482
INSTITUTE FOR COMPUTER APPLICATION RESEARCH AND UTILIZATION IN SCIENCE, INC., BOSTON, MASS.
Scalar/Vector potential formulation for compressible viscous unsteady flows
[NASA-CR-3921] N85-34113
INSTITUTE OF OCEANOGRAPHIC SCIENCES, WORMLEY (ENGLAND).
A manual of methods for the continuous flow determination of ammonia, nitrate-nitrite, phosphate and silicate in seawater
[IOS-177] N85-34243
Research at the Institute of Oceanographic Sciences related to the possible disposal of radioactive waste on or beneath the seafloor
[IOS-204] N85-34528
INSTITUTE OF PHYSICAL AND CHEMICAL RESEARCH, SAITAMA (JAPAN).
Dissipation terms in one-dimensional hydrodynamic code for ICF target N85-34677
INSTITUTE OF PHYSICAL AND CHEMICAL RESEARCH, TOKYO (JAPAN).
Coronal propagation of solar flare particles observed by satellite
[SH-3.1-2] N85-34807
Diurnal variations from muon data at Takeyama underground station
[SH-4.5-13] N85-35030
Transient cosmic ray increase associated with a geomagnetic storm
[SH-5.1-8] N85-35062
Altitude variations of cosmic-ray soft and hard components observed by airborne detectors
[SH-6.1-5] N85-35079
INSTITUTO NACIONAL DE TECNICA AEROESPACIAL, MADRID (SPAIN).
A silicon surface barrier telescope for solar particles identification
[SH-9.1-3] N85-35118
INTERAMERICA RESEARCH ASSOCIATES, ROSSLYN, VA.
Climate modeling: A retrospective-prospective view with consideration for the atmospheric carbon dioxide-climate issue
[DE85-011532] N85-34481
IWATE UNIV., MORIOKA (JAPAN).
Characteristics of cosmic ray pole-equator anisotropy derived from spherical harmonic analysis of neutron monitor data
[SH-4.3-12] N85-34996
First zonal harmonic component of cosmic ray neutron intensity
[SH-4.3-13] N85-34997

J

JET PROPULSION LAB., CALIFORNIA INST. OF TECH., PASADENA.
Spacecraft (Mobile Satellite) configuration design study
[NASA-CR-176153] N85-34152
Method and apparatus for Delta Kappa synthetic aperture radar measurement of ocean current
[NASA-CASE-NPO-15704-1] N85-34327
Method and apparatus for transfer function simulator for testing complex systems
[NASA-CASE-NPO-15696-1] N85-34333
Evaluation of half wave induction motor drive for use in passenger vehicles
[NASA-CR-176119] N85-34334
Evaluation of semiconductor devices for Electric and Hybrid Vehicle (EHV) ac-drive applications, volume 1
[NASA-CR-176118] N85-34335
Instrumentation for sensing moisture content of material using a transient thermal pulse
[NASA-CASE-NPO-15493-2] N85-34373
STACBEAM 2
[NASA-CR-176126] N85-34442
Flat-plate solar array project process development area process research of non-CZ silicon material
[NASA-CR-176117] N85-34445
Investigation of test methods, material properties, and processes for solar cell encapsulants
[NASA-CR-176132] N85-34446
Development of metallization process: FSA project, cells and module formation research area
[NASA-CR-176136] N85-34447
Ranging system which compares an object reflected component of a light beam to a reference component of the light beam
[NASA-CASE-NPO-15865-1] N85-34629
Shuttle car loading system
[NASA-CASE-NPO-15949-1] N85-34722
Low energy proton bidirectional anisotropies and their relation to transient interplanetary magnetic structures: ISEE-3 observations
[SH-3.1-9] N85-34813
Interstellar turbulence, random density variations, and scintillation measurements
[OG-7.2-13] N85-34880
Gradients and anisotropies of high energy cosmic rays in the outer heliosphere
[SH-4.3-7] N85-34992
JOINT PUBLICATIONS RESEARCH SERVICE, ARLINGTON, VA.
USSR report: Life sciences. Biomedical and behavioral sciences
[JPRS-UBB-85-021] N85-34489
Microorganisms in space flight N85-34490
USSR report: Space Biology and Aerospace Medicine, vol. 19, no. 3, May - June 1985
[JPRS-USB-85-005] N85-34494
Fluid-electrolyte metabolism and renal function in cosmonauts following 185-day spaceflight N85-34495
Tolerance to +Gz and +Gx accelerations of individuals in older age groups in good health and with early signs of arteriosclerosis N85-34496
Effect of hypokinesia and +Gz accelerations on transport function of human blood N85-34497
Oxygenation and regional circulation in gingival mucosa during exposure to lower body negative pressure N85-34498
Effect of water immersion of parameters of central hemodynamics in individuals over 45 years old N85-34499
Lipid hydrolysis in man during antiorthostatic hypokinesia N85-34500
Dissociation of autonomic and sensory vestibular reactions N85-34501
Rat skeletal muscles with simulation of physiological effects of weightlessness (morphological study) N85-34502
Effect of acute hypoxia on coronary and systemic hemodynamics N85-34503
Effect of dibazol on parameters of nonspecific resistance of subjects in pressurized cabins N85-34504
Effect of seeds of heavy charged particles of galactic cosmic radiation N85-34505
Monitoring dosage of volatile compounds in tests at low barometric pressure N85-34506
Determination of individual tolerance in hyperbaric oxygen N85-34507
Lipogenesis in rat liver after flight aboard Cosmos-1129 biosatellite N85-34508
Problems of aviation and space medicine and psychology discussed at 14th Gagarin lectures N85-34509

K

KALININ (M. I.) POLYTECHNICAL INST., LENINGRAD (USSR).
On the connection between the 3HE-enrichment and spectral index of solar energetic particles
[SH-2.2-9] N85-34804
The plasma mechanism for preferential acceleration of heavy ions
[SH-2.2-10] N85-34805
On the cosmic ray diffusion in a violent interstellar medium
[OG-7.2-14] N85-34881
KAMAN AEROSPACE CORP., BLOOMFIELD, CONN.
Automated dynamic analytical model improvement for damped structures
[NASA-CR-177945] N85-34425
KANAGAWA UNIV., YOKAHAMA (JAPAN).
The cosmic ray composition as viewed from the chemical abundances of the solar system
[OG-7.1-8] N85-34869
The 4He1H ratios in the chemical compositions of solar flare particles and the primordial solar nebula
[SH-7.1-12] N85-35104
A possible mechanism to cause the quasi-biennial variability on the solar neutrino flux
[SH-8.1-5] N85-35110
KANAZAWA INST. OF TECH. (JAPAN).
Statistical pooling method of fatigue data for reliability design N85-34198
KANSAS UNIV., LAWRENCE.
Particle acceleration due to shocks in the interplanetary field: High time resolution data and simulation results
[SH-1.5-5] N85-34774
Solar and interplanetary particles at 2 to 4 MEV during solar cycles 21, solar cycle variations of event sizes, and compositions
[SH-1.5-16] N85-34779
KAZAN STATE UNIV. (USSR).
Additional flux of particles and albedo-electrons in upper atmosphere
[SH-6.1-6] N85-35080
KEIO UNIV., YOKAHAMA (JAPAN).
On the heat flux derived by the moment method in Lorentzian plasma between hot and cold walls N85-34682
KENT STATE UNIV., OHIO.
Robot environment expert system
[NASA-CR-3915] N85-34593
KENTUCKY UNIV., LEXINGTON.
Electron photoejection in carbanions
[DE85-011747] N85-34230
Electron photoejection in carbanions
[DE85-011748] N85-34237
KHARKOV STATE UNIV. (USSR).
Sporadic radio emission connected with a definite manifestation of solar activity in the near Earth space
[SH-10.1-8] N85-35139
Near Earth space sporadic radio emission busts occurring during sunrise
[SH-10.1-9] N85-35140
KIEL UNIV. (WEST GERMANY).
Injection of energetic particles following the gamma-ray flares on June 7, 1980, as observed on Helios 1
[SH-1.3-9] N85-34756

Coronal propagation of flare associated electrons and protons
[SH-3.1-3] N85-34808
Pitch angle distributions of solar energetic particles and the local scattering properties of the interplanetary magnetic field
[SH-3.1-13] N85-34816
The local characteristic function of interplanetary particle propagation
[SH-3.2-8] N85-34823
Pulsars as cosmic ray particle accelerators: Proton orbits
[OG-8.2-21] N85-34917
Pulsars as cosmic ray accelerators: Energy development of protons
[OG-8.2-22] N85-34918
Pulsars as cosmic ray particle accelerators: Dynamics of electrons
[OG-8.2-23] N85-34919
Cherenkov-dE/dx-range measurements on cosmic ray iron group nuclei
[OG-9.1-12] N85-34937
An EAS experiment at mountain altitude for the detection of gamma-ray sources
[OG-9.4-5] N85-34972
Measurement of low energy cosmic rays aboard Spacelab-1
[SH-10.1-6] N85-35137
Heavy cosmic ray measurement aboard Spacelab-1
[SH-10.1-7] N85-35138

KMS FUSION, INC., ANN ARBOR, MICH.
Modular digital holographic fringe data processing system
[NASA-CR-177952] N85-34376

KOBE UNIV. (JAPAN).
Behaviors of stress waves in a conical bar N85-34182
Neutrino production from the solar atmosphere
[SH-8.1-9] N85-35114

KOCHI UNIV., AKEBONO (JAPAN).
On the solar cycle variation in the barometer coefficients of high latitude neutron monitors
[SH-6.1-2] N85-35077
Burst size distributions in the digitized data of the ion chambers t Mt. Norikura and sea level stations
[SH-9.1-9] N85-35124

KUNSAN NATIONAL UNIV., MIRYOUN-DONG, KUNSAN-CITY (SOUTH KOREA).
Comparisons of monthly mean cosmic ray counting rates observes from worldwide network of neutron monitors
[SH-9.1-7] N85-35122

KYOTO INST. OF TECH. (JAPAN).
Numerical solutions of the Vlasov equation N85-34672

KYOTO UNIV. (JAPAN).
The influence of temperature on static and dynamic SCC crack growth behavior in aluminum alloy N85-34190
A fractographic study on mode 2 and mode 3 SCC crack growth in an Al-Zn-Mg alloy N85-34191
Strength properties of glassfiber reinforced thermoplastics N85-34212
Computational study on excitation, propagation and 3 omega -heating due to the ion Bernstein wave
[IPPJ-733] N85-34641
Behavior of helically-trapped fast ion orbits in heliotron E N85-34666
Neoclassical diffusion including ellipticity in a heliotron-like configuration N85-34667
Numerical simulation in astrophysics: Smoothed particle methods N85-34674

KYUSHU UNIV., FUKUOKA (JAPAN).
Negative flexural behavior of precase composite slabs with steel joint N85-34183

L

LAMONT-DOHERTY GEOLOGICAL INST., PALISADES, N. Y.
Scaling differences between large interplate and intraplate earthquakes
[NASA-CR-176149] N85-34467

LEEDS UNIV. (ENGLAND).
A new array for the study of ultra high energy gamma-ray sources
[OG-9.4-7] N85-34974
Cerenkov light images of EAS produced by primary gamma
[OG-9.5-3] N85-34979
Shower disc sampling and the angular resolution of gamma-ray shower detectors
[OG-9.5-2] N85-34980

LEHIGH UNIV., BETHLEHEM, PA.
Designing a graphics application interface N85-34574

LIEGE UNIV. (BELGIUM).
Germanium and lead: Significant differences between meteoritic and photospheric abundances?
[OG-7.1-2] N85-34864

LINCOLN LAB., MASS. INST. OF TECH., LEXINGTON.
Effect of interference on the performance of a minimum TCAS 2
[FAA/PM-84/33] N85-34131

LIVERPOOL POLYTECHNIC (ENGLAND).
Intermittent motion N85-34323

LODZ UNIV. (POLAND).
Propagation and nucleosynthesis of ultraheavy cosmic rays
[OG-7.1-5] N85-34867
Secondary to primary ratio and the continuous acceleration
[OG-8.3-4] N85-34923

LOS ALAMOS NATIONAL LAB., N. MEX.
Three-dimensional hydrodynamic hot-spot model
[DE85-009587] N85-34301
Effect of precipitation variables on the specific surface and explosion characteristics of pentaerythritol tetranitrate
[DE85-009620] N85-34302
CYLTRAN calculations of electron effects on XD detectors
[LA-10264-MS] N85-34601
General-purpose heat source development: Safety test program. Postimpact evaluation, design iteration test
[LA-10034-SR] N85-34606

LOS ALAMOS SCIENTIFIC LAB., N. MEX.
Iron and manganese in oxide minerals and in glasses: Preliminary consideration of Eh buffering potential at Yucca Mountain, Nevada
[DE85-011892] N85-34271
Intermolecular explosives
[DE85-009609] N85-34296
Detonation in tungsten-loaded HMX
[DE85-009606] N85-34299
Modeling heterogeneous high explosive burn with an explicit hot-spot process
[DE85-009593] N85-34300
Real time analysis of PETN detonation products
[DE85-009581] N85-34303
Vapor phase heat transport concepts
[DE85-009550] N85-34366
Workshop on Recent Research in the Valles Caldera
[DE85-010569] N85-34472
Electron density distribution analysis for nitroguanidine
[DE85-009598] N85-34603
Observations on (3)He neutron spectrometry
[DE85-010731] N85-34608
Synthesis of ultrafine ceramic and metallic powders in a thermal argon rf plasma
[DE85-009634] N85-34696
Cosmogenic-nuclide production by primary cosmic-ray protons
[SH-7.1-6] N85-35098
Cosmic-ray exposure records and origins of meteorites
[SH-7.1-7] N85-35099

LOUGHBOROUGH UNIV. OF TECHNOLOGY (ENGLAND).
A versatile computer package for mechanism analysis N85-34314
A versatile computer package for mechanism analysis, part 2: Dynamics and balance N85-34315

LOWELL OBSERVATORY, FLAGSTAFF, ARIZ.
The 13 November 1984 occultation of BD +08 deg 0471 by (1) Ceres
[NASA-CR-176106] N85-34725

M

MALAYA UNIV., KUALA-LUMPUR.
Second-order Compton-Getting effect on arbitrary intensity distribution
[SH-3.1-10] N85-34814
Determination of the pitch-angle distribution and transverse anisotropy of interplanetary particles
[SH-3.1-11] N85-34815

MARTIN MARIETTA AEROSPACE, DENVER, COLO.
Box truss analysis and technology development. Task 1: Mesh analysis and control
[NASA-CR-172570] N85-34156

MARYLAND UNIV., COLLEGE PARK.
Spatial dependence of the local diffusion coefficient measured upstream of the November 12, 1978 interplanetary traveling shock
[SH-1.5-12] N85-34776
Constraints of solar flare particle transport models from anisotropy observations at Voyager 1
[SH-3.1-8] N85-34812
Radial transport of approximately 1 MeV/nucleon ions during the 22 November 1977 solar particle event
[SH-3.2-5] N85-34821
The dispersive evolution of charged-particle bunches in random magnetic fields
[SH-4.1-2] N85-34828
Numerical descriptions of cosmic-ray transport
[SH-4.1-3] N85-34829
Numerical and analytic descriptions of cosmic-ray transport
[SH-4.1-4] N85-34830
Relativistic cosmic ray spectra in the full non-linear theory of shock acceleration
[OG-8.1-6] N85-34896
Temporal variations of the anomalous oxygen component, 1977 - 1984
[SH-4.6-3] N85-35041

MASSACHUSETTS INST. OF TECH., CAMBRIDGE.
Towards an integrated view of 3-D computer character animation N85-34538
The idea of space exploration N85-35150

MAX-PLANCK-INST. FUER AERONOMIE, KATLENBURG-LINDAU (WEST GERMANY).
Possible detection of flare-generated positrons by Helios 1 on 3 Jun 1982
[SH-1.4-10] N85-34770

MAX-PLANCK-INST. FUER ASTROPHYSIK, GARCHING (WEST GERMANY).
Do supernovae of type 1 paly a role in cosmic-ray production?
[OG-8.2-5] N85-34905

MAX-PLANCK-INST. FUER EXTRATERRESTRISCHE PHYSIK, GARCHING (WEST GERMANY).
The mean ionic charges of N, Ne, MG, SI and S in solar energetic particle events
[SH-2.1-11] N85-34792
Calculations of heavy ion charge state distributions for nonequilibrium conditions
[SH-2.1-12] N85-34793
The mean ionic charge of silicon in 3HE-rich solar flares
[SH-2.2-8] N85-34803
Cosmic ray secondary nuclei and the structure of the galaxy
[OG-7.2-4] N85-34876
Observation of pick-up ions in the solar wind: Evidence for the source of the anomalous cosmic ray component?
[SH-4.6-5] N85-35043
Monte Carlo calibration of the SMM gamma ray spectrometer for high energy gamma rays and neutrons
[SH-9.1-6] N85-35121

MAX-PLANCK-INST. FUER KERNPHYSIK, HEIDELBERG (WEST GERMANY).
Time-dependent nonlinear cosmic ray shocks confirming abstract
[OG-8.1-3] N85-34893
Selfsimilar time dependent shock structures
[OG-8.1-4] N85-34894
Acceleration of cosmic rays in supernova-remnants
[OG-8.1-9] N85-34899
Onion-shell model for cosmic ray electrons and radio synchrotron emission in supernova remnants
[OG-8.1-10] N85-34900
Approximate supernova remnant dynamics with cosmic ray production
[OG-8.1-12] N85-34901
Results of ultra-low level 71ge counting for application in the Gallex-solar neutrino experiment at the Gran Sasso Underground Physics Laboratory
[SH-8.1-2] N85-35108

MAX-PLANCK-INST. FUER PHYSIK UND ASTROPHYSIK, GARCHING (WEST GERMANY).
The final COS-B database now publicly available
[OG-9.3-8] N85-34963
The final COS-B database: In-flight calibration of instrumental parameters
[OG-9.3-9] N85-34964

MAX-PLANCK-INST. FUER RADIOASTRONOMIE, BONN (WEST GERMANY).
Stochastic particle acceleration in solar flares
[SH-1.1-4] N85-34731
Why do leaky-box models work so fine?
[OG-7.2-8] N85-34877

MCGILL UNIV., MONTREAL (QUEBEC).
Non-rigid body motion N85-34576
Multi-robot assembly of IC's N85-34577

MEIDENSHA ELECTRIC MFG. CO. LTD., TODYO (JAPAN).
X-ray residual stress analysis on the coarse grain of copper and its application to the brazed copper N85-34202
Study on fracture behavior of epoxy resin N85-34216

MEMORIAL UNIV. OF NEWFOUNDLAND, ST. JOHNS.
Interfacing interactive circuit simulation with standard graphics facilities N85-34529

MERIDIAN CORP., FALLS CHURCH, VA.
Ocean thermal energy conversion
[DE85-012291] N85-34456
MICHIGAN STATE UNIV., EAST LANSING.
Sequential regularization solution of the inverse heat conduction problem
[DE85-010657] N85-34362
MICHIGAN UNIV., ANN ARBOR.
The origins of cosmic rays and quantum effects on gravity
[OG-8.2-15] N85-34911
MIDWEST RESEARCH INST., GOLDEN, COLO.
Resource evaluation and site selection for microalgae production systems
[DE85-006807] N85-34485
MINNESOTA UNIV., MINNEAPOLIS.
Variations in the propagation of UH-nuclei
[OG-7.1-1] N85-34863
Interactions of heavy nuclei, Kr, Xe and Ho, in light targets
[OG-7.2-21] N85-34888
MISSOURI UNIV., COLUMBIA.
Evaluation of half wave induction motor drive for use in passenger vehicles
[NASA-CR-176119] N85-34334
MISSOURI UNIV., ST. LOUIS.
Low-excitation Herbig-Haro objects and interstellar extinction
[NASA-CR-176142] N85-34726
MONTREAL UNIV. (QUEBEC).
Computer graphics for multivariate data N85-34528
Graphics Interaction in databases N85-34534
3D computer animation: More an evolution problem than a motion problem N85-34536
Design and implementation of an interactive route editor N85-34559
Strategic use of business graphics: A stakeholder approach N85-34566
Shadow volumes for non-planar polygons N85-34580
MOSCOW STATE UNIV. (USSR).
Two types of electron events in solar flares
[SH-1.2-11] N85-34746
Observation of the fluxes of nuclei with energies 10-20 MEV per nucleon during the solar flare of April 26, 1984
[SH-2.1-1] N85-34783
On the retention of high-energy protons and nuclei with charges Z or equal to 2 in large solar flares after the process of their acceleration
[SH-2.1-8] N85-34789
Variations of the cosmic ray general component in Antarctica
[SH-4.4-17] N85-35013
Dynamics of two-year cosmic ray variations inferred from the data of spacecraft and stratospheric measurements and from the neutron monitor data in 1959-1981
[SH-4.4-21] N85-35017
Penetration of solar protons into the Earth's magnetosphere on November 22, 1977
[SH-6.1-15] N85-35088
Observation of nuclei with energies 8-30 MeV per nucleon in the Earth's magnetosphere at the altitudes 350 KM
[SH-10.1-5] N85-35136
MUSASHI INST. OF TECH., TOKYO (JAPAN).
Monotonous stress-strain properties of structural steel subjected to nonstationary repetitive pre-loading N85-34185
Multiaxial stress analysis taking account of penetration depth of X-rays. A solution by means of polynomial approximation N85-34204

N

NAGASAKI UNIV. (JAPAN).
On the methods to determine the stress intensity factors in boundary element method N85-34189
NAGOYA UNIV. (JAPAN).
Collisional relaxation of electron tail distribution
[IPPJ-729] N85-34635
Nonlocal and nonadiabatic expression for the ponderomotive force near cyclotron resonance
[IPPJ-736] N85-34636
Some physical differences between sheet plasma and multicusp plasma as volume produced H- or D- ion sources
[IPPJ-728] N85-34637
Measuring method and confirmation of H- (D-) ion current by sheet plasma 1
[IPPJ-730] N85-34638
Size effects of vacuum chamber for H- (D-) ion volume production by sheet plasma 1
[IPPJ-731] N85-34639
A curvilinear coordinate method for the solutions of initial value problems using the third-order upwind differencing scheme
[IPPJ-734] N85-34642
Resonant ion acceleration by oblique magnetosonic shock wave in a collisionless plasma
[IPPJ-735] N85-34643
Proceedings of the US-Japan Workshop on Transport in Open-Ended Systems
[IPPJ-727] N85-34644
Azimuthal uniformity and current balance study of ICRH-produced plasma in RFC-XXM N85-34659
Breakdown of intrinsic ambipolarity for the radial diffusion due to a rotating RF field N85-34660
Effect of ECH and ICH on ambipolar potential in NBT-1M N85-34661
Transports studies of ECH and ICRH-heated bumpy torus plasma in NBT-1M N85-34662
Guiding center distribution function and longitudinal invariant N85-34663
Simulation studies on stability of hot electron plasma N85-34664
Observation of mode-converted by ion Bernstein wave by an HCN laser scattering
[IPPJ-724] N85-34668
Fokker-Planck calculation of hot electron formation in the thermal barrier region of tandem mirror Gamma-10
[IPPJ-726] N85-34669
Workshop report on Simulation Techniques for Shock Wave Phenomena and Characteristics of Plasmas in Inertial Confinement Fusion
[IPPJ-725] N85-34670
Data on the backscattering coefficients on light ions from solids: A revision
[IPPJ-AM-41-REV] N85-34689
Low-energy sputterings with the Monte Carlo Program ACAT
[IPPJ-AM-40] N85-34690
IMF-sense-dependent cosmic ray anisotropy produced from diffusion-convection in heliosphere
[SH-4.3-9] N85-34994
Sidereal anisotropies in the median rigidity range 60-600GV in 1978-1983
[SH-4.4-3] N85-35001
The first three harmonics of solar daily variation caused by the diffusive propagation of galactic cosmic rays through the heliosphere
[SH-4.5-1] N85-35019
Formulation of cosmic-ray solar daily variation and its seasonal variation, produced from generalized stationary anisotropy of solar origin
[SH-4.5-2] N85-35020
Anomalous increase of solar anisotropy above 150GV in 1981-1983
[SH-4.5-18] N85-35035
Rigidity spectrum of Forbush decrease
[SH-5.1-6] N85-35060
The solar wind effect on cosmic rays and solar activity
[SH-5.1-13] N85-35066
NATAL UNIV., DURBAN (SOUTH AFRICA).
The role of cosmic rays and Alfven waves in the structure of the galactic halo
[OG-7.2-18] N85-34885
Instabilities in decelerating supersonic flows with applications to cosmic ray shocks
[OG-8.1-2] N85-34892
NATIONAL ACADEMY OF SCIENCES - NATIONAL RESEARCH COUNCIL, WASHINGTON, D. C.
Space Station Engineering and Technology Development: Proceedings of the Panel on In-Space Engineering Research and Technology Development
[NASA-CR-176110] N85-34153
Fire-resistant phosphorus containing polyimides and copolyimides
[NASA-CASE-ARC-11522-2] N85-34280
Metal (2) 4,4',4',4'' phthalocyanine tetraamines as curing agents for epoxy resins
[NASA-CASE-ARC-11424-1] N85-34281
NATIONAL AERONAUTICS AND SPACE ADMINISTRATION, WASHINGTON, D. C.
A life-saving device for ships
[NASA-TM-77670] N85-34129
The effect of liquid-liquid phase separation of glass on the properties and crystallization behavior
[NASA-TM-77890] N85-34285
Snow cover in the Siberian forest-steppe
[NASA-TM-77914] N85-34435
Aerospace Medicine and Biology: A continuing bibliography with indexes (supplement 274)
[NASA-SP-7011(274)] N85-34491
The large scale dynamics of the outer heliosphere and the long-term modulation of galactic cosmic rays
[SH-4.7-3] N85-35048
A spacefaring people: Perspectives on early spaceflight
[NASA-SP-4405] N85-35142
Management of large-scale technology N85-35145
NATIONAL AERONAUTICS AND SPACE ADMINISTRATION. AMES RESEARCH CENTER, MOFFETT FIELD, CALIF.
An evaluation of three helicopter rotor sections
[NASA-TM-86719] N85-34115
Use of a hyperbolic grid generation scheme in simulating supersonic viscous flow about three-dimensional winged configuration
[NASA-TM-85344] N85-34116
Flight testing the fixed-wing configuration of the Rotor Systems Research Aircraft (RSRA)
[NASA-TM-86762] N85-34135
Prediction of the flow-field interference induced by the long-range laser velocimeter in the Ames 40- by 80-foot and the 80- by 120-foot wind tunnels
[NASA-TM-86763] N85-34146
Fire-resistant phosphorus containing polyimides and copolyimides
[NASA-CASE-ARC-11522-2] N85-34280
Metal (2) 4,4',4',4'' phthalocyanine tetraamines as curing agents for epoxy resins
[NASA-CASE-ARC-11424-1] N85-34281
A three-dimensional turbulent boundary layer undergoing transverse strain and streamwise pressure gradient
[NASA-TM-86768] N85-34358
Modulated voltage metastable ionization detector
[NASA-CASE-ARC-11503-1] N85-34374
Practical aspects of laser holographic interferometry in wind tunnels
[NASA-TM-86788] N85-34378
Nonsimultaneous coupled laser velocimeter measurement technique: Error prediction for spatially noncoincident measurements
[NASA-TM-86718] N85-34379
The impact of supercomputers on experimentation: A view from a national laboratory
[NASA-TM-86822] N85-34510
NATIONAL AERONAUTICS AND SPACE ADMINISTRATION. GODDARD SPACE FLIGHT CENTER, GREENBELT, MD.
Performance interface document for the S-band diplexer for space users of NASA networks
[NASA-TM-86224] N85-34155
Solar maximum: Solar array degradation
[NASA-TM-86194] N85-34175
The International Cometary Explorer (ICE)wallsheet teacher's guide
[NASA-TM-87498] N85-34727
Comparisons of the North Polar Cap of Mars and the Earth's Northern Hemisphere snow cover
[NASA-TM-86191] N85-34728
Ninteenth International Cosmic Ray Conference. SH sessions, volume 4
[NASA-CP-2376-VOL-4] N85-34729
First-order shock acceleration in solar flares
[SH-1.1-5] N85-34732
Fast drift kilometric radio bursts and solar proton events
[SH-1.1-7] N85-34734
Spectral and spatial properties of solar microflares
[SH-1.2-4] N85-34740
Two classes of solar energetic particle events associated with impulsive and long duration soft X-ray flares
[SH-1.2-12] N85-34747
Energetic protons from a disappearing solar filament
[SH-1.3-7] N85-34754
Helios 1 energetic particle observations of the solar gamma ray flare events of 7, 21 June 1980 and 3 June 1982
[SH-1.3-8] N85-34755
Elemental abundances in corotating events
[SH-1.5-15] N85-34778
Energetic particle observations of the solar-gamma ray/neutron flare events of 3 Jun 1982 and 21 June 1980 isotopic and chemical composition
[SH-2.1-3] N85-34784
Variations in elemental composition of several MEV/nucleon ions observed in interplanetary space
[SH-2.1-7] N85-34788
Abundances from solar-flare gamma-ray line spectroscopy
[SH-2.1-13] N85-34794
Solar flare gamma-ray line spectroscopy
[SH-2.1-14] N85-34795
Type 3 solar radio bursts and 3HE-rich events
[SH-2.2-3] N85-34798
Solar source regions of 3HE-rich particle events
[SH-2.2-4] N85-34799
The 3HE in solar non-relativistic electron events
[SH-2.2-5] N85-34800
The heavy ion composition in 3HE-rich solar flares
[SH-2.2-7] N85-34802

Some characteristics of the solar flare event of February 16, 1984
[SH-3.1-7] N85-34811
The propagation of solar energetic particles in magnetic channels
[SH-3.2-4] N85-34820
Cosmic ray modulatin and merged interaction regions
[SH-4.1-11] N85-34834
Propagation of the phase of solar modulation
[SH-4.1-12] N85-34835
Differential measurement of cosmic-ray gradient with respect to interplanetary current sheet
[SH-4.2-9] N85-34847
Ninteenth International Cosmic Ray Conference. OG sessions, volume 3
[NASA-CP-2376-VOL-3] N85-34862
The central engine of quasars and AGNs: A relativistic proton radiative shock
[OG-8.1-7] N85-34897
The design of an experiment to detect low energy antiprotons
[OG-9.1-1] N85-34928
High resolution Cherenkov detectors for cosmic ray isotope experiment
[OG-9.1-4] N85-34930
Mass resolution optimization in a large isotopic composition experiment
[OG-9.1-9] N85-34935
A coded aperture imaging system optimized for hard X-ray and gamma ray astronomy
[OG-9.2-3] N85-34942
The Gamma-Ray Imaging Spectrometer (GRIS): A new balloon-borne experiment for gamma-ray line astronomy
[OG-9.2-4] N85-34943
High energy gamma ray balloon instrument
[OG-9.2-12] N85-34951
A star camera aspect system suitable for use in balloon experiments
[OG-9.3-10] N85-34965
Ninteenth International Cosmic Ray Conference. SH sessions, volume 5
[NASA-CP-2376-VOL-5] N85-34991

NATIONAL AERONAUTICS AND SPACE ADMINISTRATION. JOHNSON (LYNDON B.) SPACE CENTER,
Reactant pressure differential control for fuel cell gases
[NASA-CASE-MSC-20127-2] N85-34403
Space activities in the Soviet Union, Japan, and the People's Republic of China N85-35149

NATIONAL AERONAUTICS AND SPACE ADMINISTRATION. LANGLEY RESEARCH CENTER, HAMPTON, VA.
Ground-based and in-flight simulator studies of flight characteristics of a twin-fuselage passenger transport airplane during approach and landing
[NASA-TP-2451] N85-34144
Process for improving moisture resistance of epoxy resins by addition of chromium ions
[NASA-CASE-LAR-13226-1] N85-34282
A review of spectral methods
[NASA-CR-172502] N85-34350
Experimental aerodynamic heating to simulated space shuttle tiles in laminar and turbulent boundary layers with variable flow angles at a nominal Mach number of 7
[NASA-TP-2307] N85-34351
Nozzle wall roughness effects on free-stream noise and transition in the pilot low-disturbance tunnel
[NASA-TM-86389] N85-34355
Tensile testing apparatus
[NASA-CASE-LAR-13243-1] N85-34375
Nonlinear adhesive behavior effects in a cracked orthotropic sheet stiffened by a semi-infinite orthotropic sheet
[NASA-TM-87584] N85-34426
The parser generator as a general purpose tool
[NASA-CR-177955] N85-34521
Reordering computations for parallel execution
[NASA-CR-177961] N85-34522
Langley aeronautics and space test highlights, 1984
[NASA-TM-87585] N85-35151

NATIONAL AERONAUTICS AND SPACE ADMINISTRATION. LEWIS RESEARCH CENTER, CLEVELAND, OHIO.
Telecommunications forecast for ITU Region 2 to the year 1995
[NASA-TM-87077] N85-34150
Optical analysis of parabolic dish concentrators for solar dynamic power systems in space
[NASA-TM-87080] N85-34176
Heaterless ignition of inert gas ion thruster hollow cathodes
[NASA-TM-87086] N85-34177
Electrode erosion in arc discharges at atmospheric pressure
[NASA-TM-87087] N85-34178
Hollow cathodes in high pressure arc discharges
[NASA-TM-87098] N85-34179
Mechanical properties of SiC fiber-reinforced reaction-bonded Si3N4 composites
[NASA-TM-87085] N85-34223
Aluminum work function: Effect of oxidation, mechanical scraping and ion bombardment
[NASA-TM-87079] N85-34265
Microstructures in rapidly solidified Ni-Mo alloys
[NASA-TM-87100] N85-34266
Reliability of two sintered silicon nitride materials
[NASA-TM-87092] N85-34284
Refrigerated dynamic seal to 6.9 MPa (1000 psi)
[NASA-TM-87108] N85-34356
Surface temperature distribution along a thin liquid layer due to thermocapillary convection
[NASA-TM-87115] N85-34357
Oxidizing seal for a turbine tip gas path
[NASA-CASE-LEW-14053-1] N85-34402
Generated spiral bevel gears: Optimal machine-tool settings and tooth contact analysis
[NASA-TM-87075] N85-34405
Thermal stress analysis of a new turbine shroud seal concept
[NASA-TM-87082] N85-34406
Lubrication and cooling for high speed gears
[NASA-TM-87096] N85-34407
Elastohydrodynamic lubrication calculations used as a tool to study scuffing
[NASA-TM-87097] N85-34408
Design and lubrication of high-speed rolling-element bearings
[NASA-TM-87107] N85-34409
Nonlinear flap-lag-extensional vibrations of rotating, pretwisted, preconed beams including Coriolis effects
[NASA-TM-87102] N85-34427
Thermionic photovoltaic energy converter
[NASA-CASE-LEW-14077-1] N85-34441
Evaluation of developmental membranes for the mixed reactant iron-chromium redox system
[NASA-TM-87074] N85-34443
Reflection plane tests of a wind turbine blade tip section with ailerons
[NASA-TM-87018] N85-34444
Diamondlike carbon protective coatings for IR materials
[NASA-TM-87083] N85-34631

NATIONAL AERONAUTICS AND SPACE ADMINISTRATION. MARSHALL SPACE FLIGHT CENTER, HUNTSVILLE, ALA.
Space station rotational equations of motion
[NASA-TP-2511] N85-34148
Potential spin-offs of the carbon dioxide observational platform system (CO-OPS) for remote sensing opportunities
[NASA-TP-2510] N85-34149
The role of tethers on space station
[NASA-TM-86519] N85-34154
Soft X-Ray Telescope (SXRT) N85-34159
Solar Ultraviolet Spectral Irradiance Monitor (SUSIM) N85-34160
White Light Coronograph (WLC) and Ultra-Violet Coronal Spectrometer (UVCS) N85-34161
High Resolution Telescope and Spectrograph (HRTS) N85-34162
Active Cavity Radiometer (ACR) N85-34163
Space Experiments with Particle Accelerators (SEPAC) N85-34165
Theoretical and Experimental Beam Plasma Physics (TEBPP) N85-34166
Recoverable Plasma Diagnostics Package (RPDP) N85-34167
Electrodynamic tether N85-34168
Imaging Spectrometric Observatory (ISO) N85-34169
Atmospheric Emission Photometric Imaging (AEPI) N85-34170
Wide Angle Michelson Doppler Imaging Interferometer (WAMDII) N85-34172
Vehicle Charging And Potential (VCAP) N85-34173
Initial placement of STO instruments N85-34174
Variable length strut with longitudinal compliance and locking capability
[NASA-CASE-MFS-25907-1] N85-34401
Hardware math for the 6502 microprocessor
[NASA-TM-86517] N85-34511
Burst and Transient Source Experiment (BATSE) for the Gamma Ray Observatory (GRO)
[OG-9.2-14] N85-34953
Gamma-ray burst spectroscopy capabilities of the BATSE/GRO experiment
[OG-9.2-15] N85-34954
Capabilities of the GRO/BATSE for monitoring of discrete sources
[OG-9.2-16] N85-34955

NATIONAL AERONAUTICS AND SPACE ADMINISTRATION. PASADENA OFFICE, CALIF.
Method and apparatus for Delta Kappa synthetic aperture radar measurement of ocean current
[NASA-CASE-NPO-15704-1] N85-34327
Method and apparatus for transfer function simulator for testing complex systems
[NASA-CASE-NPO-15696-1] N85-34333
Instrumentation for sensing moisture content of material using a transient thermal pulse
[NASA-CASE-NPO-15493-2] N85-34373
Ranging system which compares an object reflected component of a light beam to a reference component of the light beam
[NASA-CASE-NPO-15865-1] N85-34629
Shuttle car loading system
[NASA-CASE-NPO-15949-1] N85-34722

NATIONAL BUREAU OF STANDARDS, GAITHERSBURG, MD.
The application of models to the assessment of fire hazard from consumer products
[NBSIR-85-3219] N85-34325

NATIONAL CENTER FOR ATMOSPHERIC RESEARCH, BOULDER, COLO.
Latitudinal gradients of cosmic rays and the polarity reversal of the heliospheric magnetic field: A preliminary evaluation
[SH-4.2-16] N85-34853
Stochastic particle acceleration in flaring stars
[OG-8.3-9] N85-34927

NATIONAL CHEMICAL LAB. FOR INDUSTRY, TSUKUBA (JAPAN).
Numerical calculations on shock loaded materials N85-34676

NATIONAL DEFENCE ACADEMY, TOKYO (JAPAN).
Electrical resistivity and hysteresis of the equiatomic nickel-titanium alloy near the martensitic transformation temperature N85-34181

NATIONAL PHYSICAL LAB., TEDDINGTON (ENGLAND).
Recommendations for the design and equipping of engineering metrology laboratories
[NPL-MOM-22] N85-34145
Production of initial estimates of photogrammetric variables
[NPL-MOM-66] N85-34434
A prototype PASCAL program validation system
[NPL-DITC-57/85] N85-34513
Experiments and discussions on the analysis of interferograms with closed-loop fringes
[NPL-MOM-68] N85-34515
Polarisation insensitive achromatic cube beamsplitter
[NPL-MOM-72] N85-34630

NATIONAL RADIO ASTRONOMY OBSERVATORY, CHARLOTTESVILLE, VA.
The extent of the local hi halo
[NASA-CR-176115] N85-34724

NATIONAL RESEARCH COUNCIL OF CANADA, OTTAWA (ONTARIO).
Short-time creep of ice
[NRC/CNR-TT-2111] N85-34428
Selection of segment similarity measures for hierarchical picture segmentation N85-34548
Acoustical absorption coefficient in a diffuse field of a plane, rectangular material of finite dimensions placed on an infinite perfectly reflecting surface
[NRC/CNR-TT-2113] N85-34599

NAVAL RESEARCH LAB., WASHINGTON, D. C.
Theoretical and computational research on the focused transport of intense charged particle beams
[DE85-012980] N85-34621
Calculation of improved spallation cross sections
[OG-7.2-23] N85-34890
Propagation of cosmic rays and new evidence for distributed acceleration
[OG-8.3-5] N85-34924

NEUSER (ROLF), ESSEN (WEST GERMANY).
A user-friendly computer-aided construction of boundaries N85-34564

NEW HAMPSHIRE UNIV., DURHAM.
Magnetic search system
[PB85-185108] N85-34477
The propagation of solar flare particles in a turbulent coronal loop
[SH-1.1-3] N85-34730
Time extended production of neutrons during a solar flare
[SH-1.4-1] N85-34782
Neutral pion production in solar flares
[SH-1.4-7] N85-34787
Energetic solar particle fluxes out to 3 AU during the 7 May 1978 flare event
[SH-3.2-6] N85-34822
The intensity recovery of Forbush-type decreases as a function of heliocentric distance and its relationship to the 11-year variation
[SH-4.1-9] N85-34832

Drift and observations in cosmic-ray modulation, 1
[SH-4.2-4] N85-34842
Drift and observations in cosmic-ray modulation, 2
[SH-4.2-5] N85-34843
The effects of newly measured cross sections in hydrogen on the production of secondary nuclei during the propagation of cosmic rays through interstellar H
[OG-7.2-2] N85-34874
Measurements of the fragmentation of (40)Ar, (28)Si and (12)C in CH2C and H targets between 300 and 1500 MeV/nuc at the Bevalac
[OG-7.2-19] N85-34886
Radial and latitudinal gradients of anomalous oxygen during 1977 - 1985
[SH-4.6-4] N85-35042
On the anomalous component
[SH-4.6-6] N85-35044
The cosmic ray interplanetary radial gradient from 1972 - 1985
[SH-4.7-1] N85-35046

NEW MEXICO UNIV., ALBUQUERQUE.
North-south asymmetry in activity on the Sun and cosmic ray density gradients
[SH-4.2-7] N85-34845
Mini and super mini arrays for the study of highest energy cosmic rays
[OG-9.4-9] N85-34976
Detection of 10 (1) GeV cosmic neutrinos with a space station
[OG-9.4-10] N85-34977
Angular resolution of air-shower array-telescopes
[OG-9.5-6] N85-34983
Astrophysical applications of high angular resolution array-telescopes
[OG-9.5-7] N85-34984
Corrected sidereal anisotropy for underground muons
[SH-4.4-7] N85-35005
Upper cut-off rigidity for corotation anisotropy during solar activity cycles 20 and 21
[SH-4.5-4] N85-35022
Solar wind velocity and daily variation of cosmic rays
[SH-4.5-6] N85-35024
Diurnal anisotropy during solar activity cycle twenty and diffusion-convection model
[SH-4.5-7] N85-35025

NEW YORK STATE DEPT. OF EDUCATION, ALBANY.
Solar energy education. Renewable energy: A background text
[DE85-010365] N85-34452

NEW YORK UNIV., NEW YORK.
Stability of two-dimensional immiscible flow to viscous fingering
[DE85-011403] N85-34364
Image synthesis: Optical identity or pictorial communication? N85-34565

NEWCASTLE-UPON-TYNE UNIV. (ENGLAND).
The balancing of complex linkage mechanisms N85-34313

NIHON UNIV., SHINEI (JAPAN).
FEMALE: Finite Element Method for Arbitrary Lagrangian and Eulerian elements N85-34671
A relation between the short time variations of cosmic rays and geomagnetic field change
[SH-5.1-14] N85-35067

NIHON UNIV., TOKYO (JAPAN).
Electrolytic synthesis of colored eta alumina film N85-34201
Radial transport caused by collision N85-34652
Electron dynamics and transport in a mirror field N85-34656

NIIGATA UNIV. (JAPAN).
Low frequency instability in a mirror field N85-34657

NIIHAMA TECHNICAL COLL. (JAPAN).
X-ray measurement of thermal stresses in tungsten fiber-copper composites N85-34205

NIPPON ELECTRIC CO. LTD., KAWASAKI (JAPAN).
How map designers can represent their ideas in thematic maps: Effective user interfaces for thematic map design N85-34562

NORTH CAROLINA STATE UNIV., RALEIGH.
Analysis of transient radiation upset in a 16K SRAM
[DE85-009442] N85-34586
Circuit approaches to increasing SRAM performance in total dose environments
[DE85-009441] N85-34588

NORTH STAFFORDSHIRE POLYTECHNIC, STAFFORD (ENGLAND).
Re-designing a mechanism for higher speed: A case history from textile machinery N85-34310

NOTRE DAME UNIV., IND.
Scaling parameters of flashover
[NBS-GCR-85-497] N85-34229

NUCLEAR UTILITY SERVICES, INC., GAITHERSBURG, MD.
User's guide to the MATHEW/ADPIC models
[DE85-012952] N85-34587

O

OAK RIDGE NATIONAL LAB., TENN.
Method for removing oxide contamination from silicon carbide powders
[DE85-011648] N85-34287
Advanced heat pump research and development
[DE85-009540] N85-34372
The 1983 international intercomparison of nuclear accident dosimetry systems at Oak Ridge National Laboratory
[DE85-011303] N85-34382
Effect of stainless steel weld overlay cladding on the structural integrity of flawed steel plates in bending, series 1
[TI85-010349] N85-34418
Characterization of modified 9 Cr Mo steel extruded pipe
[DE85-012056] N85-34430
Effects of acid rain on forest nutrient status
[DE85-012486] N85-34463
Two dimensional CO2-ocean model including the biological processes
[DE85-012341] N85-34483
Monte Carlo techniques for analyzing deep penetration problems
[DE85-011426] N85-34598
Capture in the 1.15-keV iron resonance
[DE85-011913] N85-34612
Calculation of mixed depth for some metal-Si systems
[DE85-011907] N85-34616
Negative ion sources equipped with continuous annular and spherical geometry surface ionizers
[DE85-011939] N85-34619
Pairing correction of particle-hole state densities for two kinds of fermions
[DE85-011549] N85-34620
Electron impact ionization of multicharged ions at ORNL: 1980-1984
[DE85-013104] N85-34622
Analytic and numerical calculations of the ambipolar electric field in a stellarator N85-34665
Compact DT fusion spherical tori at modest field
[DE85-011568] N85-34692
Experimental measurements of the ion cyclotron antennas' coupling and RF characteristics
[DE85-011569] N85-34694
Shield design for next-generation, low-neutron-fluence, superconducting tokamaks
[DE85-011409] N85-34695
Langmuir probe on ISX-B
[DE85-012066] N85-34697
Advanced Toroidal Facility (ATF)
[DE85-011567] N85-34699
Multiple-frequency electron cyclotron heating of hot electron rings in EBT-1
[DE85-011302] N85-34701
Stellarator approach to fusion plasma confinement
[DE85-011420] N85-34704
Assessment of magnetic field asymmetries in ELMO Bumpy square
[DE85-011559] N85-34705
Instrument to synchronize Thomson scattering diagnostic measurements with MHD activity in a Tokamak
[DE85-012082] N85-34708
Confinement experiments on ISX-B
[DE85-012346] N85-34709
Flux-line lattice anisotropy in V3Si: Observation and interpretation
[DE85-011935] N85-34713
Survey of mixing in metal/insulator systems
[DE85-011938] N85-34714

OAK RIDGE Y-12 PLANT, TENN.
Experimental attempt to achieve microstructure variations through temperature/time permutations for a nonwrought powder metallurgy uranium-6 niobium alloy
[DE85-013166] N85-34272

OBSERVATOIRE DE PARIS-MEUDON (FRANCE).
Temporal evolution of an energetic electron population in an inhomogeneous medium: Application to solar hard X-ray bursts
[SH-1.2-6] N85-34741
Quantitative analysis of flare accelerated electrons through their hard X-ray and microwave radiation
[SH-1.2-7] N85-34742

OBSERVATOIRE DU PIC-DU-MIDI, BAGNERES DE BIGORRE (FRANCE).
Diffusion in the chromosphere and the composition of the solar corona and energetic particles
[SH-2.1-9] N85-34790

OHIO STATE UNIV., COLUMBUS.
Experimental evaluation of the thermodynamic properties of concentrated aqueous potassium hydroxide solutions
[DE85-010628] N85-34238
Adaptive antenna arrays for satellite communications: Design and testing
[NASA-CR-176162] N85-34329
The design and analysis of single flank transmission error testor for loaded gears
[NASA-CR-176163] N85-34404

OPEN UNIV., MILTON (ENGLAND).
Computer animation in distance teaching N85-34581

OREGON STATE UNIV., CORVALLIS.
Increase of total CO2 in the World ocean
[DE85-007756] N85-34484

OKAYAMA UNIV. OF SCIENCE (JAPAN).
The read-out system of spatial distribution of thermoluminescence in meteorites
[SH-9.1-16] N85-35131

OSAKA CITY UNIV. (JAPAN).
Stress distribution of fiberglass reinforced plastic beam with a delamination under three-point bending N85-34210
A new ultra high energy gamma ray telescope at Ohya mine
[OG-9.4-3] N85-34970

OSAKA UNIV. (JAPAN).
Experimental study of collapse of thick-walled tube under external pressure and axial force N85-34186
Integral representation for nonlinear heat transport N85-34683

OSAKA UNIV., SUITA (JAPAN).
Cubic interpolated pseudo-particle method (CIP) for solving hyperbolic-type equation N85-34673
Stability of implosion dynamics N85-34680
Multiple inner shell vacancies in laser-irradiated Au plasma N85-34687
Vector calculation of particle code N85-34688

P

PACIFIC NORTHWEST LAB., RICHLAND, WASH.
Separation of gas mixtures by supported complexes
[DE85-011996] N85-34236

PECHAN (E. H.) AND ASSOCIATES, INC., SPRINGFIELD, VA.
Forecasting future industrial SO2 and NC/sub x/ emissions, revised N85-34461

PENNSYLVANIA STATE UNIV., UNIVERSITY PARK.
Grain boundary and surface diffusion in oxide systems
[DE85-007291] N85-34715

PENNSYLVANIA UNIV., PHILADELPHIA.
Three dimensional calculation of flux of low energy atmospheric neutrinos
[SH-8.1-11] N85-35116
Satellites and politics: Weather, communications, and earth resources N85-35144

PERCEPTION COMPUTING, INC., DOWNSVIEW (ONTARIO).
The scientific and technical issues in integrating remotely sensed imagery with geocoded data bases N85-34547

PITTSBURGH UNIV., PA.
Infrared studies of the influence of alkali metals on the C-O bond in chemisorbed carbon monoxide
[DE85-005306] N85-34232

POLITECNICO DI MILANO (ITALY).
The CADME approach to the interface of solid modellers N85-34554

POTCHEFSTROOM UNIV. FOR CHRISTIAN HIGHER EDUCATION (SOUTH AFRICA).
Spectra of solar proton ground level events using neutron monitor and neutron moderated detector recordings
[SH-1.3-14] N85-34759
Notes on drift theory
[SH-4.2-3] N85-34841
Drift and Forbush decreases
[SH-5.1-2] N85-35056
The neutron moderated detector and groundbased cosmic ray modulation studies
[SH-9.1-13] N85-35128

PRC KENTRON, INC., HAMPTON, VA.
User's operating procedures. Volume 1: Scout project information programs
[NASA-CR-177948] N85-34518
User's operating procedures. Volume 1: Scout project financial analysis program
[NASA-CR-177949] N85-34519
User's operating procedures. Volume 3: Projects directorate information programs
[NASA-CR-177950] N85-34520

PUERTO RICO UNIV., HUMACAO.
Evaluation of parameters for particles acceleration by the zero-point field of quantum electrodynamics
[OG-8.2-16] N85-34912
PURDUE UNIV., LAFAYETTE, IND.
Geophysical-geological studies of possible extensions of the New Madrid fault zone
[TI85-901341] N85-34475

R

RADIATION MONITORING DEVICES, INC., WATERTOWN, MASS.
Applications of CdTe to nuclear medicine
[DE85-011877] N85-34492
RANI DURGAVATI UNIV., JABALPUR (INDIA).
Comparative study of the phase of diurnal anisotropy on quiet and disturbed days on a long term basis up to recent period
[SH-4.5-9] N85-35027
Study of spectral exponent on quiet and disturbed days
[SH-4.5-10] N85-35028
Diurnal variation of galactic cosmic ray intensity on quiet days
[SH-4.5-11] N85-35029
RCA ASTRO-ELECTRONICS DIV., PRINCETON, N. J.
Spacecraft (Mobile Satellite) configuration design study
[NASA-CR-176153] N85-34152
REGINA UNIV. (SASKATCHEWAN).
Hologram-like transmission of pictures N85-34552
RENSSELAER POLYTECHNIC INST., TROY, N. Y.
The automatic labeling of geographic maps: A problem in computer aesthetics N85-34561
Building an octree from a set of parallelepipeds N85-34572
RIKKYO UNIV., TOKYO (JAPAN).
Observations of solar flare photon energy spectra from 20 keV to 7 MeV
[SH-1.2-9] N85-34744
Observations of solar flare gamma-rays and protons
[SH-1.3-6] N85-34753
ROCHESTER UNIV., N. Y.
Photoionization-pumped, Ne 2, X-ray laser studies project
[DE85-012973] N85-34399
ROCKEFELLER UNIV., NEW YORK.
Thermal transport measurements of UV laser irradiated spherical targets
[DE85-011038] N85-34365
ROCKWELL INTERNATIONAL CORP., RICHLAND, WASH.
Review of zirconium-zircaloy pyrophoricity
[DE85-011169] N85-34270
ROCKY MOUNTAIN BILOGICAL LAB., CRESTED BUTTE, COLO.
Small Hydroelectric Power Plan Demonstration Project
[DE85-011343] N85-34454
ROLLS-ROYCE LTD., DERBY (ENGLAND).
Performance improvements from surfacing in aero engine components
[PNR-90257] N85-34142
Shroud segments for unshrouded blade turbines
[PNR-90260] N85-34143
Design, development and operation of a high simultaneous capacity digital telemetry system
[PNR-90261] N85-34151
The development and evaluation of the creep and corrosion resistant alloy IN6201
[PNR-90253] N85-34278
Directionally solidified gas turbine alloys
[PNR-90264] N85-34279
Towards the year 2000: Developments in inspection and product assurance to be anticipated during the next 15 years
[PNR-90258] N85-34421
The stress pattern analysis of coarse grain titanium specimens
[PNR-90250] N85-34433
Cost effective single crystals: The Rolls Royce approach
[PNR-90262] N85-34717
Discrete simulation models - their role in the design, development and management of inventory control systems
[PNR-90249] N85-34719
ROYAL SIGNALS AND RADAR ESTABLISHMENT, MALVERN (ENGLAND).
A device-independent 2D plotting package written in FORTRAN
[RSRE-MEMO-3776] N85-34514

S

SAN ANDRES UNIV., LA PAZ (BOLIVIA).
Search for solar neutrons using NM-64 equipment
[SH-1.4-5] N85-34765
SANDIA LABS., ALBUQUERQUE, N. MEX.
Time-resolved spectroscopic studies of detonating heterogeneous explosives
[DE85-009760] N85-34297
Pressure-shear loading of PBX-9404
[DE85-009982] N85-34298
New directional couplers for multimode circular waveguides applied to intense pulsed microwave systems
[DE85-011753] N85-34330
Technical assessment of thermal-hydraulics for high heat flux fusion components
[DE85-013178] N85-34359
Preliminary SPR thermal model description and results for WH-11 and BM-4
[DE85-013171] N85-34360
Degradation mechanisms and accelerated aging test design
[TI85-003251] N85-34420
Shock and release equation of state of calcite
[DE85-013151] N85-34432
Graph-theoretical exorcism
[DE85-011916] N85-34512
Coupled electron-photon transport calculations using the method of discrete ordinates
[DE85-009444] N85-34597
Rapid annealing of temperature-compensated, precision voltage references following fast-neutron irradiation
[DE85-009821] N85-34609
RADLAC technolgy review
[DE85-011995] N85-34691
Repetitive pulse accelerator technology for light ion inertial confinement fusion
[DE85-012030] N85-34693
Measurement and interpretation of electron angle at MABE beam stop
[DE85-011918] N85-34698
Light ion sources for ICF
[DE85-011544] N85-34702
SANDIA LABS., LIVERMORE, CALIF.
Numerical model of a pulse combustor
[DE85-011717] N85-34240
SAO PAULO UNIV. (BRAZIL).
Project management using graphics N85-34560
SCHOLL (LAURA) AND ASSOCIATES, SAN FRANCISCO, CALIF.
Heuristic rules for visualization N85-34584
SCHWEITZER (UDO), ESSEN (WEST GERMANY).
A user-friendly computer-aided construction of boundaries N85-34564
SCIENCE APPLICATIONS, INC., BOULDER, COLO.
Potential effect in transport due to non-axisymmetric confining field N85-34645
Induced azimuthal electric field effects on tandem transport and ambipolarity N85-34650
SCIENCE UNIV. OF TOKYO (JAPAN).
Electron loss process and cross section of multiply charged ions by neutral atoms N85-34685
SCIENTIFIC RESEARCH ASSOCIATES, INC., GLASTONBURY, CONN.
A three-dimensional viscous flow analysis for the helicopter tip vortex generation problem
[NASA-CR-3908] N85-34114
SEVERN COMMUNICATIONS CORP., SEVERNA PARK, MD.
Electron capture decay of cosmic rays: A model of the inhomogeneous interstellar medium
[OG-7.1-10] N85-34871
Implications of cross section errors for cosmic ray propagation
[OG-7.2-3] N85-34875
SHENANDOAH SYSTEMS CO., VIENNA, VA.
Magnetic search system
[PB85-185108] N85-34477
SHINSHU UNIV., MATSUMOTO (JAPAN).
Cosmic ray intensity variations observed at Matsushiro (220 M.W.E. in depth)
[SH-4.4-9] N85-35007
Solar tri-diurnal variation of cosmic rays in a wide range of rigidity
[SH-4.5-3] N85-35021
New Matsushiro underground cosmic ray station (220 M.W.E. in depth)
[SH-9.1-14] N85-35129
SHIP RESEARCH INST., TOKYO (JAPAN).
Mechanical properties of plasma arc cut steel N85-34188
SIEGEN UNIV., (WEST GERMANY).
Cross sections for the production of fragments with Z greater than or equal to 8 by fragmentation of Z greater than or equal to 9 and less than or equal to 26 nuclei
[OG-7.2-22] N85-34889
Propagation of injected cosmic rays under distributed reacceleration
[OG-8.3-3] N85-34922
SIKORSKY AIRCRAFT, STRATFORD, CONN.
Flight service evaluation of composite helicopter components
[NASA-CR-172562] N85-34222
SIMULA, INC., PHOENIX, ARIZ.
Design and testing of an energy-absorbing crewseat for the F/FB-111 aircraft, volume 1
[NASA-CR-3916] N85-34133
Design and testing of an energy-absorbing crewseat for the F/FB-111 aircraft. Volume 3: Data from crew module testing
[NASA-CR-3918] N85-34134
SMITHSONIAN ASTROPHYSICAL OBSERVATORY, CAMBRIDGE, MASS.
Results of a study to build a gamma-ray telescope in an external tank
[OG-9.3-3] N85-34958
Research of advanced techniques for X-ray detectors and telescopes with applications to rockets and the LAMAR facility
[NASA-CR-176161] N85-35141
SOCIETE FRANCAISE D'INSTRUMENTS DE MESURE, MASSY (FRANCE).
Implications of artificial intelligence on the design of future onboard systems
[SFENA-DPS/C/S3/84252A] N85-34596
SOCIETE NATIONALE INDUSTRIELLE AEROSPATIALE, ISSAC (FRANCE).
Centralized surveillance of flexible workshops for the manufacturing of composite materials
[SNIAS-851-430-103] N85-34227
Product definition: Technical specification of needs
[SNIAS-851-430-104] N85-34228
SOCIETY OF MATERIALS SCIENCE, KYOTO (JAPAN).
Proceedings of the Twentyseventh Japan Congress on Materials Research
[ISSN-0368-3141] N85-34180
SOUTH CAROLINA UNIV., COLUMBIA.
Influence of the source distribution on the age distribution of galactic cosmic rays
[OG-8.3-1] N85-34920
Explanation of the secondary to primary ratio within the continuous Fermi accelerator model
[OG-8.3-2] N85-34921
SOUTH DAKOTA SCHOOL OF MINES AND TECHNOLOGY, RAPID CITY.
Thermally induced chemical migration: A natural analog approach
[DE85-012308] N85-34474
SOUTHAMPTON UNIV. (ENGLAND).
A comparison of calculated and measured background noise rates in hard X-ray telescopes at balloon altitude
[OG-9.3-7] N85-34962
A position sensitive phoswich hard X-ray detector system
[OG-9.3-12] N85-34967
SOUTHWEST RESEARCH INST., SAN ANTONIO, TEX.
Magnetospheric multiprobes: MMP/CHEMSAT N85-34171
SPECTROLAB, INC., SYLMAR, CALIF.
Development of metallization process: FSA project, cells and module formation research area
[NASA-CR-176136] N85-34447
SPRINGBORN LABS., INC., ENFIELD, CONN.
Investigation of test methods, material properties, and processes for solar cell encapsulants
[NASA-CR-176132] N85-34448
STANFORD LINEAR ACCELERATOR CENTER, CALIF.
Using LINE as an interactive graphics package. Interfacing line and Topdraw in 43 and 24 VM
[DE85-012007] N85-34585
STANFORD UNIV., CALIF.
Depletion modeling of liquid dominated geothermal reservoirs
[DE85-009923] N85-34437
STATE UNIV. OF NEW YORK, ALBANY.
Solar energy education: Renewable energy activities for chemistry and physics
[DE85-010371] N85-34455
Throughfall rate and chemistry studies: Whiteface Mountain
[DE85-012407] N85-34464
STATE UNIV. OF NEW YORK, STONY BROOK.
Applications of holography to X-ray imaging
[DE85-010984] N85-34384

STEVENS INST. OF TECH., HOBOKEN, N. J.
The electromagnetic ram action of the plasma focus as a paradigm for the generation of cosmic rays and the gigantic jets in active galaxies
[OG-8.2-14] N85-34910
STOTTLER, STAGG AND ASSOCIATES, INC., SAN ANTONIO, TEX.
Hydrology
[PB85-182954] N85-34440
SURREY UNIV., GUILDFORD (ENGLAND).
A rational approach to cam design N85-34311
SUZUKA COLL. OF TECHNOLOGY (JAPAN).
Fractographic analysis for nonpropagating conditions of fatigue crack at high stress ratios in mild steel N85-34194
SYRACUSE UNIV., N. Y.
Unsteady transonic heat transfer in a transient facility
[NASA-CR-176145] N85-34354
SYSTEMS DESIGNERS LTD., FARNSBOROUGH (ENGLAND).
AMI calibration study. Volume 1: SAR calibration. Volume 2: Ground Targets. Volume 3: Scatterometer calibration
[C2248/4/4-VOL-1] N85-34394

T

TASHKENT V. I. LENIN STATE UNIV., VUZGORODOK (USSR).
Dynamics of the penetration boundaries of solar protons during a strong magnetic storm
[SH-6.1-16] N85-35089
TASMANIA UNIV., HOBART (AUSTRALIA).
Energetic solar particle events
[SH-3.2-2] N85-34818
Isotropic intensity waves and features of their occurrence
[SH-4.3-8] N85-34993
Sidereal variations deep underground in Tasmania
[SH-4.4-4] N85-35002
The effect of the interplanetary magnetic field on sidereal variations observed at medium depth underground detectors
[SH-4.4-5] N85-35003
The sidereal semi-diurnal variation observed at high zenith angles at Mawson, 1968-1984, and the polarity of the solar main field
[SH-4.4-6] N85-35004
Long-term modulation of cosmic rays during solar cycle 21
[SH-4.4-10] N85-35008
Atmospheric effects on the underground muon intensity
[SH-6.1-3] N85-35078
TATA INST. OF FUNDAMENTAL RESEARCH, BOMBAY (INDIA).
Silicon to iron abundances in solar cosmic rays and in the sun
[SH-2.1-6] N85-34787
Lead and uranium group abundances in cosmic rays
[OG-7.1-3] N85-34865
Exact solutions for sporadic acceleration of cosmic rays
[OG-8.3-7] N85-34925
Angular resolution of an EAS array for gamma ray astronomy energies 5 x 10 (13) eV
[OG-9.5-8] N85-34985
Possible origin of the anomalous component of cosmic rays
[SH-4.6-7] N85-35045
Detector calibration of the Indian cosmic ray experiment (IONS) in Space-Shuttle Spacelab-13
[SH-9.1-2] N85-35117
TECHNISCHE HOGESCHOOL, EINDHOVEN (NETHERLANDS).
Conjugated symmetrical coupler curves, produced by 4-bar linkages having the same transmission angles N85-34322
TECHNISCHE HOGESCHOOL TWENTE, ENSCHEDE (NETHERLANDS).
Realization and linearization of a hyperfrequency power amplifier implemented with bipolar transistors in class C polarization
[CNES-NT-114] N85-34346
TENNESSEE UNIV., KNOXVILLE.
Shape memory effect in uranium-niobium alloys below room temperature
[DE85-012964] N85-34268
TEXAS A&M UNIV., COLLEGE STATION.
A theoretical study of non-adiabatic surface effects for a model in the NTF cryogenic wind tunnel
[NASA-CR-3924] N85-34352
Application of evaluated fission-product delayed-neutron precursor data in reactor kinetics calculations
[DE85-012728] N85-34624
TOHOKU UNIV., SENDAI (JAPAN).
Cosmic ray intensity and the tilt of the neutral sheet
[SH-4.2-8] N85-34846
TOKUSHIMA UNIV. (JAPAN).
Fracture behavior of aluminum composites reinforced with fiber N85-34207
TOKYO INST. OF TECH. (JAPAN).
Anti wear property of two phasic metal composite N85-34199
Three body abrasive wear in various metal combinations N85-34200
Moving finite element method for ICF target implosion N85-34675
TOKYO INST. OF TECH., YOKAHAMA (JAPAN).
Two-dimensional simulation of LIB target implosion N85-34678
TOKYO UNIV. (JAPAN).
Animengine: An engineering animation system N85-34535
A simple but systematic CSG system N85-34569
Magnetohydrodynamic equilibrium and stability of spheromak with spheroidal plasma-vacuum interface
[IPPJ-732] N85-34640
Simulation of instability of cylindrically converging shock waves N85-34679
Stability of ion distribution in strong ion shock structure N85-34681
X-ray spectra of bursting neutron stars N85-34686
Akeno 20 km (2) air shower array (Akeno Branch)
[OG-9.4-8] N85-34975
TOKYO UNIV., TANASHI (JAPAN).
Note on the detection of high energy primary cosmic gamma rays by air shower observation
[OG-9.5-9] N85-34986
TORONTO UNIV. (ONTARIO).
Tabular and graphical solutions of regular and Mach reflections in pseudo-stationary frozen and vibrational-equilibrium flows, part 1
[UTIAS-283-PT-1] N85-34117
Tabular and graphical solutions of regular and Mach reflections in pseudo-stationary frozen and vibrational-equilibrium flows, part 2
[UTIAS-283-PT-2] N85-34118
A model of hypersonic two-dimensional oblique detonation wave ramjet
[UTIAS-TN-257] N85-34139
Frame buffer algorithms for stochastic models N85-34525
Issues and techniques in touch-sensitive tablet input (executive summary) N85-34543
Using percent-done program indicators to enhance user interfaces N85-34546
A multi-touch three dimensional touch-sensitive tablet (executive summary) N85-34553
Colour spaces and colour contrast N85-34567
Geometric continuity with interpolating Bezier curves N85-34570
TOSHIBA CORP., FUCHU (JAPAN).
Safety and reliability of steel structural materials under random service impact loads N85-34197
TOSHIBA CORP., TOKYO (JAPAN).
Knowledge engineering application in image processing N85-34583
TOYAMA UNIV. (JAPAN).
Corrosion fatigue strength and crack growth in prestrained 0.16% C carbon steel N85-34192
TRW, INC., REDONDO BEACH, CALIF.
Waves In Space Plasmas (WISP) N85-34164
Investigation of non-intrusive radiometers for entrained gasifier temperature measurement, revision 3
[DE85-011795] N85-34385
TSUKUBA UNIV. (JAPAN).
Plug and thermal barrier potential formation in Gamma 10 N85-34648
Recent experiments in Gamma-10 N85-34651
TUEBINGEN UNIV. (WEST GERMANY).
On the statistical significance of excess events: Remarks of caution and the need for a standard method of calculation
[OG-9.5-10] N85-34987
TURKU UNIV. (FINLAND).
Monte Carlo calculations of relativistic solar proton propagation in interplanetary space
[SH-3.2-11] N85-34826
Spectral analysis of the Forbush decrease of 13 July 1982
[SH-5.1-7] N85-35061
Observations of cosmic-ray modulations in the fall, 1984
[SH-5.1-16] N85-35069
Empirical model for the Earth's cosmic ray shadow at 400 KM: Prohibited cosmic ray access
[SH-6.1-14] N85-35087

U

UNITED KINGDOM ATOMIC ENERGY AUTHORITY, HARWELL (ENGLAND).
Calculations on the feasibility of ultrasonic inspection of steam generator tubing in pressurized water reactors
[AERE-R-10960] N85-34419
UNITED TECHNOLOGIES CORP., SOUTH WINDSOR, CONN.
Reactant pressure differential control for fuel cell gases
[NASA-CASE-MSC-20127-2] N85-34403
UNIVERSIDAD NACIONAL AUTONOMA DE MEXICO, MEXICO CITY.
Study of photon emission by electron capture during solar nuclei acceleration, 1: Temperature-dependent cross section for charge changing processes
[SH-1.1-8] N85-34735
Study of photon emission by electron capture during solar nuclei acceleration. 2: Delimitation of conditions for charge transfert establishment
[SH-1.1-9] N85-34736
Study of photon emission by electron capture during solar nuclei acceleration. 3: Photon production evaluations
[SH-1.1-10] N85-34737
Study of non-thermal photon production under different scenarios in solar flares. 1: Scenarios and formulations
[SH-1.2-2] N85-34738
Study of non-thermal photon production under different scenarios in solar flares. 2: The Compton inverse and Bremsstrahlung models and fittings
[SH-1.2-3] N85-34739
Onset of solar flares as predicted by two-dimensional MHD-models of quiescent prominences
[SH-1.3-1] N85-34750
Source energy spectra from demodulation of solar particle data by interplanetary and coronal transport
[SH-1.3-13] N85-34758
UNIVERSIDAD NACIONAL AUTONOMA DE MEXICO, VILLA OBREGON.
Shock and statistical acceleration of energetic particles in the interplanetary medium
[SH-1.5-1] N85-34771
Isotopic overabundances and the energetic particle model of solar flares
[SH-2.2-1] N85-34796
the role of shock waves in modulation of galactic cosmic rays
[SH-4.1-7] N85-34831
Difference between even and odd 11-year cycles in cosmic ray intensity
[SH-4.2-22] N85-34859
UNIVERSITY COLL., DUBLIN (IRELAND).
GeV gamma-ray astronomy telescopes with high angular resolution
[OG-9.3-4] N85-34959
Application of imaging to the atmospheric Cherenkov technique
[OG-9.5-4] N85-34981
UOP, INC., DES PLAINES, ILL.
Development and demonstration of a spiral-wound thin-film composite membrane system for the economical production of oxygen-enriched air, phase 4
[DE85-012380] N85-34288
UOP, INC., SAN DIEGO, CALIF.
Development and demonstration of a spiral-wound thin-film composite membrane system for the economical production of oxygen-enriched air, phase 4
[DE85-012380] N85-34288
UTAH GEOLOGICAL AND MINERALOGICAL SURVEY, SALT LAKE CITY.
Evaluation of low-temperature geothermal potential in Utah and Goshen Valleys and adjacent areas, Utah. Part 2: Water temperature and chemistry
[DE85-009344] N85-34438
UTAH UNIV., SALT LAKE CITY.
A method to improve observations of gamma-ray sources near 10 (15) eV
[OG-9.5-5] N85-34982
Re-evaluation of cosmic ray cutoff terminology
[SH-6.1-11] N85-35084

V

VICTORIA UNIV. (BRITISH COLUMBIA).
Generative design in architecture using an expert system N85-34582
VIKING ENGINEERING, GARRETSON, S. DAK.
Solar heat pump
[DE85-011323] N85-34453

VIRGINIA POLYTECHNIC INST. AND STATE UNIV., BLACKSBURG.
Hydrogen embrittlement testing
[DE85-007352] N85-34273
Evaluation of semiconductor devices for Electric and Hybrid Vehicle (EHV) ac-drive applications, volume 1
[NASA-CR-176118] N85-34335
VIRGINIA UNIV., CHARLOTTESVILLE.
Duality of two-point functions for confined non-relativistic quark-antiquark systems
[DE85-012334] N85-34618
VONIER (THOMAS) ASSOCIATES, INC., WASHINGTON, D.C.
Monitoring building energy performance: An informal review and characterization of research in progress
[BNL-51765] N85-34308
VRIJE UNIVERSITEIT, BRUSSELS (BELGIUM).
Bursting star formation and the overabundance of Wolf-Rayet stars
[OG-8.2-8] N85-34907

W

WASEDA UNIV., TOKYO (JAPAN).
Crystallographic orientation dependence of fatigue crack propagation in extremely low carbon steel N85-34195
Fatigue crack retardation phenomenon caused by single-multiple overloads in 2017-T3 aluminum allow N85-34196
Evaluation methods of ceramic fiber reinforced metal matrix composite N85-34206
Effect of strain rate on the initial failure of notched GRP laminates N85-34214
Impact fracture mechanism of polymer plates containing a heavy inner material N85-34215
Pulse effect in a light ion beam propagation through a Z-discharge plasma channel N85-34684
Observations of solar energetic particles at a synchronous orbit
[SH-3.1-1] N85-34806
WASHINGTON UNIV., SEATTLE.
High resolution electron microscopic characterization of interfaces in ceramics
[DE85-011207] N85-34289
Gauge invariance and fractional quantized Hall effect
[DE85-007832] N85-34716
WASHINGTON UNIV., ST. LOUIS, MO.
Implications of source abundances of ultraheavy cosmic rays
[OG-7.1-4] N85-34866
Sources of the ultraheavy cosmic rays
[OG-7.1-7] N85-34868
The model-independence of cosmic ray source determinations
[OG-7.2-1] N85-34873
Alfven wave scattering and the secondary to primary ratio
[OG-7.2-9] N85-34878
Bevalac calibration of the SOFIE range and hodoscope detectors
[OG-9.1-7] N85-34933
WESTINGHOUSE ELECTRIC CORP., PITTSBURGH, PA.
Flat-plate solar array project process development area process research of non-CZ silicon material
[NASA-CR-176117] N85-34445
WIEN UNIV. (AUSTRIA).
A cosmic ray driven instability
[OG-8.1-5] N85-34895
WILSON (JAMES E.), LA PLATA, MD.
Study to encourage and facilitate industrial investment and involvement in space
[NASA-CR-176152] N85-34147
WISCONSIN UNIV., MADISON.
Transport issues in Phaedrus-type plasmas N85-34653
Observation of helical sawtooth oscillations in a tokamak
[DE85-012062] N85-34703
WISCONSIN UNIV., MILWAUKEE.
A study of the second and third order closure models of turbulence for prediction of separated shear flows
[NASA-CR-176127] N85-34353

Y

YAKUTSK STATE UNIV. (USSR).
Sidereal anisotropy of cosmic rays
[SH-4.4-8] N85-35006
Galactic cosmic ray currents and magnetic field irregularity degree in high-speed solar wind streams
[SH-5.1-9] N85-35063
YALE UNIV., NEW HAVEN, CONN.
Research on gyrotrons
[AD-A154032] N85-34380
YUNNAN UNIV., KUNMING (CHINA).
Nucleosynthesis in the terrestrial and solar atmospheres
[SH-2.2-2] N85-34797
A very important process of nucleosynthesis in stars
[OG-7.1-11] N85-34872

CONTRACT NUMBER INDEX

Typical Contract Number Index Listing

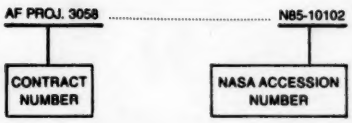

Listings in this index are arranged alphanumerically by contract number. Under each contract number the NASA accession numbers denoting documents that have been produced as a result of research done under that contract are arranged in ascending order. The NASA accession number denotes the number by which the citation is identified.

AF-AFOSR-82-0096 ..... N85-34117
AF-AFOSR-001-83-C-0266 ..... N85-34118
AF-AFOSR-1089-85 ..... N85-34522
CMA-82-396 ..... N85-34466
DAJA45-84-M-0446 ..... N85-34125
DE-AC01-77CS-34039 ..... N85-34452
N85-34455
DE-AC01-79CS-40294 ..... N85-34288
DE-AC01-79ER-10511 ..... N85-34225
DE-AC01-82ER-60081 ..... N85-34481
DE-AC02-76CH-00016 ..... N85-34217
N85-34290
N85-34292
N85-34308
N85-34326
N85-34384
N85-34451
N85-34486
N85-34613
N85-34615
N85-34710
DE-AC02-76ER-03077 ..... N85-34364
DE-AC02-76ET-53051 ..... N85-34703
DE-AC02-76EV-02541 ..... N85-34492
DE-AC02-76EV-02986 ..... N85-34464
DE-AC02-78ER-04998 ..... N85-34715
DE-AC02-80ER-10639 ..... N85-34269
DE-AC02-80ET-17019 ..... N85-34460
DE-AC02-81ER-10877 ..... N85-34235
DE-AC02-82ER-13017 ..... N85-34232
DE-AC02-82ER-60084 ..... N85-34611
N85-34614
DE-AC02-83CH-10093 ..... N85-34458
N85-34485
N85-34488
DE-AC02-83EB-40105 ..... N85-34618
DE-AC02-83ER-60106 ..... N85-34480
DE-AC03-76SF-00098 ..... N85-34219
N85-34238
N85-34289
N85-34368
N85-34384
N85-34392
N85-34412
N85-34431
N85-34439
N85-34473
N85-34605
N85-34623
DE-AC03-76SF-00515 ..... N85-34585
DE-AC03-83SF-11919 ..... N85-34448
DE-AC03-84SF-11906 ..... N85-34625
DE-AC03-84SF-12192 ..... N85-34625
DE-AC03-84SF-12193 ..... N85-34625
DE-AC04-76DP-00053 ..... N85-34274
DE-AC04-76DP-00613 ..... N85-34413
DE-AC04-76DP-00785 ..... N85-34388
DE-AC04-76DP-00789 ..... N85-34286
N85-34293
N85-34297
N85-34298
N85-34330
N85-34359
N85-34360
N85-34362
N85-34389
N85-34432
N85-34450
N85-34470
N85-34512
N85-34586
N85-34588
N85-34597
N85-34609
N85-34691
N85-34693
N85-34698
N85-34702
DE-AC04-76DR-00789 ..... N85-34240
DE-AC05-76OR-00001 ..... N85-34386
DE-AC05-76SR-00001 ..... N85-34234
DE-AC05-84CR-21400 ..... N85-34382
N85-34415
N85-34692
N85-34704
DE-AC05-84OR-21400 ..... N85-34221
N85-34287
N85-34372
N85-34418
N85-34430
N85-34463
N85-34483
N85-34598
N85-34604
N85-34612
N85-34616
N85-34619
N85-34620
N85-34622
N85-34627
N85-34694
N85-34695
N85-34697
N85-34699
N85-34701
N85-34705
N85-34708
N85-34709
N85-34713
N85-34714
DE-AC05-84OS-21400 ..... N85-34272
DE-AC06-76FF-02170 ..... N85-34411
N85-34626
DE-AC06-76RL-01830 ..... N85-34236
DE-AC06-77RL-01030 ..... N85-34270
DE-AC06-81ER-40048 ..... N85-34716
DE-AC07-76ID-01570 ..... N85-34341
N85-34371
N85-34393
DE-AC07-79ID-01675 ..... N85-34241
DE-AC08-83NV-10282 ..... N85-34487
N85-34589
DE-AC12-76SN-00052 ..... N85-34267
DE-AC21-79FT-15440 ..... N85-34459
DE-AC21-83MC-20468 ..... N85-34385
DE-AI01-78CS-54209 ..... N85-34334
DE-AI01-79ET-20320 ..... N85-34444
DE-AI01-83PE-70494 ..... N85-34461
DE-AI04-80AL-12726 ..... N85-34443
DE-AI05-83ER-40112 ..... N85-34621
DE-AI08-78ET-44802 ..... N85-34471
DE-AS05-78ER-06039 ..... N85-34273
DE-AS05-79ER-10424 ..... N85-34230
N85-34237
DE-AS07-77ET-28393 ..... N85-34438
DE-AS08-82DP-40175 ..... N85-34365
DE-AT03-80ER-10634 ..... N85-34370
DE-AT03-80ER-52061 ..... N85-34707
DE-AT03-80SF-11459 ..... N85-34437
DE-AT06-81EV-10611 ..... N85-34484
DE-FC07-79ID-12026 ..... N85-34436
DE-FC08-85DP-40200 ..... N85-34365
DE-FG01-84ER-13259 ..... N85-34474
DE-FG22-81PC-40781 ..... N85-34218
DE-FG48-79R8-00434 ..... N85-34454
DE-FG48-81R8-06041 ..... N85-34453
DFVLR-IB-129-84/5 ..... N85-34127
DNA001-83-C-0266 ..... N85-34117
N85-34118
DOE-40-550-70 ..... N85-34420
DOT-FA77WAI-817 ..... N85-34131
DRET-82-318 ..... N85-34128
DRET-83-1160 ..... N85-34395
DRET-83-1423 ..... N85-34596
DTFH61-83-C-00118 ..... N85-34440
EPRI PROJ. 1813 ..... N85-34463
ESA-5276/82 ..... N85-34394
F19628-81-K-0020 ..... N85-35084
F19628-82-K-0039 ..... N85-35085
N85-35086
F19628-85-C-0002 ..... N85-34131
JPL PROJ. 9950-1152 ..... N85-34447
JPL-956205 ..... N85-34447
MIN-DEF-2037/0218/XR/STR N85-34423
MIN-DEF-2048/O26XR/STR N85-34123
MIN-DEF-2048/026XR/STR N85-34124
NAGW-101 ..... N85-34776
N85-34802
N85-34821
NAGW-122 ..... N85-34933
NAGW-451 ..... N85-34944
N85-34945
N85-34946
NAGW-567 ..... N85-34723
NAG1-341 ..... N85-34593
NAG1-417 ..... N85-34352
NAG1-534 ..... N85-34521
NAG3-488 ..... N85-34295
NAG3-536 ..... N85-34329
NAG3-541 ..... N85-34404
NAG3-546 ..... N85-34353
NAG3-621 ..... N85-34354
NAG5-255 ..... N85-34724
NAG5-374 ..... N85-34817
N85-34860
NAG5-376 ..... N85-34819
NAG5-446 ..... N85-34467
NAG5-461 ..... N85-34726
NAG8-451 ..... N85-34866
NAG8-497 ..... N85-34723
NAG8-498 ..... N85-34936
N85-34939
NAG8-500 ..... N85-34938
N85-34939
NAG8-502 ..... N85-34938
N85-34939
NAG9-33 ..... N85-35097
NAG9-41 ..... N85-35097
NASA ORDER S-70926-A N85-34762
N85-34767
N85-35121
NASA ORDER W-14084 ..... N85-35098
N85-35099
NASW-3873 ..... N85-34147
NASW-4003 ..... N85-34153
NASW-4004 ..... N85-34285
N85-34435
NASW-4006 ..... N85-34129
NAS1-14904 ..... N85-34114
NAS1-15325 ..... N85-34517
NAS1-15805 ..... N85-34425
NAS1-16542 ..... N85-34222
NAS1-17070 ..... N85-34350
N85-34521
N85-34522
NAS1-17317 ..... N85-34113
NAS1-17387 ..... N85-34133
N85-34134
NAS1-17551 ..... N85-34156
NAS1-17945 ..... N85-34378
NAS1-18000 ..... N85-34518
N85-34519
N85-34520
NAS2-153 ..... N85-34992
NAS2-4354 ..... N85-35046
NAS2-11126 ..... N85-35050
NAS2-12081 ..... N85-34136

NAS3-20643 ..... N85-34138
N85-34141
NAS3-23687 ..... N85-34140
NAS5-23761 ..... N85-35121
NAS5-24354 ..... N85-34832
NAS5-25731 ..... N85-34853
NAS5-26680 ..... N85-34749
N85-34763
N85-34782
NAS5-27996 ..... N85-34933
NAS5-28441 ..... N85-35040
NAS5-28442 ..... N85-34838
N85-34860
N85-35050
NAS5-28449 ..... N85-35040
NAS5-28500 ..... N85-34860
NAS5-28609 ..... N85-34762
N85-34767
N85-34794
N85-34795
NAS5-28704 ..... N85-34776
N85-34802
N85-34812
N85-34821
NAS7-100 ..... N85-34335
NAS7-918 ..... N85-34781
N85-34785
N85-34786
N85-35039
N85-35042
N85-35049
NAS8-488 ..... N85-34158
NAS8-27976 ..... N85-34938
N85-34939
NAS8-27977 ..... N85-34938
N85-34939
NAS8-27978 ..... N85-34938
N85-34939
NAS8-32828 ..... N85-34934
NAS8-36144 ..... N85-34377
NA81AA-D-00035 ..... N85-34477
NGL-05-005-007 ..... N85-34992
NGL-14-01-005 ..... N85-34782
NGL-14-001-005 ..... N85-34749
N85-34763
N85-34860
NGL-14-001-006 ..... N85-34836
N85-34860
N85-35143
NGL-14-001-258 ..... N85-34931
NGR-05-002-160 ..... N85-34781
N85-34785
N85-34786
N85-34938
N85-34939
N85-34940
N85-34941
N85-34966
N85-35039
N85-35040
N85-35042
N85-35049
NGR-05-005-004 ..... N85-34916
NGR-05-008-022 ..... N85-34961
NGR-21-002-066 ..... N85-34828
N85-34830
NGR-21-002-224 ..... N85-34776
N85-34802
N85-34821
NGR-21-002-316 ..... N85-34788
N85-34802
N85-34821
NGR-24-005-050 ..... N85-34938
N85-34939
NGR-26-006-001 ..... N85-34933
N85-34938
N85-34939
NGR-30-002-052 ..... N85-34886
NR PROJ. 632-001 ..... N85-34360
NRC-FIN-A-1051 ..... N85-34420
NRC-FIN-A-2238 ..... N85-34369
NRC-FIN-A-6043 ..... N85-34371
NRC-FIN-B-0119 ..... N85-34418
NRC-FIN-B-8077 ..... N85-34475
NRC-04-81-196-01 ..... N85-34475
NSF ATM-79-25987 ..... N85-34774
NSF ATM-82-06044 ..... N85-34766
NSF ATM-82-06418 ..... N85-34853
NSF ATM-83-03758 ..... N85-34817
N85-34844
N85-35038
NSF ATM-83-04486 ..... N85-34832
N85-34853
N85-35046
NSF ATM-83-05098 ..... N85-34846
N85-35005
NSF ATM-83-05537 ..... N85-34772
N85-34779
N85-35051
NSF ATM-83-11241 ..... N85-34891
N85-34926
NSF ATM-83-17701 ..... N85-34832
NSF ATM-83-24486 ..... N85-34822
NSF ATM-84-01427 ..... N85-34860
NSF ATM-84-07546 ..... N85-34802
N85-34821
NSF ATM-84-12382 ..... N85-34860
NSF DMR-79-20735 ..... N85-34716
NSF DPP-83-00544 ..... N85-34817
N85-34844
NSF ECS-82-04381 ..... N85-34524
N85-34551
NSF INT-81-18555 ..... N85-34822
NSF INT-84-00591 ..... N85-34849
NSF MCS-83-04185 ..... N85-34538
NSF PHY-80-25605 ..... N85-34723
NSF PHY-84-15294 ..... N85-34982
NSF-ATM-83-05537 ..... N85-34837
NSG-1435 ..... N85-34521
NSG-5049 ..... N85-34397
NSG-7101 ..... N85-34832
N85-34848
N85-34898
N85-34903
NSG-7464 ..... N85-34931
NSG-7603 ..... N85-34725
NSG-7653 ..... N85-34723
NSG3-48 ..... N85-34405
NSG5-138 ..... N85-35141
N00014-78-C-0306 ..... N85-34539
N00014-80-C-0075 ..... N85-34380
N00014-84-C-0149 ..... N85-34336
N00024-78-C-5384 ..... N85-35051
N00024-83-C-5301 ..... N85-34772
N85-34777
N00024-83-E-5301 ..... N85-34773
N00024-85-C-5301 ..... N85-34837
N85-34840
N85-34992
N00030-82-C-0235 ..... N85-34524
STU-81-4626 ..... N85-34126
W-31-108-ENG-38 ..... N85-34602
W-31-109-ENG-38 ..... N85-34220
N85-34226
N85-34233
N85-34275
N85-34291
N85-34391
N85-34417
N85-34456
N85-34469
N85-34493
N85-34516
N85-34607
N85-34617
N85-34712
W-7405-ENG-36 ..... N85-34271
N85-34296
N85-34299
N85-34300
N85-34301
N85-34302
N85-34303
N85-34305
N85-34306
N85-34342
N85-34343
N85-34344
N85-34345
N85-34366
N85-34390
N85-34414
N85-34416
N85-34472
N85-34601
N85-34603
N85-34606
N85-34608
N85-34624
N85-34696
W-7405-ENG-38 ..... N85-34363
W-7405-ENG-48 ..... N85-34231
N85-34239
N85-34268
N85-34304
N85-34361
N85-34367
N85-34383
N85-34398
N85-34399
N85-34457
N85-34462
N85-34465
N85-34587
N85-34590
N85-34595
N85-34633
N85-34700
N85-34706
W-7405-ENG-82 ..... N85-34242
146-20-1A N85-34150
307-04-1 ..... N85-34136
324-01-00-01 ..... N85-34376
384-55-62 ..... N85-34176
505-31-01 ..... N85-34116
N85-34358
505-31-13-06 ..... N85-34355
505-31-21 ..... N85-34115
505-31-51 ..... N85-34146
N85-34378
N85-34379
505-31-53-10 ..... N85-34352
505-31-83-01 ..... N85-34522
505-33-7B N85-34427
505-33-7C N85-34409
505-33-43-12 ..... N85-34113
505-33-62 ..... N85-34266
N85-34408
505-34-03-03 ..... N85-34144
505-40-22 ..... N85-34295
505-42-92 ..... N85-34406
505-42-94 ..... N85-34405
N85-34407
506-51-23-03 ..... N85-34351
506-53-1B N85-34265
506-53-23 ..... N85-34426
506-53-43-15 ..... N85-34425
506-55-22 ..... N85-34177
N85-34178
N85-34179
506-55-72 ..... N85-34631
533-04-1A N85-34140
533-05-12 ..... N85-34223
N85-34284
542-05-12 ..... N85-34443
553-13-00 ..... N85-34356
563-22-68-88 ..... N85-34518
N85-34520
563-22-69-88 ..... N85-34519
674-25-05 ..... N85-34357
727-310-20-46 ..... N85-34155
776-33-41 ..... N85-34444
997-21-01 ..... N85-34510

REPORT / ACCESSION NUMBER INDEX

Typical Report / Accession Number Index Listing

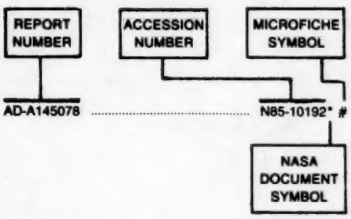

Listings in this index are arranged alphanumerically by report number. The NASA accession number denotes the number by which the citation is identified. An asterisk (*) indicates that the item is a NASA report. A pound sign (#) indicates that the item is available on microfiche.

AD-A154032 ..... N85-34380 #
AD-A154748 ..... N85-34336 #

AD-D011719 ..... N85-34224 #
AD-D011720 ..... N85-34337 #
AD-D011721 ..... N85-34338 #
AD-D011722 ..... N85-34410 #
AD-D011723 ..... N85-34339 #
AD-D011724 ..... N85-34594 #
AD-D011725 ..... N85-34381 #
AD-D011726 ..... N85-34340 #
AD-D011727 ..... N85-34632 #

AERE-R-10960 ..... N85-34419 #

AERONOMICA-ACTA-A-287-1984 ..... N85-34466

AMTE(S)-R-84104 ..... N85-34424

ANL-84-24 ..... N85-34602 #
ANL-84-56 ..... N85-34516 #

ANL/ACL-85-2 ..... N85-34233 #

ANL/EES-TM-276 ..... N85-34493 #

ANL/ES-146 ..... N85-34469 #

ANL/OTEC-TM-4 ..... N85-34456 #

APR-2 ..... N85-34480 #

AQEF-783/84 ..... N85-34228 #

AR-8 ..... N85-34446* #
AR-003-962 ..... N85-34132 #
AR-003-968 ..... N85-34137 #
AR-003-999 ..... N85-34119 #
AR-004-018 ..... N85-34429 #

ARL-AERO-R-162 ..... N85-34137 #

ARL-STRUC-R-416 ..... N85-34119 #

ARL-STRUC-TM-409 ..... N85-34429 #

ARL-SYS-R-32 ..... N85-34132 #

ASR-1 ..... N85-34140* #

ATC-132 ..... N85-34131 #

BBC-RD-1985/5 ..... N85-34328

BDX-613-3115 ..... N85-34413 #

BGSD-MO-7035 ..... N85-34377* #

BLL-M-35776-(5828.4) N85-34260

BLL-M-35781-(5828.4) N85-34283
BLL-M-35786-(5828.4) N85-34349
BLL-M-35795-(5828.4) N85-34711
BLL-M-35808-(5828.4) N85-34259
BLL-M-35809-(5828.4) N85-34258
BLL-M-35810-(5828.4) N85-34257
BLL-M-35819-(5828.4) N85-34348
BLL-M-35825-(5828.4) N85-34256
BLL-M-35829-(5828.4) N85-34251
BLL-M-35843-(5828.4) N85-34249
BLL-M-35844-(5828.4) N85-34250
BLL-M-35850-(5828.4) N85-34252
BLL-M-35868-(5828.4) N85-34253
BLL-M-35874-(5828.4) N85-34261
BLL-M-35875-(5828.4) N85-34254
BLL-M-35878-(5828.4) N85-34347
BLL-M-35894-(5828.4) N85-34263
BLL-M-35896-(5826.4) N85-34262
BLL-M-35897-(5828.4) N85-34255
BLL-M-36296-(5828.4) N85-34247
BLL-M-36304 ..... N85-34422
BLL-M-36315-(5828.4) N85-34248
BLL-M-36317-(5828.4) N85-34246

BLL-OA-TRANS-3226-(6196.3) N85-34244

BLL-RARDE-TR-1220-(7291.7965) N85-34245

BMFT-FB-T-85-006 ..... N85-34294 #

BMI-2126 ..... N85-34592 #

BNL-36089 ..... N85-34217 #
BNL-36369 ..... N85-34451 #
BNL-36395 ..... N85-34613 #
BNL-36439 ..... N85-34615 #
BNL-51765 ..... N85-34308 #

BR94017 ..... N85-34424
BR94778 ..... N85-34423
BR95018 ..... N85-34514

CNES-NT-113 ..... N85-34157 #
CNES-NT-114 ..... N85-34346 #

CONF-841201-32-APP ..... N85-34370 #
CONF-850137-3 ..... N85-34384 #
CONF-850270-1 ..... N85-34368 #
CONF-850280-1 ..... N85-34217 #
CONF-850283-1 ..... N85-34512 #
CONF-850301-3 ..... N85-34372 #
CONF-850301-7 ..... N85-34704 #
CONF-850310-92 ..... N85-34695 #
CONF-850310-97 ..... N85-34705 #
CONF-850310-98 ..... N85-34694 #
CONF-850310-99 ..... N85-34699 #
CONF-850310-100 ..... N85-34692 #
CONF-850311-8 ..... N85-34277 #
CONF-850312-2 ..... N85-34439 #
CONF-850315-3 ..... N85-34615 #
CONF-850351-6 ..... N85-34276 #
CONF-850388-4 ..... N85-34366 #
CONF-850406-10 ..... N85-34617 #
CONF-850411-12 ..... N85-34596 #
CONF-850421-6 ..... N85-34451 #
CONF-850421-8 ..... N85-34623 #
CONF-850504-26 ..... N85-34702 #
CONF-850504-27 ..... N85-34330 #
CONF-850504-32 ..... N85-34691 #
CONF-850504-33 ..... N85-34700 #
CONF-850504-36 ..... N85-34619 #
CONF-850504-37 ..... N85-34698 #
CONF-850504-39 ..... N85-34693 #
CONF-850507-3 ..... N85-34608 #
CONF-850507-7 ..... N85-34620 #
CONF-850507-10 ..... N85-34612 #
CONF-850507-17 ..... N85-34624 #
CONF-850533-6 ..... N85-34589 #
CONF-850533-7 ..... N85-34613 #
CONF-850706-2 ..... N85-34304 #
CONF-850706-4 ..... N85-34603 #
CONF-850706-5 ..... N85-34300 #
CONF-850706-6 ..... N85-34301 #

CONF-850706-7 ..... N85-34299 #
CONF-850706-8 ..... N85-34303 #
CONF-850706-10 ..... N85-34296 #
CONF-850706-14 ..... N85-34297 #
CONF-850706-15 ..... N85-34298 #
CONF-850711-4 ..... N85-34597 #
CONF-850711-5 ..... N85-34586 #
CONF-850711-6 ..... N85-34588 #
CONF-850711-8 ..... N85-34609 #
CONF-850712-2 ..... N85-34363 #
CONF-850714-1 ..... N85-34696 #
CONF-850742-1 ..... N85-34302 #
CONF-850745-4 ..... N85-34362 #
CONF-850745-5 ..... N85-34367 #
CONF-850745-6 ..... N85-34361 #
CONF-8405144-4 ..... N85-34473 #
CONF-8407123-1 ..... N85-34289 #
CONF-8409121-2 ..... N85-34431 #
CONF-8410265-SUMMS ..... N85-34472 #
CONF-8411134-1 ..... N85-34231 #
CONF-8411148-1 ..... N85-34600 #
CONF-8503105-2 ..... N85-34706 #
CONF-8504113-6 ..... N85-34240 #
CONF-8504116-2 ..... N85-34616 #
CONF-8504116-3 ..... N85-34714 #
CONF-8504135-1 ..... N85-34465 #
CONF-8505115-5-PT-2 ..... N85-34470 #
CONF-8505131-3 ..... N85-34595 #
CONF-8505138-1 ..... N85-34713 #
CONF-8505138-2 ..... N85-34712 #
CONF-8505139-1 ..... N85-34234 #

CT-585 ..... N85-34482 #

C2248/4/4-VOL-1 ..... N85-34394 #
C2248/4/4-VOL-2 ..... N85-34394 #
C2248/4/4-VOL-3 ..... N85-34394 #
C2248/4/5-VOL-1 ..... N85-34394 #
C2248/4/5-VOL-2 ..... N85-34394 #
C2248/4/5-VOL-3 ..... N85-34394 #
C2685/4/2-VOL-1 ..... N85-34394 #
C2685/4/2-VOL-2 ..... N85-34394 #
C2685/4/2-VOL-3 ..... N85-34394 #

DE85-003047 ..... N85-34363 #
DE85-004987 ..... N85-34231 #
DE85-005005 ..... N85-34436 #
DE85-005306 ..... N85-34232 #
DE85-005734 ..... N85-34417 #
DE85-005736 ..... N85-34460 #
DE85-005738 ..... N85-34306 #
DE85-005740 ..... N85-34393 #
DE85-005749 ..... N85-34387 #
DE85-005756 ..... N85-34290 #
DE85-005757 ..... N85-34626 #
DE85-005759 ..... N85-34218 #
DE85-005760 ..... N85-34457 #
DE85-005762 ..... N85-34275 #
DE85-005763 ..... N85-34220 #
DE85-005765 ..... N85-34633 #
DE85-005766 ..... N85-34293 #
DE85-005987 ..... N85-34458 #
DE85-005988 ..... N85-34391 #
DE85-005991 ..... N85-34459 #
DE85-005992 ..... N85-34416 #
DE85-006001 ..... N85-34345 #
DE85-006002 ..... N85-34392 #
DE85-006018 ..... N85-34411 #
DE85-006361 ..... N85-34291 #
DE85-006400 ..... N85-34226 #
DE85-006401 ..... N85-34292 #
DE85-006406 ..... N85-34286 #
DE85-006407 ..... N85-34390 #
DE85-006408 ..... N85-34326 #
DE85-006409 ..... N85-34344 #
DE85-006411 ..... N85-34604 #
DE85-006412 ..... N85-34242 #
DE85-006420 ..... N85-34219 #
DE85-006423 ..... N85-34305 #
DE85-006434 ..... N85-34412 #
DE85-006438 ..... N85-34342 #
DE85-006443 ..... N85-34274 #
DE85-006445 ..... N85-34241 #

DE85-006499 ..... N85-34627 #
DE85-006501 ..... N85-34343 #
DE85-006502 ..... N85-34389 #
DE85-006505 ..... N85-34388 #
DE85-006508 ..... N85-34414 #
DE85-006511 ..... N85-34607 #
DE85-006518 ..... N85-34415 #
DE85-006519 ..... N85-34710 #
DE85-007266 ..... N85-34304 #
DE85-007291 ..... N85-34715 #
DE85-007352 ..... N85-34273 #
DE85-007756 ..... N85-34484 #
DE85-007832 ..... N85-34716 #
DE85-008306 ..... N85-34614 #
DE85-008787 ..... N85-34488 #
DE85-008807 ..... N85-34485 #
DE85-009344 ..... N85-34438 #
DE85-009441 ..... N85-34588 #
DE85-009442 ..... N85-34586 #
DE85-009444 ..... N85-34597 #
DE85-009476 ..... N85-34370 #
DE85-009540 ..... N85-34372 #
DE85-009550 ..... N85-34366 #
DE85-009581 ..... N85-34303 #
DE85-009587 ..... N85-34301 #
DE85-009593 ..... N85-34300 #
DE85-009598 ..... N85-34603 #
DE85-009606 ..... N85-34299 #
DE85-009609 ..... N85-34296 #
DE85-009620 ..... N85-34302 #
DE85-009634 ..... N85-34696 #
DE85-009753 ..... N85-34450 #
DE85-009760 ..... N85-34297 #
DE85-009770 ..... N85-34217 #
DE85-009821 ..... N85-34609 #
DE85-009901 ..... N85-34368 #
DE85-009903 ..... N85-34431 #
DE85-009904 ..... N85-34361 #
DE85-009923 ..... N85-34437 #
DE85-009982 ..... N85-34298 #
DE85-010365 ..... N85-34452 #
DE85-010371 ..... N85-34455 #
DE85-010569 ..... N85-34472 #
DE85-010628 ..... N85-34238 #
DE85-010657 ..... N85-34362 #
DE85-010731 ..... N85-34608 #
DE85-010926 ..... N85-34367 #
DE85-010984 ..... N85-34384 #
DE85-011038 ..... N85-34365 #
DE85-011169 ..... N85-34270 #
DE85-011185 ..... N85-34611 #
DE85-011207 ..... N85-34289 #
DE85-011233 ..... N85-34225 #
DE85-011302 ..... N85-34701 #
DE85-011303 ..... N85-34382 #
DE85-011323 ..... N85-34453 #
DE85-011343 ..... N85-34454 #
DE85-011368 ..... N85-34269 #
DE85-011403 ..... N85-34364 #
DE85-011409 ..... N85-34695 #
DE85-011420 ..... N85-34704 #
DE85-011426 ..... N85-34598 #
DE85-011506 ..... N85-34234 #
DE85-011532 ..... N85-34481 #
DE85-011544 ..... N85-34702 #
DE85-011549 ..... N85-34620 #
DE85-011559 ..... N85-34705 #
DE85-011567 ..... N85-34699 #
DE85-011568 ..... N85-34692 #
DE85-011569 ..... N85-34694 #
DE85-011586 ..... N85-34221 #
DE85-011648 ..... N85-34287 #
DE85-011649 ..... N85-34267 #
DE85-011683 ..... N85-34589 #
DE85-011707 ..... N85-34470 #
DE85-011715 ..... N85-34487 #
DE85-011717 ..... N85-34240 #
DE85-011747 ..... N85-34230 #
DE85-011748 ..... N85-34237 #
DE85-011753 ..... N85-34330 #
DE85-011795 ..... N85-34385 #
DE85-011826 ..... N85-34451 #
DE85-011830 ..... N85-34613 #
DE85-011837 ..... N85-34615 #
DE85-011849 ..... N85-34706 #
DE85-011855 ..... N85-34465 #
DE85-011856 ..... N85-34595 #
DE85-011857 ..... N85-34700 #
DE85-011863 ..... N85-34398 #
DE85-011877 ..... N85-34492 #
DE85-011879 ..... N85-34235 #
DE85-011892 ..... N85-34271 #
DE85-011907 ..... N85-34616 #
DE85-011913 ..... N85-34612 #
DE85-011916 ..... N85-34512 #
DE85-011918 ..... N85-34698 #
DE85-011935 ..... N85-34713 #
DE85-011938 ..... N85-34714 #
DE85-011939 ..... N85-34619 #
DE85-011954 ..... N85-34341 #
DE85-011964 ..... N85-34718 #
DE85-011995 ..... N85-34691 #
DE85-011996 ..... N85-34236 #
DE85-012007 ..... N85-34585 #
DE85-012009 ..... N85-34448 #
DE85-012015 ..... N85-34233 #
DE85-012019 ..... N85-34413 #
DE85-012030 ..... N85-34693 #
DE85-012056 ..... N85-34430 #
DE85-012062 ..... N85-34703 #
DE85-012066 ..... N85-34697 #
DE85-012074 ..... N85-34707 #
DE85-012082 ..... N85-34708 #
DE85-012124 ..... N85-34617 #
DE85-012253 ..... N85-34449 #
DE85-012284 ..... N85-34712 #
DE85-012291 ..... N85-34456 #
DE85-012293 ..... N85-34493 #
DE85-012308 ..... N85-34474 #
DE85-012311 ..... N85-34625 #
DE85-012320 ..... N85-34610 #
DE85-012334 ..... N85-34618 #
DE85-012341 ..... N85-34483 #
DE85-012346 ..... N85-34709 #
DE85-012380 ..... N85-34288 #
DE85-012407 ..... N85-34464 #
DE85-012486 ..... N85-34463 #
DE85-012553 ..... N85-34439 #
DE85-012555 ..... N85-34473 #
DE85-012605 ..... N85-34623 #
DE85-012728 ..... N85-34624 #
DE85-012788 ..... N85-34591 #
DE85-012789 ..... N85-34486 #
DE85-012796 ..... N85-34386 #
DE85-012817 ..... N85-34239 #
DE85-012937 ..... N85-34383 #
DE85-012952 ..... N85-34587 #
DE85-012964 ..... N85-34268 #
DE85-012973 ..... N85-34399 #
DE85-012980 ..... N85-34621 #
DE85-012987 ..... N85-34480 #
DE85-013038 ..... N85-34469 #
DE85-013039 ..... N85-34471 #
DE85-013104 ..... N85-34622 #
DE85-013151 ..... N85-34432 #
DE85-013166 ..... N85-34272 #
DE85-013171 ..... N85-34360 #
DE85-013176 ..... N85-34462 #
DE85-013178 ..... N85-34359 #
DE85-013182 ..... N85-34590 #

DGR-481/176 ..... N85-34628 #
DGR-481/177 ..... N85-34628 #
DGR-481/178 ..... N85-34628 #
DGR-481/179 ..... N85-34628 #

DIT-3 ..... N85-34606 #

DOE/CE-0110 ..... N85-34449 #

DOE/CH-00016/T6 ..... N85-34486 #

DOE/CS-34039/T6 ..... N85-34455 #
DOE/CS-34039/T9 ..... N85-34452 #
DOE/CS-40294/1 ..... N85-34288 #
DOE/CS-54209/27 ..... N85-34335* #
DOE/CS-54209/28 ..... N85-34334* #

DOE/DP-40200/T1 ..... N85-34365 #

DOE/ER-0222 ..... N85-34591 #
DOE/ER-03077/244 ..... N85-34364 #
DOE/ER-04998/T5 ..... N85-34715 #
DOE/ER-06039/T2 ..... N85-34273 #
DOE/ER-10424/4 ..... N85-34237 #
DOE/ER-10424/5 ..... N85-34230 #
DOE/ER-10511/T6 ..... N85-34225 #
DOE/ER-10639/T2 ..... N85-34269 #
DOE/ER-10877/3 ..... N85-34235 #
DOE/ER-13017/T1 ..... N85-34232 #
DOE/ER-13259/T1 ..... N85-34474 #
DOE/ER-40048/10-P4 ..... N85-34716 #
DOE/ER-40105/462 ..... N85-34618 #
DOE/ER-40112/T1 ..... N85-34621 #
DOE/ER-60081/T2 ..... N85-34481 #
DOE/ER-60084/T2 ..... N85-34614 #
DOE/ER-60084/4 ..... N85-34611 #
DOE/ER-60106/2 ..... N85-34480 #

DOE/ET-28393/T7-PT-2 ..... N85-34438 #
DOE/ET-53051/79 ..... N85-34703 #
DOE/EV-02541/T2 ..... N85-34492 #
DOE/EV-02986/T1 ..... N85-34464 #
DOE/EV-10611/T1 ..... N85-34484 #

DOE/ID-12026/T9 ..... N85-34436 #

DOE/JPL-954527-84/27 ..... N85-34446* #
DOE/JPL-956205-85/9 ..... N85-34447* #
DOE/JPL-956616-85/5 ..... N85-34445* #

DOE/MA-0184 ..... N85-34718 #

DOE/NASA/12726-26 ..... N85-34443* #
DOE/NASA/20320-65 ..... N85-34444* #

DOE/NBB-0070 ..... N85-34483 #

DOE/OR-21400/T123 ..... N85-34463 #
DOE/OR-21400/T125 ..... N85-34709 #

DOE/RL-01830/T35 ..... N85-34236 #

DOE/RW/85/003 ..... N85-34628 #

DOE/R8-00434/T1 ..... N85-34454 #
DOE/R8-06041/T1 ..... N85-34453 #

DOE/SF-11919/T2 ..... N85-34448 #

DP-MS-85-37 ..... N85-34234 #

DRD-SE-5 ..... N85-34445* #

DRL-206 ..... N85-34445* #

D6-51089 ..... N85-34517* #

E-2325-1 ..... N85-34284* #
E-2506 ..... N85-34631* #
E-2564 ..... N85-34444* #
E-2598 ..... N85-34427* #
E-2646 ..... N85-34443* #
E-2648 ..... N85-34405* #
E-2653 ..... N85-34150* #
E-2657 ..... N85-34265* #
E-2658 ..... N85-34408* #
E-2659 ..... N85-34176* #
E-2660 ..... N85-34407* #
E-2666 ..... N85-34406* #
E-2670 ..... N85-34409* #
E-2671 ..... N85-34223* #
E-2672 ..... N85-34177* #
E-2673 ..... N85-34178* #
E-2689 ..... N85-34179* #
E-2694 ..... N85-34266* #
E-2708 ..... N85-34356* #
E-2715 ..... N85-34357* #

EGG-SE-6764 ..... N85-34341 #

EGG-2245 ..... N85-34371 #
EGG-10282-2056 ..... N85-34589 #

EGG/10282-2057 ..... N85-34487 #

EML-437 ..... N85-34610 #

ENST-83E018 ..... N85-34331 #

EOSL-85-006 ..... N85-34397* #

ESA-CR(P)-2009-C-VOL-3 ..... N85-34394 #
ESA-CR(P)-2009-VOL-1 ..... N85-34394 #
ESA-CR(P)-2009-VOL-2 ..... N85-34394 #

ESL-716109 ..... N85-34404* #
ESL-716111-3 ..... N85-34329* #

FAA/PM-84/33 ..... N85-34131 #

FFA-TN-1985-4 ..... N85-34126 #

FHWA/IP-84/15 ..... N85-34440 #

FI-447-TBR-18 ..... N85-34332 #

FS-196 ..... N85-34449 #

GA-A-17773 ..... N85-34625 #

GAT-T-3297 ..... N85-34386 #

GPO-39-847 ..... N85-34130 #

GU-AERO-8408 ..... N85-34120 #
GU-AERO-8410 ..... N85-34121 #

GU-AERO-8412 N85-34122 #
GU-AERO-8413-VOL-1 N85-34123 #
GU-AERO-8414 N85-34124 #
GU-AERO-8501 N85-34125 #

G85F-0299 N85-34155* #

HR-73600253 N85-34136* #

IAG-85-282 N85-34357* #

ICASE-84-59 N85-34350* #
ICASE-85-35 N85-34522* #
ICASE-85-36 N85-34521* #

INVESTIGATIONS-26 N85-34436 #

IOS-177 N85-34243 #
IOS-204 N85-34628 #

IPPJ-AM-40 N85-34690 #
IPPJ-AM-41-REV N85-34689 #

IPPJ-724 N85-34668 #
IPPJ-725 N85-34670 #
IPPJ-726 N85-34669 #
IPPJ-727 N85-34644 #
IPPJ-728 N85-34637 #
IPPJ-729 N85-34635 #
IPPJ-730 N85-34638 #
IPPJ-731 N85-34639 #
IPPJ-732 N85-34640 #
IPPJ-733 N85-34641 #
IPPJ-734 N85-34642 #
IPPJ-735 N85-34643 #
IPPJ-736 N85-34636 #

ISBN-3-88148-214-8 N85-34478
ISBN-3-88148-216-4 N85-34479

ISL-CO-219/84 N85-34127 #
ISL-CO-223/84 N85-34634 #
ISL-CO-225/84 N85-34128 #
ISL-CO-226/84 N85-34395 #
ISL-CO-227/84 N85-34396 #
ISL-CO-228/84 N85-34307 #

ISL-R-107/84 N85-34400 #

ISSN-0069-5882 N85-34476 #
ISSN-0072-4130 N85-34478
ISSN-0072-4130 N85-34479
ISSN-0077-5606 N85-34428 #
ISSN-0077-5606 N85-34599 #
ISSN-0082-5255 N85-34117 #
ISSN-0082-5255 N85-34118 #
ISSN-0082-5263 N85-34139 #
ISSN-0262-5369 N85-34513
ISSN-0309-3069 N85-34145
ISSN-0309-3069 N85-34434
ISSN-0309-3069 N85-34515
ISSN-0309-3069 N85-34630
ISSN-0340-7608 N85-34294 #
ISSN-0368-3141 N85-34180 #
ISSN-0713-5424 N85-34523 #
ISSN-0751-1353 N85-34331 #

JPL-9950-1038 N85-34335* #
JPL-9950-1039 N85-34334* #
JPL-9950-1151 N85-34446* #
JPL-9950-1159 N85-34442* #
JPL-9950-1161 N85-34445* #

JPRS-UBB-85-021 N85-34489 #

JPRS-USB-85-005 N85-34494 #

L-15781 N85-34351* #
L-15903 N85-34355* #
L-15941 N85-34144* #

LA-UR-85-742 N85-34301 #
LA-UR-85-769 N85-34300 #
LA-UR-85-860 N85-34303 #
LA-UR-85-887 N85-34366 #
LA-UR-85-981 N85-34696 #
LA-UR-85-1023 N85-34302 #
LA-UR-85-1088 N85-34603 #
LA-UR-85-1122 N85-34299 #
LA-UR-85-1130 N85-34296 #
LA-UR-85-1476 N85-34608 #
LA-UR-85-1730 N85-34624 #

LA-10034-SR N85-34606 #
LA-10264-MS N85-34601 #
LA-10339-C- N85-34472 #
LA-10369-MS N85-34271 #

LBL-17473 N85-34473 #
LBL-18268 N85-34439 #
LBL-18457 N85-34431 #
LBL-18500 N85-34605 #
LBL-18833 N85-34368 #
LBL-19146 N85-34238 #
LBL-19319 N85-34384 #
LBL-19396 N85-34289 #
LBL-19468 N85-34623 #

LC-84-979 N85-35142* #

MCR-85-533 N85-34156* #

MITT-42 N85-34476 #

MPN-764038 N85-34404* #

M85901341 N85-34475 #
M85901384 N85-34276 #

NAS 1.12/6:4405 N85-35142* #
NAS 1.15:77670 N85-34129* #
NAS 1.15:77890 N85-34285* #
NAS 1.15:77914 N85-34435* #
NAS 1.15:85344 N85-34116* #
NAS 1.15:86191 N85-34728* #
NAS 1.15:86194 N85-34175* #
NAS 1.15:86224 N85-34155* #
NAS 1.15:86389 N85-34355* #
NAS 1.15:86517 N85-34511* #
NAS 1.15:86519 N85-34154* #
NAS 1.15:86718 N85-34379* #
NAS 1.15:86719 N85-34115* #
NAS 1.15:86762 N85-34135* #
NAS 1.15:86763 N85-34146* #
NAS 1.15:86768 N85-34358* #
NAS 1.15:86788 N85-34378* #
NAS 1.15:86822 N85-34510* #
NAS 1.15:87018 N85-34444* #
NAS 1.15:87074 N85-34443* #
NAS 1.15:87075 N85-34405* #
NAS 1.15:87077 N85-34150* #
NAS 1.15:87079 N85-34265* #
NAS 1.15:87080 N85-34176* #
NAS 1.15:87082 N85-34406* #
NAS 1.15:87083 N85-34631* #
NAS 1.15:87085 N85-34223* #
NAS 1.15:87086 N85-34177* #
NAS 1.15:87087 N85-34178* #
NAS 1.15:87092 N85-34284* #
NAS 1.15:87096 N85-34407* #
NAS 1.15:87097 N85-34408* #
NAS 1.15:87098 N85-34179* #
NAS 1.15:87100 N85-34266* #
NAS 1.15:87102 N85-34427* #
NAS 1.15:87107 N85-34409* #
NAS 1.15:87108 N85-34356* #
NAS 1.15:87115 N85-34357* #
NAS 1.15:87498 N85-34727* #
NAS 1.15:87584 N85-34426* #
NAS 1.15:87585 N85-35151* #
NAS 1.21:7011(274) N85-34491*
NAS 1.26:3906 N85-34114* #
NAS 1.26:3915 N85-34593* #
NAS 1.26:3916 N85-34133* #
NAS 1.26:3918 N85-34134* #
NAS 1.26:3921 N85-34113* #
NAS 1.26:3924 N85-34352* #
NAS 1.26:168070 N85-34141* #
NAS 1.26:168245 N85-34138* #
NAS 1.26:172502 N85-34350* #
NAS 1.26:172562 N85-34222* #
NAS 1.26:172570 N85-34156* #
NAS 1.26:174765 N85-34140* #
NAS 1.26:174911 N85-34295* #
NAS 1.26:176106 N85-34725* #
NAS 1.26:176110 N85-34153* #
NAS 1.26:176115 N85-34724* #
NAS 1.26:176117 N85-34445* #
NAS 1.26:176118 N85-34335* #
NAS 1.26:176119 N85-34334* #
NAS 1.26:176126 N85-34442* #
NAS 1.26:176127 N85-34353* #
NAS 1.26:176132 N85-34446* #
NAS 1.26:176136 N85-34447* #
NAS 1.26:176138 N85-34723* #
NAS 1.26:176142 N85-34726* #
NAS 1.26:176143 N85-34377* #
NAS 1.26:176145 N85-34354* #
NAS 1.26:176149 N85-34467* #
NAS 1.26:176152 N85-34147* #
NAS 1.26:176153 N85-34152* #
NAS 1.26:176159 N85-34397* #
NAS 1.26:176160 N85-34158* #
NAS 1.26:176161 N85-35141* #
NAS 1.26:176162 N85-34329* #
NAS 1.26:176163 N85-34404* #
NAS 1.26:176263 N85-34264* #
NAS 1.26:177366 N85-34136* #
NAS 1.26:177945 N85-34425* #
NAS 1.26:177948 N85-34518* #
NAS 1.26:177949 N85-34519* #
NAS 1.26:177950 N85-34520* #
NAS 1.26:177952 N85-34376* #
NAS 1.26:177955 N85-34521* #
NAS 1.26:177961 N85-34522* #
NAS 1.26:178224 N85-34517* #
NAS 1.55:2376-VOL-3 N85-34862* #
NAS 1.55:2376-VOL-4 N85-34729* #
NAS 1.55:2376-VOL-5 N85-34991* #
NAS 1.60:2307 N85-34351* #
NAS 1.60:2451 N85-34144* #
NAS 1.60:2510 N85-34149* #
NAS 1.60:2511 N85-34148* #
NAS 1.71:NPO-15493-2 N85-34373*

NASA-CASE-ARC-11424-1 N85-34281*
NASA-CASE-ARC-11503-1 N85-34374*
NASA-CASE-ARC-11522-2 N85-34280*

NASA-CASE-LAR-13226-1 N85-34282*
NASA-CASE-LAR-13243-1 N85-34375*

NASA-CASE-LEW-14053-1 N85-34402*
NASA-CASE-LEW-14077-1 N85-34441*

NASA-CASE-MFS-25907-1 N85-34401*

NASA-CASE-MSC-20127-2 N85-34403*

NASA-CASE-NPO-15493-2 N85-34373*
NASA-CASE-NPO-15696-1 N85-34333*
NASA-CASE-NPO-15704-1 N85-34327*
NASA-CASE-NPO-15865-1 N85-34629*
NASA-CASE-NPO-15949-1 N85-34722*

NASA-CP-2376-VOL-3 N85-34862* #
NASA-CP-2376-VOL-4 N85-34729* #
NASA-CP-2376-VOL-5 N85-34991* #

NASA-CR-3906 N85-34114* #
NASA-CR-3915 N85-34593* #
NASA-CR-3916 N85-34133* #
NASA-CR-3918 N85-34134* #
NASA-CR-3921 N85-34113* #
NASA-CR-3924 N85-34352* #
NASA-CR-168070 N85-34141* #
NASA-CR-168245 N85-34138* #
NASA-CR-172502 N85-34350* #
NASA-CR-172562 N85-34222* #
NASA-CR-172570 N85-34156* #
NASA-CR-174765 N85-34140* #
NASA-CR-174911 N85-34295* #
NASA-CR-176106 N85-34725* #
NASA-CR-176110 N85-34153* #
NASA-CR-176115 N85-34724* #
NASA-CR-176117 N85-34445* #
NASA-CR-176118 N85-34335* #
NASA-CR-176119 N85-34334* #
NASA-CR-176126 N85-34442* #
NASA-CR-176127 N85-34353* #
NASA-CR-176132 N85-34446* #
NASA-CR-176136 N85-34447* #
NASA-CR-176138 N85-34723* #
NASA-CR-176142 N85-34726* #
NASA-CR-176143 N85-34377* #
NASA-CR-176145 N85-34354* #
NASA-CR-176149 N85-34467* #
NASA-CR-176152 N85-34147* #
NASA-CR-176153 N85-34152* #
NASA-CR-176159 N85-34397* #
NASA-CR-176160 N85-34158* #
NASA-CR-176161 N85-35141* #
NASA-CR-176162 N85-34329* #
NASA-CR-176163 N85-34404* #
NASA-CR-176263 N85-34264* #
NASA-CR-177366 N85-34136* #
NASA-CR-177945 N85-34425* #
NASA-CR-177948 N85-34518* #
NASA-CR-177949 N85-34519* #
NASA-CR-177950 N85-34520* #
NASA-CR-177952 N85-34376* #
NASA-CR-177955 N85-34521* #
NASA-CR-177961 N85-34522* #
NASA-CR-178224 N85-34517* #

NASA-SP-4405 N85-35142* #
NASA-SP-7011(274) N85-34491*

NASA-TM-77670 ..... N85-34129* #
NASA-TM-77890 ..... N85-34285* #
NASA-TM-77914 ..... N85-34435* #
NASA-TM-85344 ..... N85-34116* #
NASA-TM-86191 ..... N85-34728* #
NASA-TM-86194 ..... N85-34175* #
NASA-TM-86224 ..... N85-34155* #
NASA-TM-86389 ..... N85-34355* #
NASA-TM-86517 ..... N85-34511* #
NASA-TM-86519 ..... N85-34154* #
NASA-TM-86718 ..... N85-34379* #
NASA-TM-86719 ..... N85-34115* #
NASA-TM-86762 ..... N85-34135* #
NASA-TM-86763 ..... N85-34146* #
NASA-TM-86768 ..... N85-34358* #
NASA-TM-86788 ..... N85-34378* #
NASA-TM-86822 ..... N85-34510* #
NASA-TM-87018 ..... N85-34444* #
NASA-TM-87074 ..... N85-34443* #
NASA-TM-87075 ..... N85-34405* #
NASA-TM-87077 ..... N85-34150* #
NASA-TM-87079 ..... N85-34265* #
NASA-TM-87080 ..... N85-34176* #
NASA-TM-87082 ..... N85-34406* #
NASA-TM-87083 ..... N85-34631* #
NASA-TM-87085 ..... N85-34223* #
NASA-TM-87086 ..... N85-34177* #
NASA-TM-87087 ..... N85-34178* #
NASA-TM-87092 ..... N85-34284* #
NASA-TM-87096 ..... N85-34407* #
NASA-TM-87097 ..... N85-34408* #
NASA-TM-87098 ..... N85-34179* #
NASA-TM-87100 ..... N85-34266* #
NASA-TM-87102 ..... N85-34427* #
NASA-TM-87107 ..... N85-34409* #
NASA-TM-87108 ..... N85-34356* #
NASA-TM-87115 ..... N85-34357* #
NASA-TM-87498 ..... N85-34727* #
NASA-TM-87584 ..... N85-34426* #
NASA-TM-87585 ..... N85-35151* #

NASA-TP-2307 ..... N85-34351* #
NASA-TP-2451 ..... N85-34144* #
NASA-TP-2510 ..... N85-34149* #
NASA-TP-2511 ..... N85-34148* #

NBS-GCR-85-497 ..... N85-34229 #

NBSIR-85-3219 ..... N85-34325 #

NPL-DITC-57/85 ..... N85-34513

NPL-MOM-22 ..... N85-34145
NPL-MOM-66 ..... N85-34434
NPL-MOM-68 ..... N85-34515
NPL-MOM-72 ..... N85-34630

NRC/CNR-TT-2111 ..... N85-34426 #
NRC/CNR-TT-2113 ..... N85-34599 #

NUREG/CR-3174-VOL-2 ..... N85-34475 #
NUREG/CR-3193 ..... N85-34371 #
NUREG/CR-4015-SER-1 ..... N85-34418 #
NUREG/CR-4120 ..... N85-34369 #
NUREG/CR-4211 ..... N85-34592 #

OG-7.1-1 ..... N85-34863* #
OG-7.1-2 ..... N85-34864* #
OG-7.1-3 ..... N85-34865* #
OG-7.1-4 ..... N85-34866* #
OG-7.1-5 ..... N85-34867* #
OG-7.1-7 ..... N85-34868* #
OG-7.1-8 ..... N85-34869* #
OG-7.1-9 ..... N85-34870* #
OG-7.1-10 ..... N85-34871* #
OG-7.1-11 ..... N85-34872* #
OG-7.2-1 ..... N85-34873* #
OG-7.2-2 ..... N85-34874* #
OG-7.2-3 ..... N85-34875* #
OG-7.2-4 ..... N85-34876* #
OG-7.2-8 ..... N85-34877* #
OG-7.2-9 ..... N85-34878* #
OG-7.2-11 ..... N85-34879* #
OG-7.2-13 ..... N85-34880* #
OG-7.2-14 ..... N85-34881* #
OG-7.2-15 ..... N85-34882* #
OG-7.2-16 ..... N85-34883* #
OG-7.2-17 ..... N85-34884* #
OG-7.2-18 ..... N85-34885* #
OG-7.2-19 ..... N85-34886* #
OG-7.2-20 ..... N85-34887* #
OG-7.2-21 ..... N85-34888* #
OG-7.2-22 ..... N85-34889* #
OG-7.2-23 ..... N85-34890* #
OG-8.1-1 ..... N85-34891* #
OG-8.1-2 ..... N85-34892* #
OG-8.1-3 ..... N85-34893* #
OG-8.1-4 ..... N85-34894* #
OG-8.1-5 ..... N85-34895* #
OG-8.1-6 ..... N85-34896* #
OG-8.1-7 ..... N85-34897* #
OG-8.1-8 ..... N85-34898* #
OG-8.1-9 ..... N85-34899* #
OG-8.1-10 ..... N85-34900* #
OG-8.1-12 ..... N85-34901* #
OG-8.1-13 ..... N85-34902* #
OG-8.2-2 ..... N85-34903* #
OG-8.2-3 ..... N85-34904* #
OG-8.2-5 ..... N85-34905* #
OG-8.2-6 ..... N85-34906* #
OG-8.2-8 ..... N85-34907* #
OG-8.2-12 ..... N85-34908* #
OG-8.2-13 ..... N85-34909* #
OG-8.2-14 ..... N85-34910* #
OG-8.2-15 ..... N85-34911* #
OG-8.2-16 ..... N85-34912* #
OG-8.2-18 ..... N85-34914* #
OG-8.2-19 ..... N85-34915* #
OG-8.2-20 ..... N85-34916* #
OG-8.2-21 ..... N85-34917* #
OG-8.2-22 ..... N85-34918* #
OG-8.2-23 ..... N85-34919* #
OG-8.3-1 ..... N85-34920* #
OG-8.3-2 ..... N85-34921* #
OG-8.3-3 ..... N85-34922* #
OG-8.3-4 ..... N85-34923* #
OG-8.3-5 ..... N85-34924* #
OG-8.3-7 ..... N85-34925* #
OG-8.3-8 ..... N85-34926* #
OG-8.3-9 ..... N85-34927* #
OG-9.1-1 ..... N85-34928* #
OG-9.1-3 ..... N85-34929* #
OG-9.1-4 ..... N85-34930* #
OG-9.1-5 ..... N85-34931* #
OG-9.1-6 ..... N85-34932* #
OG-9.1-7 ..... N85-34933* #
OG-9.1-8 ..... N85-34934* #
OG-9.1-9 ..... N85-34935* #
OG-9.1-10 ..... N85-34936* #
OG-9.1-12 ..... N85-34937* #
OG-9.1-13 ..... N85-34938* #
OG-9.1-13 ..... N85-34939* #
OG-9.2-1 ..... N85-34940* #
OG-9.2-2 ..... N85-34941* #
OG-9.2-3 ..... N85-34942* #
OG-9.2-4 ..... N85-34943* #
OG-9.2-5 ..... N85-34944* #
OG-9.2-6 ..... N85-34945* #
OG-9.2-7 ..... N85-34946* #
OG-9.2-8 ..... N85-34947* #
OG-9.2-9 ..... N85-34948* #
OG-9.2-10 ..... N85-34949* #
OG-9.2-11 ..... N85-34950* #
OG-9.2-12 ..... N85-34951* #
OG-9.2-13 ..... N85-34952* #
OG-9.2-14 ..... N85-34953* #
OG-9.2-15 ..... N85-34954* #
OG-9.2-16 ..... N85-34955* #
OG-9.3-1 ..... N85-34956* #
OG-9.3-2 ..... N85-34957* #
OG-9.3-3 ..... N85-34958* #
OG-9.3-4 ..... N85-34959* #
OG-9.3-5 ..... N85-34960* #
OG-9.3-6 ..... N85-34961* #
OG-9.3-7 ..... N85-34962* #
OG-9.3-8 ..... N85-34963* #
OG-9.3-9 ..... N85-34964* #
OG-9.3-10 ..... N85-34965* #
OG-9.3-11 ..... N85-34966* #
OG-9.3-12 ..... N85-34967* #
OG-9.3-13 ..... N85-34968* #
OG-9.4-2 ..... N85-34969* #
OG-9.4-3 ..... N85-34970* #
OG-9.4-4 ..... N85-34971* #
OG-9.4-5 ..... N85-34972* #
OG-9.4-6 ..... N85-34973* #
OG-9.4-7 ..... N85-34974* #
OG-9.4-8 ..... N85-34975* #
OG-9.4-9 ..... N85-34976* #
OG-9.4-10 ..... N85-34977* #
OG-9.5-1 ..... N85-34978* #
OG-9.5-2 ..... N85-34980* #
OG-9.5-3 ..... N85-34979* #
OG-9.5-4 ..... N85-34981* #
OG-9.5-5 ..... N85-34982* #
OG-9.5-6 ..... N85-34983* #
OG-9.5-7 ..... N85-34984* #
OG-9.5-8 ..... N85-34985* #
OG-9.5-9 ..... N85-34986* #
OG-9.5-10 ..... N85-34987* #
OG-9.5-11 ..... N85-34988* #
OG-9.5-13 ..... N85-34989* #
OG-9.5-14 ..... N85-34990* #

ORNL-6154 ..... N85-34430 #
ORNL-6164 ..... N85-34382 #

ORNL/TM-8938 ..... N85-34697 #
ORNL/TM-9372 ..... N85-34701 #
ORNL/TM-9397 ..... N85-34708 #
ORNL/TM-9501 ..... N85-34622 #

P/85/8/132 ..... N85-34723* #

PB85-182954 ..... N85-34440 #
PB85-185108 ..... N85-34477 #

PECD7/9/023 ..... N85-34628 #

PNR-90249 ..... N85-34719 #
PNR-90250 ..... N85-34433 #
PNR-90253 ..... N85-34278 #
PNR-90257 ..... N85-34142 #
PNR-90258 ..... N85-34421 #
PNR-90260 ..... N85-34143 #
PNR-90261 ..... N85-34151 #
PNR-90262 ..... N85-34717 #
PNR-90264 ..... N85-34279 #

QR-4 ..... N85-34385 #
QR-5 ..... N85-34445* #

R-1810 ..... N85-34425* #

REPT-85-GT-201 ..... N85-34276 #
REPT-85B0257 ..... N85-34175* #
REPT-255 ..... N85-34428 #
REPT-257 ..... N85-34599 #
REPT-6329-29 ..... N85-34447* #
REPT-85217 ..... N85-34379* #
REPT-85219 ..... N85-34115* #
REPT-85283 ..... N85-34135* #
REPT-85286 ..... N85-34146* #
REPT-85323 ..... N85-34358* #
REPT-85344 ..... N85-34116* #
REPT-85365 ..... N85-34378* #
REPT-85377 ..... N85-34510* #

RHO-RE-ST-31P ..... N85-34270 #

RSRE-MEMO-3776 ..... N85-34514

R82AEB408 ..... N85-34141* #
R82AEB437 ..... N85-34138* #

S-REPT-99-129 ..... N85-34720 #

SAND-84-0159 ..... N85-34359 #
SAND-84-1741C ..... N85-34297 #
SAND-84-1825C ..... N85-34298 #
SAND-84-1957 ..... N85-34360 #
SAND-84-2115C ..... N85-34420 #
SAND-84-2272C ..... N85-34362 #
SAND-84-2421C ..... N85-34696 #
SAND-84-8971 ..... N85-34240 #
SAND-85-0039C ..... N85-34330 #
SAND-85-0040C ..... N85-34693 #
SAND-85-0564C ..... N85-34597 #
SAND-85-0821C ..... N85-34609 #
SAND-85-0945C ..... N85-34702 #
SAND-85-0947 ..... N85-34432 #
SAND-85-0990C-PT-2 ..... N85-34470 #
SAND-85-1110C ..... N85-34512 #
SAND-85-1133C ..... N85-34691 #
SAND-85-7164 ..... N85-34450 #
SAND-85-7182C ..... N85-34588 #
SAND-85-7183C ..... N85-34586 #

SAR-16 ..... N85-35141* #
SAR-17 ..... N85-35141* #

SER-510117 ..... N85-34222* #

SERI/STR-231-2657 ..... N85-34488 #

SERI/TR-215-2484 ..... N85-34485 #

SFENA-DPS/C/S3/84252A N85-34596

SGP-TR-80 ..... N85-34437 #

SH-1.1-3 ..... N85-34730* #
SH-1.1-4 ..... N85-34731* #
SH-1.1-5 ..... N85-34732* #
SH-1.1-6 ..... N85-34733* #
SH-1.1-7 ..... N85-34734* #
SH-1.1-8 ..... N85-34735* #
SH-1.1-9 ..... N85-34736* #

SH-1.1-10 ..... N85-34737* #
SH-1.2-2 ..... N85-34738* #
SH-1.2-3 ..... N85-34739* #
SH-1.2-4 ..... N85-34740* #
SH-1.2-6 ..... N85-34741* #
SH-1.2-7 ..... N85-34742* #
SH-1.2-8 ..... N85-34743* #
SH-1.2-9 ..... N85-34744* #
SH-1.2-10 ..... N85-34745* #
SH-1.2-11 ..... N85-34746* #
SH-1.2-12 ..... N85-34747* #
SH-1.2-13 ..... N85-34748* #
SH-1.2-14 ..... N85-34749* #
SH-1.3-1 ..... N85-34750* #
SH-1.3-2 ..... N85-34751* #
SH-1.3-5 ..... N85-34752* #
SH-1.3-6 ..... N85-34753* #
SH-1.3-7 ..... N85-34754* #
SH-1.3-8 ..... N85-34755* #
SH-1.3-9 ..... N85-34756* #
SH-1.3-11 ..... N85-34757* #
SH-1.3-13 ..... N85-34758* #
SH-1.3-14 ..... N85-34759* #
SH-1.3-15 ..... N85-34760* #
SH-1.3-17 ..... N85-34761* #
SH-1.4-1 ..... N85-34762* #
SH-1.4-2 ..... N85-34763* #
SH-1.4-3 ..... N85-34764* #
SH-1.4-5 ..... N85-34765* #
SH-1.4-6 ..... N85-34766* #
SH-1.4-7 ..... N85-34767* #
SH-1.4-8 ..... N85-34768* #
SH-1.4-9 ..... N85-34769* #
SH-1.4-10 ..... N85-34770* #
SH-1.5-1 ..... N85-34771* #
SH-1.5-3 ..... N85-34772* #
SH-1.5-4 ..... N85-34773* #
SH-1.5-5 ..... N85-34774* #
SH-1.5-6 ..... N85-34775* #
SH-1.5-12 ..... N85-34776* #
SH-1.5-14 ..... N85-34777* #
SH-1.5-15 ..... N85-34778* #
SH-1.5-16 ..... N85-34779* #
SH-1.5-17 ..... N85-34780* #
SH-1.5-18 ..... N85-34781* #
SH-1.5-19 ..... N85-34782* #
SH-2.1-1 ..... N85-34783* #
SH-2.1-3 ..... N85-34784* #
SH-2.1-4 ..... N85-34785* #
SH-2.1-5 ..... N85-34786* #
SH-2.1-6 ..... N85-34787* #
SH-2.1-7 ..... N85-34788* #
SH-2.1-8 ..... N85-34789* #
SH-2.1-9 ..... N85-34790* #
SH-2.1-10 ..... N85-34791* #
SH-2.1-11 ..... N85-34792* #
SH-2.1-12 ..... N85-34793* #
SH-2.1-13 ..... N85-34794* #
SH-2.1-14 ..... N85-34795* #
SH-2.2-1 ..... N85-34796* #
SH-2.2-2 ..... N85-34797* #
SH-2.2-3 ..... N85-34798* #
SH-2.2-4 ..... N85-34799* #
SH-2.2-5 ..... N85-34800* #
SH-2.2-6 ..... N85-34801* #
SH-2.2-7 ..... N85-34802* #
SH-2.2-8 ..... N85-34803* #
SH-2.2-9 ..... N85-34804* #
SH-2.2-10 ..... N85-34805* #
SH-3.1-1 ..... N85-34806* #
SH-3.1-2 ..... N85-34807* #
SH-3.1-3 ..... N85-34808* #
SH-3.1-5 ..... N85-34809* #
SH-3.1-6 ..... N85-34810* #
SH-3.1-7 ..... N85-34811* #
SH-3.1-8 ..... N85-34812* #
SH-3.1-9 ..... N85-34813* #
SH-3.1-10 ..... N85-34814* #
SH-3.1-11 ..... N85-34815* #
SH-3.1-13 ..... N85-34816* #
SH-3.2-1 ..... N85-34817* #
SH-3.2-2 ..... N85-34818* #
SH-3.2-3 ..... N85-34819* #
SH-3.2-4 ..... N85-34820* #
SH-3.2-5 ..... N85-34821* #
SH-3.2-6 ..... N85-34822* #
SH-3.2-8 ..... N85-34823* #
SH-3.2-9 ..... N85-34824* #
SH-3.2-10 ..... N85-34825* #
SH-3.2-11 ..... N85-34826* #
SH-3.2-13 ..... N85-34827* #
SH-4.1-2 ..... N85-34828* #
SH-4.1-3 ..... N85-34829* #
SH-4.1-4 ..... N85-34830* #
SH-4.1-7 ..... N85-34831* #
SH-4.1-9 ..... N85-34832* #
SH-4.1-10 ..... N85-34833* #
SH-4.1-11 ..... N85-34834* #
SH-4.1-12 ..... N85-34835* #
SH-4.1-13 ..... N85-34836* #
SH-4.1-14 ..... N85-34837* #
SH-4.1-16 ..... N85-34838* #
SH-4.1-20 ..... N85-34839* #
SH-4.1-21 ..... N85-34840* #
SH-4.2-3 ..... N85-34841* #
SH-4.2-4 ..... N85-34842* #
SH-4.2-5 ..... N85-34843* #
SH-4.2-6 ..... N85-34844* #
SH-4.2-7 ..... N85-34845* #
SH-4.2-8 ..... N85-34846* #
SH-4.2-9 ..... N85-34847* #
SH-4.2-10 ..... N85-34848* #
SH-4.2-11 ..... N85-34849* #
SH-4.2-12 ..... N85-34850* #
SH-4.2-13 ..... N85-34851* #
SH-4.2-14 ..... N85-34852* #
SH-4.2-16 ..... N85-34853* #
SH-4.2-17 ..... N85-34854* #
SH-4.2-18 ..... N85-34855* #
SH-4.2-19 ..... N85-34856* #
SH-4.2-20 ..... N85-34857* #
SH-4.2-21 ..... N85-34858* #
SH-4.2-22 ..... N85-34859* #
SH-4.2-23 ..... N85-34860* #
SH-4.2-24 ..... N85-34861* #
SH-4.3-7 ..... N85-34992* #
SH-4.3-8 ..... N85-34993* #
SH-4.3-9 ..... N85-34994* #
SH-4.3-10 ..... N85-34995* #
SH-4.3-12 ..... N85-34996* #
SH-4.3-13 ..... N85-34997* #
SH-4.3-14 ..... N85-34998* #
SH-4.3-15 ..... N85-34999* #
SH-4.4-2 ..... N85-35000* #
SH-4.4-3 ..... N85-35001* #
SH-4.4-4 ..... N85-35002* #
SH-4.4-5 ..... N85-35003* #
SH-4.4-6 ..... N85-35004* #
SH-4.4-7 ..... N85-35005* #
SH-4.4-8 ..... N85-35006* #
SH-4.4-9 ..... N85-35007* #
SH-4.4-10 ..... N85-35008* #
SH-4.4-12 ..... N85-35009* #
SH-4.4-14 ..... N85-35010* #
SH-4.4-15 ..... N85-35011* #
SH-4.4-16 ..... N85-35012* #
SH-4.4-17 ..... N85-35013* #
SH-4.4-18 ..... N85-35014* #
SH-4.4-19 ..... N85-35015* #
SH-4.4-20 ..... N85-35016* #
SH-4.4-21 ..... N85-35017* #
SH-4.4-22 ..... N85-35018* #
SH-4.5-1 ..... N85-35019* #
SH-4.5-2 ..... N85-35020* #
SH-4.5-3 ..... N85-35021* #
SH-4.5-4 ..... N85-35022* #
SH-4.5-5 ..... N85-35023* #
SH-4.5-6 ..... N85-35024* #
SH-4.5-7 ..... N85-35025* #
SH-4.5-8 ..... N85-35026* #
SH-4.5-9 ..... N85-35027* #
SH-4.5-10 ..... N85-35028* #
SH-4.5-11 ..... N85-35029* #
SH-4.5-13 ..... N85-35030* #
SH-4.5-14 ..... N85-35031* #
SH-4.5-15 ..... N85-35032* #
SH-4.5-16 ..... N85-35033* #
SH-4.5-17 ..... N85-35034* #
SH-4.5-18 ..... N85-35035* #
SH-4.5-19 ..... N85-35036* #
SH-4.5-20 ..... N85-35037* #
SH-4.5-21 ..... N85-35038* #
SH-4.6-1 ..... N85-35039* #
SH-4.6-2 ..... N85-35040* #
SH-4.6-3 ..... N85-35041* #
SH-4.6-4 ..... N85-35042* #
SH-4.6-5 ..... N85-35043* #
SH-4.6-6 ..... N85-35044* #
SH-4.6-7 ..... N85-35045* #
SH-4.7-1 ..... N85-35046* #
SH-4.7-2 ..... N85-35047* #
SH-4.7-3 ..... N85-35048* #
SH-4.7-4 ..... N85-35049* #
SH-4.7-5 ..... N85-35050* #
SH-4.7-6 ..... N85-35051* #
SH-4.7-7 ..... N85-35052* #
SH-4.7-9 ..... N85-35053* #
SH-4.7-10 ..... N85-35054* #
SH-4.7-11 ..... N85-35055* #
SH-5.1-2 ..... N85-35056* #
SH-5.1-3 ..... N85-35057* #
SH-5.1-4 ..... N85-35058* #
SH-5.1-5 ..... N85-35059* #
SH-5.1-6 ..... N85-35060* #
SH-5.1-7 ..... N85-35061* #
SH-5.1-8 ..... N85-35062* #
SH-5.1-9 ..... N85-35063* #
SH-5.1-11 ..... N85-35064* #
SH-5.1-12 ..... N85-35065* #
SH-5.1-13 ..... N85-35066* #
SH-5.1-14 ..... N85-35067* #
SH-5.1-15 ..... N85-35068* #
SH-5.1-16 ..... N85-35069* #
SH-5.1-17 ..... N85-35070* #
SH-5.1-18 ..... N85-35071* #
SH-5.1-20 ..... N85-35072* #
SH-5.1-21 ..... N85-35073* #
SH-5.1-22 ..... N85-35074* #
SH-5.1-23 ..... N85-35075* #
SH-6.1-1 ..... N85-35076* #
SH-6.1-2 ..... N85-35077* #
SH-6.1-3 ..... N85-35078* #
SH-6.1-5 ..... N85-35079* #
SH-6.1-6 ..... N85-35080* #
SH-6.1-7 ..... N85-35081* #
SH-6.1-8 ..... N85-35082* #
SH-6.1-10 ..... N85-35083* #
SH-6.1-11 ..... N85-35084* #
SH-6.1-12 ..... N85-35085* #
SH-6.1-13 ..... N85-35086* #
SH-6.1-14 ..... N85-35087* #
SH-6.1-15 ..... N85-35088* #
SH-6.1-16 ..... N85-35089* #
SH-6.1-18 ..... N85-35090* #
SH-6.1-19 ..... N85-35091* #
SH-6.1-21 ..... N85-35092* #
SH-6.1-22 ..... N85-35093* #
SH-7.1-1 ..... N85-35094* #
SH-7.1-2 ..... N85-35095* #
SH-7.1-3 ..... N85-35096* #
SH-7.1-4 ..... N85-35097* #
SH-7.1-6 ..... N85-35098* #
SH-7.1-7 ..... N85-35099* #
SH-7.1-8 ..... N85-35100* #
SH-7.1-9 ..... N85-35101* #
SH-7.1-10 ..... N85-35102* #
SH-7.1-11 ..... N85-35103* #
SH-7.1-12 ..... N85-35104* #
SH-7.1-14 ..... N85-35105* #
SH-7.1-15 ..... N85-35106* #
SH-7.1-17 ..... N85-35107* #
SH-8.1-2 ..... N85-35108* #
SH-8.1-5 ..... N85-35110* #
SH-8.1-6 ..... N85-35111* #
SH-8.1-7 ..... N85-35112* #
SH-8.1-8 ..... N85-35113* #
SH-8.1-9 ..... N85-35114* #
SH-8.1-10 ..... N85-35115* #
SH-8.1-11 ..... N85-35116* #
SH-9.1-2 ..... N85-35117* #
SH-9.1-3 ..... N85-35118* #
SH-9.1-4 ..... N85-35119* #
SH-9.1-5 ..... N85-35120* #
SH-9.1-6 ..... N85-35121* #
SH-9.1-7 ..... N85-35122* #
SH-9.1-8 ..... N85-35123* #
SH-9.1-9 ..... N85-35124* #
SH-9.1-10 ..... N85-35125* #
SH-9.1-11 ..... N85-35126* #
SH-9.1-12 ..... N85-35127* #
SH-9.1-13 ..... N85-35128* #
SH-9.1-14 ..... N85-35129* #
SH-9.1-15 ..... N85-35130* #
SH-9.1-16 ..... N85-35131* #
SH-9.1-17 ..... N85-35132* #
SH-10.1-1 ..... N85-35133* #
SH-10.1-2 ..... N85-35134* #
SH-10.1-3 ..... N85-35135* #
SH-10.1-5 ..... N85-35136* #
SH-10.1-6 ..... N85-35137* #
SH-10.1-7 ..... N85-35138* #
SH-10.1-8 ..... N85-35139* #
SH-10.1-9 ..... N85-35140* #

SNIAS-851-430-103 ..... N85-34227 #
SNIAS-851-430-104 ..... N85-34228 #

SPE-13894-PT-2 ..... N85-34470 #

SU-SLAC-TM-85-3 ..... N85-34585 #

TG-101/9-85 ..... N85-34727* #

TI85-003251 ..... N85-34420 #
TI85-006132 ..... N85-34600 #
TI85-006884 ..... N85-34277 #
TI85-009331 ..... N85-34371 #
TI85-009747 ..... N85-34369 #

TI85-010349 ..... N85-34418 #
TI85-901341 ..... N85-34475 #
TI85-901384 ..... N85-34276 #
TI85-901402 ..... N85-34592 #

TMS-PAPER-F84-14 ..... N85-34264* #

TR-83-4975-02 ..... N85-34352* #
TR-84-01 ..... N85-34113* #
TR-84428 ..... N85-34133* #
TR-84428 ..... N85-34134* #

TRW-SN-39146-REV-3 ..... N85-34385 #

UCID-20381 ..... N85-34462 #
UCID-20385 ..... N85-34239 #
UCID-20400 ..... N85-34590 #
UCID-20415 ..... N85-34587 #

UCLA/PPG-860 ..... N85-34707 #

UCRL-15666 ..... N85-34268 #
UCRL-15668 ..... N85-34399 #
UCRL-15672 ..... N85-34383 #
UCRL-53541-84 ..... N85-34398 #
UCRL-91402 ..... N85-34465 #
UCRL-91617 ..... N85-34361 #
UCRL-91831 ..... N85-34231 #
UCRL-91936 ..... N85-34700 #
UCRL-92102 ..... N85-34304 #
UCRL-92505 ..... N85-34367 #
UCRL-92532 ..... N85-34706 #
UCRL-92624 ..... N85-34595 #

UNH-MP-TR-SG-84-9 ..... N85-34477 #

US-PATENT-APPL-SN-359382 ..... N85-34327*
US-PATENT-APPL-SN-387647 ..... N85-34333*
US-PATENT-APPL-SN-425202 ..... N85-34629*
US-PATENT-APPL-SN-457990 ..... N85-34722*
US-PATENT-APPL-SN-510137 ..... N85-34401*
US-PATENT-APPL-SN-548583 ..... N85-34282*
US-PATENT-APPL-SN-559501 ..... N85-34627 #
US-PATENT-APPL-SN-563890 ..... N85-34373*
US-PATENT-APPL-SN-580573 ..... N85-34441*
US-PATENT-APPL-SN-582643 ..... N85-34374*
US-PATENT-APPL-SN-590923 ..... N85-34375*
US-PATENT-APPL-SN-598777 ..... N85-34281*
US-PATENT-APPL-SN-602050 ..... N85-34402*
US-PATENT-APPL-SN-605950 ..... N85-34345 #
US-PATENT-APPL-SN-606037 ..... N85-34387 #
US-PATENT-APPL-SN-606038 ..... N85-34241 #
US-PATENT-APPL-SN-608282 ..... N85-34392 #
US-PATENT-APPL-SN-609685 ..... N85-34391 #
US-PATENT-APPL-SN-609686 ..... N85-34458 #
US-PATENT-APPL-SN-610905 ..... N85-34242 #
US-PATENT-APPL-SN-611557 ..... N85-34306 #
US-PATENT-APPL-SN-611558 ..... N85-34305 #
US-PATENT-APPL-SN-611772 ..... N85-34286 #
US-PATENT-APPL-SN-611773 ..... N85-34274 #
US-PATENT-APPL-SN-612199 ..... N85-34220 #
US-PATENT-APPL-SN-612951 ..... N85-34460 #
US-PATENT-APPL-SN-612953 ..... N85-34218 #
US-PATENT-APPL-SN-612954 ..... N85-34457 #
US-PATENT-APPL-SN-612955 ..... N85-34412 #
US-PATENT-APPL-SN-614507 ..... N85-34417 #
US-PATENT-APPL-SN-614508 ..... N85-34290 #
US-PATENT-APPL-SN-615210 ..... N85-34626 #
US-PATENT-APPL-SN-615486 ..... N85-34390 #
US-PATENT-APPL-SN-617197 ..... N85-34604 #
US-PATENT-APPL-SN-617652 ..... N85-34416 #
US-PATENT-APPL-SN-617653 ..... N85-34344 #
US-PATENT-APPL-SN-617656 ..... N85-34326 #
US-PATENT-APPL-SN-617658 ..... N85-34342 #
US-PATENT-APPL-SN-617660 ..... N85-34292 #
US-PATENT-APPL-SN-617781 ..... N85-34226 #
US-PATENT-APPL-SN-619759 ..... N85-34393 #
US-PATENT-APPL-SN-619886 ..... N85-34219 #
US-PATENT-APPL-SN-620287 ..... N85-34414 #
US-PATENT-APPL-SN-620305 ..... N85-34633 #
US-PATENT-APPL-SN-620306 ..... N85-34293 #
US-PATENT-APPL-SN-620308 ..... N85-34607 #
US-PATENT-APPL-SN-623874 ..... N85-34710 #
US-PATENT-APPL-SN-623875 ..... N85-34415 #
US-PATENT-APPL-SN-624085 ..... N85-34275 #
US-PATENT-APPL-SN-625321 ..... N85-34389 #
US-PATENT-APPL-SN-625322 ..... N85-34343 #
US-PATENT-APPL-SN-625324 ..... N85-34291 #
US-PATENT-APPL-SN-625325 ..... N85-34411 #
US-PATENT-APPL-SN-625326 ..... N85-34388 #
US-PATENT-APPL-SN-636658 ..... N85-34287 #
US-PATENT-APPL-SN-636659 ..... N85-34267 #
US-PATENT-APPL-SN-641143 ..... N85-34280*
US-PATENT-APPL-SN-646044 ..... N85-34403*
US-PATENT-APPL-SN-649623 ..... N85-34221 #
US-PATENT-APPL-SN-721836 ..... N85-34340 #
US-PATENT-APPL-SN-721977 ..... N85-34632 #
US-PATENT-APPL-SN-724714 ..... N85-34337 #
US-PATENT-APPL-SN-724719 ..... N85-34224 #
US-PATENT-APPL-SN-726558 ..... N85-34338 #
US-PATENT-APPL-SN-729389 ..... N85-34410 #
US-PATENT-APPL-SN-731646 ..... N85-34339 #
US-PATENT-APPL-SN-733991 ..... N85-34594 #
US-PATENT-APPL-SN-737377 ..... N85-34381 #
US-PATENT-APPL-SN-814505 ..... N85-34459 #

US-PATENT-CLASS-73-75 ..... N85-34373*
US-PATENT-CLASS-73-831 ..... N85-34375*
US-PATENT-CLASS-73-856 ..... N85-34375*
US-PATENT-CLASS-136-253 ..... N85-34441*
US-PATENT-CLASS-137-99 ..... N85-34403*
US-PATENT-CLASS-137-116.3 ..... N85-34403*
US-PATENT-CLASS-244-118.1 ..... N85-34401*
US-PATENT-CLASS-244-158R N85-34401*
US-PATENT-CLASS-248-550 ..... N85-34401*
US-PATENT-CLASS-250-374 ..... N85-34374*
US-PATENT-CLASS-250-379 ..... N85-34374*
US-PATENT-CLASS-267-8R N85-34401*
US-PATENT-CLASS-267-150 ..... N85-34401*
US-PATENT-CLASS-324-65-P N85-34373*
US-PATENT-CLASS-343-5-CM N85-34327*
US-PATENT-CLASS-343-5-W N85-34327*
US-PATENT-CLASS-343-13-R N85-34629*
US-PATENT-CLASS-343-17.2-PC N85-34327*
US-PATENT-CLASS-356-5 ..... N85-34629*
US-PATENT-CLASS-364-571 ..... N85-34333*
US-PATENT-CLASS-364-578 ..... N85-34333*
US-PATENT-CLASS-372-32 ..... N85-34333*
US-PATENT-CLASS-410-156 ..... N85-34401*
US-PATENT-CLASS-414-288 ..... N85-34722*
US-PATENT-CLASS-414-328 ..... N85-34722*
US-PATENT-CLASS-414-373 ..... N85-34722*
US-PATENT-CLASS-414-786 ..... N85-34722*
US-PATENT-CLASS-415-170-R N85-34402*
US-PATENT-CLASS-415-174 ..... N85-34402*
US-PATENT-CLASS-415-196 ..... N85-34402*
US-PATENT-CLASS-415-200 ..... N85-34402*
US-PATENT-CLASS-416-174 ..... N85-34402*
US-PATENT-CLASS-428-260 ..... N85-34281*
US-PATENT-CLASS-428-408 ..... N85-34281*
US-PATENT-CLASS-428-413 ..... N85-34281*
US-PATENT-CLASS-523-454 ..... N85-34282*
US-PATENT-CLASS-523-458 ..... N85-34282*
US-PATENT-CLASS-525-107 ..... N85-34281*
US-PATENT-CLASS-525-113 ..... N85-34281*
US-PATENT-CLASS-525-119 ..... N85-34281*
US-PATENT-CLASS-525-186 ..... N85-34281*
US-PATENT-CLASS-525-229 ..... N85-34281*
US-PATENT-CLASS-528-92 ..... N85-34282*
US-PATENT-CLASS-528-94 ..... N85-34281*
US-PATENT-CLASS-528-106 ..... N85-34282*
US-PATENT-CLASS-528-113 ..... N85-34281*
US-PATENT-CLASS-528-117 ..... N85-34281*
US-PATENT-CLASS-528-168 ..... N85-34280*
US-PATENT-CLASS-528-229 ..... N85-34280*
US-PATENT-CLASS-528-229 ..... N85-34282*
US-PATENT-CLASS-528-352 ..... N85-34280*
US-PATENT-CLASS-528-353 ..... N85-34280*
US-PATENT-CLASS-528-407 ..... N85-34281*
US-PATENT-CLASS-528-407 ..... N85-34282*

US-PATENT-4,509,048 ..... N85-34327*
US-PATENT-4,509,132 ..... N85-34333*
US-PATENT-4,509,548 ..... N85-34403*
US-PATENT-4,510,277 ..... N85-34282*
US-PATENT-4,528,417 ..... N85-34441*
US-PATENT-4,532,797 ..... N85-34373*
US-PATENT-4,533,242 ..... N85-34629*
US-PATENT-4,535,636 ..... N85-34375*
US-PATENT-4,536,114 ..... N85-34401*
US-PATENT-4,536,365 ..... N85-34280*
US-PATENT-4,537,554 ..... N85-34722*
US-PATENT-4,537,834 ..... N85-34281*
US-PATENT-4,538,066 ..... N85-34374*
US-PATENT-4,540,336 ..... N85-34402*

USAAVSCOM-TM-85-A-4 ..... N85-34135* #

USAAVSCOM-TR-85-C-9 ..... N85-34405* #
USAAVSCOM-TR-85-C-14 ..... N85-34223* #
USAAVSCOM-TR-85-C-16 ..... N85-34406* #

USGS-CIRC-945 ..... N85-34468 #

USGS-OFR-85-224 ..... N85-34471 #

UTIAS-TN-257 ..... N85-34139 #

UTIAS-283-PT-1 ..... N85-34117 #
UTIAS-283-PT-2 ..... N85-34118 #

Y/DV-427 ..... N85-34272 #

☆U.S. GOVERNMENT PRINTING OFFICE: 1985-491-575/20022

FEDERAL DEPOSITORY LIBRARY PROGRAM

The Federal Depository Library Program provides Government publications to designated libraries throughout the United States. The Regional Depository Libraries listed below receive and retain at least one copy of nearly every Federal Government publication, either in printed or microfilm form, for use by the general public. These libraries provide reference services and inter-library loans; however, they are *not* sales outlets. You may wish to ask your local library to contact a Regional Depository to help you locate specific publications, or you may contact the Regional Depository yourself.

ARKANSAS STATE LIBRARY
One Capitol Mall
Little Rock, AR 72201
(501) 371-2326

AUBURN UNIV. AT MONTGOMERY LIBRARY
Documents Department
Montgomery, AL 36193
(205) 279-9110, ext. 253

UNIV. OF ALABAMA LIBRARY
Documents Dept.—Box S
University, AL 35486
(205) 348-7369

DEPT. OF LIBRARY, ARCHIVES AND PUBLIC RECORDS
Third Floor—State Cap.
1700 West Washington
Phoenix, AZ 85007
(602) 255-4121

UNIVERSITY OF ARIZONA LIB.
Government Documents Dept.
Tucson, AZ 85721
(602) 626-5233

CALIFORNIA STATE LIBRARY
Govt. Publications Section
P.O. Box 2037
Sacramento, CA 95809
(916) 322-4572

UNIV. OF COLORADO LIB.
Government Pub. Division
Campus Box 184
Boulder, CO 80309
(303) 492-8834

DENVER PUBLIC LIBRARY
Govt. Pub. Department
1357 Broadway
Denver, CO 80203
(303) 571-2131

CONNECTICUT STATE LIBRARY
Government Documents Unit
231 Capitol Avenue
Hartford, CT 06106
(203) 566-4971

UNIV. OF FLORIDA LIBRARIES
Library West
Documents Department
Gainesville, FL 32611
(904) 392-0367

UNIV. OF GEORGIA LIBRARIES
Government Reference Dept.
Athens, Ga 30602
(404) 542-8951

UNIV. OF HAWAII LIBRARY
Govt. Documents Collection
2550 The Mall
Honolulu, HI 96822
(808) 948-8230

UNIV. OF IDAHO LIBRARY
Documents Section
Moscow, ID 83843
(208) 885-6344

ILLINOIS STATE LIBRARY
Information Services Branch
Centennial Building
Springfield, IL 62706
(217) 782-5185

INDIANA STATE LIBRARY
Serials Documents Section
140 North Senate Avenue
Indianapolis, IN 46204
(317) 232-3686

UNIV. OF IOWA LIBRARIES
Govt. Documents Department
Iowa City, IA 52242
(319) 353-3318

UNIVERSITY OF KANSAS
Doc. Collect—Spencer Lib.
Lawrence, KS 66045
(913) 864-4662

UNIV. OF KENTUCKY LIBRARIES
Govt. Pub. Department
Lexington, KY 40506
(606) 257-3139

LOUISIANA STATE UNIVERSITY
Middleton Library
Govt. Docs. Dept.
Baton Rouge, LA 70803
(504) 388-2570

LOUISIANA TECHNICAL UNIV. LIBRARY
Documents Department
Ruston, LA 71272
(318) 257-4962

UNIVERSITY OF MAINE
Raymond H. Fogler Library
Tri-State Regional Documents Depository
Orono, ME 04469
(207) 581-1680

UNIVERSITY OF MARYLAND
McKeldin Lib.—Doc. Div.
College Park, MD 20742
(301) 454-3034

BOSTON PUBLIC LIBRARY
Government Docs. Dept.
Boston, MA 02117
(617) 536-5400 ext. 226

DETROIT PUBLIC LIBRARY
Sociology Department
5201 Woodward Avenue
Detroit, MI 48202
(313) 833-1409

MICHIGAN STATE LIBRARY
P.O. Box 30007
Lansing, MI 48909
(517) 373-0640

UNIVERSITY OF MINNESOTA
Government Pubs. Division
409 Wilson Library
309 19th Avenue South
Minneapolis, MN 55455
(612) 373-7813

UNIV. OF MISSISSIPPI LIB.
Documents Department
University, MS 38677
(601) 232-5857

UNIV. OF MONTANA
Mansfield Library
Documents Division
Missoula, MT 59812
(406) 243-6700

NEBRASKA LIBRARY COMM.
Federal Documents
1420 P Street
Lincoln, NE 68508
(402) 471-2045
In cooperation with University of Nebraska-Lincoln

UNIVERSITY OF NEVADA LIB.
Govt. Pub. Department
Reno, NV 89557
(702) 784-6579

NEWARK PUBLIC LIBRARY
5 Washington Street
Newark, NJ 07101
(201) 733-7812

UNIVERSITY OF NEW MEXICO
Zimmerman Library
Government Pub. Dept.
Albuquerque, NM 87131
(505) 277-5441

NEW MEXICO STATE LIBRARY
Reference Department
325 Don Gaspar Avenue
Santa Fe, NM 87501
(505) 827-2033, ext. 22

NEW YORK STATE LIBRARY
Empire State Plaza
Albany, NY 12230
(518) 474-5563

UNIVERSITY OF NORTH CAROLINA AT CHAPEL HILL
Wilson Library
BA/SS Documents Division
Chapel Hill, NC 27515
(919) 962-1321

UNIVERSITY OF NORTH DAKOTA
Chester Fritz Library
Documents Department
Grand Forks, ND 58202
(701) 777-2617, ext. 27
(In cooperation with North Dakota State Univ. Library)

STATE LIBRARY OF OHIO
Documents Department
65 South Front Street
Columbus, OH 43215
(614) 462-7051

OKLAHOMA DEPT. OF LIB.
Government Documents
200 NE 18th Street
Oklahoma City, OK 73105
(405) 521-2502

OKLAHOMA STATE UNIV. LIB.
Documents Department
Stillwater, OK 74078
(405) 624-6546

PORTLAND STATE UNIV. LIB.
Documents Department
P.O. Box 1151
Portland, OR 97207
(503) 229-3673

STATE LIBRARY OF PENN.
Government Pub. Section
P.O. Box 1601
Harrisburg, PA 17105
(717) 787-3752

TEXAS STATE LIBRARY
Public Services Department
P.O. Box 12927—Cap. Sta.
Austin, TX 78753
(512) 471-2996

TEXAS TECH UNIV. LIBRARY
Govt. Documents Department
Lubbock, TX 79409
(806) 742-2268

UTAH STATE UNIVERSITY
Merrill Library, U.M.C. 30
Logan, UT 84322
(801) 750-2682

UNIVERSITY OF VIRGINIA
Alderman Lib.—Public Doc.
Charlottesville, VA 22901
(804) 924-3133

WASHINGTON STATE LIBRARY
Documents Section
Olympia, WA 98504
(206) 753-4027

WEST VIRGINIA UNIV. LIB.
Documents Department
Morgantown, WV 26506
(304) 293-3640

MILWAUKEE PUBLIC LIBRARY
814 West Wisconsin Avenue
Milwaukee, WI 53233
(414) 278-3000

ST. HIST LIB. OF WISCONSIN
Government Pub. Section
816 State Street
Madison, WI 53706
(608) 262-4347

WYOMING STATE LIBRARY
Supreme Ct. & Library Bld.
Cheyenne, WY 82002
(307) 777-6344

National Aeronautics and
Space Administration
Code NIT-4
Washington, D.C.
20546

Official Business

Penalty for Private Use, $300

SPECIAL FOURTH-CLASS RATE
POSTAGE & FEES PAID
NASA
WASHINGTON, D.C.
PERMIT No. G 27

NASA

POSTMASTER: If Undeliverable (Section 158
Postal Manual) Do Not Return